Geotechnical Engineering for the Preservation of Monuments and Historic Sites

Editors:
Emilio Bilotta
Alessandro Flora
Stefania Lirer
Carlo Viggiani

CRC Press
Taylor & Francis Group
A BALKEMA BOOK

GEOTECHNICAL ENGINEERING FOR THE PRESERVATION OF MONUMENTS AND HISTORIC SITES

This page intentionally left blank

PROCEEDINGS OF THE SECOND INTERNATIONAL SYMPOSIUM ON GEOTECHNICAL ENGINEERING FOR THE PRESERVATION OF MONUMENTS AND HISTORIC SITES, NAPOLI, ITALY, 30–31 MAY 2013

Geotechnical Engineering for the Preservation of Monuments and Historic Sites

Editors

Emilio Bilotta, Alessandro Flora, Stefania Lirer & Carlo Viggiani

University of Naples Federico II, Napoli, Italy

CRC Press
Taylor & Francis Group
Boca Raton London New York Leiden

CRC Press is an imprint of the
Taylor & Francis Group, an **informa** business

A BALKEMA BOOK

CRC Press
Taylor & Francis Group
6000 Broken Sound Parkway NW, Suite 300
Boca Raton, FL 33487-2742

© 2013 by Taylor & Francis Group, LLC
CRC Press is an imprint of Taylor & Francis Group, an Informa business

No claim to original U.S. Government works
Version Date: 20130625

International Standard Book Number-13: 978-1-315-88749-4 (eBook - PDF)

This book contains information obtained from authentic and highly regarded sources. Reasonable efforts have been made to publish reliable data and information, but the author and publisher cannot assume responsibility for the validity of all materials or the consequences of their use. The authors and publishers have attempted to trace the copyright holders of all material reproduced in this publication and apologize to copyright holders if permission to publish in this form has not been obtained. If any copyright material has not been acknowledged please write and let us know so we may rectify in any future reprint.

Except as permitted under U.S. Copyright Law, no part of this book may be reprinted, reproduced, transmitted, or utilized in any form by any electronic, mechanical, or other means, now known or hereafter invented, including photocopying, microfilming, and recording, or in any information storage or retrieval system, without written permission from the publishers.

For permission to photocopy or use material electronically from this work, please access www.copyright.com (http://www.copyright.com/) or contact the Copyright Clearance Center, Inc. (CCC), 222 Rosewood Drive, Danvers, MA 01923, 978-750-8400. CCC is a not-for-profit organization that provides licenses and registration for a variety of users. For organizations that have been granted a photocopy license by the CCC, a separate system of payment has been arranged.

Trademark Notice: Product or corporate names may be trademarks or registered trademarks, and are used only for identification and explanation without intent to infringe.

Visit the Taylor & Francis Web site at
http://www.taylorandfrancis.com

and the CRC Press Web site at
http://www.crcpress.com

Geotechnical Engineering for the Preservation of Monuments and Historic Sites – Bilotta, Flora, Lirer & Viggiani (eds)
© 2013 Taylor & Francis Group, London, ISBN 978-1-138-00055-1

Table of contents

Preface xi

Organization xiii

Opening address

Cultural heritage and geotechnical engineering: An introduction 3
C. Viggiani

Special lectures

Influence of the subsoil on the urban development of Napoli 15
S. Aversa, A. Evangelista & A. Scotto di Santolo

Local site conditions and seismic risk assessment of historic buildings 45
D. D'Ayala & A. Ansal

The role of monitoring and identification techniques on the preservation of historic towers 57
R. Lancellotta & D. Sabia

Intervention techniques 75
E. Ovando-Shelley, E. Santoyo & M.O. Pinto de Oliveira

Papers

New underground lines in historic centres: Experiences in Brescia 95
A.M. Ajmone Cat, E. Campa, M. Lodico & C. Umiliaco

Safeguarding the historic town of San Fratello, Sicily 105
C. Airò Farulla & F. Cafiso

Stability analysis of the underground masonry tunnel of Ancient Nemea 113
H. Alexakis & N. Makris

Foundation systems of some heritage buildings in Najaf/Iraq case study: Al Shelan Khan 123
N.K.S. AL-Saoudi & M.Sh. AL-Shakerchy

Seismic vulnerability reduction for historical buildings: The case study of house of mosaics 129
L. Alterio, L. Evangelista, G. Russo & F. Silvestri

New evidences on the Phlegraean bradyseism in the area of *Puteolis* harbour 137
L. Amato & C. Gialanella

Important works in the town centre and preservation of existing heritage:
The Grand Carré Jaude in Clermont-Ferrand (France) 145
F. Ambrosini, P. Berthelot, F. Durand & A. Reynaud

Drilled spiral piles in St. John's Church of Tartu, Estonia 149
K. Avellan

Settlement induced by TBM excavation under the Vittoria's Church in Napoli 157
S. Aversa, E. Bilotta, G. Russo & A. di Luccio

Ground improving injections underneath historical buildings: Five case histories as an overview of a technique 165
V. Berengo

Monitoring of the temperature-moisture regime of rock dwellings in Brhlovce village (Slovakia) 175
V. Boháč, D. Fidríková, V. Vretenár, T. Durmeková, I. Šimková, V. Greif & J. Vlčko

Restoration projects and remedial works in the historical island of Ventotene 183
N. Bosco, P. Croce, B. Palma, D. Pingitore & M. Ramondini

19th and 20th century coastal military installations affected by coastal erosion in the UK 191
E.N. Bromhead, M-L. Ibsen & D. Tapete

Interpretation and modelling of the subsidence at the archaeological site of Sybaris (Southern Italy) 199
F. Cafaro, F. Cotecchia, V. Lenti & R. Pagliarulo

Geotechnical aspects in the preservation of the *Domus Tiberiana* in Rome 207
G. Calabresi, L. Cavalera, V. Ascoli Marchetti & M.G. Filetici

New underground lines in historic centres: Experiences in Naples 215
E. Campa, A.M. Ajmone Cat, C. Fioretti & L. Mormone

The Benedictine Basilica of S. Angelo in Formis (Southern Italy): A therapy without diagnosis? 225
A. Cammarota, G. Russo, C. Viggiani & M. Candela

The vineyard of the monastery of S. Martino in Napoli 233
M. Candela, C. Viggiani & R. Viparelli

Site characterization by in situ and laboratory tests for the structural & architectural restoration of Saint Nicholas Church, Nicosia, Cyprus 241
A. Cavallaro, L. Cessari & E. Gigliarelli

Long-term mechanical behavior of wooden pile foundation in Venice 249
F. Ceccato, P. Simonini & A. Lionello

Cultural Heritage and physical environment: A geo-archaeological approach to the analysis of interaction and risk factors 257
A. Cinti, L. Coppola & E.N. Bromhead

Settlement response of masonry constructions 265
M. Como

Assessment of geological and geotechnical conditions for rebuilding Avala's television tower 273
S. Ćorić, D. Rakić, G. Hadži-Niković, T. Janković, V. Filipović & B. Marjanović

Afghanistan, Buddhas of Bamiyan: Emergency consolidation of the cliffs and niches 279
C. Crippa, R. Granata & C. Margottini

Archaeology and geotechnical engineering 289
S. D'Agostino & G. Tocco

Long-term stability of old cathedrals in St. Petersburg 299
R.E. Dashko & A.V. Shidlovskaya

A study for the requalification and safety against natural hazards of the environmental and building heritage of Sant'Agata de' Goti (Italy) 307
F. de Silva, M. Melillo, D. Calcaterra, F. Fascia, A. Scotto di Santolo, F. Silvestri & L. Stendardo

Study and monitoring for conservation of Sanctuary of Santa Maria Assunta at Monteortone (Abano Terme, Padova) 317
A. Dei Svaldi & A. Mazzucato

Slope dynamics, monitoring and geological conservation of the Siq of Petra (Jordan) 325
G. Delmonaco, C. Margottini & D. Spizzichino

Historic and non-historic building impact assessment methodology for major tunnelling infrastructure projects 335
M. Devriendt, E. Palmer, R. Hill & D. Lazarus

Dynamic identification and seismic behaviour of the Ghirlandina tower in Modena (Italy) 343
A. Di Tommaso, R. Lancellotta, D. Sabia, D. Costanzo, F. Focacci & F. Romaro

Performance evaluation of bending strength to predict durability of ornamental gneiss from Santo Antônio de Pádua, RJ, BR 353
J.L.E. Dias Filho, P.C.A. Maia, G.C. Xavier & P.A.M. Fernandes

The role of the geotechnical engineer in archaeological work: The Greek experience 359
D. Egglezos, D. Moullou & M. Ioannidou

Re-burial of the Arrephorion on the Athenian Acropolis: An in situ rescue intervention against degradation 367
D.N. Egglezos

Egyptian experience in the preservation of monuments and historic structures. A case study: Hibis Temple, El-Kharga—Egypt 377
M.K. El-Ghamrawy, M.A. Sakr & S.A. Gad

Diagnostic of the colonial structure "Palacio del Segundo Cabo" in Havana, Cuba 385
S. Figueredo, Y. Gámez, R. Lorenzo, J. de la Rosa & R.P. da Cunha

Softening and swelling mechanism affecting south slope of Civita di Bagnoregio (VT) 395
F. Garbin, C. Margottini, R. Brancaleoni & A. Sonnessa

Evaluation of the soil disturbance due to the installation of prefabricated vertical drains: An analytical approach applied to case histories 403
A. Ghandeharioon

Preservation and monitoring of the Frari bell tower in Venice 411
G. Gottardi, M. Marchi, A. Lionello & P.P. Rossi

Collapse of a backfilled wall at the Castle Wespenstein 425
I. Herle, J. Männer, E. Schwiteilo & J. Wehr

Geotechnical problems on historical buildings from Transylvania 431
N.M. Ilieş & A. Popa

Research and advanced technology in the restoration of the monuments of the Athenian Acropolis 437
M. Ioannidou

Estimation of moisture condition with salinity in the ground behind the Dunhuang Mogao Grottoes using the electrical resistivity method 447
M. Ito, K. Koizumi, K. Oda, T. Miyawaki, C. Piao, C. Tanimoto, Y. Iwasaki, X. Wang, Q. Guo & S. Yang

Dismantling for reconstitution of N1 Tower of Prasat Suor Prat, Angkor Thom, Cambodia 455
Y. Iwasaki, Y. Akazawa, M. Fukuda, J. Nakazawa, K. Nakagawa, I. Shimoda & T. Nakagawa

A variegated embankment dam in a historical territory 465
R. Jappelli

Safety and/or security of monuments? An apparent dilemma 473
R. Jappelli

Strong motion record processing for the Athenian Acropolis seismic response assessment 483
I.S. Kalogeras & D. Egglezos

Settlements due to tail gap of shield tunnelling 493
D. Kolymbas

An innovative approach for reducing the seismic risk of existing buildings and historic sites 507
D. Lombardi, A. Flora, S. Lirer & F. Silvestri

Preservation of historic structures and monuments using minimally invasive Screw-Piles and Helical Anchors—two cases 515
A.J. Lutenegger, D. Robson & P. Mohan

Seismic risk assessment of San Gimignano towers: Geotechnical aspects and soil-structure interaction 523
C. Madiai, S. Renzi & G. Vannucchi

Analytical modelling of the creep-rotation rate for leaning towers 531
M. Marchi, I. Fabbi, G. Gottardi, R. Butterfield & R. Lancellotta

Geotechnical and geophysical characterization of Moai statues—Rapa Nui Easter Island (Chile) 539
C. Margottini, D. Spizzichino, L. Orlando, M. Marsella, B. Renzi, A. Sonnessa, O. Pandolfi & P. Soddu

Landslide risk and monitoring system for conservation of Vardzia monastery, Georgia 549
C. Margottini, D. Spizzichino & A. Sonnessa

Strength and structure of the roofed mud-walls of Toji Temple 559
M. Mimura, M. Yoshimura & T. Terao

Spatial-temporal analysis of the subsidence in the city of Bologna 565
G. Modoni, G. Darini, R.L. Spacagna, M. Saroli, G. Russo & P. Croce

Repair works at Saint Claire Convent in Chinchón (Madrid, Spain) 573
P.R. Monteverde & J.M. Avila-Jalvo

Groundwater management during excavations of S. Pasquale station in Naples 579
L. Mormone, G. Falconio & A. Mandolini

Offshore soil investigations on the bottom of Ohrid Lake and authentic reconstruction of timber piles settlement 589
D. Nikolovski, B. Veljanovski & A. Stojkovska

Groundwater development and management in Siem Reap, Cambodia: Impacts of groundwater pumping on Angkor Wat 595
M. Nishigaki, S. Takahashi, M. Takahashi & Y. Maruo

Unsaturated sand in the stability of the cuesta of the Temple of Hera (Agrigento) 603
N. Nocilla, L. Ercoli, M. Zimbardo, A. Nocilla, P. Meli, G. Grado, G. Parello & G. Presti

Slope consolidation of Monteagudo de las Vicarías castle (Soria) 613
C.S. Oteo & P. de la Fuente

Load transfer in micropile underpinning of old foundations 621
J.M. Rodríguez Ortiz

Construction of the Line C San Giovanni station in Rome 627
E. Romani & N. Miniero

Permanence and preservation of the Metztitlán convent in Hidalgo, Mexico 633
E. Santoyo-Villa & E. Ovando-Shelley

The Fontanelle Cemetery: Between legend and reality 641
A. Scotto di Santolo, L. Evangelista & A. Evangelista

A class C prediction of the settlements induced in a historical masonry structure by the excavation of shallow twin tunnels 649
M. Sebastianelli, G. de Felice, M. Malena, A. Amorosi, D. Boldini & G.Di Mucci

Soil structure interaction on the dynamic behavior of two historic masonry structures 657
S. Sica, F. Ceroni & M.R. Pecce

New Lanark Walls: Examples of sustainable design for a World Heritage Site 669
M.J. Smith

Evaluating the effects of tunnel construction on monuments: The example of the Basilica di Massenzio in Rome 675
F.M. Soccodato, L. Callisto, S. Rampello & G.M.B. Viggiani

The preservation of the historical, archeological and artistic heritage of Orvieto: An interdisciplinary project 683
F.M. Soccodato, E. Martini, L. Tortoioli & A.M. Mazzi

Landslide risk assessment and management in the archaeological site of Machu Picchu (Peru) 697
D. Spizzichino, C. Margottini & L.M. Puzzilli

The rebuilding of San Piero a Grado bell tower 709
N. Squeglia

Safeguard stories of living monuments (unstable towns of the region of Umbria) 717
P. Tamburi & E. Martini

Geohazards and climate change issues for the preservation of the Saxon Shore in South Britain 725
D. Tapete & E.N. Bromhead

Preservation and reconstruction of historic monuments in Saint Petersburg with provisions for soil-structure interaction 735
V.M. Ulitsky, A.G. Shashkin, K.G. Shashkin & M.B. Lisyuk

Localized settlements of an ancient hospital foundation: Analysis of the problem to assess a possible reinforcement intervention 743
R. Valentino, E. Coïsson, F. Freddi & F. Ottoni

Geotechnical investigation and stabilization of the foundations of a World Heritage in Portugal, the Guimarães Castle 751
A. Viana da Fonseca, A. Arêde, E. Paupério & A. Costa

Safeguarding interventions for two historical sites in the Middle East 761
B. Vingiani & G. Salerno

Use of jet grouting technique to realize substructures of historic buildings: The example of an apartment building in Warsaw 769
K. Wanik

Geotechnical and structural investigations of historical monuments of Kazakhstan 779
A. Zh. Zhussupbekov, T.O. Zhunisov, A.Z. Issina & T. Awwad

The safety of an industrial archaeological heritage: The underground quarries in Marsala (Sicily) 785
M. Zimbardo, L. Ercoli, C. Cannone & A. Nocilla

Author index 793

This page intentionally left blank

Geotechnical Engineering for the Preservation of Monuments and Historic Sites – Bilotta, Flora, Lirer & Viggiani (eds)
© 2013 Taylor & Francis Group, London, ISBN 978-1-138-00055-1

Preface

The Technical Committee on Preservation of Monuments and Historic Sites was established by the International Society of Soil Mechanics and Geotechnical Engineering in 1981 with the mark TC19. It was renamed TC301 in 2010, and it is the first of a group of Technical Committees related to the impact of Geotechnical Engineering on society.

TC301 is intended to provide a forum for interchange of ideas and discussion, to collect case histories and to promote and diffuse the culture of conservation within the geotechnical community. More specifically, it focuses on geotechnical factors affecting historic sites, monuments and cities. TC301 searches for design criteria and construction methods of our ancestors, and reports on specific techniques adopted to preserve ancient sites and constructions. TC301 should also select special requirements and constraints to be considered in any rehabilitation intervention on monuments in order to preserve their cultural and historical integrity.

The Committee is supported by the Italian Geotechnical Society (AGI); it has been chaired in the past by Jean Kerisel (France, 1981–1984), Arrigo Croce (Italy, 1985–1989), Ruggiero Jappelli (Italy, 1990–1994), Carlo Viggiani (Italy, 1995–2003; 2009 to present). Yoshimori Iwasaki, Japan, acts as vice chairman and Alessandro Flora, Italy, is the secretary.

Among its terms of reference for the period 2010–2013, the Committee included the production of guidelines and a theme Conference to share experiences and research on the Preservation of Monuments and Historic Sites.

Conservation is actually one of the most challenging problems facing modern civilization. It involves a number of factors belonging to different fields (cultural, humanistic, social, technical, economical and administrative), intertwining in inextricable patterns. The complexity of the topic is such that it is difficult to imagine guidelines or recommendations summarizing what should be done and prescribing activities to carry on, intervention techniques, design approaches. Instead of this ambitious undertaking, the Committee resolved to produce a volume, *Geotechnics and Heritage*, collecting a number of relevant case histories of the role of Geotechnical Engineering in the preservation of monuments and historic sites. It is offered as a collection of paradigmatic examples which may inspire the geotechnical engineer dealing with monuments and historic sites, suggesting an approach rather than a solution. The volume is now available at Taylor & Francis.

The final decision to organize the theme conference was taken in Rome in May 2011, during a meeting of TC301. It was agreed to hold it in Napoli (Italy) where a first conference on the same topic, dedicated to the memory of Arrigo Croce, had already been held in 1997.

After a process of peer reviewing, more than 80 papers have been accepted, reporting experiences on some of the most famous monuments and historic sites of the world. This volume contains all of them, and includes also the special and key note lectures presented in Napoli.

The Symposium has been organized to report on the progress of our community in the development of a culture of conservation and preservation of heritage. It has shown that, in a period in which future seems to absorb all the efforts and resources of the mankind, there are people who do care about our past and its preservation. This confirms the statement by Edmund Burke (1790), in his famous "Reflection on the revolution in France": "*People will not look forward to posterity, who never look backward to their ancestors*".

New ideas and fruitful discussion have come up. For instance, since many relevant sites are located in highly seismic areas, the issue of the seismic risk mitigation has been clearly put forward.

The Symposium would not have been possible without the hard work of the Scientific and Organizing Committees, as well as of Claudio Soccodato, secretary of AGI. The contribution of all peoples involved is gratefully acknowledged.

This page intentionally left blank

Geotechnical Engineering for the Preservation of Monuments and Historic Sites – Bilotta, Flora, Lirer & Viggiani (eds)
© 2013 Taylor & Francis Group, London, ISBN 978-1-138-00055-1

Organization

ORGANISING COMMITTEE

Carlo Viggiani (Italy, TC301 chair)
Stefano Aversa (Italy, AGI President)
Emilio Bilotta (Italy)
John Burland (UK)
Giovanni Calabresi (Italy)
Michele Candela (Italy)
Salvatore D'Agostino (Italy)
Alessandro Flora (Italy, TC301 Secretary)
Yoshinori Iwasaki (Japan, TC co-chair)
Michele Jamiolkowski (Italy)
Stefania Lirer (Italy)
Efren Ovando-Shelley (Mexico)
Gianpiero Russo (Italy)
Claudio Soccodato (Italy, AGI General Secretary)

TC 301

Carlo Viggiani (Italy, TC chair)
Yoshinori Iwasaki (Japan, TC co-chair)
Alessandro Flora (Italy, TC secretary)
Namir Al-Sa'oudi (Iraq)
Atilla Ansal (Turkey)
Laszlo Aradi (Hungary)
Charles Augarde (UK)
Kari Avellan (Finland)
Frans Barends (Netherlands)
Jens Brendstrup (Denmark)
John Burland (UK)
Giovanni Calabresi (Italy)
Dimitris Egglezos (Greece)
Moustafa K. El Ghamrawy (Egypt)
Nicoleta Ilies (Romania)
Askar Khasanov (Uzbekistan)
Renato Lancellotta (Italy)
Jean Launay (France)
Michael Lisyuk (Russia)
Masoud Makarchian (Iran)
Sandro Martinetti (Italy)
Mamoru Mimura (Japan)
Efrain Ovando Shelley (Mexico)
Dick Parry (UK)
Jose M. Rodriguez Ortiz (Spain)
Chikaosa Tanimoto (Japan)
Christos Tsatsanifos (Greece)
Vladimir Ulitsky (Russia)
T.O. Zhunisov (Kazakhstan)

This page intentionally left blank

Opening address

This page intentionally left blank

Geotechnical Engineering for the Preservation of Monuments and Historic Sites – Bilotta, Flora, Lirer & Viggiani (eds)
© 2013 Taylor & Francis Group, London, ISBN 978-1-138-00055-1

Cultural heritage and geotechnical engineering: An introduction

C. Viggiani
Emeritus Professor of Geotechnics, University of Napoli Federico II, Italy
Chairman, TC301, ISSMGE

ABSTRACT: One of the fields of activity of Civil Engineering is the maintenance of existing constructions and infrastructures; among these, the Cultural Heritage. In particular, Geotechnical Engineering plays a significant role in a number of relevant cases. The conservation of Heritage is one of the most challenging problems facing modern civilization. It involves a number of factors belonging to different fields (cultural, humanistic, social, technical, economical and administrative), intertwining in inextricable patterns. From the point of view of an engineer, the peculiarity of this type of intervention is the requirement of respecting the integrity, besides guaranteeing the safe use. This requirement is analysed and discussed. It is concluded that the development of a shared culture between engineers and other professionals such as archaeologists, art historians and architects is a necessary condition for a successful conservation. To become sufficient too, the conservation culture should be spread widely and become a common sentiment amongst the majority of people.

1 INTRODUCTION

Geotechnical Engineering is part of Civil Engineering, the oldest branch of Engineering. As early as 30 centuries BC Egyptian engineers conceived and directed large constructions, as the great pyramids, the river Nile regulation and huge irrigation projects.

During the centuries, civil engineers have used the resources of Nature for the progress of mankind. At present, however, they are generally considered to operate in a "mature" sector, where mature is just an euphemism meaning outdated, behind the times, out of the mainstream of modernity. Till a few decades ago, the public perception of civil engineer was the man of progress; at present, this image is gradually changing into that of a cementifier, dangerous for the environment, operating in a routine sector of activity not worthy of investing financial and human resources; these on the contrary are reserved for fields such as aerospace, informatics, biomedicine.

We all know that this picture is utterly in error. According to the American Peoples Encyclopedia, Engineering "… applies scientific knowledge to the practical problems of creating, operating and maintaining structures, devices and services". Civil Engineers have thus still a fundamental role not only (i) in constructing new structures and (ii) in dealing with new problems, but also (iii) in taking care of the existing infrastructures and heritage.

As for new structures, just to quote a few examples, structures such as the Messina Strait suspension bridge, with its 3.3 km span (fig. 1), or

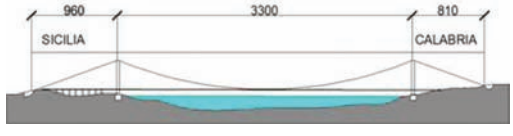

Figure 1. Sketch of the intended suspension bridge across Messina Strait, Italy.

skyscrapers such as the Burji Khalifa, with its 830 m height (fig. 2), will continue to require high level knowledge. Less visible (there is no glory in foundations, said Terzaghi), but probably equally demanding and more important and widespread are other works, as for instance the shallow urban tunnels for transportation and other purposes that are being excavated under all the great cities of the world.

New problems are continuously posed to civil engineers by the evolution of Society. For instance, environmental problems were not included in the engineering curricula when I was a student (admittedly, very long ago), in spite of them being described at the best as early as in Shakespeare's Hamlet. "*This goodly frame, the earth, seems to me a sterile promontory, this most excellent canopy, the air, look you, this brave overhanging firmament, this majestical roof fretted with golden fire, why, it appears no other thing to me than a foul and pestilent congregation of vapours*" says Hamlet entering the scene at the beginning of the second act.

We are used to associate sea gulls with blue skies and uncontaminated seas (fig. 3); but nowadays, on the contrary, they often deal with things such

Figure 2. The Burj Khalifa, the tallest building in the world.

Figure 3. Blue skies and uncontaminated seas.

Figure 4. One of the present jobs of the seagulls.

as solid urban wastes (fig. 4). Seagulls undertake a dirty job, just as we civil engineers do in addition to conceiving and constructing suspension bridges, skyscrapers, tunnels.

At a first glance, taking care of (maintaining, upgrading, reinforcing) existing structures, devices and services appears a minor field of activity; but there are many arguments proving the contrary. Apart from ordinary maintenance, puzzling problems are posed by new destinations of the existing structures or by more demanding safety requirements (for instance, in connection with the seismic safety of existing dams).

Within this sector, there is the sub sector of taking care of (maintaining, preserving, conserving, restoring, improving) monuments and historic sites. Again, an apparently minor sub sector, and again, on the contrary, one of the utmost importance—may be the most significant contribution that Civil Engineering can give to mankind in our time.

2 ITALIANS DO IT BETTER?

Italy has a long history of conservation; there is a widespread belief that the national heritage is very important. Let us examine a few quotations: "*According to UNESCO's estimates, Italy has between 60 and 70 per cent of the world's cultural assets*" (Eurispes Report, 2006). "*72% of Europe's cultural heritage is to be found in Italy and as much as 50% of the world's*" (Berlusconi, press conference held in London on 10 September 2008). According to a Sicilian minister, "*60 per cent of the world's cultural assets are in Italy and of these, 60 per cent are in Magna Grecia and of these last ones 60 per cent are in Sicily*". According to the councilor responsible for culture in the Regione Toscana, "*Italy alone has 60% of the world's cultural assets, but 50% of those Italian cultural*

assets are concentrated in Tuscany"; according to the Deputy Mayor of Rome, Rome by itself "*has 30-40% of the world's cultural assets*". If we add all the percentages together, it would appear that Italy somehow manages to encompass more than 100 per cent of the planet's cultural heritage!

Obviously these "UNESCO statistics" do not exist, and the figures, invariably inconsistent with one another, are shamelessly concocted on various occasions; perhaps the symptom of national pride, but certainly of ill-conceived superficiality. Yet Italy does have a very significant position because of its cultural heritage, whose central importance, however, is not based on its quantity but rather on its quality. There are three different reasons for this: first, the time-honored harmony between the city and the wider landscape; second, the spread of this heritage throughout the country and down to the smallest towns and villages; third, the continuity in the use of churches, mansions, statues and paintings. Italian museums only contain a small portion of the country's artistic heritage, which is spread throughout the cities and the countryside: within this context—the product of many centuries of accumulated wealth and civilization—the whole is far more than the sum of its parts.

There is, however, a fourth factor at play, which is no less important: the "Italian model" of conservation of cultural heritage. Long before Italian unification, the Italian states formulated rules and set up public institutions to regulate and engage in this area of activity. Italy (as a state) was the first country to include the preservation of its landscapes and its cultural heritage amongst the founding principles of its Constitution. Article 9 of the Italian Constitution (which came into effect on January 1st, 1948) states: "The Republic promotes the development of culture and scientific and technical research. It protects the landscape and the Nation's historical and artistic heritage." (in the Italian original: *La Repubblica promuove lo sviluppo della cultura e la ricerca scientifica e tecnica. Tutela il paesaggio e il patrimonio storico e artistico della Nazione*). The Constituent Assembly arrived at this formulation after a long debate and eleven different proposed texts. Members of all parties contributed to the final wording, particularly the communist Concetto Marchesi, a professor of Latin from Sicily who had been rector at the University of Padua, and a very young Christian-democrat, later to be prime minister, Aldo Moro.

3 GEOTECHNICS AND HERITAGE

There are quite a number of monuments, monumental buildings, historical cities and sites affected by geotechnical risks of various types, so that Geotechnical Engineering is called to play a very important role in their safeguard. Just to quote some examples, the village of Terra Murata (Walled Land) in the island of Procida in the bay of Napoli, is a settlement dating back to the X century and includes the Abbey of S. Michele and a number of churches. The Abbey and other churches are exposed to the risk of collapse by the action of the sea, undermining the steep cliffs over which they were erected (fig. 5); a problem of stabilisation of rock slopes. Very frequently, in historical cities there are a number of superimposed remains; in fig. 6 a Roman villa of the imperial age found just below a church in a seaside resort near Napoli is reported.

The villa had been buried by the Vesuvius eruption of 69 AD, and the church has been built in the Middle Age on a thin tuff layer covering it.

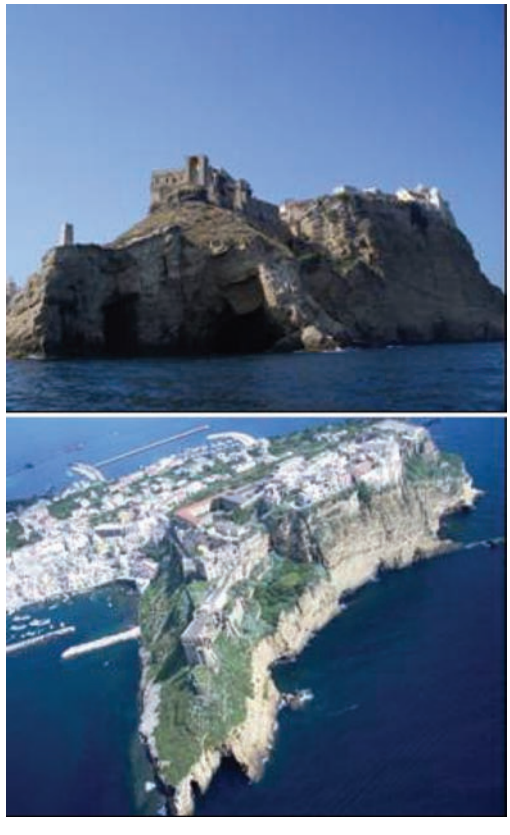

Figure 5. The village of Terra Murata in the island of Procida. (above) view from the sea; in the foreground, the remains of the church of S. Margherita Nuova; in the background, at the right of the picture, the Abbey of S. Michele. (below) bird's eye view.

Figure 6. (a) the Church of S. Maria Assunta at Positano, near Napoli. (b) the remains of a Roman villa of imperial age found just a couple of meters below the foundation of the church.

It is evident that the solution of any foundation problem for the church needs the use of sophisticated geotechnics.

The famous Leaning Tower of Pisa is depicted in fig. 7; it has been recently stabilised by slightly decreasing its inclination by underexcavation. The inclination of the Big Ben clock tower (fig. 8) caused by the nearby excavation of the tunnels of the Jubilee Line Extension has been controlled by compensation grouting.

Both these case histories are reported in details in two contributions in this volume.

The road tunnels excavated by the Romans in the Phlegrean Fields, east of Napoli, are unprecedented and unequalled masterpieces of ancient geotechnical engineering. Some of them have been in regular use till the XIX century! The so called Grotta di Cocceio, linking the Avernus lake to the citadel of Cumae (fig. 9), includes an enormous explosion cavern caused by the firing of explosives stored there during World War II.

Figure 7. The Leaning Tower of Pisa.

The cavern is now inhabited by chiroptera (bats) who are a protected species; their protection is at present conflicting with the stabilisation of the cavern, epitomizing the complexity and variety of conservation problems.

Many other examples could be quoted, there are omitted here for space reason.

4 INTEGRITY

The conservation of monuments and historical sites is one of the most challenging problems facing modern civilization. It involves a number of factors belonging to different fields (cultural, humanistic, social, technical, economical and administrative), intertwining in inextricable patterns.

From the point of view of an engineer, the peculiarity of this type of intervention is the requirement of respecting the integrity, besides guaranteeing the safe use. The latter requirement is relatively straightforward for a well trained and experienced engineer. The former one, on the contrary, is worth of some discussion.

Figure 8. The Big Ben Clock Tower.

A prerequisite is the comprehension of the concept of integrity; one soon discovers that it has many facets and is rather elusive. Formal or iconic integrity is the first and most obvious facet; the external aspect, the original form should not be altered by the engineering intervention. Let us imagine an old, experienced civil engineer contemplating Leonardo's Mona Lisa, in the Museum of Louvre in Paris. Let us also imagine that his expert eye discovers that the wall hook to which the picture is hanging is near to collapse, with the risk of the masterpiece falling on the floor and possibly being damaged. What horror! The expert engineer takes a new large nail, plants it in the forehead of the lady and knocks it into the wall (fig. 10). "Now it is safe", he concludes with a legitimate satisfaction; but the visitors of the Museum would probably be much less satisfied.

Unfortunately formal integrity, though being very important, is not all, otherwise a copy would have the same value as the original.

Another important facet of integrity is historical integrity; it can be best illustrated by an example, taken from the history of Napoli.

The church of Santa Chiara was founded in 1310 by Robert the Wise and Sancia of Mallorca as

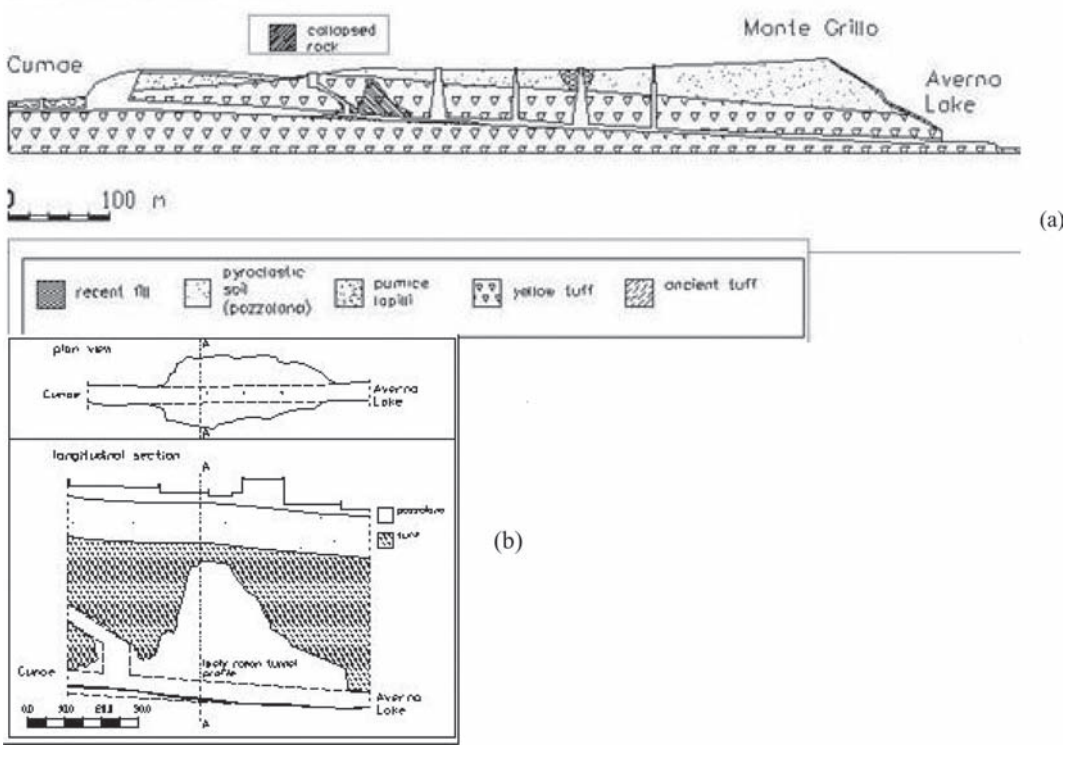

Figure 9. The grotta di Cocceio, a Roman tunnel in the Phlegrean Fields east of Naples. (a) longitudinal profile of the tunnel. (b) the explosion cavern in the mid of the tunnel.

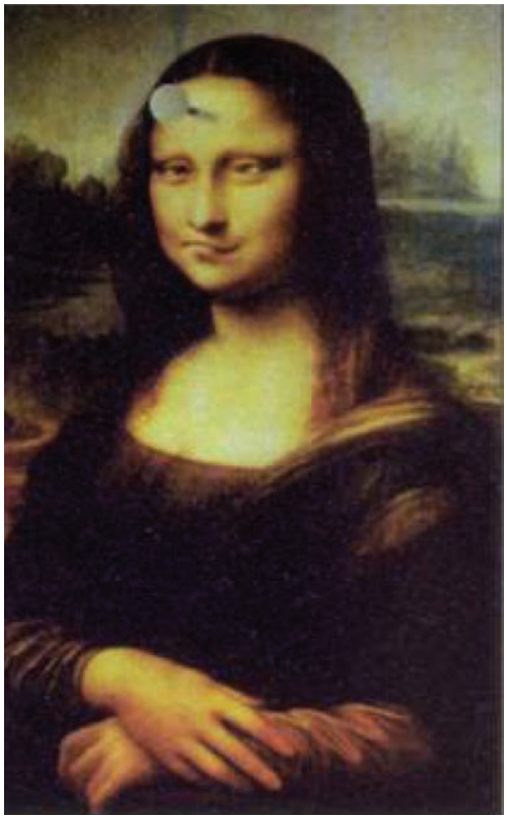

Figure 10. Mona Lisa stabilised.

Figure 11. The Angevin church of Santa Chiara in Napoli.

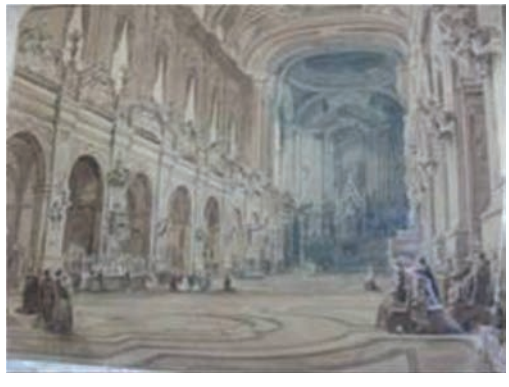

Figure 12. The interior of Santa Chiara in 1942.

a double convent for the Poor Clares and Franciscans. The church exceeded in scale any other church in the kingdom; it loomed over medieval Naples and still presides over the modern city (fig. 11). It was intended not only to host the tombs of the royal family but probably as part of a program to propose a Franciscan alternative to the authority of the papacy, by this time displaced to Avignon.

The project of Santa Chiara, initiated soon after the arrival of Robert and Sancia in Napoli, reflected a new trend in the spiritual life of the kingdom, now strongly inclined towards the Franciscan and in particular towards the Spirituals. According to some historians, Santa Chiara was perhaps nothing less than the setting for a brave and doomed attempt to reform the Church. Before 1943, the medieval interior of Santa Chiara was actually invisible, encased in a sumptuous baroque decoration designed by Domenico Antonio Vaccaro in 1744 and executed by Giovanni del Gaizo and others (fig. 12). It perfectly epitomized the defeat of the Franciscan party and the historical victory of the Rome papacy.

The original structure underneath the baroque decoration was revealed to modern eyes only on 4 August 1943, after American incendiary bombs caused a fire that burned continuously for 36 hours.

The eighteenth century stucco was entirely destroyed and the medieval walls behind severely calcinated (fig. 13). In keeping with the post-war preferences for streamlined design, and principally because of the cost and complexity of re-creating the splendors of the baroque interiors, the church was reconstructed instead to an austere medieval shell, a loss still lamented by most Neapolitans lovers of the Baroque. Has the historical integrity been respected? (fig. 14).

A further facet of the integrity is the material integrity. It is at present acknowledged that the materials, the construction techniques, the structural scheme are original features of the monument as significant as its appearance and history. An arch should not be transformed into a garland of stones hanging from a hidden beam; a direct foundation should not be transformed into a piled

Figure 13. Santa Chiara in August 1943.

Figure 14. Has the historical integrity been respected?

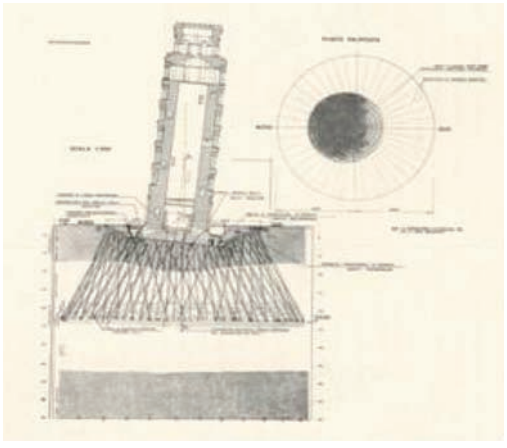

Figure 15. One of the solution proposed in the 1970's for the stabilization of the Tower of Pisa.

Figure 16. Pienza.

one, unless this is the only way to save it, and in any case at the price of a defeat.

Fig. 15 shows one of the solutions proposed in the 1970's to stabilize the leaning tower of Pisa; while completely exhaustive from a merely technical viewpoint, it would have deprived the visitors of the tower of the subtle sensation of risk when climbing the spiral stairs!

Finally, we have already mentioned the harmony between the city and the wider landscape that is one of the factors making Italy so important from the point of view of cultural heritage.

Fig. 16 shows a quintessentially Italian landscape: Pienza in Tuscany, a small city founded by Pope Pius II in 1462 and still gloriously emerging from the surrounding landscape on top of a hill, in the Senese Val d'Orcia. The balance of countryside and cityscape is so admirably preserved that in 2004 the entire Val d'Orcia was included among the UNESCO sites. Geotechnical interven-

tions may significantly affect the landscape; this is another important facet of integrity to take into account.

The cliff below Terra Murata mentioned above, for instance, could be protected from the sea action lining it by reinforced concrete, but this would be an irreparable wound to the landscape.

5 SHARED CULTURE

The requirements of safety and use, in the majority of cases the Author has experienced, appear (and often actually are) in conflict with the respect of the iconic, historical and material integrity of the monuments. In almost all countries of the world conservation is looked after by an official trained in Art History or Archaeology.

Generally (e.g., this is the case in Italy) he has an absolute control on any action to be undertaken, and imposes constraints and limitations that sometimes appear unreasonable to the engineer. The engineer, in turn, tends to achieve safety by means of solutions which appear unacceptable to the official in charge of conservation, sometimes mechanically applying procedures and regulations conceived for new structures. With a misused word, he tends to cementify.

It is evident that some equilibrium has to be found. Conservation requires on one hand the safeguard of the formal, material and historical integrity of the monument, while on the other its survival and safe fruition. The difficulty of the problem is increased by the lack of a general theory, guiding the behaviour of the various actors involved as Mechanics does with the structural engineer. The lack of unicity of the solution of preservation and conservation problems, vividly exemplified by the case of Santa Chiara, is in particular rather disturbing for us engineers.

It is a deep belief of the author that a satisfactory equilibrium between safety and conservation, between engineers and restorers, may be found only in the development of a shared culture. In the last decades, significant advancements have been actually registered in this direction between the realm of conservation ant that of engineering, and a number of associations, conferences, seminars have contributed to these advancements.

ISSMGE is pursuing this goal in different ways; among them, the institution of a Technical Committee on Geotechnical Engineering for the Preservation of Monuments and Historic Sites (TC301, formerly TC29), started many years ago by Jean Kerisel and Arrigo Croce and sponsored by the Italian Geotechnical Society. This volume is intended as a contribution to the effort.

6 NECESSITY AND SUFFICIENCE

Unfortunately, the development of a shared culture of conservation is a necessary, but far from sufficient condition. Immediately after the inclusion among the UNESCO sites, the area around Pienza was involved in a real estate project (fig. 17).

The new settlement, the *Casali di Monticchiello,* were advertised as "your new home in a Unesco site". In other words, the UNESCO label, that the Val d'Orcia earned for its preservation, was immediately exploited for commercial reasons.

The eighteen-year-old king Charles of Bourbon, who entered Naples to great celebrations in 1734, inaugurated a new era in the history of the Kingdom which was now once more independent after centuries of being a Spanish viceroyalty. He initiated the digs in Herculaneum (from 1738) and Pompeii (from 1748), which produced an enormous quantity of new antiquities. This situation gave rise to Neapolitan legislation to protect the cultural heritage (1755), expressing the King's "profound regret" over the past export of antiquities from the Kingdom and establishing new rules to prevent it to happen again in the future.

Indeed, when Charles III became King of Spain (1759), in his new capacity he did not issue any provisions to safeguard artifacts there. Had his "profound regret" over the lack of protection for works of art in Naples vanished once he got to Madrid? No. In both cases, the monarch had not been writing the legislation personally, but expressing through it the civic and juridical traditions and practice of the place in which he was ruler. In Italy, there is a sharp contrast between a long history of preservation and its decline over the last few years. The roots of the civic, cultural and juridical aptitude to preservation are to be found in the spirit and tradition of the Italian cities, which, at least from the twelfth century on, had been developing a deeply held and highly sophisticated concept of citizenship, in which the monuments were the basis for civic pride and identity and a sense of belonging which were closely linked to the very idea of a well governed community. In this connection, it is interesting to quote two documents:

(i) the Commune of Rome (1162), concerning Trajan's Column (fig.18), states: "In order that the public honor of the City of Rome is preserved, the Column shall never be damaged or knocked down, but must remain as it is for eternity, intact and unspoiled for as long as the world shall exist. Should anyone inflict or attempt to inflict damage on it, they shall be condemned to death and their assets confiscated by the treasury";

(ii) the Constitution of the Commune of Siena (1309) says that "those who govern the city must above all ensure its beauty and ornament (fig. 19),

Figure 17. Commercial exploitation of Val d'Orcia near Pienza.

Figure 18. The Trajan column in Rome.

Figure 19. Siena.

which is essential for the delight and amusement of foreigners, but also for the honor and prosperity of the Sienese themselves".

Very similar principles are found in hundreds of documents: beauty, decorum, suitability, public honor, the common good or *public benefit*, for which the classical Roman formula *publica utilitas* was often employed.

There is a perfect continuity between the conservationist laws of Italy's liberal governments, the two laws passed by Mussolini's regime and finally Article 9 of the Republic's Constitution; this come as a surprise only to those who think in terms of labels and affiliations, and fail to enter into the complexities of the history of ideas.

What might be even more surprising is the evident continuity between the conservationist legislation of the Italian states of the *Ancien Régime* (for instance, papal Rome and Bourbon Naples) and the heritage and conservation culture that spread around Europe after the French Revolution.

The latter was definitely not a "restoration" of previous laws, but a radical rethinking of the language and rules of the *Ancien Régime* in the light of new guiding principles, such as the concepts of nation, of popular sovereignty and of citizenship, which the events of the French Revolution had

changed forever, while giving new meaning to the notion of the "common good" and encapsulating it, among other things, also in historical monuments.

However, this complex system is operating in an increasingly ineffective manner. The devastation of the landscape in Italy has become dramatic. The harmonious relationship between the Italian cities and their countryside, established over many centuries, is giving way to an uncontrolled urban sprawl, which is now home to a large proportion of the population. Although the conservationist laws remain in force and indeed are constantly improved (on paper), "derogations", "exceptions" and even "amnesties" (*condoni*) for the infringement of building regulations are continuously enacted. At the same time, conservation of the cultural heritage is undergoing a deep crisis caused by a lack of human and financial resources.

I have a dream. The international geotechnical community, besides contributing to the development of a shared culture of conservation, plays an active role in the re-establishment of these principles in the common sentiment of people in Italy and all over the world.

ACKNOWLEDGMENT

The author owes a deep debt for their teaching and for stimulating discussions over the years to masters as Arrigo Croce, Ruggiero Jappelli, Jean Kerisel and to friends as Giovanni Calabresi, Salvatore D'Agostino and Salvatore Settis; their inspiration is gratefully acknowledged.

Special lectures

This page intentionally left blank

Geotechnical Engineering for the Preservation of Monuments and Historic Sites – Bilotta, Flora, Lirer & Viggiani (eds)
© 2013 Taylor & Francis Group, London, ISBN 978-1-138-00055-1

Influence of the subsoil on the urban development of Napoli

S. Aversa
Dipartimento di Ingegneria, Università di Napoli Parthenope, Italy

A. Evangelista & A. Scotto di Santolo
Dipartimento di Ingegneria Civile Edile e Ambientale, Università di Napoli Federico II, Italy

ABSTRACT: This report is devoted to the role that the subsoil of Napoli has had in the development of the city. The topic is considered mainly from the geotechnical point of view, also if geological, structural, architectural and historical points of view are dealt too. First the geological peculiarities of the ground of Napoli, located between two active volcanic districts, are described. A short synthesis of the mechanical behaviour of the soils and rocks of the subsoil of Napoli is presented. The report ends with the main part dedicated to the effect of the subsoil on the historical development of the city through the centuries and on the geotechnical problems of Napoli at present time.

1 INTRODUCTION

The history of Napoli dates since IX century b.C., when Greeks founded Partenope on the Pizzofalcone Hill in front of the small island of Megaride, where the well known Castel dell'Ovo was built some centuries later. This castle (see Fig. 1), with the strong continuity between the base tufaceous rock and the construction stones, within the wonderful scenario of the Bay of Napoli, can be considered as a very effective synthesis of this report, devoted to the influence of the subsoil on the urban development of the city.

The choice of Pizzofalcone hill as the site of the first settlement was probably due (de'Seta, 1969) to the fact that, at that time, the hill was surrounded by the sea along three sides, with the fourth one of difficult access because of the steepness of the hill. Partenope, which derived its name from that of one of the Mermaids, was a classic example of archaic settlement with a small harbour just beneath the urban area on the tufaceous hill. The role of this soft rock in the development of the city is clear since that time.

After the victory against Etruscans in 474 b.C., the Greeks of Siracuse extended the city in the plan area located at the East of Partenope, founding the so-called *Neapolis* (Fig. 2), to be distinguished from the old one, that was also indicated with the name of *Palaepolis*.

The role of subsoil is apparently less evident in the choice of the location of Neapolis. The New-City was located between two small rivers at the two sides. It is interesting to stress that, according to Di Stefano (1971), in the large part of Neapolis,

Figure 1. Picture of Castel dell'Ovo, Napoli, Italy.

Neapolitan Yellow Tuff outcropped (see Fig. 3), while in the surroundings alluvium and marine deposits characterise the subsoil. Greeks preferred to build up the city on the rock.

The aim of this report is to show the role that the subsoil has had on the birth and growth of the city of Napoli where, owing to the large diffusion pyroclastic rocks, a significant number of building has been constructed using these materials. Old quarries, tunnels and other underground works frequently involve these formations; cliffs and slopes of these rocks are often present into urban areas. Pyroclastic soils also influences the behaviour of buildings and other structures present in the city, especially when these soils, originally unsaturated, experience significant increase of water content.

The general theme of the Conference is dealt throughout all the paper, stressing the very relevant role that knowledge, investigation, monitoring and can have in a site like Napoli, where the history of mankind flows continuously since some thousands of years.

Figure 2. Plan view of Napoli IV sec. (after Di Stefano 1971).

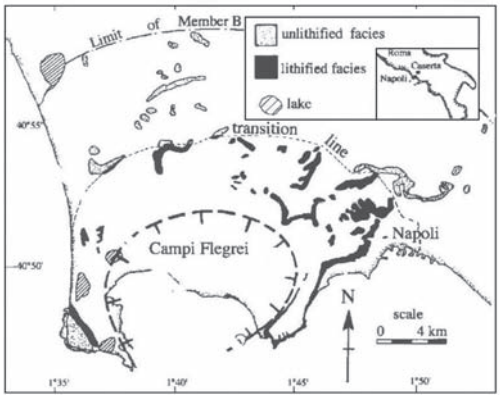

Figure 3. Pyroclastic outcrops and transition between lithified and unlithified face of Yellow Tuff in Napoli (after Picarelli et al. 2006).

The report is subdivided into four parts related to:

- the geology of the area where Napoli is located;
- the properties of tuff and pyroclastic soils found in this area;
- the influence of these materials, with special regard to the tuff, on the urban structure and on the monuments of Napoli;
- the description of some of the geotechnical problems due to the actual condition of the subsoil.

Geotechnical studies on the behaviour of Neapolitan tuff have been carried during the last 50 years by many Neapolitan geotechnical researchers (Pellegrino 1967, 1968, 1970a, b, 1974; Evangelista 1980, Evangelista et al. 1980, 2000, 2002a, c, 2003, 2004, 2006, 2007, 2009, Evangelista & Pellegrino 1986, Evangelista & Aversa 1993, Aversa 1989, 1991, Evangelista & Pellegrino 1990, Aversa et al., 1990, 1991, 1993, Aversa & Evangelista, 1993, 1998, Aversa & Lagioia 2000, Aurisicchio et al.,1982a, b, 1985).

The investigation on the behaviour of pyroclastic soils present in the city of Napoli and in the surrounding areas also started many years ago (Croce 1954, Croce & Pellegrino, 1967; Pellegrino, 1967, 1970a, b and c), but only in the last decades, with the improvement of knowledge on the behaviour of unsaturated soils, it received more significant developments (Nicotera 1998, 2000, Nicotera et al. 1999a, b, Scotto di Santolo 2000a, b, Aversa et al. 1998, Aversa & Nicotera 2002, Picarelli et al. 2006, Evangelista & Scotto di Santolo 2000, 2001, 2010, Papa 2007, Papa et al. 2008).

In recent years the relationship between the subsoil of the city and the urban development has been already discussed in papers written by many Neapolitan geotechnics (Evangelista et al. 2002a, b, c; Scotto di Santolo & Evangelista 2010, Aversa et al. 2013, Evangelista & Viggiani 2013, Scotto di Santolo et al. 2012). Some papers (Scotto di Santolo et al. 2013, Campa et al. 2013, Sica et al. 2013, Candela, Viggiani & Viparelli 2013, Aversa et al. 2013, Amato & Gialanella 2013, Alterio et al. 2013) are also in the Proceedings of this Conference.

2 GEOLOGY OF THE SUBSOIL OF NAPOLI

Pyroclastic rocks and soils are present in the volcanic areas located along the western slope of the Apennine chain. Pyroclastic rocks outcrop mainly in the Campanian Region; their presence is primarily related to volcanic activity of the Phlegrean Fields and only in a few cases of Vesuvius.

The volcanic activity in the Phlegrean Fields started 130.000 years b.p. in the island of Ischia. The last volcanic event in this area happened in 1538, with the Monte Nuovo eruption.

In a simplified scheme, in the subsoil of Napoli, it is possible to distinguish different volcanic formations (see Fig. 4):

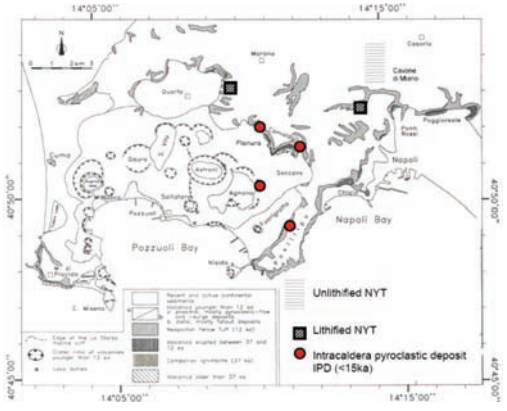

Figure 4. Simplified geological map of Phlegrean Fields (after Picarelli et al., 2006).

- Campanian Ignimbrite (35.000 years b.p.);
- Pre Neapolitan Yellow Tuff (35.000–12.000 years b.p.);
- Neapolitan Yellow Tuff (12.000 years b.p.);
- Pyroclastic soils due to the last period of Phlegrean activity, known as the third period (<12.000 b.p.).

2.1 *Campanian Ignimbrite*

The Campanian Ignimbrite originated from the pyroclastic flows of an impressive eruption which occurred 35.000 years b.p. The pyroclastic deposits covered a wide area of approximately 10.000 km^2, to a thickness often exceeding 50 m. This material has been used for constructions since antiquity.

A very hard variety of the Campanian Ignimbrite is the so-called Piperno, characterised by the presence of lava scoriae. It outcrops in Napoli in a localised bank between Pianura and Soccavo, at the base of the Camaldoli hill. For its strength and resistance to weathering, Piperno has been used for balconies, frames, and for many other decorations also in buildings in which tuff walls are plastered.

2.2 *Pre Neapolitan Yellow Tuffs*

These rocks lay beneath the subsequent Neapolitan Yellow Tuff formation. They are due to the autochthonous volcanic activity and are 35.000–12.000 years old. In a few cases these rocks outcrop in the urban area, mainly due to artificial cuts. Among these tuffs it is possible to distinguish the layered tuff, the coloured (green or pink) tuff and the fine-grained tuff, which is the most valuable variety, not only for its excellent physical and mechanical properties (Aversa et al., 1991, Aversa 1991, Aversa & Evangelista 1998).

2.3 *Neapolitan Yellow Tuff*

The Neapolitan Yellow Tuff covers approximately 300 km^2. It forms the most important hills in the Phlegrean areas and in the city of Napoli. The NYT originated approximately 13.000–11.000 years b.p. during one or more volcanic eruptions in the Phlegrean Fields.

It is possible to distinguish different varieties of Neapolitan Yellow Tuff with different characteristics. This rock has been extensively used since antiquity as building material.

Neapolitan Yellow Tuff formation is not always lithified (Fig. 3). The intensity of lithifications reduces the further one gets from the Phlegrean Fields. In the subsoil of Napoli, very often, it is possible to distinguish a thin zone of transition that separates lithic facies from incoherent ones. In some sites NYT outcrops for several reasons:

- tectonic volcanic collapses;
- erosion of the uncemented pyroclastic materials above it;
- limited thickness of pyroclastic covers along steep gradient slopes;
- superficial water action that erodes uncemented soils down to the tuff formation and beyond it;
- sea wave erosion;
- anthropic action (open quarries, excavations to build roads, etc.).

Among the lapideous rocks, the Neapolitan Yellow Tuff is the most superficial.

In the NYT formation it is possible to distinguish some discontinuities connected to the formation of the rock mass:

- *Scarpine*: sub-vertical discontinuities generally attributed to the effect of the reduction of the temperature after the tuff has been lithified;
- *Suoli*: sub-horizontal discontinuities at the contact between different erupted materials.

Sub-vertical discontinuities are more frequent in the proximity of natural cliffs, due to the effect of stress reduction. Only recently, thanks to the developments in the techniques of surveying and photogrammetry, an oriented structure has been identified in sub-vertical cliffs with the identification of at least three families of discontinuities and of removable blocks (Nocilla et al 1999, Evangelista et al., 2002, 2003, 2004, 2006, 2009, Nocilla et al., 2009).

2.4 *Pyroclastic cover (3rd Phlegrean period)*

The post NYT intracaldera pyroclastic deposits were produced by the overall eruptive centres of Phlegrean Fields.

The thickness of these deposits varies from about 20 m in areas close to the eruptive centres, to about 4 m, in distal outcrops. The sequence, well described by Picarelli et al. (2006), is composed by at least six fall units, interbedded with numerous ash layers and pumice fall layers.

These deposits are delimited by either thin paleosoils or erosional discontinuities that provide clear demarcations between the various eruptions of the recent volcanic history. In general, they consist of a sequence of fine to coarse unsaturated ash with intercalated pumice layers.

3 PROPERTIES OF VOLCANIC TUFFS

3.1 *Generality*

Volcanic tuffs are porous siliceous rocks generated by fragments which underwent a lithification process. Their structure may be defined by three components: an ashy matrix, high porous inclusions (pumices and/or scoriae) and lithic inclusions.

The quality and abundance of porous and lithic inclusions characterise the particular type of tuff and, in the same formation, depend on the distance from the volcanic source. The minerals present in the ashy matrix have a strong influence on the tuff's properties. The role of zeolites as a cementing agent is generally accepted according to the mineralogic studies (de Gennaro et al. 1995).

A concise view of the properties of Neapolitan tuffs is given by the diagrams of Figure 5 where uniaxial compressive strength is plotted against dry density, where any single dot represents the mean value for a homogeneous group of samples. It may be observed that uniaxial compressive strength is very dependent on dry density. At the same dry density Fine-Grained Tuff reaches the highest values of uniaxial strength. According to Evangelista et al. (2000) it is possible to assert that the strength is not only influenced by the dry density but also by the structure of the material.

3.2 *Yield surface and failure criterion*

Pellegrino (1968, 1970a, 1970b) first individuated, for Neapolitan Yellow Tuff, two different stress dominions where soft rocks have different types of behaviour: «rock-like behaviour» at small mean stress and «soil-like behaviour» at high mean stress (see Fig. 6). The transition from «rock-like behaviour» to «soil-like behaviour» happens because the stressed bonded mass is transformed progressively into an assembly of fragments. The mechanical properties change and it behaves like an unbounded soil. According to Leroueil and Vaughan (1990), this phenomenon could be named «destructuration». Figure 7 shows results of isotropic compressive tests performed on Fine Grained Tuff. This figure shows very clearly the difference in behaviour before and after yield.

Figure 8 shows the yield surface of Neapolitan Fine Grained Tuff in the dimensionless plane where p'_o represents the mean pressure at the inter-

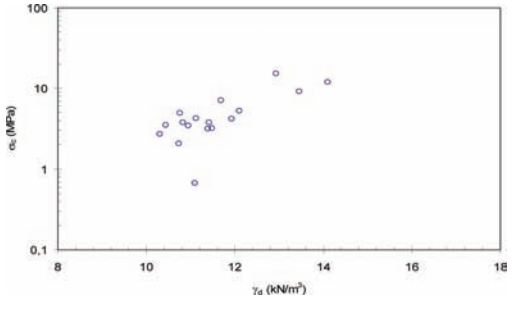

Figure 5. Uniaxial compressive strength of lithified tuff vs. dry unit weight (modified from Evangelista et al. 2000).

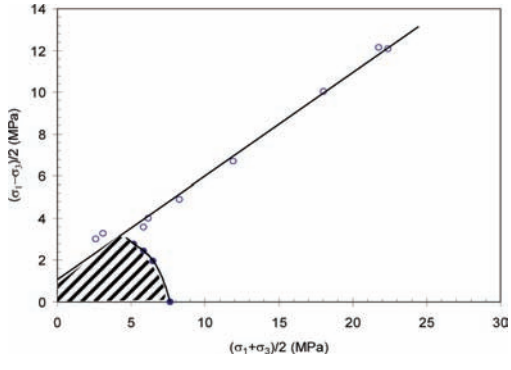

Figure 6. Rock-like and soil-like domains for the lithified tuff (modified from Pellegrino 1970b).

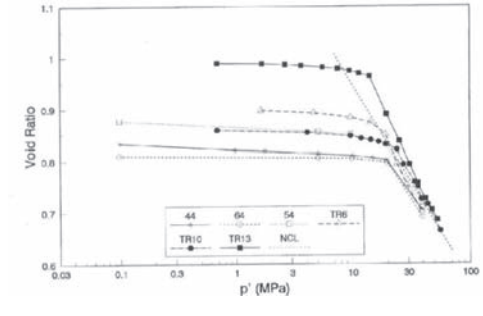

Figure 7. Isotropic compression test on a Neapolitan tuff (after Aversa et al. 1991).

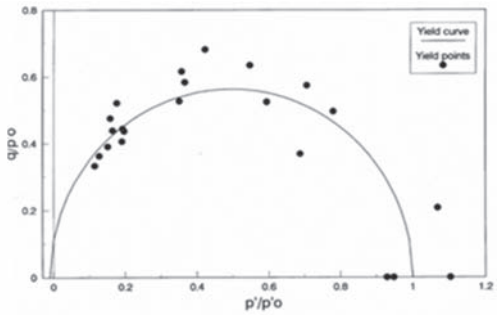

Figure 8. Yield surfaces of Fine-Grained Tuff (after Aversa et al. 1991).

section of the unloading-reloading curve with the normal compression line in isotropic compression (Aversa & Evangelista 1998). Before yield, the material exhibits a linear behaviour (Tatsuoka 1995) with the uniaxial modulus of deformability practically independent of both deviatoric and mean effective stresses.

At small mean stress level, after peak, the strength suddenly decreases significantly, as shown in Figure 9 (brittle behaviour). Brittleness decreases as the effective confining pressure rises. The stress-strain curves approach a constant strength value.

At higher values of the effective confining pressure, the behaviour is significantly different. The material shows a linear-elastic behaviour only in the first part of the stress-strain curve (see Fig. 9), which then turns into a strain hardening elasto-plastic behaviour.

To characterise the deformability of Neapolitan tuffs it is possible to refer to elastic moduli within yield surface. They may be assumed constant from a practical point of view and, for this reason, in this stress domain the Young modulus may be considered a property of the rock. Values of the ratio E/σ_c vary between 500 and 1.000.

Evangelista & Aversa (1993) and Aversa & Evangelista (1994) proposed bilinear envelope as peak strength criterion for Fine Grained Tuff (see Fig. 10). The scattering of strength is usually very high and for this reason it is difficult to define strength parameters of bilinear envelopes and the simple Mohr-Coulomb criterion has been used. Figure 11 shows the strength envelope obtained for a Neapolitan Yellow Tuff. The angle of shearing resistance varies between 22° and 30°. Cohesion is seen to be generally related to dry density (see box in Fig. 11).

Aversa & Evangelista (1998) showed that after yielding in isotropic compression the evolution of the yield curve is not homothetic, being affected by destructuration, as shown in Figure 12, where

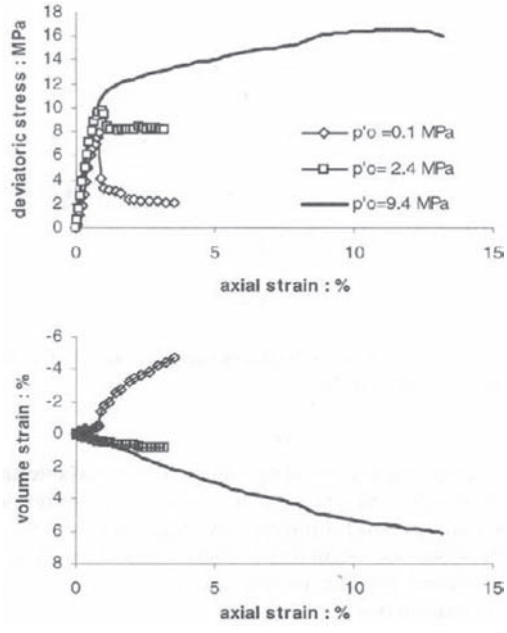

Figure 9. Drained triaxial tests on FGT at low: a) deviatoric stress vs. axial strain; b) volumetric strain vs. axial strain (after Aversa & Lagioia, 2000).

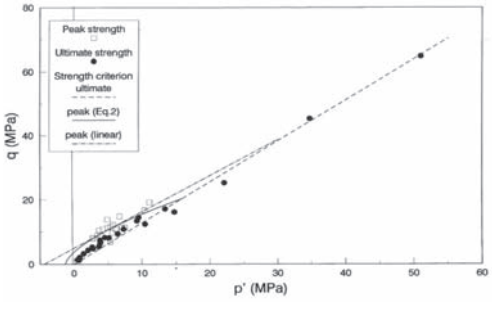

Figure 10. Bilinear strength envelope for Fine-Grained Tuff (after Aversa et al., 1991).

the intact and destructured material yield curves are represented in the q-p′ plane. It is evident the combined effect of "destructuration" and porosity reduction.

3.3 *Long-term strength*

The dependence of strength on the time to reach failure obtained for Neapolitan Yellow Tuff, reported in Figure 13, was evaluated on the basis of strain control tests and creep tests (Evangelista & Aversa 1993). Experimental data show that the

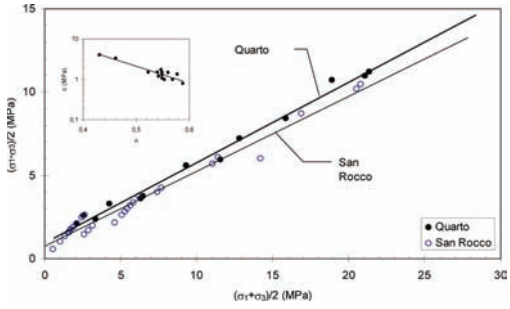

Figure 11. Strength envelope of two types of lithified tuff: San Rocco tuff and Quarto tuff and influence of porosity on cohesion (modified from Evangelista & Pellegrino 1990).

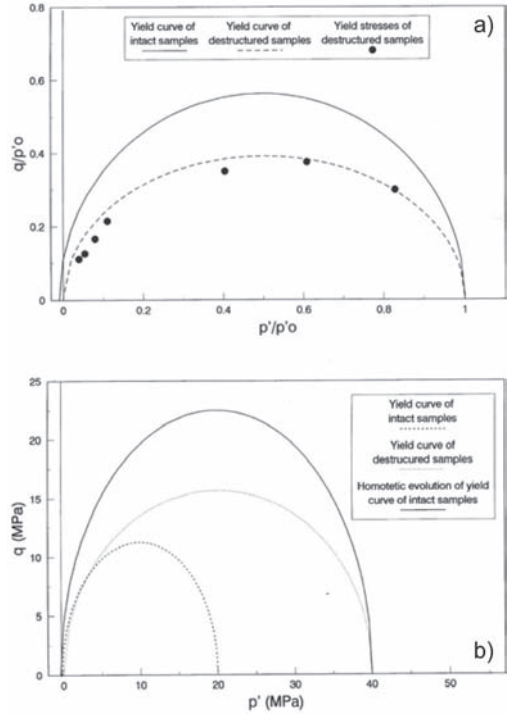

Figure 12. Evolution of the yield curve intact and destructured material: a) in the normalised plane; b) in the q-p′ plane (Aversa & Evangelista 1998).

uniaxial strength decreases with the logarithm of time, t. To evaluate the decrease of uniaxial strength, it is possible to define the ratio K as shown in Figure 13 (with t_1 = reference time) that assumes a value equal to 8÷11%, for the Neapolitan Yellow Tuff.

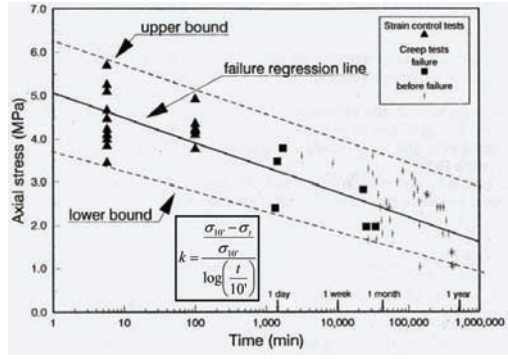

Figure 13. Influence of time on uniaxial compressive strength of Neapolitan Yellow Tuff: Uniaxial strength vs. time to failure (after Evangelista & Aversa 1993).

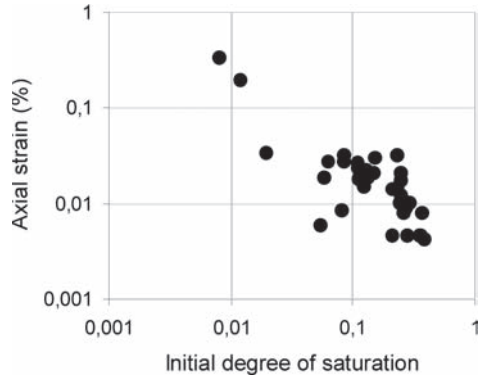

Figure 14. Uniaxial expansion of lithified tuff due to saturation as a function of the degree of saturation (after Evangelista & Aversa 1993).

3.4 *Alteration of soft rocks and interference with water*

Interaction between Neapolitan Yellow Tuff (NYT) and water was first investigated by Evangelista (1980). It was noticed that unsaturated samples of tuff are subject to expansion if soaked with water. Intensity of expansion is indirectly proportional to the initial degree of saturation (see Fig. 14).

Experimental data obtained by Evangelista (1980) showed a reduction of peak strength and shrinkage of the yield surface for saturated tuff. The effect of wetting-drying cycles on the strength of tuff samples is not evident only if samples are dried at room temperature (Evangelista 1980).

3.5 *Behaviour of tuff mass*

Figure 3 shows the outcrops of NYT in distal and proximal areas with a clear interface between

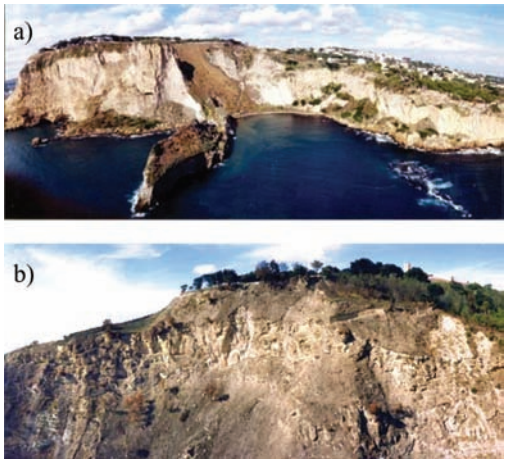

Figure 15. Cliff of Neapolitan Yellow Tuff: a) Posillipo hill; b) Camaldoli hill.

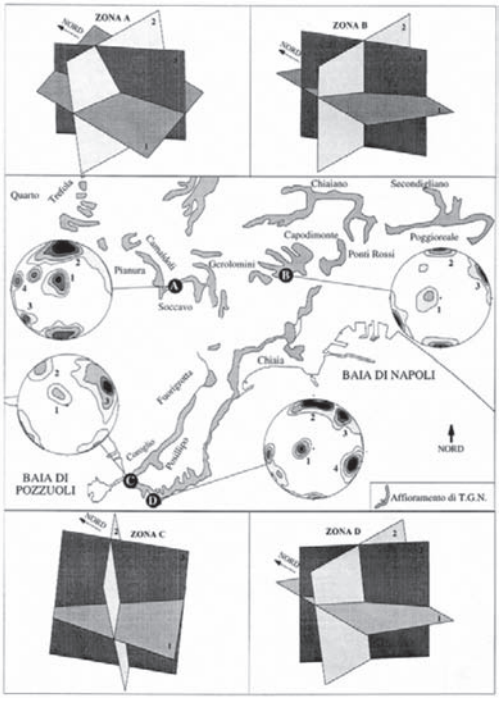

Figure 16. Structural characteristics of NYT (after Evangelista et al. 2002a).

lithified and unlithified zones throughout the city. In particular, NYT is exposed along natural cliffs, some of them facing the sea, and along man-made cuts of significant height (Fig. 15).

The mesostructure of the tufaceous mass, in the proximity of the cliffs, is characterized by a system of nearly vertical discontinuities (set 1) that are normal (set 2 and 4) to the slope surface (see Fig. 16). These discontinuities delimit removable rock blocks with parallelepiped or slab-like shapes (Evangelista et al. 2002a). The base of such blocks consists of sub-horizontal discontinuities, dipping between 5° and 38°, which lead to planar sliding. Block size is determined by the spacing which ranges from a few decimeters up to 3–5 meters in the subvertically-oriented discontinuities.

4 PROPERTIES OF PYROCLASTIC SOILS

4.1 *Generality*

A review of the mechanical properties of pyroclastic soils outcropping in the town of Naples and in its neighbours has been recently presented by Picarelli et al. (2006). In this report, pyroclastic soils are subdivided in:

1. unlithified Neapolitan Yellow Tuff, or Pozzolana (YTP);
2. pyroclastic products of the volcanic activity of Campi Flegrei younger than 15.000 years (Intracaldera Phlegrean pyroclastic Deposits, IPD), overlying the Neapolitan Yellow Tuff formation.

4.2 *Physical properties*

The grain size distribution of YTP, as shown by Evangelista et al. (2002b), taking into account experimental results obtained on a large number of samples recovered in a wide area located in the Northern part of Napoli, exhibits a limited scatter (see Fig. 17). The material is well graded and is mainly constituted by sand and silt with a little amount of clay fraction. This type of distribution is probably related to the origin of the YTP as massive pyroclastic flow. Figure 18 reports the frequency distribution of dry unit weight, void ratio and degree of saturation. It is possible to see that these properties vary very significantly.

As shown by Picarelli et al. (2006), because of this variance, it is not possible to determine any trend in their variation with depth.

The grain size distribution of some samples of intracaldera deposits of Phlegrean Fields (IPD) is reported in Figure 19. As it can be seen the material is not homogeneous: it ranges from fine sandy silt to well graded silty sand, and finally to sandy gravel. This variability it could be observed also from the physical properties reported in Fig. 20. The histograms in this figure report the frequency distribution of dry unit weight, void ratio and

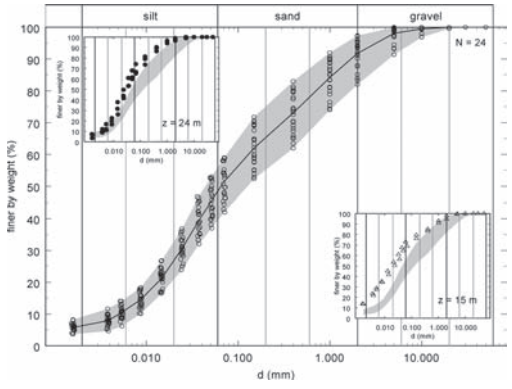

Figure 17. Grain size distribution of Pozzolana (after Picarelli et al. 2006).

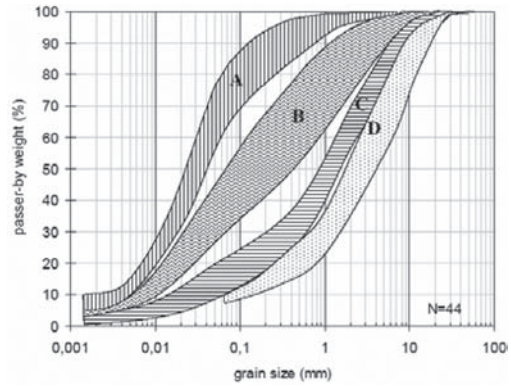

Figure 19. Grain size distribution curves of IPD deposits (after Picarelli et al. 2006).

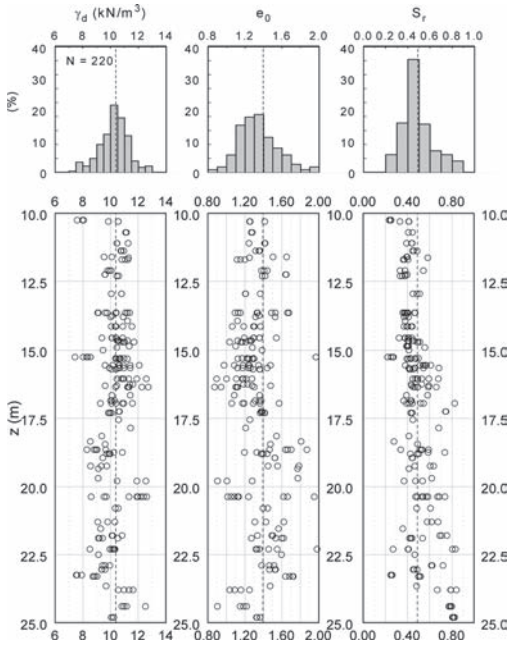

Figure 18. Main physical properties of pozzolana (after Picarelli et al. 2006).

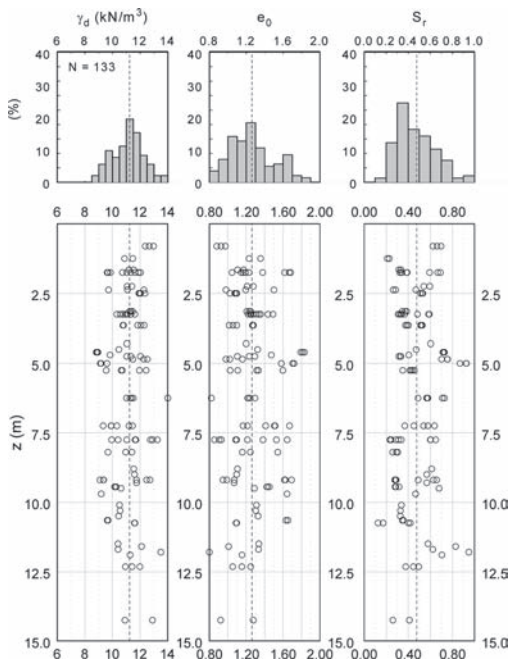

Figure 20. Main physical properties of IPD (after Picarelli et al. 2006).

degree of saturation. The same data have been drawn as a function of depth below the ground level.

4.3 *Water retention curve and permeability function*

Some Neapolitan researchers (Aversa et al. 1998, Nicotera 1998, Nicotera et al. 1999a, b, Papa, 2007) determined the water retention curve and the permeability function of YTP. The empirical expression suggested by Brooks & Corey (1964) has been used to interpolate all the experimental data, obtaining the water retention curve reported in Figure 21a. The best estimate of the permeability function (Aversa et al. 1998, Nicotera et al. 1999) is reported in Fig. 21b.

The permeability varies in a very wide range, assuming a value of 1.4×10^{-4} cm/s for saturated soil, and a value of ~1.0×10^{-9} cm/s for a suction of

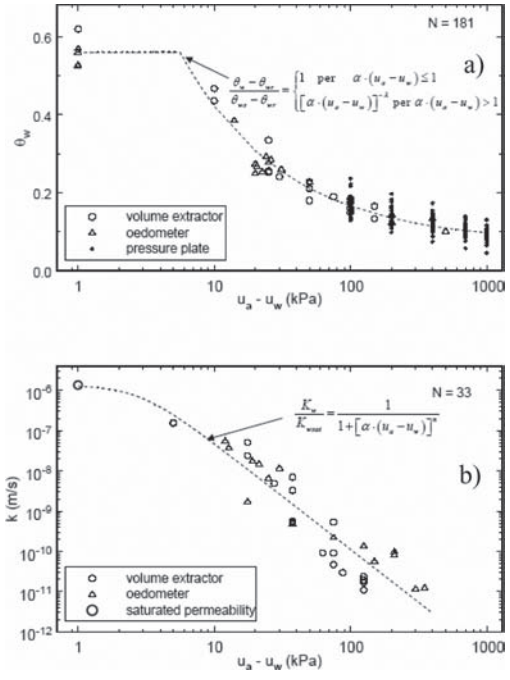

Figure 21. Water retention curve (a) and permeability function (b) of pozzolana (after Aversa et al. 1998).

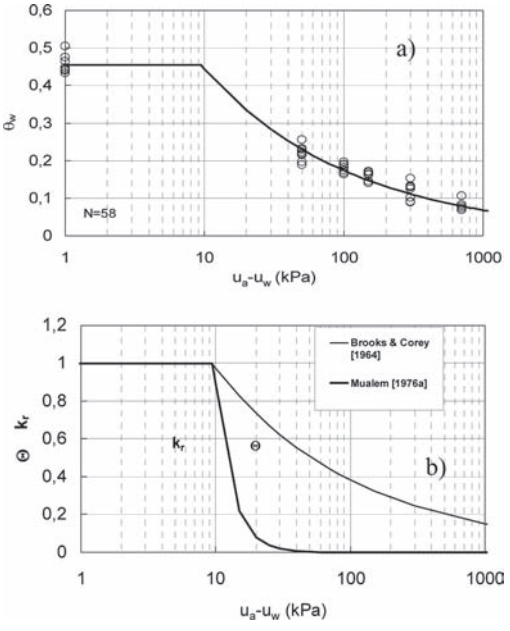

Figure 22. Water retention curve (a) and relative permeability and WRC (b) of IPD (after Scotto di Santolo et al. 2000).

350 kPa. The large part of the reduction in permeability is in the range 0–50 kPa. As already stressed by Picarelli et al. (2006), the main features of the water retention curve and of the permeability function are the very low air entry value (approximately 5 kPa), the very quick drying that is almost completed in a few tens of kPa, and the consequently sudden reduction of permeability.

The water retention curve of some samples of IPD has been determined by Scotto di Santolo (2000b) and is shown in Figure 22. As in the case of YTP, the air-entry pressure is very low (less than 10 kPa but the control at very low value of suction is not accurate) and the large part of the decrease of saturation occurs in the range 0–100 kPa of suction The hysteresis is negligible. The permeability function in terms of k_r (k_w/k_{sat}), plotted in Figure 22b; the saturated permeability k_{sat} is equal to 5.4 · 10E-5 m/s.

4.4 *Compressibility*

Compressibility of YTP was investigated since many years in order to evaluate foundations settlements and problems of soil-structure interaction (Croce 1954; Penta et al. 1961; Pellegrino 1967).

Typical results of standard oedometer tests on unsaturated specimens are reported in Figure 23.

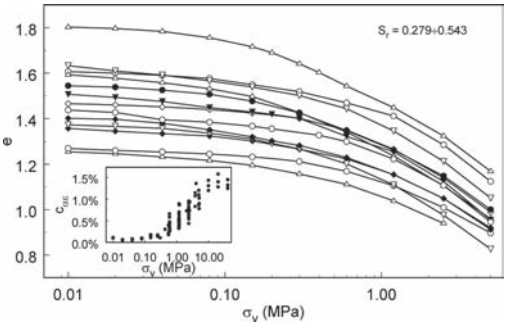

Figure 23. Results of standard oedometer tests on unsaturated pozzolana, and secondary compression index as a function of the vertical stress (after Picarelli et al. 2006).

Pellegrino (1967) has shown the structural collapse of unsaturated pozzolana upon wetting. Some experimental results are reported in Figure 24, where the results of three standard oedometer compression tests on unsaturated natural specimens are compared to those of three tests in which the soil has been submerged under water at a constant vertical net load. The reduction in void ratio caused by wetting decreases as the initial void ratio decreases. A more clear insight into YTP collapse has been obtained by Nicotera (1998), performing tests in suc-

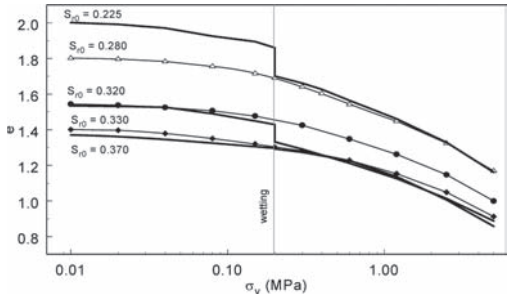

Figure 24. Results of oedometer compression tests on unsaturated pozzolana with a wetting phase (after Picarelli et al. 2006).

tion controlled oedometer (Aversa & Nicotera 2002). Experimental results obtained by Nicotera (1998), shows that collapse mostly occurs in proximity of zero suction, with the larger saturation increase (i.e. the suction effect is clearly non linear for structural collapse).

Croce (1954) and Pellegrino (1967) have shown that both unsaturated and saturated pozzolana display significant creep deformations. These observations have been confirmed by Nicotera (1998), who proposed the relationship between $c_{\alpha\varepsilon}$ and the vertical net stress, inserted in the box of Figure 23. Similar results have been obtained by Scotto di Santolo (2000a) with reference to IPB.

4.5 *Shear strength*

A number of data coming out from standard triaxial compression tests performed on specimens at natural water content or on previously saturated specimens have been collected by Picarelli et al. (2006). Strength envelopes (Fig. 25) clearly show the influence of the initial dry unit weight. A significant cohesive intercept comes out from the linear regression of the data for higher density. This intercept should be mainly attributed to the coupled effect of dilatancy and matric suction, being negligible the presence of bonds among particles.

In more recent years, suction controlled triaxial tests (Nicotera 1998, Papa 2007, Papa et al. 2008) have been performed by means of an apparatus developed by Aversa and Nicotera (2002). Some results of suction controlled triaxial tests are reported in Figure 26. From these test results, Picarelli et al. (2006), concluded that, for YTP, the matric suction does not affect the critical friction angle but only the peak strength, and that there is no "apparent cohesion" due to suction at the critical state. Picarelli et al. (2006) compared also shear strength parameters obtained by suction controlled triaxial tests with those determined by standard triaxial tests, obtaining a fairly good agreement.

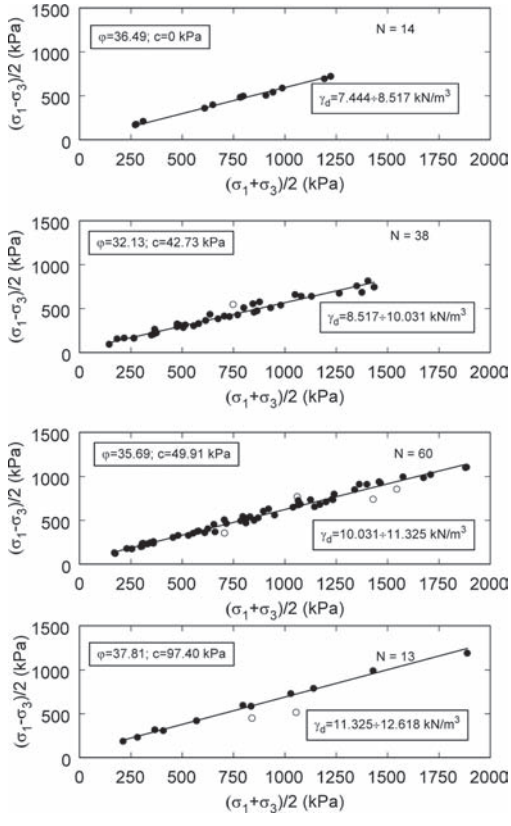

Figure 25. Strength envelopes of unsaturated undisturbed pozzolana specimens (empty circles indicate outliers data identified by the regression analysis) (after Picarelli et al. 2006).

Some considerations on the shear strength of IPD have been already presented by Picarelli et al. (2006) The results of 175 triaxial tests (CID) are shown in Figure 27. This behaviour is consistent with similar ones obtained on YTP. As for the YTP the specimens have been subdivided into four classes as a function of γ_d. If a linear strength envelope is assumed, the peak friction angle rises as density increases. The value of the critical state angle is around 35°.

These materials have been tested also by means of direct shear tests: Four types of tests have been performed (Pellegrino 1967, Nicotera 1998, 2000, Scotto di Santolo 2000a, b; Evangelista & Scotto di Santolo 2001; Calcaterra et al., 2010): a) on specimens wetted at peak during the shear stage; b) on specimens saturated in the consolidation stage; c) on specimens at their natural water content; d) on specimens dried in the pressure plate apparatus at different matric suction values. Figure 28 shows the results of tests of types a, b, and c carried out at

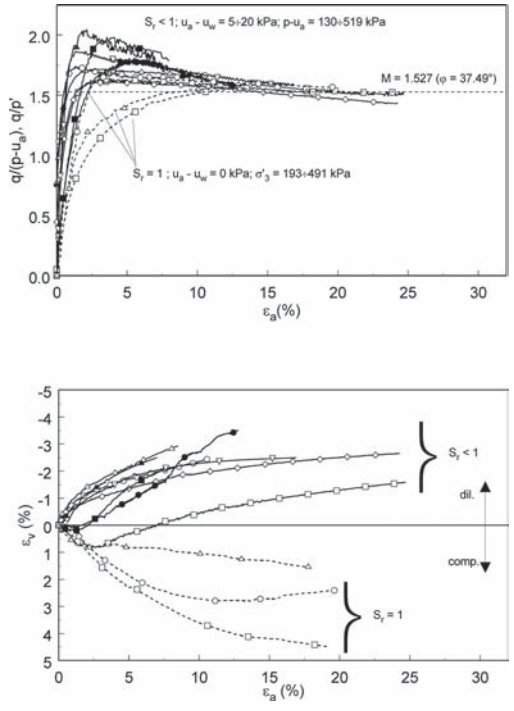

Figure 26. Results of suction controlled triaxial tests (continuous lines) versus standard triaxial tests on saturated pozzolana specimens (dashed lines) (modified from Nicotera 1998).

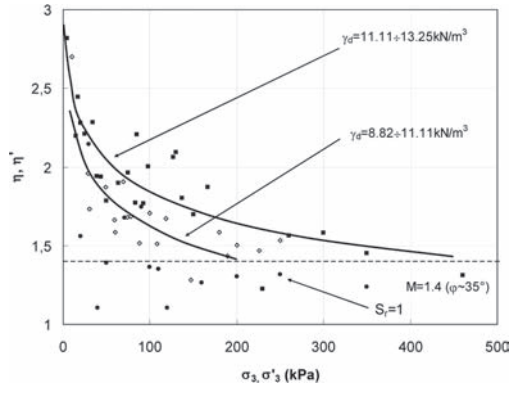

Figure 27. Stress ratio (η = q/p; η′ = q/p′) vs. confining stress for specimens of IPD characterised by a different density and degree of saturation (after Picarelli et al. 2006).

the same vertical stress (Scotto di Santolo 2000a). Any increase of the degree of saturation causes a change of the soil behaviour which turns from brittle to ductile. Wetting at peak causes a relevant compression and a strength decrease. However,

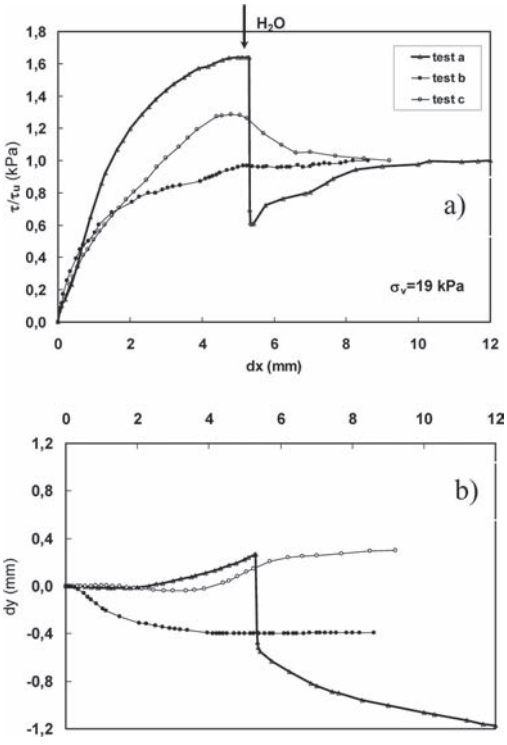

Figure 28. Results of direct shear tests on IPD carried out for different saturation conditions (after Scotto di Santolo 2000).

as the shear displacement increases, a progressive recovering of the shear strength occurs until the steady state value is attained.

5 URBAN DEVELOPMENT OF NAPOLI

5.1 *Generality*

Napoli developed in favourable geographic, climatic and geological conditions. Among the reasons which made the Neapolitan area very attractive for city building, it is possible to include the presence of very good construction materials: yellow tuff for bricks and pozzolana for mortar.

The presence of the volcanic tuff strongly determined the urban structure. According to Evangelista et al. (2000), Napoli could be called the «Tuff City».

As we have seen before, the yellow variety of tuff can be found in:

- ancient buildings and monuments;
- natural outcrops and excavated cliffs;
- quarries and cavities;
- subsoil utilities (tunnels, aqueducts, sewers).

In the following only some aspects of different ages and different works will be discussed.

5.2 *Origin—Greek settlements*

Greeks colonised Napoli in several phases from the 9th to the 7th century b.C. Coming from the island of Ischia and Cuma, they founded Partenope in front of the island of Megaride.

Only in 470 B.C. they founded Neapolis in the eastern zone, from which the present city developed. In Figure 29 it is possible to see the extension of the Hellenic settlements.

Neapolis was organised following a regular network of streets, three long main streets called "*Decumani*" oriented from West to East, and many orthogonal ones, named "*Cardini*", from North to South. The scheme of the city is similar to those present in many Greek cities at that time and is called *Ippodameus* (Di Stefano 1971), from the name of the famous architect Ippodamo of Mileto.

The distance between Cardini is variable, as a function of the destination of the inner "*insula*", larger in the case of public and religious destinations, smaller for private buildings.

Greeks built up fortified walls around Neapolis. Remains of the Greek walls are still present in the subsoil of the actual city. Some of those walls, built up in the 5th century b.C., are present in the actual Piazza Cavour and were also described in the opera of Palladio (1570). Some other walls were erected in the 4th century b.C. and some remains are present in the actual Piazza Bellini (see Fig. 30). The availability of tuff in the subsoil of the city permitted the construction of these massive walls, which resulted very effective to defend the city from enemies. According to Di Stefano (1971) the Romans conquered the city only because of the capitulation of the inhabitants and not because of any failure in the wall defensive system.

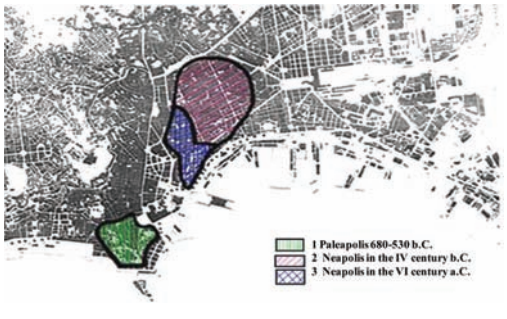

Figure 29. Hellenic settlements (IX—V century b.C.).

Figure 30. Hellenic settlements in Piazza Bellini, Napoli.

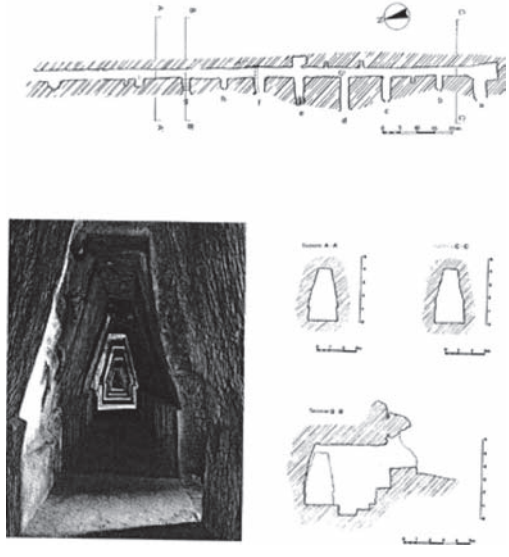

Figure 31. View of the cave of Sybilla at Cuma.

During the Greek period other cities were built up in the area interested by the presence of pyroclastic soils and rocks. Among these settlements we must remember *Pithecusa* (Ischia), probably the first Greek settlement in Campania, *Kyme* (Cuma) and *Dikaiarcheia* (Pozzuoli).

Greek necropolis were excavated at the boundaries of Neapolis, with the largest one in the area of Castel Capuano.

The fascinating cave in Cuma (see Fig. 31) was also excavated in this period. This cave was the site of the Sibilla who was used to answer to the question in a sibylline way. For example when requested to answer to the destiny of a person going for a

Segmento della tavola Peutingeriana. Si leggono le vie di addutione a Napoli: la strada Capua-Atella, quella proveniente da Ercolano e quella proveniente da Pozzuoli. La tavola Peutingeriana è una copia medievale (sec. XI-XII) di una carta di età imperiale.

Figure 32. Peutingeriana Table.

war, she answered in Latin "*ibis redibis non morieris in bello*", that can be translated in English alternatively as "*you will go you will return, you will not die in war*" or "*you will go you will not return, you will die in war*".

5.3 *Roman period*

The structure of the Greek settlement was preserved during the Roman age, and is still present in the Old Centre (*Centro Antico*) of Napoli, where in place of old temples (Apollo, Demetra, Dioscuri), very impressive Christian Churches characterise the morphology of the area.

Due to the different political conditions the defensive walls were less important during this period. The city was enlarged mainly in the direction of the sea, following the morphology of the sites, abandoning the regular network of the previous Greek period. Some thermal, public and residential buildings were constructed.

The peace permitted also the expansion out from the centre of Neapolis, mainly with vacation villas of rich Romans. Remains of these villas (de'Seta, 1969) are still present in the most beautiful sites around the Old Napoli: Posillipo, especially in the Gaiola, Capodimonte, S. Rocco, etc.

The relationship with other Roman cities required the construction of many roads. Some of these roads are sketched in a qualitative way in the Peutingeriana Table, which is a copy of an old map of the Roman Period (see Fig. 32).

In order to facilitate the relationship with Pozzuoli, without passing over the Vomero hill, Romans decided to excavate a tunnel, between the actual Mergellina and Fuorigrotta, called *Crypta Neapolitana*. This tunnel crosses the Posillipo Hill and is shown in Figure 33.

Romans realised also many other underground works: they built the first aqueducts, excavating them as channels in tuff, and several tunnels for civil and military traffic. Among these, beside the Crypta Neapolitana, it is possible to quote the Seiano tunnel (see Fig. 33), which crosses the same hill, connecting Posillipo to Bagnoli, and the tunnel network in Cuma: the Crypta cumana; the Cuman tunnel; the Cocceio's grotto. The latter is particularly interesting because, due to an explosion of German weapons during the last war, a very huge room was created in the central part of the tunnel.

Paleochristian catacombs (see Fig. 34) also date from the Roman period. Most of the catacombs are located in the North side of Neapolis, close Via Vergini and Via Fontanelle, in the area called Sanità.

The presence of catacombs was so relevant in the social life of the city, that—when the Christian religion was permitted after Costantino—first Christian Churches were built at the entrance of the Catacombs. The oldest one is the S. Gennaro Church, but some others (S. Vito, S. Gaudioso, S. Maria della Sanità, S. Efremo Vecchio, S. Maria del Pianto) must be also quoted as first examples of Churches in Napoli. The structure of these churches was realised with tuff.

5.4 *Middle age*

The maximum effort in the building activities during Middle Age was devoted to the reconstruction and the extension of fortified walls in order to defend Napoli. The city had its centre close to the seat of Bishop, in the church of S. Restituta. Many monasteries were built out from the walls of the city on the Pizzofalcone Hill, in Santa Lucia or in the area of Chiaia, with the Church of S. Maria a Cappella Vecchia. This church is located beneath a subvertical tufaceous cliff, where a manmade (not natural, as wrongly stated by de'Seta, 1969) cavity hosted a "Cenobio".

5.5 *Norman Svevian Period*

In the Norman-Svevian Period the city extended towards the inland. In order to defend the city, a castle, named Castel Capuano, was built up. Castel Capuano is located at the end of the Decumano Maggiore, close to one of the main entrance of the city: Porta Capuana (see. Fig. 35). Normans enlarged and reconstructed also Castel dell'Ovo on the island of Megaride. Both these castles were used as Royal Palaces.

During this Period, in 1224, Federico II founded the University of Napoli, the first non clerical University in Europe. In this report, it is relevant because, many centuries later, first systematic studies on mechanical behaviour of NYT and on pyroclastic soils started in this University.

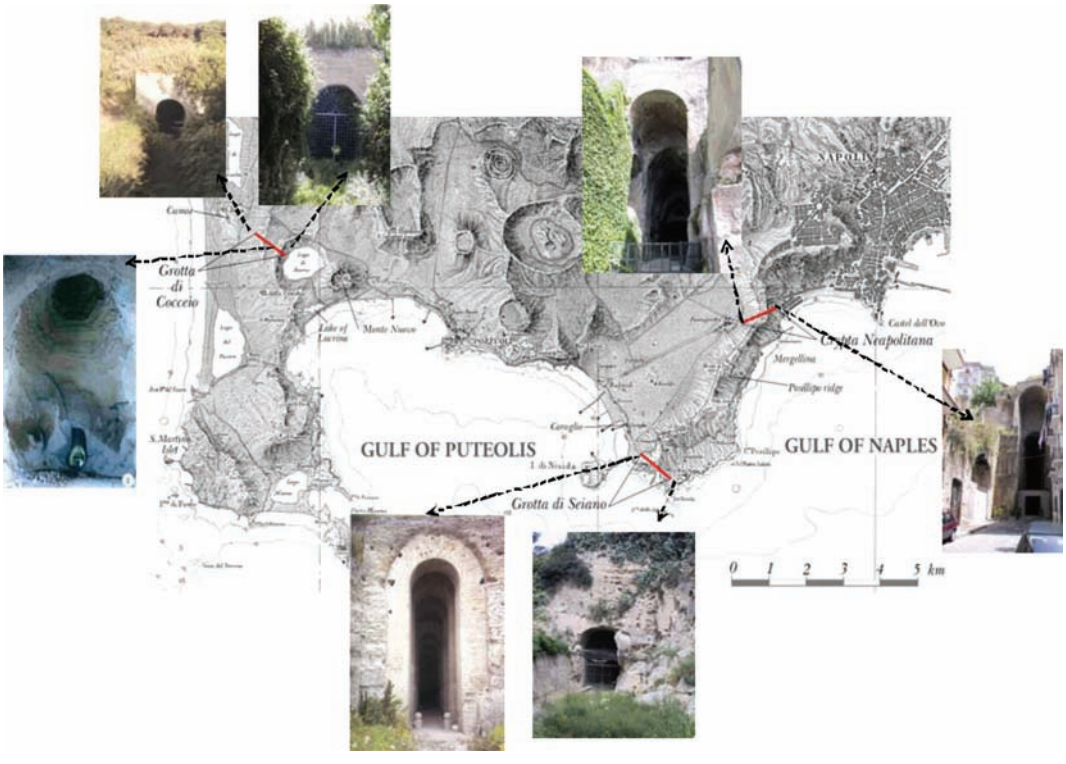

Figure 33. Plan and pictures of the entrances of the Roman tunnels.

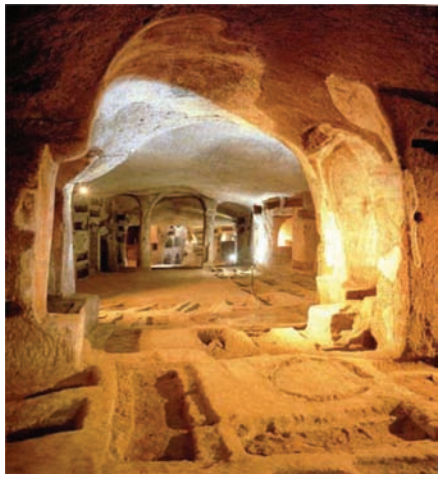

Figure 34. View of a paleochristian catacomb (Catacombe di S. Gennaro) 2nd century a. C.

Figure 35. Picture of Porta Capuana.

5.6 *Angioin period*

The Angioin period was a prosperous time for the city, when Napoli was an important centre for architecture and sculpture.

Starting from the German Gothic, a Neapolitan Gothic was developed in the city with some modifications with respect to the original due to the peculiarities of the available materials.

In this period undressed local stone «a faccia vista» was used for many structures, particularly in the fortified castles, like "Maschio Angioino" (see Fig. 36) and Castel Sant'Elmo (see Fig. 37). In this

Figure 36. Castel Nuovo.

Figure 37. View of Castel S. Elmo.

case, like in Castel dell'Ovo (see Fig. 1), there is a strong continuity between in situ rock and tuff bricks.

Among the churches, particularly valuable are: S. Chiara (see Fig. 38), S. Domenico Maggiore (see Fig. 39) and S. Lorenzo, completely built of yellow tuff «a faccia vista». Other impressive churches were built or renewed in this period (S. Giovanni Maggiore, Donna Regina, Donna Restituta, Gerolamini, S. Agostino alla Zecca, S Pietro a Maiella, S. Gregorio Armeno).

In churches and monumental buildings Piperno and Nocera Grey Tuff have been used for decorations.

A great improvement of the quality of the city was given with realization of a sewer network. Napoli was enlarged as it is possible to see on the Lafrery Chart (see Fig. 40). Fortified walls were reinforced and extended both to West and to East.

5.7 *Aragonese period*

During the Aragonese period a new wall defensive system was built on. It is still visible in some part

Figure 38. Santa Chiara Church.

Figure 39. San Domenico Maggiore Church.

Figure 40. Lafrery chart.

of the city, especially in the proximity of Castel Capuano and close to the harbour. The wall was characterised by the presence of 22 towers.

Napoli became one of the principal cities of the Italian Renaissance, with the presence of many important artists and intellectuals. From the architectonical point of view it must be highlighted some interventions on Castel Nuovo, especially with the addition of the very relevant entrance arch (*Arco di trionfo*) and with the wonderful and wide Hall, actually called "*Sala dei Baroni*". Aragonese operated also on Castel dell'Ovo. Among the main buildings of this period it is interesting to recall Palazzo dei Principi di Salerno, whose facade is now that of the Gesù Nuovo Church, with its characteristic "*bugnato*" (see Fig. 41).

5.8 *Spanish domination*

During the Spanish domination the city enlarged, with the realisation of Toledo Street and the District for the Spanish army, located between this street and the Vomero hill. It occupies an area of 150 hectares, part of which included within the new city walls built by Don Pedro de Toledo. The district (see Fig. 42) was designed as a regular grid of perpendicular streets, defining almost square internal blocks (for the troopers) and rectangular external blocks (for the Spanish nobles' houses) along Toledo Street. After this development, for almost two centuries (from 1566 to 1700), the city was forced into its boundaries by several laws, called «*prammatiche*», forbidding building activity near or outside the city walls. Therefore, in the city every bit of space was used to build houses as tall as the techniques of the time allowed. On this subject, it has been already noticed (Evangelista et al., 2000) that the use of tuff as construction material made possible to build up houses to a height of five or six floors, which could not be seen elsewhere in the world at that time.

Figure 41. Gesù Nuovo Church.

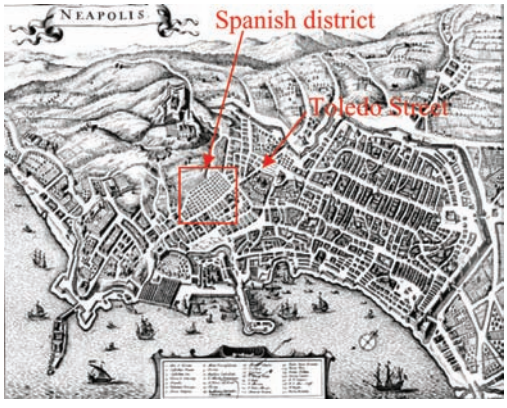

Figure 42. Plan of Neapolis with localization of the Spanish district.

The first Borbonic period, under Carlo di Borbone, was characterised by great architectural works always involving pyroclastic rocks. He promoted the construction of the S. Carlo Theatre and of several Royal Palaces (Napoli, Caserta, Portici). In this period the archaeological excavations of Ercolano and Pompei took place.

The Theatre of Ercolano was discovered by chance by the prince of Elboeuf. During the excavation of an artesian shaft, he ended up in the stage of the theatre. The theatre is totally buried, yet partially visible through tunnels excavated by the Borbone. It is covered by layers of weakly cemented pyroclastic soils and tuffs with very variable mechanical properties.

It was really sad having read on newspapers in recent time that the wonderful "*Palazzo Elboeuf*" is completely abandoned, in a state of disrepair. Historic sites need continuous attention and maintenance.

5.9 *Kingdom of Italy*

The period of Kingdom of Italy was characterised by tuff excavation to build utilities to improve the viability of the city. For example:

- excavation of tunnels for three funiculars connecting the Vomero hill to the lower part of the city;
- excavation of rail and street tunnels crossing the Posillipo hill;
- building of the two urban tunnels.

During this period some relevant buildings were designed by the architect Lamont Young,

among which it is possible to quote the Castello Anselmeyer on Corso Vittorio Emanuele and the actual seat of the Istituto Grenoble in Napoli. The facade of this building is realised with "a faccia vista" tuff (see Fig. 43). Lamont Young was a dreamer: he designed an underground railway, not realised (see Fig. 44).

5.10 *Italian Republic*

Between 1950–1970, due to the corruption of politicians, the city enlarged in an extremely disordered way, especially on the Vomero and Posillipo hills, without any regulation plan. The situation was well described in some books and movies (i.e., Rosi 1963). No attention was given to the subsoil condition and also to the presence of cavities. The increase of residential buildings on the Vomero hill created many problems to the sewers coming down from this hill. Some of them collapsed and produced damages to roads and structures.

In this period the ring road "Tangenziale" and several tunnels of the new underground railways have been constructed; some others are still under construction. Some cavities have been used for parking and also for a cinema.

Figure 43. Grenoble Institute.

Figure 44. Picture of the underground railway thinking by Young at the Toledo station.

6 UNDERNEATH NAPOLI

Particularly fascinating is the underground of Napoli (e.g. Melisurgo 1889). It consists of the combination of different cavities excavated in the tuff for different purposes:

- old aqueducts;
- quarries for the extraction of tuff blocks;
- hypogeans;
- ancient cult places.

The planimetric and volumetric extension of the cavities is very variable because it is possible to find small tunnels of the old aqueducts and very large obsolete quarries, with an overall volume of approximately 6 millions of cubic meters.

In Figure 45 it is possible to see the close interrelationship between underground cavities and the urban structure. Many cavities are inaccessible or partially full of building detritus or other materials. Often the cavities are subjected to inner instability phenomena (see Fig. 46).

The construction of the urban internal water distribution network goes back to the Roman period; it developed during the Angioin period (1200–1300), with the Bolla aqueduct (see Fig. 47); and it was completed late in the XVII century,

Figure 45. Map of underground cavities.

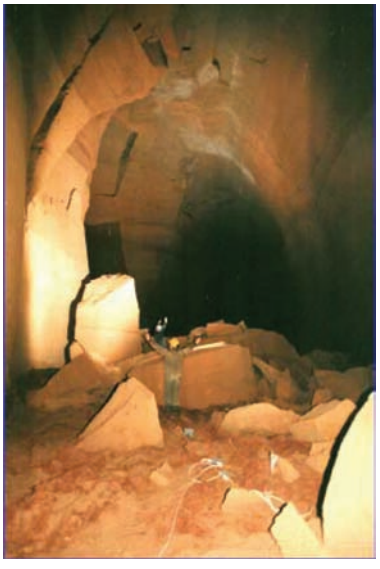

Figure 46. Instability phenomena in a cavity.

Figure 47. Plan view of acqueducts: della Bolla, Carmignano e Serino (after Di Stefano 1967).

during the vice-royal period, with the Carmignano aqueduct.

All the buildings in the lower part of the city, at the toe of the Vomero hill, received water via a narrow net of modestly inclined channels excavated in tuff, running beneath the streets. Those channels fed some tanks, from which inhabitants took water through wells excavated in the upper soils (consisting of pozzolana and reports), placed into the inner yards of the buildings or directly in the flats.

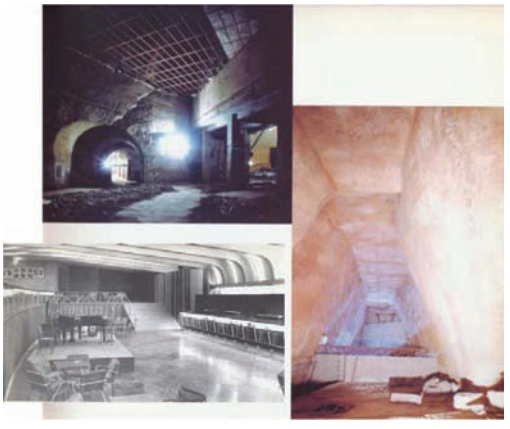

Figure 48. Example of a cavity turned into a cinema (Metropolitan 1950).

This aqueduct was managed by the «pozzari» (shaft men) who knew this complicated network very well. The city under siege was conquered twice, in 536 and in 1442, due to the betrayal of «pozzari» who indicated underground paths to the invaders.

During the last World war the tanks were turned into air-raid shelters; moreover, large amounts of rubbish and debris from collapsed buildings caused by bombing were thrown into the old aqueduct.

Right after the cholera epidemic of 1884, the city finally had a modern pressure aqueduct. Even in this case the weak lapideous rock of the Neapolitan hills gave its contribution since almost all tanks have been excavated in tuff. The aqueduct consists of several tunnels along which pipes and channels are located.

After the II World War one of the most important cavity, previously used as war recover, was transformed in the largest Cinema in Europe and, in more recent times, transformed in a Multiplex (see Fig. 48).

Some of the Cavities have been used as parking, one of them, Parcheggio Morelli, recently constructed. From this parking it is possible to visit the so called "*Borbonic tunnel*", passing beneath the Pizzofalcone Hill.

7 GEOTECHNICAL PROBLEMS IN NAPOLI

7.1 *Generality*

Main geotechnical problems in the city consist in:

- stability of old cavities;
- underground works;

- stability of rock cliffs;
- landslides in pyroclastic soils;
- foundation settlements due to saturation of pyroclastic soil;
- collapse of retaining walls due to saturation of the backfill.

7.2 *Cavities and tunnels*

The presence of cavities causes several types of damage. Frequently a cavity represents an address for water that seeps through the pyroclastic soils overlying the tufaceous bedrock, eroding incoherent soils and causing subsidence or chasms in streets and damage to buildings.

For economical reasons, excavations in the quarries have been so extensive as to induce high stresses both in the pillars and vaults, thus frequently causing a dense network of large fractures, and falls of large blocks from the vaults and the pillars. This phenomenon, especially in the vaults is due to the presence of thin discontinuities or disomogeneties, such as micro-fractures or pumiceous intercalations.

Instability phenomena sometimes occur a long time after the excavation. For instance cavities excavated over a hundred years ago are actually interested by new damage. This is due to the influence of time on the strength of tuff already studied by Evangelista and Aversa (1994) and discussed in a previous section.

A very interesting case history is that of the Fontanelle Cemetery, illustrated in a paper (Scotto di Santolo et al. 2013) presented in this conference.

Important stabilization works were carried out on a cavity along the Posillipo rim, located beneath the "*Fenestella 'e Marechiaro*", famous for the presence of a little window that inspired a song of Salvatore di Giacomo (Fig 49a). The cavity has a rectangular plan shape; it has almost vertical walls and it is characterised by an isolated pillar eroded by meteorological agents to form a helix (Fig. 49b). The conditions of stability are aggravated by the large number of discontinuities. They required an intervention of consolidation of the natural pillar completed with a series of rock bolts on the roof and deep nails on the retaining wall above the cavity (Fig. 49c). The intervention was completed by a protection of the entire ridge from sea erosion and a revitalization of the marine environment.

Not always the cavities have an environmental value. This is the case of Cupa Spinelli: a huge cavity, of about 60.000 m^3, excavated around a single pillar in the central part beneath an inhabited area (Fig. 50a). The cavity is accessible through a well (Fig. 50b). The floor of the cavity is located at about 40 m deep from the ground level with an average height of 20 m. The poor stability conditions of the

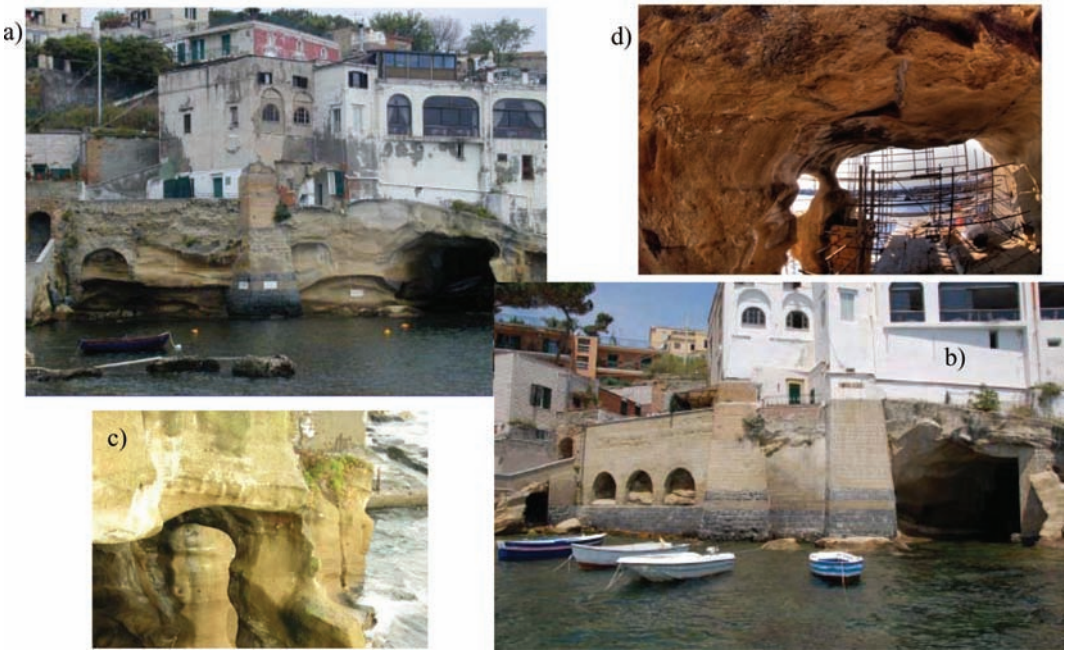

Figure 49. Cavity below the "*Fenestella 'e Marechiaro*": a) before and b) after consolidation works; c) eroded pillar and d) fractures inside the cavity.

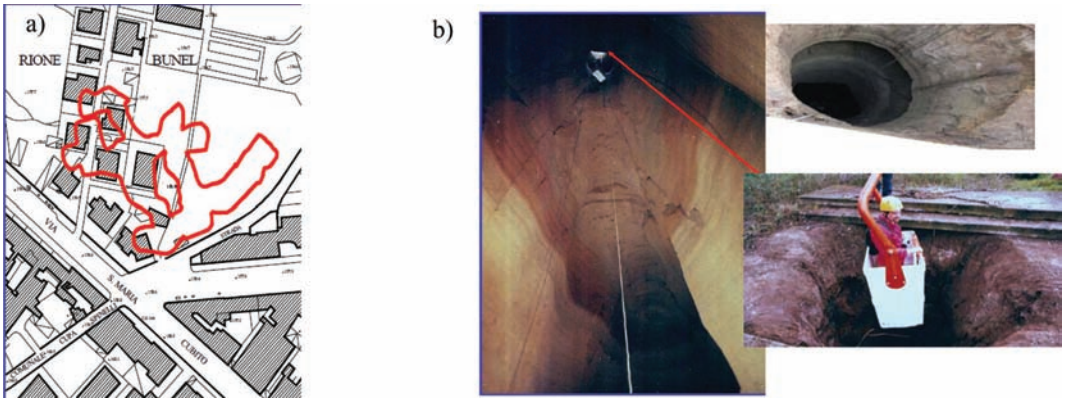

Figure 50. Cupa Spinelli cavity: a) plan view; b) pictures of the well entrance.

cavity were evident also because of the presence of numerous tuff blocks on the floor (see Fig. 46). In order to reduce the risk for the inhabitants of this part of the city, it was decided to fill the cavity (Evangelista et al. 2002).

Some problems have arisen also during the excavation of tunnels, or just after the excavation were completed; in other cases accidents occur several years after the construction, as it happens for some of them excavated under Posillipo hill (Evangelista et al. 2000).

7.3 *Cliffs*

Volcanic rock formations outcrop for different reasons with vertical and sub-vertical cliffs.

As already written in § 3.5 the Neapolitan Yellow Tuff formation is affected by random subvertical discontinuities named «*scarpine*», and by horizontal planes of discontinuities named «*suoli*». Isolated blocks fall down the cliffs; sometimes the cliffs can be subjected to overall rockfalls.

High instability conditions are present also along the coastal cliffs over a wide extension (Fig. 15a).

Cliffs hanging on urban areas or on the coasts have to be stabilised by means of expensive works, comprising masonry and concrete retaining structures, lining, rock anchors, rock bolts. These works have been realised in areas of landscape interest and, for this reason, they needed accurate evaluations from the environmental point of view. Some examples are shown in Figure 51.

A rock falls involved the tuff mass at the top of Camaldoli hill made of Neapolitan Yellow Tuff (see Fig. 15b). Survey techniques and analyses, based on terrestrial photogrammetry (Nocilla et al. 1999), were used to define the oriented structure of the rock mass and thus the removable blocks present in the detachment area (Evangelista et al. 2002a, 2004, 2007). A detailed investigation was carried out on this rockfall, also by means of in situ full scale tests (Nocilla et al. 2003). The data showed a reduction in block volume during run out.

An empirical relationship of volume reduction versus travel distance was proposed (see Fig. 52). This relationship was also validated by comparing the population volumes of fallen blocks along the slope, with the population of removable ones on the rock face, (Nocilla et al. 2009).

Interventions of stabilization posed difficult problems of landscape character especially for the coastal cliffs of Posillipo, of great environmental value.

7.4 *Landslides in pyroclastic soils*

In the city of Naples there are hilly areas of variable height ranging from the 100 to 500 m. These slopes consist of a rocky skeleton of volcanic nature (tuffs of different age) and are covered by pyroclastic products of the activity of the Third Phlegrean period (<12,000 years). They are characterized by high porosity and are partially saturated. The thickness is very variable, ranging from one meter to some tens of meters on the hills of Camaldoli and Posillipo, and up to several tens of meters in the Conca di Agnano.

In such areas landslides are widespread (Beneduce et al., 1988; Pellegrino 1994; Calcaterra and Guarino 1999; Scotto di Santolo 2000a, 2002). The standard type of the phenomena is for 30% complex landslides (translational or rotational slide, or falls that lead to debris flows). The volumes are generally reduced (reaching the maximum rates of 1000 m^3) and only in some cases the covered distances exceed the foot of the hill. The geometric feature of landslides is compared in Figure 53 with what occurred in the Campania region (Monti Lattari and Monti di Sarno) in recent years. More

Figure 51. Cliff in NYT: a) Posillipo; and b) Camaldoli hill.

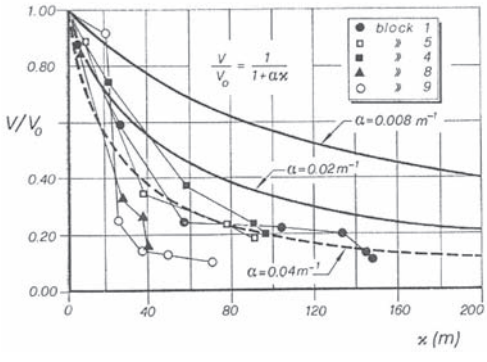

Figure 52. Camaldoli hill: Theoretical fragmentation curve of the blocks during rockfall (after Nocilla et al. 2009).

consideration on this topic can be found in the paper by Scotto di Santolo and Evangelista (2008). The risk of these landslides is high because of the intense urbanization of the hilly area.

The landslides occurred in the rainy period: in Figure 54 the frequency of the landslides in the months of the year are reported for 101 complex landslides which occurred in this deposit in the period between 1986 and 2009 (Scotto di Santolo and Evangelista 2009). It has been observed that the phenomena mainly take place in winter and at the beginning of spring. If compared with average monthly rainfall, as shown in Figure 55, it can be observed that the landslides do not occur in correspondence with the wettest period (October–December), but are delayed by several months. The delay between rainfall and landslides is a function of climatic conditions and the hydraulic characteristics of the cover.

The triggering of landslides is strongly related to rainfall. Infiltration of rainfall leads

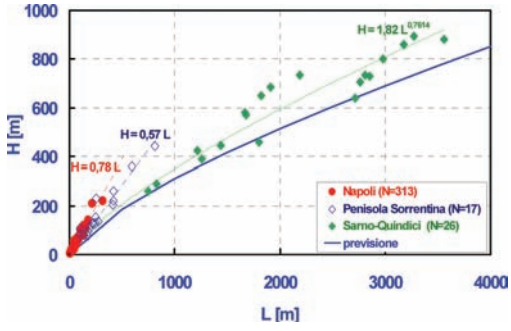

Figure 53. Relation between the height and horizontal travel distance of landslides in Campania Region (after Scotto di Santolo 2000).

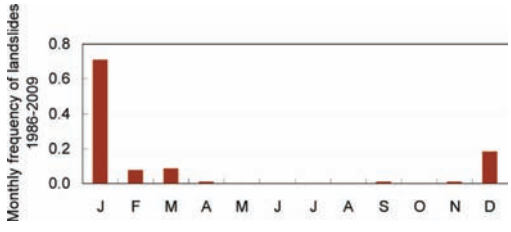

Figure 54. Distribution of landslides (1986–2009) (after Scotto di Santolo & Evangelista 2011).

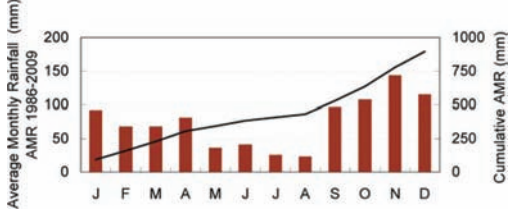

Figure 55. Average monthly rainfalls (1986–2009) (after Scotto di Santolo & Evangelista 2011).

to a decrease in suction which reduces the shear strength of the shallow soils (e.g. Fredlund et al., 1978; Evangelista & Scotto di Santolo, 2001; Papa et al., 2008). The prediction of triggering factors is of extreme importance for hazard mitigation, due to the dynamic features that characterize these phenomena during their evolution (Scotto di Santolo 2000, 2002; Scotto di Santolo et al. 2012).

Four sites which are representative of the morphologic and stratigraphic conditions of slopes susceptible to debris flows in Naples were monitored with rain gauges, tensiometers, psychrometers, tiltmeters and TDR probes (see red circle in Fig. 4). More details on these test sites can be found in the papers by Evangelista et al. (2003), Scotto

di Santolo et al. (2005) and Scotto di Santolo & Evangelista (2010).

7.5 *Foundation settlements*

In the large part of the city of Napoli pyroclastic soils are unsaturated since their deposition. When saturated they can experience a collapse as shown previously. This is the reason for which sometimes in Napoli old buildings with shallow foundations on pyroclastic soils can experience large settlements due to saturation of subsoil produced by aqueduct and sewer leakage or by infiltration trough open excavations close to their foundations.

Many cases of settlement have been recorded in the historical centre of Napoli on September 15, 2001 when the city was hit by an exceptional rainstorm, with 130–160 mm of rain in three hours. It was an event with an occurrence period of 400–500 years. Following this events some buildings in the area of via Duomo—via Foria underwent some damages. Between them a historic building of via Settembrini suffered settlement larger than 20 cm that became progressively worst with elapsing time, Figure 56. It is interesting to notice that Via Settembrini is out but close to the original Greek city, whose walls are still visible in the basements of the buildings and courtyards present (Fig. 57). The subsoil is composed by (Fig. 56b) land fill (MC) with thickness of tens of meters, few meters of pozzolana and pomices (P) resting on the NYT (TGN in the Fig. 56). The thickness of the layer of pozzolana grows moving along via Settembrini.

The original ground water level was at the depth of 25–27 m below the ground level. In this area the roof of the tuff is highly irregular. Within this formation some cavities were found; they represent water-tanks of the old aqueduct ("*della Bolla*") working until the second half of the nineteenth century (Fig. 47). Moreover within the pozzolana tombs of the Greek period were found, at depth between 10 and 17 m below the actual ground level. The presence of such funerary works, which originally were made at a maximum depth of the order of a couple of meters, suggests that fills of 10 ÷15 meters of thickness are present in this area. Due to the rainfall and to the presence of debris in the tuff channels and in the tank, the level of water increased very quickly, producing the saturation of the upper soils. The settlement was caused by the collapse of in situ Pozzolana, produced by its saturation.

A very strong reinforcement of foundations was designed (Feola et al. 2004) due to the need of not wanting to demolish the building in order to preserve the urban fabric. Therefore, all the cavities intercepted were filled with lightweight concrete (about 3000 m^3) instead some catacombs have been preserved. The buildings have been founded on micropiles connected to the masonry through reinforced concrete beams.

This very massive intervention, not very respectful of the material integrity of the building in the spirit of what affirmed about the Ground-Monument System in many documents of TC301 (Jappelli 1991, 1997, Viggiani 1994, Calabresi & D'Agostino 1994, Aversa 2007, Aversa et al. 2012a), was probably mandatory due to the severe damages occurred and to the residual risk still present after the event.

It must be stressed that, if a correct maintenance of the subsoil had been done, without permitting the obstruction of old channel with man-made debris, and with an adequate design of sewer, no problems would have occurred.

Another interesting case, that shows the role of the subsoil in the urbanisation of Napoli, is that of an r.c. building realised in the second half of 20th century in Via Jannelli. On December 1992 some cracks appeared on some of the inner partition walls. Many of the cracks showed inclination to the vertical very close to 45° and descending towards the interior of the building (Fig. 58). An evident rotation of the exterior wall was also observed. This phenomenon was quickly related to a relevant water infiltration from a pipe that runs along the Camaldolilli Street. The subsoil beneath the building is very irregular; tuff outcrops in a part of the building area, but it rapidly deepens at a depth varying between 20 and 28 m in the other parts.

The building had mixed foundations: on piles, not always interesting the tuff formation, along via Camaldolilli and direct foundations on tuff in the other sides. The infiltration of the unsaturated pyroclastic soils has resulted in a collapse and in a decrease of the shear strength as reported in § 4. At the same time this produces a reduction of the limit load of the piles due to a negative friction phenomenon. The foundation was integrated with micropiles embedded in the tuff for approximately 5 m (Fig. 59).

7.6 *Collapse of retaining walls*

Old retaining walls in Napoli are made by a NYT masonry, very often unplastered ("*faccia vista*"). More than 260 km in length of this type of walls are present in the city.

The height of these walls varies significantly, with maximum values up to 20 m. The ratio between the width B at the base and the height H varies in a wide range, with a mean value between 0.2 and 0.3 (Evangelista et al. 2002a, Scotto di Santolo et al. 2012, 2013). The backfill is very often constituted by unsaturated pyroclastic soils.

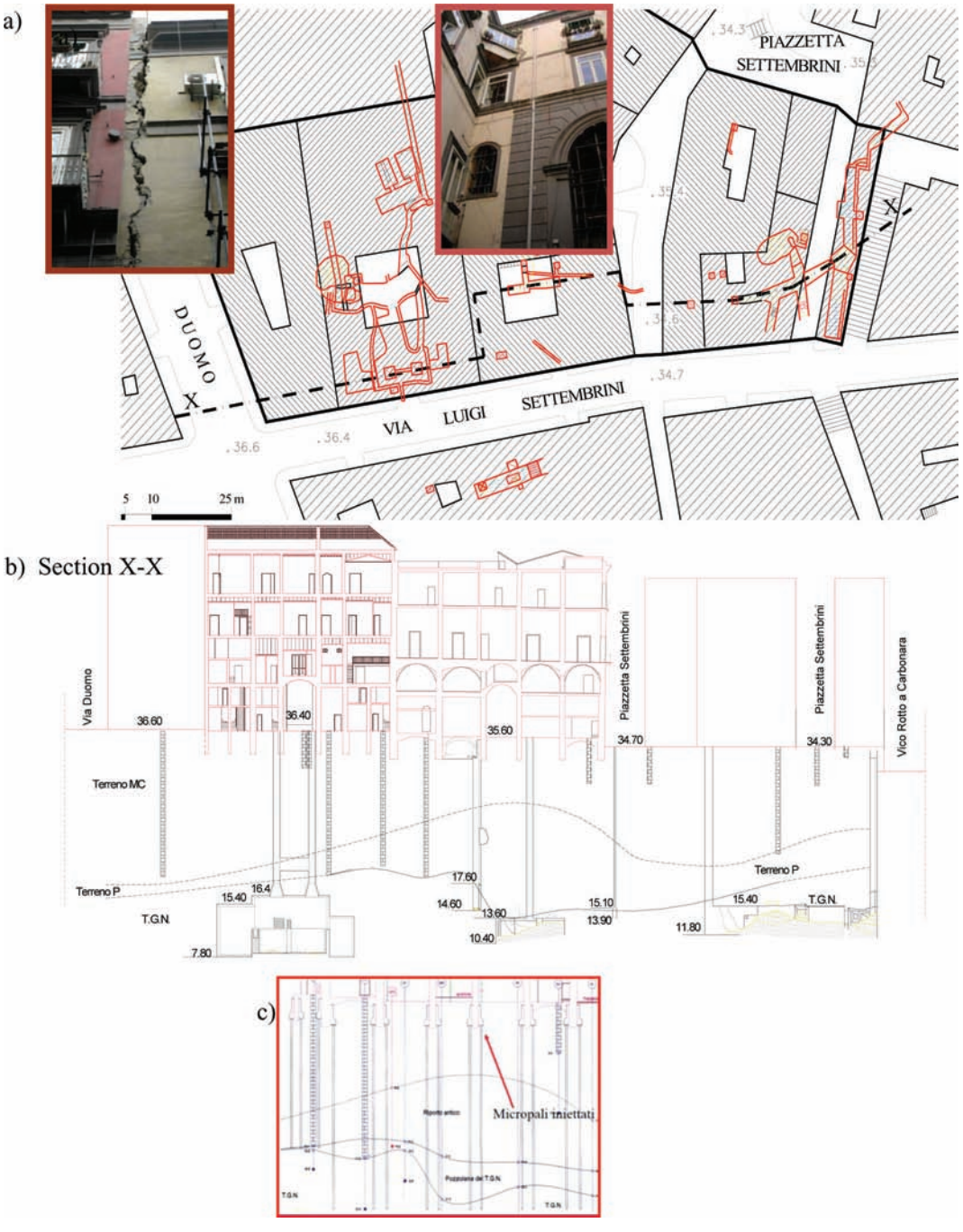

Figure 56. a) Plan view of the area and pictures of the damages; b) Stratigraphic sections of Via Settembrini; c) consolidation works (modified from Feola et al. 2004).

If stability of these walls is checked, without considering the positive effect of matric suction, the large part of the Neapolitan tuff retaining walls results not stable, with geotechnical safety factors against sliding, toppling and bearing capacity lower than 1.0. The structures appear

Figure 57. Contours of the Greek walls.

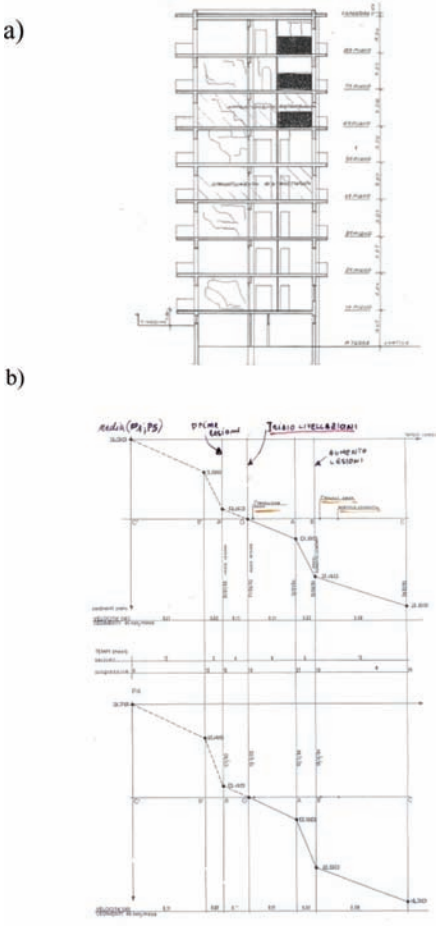

Figure 58. Via Jannelli: a) section with table cracks; b) monitoring displacements of the pillars.

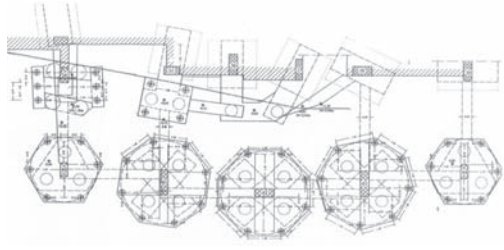

Figure 59. Via Jannelli: Stabilisation works.

not safe also from the structural point of view. Many stability analyses of these walls using classical geotechnical approaches have been performed by Evangelista et al. (2002c) and Scotto di Santolo et al. (2012).

As obvious, the suction decreases when the degree of saturation increases and it disappears with the full saturation. Aversa and Nicotera (2013) showed that it is very difficult that saturation of the backfill and collapse of the wall can occur only because of infiltration from the ground level of the backfill, unless incredibly prolonged rains will occur. Generally, collapses occur due to leakage from sewer or aqueducts, located close to retaining walls. This is another proof that the regular maintenance of hydraulic systems is very important in historic sites.

Scotto di Santolo et al. (2013) reported the results of a coupled parametrical numerical analyses taking into account the unsaturated behaviour of the backfill and of the masonry tuff. They observed that the relative permeability between them (wall and backfill) played a predominant role on the seepage of the systems besides the parameters that influence the process of infiltration in unsaturated soil. The role of the permeability of the interface between wall and backfill has been shown also by Aversa and Nicotera (2013).

8 RECENT EXCAVATIONS

New excavations have been done in the city for the Neapolitan underground railway system, currently under construction (see Fig. 60), and for highway and urban road tunnels.

The presence of a soft rock, like NYT, in the subsoil of the city can be considered as a lucky condition, both in the upper part of the city where the underground has been excavated well above the water table and in the proximity of the sea where the line has been realised below the water table.

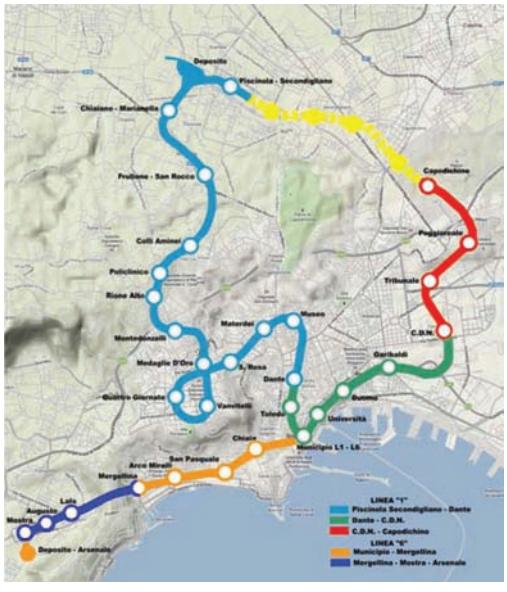

Figure 60. Plan of the new underground railway.

The main problem during excavation in the upper part of the city was due to the presence of unknown cavities and fills.

The instability in road tunnels in NYT (Di Stefano 1967) should be also mentioned. In the '70s as a result of work on the construction of the ring road of Napoli (Tangenziale), for instance the cavity of the Scudillo No. 22 was intersected. This cavity in the past was used as a weapons depot of the Navy, and experienced a partial collapse due to their explosion. The discovery of the cavity created many problems to the designers, who provided the partial filling of the cavity.

The Cumana railways was initially a one-way rail tunnel, subsequently (in 1975) doubled because of the growth of transport demand. All these galleries are at the base of the hills of Vomero and Posillipo and are above the water table. With reference to the tunnels crossing the hill of Posillipo (Fig. 61), it is possible to recall:

1. the road tunnel of Quattro giornate, opened in 1884 and closed because of a rockfall in 1890, subsequently restored and re-opened;
2. the tunnel Direttissima of the railway Napoli-Roma, built up in 1917, which presentes some damages in 1922;
3. the road tunnel Laziale completed in 1926, which suffered some damages in 1932.

Some of this failures can be related to the effect of time on the strength of NYT, already discussed in a previous section (see § 3.3).

Figure 61. Plan of some tunnels crossing the Posillipo Hill excavated during the Kingdom of Italy.

In the lower part of the city, in recent times, the railway tunnels were excavated using Tunnelling Boring Machines with blind heads, mainly passing through the tuff formation, without any problem to the urban environment. This is the reason for which Line 1 of the Metro line is very deep, with very deep stations. These stations have been realised with a shaft and enlargements of the line tunnels for accommodating the walkways. The realisation of these enlargements was done by means of soil freezing. A great attention was given to the design of these stations and to the monitoring of induced displacements.

In the part of Line 6 close to the sea the tunnel mainly passes above the tuff formation, luckily not very close to historic buildings. Only in the stretch between Piazza Vittoria and Via Calabritto, the line underpasses some old buildings and a church of 16th century. More details on this situation are in the paper of Aversa et al. (2013) presented at this Conference. No problems were created to the church and to the buildings, but it must be stressed that the design was based on specific geotechnical, structural and historic invest and that the relevance of the buildings required an accurate monitoring.

Excavation of the underground stations of metro permitted to go back in the history of the city. This is especially true in the case of the Municipio Station, where it was possible to bring to light the old walls of the fortress around the Castel Nuovo (see Fig. 36), built up during the Aragonese period, and an old necropolis. During the excavation of the shaft of the station (see Fig. 62) old roman boats appeared, fortunately not cut by diaphragm walls.

Similarly, during the excavation of the station in Piazza Nicola Amore an old Temple was found. In this case, unfortunately, diaphragm walls cut the remains. The temple will be partly reconstructed within the underground station.

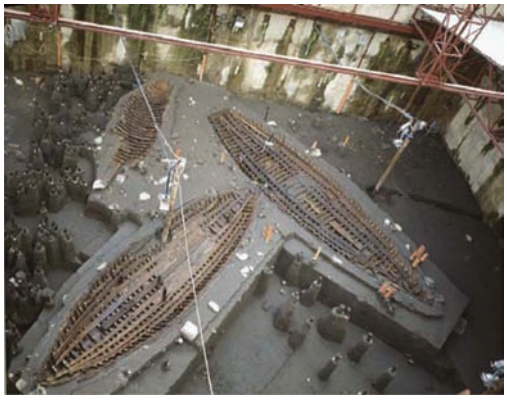

Figure 62. View of roman boats found during the excavation of the underground.

9 CONCLUSIONS

The history of Napoli dates since approximately three thousand years, during which different many events have happened, peoples and dominations have followed, the city grew spreading and stratifying, changing the allocation of sites and modifying the morphology of the landscape.

The current situation is the result of all these events, some of them briefly recalled in this report, aimed to show how this history must be considered not only in the examination of what is above the ground level, but also what is buried in the subsoil.

When dealing with interventions on monuments and historic sites, investigation of the subsoil is very relevant. The higher is the knowledge of the subsoil, the better is the geotechnical model of the subsoil, the greater is the confidence in designing, and the more respectful these interventions will be. Good information on history of the monuments and of the urban changes of the sites is essential in these cases.

Documentation and monitoring of he interventions is fundamental in order to improve the knowledge and to permit to operate always in a better way.

As shown very clearly in the paragraph dedicated to the construction of the underground railway system, the realization of these structures is also the occasion to go back in the history, increasing the awareness of our past. In some cases it could be also the occasion to enrich the very large archeological patrimony of our Country.

Two final considerations, of opposite sign. Italians do not like maintenance; this is especially true for Neapolitans. The huge architectural, environmental and historical heritage is not adequately preserved. Many monuments and historic sites are abandoned.

From the other side the knowledge on the subsoil of the city of Napoli is very high, not only because of what has been done by researchers at the University but also because of the database of information recovered at the Municipality of Napoli, thanks to the "Commissione sottosuolo", chaired for many years by Prof. Arturo Pellegrino, the researches performed by C.U.G.Ri. and the "Ufficio Sottosuolo" of the Municipality of Napoli, under the guidance of Ing. Goffredo Lombardi. The amount of information is much larger than that recovered in many other cities in Italy and worldwide (Evangelista & Viggiani 2013). The authors hope that this very significant heritage will be preserved and increased in the future.

ACKNOWLEDGEMENTS

The authors would like to acknowledge all the colleagues and friends, who gave them suggestions and materials for preparing this report. Some of the data have been originated in the framework of a research convention of C.U.G.Ri., which is deeply acknowledged.

REFERENCES

Alterio, L., Russo, G., Silvestri, F. 2013. Seismic vulnerability reduction for historical buildings: the case study of Villa Favorita (Ercolano). *Proc. 2nd Inter. Symposium on Geotechnical Engineering for the preservation of Monuments and Historic Sites, TC301*, Naples 2013.

Amato, L. & Gialanella, C. 2013. New evidences on the area of Puteolis harbour referring to Serapeum in connection with the different phases of Phlegraean bradyseism. *Journal, GTJODJ*, 25(1): 3–15.

Aurisicchio, S., Evangelista, A., Masi, P. 1982a. Il Tufo Giallo Napoletano: permeabilità ed impregnabilità con monomeri acrilici. *Rivista Italiana di Geotecnica* Anno XVI N.1.

Aurisicchio, S., Masi, P., Nicolais, L., Evangelista, A., Pellegrino, A. 1982b. *Polymer impregnation of Tuff.* Polymer Composites J., July, Vol.3, N.3.

Aurisicchio, S., Evangelista, A., Nicolais, L. 1985. Comportamento meccanico del tufo trattato con polimeri. *Rivista Italiana di Geotecnica*, Anno XIX, n. 2.

Aversa, S. 1989. *Comportamento del Tufo Giallo Napoletano ad elevate temperature.* Tesi di Dottorato di Ricerca in Ingegneria Geotecnica, Università di Napoli 1989.

Aversa, S. 1991. Mechanical behaviour of soft rocks: some remarks. *Proc. of the Workshop on "Experimental characterisation and modelling of soils and soft rocks", 191–223, Napoli.*

Aversa, S. & Evangelista, A. 1993. Thermal expansion of Neapolitan Yellow Tuff. *Rock Mechanics and Rock Engineering*, vol. 26 (4): 281–306.

Aversa, S. & Evangelista, A. 1998. Mechanical behaviour of a volcanic tuff: yield, strength and "destructuration" effects. *Rock Mechanics and Rock Engineering*, vol. 31 (1): 25–42.

Aversa, S., Evangelista, A., Ramondini, M. 1990. Influenza della struttura sulla compressibilità di un tufo vulcanico. *Atti della Riunione Annuale dei Ricercatori del G.N.C.S.I.G. del C.N.R., 157–160, Roma*.

Aversa, S., Evangelista, A., Ramondini, M. 1991. Snervamento e resistenza a rottura di un tufo a grana fine. *Atti del II Convegno dei Ricercatori del G.N.C.S.I.G. del C.N.R., Vol. 1: 3–22, Ravello*.

Aversa, S., Evangelista, A., Leroueil, S., Picarelli, L. 1993. Some aspects of the mechanical behaviour of "structured" soils and soft rocks. *Proc. of International Symposium on "Geotechnical Engineering of Hard Soils and Soft Rocks", vol.1: 359–366, Athens*.

Aversa, S., Candela, M., Nocilla, N., Urciuoli, G. 1997. Stability of the vertical cliff overhanging Via Krupp in Capri. *Geot. Eng. for the Preservation of Monuments and Historic Sites*. Vol. 1, p. 49–60, ISBN: 90–5410–871–1.

Aversa, S., Evangelista, A. & Nicotera, M.V. 1998. Experimental determination of characteristic curves and permeability functions of partially saturated pyroclastic soil. In *Unsaturated Soils, Proc. 2nd Int. Conf., Beijing, 1: 13–18.*

Aversa, S. & Lagioia, R. 2000. Model requirements and design criteria for soft rocks. *Proc. of the II Int. Symp. on "The Geotechnics of Hard Soils and Soft Rocks", Napoli, Vol. 3: 1483–1497*. Rotterdam: Balkema.

Aversa, S. & Nicotera, M.V. 2002. A triaxial and oedometer apparatus for testing unsaturated soils. *Geotechnical Testing Journal* 25 (1):. 3–15.

Aversa, S. & Russo, G. 2006. Il ruolo delle indagini nella valutazione delle condizioni di sicurezza delle opere esistenti. *Rivista Italiana di Geotecnica*, vol. 4/06, ISSN: 0557–1405.

Aversa, S. 2007. Preserving cities and monuments. In: Geotechnical Engineering in Urban Environments. Madrid, 24–27 September 2007, vol. 5, p. 453–462, Rotterdam: Millpress, ISBN: 978–90-5966-055-7

Aversa, S., Flora, A., Viggiani, C. 2012. Il ruolo della Geotecnica nella conservazione del patrimonio architettonico ed ambientale. In A. Aveta & B.G. Marino Eds: "Restauro e Riqualificazione del Centro storico di Napoli Patrimonio dell'Unesco tra Conservazione e Progetto. Edizoni Scientifiche Italiane, 159–169.

Aversa, S., Flora, A, Viggiani, C. 2012. Il sottosuolo della città di Napoli: pericolo o risorsa? A. Aveta & B.G. Marino Eds. "Restauro e Riqualificazione del Centro storico di Napoli Patrimonio dell'Unesco tra Conservazione e Progetto. Edizoni Scientifiche Italiane, 140–158.

Aversa, S. & Nicotera, M.V. 2013. On the effects of suction on the stability of ancient retaining walls. *Proc. 15th ECSMGM. Athens 2011*. Amsterdam: Mill Press (In press).

Aversa, S., Bilotta, E., Di Luccio, A., Russo, G. 2013. Settlement induced by TBM excavation under the Vittoria's Church in Napoli. *Proc. 2nd Inter. Symposium on Geotechnical Engineering for the preservation of Monuments and Historic Sites, TC301*, Naples 2013.

Beneduce, P., D'Elia, G., Guida, M. 1988. Morfodinamica dei versanti dell'area flegrea (Campania): erosione in massa ed erosione lineare. Mem. Soc. Geol. It., 41.

Brooks, R.H. & Corey, A.T. 1964. Hydraulic properties of porous media. *Hydrology Paper No.3*, Colorado State Univ., Fort Collins, Colorado.

Burland, J.B., Standing, J.R. 1997. Geotechnical monitoring of historic monuments. *Proc. of the Arrigo Croce Memorial Symposium—Geotechnical Engineering for the Preservation of Monuments and Historic Sites, Napoli, 1996., A.A*. Rotterdam: Balkema.

Calabresi, G., D'Agostino, S. 1997 Monuments and historic sites: Intervention techniques. *Proc. of the Arrigo Croce Memorial Symposium—Geotechnical Engineering for the Preservation of Monuments and Historic Sites, Napoli, 1996.,* A.A. Rotterdam: Balkema.

Calcaterra, D., Guarino, P.M. 1999. Dinamica morfologica e fenomeni franosi recenti nell'area collinare napoletana (settore occidentale). Geologia Tecnica ed Ambientale 2/99, Roma.

Calcaterra, D., de Luca Tuppini, F., Evangelista, A., Ruopolo, S., Scotto di Santolo, A. 2010. Modellazione di frane superficiali da scorrimento—colata ad innesco meteorico nei depositi piroclastici del cratere degli Astroni (Campi Flegrei). *Proc. 1st Italian Workshop on Landslides, Rainfall—Induced Landslides: Mechanisms, monitoring techniques and nowcasting models for early warning systems Naples, 8–10 June 2009*.

Campa, E., Ajmone, A.M., Fioretti, C., Mormone L. 2013. New undergrounds in historic centres: experiences in Naples. *Proc. 2nd Inter. Symposium on Geotechnical Engineering for the preservation of Monuments and Historic Sites, TC301*, Naples 2013 (in Press).

Candela, M. Viggiani, C. & Viparelli, R. 2013. The vineyard of the monastery of S. Martino in Napoli. *Proc. 2nd Inter. Symposium on Geotechnical Engineering for the preservation of Monuments and Historic Sites, TC301*, Naples 2013.

Croce, A. 1954. Sulla compressibilità delle pozzolane quali terreni di fondazione. *Geotecnica*, 1(1): 6–16.

Croce, A, 1985. Old monuments and cities. Research and preservation. Geotechnical Engineering in Italy—An overview—AGI Associazione Geotecnica Italiana, 1985.

Croce, A. & Pellegrino, A. 1967. Il sottosuolo della città di Napoli. Caratterizzazione geotecnica del territorio urbano. *Atti VIII Convegno Nazionale di Geotecnica, Cagliari, Vol. 3., pag. 165*.

de Gennaro, M., Coltella, C., Langella, A., Cappelletti, P. 1995. Decay of campanian ignimbrite stoneworks in some monuments of the Caserta area. *Science and Technology for Cultural Heritage*, 4 (2): 75–86.

de Gennaro, M., Incoronato, A., Mastrolorenzo, G., Adabbo, M. & Spina, G. 1999. Depositional mechanisms and alteration processes in different types of pyroclastic deposits from Campi Flegrei volcanic field (Southern Italy). *J. Volcanol. Geotherm. Res.*, 91: 303–320.

de Riso, R., Evangelista, A., Mazzoleni, S., Pellegrino, A. 2002. Stabilità delle coltri piroclastiche. *XXI Convegno di Geotecnica, L'Aquila, 143–156.* Bologna: Pàtron.

de' Seta, C. 1969. *Cartografia della città di Napoli. Lineamenti dell'evoluzione urbana*. Napoli: Edizioni Scientifiche Italiane.

Di Girolamo, P. 1968. Petrografia dei tufi campani: il processo di pipernizzazione. *Rendiconti dell'Accademia di*

Scienze Fisiche e Matematiche della Società Nazionale di Scienze, Lettere ed Arti in Napoli, serie 4, vol. 35.

Di Girolamo, P., Ghiara, M.R., Lirer, L., Munno, R., Rolandi, G. & Stanzione, D. 1984. Vulcanologia e Petrologia dei Campi Flegrei. *Boll. Soc. Geol. It*., 103: 349–413.

Di Stefano, R. 1967. Il sottosuolo di Napoli. Le gallerie sotterranee in rapporto allo sviluppo urbanistico nel tempo. *Atti VIII Convegno Nazionale di Geotecnica, Cagliari.*

Di Stefano, R. 1971. Lineamenti di storia urbanistica. In: *Il centro antico di Napoli* A.A.V.V. Napoli: Edizioni Scientifiche Italiane.

De Vivo, B., Rolandi, G., Gans, P.B., Calvert, A., Bohrson, B.A., Spera, F.J. & Belkin, H.E. 2001. New constraints on the pyroclastic eruptive history of the Campanian volcanic Plain (Italy). *Mineralogy and Petrology*, 73: 47–65.

Evangelista, A. 1980. Influenza del contenuto d'acqua sul comportamento del tufo giallo napoletano. *Atti del XIV Convegno Nazionale di Geotecnica, Firenze.*

Evangelista, A. & Pellegrino, A. 1986. Ripartizione delle tensioni tra scheletro solido ed acqua nel tufo giallo napoletano. *Atti del Convegno "Bradisismo e fenomeni connessi", Napoli, 1986*.

Evangelista, A., & Pellegrino, A. 1990. Caratteristiche geotecniche di alcune rocce tenere italiane. *Atti del terzo ciclo di Conferenze di Meccanica e Ingegneria delle Rocce MIR90, Torino*.

Evangelista, A. & Aversa, S. 1993. Experimental evidence of non-linear and creep behaviour of pyroclastic rocks. *Proc. of CISM Course on "Time dependent behaviour of geomaterials", CISM, Udine*. Springer-Verlag.

Evangelista, A., Lapegna, U., Pellegrino, A. 1980. Problemi geotecnici nella città di Napoli per la presenza di cavità nella formazione del Tufo. *Atti del XIV Convegno Nazionale di Geotecnica, Firenze*. Bologna: Pàtron.

Evangelista, A., Aversa, S., Pescatore, T.S. & Pinto, F. 2000. Soft rocks in southern Italy and role of volcanic tuffs in the urbanization of Naples. *Proc. of the II Int. Symp. on "The Geotechnics of Hard Soils and Soft Rocks", Napoli, Vol. 3: 1243–1267*. Rotterdam: Balkema.

Evangelista, A., Nocilla, N., Scotto di Santolo, A., Danzi, M., Viviano, D. 2002a. Sui fenomeni di instabilità nei costoni di Tufo Giallo Napoletano. *Atti del XXI Convegno Nazionale di Geotecnica, L'Aquila*, *11–14 settembre 2002, pp. 157–164,* ISBN 88 555 26634. Bologna: Pàtron Ed.

Evangelista, A., Nicotera, M.V., Scotto di Santolo, A., 2002b. Caratteristiche Geotecniche dei Terreni piroclastici della città di Napoli. *Atti del XXI Convegno Nazionale di Geotecnica, L'Aquila*, *11–14 settembre 2002, pp. 45–52*. Bologna: Pàtron Ed. ISBN 88 555 26634.

Evangelista, A., Flora, A., Lirer, L., de Sanctis, F. 2002c. Studi ed interventi per la tutela di un patrimonio sotterraneo: l'esempio delle cavità di Napoli. *Atti del XXI Convegno Nazionale di Geotecnica, L'Aquila*, *11–14 settembre 2002, pp. 579–588.* Bologna: Pàtron Ed. ISBN 88 555 26634.

Evangelista, A., Pellegrino, A., Perrella, A., Viggiani, C. (2002d) Un paradiso abitato da diavoli? I problemi geotecnici della città di Napoli. *XXI Convegno di Geotecnica, L'Aquila, 53–62*. Bologna: Pàtron.

Evangelista, A., Nocilla, N., Scotto di Santolo, A., Susani, A. 2003. Analysis of rockfall phenomena in soft and hard rocks. Proc. Intern. Conf. on Fast Slope Movements-Prediction and Prevention for Risk Mitigation, IC-FSM, Naples, May, 11–13, 2003, pp. 379–382. Bologna: Pàtron Ed. ISBN 88 555 2699 5.

Evangelista, A., Nocilla, N., Scotto di Santolo, A., Feola, A., Messineo, S. 2004. Sperimentazione ed osservazioni in sito sulla caduta massi dai costoni di Tufo Giallo Napoletano. *Atti XXII Convegno Nazionale di Geotecnica, Palermo*, *22–24 settembre 2004, pp. 99–106.* Bologna: Pàtron Ed. ISBN 88 555 2770 3.

Evangelista, A., Nocilla, N., Scotto di Santolo, A., 2006. *Sperimentazione e osservazioni in sito sulla caduta massi.* Questioni di Ingegneria Geotecnica – Hevelius Edizioni, febbraio 2006, pp 555–574 ISBN 88 86977 76X.

Evangelista, A., Nocilla, N., Scotto di Santolo, A. 2007. *Caratterizzazione meccanica dei tufi di Trentaremi, Napoli*. Memorie in ricordo di Renato Ribacchi, Roma 2007, pp. 99–108. Bologna: Pàtron.

Evangelista, A. & Viggiani, C. 2013. A paradise inhabited by devils? The geotechnical risks in the city of Napoli and their mitigation. *TC301 Exemplary case histories volume*. Rotterdam: CRC Press.

Feola, A., Lombardi, G., Pellegrino, A., Viggiani, C. 2004. I dissesti di via Settembrini a Napoli a seguito dell'evento piovoso del 15 settembre 2001. *Atti del XXII CNG, Palermo*, pp. 107–117. Bologna: Pàtron Ed.

Fredlund, D.G. & Rahardjo, H. 1993. *Soil mechanics for unsaturated soils*. Wiley & Sons, Toronto.

Jappelli, R. 1991. The Contribution of Geotechnical Engineering to the Preservation of Italian Historic Sites. *Associazione Geotecnica Italiana*.

Jappelli, R. 1997. An integrated approach to the safeguard of monuments: the contribution of Arrigo Croce. *Proc. of the Arrigo Croce Memorial Symposium—Geotechnical Engineering for the Preservation of Monuments and Historic Sites, Napoli*, 1996., A.A. Balkema, Rotterdam 1997.

Leroueil, S. & Vaughan, P.R. 1990. The general and congruent effects of the structure in natural soils and weak rocks. *Géotechnique*, Vol. 40 (3): 467–488.

Melisurgo, G. 1889. *Napoli Sotterranea*. Napoli: R. Tipografia F. Giannini e Figli, pp. 61.

Nicotera, M.V. 1998. Effetti del grado di saturazione sul comportamento meccanico di una pozzolana del napoletano. *PhD Thesis, Università di Napoli Federico II.*

Nicotera, M.V. 2000. Interpretation of shear response upon wetting of natural unsaturated pyroclastic soils. In Tarantino and Mancuso (eds.) *proc. int. workshop on Unsaturated Soils, Trento: 177–192.* Rotterdam: Balkema.

Nicotera, M.V. & Aversa, S. 1999. Un laboratorio per la caratterizzazione fisico—meccanica dei terreni piroclastici non saturi. In *proc. 20th Italian Geotechnical Conf.*, *Parma*: 200–212. Bologna: Pàtron.

Nicotera, M.V., Evangelista, A. & Aversa, S. 1999a. Determinazione della curva caratteristica e delle funzioni di permeabilità di una pozzolana non satura. In *proc. 20th Italian Geotechnical Conf., Parma*: 213–221. Bologna: Pàtron.

Nicotera, M.V., Evangelista, A. & Aversa, S. 1999b. Osservazioni sperimentali sulla risposta meccanica di una pozzolana in condizioni lontane dalla saturazi-

one. In *proc. 20th Italian Geotechnical Conf*., *Parma*: 222–230. Bologna: Pàtron.

Nocilla, N. & Urciuoli, G. 1997. *Stabilità dei pendii in roccia: Rilievi strutturali e spostamenti ammissibili*. Benevento: Hevelius.

Nocilla, N., Viviano, D., Aversa, S. 1999. Applicazione della fotogrammetria al rilievo strutturale di costoni rocciosi. In: *Atti del XX Convegno Nazionale di Geotecnica, Parma 1999, 231–238*. Bologna: Pàtron.

Nocilla, N., Evangelista, A., Scotto di Santolo, A., Susani, A. 2003. Analysis of rockfall phenomena in soft and hard rocks. In: *Picarelli L. (ed) Proc. of Int. Conf. on Fast Slope Mouvements Prediction and Prevention for Risk mitigation, Naples, May 11–13 2003, 379–382*. Bologna: Pàtron.

Nocilla, N., Evangelista, A., Scotto di Santolo, A. 2009. Fragmentation during rock falls: two Italian case studies for hard and soft rocks. *Int. Journal of Rock Mechanics and Rock Engineering: Volume 42, Issue 5*, Page 815.

Orsi, G., de Vita, S. & Di Vito, M. 1996. The restless, resurgent Campi Flegrei nested caldera (Italy): constraints on its evolution and configuration. *J. Volcanol. Geotherm. Res*., 74: 179–214.

Palladio, A. 1570. I *quattro libri di Architettura*.

Papa, R. 2007. Indagine sperimentale sulla Coltre piroclastica di un versante della Campania. *PhD Thesis, Università di Napoli Federico II*.

Papa, R., Evangelista, A. Nicotera, M.V. Urciuoli, G. 2008. Mechanical properties of unsaturated pyroclastic soils affected by fast landslide phenomena Proc. 1st European Conference on Unsaturated Soils, E-UNSAT 2008, pp. 917–923.

Pellegrino, A. 1967. *Proprietà fisico-meccaniche dei terreni vulcanici del napoletano.* Atti del VIII Convegno Nazionale di Geotecnica, Cagliari.

Pellegrino, A. 1968. *Compressibilità e resistenza a rottura del Tufo Giallo Napoletano*. Atti del IX Convegno Nazionale di Geotecnica-Genova.

Pellegrino, A. 1970a. *Le rocce lapidee tenere.* Ricerche in corso: risultati e linee di sviluppo del Gruppo di ricerche Terreni e Strutture del CNR, Napoli.

Pellegrino, A. 1970b. *Mechanical behaviour of Soft Rocks under high stresses.* Proc. of the 2nd. Congress of the Int. Soc. for Rock Mech., Vol. 3–25, Belgrade, 1970.

Pellegrino, A. 1974. *Surface footings on Soft Rocks.* Proc. of the Third Congress of the International Society of rock Mechanics, Denver.

Pellegrino, A. 1994. *I Fenomeni Franosi nell'area Metropolitana Napoletana.* Acta Nepolitana, Napoli: Guida Ed, 18, 237–25.

Pellegrino, A. 2002. Dissesti idrogeologici nel sottosuolo della città di Napoli; analisi e interventi. *XXI Convegno di Geotecnica, L'Aquila, vol. II, 326–346*. Bologna: Pàtron.

Penta, F., Croce A., Esu, F. 1961. Engineering properties of volcanic soils. *Proc. V Int. Conf. Soil Mech. Found. Eng.* Paris.

Picarelli, L., Evangelista, A., Rolandi, G., Paone, A., Nicotera, M.V., Olivares, L., Scotto di Santolo, A., Lampitiello, S., Rolandi, M. 2006. *Mechanical properties of pyroclastic soils in Campania Region.* Proc. Int. Workshop on Characterisation & Engineering Properties of Natural Soils November- 1 December 2006, pp. 2331–2383, ISBN 978–0-415–47692–8. London: Taylor & Francis Group plc.

Rosi, F. 1963. *Le mani sulla città*.

Scotto di Santolo, A. 2000a. Analisi geotecnica dei fenomeni franosi nelle coltri piroclastiche della Provincia di Napoli. *Ph. D. Thesis, Università di Napoli Federico II.*

Scotto di Santolo, A. 2000b. Analysis of a steep slope in unsaturated pyroclastic soils. *Asian Conference on Unsaturated Soils, UNSAT-ASIA2000/ Singapore, 18–19 May 2000, p. 569–574*. Rotterdam: Balkema.

Scotto di Santolo, A. 2002. *Le colate rapide*. pp. 119. Benevento: Hevelius.

Scotto di Santolo, A., Nicotera, M.V., Ramondini M. 2000a. Analysis of instability phenomena affecting a cut slope in unsaturated pyroclastic soils. *8th Inter. Symposium on Landslides, Cardiff, 26–30 June 2000, pp. 1353–1360.* London: Thomas Telford. ISBN 0 7277 2872 5.

Scotto di Santolo, A., Nicotera, M.V., Evangelista, A., Pellegrino, A., Ramondini, M., Urciuoli, G. 2000b. Some remarks on the shear strength of neapolitan pyroclastic deposits. *Inter. Conference on Geotechnical Engineering GeoEng 2000, Melbourne*.

Scotto di Santolo, A. & Evangelista A. 2000. Mechanical behaviour of unsaturated pyroclastic soil. Proc. *Int. Conference on Landslides: Causes, Impacts and Countermeasures, Davos 17–21 June 2001,* pp. 35–44, UEF, VGE Verlag Glückauf Essen, ISBN 3–7739–5969–9.

Scotto di Santolo, A., Evangelista, A. & Nicotera, M.V. 2005. Monitoring matric suction profiles into partially saturated pyroclastic topsoil slope. In *Advanced Experimental Unsaturated Soil Mechanics, EXPERUS 2005, proc. int. symp., Trento*: 533–539. Rotterdam: Balkema.

Scotto di Santolo, A. & Evangelista, A. 2011. Matric suction in unsaturated pyroclastic slopes. *Proc. of Fifth International Conference on Unsaturated Soils UNSAT 2010, Barcelona, Spain, September* 6–8, 2010, 1285–1290.

Scotto di Santolo, A., Pellegrino, A.M., Evangelista A., Coussot, P. 2012. Rheological behaviour of reconstituted pyroclastic debris flow. *Géotechnique* 62, No. 1, 19–27.

Scotto di Santolo, A., Evangelista, L., Evangelista, A. 2012. Influence of suction on the behaviour of retaining walls in the city of Naples, Italy. *Proc. E-Unsat, Naples 20–22 June 2012, pp. 275–282,* ISBN 978–3-642-31342–4.

Scotto di Santolo, A., Evangelista, L., Evangelista, A. 2013. The Fontanelle Cemetery: between legend and reality. *Proc. 2nd Inter. Symposium on Geotechnical Engineering for the preservation of Monuments and Historic Sites, TC301*, Naples 2013.

Scotto di Santolo, A., Evangelista, L., Evangelista, A., 2013 Retaining walls of unsaturated pyroclastic soil: comparison between observation and theoretical results. *Submitted to int. journal.*

Sica, S., Ceroni, F., Pecce, M.R. 2013. Soil structure interaction on the dynamic behavior of two historic masonry structures. *Proc. 2nd Inter. Symposium on Geotechnical Engineering for the preservation of Monuments and Historic Sites, TC301*, Naples 2013.

This page intentionally left blank

Geotechnical Engineering for the Preservation of Monuments and Historic Sites – Bilotta, Flora, Lirer & Viggiani (eds)
© 2013 Taylor & Francis Group, London, ISBN 978-1-138-00055-1

Local site conditions and seismic risk assessment of historic buildings

D. D'Ayala
University College London, London, UK

A. Ansal
Ozyegin University, Istanbul, Turkey

ABSTRACT: The objectives of the Istanbul Seismic Risk Mitigation and Emergency Preparedness Project are to improve Istanbul's preparedness for a potential earthquake. Within this framework "Risk Assessment of Cultural Heritage Buildings" was designed to address the vulnerability of cultural assets, specifically buildings with global cultural heritage value. One of the components of the project was the vulnerability and risk assessment of 170 historic buildings of varied age, value and state of conservation, distributed over several square miles. Many of these buildings have public functions such as museums or education establishments. Among the most famous are Topkapı Palace and Hagia Irene museum. After a discussion of the choice of the most appropriate earthquake scenario, the methodology used for assessing the effects of local site conditions on the seismic performance of selected cultural heritage buildings is presented. The purpose is to estimate the earthquake characteristics on the ground surface based on the probabilistic and deterministic hazard studies. The site specific elastic design spectra for each site are then manipulated to obtain site specific nonlinear displacement spectra, so that these can be directly compared with capacity curves for the buildings obtained by using mechanism approach limit state analysis. The procedure for obtaining the capacity curves is described and the choice of the most appropriate level of ductility and the equivalent reduction coefficient are discussed. A procedure to evaluate performance points and to define safety factors based on lateral acceleration, drift or expected damage level, is presented. The process of arriving at a risk evaluation and hence recommendation for strengthening or otherwise, is finally highlighted with respect to four comparable case studies.

1 INTRODUCTION

Historic buildings in countries boarding the Mediterranean basin span several centuries, styles and cultures, from pre-historic settlements to Persian, Greek and Roman urban developments to the Christians and Muslim eras, up to the Renaissance and Baroque period.

While the architectural typologies and styles differ substantially, the construction materials and associated structural principles remain substantially the same. Within the architectural heritage classes of buildings can be defined, which have homogeneous morphology, materials, values and use and that suffer similar damage in the event of an earthquake and for a given seismic intensity.

The concept that an existing building should be assessed and upgraded using different parameters from the design of new buildings is nowadays recognised also for ordinary structures in a number of national and international seismic codes, such as Eurocode 8 part 3 (2005), or the ASCE 41-06(2007). In Italy, given the large number of historic buildings at risk of seismic damage and the need to keep them in use, the concept of improvement rather than upgrading has been introduced with a Directive PCM 12/10/2007 (2007). This document also introduces the concepts, already present in the EC8-3, of level of knowledge and level of use in relation to the type of analysis to be carried out and the level of hazard to be considered. Moreover the level of hazard is also a function of the performance requirement for the asset.

This approach was chosen as the framework within which to carry out the seismic risk assessment of a large number of historic buildings in Istanbul, Turkey, in the care of the Ministry of Culture and Tourism.

Studies on the seismic vulnerability of the urban fabric of historic centres have been developed in the past fifteen years for many European and other city centres, but these studies usually relate to residential and ordinary historic buildings. Given the large number of them usually in any given centre, vulnerability and fragility assessment can rely on statistical approach, by defining a few common typologies (D'Ayala et al., 1997, D'Ayala, 2004, Lang & Bachmann, 2004).

The ISMEP project however presented a specific challenge, as the number of buildings to be considered is relatively large, close to 200, while due to the nature of the sample is very difficult to identify common typologies and generalize behaviours within it, reducing the analysis to the choice of a small number of parameters. At the same time given the time frame of the project and its resources was unconceivable to run specific level 3 or above vulnerability assessment analysis for each of the buildings, i.e. collecting sufficient information to conduct nonlinear finite element push-over or time-histories analysis. It was therefore decided to carry out a quantitative assessment using a numerical approach based on failure mechanisms and limit state analysis, called FaMIVE, whose robustness and reliability has already been proven in past studies for more homogeneous samples of historic masonry buildings (D'Ayala, Speranza 2003). Hence the procedure adopted is:

- Define soil profile and shearwave velocity profile down to bedrock (750 m/s) for all building sites;
- Evaluate regional seismic hazard for 475y return period using as intensity measure (IM) PGA and spectral acceleration at T = 0.2, 1 sec at bedrock;
- Choose a selection of spectra compatible acceleration time histories and scale them to provide target NEHRP equivalent bedrock spectrum;
- Use 1D equivalent linear model and a selection of compatible acceleration time histories to determine site response as free-field surface NEHRP equivalent elastic spectrum;
- Define building response in terms of most likely collapse mechanism with associated ultimate capacity load factor;
- Represent collapsing portion as equivalent SDOF nonlinear oscillator, identifying T, μ, R;
- Define tri-linear capacity curve for each collapsing portion and identify damage thresholds on it;
- Manipulate elastic spectrum using N2 method to obtain equivalent nonlinear spectrum for given ductility and reduction factor for each building on site;
- Compute performance points and define damage state;
- Compute safety factors and define level of risk.

This procedure is explained in details in the following section and illustrated in relation to four different building sites.

2 SITE RESPONSE ANALYSIS

Local geological and geotechnical site conditions were evaluated using all the available and relevant information and representative soil profiles with shear wave velocity profiles extending down to the engineering bedrock with estimated shear wave velocity of 750 m/s are determined for all building sites. The variation of shear wave velocity with depth was determined from SPT-N blow counts using an empirical relationship proposed by Iyisan (1996) as well as based on in-hole and surface shear wave velocity measurements conducted in the vicinity of the borings. The shear wave velocity profiles determined from SPT values were compared with measured or calculated shear wave velocity data reported in available geophysical reports and modifications were made if necessary.

Site specific response analyses were carried out at each building site using these representative soil profiles and regional seismic hazard parameters. Regional seismic hazard was evaluated using deterministic as well as probabilistic time dependent Poisson model for the return period of 475 years that corresponds approximately to 10% probability of exceedance in 50 years by Erdik et al. (2007). Seismic hazard parameters in terms of PGA and spectral accelerations at periods T = 0.2 s and T = 1 s on the engineering bedrock outcrop were assigned at each site. 1D equivalent-linear model site response code Shake91 (Idriss and Sun, 1991) was used to conduct site response analyses.

2.1 *Earthquake input*

Twenty four acceleration time histories compatible with the earthquake hazard in terms of probable magnitude, distance and fault mechanism were selected as the input rock outcrop motion (Ansal and Tönük, 2007). The main purpose was to account for the variability arising from the differences observed in the real acceleration time histories (Table 1).

2.2 *Input motion scaling*

The seismic hazard compatible input motions listed in Table 1 are used for site response analysis for each location. However, the selected set of acceleration time histories are scaled with respect NEHRP design spectrum specified at each location by Erdik et al (2007) to be used for 1D site response analyses.

In this procedure strong motion acceleration are modified to have better outcrop NEHRP hazard spectra compatibility by using a simple optimization scheme based on PGA scaling to have the best fit of the mean acceleration spectrum with respect to the target outcrop NEHRP hazard spectra.

Table 1. Acceleration time histories that were used for site response analysis (from PEER data bank).

Earthquake	Station	Mw	Comp.	PGA(g)
Duzce 11/12/99	375 Lamont	7.1	375E	0.514
Duzce 11/12/99	375 Lamont	7.1	375N	0.970
Duzce 11/12/99	531 Lamont	7.1	531E	0.118
Duzce 11/12/99	531 Lamont	7.1	531N	0.159
Duzce 11/12/99	1059 Lamont	7.1	1059E	0.133
Duzce 11/12/99	1059 Lamont	7.1	1059N	0.147
Duzce 11/12/99	1061 Lamont	7.1	1061E	0.134
Duzce 11/12/99	1061 Lamont	7.1	1061N	0.107
Duzce 11/12/99	1062 Lamont	7.1	1062E	0.254
Duzce 11/12/99	1062 Lamont	7.1	1062N	0.114
Duzce 11/12/99	Bolu	7.1	BOL000	0.728
Duzce 11/12/99	Bolu	7.1	BOL090	0.822
Kocaeli 8/17/99	Arçelik	7.4	ARC000	0.219
Kocaeli 8/17/99	Arçelik	7.4	ARC090	0.150
Kocaeli 8/17/99	Gebze	7.4	GBZ000	0.244
Kocaeli 8/17/99	Gebze	7.4	GBZ270	0.137
Kocaeli 8/17/99	Duzce	7.4	DZC180	0.312
Kocaeli 8/17/99	Duzce	7.4	DZC270	0.358
Imp.Val. 5/19/40	El Centro #9,	7.0	I-ELC180	0.313
Imp.Val. 5/19/40	El Centro #9,	7.0	I-ELC180	0.215
Landers 6/28/92	Morango Valley	7.3	MVH090	0.182
Landers 6/28/92	Morango Valley	7.3	MVH000	0.138
Landers 6/28/92	Joshua Tree	7.3	JOS000	0.274
Landers 6/28/92	Joshua Tree	7.3	JOS090	0.284

3 BUILDING RESPONSE ANALYSIS

The first step in any analytical vulnerability assessment is to categorise the buildings by structural system, construction material, but also layout, typology and period of construction.

It is difficult to reduce the ISMEP sample to only few typologies as they vary greatly by all criteria identified above.

For instance one typological class is formed by the five Byzantine churches included in the sample. While they have similar construction layout and materials, their scale range from the few meters of the Fethiye museum to the 43 meter diameter dome of Hagia Sophia. One other typology class can be identified by the Ottoman libraries such as Atif Efendi, Ragip Pasha, Semsy Pasha Library and Beyazit Library. Some of the other buildings included in the assessment were more complex, such as Topkapi Palace or had different structural configurations, such as the relative large numbers of 19th century buildings. Some of the buildings also had a prevalent timber structure loadbearing system and were not anlaysed with this approach.

To increase the complexity of the study is the issue that a large proportion of the building analysed had floors and roof made of masonry vaulted structures. This was taken into account by computing the thrust transferred by the vault to the vertical structures both for gravity and lateral loads, and assessing their likelihood of collapse by using a limit state based numerical procedure, VULVAULT (see ISMEP 2008, D'Ayala & Ansal 2012).

The FaMIVE procedure is based on the lower bound approach of limit state analysis and identifies all possible mechanisms that can occur for an elevation in a building given its connections to other elevations and horizontal structures and the layout of openings (D'Ayala & Speranza, 2003). Among all possible mechanisms for each wall the one that has the worst combination of load factor and damage extension, is considered as defining the vulnerability of the wall.

The fundamental assumption is that the seismic capacity of masonry walls is highly reliant on the possibility of considering post elastic behaviour, and specifically extensive cracking under relatively stable loading conditions (D'Ayala 2005). The frictional model introduced to describe the structural behaviour, at the basis of both FaMIVE and VULVAULT, indeed assumes that any mechanism is stable until the "plastic hinges" needed to define the mechanism are fully developed, i.e for in plane mechanisms, for instance, failure will not occur until the width of the crack is greater than the staggering of the units. This allows considering capacity curves for each wall which are characterised by post peak behaviour. From a mechanical point of view the collapse load factor as calculated in FaMIVE and assumed as the ultimte acceleration capacity of the wall, corresponds to the inception of collapse and hence to a condition of "repairable damage", characterised by damage to nonstructural and structural elements, depending on the type of structural typology and the mechanisms considered.

The ultimate capacity can be measured in three ways: a) as ratio of nonlinear acceleration demand obtained from a NEHRP-like (National Earthquake Hazard Reduction Program) spectrum against acceleration capacity measured as the collapse load factor; b) as a comparison between capacity and demand in spectral displacement terms by checking the performance point on the nonlinear displacement spectrum obtained starting with the NHERP equivalent spectrum (Ansal et al. 2006) and using the procedure outlined in D'Ayala (2005) and the N2 procedure (Fajfar, 2000) to derive the non-linear displacement spectra; c) in terms of damage grades and corresponding damage states, using for instance the damage scale proposed in EMS '98 (Grünthal, 1998). For

the analytical details of the procedure the reader is referred to D'Ayala & Ansal (2012).

However the calculation of safety factor in terms of lateral acceleration does not completely depict the behaviour of the façades or building, as it does not take into account the associated demand in terms of displacement, whether this displacement occurs in the elastic range of behaviour of the buildings or it is associated with cracking, and hence the corresponding level of damage reached. For a given level of lateral ultimate capacity, lateral displacement and level of damage will be dependent on the partialised stiffness of the walls and their ultimate displacement D_u dependent on construction details.

In order to compare behaviour for different walls and buildings in terms of lateral displacement, a drift is defined as the ratio of the performance point displacement over the height of the façade.

Given the fact that buildings, given their monumental character, might have large heights over single storeys, a drift defined as roof displacement over total height appear to be the most representative measure.

The expected damage is defined in terms of % of ultimate displacement. For simplicity, if the capacity curve meets the spectral curve for a value smaller or equal than the limit elastic displacement, it is assumed that the damage will be non-structural, corresponding to level D2 or the limit state of damage limitation DL, if the performance point is between this limit and 50% of the ultimate displacement, the damage level is D3, or past the threshold of significant damage if it is between 50% and 75% the damage level is D4, or Near Collapse, if greater D5. The corresponding classes of limit drift assumed are respectively smaller that 0.3%, between 0.3% and 0.6%, between 0.6% and 1.2%, or greater. Correlating damage and drift allows drawing comparison with other classes of building evaluated with other procedures using only a damage criterion.

As it can be seen in Figure 2, the classes so defined correspond well in terms of sample percentage, not just between damage level and drift, but also between these two and the corresponding acceleration capacity classes. These values have been obtained using throughout a ductility factor of 2.5 and a corresponding maximum reduction factor R_{max} = 2.5. In reality the ductility of some of the façades can be greater, so the value chosen represent a minimum threshold rather than an upper limit.

The results show that under these conditions 30% of the sample has a capacity comprised between 0.08 and 0.15, a required drift greater than 1.2% and damage state near collapse or greater is expected for the earthquake scenario chosen. Buildings to suffer non-structural damage are 10% of the sample, while building suffering significant damage to near collapse or greater are 33% and 30% respectively.

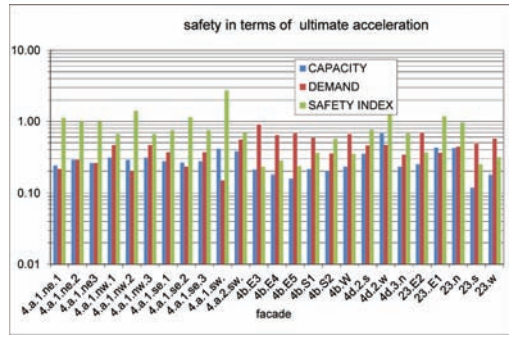

Figure 1. Building response in terms of ultimate lateral capacity and safety factor.

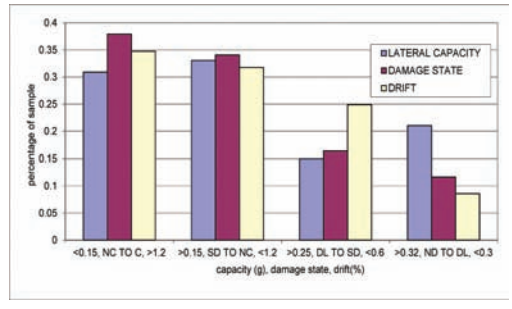

Figure 2. Comparison of force capacity, damage level and drift in relation to damage states.

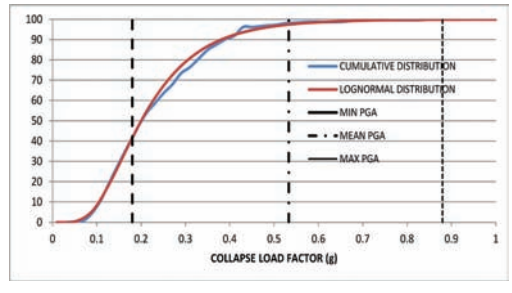

Figure 3. Cumulative distribution for ultimate acceleration and range of values of PGA at the sites.

The cumulative distribution for the ultimate capacity and drift for significant damage are compared with the corresponding normal distribution in Figures 3 and 4, respectively. It can be seen that in both cases the lognormal distribution represent a good fit of the actual data.

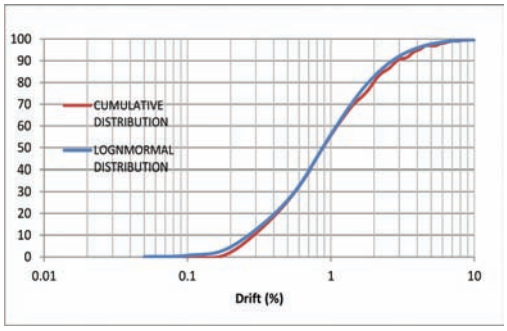

Figure 4. Cumulative distribution for drift at significant damage.

Figure 5. Kariye Museum (ISMEP, 2007).

4 KARIYE MUSEUM

One of the historical heritage buildings investigated was the Kariye Museum located on the north part of the Istanbul historical peninsula very near to the outer city walls of that period. The Kariye Museum was constructed as a church during sixth century. The main building is dated to 11th century. Second church, inner and outer narthexes, parecclesion and northern annex are dated 14th century. To structurally strengthen the bema section an abutment was placed on 14th century. The church was converted into a mosque on 15th century and later to museum.

After 1766 earthquake extensive repairs have been undertaken, including the replacement of the brick dome of naos with a timber dome. According Oztin (1994) the minaret of the museum partially collapsed and some cracking was observed in different parts of the museum during the 1894 earthquake.

Based on the available borings in the vicinity of the investigation area (app. 150 m), the representative soil profile consists of approximately 9 m of sandy clay overlying 7.5 m of sandy layers, upper 3 m of which is sand with clay, underlain by 1.5 m of sandstone and the lower 3 m is with sand (Figure 6).

The profile enters a layer of clay with sand starting from 16.5 m and continues until 30 m depth. Beneath clay layer claystone is encountered that was assumed as the engineering bedrock. Ground water table is at 5 m below the ground surface. The site is located on the Güngören Formation (Ansal et al, 2007).

Shear wave velocities in the transitional clayey and sandy soil layers over claystone vary between 254–550 m/s. Equivalent shear wave velocity was estimated as 405 m/s. The NEHRP site classification is class C, described as stiff soils. The spectra of all scaled strong motion records and the mean

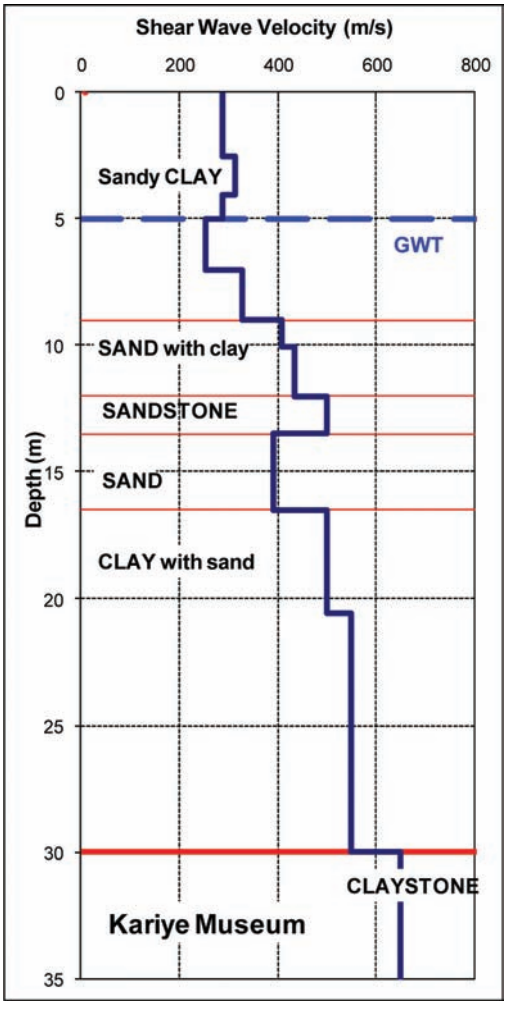

Figure 6. Soil profile for Kariye Museum.

spectrum with respect to outcrop hazard spectrum are shown in Figures 7 for Kariye Museum.

The average PGA on the ground surface was calculated as 0.34 g for the probabilistic earthquake scenarios. The acceleration response spectra obtained on the ground surface from site response analysis for all of the input motions, the average of these spectra and the best fit envelope NEHRP spectrum on the average are shown in Figure 8.

In Figure 9 the capacity curves obtained with the FaMIVE procedure are shown together with the nonlinear spectrum obtained for a value of ductility of 2.5 and the corresponding performance points.

It can be seen that the 3 elevation would be at diverse level of damage for the corresponding spectral displacement, with elevation 4d3.n identified as the most vulnerable. However given that this façade is supporting the presbiterium of the building but not the main space and dome, its failure might be considered as local, and hence the overall capacity of the complex can be related to the other 2 façades.

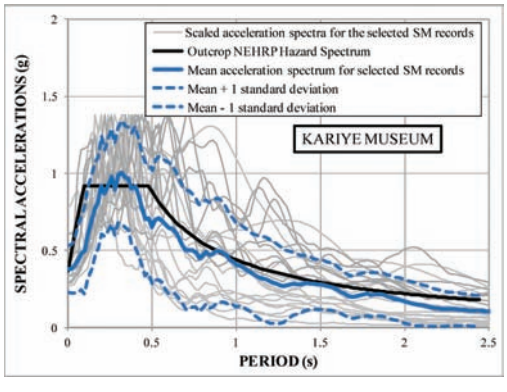

Figure 7. Acceleration spectra of for input acceleration records obtained for best fit mean spectra for Kariye Museum.

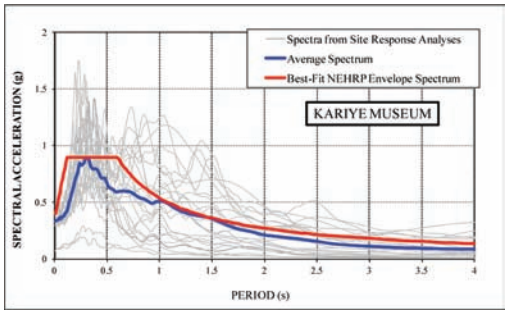

Figure 8. Acceleration response spectra on the ground surface based on site response analysis for Kariye Museum.

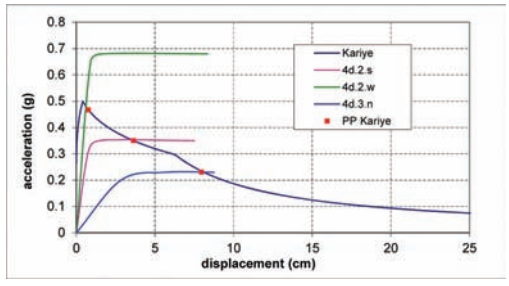

Figure 9. Capacity curves and performance points for 3 elevations of Kariye museum.

5 SEMSI PASA LIBRARY

Semsi Ahmet Pasha had Mimar Sinan build Semsi Pasha Madrasa which consists of mosque, tomb, and Ottoman elementary-primary school and forms some part of Semsi Pasha Complex in 1580.

The madrasa was damaged in the earthquake of 1894 with Semsi Pasha Complex and restored by Sureyya Yucel, the architect of Istanbul Head Management of Foundations, in 1940. The Madrasa has been used as Semsi Pasha Public Library since 1953 (Figure 10).

Based on the available borings in the vicinity of the investigation area (app. 450 m), the representative soil profile consists of approximately 3.5 m of artificial fill overlying 3 m deep sandy gravel layer. Claystone-Siltstone layers are encountered at 29.5 m depth and were assumed as the engineering bedrock. Ground water table is at 1.2 m below the ground surface. The surface gravel layers are part of Güngören Formation where greywacke layers encountered deeper belong to Trakya Formation.

Shear wave velocities in the artificial fill and gravel layer vary between 130–550 m/s. Equivalent shear wave velocity (weighted average for the uppermost 30 m from the ground) was estimated as 272 m/s. The NEHRP site classification is class D, described as stiff soils Figure 11). The spectra of all scaled strong motion records and the mean spectrum with respect to outcrop hazard spectrum are shown in Figure 12 for Semsi Pasa Library.

The average PGA on the ground surface was calculated as 0.47 g for the probabilistic earthquake scenarios. The acceleration response spectra obtained on the ground surface from site response analysis for all of the input motions, the average

Figure 10. Şemsi Paşa Library (ISMEP, 2007).

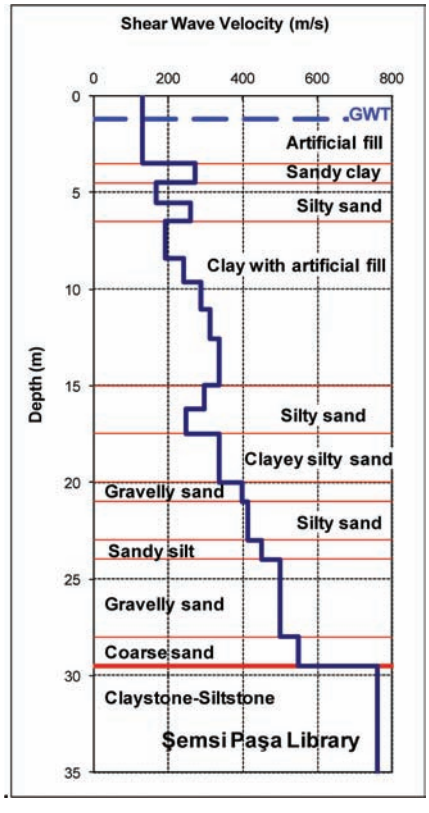

Figure 11. Soil profile for Semsi Pasa Library.

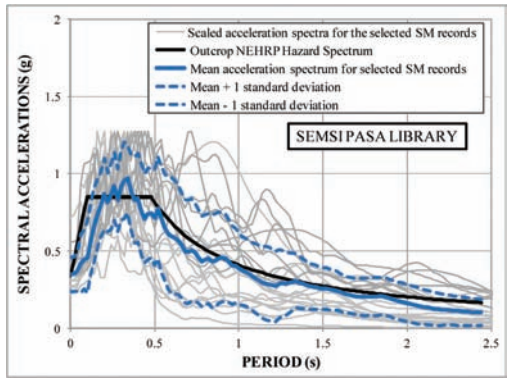

Figure 12. Acceleration spectra of for input acceleration records obtained for best fit mean spectra for Semsi Pasa Library.

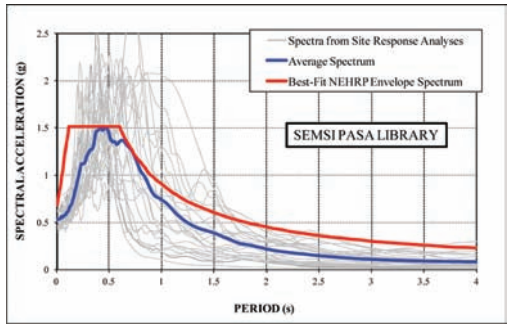

Figure 13. Acceleration response spectra on the ground surface based on site response analysis for Semsi Pasa Library.

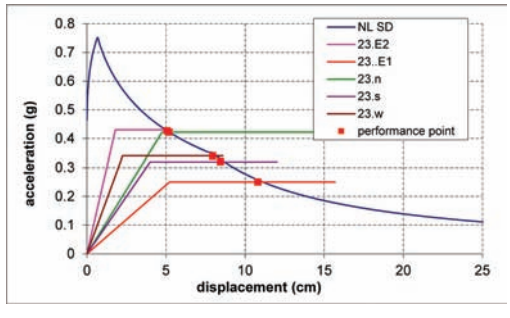

Figure 14. Capacity curves and performance points for 3 elevations of Semsi Pasa Library.

of these spectra and the best fit envelope NEHRP spectrum on the average are shown in Figure 13.

Figure 14 shows the capacity curves and corresponding performance points for Semsi Pasa Library. Range of ultimate capacity and displacement are more homogeneous than in the case of Kariye Museum with a maximum capacity just about 0.4 g and a maximum displacement at NC of 15 cm relating to the maximum overlapping of stones. The performance points are very close and hence the vulnerability of the building as a whole is well represented by the average vulnerability of its facades.

6 FETIYE MUSEUM

The building located in Yedikule is one of the oldest buildings of Byzantine in Istanbul. It was built in the 5th century, Byzantine miniature depicting the Stoudios Monastery and the Propontis (Sea of Marmara). Saint John the Forerunner at Stoudios, often shortened to Stoudios or Stoudion (Latin: Studium), was historically the most important monastery of Constantinople (modern-day Istanbul), the capital of the Eastern Roman Empire.

After Istanbul was conquered, the building was converted into mosque by İlyas Bey in 1486.

The building suffered considerable earthquake damages from earthquakes and fires occurred in various periods and the roof of the building was demolished in 1908, and as it was not repaired the building has come to the present time with its today's appearance (Figure 15).

Based on the available borings in the vicinity of the investigation area (app. 200 m), the representative soil profile consists of 5.5 m of artificial fill overlying on approximately 30 m thick soil layers where limestone, clay, clayey sand, clay stone, clay with gravel and clay layers are encountered with depth for which the thickness of layers vary between 2 m and 8.5 m. Greywacke layers are encountered starting from 45 m depth and was assumed as the engineering bedrock. Ground water table is at 10 m below the ground surface. The site is located on the Güngören Formation underlain by Trakya Formation. Shear wave velocities in the artificial fill and transitional clayey and sandy surface layers vary between 151–450 m/s. Equivalent shear wave velocity (weighted average for the uppermost 30 m from the ground) was estimated as 277 m/s. The NEHRP site classification is class D, described as stiff soils (Figure 16). The spectra of all scaled strong motion records and the mean spectrum with respect to outcrop hazard spectrum are shown in Figure 17 for Fetiye Museum.

The average PGA on the ground surface was calculated as 0.73 g for the probabilistic earthquake scenarios. The acceleration response spectra obtained on the ground surface from site response analysis for all of the input motions, the average of these spectra and the best fit envelope NEHRP spectrum on the average are shown in Figure 18.

Figure 15. Fetiye Museum (ISMEP, 2007).

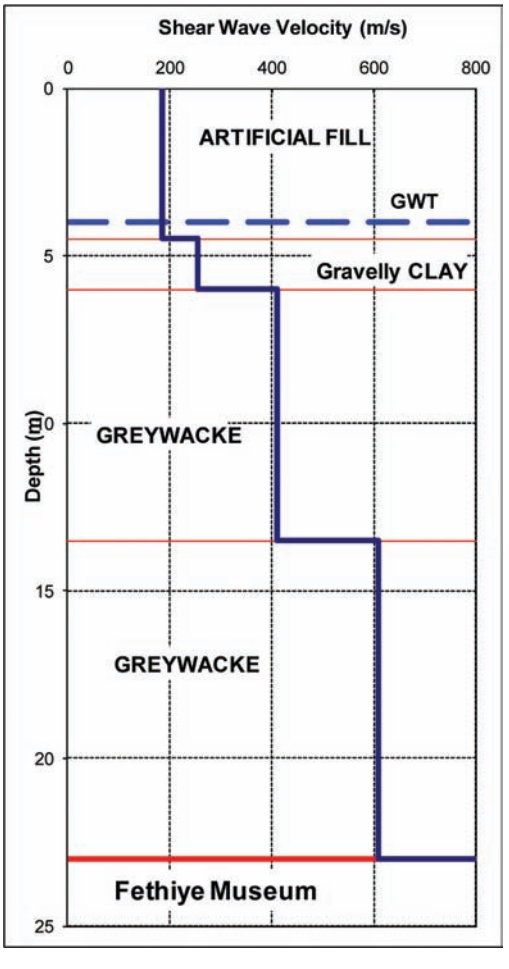

Figure 16. Soil profile for Fetiye Museum.

Fetiye museum results as the most at risk of the four buildings presented here. Indeed the local amplification is the highest while the capacity of the building is among the lowest with no single elevation achieving a lateral capacity greater than 0.25 g.

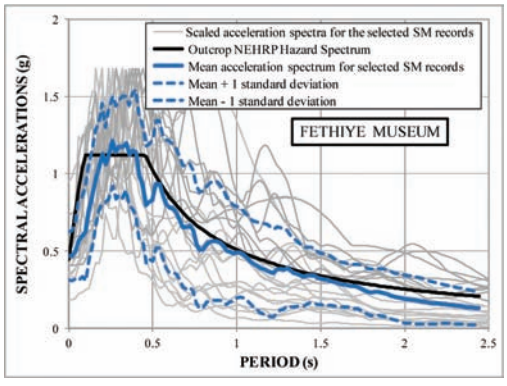

Figure 17. Acceleration spectra of for input acceleration records obtained for best fit mean spectra for fetiye museum.

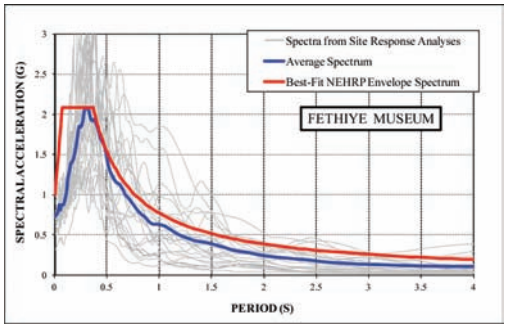

Figure 18. Acceleration response spectra on the ground surface based on site response analysis for Imrahor Monument.

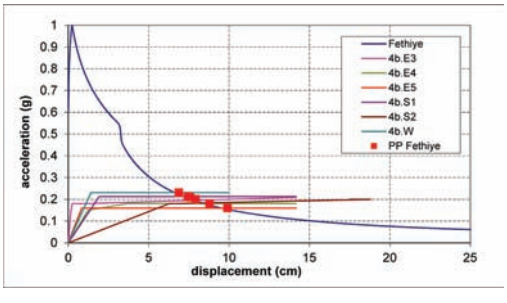

Figure 19. Capacity curves and performance points for 3 elevations of Fetiye Museum.

The facades are comparatively less rigid than the other buildings and have good margin of displacement. The position of the performance points indicates that the condition would be of very serious structural damage and nearing collapse.

7 ST. IRENE MUSEUM

This church is one of the earliest Christian buildings of Istanbul. It is located in the enclosure of the Topkapi Palace. The church was founded by the emperor Constantine in the year of 330 on the site of the temple of Aphrodite. In 532 the church was completely destroyed by a fire, and was rebuilt by Justinian. Although the Emperor Justinian had the St. Irene restored, it suffered significant damages in fires and earthquakes in later years. Fortunately, the church was renewed each time it was damaged, and, after the conquering of Istanbul, for a long period, the St. Irene was used as a weapons depot, and finally, in 1869, it was converted into a museum. It became the first museum in the Ottoman Empire, and has been used as such for quite a long time. Furthermore, it is the only church surviving today with an atrium. Due to its extraordinary acoustics, it often plays host to a variety of concerts and cultural/artistic events.

Based on the available borings in the vicinity of the investigation area (app. 200 m), the representative soil profile consists of approximately 4.5 m of artificial fill overlying 6 m thick gravel layer. Beneath the weathered portion, the greywacke layers were assumed as the engineering bedrock located at 17 m depth. Ground water table is at 5 m below the ground surface. The greywacke layers belong to the Trakya Formation.

Shear wave velocities in the artificial fill and gravel layer vary between 160–650 m/s.

Figure 20. St. Irene Museum (ISMEP, 2007).

Equivalent shear wave velocity (weighted average for the uppermost 30 m from the ground) was estimated as 498 m/s. The NEHRP site classification is class C, described as very dense soil and soft rock (Figure 21).

The spectra of all scaled strong motion records and the mean spectrum with respect to outcrop hazard spectrum are shown in Figure 22 for St. Irene Museum.

The average PGA on the ground surface was calculated as 0.59 g for the probabilistic earthquake scenarios. The acceleration response spectra obtained on the ground surface from site response analysis for all of the input motions, the average of these spectra and the best fit envelope NEHRP spectrum on the average are shown in Figure 23.

The capacity curves for the facades of Irene Museum are shown in Figure 24. There is one elevation which has very modest lateral capacity and very little ductility. Some of the facades given their height and substantial thickness can accommodate rather large displacement and they are relatively flexible given their slenderness. However there are also some elevation with a good lateral capacity

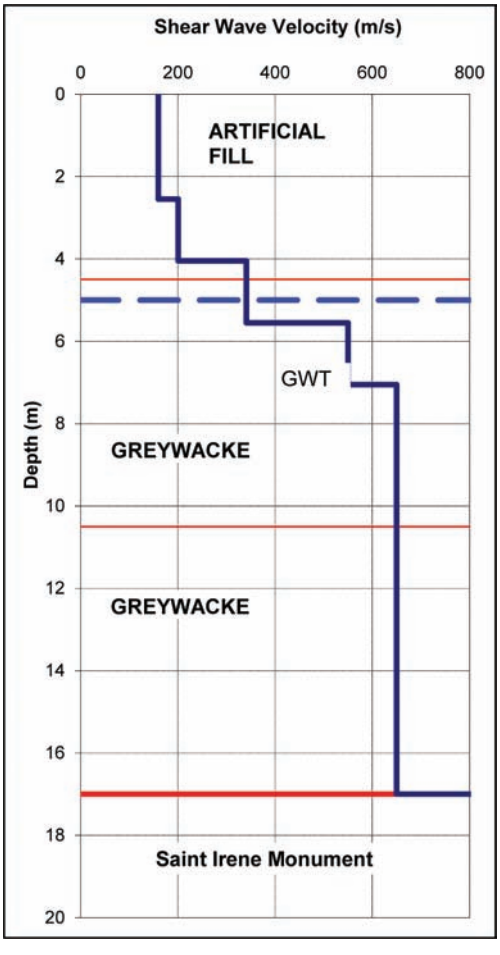

Figure 21. Soil profile for St. Irene Museum.

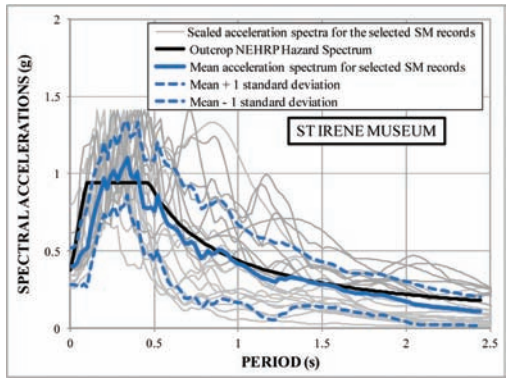

Figure 22. Acceleration spectra of for input acceleration records obtained for best fit mean spectra for St. Irene Museum.

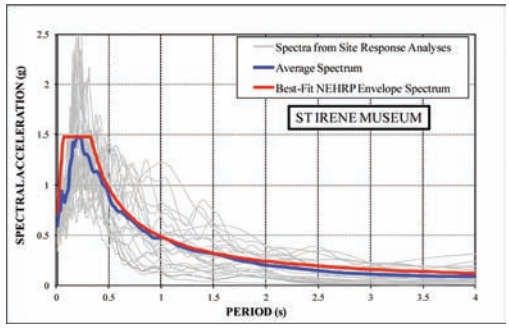

Figure 23. Acceleration response spectra on the ground surface based on site response analysis for St. Irene Museum.

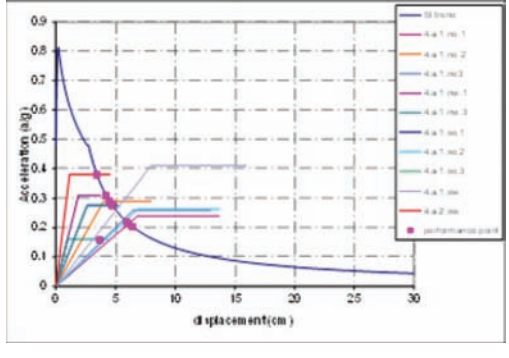

Figure 24. Capacity curves and performance points for 3 elevations of Irene Museum.

but modest ductility which would undergo serious structural damage. Given the complexity of the building and the diverse behaviour of its façade, notwithstanding the apparent symmetry of its plan, it is appropriate to undergo a much more in depth analysis of this building.

8 CONCLUSIONS

A detailed study was conducted to evaluate site-specific ground shaking parameters at the cultural heritage building sites based on available geotechnical and geophysical data. The results obtained from the probabilistic earthquake hazard study for a Poisson model with a return period of 475 years that corresponds to 10% probability of exceedance in 50 were used to define the earthquake hazard at NEHRP (2001) B/C boundary site conditions. 24 real earthquake records that are compatible with the earthquake hazard in terms of probable magnitude, distance and fault mechanism were selected and scaled with respect to the target hazard spectra from hazard studies and were used as outcrop input motions for site response analyses.

Site response analyses based on 1D equivalent-linear model was used to predict free-field earthquake shaking parameters on the ground surface.

The overall cumulative distribution of drift lateral capacity and expected damage show good agreement for the expected 5 damage states of the EMS '98 scale. The two cumulative distribution in terms of displacement for structural damge and ultimate lateral acceleration show that a large proportion of the buildings has a medium high value of vulnerability and that a lognormal distribution well represent the fragility curves of the overall sample. The four examples shown in the paper provide good insight in the relative vulnerability of buildings even when they have very similar typologies, such as the St. Irene, Fetiye and Kariye Museums. The better performance of some of the buildings and elevation is directly related to the presence of historic or modern anchor ties that help resisting the thrust of the vaults above the walls, but also provide restraint in overturning in presence of lateral acceleration.

REFERENCES

Ansal, A., Durukal, E. & Tönük, G. (2006) "Selection and Scaling of Real Acceleration Time Histories for Site Response Analyses", *Proc. of ETC12 Workshop*, Athens, Greece.

Ansal, A., Tönük, G., Demircioglu, M., Bayraklı, Y., Sesetyan, K. & Erdik, M. (2006) "Ground Motion Parameters for Vulnerability Assessment", *Proceedings of the First European Conference on Earthquake Engineering and Seismology*, Geneva, Paper Number: 1790.

Ansal, A. & Tönük, G. (2007) "Source And Site Effects For Microzonation", *Earthquake Geotechnical Engineering, 4th International Conference on Earthquake Geotechnical Engineering-Invited Lectures*, Springer Editor.: K. Pitilakis, Chapter 4, 73–92.

Ansal, A., Kurtuluş, A., & Tönük, G. (2007a) Earthquake Damage Scenario Software for Urban Areas. Keynote Lecture, Computational Methods in Structural Dynamics and Earthquake Engineering, M. Papadrakakis, D.C.

Ansal, A., Kurtuluş, A. & Tönük, G. (2007b) "Evaluation Of Site-Specific Earthquake Characteristics On The Ground Surface", *Istanbul Seismic Risk Mitigation and Emergency Preparedness Project (ISMEP) on Inventorization and Multi-Hazard and Earthquake Performance Evaluation of the Cultural Heritage Buildings in Istanbul*, the Ministry of Culture and Tourism.

ASCE 41–06 Seismic Rehabilitation of Existing Buildings, Edition: 1st, American Society of Civil Engineers/15-May-2007/423 pages, ISBN: 9780784408841.

Borcherdt, R.D. (1994) "Estimates of Site Dependent Response Spectra For Design (Methodology And Justification)" *Earthquake Spectra*, 10(4), 617–654.

BSSC-Building Seismic Safety Council (2001) NEHRP (National Earthquake Hazards Reduction Program) Recommended Provisions for Seismic Regulations for new buildings and other structures, 2000 Edition, Part 1: Provisions (FEMA 368), Ch. 4, Washington, D.C.

Darendeli, M.B. (2001) A New Family of Normalized Modulus Reduction and Material Damping Curves, PhD Dissertation, University of Texas at Austin, 362 p.

D'Ayala, D.F. & Casapulla, C. Limit state analysis of hemispherical domes with finite friction *In Historical Constructions, Possibilities of Numerical and Experimental Techniques*, pp. 617–626.

D'Ayala, D. & Speranza, E. (2003) Definition of Collapse Mechanisms and Seismic Vulnerability of Historic Masonry Buildings. *Earthquake Spectra*, 19, 479–509.

D'Ayala, D. (2004). Correlation of fragility curves for vernacular building types: Houses in Lalitpur, Nepal and in Istanbul, Turkey. *In*: *Proceedings of the 13th World Conference of Earthquake Engineering*, Vancouver Canada.

D'Ayala, D.F. (2005) *Force and Displacement Based Vulnerability Assessment for Traditional Buildings*. Bulletin of Earthquake Engineering, 3(3): 235–265.

D'Ayala, D.F. (2008) *Seismic vulnerability and risk assessment of cultural heritage buildings in Istanbul, Turkey*. in 14th WCEE, Beijing October 2008.

D'Ayala, D. & Ansal, A. (2009) "Non linear push over assessment of historic buildings in Istanbul to define vulnerability functions" *Proceedings of the Conference on Earthquakes and Tsunamis—Civil Engineering Disaster Mitigation Activities—Implementing Millennium Development Goals.*, Paper No. 128.

D'Ayala, D. & Ansal, A. (2012) Non linear push over assessment of heritage buildings in Istanbul to define seismic risk. Bulletin of Earthquake Engineering; Feb 2012, Vol. 10 Issue 1, p. 285.

Directive of the PCM 12 October 2007 (2007) Evaluation and Reduction of Seismic Risk of Cultural Heritage with reference to the Technical Standard for

Construction (in Italian) G.U.R.I. n. 24, 9 January 2008.

Durukal, E., Ansal, A. & Tönük, G. (2005) "Effect of Ground Motion Scaling in Site Response Analyses", *Proceedings of the Earthquake Geotechnical Engineering Satellite Conference*, 16th ICSMGE, Osaka, Japan.

EPRI (1993) "Guidelines for Determining Design Basis Ground Motions", Electric Power Research Institute, Palo Alto, CA, Vol1, EPRI TR-102293.

Erdik, M. & Fahjan, Y. (2006) Damage Scenarios and Damage Evaluation, *Assessing and Managing Earthquake Risk Geo-scientific and Engineering Knowledge for Earthquake Risk Mitigation: developments, tools, techniques*, Ch.10, Book Series: Geotechnical, Geological, and Earthquake Engineering, Eds: Oliveira CS, Roca A, Goula X (Eds.).

Erdik, M., Durukal, E., Şeşetyan, K. & Demircioğlu, M.B. (2007) "Assessment Of Site-Specific Earthquake Hazard At Reference Ground Conditions", *Istanbul Seismic Risk Mitigation and Emergency Preparedness Project (ISMEP) on Inventorization and Multi-Hazard and Earthquake Performance Evaluation of the Cultural Heritage Buildings in Istanbul*, the Ministry of Culture and Tourism.

Eurocode 8, 2002004, BS EN 1998–3:2004, *Design of structures for earthquake resistance—Part 3: Assessment and retrofitting of buildings*, British Standard Institution, London.

Fajfar, P. (2000) A nonlinear analysis method for performance-based seismic design, *Earthquake Spectra* **16**(3); 573–592.

Grünthal, G. (ed.), (1998) European Macroseismic Scale 1998 (EMS-98). Cahiers du Centre Européen de Géodynamique et de Séismologie 15, Centre Européen de Géodynamique et de Séismologie, Luxembourg, 99 pp.

Idriss, I.M. & Sun J.I. (1992) "Shake91, A Computer Program for Conducting Equivalent Linear Seismic Response Analysis of Horizontally Layered Soil Deposits Modified based on the original SHAKE program Published in December 1972 by Schnabel, Lysmer and Seed".

ISMEP (2008) Inventorization and Multi-Hazard and Earthquake Performance Evaluation of the Cultural Heritage Buildings in Istanbul, Istanbul Seismic Risk Mitigation And Emergency Preparedness Project Reports, Republic of Turkey, Ministry of Culture and Tourism, Istanbul Directorate of Surveying and Monuments.

Iwasaki, T., Tokida, K., Tatsuoka, F., Watanabe, S., Yasuda, S. & Sato, H. (1982) "Microzonation of Soil Liquefaction Potential Using Simplified Methods", *Proc. 3rd Int. Conf. On Microzonation*, Seattle, 3:1319–1330.

Iyisan, R. (1996) "Correlations between Shear Wave Velocity and In-situ Penetration Test Results", *Technical Journal of Turkish Chamber of Civil Engineers*, 7(2),1187–1199 (in Turkish).

Menq, F.Y., Stokoe, K.H. & Kavazanjian, E. (2003) "Linear dynamic properties of sandy and gravelly soils from largescale resonant tests," *International Symposium IS Lyon 03, Deformation Characteristics of Geomaterials*, (Lyon, France).

Oztin, F. (1994) 10 July 1894 Istanbul Earthquake Report, Ministry of Construction and Settlement, General Directorate of Disaster Affairs, Earthquake Research Division.

PEER Strong Motion Data Bank, http:// peer.berkeley.edu.

Seed, H.B., Wong, R.T., Idriss, I.M. & Tokimatsu, K. (1986) "Moduli and Damping Factors for Dynamic Analyses of Cohesionless Soils", Univ. of California, Berkeley, Earthquake Engineering Research Center, Report No. UCB/EERC-84/14, 37 p.

Turkish Earthquake Code (2007) "Specification for Structures to be Built in Earthquake Areas", Ministry of Public Works and Settlement, Government of Republic Turkey.

Vucetic, M., & Dobry, R. (1991) "Effect of soil plasticity on cyclic response", *Journal of Geotechnical Engineering*, American Society of Civil Engineers, 117(1), 89–107.

Geotechnical Engineering for the Preservation of Monuments and Historic Sites – Bilotta, Flora, Lirer & Viggiani (eds)
© 2013 Taylor & Francis Group, London, ISBN 978-1-138-00055-1

The role of monitoring and identification techniques on the preservation of historic towers

R. Lancellotta & D. Sabia
Politecnico di Torino, Italy

ABSTRACT: The historic towers today we observe survived the initial period in which they could have been not so far from a *bearing capacity* collapse, due to *lack of strength*. And due to uneven settlements, they appear today to survive at an alarming angle of inclination, in some cases not so far from the danger of a *leaning instability*, due to *lack of stiffness* of the soil. Since these towers are quite often the symbol of the town and sometime they represent the local community as a whole, their preservation deserves special attention and efforts. Within the context of the restoration principles, preserving the whole integrity of the monument should be a well accepted concept and this requires not to rush in deciding the stabilizing measures until the behaviour of the monument is properly understood. A long term monitoring should then be aimed at identifying the causes of movements and their potential increase in rate in order to distinguish the normal physiological behaviour from deviations. In addition, these observations can be complemented with experimental identification analyses, performed in the presence of ambient vibration, that allow to explore in a rather effective way the response of the structure and its interaction with the soil.

1 INTRODUCTION

Historic masonry towers are an important part of our cultural heritage. Some of them originated as bell towers, and among the oldest examples there are the campaniles in Ravenna, well known for their peculiar cylindrical shape and for not being structurally connected to the church. During X and XI centuries there was an impressive development of private towers (this was the case of Bologna, S. Gimignano, Florence, Lucca, Pisa, Pavia and many other cities), used by families as their house in case of strife within the medieval commune and as a symbol of their power and prosperity. In the thirteenth century the landscape of the commune was being dominated by the civic tower and the bell tower of the cathedral. Some others were defense tower, as it was the case of the fortified town of Monteriggioni (Siena) with fourteen towers at the corner of the defence wall. All these example, and many others, tell us that historic masonry towers are part of our history and our culture, i.e. they are an important cultural heritage; they are not only a distinctive feature of the old town centre but quite often they are the symbol of the town and represent the local community as a whole. For all these mentioned aspects their preservation deserves special attention and efforts.

It seems evident that the towers today we observe survived the initial period in which they could have been not so far from a *bearing capacity* collapse, due to *lack of strength* of the soil. Delay or interruption of the building process allowed the foundation soil to improve its strength and the tower to be successfully finished. And due to uneven settlements, they appear today in some circumstancies to survive at an alarming angle of inclination. This highlights the danger of a *leaning instability*, that increases if there is *lack of stiffness* of the soil. In this respect the leaning tower of Pisa represents a powerful example, because the preservation of the tower was recognised as being a problem of leaning instability (Hambly, 1985; Lancellotta, 1993; Como, 1993; Desideri and Viggiani, 1994; Nova and Montrasio, 1995; Pepe, 1995; Federico and Ferlisi, 1999; Burland et al., 2003; Marchi et al., 2011).

Obviously, there are also problems of structural nature interacting with these geotechnical aspects. They depend on the masonry behaviour as a unilateral material and deserve special attention as proved by the collapse of the Campanile in Venice in 1902 and the Civic Tower in Pavia in 1989 (Heyman, 1992; Binda et al., 1992; Macchi, 1993). And it must be outlined the severe damage that occurred and may occur to monument and cultural heritage during the seismic events, as well as the need for the stabilization as a result of soil movements, induced by subsidence due to ground water lowering, underground works and seasonal effects such as swelling and shrinking.

In all the mentioned cases, a prerequisite for devising appropriate stabilizing measures requires

careful and long term monitoring, in order to identify at least the causes of the movements and their rate. But monitoring is also an essential component of our studies when exploring the role of soil-structure interaction in the long term performance or when assessing the seismic vulnerability, since it can contribute to establish a reliable response for the soil-foundation system.

This keynote is intended to contribute to these aspects and it is conceptually divided in two parts: the first one focuses on the role of long term monitoring aimed at identifying the causes of movements and their potential increase in rate and at distinguishing the normal physiological behaviour from deviations.

The second part focuses on the rather significant and more recent contributions coming from experimental identification analyses, performed in the presence of ambient vibration.

2 WHAT WE ARE MEASURING FOR

In order to illustrate in a more effective way the role of long term monitoring and identification analyses in forecasting the behaviour of historic towers, reference will be made to two case histories. The first one, the tower of Pisa, is well described in the literature (MLLPP, 1971; Burland and Viggiani, 1994; Jamiolkowski, 2001; Burland et al., 2003), and there is no need to recall the history of construction, details of the structure or the subsoil conditions. Therefore, few introductory notes will be only limited to the description of the second case, that of the Ghirlandina tower in Modena (see Cadignani, 2009; Piccinini, 2009; Lancellotta, 2009; Di Tommaso et al., 2013; Lancellotta, 2013).

The Ghirlandina tower (figure 1) and the Cathedral of Modena are part of the Unesco site of Piazza Grande and during the last decade there has been an increased interest towards the potential seismic vulnerability of the tower, by also considering its interaction with the Cathedral. The Ghirlandina tower is a square based (side: 11,0 m) structure, 88.82 m high, with a hollow cross section (figure 2), thicker on the corner because of the presence of four masonry pillars. In the inner part, an open stair runs along the tower from the base to the higher part where the belfry and the spire roof complete the structure.

There are three masonry diaphragms built in the tower: the vault on the first floor, the floor of the Torresani cell and the vault above the belfry (the deck instead is a timber structure). At ground level, two masonry arches connect the tower with the adjacent Cathedral (figure 3).

The Tower was started at the same time the Cathedral was by Lanfranco (i.e. 1099) and reached his final stage in 1319 (see for more details Dieghi, 2009; Piccinini, 2009; Labate, 2009).

Figure 1. The Ghirlandina tower in Modena.

It is argued that the first five floors were successful standing in 1169 or 1184 and the tower reached the height corresponding to the sixth floor in 1216.

In 1338 the arches connecting the southern side of the tower to the Cathedral were already in place, eventually to prevent additional tilt of the tower towards the Cathedral. There is in fact evidence that the tower begun to tilt during the construction and the ancient masons made some corrections accordingly.

Soil profile down to the investigated depth of 80 m (see figure 4) is composed of a first horizon of medium to high plasticity inorganic clays, with an abundance of laminae of sands and peat, only millimetres thick. The upper portion of this horizon, whose thickness ranges from 5 to 7 meters, is known as Modena Unit and is linked to the flooding events (of post-Roman age) produced by minor streams (Fossa-Cerca).

The subsequent underlaying horizons, ranging in depth from 22 to 54 m, represent the result of a complete transgressive-regressive cycle: the fine-grained sediments, belonging to the horizon known as Niviano Unit, were deposited during the penultimate interglacial cycle, and the superimposed coarse-grained materials, belonging to the

Vignola Unit, are linked to transport activities of the Secchia River (Lugli et al., 1984).

A second horizon of coarse-grained materials is encountered at depths ranging from 54 to 63 m, and thereafter a fine-grained materials horizon is found down to a depth of 78 m, here again characterized by a diffuse presence of laminae of sand.

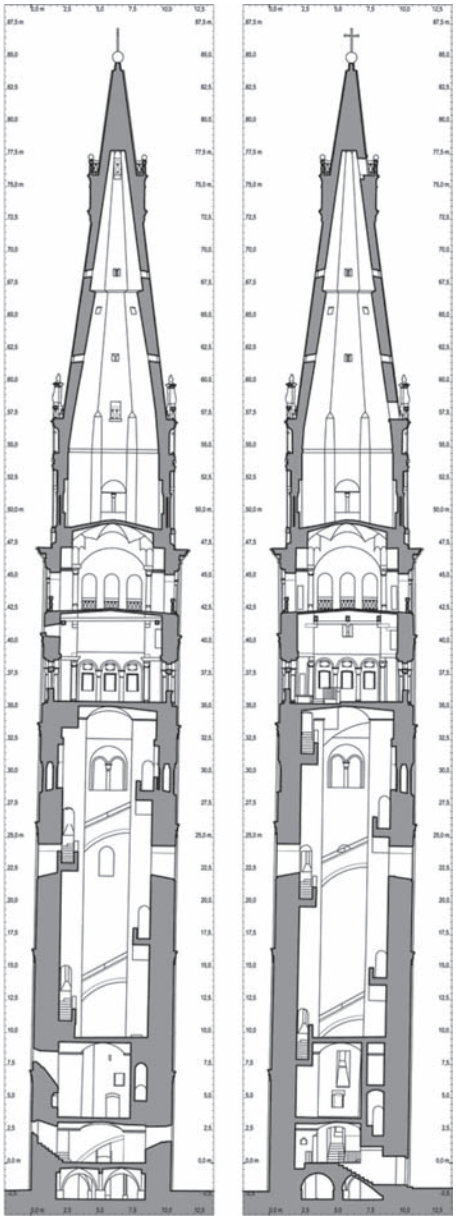

Figure 2. Vertical sections of Ghirlandina tower: From the left, view towards South, view towards East (Giandebiaggi et al. 2009).

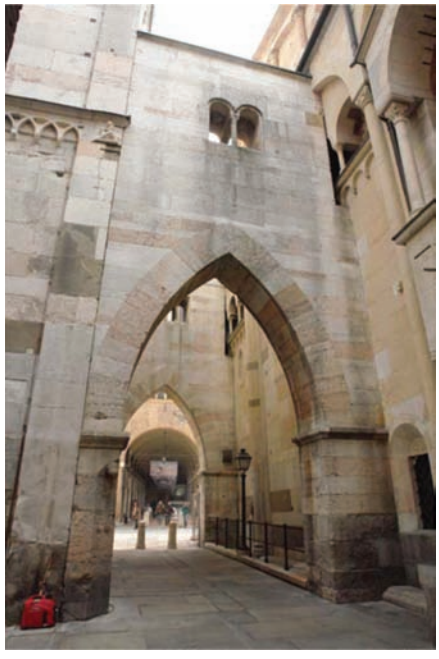

Figure 3. The gotic arches connecting the Ghirlandina tower and the Cathedral (first constructed in 1338 and rebuilt in 1905).

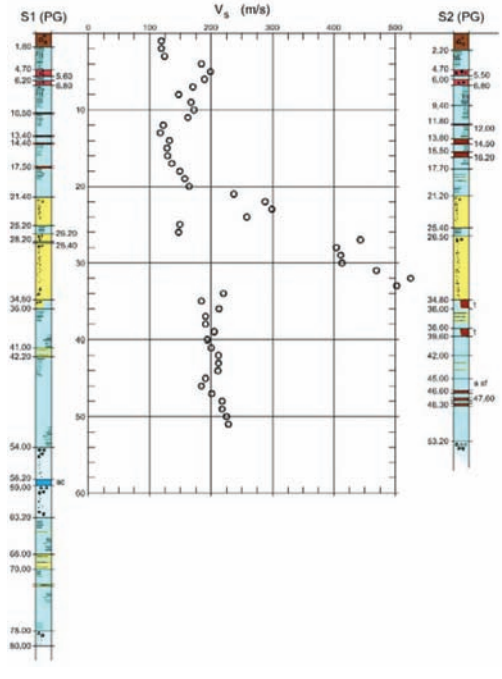

Figure 4. Soil profile and cross-hole tests (Lancellotta, 2009).

The soil profile, shown in figure 4, has been complemented with the results of cross-hole tests, because of their non-invasive character. These tests allow for preservation of the initial structure of soil deposits as well as the influence of all diagenetic phenomena contributing to a stiffer mechanical response, and for this reason they represent one of the most reliable methods of determining the shear modulus at small strain amplitude.

2.1 *Example of long term monitoring*

As already mentioned in the introduction, the danger of a *leaning instability* increases if there is *lack of stiffness* of the soil. In addition, initial imperfections and non-uniform foundations very often generated differential settlements which, coupled with low stiffness of the soil-foundation system and delayed deformations due to soil creep, can led to long-term critical conditions. Therefore, depending on the elasto-plastic soil stiffness and on viscous properties, we can reach a long term stable condition as well we can approach an instability condition (figure 5).

The case of Pisa tower provides a relevant example to show how long-term monitoring was of benefit in assessing the need for stabilisation measures. As it is well known (Burland and Viggiani, 1994), we can read the history of the tilt in the adjustment made to the masonry levels during the construction and in the shape of the axis of the tower.

Monitoring started in 1911 and the inclination of the tower was measured by means of a theodolite (figure 6). In 1934 a plumb-line, known as Girometti-Bonechi pendulum was installed in the tower, suspended from the sixth floor and observed in an instrument room. At that time, a 4.5 m long

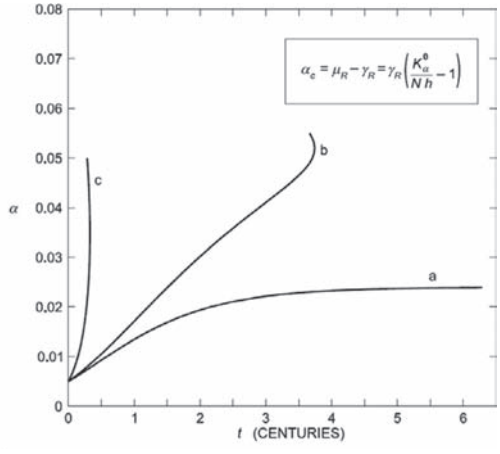

Figure 5. Time evolution of the stability conditions (Como, 1993; Lancellotta, 2013).

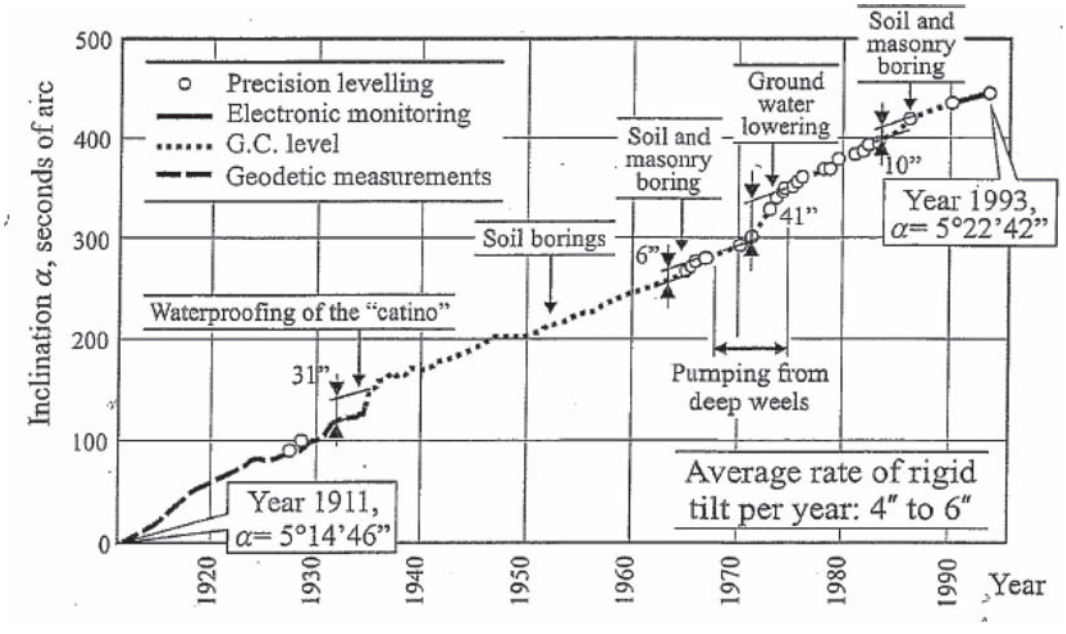

Figure 6. Time evolution of the tilt of Pisa tower since 1911 in seconds of arc (MLLPP, 1971; Burland and Viggiani, 1994; Jamiolkowski, 2001).

spirit level (known as GC level) was also installed within the instrument room, to measure both the north-south and the east-west inclination.

As it is shown in figure 6, the evolution of the tilt was measured from 1934 to 1969 by using the GC level once or twice a year, and unfortunately these measurements ceased in 1969. From 1965 till 1985 the tilt evolution was based on precision levelling on the fifteen points around the Tower, and in more recent years (from 1990) both reading of GC level and precision levelling recommenced.

It is apparent from figure 6 that the tilt trend contains some events of interest: in 1934 the foundation masonry was grouted and the catino waterproofed; in early 1970's pumping from the lower sands caused subsidence and tilting of the Piazza towards south-west (Croce et al., 1981); in 1985 an increase of tilt resulted from boring through the foundation.

In any case, it is also apparent that, even corrected for these increments and other minor perturbations, the tilt was steadily increasing and in early 1990's the rate of inclination was about 6 seconds per year and has doubled since the 1930's (figure 7), i.e. an emerging alarming trend towards instability (curve b in figure 5).

2.2 *Detecting normal physiological trend from deviations*

Continuous movements of historic towers tend to be seasonal and for this reason it is again very important to have reliable measurements over a long term period, in order to distinguish between components of different frequency. The example in figure 8 refers to Ghirlandina tower and clearly shows the seasonal trend superimposed to a long period one (Blasi et al., 2009).

In this case, investigations aimed at clarifying the stability of the tower and measurements of tilt started at the end of the XIX century. At that time, prof. Cavani (from the University of Bologna) reached the conclusion in 1903 that the tilt was equal to 1°14'16" and the vertical plane of tilt was approximately oriented along the North-East to South-West direction (the deviation from this direction was of about 7°5' from South-West towards West).

More recently, in 2003 a plumb-line, 23 meter length, has been installed in the tower, suspended from the *Torresani* cell and the coordinates of the plumb-line are read automatically by means of a telecoordinometer with the sensitivity of 1/100 mm. It appears from figure 8 that during August the tower tends to move southwards and westwards and this trend continues till January.

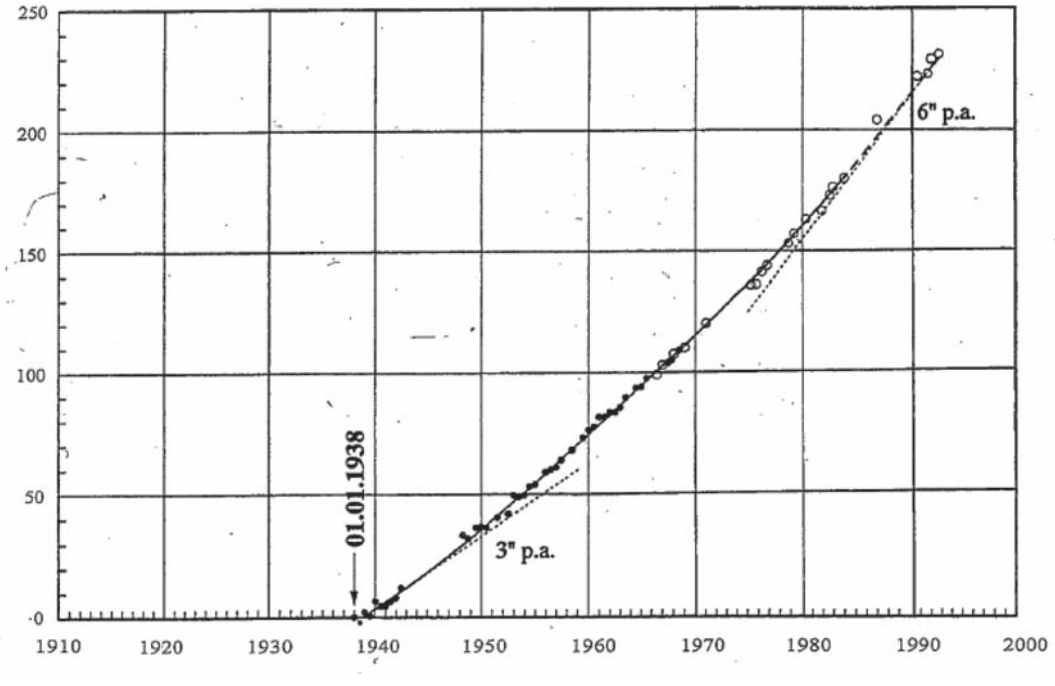

Figure 7. The evolution of the inclination of the base of the tower corrected from incidental increments (Burland and Viggiani, 1994; Jamiolkowski, 2001).

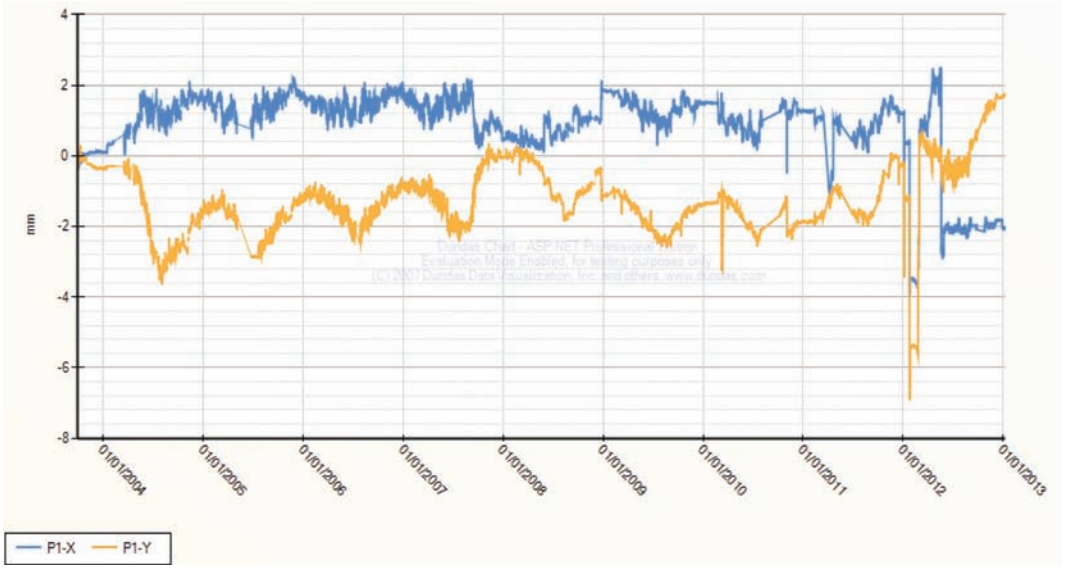

Figure 8. Seasonal movements of Ghirlandina tower as measured by means of a pendulum (P1-X north-south inclination; P1-Y: east-west inclination).

The long period trend appear to be more pronounced in the plane parallel to the side of the Cathedral, at a rate of about 0.25 mm/year, whereas in the plane orthogonal to the Cathedral side there is not a definite trend and cyclic seasonal movements also appear to be less pronounced, due to the presence of the arches between the Tower and the Cathedral that may partially act as constraint for the Tower.

2.3 *Redundancy of measurements*

Sensors have to be positioned in such a way that any movement should give rise to a consistent set of readings in different locations, providing in this way redundancy of informations. In particular, an aspect that deserves attention is the possibility of a distinction between the movement of the structure and that of its foundation.

This was done with noticeable care for the Pisa tower (Burland and Viggiani, 1994), and the theodolite and precision levelling measurements helped to clarify that the seat of the continuous tilting of the tower was in the horizon A. This conclusion provided a sound basis for the analysis of leaning instability and suggested the even a small decrease of the inclination would result in a substantial increase against the phenomenon of instability.

2.4 *Causes of movements*

Additional requirements to forecast potential threshold functions include monitoring of basic physical conditions, such as water table fluctuation, temperature, solar radiation, wind.

How important can be the link between the specific local geotechnical problem to the environment (territory) was clearly shown by prof. Arrigo Croce (see Jappelli, 1997) for the safeguard of Milan Cathedral, one of the most impressive medieval architecture in Italy (started in 1386).

The observed cracks and fissures became so important in 1969 that concrete casing were put in place to safeguard the integrity of the pillars and the whole Cathedral. Focusing the attention in the groundwater conditions existing in the alluvial subsoil, there was a strong evidence that the settlements of the Cathedral had to be considered within the context of the subsidence of a large area, induced by pumping started in 1922 and progressively increased in 1950's. Reduction of water withdrawal was imposed in the following years, and these measures allowed to slow down the settlements of the structure, to remove the casing of the pillars and in 1986 the Cathedral was returned to visitors.

Back to seasonal movements superimposed to a steadily long term movement, a trend similar to that reported in figure 8 was also observed for Pisa tower (Burland and Standing, 1997), and in that case the most likely cause of seasonal movements was believed to the fluctuations of water table in horizon A. In particular, it was observed that peaks of water level corresponding to intense rainfall events produced instantaneous southward

tilting of the tower, with an increment not completely recovered.

The gradual accumulation of such small irreversible rotations was believed to be one of main factors for the steady increase of the inclination experienced by the tower in the past and this conclusion suggested the drainage system north of the tower to mitigate the effects of the fluctuations of the water table (Burland et al., 2003).

A similar experience is now being to be gained with the case of the Ghirlandina in Modena, where since 1980 the town council promoted studies and investigations related to the subsidence of the alluvial plain (Russo, 1985; Cancelli, 1986; Cancelli and Pellegrini, 1984). Significant changes of piezometric levels within the major aquifers occurred during the mid 1970's due to municipal water supply purposes, lowering down to 10 m the original level and the old town centre experienced a subsidence phoenomenon of up to 80 to 90 cm (Cancelli, 1986; Russo, 1985).

This claimed for controls in order to reduce or prevent further negative effects, so that the piezometric level of the two aquifers, ranging from 22 to 34 m and from 54 to 63 m, rised progressively by reaching at present an elevation of +0.5 m from ground level, whereas within the first horizon the groundwater level oscillates from depth of 1.50 to 1.2 m.

Since the subsidence phenomenon was very pronounced, the Municipality of Modena decided to monitor the vertical movements within the historical area, with the aim of detecting the differential vertical displacements, producing detrimental effects on the stability of the Cathedral and the Ghirlandina tower. A high precision levelling network made by 29 benchmarks was originally installed in 1984.

It is now comprehensive of 24 benchmarks (figure 9) and it is surveyed with levelling of high precision (standard deviation of 0.1 mm in height difference determination).

As can be inferred from figure 9, the tower exhibits vertical displacements more pronounced that the surrounding area, but, in any case, a great benefit was reached as result of the counteracting measures since the rate of settlement reduced by an order of magnitute with respect to the trend observed during 70's and 80's (Russo, 1985).

A further relevant aspect is represented by the correlation between seasonal movements and solar radiation and is highlighted by data reported in figure 10, where the seasonal movements of the Ghirlandina tower (previously shown in figure 8) are superimposed to the trend of temperature, as measured by a thermometer (TG1) installed of

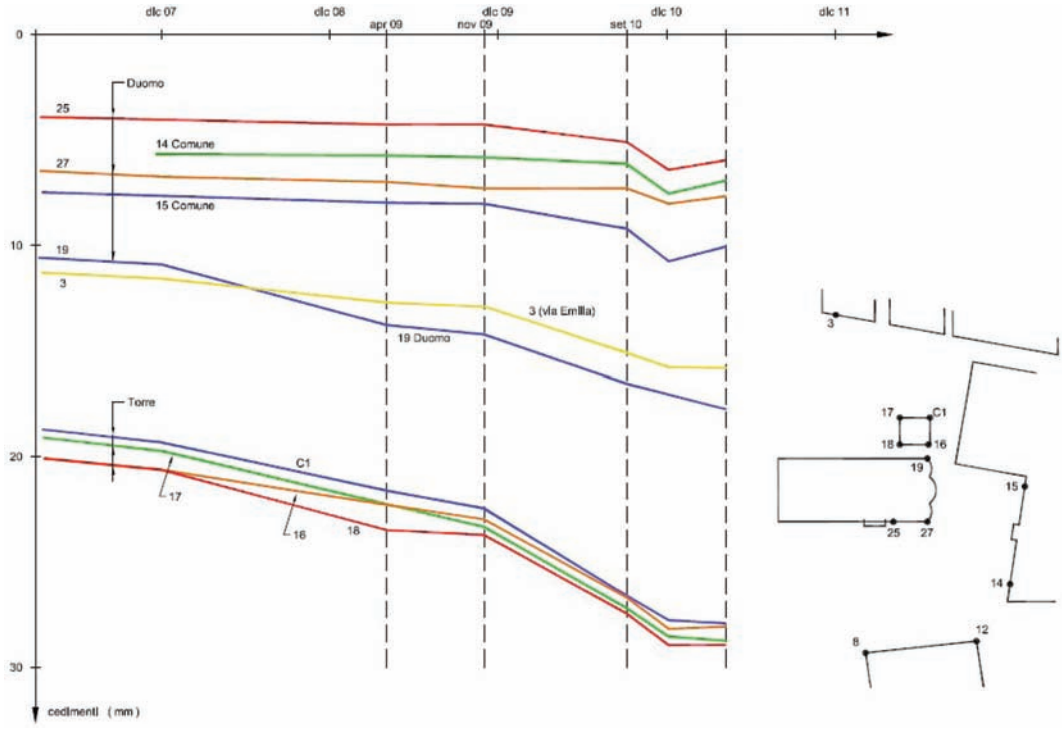

Figure 9. Trend of subsidence during the last decade in Modena (data provided by Capra and Castagnetti, 2011).

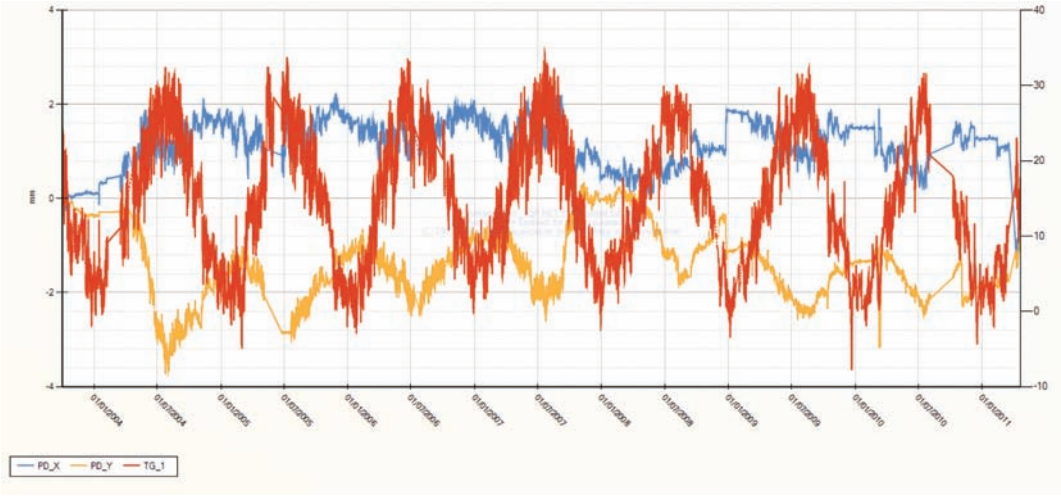

Figure 10. Seasonal movements (PD_X, PD_Y) of the Ghirlandina tower and correlation with the trend of the temperature (TG_1).

the south-east masonry wall of the structure (the temperature scale on the right axis of the plot is Celsius degree).

3 MODELLING, DYNAMIC TESTS AND IDENTIFICATION ANALYSIS

In order to forecast the long term behaviour of an historic tower, as well as its vulnerability with respect to seismic actions, there is a need to model the interaction with the supporting soil and here again monitoring is an essential component to validate any conceptual model as well as subsequent numerical analyses. In addition, a complimentary and effective tool to investigate the material properties and the structural behaviour as a whole comes from identification analyses, as it will be discussed in the sequel for the case of the Ghirlandina tower in Modena.

A first convenient way to explore the leaning instability mechanism is to make reference to the inverted pendulum model (figure 11). The tower is represented by a rigid column of length *h*, connected at its base to a rotational spring, representing the soil-foundation system, and a crucial step in the analysis is therefore to establish a reliable response for the tower foundation.

In this respect, strain-hardening plasticity models, developed in relation to the overall soil-footing system (i.e. the so-called "macro-element" model), can provide such a relationship (Prager, 1955; Butterfield, 1980; Desideri and Viggiani, 1994; Nova and Montrasio, 1991; Paolucci et al., 1999; Como, 2010; Marchi et al., 2011), and allow to take into

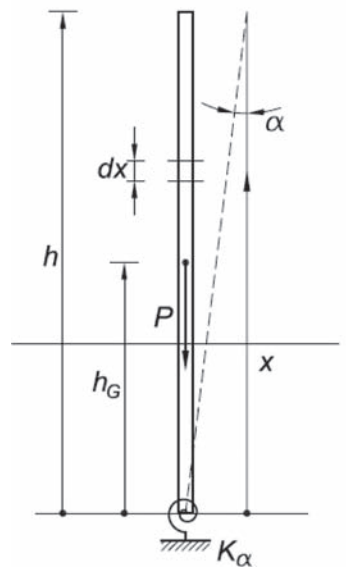

Figure 11. The inverted pendulum model.

account the main aspects of soil behaviour: non-linearity, irreversibility and coupling between settlement and rotation.

However, by considering the 3D nature of the problem, the mechanical heterogeneity induced by the applied stresses as well as the effectiveness of the soil contact along the the vertical sides of the embedded foundation, a complimentary approach comes from experimental identification analyses, that allow to estimate the dynamic parameters of

the structure, such as natural frequencies of vibration, mode shapes and damping.

These tests can be performed under known or unknown input. In the first case the tests are performed using artificially produced excitation of harmonic type at variable frequency, usually by applying to the structure an eccentric mass rotating machine (vibrodine), or by producing a pulse load by means of a dropping weight. Although they offer considerable advantages, i.e. the different modes can be excited individually, modal shapes and damping can then directly be identified and non linear behaviour can be also explored, these tests involve several shortcomings. These include difficulties in setting up the testing equipment, the need to prevent the use of the structure during testing, resolution problems associated with coupled modes, very long execution times.

In contrast, dynamic tests with environmental excitation are performed through identification techniques that do not require a knowledge of the input, the results can be continuously recorded and it is possible to perform an unlimited number of tests without impairing the integrity of the structure.

Making reference to the case of Ghirlandina tower, the experimental tests were performed by recording time histories of acceleration along the three coordinate directions x, y and z, as shown in Figure 12 (x axis points towards North).

The position of the sensors on the structure was identified in advance by performing a sensitivity analysis by means of a numerical model (FEM) of the tower, composed of 24296 solid elements (SOLID186 and SOLID187), that was also used for a quality control of the mode shapes.

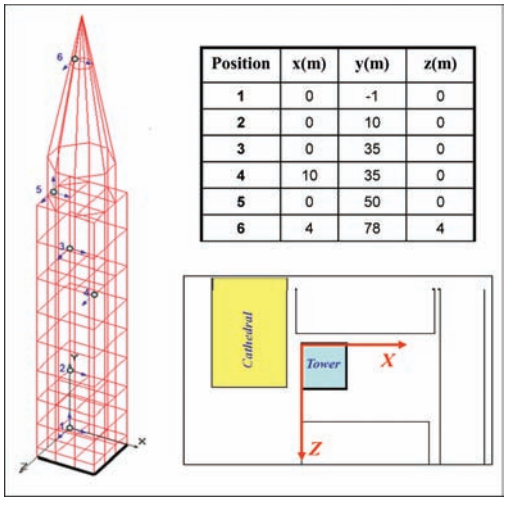

Figure 12. Ghirlandina tower: Layout of measurement points (Sabia, 2012).

This preliminary analysis was particularly relevant in order to detect the mode shapes and to avoid ambiguous estimates resulting from insufficiency of points or by an incorrect distribution on these point on the structure (space aliasing).

The measuring system required the use of a data logger NI PXI-1033 Series, 2 data acquisition cards NI PXI-449 PXIe-449x (16 channels, 24 bit resolution, antialiasing filter), and triaxial accelerometers PCB: ICP M.N. 356B18 (sensitivity: 1 V/g; measure range ±5 g pk; frequency range: 0.3–5000 Hz).

In order to show the capability of this analysis in an rather simple, introductory but effective way, let explore the problem by considering in figure 12 only the accelerometers at location 5, 4 and 3. If $Y(f)$ is the Fourier transform of a signal $Y(t)$ and $\overline{Y}(f)$ is its complex conjugate, the autospectra of each signal $G_{yy}(f)$ is defined as

$$G_{yy}(f) = Y(f)\overline{Y}(f)$$

and the frequency response spectra in figure 13 reveal peaks that can generally be assumed to represent either peaks in the excitation spectrum or normal modes of the structure (see Bendat and Piersol, 1993).

To distinguish peaks linked to structural response from peaks in the excitation, we have to observe that points in a lightly damped normal mode of vibration will be in phase or 180° out of phase, depending only on the the shape of the normal mode. In particular, a distinction between bending and torsional modes requires phase measurements between two points on the opposite side of the structure but at same elevation. In this respect, the autospectra of the signals do not provide information to identify the normal modes and this is the reason why reference is made to the cross-spectrum $G_{yz}(f)$ function, defined as

$$G_{yz}(f) = Y(f)\overline{Z}(f)$$

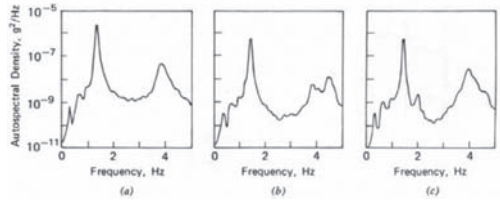

Figure 13. Autospectra of signals from 3 accelerometers located along the axis of the structure, (a) and (b), and at the same level but opposite side, (b) and (c) (Bendat and Piersol, 1993).

By referring to the example in figure 14, the peak at frequency 1.4 Hz indicates a bending mode, because all measurements are in phase. On the contrary, the peak at 3.9 Hz would suggest a torsional mode, because the measurements along longitudinal separation are in phase, while points on the opposite sides are 180° out of phase. The peak at 4.5 Hz would suggest a higher order bending mode, but in this case the coherence function

$$\gamma^2(f) = \frac{\left|G_{yz}(f)\right|^2}{G_{yy}(f)G_{zz}(f)}$$

is as low as 0.25, that indicates that autospectra at this frequency includes substantial extraneous noise.

The analysis of the seismic response of the Ghirlandina tower, measured during the earthquake of October 3th 2012 (with epicenter in Piacenza and magnituto M = 4.5) proves the capability of spectral analysis to detect the dynamic parameters of the structure. As an example, figure 15 shows the cross-spectra of acceleration time histories measured at points 1, 3 and 4 and an inspection of

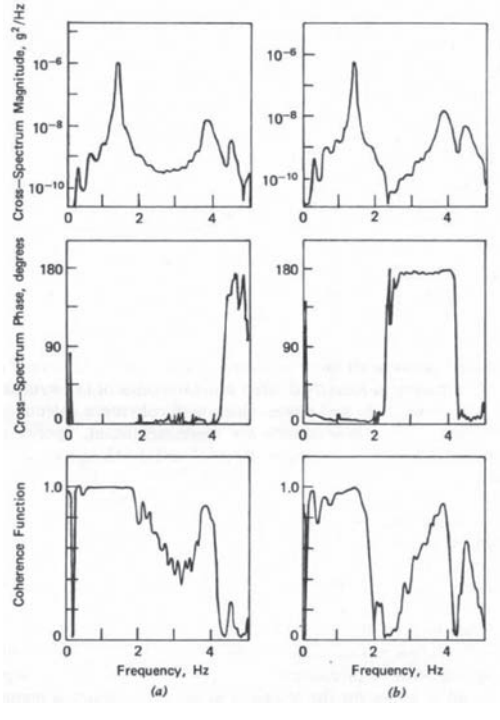

Figure 14. Cross-spectra and coherence functions between outputs of previous figure: a versus b; b versus c (Bendat and Piersol, 1993).

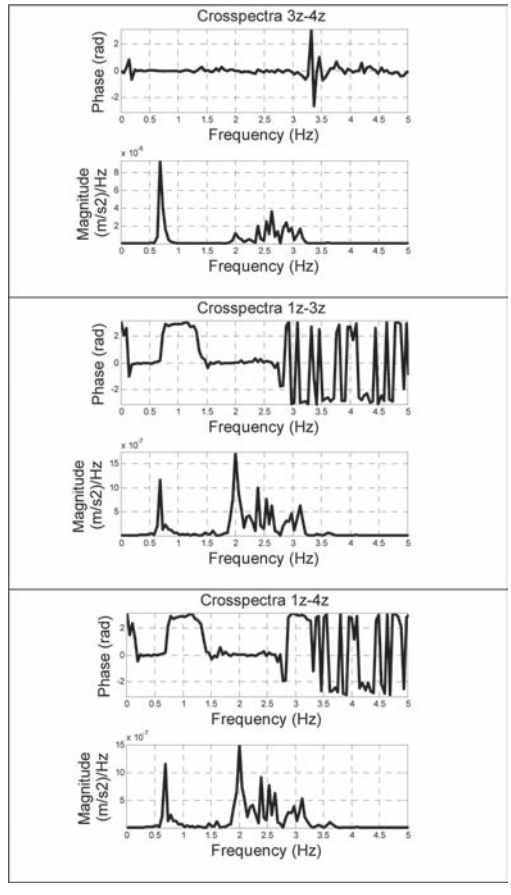

Figure 15. Ghirlandina tower: Cross-spectra functions between points 1, 3 and 4 of figure 12.

this spectra reveals peaks associated to structural response.

In order to estract from these measurements modal frequencies, shapes and damping parameters of the structure, a Stochastic Subspace Identification Method (Van Overschee and De Moor, 1996; Aoki et al., 2007, 2008) was used, and example of mode shapes, as detected on the plane (z, y) parallel to the Cathedral nave and on its orthogonal plane (x, y), are shown in figure 16.

In particular, referring to the modal shapes 1 and 2, with associated frequencies of 0.74 Hz and 0.85 Hz, it can be observed that the first one outlines the rotation at the tower basis due to soil deformability, whereas the second one claims for the presence of the arches connecting the Tower and the Cathedral.

In the figure 16b the first two modal shapes related to vibrations along the tower axis are also shown (mode 8 and 9), the related frequencies now

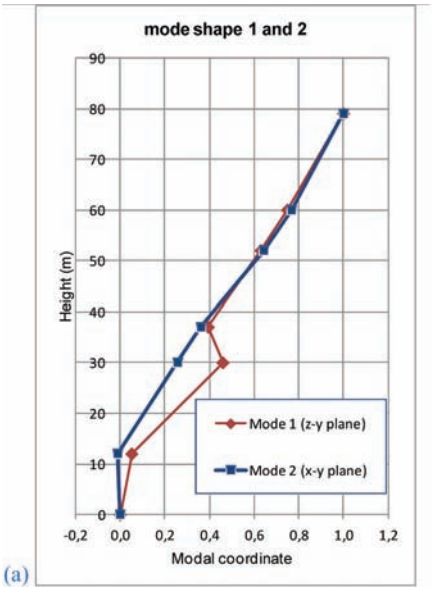

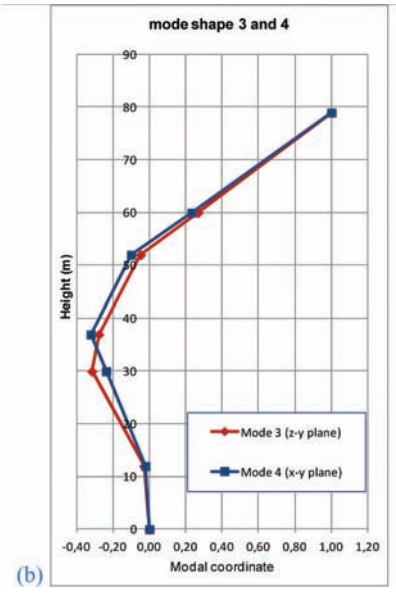

Figure 16a–b. Bending modal shapes (Sabia, 2012).

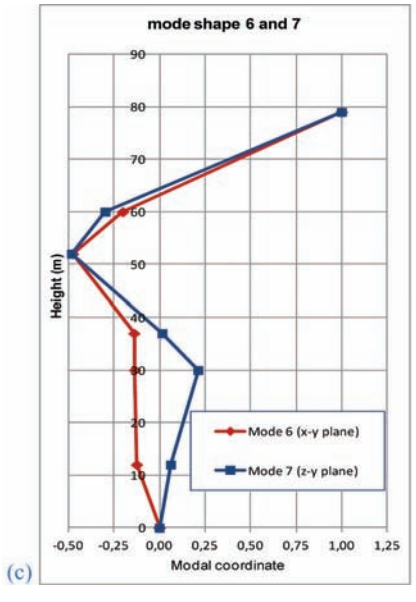

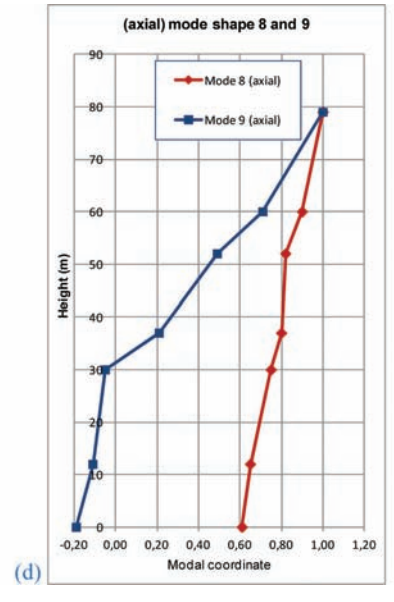

Figure 16c–d. Bending (c) and axial (d) modal shapes (Sabia, 2012).

being 4.51 Hz and 9.81 Hz, and here againg the displacements at the tower basis outline the contribution of soil deformability.

The main conclusion reached is therefore that the soil structure interaction cannot be neglected, in contrast to most published identification analyses that usually assume the structure with rigid constraint at its base.

Note that these latter results (i.e. longitudinal mode shapes and related frequencies) are of

particular interest because they allow to make an estimate of the lower bounds of both the soil-foundation stiffness and the masonry modulus in a simple but effective manner.

Let first assume the tower as a rigid body resting on a deformable soil, then the frequency and the soil-foundation stiffness will be linked through the relation

$$f = \frac{1}{2\pi}\sqrt{\frac{K_{yy,lower}}{M}}$$

being K_{yy} the axial stiffnes of the soil-foundation system and M the mass of the tower. Since $M = 8525 \cdot 10^3\ kg$ and the measured frequency is $f = 4.51\ Hz$ one gets

$$K_{yy,lower} = 6.84\ GN/m$$

On the contrary, by assuming the soil as a rigid constraint while the tower is being represented with beam elements and lumped masses, a lower bound of the masonry modulus can be estimated, this being equal to

$$E_{m,lower} = 1.7 GPa$$

Obviously, soil and masonry deformability both contribute to the dynamic response of the structure, so that an optimization analysis has been performed, by considering both bending and axial modes.

The obtained results prove that the first modes (in both cases of bending and longitudinal vibrations) are sensitive to soil stiffness, whereas the higher modes depend on masonry deformability and we can optimize the response of the soil-structure system by using the masonry modulus E_m ranging from 3 to 4 *GPa* and the following values of the axial and rotational stiffness of the soil-foundation system:

$$K_{yy} = 7.8\ GN/m$$

$$K_{\alpha} = 240\ GN \cdot m/rad$$

Note that these value must be considered as representative of an elastic response, to be used with reference to serviceability limit states or in presence of low intensity seismic events. In presence of strong motion we need to properly take into account the decay of soil stiffness with shear strain (Lancellotta, 2009a).

4 THE BEHAVIOUR OF THE GHIRLANDINA TOWER DURING RECENT SEISMIC EVENTS

At present there is a dynamic system continously operating since August 2012 that detects, with a sampling frequency of 100 Hz, the accelerations at 6 locations along the vertical wall of the structure (figure 12).

Figures 17, 18 and 19 show the measured time histories of acceleration and the corresponding derived time histories of velocity and displacement, detected during the earthquake of January 25, 2013 (epicenter in Garfagnana with magnitude M = 4.8) at points 6 (elevation h = 78 m, from the level of the square), 5 (h = 50 m) and 1 (base of the tower, see figure 12 for details).

It is worth to note that the maximum acceleration detected in point 6 in the Z direction is amplified by about 10 times if compared to the corresponding value detected at point 1.

It is also of interest to observe the detail of the seismic response of the tower at the base and at the top, as shown in figure 20. The analysis of the signal clearly confirms the value of the frequency of the first vibration mode as was estimated by the identification procedure performed with the environment excitation.

Furthemore, the spectra of the time histories, shown in figures 21 and 22, and in particular the amplification measured moving from the base to the belfry of the the tower, are of particular value for the following reasons.

Tower are peculiar structures characterized by the vertical dimension much greater if compared with the base sides. It implies that, because of uneven settlements, the tower is prone to global instability problems. In addition, any stress analysis proves that there is usually stress concentration on the brickwork of facing of the walls, and this may be the reason for local instability, as it was the case of the Pavia civic tower.

Additional causes of local damage or failure are linked to deterioration in time of the external facing, as well of the mortar. Further on we have to consider the reduction of the resistant horizontal section along the axis of the tower, due to reduction of the wall thikness or due to the presence of openings.

All these aspects deserve special attention because they can induce local instability phoenomena or weakness points, that are difficult to forecast, because of the absence of any evidence in advance.

The recent earthquake in Emilia Romagna region (May 2012) is a significative example in this respect, because we had the collapse of many cam-

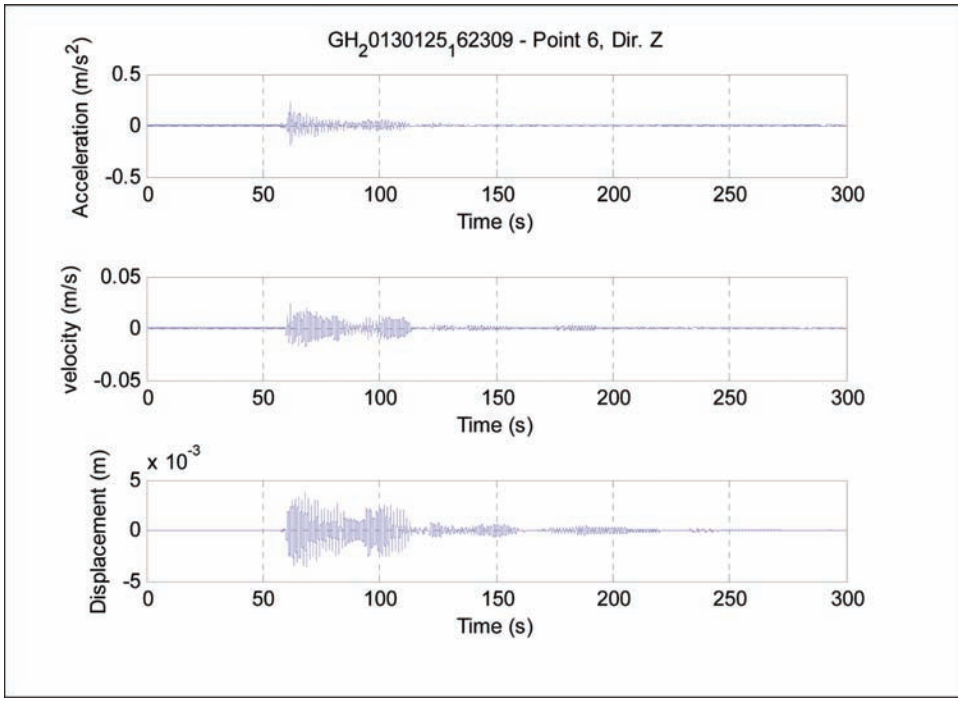

Figure 17. Time histories of acceleration, velocity and displacement along the Z direction at point 6.

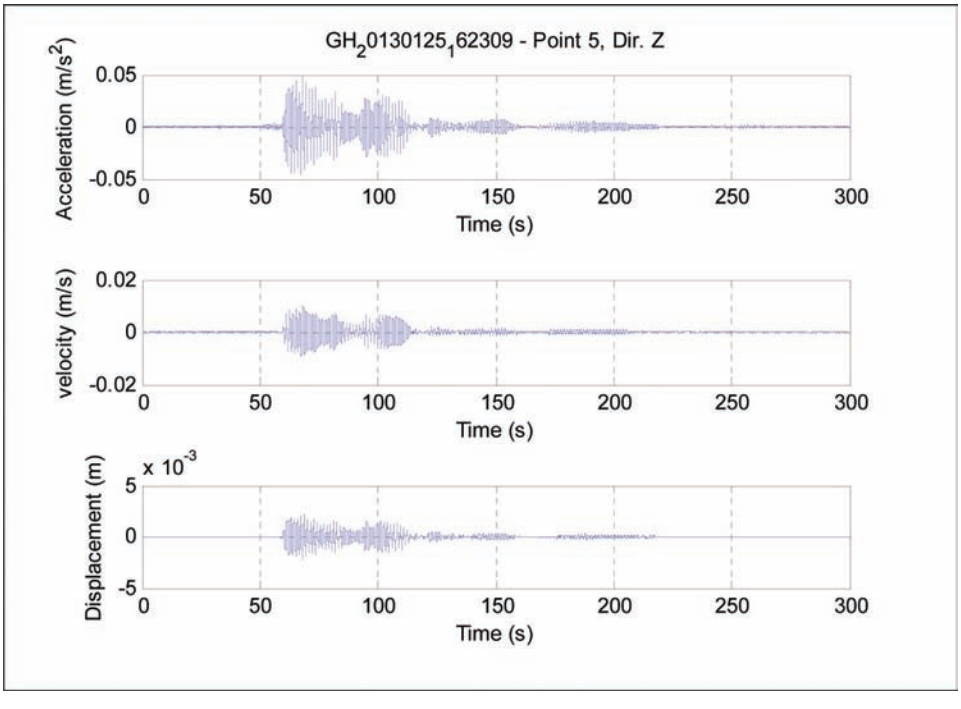

Figure 18. Time histories of acceleration, velocity and displacement along the Z direction at the point 5.

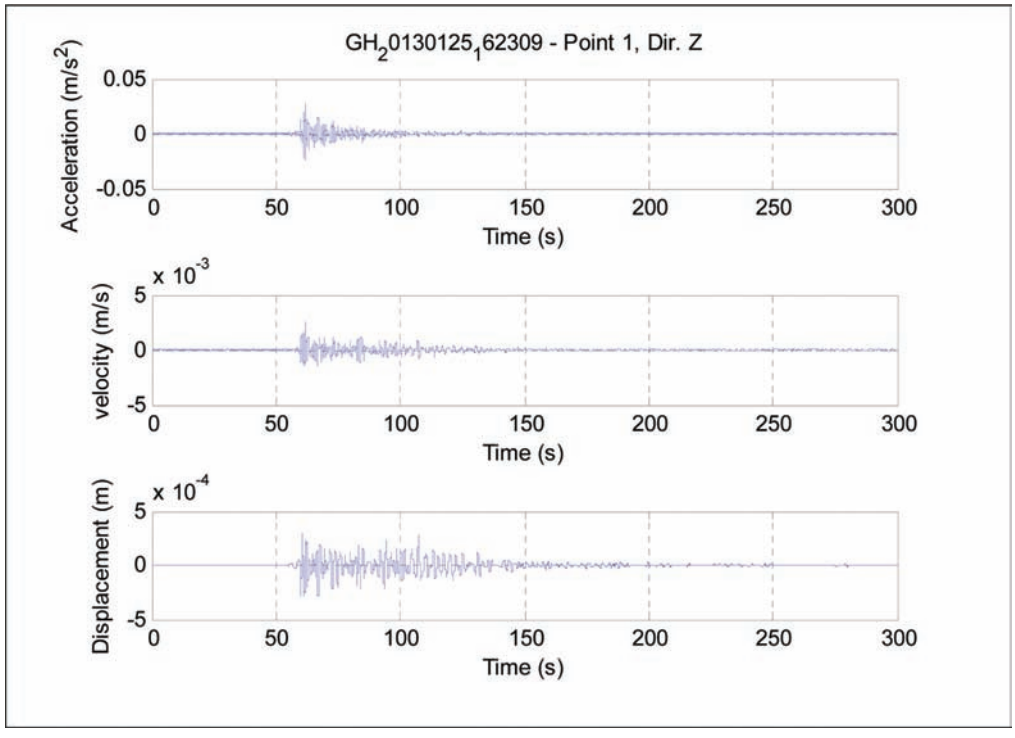

Figure 19. Time histories of acceleration, velocity and displacement along the Z direction. at the base.

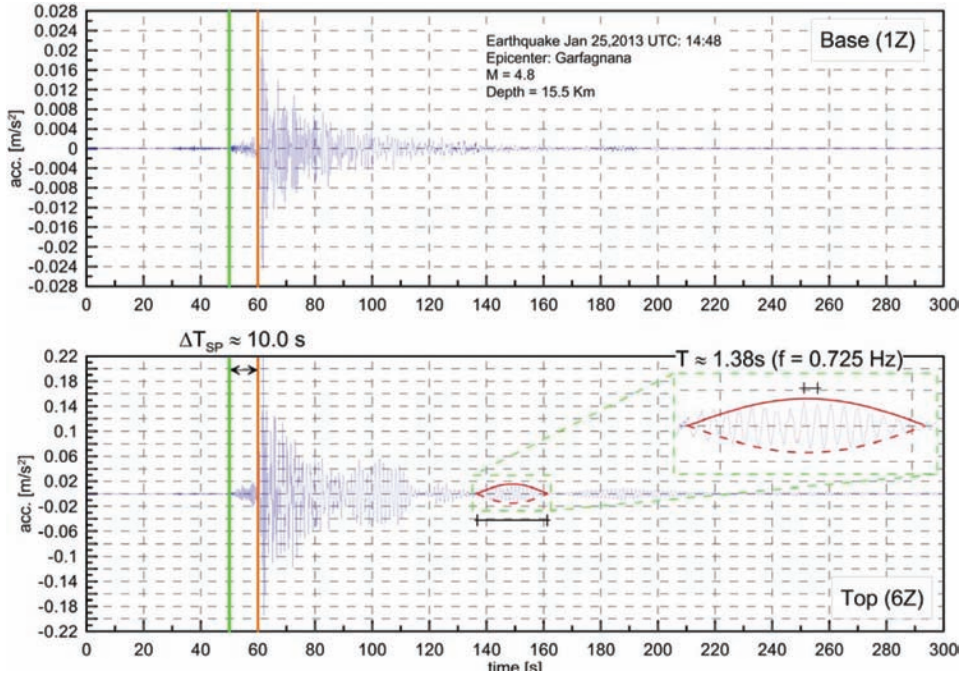

Figure 20. Seismic response of the tower.

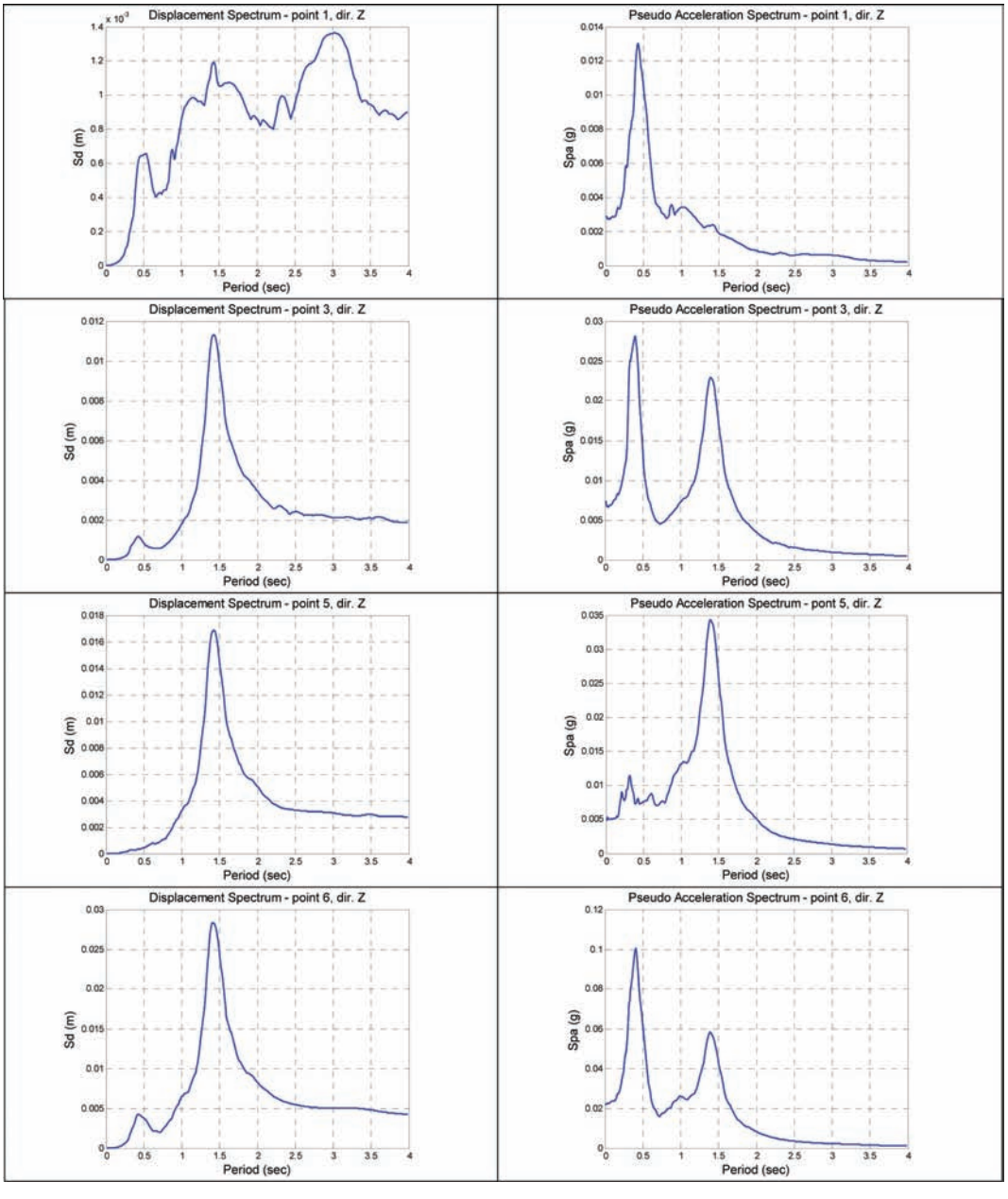

Figure 21. Elastic responce spectra, horizontal direction Z.

paniles, despite the moderate magnitude (M = 5.9) of the seismic event.

Therefore, the possibility to have measurements of acceleration spectra along the axis of the tower greatly enhances our capability of preserving the local and global integrity of the structure.

5 FINAL REMARKS

The case histories, here briefly recalled, prove how monitoring can help in understanding the behaviour of historic towers, in capturing the normal physiological trend, in distinguishing deviations

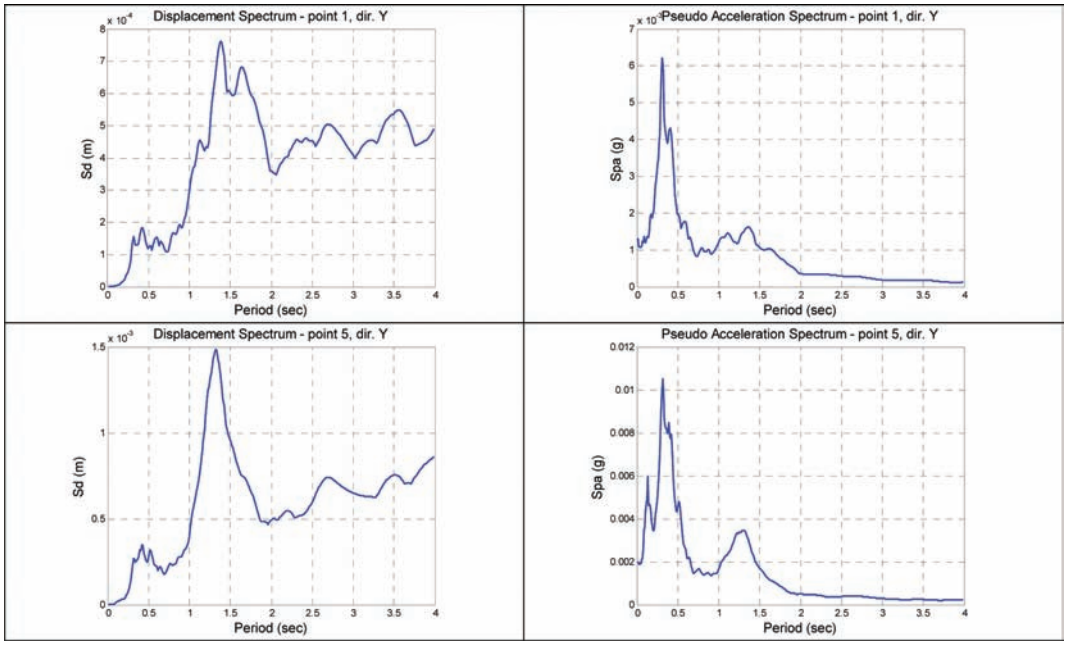

Figure 22. Elastic responce spectra, vertical direction Y.

from this trend and in highlighting the causes of movements. By only devising a diagnosis of these causes the choice of remedial measures can be fully consistent with the principles of restoration and can fullfill both the requirements of survival and integrity of the monument, as it was the case of the tower of Pisa.

There should be no need to stress the importance of the concept of integrity, but quite often this is only interpreted as the requirement of preserving the shape and the appearance of the monument. The requirement of integrity is not so simple, because it also implies historic integrity, by considering the changes the monument experienced with time, as well as material integrity, that means construction techniques, materials and structural scheme. Therefore, preserving integrity requires a multidisciplinary approach as well as to develop the attitude not to rush in deciding the stabilizing measures until the behaviour of the monument is properly understood (Calabresi and D'Agostino, 1997).

The historic towers today we observe survived the initial period in which they could have been not so far from a *bearing capacity* collapse, due to *lack of strength*. And due to uneven settlements, quite often they appear today to survive at an alarming angle of inclination, in some cases not so far from the danger of a *leaning instability*, that increases if there is *lack of stiffness* of the soil.

In order to forecast their long term behaviour as well as their vulnerability with respect to seismic actions, there is a need to model the interaction with the supporting soil and here again monitoring is an essential component to validate any conceptual model as well as subsequent numerical analyses. In addition, a complimentary and effective tool to investigate the material properties and the structural behaviour as a whole comes from identification analyses, as it has been shown for the case of the Ghirlandina tower in Modena.

ACKNOWLEDGMENTS

Most of the results presented in this paper are from the research carried out at Politecnico di Torino for the Municipality of the Modena City. For this reason, the authors are indebted to arch. R. Cadignani, which allowed to perform these tests, and to our collegues Takayoshi Aoki, Daniele Costanzo, Renato Cosentini and dr. eng. Marco Alessio, for their assistance during the execution of the experimental tests.

REFERENCES

Aoki T, Sabia D, Rivella D, Komiyama T. (2007). Structural caracterization of a stone arch bridge by experimental tests and numerical model updating. International Journal of Architectural Heritage, vol. 1, p. 227-250, ISSN: 1558–3058.

Aoki T, Sabia D, Rivella D. (2008). Influence of experimental data and FE model on updating results of a brick chimney. Advances in Engineering Software, vol. 39, p. 327–335, ISSN: 0965–9978.

Bendat J.S., Piersol A.G. (1993). Engineering applications of correlation and spectral analysis. Ed. J Wiley.

Binda L., Gatti G., Mangano G., Poggi C., Sacchi Mandriani G. (1992). The collapse of the Civic Tower of Pavia: a survey of the materials and structure. Masonry Int., 20, 6, 11–20.

Blasi C., Capra A., Coisson E., Lancellotta R. (2009). I dati del monitoraggio per la comprensione dei movimenti della torre Ghirlandina. In La Torre Ghirlandina. Un progetto per la conservazione, Ed. Sossella, Roma, 194–205.

Burland J.B., Viggiani C. (1994). Osservazioni sul comportamento della Torre di Pisa. Rivista Italiana di Geotecnica, 28, 3, 179–200.

Burland J.B., Standing J.R. (1997). Geotechnical monitoring of historic monuments. Proc. of Int. Symp. on Geotechnical Engineering for the preservation of Monuments and Historic Sites, Viggiani C. Ed., Balkema, 321–341.

Burland J.B., Jamiolkowski M., Viggiani C. (2003). The stabilization of the leaning Tower of Pisa. Soils and Foundations, 43, 5, 63–80.

Butterfield R. (1980). A simple analysis of the load capacity of rigid footings on granular materials. Journeé de Géotechnique, 128–134.

Cadignani R. (2009). Un progetto per la conservazione. In La Torre Ghirlandina: un progetto per la conservazione. Vol. 1, 28–39, Sossella Editore, Roma.

Calabresi G., D'Agostino S. (1997). Monuments and historic sites: intervention techniques. Proc. of Int. Symp. on Geotechnical Engineering for the preservation of Monuments and Historic Sites, Viggiani C. Ed., Balkema, 409–425.

Cancelli A. (1986). Aspetti geotecnici della subsidenza. Ambiente: Protezione e Risanamento. Atti 2° Corso di Aggiornamento per tecnici di igiene ambientale. Modena. Ed. Pitagora, Bologna.

Cancelli A., Pellegrini M. (1984). Problemi geologici e geotecnici connessi al territorio della città di Modena. Atti 2° Congr. Naz. ASS.I.R.C.CO., Ferrara, 53–64.

Capra A., Castagnetti C. (2011). Personal communication.

Cavani F. (1903). Pendenza, stabilità e movimento delle torri. La Garisenda di Bologna e la Ghirlandina di Modena. Bologna.

Como M. (1993). Plastic and visco-plastic stability of leaning towers. Int. Conf. Physic-Mathematic and Structural Engineering, in memory of G. Krall, Elba.

Como M. (2010). Statica delle costruzioni storiche in muratura. Aracne, Roma, 902 pp.

Croce A., Burghignoli A., Calabresi G., Evangelista A., Viggiani C. (1981). The Tower of Pisa and the surrounding square: recent observations. Proc. X ICSMFE, Vol. 3.

Desideri A., Viggiani C. (1994). Some remarks on the stability of towers. Symp. on Development in Geot. Eng. (from Harvard to New Delhi, 1936–1994), Bangkok.

Desideri A., Russo G., Viggiani C. (1997). La stabilità di torri su terreno deformabile. RIG, 1, 5.

Dieghi C. (2009). Fonti e studi per la storia della ghirlandina. La Torre Ghirlandina: un progetto per la conservazione. Vol. 1, 48–65, Luca Sossella Editore.

di Prisco C., Nova R., Sibilia A. (2002). Analysis of soil-structure interaction of towers under cyclic loading. Proc. NUMOG 8, Roma, Pande & Pietruszczak eds., Balkema, 637–642.

Di Tommaso A., Lancellotta R., Focacci F., Romano F. (2010). Uno studio sulla stabilità della Torre Ghirlandina. in La Torre Ghirlandina. Storia e Restauro, Ed. Sossella, Roma, 204–217.

Di Tommaso A., Lancellotta R., Sabia D., Costanzo D., Focacci F., Romano F. (2013). Dynamic identification and seismic behaviour of Ghirlandina Tower in Modena (Italy). 2nd Int. Symposium on Geotechnical Engineering for the Preservation of Monuments and Historic Sites, Napoli.

Federico F., Ferlisi S. (1999). Time evolution of stability of leaning towers. VI Int. Conf. STREMAH, Dresden, Brebbia and Jager Edrs, 485–494, WIT Press.

Federico F., Ferlisi S., Jappelli R. (2001). Safety evolution of masonry leaning towers on deformable soils. Proc. ICSMGE, Istanbul, Balkema, 1, 679–682.

Giandebiaggi P., Zerbi A., Capra A. (2009). Il rilevamento della torre Ghirlandina. In La Torre Ghirlandina. Un progetto per la conservazione, Ed. Sossella, Roma, 78–87.

Hambly E.C. (1985). Soil buckling and the leaning instability of tall structures. The Structural Engineer, 63, 3, 77–85.

Heyman J. (1992). Leaning towers. Meccanica, 27, 153–159.

Jamiolkowski M. (2001). The leaning tower of Pisa: End of an Odyssey. Terzaghi Oration, XV ICSMGE Instanbul, Turkey, 4, 2979–2996.

Jappelli R. (1997). An integrated approach to the safeguard of monuments: the contribution of Arrigo Croce. Proc. of Int. Symp. on Geotechnical Engineering for the preservation of Monuments and Historic Sites, Viggiani C. Ed., Balkema, 11–27.

Labate D. (2009). Il contributo dell'archeologia alla lettura di un monumento. La Torre Ghirlandina: un progetto per la conservazione. Vol. 1, 66–77, Sossella Editore, Roma.

Lancellotta R. (1993). The stability of a rigid column with non linear restraint. Géotechnique, 33, 2, 331–332.

Lancellotta R. (2009). Aspetti geotecnici nella salvaguardia della torre Ghirlandina. In La Torre Ghirlandina. Un progetto per la conservazione. Ed. Sossella, Roma, 178–193.

Lancellotta R. (2009.a). Geotechnical Engineering. Taylor and Francis, London, 499 pp.

Lancellotta R. (2013). La torre Ghirlandina: una storia di interazione struttura-terreno. XI Croce Lecture, to appear on Rivista Italiana di Geotecnica.

Lugli S., Marchetti Dori S., Fontana D., Panini F. (2004). Composizione dei sedimenti sabbiosi nelle perforazioni lungo il tracciato ferroviario ad alta velocità: indicazioni preliminari sull'evoluzione sedimentaria della media pianura modenese. Il Quaternario, Italian Journal of Quaternary Sciences, 17, 379–389.

Macchi G. (1993). Monitoring medieval structures in Pavia. Structural Engineering International, 1, 9–9.

Marchi M., Butterfield R., Gottardi G., Lancellotta R. (2011). Stability and strength analysis of leaning towers. Géotechnique, 61, 12, 1069–1079.

Ministero dei Lavori Pubblici (MLLPP) (1971). Ricerche e studi sulla Torre Pendente di Pisa e i Fenomeni Connessi alle Condizioni d'Ambiente.

Nova R. (1982). A viscoplastic constitutive model for normally consolidated clay. Proc. IUTAM Symp. on Deformation and Failure of Granular Materials, P.A. Vermeer Luger eds, Delft, 287–295.

Nova R., Montrasio L. (1995). Un'analisi di stabilità del campanile di Pisa. Rivista Italiana di Geotecnica, 2, 83–93.

Paolucci R., di Prisco C., Figini R., Petrini L., Vecchiotti M. (2009). Interazione dinamica non lineare terreno-struttura nell'ambito della progettazione sismica agli spostamenti. Progettazione Sismica, 2, 83–103.

Pepe M. (1995). La Torre pendente di Pisa. Analisi teorico-sperimentale della stabilità dell'equilibrio. Tesi di Dottorato, Politecnico di Torino.

Piccinini F. (2009). Note sul cantiere del Duomo e della Ghirlandina: Lanfranco, Wiligelmo, i Campionesi e il Comune medievale a Modena. La Torre Ghirlandina: un progetto per la conservazione. Vol. 1, 42–65, Luca Sossella Editore.

Prager W. (1955). The theory of plasticity: a survey of recent achievements. Proc. Inst. Mech. Eng., 169, 41–57.

Righi P.V. (1980). Rilevamenti geotecnici nel sottosuolo del Palazzo Nazionale di Modena. Atti XIV Conv. Naz. Geotecnica, Firenze, 1, 257–266.

Russo P. (1985). L'abbassamento del suolo nella zona di Modena (1950–1982). Tecnica Sanitaria, XXIII, 293–3.

Sabia D. (2012). Rilievo e analisi delle vibrazioni della Torre Ghirlandina di Modena. Contratto di Ricerca tra Comune di Modena e Politecnico di Torino.

Van Overschee P. and De Moor B., (1996) Subspace Identifcation for linear Systems: theory-Implementation-Applications. Dordrecht, Netherlands: Kluwer Academic Publishers.

Geotechnical Engineering for the Preservation of Monuments and Historic Sites – Bilotta, Flora, Lirer & Viggiani (eds)
© 2013 Taylor & Francis Group, London, ISBN 978-1-138-00055-1

Intervention techniques

E. Ovando-Shelley
Instituto de Ingeniería, Universidad Nacional Autónoma de México, Mexico City, Mexico

E. Santoyo
TGC Geotecnia, Geotechnical Consultants, Mexico City, Mexico

M.O. Pinto de Oliveira
Formerly at Instituto de Ingeniería, Universidad Nacional Autónoma de México, Mexico City, Mexico

ABSTRACT: In this paper we review the factors that produce damage in architectural monuments and ponder on how they should be assessed in order to put forth solutions that are not only technically acceptable but that are also satisfactory from the view point of conservationists, archaeologists, historians and even politicians. Intervention techniques must consider the extent and nature of damage in the monument from which a range of technically feasible solutions can emerge. Certain solutions may be rendered as temporary or as permanent, depending on circumstances which may not be solely technical. We discuss interventions that are intended to correct or mitigate the effects of the damaging agents. We also review actions that aim at preventing the accumulation of further damage. In this paper we also look at some solutions that are less commonly used and in which soil properties or stress states are modified conveniently to achieve the proposed goals.

1 INTRODUCTION

Interventions in architectural monuments are indefectibly associated to the notions of restoration and preservation. To restore and preserve, actions on monuments must prevent, avoid or mitigate structural damage. A necessary first step towards restoring and preserving a monument is to identify the factor or factors that bring about damage. On many occasions those factors fall within the sphere of Geotechnical Engineering. According to some specialists, "the origins and general cause of damages are in general of geotechnical nature" (Calabresi and D'Agostino, 1997). Interventions however, can fall within a broader range of areas, most notably, in the field of Structural Engineering but the participation of architects, archaeologists, historians, restoration experts is vital in many cases.

Structural damage can be usually related to either stress or strain concentrations which are the result of the accumulation of unwanted deformations. The latter may result because supporting elements are undergoing deformation caused by stress and strain changes in the ultimate supporting element, the soil. Geotechnical engineers may then collaborate with structural experts to determine whether the situation involves risk or not, in the present and in the future. They may also provide estimates about the evolution of security conditions with time. The selection of the intervention technique to be applied may not only be left to the geotechnician and or the structural experts: it may be required that architects, archaeologists, conservationists, historians and even politicians participate in this decision.

Solutions to geotechnical problems in architectural monuments have almost entirely been drawn from the field of Foundation Engineering so that the resulting intervention techniques constitute applications of that branch of geotechnics giving due consideration is given to the notions of preservation and conservation, as stated previously. These techniques have been comprehensively described in the past and their relative merits and drawbacks have also been discussed previously (Calabresi and D'Agostino, 1997; Pinto de Oliviera, 2008; Santoyo, 2010). Rather than providing yet another catalogue of intervention techniques, in this paper we review the causes that originate problems in architectural monuments and point out a possible manner in which the identification of the factors originating these problems relate to the selection of adequate corrective or preventive measures. We also describe a set of less used or less known intervention techniques.

2 CONCEPTUAL FRAMEWORK

Before acting on a monument it is useful to have a conceptual framework with which geotechnical engineers will gain insight into the nature of the problem and within which the applicability and efficacy of plausible intervention techniques to solve the problem under consideration can be assessed qualitatively. However, field exploration and testing as well as laboratory studies must precede the building up this framework since it requires a detailed knowledge of the geological and geotechnical environment at the site. Soil and foundation conditions must be determined in as much detail as possible. Soundings, pits, exploratory shafts can all be used but field investigation must be planned and executed carefully, to avoid damaging the monument. The study of soil conditions must also aim at the reconstruction of the effective-stress-history at the site. In this context historical research must not be limited to the building, it must also include the soil. Historians and archaeologists can provide useful data and information. Documentary research is also required in this respect. Take for example the graphs shown in Figure 1 where both historical data and engineering criteria were used to reconstruct stress paths for typical soil elements under the western tower of the Metropolitan Cathedral in Mexico City from its depositional stage to the present. The effects of the intervention with mortar grouts which are discussed later, were taken into account. As seen in Figure 1, stress conditions result from a complex process that can be schematically divided into the following stages:

a) The deposition of the clays in the lacustrine environment, undergoing large vertical deformations but with no lateral strains is represented by segment 0–1 in Figure 1. It can be expected that in the early stages of human occupation in the Basin of Mexico in pre-Aztec times, about 1200 years ago, the soil was normally consolidated or even underconsolidated. Long periods under sustained stresses also induced important deformations due to secondary consolidation during which, according to some authors (Mesri, 1993), horizontal stresses tend to increase (segment 1–2 in Fig 24).
b) Stress changes produced by the construction of prehispanic structures became significant early in the XIVth century (segment 2–3 in Figure 1). In the specific case of the site where the Cathedral was later erected, it is very likely that prior to the edification of pyramids and palaces within the Aztec ritual precinct, a large earthen platform was first erected to reclaim land from the lake (Mazari et al, 1985). The pyramids were then built and it is also likely that, at least during some periods, construction was so fast that the subsoil was, in some cases, close to an undrained failure condition. Archaeological and geotechnical data give a fair idea of the general distribution of the ancient prehispanic structures but their actual volumes and, hence, the magnitude of the surcharges imposed by them can only be very roughly approximated (Ovando-Shelley and Manzanilla, 1997).
c) After the Spanish Conquest in the XVIth century, the prehispanic structures were almost totally demolished. Re-loading of the subsoil during the construction of the Cathedral (1573-1813) is represented by segment 3–4 in Figure 1. Again, fast construction periods induced local failures (architectonic evidence and historical chronicles suggest, for example, that the western tower tilted dangerously towards the northwest when the vaults were nearly finished, before the Cathedral's second dedication in 1666). Other portions of the subsoil may have been left in a close to failure condition before excess pore pressures dissipated.
d) By the mid XIXth century self weight consolidation was over. At that time water pumping began in the city and a regional consolidation process began, due to the gradual depletion of pore water pressure within the clay masses (segment 4–5 in Figure 1). The process continues to this day and it has induced large differential settlements due to the non uniform distribution of compressibilities at the site (a consequence of the previous loading stages before and after the construction of the Cathedral and the Sagrario Church).
e) Further changes in stress conditions were brought about by interventions in the foundations during the 1940s and the 1970s, as described previously but these are difficult to assess and as described previously, their effects were unimportant. After the 1970s intervention, the structures were again exposed to the effects of regional subsidence until underexcavation began in September, 1993. Underexcavation produced more changes in stress conditions. These are mainly due to local pumping from the bottom of the soil extraction shafts over a nearly five years. At locations that were not underexcavated, like the base of the western tower, these effects are minor.
f) Injection of mortars increases total lateral stresses and consequently shear stresses will reduce (segment 5–6). Dissipation of excess pore pressures induced during mortar injection then follows (segment 6–7).
g) Results of topographical levellings showed that it took between 200 and 300 days to appreciate reductions in settlement rates (Ovando and

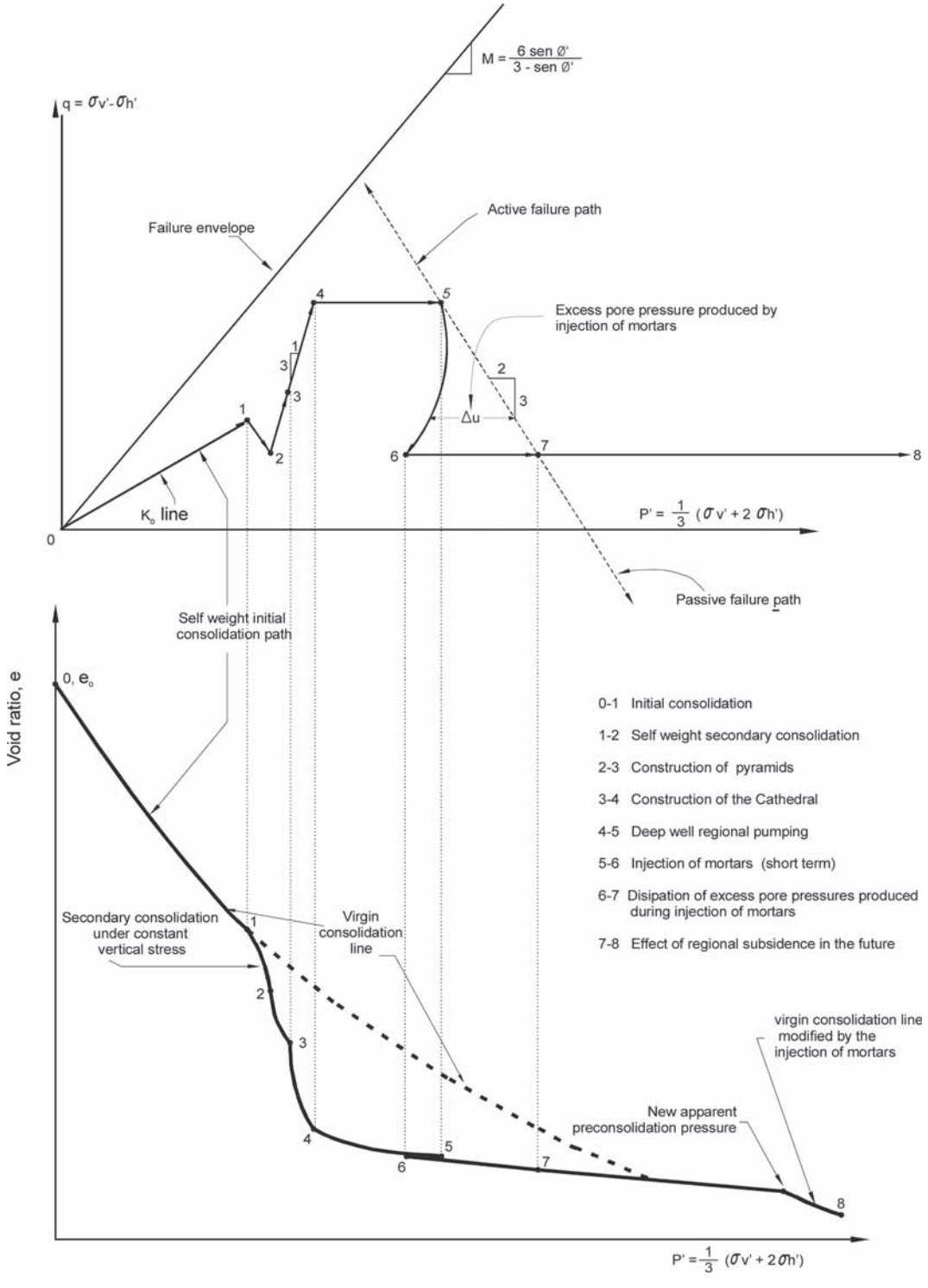

Figure 1. Historical and geotechnical reconstruction of typical soil conditions at the Metropolitan Cathedral in Mexico City.

Santoyo, 2001; Santoyo and Ovando, 2004). Once this stage is reached, the treated clay mass is again exposed to the effects of regional subsidence. In the future, as the exploitation of the aquifers continues consolidation under constant deviator stress will again be present but the injected clays will follow a new consolidation path in the p'-e space.

They will now be less compressible and will also exhibit a higher apparent preconsolidation pressure, as discussed previously (segment 7–8).

3 BEARING CAPACITY PROBLEMS

In old buildings bearing capacity problems are by far the less frequent—they occur mainly in the short term. They usually arise if a disrupting agent introduces changes in the prevailing geotechnical conditions. Natural agents like torrential rains, flooding or earthquakes, even tsunamis in coastal areas, may reduce shear strength or increase applied stress leading to bearing capacity failures. Anthropic agents can be equally disrupting and in the case of bearing capacity problems, are mainly related to man-induced changes in water content within soil masses like leakage from cisterns, sewage or water supply lines, construction of dams or channels, or, among others, excavations in neighbouring sites, construction of buildings in the vicinity or tunnelling under the monument.

4 SETTLEMENT RELATED PROBLEMS

Regarding foundations, a large number of problems in architectural monuments have their origin in the accumulation of differential settlement which may give rise to inclinations, tilts and eventually to structural damage. Even if a monument settles more or less uniformly without undergoing significant structural damage itself, settlement troughs around it can disrupt service lines (gas, telephone, water supply, and sewage) and damage neighbouring structures or urban infrastructure.

Differential settlements increase vulnerability to environmental hazards such as earthquakes or flooding. Significant differential settlements are present in many ancient buildings and their importance, seen in terms of their detrimental effects, depend as much on local soil conditions as on the structural and geometrical characteristics of the building. Building materials, construction techniques and structural systems must be studied and investigated. Many other factors can influence the apparition, evolution and consequences of differential settlements. The key point in dealing with a differential settlement-related problem is to identify the factors or sources that originate settlement differentials. Specificity and precision in this respect are necessary. However, in a large number of cases it is impossible to point out a single source or origin because the factors that originate differential settlements usually turn up combined or are interrelated.

We discuss and comment briefly on some of the most common factors originating the apparition of differential settlements:

Design errors. Normally, design errors affect a structure shortly after its construction but their effects and consequences may span over much longer periods of time. It has even suggested that it may take a very short time for trouble to turn up, as postulated by Heyman (1995), in his five minute rule. Some of these arise from lack of technical elements to assess working conditions in structural elements or in the foundation. The structure may remain stable for decades or even centuries but external factors (natural or anthropic) may eventually trigger unwanted or potentially dangerous situations that may have otherwise remained dormant.

Construction errors. These result from either technological limitations or shortages to guarantee proper craftsmanship; examples: the inability to obtain fully vertical columns or to achieve right angles at corners, the lack of proper compaction of fills, remoulding of soils at foundation level, etc. Figure 2 shows an example in which right angles were not achieved in walls and there is misalignment of structural axes. In this case, the House of Tiles in Mexico City (Casa de los Azulejos), these details had no major effect on the behaviour of this structure, a XVIIth century construction (Pinto de Oliveira, 2008).

Changes in buildings. They refer to changes in use and in general refer to modifications in the loads carried by the structure and their distribution within it. Structural modifications may also change loads transmitted to foundation elements and, eventually, to the subsoil. Many structures

Figure 2. Plan view of the XVIIth century House of Tiles (casa de los azulejos) in Mexico City showing construction errors.

underwent these changes in the past. Presently authorities and international organizations tend to impose strict regulations to allow alterations in architectural monuments. Changes in buildings also refer to use. It is not uncommon that ancient structures become museums, offices, shops, stores or factories. Operation of such establishments or businesses may require that live loads be concentrated in spaces and zones not originally conceived to bear heavy weights which can eventually overstress foundation elements and produce settlements in the supporting soil.

Increase of water content or humidity. Removal of large trees near structures may induce swelling, a situation that has been identified as a major contributor to damage in many countries. Dam impoundment will flood large areas and may give rise to regional changes in hydraulic conditions in the subsoil that can conceivably affect architectonic monuments. Flooding originated by meteorological phenomena can produce similar effects. Water penetrating into open fractures or fissures in the soil mass can de-stabilize slopes as a result of alterations in pore pressure distribution. Leakage from cistern, water depositories, and septic tanks or from sewage or water supply lines will also have detrimental effects.

Existence or construction of underground structures. Existence of buried structures or conspicuous geotechnical heterogeneities should be identified in field investigations. Construction of tunnels or underground structures of any kind in the vicinity of the monument must always be designed to avoid any damage to the monument, including the design of suitable construction procedures. Preventive rather than corrective measures are required in this respect. Pre-existing underground structures must be inspected and monitored to prevent unwanted conditions in the monument, looking carefully at agents, factors or conditions that could possibly bring about potentially dangerous changes in effective stresses.

Geotechnical peculiarities at the site. Usual techniques to define stratigraphy, soil properties, and hydraulic conditions may not always be applied to avoid damage in the monument or its surroundings. It may also be necessary to investigate and identify geological processes or geological structures affecting the monument. Erratic distribution of soil properties, mainly strength and compressibility, can have a major influence on the behaviour of a monument as well as variations in the thicknesses of relevant soil strata.

Extraction of water from soil mass or soil drying. Introduction of vegetation, mainly trees, will modify the distribution of water content within the underlying soil mass, a situation that can induce differential deformation of the bearing soil mass (see Figure 3). This factor is frequently overlooked. Repair of water leaks in flooded basements will also change water content locally, under and around the structure. Operation of water wells in the vicinity of the structure may also induce detrimental settlements. Regional subsidence produce by extraction of water on a larger scale will most likely induce the apparition of differential settlements which can affect the monument.

Excavations. Retaining structures or systems in large excavations near monuments should be carefully designed, including a careful evaluation of the effects of de-watering systems. Construction procedures should also be designed to avoid damage in the monument or its surroundings. The case shown in Figure 4 illustrates an excavation in volcanic rocks for an open pit mine performed next to a XVIIth century church in San Luis Potosí, Mexico. The excavation is programmed to reach a maximum depth of about 300 m. Even though analyses performed by the mining company showed that the safety and permanence of the church are not endangered, the case has caused concern in social groups and in the institutions charged with preserving cultural heritage in Mexico.

Construction of new structures. New structures built near a monument may also affect it. This situation not only refers to the interaction

Figure 3. Large trees may endanger old buildings and important architectonic monuments.

between the ancient and the new structure, it should also consider the effects of construction and operation of service lines (gas, electricity, telephone, water supply, sewage).

Slope instability. Many important architectural monuments are located on or near sloping grounds that can eventually be subjected to unwanted deformations. Safety conditions will be altered by the same factors that affect any slope and standard stabilization procedures will in general be applicable for deep seated failure mechanisms; local failure mechanisms affecting the monument may require special attention. In the case shown in Figure 4, a deep seated failure would inevitably imply the destruction of the church and remedial measures to prevent it would be highly costly and surely impractical. Local mechanisms could be dealt with more easily, as in the case illustrated in Figure 5, a XVIth century convent south of Mexico City (Santoyo, 2010). Local failures were stabilized with retaining structures, but stabilizing the deep seated mechanism would probably require a combination of anchors and deep horizontal drains.

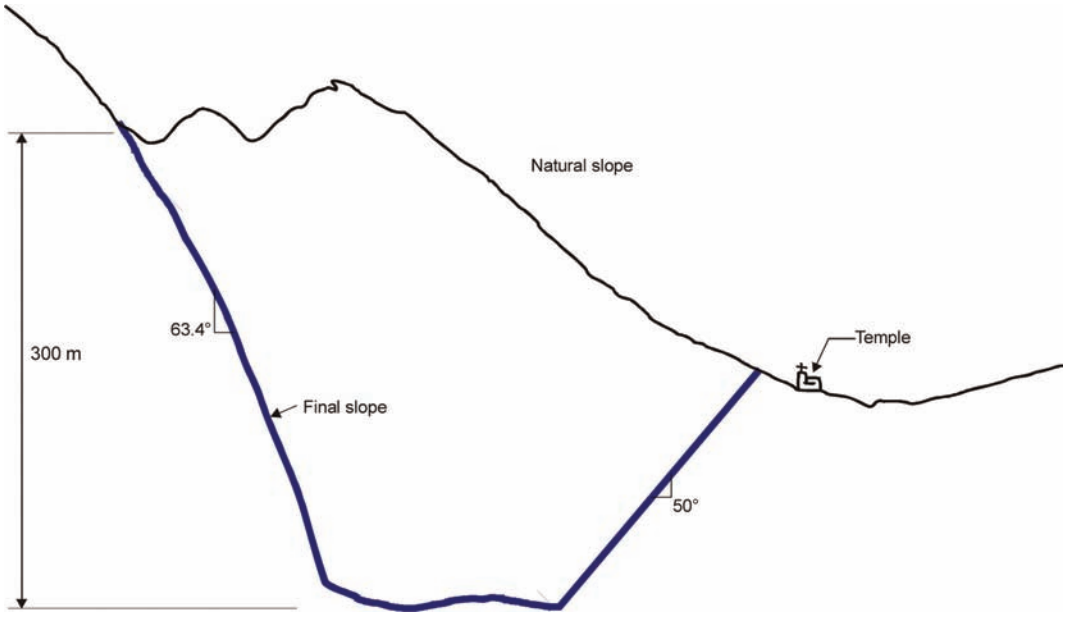

Figure 4. Excavation in volcanic rocks for an open pit mine performed next to a XVIIth century church in San Luis Potosí, Mexico.

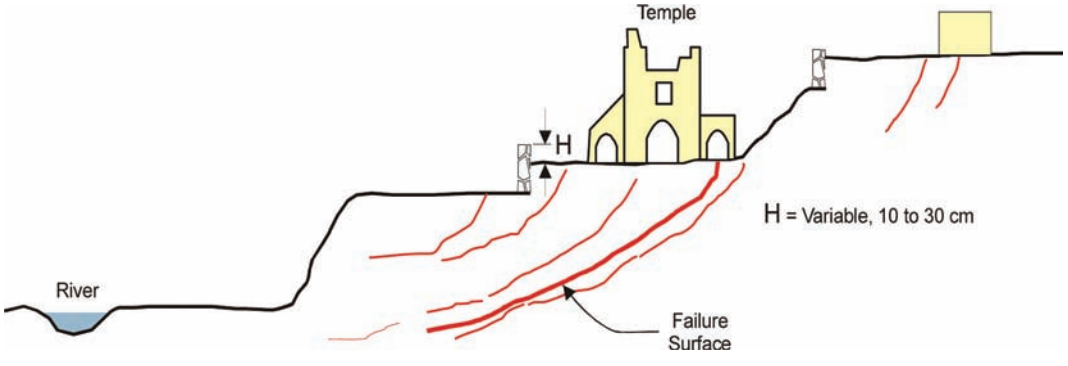

Figure 5. Local and deep seated failure mechanisms affecting a XVIth century temple south of Mexico City (Santoyo, 2010).

Earthquakes. Seismic events affect architectural monuments successively over long periods of time. Gradual accumulation of damage brings increases seismic vulnerability as a building deteriorates through time (Ovando-Shelley et al, 2007). One of the causes of concern regarding the safety of the tower of Pisa was its exposure to seismic events given that its vulnerability to such phenomena had been continuously increasing with time, (Jamiolkowsky et al, 1999, 2001). Similarly, the seismic vulnerability of the west tower of the Metropolitan Cathedral became unacceptable in 1989 and it was one of the factors that prompted a major intervention in the temple afterwards (Tamez et al, 1997). All the other factors listed previously can affect seismic stability. Preventive rather than corrective measures must be sought in dealing with seismic hazard.

Assuming that the originating factors have been identified, interventions in the soil may be grouped according to the nature and magnitude of the damage and depending, also, on the scope and magnitude of the project, not forgetting budgetary considerations. Interventions can, in general, be arranged into four groups, according to Calabresi and D'Agostino (1997).

a) Installation of rigid elements into the soil in order to transfer loads to deeper strata, or to modify stress distributions within the soil mass, typically any form of rigid inclusion such as shafts, piles, micropiles, tendons, piles not connected to the structure, etc. These measures can also include underpinning or enlarging existing foundations.
b) Addition of substances to modify soil properties, i.e., chemical or cement grouts, or jet grouting.
c) Modification of stress state inside the soil mass by inducing changes in pore pressure, induction of water flow by electro-osmosis or by applying external loads (pre-loading), by inducing discontinuities in the soil mass, by the use of compensation grouting or injections to modify the compressibility of the soil mass.
d) Measures to control the original conditions of the soil strata or the structure: humidity control, restoration or removal of vegetation, bacterial protection in foundation elements, removal of added non-original elements, etc.

Intervention techniques based on the installation of rigid elements are still very common. Driving piles or drilling boreholes to install pre-cast or cast-in-situ elements may damage culturally rich strata and that is why conservationists tend to favour other less obstructive techniques. Improved techniques for drilling small diameter micro-piles or inclusions are less intrusive but they can still damage historical or archaeological elements. Jet grouting and the injection of cement, lime or grouts with other chemicals can modify soil properties and are less common. Techniques of the third group are also less popular. They aim at modifying effective stresses or displacement fields in the soil mass, to correct unwanted deformation. Interventions of the last group aim at maintaining favourable present condition or at preventing exposure of the monument to future risks.

5 SELECTION OF INTERVENTION TECHNIQUES

The level and scope of the intervention must be pondered carefully. Apart from other factors, selecting the type, magnitude and nature of any remedial measure to eliminate, counteract or mitigate the effects of differential settlements and/or to increase bearing capacity, is a process influenced by the degree of damage already present in the monument.

Drastic measures may be required in highly damaged structures. In any case, non obtrusive techniques must be preferred. Economic or budgetary restrictions may also limit the level and scope of the intervention at the foundation level. Remedial measures may act over limited periods of time, interim or temporary solutions, or may have irreversible effects and be permanent.

Interim or temporary solutions. These can be adopted if the causes originating damage are not fully understood or have not been precisely identified. Solutions of this nature can also be adopted as part of a well defined project in which the specific causes originating the problem have been identified and are well established.

Ballast, applied on certain areas in a monument or next to it to induce corrective settlement to compensate inclinations and tilts may very seldom be conceived as a permanent solution (e.g. the Tower of Pisa, and many buildings in Mexico City). Water pumping at selected sites and electro osmosis are also, by nature, interim or temporary solutions.

The application of these measures spans over a limited, well defined period of time but some of its effects may prevail or be effective far longer.

In what refers to its effects, also intended to produce corrective settlements, underexcavation is also a temporary measure which may even require its periodic application.

Permanent solutions. These refer to those that imply modifications in the original foundations in which no come back is possible or in which no such possibility is considered in the project. Examples of these are underpinning, broadening of footings, addition of new footings, of piles or interventions

Table 1. Origin of differential settlements and influencing factors.

Origin or source	Influencing factors
Design errors	1. Architectonic, geotechnical, structural (combinations of any of these)
Construction errors	2. Inability to obtain verticality or right angles in walls, ceilings, etc.
	3. Alteration (remoulding) of soil at foundation level
Changes in buildings	4. Increase of dead weight
	5. Flooding of basements
	6. Architectural or structural alterations
Increase in water content or humidity in the soil mass	7. Removal of trees
	8. Dam impoundment
	9. Flooding
	10. Water penetrating into open fractures or fissures in soil mass
	11. Breakage of sewage or water supply lines
	12. Leakage from cisterns or water depositories
Existence or construction of underground structures	13. Construction of underground structures (car parks, shafts, structures for hydropower projects)
	14. Tunnelling (mines, railways, roads, sewage or water supply)
Geotechnical peculiarities at the site	15. Buried structures
	16. Erratic distribution of compressibilities
	17. Variations of thicknesses of soil strata
Extraction of water from soil mass, soil drying	18. Introduction of vegetation (mainly trees)
	19. Removal of water from flooded basements
	20. Local influence of pumping wells
	21. Regional subsidence
Excavations	22. Excavations near the monument, mainly in urban areas
Construction of new buildings	23. Obliteration of archaeological evidence
	24. Unwanted effects on existing monument
Slope instability	25. Cuts to modify slope inclination
	26. Humidity at slope feet along rivers, seafront, lakes
	27. Leakage from sewage or water supply systems
	28. Deforestation leading to erosion
	29. Slope subjected to long term geological processes (creep)
Earthquakes	30. Accumulated tilt
	31. Low bearing capacity
	32. Low factor of safety in slopes

to modify soil properties (soil improvement), etc. Remedial measures may also be classified as preventive or corrective.

Corrective measures. These arrest or mitigate the effects of differential settlements, tilts or structural damage arising from them, as indicated in Table 2. They may not necessarily eliminate the factors that originate differential settlements. On occasions corrective measures are necessary when unforeseen factors modify the conditions at the site (e.g. by leakages from cisterns, water supply or sewage lines, removal or addition of trees, etc.). Underexcavation, for example, may need to be applied periodically in many cases since it does not eliminate the factor that gives rise to differential settlements.

Preventive measures. These are intended to prevent the detrimental effects of differential settlements or to prevent further accumulation of damage. Preventive measures may be applicable when conditions at the site are somehow modified (e.g. by nearby cuts, excavations, tunneling, etc.). In many cases adoption of these measures also implies elimination of the originating factor (see Table 3).

6 NON CONVENTIONAL TECHNIQUES

Most corrective or preventive intervention techniques described in Tables 2 and 3, are commonly

Table 2. Intervention techniques to correct, arrest or mitigate the effects of differential settlements.

Method	Advantages/disadvantages	Important examples
Underexcavation	Effects may be difficult to predict or estimate. Relies heavily on observational method. Adaptable to a large variety of conditions. May require auxiliary works (trenches, shafts) or specialized drilling equipment. Non obtrusive. Rate of induced corrective settlements may be controlled.	Oldest documented case dating back to 1835 (St. Chad's Bell Tower in the UK); Tower of Pisa, Mexico City Cathedral.
Jacking from pile heads	Piles must first be installed or cast in place. Major structural modifications required in the monument's foundation system. Superstructre must be adapted and/or reinforced to tolerate imposed movements. Rate and magnitude of corrective vertical displacement can be accurately controlled.	Has been applied successfully in several parts of the world.
Control piles	Piles connected indirectly to the building by means of a frame. May be used to regulate loads applied at the pile heads or to directly control settlements. Modifications at foundation and at the superstructure level required. Permanent maintenance required.	Developed in the late 1940's in Mexico City. Used successfully in several monuments.
Piles at selected sites	Special and very specific geotechnical conditions must be met in order to use this technique, e.g. at sites undergoing regional subsidence.	Several important buildings and monuments in Mexico City. Used as an interim solution in Mexico City's Sagrario Church.
Local injection of water	Intended to restore pore pressure at selected locations in sites undergoing regional consolidation. Induced corrective settlements are difficult to control.	Used experimentally in Mexico City's National Palace (1978) and in a late XVIIth century house (1984). Results up to date are not conclusive.
Electro-osmosis	Put forth to induce water flow and changes in effective stress and, hence, corrective settlements. Difficult to control	Tried and abandoned in Mexico City in the seventies. Used experimentally at the Tower of Pisa.

used in Foundation Engineering and have been described comprehensively by many authors (for example by Calabresi and D'Agostino, 1997; Pinto de Oliveira, 2008; Santoyo, 2010).

In what follows, se discuss some lesser known techniques that have been applied by the authors over the last few years, mainly in Mexico.

6.1 *Control piles*

These piles were created by a Mexican engineer, Manuel González Flores and were first used in the late 1940s. They are driven into the soil and are not connected structurally to the foundation slab. Loads on the pile are applied by means of the reaction frame illustrated in Figure 6. As seen there, the pile head will emerge relative to the slab floor, as the structure settles. Layers of deformable wooden cubes are placed between the pile head and the transversal steel beam. The magnitude of the load applied on the pile head depends on the mechanical properties of the wooden blocks and the number of them.

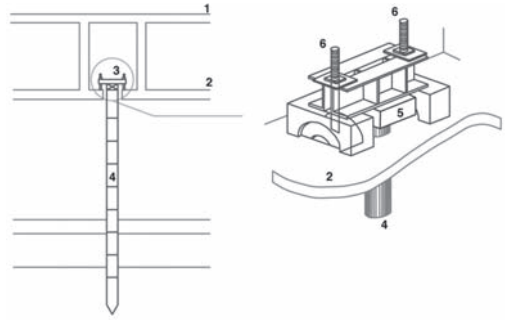

Figure 6. Schematic representation of a control pile. Key: 1) top slab of box foundation; 2) base slab; 3) control device; 4) semented pile; 5) array of wooden blocks; 6) reaction frame.

The graph in Figure 7 shows schematically a load-deformation curve for a typical array of wooden cubes. The yield load of the array will limit the magnitude of the load applied at the pile

Table 3. Intervention techniques to prevent the detrimental effects of differential settlements.

Method	Advantages/disadvantages	Important examples
Underpinning: broadening of footings, restoration of origi nal foundation elements	Used to restore or improve condition of existing foundation. Effective, depending on proper identification of originating factor and on good knowledge of geotechnical conditions.	Has been used in many monuments and historical buildings around the world.
Addition of piles, micropiles or other deep foundation elements	Can usually eliminate the originating factor giving rise to differential settlements. Can disrupt, damage or even completely destroy archaeological data.	Has been used in many monuments and historical buildings around the world.
Soil improvement: jet grouting, deep mixing	Can be difficult to implement; it is sometimes intrusive (can produce damage to archaeologically rich deposits or ancient buried structures).	Mortar injection by hydrofacturing Cathedral.
Injection of mortars by hydrofracturing in soft soils	Can be difficult to implement; it is sometimes intrusive (can produce damage to archaeologically rich deposits or ancient buried structures).Overall intended effect: to attain a more uniform distribution of settlement or vertical deformation fields.	Used successfully at the Metropolitan Cathedral and the San Agustín Church in Mexico City.
Compensation grouting	Can be difficult to implement; it is sometimes intrusive (can produce damage to archaeologically rich deposits or ancient buried structures). Overall intended effect: to induce corrective vertical deformations to compensate other non wanted movements.	Used in the Jubilee line in London.
Rigid inclusions	Can be difficult to implement; it is sometimes intrusive (can produce damage to archaeologically rich deposits or ancient buried structures). Overall intended effect: to attain a more uniform distribution of settlement or vertical deformation fields. Rigid inclusions are not connected to structure.	Not proven in Architectural Monuments. Several projects have been put forth in several ancient structures in Mexico City.
Isolation or separation trenches	Slurry trenches can be used to separate or isolate displacement fields of two or more structures. Non setting gels may be also used.	Used at the Capilla de las Ánimas and the Casa de Los Azulejos, Mexico City. Results are still being evaluated. Suggested as a means to correct the inclination of the Tower of Pisa.

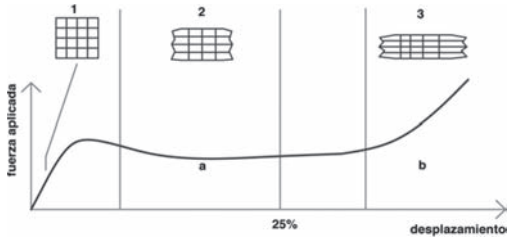

Figure 7. Load deformation curve of an array of wooden blocks in a control pile. After yielding, the blocks will deform continually and will take further load when deformation exceeds 25% of the cube side.

head. Yielding of the array depends on the number of cubes, so the magnitude of the applied load can be readily calculated if the load-deformation properties of the cubes are known. As yielding takes place, the wooden curves deform and will eventually harden when reaching a deformation of about 25% of the cube's side; the pile will again take load unless the cubes are replaced. Cubes need to be replaced at least once a year throughout life time of the building.

I should be noted that control piles cannot carry tension loads and this is a major drawback in seismically active regions where tension capacity is

required to equilibrate overturning moments during earthquakes. Referring back to Figure 6, it is also evident that another limitation of system is its restricted capacity for taking horizontal loads perpendicular to the plane of the reaction frame, i.e. it won´t be capable of taking seismic base shears.

Control piles are point bearing elements and their capacity can be seriously reduced by negative friction (down drag) if their tips underlie soft materials subjected to a consolidation process. This condition can be overcome by surrounding the pile with a deformable, external sheath, as shown schematically in Figure 8. The annular space between the sheath and the pile is filled with grease so that negative friction forces will not be transferred to the pile.

Despite its limitations, control piles have been used in a rather large number of buildings in Mexico City, some of which have had a less than satisfactory behavior during large earthquakes. Control piles have been also used for underpinning rigid modern buildings that can allow continued maintenance operation for these piles which imply the temporary removal of the reaction frames and eventually, the trimming of the pile caps.

Regarding architectural monuments, control piles were successfully used to level the bishopric next to the Guadalupe Basilica in Mexico City (Santoyo, 2010). They have also been used in at least five other important monuments, most notably the Metropolitan Cathedral where 390 of them were installed in the mid 1970s and only about one third worked properly (Tamez et al, 1997; Ovando-Shelley and Santoyo 2001). That is one of the reasons that later (early 1990s) prompted the next major intervention in the Cathedral.

6.2 *Underexcavation*

According to Johnston and Burland (2000), the late Prof. Skempton discovered what is possibly the earliest documented example of underexcavation, the inclined tower at St Chad's church in Wybunbury in South Chesire, England that was underexcavated by Charles Trubshaw in 1832. There is also evidence to the use of the method in 1866, on a 100m chimney at the Bochum cast steel works in Germany and in the same year on an inlcined church tower in the Netherlands.

This technique was suggested as a means for correcting some of the inclination of the Tower of Pisa by the Italian engineer, Ferando de Terracina, as illustrated in Figure 9 (Terracina, 1962).

For the Mexican Cathedral it required drilling 10 cm diameter "micro-tunnels" that would close due to plastic deformation or failure of the soft clays; successive opening and closure of the tunnels

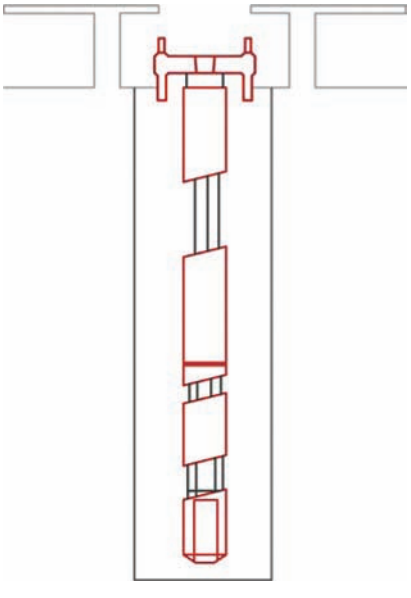

Figure 8. Control pile with an external deformable sheath for carrying negative friction (down drag).

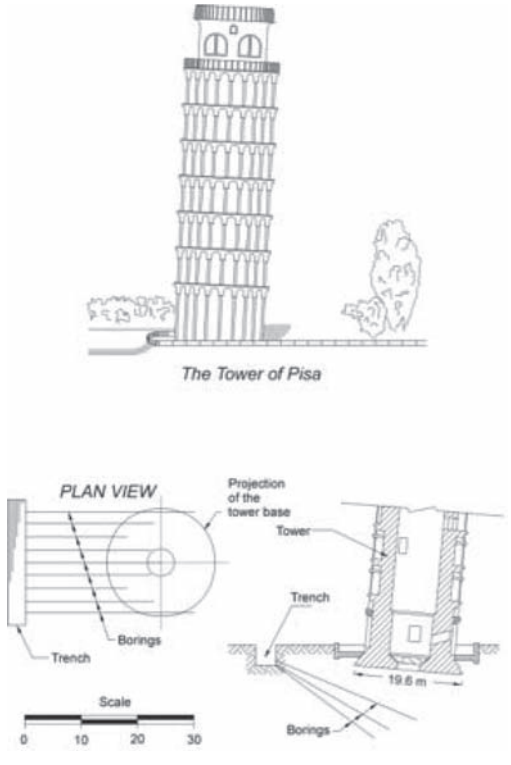

Figure 9. An early proposal for underexcavating the tower of Pisa (Terracina, 1962).

would gradually induce corrective settlements until reaching the deformation targets fixed according to structural considerations. The procedure is described graphically in Figure 10; a view of one of the shafts from which soil was extracted is provided by the photograph in Figure 11. Details of underexcavation at the Metropolitan Cathedral have been published elsewhere (Ovando-Shelley and Santoyo, 2001; Santoyo and Ovando-Shelley, 2004).

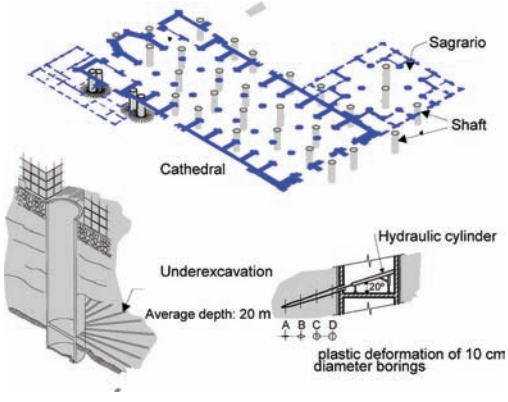

Figure 10. Schematic representation of the procedure to underexcavate the Metropolitan Catehdral in Mexico City.

Underexcavation was later applied at the Tower Pisa later, as discussed in several other papers (e.g., Jamiolkowsky et al, 1999; Burland, 2002). The general layout for underexcavaing the tower is shown in Figure 12. Underexcavation of the Metropolitan Cathedral and of the tower of Pisa are both success stories which are described in greater detail in the companion volume on case histories.

The techniques developed at the Metropoilitan Cathedral have been improved and their continued evolution over the last couple of decades has been used advantageously for correcting the inclination of nearly 80 modern buildings in Mexico City. The photographs and the drawing in Figure 13 show the newer high speed rotary tools presently being used.

6.3 *Grouting with hydro-fracturing*

Fluids injected under pressure into soft materials having low shear strengths, like Mexico City clay, produce hydraulic fracturing. Injected grout penetrates into the fissures and cracks and when it sets, the compressibility of the soil treated in this way will reduce. Mortars injected into the soil form sheets whose orientations depend on the stress state

Figure 11. View of one of the underexcavation shafts in the Metropolitan Cathedral. There 36 shafts, 14 to 25 m deep.

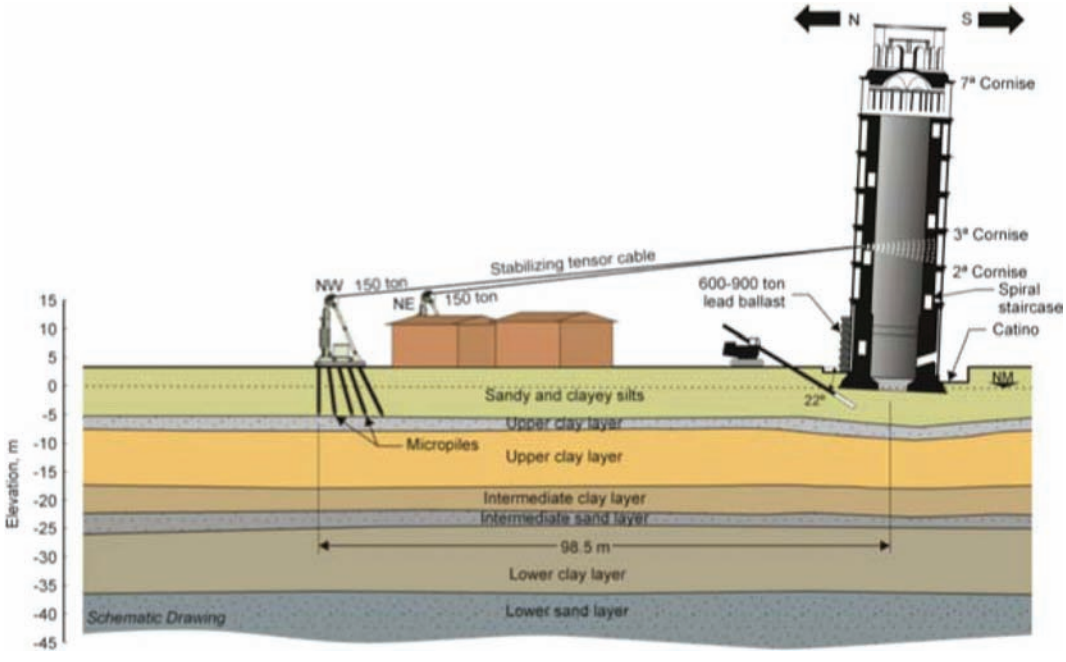

Figure 12. The general layout for underexcavaing the tower of Pisa (adapted from Jamiolkowsky, et al, 1999).

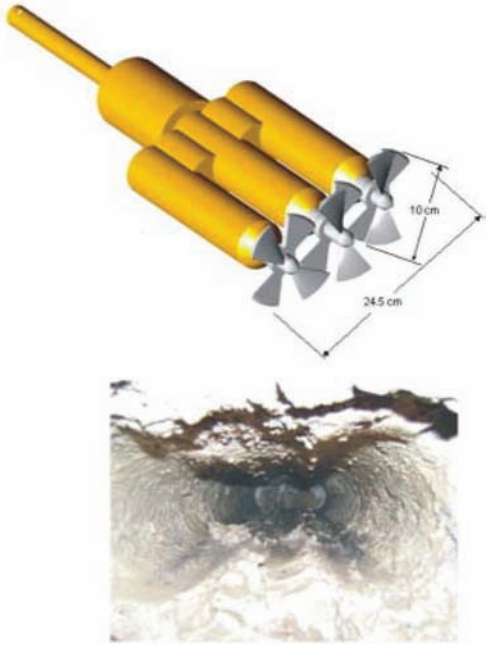

Figure 13. Rotary tool used for underexcavating buildings in Mexico City (Santoyo, 2010).

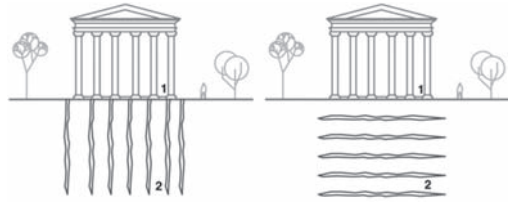

Figure 14. Grouting with hydro-fracturing produces vertical mortar sheets when the major principal stress is vertical (left hand side) and horizontal sheets at sites in which the major principal stress is horizontal (right hand side).

within the soil. Basic fracture mechanics showed that in this case (normally consolidated or lightly overconsolidated materials) they would be vertical or nearly so, as illustrated in the left hand side of Figure 14. Hydro fracturing of overconsolidated clays where the principal stress is horizontal will produce horizontal fracture planes, as seen in the right hand side of Figure 14.

Grouting with hydro-fracturing was used at the Metropolitan Cathedral in Mexico City as a preventive method to preserve the corrective deformations achieved with underexcavation and to prevent

the accumulation of differential settlements in the future. The experience gained from the mortar injection at the Palace of Fine Arts was taken into account and an investigation was made to determine the amounts and characteristics of the grout needed to reduce the compressibility of the clays under the Cathedral. Field tests were initially carried out at the former Texcoco Lake bed, as well as complementary laboratory tests; numerical simulations on the effect of introducing fluid mortars in the subsoil were also performed.

Injection was carried out from a cast-in-situ central mortar nucleus (diameter = 26 cm) that acts as a rigid intrusion in the soil. The mortars were injected using perforated PVC tubes (tubes á manchette) placed at the side of the nucleus. The mortar formed sheets that spanned 2.0 to 3.0 m laterally from the nucleus, as indicated in Figure 15. Successive injections produce a family of mortar sheets which will modify the overall properties of the clay mass (Santoyo and Ovando-Shelley, 2004). The sketch in Figure 16 shows the array of mortar sheets. A typical profile included in this figure shows the significant soil strata along the Cathedral's west atrium. The mortar nuclei and sheets were injected over the thickness of the first clay formation (24.0 to 27.0 m) in which the softer and more compressible clays are found.

Mortars were injected at the places where the softer materials were found and the volumes of injected mortar were distributed to achieve a uniform distribution of compressibilities within the soil. Further details of the procedure can be in previous publications (Ovando-Shelley and Santoyo, 2001; Santoyo and Ovando-Shelley, 2004). Other facts are given in the companion volume on case histories where the efficacy of the procedure is demonstrated by showing that for all practical purposes, the Metropolitan Cathedral was sinking uniformly, i.e. differential settlement rates are presently negligible.

Horizontal sheets are obtained when injection is carried out in highly overconsolidated clays like those that are common in the northern hemisphere. The sketch in Figure 17 illustrates schematically the concept of compensation grouting to correct

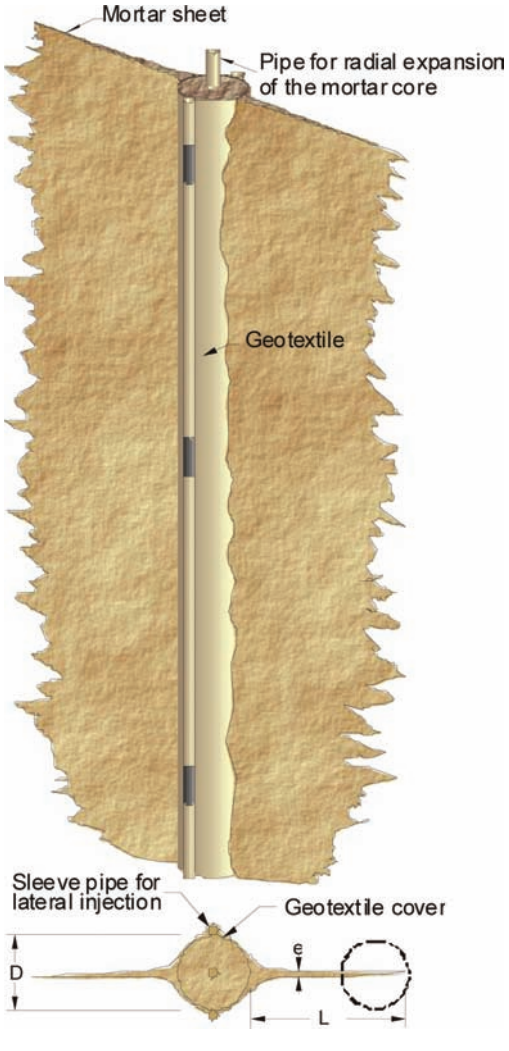

Figure 15. Central mortar nucleus to carry out injection with hydro-fracturing at the Metropolitan Cathedral.

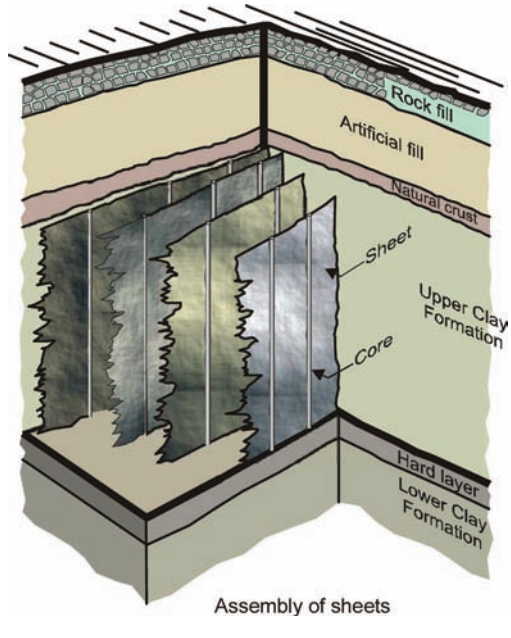

Figure 16. Assembly of mortar sheets.

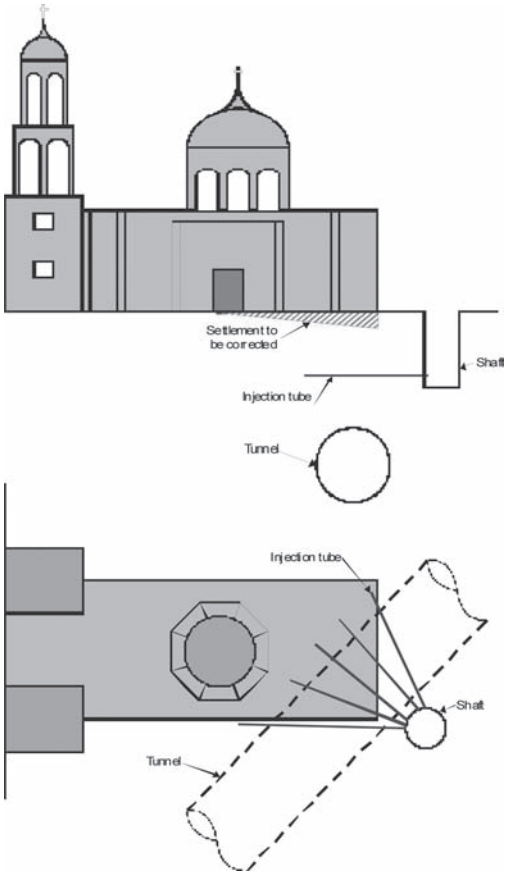

Figure 17. Schematic representation of compensation grouting under a monument due to construction of a tunnel nearby.

settlements in a structure induced by tunnelling. Compensation grouting was successfully applied in the Jubilee Line of London´s Underground, as described in other publications (Burland, 2002; Mair, 2003).

6.4 *Isolation and separation trenches*

Separation trenches have been used by the authors to modify the manner in which two adjoining structures interact. A trench is opened in the ground (30 to 60 cm wide) down to an adequate depth and it is filled with a non setting gel which is not capable of bearing shear stresses. As a result the displacement fields of both structures will be modified and a redistribution of stresses inside the soil will occur. Alternatively, a series of injection wells can be utilized to create the weak no-shear-stress plane using the hydro fracturing mechanism described previously albeit this technique can in theory only be

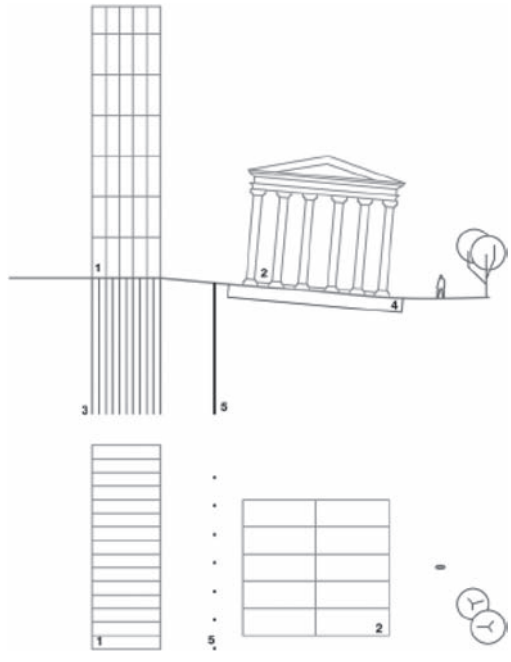

Figure 18. A modern building with point bearing piles in a site undergoing regional subsidence shows a relative emergence with respect to its surroundings.

used at sites with normally consolidated materials or materials only slightly overconsolidated.

The sketch in Figure 18 shows schematically a site undergoing regional subsidence where a modern building founded on point bearing piles is emerging relative to its surroundings and by doing so is affecting an adjoining monument. Point 4 under the monument on the right settles faster than point 2 which affected by the settlement trough produced be the tall building. Injection wells on and along point 5 create a weak plane thus allowing the monument to settle freely. Stress redistribution also occurs. Corrective differential settlements in the monument ensue.

Inclination in the monument will also reduce and it may even regain the vertical. Conceptually this is the case of the House of Tiles (Casa de los Azulejos) whose plan was illustrated in Figure 2. The same solution was used at a small chapel located northwest of the Metropolitan Cathedral, the Capilla de Ánimas (All Souls Chapel). A weak plane was created to facilitate the movements of the chapel relative to an underground railway line (Ovando-Shelley and Santoyo, 2001).

The temple of Corpus Christi in downtown Mexico City is a XVIIIth century structure (25 m wide and 37 m long) that is surrounded by two high rise modern buildings 26 and 23 storey high

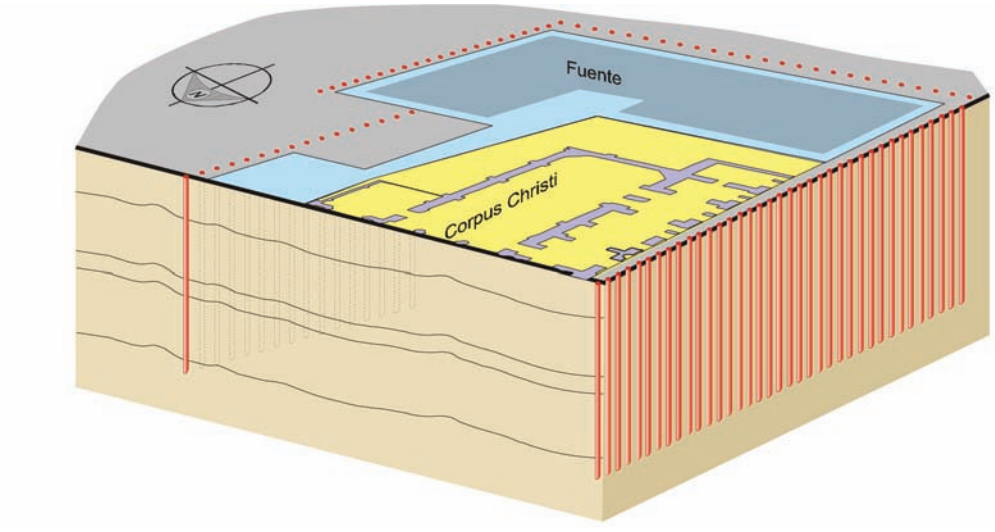

Figure 19. Perimetral injection wells were used in the church in Corpus Chisti to isolate it from the consolidating clay mass surrounding it.

founded with cast-in-situ point bearing shafts and by other shorter structures supported by precast piles. The site is exposed to regional subsidence brought about by extraction of water from the aquifer that underlies the layers of very soft and highly compressible Mexico City Clay. Sinking rates in the large structures and in the temple would induce damaging differential settlements in the church that would seriously compromise its permanence in just a couple of decades.

The programme for salvaging the temple included the reinforcement of the original foundation and the addition of 65 micropiles. The piles are made with steel tubes, 6" in diameter in-filled with mortar and with an external mortar sheath confined by a geotextile; their overall external diameter is 25 cm and their tips are located 25 m below the surface, i.e. they are friction elements.

A weak no-shear-plane was also created by injecting a non setting gel from 96 PVC tubes, with a diameter of 5 cm. The efficiency of the weak plane is guaranteed by performing periodic re-injections, typically every three to four months.

7 CONCLUSIONS

It is not uncommon that the factors that produce damage in an architectonic monument fall within the field of Geotechnical Engineering. In this paper we reviewed those factors and pondered on how they should be assessed in order to put forth solutions that are not only technically acceptable but that are also satisfactory from the view point of conservationists, archaeologists, historians and even politicians. Evaluation of intervention solutions must consider the extent and nature of damage in the monument from which a range of technically feasible solutions can emerge. To implement them, Geotechnical Engineers must reconstruct the geotechnical history at the site and may require the participation of experts in other fields.

Even though the ultimate goal of an intervention is to preserve a monument, circumstances (economical, political, social) may render certain solutions difficult to implement. Hence, technicians may need to resort to temporary solutions, preferably with non permanent effects. Similar situations can arise when the factors that originate damage have not been clearly identified or when they have not been fully understood.

Interventions may also be aimed at correcting or at least mitigating the effects of the damaging agents. If no other measures are taken, corrective measures may need to be applied periodically. Preventive interventions, on the other hand, aim at preventing the accumulation of further damage and on many occasions they imply the obliteration of the damaging factor or factors. Corrective and preventive interventions can also be applied successively.

Many of the interventions resort to the use of solutions taken from classical Foundation Engineering, adapted to the circumstances inherent in a project to preserve an architectonic monument. In this paper we also reviewed some solutions that are less commonly used. We describe and discussed control piles and underexcavation which induces

corrective deformations and mortar injections with hydro fracturing and the use of isolation trenches which modify in situ stress states and/or soil properties to achieve the proposed goals.

Finally, geotechnical engineers must always consider the installation of appropriate instruments to monitor the subsoil and the structure before, during and after the intervention. The observational method must therefore be present during the totality of the project to assess the efficacy of the intervention or as a means to identify unexpected situations or unwanted conditions. Modifications or adjustments to the project can then be made on the basis of analyses of instrumental observations rather than on mere intuition.

REFERENCES

Burland, J. 2002. A Tale of Two Towers: Big Ben and Pisa. *The Royal Academy of Engineering and the Royal Society of Edinburgh*. London: The Royal Academy of Engineering.

Heyman, J. 1995. *The Stone Skeleton—Structural Engineering of Masonry Architecture*. Cambridge, U.K: Cambridge University Press.

Jamiolkowsky, M., Viggiani, C., and Burland, J. 1999. Geotechnical aspects. *Proc. Workshop on the Restoration of the Leaning Tower: Present Situation and Perspectives*, pre-prints Volume, Pisa.

Jamiolkowski, M. 2001. The leaning tower of Pisa: End of an Odyssey. *Proc. International Conference on Soil Mechanics and Foundation Engineering*. Istanbul.

Johnston, G. and Burland, J. 2000. An Early Example of the Use of Underexcavation to Stabilize the Tower of St. Chad, Wybunbury in 1832. *In: ICOMOS, in partnership with the Bethlehem 2000 Project Authority. International Millennium Congress,* Selected Papers Volume II, Session 4. Bethlehem.

Mair, R.J. 2003. Research on Tunneling—Induced Ground Movements and their effects on buildings—lessons from the Jubilee Line extension. In: R, Jardine, (ed.), *Response of buildings to excavation-induced ground movements. Proceedings of the International Conference held at Imperial College. London.*

Mazari M, Marsal R.J. and Alberro J. 1985. *The settlements of the Aztec great temple analyzed by soil mechanics,* Mexico: Mexican Society for Soil Mechanics.

Mesri, G. and Hayat, T.M. 1993. The coefficient of earth pressure at rest. *Canadian Geotechnical Journal*, 30, 647–666.

Ovando-Shelley, E. and Manzanilla, L. 1997. Archaeological interpretation of geotechnical soundings in the Metropolitan Cathedral, Mexico City, *Archaeometry*, (39), 1,221–235.

Ovando-Sehlley, E. and Santoyo, E. 2001. Underexcavation of buildings in Mexico City: the Case of the Metropolitan Cathedral and the Sagrario church. *Proc. ASCE*, *Journal of Architectural Engineering,* 7, (3), 61–70.

Ovando-Shelley, E. and Santoyo, E. 2001. Salvaging the Capilla de las Ánimas in México City. In: *Proc. UNESCO-ICOMOS International Congress on Safeguarding the structures of our Cultural Heritage*, selected paper. Vol II, session 4.

Ovando Shelley, E., Pinto de Oliveira, M. and Santoyo, E. "Regional Subsidence and Earthquakes as Threats to Architectural Monuments in Mexico City". *Proc. 4th International Conference on Earthquake Geotechnical Engineering, Paper No. W2-1005*. Thessaloniki, 410–426.

Ovando-Shelley, E., Pinto Oliveira, M.O., Santoyo Villa, E. and Hérnández, V. 2008. Mexico city: Geotechnical concerns in the preservation of monuments. *International Journal of Architectural Heritage,* 2, 1–23.

Pinto de Oliveira, M.O. 2008. *La geotecnia en los monumentos históricos (Geotechnics in historical monuments)*. MSc Thesis, División de estudios de posgrado, Facultad de Ingeniería, Univerisda Nacional Autónoma de México, August, 2008.

Santoyo, E. and Ovando-Shelley, E. 2004. Geotechnical considerations for hardening the subsoil in Mexico City's Metropolitan Cathedral". In: *Advances in Geotechnical Engineering: The Skempton Conference, Vol. 2*. London: Thomas Telford, 1155–1168.

Santoyo, E. 2010. *Cimentaciones de templos y conventos de los siglos XVI a XVIII (Foundations of temples and convents from the XVIth to the XVIIIth century)*. Doctoral Thesis, School of Architecture, Universidad Nacional Autónoma de México.

Tamez, E., Santoyo, E. and Ovando, E. 1997. Underexcavation of Mexico City's Metropolitan Catedral and Sagrario Church". *Proceedings of the Fourteenth International Conference on Soil Mechanics and Foundation Engineering, Special invited lecture, Volume 4*. 2105–2126, Hamburg.

Terracina, F. 1962. Foundations of the Tower of Pisa, *Geotechnique,* London, 12(3), 336–339.

This page intentionally left blank

Papers

This page intentionally left blank

Geotechnical Engineering for the Preservation of Monuments and Historic Sites – Bilotta, Flora, Lirer & Viggiani (eds)
© 2013 Taylor & Francis Group, London, ISBN 978-1-138-00055-1

New underground lines in historic centres: Experiences in Brescia

A.M. Ajmone Cat, E. Campa, M. Lodico & C. Umiliaco
Astaldi S.p.A., Engineering Department, Rome, Italy

ABSTRACT: The field of engineering the "preservation" of historic or artistic heritage need not be confined only to "structural" interventions. In recent years in Brescia (North Italy), an excavation of several kilometres was completed by TBM in delicate geological and geotechnical conditions, in interaction with a historic centre dense with buildings of considerable importance, in masonry and with superficial foundations. When operating in sensitive areas, a reliable reconstruction of the setting's history, through the integration of skills with the local administrations, universities and specific experts, is a key basis for studying the appropriate work sequences and identifying the best technologies of operation. In Brescia, Astaldi S.p.A., with its consultants, has played an active part in this process, coordinating and synthesizing the contributions of all the local stakeholders involved; the capacity for collaboration and coordination of a broad spectrum of disciplines and contributions allowed some very complex interactions to be successfully resolved.

1 INTRODUCTION

Astaldi S.p.A. (AST) has gained broad experience in the design and implementation of undergrounds in major Italian and European cities; these works often interact with sites and structures belonging to the historic and artistic heritage (in Italy, for example, in Rome, Milan, Turin, and abroad in Bucharest, Warsaw and Istanbul).

Recently, AST, with its consultants, completed a "light" underground railway line in the historic centre of Brescia (North Italy), relying on its execution and management capabilities on one hand and, on the other, actively promoting and playing a main role in the process of coordinating the contributions, skills and specific knowledge of all the local bodies, authorities, stakeholders and academic consultants involved.

In fact, as a result of their stress/strain history, the historic buildings often cannot sustain even small settlements or vibrations, but their static/dynamic behaviour are difficult to investigate and predict.

The work referred to in this article is thus the result of the interaction of different expertises (historic, geotechnical, structural…), to guide the design choices and optimize the steps of execution for realizing the work in conditions of safety.

This approach makes it possible to identify appropriate solutions in complex conditions.

2 THE NEW UNDERGROUND IN BRESCIA

2.1 *Overview*

The town of Brescia (BS) developed starting from the third–fourth century, in a flat area at the border of the Po River Valley in Lombardy (northern Italy).

Here, starting in i2004, AST carried out the civil works for a underground line (13 km), which in its central section passes beneath the Medieval or Renaissance epochs urban centre, dense with buildings of considerable importance, in masonry and with superficial foundations (Figs. 1, 2).

Figure 1. Brescia (Italy), alignment of the new underground line beneath the historic centre.

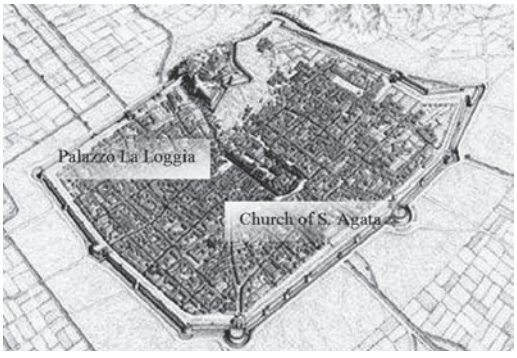

Figure 2. Brescia in the XVI–XVII century.

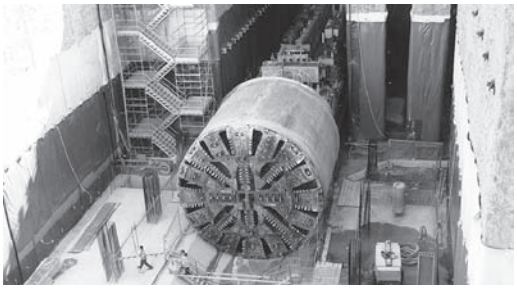

Figure 3. The TBM (Herrenknecht S-260) operating in Brescia. The picture refers to "La Marmora" Station.

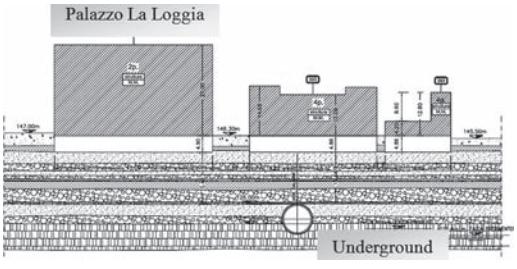

Figure 4. Typical geotechnical cross section.

Along the route there are about 6 km of tunnels (8 stations), bored in about three years by a TBM (EPB-S type), with a diameter D = 9.15 m (Fig. 3).

The excavation depth beneath the historic centre, optimized with a view to this interaction, was on the order of 15–20 m, which is to say up to 2 × D. The intervention involved gravelly alluvial terrains in silty—sandy matrix typical of the area, with stretches in partialized section due to the presence of banks of limestone at the excavation level (Mesozoic carbonate formations constituting the reliefs surrounding the plain, Fig. 4).

These alluvia present frequent alternations among the various lithotypes, as they are classic foothill deposits resulting from major erosion and depositing processes in the ancient river beds and conoids of a complex system of streams (Mella, Garza) and channels. Buried traces of Medieval and later works (bridges, towers, mills) are present. The water table depth (15–20 m below ground level), generally was a little within the range of tunneling excavation.

This realisation was possible through a close collaboration between the Municipality (and its Technical Commission), the Client (Brescia Mobilità), the Heritage authorities, the University of Brescia (UNI_BS), other bodies and AST. AST then relied up on the support of various specialists (e.g. Stone S.p.A. for the tunnel design, P & P Eng. Cons. for vibration monitoring and analysis, Studio Balossi Restelli for the consolidation works).

The stratum of direct archaeological interest has an average thickness of 3–4 m, and up to 6–8 m in sections. The excavation, however, also had to overcome various cases of interaction with ancient and recent surface buildings. Among others, mention should be made of Palazzo Avogadro with frescoes (1340), the "S. Agata" and "del Carmine" churches, Palazzo La Loggia (the municipality's city hall since 1500), and the "S. Faustino" church (1620). In this areas the excavation of tunnels and stations was a complex task, due to the superficial foundations and masonry structures, and their previous stress—strain paths. The work proceeded with careful monitoring and targeted interventions, adjusting to the criteria and procedures suggested by the Municipality and by the specialists hired for the purpose.

The remains of a Medieval tower buried at 7–8 m depth in the vicinity of S. Agata (Vittoria station) were disassembled block by block (work organised and supervised by Brescia Mobilità, with consulting from local Academic specialists—Zanirato 2009, 2010), to be rebuilt in a suitable location (Fig. 5).

At the San Faustino station, the layout was modified during the work to include sections of ancient Venetian walls with a former gate to the city, as well as some spans of a bridge on the defensive moat (e.g. Zanirato 2010).

Hereinafter, the cases of Palazzo "La Loggia" (Fig. 6) and of the Church of Sant'Agata are highlighted in some detail (Fig. 7).

2.2 *Design phases, tunneling and monitoring*

The interventions were performed on the basis of a careful historic research and field surveys carried out in collaboration with, or directly by the local University and specialists (e.g., UNI_BS 1997,

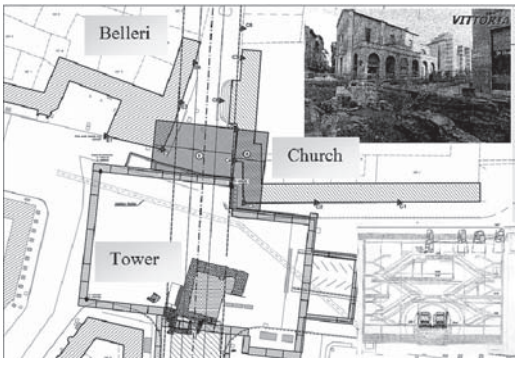

Figure 5. Disassembling of the Medieval tower in the vicinity of Sant'Agata, and typical cross section of the Vittoria Station.

Figure 6. Palazzo La Loggia.

Figure 7. Church of Sant'Agata.

1999, 2004; Giuriani 2007). Ancient morphologies and orography (e.g., former river beds or channels, and the hydraulic works now buried, possible presenting obstacles), were studied in detail, as well as the type, geometry, and current state of consistency of the foundations and structures of the buildings nearby the line.

Some general precautions were adopted on this basis, e.g. the prior sealing of all the "historic" wells identified (to avoid flooding in the basements near the TBM excavation front under pressure, or other interferences). The surveys overcame the difficulty of finding suitable accesses and operating in an urban setting marked by tight spaces. A careful organization made it possible to carry out 13 boreholes in less than 2 km, necessary for soil characterization and monitoring.

The specialist surveys on the historic buildings were carried out in cooperation with the University.

The evaluation of interference with buildings, the structural verification or design for interventions, and the back analysis on monitoring data were done as usual in phases.

The first phase, for the buildings within ±20 m from the line, included the survey of the conditions ante operam and a "green field" study of the longitudinal and transversal subsidences (lost volume hypothesis, Vp = 0.5%), with the forecast of strains and possible damage categories, based on elements known in the literature (a recent overview in Tanzini 2012). The damage classes Cd admissible for valuable masonry buildings were assumed as less than 1 (Cd down to "zero" for buildings with frescoes, churches etc. – e.g. Merlanti et al. 2008).

The second phase (for more "sensitive" buildings) included careful surveys and investigations as basis for detailed FEM 3D analyses, studying the effect of subsidences foreseen when combined with existing conditions of cracking or previous strains. These evaluations brought about lowering of several metres the tunnel design depth in the "historic" stretch.

In the third phase, for the more complex cases, the buildings with structures at risk were cleared, cordoned off, or protected by ancillary or long term works: design was based on studies and surveys carried out in an initial section of TBM excavation, including specific vibratory analyses.

In fact, in this first section (Volta – La Marmora stations), a "test field" was realised, calibrating the forecast models and the tunneling parameters/drilling tools during the TBM's advance, depending on the stress—strain responses of soil as monitored using inclinometers, multibase extensometers, topographic surveys, etc. The design hypotheses were verified (Vp of preconvergence, shield passage and post, in total 0.5%; k of Peck 1969, 0.35–0.45; transversal amplitude of subsidence basin, for excavations 15 to 20 m depth, between 45 and 55 m; settlements between 1 and 2 cm, Stone & AST, unpubl.). The pressures at the bottom in the excavation chamber were between 2.0 and 2.5 bars.

The grout injected behind the lining varied from 6.5 to 8.5 m^3 at each thrust (AST data).

In the same stretch, with a view to excavation beneath sensitive buildings, a monitoring survey was also performed with seismometers to characterize the vibration levels introduced in the "free field" by the TBM tunneling operation and its supporting equipments, in the phases of boring, mucking out, and assembling the lining segments. The tests, compared with similar parallel investigations on various buildings, confirmed the representativeness of the survey data (appropriate levels of relationship between records for "active source" and "environmental noise"). The vibratory effects during the lining assembly were negligible.

The peak levels of vibration induced at ground level (free field), were higher than those usually measured on buildings in the observed cases (due to attenuation induced by their structural masses – AST data and technical reports, unpubl.).

Topographical monitoring of the buildings in the interaction area (integrated with inclinometers and fissurimeters for sensitive buildings) was performed constantly during the excavation, up to the complete TBM passage and stabilization of settlements, in comparison with the numerical forecasts and alarm thresholds (periodic reports were made available).

Lastly, having defined the vibrating behaviours ante operam and those expected in the excavation phase for the main buildings, it was verified that pre-established response thresholds were not exceeded during the excavation, by adopting appropriate "guide rules" for the TBM, verifying their suitability through appropriate monitoring operations.

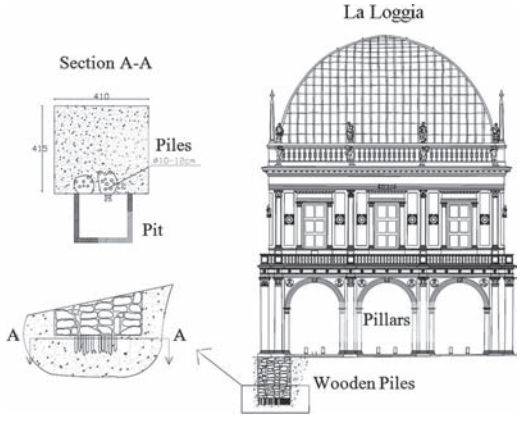

Figure 8. Palazzo La Loggia. Typical foundation of pillars.

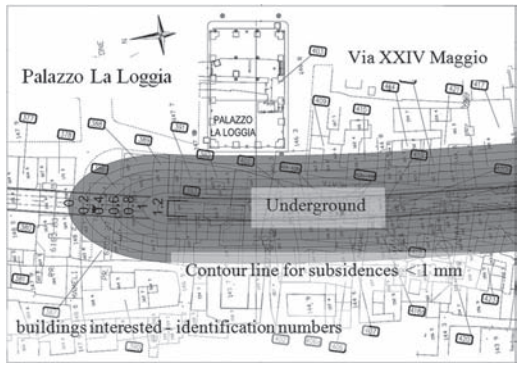

Figure 9. Palazzo La Loggia. No subsidences expected.

3 EXCAVATION NEAR "LA LOGGIA"

Palazzo La Loggia is a large stone masonry structure with 2 floors in wood (measuring 30 × 47 m, 20 m tall, plus 18 m of roofing). When the building was being constructed (1400–1500), the bed of the Garza had been covered and channelled into a tunnel integrated into the building foundations (Palladio & Rusconi 1570). Laterally, the building has large arches on pillars (4 × 4 m), founded at a depth of 4–5 m below g.l., at the bottom of these ancient fills, on sandy and gravelly alluvial deposits alternating with silty—clayey levels, having homogeneous thickness; the water table is at a depth of 20–25 m.

The granular soil under the pillar basements had been consolidated as typical of the time, using some 1600 wooden piles (on historic data, expected L = 2 m, diam. 10 cm), driven into the sands to increase their density (Zamboni 1778, Fig. 8).

The load acting at the foundation level is 0.5 MPa, comparing to the static bearing capacities at collapse estimated for these dense sands at 2.7 MPa (e.g., Marini & Riva 2000). Moreover, the TBM had to excavate at least 20 m distant from the pillars, and at about 15 m in depth; thus the subsidences expected beneath the foundations were negligible (<2 mm, Fig. 9), as confirmed by the test field.

The conditions of these piles and of surrounding soil beneath the pillars have then been the object of mentioned investigations since 1990, made by the University under the supervision of the Heritage authorities (e.g., Franchi et al. 1993).

This survey included two initial direct exploration pits (with concrete walls connected to the basements, to counter balance the reduction of bearing capacity due to the lateral excavation), some sub horizontal micro drilling bored using a specifically designed probe (dia. 26 mm), equipped with video camera, and sampling (taking care not

to change the bearing capacity of the pillars, not to induce vibrations nor settlements). Some tests were also carried out filling the voids with injections. The piles (spaced at 25 × 25 cm) were found too short (1 m) and largely deteriorated (UNI_BS 1999), with many residual cavities beneath the pillars (Fig. 10).

Anyway, in static conditions the foundation pressures σ_f would not have exceed levels of 0.5–0.6 MPa, remaining in a range "acceptable".

The cavities, however, were at risk of collapse with sudden loss of volume in the event of disturbance of the brittle residual "septa" of terrain between the piles (e.g. in the case of earthquake, with estimates of possible settlement for a pillar up to 10 cm).

Therefore a number of simulations were performed with complex numerical elastic—plastic models of the building (also calibrated with sophisticated physical models on a reduced scale—e.g. Giuriani et al. 2004). Upon the settlement of one or more pillars, there was the risk of reaching conditions of final limit status of some foundations (σ_f exceeding 1.9 MPa). Although planning structural interventions with chains in the masonry, settlements of even 2–3 cm on a single pillar could cause serious overall structural damage to the Palazzo (ref. above).

The forecast and monitoring of the vibrating regime induced by the TBM boring at a relatively "short" distance thus held more importance than that of the subsidences; in concert with all the experts, action was then taken with filling of the voids beneath the pillars, and with strict control of tunneling conditions, depending on the structure vibratory "response". Moreover, during the investigation, reliance on lime mortar to fill the voids had been already successfully tested (on models and on site—references above). However, it was necessary to accurately drill a high number of sub-horizontal

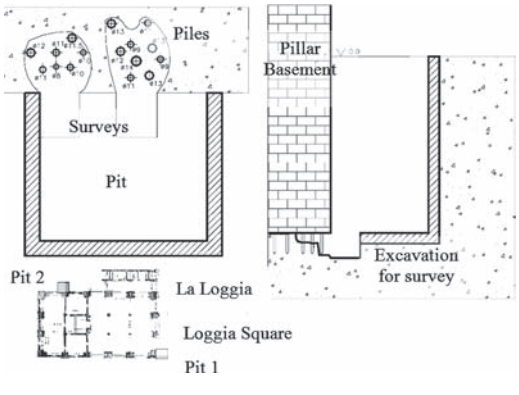

Figure 10. Scheme of investigations on pillar foundations.

holes (operating in tight available spaces), and to inject the mortar without modifying the existing equilibrium (e.g. by "breaking" too quickly, and in too widespread a fashion, the residual septa of terrain between void and void). This operation was carried out successfully under direct supervision of UNI_BS and Municipality consultants, operating with particular equipments from a few surrounding pits (located for the purpose in the limited accessible points; see Zanirato 2010).

The Palazzo's foundation system, its bearing walls and the floors were then equipped by AST and P & P Eng. with 4 to 6 seismometers (Si, i = 1 to 6). The sensors were placed in three directions respect to the excavation axis: vertical, V, parallel, L and transversal, T. The 18-channel recordings, acquired, filtered, and remotely analysed with a specific software, lasted 60 s each (during the excavation, every 6 minutes – AST with P & P Eng., unpubl.).

The processing operations were able to regard the peak values of the three components of vibration speed (Vv, Vl, Vt), the data spectrum and other typical evaluations (see for instance UNI 9614, UNI 11048). The objective was to assess and characterize the level of environmental and induced vibrations, and evaluate the possible effects on the building (as for UNI 9916 and similar regulations BS 5228, BS 6472, BS 7385, DIN 4150, ISO 4866).

These regulations suggest indicative thresholds of reference, e.g. max value of the velocity vector (Peak Particle Velocity, p.p.v.), or the max value of a component (p.c.p.v.), with which to pre-assess the compatibility of transitory or "continuous" vibration regimes. In Italy, the main regulation applicable in this field is the UNI 9916 (e.g. its Appendix D).

When the p.c.p.v. induced do not overcome the thresholds suggested for each type of building and vibrational conditions, only a limited, "cosmetic" damage should usually occur (e.g. Tab. 1; see Fig. 11 for the installations at the La Loggia base level).

Between December 2007 and February 2008, recordings of the "environmental" vibration levels were acquired in the building (e.g. upon the transit of motor vehicles, or for other typical events in the adjacent piazza, such as fairs). These recordings calibrated the estimate on building vibration behaviour (response spectra),processed with specific numerical models (including the functioning of the trains for supplying the TBM and mucking out).

A dampening "mass effect" was detected, as well as certain amplification behaviours by the structure (foundations and floors), and by the ground—building system (at about 8 Hz – AST with P & P Eng., report unpubl.).

Table 1. Thresholds for peak component particle velocities.

Class	Type of building	Thresholds suggested for p.c.p.v. induced in every frequency range (Hz)
		Peak of velocity [mm/s]
1	Industrial and commercial (reinforced or framed structures)	10
2	Residential or similar	5
3	Historic monuments, buildings or other structures to be preserved	2.5 or less (for churches, in presence of frescoes ..)
The values suggested are referred to continuous vibration regimes and suitable for every floor and for the foundation level (DIN 4150).		

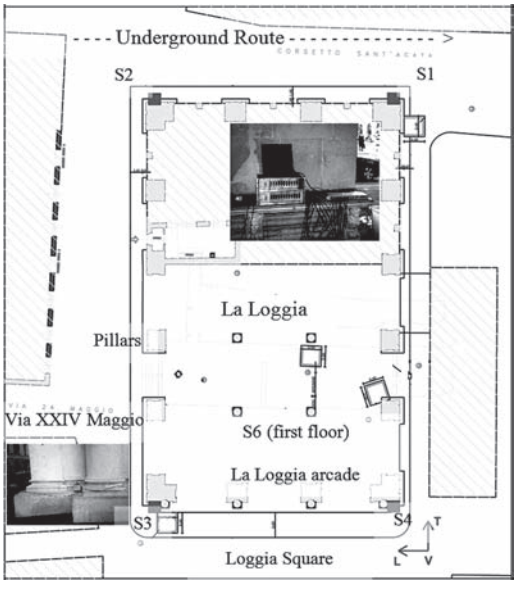

Figure 11. Vibrational monitoring at the base of pillars.

The 50 m tunnel section closest to the building was then excavated under monitoring in about 8 days (May 2008), comparing the values recorded with the thresholds based on the aforementioned simulations and recommendations (Fig. 12).

Any damage was induced. From 3 to 4 lining rings were completed in a day, as against the 6–8 usually reached in other stretches.

While the p.c.p.v. measured at the transit of vans or buses presented sporadic transitory peaks exceeding 4500 μm/s, during excavation the sensors in the foundation (S1, S2) did not exceed 300 μm/s;

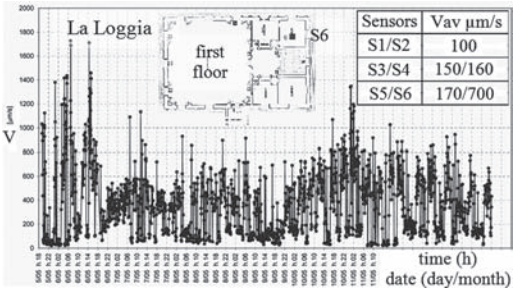

Figure 12. Seismometer S6, vibration record during excavation.

in S6, at the centre floor, first level (mayor's office), 1750 μm/s (less than the attention threshold proposed for "historic" buildings, 2500 μm/s).

4 EXCAVATION NEARBY "SANT'AGATA"

The excavation at the church of Sant'Agata (sixth–seventh century) took place in a similar geological—geotechnical setting and with analogous phases of design or control during the work.

The design water table was expected above the excavation bottom, therefore continuous piezometric monitoring was performed (excavation above the water table during the work).

Surficial loose soils fill an ancient bed of the Garza stream and channels, in thicknesses of up to 8 m, thus susceptible to induce significant settlement beneath the building shallow foundations.

The TBM here bored at a 20 m depth between the church and a building, "Ottica Belleri", heavily ruined and unviable; the Vittoria station, named as the square nearby, had also to be realised up against those buildings (Fig. 13, Fig. 14).

The structure of the church showed signs of past interventions and previous significant states of stress, strain and cracks (e.g. the portico, built to counterbalance and retrieve the damage caused by previous demolitions of other structures on that side, or the remains of one arcade of a bridge on the ancient Garza stream, see apse wall in Fig. 15).

Historic and geotechnical analyses and complex FEM 3D digital simulations thus suggested containing the additional settlements that the TBM and station excavations could have caused to these buildings, right from the construction of the diaphragms. These FEM simulations took into account the various structural parts present, from different epochs, with different material characteristics and various stress—strain paths (for "Ottica Belleri", see Fig. 16). The works schedule was thus modified to limit the expected damage classes ($\varepsilon_{max} < 0.015\%$).

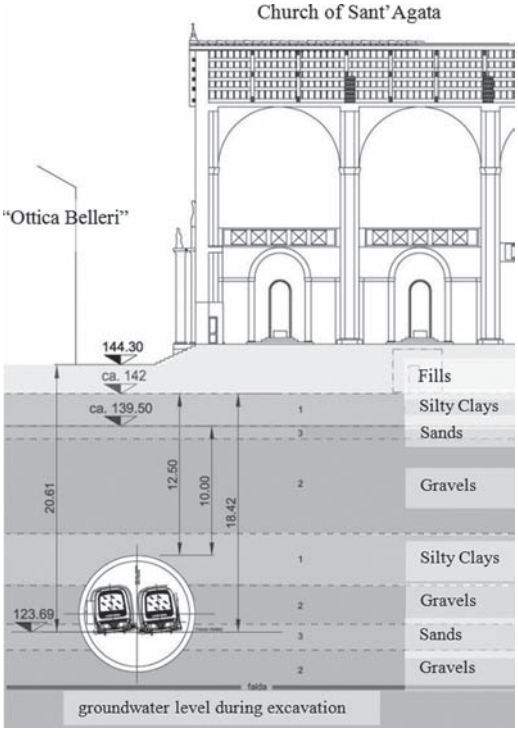

Figure 13. Geotechnical cross section beneath Sant'Agata.

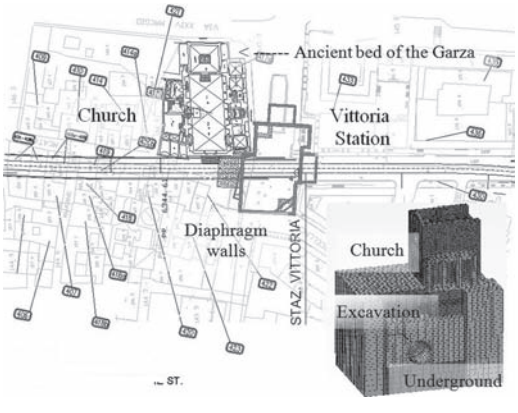

Figure 14. Church of Sant'Agata and Vittoria Station. Layout and FEM 3D model for analysis of the steps of excavation.

In order, the following operations were carried out: major consolidations with grouting (in the soil volume behind the diaphragms, to ease the breaking through of the TBM; injections beneath the church foundations, to allow the subsequent excavation of the station); excavation of the diaphragms; TBM passing beneath the square before

Figure 15. Church of Sant'Agata.

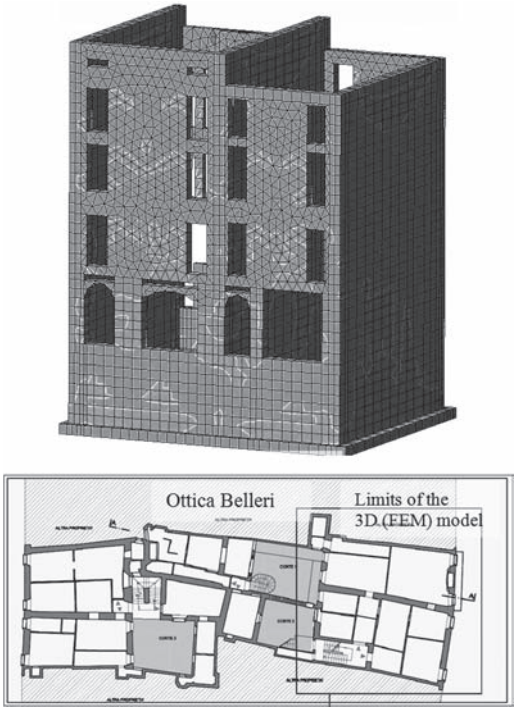

Figure 16. Ottica Belleri. FEM 3D studies of the structural effects of excavation and evaluation of the risk of damage.

the excavation of the station area, to limit all interactions; station excavation with final demolition of the lining inside.

Given the 20% of fine particles in the soil, microfine concrete mixes with high penetrability, and bi-component silicate mixes with high saturation penetrability (radii of action, 0.8 m) were used, to avoid both "*claquage*" (max pressure, around.

14–16 bars) and the risk of segregation by loss of water.

The grouting operations (in two steps, with controlled volume, each at a theoretical 6–8% of the volumes to be treated) were performed realising 12 sets of drills with complex geometries and sequences, due to the presence of the ruins of the Medieval tower and of some main phone cables (Fig. 17–AST and Studio Balossi Restelli, data unpubl.).

The operation required the constant verification of the mixes, sequences and timing for the injectors, as well as of the pressures and volumes injected (max flow rates, 400 l/h). A topographical levelling and continuous checks with fissurimeters (for the church) were performed on the two structures. The treated volumes were significant (depths reached near the excavation bottom, about 30 m below g.l.), and yet the settlements in the surrounding area were limited to within a maximum of ± 1 cm.

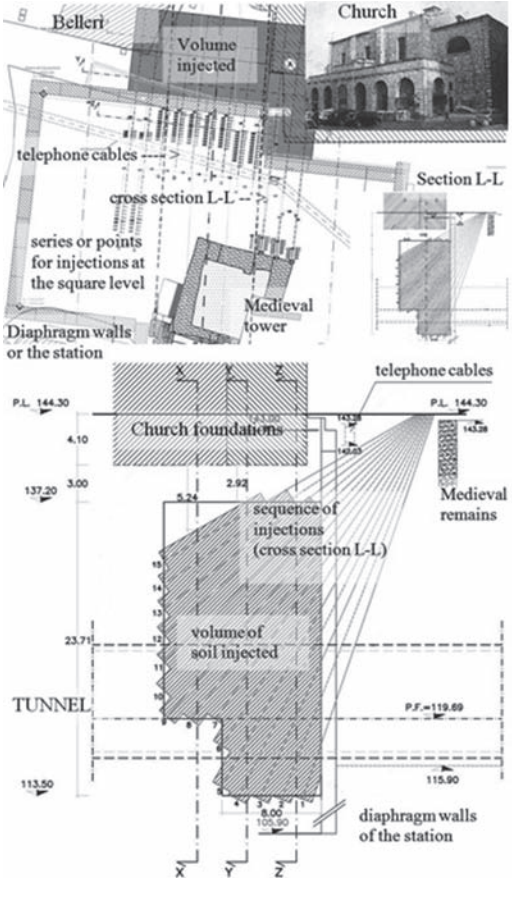

Figure 17. Vittoria station. Schemes of consolidations beneath the Church of Sant'Agata and "Ottica Belleri".

Figure 18. Excavation nearby the Church of Sant'Agata.

The effect of these consolidations and work phases made it possible to limit the settlements during tunneling and station excavation, to less than 0.5 cm (Fig. 18).

5 CONCLUSIONS

"Preservation" of the historic or artistic heritage requires not only heavy, "structural" interventions. When operating in sensitive areas, a reliable reconstruction of the setting's history (e.g. of the construction typologies, techniques and events), mainly through the integration of skills with the administrations, universities and specific experts, is a priority. It is also a key basis for the study of the appropriate work sequences and identification of the best technologies of operation. Preliminary test fields and careful monitoring have to be conceived as a main, active part of the intervention. TBM tunneling at a "shallow" depth near historic or "delicate" buildings can thus be done successfully if carefully analysed, planned, performed and controlled, including the forecasting and monitoring of the induced vibrations. Moreover, these consolidations gave the TBM as gradual as possible a transition of stiffness towards the soil behind, when crossing the diaphragms (reinforced with VTR bars in the excavation sections). The historic buildings were safeguarded, and the station was successfully completed.

REFERENCES

AA.VV. 1987 Ricostruire una chiesa. In "*Bollettino pastorale S. Maria del Suffragio*". Milano.

Franchi, A.; Giuriani, E.; Gubana, A.; Lupo, G.; Mezzanotte, G.; Ronca, P.; Volta, V. 1993 Per la conservazione del Palazzo della Loggia di Brescia – Parere sulla stabilità strutturale. Centro Studio e Ricerca per Conservazione e Recupero Beni Architettonici e Ambientali (Ce.S.Ri.CR), UNI_BS. Brescia: Grafo Edizioni.

Giuriani, E.; Coleselli, F.; Gelfi, P.; Meda, A.; Poli, A. 2000 Relazione sulla prova sperimentale per la messa a punto della tecnica di consolidamento del terreno sotto le fondazioni del Palazzo Loggia di Brescia. UNI_BS. Brescia.

Giuriani, E.; Marini, A.; Minini, C.; Riva, P. 2004 Studio del comportamento sperimentale del modello in scala 1:20 della facciata del Palazzo della Loggia nell'ipotesi di cedimento differenziale di un pilastro. *Technical Report n. 2*. UNI_BS, Dipartimento Ingegneria Civile. Brescia.

Giuriani, E. 2007 Il percorso delle indagini e degli studi per gli interventi sulla struttura del Palazzo della Loggia. In *Atti del Convegno "Il Palazzo della Loggia di Brescia. Indagini e progetti per la conservazione":109–140. UNI_BS. Brescia*.

Marini, A. & Riva, P. 2000 Comportamento della facciata della Loggia soggetta a cedimenti differenziali. *In Atti del Convegno "Storia e problemi statici del Palazzo della Loggia di Brescia": 141–154. UNI_BS. Brescia.*

Merlanti, P.; Bellocchio, A.; Sicilia, R. 2008 Analysis and prediction of subsidence phenomena induced by excavation employing an EPB-S in the works to construct the Brescia metro. Design predictions – back analysis. *In Congrès Int. "Le souterrain: espace d'avenir", Oct. 2008. Monaco*.

Palladio, A. & Rusconi, G. 1570 Gli edifici pubblici di Andrea Palladio, Documento "I", In Scrittura su alcuni quesiti a noi sottoposti dai Deputati alle Fabbriche di Brescia.

Peck, R.B. 1969 Deep Excavations and Tunneling in Soft Ground. In Proc. 7th Int. Conf. S.M.F.E., *In State of the Art Volume: 225–290, Mexico City*.

Studio Franzoni 1989 Relazione Tecnica relativa alle indagini geognostiche eseguite nel terreno di fondazione del Palazzo della Loggia a Brescia. Brescia, 4 Marzo 1989.

Tanzini, M. 2012 Tunneling—induced ground movements and evaluation of risk of dam age to buildings owing to subsidence. In *Gallerie e grandi opere sotterranee*, n. 103: 27–58. Bologna: Patròn Ed.

UNI_BS 1997 Rapporto Tecnico Loggia 2/97. Relazione Tecnica e Illustrativa sulle indagini per la valutazione dello stato di conservazione dei pali in legno delle fondazioni del Palazzo della Loggia (Ce.S.Ri.CR). Brescia.

UNI_BS 1999 Progetto di consolidamento delle fondazioni del Palazzo della Loggia. Stato di conservazione pali di fondazione, Prime Valutazioni sulla Situazione delle fondazioni e Relazione Fotografica. (Ce.S.Ri. CR). Brescia.

UNI_BS 2003 Supplemento di indagini alla palificata in legno delle fondazioni del Palazzo Loggia. (Ce.S.Ri. CR). Brescia.

UNI_BS 2004 Rapporti tecnici Loggia 3/2004 Prove sperimentali di consolidamento terreno di fondazione; 4/2004 Indagini endoscopiche terreno fondazione; 5/2004 Riempimento delle cavità dei pali mediante iniezioni a bassa pressione di malta di calce; 6/2004 Studio dissesto facciata mediante modello fisico 1:20. (Ce.S.Ri.CR). Brescia.

Zamboni, B. 1778 Memorie intorno alle pubbliche fabbriche più insigni della città di Brescia: 50, e App. II, III. Brescia.

Zanirato, L. 2009 Metropolitana leggera automatica di Brescia. Nel cuore della Talpa. Il viaggio della TBM a Brescia Tech. contribution Umiliaco C. Brescia: Brescia Mobilità (BSM).

Zanirato, L. 2010 Metropolitana leggera automatica di Brescia. MetroBrescia. Un passo verso il futuro. Brescia: BSM.

This page intentionally left blank

Geotechnical Engineering for the Preservation of Monuments and Historic Sites – Bilotta, Flora, Lirer & Viggiani (eds)
© 2013 Taylor & Francis Group, London, ISBN 978-1-138-00055-1

Safeguarding the historic town of San Fratello, Sicily

C. Airò Farulla
Università degli Studi di Palermo, Italy

F. Cafiso
PRO-GEO, Palermo, Italy

ABSTRACT: The paper presents the case history of San Fratello, a small town on the Nebrodi Mountains in Sicily rich in history and with very peculiar environmental and cultural characteristics. Both slopes of the narrow ridge where San Fratello is seated had been affected in 1754, 1922, 1986 and 2010 by very large landslides which caused the failure of a lot of buildings and historical monuments in the town. The paper illustrates the analyses carried out in the 2010 landslide and the design of stabilization works still in progress. Some problematic aspects related to the decision to safeguard San Fratello are discussed.

1 INTRODUCTION

In Italy a lot of towns of historical and artistic importance were seated in the past for defence or climatic purposes on the top of hills usually of very difficult access. A lot of them are now affected by very extensive landslides, depending mainly on morphological evolution of slopes and changes in climatic and environmental conditions. From this point of view, causes deriving from man's activity can be very significant and dangerous. Besides, with reference to several historical towns sited on the Apennine chain and in Sicily, outcropping soils belonging to structurally complex formations (AGI, 1979) are more or less extensively involved by weathering and softening processes. The safeguarding and conservation of these historical towns poses very difficult problems from both economic and social points of view. In these cases, a dilemma rises: abandoning historical towns, moving the inhabitants to new buildings in safer places, or defending and preserving them in order to delay as much as possible their end. Such choices depend on conflicting factors: on the one hand, safeguarding these towns is usually very expensive; on the other hand, the inhabitants want their villages to be preserved, for those are made not only of buildings, but also of traditions, emotional and cultural roots, which represent the identity and soul of a people. Although it is a difficult choice, the preference is to let the historical towns survive as long as possible, for they are the goods and legacy of the mankind. In such cases, the role of geotechnical engineering is essential for investigating causes of landslides and choosing and designing safeguarding works. It is also central in carrying out stabilization works by means of both traditional and innovative techniques at bearable costs. These problems are discussed with reference to the case of the historical town of San Fratello in Sicily, seriously damaged by a large landslide in February 14th 2010, which caused the failure of numerous buildings.

This paper, after a short presentation of the history of San Fratello and physical characteristics of its site, illustrates the results of the analyses carried out to investigate the landslide mechanisms and to design the stabilization works still in progress. The monitoring system installed and the first data recovered from measures are presented.

2 HISTORY AND PHYSICAL CONDITIONS

San Fratello is a small town situated on the Nebrodi Mountains just on the northern coast of Sicily at about 700 m a.s.l. It is placed in a commanding position to control lines of communication from Palermo to Messina. For this reason, it was inhabited during the Greek and Roman ages, when was named *Apollonia*. It was destroyed during Arabic domination in Sicily, and rebuilt between XI and XIII centuries by a group of soldiers coming from the North of Italy and France to conquer Sicily, guided by the Norman Count Roger. The Normans built a fortress in San Fratello, whose defence was entrusted to Longbard and French mercenary troops. Because of their origin, the inhabitants of San Fratello, speaking a dialect of Gallic origin, are considered as foreigners by Sicilian people and named *"the French"*. San Fratello is rich in history and tradition which testifies the passage of several

dominations and civilizations from Europe, Asia and Africa through Sicily.

The slopes on both sides of the ridge where San Fratello is sited have been involved in very large landslides, which have caused serious damage to buildings in the town and to agricultural and breeding activities of inhabitants. There is evidence of three large landslides which happened in 1754, on the eastern slope, and in 1922 and in 1986, on the western. The contour of the 1754 landslide has been reconstructed on the basis of a few historical chronicles and actual morphological evidences (Fig. 1). According to some sources, it destroyed San Filadelfio fortress, one of the first Middle Age buildings in San Fratello. The 1922 landslide involved the city centre, destroying several buildings and the cathedral (Crinò, 1922). In the city centre on the 7th January 1922 very deep tension cracks appeared on the ground and authorities commanded the citizens to leave the town. The following day in few hours the central and western part of the town slid down the slope. On the crest of the slide area, a 400 m long and 40 m high scarp appeared. Crinò reports that in the previous days the region of San Fratello was affected by prolonged rainfall and huge snowfall, which occurred after a prolonged drought. Because of the severe damage, authorities decided to abandon the area, moving the people to the village of Acquedolci, built for this purpose on the sea cost. However, the inhabitants moved back after the Second World War, exploiting the eastern slope as an expanding urban area.

3 THE 14TH FEBRUARY 2010 LANDSLIDE

In February 2010 a very large landslide occurred on the eastern slope of the ridge involving an overall area 100 ha wide, 10 ha in the town. The slide extended 1500 m from hill to valley and was about 950 m at the crest. It damaged more than 300 buildings and caused the evacuation of a quarter of four thousand inhabitants. The waterworks, sewer pipes and access roads to the East zone of the town were ruined.

The mechanism of the landslide is very complex and can be considered the reactivation of movements in several zones of the 1754 landslide. With reference to the Fig. 1, the landslide started in zone A, where large surface movements were evident on the 12th of February 2010. Next day it regressed upslope and zone B moved, while very large and deep cracks appeared on the ground surface. On 14th February, movements reached the city center. Tension cracks appeared along squares and streets and a lot of buildings were badly damaged or ruined in the city areas C (Fig. 2), D and E (Figs. 3 and 4). The mean displacement rate in these zones was evaluated as about 3,5 cm/h.

In the next months the landslide became larger at the crest, involving zone F, at the southern border of the town (Fig. 1). Mean displacement vectors in zone F pointed to the North-East and pointed to the East in the previously moved zones. That is, zone F movements developed as consequence of the sliding of zone C, which retained its foot (Fig. 1).

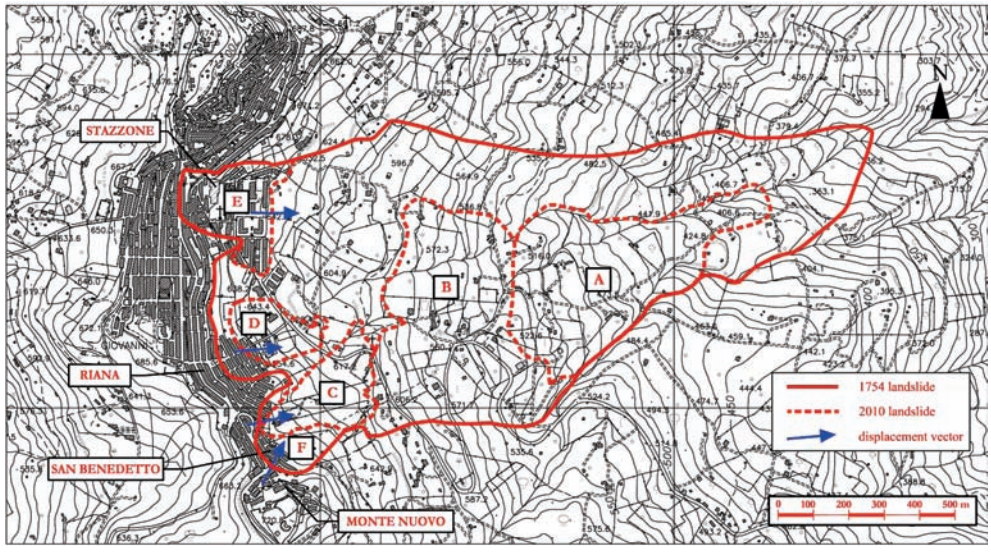

Figure 1. Contour of the 1754 landslide and the zones reactivated in the February 2012 landslide.

Figure 2. Destroyed buildings in San Benedetto.

Figure 3. Destroyed buildings in Stazzone.

Figure 4. Damage to streets and water pipes in Stazzone.

4 LANDSLIDE ANALYSIS

4.1 *Geology*

San Fratello is seated on a narrow ridge oriented approximately in the North-South direction separating two long slopes degrading to the valleys of two streams. Beyond the town, the ridge rises further to the South towards Pizzo Costanzo mountain (841 m a.s.l.), which dominates the region and, probably, feeds the ground water detected in the overall city subsoil. In the town site, three different structurally complex formations (Jappelli et al., 1977) belonging to the Apennine Units are present in tectonic contact. In particular, they are:

- Monte Soro Flysch (Sicilide—Cretaceous Complex), consisting mainly of alternating quartzarenites and clays (MS).
- Scaly Clays (Sicilide—Cretaceous Complex), consisting of stiff highly fissured clays with interbedded strata of jointed limestones and marly limestones (SC).
- Frazzanò Flysch (Calabride—Upper Eocene Complex), consisting of alternating sandstones and clays with interbedded layers of conglomerates and gneiss (FF).

The February 2010 landslide developed for the most part in the Scaly Clays, that in the upper layer are generally altered (SCa). Above the SC formation there is a superficial layer of soils, consisting mainly of remoulded and softened clays and silty clays (RC). Usually, the overall thickness of RC soils does not exceed 10 m. Heterogeneity and structural characteristics rule mechanical behavior of Scaly Clays with reference to stiffness, shear strength and permeability, and influence deeply stability of the slope. The interbedded strata of limestone, sometimes of high thickness, lack continuity both in vertical and horizontal directions, determining different conditions in the movements and pore pressures intensity in the different zones of the slope. Besides it has to be considered that the various geological formation outcropping in the San Fratello site are in contact along faults, some of them at present active in both ridge slopes.

4.2 *Geotechnical investigations*

To investigate geological and geotechnical characteristics of soils involved by movements in zones C, D and E, about 50 boreholes were drilled in successive phases between 2010 and 2012; some of boreholes were equipped with inclinometers and stand pipes.

On undisturbed samples recovered from boreholes an extensive program of geotechnical laboratory tests were carried out. Peak and residual shear strength of the Scaly Clay samples were extensively investigated by direct shear tests.

A peculiar aspect of site investigations was represented by the survey of about one hundred wells excavated in the historic town. By ancient tradition, houses in San Fratello have a private well because ground water level is very near to ground level for the most part of the year. By means of well survey

carried out in the month following landslide, it was observed that the ground water level was deep only a few ten of centimeters from ground surface. Inhabitants relate that sometimes in the past water came out from wells, that is artesian conditions prevailed and piezometric level rose over ground surface.

4.3 *Landslide kinematics*

According to the suggested glossary of landslides (WP, 1995) the February 2010 landslide in San Fratello is a complex, regressive and reactivated slide.

Movements in the area of San Benedetto (Area C—Fig. 1), had a rotational character. A clear rear scarp was observed which settled more than 6 m and a foot zone which raised about 5 m; the buildings on the slide zone were destroyed or severely damaged (Fig. 2). On the basis of the analyses of inclinometer and natural water content (w_n) versus depth profiles, the slip surface was inferred to develop to a maximum depth of 11.50 m, along the contact between RC and SCa soils, and within the latter.

In the Riana area (Zone D—Fig. 1), a clear slip surface was not identified either by inclinometer or w_n versus depth profiles. Inspections carried out by means of video recording in a number of wells damaged by the landslide did not provide significant data. On the basis of ground evidence (cracks, damage to buildings, etc), field surveys and back analyses, the slip surface was inferred at a maximum depth of about 14 m.

In the Stazzone area (Zone E—Fig. 1), movements shared characteristics of rotation in the top and middle part and of translation in the low part of slide area. Data recovered from inclinometer readings inferred a slip surface, mostly flat with a trend sub parallel to the ground surface in the low part, developed to a depth of about 10 m at the contact between RC and SC soils.

4.4 *Back analyses*

The results of the back analyses of the single slide zones have been used to obtain information about shear strength parameters mobilized at failure. For zones C and E, where the slip surfaces have been identified with sufficient accuracy, assuming piezometric lines at the ground level, back analyses resulted in: $c' = 0$ and $\varphi' = 20°$. Such values accord very well with data obtained by direct shear tests, which gave values of peak shear strength angle of about 20° for remoulded superficial soils (RC) and of about 18° for the residual shear strength of Scaly Clays. With reference to zone D, the analyses were carried out by fixing the position of the slip surface crest and foot, assuming a piezometric line at the ground level and assigning to c' and φ' the above values. A factor of safety equal to 1 was achieved for a slip surface seated along the contact between the RC and SC soils at a maximum depth of 14 m. Back analyses were carried out by a software using the Spencer method.

5 STABILIZATION WORKS

The design of stabilization works depended on the decision to safeguard the town by blocking the upslope regression of soil movements. It was believed that the landslide, in absence of any intervention, could regress upstream, involving the collapse of other buildings. This hypothesis was confirmed by the movement occurred in zone F (Fig. 1) a few months after the main event of 14th February. On the other hand, the extent of the landslide and the difference in its characteristics in the single zones made very difficult and almost impossible work aiming to stabilize the overall area. On the basis of such consideration, designed works, still in progress, were devised according to two lines of defence: retaining the upslope soils by means of massive retaining structures placed just up of the rear scarps of landslide in the zones C, D, E; lowering the ground water level in the town site by an articulated net of trench drains and draining secant piles. The layout of stabilization works designed in zone E is shown in Fig. 5. Retaining structures, set along the boundary of the urbanized area, include circular structural caissons, placed at a distance of 22 m, having an external diameter of about 12 m and a depth of about 24 m. Caissons were built inside a ring of piles with a diameter of 800 mm and a length of 28 m (Figs. 5 and 6). Caissons were connected by semicircular pile walls consisting of piles with a diameter of 800 mm and a length of 28 m (Fig. 5).

Just behind the retaining structures, draining secant piles are placed, made of permeable concrete (made of gravel and cement), with a diameter of 600 mm and a length of 12 m, located at intervals of 45 cm (Figs. 5 and 6). The choice of the draining secant piles depends on avoiding excavation in the moved zones. Micro perforated pipes 4 m in length set at different depths enable hydraulic connection between the draining secant piles and the structural caissons (Fig. 6). It is evident that caissons have both a retaining and a draining function.

In the town along some streets aligned with the rear scarps of slide areas, some trench drains 5 m deep have been built using permeable concrete. In order to defend stability of buildings seated on both sides during trench excavation and

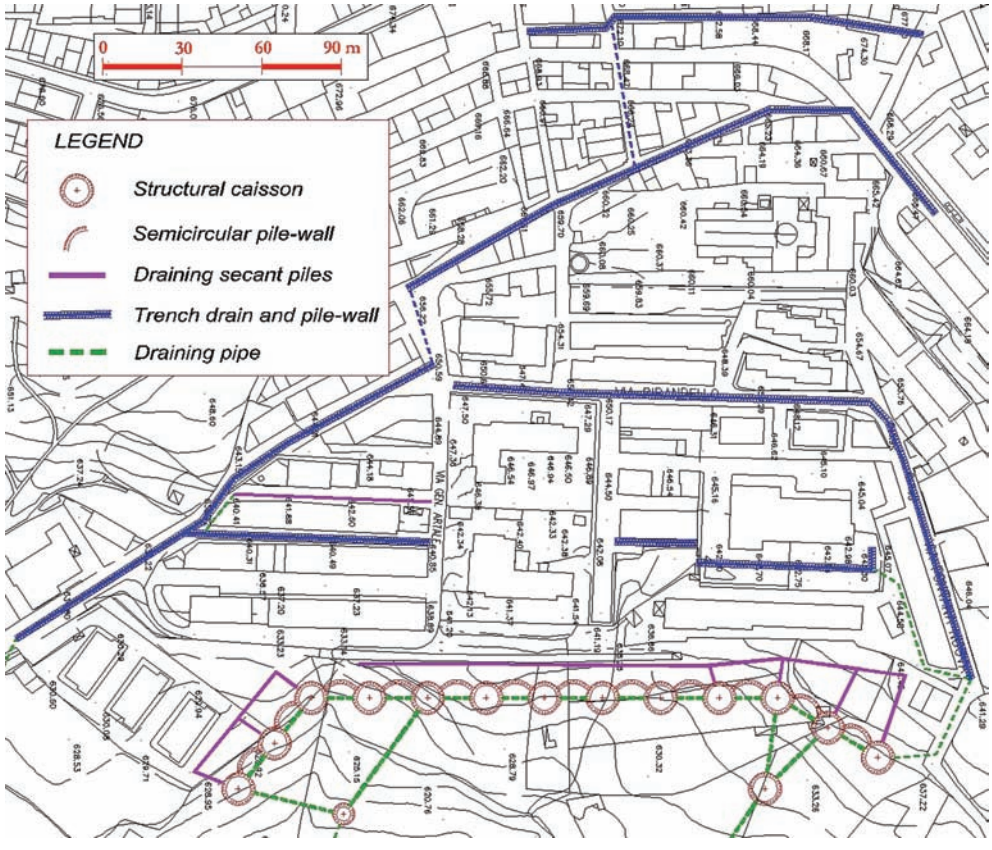

Figure 5. Stabilization works in Stazzone.

limit foundation movements induced by drainage, pile-walls are built, formed by two rows of piles with a diameter of 600 mm and a length of 21 m connected by a reinforced concrete beam. Trench drains are excavated between the two pile walls. The layout of stabilization works is the same for zones D and C. However, the number of caissons, retaining and draining secant piles and trench drains varies according to the zone width and calculated factor of safety increments. Stabilization works consist of modules of retaining and draining works, which can be repeated until a satisfactory stability level is achieved in the considered zones. With reference to the large landslide area below the ridge, analyses are still continuing in order to detect causes of movement reactivation at the foot of the landslide and in the upslope zones. On the basis of collected results, it will be possible to devise suitable works aiming at controlling and limiting movements. In this case, preferred solutions will be addressed to surface arrangement, as slope profiling, and naturalistic engineering works. The main objectives are related to the arrangement of the forest and the recovery of the land area used for agriculture and the breeding of the selected breeds that have made famous San Fratello in Sicily.

6 MONITORING SYSTEM

A monitoring system is still in progress devoted to control: effects of stabilization works on buildings both during construction phase and in the long-term conditions; the effectiveness of stabilization works during the time with reference to the overall stability.

A survey of surface movements on the overall ridge has been active since April 2010 by using ground-based SAR interferometry, whose instrumentation was installed on the slope in front of San Fratello. At the same time, high precision traditional topographic surveys were carried out to monitor displacements of ten selected points in the town.

In the summer 2010 and in the spring 2011, as previously noted, stand pipe piezometers and

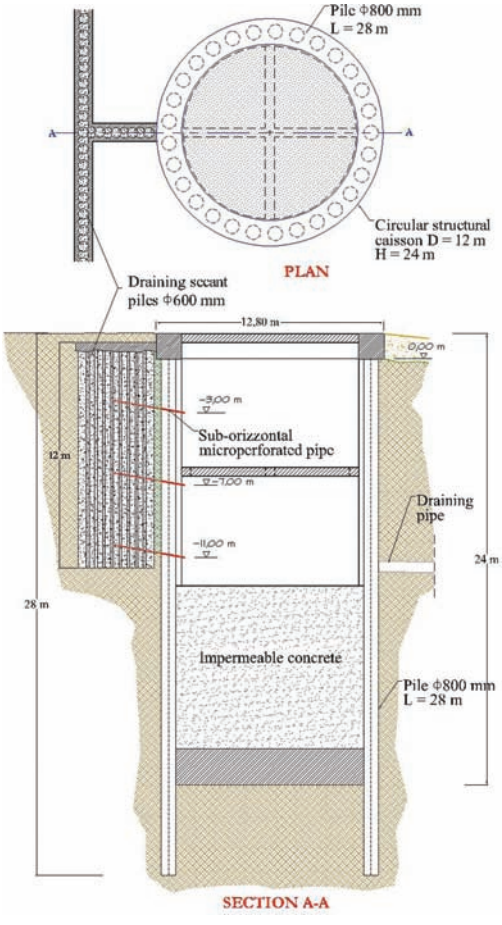

Figure 6. Trench drain and circular structural caisson.

inclinometers were installed in some boreholes. At the beginning of trench drain construction, accelerometers have been placed in the buildings closest to the pile walls in order to control vibration effects on buildings. Topographic surveying is continuing to monitor building settlements induced by drainage. Recently, a GPS technology was implemented to control movements of a net of points sited in the town, in correspondence of stabilization works and on the landslide zones. The monitoring system is believed of paramount importance in order to achieve deeper information on the mechanisms determining activation of movements in the landslide zone and to control the effectiveness of stabilization works. In this respect collected measurements of movements in zone E, where the stabilization work construction has gone forward, point out a very significant reduction of the displacement rates as shown in Fig 7.

Figure 7. Displacement-time of a selected point.

7 CONCLUSION

San Fratello is an ancient town probably not famous as other historical towns in Sicily like Agrigento, Taormina, Erice and so on. However, it is rich in interesting traditions and cultural heritage going back to the Greek and Roman ages and to the Norman Conquest of Sicily. Besides it is the centre of an environmental and economical system which includes a wide region. This system is interesting not only from a historical and cultural points of view, but also because it could be the nucleus of a new economy based on environment exploitation, cultural tourism and breeding of selected breed of animals. In fact San Fratello is in the middle of a wide wood and is the principal centre of the breed of an horse, just named *"of San Fratello"*, which the tradition believes to go back to the Normans or, further back in the time, to Sicani, the ancient inhabitants of Sicily.

In this regard, the decision to safeguard San Fratello is important from a cultural, social and economical points of view, because it could be an interesting attempt to begin a new economy in an habitat typical of Sicily, based on the exploitation of the territory and its traditional economic activity like agriculture and breeding. In this perspective, gaining some more years of life of San Fratello could be successful at designing such a new economy model and determining with more confidence the definitive arrangement of the whole region.

ACKNOWLEDGMENTS

The authors would like to thank the Department of Civil Protection of Sicily and, in particular, the Eng. Mr. P. Lo Monaco and the Geologist Dr. G. Basile for their contribution to the drafting of this paper.

REFERENCES

AGI, Associazione Geotecnica Italiana. (1979). *Some Italian experiences on the mechanical characterization of structurally complex formations.* Proc. IV Int. Congr. Soc. Rock Mech., Motreux, vol. 1, 827–846.

Cafiso F. (2011). *New technologies employed in studying, monitoring and stabilizing the San Fratello landslide (Sicily, Italy).* The Second World Landslide Forum, Rome (in progress).

Cafiso F., Basile G., Lo Monaco P., (2011). *La frana di San Fratello (ME): studio, monitoraggio ed interventi di stabiliz-zazione*. XXIV Convegno Nazionale di Geotecnica, Napoli, vol. II, 641–648.

Crinò S. (1922). *La frana di San Fratello*. Rivista Geografica Italiana, vol. XXIX, 63–66.

Croce A. (1985). *Antichi monumenti e città. Ricerca e conservazione*. AGI, Geotechnical Eng. in Italy. An overview. Published on the occasion of the ISSMFE Golden Jubily, 57–110.

Jappelli R., Liguori V., Umiltà G., Valore C. (1977). A survey of geotechnical properties of a stiff highly fissured clay. Proc. Int. Symp. "*The Geotechnics of Structurally complex formations*", Capri, vol. II, 91–106.

WP/WLI. (1993). *Multilingual landslide glossary.* Bi-Tech Publishers, Richmond, British Columbia, Canada, 59 pp.

This page intentionally left blank

Geotechnical Engineering for the Preservation of Monuments and Historic Sites – Bilotta, Flora, Lirer & Viggiani (eds)
© 2013 Taylor & Francis Group, London, ISBN 978-1-138-00055-1

Stability analysis of the underground masonry tunnel of Ancient Nemea

H. Alexakis & N. Makris
University of Patras, Patras, Greece

ABSTRACT: In the archaeological site of Ancient Nemea, Greece, southeast of the Temple of Zeus, there is an ancient tunnel that was buried with earth until it was discovered in 1978. At present, some limestone blocks of the tunnel show appreciable damage mainly due to the humidity fluctuation within the tunnel. In this paper we present a comprehensive structural analysis of the underground tunnel based on the thrust line limit-analysis of the masonry arch and its surrounding soil. The study concludes that the tunnel with its overburden-surrounding soil is structurally stable and has ample bearing capacity. At the same time the study shows that the stones which suffer the most noticeable exfoliation due to the humidity fluctuation are those that their visible surface from the inside of the tunnel is in compression. In conclusion, selective stones of the structure need to be retrofitted in order to avoid further local failures, while the humidity fluctuation inside the tunnel needs to be minimized.

1 INTRODUCTION

The entrance from the west to the ancient stadium at Nemea, Greece (see Fig. 1), is a 36.35 m long vaulted tunnel with inner width that is approximately 2.10 m and with inner height that is approximately 2.45 m.

The tunnel was constructed during the 4th century B.C. as a cut-and-cover structure and subsequently was covered with earth. Both ends of the tunnel were discovered in 1978 (Miller 2001). They were completely filled with and covered over by silty soil. The interior however, had not completely filled. According to Miller (2001), the earth above the tunnel has stabilized over the past 2300 years. Figure 2 shows a section of the tunnel along its longitudinal axis, together with the overburden earth, as was measured in 1978 (Miller 2001). No excavation over it has been attempted until now, because there was the fear that this could affect the stability of the structure with destructive consequences. Part of the motivation of this work is to analyze the structural behavior and offer a dependable load bearing capacity estimate of the tunnel in order to reach conclusions on the stability of the tunnel based on technical arguments.

The fact that the ends of the tunnel were completely filled and prevented the circulation of air had a most beneficiary role on the structural integrity of the tunnel since it minimized the fluctuation of humidity. Although the tunnel was remarkably well preserved, a few of the blocks of the vault were

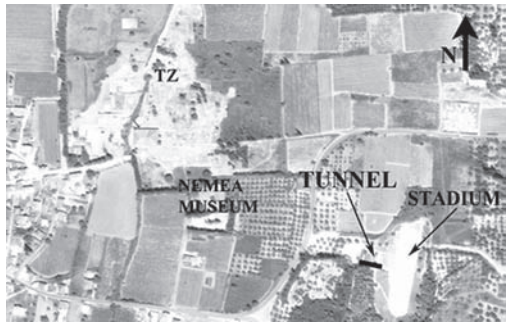

Figure 1. Aerial view of part of the valley of Ancient Nemea, showing the locations of the sanctuary of the Temple of Zeus (TZ), the stadium and its tunnel entrance from the west.

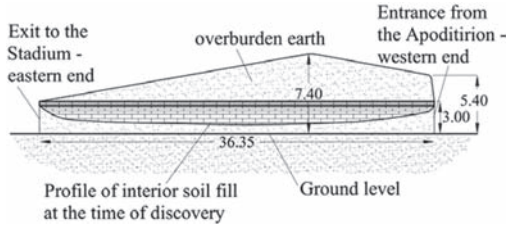

Figure 2. Schematic section of the tunnel along its longitudinal axis showing the levels of earth fill inside and above the tunnel.

Figure 3. Current view of the entrance of the tunnel (western end-top), the exit to the stadium (eastern end-center) and the interior of the tunnel (bottom).

missing, while the face of many of the voussoirs had split off (Miller 2001, see also Fig. 3 bottom). Figure 3 (top) shows the entrance of the tunnel (western end), while Figure 3 (center) shows the exit of thetunnel to the stadium (eastern end) as they appear today. Upon the removal of the earth that filled the entrance, the tunnel was subjected to a more intense fluctuation of humidity and further exfoliation of stones has been observed during the recent years.

2 DESCRIPTION OF THE TUNNEL STRUCTURE AND ITS INTERACTION WITH THE SURROUNDING SOIL

The tunnel was initially constructed in a straight trench that was excavated in a firm soil/soft rock. It consists of two vertical stone walls which support the cylindrical vault (see Fig. 3). The vertical wall and the cylindrical vault consists of limestone blocks of about the same size, with dimension of the order of 40 cm, built in horizontal rows, as shown in Figure 3 (bottom). Figure 4 shows a drawing with the average dimensions of the stone blocks at a given cross section of the tunnel. At each side, the lower stone row is the foundation and the above four (4) rows form the walls of the tunnel, as shown in Figure 3. The cylindrical vault consists of a central row of key stone and four (4) rows of voussoirs on each side. The width of the voussoirs at the extrados exceeds 42 cm, while the width of the voussoirs at the intrados is of the order of 30 cm.

Between the vertical walls of the tunnel and the near vertical surface of the excavated soft rock, there is a gap with variable width between 20 and 40 cm. Upon construction of the walls, this gap was filled with silt (probably from the excavated material from the trench), which appears to be well compacted. Accordingly, the backfill soil between the vertical walls and the soft rock initially was in a triaxial stress state. The good construction of the tunnel in association with the shape of the thrust line of the free standing tunnel before the backfill was placed (see Fig. 6 top) together with the relative high value of the coefficient of the friction along limestone surface $\mu_{LS} > 0.7$ (Konstantinidis & Makris 2005) opposes any potential movement of the stones of the walls to the inside; therefore it is unlikely that the backfill soil deteriorated to an active state of stress (point 1 in Fig. 5). Therefore, in addition to the active limit case we examine the case where the horizontal soil stresses $\sigma_h \geq K_a \sigma_v$, where

$$K_a = \frac{1 - \sin\phi}{1 + \sin\phi} \tag{1}$$

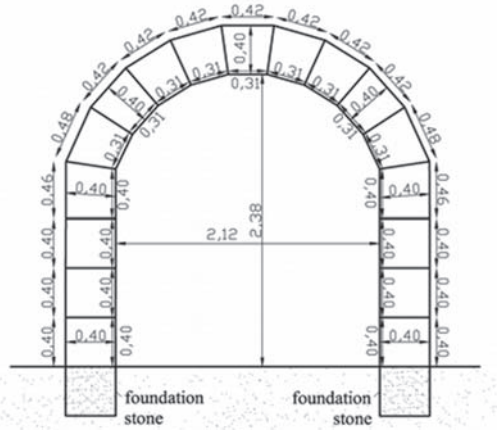

Figure 4. Schematic of a tunnel section showing the dimensions of the stone blocks used in the analysis.

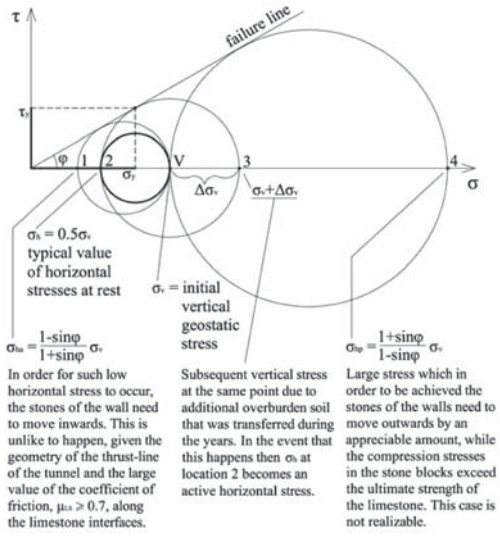

Figure 5. Admissible state of stresses under geostatic conditions.

is the coefficient of active stress. Accordingly, at rest we assume a horizontal stress $\sigma_h = 0.5\sigma_v$ (point 2 in Fig. 5—see also Jaky 1944).

Within the context of the limit analysis for the tunnel-surrounding soil system that this work offers, we adopt for the soil the Mohr–Coulomb failure law

$$\tau_y = c + \sigma_y \tan\phi \tag{2}$$

where c is the cohesion intercept of the failure line with the shear-stress axis and ϕ is the friction angle (angle of shearing resistance) of the soil. Given the lack of information regarding the exact behavior of the backfill soil at failure, we assume that the cohesion intercept $c = 0$ and the failure law for the backfill soil simplifies to

$$\tau_y = \sigma_y \tan\phi \tag{3}$$

The simplified failure law given by Eq. (3) and shown schematically in Figure 5 is attractive since the same expression (with a different value for the friction angle ϕ) is used for the shearing resistance along the interfaces of the limestones of the tunnel; while the reasoning regarding the state of horizontal stresses is not affected by the assumption $c = 0$. With reference to Figure 5 the vertical σ_v and horizontal $\sigma_h = 0.5\sigma_v$ geostatic stresses of the backfill soil are shown respectively with point V and point 2 along the horizontal σ-axis. It is worth mentioning that an analysis with $\sigma_h = 0.5\sigma_v$ and a given value of friction angle ϕ corresponds to a case where σ_h is now an active stress in association with a lower value of ϕ.

Through the years, additional soil was transferred over the tunnel and the initial vertical stress at a point σ_v (point V in Fig. 5) may have increased to $\sigma_v + \Delta\sigma_v$ (point 3 in Fig. 5). Such an increase in the vertical stress may create a sufficient difference between $\sigma_v + \Delta\sigma_v$ and σ_h (segment 2–3) so that σ_h at point 2 becomes an active stress due to the new stress state. It should be noted however that the narrow gap between the wall of the tunnel and the vertical surface does not allow for a linear increase of the vertical stress ($\sigma_v = \gamma z$) as z increases, given that there is substantial friction of the soil with the stone wall of the tunnel and the neighboring excavated vertical wall of the soft rock. The study also examines the unfavourable situation were all the overburden load above the gap is diverted to neighbouring locations due to a possible arching of the consolidated soil above the gap and in this case the lateral stresses σ_h are limited to the value that correspond to the case where the gap is filled only up to the keystone level and the influence of any overburden soil to the lateral stresses on the walls of the tunnel is neglected. Based on the above discussion the structural analysis that follows, in addition to the active limit state $\sigma_h = \sigma_v(1 - \sin\phi)/(1 + \sin\phi)$, investigates the vertical load carrying capacity of the tunnel where the horizontal soil stress $\sigma_h = 0.5\sigma_v$. In the analysis that follows the friction angle for the backfill is assumed $\phi = 30^o$. Consequently the results for the geostatic case $K_0 = 0.5$ (σ_h is point 2 in Fig. 5) corresponds to a conservative active limit state ($K_a = (1 - \sin\phi)/(1 + \sin\phi)$) where $\phi \approx 20°$ (Gazetas & Kavvadas 2009). Accordingly, the analysis presented in this work covers a reasonable range of the angle of internal friction which is on the safe side. The forthcoming analysis shows that the results depend mildly on the value of the coefficient of friction; nevertheless, this dependence is not critical.

The evolution of the thrust line as the backfill height increases in association with the inclination of the limestone interfaces with the thrust line and the typical value of the coefficient of friction along the limestone interfaces indicate that it is unlike that the stones of the walls have move out by an appreciable amount due to hinging of the tunnel, therefore the possibility of encountering a passive failure is excluded (point 4 in Fig. 5). Interestingly, this paper shows that hinging of the tunnel may only happen under very large overburden loads which exceed by far the values of the overburden loads that generate compression failure of the stone blocks of the tunnel.

3 BACKGROUND ON THE STRUCTURAL ANALYSIS OF MASONRY ARCHES AND VAULTED STRUCTURES

The two main approaches for the structural analysis of arches and vaulted structures are: (a) the ultimate stability analysis—also reported as limit stability/equilibrium analysis, rigid-plastic analysis or thrust line method (Heyman 1966, Harvey 1991, Boothby 2001, Block et al. 2006, Roca et al. 2010, among others) and (b) a stress analysis of the structure.

For historic masonry structures in general and more specifically for those constructed from massive bearing stones, the thrust line method is the choice, since compressive stresses are an order of magnitude smaller than the failure stress of the masonry and the issue of stability prevails.

In this paper the loading resistance/capacity of the tunnel-entrance to the Stadium of Ancient Nemea is examined via an ultimate stability analysis. The ultimate stability analysis is first implemented through its classical formulation, using the simplifying assumptions advanced by Heyman (1966) and subsequently via an elaborated formulation presented by Livesley (1978). Using linear programming method based on the kinematic approach, in association with an optimization process Livesley (1978) calculated the limit load on a rigid block structure prior to failure. This work was subsequently followed by several other investigators (Gilbert & Melbourne 1994, Baggio & Trovalusci 1998, Ferris & Tin-Loi 2001, Orduña & Lourenço 2003, among others).

4 LIMIT EQUILIBRIUM ANALYSIS—THE THRUST LINE APPROACH

The thrust line (limit-state) approach has been widely used for the stability of masonry structures since the years of Hooke (1675), who described the analogy between the tension in a hanging chain due to its own weight and the compression along the thrust line of a masonry arch. Heyman (1966) was apparently the first who proposed that the limit equilibrium analysis, which derives from the plastic theory of metal structures, may also be applied for the analysis of stone and masonry structures such as masonry arches and vaults provided that three (3) basic assumptions are introduced (see also Boothby 2001, Block et al. 2006, Roca et al. 2010):

a. the joints of the masonry blocks do not transmit tension (zero tensile tension).
b. the masonry blocks are rigid and incompressible.
c. the masonry blocks do not slide at the joints.

In the case of the vaulted tunnel of Nemea, the assumptions (a) and (b) apply since the working stress along the tunnel (~1.0 MPa) are more than an order of magnitude less than the average strength of the limestone (~10 MPa) (Makris & Psychogios 2004). Moreover, given that there is no mortar at the stone block interfaces in association with the relative high value of the modulus of elasticity (~E = 6.5 GPa) to the working stresses (~1.0 MPa), the stone blocks may considered as rigid.

The equilibrium-stability of a stone arch is established via the thrust line. This is a physically realizable line that represents the load path of the resultant of the compressive forces through the stone skeleton. For a structure in pure compression to be in equilibrium with the applied loads there must be a line of thrust that lies entirely within the section of the structure.

In this work the limit equilibrium analysis is performed with two validated computer codes known as ARCO v1.1 (Gelfi 2002) and RING v1.5 (Gilbert et al. 2005). Both codes idealize a vaulted structure as an assemblage of rigid blocks. Software ARCO assumes that no sliding occurs at the block interfaces and computes the optimum thrust line via an optimization process which converges to the thrust line that minimizes the normal stresses at the extrados and intrados of each block interface. When the thrust line is eccentric in association that the stone interface does not take any tension, the stress distribution is assumed to be triangular with the resultant force, N, passing through the 1/3 of the base of the triangle. Accordingly, the width of the base of the triangular distribution is $3d$; and from equilibrium $N = \sigma_{max}\ 3d/2$. Software RING analyses only the collapse state of the structure. In addition to basic equilibrium considerations, two conditions are examined to test for ultimate collapse: (a) hinging where the line of thrust can be transmitted through a hinge point lying on (infinite strength) or near (finite strength) an exterior face of the arch and (b) sliding (assuming that sliding failures obey an associative flow rule).

5 LIMIT EQUILIBRIUM ANALYSIS OF THE IDEALIZED TUNNEL

The thrust line can be graphically described by the use of the force polygon. Figure 6 (top) shows the thrust line of the free-standing tunnel (no backfill—there is no vertical or lateral earth pressure) where the only load is the weight of each block (W1–W9). Figure 6 (top-right) shows graphically the vector summation of forces (force polygon) as we move from the keystone (No 9) to the above-the-foundation stone of the wall (No 1). With reference to Figure 6, note that the thrust line meets the interfaces of the stone blocks at various angles ψ.

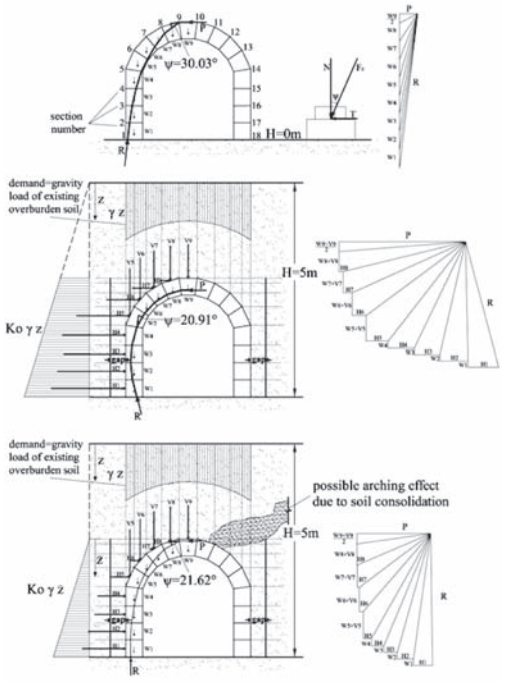

Figure 6. Top: Thrust line and force polygon of the free-standing tunnel (no backfill). Center: With 5 m backfill-overburden soil assuming that the entire overburden vertical load enters through the gap. Bottom: With 5 m of backfill-overburden soil assuming that the path of overburden vertical load is arrested due to some arching effect between the top voussoirs and the excavated wall of the gap.

The force normal to the stone interface (potential failure plane) is $N = F_c \cos\psi$, while the force tangential to the stone interface is $T = F_c \sin\psi$. Assuming that the coefficient of friction at the stone interface is μ, sliding along the interface will not happen as long as

$$T = F_c \sin\psi < \mu N = \mu F_c \cos\psi \text{ or } \tan\psi < \mu \qquad (4)$$

When the thrust line is inclined enough ($\tan\psi = \mu$), sliding = failure occurs and in this case

$$T = N \tan\psi \qquad (5)$$

Eq. (5) is the same expression (in terms of forces) as Eq. (3) and indicates that upon dividing the forces with the contact surface of the adjacent stones, the Mohr–Coulomb criterion introduced earlier as the failure law for the backfill soil is also valid for the limestone where the angle of shearing resistance ϕ for the soil is replaced with the angle for shearing resistance ψ for the limestone. For limestones, a conservative value for the coefficient of friction is $\mu_{LS} = 0.7$, therefore sliding will occur for an angle $\psi > \tan^{-1}\mu_{LS} = 35°$ (capacity). Figure 6 (top) shows that the larger angle of incidence of the thrust line (demand) is $\psi_{max} = 30.03°$, therefore assuming that all stones are in healthy condition ($\mu_{LS} = 0.7$) the possibility of sliding is excluded given that $\psi_{max} = 30.03° < \tan^{-1}\mu_{LS} = 35°$. Figure 6 (top) also shows that the geometry of the thrust line of the free-standing tunnel (no backfill soil) is such that the tangential-to-the-stone interface forces along the walls of the tunnel are towards the outside. Accordingly, upon the tunnel was constructed and the backfill soil was placed the situation where the stones of the wall move to the inside leading to an active failure of the soil is excluded. Figure 6 (center) shows the thrust line of the tunnel where there is 5 m high of backfill ($\rho = 1.8$ Mg/m^3) and the horizontal soil stresses $\sigma_h = 0.5\sigma_v = 0.5\gamma z$ (point 2 in Fig. 5, $\phi = 30°$). As we move from the keystone to lower stones of the walls, in addition to the gravity loads, the stones are subjected to horizontal forces from the backfill soil. This coexisting lateral thrust bends the thrust line to the inside as depicted schematically in the vector summation of forces shown at the center-right of Figure 6. Note that for this case the largest deviation of the thrust line from the perpendicular to the stone interface is at the first stone of the vault (springer), where $\psi_{max} = 20.91°$, a value that is appreciable lower than the 35° of available frictional resistance. Figure 6 (bottom) shows the thrust line of the tunnel where there is 5 m height of backfill-overburden soil ($\rho = 1.8$ Mg/m^3) but now the horizontal soil stresses σ_h are limited to the case where the gap is filled only up to the keystone level of the tunnel and the effect on the lateral stresses on the walls of the tunnel of any overburden soil is neglected. This situation results to smaller lateral stresses than those shown in Figure 6 (center) and the corresponding thrust line assumes a shape that is in between the shape shown in Figure 6 (top) and 6 (center). Note that even in the unfavorable situation shown in Figure 6 (bottom) the maximum angle that the thrust line meets the stone interfaces is $\psi = 21.62°$ which is much lower than the typical values of internal friction for limestone. The findings shown in Figure 6 indicate that the tunnel is a well engineered "self-locking" structure which does not allow any movements of its constituents stones neither to the outside nor to the inside; therefore the outside backfill soil shall remain at rest ($K_o = 0.5$).

Figure 7 shows the evolution of the thrust line of the tunnel as the backfill height increases from $H = 1$ m to $H = 9$ m. Note that as the backfill height increases the largest deviation of the thrust line from the perpendicular to the stone interface

Table 1. Maximum compressive stresses at the extrados and the intrados together with the angle ψ of thrust line with the normal to the contact surface of the stones.

H m	max σ_{ex} MPa	S.n*	max σ_{in} MPa	S.n*	max ψ demand (°)	min μ for no sliding	S.n*
0	0,380	1, 18	0,380	5, 14	30,03	0,5780	9, 10
1	0,205	9, 10	0,205	5, 14	28,06	0,5331	9, 10
2	0,174	4, 15	0,174	1, 18	24,53	0,4564	5, 14
3	0,304	3, 16	0,304	9, 10	24,35	0,4526	5, 14
5	0,447	3, 16	0,447	1, 18	20,91	0,3821	5, 14
7	0,683	3, 16	0,683	1, 18	18,92	0,3428	5, 14
9	0,921	3, 16	0,921	1, 18	18,06	0,3261	5, 14

* Section number (see Figure 6-top).

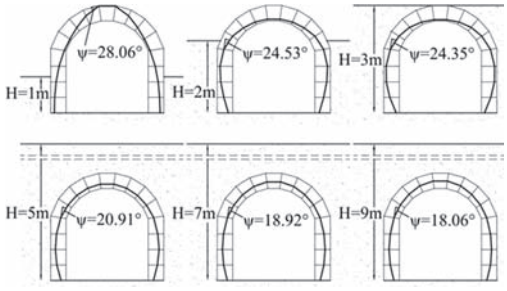

Figure 7. Evolution of the thrust line of the Nemea tunnel as the backfill height H increases. As H increases the longest deviation of the thrust line from the perpendicular to the stone interface decreases, leading to a more stable configuration.

decreases, leading to a more stable configuration. Table 1 offers the maximum values of angle ψ and the interfaces where they appear together with the corresponding values of coefficient of friction needed for no sliding and the maximum compressive stresses that develop at the stone interfaces. Note that even when the backfill soil reaches a height H = 9 m the maximum compressive stress is below 1.0 MPa—that is an order of magnitude less than the compressive strength of the Nemea limestone.

Figure 3 (bottom) shows clearly the loss of material at the bottom of the walls and in the vicinity of the springer stone. This exfoliation pattern is in direct correlation with the shape of the thrust line of the underground tunnel (Figure 7), which reveals that the visible surfaces of the stones which have suffered most are those in compression. Alexakis & Makris (2013) confirm this finding with finite element analysis.

Our limit equilibrium analysis proceeds with the limit analysis of a slice of the tunnel that is 1 m thick and with variable backfill height H, that is further loaded with a distributed load that ranges over the 3 m width of the tunnel. What is interesting is to compute what additional distributed load will take to fail the tunnel. For instance, Figure 8 (top) shows that when there is 5 m of backfill the gravity load of the existing overburden soil along 1 m of tunnel depth is 133 kN whereas it takes 773 kN distributed load over the 3 m-width of the tunnel (that is an additional column of soil 3 m × 1 m × 14.31 m) to fail the 1 m thick tunnel section. In this calculation the lateral stresses on the wall of the tunnel are those that correspond to the existing 5 m high overburden soil assuming that the entire overburden load penetrates into the gap. It is important to note that under this very high additional overburden load the tunnel fails because we exceed the compressive strength of the limestones (say σ_{max} = 10 MPa)—not because we reached instability due to hinging of the tunnel. At the bottom stone and the springer where the compressive stresses reach 10 MPa, there is still a finite distance $d \neq 0$ between the thrust line and the extrados and intrados respectively, so that $\sigma = 2N/3d = \sigma_{max}$. Figure 8 (bottom) shows the unfavorable limit state by assuming that the backfill is

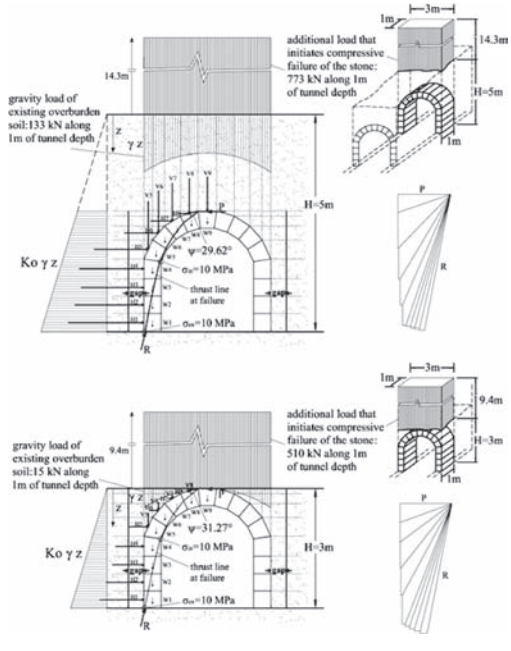

Figure 8. Thrust lines of the Nemea tunnel when compressive failure of the stone blocks is reached, together with the loads needed to fail a 1.0 m thick section of the tunnel. Top: The entire overburden vertical load from a 5 m backfill-overburden soil enters through the gap. Bottom: Lateral loads on the walls of the tunnel are limited to the backfill up to the keystone level.

only up to the level of the keystone of the tunnel. In this case it takes 510 kN distributed load over the 3 m-width of the tunnel (that is a column of soil 3 m × 1 m × 9.4 m) to fail the 1 m thick tunnel section. Consequently, regardless of what is the exact value of the compressive strength (σ_{max} = 10 MPa), the tunnel has ample bearing capacity even when we assume an unfavorable situation for the lateral soil pressure. Again, as in Figure 6, the larger angle of incidence of the thrust line is in the neighborhood of 30°; therefore, assuming that all stones are in healthy condition, the possibility of sliding is excluded given that with μ_{LS} = 0.7, ψ_{max}< $\tan^{-1}\mu_{LS}$ = 35°.

Figure 9 shows that the additional load that is needed to fail the Nemea tunnel is an increasing function of the existing backfill height. All lines except the demand (dotted) line in Figure 9 show the entire vertical load that a one-meter-thick slice of the tunnel can sustain (see Fig. 8). The continuous dark and gray lines are computed with software ARCO which assumes that no sliding occurs

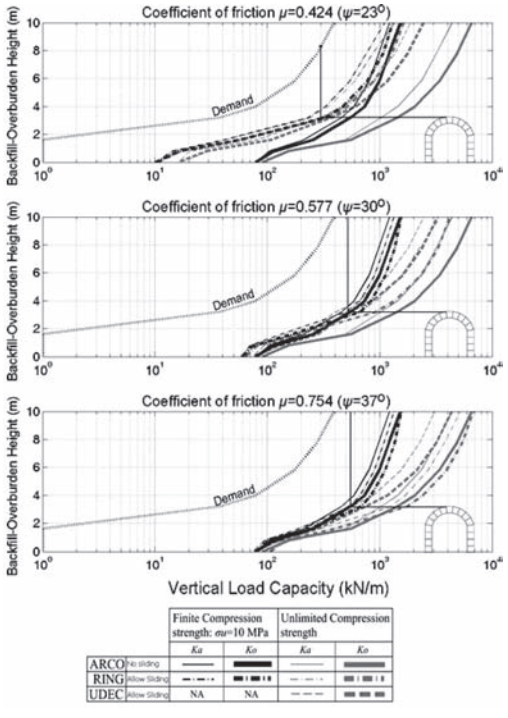

Figure 9. Vertical load carrying capacity as a function of the backfill-overburden soil height next and above the tunnel. The center plot shows that even for a value of ψ = 30° which is below the typical values of friction angle for limestone and even when the backfill is only up to the keystone level, the tunnel can sustain a demand of overburden soil with height larger than 10 m.

along the stone interfaces. The dark lines show the ultimate load which is controlled by the compressive failure of the limestone (σ_{max} = 10 MPa), while the gray lines show a fictitious ultimate load which is controlled from the hinging of the tunnel assuming building blocks with unlimited compressive strength. The thick lines is when the lateral soil stress ratio $K = K_o$ = 0.5; whereas, the thin lines is when the lateral soil stress ratio $K = K_a$ (ϕ = 30°). The corresponding chain lines are computed with the software RING which also examines whether sliding occurs. The results presented in Figure 9 (bottom) are for a relative high value of the coefficient of friction μ = 0.754 (ψ = 37°). The results from both computer codes are in good agreement. Next to these lines, the dashed lines are the results from a distinct element method (Alexakis & Makris 2013), which are in good agreement with the thrust line analysis.

Figure 9 (centre and top) plots the same results as those presented in Figure 9 (bottom), whereas now the coefficient of friction along the block interfaces is μ = 0.577 (ψ = 30°) and μ = 0.424 (ψ = 23°) respectively. Note now the results obtained with software RING which allows for sliding along the block interfaces predict a bearing capacity lower than the bearing capacity predicted with ARCO, since the lower value of friction coefficient assumed in this analysis (μ = 0.577 and μ = 0.424) may allow for some sliding along the stone interfaces. In any event, Figure 9 shows that regardless of what is the exact value of the horizontal soil stresses, the tunnel at Nemea has ample vertical load carrying capacity.

6 CORRELATION OF COMPUTED LOAD PATHS WITH OBSERVED/REPORTED DAMAGE

The vaulted tunnel next to the stadium of Ancient Nemea was discovered in 1978 by S.G. Miller (2001). In volume II of his work "*Excavations at Nemea*" entitled "*The Early Hellenistic Stadium*", Miller (2001) offers a thorough description of the observed damage of the tunnel with emphasis on a keystone block and its adjacent voussoir stone which had fallen down about 25 m from the eastern end of the tunnel. Miller indicates that the fallen stones had disintegrated while structural problems in this part of the tunnel must have begun very early in its history given that large fragments of the one or more voussoirs were found in layers as low as only 20 cm above the floor of the tunnel.

There are several possible causes of these reported failures. Nevertheless, the structural analysis presented in this paper may offer a plausible convincing explanation. Figure 6 (top) shows that

when the tunnel is without backfill, its thrust line at the keystone approaches the extrados and exerts a compressive force at the outer corner of voussoir stone, No 8, adjacent to the keystone, No 9. Given the local character of this thrust in association with a possible poor quality of this specific stone, yielding or crashing of the corner of this voussoir No 9 at the extrados may have occurred. Figure 6 (top) also indicates that when the tunnel is free-standing (no backfill) the thrust line meets the interfaces of the voussoir stone No 8 and the keystone No 9 at the higher angle $\psi = 30.03°$. A value of $\psi = 30.03°$ corresponds to a demand friction coefficient $\mu = \tan\psi > 0.578$ for sliding not to happen. In the event that this specific voussoir stone is of poor quality it is possible that such a value of coefficient of friction ($\mu = 0.578$) did not develop at this specific interface and in association with the possibility that its upper extrados corner has crashed, the result was that this voussoir stone to slide inwards. Figure 7 indicates that as the backfill height increases the thrust line at the key stone lowers towards the intrados. The presence of these compressive forces in association with the fluctuation of humidity may have further chipped the voussoir stone or the keystone at the intrados. It is this combined effect of a premature sliding of the voussoir to the inside due to the relative high value of the incident angle ψ before the backfill was placed in association with the humidity fluctuation that may have caused the local failures reported by Miller (2001). The alternative explanation for the observed failure offered by Miller (2001)—that due to the settling weight of the earth above the vault forced the walls of the tunnel to bow out (therefore reaching a passive limit state of the soil in the vicinity of the springer), thus increasing the width of the tunnel and opening the vault enough so that the wedge shape block could fall in—is most unlikely since as the value of the backfill increases the value of the maximum incident angle ψ decreases (see Figure 7); therefore the tunnel becomes even more stable and the possibility of the stone blocks to move out is further reduced. Consequently, Figure 10 plots the width of the tunnel measured at the bottom stones of the walls (line 2–17) and the width of the tunnel measured below the springer stones (line 4–15) as a function of the length of the tunnel. These values are measured with a laser pointer which occasionally was pointing to local indentations of the weathered stones. Despite the presence of these local indentations, the bottom and the top width of the tunnel is remarkable close and any possibility that the vault opened is excluded. In fact, the measurements reported in Figure 10 show larger variations of the measured distances close to the East exit of the tunnel where no damage of the vault has been observed.

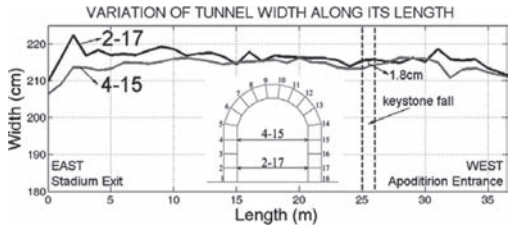

Figure 10. Variation of the width of the tunnel along its length as measured at the bottom stones of the walls (distance 2–17) and below the springers of the vault (distance 4–15). The neighborhood defined with the vertical dashed lines is where the keystone block and its adjacent voussoir stone had fallen.

The failure mode conceived intuitively by Miller which requires the development of passive soil stresses in the neighborhood of the springer stone is a fictitious mode which cannot be reached given that: (a) the tunnel will have failed earlier (under lower overburden loads) due to compressive failure of the stone blocks as shown in Figure 8; and (b) there is no evidence that the vault opened allowing for the falling of the wedged-shaped voissoirs.

7 CONCLUSIONS

In this paper we present a comprehensive structural analysis of the underground tunnel based on the thrust line limit-analysis of the masonry arch and its surrounding soil.

The study concludes that for all levels of the overburden soil, the thrust line meets the normal-to-the interfaces of the stone blocks at angles ψ which are lower than the available frictional resistance. Consequently the tunnel is a well engineered "self-locking" structure which does not allow any movements of its constituent stones either to the outside or to the inside. This finding implies that the soil next and above the tunnel remained through the years at rest and that the possibility that it deteriorated to an active limit state is remote. The limit equilibrium analysis shows that even when an active limit state for the soil has been assumed (most conservative scenario) the tunnel at Nemea has ample vertical load carrying capacity.

Assuming that the overburden load above the tunnel increases, the tunnel will eventually fail due to compression failure of its stone blocks—not due to hinging of the tunnel. This is true even for the unfavourable case where the vertical loads from the overburden soil do not penetrate in the gap between the tunnel walls and the nearly vertical excavated surface; and in this case the lateral stresses on the walls of the tunnel may be limited to the values that corresponds to the case where

the gap is filled only up to the keystone level. This finding concludes that the development of passive soil stresses is not physically realizable.

The thrust line analysis reveals that the surfaces of the stones of the tunnel which have suffered from exfoliation are those in compression. Given that the exfoliation is the result from a combination of the fluctuation of humidity and compressive stresses, the study concludes that the fluctuation of humidity needs to be minimizes by preventing the active circulation of air through the tunnel.

REFERENCES

Alexakis, H. & Makris, N. 2013. Structural Stability and Bearing Capacity Analysis of the Tunnel-Entrance to the Stadium of Ancient Nemea. *Int. J. Arch. Her*. Vol.7 (in press).

Baggio, C. & Trovalusci, P. 1998. Limit Analysis for No-Tension and Frictional Three-Dimensional Discrete Systems. *Mech. Struct. Mach. 26*(3):287–304.

Block, P., Dejong, M. & Ochsendorf, J. 2006. As Hangs the Flexible Line: Equilibrium of Masonry Arches. *Nexus Network J.* 8(2):13–24.

Boothby, T.E. 2001. Analysis of masonry arches and vaults. *Prog. Struct. Engng Mater* 3:246–256.

Ferris, M.C. & Tin-Loi, F. 2001. Limit analysis of frictional block assemblies as a mathematical program with complementarity constraints. *Int. J. of Mech. Sci.* 43:209–224.

Gazetas, G. & Kavvadas, M. 2009. *Soil-Structure Interaction*. Monograph, Published by the National Technical University of Athens, Greece (in Greek).

Gelfi, P. 2002. Program ARCO: Assessment of masonry arches and vaults, Version 1.1 (free distribution), <http://dicata.ing.unibs.it/gelfi/arco.htm>, University of Brescia.

Gilbert, M. & Melbourne, C. 1994. Rigid-block analysis of masonry structures. *Struct. Eng.* 72(21):356–361.

Gilbert, M., Ahmed, H.M. & Sollis, A.J. 2005. RING: Analysis software for masonry arch bridges, Version 1.5 (free distribution), <http://www.ring.shef.ac.uk/index.html>, University of Sheffield.

Harvey, W.J. 1991. Stability, strength, elasticity and thrustlines in masonry structures. *Struct. Eng.* 69(9):181–184.

Heyman, J. 1966. The Stone Skeleton. *Int. J. Solids Struct*. 2(2):249–279.

Hooke, R. 1675. A description of helioscopes, and some other instruments. London.

Jaky, J. 1944. The coefficient of earth pressure at rest. *J. Soc. Hungarian Archit. Eng.* 78(22):355–358.

Konstandinidis, D. & Makris, N. 2005. Seismic Response Analysis of Multidrum Classical Columns. *Earthq Eng Struct Dyn* 34:1243–1270.

Livesley, R.K. 1978. Limit analysis of structures formed from rigid blocks. *Int. J. Numer. Methods Eng.* 12(12):1853–1871.

Makris, N. & Psychogios, T. 2004. Static and dynamic analysis of columns and part of the entablature of the NE corner of the temple of Zeus at Nemea. Report to American School of Classical Studies, Athens.

Miller, S.G. 2001. *Excavations at Nemea II: The early Hellenistic Stadium*. Berkeley and Los Angeles, California: University of California Press.

Orduña, A. & Lourenço, P.B. 2003. Cap Model for Limit Analysis and Strengthening of Masonry Structures. *J. Struct. Eng.* 129(10):1367–1375.

Roca, P., Cervera, M., Gariup, G. & Pela', L. 2010. Structural Analysis of Masonry Historical Constructions. Classical and Advanced Approaches. *Arch Comput Methods Eng* 17:299–325.

This page intentionally left blank

Geotechnical Engineering for the Preservation of Monuments and Historic Sites – Bilotta, Flora, Lirer & Viggiani (eds)
© 2013 Taylor & Francis Group, London, ISBN 978-1-138-00055-1

Foundation systems of some heritage buildings in Najaf/Iraq case study: Al Shelan Khan

N.K.S. AL-Saoudi
Building and Construction Engineering Department, University of Technology, Baghdad, Iraq

M.Sh. AL-Shakerchy
Civil Engineering Department, University of Kufa, Najaf, Iraq

ABSTRACT: The word "Khan" refers to the place where visitors to Najaf city will rest for few days. Historically visitors with their animals, as the only means of transport, usually come to Najaf city in certain religious occasions, rest and settle down in Al Shelan Khan. The Khan was constructed in 1895 by the governor (Wally) Muhammad Mueen Aga during the last years of the Ottoman Empire. The Khan is distinguished by its architectural design and the configuration of the types of columns and arches. The structure has an overall area of 1500 m^2 consisting of two floors and three basements located at different places in the structure layout. The foundation of the structure is strip type extended approximately 5.5 m below ground level. Bricks of dimensions 22 cm ∗ 10 cm ∗ 4.5 cm are the building units with a mixture of "juss", lime as binding material. The paper focuses on the overall structural skeleton of the Khan and on the analysis of foundation system.

1 INTRODUCTION

Najaf is one of the most important cities in Iraq due to its spiritual and religious reputation. It is located in middle of Iraq and south of Baghdad in the west of the Euphrates River. Locally Najaf extends between 44° 15′ 23″– 44° 25′ 25″ longitude and 31° 54′ 25″–32° 02′ 45″ latitude and lies on the edge of the sedimentary plain of the lower Mesopotamian. Figure 1 demonstrates the location of Najaf city with respect to Iraq.

Najaf city has a remarkable historical background. It is a holy town containing the shrine of Imam Ali Bin Abe Talib, the fourth Caliph and the cousin of Prophet Muhammad. The city is distinguished by its religious reputation which makes it a respectable place for all mausoleums. The city host many archeological monuments and heritage structures, among these is Al Shelan Khan. The Khan was constructed in 1895 by the governor (Wally) Muhammad Mueen Aga during the last years of the Ottoman Empire to serve as a rest house for the visitors of the holy shrine of Imam Ali Bin Abe Talib and sometimes by merchants travelling between different places; as part of the trading activities. After many years, the Ottoman government decided to make the Khan as head quarters of the Ottoman government. (A1-Khalidi 2010)

From 1915 till 1920, the Khan was the centre of the local government under the control of the

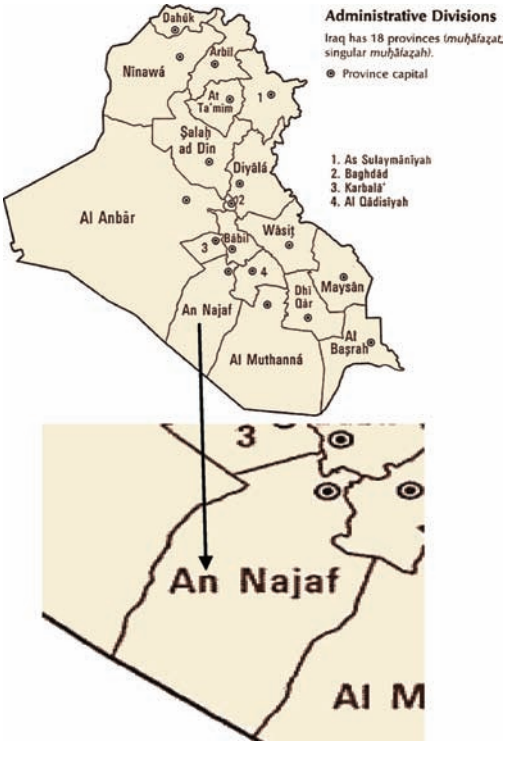

Figure 1. Location of Najaf city in Iraq.

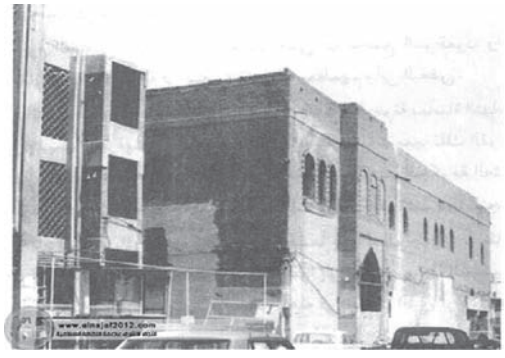

Figure 2. Old photo of Khan Shelan.

Figure 3. Damaged parts of Khan Shelan.

British authority. In 1920 and after the Najaf revolution, the Khan had been used for different purposes. Figure 2 shows one of the oldest photos of the Khan (Al-Arraji 2011).

As many other historical and cultural places the Khan suffers from the lack of rehabilitation and maintenance. During the past decades, it was used by the local people of Najaf in an illegal way. Parts of the ground floor were modified into a number of stores that damaged its architectural presence as a heritage symbol of Najaf city. Parts of the Khan were also subjected to devastation by vandalism actions and many others were damaged due to the long period of different environmental conditions. Figure 3 shows parts of the devastated arches and walls (Shinan 2012).

Currently the local government of Najaf is rehabilitating and redecorating this heritage structure. After the rehabilitation is completed, the Khan is going to be the historical museum housing the panorama of the Najaf revolution in 1920 and many archeological and cultural pieces of the city.

2 GENERAL DESCRIPTION OF THE KHAN

The Khan is an old bearing type structure of plan dimensions 45 m by 46.5 m, consists of two floors with open yard 20 m by 22.66 m in the middle of the structure, figure 4. The total height of the Khan is about 11.5 m above natural ground level. The Khan contains many rooms of different dimensions with two distinguished large rooms on the ground floor of dimensions 9 m ∗ 9 m and double height ceiling, which were probably used as meeting halls.

There are three basements extending in depth to about 5 m below natural ground level, two of dimensions 9.18 m ∗ 10.15 m and the other 9 ∗ 11.5 m. Figure 5 shows the location of the basements.

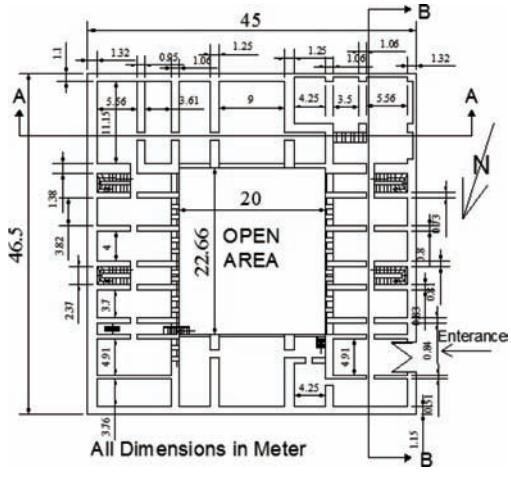

Figure 4. General plan of Khan Shelan.

Figure 5. Location of the three basements.

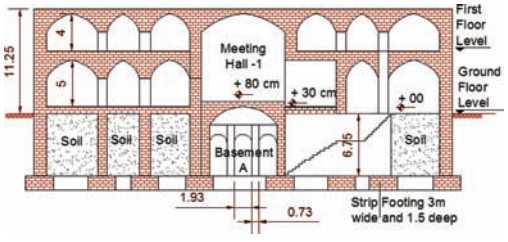

Figure 6. Section A-A in figure 4.

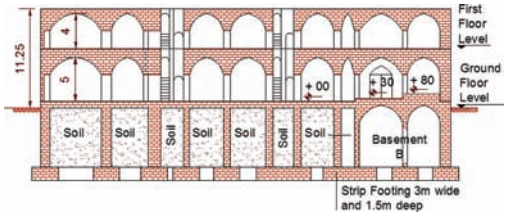

Figure 7. Section B-B in figure 4.

Figures 6 and 7 show the details of the sections A-A and B-B in figure 4. The two sections in figures 6 and 7 clearly demonstrate the different arches used in the Khan and all foundations are placed on the same level.

3 THE STRUCTURAL ANALYSIS OF THE KHAN

The whole structure was constructed of bearing walls made of bricks of dimensions 22 cm ∗ 10 cm ∗ 4.5 cm. These dimensions are not the same as the current standard brick dimensions. The mortar between the bricks is a mixture of lime and "juss". The structure is distinguished by its architectural and structural design. The ceilings of the rooms are basically a combination of arches and domes, supported by different sizes of embedded columns in the walls. The different patterns of ceilings are discussed separately according to their existence in the structure.

3.1 *The basements*

A typical section in basement A of dimensions 9 m by 11.15 m is shown in figure 8.There are two types of embedded columns in the walls; the major ones are 1.06 m ∗ 2.20 m and 2.5 m apart along the long sides and the minor ones are 0.52 m ∗ 2.00 m along the short side, 2.45 m apart. Each two opposite columns support a complete arch, and the number of arches forms the ceiling of the basement. Figure 9 shows the merging of two arches from the top of a column.

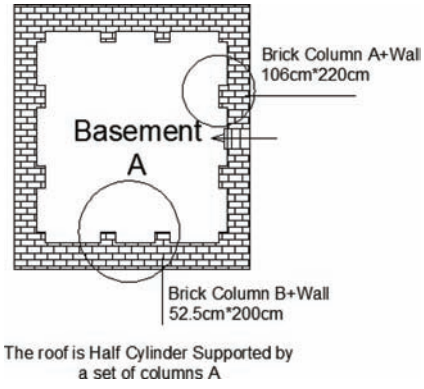

Figure 8. Section through basement A.

Figure 9. Two arches in different directions merging from one column.

Figure 10. Patterns of decorations on the walls of the basments.

Figure 10 demonstrates the different patterns of decoration observed on the walls of the basement and in many other walls of the Khan, with inner circular arches between the columns. All these decorations were made using the same building unit with perfect measurements and stiles.

3.2 *The meeting halls*

The two meeting halls in the ground floor, figure 11, have similar pattern of columns to those

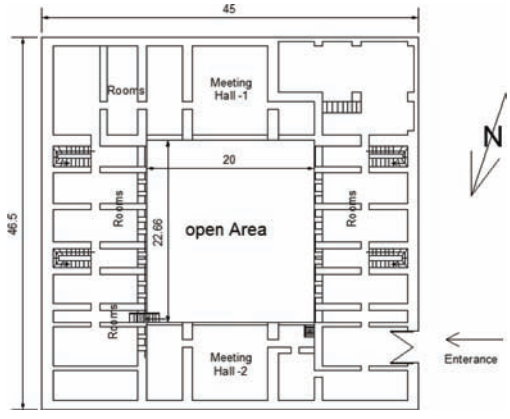

Figure 11. Location of meeting halls.

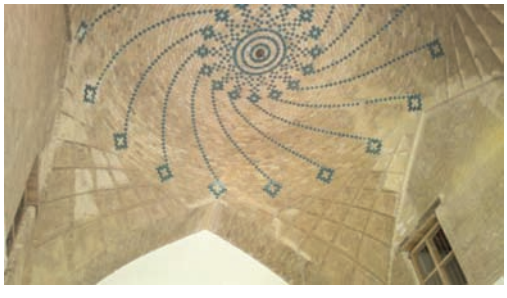

Figure 12. Original decoration of meeting hall 2.

in the basements but the columns are higher since these two halls are designed to have double height ceiling as shown in section A-A of figure 6.

The ceiling of meeting halls has the shape of a dome with real artistic patterns of decorations. The dome of meeting hall 2 remained in its original shape and decoration as shown in figure 12, indicating high quality of artistic proficiency.

Meeting hall 1 was subjected to serious damage and during rehabilitation it was nearly removed and reconstructed using the same size of building units. In spite of the great efforts made by the working crew to get as close as possible, the same decoration of the dome of meeting hall 2, the builders were unable and unsuccessful in achieving the same pattern of decoration as shown in figure 13. The difference in the quality and patterns of decorations can clearly be observed in the two figures.

3.3 *Rooms*

The same construction approach was used in all rooms. The ceiling of all rooms is made of close arches. The space between two adjacent arches

Figure 13. Decorated ceiling of meeting hall 1 after rehabilitation.

Figure 14. The inside of a typical room after plastering.

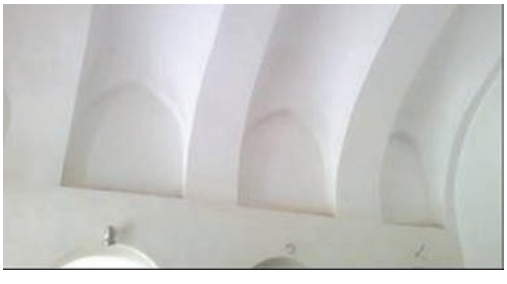

Figure 15. Typical ceiling of room-arches in the form of ribs.

depends on the dimensions of the room. These arches act as ribs and the bricks filled the space between them taking the curvature of the arches. Figures 14 and 15 demonstrate the pattern of arches in a typical room after rehabilitation.

Most of the walls in the rooms were constructed with high artistic decoration similar to those shown in figure 10. The working crew was unable to restore and preserve these original fantastic decorations due to the lack of experience and most of these decorations were covered by a layer of "juss" and lime as shown in figure 14.

4 FOUNDATION SYSTEM OF THE KHAN

All the walls are of bearing type extending approximately to a depth 5 m below natural ground level, resting on a strip footing 3 m wide and 1 to 1.5 m thick. The walls and the footings are all constructed from bricks with "juss" and lime as mortar. It is hard to inspect the durability of the building materials of the footings under such high stress, but since they remained sound for more than 100 years, it is thus expected that both walls and footings had integrated and interacted, in such a way that they formed a rigid pad able to sustain high stress under sever environmental conditions.

There are no geotechnical data reflecting the current geotechnical properties of the soil underneath the Khan as it is impossible to get the drilling facilities inside the building. It was suggested that the soil investigation report of the multistory building close to the khan, shown in figure 2, can be adopted. The report was prepared in the sixties, and revealed the soil stratification shown in figure 16.

Figure 17 demonstrates that the top 5 m has an SPT-N value between 10 and 30, overlaying a strong layer of SPT-N—value >50.

Since the base of all footings of the Khan is located approximately 5.5 m below natural ground surface, then the footings of the whole structure are resting on the strong layer of medium to very dense silty sand mixed with pebbles and gypsum. Previous studies on Najaf soil (Al-Shakerchy 2007), showed that the presence of high gypsum created lumps of cemented material that exhibit high resistance to penetration.

For this particular case where the strip footing 3 m wide, placed at a depth D = 5.5 m, below natural ground level, the allowable bearing capacity based on 25 mm settlement can better be estimated using the equations proposed by Meyerhof 1956, 1974. The proposed equations shown below are based on SPT data corrected to N_{55} or N_{70} as reported by (Bowles 1996).

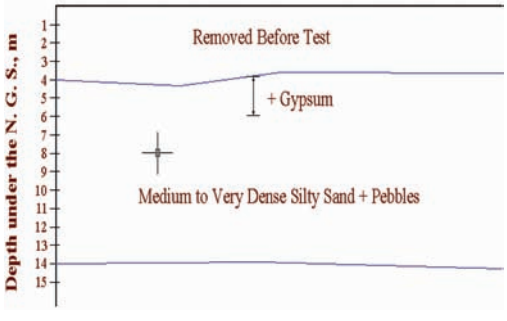

Figure 16. Soil stratification from a nearby site to the Khan.

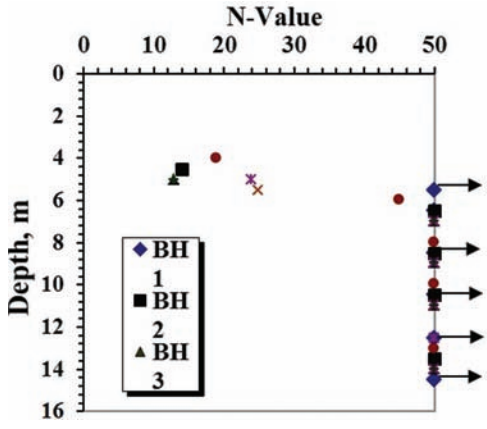

Figure 17. SPT versus depth.

$$q_a = (N/F_1) * K_d \ldots \quad \text{for} \quad B \le F_4 \tag{1}$$

$$q_a = (N/F_2) * ((B + F_3)/B)) * K_d \ldots \quad \text{for} \quad B > F_4 \tag{2}$$

where q_a = allowable bearing capacity in kPa for settle ment 25 mm.

$$K_d = 1 + 0.3\,(D/B) \le 1.33 \tag{3}$$

Since the geotechnical report was written in the late sixties, it is more reliable to consider the F factors corresponding to N_{55} rather than $N_{70.}$ The quoted values are $F_1 = 0.05$, $F_2 = 0.08$, $F_3 = 0.3$ and $F_4 = 1.2$ (Bowles 1996).

Substituting for D = 5.5 m, B = 3 m and N = 50 in equations 2 and 3, the obtained allowable bearing capacity is 1006 kPa.

According to the measured dimensions of the structure shown in figures 4, 5, and 6, an estimate was made of the average total applied stress generated from live and dead loads of the different structural elements. The outcomes of the analysis revealed a total stress of 775 kPa on a strip footing 3 m wide. Since the depth of the footing is 5.5 m below natural ground level and the submerged unit weight of the soil approximately equal to 10 kN/m^3, the net applied stress at base level is determined as

$$q_{applied} = q_{total} - (\gamma)(D)$$

$$q_{applied} = 775 - (10)(5.5) = 720\ \text{kN/m}^2 \tag{4}$$

The settlement corresponding to this net applied stress will be

$$S = (720/1006) * (25) = 18\ \text{mm}$$

Meyerhof 1965 proposed another approach for estimating the compressibility of cohesionless soil.

The proposed equation, shown below, was applied for the current foundation keeping N = 50.

$$S = (2q/N_{60})(B/(B+0.3))^2 \quad \text{for} \quad B > 1.22\,\text{m}$$
$$S = (2 * 720/50)(3/3.3)^2 = 24\,\text{mm} \qquad (5)$$

In terms of settlement calculations the two values can be averaged to 21 mm. In case this settlement had occurred during the life time of the structure, nearly 100 year, its influence is inconsiderable in causing any serious structural damage to the skeleton of the structure. Close inspection of the whole structure from the inside and outside, did not show any significant cracks or signs of excessive settlement or tilting.

The ground floor level experienced some heaving, in the open areas, due to the lack of proper drainage system. Some deterioration of the walls was also observed due to capillary rise. It can be stated that the Khan was damaged by environmental conditions and by local people taking parts of it as small shops and changing its original architectural appearance. Rehabilitation process is in the final stages and figure 18 shows the new appearance of the Khan from the interior open yard.

Figure 18. View of the Khan from the inside yard.

5 CONCLUSIONS

All nations must be proud of their ancient history as it represents the period where man began to set up the paths of the civilized life. Conservation of cultural and historical sites must be well preserved and passed to the new generations. The paper presents a review of the rehabilitation process taking place in Khan Al-Shelan, one of the heritage structures in Najaf city in Iraq. The paper sheds the light on the quality of the structural elements, types of arches, the difference in the quality and proficiency of the workmanship in terms of architectural decorations.

In terms of structural analysis, the net applied stress on the base of the strip footing was calculated and found to be 720 kPa. This value is less than the calculated allowable bearing capacity, 1006 kPa. The compressibility was also calculated by two methods revealing an average settlement of 21 mm. This value is fairly small and caused no significant impact on the structure. The major source of damage was by the environmental agents.

REFERENCES

Al-Arraji, A. 2011. Khan Al Shilan the new cultural museum of Najaf city, http://cicnajaf.com/index.aspx?siteid = 3&pageid = 981&newsview = 42

Al-Khalidi H. 2010. History of Khan Al Shilan, http://www.najaf2012.com/artc/50/news/default/index.html

Al-Shinan, A.M. 2012. The future of Khan Al Shilan, http://www.aliraqnet.net/arabic/index.php/2011-08-30-14-05-27/4479-2012-11-19-20-18-45

Al-Shakerchi, M.SH. 2007. Geotechnical properties of Najaf city soil with emphasis on infiltration and strength characteristics, PhD. Thesis University of Technology, Baghdad, Iraq.

Bowles, J.E. 1996. *Foundation analysis and design*, fifth edition, The McGraw Hill Companies Inc.

Meyerhof, G.G. 1956. Penetration tests and bearing capacity of cohesionless soils, *JSMFE, ASCE*, Vol. 82, SM1, pp. 1–19.

Meyerhof, G.G. 1974. General report, Outside Europe, 1st ESOPT, Stockholm, vol 2.1, pp. 40–48.

Meyerhof, G.G. 1965. Shallow foundations, *JSMFE, ASCE*, Vol. 91, SM2.

Geotechnical Engineering for the Preservation of Monuments and Historic Sites – Bilotta, Flora, Lirer & Viggiani (eds)
© 2013 Taylor & Francis Group, London, ISBN 978-1-138-00055-1

Seismic vulnerability reduction for historical buildings: The case study of house of mosaics

L. Alterio
Altran s.p.a. c/o Tecnimont Civil Construction s.p.a., Milano, Italy

L. Evangelista, G. Russo & F. Silvestri
University of Napoli "Federico II", Italy

ABSTRACT: The present paper explores the possibility to obtain the reduction of seismic vulnerability of historical buildings through subsoil treatments, in order to reduce the seismic actions. The study is motivated by the unsatisfactory degree of protection of many historical buildings with respect of seismic risk, and by the inadequacy and/or the inability to adopt the reinforcement or base isolation methodologies used on the new constructions. The issue has been addressed through a multi-disciplinary approach. A suitable case study was selected, i.e. the ancient Villa Favorita park on the sea in Herculaneum, a site well-characterized in terms of geology, stratigraphy, and mechanical properties of the soil. These features allowed to simulate the seismic subsoil response by 1D modeling, with site effects exclusively induced by the stratigraphy. The seismic behaviour of the building, with high historical-architectural value, was accurately reproduced by a 3D model. The study was conducted through uncoupled numerical analysis of the site response and the structure in elevation, analyzing the effects of possible artificial variations of soil properties on the seismic safety of the building.

1 INTRODUCTION

1.1 *Preliminary remarks and purposes*

The seismic protection of cultural heritage is an outstanding problem in Italy. The structural vulnerability of most of the built heritage, together with the frequent seismic activity in Italian territory, are, in fact, two factors inducing high seismic risk in many historical centers (e.g. Costanzo et al. 2007). Many systems and devices have been developed in recent decades, in order to obtain the energy dissipation and seismic base-isolation. The use of the aforesaid systems is still limited for historical buildings, due to the need for respecting the conservation requirements, strictly specified by the Ministry of cultural heritage and environmental conservation. Furthermore, dissipation devices do not reduce the seismic action on the structure, but only its consequences.

Base isolation concept, instead, presents the advantage of limiting the intervention only in foundation, avoiding the traditional reinforcement of structural elements or the introduction of new elements which are expressly prohibited by the Code (Linee Guida 2010). Moreover, the design and calculation of the dynamic behaviour of a base-isolated structure are easier than those of conventional earthquake-reinforced structure. The only drawback is the need to create a joint around the building. Hence, the use of this type of intervention is possible only for buildings that are not bound laterally by other buildings. At present, base isolation is usually obtained for buildings either through the cutting of the foundations or load-bearing structures (columns and walls) positioned at the lower floor (which is not allowed by the Italian code), or by excavating a new underground floor for inserting the isolators, with significant executive difficulties and high total expenses (Martelli 2009, Clemente, ENEA 2010).

Based on the principle of isolation, i.e. creating a disconnection between the structure and the soil, and inspired by various studies (Muir Wood, 2006), the present work investigates the possibility to obtain an attenuation of the seismic signal by means of soil treatment interventions.

2 CASE STUDY

2.1 *Description*

The case study selected is the park of Villa Favorita in Hercolaneum, located on the seashore, along the ancient royal road of Calabria, in the stretch that connects Napoli to Torre Annunziata, called Golden Mile. This latter name derives from the

extensive building by the XVIII century Neapolitan aristocracy, of villas for residence and "delight" near the Royal Palace built by Charles III of Bourbon at Portici.

The 122 Vesuvian villas are an important artistic and cultural heritage which, for its specific character, is a unique testimony of the development in architectural, technical, urban planning and the landscape terms of the Vesuvius area. The site has a unique connotation also from seismic and geological point of view, related to the presence of the Somma-Vesuvius volcanic complex (Fig. 1).

In the park the following buildings are also located: the Mosaics Palace (annex of the most sumptuous Villa), two Coffee Houses near to the coast, the Chapel, the building known as the "Rollercoaster", and the Laundry.

The most interesting building, in the park by an architectural and a decorative point of view, is certainly the Mosaics Palace. The building has a compact rectangular plan, developed on two storeys, with dimension 31.20 m × 20.95 m. The interstorey height decreases from 5.10 m–5.60 m at ground floor, to 4.90 m at first, to 3.75 in the attic, for a total height of 14.30 m.

At the ground floor, there is a large vaulted atrium, which divides the building into two equal portions along E-W direction and leads to the great hall of the mosaic in front of the sea. Some of the remaining rooms are covered by barrel or sail brick vaults, some others by flat slabs. At the first floor the rooms match those on the lower floor, except for the great hall of the mosaic, here replaced by a large terrace (Fig. 2). Finally, the attic floor consists of one room with dormer windows on all four sides of the building.

By a structural point of view the villa is characterized by a sack masonry, made by an external framework in yellow Neapolitan tuff and an inner core with chaotic structure filled by lava fragments. The primary horizontal structures are plane steel floors, with the exception of some ground floor rooms. The binder is a mixture of pozzolana and lime mortar. The documents of the archive of the Vesuvian Villas Institution reports that the masonry is founded at a depth around 1.5 m under the ground surface, the thickness being equal to the wall in elevation.

In 1990, the palace was completely restored as the state of stability and conservation of the structure appeared unsatisfying (Fig. 3).

Many walls, especially those not protected by the plaster, presented the exterior face strongly eroded by the wind and marine agents, while the state of conservation of the mortar was enough good. Regarding the horizontal structures, the original wooden floors were collapsed or irreparably damaged, while the iron beams included in the remaining floor slabss were highly oxidized and therefore not able to withstand the overload. The brick vaults had a crack pattern which, however, allowed the repair and recover works. Finally, the attic floor had been demolished in 1962, because it was judged as unsafe and not recoverable.

Figure 1. Geo-lithological characterization of the studied area and localization of building under study (modified from I.S.P.R.A.1967).

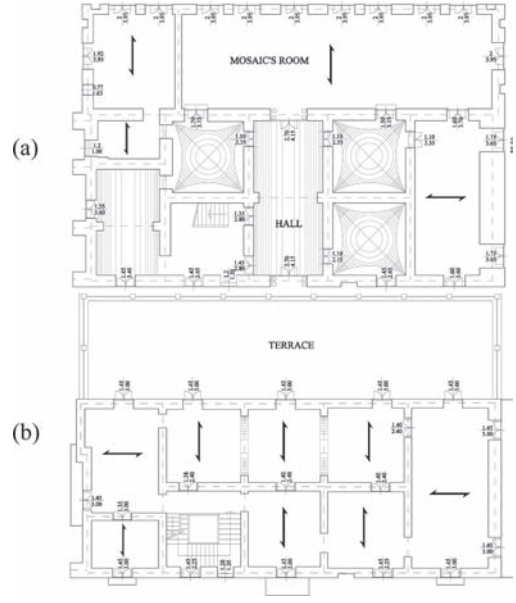

Figure 2. The Mosaics Palace: (a) ground floor and (b) first floor plan.

Figure 3. The Mosaics Palace before and after the restoration.

In order to recover the original static scheme of the building, without altering the characteristics of the bearing elements, the following reinforcement interventions were executed: armed injections to restore the cantonal detachments; unarmed injections to strengthen the walls with degraded mortar; reconstruction of collapsed or excessively damaged walls, using tuff square blocks and willing bound by lime mortar; lintels made of steel UPN profiles; replacement of wooden floors with new ones steel made; wooden roof reconstruction respecting the original typological scheme; realization of a crowing curb.

2.2 *Geotechnical model*

Due to the location of the city of Hercolaneum at the foot of the volcanic complex of Somma-Vesuvius, the geology of the place is closely linked to the eruptions that occurred over the centuries.

The subsoil of the investigated area is characterized by the products of the Vesuvius eruptions that in various stages reached the coastline (Fig. 1). The outcropping lithologies in the area consist of lava flows subsequent to 79 AD and prior to 1631, and by thick pyroclastic flow (ash clouds, lahars) of the 1631 eruption, which frequently cover these lavas.

Figure 4 shows the stratigraphy, as derived from a borehole near to the palace. The subsoil is made by alternating layers deriving partially by the volcanic flows (fractured and intact lava) and partially by fall products consisting of pyroclastic sands and ashes (pozzolana).

A MASW test was carried out on purpose, to increase the knowledge about the mechanical properties of the various layers. The profile of shear wave velocity, V_S, shown in Fig. 4, was obtained by a constrained inversion of the dispersion curve measured in situ. Once the thickness for each layer

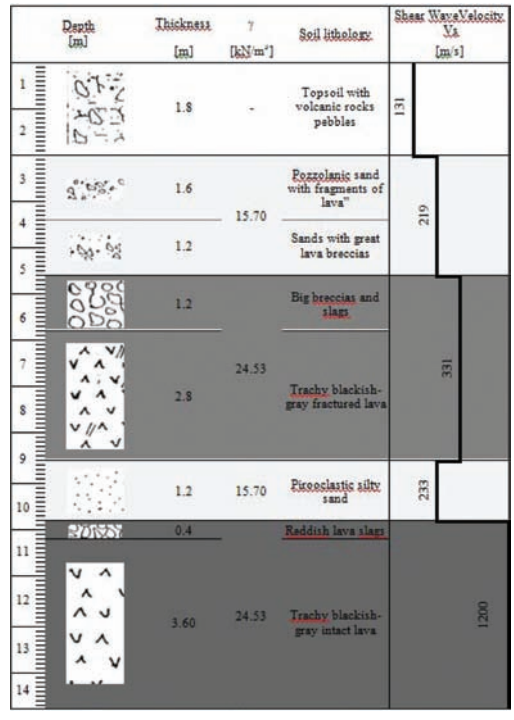

Figure 4. Layering and shear wave velocity profile of the site.

was set consistent to the layering, the solution was obtained by letting the velocity to vary within a reasonable range of values, appropriate to the materials constituting each layer, until obtaining the best fit with the experimental dispersion curve.

It can be noted that the shear wave velocity profile results characterized by an increase with depth, except for the velocity inversion across a pozzolana layer interbedded between the fractured and the intact lava, this latter corresponding to the seismic bedrock.

2.3 *Seismic input*

An original procedure to select the reference input motion was implemented (Alterio, 2012). The seismic hazard of the site was first evaluated from the recent Italian building code (D.M. 14.01.2008). The return period, T_R, and the peak horizontal ground acceleration, PHA, for the site, were identified according to different ratios of exceedance, P_{VR}: 5% for the collapse limit state, SLC, and 63% for the damage limit state, SLD. With reference to such percentages of exceedance, P_{VR}, events contributing most to the seismic hazard of the site were identified from the dominant modes of the relevant disaggregation distributions (Spallarossa &

Barani, 2007), in terms of ranges of magnitude, M, and source-site distance, R. The ranges were found to correspond to M = 4.5–5.0 and R = 0–10 km, M = 6.0–7.0 and R = 60–80 km, for SLC and SLD respectively. On the basis of the local seismic history, it can be inferred that the first ranges correspond to near-field earthquakes with relatively low energy, related to the volcanic activity of Somma-Vesuvius; the second ranges apparently refer to far-field strong-motion events, originated by the seismogenetic Irpinia area.

A large number of seismic records compatible with the above ranges was then selected from the ITalian ACcelerometric Archive (Working Group ITACA, 2010). For each couple of horizontal records found, the NS and EW components were composed to obtain the resultant motion along the direction for which the spectral intensity (Housner, 1952) was found maximized. A cluster of projected records was then extracted, according to the following criteria:

1. Combination of at least seven accelerograms;
2. Value of scale factor, F_{SC} (i.e. the ratio between the reference design peak horizontal acceleration, PHA_0, and that corresponding to the selected event, PHA_S) lower than 4 and as close as possible to 1;
3. Minimum deviation between the average spectrum of the combination of accelerograms and the target code spectrum;
4. Duration of the pseudo-stationary part of the accelerograms at least equal to 10 s.

Spectrum-compatibility (i.e. requirement n.3) was evaluated with three different statistical indicators: the average root-mean-square deviation, D_{rms} (Bommer & Acevedo, 2004), the average spectrum deviation, δ_i (Iervolino et al, 2009), and the Pearson correlation coefficient, R^2. The cluster combination most compatible to the above requirements was represented by the records listed in Table 1, including the long duration record of the well-known Irpinia earthquake (1980) at a station very close to the site.

Table 1. Selected records from ITACA database.

Event name	Date	M_W	Station (code)	D (km)	PHA (g)
Aquila	2009-04-07	4.6	Pettino (AQP)	0.7	0.13
Massiccio Meta	1984-05-11	4.8	Villetta Barrea (VLB)	5.9	0.12
App. Umbro-March.	1998-04-05	4.8	Nocera Umbra Salmata (NCM)	5.1	0.10
Irpinia	1980-12-01	–	Oppido-Balzata (OPB)	8.7	0.08
App. Umbro-March.	1998-03-21	5	Cesi Monte (CESM)	6.3	0.08
App. Parmense	2008-12-23	4.9	Neviano degli Arduini (NEVI)	9.2	0.07
Irpinia	1980-11-23	6.9	Torre del Greco (TDG)	78.3	0.06

2.4 *Building modeling*

In order to define the capacity curve of the building and, consequently, to assess its seismic vulnerability, a numerical model was implemented on the basis of the data obtained from the historical research and a careful geometric survey, as well as from a detailed analysis of the working loads (Alterio, 2012). A confidence factor was applied to the properties of the materials, thus reducing their resistance, in order to take into account the model uncertainties with reference to the knowledge level reached. Values of this factor are specified in the Italian Guidelines for the evaluation and the reduction of the seismic vulnerability of artistic and historical heritage (Linee Guida 2010). A confidence factor of 1.35 was adopted, i.e. the most conservative according to the above mentioned guidelines, since it was neither possible to deepen the crack surveys, nor to exactly define the construction steps and the building materials. The reduced strength properties of the masonry were derived applying the confidence factor to the mean values of the ranges proposed in the table C8.A.2.1 of the Circular 02/02/2009, N. 617, referred to different types of masonry found in the construction practice.

To implement the numerical model of the building under study, the 'Tremuri' code (Galasco et al. 2001) was used. The code adopts an equivalent 3D frame approach based on the theory of the macro-elements: its theoretical formulation is derived directly from observations and from experimental tests of masonry behavior in buildings under seismic actions. The model of the Mosaics Palace is shown in Figure 5, where the absence of the wooden inclined roof can be noted. Its presence was simply modeled by applying the loads of the roof on the underlying walls.

2.5 *Seismic building capacity (pushover analysis)*

The seismic vulnerability of a building is typically defined through a non-linear static analysis (pushover)

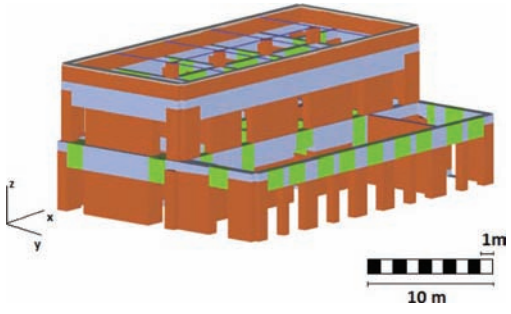

Figure 5. Tremuri 3D model of building.

consisting of applying increasing horizontal loads to the structural model, until collapse occurs. The distribution of the horizontal loads among the various storeys is preliminarily fixed. Generally, two different horizontal loads distributions are considered and analyzed separately for each direction:

- the first one is proportional to the masses,
- the second one is proportional to the product of the masses the shape of the first mode of vibration.

The amplitude increase of the load distribution is typically represented by its resultant, V_b, i.e. the shear force at the base of the building. The so-called "capacity curve" describes the relationship, obtained along each direction, between V_b and the horizontal displacement, d, of a control point fixed on the structure. The control point must be chosen so that its displacement is significant for the global behavior of the structure, the gravity centre of the last floor being one of the typical choices (Manfredi et al. 2007). Following the building code (DM 14.I.2008), for each direction an accidental eccentricity of the centre of mass was assumed equal to 5% of the maximum size of the building in the direction perpendicular to the earthquake.

As a consequence of the combinations between the distribution of loads and the directions of the additional accidental eccentricity, 24 different analyses were performed. The results of the analyses show that the weakest direction of the building is the transverse one (Y direction), where the total area of resistant masonry is less than the area in the longitudinal direction (X direction). As a matter of fact, the most severe analyses in terms of both yielding shear force, V_{bu}, and capacity ultimate displacement, d_u, were relative to the Y direction.

Figure 6 shows the capacity curves relevant to each analysis: in most cases, they show localized irregularities, corresponding to the symptom of

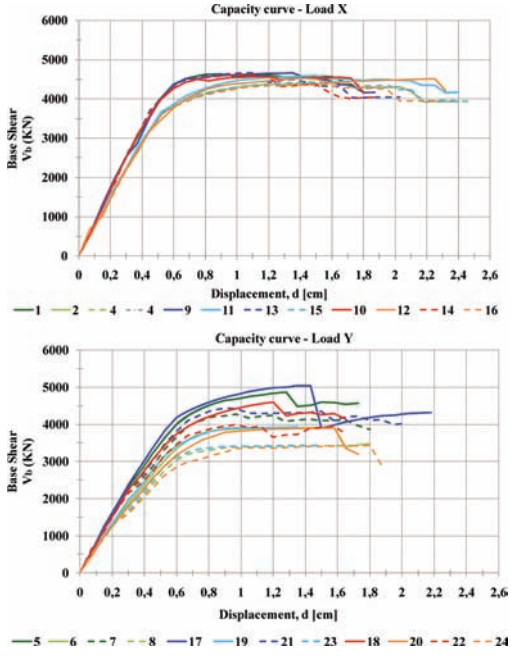

Figure 6. Building capacity curves along X and Y directions.

failure mechanisms, involving one or more significant structural elements, and giving rise to a sudden drop of resistance.

2.6 *Seismic demand (site response analyses)*

For seismic safety assessment, it is necessary to compare the capacity curve with the demand, represented by the design seismic action including site amplification. To define this latter, 1D linear equivalent seismic response analyses were carried out with the EERA code (Bardet et al., 2000); they were based on the subsoil model and the seismic input motion defined in § 2.2. and § 2.3 respectively.

A first analysis was executed on the 'natural soil' model (case 0), corresponding to the subsoil profile without treatments, while the other analyses were carried out on 'modified soil' models, corresponding to different hypotheses of soil treatments. The treatment effectiveness was expressed as the ratio, E_V, between the shear wave velocity in the treated soil, V_{Streat}, and the value in the natural soil, V_{S0}:

$$E_V = \frac{V_{Streat}}{V_{S0}} \quad (1)$$

Three different options were evaluated: two types of interventions increasing the stiffness of the treated layer (E_v = 1.4 and 3.0), and one that, instead, would reduce it (E_v = 0.5) through installation of a soft layer. For each type of treatment, three different depths of interventions were considered, for a total number of 9 analyzed cases, the characteristics of which are summarized in Figure 7. Cases A and B refer to treatments of the shallowest pozzolana layers, while case C assumes a deep treatment in the layer between the fractured lava and the bedrock.

For each of the 10 profiles (9 treatments plus the natural soil), analyses were performed for both design limit states, SLC and SLD, and for each of the 7 selected accelerograms, resulting in 140 ground motions. The results were expressed in terms of response spectra for acceleration, $S_a(T)$, and displacement, $S_d(T)$. For each soil profile, the average spectra resulting from the seven input accelerograms were then considered as representative of the seismic demand.

2.7 *Comparison between demand and capacity*

The average seismic demand predicted for the different soil profiles was then compared with the building capacity, by assuming the behavior of the structure with multiple degrees of freedom (MDOF) as simplified to that of an equivalent model with one degree of freedom (SDOF).

The capacity curve was therefore transformed in terms of SDOF acceleration-displacement relationship, by dividing the shear force, V_b, for the value of the total mass of bearing walls along the analized direction, m*.

Figure 8 shows the comparison between the capacity curve of the building, corresponding to the most conservative value of $PGA_c = V_{bu}/m^*$, and the seismic demand at the damage limit state (SLD), expressed in terms of S_a and S_d computed at the same T values, for each case of soil treatment analyzed. In the figure D_{dmin} represents the damage limit displacement tolerable by the building and its

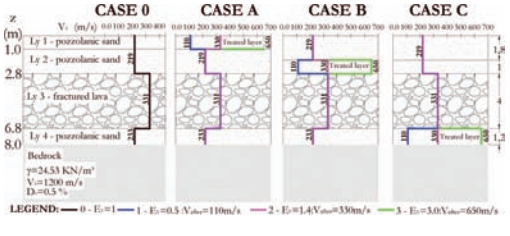

Figure 7. Layering and shear wave velocity profiles for the analyzed cases.

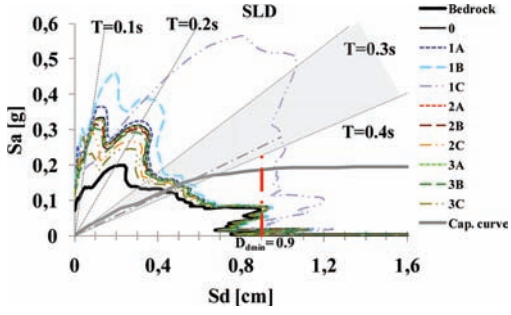

Figure 8. Comparison at the SLD between the most conservative capacity curve (analysis n. 24, Y direction) and the S_a:S_d demand spectrum for different soil treatments.

Table 2. Comparison between the building capacity and the spectral displacement demand for different soil treatments at SLD.

24 – Load +Y (1°Mode); T* = 0.373		$S_d(T^*)$ vs d_{dmin} = 0.90 cm			
Depth of interv. (m)		Case 0 Ev = 1	Case 1 Ev = 0.5	Case 2 Ev = 1.4	Case 3 Ev = 3
A	1.8		0.50	0.49	0.49
B	3.6	0.49	0.53	0.49	0.48
C	8.6		**0.99**	0.47	0.46

value is the minor between that corresponds to the maximum shear and that would exceed the maximum value of the storey drift (0.003).

It can be noted that the cases 1 A/B/C, where the treatment is supposed to cause a decrease of the stiffness of the soil, always involve an overall higher demand compared to the reference case (0) with the natural soil; the opposite occurs when the soil treatment is supposed to provide an increase in soil stiffness (2 A/B/C and 3 A/B/C).

Tables 2–3 report the numerical values of the spectral ordinates with reference to the fundamental period T* = 0.373 s, computed by the Tremuri model. It can be noted that the overall minimum demand corresponds to the case 3C, while the largest corresponds to case 1C.

The comparison in terms of displacement (Table 2) shows that the structure, characterized by a yield displacement d_{dmin} = 0.9 cm, shows a satisfactory behavior in all the cases, with the only exception of the case 1C (E_v = 0.5 in the deep pozzolana layer). On the other hand, the comparison in terms of acceleration (Table 3) is not as satisfactory, the demand being always greater than the capacity, corresponding to a PGA_c = 0.12 g.

Table 3. Comparison between the building capacity and the spectral acceleration demand for different soil treatments at SLD.

24 − Load + Y (1°Mode); T* = 0.373		$S_a(T^*)$ vs PGA_C = 0.12 g			
Depth of interv. (m)		Case 0 Ev = 1	Case 1 Ev = 0.5	Case 2 Ev = 1.4	Case 3 Ev = 3
A	1.8		0.15	0.14	0.14
B	3.6	0.14	0.15	0.14	0.14
C	8.6		**0.29**	0.14	0.14

Table 4. Comparison between the building capacity and the spectral acceleration demand for different soil treatments at SLC.

T* = 0.34		$S_a(T^*)$ vs PGA_C = 0.22 g			
Depth of interv. (m)		Case 0 Ev = 1	Case 1 Ev = 0.5	Case 2 Ev = 1.4	Case 3 Ev = 3
A	1.8		0.53	0.51	0.51
B	3.6	0.53	0.59	0.52	0.52
C	8.6		**0.98**	0.49	0.47

Table 5. Comparison between the building capacity and the spectral displacement demand for different soil treatments at SLC.

19 − Load + Y (1°Modo); T* = 0.338 s		$S_d(T^*)$ vs d_{umin} = 1.35 cm			
Depth of interv. (m)		Case 0 Ev = 1	Case 1 Ev = 0.5	Case 2 Ev = 1.4	Case 3 Ev = 3
A	1.8		1.54	1.47	1.47
B	3.6	1.47	1.70	1.48	1.49
C	8.6		**2.80**	1.41	1.36

Similar considerations can be drawn, also, for the assessment relevant to SLC. Tables 4–5 and Figure 9 show that the capacity of the structure is always less than the demand both in terms of acceleration PGA_c than in terms of ultimate displacement $D_{umin,}$ defined as the minor value of displacement corresponding to 80% of maximum shear force V_{bu}.

3 CONCLUSIONS

The study presented in this paper has investigated the possibility of obtaining a seismic vulnerability reduction of historical-monumental buildings, by subsoil treatments. For this purpose, seismic site response analyses were carried out at the selected site, taking into account various treatments hypotheses The results, expressed in terms of response spectra, show that for the damage limit state (SLD), a superficial treatment producing an increase of the soil stiffness does not significantly reduce the spectral acceleration at surface, while a reduction in stiffness can even amplify it.

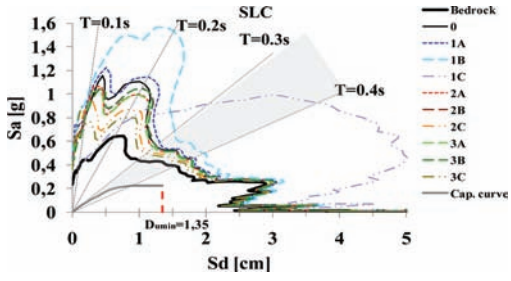

Figure 9. Comparison at the SLC between the most conservative capacity curve (analysis n. 19, Y direction) and the S_a:S_d spectrum for different soil treatments.

Deep treatments, instead, produce more beneficial effects. The reduction of surface acceleration is, however, not proportional to the increase of stiffness of the treated layer. Stiffening above a certain level or beyond a certain depth would imply an economic charge not justified by a comparable benefit.

The analyses carried out also show that at SLC a stiffness reduction could lead to a reduction of the horizontal surface acceleration due to non-linearity of soil behaviour. This aspect should be better investigated considering also the effects of the treatments on the damping ratio of the soil.

Finally, comparing the results with the structural capacity of the building, it was possible to note that for SLD (damage limit state) the capacity was higher than the demand in terms of displacements, except in the case of reduced stiffness in the superficial layer. On the contrary, the assessment was never satisfied in terms of acceleration, being the demand always greater than the structural capacity.

It should be emphasized that, even if not fully satisfying the safety assessment in the case study analyzed, the soil treatments may contribute to reduce the seismic demand, and thus to decrease the total cost of the structural intervention. It is also worth mentioning that the effects of the soil treatments do not only modify the surface acceleration amplitude, but also shifts the resonant period of the soil, usually corresponding to the peak spectral amplitudes. The soil treatments could thus be

adopted to appropriately move the subsoil period away from the fundamental period of the structure, avoiding double resonance mechanisms.

The effectiveness and efficiency of each treatment on the seismic protection of historical buildings can be said as strongly influenced by local stratigraphic details: the surface seismic response of the deposit is, in fact, linked, not only to the characteristics of the single treated layer, but also to those of the adjacent soil and to the relative impedance ratios between them. This suggests, therefore, that while the proposed procedure can be exported to other cases, the specific conclusions on this case study cannot be generalized.

REFERENCES

Alterio L. (2012). "Seismic vulnerability reduction of monumental building by soils treatments" *Ph.D. thesis*—University of Naples "Federico II" – Italy.

Bardet, J.P., Ichii, K., Lin, C.H. (2000). EERA a Computer Program for Equivalent-linear Earthquake site Response Analyses of Layered Soil Deposits. *Univ. of Southern California, Dep. of Civil Eng.*

Bommer J.J., Acevedo A.B. (2004). "The use of real earthquake accelerograms as input to dynamic analysis"—*Journal of Earthquake Engineering*, 8, special issue 1: 43–91.

Circolare n. 617 del 2.II.2009—"Istruzioni per l'applicazione delle nuove norme tecniche per le costruzioni." *Ministero delle infrastrutture e dei trasporti—G.U,n. 47 of 26.II.2009* Suppl. *Ordinario n.27—Italy (in italian).*

Clemente P., ENEA. (2010). Internal technical note (in italian).

Costanzo A., d'Onofrio A., Lanzo G., Pagliaroli A., Penna A., Puglia R., Santucci De Magistris F., Sica S., Silvestri F., Tommasi P. (2007). "Seismic response of historical centers in Italy: selected case studies."—*Workshop on 'Geotechnical Earthquake Engineering related to Monuments and Historical Centers'*, IV ICEGE, Thessaloniki.

DM 14/1/2008. Norme Tecniche per le Costruzioni. S.O. n. 30-*Gazzetta Ufficiale della Repubblica Italiana*, No. 20-4/2/2008 (in italian).

Galasco, A., Lagomarsino, S. and Penna, A. (2002). TREMURI Program: Seismic Analyser of 3D Masonry Buildings, University of Genoa.

Housner, G.W. (1952). Spectrum intensity of strong-motion earthquakes. *Proc.. Symp. on Earthquakes and Blast Effects on Structures*, EERI, Univ. of California at Los Angeles, Earthquake Engineering Research Institute, Oakland, Calif., 26–36.

Iervolino I, Galasso C., Cosenza E. (2009). "Rexel 2.3.1(beta) e la selezione normativa dell'input sismico per analisi dinamica non lineare delle strutture" – *Proceedings of ANIDIS XIII Convegno ANIDIS "L' ingegneria Sismica in Italia"*—Bologna, 28 June-2 July 2009, Italy.

I.S.P.R.A. (1967). Italian Geologichal map, 1:100000-Sheet 183–184, Napoli (http://www.isprambiente.gov.it/it/cartografia/carte-geologiche-e-geotematiche/carta-geologica-alla-scala-1-a-100000).

"Linee Guida per la valutazione e riduzione del rischio sismico del patrimonio culturale—allineamento alle nuove Norme tecniche per le costruzioni"-*Ministero per i Beni e le Attività Culturali*—Circolare n. 26 del 2.12.2010 (in italian).

Manfredi G., Masi A., Pinho R., Verderame G.M., Vona M. (2007). "Valutazione di edifici esistenti in cemento armato."—*IUSS Press*—Pavia, Italy pp. 87–91(in italian).

Martelli, A., (2009). "Development and application of innovative anti-seismic systems for the seismic protection of cultural heritage"—*Proceedings of International Conference Prohitech09*. Rome—June 2009 Italy. Volume I.F.M. Mazzolani editor.

Muir Wood, D. (2006). Invited Lecture-*4th International Conference on Earthquake Geotechnical Engineering*, June 2006 Thessaloniki, Greece, Kryazis D. Pitilakis editor.

Spallarossa, D. & Barani, S. (2007). Disaggregazione della pericolosità sismica in termini di M-R-ε. Deliverable D14, *Progetto DPC-INGV S1, http://esse1.mi.ingv.it/d14.html (in italian).*

Working Group ITACA (2010). ITACA (Italian strong motion database) User Manual, Project S4, by Lucia Luzi, Francesca Pacor, Rodolfo Puglia, and Roberto Paolucci *(http://itaca.mi.ingv.it/ItacaNet/).*

Geotechnical Engineering for the Preservation of Monuments and Historic Sites – Bilotta, Flora, Lirer & Viggiani (eds)
© 2013 Taylor & Francis Group, London, ISBN 978-1-138-00055-1

New evidences on the Phlegraean bradyseism in the area of *Puteolis* harbour

L. Amato
Tecno in Servizi di Ingegneria S.p.A, Milano Napoli, Italy

C. Gialanella
Soprintendenza Speciale per i Beni Museali di Napoli e Pompei, Italy

ABSTRACT: Puteolis, the modern Pozzuoli, is located in the centre of Phlegrean Fields; because of this geographical position, it was the main seaport of the ancient Rome, so as to be remembered by the historian Polybius and by the poet Lucilius as "Delus minor". The data resulting from a series of investigations for the design of infrastructures allowed to re-elaborate the complex paleomorfology of the area and New reconstractions thesis, thus affecting the succession of natural processes and human activities which have profoundly changed the coastal area of Pozzuoli from ancient times to the present. It is shown that bradyseismic processes were already active in The Roman Republican Age and probably influenced the urban expansion, having an impact on the various the various stages of development and restoration of the city. On the basis of reported data, a reconstruction is proposed by the uplift and downward distortion of the ground surface during the centuries, with particular reference to the Macellum, that has been often used as a "marker" for the reconstruction of the movements of the Phlegraean area. In addition, and specifically the analysis of the materials of the old port quays confirm the indications reported by Vitruvius *(De Architectura, V, XII*), which was the only literary source on the construction of harbours in ancient times.

1 OVERVIEW OF THE LOCATIONS

1.1 *Geological geographical overview*

The area in consideration is located in the western sector of the still active volcanic district of the Phlegraean. Specifically, the study area belongs to the town of Pozzuoli (NA) along the coast and near the dock below the promontory of Rione Terra (Fig. 1). The key feature of the Phlegraean area, and of the its main town Pozzuoli, is the phenomenon of volcanic bradyseism (slow movement of soil) which caused an uplift of the ground of about 90 m in the last 10,000 years. In the caldera of the Neapolitan Yellow Tuff the bradyseism began between 10,500 and 8,000 years ago; the peak of upheaval was reached about 5,000 years ago.

Direct observations of the soil displacements have been recently carried out in the Phlegraean Fields, starting in 1969–1982. The coast line of the Roman period is found at an average depth of 3–5 m below sea level, and numerous ruins of Roman and medieval times at different depths below the sea level furnish evidence of general subsidence in the last 2,000 years. A reversal of this trend occurred before the eruption of Monte Nuovo (Fig. 1) in 1538, since the beginning of the XIV century, there had been a slow uplift of ground, with an advance of the shore line in the coast stretch between Baiae and Pozzuoli. The eruption was followed by a slow subsidence that stopped only in 1969, when a new phase of rising started. Between 1969 and mid-1972, the Phlegraean Fields were interested by a first bradyseismic crisis, with upward displacements up to 1.7 m in the area of Pozzuoli.

In early 1982 a new phase of intense upheaval began, that reached a value of 1.8 m at the end of 1984. Since the end of 1984, a general slow subsidence resumed, interrupted only by occasional negligible uplifts.

The phenomenon of rising bradyseism is always accompanied by seismic activity earthquakes with a variable intensity, depending on the magnitude of the event.

In early 1982 began a new phase of intense, that at the end of 1984 reached a value of 1.8 m. Since the end of 1984, a general slow subsidence resumed and interrupted only by occasional negligible uplifts.

The phenomenon of bradyseism ascendant is always accompanied by the occurrence of earthquakes with a variable magnitude, depending on the extent of the event.

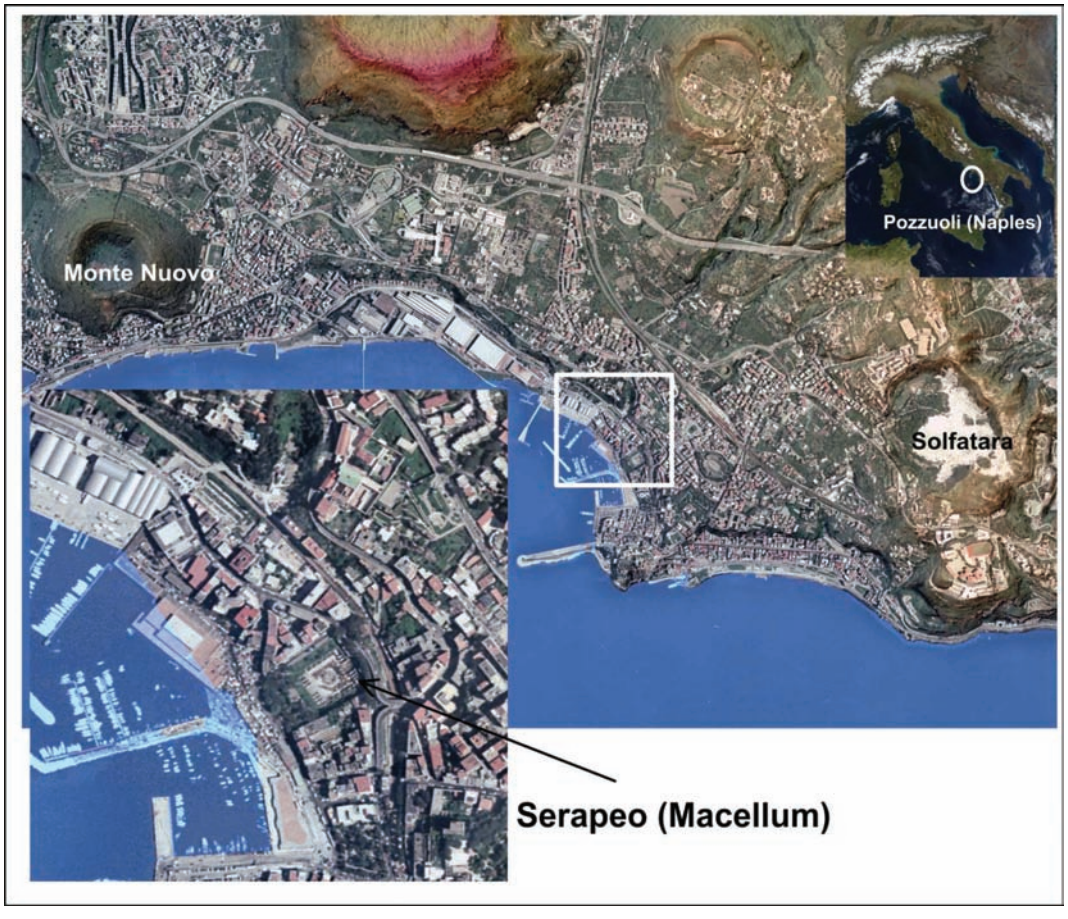

Figure 1. General overview of the Puteolis coast.

1.2 *Historical overview*

Information about the pre-Roman Pozzuoli is poor. In Roman times, the unique geographic position of the city and its status as a Roman colony, together with the increase of trade in the western Mediterranean, made the city soon became the main port of Rome, collecting the intense maritime traffic from Sicily, Africa and Orient to (supply) provide Rome of any kind of goods. Throughout the second century AD and up to Severian Age, Puteolis experienced a great edification phase. A restoration of the port establishments placed near Macellum, attested by an inscription (394 AD CIL X, 1692), shows that at the end of the fourth century AD the port was still in activity. Not many years later, however, the decline of the commercial activities of Puteolis and the increasing bradyseismic movements led to a progressive deterioration of the coastal district.

The so called Emporium, the great harbor district of Puteoli, developed along the coast north of the piers and north west of the acropolis; commercial traffic was concentrated in the Emporium, and large warehouses were built behind (at the back) starting probably in I or II century BC. Macellum (Serapeum) was its main building. The whole area was surrounded by piers with arcades towards the sea.

Little is left of Emporium and ripa structures. At present they are partly under water, partly covered by major reclamation works carried out over the centuries in order to raise the ground surface as a result of subsidence phenomena. Macellum (so-called Serapeum) is still visible; it was found in the mid-700 and early 800. The building, one of the largest known in the Roman world, is dated between the late first and second century AD. As we will see later, during the Saverian age substantial works of resettlement were carried out. The floor now visible and the central tholos with columns

that have always been considered the measure and the symbol of bradyseism, belong to this period.

2 RESULTS OF INVESTIGATIONS

2.1 *The reconstruction of the coastline*

The reconstruction of the coast line during the Roman Republican Era is characterised by a coastal strip much smaller than the reconstructions made in the past (fig. 2); The analysis of the sediments of the enviroment under water allows us to assume a bradyseismic uplift between The Republican and Augustus Giulius Claude Era, testified of sedimentary transition environment. Such phenomenon causes an advance of the coast line (to go forward).

The bradyseismic uplift, together with the development of the port of *Puteoli* and in relationship to the stockage of wheat in Rome, could be one of the factors which has contributed to the high development of the city plan and has radically changed the lower part of the city. The significant presence of structures found through the surveys, especially in unknown areas, confirm the conservation intervention of the *ripa*, with the accomplishment of an enormous system of quays, which allows to gain ground and therefore let the costal line go forward.

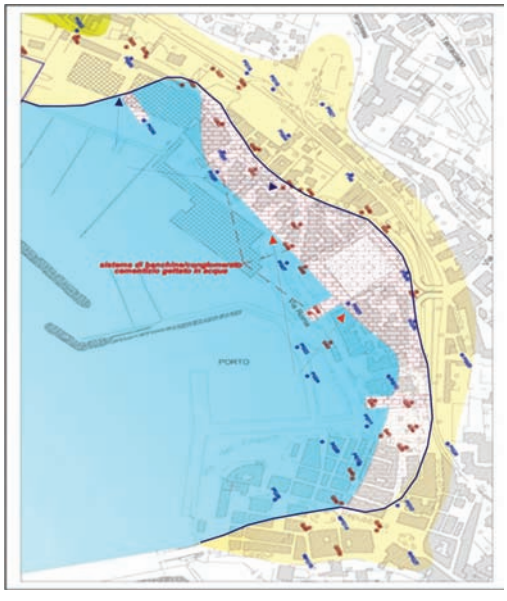

Figure 2. Reconstruction of the costal line in The Republican Age and development of the extension of the port quays towards the sea during the Imperial Age.

Survey, in fact, intercept a first level of structures made of conglomerate cement (opus caementicium) of substantial thickness.

The characteristics of the material, as well as the height of placement above the grade level built by submersed sands,thrown in water, within wooden formworks. The dating of archaeological material unearthed, consisting of fragments of Italian ceramic and sealed thin walls, allows you to frame the complex of actions at the first Imperial age, starting from the Augustan period.

It is on this impressive work of filled that builds the Macellum (market), prominent position overlooking the sea. Below, in order to clarify the development over the centuries of bradyseism phenomenon and, therefore, of the various phases of the monument, referring to the annexed section rebuilt sequence (fig. 3), positioned on the Macellum has always been used as a "marker" for the study of the deformation area. Recent surveys made it possible to clarify the development over time of the area and to add new information to those deriving from the eighteenth and nineteenth century excavations that signalled a further floor subjected to 2 metres at that age currently visible Old Flavia-Trajan.

In particular, it was found a floor plan in Opus signinum (cocciopesto) at about –3.5 MASL (I floor-cf. S21 S23 and S24), place in opera immediately above the quay of the Augustan period, created by a thrown overboard in opus caementicium.

The discovery of the same floor with more core, located further north, suggests that this pavement was extended to cover the entire surface of the platform. In such a case, unless caught, the flooring was destroyed or eroded by the sea during the next phase of subsidence.

Returning to the area of the Macellum, the floor above was the first floor of frequentation, dating probably to the Augustan period. The tempering of the roof of the docks (about –3.5 MASL.), together with the pavement plans dimensions allow to hypothesise an average sea level to an altitude of era –5.00/–5.50 m than at present.

Next, you pick the signs of a cleanup construction, probably made in Old Flavia, suspect in S21 (fig. 3) the construction of a structure resting on the floor in *Opus signinum* described above.

This structure was to be part of a broader intervention including the walls intercepted in PG23 and S22 (collapse); there are no items to define whether the structure caught in S24 was in the same building or stage, being more backward, might be already there.

Noting that survey PG23, S21 and S22 are located in the most advanced portion towards the sea, although missing clues of a marine ingression

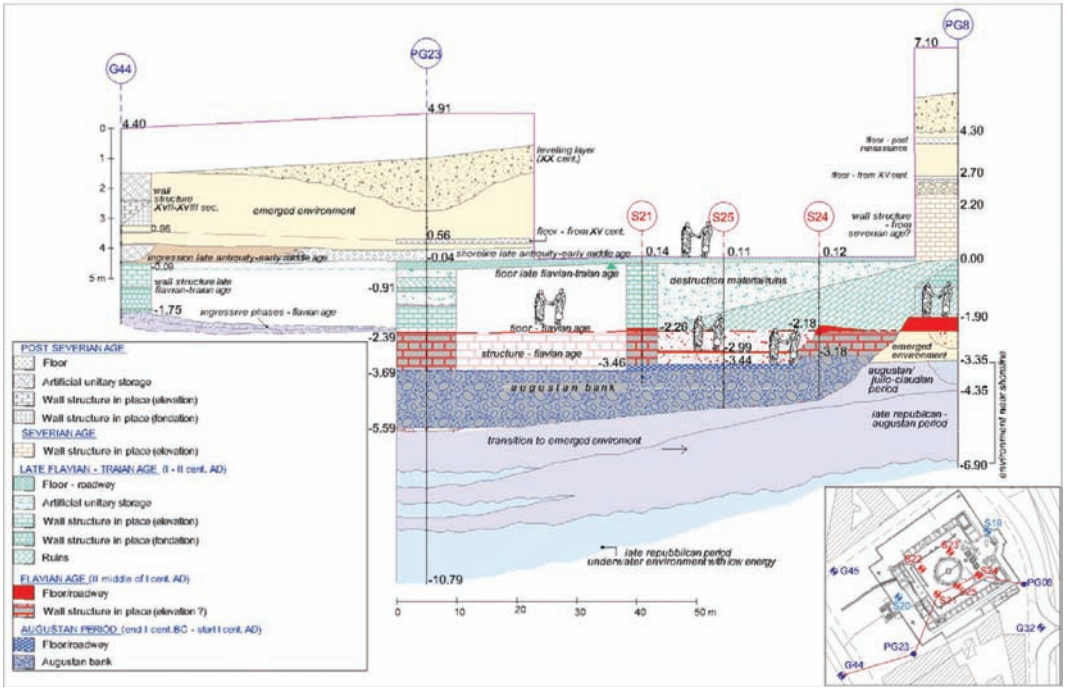

Figure 3. Geoarchaeologic and lithostratigraphic section in correspondence to the Macellum (Serapeum) of Pozzuoli.

and subsidence phenomena, we cannot exclude the possibility that these structures represent the elevation of the platform in order to counter the advance of the sea and protect the rear area of the *Macellum*. The hypothesis is comforting in its evidence of attendance plans makeover of *Macellum* in higher dimensions (S25:–2.99/–3.09 MASL) first at about -3 MASL current (II floor) and later a –2.2 MASL current (3rd floor). The latter level is well connected with the dimensions of these floors to the top of the structure in high on the quayside. They stood at about-current 2.3 MASL—about 1 m above the previous 1st floor in Opus signinum (S23:–2.07/–2.27 MASL; PG23:-/–2.44 2.39 MASL.; PG21–2.26/–2.36 MASL), almost the same hight of a stone pavement, that can be related to a road plan, found in PG8 (–2.35/–2.60 MASL).

Unfortunately, the absence of material dating in accumulations ranging from floor plans of the *Macellum* does not allow a precise chronological sweep of remakes. However, the finding of coarse sands in the accumulation on which rested the last floor in S25, strengthens the hypothesis of marine ingression as determining cause of resets, which would then be linkable to the Late age of Flavia—Trajan subsidence.

The data is also consistent with the lower floor plan of *Macellum*, unearthed in the excavations made in the last centuries, dating to the flavian time, testified about – 2.00 MASL. (fig. 4).

Already in Late Flavia Age, the data indicate a reversal of the processes for all bradyseism, with the beginning of a phase of subsidence which causes the surfacing of the aquifer. The deposition of silt on the quays leads to significant works of renovation and elevation of floor plans. The investigations have identified, in coastal areas affected by the construction of the quays in the Augustan Age, levels of collapse and breakup with silt and deposits silt-sandy soils, with thicknesses ranging from a few centimeters to about 2.00 m. The characteristics of these deposits bear witness to the presence of ingressive phenomena of an aquifer outcrop, sub-that does not cause the submergence and the abandonment of the area, but require a series of interventions by raising and reconstruction of port facilities and their floor plans.

In this phase can be attributed the current flooring (4th floor) of the monument, come to light as a result of the excavations taken in 1750 by Charles III of Bourbon, King of Naples, and later King of Spain, in the place known as la Vigna of the three columns. The most backward sectors, on the other

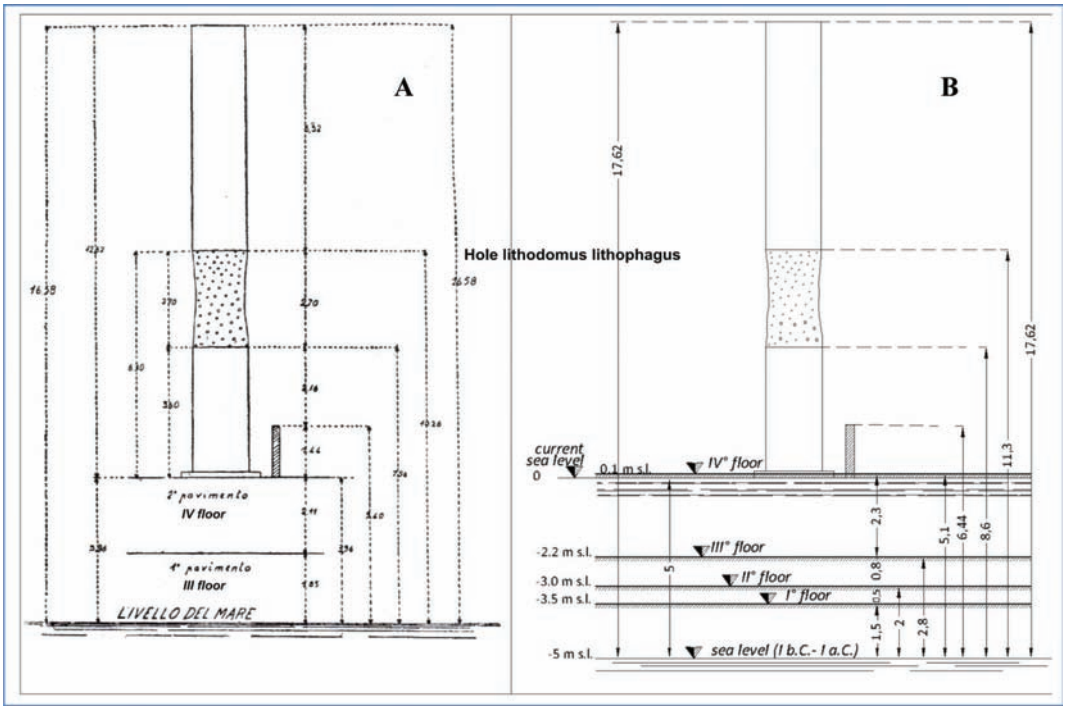

Figure 4. A) Section of the columns of the *Macellum* (Temple of Serapis) with highlighted dimensions for the holes of litodomi, the first floor of Flavia Age and the second of Late Flavia-Trajan *(Parascandola*). B) Modified Section in relation to 2012 data with evidence of four trampling found plans and quotas.

hand, for all bradyseism movements are witnessed by the presence of thin layers of silty granulometry abandonment, but without the powerful meltdowns that characterize the coastal area.

Currently available data indicate a partial rearrangement of some surrounding areas the *Macellum* is rearranged, too, as evidenced by a fistula plumbea with the name of Septimius Severus and the construction of the tholos in the middle of the marble Court.

In ancient and medieval age the negative bradyseism phenomena, well attested and known from the analysis of the sources, as well as the study of the traces of the litodomi (lithodomus lithophagus) on the columns, cause sea level rise up to +7/+8 m and abandonment and the submergence of the lower town. That period does not have testimony from investigations being predominantly erosional ingressive this stage.

During Vicereal and Bourbon Age, sedimentation consists generally of beach sands, which testify to the emergence of post medieval city, with an advancement of the coastline. These are, in fact, the full emergence stages of lower town area in relation to the eruption of Monte Nuovo (1538). This leads to a new urban development plan of the city, of which we find traces in the investigation with the discovery of remains of structures in the area in front of the *Macellum*. Later, between the 18TH and 20th century large sectors of the coastal area of Pozzuoli are affected by drainage and levelling works tending to raise the floors, in relation to new stages of active subsidence since the first half of the 20th century, when the well-known lifting crisis between 1984 and 1972 have reversed the "trend".

3 THE FILLED OF QUAYSIDE

Particularly important is Pozzuoli in the history of port engineering, for the use of Opus caementicium in dispose of wharves and dams. The fact is already highlighted by Strabo (V,4,6) that, talking about the "huge" trading port of Pozzuoli, recalls the "artificial anchors (which could do) thanks to the favourable nature of the dust", the pulvis Puteolanus, still called pozzolan.

We have already mentioned material characteristics of opus caementicium consisting of building debris of tufa, in plenty of Pozzolanic mortar, extremely rich in lime nuclei not dissolved and, in some cases, not completely wrinkled, which is the

backbone of making enlargement of the quays in the Augustan period. The material composition confirmed as reported by ancient sources, in particular by Vitruvius, on the implementation of ports, describing in De Architectura, V, XII fundamental techniques of construction of water structures, based on three methods: the first two illustrate the works to be done directly at the point of destination, using discarded in wooden formworks; the third contemplates the implementation ashore of prefabricated blocks to throw then into the water. Only for the first way, Vitruvius explicitly prescribes the use of opus caementicium with pozzolana: "*the structure of the pier will remain under water must be made with powdered pozzolana imported from that region that stretches from Cuma until Minerva promontory (Punta della Campanella—Sorrento), mixing it so that it is in proportion of two parts for one (lime)*".

The same author also describes the properties of *pulvis Puteolanus*, implying: Pozzolanic aggregate quality that allows the mortar to resist water and solidify even in very humid environments, thanks to the presence in a considerable quantity pulvis of aluminium silicate. In summary, adding the pozzolan lime to lime, this is transformed into hydraulic lime.

In our case, the manufacturers had added as *caementa* and fragments, blocks of tufa, material rich in zeolites, which are of silico-aluminate hydrates of alkali metals and/or alkaline-earth metals (chabazite and phillipsite). It follows, unknowingly, an improvement of the hydraulic reaction.

The pozzolan was also exported from Pozzuoli to the shores of Palestine, such as the construction of the port of Herod to Caesarea Maritima, as was, in fact, a perfect return for cargo ships carrying grain from Alexandria to Puteoli.

As regards the construction of docks, given the opportunity of convenient supply of *pulvis Puteolanus* and thrown directly on the sand, we can assume that the realization has occurred according to the dictates of the first method illustrated by Vitruvius, or "formwork flooded". This was, in fact, the simplest and cheapest method. The salient feature for the thrown in water consists in absence of tinning of this type of case, which, according to Vitruvius, was not to even get the Fund.

In fact, once assembled the structure, "(the) *inferior pars sub aqua was exaequanda et purganda*. Quote: "then, at that point, you must sink and secure with safety of formwork systems held together by oak uprights and cross ties; then, in the inner compartment, (working) from sleepers to level and clean the bottom (*exaequanda et purganda*) and throw the mortar, prepared as is explained above, mixed in the debris of stone, until the space between the bulkheads is not filled with concrete". Vitruvius gives, however, a "partially improper" explanation of the chemical quality of the pozzolan: improper, because he doesn't know the reaction that occurs in the transformation from the lime hydraulic lime and the chemistry that implies; partly because in his description of *pulvis Puteolanus* (*De Architectura, II, VI.1*) writes: "*and this seems possible because on the slopes of Mount there are lands and hot springs for the presence of underground deposits of sulfur, alum and bitumen that feed huge fires*".

4 DATA ANALYSIS

4.1 *The curve of ground deformations over time*

As already stated, the *Macellum* is always identified as "marker" for the study of deformative movements the Phlegraean area. The importance of Phenomenology of bradyseism is presented in the masterful artwork of C. Lyell, 'Principles of geology' of 1830–33, in which the author, in order to support the principle of actualism which interpretation of the phenomena of the past, as an example the bradyseism phenomenon of Pozzuoli, where the columns of the *Macellum* had recorded the slow and steady ground motion over the centuries. (Lirer, et al. 2010). It is worth mentioning that, along with a number of distinguished scientists, even W. Goethe had expressed his opinion on the Phenomenology, however, attributing the cause to changes in sea level.

The data emerged from the studio, allow a rereading of the curve of ground deformations over time (fig. 5).

Rebuilding takes as its reference the first floor of the Augustan period, assuming a share of tax of 1.5 MASL. This was necessary in order to reconstruct the pattern of landuse changes in ancient times, and have a reference level of course. On the basis of those data also the curve is rebuilt on the 4TH floor (currently visible) dated to late Flavian-Trajan Age.

The two curves are proposed in consideration that you can rebuild properly the ground deformations without considering the fillings made in ancient times.

Currently the floor is at an altitude of around –3.5 MASL. The values on the curve are relative to the likely location of the floor in relation to the distances that separate it from "markers" above. For example, in the case of the fourth floor, there is a thickness of 3.5 m. Assuming, then, a set of the fourth floor of 1.5 m above sea level, the floor will be at an altitude of –2.0 MASL.

The maximum depth of sinking is normally considered about –6.3 m, in relation to the litodomi holes present on the columns of cipollino marble of the *Macellum* from current level of marble flooring (in this note IV floor—fig. 4), which are

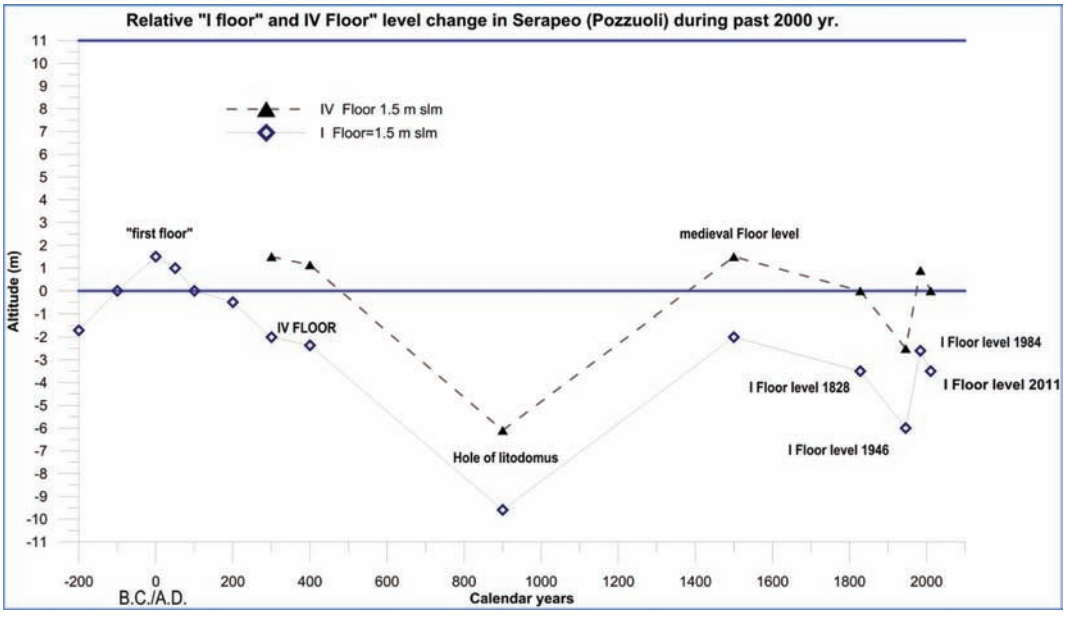

Figure 5. Curve reconstruction of ground deformations with reference to the fourth floor and the Augustan age of the *Macellum*.

supported by columns, which, as we have seen, is placed on an artificial grabbing works of about 3.5 meters compared to the floorto counteract the phenomena of soil sinking. Therefore we believe that the correct measure of maximum depth of soil sinking, with reference to the floor plan (fig. 4), or –9.8 m, or –11.3 m if referring to likely sea level.

If we take into account the curve on the 4th floor of the late Severan flavia-age, placing it at an altitude of 1.5 MASL. at the time of its realization and maintaining intact the relations underlying floored, it notes that the proportion of an litodomi holes on the curve at a depth of –6.2 m, very close to the real measured as distance from the 4th floor and also by the reported *Parascandola* (1983). Analogue of speech can be done to the medieval floor, whose share was approximately 1.3 MASL. As regards the measures starting in 1828, they know the odds of the fourth floor and then is easy to reconstruct both curves.

ACKNOWLEDGEMENTS

The authors would like to thank Maria Luisa Tardugno, researcher at the Università degli Studi di Napoli "Federico II" and geologists Carla Palomba and Carmela Guastaferro, without whose help this work would not have been able to complete.

REFERENCES

Amato L. (2012). Nuove evidenze connesse ai fenomeni di deformazione del suolo nell'ambito del bradisismo Flegreo. *31° Congresso Gruppo di Geofisica della Terra Solida.*

Gianfrotta P. (1991). Navi, flotte, porti e il viaggio per mare. In: Settis S., Civiltà dei Romani. *La città, il territorio, l'impero*, Electa Milano Ed..

Lirer L., Petrosino P., Armiero V, (2010). Ital. J. Geosci. *(Boll.Soc.Geol.It.)*, Vol. 129, No. 2.

Lyell C. (1830–33). Principles of Geology, Being an Attempt to Explain the Former Changes of the Earth's Surface, by Reference to Causes Now in Operation. John Murray, London.

Morhange C., Bourcier M., Laborel J., Gialanella C., Goiranj P., Crimaco L. (1999). New data on historical relative sea level movements in Pozzuoli, Phlaegrean Fields, Southern Italy. *Phys. Chem. Earth, Part A*: Solid Earth and Geodesy, 24.

Parascandola A. (1983). I fenomeni bradisismici del Serapeo di Pozzuoli; *Acta Neapolitana* Guida editore.

Vitruvio Pollione M. (1990). *De Architectura*. Edizione studio Tesi.

This page intentionally left blank

Geotechnical Engineering for the Preservation of Monuments and Historic Sites – Bilotta, Flora, Lirer & Viggiani (eds)
© 2013 Taylor & Francis Group, London, ISBN 978-1-138-00055-1

Important works in the town centre and preservation of existing heritage: The Grand Carré Jaude in Clermont-Ferrand (France)

F. Ambrosini
Vipp Lavori, Angiari (VR), Italy

P. Berthelot
Bureau Veritas, Paris, France

F. Durand
Structures Geotechnics, Rueil Malmaison, France

A. Reynaud
Fugro GeoConsulting, Nanterre, France

ABSTRACT: In the town centre of Clermont-Ferrand, the realization of a large building complex with 8/9 levels on 2 basement levels and a footprint of over 11 000 m^2 required the execution of works with a complex infra-structure. The particular geology and hydrogeology related to the presence and the filling of an ancient volcano has forced the designers to adopt very specific constructive solutions. The constructive environment they wanted to keep, forced the designers to adapt these solutions even more precisely and especially their implementation. The buildings with 3 to 7 levels in the neighbourhood situated between 5 and 15 m from the Project north and west of the site were primarily based on shallow foundations anchored at 2 m depth in the area of the water layer in a 'travertinised' silt. South of a mall type construction on the ground floor and topped by residential buildings with five levels is based, through a basement, on a raft of floating piles of 10 m deep. East of the site is situated near the tramway on pneumatics and powered by rails guided by the soil. All these works have been equipped with instrumentation for monitoring and controlling the stability and deformation during all phases of implementation of the infrastructure works, banking and construction of the super-structure. At the start of the works several floor tests were needed to confirm the requested preferential demanding and to control the inter-actions with existing structures.

1 INTRODUCTION

One of the most important real estate projects has been launched in France in 2010. This project has a size on ground of more than 11 000 m^2 and is situated at Clermont-Ferrand, in the Middle of France and in edge of the main place in the downtown: place of Jaude. Several 6 or 7-level buildings with flats, offices and functional structures must be realized on two levels of shops and 2 levels of basement.

The achievement of such a project in the city centre requires a perfect control of the deformations of the project itself but also of the neighbouring works.

To the north of the project (Julien Avenue) the nearby buildings are located at less than 15 meters: R + 3 to R + 7 concrete buildings of 20 years old. In the south of project, existing R + 8 buildings

Figure 1. Presentation of the project.

(Giscard de la Tour Fondue street) are located at a distance between 5 and 10 meters from the project.

To the west (Bonnabaud street) it exists an old R + 2 masonry building.

To the east on the Gonod street circulates a pneumatic tramway at least at 10 meters.

The main difficulty of this project is to realize the 2 basement levels with an under-water excavation with the water table that is near the naturel ground and could be artesian locally.

2 PRESENTATION OF THE SITE

2.1 *Geology: The Jaude maar*

The site is geologically atypical because it is on an ancient maar. An old volcanic chimney with a cylindrical or conical shape has stamped out the pre-eruptive substratum from Marls and marl-limestone.

On about one hundred meters, the central depression has been filled up by water then by lake sediments (silts and sands) and probably by river sediments (coarse sands, silts and soft clays).

2.2 *Geotechnical*

The geological campaign by FUGRO Géotechnique consisted in 44 static penetrometer tests with piezoconic head and about 10 core drillings (between 15 and 30 meters deep) to define precisely the stratigraphic section, the identification characteristics and the soil mechanics.

With the piezocone tests we can separate the different soils: sandy soils and silt or clay soils.

Under the 3 meters of backfill, the following layers has been found:

- Silts from old volcanic griffins,
- Soft upper silts which are excessively compressible and organic in some places,
- Fine sands to coarse sand more or less compact,
- Lower consolidated silts deposit of the maar.

2.3 *Artesian ground water*

Under this ancient volcano, some "chimneys" have ascending water currents charged with carbonic gas, called "griffon". The static penetration tests with U measure and the selective piezometers have permitted to measure the deep pore pressure higher to the simple hydraulic charge, which means pressure like $(1 + i) \times \gamma_w \times h$ rather than $\gamma_w \times h$.

On the surface, water table is located towards 3 meters depth. On the other hand, towards 15 meters depth, the artesian could locally reach charges higher than the natural ground charges (around 3 meters above the natural ground).

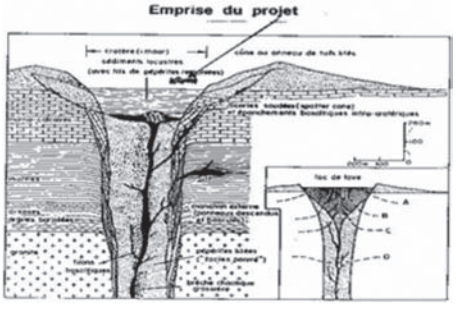

Figure 2. Geological section.

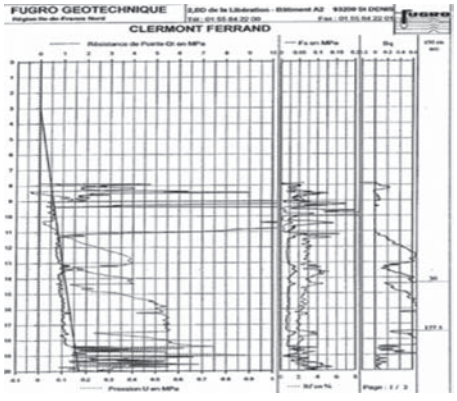

Figure 3. Typical static penetrometer test.

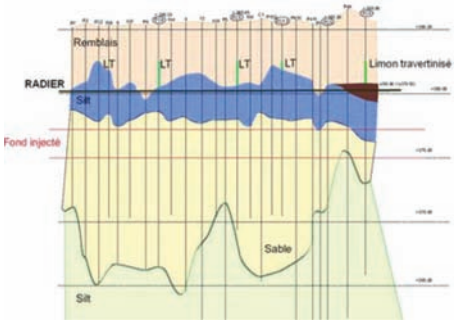

Figure 4. West-east overall geotechnical section.

3 PRESENTATION OF THE PROJECT

3.1 *General principle*

Several buildings with 6 or 7 levels and 2 levels of shops and 2 basement levels are planned.

For the 2 basement levels, an under-water excavation with a specific artesian, is needed.

The zero level of the project was fixed at +386.10NGF, which is slightly above the original ground. The final underground levels were fixed at –5,7 m compared to the zero level of the project and at some places at –6,60 m, so respectively the

final levels at the following heights +380,4NGF and +379,5NGF.

The under-water excavation obliges to realize a vertically and horizontally permeable work to isolate the parcel from the rest of the site. This work should include:

- A perimetric wall,
- An injected deep excavation.

A perimetric wall with descending sheeting piles (to avoid beating problems in urban site) in the mortar wall already drilled must be set up.

The injected deep excavation will be made with secant columns of jet-grouting.

Otherwise the general principle of the work foundation consists in realizing a compensated foundation, which means that the removed soil weight is almost equal to the work global weight deduced from Archimedes 'buoyancy.

The building foundation is made up of a concrete foundation raft to report charges on the jet-grouting transfer columns anchored in the injected deep excavation. The aim is to obtain a homogeneous stress on the injected deep excavation base.

The deep excavation made of jet-grouting columns has 3 functions:

- Water tightness function during the provisional phase
- Cross brace function to block sheeting piles bases
- Stress distribution function on the injected deep excavation base to complete the concrete foundation raft and the transfer columns.

4 THE SOLUTION

4.1 *Perimetric wall (530 ml—5 950 m²)*

Because of the locally artesian risk, the selected execution principle is a wall with grout pre-drilling and sheeting piles. The slurry wall solutions must be avoided because of the bentonitic mud needed to hold the drilling wall.

The usual density of this mud is equal to 10,2 kN/m³, so the risk is to get instability when a panel is open if it is situated on a "griffon".

The supporting and relative waterproof are obtained by the sheeting piles. The grout pre-drilling allows to cross hard bolster benches and to fix the sheeting piles without beating or high vibration. At the final stage it's planned a reinforced concrete wall.

As an alternative to the grout drilling, the company proposed a soil mixing solution which minimizes the evacuation of materials and allows a better control in case of "griffon".

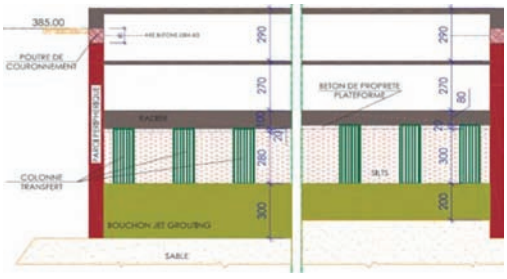

Figure 5. Infrastructure section.

4.2 *Jet grouting plug (42.000 m³)*

Because of the nature of the materials (sand, silt and soft silt) the injected deep excavation could not be done as usual by a grout injection. So it has been made of secant jet-grouting columns.

Because of the global conception of the project, the injected deep excavation and the transfer columns have 3 functions, which oblige to define efficient characteristics for the calculations:

- A injected deep excavation thickness between 2 and 3 meters depending on the loading zones brought by the building,
- An E Young modulus superior or equal to 2000 MPa. We need to obtain a modulus at least equal to 2000 MPa because of the modeling results and the relative settlements which must have a maximum slope of 1/500,
- A compressive strength equal or superior to 6 MPa,
- A permeability lower than 10^{-7} m/s to minimize flow of exhaustion and make the project hydraulically independent of the exterior,
- A column diameter in accordance with the planned objectives to ensure that the injection deep excavation device is secant,
- A transfer column diameter also in accordance to ensure a perfect load transfer between the concrete foundation raft base and the injected deep excavation roof.

5 THE EXPECTED IN TERMS OF ADJACENT TO DEFORMATION

Deformations considered different works nearby were proposed with respect to several criteria:

– Distance of existing works in relation to the perimeter wall project
– Behavior differential settlement based on the type of construction
– Evolution of deformation in time 3 years (full completion), 10 years ("garantie décennale") and 30 years ("trentennale")

5.1 *Allowable values*

By combining the distance of existing structures, construction type and behavior and differential settlement (assuming value of 1/500 of the span for reinforced concrete and 1/1000 for masonry), the allowable deductions values are the following:

5.2 *Settlements prediction*

These values depend on:

- The intensity and the asymmetry of loads provided by the project
- Phases of construction
- From sandy to silty respective layers, depending on their thickness and their distribution. Part due to the sand is almost instantaneous, due to the silt is delayed in time. Taking into account the speed of consolidation obtained through edometric tests, the following approach was chosen:
- 50% of settlement to due to silt occur during 3 years

Streets	Settlement begin the wall	Settlement for a distance		Settlement for a distance	
	mm	< 20mm	< 10mm	< 2mm/ml (<1/500)	< 1mm/ml (<1/1000)
Bonnabaud	70mm	14m	21m	10m	15m
Julien	80mm	17m	25m	10m	21m
Tour Fondue	30 mm	4m	10m	5m	11m
Gonod	30 mm	5m	10m	5m	11m

Figure 6. Allowable settlements values.

Street	Settlement begin the wall (mm)				
	for sandy layer	for silty layer	after 3 years	after 10 years	after 30 years
Bonnabaud	20 mm	50 mm	45 mm	60 mm	70mm
Julien	20 mm	60 mm	50 mm	70 mm	80mm
Tour Fondue	10 mm	20 mm	20 mm	25 mm	30mm
Gonod	10 mm	20 mm	20 mm	25 mm	30mm

Street	Settlement behind the wall (mm)			
	X m from the screen	after 3 years	after 10 years	after 30 years
Bonnabaud	18 m	10mm	13mm	15mm
Julien	18 m	12mm	16mm	18mm
Tour Fondue	5 m	13mm	17mm	20mm
Gonod	5 m	13mm	17mm	20mm

Figure 7. Settlement prediction.

Street	Settlement begin the wall (mm)		Settlement behind the wall (mm)	
	Measure	Theoritical : 90% * Value at 3 years	Measure	Theoritical : 90% * Value at 3 years
Julien	35mm	45mm	6mm	10mm

Figure 8. Measured settlements.

- After ten years, it's 80%
- And almost 100% of settlements are obtained in 30 years.

6 THE MEASURES AND COMPARISON WITH THE EXPECTED

All works nearby were under supervision in monitoring movement:

- Settlements with the installing of targets (46) on buildings and spits (58) on roads
- The water table level by an outside piezometric monitoring
- The movement of the perimetric wall by inclinometric measures.

In the late stages of excavation, the implementation of the raft and its behavior during all phases of the project were also followed by more than 50 topographic targets.

Taking for example the area more heavily loaded side Julien Avenue (north of the project) for a loading rate of 90% average, the measured settlements correspond to 75% of the expected settlement at 3 years.

7 CONCLUSION

Building in the downtown (compact and heterogeneous area with historic buildings, new constructions, means of sensitive transport…) and in a complex geological, setting hydrogeo-technics requires a "project study" extremely detailed and taking into account very precisely interaction with all neighboring. The definition of a specific target for perimetric wall and jet grouting in terms of waterproof systems, bearing capacity, allows to carry out this project in compliance with the integrity of the site.

Follow-up, monitoring and implementation of breakpoints in key phases of construction have ensured the good development of the project with the respect of thresholds defined during the study phase.

The strong reactivity of all companies and participants involved in the building project contributed to the successful infrastructure realization.

Geotechnical Engineering for the Preservation of Monuments and Historic Sites – Bilotta, Flora, Lirer & Viggiani (eds)
© 2013 Taylor & Francis Group, London, ISBN 978-1-138-00055-1

Drilled spiral piles in St. John's Church of Tartu, Estonia

K. Avellan
KAREG Consulting Engineers, Helsinki, Finland

ABSTRACT: This article focuses on original working method devised for an important underpinning project in Tartu, Estonia in the 1990s. Because of the sinking and uneven settlement of St. John's Church of Tartu, jacked piles, and especially designed drilled spiral piles, were used to strengthen its foundations. The drilled spiral pile was developed for a particular circumstance, in this case the underpinning of a long massive stone wall without lateral bracing and for rebuilt columns. The piles were drilled down with a hydraulic machine after each segment was welded to the previous one and to the prefabricated spiral treaded close toe of the pile. Practical pretesting and end jacking procedures for drilled spiral piles were developed. Every single installed drilled spiral pile was pretested and end jacked to a dense layer. In addition, other attributes of the new technique is its low cost, portability of equipment and small space requirement for its implementation.

1 INTRODUCTION

1.1 *Foundation strengthening in historic structures*

In many cases historic buildings or monuments are founded on compressible soil, the result of which is uneven settlement over time and, at worst, building failure or collapse. A common case involves buildings or monuments originally founded on wooden structures such as timber piles or platforms.

The strengthening of historic building foundations is a field of engineering where every site is more or less different from another. The variation of the substructure, foundation, and superstructure make every case unique. Preserving heritage buildings by preventing structural decay requires know-how and suitable strengthening methods.

1.2 *The case of St. John's Church of Tartu*

The strengthening of foundations for St. John's Church of Tartu was a project of historic significance which presented many challenges. To underpin the foundations of this massive structure, original solutions had to be devised throughout the work period.

2 HISTORY OF ST. JOHN'S CHURCH

2.1 *Significance from early history*

Among the many examples of medieval architecture in Estonia, St. John's Church in Tartu remains an outstanding piece of art within the European context. It is the most prominent Gothic style building in Estonia and is renowned for its terracotta sculptures and decorative details, as shown in Figure 1.

It is understood through written records that a congregation already existed in the area of present day St. John's Church in 1323. The fragments of wooden buildings found on the site are considered the earliest evidence of an existing church. From the

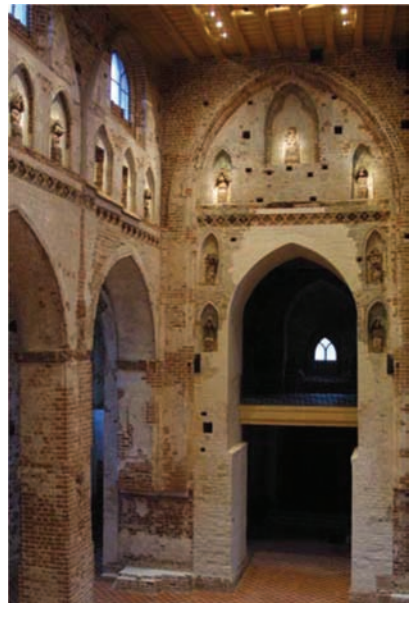

Figure 1. Today almost 1000 terracotta sculptures adorn the interior and exterior of the building. The quantity, size, and artistic quality of the figures make them unique in Europe.

evidence of archaeological findings, the building of the stone church can be firmly established as dating from the end of the 13th century at the earliest, to the beginning of the 14th century at the latest.

The church was not built according to a uniform plan and acquired its final medieval shape after several changes of design, reconstructions, and also catastrophes. In the first stage of building, the choir of the church was established on a foundation of sand and granite stones. Since Tartu is located on relative loose ground, the stability of the building was achieved by having wooden rafts underneath the stone foundations.

The dominant feature of the building is its massive western tower which rests on four pillars. The tower was found to have a weight of 5500 tons

The story of the church in the post-medieval period is a history of multiple destructions and rebuilding, with many of the original features being lost during the process. The church suffered seriously in the Northern War in 1708. Probably the upper part of the tower fell on the nave and its vaults, causing the choir to cave in. Due to the need for urgent repair, the nave was built lower than previously. From 1899–1904 the church facades were rebuilt under the direction of Latvian architect W. Bockslaff. A buttress (seen in Figure 2 between grid lines 4 and 5) was added in the 1800s. It was subsequently deemed unnecessary and was removed during the underpinning project in the 1990s.

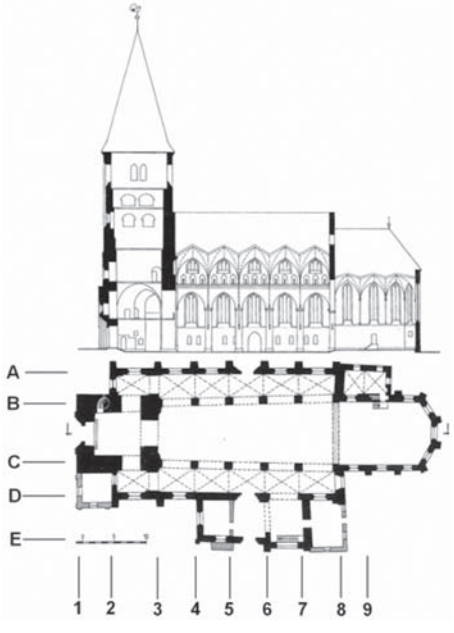

Figure 2. Plan and section of St. John's Church. The buttress between grid lines 4 and 5 was added in the 1800s.

2.2 *Conditions of St. John's post WWII*

In 1944 the church burned down and remained in ruins for the whole period of the Soviet occupation. During the following decades more than one plan for the restoration of the church was drawn up. Some practical measures connected to the restoration of the church were already taken during the late Soviet era, including some surveying of the building done in the 1970s (Alttoa 1994).

Figures 3, 4, and 5 show the state of the church before strengthening in the 1990s.

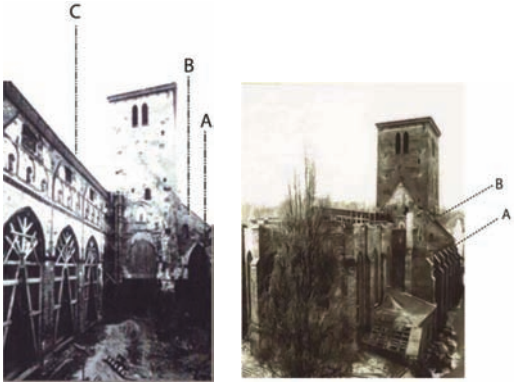

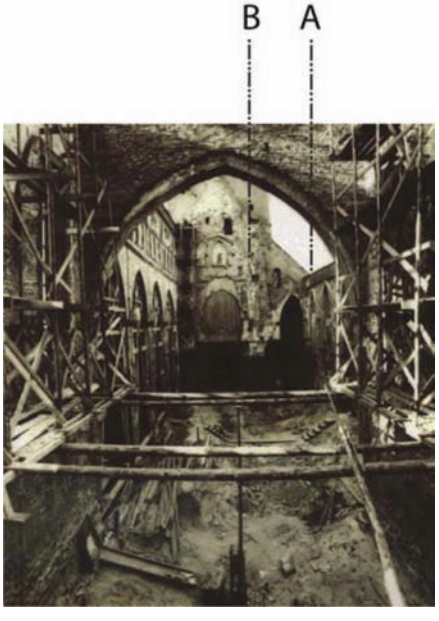

Figures 3, 4, 5. St. John's Church before the strengthening work. Line A is on the right side without roof. Line B had to be entirely rebuilt (see Fig 7).

3 REASONS FOR STRENGTHENING THE FOUNDATIONS

The existing foundations of the church are on massive stones, which themselves laid on wooden rafts. The height of the stone setting is approximately 3 m. On the lowest parts of the building, situated in the south-western and south-eastern corners, the stone setting is 1.5–2 m high. On the top layer these stones are joined together with mortar, but at the lower level the joints are filled only with sand. The double wooden raft under the stone setting was made from Ø 30–40 cm wood trunks. The ground under the church consists of a variety of different soil layers. The approximate thicknesses of the soil layers under the wooden rafts are shown in Figure 6.

It was known that the consolidation process of the loose sandy silt (tufa layer) had ended because of its thickness (5 m) and time-lapse (more than five hundred years). The outside earth surface of the church has risen in the past because of the addition of "cultural layers."

During recent industrialisation decades, the building began to sink because of the lowering of the ground water table. In the last few years before the strengthening work was started the water level had dropped below the level of the wooden rafts. As the result, the wooden rafts had begun to rot, thus accelerating the sinking process. The settlement map in the church area for the period from 1963 to 1987 is shown in Figure 7 as contour lines.

To stop the sinking of the church, work began by strengthening the foundations—a project which took place from 1993–96. The underpinning of the tower was mainly executed in 1993–94. The last supporting structures and concrete pours were realized at the beginning of 1996. The foundations of the choir were not underpinned since they lie on hard soil and were not considered to be in immediate need of strengthening.

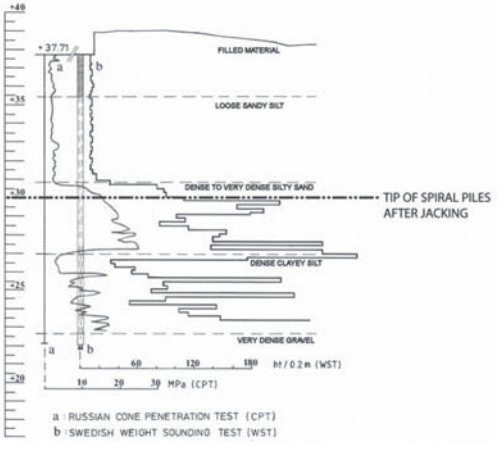

Figure 6. Russian cone penetration test (CPT) and Swedish weight sounding test (WST). Soil explorations results at sample point near the church wall.

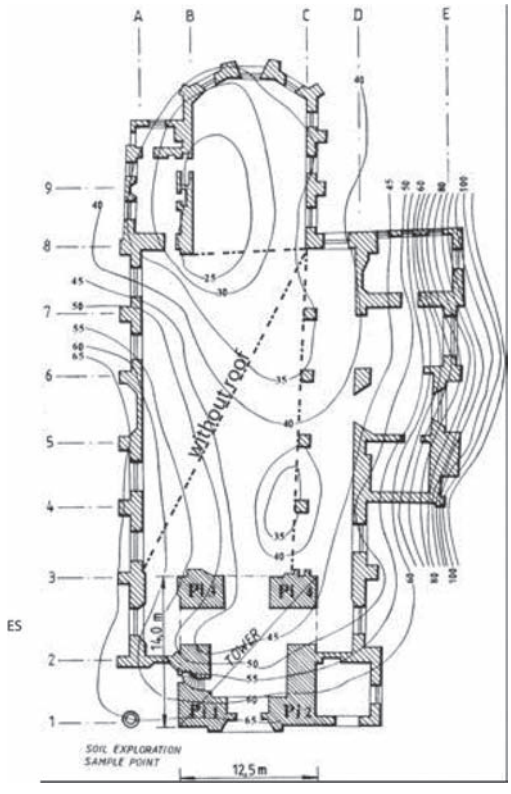

Figure 7. Contour lines of settlement (mm) in the area of the church during the years 1963–87 (Avellan 1992). Line A is on the left side without roof. Line B, where the columns were d stroyed, had to be completely rebuilt.

4 UNDERPINNING METHODS

The foundations of the church were underpinned by piling, using jacked piles and drilled spiral piles. These pile types were employed because, in its fragile state, the building could tolerate neither the vibration of driven piles nor drilling using flushing water or air techniques. The layer of dense to very dense silty sand starting at approximately 6 m below the old foundation level was chosen as the bearing stratum as the first 4–5 m layer of loose sandy silt (tufa layer) did not have enough bearing capacity.

The deformation model (E_d) of the dense to very dense silty sand was found to be approximately

Figure 8. Simple screw driving equipment for drilled spiral piles.

50–60 MPa. Additionally, the old block foundation could not have withstood the greater forces which would have been needed to jack piles through the compact silty sand layer.

The piles were embedded in the soil by twirling. The joints of the spiral drilled piles were made by welding the parts together and jacking them. The completed piles were filled with concrete. The total length of the piles on line A varied from 5.5 m to 6.5 m. A practical technique and simple equipment was devised to enable the assembly of the spiral-drilled piles by screwing in very limited workspaces. It was important that workmen could carry all the parts of the necessary equipment.

5 WORK DESCRIPTION OF DRILLED SPIRAL PILES

The underpinnings at lines A and B and the columns of line C were made with drilled spiral piles. The steel piles had a diameter of 218 mm and a thickness of 10 mm. The first section (1 m) had a welded spiral 25 mm × 10 mm. Because of the lack of a sufficient counterweight of the spiral piles in line B, where the columns were rebuilt, the work was different from that of lines A and C. In line A, the walls were pre-injected with a water-cement-sand mixture. In the first stage, the pile locations were jetted and the piles were screwed as deep as possible because of adequate torque moment of the equipment. Reinforced concrete beams were cast on both sides of the wall above the piles, against an injected stone composition; see Figure 10.

The concrete beams were forced against the old structure with pre-stressed anchorage. As the timber material of the plank foundations rots, all the vertical loads will gradually be taken on by the piles. At line A, the piles also counteract lateral loads (Fyk) and moments (Myk) from the rebuilt arch. The lateral load is Fyk = 51 kN and the moment Myk = 624.5 kNm. In line A, three piles of 340 kN allowable load each, and two piles of 360 kN outside the line work in combination. The lateral load of 10.2 kN for each pile is neglected in the design considerations.

The creep load, Qc = 525 kN, was defined beforehand without the pretesting and end-jacking procedures. The creep load of curvature is showed in Figure 9. The creep pressure under the spiral tip was 13.9 MPa.

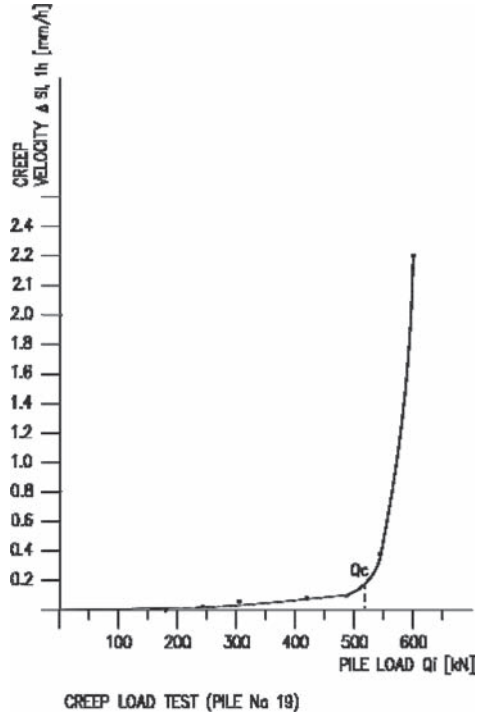

Figure 9. Creep velocity in the creep load Qc is the load which the curvature of the diagram corresponds to the minimum radius of the curvature.

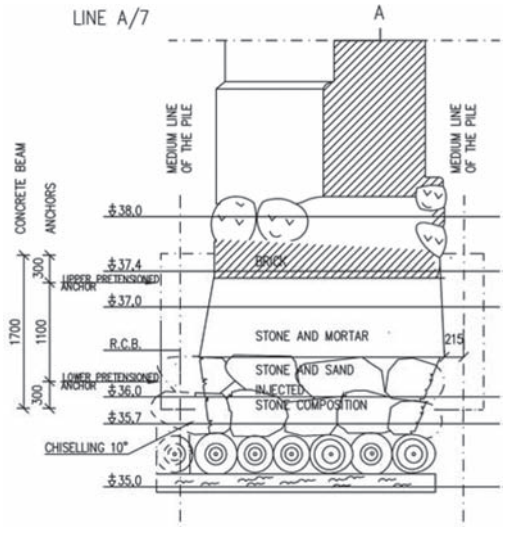

Figure 10. Section from line A, the injected stone composition, lower and upper pre-tensioned anchors and beams. Chiselling was required prior to fabricating the concrete beams for them to carry the load to the piles from superstructure.

The drilled spiral piles under the concrete beams were test-loaded, pretested and end-jacked subsequently wedged against them. The steel wedges were embedded inside concrete. The second anchorage pre-stressing sequence was carried out six months later to eliminate any loss of pre-stressing force resulting from the creep effect in the previously injected stone foundation. After pre-stressing, the drilled holes were injected with cement mortar and concrete was cast on the anchor clamps. The sequence of the work on line A is shown in Figure 11.

The sequence of the work on the line A (part of the work could be done simultaneously)

1. Digging, first outside, then inside
2. Injection of wall day 1: erection of pipes and shotcreting by hand; day 2: waiting for shot creting to mature; day 3: injection of lower part; day 4: injection of upper part
3. Preparation of pile locations and cutting
4. Jetting of pile locations and installation of piles
5. Torqueing the pile step by step
6. Boring of openings for anchors
7. Chiselling of the old stone foundation
8. Casting of concrete beams
9. Prestressing of the concrete beams together
10. Jacking the piles using a special pretesting procedure in line A in incremental loading steps at 15 minutes intervals
11. End jacking procedure

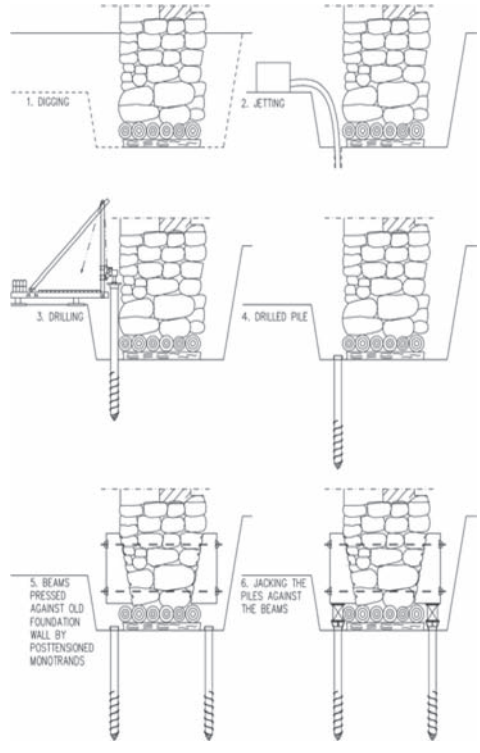

Figure 11. Working phases of drilled and jacked spiral piles.

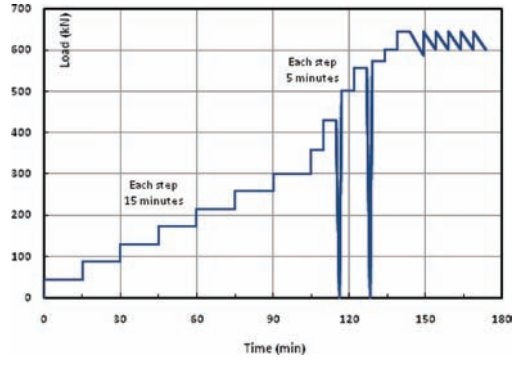

Figure 12. Time intervals for test loading of each of the drilled spiral piles in the line A.

The pretesting procedure is illustrated in diagram in Figure 12, which also includes the end jacking procedure. The pressure was held constant for 15 minutes at each step and the settlement was measured at 3 intervals (5, 10, and 15 min). When the pressure of 450 bar (644 kN) decreased in 5 minutes by less than 50 bar (72 kN) to 400 bar (572 kN), the end jacking could start.

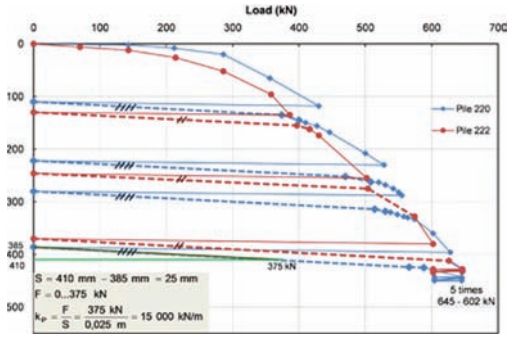

Figure 13. Load-settlement diagrams of drilled spiral piles showing the repeated load cycling between 645–602 kN and at the end of the pretesting procedure. A parallel line in the pretesting diagrams justifies the evaluation of the spring coefficient, k_P.

All of the installed drilled spiral piles went through the pretesting procedure with end jacking to ensure their functionality. An example of the pretesting and end jacking procedure of special tested piles is presented in Figure 13.

The load bearing layer, from dense to very dense silty sand, has about the same thickness (~4 m) although the upper level of the layer is slightly inclined. The area surrounding the church has the same geological strata. Near line E (Fig. 7), where the settlements were larger, there is also a clay layer formed by the presence of an ancient river. The outcome of the procedures with piles Nos. 220 and 222 indicate that using the same pretesting and end jacking procedure of the piles in line A, the allowable maximum load can be 400 kN. The safety factor gamma defined in DIN 1054 is 1.56.

$$\gamma = \frac{602\,kN + 645\,kN}{2} \times \frac{1}{400\,kN} = 1.56 \qquad (1)$$

The allowable load above is less than the creep load Qc = 525 kN (Fig. 9). The safety factor of creep is then:

$$\gamma = \frac{525\,kN}{400\,kN} = 1.31 \qquad (2)$$

The used allowable load on the spiral drilled piles that were installed was 375 kN.

6 SETTLEMENT OF DRILLED SPIRAL PILES

Based on the load settlement diagrams of the tested drilled spiral piles the author noticed that without his pretesting and end jacking procedures the settlement in line A could have been approximately 25 mm. This can be noted from the settlement diagrams in Figure 13. The surveying results from 21 October 1995 up to 9 June 2011 confirm that the pretesting and end jacking procedures worked well since there is no noticeable settlement in line A. It is therefore verifiable that the procedure is suitable for the dense to very dense silty sand layers of Tartu. One of the levelling points (No. 3) was noted to have risen, probably due the settlement in the strata of the tower. The maximum settlement during the period above mentioned is 5 mm ± 2 mm.

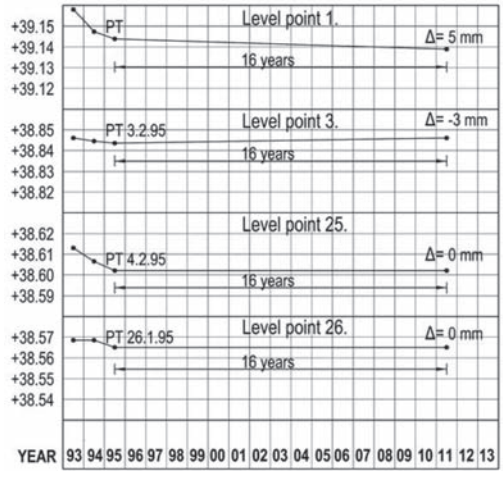

Figure 14. Data from line A: Diagrams from 1993, 1994, and 1995. Pre-testing and end-jacking date (PT). Data added from the monitoring in 2011.

Figure 15. St. John's Church was opened for visitors in May 2005 and the reopening ceremony of the church was held on 29 June 2005.

7 CONCLUSIONS

Every installed drilled spiral pile was test loaded using special pretesting and end jacking procedures. According to these, all piles function well in their respective position. The functional success of the drilled spiral piles in St. John's Church also was proven by the fact that the settling of the church has ceased. The strengthening method described in this article can be successfully employed in strengthening the foundations of other heritage structures. The methods can be applied in challenging circumstances, because of its low costs, the portability of the required equipment and minimal workspace requirements. The drilled spiral piles can be installed even where limited space is available.

The low level of investment needed to implement this method also makes it well suited for developing countries. Jetting is used to investigate if there are any boulders in the soil. It helps for drillings and to have the pile in the right direction. The main machinery involved in the installation can be placed outside the workspace. The employed drilled spiral pile is practical for the strengthening of historical foundations. Neither injection nor vibrations are involved.

REFERENCES

Alttoa, K. 1994. *St. John`s of Tartu*, St. John´s of Tartu Foundation 1994. Estonian heritage society.

Avellan, K. 1992. *Geotechnical and Structural Ultimate Limit State Design of Foundations Resting on Soil*. Licentiate thesis. Helsini University of Technology, Faculty of Civil and Environmental Engineering.

Avellan, K. & Lange, K. 1996. St. John's Church, Tartu, Estonia—Underpinning of tower. (C. Viggiani ed.) Geotechnical Engineering for Preservation of Monuments and Historic Sites. Proceedings of the International Symposium on Geotechnical Engineering for the Preservation of Monuments and Historic Sites". Naples 3–4 October 1996, 521–525.

Avellan, K. & Maanas, M. 2001. Strengthening the foundations of St. John's Church in Tartu, Estonia. "*Proceedings of the Fifteenth International Conference on Soil Mechanics and Geotechnical Engineering".* Istanbul, 27–31 August 2001, 1687–1690.

Avellan, K. 2011. Limit state design for strengthening foundations of historic buildings using pretested drilled spiral piles with special reference to St. John's Church in Tartu. Doctoral thesis. University of Oulu, Faculty of Technology. Acta Universitatis Ouluensis, C Technica 392.

This page intentionally left blank

Geotechnical Engineering for the Preservation of Monuments and Historic Sites – Bilotta, Flora, Lirer & Viggiani (eds)
© 2013 Taylor & Francis Group, London, ISBN 978-1-138-00055-1

Settlement induced by TBM excavation under the Vittoria's Church in Napoli

S. Aversa
Università di Napoli Parthenope, Italy

E. Bilotta & G. Russo
Università di Napoli Federico II, Italy

A. di Luccio
Ansaldo S.T.S., Italy

ABSTRACT: Line 6 of the Metro of Napoli underpasses one of the corner of an old church, built in the 16th century, with a tunnel of 8.5 m of external diameter at a depth of approximately 10 metres beneath its foundations. The tunnel has been excavated by means of a tunnel boring machine (TBM). During the design phase the presence of the church was carefully taken into account, with settlement predictions based on cautious range of volume loss during the construction of the tunnel. For its relevance the church was submitted to an accurate monitoring. The paper describes the monitoring system and presents the obtained results, which are also compared with the settlements measured in the greenfield sections located in the square and in the public gardens in front of the church. The influence of the stiffness of the structure and of the relative position of the underground line with respect of the plan section of the church is discussed in the last part of the paper.

1 INTRODUCTION

In the wide open space of Vittoria square in Napoli raises the façade of the church of S. Maria della Vittoria located in the corner with Vannella Gaetani street. The façade of the church is incorporated in a three-storey building which has two additional floors further to the base. The dome of the church is not longer visible because it is hidden by the different floors in elevations added over the time.

The church has been underpassed by a tunnel boring machine (TBM) dedicated to the construction of the tunnel for Line 6 of Napoli underground. The undercross was rather superficial and occurred very close to one corner of the church because no alternatives to the main route were found at the design stage. The event was carefully monitored even being the design predictions very satisfactory and no damages were expected to occur.

2 LINE 6 OF NAPOLI UNDERGROUND

2.1 *Ground conditions*

When completed, Line 6 will connect the western borough of Bagnoli to the city centre at Municipio station, with a total length of 8 km and 12 stations.

It is already operating between Mostra and Mergellina stations, while the stretch between Mergellina and Municipio stations is presently being constructed. The subsoil profile in this stretch is reported in Fig. 1. The running tunnel is a double track single tunnel with an outer diameter of 8.50 m.

Between Mergellina Station and Piazza Vittoria, the top of the tuff formation is erratic and prevalently deeper than the tunnel. A thick layer of cohesionless soils, including made ground underlain by marine sands, remoulded ashes and in situ pozzolana rests above the tuff. Between Piazza Vittoria and Municipio station, the tuff formation is found at ground level or at a depth shallower than that of the tunnel roof; here design and construction problems are thus much simpler.

2.2 *Ground displacements*

As mentioned above, in the stretch between Mergellina and Piazza Vittoria the tunnel crosses essentially granular soils at relatively shallow depth, hence surface displacements were unavoidably observed. In this stretch, however, the tunnel runs along wide streets and gardens so that surface displacements are critical only in the area of Piazza Vittoria, where historical mansions such as Palazzo Calabritto and

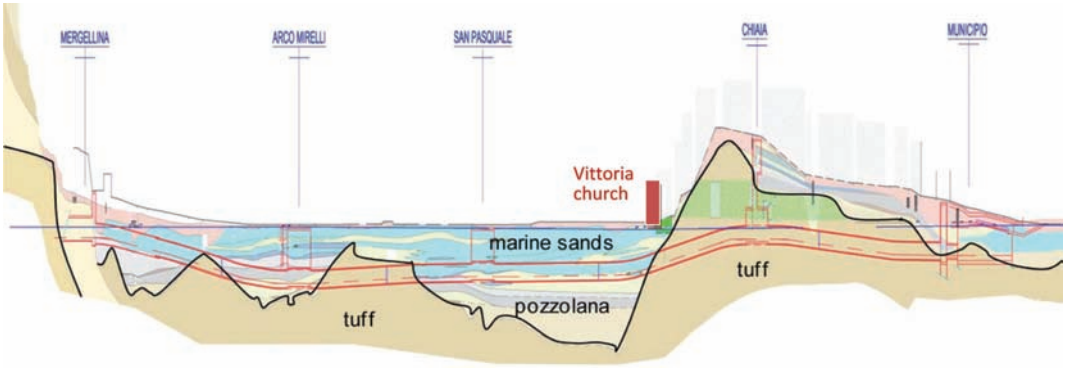

Figure 1. Subsoil profile of Line 6.

Palazzo Satriano, and the Santa Maria della Vittoria Church are close to the line. A large number of greenfield sections were monitored both before and after the passage of the TBM.

The maximum settlement along the axis of the tunnel never exceeded 15 mm. Where downwards movements were recorded, an average value of the volume loss V' equal to 0.25% has been obtained, with single values ranging between 0.07% and 0.36%. Along at least 30% of the whole stretch, however, practically zero settlement or even small upwards displacements were recorded. In any case the "negative" volume loss V' never exceeded 0.1%.

The parameter K, which represents the ratio between the width of the ground settlement trough, i, and the tunnel axis depth z_0, ranged between 0.3 and 0.7 at relatively large distances from the face.

3 THE CHURCH OF SANTA MARIA DELLA VITTORIA (VITTORIA CHURCH)

3.1 *History*

The church was built by the religious Order of Carmelites in 1573, on a site granted by the Marquis of Polignano. It was dedicated to Santa Maria della Vittoria in memory of the victory gained by the Holy League, led by don Giovanni d'Austria (1547–1578), son of Charles V, against the Turkish fleet in Lepanto, on October the 7th 1571. This victory, which marked the decline of the Turkish power on the Mediterranean sea was attributed to the intercession of the Holy Virgin.

Around 1585, the church was given to the religious Order of the Society of Jesus. Following a quarrel with the Marquis of Polignano, the members of the Society of Jesus were forced to surrender the church, which was later rebuilt in 1628 by Giovanna d'Austria, Princess of Butera, daughter of Don Giovanni, who gave the entire complex to the Order of Teatini.

In 1630, after the death of Giovanna d'Austria, the church was modified by the Teatini, who built up "a beautiful and comfortable monastery for their Order" (Celano, 1856).

Subsequently, in 1646, the church was renovated by the daughter of Giovanna, Margherita d'Austria. According to Celano, "(the church) was reduced to perfection and beauty in which can be seen today, in the year 1646 by Margherita d'Austria-Branciforte." Some documents (Savarese, 1986) show that the design can be attributed to a pupil of P. Francesco Grimaldi, the Teatino friar Pietro Caracciolo. From the middle of the '600, the church has maintained its planimetric shape, while the adjacent convent has undergone numerous changes, in particular towards the end of '700, when the Teatini friars turned the monumental complex in a residential complex.

In the 1697 Don Luigi della Cerda, duke of Medinacoeli and vice king on behalf of Carlo II from Spain ordered the modification of the Chiaia beach; the pavement was changed and willows and fountains installed to make the walking more enjoyable. Later on, about one century after, the interventions designed by Luigi Vanvitelli took place, modifying the outlook of the Royal gardens which have essentially kept the same appearance until nowadays. A plan of the area as it was after the intervention of the 1697 is reported in Figure 2.

The plan was made by P. Pietri and the area occupied by the Church of Santa Maria della Vittoria is clearly visible in the low corner on the right.

In Figure 2 a watercolour painting by John "Warwick" Smith dated about the end of the XVIII century is reported. At that time the dome was still clearly visible as it is confirmed in the Veduta by Pizzofalcone hill (Figure 4) painted in the same period by Gaspar Adriaensz van Wittel, father of the architect Luigi Vanvitelli.

The present appearance of the church is due to other changes ended in 1824. The complex was heavily modified and the dome which was clearly visible was incorporated in the courtyard of a residential building.

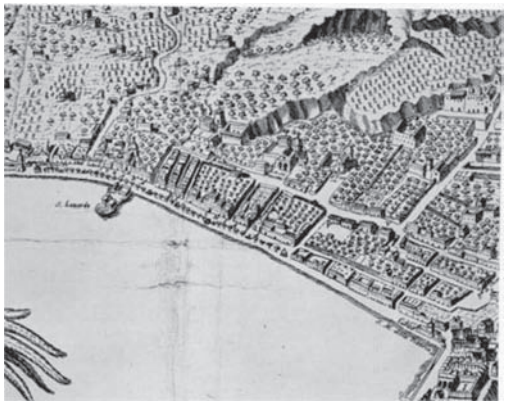

Figure 2. Plan of the area after Vanvitelli's restyling.

Figure 3. Water colour painting by J.W. Smith (1776–1781).

Figure 4. Veduta by Pizzofalcone hill by Gaspar van Wittel (1699–1702).

3.2 *Architecture*

As stated before the Church of S. Maria della Vittoria is located in the wide open space of Vittoria square in Napoli, in front of the Villa Comunale of Napoli, one of the few public gardens of the old city (Figure 5). The facade of the church is incorporated in a three-storey building (Figure 6).

The plan of the church is divided into three naves (Figure 7), the central one is covered by barrel vaults with lunettes, while the two side naves are covered by a succession of arch/vaults or basin vaults.

The naves are divided into five spans, the third one corresponding to the transept. The intersection of the nave and the transept is marked by the presence of four columns made by grey marble that end with Corinthian capitals, supporting a trabeation (Figure 8).

Figure 5. Plan view of the church and the neighborhood (modified after Sanseverino & Rahati 2012).

Figure 6. Main façade of the building.

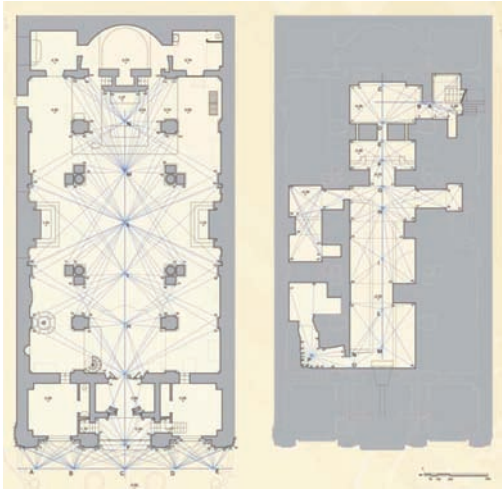

Figure 7. Plan view of the church and the crypt below (modified after Sanseverino & Rahati 2012).

Figure 8. Main nave of the church.

Above the trabeation start four spherical pendentives on which the windowed drum and the dome are built. The dome ends with one eye which diffuses the light inside the church. The dome is the central element of the composition (Figure 9).

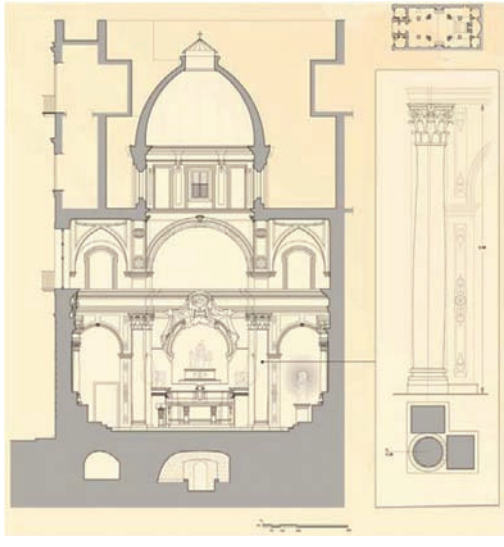

Figure 9. Transverse section of the church (modified after Sanseverino & Rahati 2012).

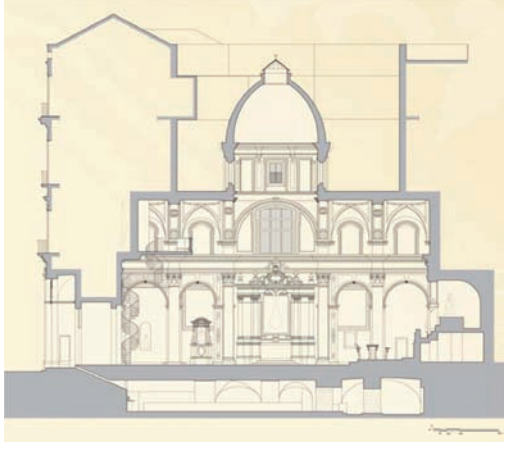

Figure 10. Longitudinal section of the church (modified after Sanseverino & Rahati 2012).

Longitudinally (Figure 10), the system ends with the altar. Below the church is located a crypt.

Throughout the whole church the floor is covered by white Carrara marble with insertion of red Verona stone.

This short description of the church architecture and history seems well justify its perception as a monument, that is an example of "firm and long-lasting mutual bond between present and past, between man and environment" (Croce, 1985, Jappelli, 1991;1997).

Nowadays, there is luckily an "increasing recognition of ancient buildings as a kind of material historic record" (Calabresi & D'Agostino, 1997), which deserves the maximum attention since the stage of design of any infrastructure interacting with it.

This issue is even more relevant in the preservation of the historic urban environments, which are increasingly often interested by extended infrastructuring (Aversa, 2007; Viggiani, 2011).

4 MONITORING OF THE CHURCH

As discussed in details by Burland & Standing (1997), geotechnical monitoring plays a vital role for the preservation of historic buildings, since it may contribute to a better understanding of the interaction between ground and structures. Monitoring appears actually a fundamental step in the search for a well founded model for analyzing the problem (Viggiani, 1997a, b).

According to this view, a monitoring programme for the church during tunnelling operations was undertaken.

4.1 *Ground conditions*

In Figure 11 a longitudinal section of the crossing under the corner of the Vittoria Church is sketched. Precision survey was conducted, in greenfield conditions, along many segments orthogonal to the tunnel axis on the square in front of the church and on targets fixed on the external walls of the church and of other buildings underpassed by the tunnel. Some targets were also located inside the church. In addition, a number of electrolevels were also located on the columns.

Some inclined boreholes have been carried out in order to detect with sufficient precision the foundation level of the church, which resulted 3 m below the ground level, and 10 m above the tunnel crown.

The observation of the measurements in the greenfield area which stretches along the tunnel path for about 100 m just before the Vittoria Church (Fig. 12) allowed the average parameters of the Gaussian fitting curve to be deduced (Peck, 1969). The parameters resulted as V' = 0.25%–0.3% and K = 0.3 to 0.4.

In Figure 13 the settlements measured at the ground surface along one transverse greenfield alignment of landmarks are shown together with a Gaussian fit (V' = 0.25%, K = 0.4). Measurements were taken at different dates, corresponding to different positions of the tunnel front, from one diameter to several diameter ahead the measuring

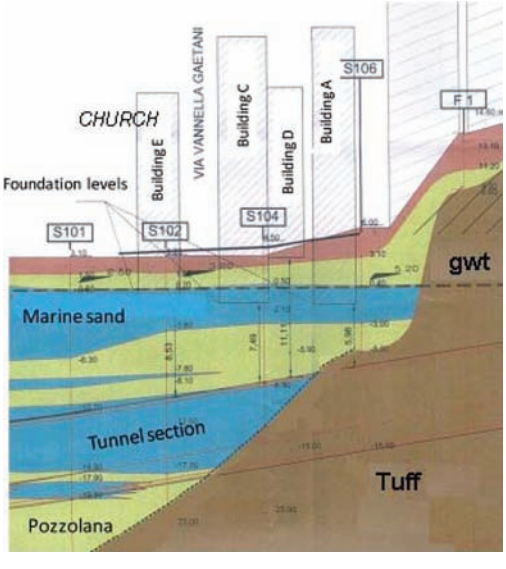

Figure 11. Geological section of the Vittoria Church (Building E) crossing.

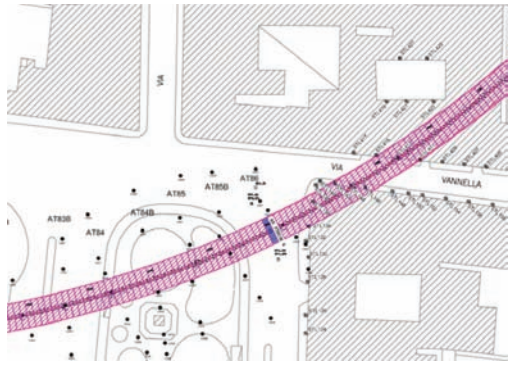

Figure 12. Location of landmarks and targets for survey.

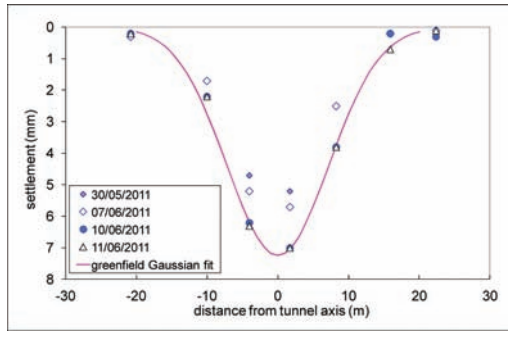

Figure 13. Measured ground settlements along a greenfield transverse section and fit (V' = 0.25% and K = 0.4).

section. The TBM passed through that section on May 25th, 2011.

It may be noticed that the Gaussian fits the settlements measured when plane strain conditions occurred around the tunnel (i.e. June 10th and 11th). The corresponding parameters were used to calculate the expected deformation of the ground level along the main façade and the lateral wall of the Vittoria Church.

The measurements of the targets on the external façade of the Church during the TBM underpass are plotted in Figure 14. The maximum observed settlement was about 16 mm, mostly developed in one week when the TBM was travelling at a speed higher than 10 m/day. It can be seen that at a distance ranging between two and three diameters the settlement caused by the excavation is negligible.

Such observed settlements along the building façades are reported in Figure 15 (closed dots from left to right: targets STL138, 136, 134, 132, 130, 128, 126) and 16 (closed dots from left to right: targets STL140, 142, 144, 146, 148, 150, 152, 154, 156, 158). The settlements measured at the ground surface in close proximity of the church main façade are also shown in Figure 15 for comparison (open dots).

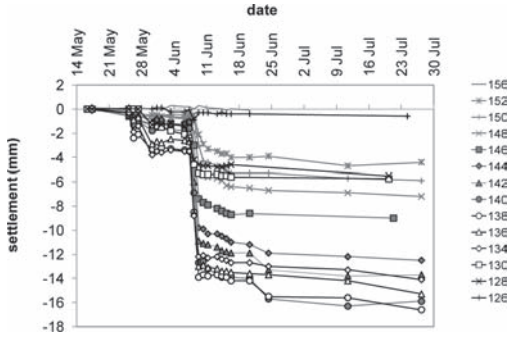

Figure 14. Measured settlements at different locations along the edges of the Vittoria Church.

The comparison with the Greenfield predictions in Figure 15 at surface (continuous line) shows that the building settled more than the ground surface: due to the presence of a Crypt, the façade settlement should compare with the maximum greenfield prediction at a lower level (about 3 m below the ground level). The latter is also shown in the figure with dashed line. However, the profile of measured building settlement shows a relatively "stiff" response of the front façade (first four targets from the left, from STL138 to STL132) to the tunnel induced deformation. This complies with the structural stiffness of the main façade in its plane.

A similar comparison is shown in Figure 16, showing a stiffening effects of the lateral continuous and massive wall of the Church.

It should be noticed that the corner of the Church (corresponding to targets 138, 140 and 142) suffered settlement larger than the predicted ones.

A special concern was related to the behaviour of the dome and its four supporting columns which appeared as being substantially independent at the head level. Furthermore the passage of the TBM was expected just below the corner of the church, as clearly indicated by the plan view of the Figure 12. The dome and its supporting columns were all placed on the right side of the underpassing tunnel in an area where presumably hogging deformations would have taken place. For all these reasons electrolevels were adopted to monitor the inclination of the column head. The installation was carried out in a traditional way by simply fixing the transducer on the column via a simple and punctual steel screw. The results obtained are reported for all the eight electrolevels in Figure 17. The passage of the TBM occurred in the first two weeks of June as clearly shown by the settlement reported in Figure 14. It can be clearly seen that the electrolevels detected only very small and almost negligible movements in this period, the maximum tilt values being below 3–4% of degree. The decision

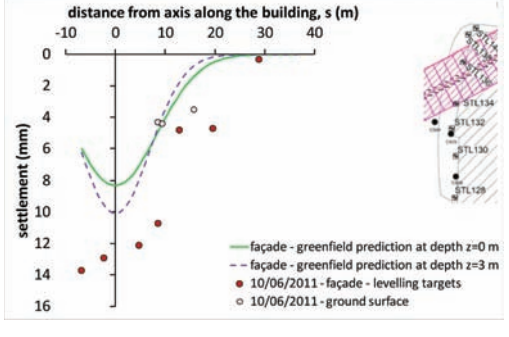

Figure 15. Measured and predicted settlements along the main façade of the Vittoria Church.

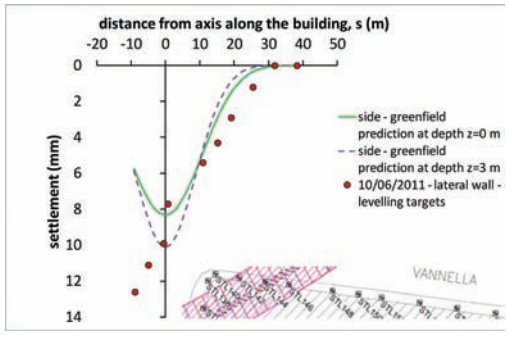

Figure 16. Measured and predicted settlements along the lateral façade of the Vittoria Church.

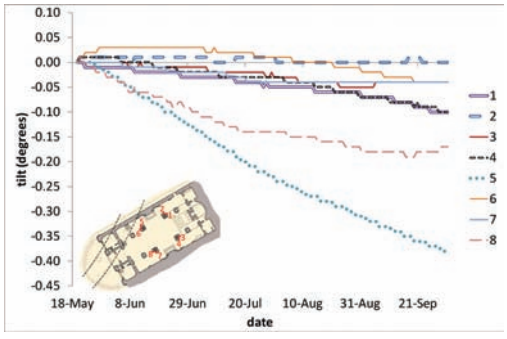

Figure 17. Tilts along two orthogonal planes measured at the head of the 4 columns supporting the dome of the Vittoria Church.

to use such instruments was mainly based on the their high resolution which was judged as opportune in a context were even small movements and trends had to be detected quickly. In the long term such instruments may suffer drift problem and, as a matter of fact, the system has been kept working for further three months during which some instruments underwent such trouble.

5 CONCLUDING REMARKS

The Church of Santa Maria della Vittoria has been underpassed by the tunnels of the Line 6 of the Metro of Napoli without suffering any static and serviceability problem. The interaction with the Church has been considered in the design phase with class A predictions. During the construction of the line the monitoring of many greenfield cross sections permitted to verify the design hypotheses in order to increase the reliability of the predictions.

An accurate monitoring was implemented on the Church, by means of high precision levelling and of electrolevels located on four inner columns.

The obtained measurements have been used to verify the effects of the excavations of the tunnel during the construction phase. The induced displacements did not produce any damage to the Church.

These measurements are also very interesting from the scientific point of view, since there are not many documented cases in which a tunnel underpasses a complex construction like an old church, in correspondence of a corner, a few meters beneath the foundation level, in a saturated sandy soil.

In particular it can be stressed that:

- in the greenfield sections in front of the church the excavation of the tunnel line with an earth pressure balance TBM produced settlements well described by the Normal distribution (Peck, 1969) with a volume loss V' of 0.3%, K = 0.4 and maximum settlement of 7 mm;
- the corner of the church suffered settlements larger than those measured in greenfield conditions;
- the settlement profiles along the two orthogonal walls of the church were different from the typical greenfield shape, due to the structural stiffness of the two walls;
- the settlements of the columns located inside the church at the base of the dome and their rotations were negligible.

The case history is also finalised to stress the importance to give to historic sites and to monuments both when operating directly on them or when operating in the proximity of them, like in this case.

Historic churches, with their particular structure, must be approached with care, taking into account that their behaviour can be different from that of residential buildings.

Investigations (geotechnical, structural and historic) are fundamental in the design process and a correct monitoring is fundamental too.

ACKNOWLEDGEMENTS

The authors would like to acknowledge the Ansaldo STS, the Municipality of Napoli, the Metropolitana di Napoli SpA for having permitted the publication of monitoring data.

REFERENCES

Aversa S. 2007. Preserving cities and monuments. In: *Geotechnical Engineering in Urban Environments*. Madrid, 24–27 September 2007, vol. 5, p. 453–462, Rotterdam:Millpress, ISBN: 978-90-5966-055-7

Burland J.B., Standing J.R. 1997. Geotechnical monitoring of historic monuments. Proc. of the Arrigo Croce Memorial Symposium—Geotechnical Engineering for the Preservation of Monuments and Historic Sites, Napoli, 1996., A.A. Balkema, Rotterdam.

Calabresi G., D'Agostino S. 1997. Monuments and historic sites: Intervention techniques. *Proc. of the Arrigo Croce Memorial Symposium—Geotechnical Engineering for the Preservation of Monuments and Historic Sites*, Napoli, 1996., A.A. Balkema, Rotterdam.

Celano C. 1856. *Notizie del bello, del l'antico e del curioso della città di Napoli* con aggiunzioni di G.B. Chiarini. Napoli, 1856-60. Reprint, 1974.

Croce A, 1985. Old monuments and cities. Research and preservation. Geotechnical Engineering in Italy—An overview. AGI Associazione Geotecnica Italiana.

Jappelli R. (Ed.), 1991. The Contribution of Geotechnical Engineering to the Preservation of Italian Historic Sites. Associazione Geotecnica Italiana.

Jappelli R. 1997. An integrated approach to the safeguard of monuments: the contribution of Arrigo Croce. *Proc. of the Arrigo Croce Memorial*

*Symposium—Geotechnical Engineering for the Preservation of Monuments and Historic Site*s, Napoli, 1996., A.A. Balkema, Rotterdam.

Peck R.B. 1969. Deep excavations and tunnelling in soft ground, *Proc. 7th ICSMFE,* Mexico City, State of the Art Volume, 225–290.

Russo, G., Viggiani, C., Viggiani, G.M.B. 2012. Geotechnical design and construction issues for lines 1 and 6 of the Naples underground. *Geomechanik und Tunnelbau*, 5 (3), pp. 300–311.

Sanseverino I. & Rahati Y. 2012. *La chiesa di S.M. della Vittoria in Napoli.* Master Thesis in Architecture. School of Architecture. University of Napoli Federico II (in Italian).

Savarese S. 1986. Francesco Grimaldi e l'architettura della Controriforma a Napoli. Roma, 1986.

Viggiani C. (Ed.). 1997a. Geotechnical Engineering for the Preservation of Monuments and Historic Sites, A.A. Balkema, Rotterdam.

Viggiani C. 1997b. Opening address-Proc. of the Arrigo Croce Memorial Symposium-Geotechnical Engineering for the Preservation of Monuments and Historic sites. A.A. Balkema, Rotterdam.

Viggiani G.M.B. 2011. General Report on Environmental geotechnical engineering and Preservation of historic sites. *European Conference on Soil Mechanics and Gotechnical Engineering, Athens* (in print).

Geotechnical Engineering for the Preservation of Monuments and Historic Sites – Bilotta, Flora, Lirer & Viggiani (eds)
© 2013 Taylor & Francis Group, London, ISBN 978-1-138-00055-1

Ground improving injections underneath historical buildings: Five case histories as an overview of a technique

V. Berengo
University of Padova, Padova, Italy

ABSTRACT: The geotechnical design approach for interventions underneath historic sites and monuments is strongly influenced by the invasiveness of the selected technique. Ground improving interventions with expansion resin injections allow for the compacting of the ground and filling of the voids underneath a foundation in a non-invasive way. In this paper several possibilities offered by this technique will be presented, describing five case histories performed all over Europe. In particular for each of these the most peculiar aspects will be highlighted in order to describe each phase of the intervention design. In terms of the design, different approaches can be used, ranging from a simple statistical approach and going as far as a 3D finite elements modelling. Due to the historical relevance of the buildings, in these cases the continuous monitoring of the job sites also plays a leading role together with comparative on-site tests to measure the effectiveness of the injections.

1 GROUND IMPROVING INJECTIONS APPLIED TO HISTORICAL BUILDINGS RESTORING

1.1 *Introduction*

Often the engineering practice leads engineers to work with the restoring of historical buildings affected by cracks which evolve over the building's lifetime.

Crack generation and evolution are in general due to differential settlements. These are caused by building modification, such as an enlargement, or by a change in the load distribution due, for instance, to ground water table fluctuation, or even by a variation in soil properties due to chemical reasons.

Regardless of the reason why settlements have occurred, there are two possible solutions: foundations strengthening or soil improvement by means of a non-invasive technique capable of guaranteeing low impact, especially in the case of historical monuments. Polyuretanic resin injections can be used to this aim, since they improve the foundation soil, causing very low vibrations.

1.2 *Uretek Deep Injections® technology*

Uretek Deep Injections® is already a well-known technology, consisting in local injections into the soil of a high-pressure expansion resin, named Geoplus®, whose properties are widely described in Favaretti et al. 2004, in order to produce a remarkable improvement in the geotechnical properties of the foundation soil.

The operation steps do not require invasive excavations or connection systems to existing and new foundation structures, so it is particularly suitable for historic buildings.

Small quantities of expanding materials are injected with precision underneath the foundation level into the soil volume where the stress state reaches its peak. After injection, resin immediately begins to expand and the high expansion pressure of the injection grout guarantees a proper compaction of the soil. The expansion process first leads to the compaction of the surrounding soil and then, in case of light overstructures, also to a lift.

This expansion process can be theoretically studied as a spherical cavity (or cylindrical, if, along a single treatment axis, injections are closely spaced) expanding in quasi-static conditions. The soil can be modelled as a linear elastic-perfectly plastic material with a non-associated Mohr-Coulomb yield criterion and it is considered initially subjected to an isotropic state of stress.

During the first part of the expansion process, when the internal pressure of the cavity increases, the soil exhibits elastic behavior. After reaching a specific value of the internal pressure plastic deformation starts, similarly to the elastic phase, until it reaches the pressure limit (σ_{lim}). It is assumed that as soon as pressure limit is reached, the resin solidifies (Dei Svaldi et al. 2005).

The analytical model of the expansion process together with the resin expansion law obtained in the laboratory were used to develop a software, Uretek S.I.M.S. 1.0, capable of predicting the

ground improvement index of a soil injected with Geoplus® resin.

Uretek S.I.M.S. 1.0 computerizes the theoretical model: During first phase injections, due to the expansion of the grout, all voids are filled, the ground is compacted and its stiffness increases. In normal consolidated ground conditions, this leads to the rise of horizontal stress to values close to the vertical one in a limited volume around the injection point. When the isotropic stress state is reached, the expansion pressure also develops in a vertical direction, inducing a surface lifting (Schweiger et al. 2004). The isotropic volume growth is clearly a simplification, because the expansion pressure first develops on the lowest stress plane in homogeneous soil conditions.

The quality of previsions provided by the analytical model has been verified in several real cases: The reliability of the theoretical previsions increases with the quality of the geotechnical investigations.

Uretek S.I.M.S. 1.0, however, enables designers to obtain improved ground parameters rapidly and those parameters can later be used in a FEM analysis to perform a stress-strain analysis.

1.3 *The restoring process phases*

The entire design process must include several phases in order to best apply the intervention technique. It is necessary to know the local conditions through preliminary testing: Both the soil profile and its mechanical properties by means of a geotechnical investigation (CPTU tests, MAIW system) and the geometry of the foundation system must be determined. Then the injection process must be modelled with the analytical model described above and/or a numerical analysis in order to understand how to best perform it in the field. During the injections the entire procedure must be monitored by electric receivers lit by a laser emitter and anchored to the building whose foundation is to be worked upon in order to measure vertical displacements. During and after the field intervention, a monitoring system called Easy Crack Monitor® is installed to guarantee an automated control of the relative movement of pairs of check points, which can be the two lips of a crack, and verify that they no longer move significantly. However, soil properties are to be investigated after the field intervention in order to verify the soil improvement in terms of strength: CPTU and pressiometer tests are performed at the end of the injection process to compare results with those performed previously.

In the following, each of these important phases will be described by presenting a specific case history in which the Uretek® technology was applied.

2 PRELIMINARY AND POST-INTERVENTION SURVEYS

2.1 *Palatium Vetus in Alessandria*

In this case history it was necessary to understand the shape of the foundations of the building in order to estimate the local stress induced on the soil, together with the soil properties, in order to plan the restoring intervention.

Palatium Vetus (Figure 1) is in fact the oldest building in Alessandria: It was built in 1170 in the heart of the town and has been refurbished and enlarged so many times that the soil stress state has changed under the foundation system. The final configuration is constituted by only one body with two levels, lying on several types of foundations. To investigate the foundation system a series of drillings were performed. A manual boring machine was used (max energy per bump: 12–14 Joule, frequency: 1200–2800 bumps per minute), making holes of 26 mm diameter (Figure 2). Drillings were performed alongside

Figure 1. Palatium Vetus in Alessandria.

Figure 2. Above: Foundation survey at Palatium Vetus. Below: Survey and intervention map.

the perimetral wall to identify the base level of the foundations and also at increasing distance from the wall to investigate the presence of enlargements or connecting beams among the plinths.

Fourteen different areas around the entire building were investigated (Figure 2): Walls were found to be constituted by bricks and binder with no discontinuities, the foundation base level varies from 0.5 m to 3.2 m depth and a 10–15 cm layer of crushed stones lies under the foundation system.

The load was estimated to increase due to the restoring intervention, up to 50% (the average value is circa 18–20%) so the final soil stress state varies more or less from 0.35 MPa to 1.19 MPa, depending on the foundation type.

A complete geotechnical survey was also performed in order to estimate the bearing capacity of the soil. Two penetrometer tests were carried out together with a borehole with SPT tests and laboratory tests (oedometer and shear tests): Under a superficial replenishment layer, whose thickness varies from 1.5 m to 2.4 m, a 3.0 m thick clayey layer and a 1.0 m silty and sandy layer were detected. Under those low resistance soil layers stiffer ones were found: More than 10.0 m thick of gravelly and sandy layers.

Since the superficial layers had little bearing resistance, soil stabilization was planned by means of the Uretek Deep Injections® technology.

The aim was to increase the mechanical properties of the ground in order to make it able to bear the stress due to the increased load transferred by the foundations. Because of the historical value of the building, the aim was not to interfere with the existing walls, so the Uretek® technology was extremely suitable.

The design was performed by means of Uretek software S.I.M.S. 1.0 described above. For further details the interested reader is referred to Pasquetto et al. (2011). The injections were performed on five different levels from the base level of the foundations until 3.5 m of depth (interaxis distance: 0.6 m) with manual boring machines identical to those used to investigate the foundations, which passed through the final part of the existing foundations themselves, as described in Figure 3. In this way only light vibrations were guaranteed.

To test the improvement of the soil resistance, fourteen comparative penetrometer tests were performed in the treated zones, in accordance with Italian regulation (NTC 2008): Figures 4 shows that mechanical properties increased more than 40% in the critical points, even though the test itself has no more than comparative meaning.

Preliminary survey has thus been found to be very important in order to correctly design the intervention (geometry and soil knowledge) and also to allow the comparison between the initial and final soil characteristics.

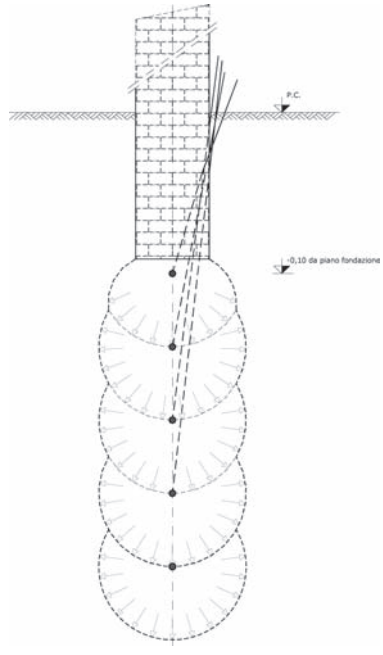

Figure 3. Injection procedure.

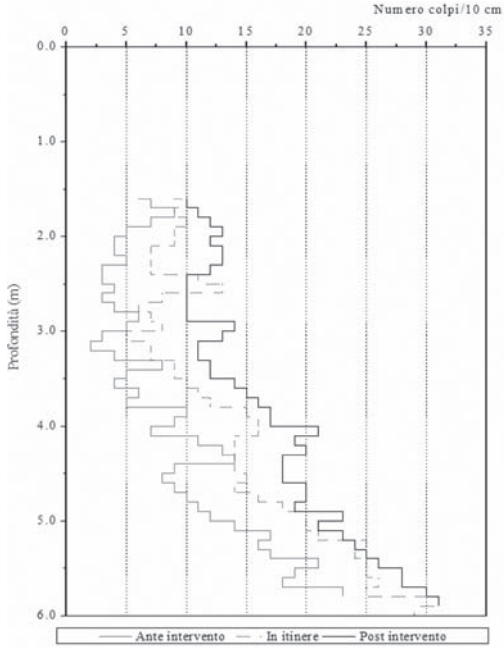

Figure 4. Penetrometer tests before and after intervention at Palatium Vetus.

3 NUMERICAL DESIGN

3.1 *The Città di Castello tower*

In the case of the Città di Castello tower, it clearly appears how helpful a 3D FEM analysis can be in making important job site decisions.

The tower, dated around the thirteenth century, is a slender structure (rectangular shape: 6.10 m × 6.8 m, maximum height: 39.8 m) leaning towards the main square and also towards the contiguous alley, and the way we see it today is the result of several collapses and reconstructions occurred over time. In particular, after the earthquake occurred in March 2007 a separation of 4 cm was detected in the seismic joint between the tower and the Bishop's Palace, due to a differential settlement. This settlement strongly increased the measured leaning of the tower from 72 cm to 78 cm towards the main square.

In order to model the actual configuration of the tower and to have a reliable prediction of the intervention effects a 3D analysis was performed using the commercial software Plaxix 3D Tunnel.

The soil profile and properties were drawn on the basis of four boreholes, ground penetration radar and laboratory tests. Under a superficial inhomogeneous replenishment layer, whose thickness varies from 1.5 m to 5.7 m, a sequence of silty sands and sandy silts layers is found, followed by a bottom layer of clay and clayey silts at depth varying from 10.0 m to 13.0 m. The soil layer parameters are summarized in Table 1 and the OCR is slightly lower than 1.

The tower was modelled in a vertical position in the input data. Afterwards, the construction phases were simulated using intermediate steps until the final configuration was reached (Figure 5).

Table 1. Soil layers properties for the Città di Castello tower FEM model.

	Parameter					
Soil type	γ_{sat} *kN/m*^{3}	E *kPa*	c′ *kPa*	ϕ °	ψ °	Constitutive law
Replenishment (Silty Clay)	19.5	6250	31	23	–	Mohr-Coulomb
Replenishment (Sandy Silt)	20.0	4000	30	28	–1	Mohr-Coulomb
Replenishment (Sand)	18.5	3000	0	32	–	Mohr-Coulomb
Sandy Silt	20.0	8000	18	30	–3	Mohr-Coulomb
Silty Sand	20.0	9000	18	30	–2	Mohr-Coulomb
Clay and Clayey Silt	21.2	13000	10	27	–	Mohr-Coulomb

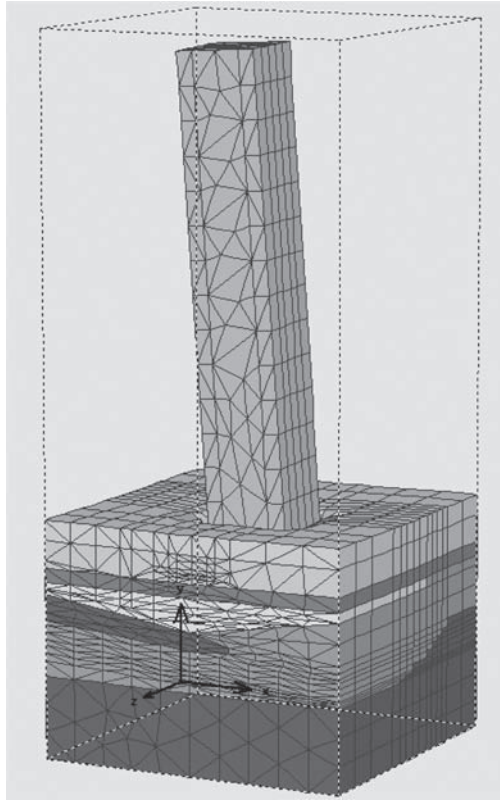

Figure 5. Città di Castello tower mesh for the FEM analysis.

The initial condition analysis pointed out that, apart from the rather complex local stratigraphy characterized by the presence of over-consolidated material lenses within much more deformable soils, the different foundation levels (higher towards the square -x < 0- and towards the alley -z > 0-) determined the tower rotation.

The error between the modelled tilting and the measured one, lower than 4%, was evaluated as acceptable.

In a higher foundation level there is a corresponding thicker layer of deformable soil. This brings about a differential settlement and the rotation of the tower, as confirmed by the leaning direction towards the shallower foundation, which is shown through the FEM analysis (Figure 5).

In correspondence to the interface between foundation and soil the stress state reaches the highest level (700 kPa) underneath the foundation facing the square, exactly where the settlement is the highest, as shown in Figure 6 (above). In particular the existing stresses are equal to the resisting ones, meaning that the soil reached a plastic equilibrium condition (full mobilization of the

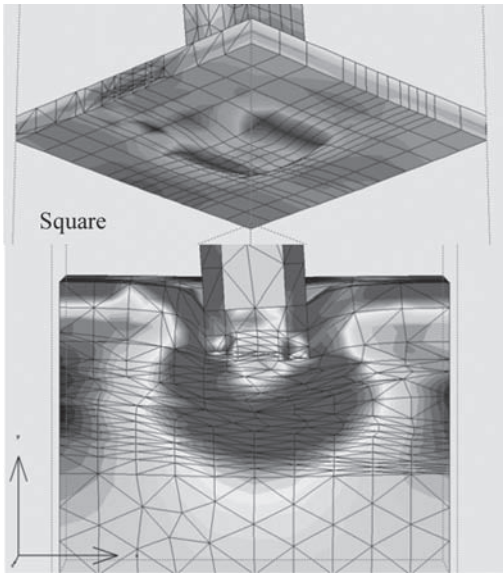

Figure 6. Relative shear stress distribution: 3D view (above), cross-section (below).

bearing capacity). These are the effects of the stress redistribution caused by the tower's eccentricity.

Figure 6 (below) shows a double failure mechanism mobilization: The superficial one, which lays just underneath the foundation level, is a typical punching failure mechanism and it is limited to the first sandy silt soil layer, while the deeper one depends from the stress state transferred to deeper soil layers. The two effects are certainly related: The second one depends on the first one.

The injections were modelled as a volumetric expansion of solid elements by forcing the volumetric strain value of the element according to the volume increase calculated with Uretek S.I.M.S. 1.0. In doing so, an accurate determination of the grout quantities to be injected was possible, given the quick reaction time of the resin preventing the material from flowing away from the injection point. A stress-strain analysis of the tower for every scheduled injection phase was thus performed, simulating the injected volume as an expansion of the soil element located exactly in correspondence of the injection point (x, y and z). The stiffness increase of both the surrounding as well as the treated soil was taken from the Uretek S.I.M.S. 1.0 output as well.

Based on the indications of the FEM analysis, an executive project was arranged, with injections performed as shown in Figure 7. The injection design was changed in real time, depending on the reaction of the tower during the different injection phases and on subsequent FEM analysis results.

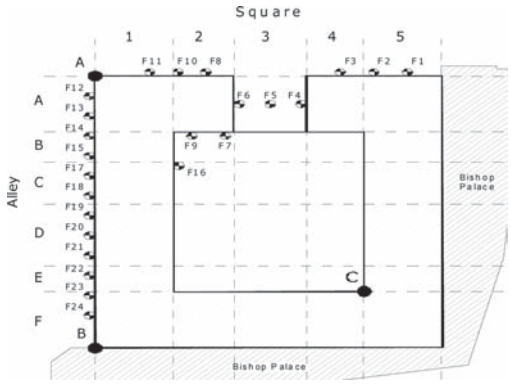

Figure 7. Injections points distribution and monitoring points.

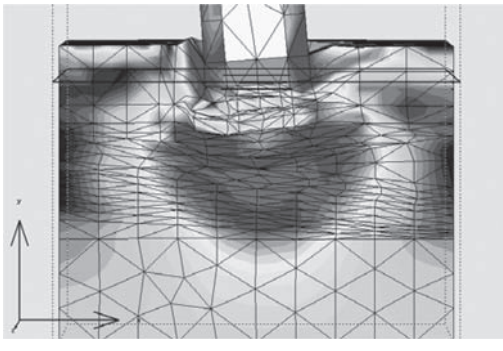

Figure 8. Relative shear stress distribution after injections.

During 14 working days, 2475.5 kg of resin were injected: The amount of injected grout per day was not constant, depending on the real time monitoring data analysis.

Figure 8, which represents FEM analysis results in terms of relative shear stress (meaning the ratio of the existing shear stresses and the resisting ones calculated with a Mohr-Coulomb failure criterion) clearly shows how the injections strongly reduce the stress state within the improved ground volume.

All throughout the work a real time electronic monitoring was operating: Figure 9 shows how slight the differences are between the calculated time/settlement curve and the real settlement measurements after every injection phase, A and B representing the conditions with zero and full expansion of the resin in two points. These results confirm the reliability of a numerical analysis in reproducing the resin injection process.

On the other hand Figure 10 shows how measured settlement rate rapidly decreases with time after injection intervention.

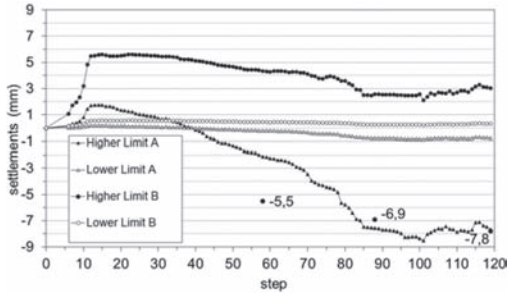

Figure 9. Time-settlement calculated curves and real measurements at Città di Castello tower.

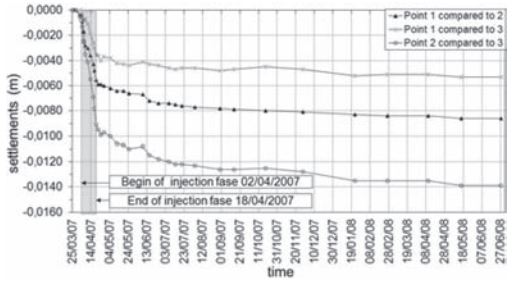

Figure 10. Measured settlements with time in controlled points.

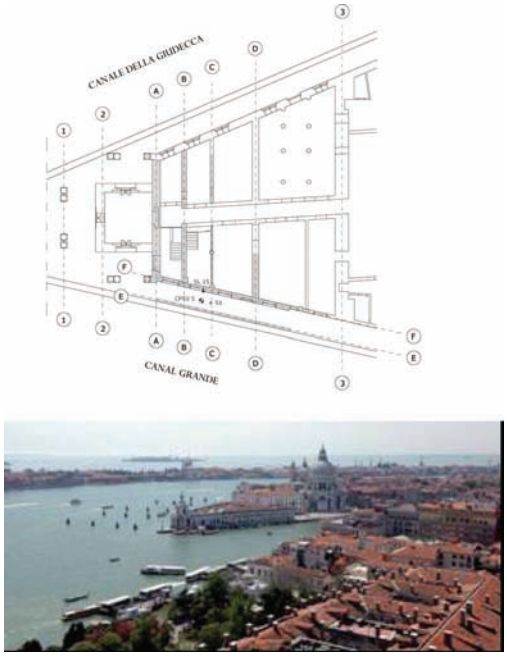

Figure 11. Punta della Dogana view (above), map (below).

4 INTERVENTION PHASES

4.1 *The Venice case at "Punta della Dogana"*

The case of "Punta della Dogana" in Venice demonstrates how sometimes the intervention must be scheduled in phases. This can be due to particular local conditions and sometimes the interventions must be changed during the execution itself.

"Punta della Dogana" is a historical place in Venice where trade occurred.

The trapezium-shaped buildings were built in 1677 on the basis of the design of the architect Giuseppe Benoni (Figure 11).

The main building has a width that varies from 16 m to 75 m and floors lie on ten brick walls, parallel to one another, as described in Figure 11. Foundations are constituted by bricks and binder walls laying on four different substrates: Directly on the soil, on a rigid shelf laid on the ground, on a shelf that lies on wooden piles or on the foundations of an existing tower. The foundation base level varies from 0.69 m to 2.84 m depending on the position.

In May 2003, during the restoring of the "Canal Grande" shore walls (the main channel in Venice) by means of micropiles, settlements of the wall near the "Punta della Dogana" together with settlements of the building itself occurred. These caused old cracks to open again, and new ones to be created. Three mechanisms were responsible for this: Vertical differential settlements, elongation in the direction of the internal walls, and rotation of the facades, especially the one towards the "Canal Grande". At that time the shore walls were already being monitored and the monitoring was continued after the episode, highlighting a settling trend. Assuming the zero corresponding to the measurement of 31.07.2002, the settlement-time curve plotted in Figure 12 shows a sharp increase in terms of settlements between April, the 30th and May, the 15th for all the anchorages, especially SL15 that is in correspondence of the "Canal Grande" and continues settling even the year later whilst the others stop.

The reason was traced to the hydraulic phenomenon of heaving. Along the shore, in fact, the soil profile is made up of a sequence of cohesive layers followed by granular ones: The top of the sandy layer is located at −6.3 m under the mean sea level.

The restoring of the shore walls had required the use of Larssen sheet piling, confining the channel zone in front of the building, and the pumping of water out and then excavating in order to reach the base of the shore wall. The water pressure in the sandy layers, deeper than the sheet piling, was kept undisturbed while the excess pore pressure

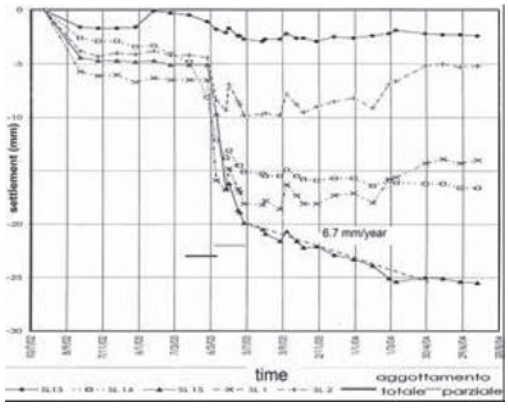

Figure 12. Time-settlement curves of several anchorages.

due to water flow concentrated in clayey layers, thus making the effective stress decrease, the equilibrium fail and the structures collapse.

To restore the building a complex series of interventions were scheduled whose aim was to arrest settlement and, in cases where the settlement had been too significant, to raise the building to its previous level. Since settlements were due to changes in soil stress state, the Uretek Deep Injections® was considered suitable to the purpose. It is in fact flexible enough to change schedule in-progress depending on the field results (foundations drillings, comparative penetrometer tests, continuous monitoring). Further, resin injections can induce swelling quite easily.

Injections were performed in three phases in order to allow excess pore pressure to dissipate. At the same time the disturbance caused by pore pressure increase could be limited by diminishing the grout quantities to be injected and by programming the injection sequence so that the same soil volume would be involved only once in the same moment.

The first phase intervention happened in November 2004. Injections were performed from the foundations base level until −8.5 m under the mean sea level in correspondence with the façade and until −5.0 m on the opposite side. Together with local injections a series of "column injections" were performed alongside the shore wall in order to create a sort of retaining structure for the following injections. The second and the third phases were performed the following year and were less invasive. The detailed description is given in Gabassi et al. (2011).

The structure response was monitored twice a day from the end of the first phase, during the injections phase, and every 15 days between the two phases. What occurred was a temporary rise in

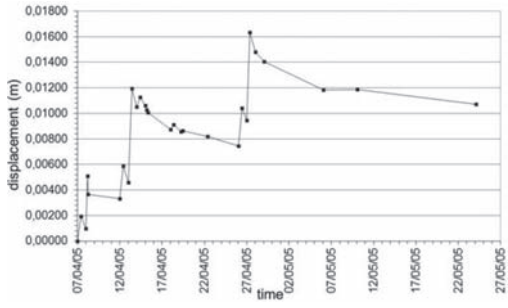

Figure 13. Time-displacement measured curve for "point 17".

the pressured water inside the injection pipes as a consequence of the resin expansion, especially during the first phase. The pore pressure increase and the consequent dissipation caused settlements to occur but in the following phases the phenomenon decreased and this trend inverted, showing also a small settlement recovery.

Figure 13 shows the time-displacement curve of the check point "17", close to the SL15 anchorage, on the "Canal Grande" side: The recovery is evident for each intervention phase.

5 DOUBLE INJECTIONS TECHNOLOGY

5.1 *Chapelle Saint Nicodème in France*

There are cases in which the soil improvement must be accompanied by a wall restoring because the structure is heavily damaged. This was the case of Chapelle Saint Nicodème in France (Figure 14).

It is located in Canton of Baud, in Brittany and its origins date back to the French Renaissance: It was built between 1520 and 1539 by the architect J. Le Layec.

From an architectural point of view the chapel forms a Latin cross: The nave is 31 m long and 7 m wide and belongs to a period of stylistic transition, since the shape is inspired by medieval architectures whilst decorations are closer to the Renaissance repertoire. The main tower reaches a height of 50 m and its rectangular base is 11 m wide and 20 m long.

In 1914 cracks due to problems in the tower foundations were detected. A geotechnical survey carried out in 1926 revealed that the ground was constituted mainly by shale which was loose and sensitive to moisture and this is probably the reason for the instability of the tower. Between 1927 and 1930 low-pressure concrete injections were performed in order to consolidate the subsoil. In 1972, however, an inclination of the chapel towards the south was detected (Figure 15). Moreover, during

Figure 14. Chapelle Saint Nicodème in France.

Figure 15. The Chapelle Saint Nicodème leaning tower.

the latest survey, cracks due to water vapour and to an incorrect water canalisation were also detected.

Because of the critical situation of the building, two types of intervention were planned: Soil improvement and wall restoring, both by means of resin injections. The first type is the previously described Uretek Deep Injections® whilst the latter is called Uretek Walls Restoring® and consists in injections whose aim is to fill voids in joints between wall blocks with binder.

Table 2. Pressiometer values at Chapelle Saint Nicodème before and after intervention.

Before (2003)	After (2009)
17.8 < E < 88.2 MPa	21.8 < E < 136 MPa
1.96 < PI < 4.01 MPa	2.96 < PI < 5.94 MPa

The procedure consists in drilling the damaged wall, inserting injection pipes and injecting the IDRO CP 200 resin, which expands thus filling every cavity in the wall.

Its mechanical properties are quite similar to mortar once solidified: When injected it is liquid, then in 60 seconds it solidifies, expands and reaches its final consistency.

The intervention was performed in two phases: In April and May 2009 and in October 2009. At the beginning and at the end, pressiometer tests were performed to compare soil resistance before and after the intervention and verify the injections performance. Results are given in Table 2 and show a significant improvement in soil properties such as elastic modulus and plastic index.

6 LONG TERM MONITORING

6.1 *A 19th century building in Genève*

The following case shows the importance of continuous monitoring of crack width with time in order to ensure crack stabilization.

The building subject to intervention in Genève (Figure 16) was affected by very long and deep cracks worsening over time. It is a residential complex constituted by nine independent parts, whose origins date back to 1828. It was built on the foundations of the city's old fortification walls. Only one side of the building, however, lays on the foundation walls, while the other side, instead, lays on an old replenishment layer: this is the cause for the cracks.

Visible differential settlements had already occurred at the time of construction, since the side laying directly on the soil started settling immediately; the first measurements go back to 1976 and now the maximum differential settlement between the two sides reaches 20 cm, while the rate of settlement is eight times faster than the initial one. The subsoil was also found to be constituted by several cavities, as detected during geotechnical preliminary surveys (Figure 17).

All this evidence, together with the strict restriction on entering the building's basement, led to the decision of using the Uretek Deep Injections® technology.

The injections were performed at different levels for an extension of 280 m long in order to fill

Figure 16. The building subject to intervention in Genève.

Figure 17. Cavities in Genève subsoil.

the voids and, as it is usual, to improve the soil mechanical properties.

In Figure 18 the settlement trend is plotted over time in correspondence to fixed control points. It is clear that the settlement stabilized after the injection procedure. The injections cause a slight localized settlement due to the procedure itself, but the graph shows that the settlements which were increasing over time prior to the intervention have almost stopped.

After the intervention a monitoring system called Easy Crack Monitor System® was installed in order to check the crack stabilization.

The system allows for the automated and continuous reading of any relative displacement between two lips of a lesion and/or two buildings and/or two structural elements, along two orthogonal directions. It is composed of one or more reading devices in correspondence of the lesions to be monitored and by a central acquisition and transmission of data (Figure 19). The reading device, rigidly connected to the masonry, detects the relative displacement between two stiff portions along two orthogonal directions at regular time intervals.

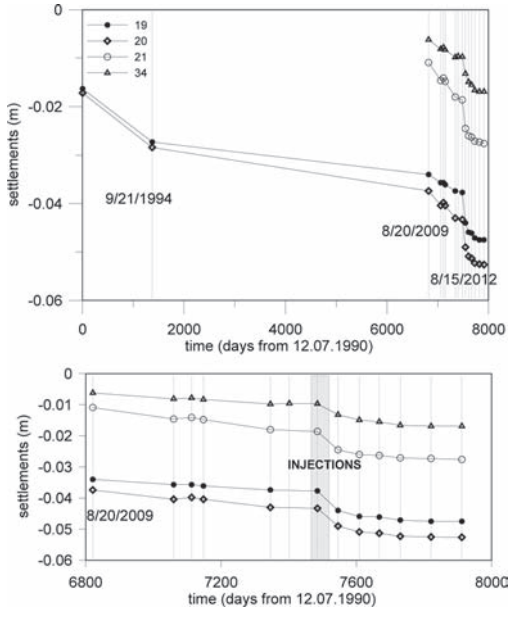

Figure 18. Above: Time-settlement curves of several anchorages. Below: Enlargement of the measurements just before and after intervention.

Figure 19. Easy Crack Monitor System®.

The reading of the movements is made at the same point for both directions, with a precision not greater than 0.5 mm. Each system is also equipped with a temperature sensor. The control unit has the function of collecting data from several reading devices and to transmit them by means of GPRS protocol, at regular intervals, to a server for storage and display.

The monitoring results are shown in Figure 20: The cracks stabilized since no more displacements occur along the X or Y directions, even when the temperature varied. Two goals were thus reached by performing the injections technique.

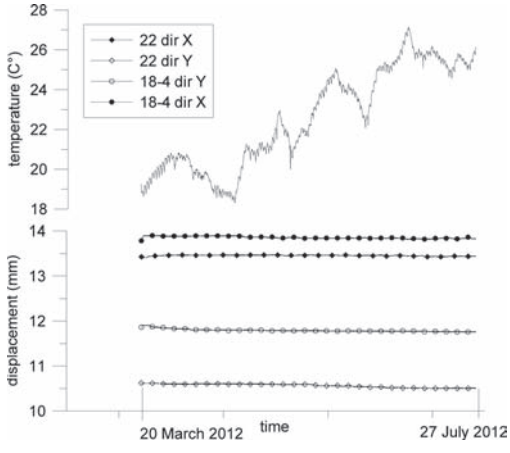

Figure 20. Time-displacement-temperature curves for two cracks (in X and Y directions).

7 CONCLUSIONS

The overall description of five case histories has allowed for the description of the main intervention phases which have to be performed when dealing with the restoring of historic buildings or monuments.Cracks are often due to differential settlements caused by excessive applied loads or by low mechanical soil properties. Ground improving interventions with expansion resin injections, such as the Uretek Deep Injections® technology, allow for the compacting of the ground and filling of the voids underneath a foundation in a non-invasive manner.

Preliminary survey is thus fundamental in order to trace the soil profile and its mechanical properties as well as to know foundation geometry in detail, as described in Palatium Vetus case.

The design must be as accurate as possible, therefore, in particular cases, a FEM analysis must be performed to best model the soil and structure response before on-field intervention. This strategy was applied in the case of the Città di Castello tower.

In the case of the Punta della Dogana building, in Venice, an accurate intervention schedule was planned both in advance as well as during the intervention itself to allow pore pressure to dissipate between one injection phase and the next. If the building is seriously damaged, the walls, too, have to be restored, as described in the case of the Chapelle Saint Nicodème in France. After each intervention a further geotechnical survey must be performed to ensure the effective performance of the injections, as was done in each of the case histories presented.

It is also beneficial to regularly monitor crack width after the intervention in order to verify that they do not move any more, as described in the case of the old building in Genève in which the Easy Crack Monitor System® was used. Accurately performing all these phases ensures the best performance of the restoring intervention, as the case histories presented here have proven.

REFERENCES

Dei Svaldi, A. Favaretti, M. Pasquetto, A. & Vinco, G. 2005. Analytical modelling of the soil improvement by injections of high expansion pressure resin. In 6th International Conference on Ground Improvement Techniques; Congress proceedings, Coimbra, 18–19 July 2005: 577–584.

Favaretti, M. Germanino, G. Pasquetto, A. & Vinco, G. 2004. Interventi di consolidamento dei terreni di fondazione di una torre campanaria con iniezioni di resina ad alta pressione d'espansione. In XXII Convegno Nazionale di Geotecnica; Congress proceedings, Palermo, 22–24 October 2004: 357–364. Bologna: Pàtron.

Gabassi M., Pasquetto A., Vinco G. & Mansueto F., 2010. 3D FEM analysis of soil improving resin injections underneath a mediaeval tower in Italy. Atti 7th European Conference on Numerical Methods in Geotechnical Engineering NUMGE 2010, Trondheim, pp. 827–832.

Gabassi M., Pasquetto A., Vinco G. & Masella A., 2011. Consolidamento del terreno di fondazione del palazzo di Punta della Dogana in Venezia realizzato con iniezioni di resina poliuretanica. In XXIV Convegno Nazionale di Geotecnica; Congress proceedings, Naples, 22–24 June 2011: 457–463. Bologna: Pàtron.

Pasquetto A., Gabassi M., Vinco G. & Massone G., 2011. Adeguamento della capacità portante del terreno di fondazione di "Palatium Vetus" ad Alessandria con iniezioni di resina espandente. In XXIV Convegno Nazionale di Geotecnica; Congress proceedings, Naples, 22–24 June 2011: 525–530. Bologna: Pàtron.

Schweiger, H. F. Kummerer, C. Otterbein, R. & Falk, E. 2004. Numerical modelling of settlement compensation by means of fracture grouting. Soils and foundations 44 (1): 71–86.

Geotechnical Engineering for the Preservation of Monuments and Historic Sites – Bilotta, Flora, Lirer & Viggiani (eds)
© 2013 Taylor & Francis Group, London, ISBN 978-1-138-00055-1

Monitoring of the temperature-moisture regime of rock dwellings in Brhlovce village (Slovakia)

V. Boháč, D. Fidríková & V. Vretenár
Institute of Physics, Slovak Academy of Sciences, Bratislava, Slovakia

T. Durmeková, I. Šimková, V. Greif & J. Vlčko
Faculty of Natural Sciences, Department of Engineering Geology, Comenius University in Bratislava, Bratislava, Slovakia

ABSTRACT: The aim of the paper is to evaluate the weathering and the damage of rock dwellings in Brhlovce village (Slovakia) based on terrain research of the natural rock mass as well as on laboratory research. A new principle of a sensor for monitoring of moisture in the porous materials/volcanic tuffs/ is presented. The sensor principle is based on hot ball method. A hot ball method is used for measuring thermal conductivity. In fact, the thermal conductivity of porous structure is dependent on moisture content in pores e.g. when pores are filled by air/vapour, water or ice. Additionally it is dependent on thermodynamic conditions like temperature gradient and temperature history. Laboratory research of moisture regime was studied using moisture sensor that was finally embedded into rock mass directly. In situ monitoring of the temperature-moisture regime of volcanoclastic rocks where the dwellings were carved out has been running more than one year. The temperature/moisture regime is monitored from October 2011 up to nowadays.

1 INTRODUCTION

1.1 *Geology of rock dwellings*

One part of the Brhlovce village in Levice district has been declared as reservation of folk architecture. "Rock dwelling in Brhlovce" and was included in the national list of cultural heritage objects. At present, many objects are abandoned derelict and neglected. The owners are using them as storeroom, summer kitchen, chambers, cellar, shed, pigsty, garage, etc. However, they are rarely preserved folk buildings of this kind in Slovakia, so it is necessary to strive for their maintenance and conservation.

The historical and cultural value of the rocky dwellings lies in the fact that they preserve memories of a way of life and living in the past. This kind of settlement documents the symbiosis of human dwellings with nature.

The rock dwelling museum was open in 1992. In 1994, the Tekov Museum in Levice was awarded with the European Union Prize for Cultural Heritage/Europa Nostra Awards as the first organization on the land of the Slovak Republic for the exposure of Rock dwelling in Brhlovce.

Locality surroundings are created by Neogene andesite volcanites (baden and sarmat). Rock dwellings are cut into pyroclastic rocks (volcanic tuffs) and redeposited tuffite sediments—sediments of peripheral parts of Štiavnica stratovolcano. Age of these neovolcanic formation products is dated about 15 milion years (Brestenská et al. 1982). All volcanoclastic complexes of strata are very heterogeneous from grain size aspect of view. The tuff in Brhlovce is lithologically described as the ash andesite tuff with variable proportion of volcanic glass matrix and crystalline sandy or fine grains. Sporadic rests of plants and wood were identified in tuffs. In studied locality volcanic sedimentary sequences is in horizontal positions.

The collapses of the rock marquis on two dwellings in a museum neighbourhood randomly happened in March 2011 and in November 2012 (Figure 1a). A large block of rocks crashed down. The reason was the simultaneous impact of water influence as well as impact of vegetation in rock discontinuities and cracks. The goal of monitoring is to prevent similar events.

Moisture in the rock walls has destructive impact that is caused by cycles of drying—wetting and freezing—thawing processes. The moisture regime is monitored by a new moisture sensor in connection with RTM electronic unit in order to understand the weathering processes of rock dwellings. A simple electronic device RTM is constructed that serve for long time monitoring of moisture in real conditions. The sensor has been placed in the wall of the rock

Figure 1a. Collapse of the rock marquis appeared over the dwellings in November 2012. The fissure in between the rock marquis and block was filled with a root that looks like a map on picture. The vegetation roots caused of marquise block separation finally.

dwellings in Brhlovce village. Moisture and temperature changes in rock mass are correlated with the meteorological data (monitoring of amount of rainfall and air temperature). In order to find out the real causes of human dwellings damage in Brhlovce village a multi-factorial assessment using geological and geotechnical parameters of rock mass in which the dwellings are cut, together with online moisture regime monitoring were evaluated. The causes of deterioration are described and commented.

1.2 *Influence of humidity*

The measurement of humidity content is a preliminary condition to investigate temperature—moisture impact on buildings. Usually the moisture and temperature depth profiles are carried out in different spots in masonry bulk in order to determine the change of moisture profile. In Brhlovce dwellings case the wall is curved out of natural tuff stone, thus the moisture and temperature were monitored directly 10 cm under the free surface to find out the changes on monitored parameters during year seasons. This paper describes a method for the in-situ monitoring of moisture in tuff. Measurements were made by moisture probe using "Hot-ball" thermal conductivity probes, which were inserted into porous rock cylinders. The principle of Hot-ball probe is based on Hot-ball method for measuring the thermal conductivity (λ, $Wm^{-1}K^{-1}$).

The moisture content of porous samples is investigated using Hot-ball method, where the measured values of thermal conductivity increase with increasing of water content in pores (Kubičár et al., 2010).

2 PHYSICAL BACKGROUND

2.1 *Relation of structure and thermophysical properties*

Thermophysical parameters (e.g. thermal diffusivity, specific heat and thermal conductivity) reflect thermodynamical state of the material structure. Various physical and chemical processes influence the thermodynamic state of material. The change of structure cause the change of thermodynamic state what is reflected in measured thermophysical parameters. In our case different climate influences are responsible for further development of structure change, degradation and finally deterioration of stone as a block. Involved particular processes invoked by temperature and moisture changes are responsible for the structure changes with the consideration of the atomic structure arrangement, arrangement of crystalline components and consideration on material defects that are created in time. By the monitoring of these properties in time we are able to follow the progress of deterioration.

Finally by measuring the change of thermal transport properties of material e.g. thermal diffusivity and thermal conductivity as well as specific heat we should conclude on structure state change. Method of the measuring and monitoring of thermophysical properties should be promoted as a measure of the quality, stability and durability of material in regarding to industrial use in civil construction on one side and the degradation or deterioration of stones on the other side. In principle the method is applicable in the investigation of degradation of any kind of materials. Process of material deterioration of stones or their state and quality comparing its basic or initial state should be monitored by continuous measurements (monitoring) of thermophysical properties too.

The sensor constructed of Hot-ball probe inserted into cylinder of porous rock can be used for the in situ monitoring of temperature—moisture regime and thus predict the material degradation in time. Analysis is based on comparison with known laboratory tests and in-situ measurements.

Measured thermal conductivity of porous tuff depends on quality of the material and the moisture content in pores.

2.2 *Principle of Hot-ball method*

Several experimental methods were developed for investigation of the heat transport properties of materials in stationary and transient (dynamic) regime (Maglić 1992, Kubičár et al. 2010, Kubičár & Boháč 1999, Krempaský 1969). The stationary methods usually operates with gradient temperature over the thickness of specimen and thus it takes reasonable time to get stable or stationary state that

increase probability of redistribution of moisture in pores. This causes moisture redistribution in material bulk and thus it is out of original moisture condition and material state is changed. In the case of transient methods we use small temperature disturbance and measuring temperature response to this disturbance. This require shorter measurement time and thus causes no or minimal redistribution of moisture, so the original state is preserved.

For the in-situ measurements of moisture content in tuff massive we used small apparatus based on the transient hot-ball method (see Figure 1b). Initially, during the measurement the temperature of specimen is stabilized, and then thermal equilibrium is disturbed by applying a step-wise heat pulse that generates heat flow.

Model of the hot ball method assumes a constant heat flux q from the empty sphere of radius r_b into the infinitive medium that starts to be generated for times $t > 0$ (Figure 2). Then the temperature

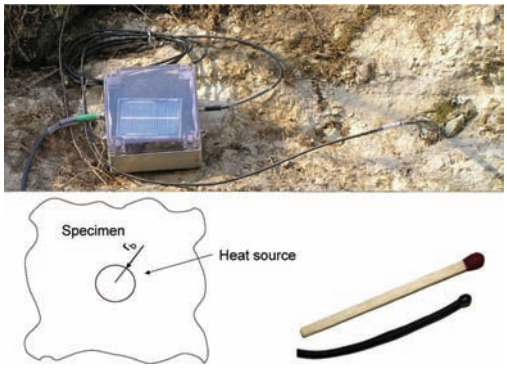

Figure 1b. RTM-solar version of electronic instrument (processor, A/D converter and memory for data storage) in connection with the hot ball arranged as moisture probe (up), model of the hot ball (down left) and probe real size picture (down right).

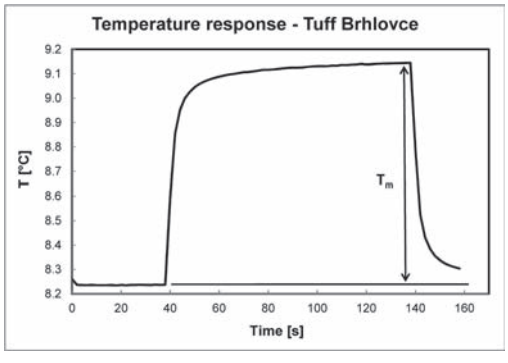

Figure 2. Temperature response measured for tuff. Measurement takes 160 s (100 s heating).

distribution within the medium is characterized by (Carslaw 1986).

$$T(r_b, t) = \frac{q}{4\pi\lambda {r_b}^2} \left\{ \sqrt{\frac{at}{\pi}} \left(1 - e^{\frac{-{r_b}^2}{\kappa t}} \right) + r_b \cdot erfc\left(\frac{r_b}{\sqrt{\kappa t}} \right) \right\} \quad (1)$$

where $erfc(x)$ isthe error function defined by $erfc(x) = \frac{2}{\pi}\int_0^x \exp(-\varsigma^2) d\varsigma$ and λ is thermal conductivity, and κ is thermal diffusivity of the surrounding medium, respectively. The long time approximation solution of function (1) was derived as the working relation of the measuring method:

$$\lambda = \frac{q}{4\pi r_b T_m (t \to \infty)} \quad (2)$$

where T_m is stabilized value of the temperature response reached in the long time limit at the surface of the empty sphere of hot ball having the radius r_b. During stabilization time the heat produced by the ball penetrates in a material volume.

The temperature response to the heat is recorded. The heat penetration depths can rich the distance less than 20 mm in a surrounding. Example of measured temperature response is shown in Figure 2 along with the maximum temperature change used to calculate the value of q/T_m and thus the thermal conductivity or moisture content according a type of calibration.

The measuring procedure consists of the measurement of initially stabilized temperature (base line), switching on the heating pulse and simultaneously scanning the temperature response. When the measured temperature is stabilized, the heating is interrupted and the temperature stabilization follows. When the temperature in the sample is stabilized, the next measurement should start again.

3 EXPERIMENT

Porous materials—rocks situated in natural conditions are exposed to the sun radiation, precipitation, evaporation, freezing and thawing phenomena. The mentioned processes are caused by the water phases found in pores (gas, liquid, solid). Then the resulting thermal conductivity of a porous material is a function of the content of pores.

3.1 *Test samples, properties of studied rocks*

For the study there were selected the cores from drilling of holes for placing the moisture sensors.

The cylinders carved in tuff from Brhlovce rock dwellings having diameter 32 mm were drilled out in a middle and hot ball probe having 2.5 mm in diameter was inserted into a centre of such a hole in rock cylinder and cables were supported by cage made of nickel wires (Figure 3).

The reason for the choice of the lithological rock types was the existence or the preparation of monitoring procedure on the temperature—moisture regime, and related laboratory research as well.

Volcanoclastic tuffs from Brhlovce belong to complex of andesite neovolcanism. In terms of descriptive characteristics of the material the colour is light grey, the grain size is ranging from 0.063 to 2.0 mm, and has the porous structure with cryptopcrystallic matrix. Physical properties of tuff from Brhlovce locations are the following: specific gravity-2.569 g.cm^{-3}, volume density-1.500 g.cm^{-3}, porosity-31.8%, water absorption-16.4% and uniaxial compression strength-17 MPa.

3.2 *Calibration procedures*

The research was focused on the study of moisture regime of tuff stone with hot ball sensor. The hot ball probe itself is calibrated in liquid media having different but known value of thermal diffusivity, in this case the water and glycerol, so one can calculate thermal conductivity from measured values of q/T_m.

Series of hand-made Hot-ball sensors were tested for reliability and calibrated in bath liquids of water and glycerol to have two calibration points for thermal conductivities and corresponding values of measured ration q/T_m in a range of thermal conductivity values that will be measured by probe. This procedure shows also the sensitivity of the probe to thermal conductivity changes.

Such a probe is inserted in a core from drilling of holes (usually carved in a form of cylinder of porous tuff stone) and moisture sensor is ready (Figure 3). It is important to use the same tuff stone drilled out from massive to have the same thermophysical properties and the same porosity as the surroundings in hole where the moisture sensor will be arranged.

Thus the next type of calibration has to be done for the use of the probe as a moisture sensor. The measured value of heat flux and temperature maximum q/T_m inside the moisture sensor represents thermal conductivity that is changing in dependency of moisture content (Figure 4). The probe sensitivity should be high enough to register the moisture content change during moisturizing process in between dry and moisture saturated state (from 0 up to 100% of moisture content). This change is measured as the difference of q/T_m. The difference of q/T_m in between maximum and minimum values is the sensitivity and in the case of this probe it was 0.93 WK^{-1}. This probe was calibrated just at room temperatures at 23 °C. This calibration serve for calculation of thermal conductivity from temperature response calculated by fitting procedure or simply by using polynomial approximation obtained from calibration constants.

After saturation by water it was inserted in the tuff massif at Brhlovce and in-situ monitoring started in October 31st 2011.

For the next future, monitoring in tuff massive in depths at 30 and 50 cm the new series of 10 probes were tested for the sensitivity. Two probes were chosen having similar sensitivity in a possible range of thermal conductivities available for measurement of tuff body in dry and moisture saturated state. The thermal conductivity value for tuff from Brhlovce is in a range of the thermal conductivity values for glycerol and water and thus they were used for Hot-Ball probe calibration. After that the chosen probes were inserted in tuff cylinders made of cores from drilling. Such moisture sensors

Figure 3. Moisture sensor with wire connections to RTM solar before inserting into rock massif.

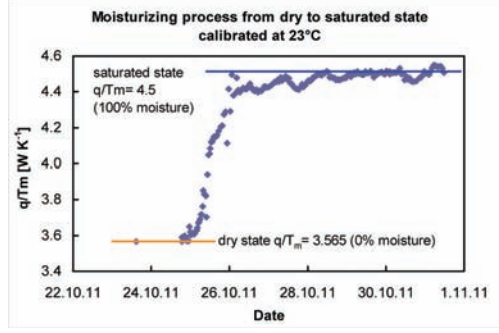

Figure 4. Calibration of probe made of tuff stone in dry and moisture saturated state. The difference of q/T_m represents 100% humidity scale in between dry and fully saturated content of pores by water.

were calibrated in dependence of temperature in both—the dry and moisture saturated regime.

The new probes have the sensitivity 1.4 WK^{-1} of q/T_m calculated from the difference of q/T_m values for dry and saturated state at 23 °C. Sensitivity of new probe is higher than the sensitivity of probe already installed for in-situ monitoring (0.93 WK^{-1}).

For different moisture content a linear dependency is valid, so one can recalculate measured values of q/T_m to the thermal conductivity or directly to moisture content from this calibration. The dry-moisture calibration was performed in laboratory conditions for the range of temperatures from –20 up to 22 °C. The calibrated temperature dependency of the thermal conductivity (or simply q/T_m) is negative in a given temperature range (Figure 5).

3.3 *Calibration results*

Humidity probes (rock bodies with hot ball probe sensor) were exposed to temperatures from –20 °C up to +22 °C in the climate chamber KD-20-T4.1. Measurements of temperature changes were performed every hour inside rock bodies to keep enough time for temperature stabilization. Temperature in the climate chamber was changed in steps of 5 °C and always lasts for 8 hours. An experiment was conducted on cylindrical test samples (moisture sensors) of length 32 mm and diameter 20 mm with built-in hot-ball sensor. Overall, the samples were calibrated in two freezing—heating cycles.

The first calibration was carried out on moisture probes dried at 105 °C till the constant weight. Constant weight was below maintenance of using silica gel in re-closable bags.

The second calibration was done for water-saturated condition when stone cylinder was packed using Parafilm. Drying process and the saturation of the samples by water was carried out according to the applicable technical standard (EN 13755). Subsequently, the experimental results were statistically processed. Result of the calibration experiment is shown in Figure 5. The figure represent the calibrated values of q/T_m that corresponds to thermal conductivity change in dependency of temperature for the materials studied in dry and moisture saturated conditions during freezing-thawing cycle. The temperature dependency of measured mean values of thermal conductivity of rock in dry as well in water saturated state is linear (Ekkertová et al., 2012).

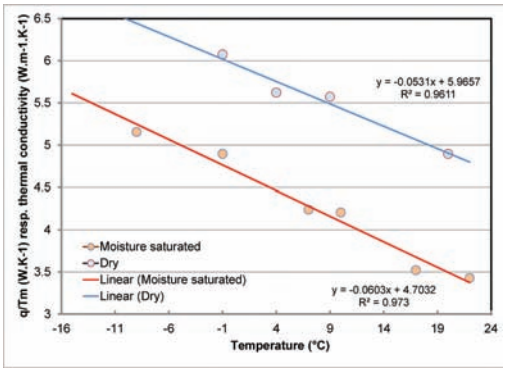

Figure 5. Temperature dependency of q/T_m measured for tuff in dry and water saturated conditions. Data were statistically averaged for a given temperature (Ekkertová et al., 2012).

The values of thermal conductivity λ in the case of water saturated probes are much higher than the dried one (see Figure 5). The high difference in the value of the q/T_m between dry and reached water-saturated state of tuff also proves its high water absorption. Based on the linear trend line equations in Figure 5 there were calculated mean values of q/T_m, e.g. the moisture content for different temperatures in the range studied. According to the difference of thermal conductivity in dry and water saturated conditions at different temperatures it was confirmed the relationship between water absorption and increase of thermal conductivity.

3.4 *In situ measurements and comparison with data from calibration of two moisture sensors having different sensitivity*

The first moisture probe with calibration in Figure 4 was inserted into a hole drilled in massive rock at locality of museum of rock dwellings in Brhlovce. The insertion depth of a moisture sensor is 10 cm. The monitoring is running since the end of October 2011 up to nowadays. The situation on locality is on Figure 6 with holes of for probe at 10 and 30 cm of depth. At the beginning the measurement started from dry state, after than the moisture probe was immersed and after saturation the sensor was placed into a massif in moisture saturated state. As the hole was drilled out under water driller system, high content of water was build up into a massif during a sensor installation. The values of thermal conductivity λ in the case of water saturated probes are much higher than the dried one (see Figure 4 and 5). The high difference in the value of the q/T_m between dry and reached water-saturated state of tuff also proves its high water absorption.

There are some gaps between the data in time that are in plot on Figure 7 as the data were downloaded manually approximately each month but not regularly and thus some breaks exists.

Nevertheless the general picture on behaviour of system with the change of temperature and moisture is evident. The data were collected along one year

Figure 6. Locality of museum. Arrows on upper and bottom part are marking position of measurement apparatus—RTM-solar device as well as meteorological station for registration of precipitation on upper part left. The detail of measurement apparatus with prepared holes is in bottom part.

and the plot represents their seasonal variation. Figure 7 show the data collected in period of one year.

The high difference in the value of the q/T_m between dry and reached water-saturated state of tuff also proves its high water absorption.

The values of q/T_m in Fig. 7. were re-plotted in dependency of temperature in Figure 8. Probe was calibrated at 23 °C and that is why values are different because of their temperature dependency. The temperature in a time of probe installation has drop down to 15 °C, and later to 0 °C, so the values of q/T_m increased because of negative temperature dependency. At 0 °C this value increased up to 5.2 WK^{-1}. The water was not evaporated for relatively long time and thus we can still attribute it to nearly 100% of moisture content at these temperatures.

In a time with monitoring of moisture changes the drying process was set up very slow and the lower values were measured in summer period when the climate in August was very dry with practically no rains and surface temperatures well above 30 °C. At the temperature 23 °C we can compare the change of monitored results with the data on calibration scale in Figure 4. At this temperature the value 3.74 WK^{-1} of q/T_m was the lowest value and correspond to 30% of humidity and the highest one was 4.2 WK^{-1} of q/T_m that corresponds to moisture content of about 70%.

Finally the monitored data from Figure 8 were compared with the new calibrated probes in

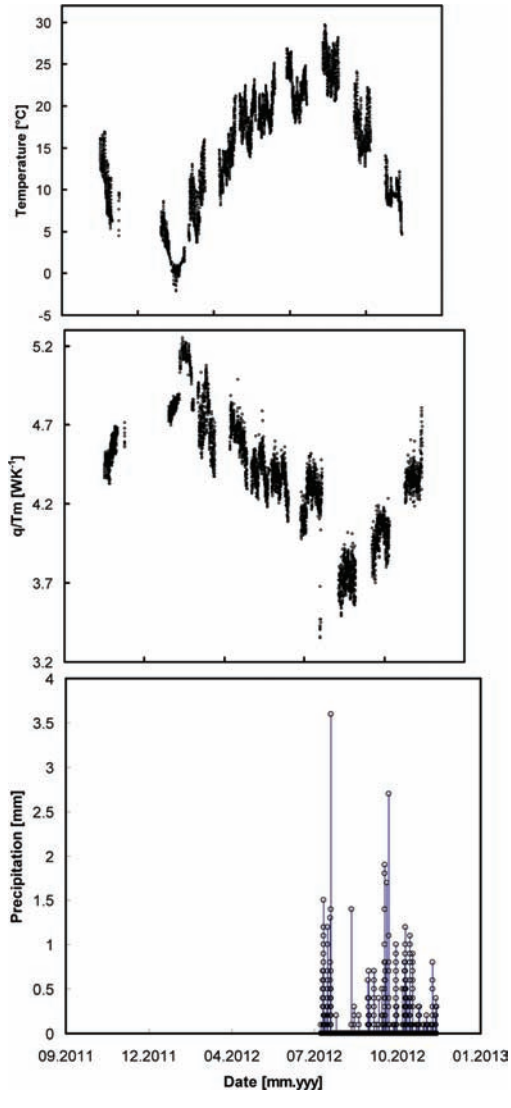

Figure 7. Data collected in time period of one year from locality Brhlovce. Upper part show temperature scattering during day-night cycles and corresponding values of q/T_m (moisture) in the middle and corresponding precipitation in the bottom. The instrument for measuring rainfall and precipitation was installed in a summer time.

Figure 9. The only problem for direct comparison is a different probe sensitivity that in the case of new ones is reasonably higher and causes a difference in between the minimal and maximum values of moisture. Data in dry and moisture state have different amplitudes for old and new probes that results from different sensitivity of moisture probes (1.4 and 0.94 WK^{-1} compared at 23 °C).

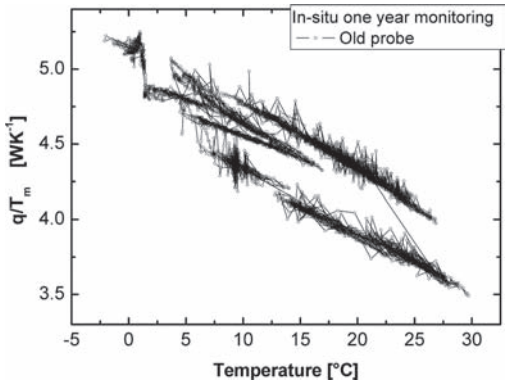

Figure 8. Data from figure 7 re-plotted in dependency of temperature collected in time period of one year from locality Brhlovce. Upper part show temperature scattering during day-night cycles and corresponding values of q/T_m (moisture) in bottom.

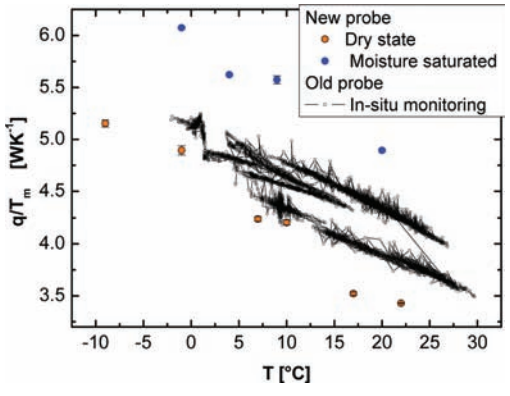

Figure 9. Comparison of scale factors of old and new probes due to different probe sensitivity. Data collected during monitoring in 10 cm of depth in massif are compared with new probes calibrated in the temperature range usual for the Brhlovce locality.

The data monitored on locality collected during one year show at least three different regions of moisture content dependent on temperature changes. The first one was recorded during period when the sensor has been installed and satisfies to highest moisture content. The slightly lower values were collected in the later spring period and show that the system was initially not dried for a long period. The only data that correspond to summer time when massif was dried enough because of high temperatures. The volume inside massif was dried well at the depth of probe at 10 cm. This corresponds to lowest values of q/T_m (moisture) in temperature dependence graph on Figure 8.

4 CONCLUSIONS

Paper presents data on moisture change in dependency of temperature. The q/T_m parameter that corresponds to change of moisture content in humidity probes was measured for calibration purposes in climatic chamber as well as in situ during monitoring of massif at locality in Brhlovce. For all of specimens or moisture sensors the dependency on humidity content variation with q/T_m parameter was found in dependency on temperature variations. Based on observed physical properties such as porosity, water absorption and thermal conductivity of studied materials; it can be assumed relationship between water absorption and increases of thermal conductivity. The experiment was carried out for the needs of correlations between laboratory and field research. This experiment will be helpful in monitoring the moisture in field research, because values of thermal conductivity are defined in extreme dry and wet conditions. On the basis of the experiment we could better eliminate linear increase in thermal conductivity due to the decrease of temperature and thus determine the actual moisture in rock massif. Thus the newly calibrated moisture probes will be inserted into a massif and monitoring of moisture content in next period. In this way we would be able get more accurate data and better possibility for calculation of moisture content from measured values of q/T_m.

ACKNOWLEDGEMENTS

This work was supported by the Slovak Research and Development Agency under the contract No. APVV-0641-10, Study of rocks properties and investigation of structural and textural characteristic in correlation with thermophysical and physico-mechanical properties.

REFERENCES

Brestenská E. et al. 1982. Geologická mapa a vysvetlivky 1:25 000 list Levice a Brhlovce. Bratislava: ŠGÚDŠ. p. 103.

Carslaw, H.S. & Jaeger, J.C. 1986. Conduction of heat in solids, Oxford, Clarendon Press, Second edition, p. 348.

Ekkertová, P., Šimková, I., Brček, M., Durmeková, T. & Boháč, V. 2012. Influences of temperature change and moisture content on the thermal conductivity of rocks. *Thermophysics 2012—Conference Proceedings, 17th International Meeting of Thermophysical Society, 31st October to 2th November 2012, Podkylava, Slovak Republic, org. Institute of Physics, Slovak Academy of Science in Bratislava, Printed by: Brno University of Technology, Faculty of Chemistry*, ISBN: 978-80-214-4599-4, p. 33–40.

EN 13755: 2008. Natural stone test methods. Determination of water absorption at atmospheric pressure.

Kubičár, Ľ. & Boháč, V. 1999. Review of several dynamic methods of measuring thermophysical parameters. In: Gaal, P.S.—Apostolescu, D.E. (eds.): *Proc. 24th Int. Thermal Cond./12 Int. Thermal Expansion Symp., Technomic Pub. Co., Pittsburgh, Pennsylvania*, p. 135–149.

Kubičár, Ľ., Vretenár, V., Štofanik & V. Boháč, V. 2010. Hot-Ball Method for Measuring Thermal Conductivity, International Journal of Thermophysics, 31, 10, p. 1904–1918.

Krempaský J. 1969. The measurements of the thermophysical Properties, SAV, Bratislava.

Maglić, K.D., Cezairliyan, A. & Peletsky, V.E. (eds.) 1992. Compendium of thermophysical property measurement methods. Volume 2: Recommended measurement techniques and practices, Plenum Press, New York, p. 643.

Geotechnical Engineering for the Preservation of Monuments and Historic Sites – Bilotta, Flora, Lirer & Viggiani (eds)
© 2013 Taylor & Francis Group, London, ISBN 978-1-138-00055-1

Restoration projects and remedial works in the historical island of Ventotene

N. Bosco
Civil Engineer, Ventotene (LT), Italy

P. Croce
DICeM, University of Cassino and Southern Lazio, Italy

B. Palma
Idrogeo s.r.l., Vico Equense (NA), Italy

D. Pingitore
CMG Testing. S.r.l., Roma, Italy

M. Ramondini
DICEA, University of Naples Federico II, Italy

ABSTRACT: Ventotene is a very small island in the Mediterranean sea and yet a very remarkable natural and historic site. In fact the peculiar volcanic nature of the island and the ruins of the Roman Empire are joined together as a single and unique jewel, which attracts enthusiastic visitors from all over the world. However, the island is subjected to the continuous dismantling action of the natural agents, which cause an accelerated sequence of erosive phenomena and landslides. This peculiar process, which is progressively reducing the dimension of the island, is undermining the stability of monuments and ruins and has recently determined several collapses including some casualties. The paper examines the case of Ventotene by considering several interconnected topics: The geological nature of the island, the characteristics of its monuments and ruins, the geotechnical properties of the volcanic deposits, the erosive process, the typical landslides mechanisms. Particular attention is given to the search for equilibrated criteria and methods for the reduction of natural hazard, as well as for the protection of the monuments and landscape. The restoration project of the ancient Roman harbour is finally presented in some detail.

1 INTRODUCTION

Ventotene is a small island rising in the Mediterranean sea, at the distance of approximately 50 km from the Italian peninsula, with a resident population of only about 600 inhabitants. The island is of volcanic origin and the present landscape is the result of the changes occurred over time, resulting from the action of the exogenous natural factors (sea waves, wind, rain) combined with the human activity which dates back to the first century b.C.

Nowadays the surface of the island is 1.24 km^2 and its maximum dimensions are: length 2.7 km, width 0.85 km, height = 135 m above sea level.

The land of the island is relatively flat but its borders are made of very steep cliffs with the exception of the north-eastern corner, which has provided the access to the island throughout its history (Fig. 1).

During the Roman Empire, Ventotene was elected to be the residence of the exiled members of the Emperor's family, such as Augustus' daughter Julia who gave the name to the beautiful Roman Palace, whose ruins stand on the north-eastern cape of the island.

The Romans constructed a wide system of cisterns and aqueducts all over the island, in order to collect rainwater and bring it to the royal palace. They also built a remarkable harbour by excavating approximately 60,000 m^3 of tuff, down to the depth of 3 m below the sea level. The harbour was equipped with a towing basin and a number of warehouses, dug into the tuff, which are still regularly used today for various commercial activities (little shops, storage facilities, etc.).

This ancient Roman harbour is still regularly used nowadays for hosting yachting and fishing boats, even if a larger port was recently constructed

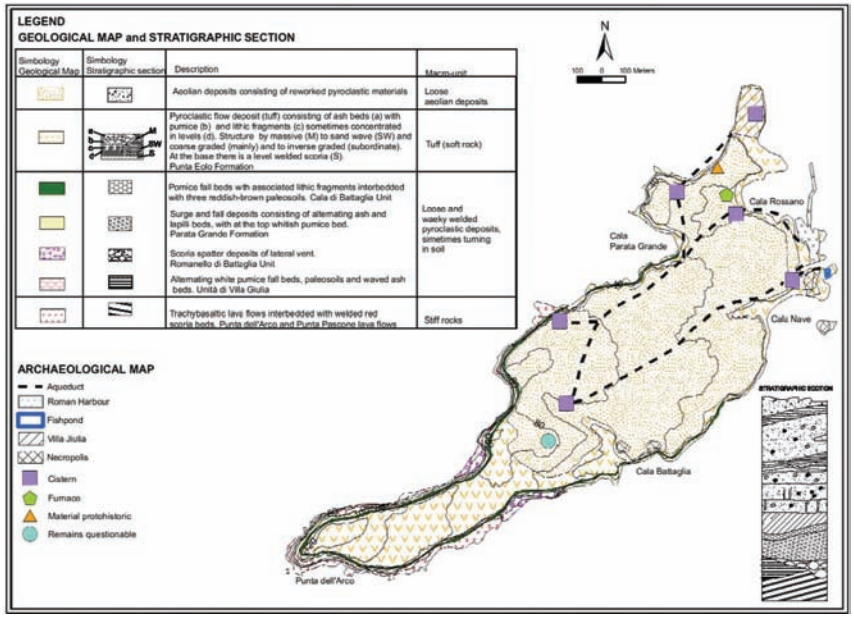

Figure 1. Geological and archeological map of Ventotene (Bellucci et al., 1999 mod).

to provide access for the large ferries connecting Ventotene to the mainland.

The Romans also excavated a large fishpond close to the port, in order to provide fresh fish to the Emperor's family.

The fishpond, located south of the entrance to the harbour was also dug into the tuff. It is composed of several pools, hydraulically interconnected and communicating with the open sea to allow a continuous supply of water to the living fauna.

After the end of the Roman Empire, Ventotene was abandoned and used only occasionally, mainly by monks, till the 18th century when the Bourbons, kings of Naples, decided to repopulate the island. The Bourbons constructed a series of buildings and roads incorporating the ancient Roman harbour, thus giving rise to the historical centre of Ventotene as it is today.

Nowadays Ventotene is a well-known touristic resort thanks to the natural beauty of the island and the transparency of the surrounding sea, combined with its unique historical and architectural features. However, the island is subjected to the continuous dismantling action of the natural agents, which cause an accelerated sequence of erosive phenomena and landslides along the coast. This peculiar process, which is progressively reducing the extension of the island, is undermining the stability of its monuments and ruins and has recently determined several collapses including some casualties.

In recent years, the writers have been engaged in the search for equilibrated criteria and methods for the reduction of the natural hazard induced by landslides as well as for the protection of the monuments and landscape. They have also contributed to the design and execution of some restoration projects. The most important project carried out so far regards the restoration of the Roman harbour.

The paper examines the case of Ventotene by considering several interconnected topics: The geological nature of the island, the location and characteristics of its monuments and ruins, the geotechnical properties of the volcanic deposits, the erosive process, the typical landslides mechanisms. Particular attention is then given to the search for equilibrated criteria and methods for the reduction of natural hazard as well as for the protection of the monuments and landscape. The restoration project of the ancient Roman harbour is finally presented in some detail.

2 EROSIVE PHENOMENA AND LANDSLIDES

The island of Ventotene is the visible part of an ancient stratovolcano (or composit volcano) resulting from effusive and explosive eruptions that occurred during the Quaternary, from 0.8 to 0.33 My. (Perrotta et al., 1996).

From the morphological point of view the island is characterized by the presence of a plateau slightly dipping towards NE, bordered by

cliffs with height ranging between 130 m (southern sector) and 10 m (northern sector). The plateau surface is grooved by flat-bottomed valleys, originated along some of the main discontinuities of the underlying tuff.

The geological formations of the island can be grouped in four main lithological units (Fig. 1):

i. Loose Aeolian Deposits made by reworked pyroclastic materials.
ii. Tuff (soft rocks) composed by layers of various lithological characteristics (*Punta Eolo* Formation).
iii. Loose and weakly welded pyroclastic deposits, consisting in a complex sequence of pumice, scoria, ash, lithic and paleosoils (*Parata Grande* Formation, *Villa Giulia* Unit, *Romanello di Battaglia* Unit and *Cala Battaglia* Unit).
iv. Lava (stiff and very stiff rocks) made of trachybasaltic lava flows interbedded with welded red scoria layers (*Punta dell'Arco* and *Punta Pascone* lava flows).

Historical studies and direct observations have pointed out the widespread occurrence of landslides along the cliffs that border the entire island of Ventotene. Such landslides, which take place with remarkable frequency, are progressively reducing the extension of the island. In fact, observations and measurements carried out in the last century have pointed out that such landslides result mainly from the natural evolution of the cliffs bordering the island. This natural process is triggered by the following main exogenous factors:

– the sea waves action, resulting in the progressive excavation of the cliffs foot, leading to the collapse of the overhanging rocks and/or soils along weak sub-vertical planes;
– the wind abrasion which determines the selective erosion of the softer rocks and soils layers, resulting in the gradual formation of protruding sub-horizontal slabs of stiffer rocks, which may then collapse by flexural or block toppling;
– the infiltration of rain water, causing the progressive alteration and weakening of rocks and enlargement of genetic fractures;
– thermoclastism and haloclastism phenomena that accelerate the state of fracturing of the rocks.

The result of the previously mentioned phenomena, however, is more or less pronounced according to the local geological structure. In particular, the overall sequence of erosion and landslide is slower in the southern sector, where the tuff rests on top of the lava, and faster in the northern one, where the entire cliff is made of pyroclastic rocks and soils.

The aeolian deposits, resting on top of the tuff, are subjected to small earth slides (Varnes 1978; Cruden and Varnes 1996) occurring mainly along the coastal perimeter between Cala Battaglia and Punta Pascone through Cala Rossano (see Fig. 1). These earth landslides are favoured by the rain water which operates both by infiltration and scouring, producing grooves and funnels which may act as triggering points. The sliding surfaces are often located along the weaker contact surfaces between the primary pyroclastic deposits and the natural soil (Palma et al, 2009).

The rock slides are diffused along the entire perimeter of the island, taking place mostly in the tuff formation with mechanisms of toppling and sliding (Varnes 1978, Cruden and Varnes 1996). These mechanisms are dictated by the sub-vertical weak planes related to cooling joints formed in the ignimbrite deposits after their emplacement. Such weak planes give rise to three principal families (k1, k2, k3) of discontinuities with dip direction of 35° (k1), 250° (k2) e 200° (k3) (Fig. 2). The single block volumes are in order of few cubic meters but the whole landslide volumes can become to hundreds of cubic meters (Fig. 3).

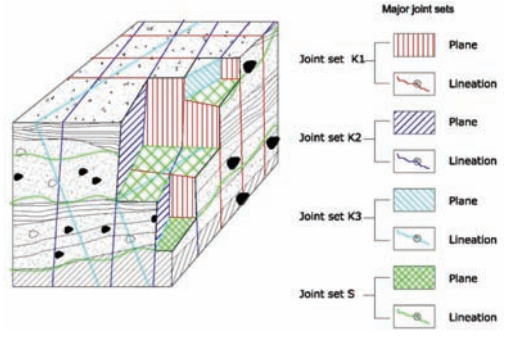

Figure 2. Schematic view of the discontinuities in the pyroclastic rocks.

Figure 3. Typical landslide of a tufaceous cliff (Parata Grande).

3 REDUCTION OF NATURAL HAZARD AND PROTECTION OF MONUMENTS

The diffused erosion process and the frequent landslides which were previously described have recently been recognized as a dramatic threat for the entire island of Ventotene, including its monuments and archaeological remains.

However, by comparing the wide extension of the natural hazards with the reasonable economical resources, it was first recognized that is not possible to stop the natural erosion process and to provide effective slope stabilization all over the island. It was then decided to identify the most valuable areas which can be effectively protected within economical availability. It was thus determined to concentrate the efforts in the north-eastern sector of the island, which is the most important from any point of view. In fact, as it was previously mentioned, this area provides the only access to the entire island, by means of two harbours, one close to the other: the ancient roman harbour and the new commercial port for the ferryboats. Moreover, the most valuable historical buildings and archaeological ruins are concentrated in this zone, as well as the most popular beaches. Four main projects were thus planned in this area as indicated in Fig. 4.

Several peculiar requirements were considered for each project, as briefly listed in the following:

i. People safety;
ii. Monuments integrity;
iii. Landscape conservation;
iv. Fauna and flora preservation;
v. Touristic industry protection,

Figure 4. Slope stabilization and protection projects: 1) stabilization of the rock cliff above Cala Nave beach; 2) stabilization of the rock cliff under a Roman necropolis; 3) restoration of the ancient Roman Harbour; 4) stabilization and rock fall protection at Cala Rossano commercial harbour.

In practice, it is necessary to satisfy the safety conditions according to the typical engineering rules and regulations but it is also required to avoid any destructive technique or possible changes to the preexisting monuments and landscape.

Another peculiar constraint is given by the diffused occurrence of archaeological remains (pottery, fragments, etc.) which may be found in the top soil layers and that should not be removed or damaged by construction works.

Finally an important requirement to be considered is the need to work in narrow spaces which cannot be closed to the public, unless for very limited time.

This restriction is imposed by the need to guarantee the fruition of the island not only by the inhabitants but also by the tourists which constitute the only economical resource of Ventotene.

4 RESTORATION PROJECT OF THE ANCIENT ROMAN HARBOUR

The most important project carried out so far is the restoration of the ancient Roman harbour, which is briefly described in the following. As it was previously mentioned, the ancient Roman harbour is one of the most characteristic historical evidence in the island of Ventotene, completely excavated in the tuff formation and equipped with a towing basin and a number of warehouses also dug into the tuff by the Romans (Fig. 5). These warehouses, which are still regularly used today for various commercial activities (little shops, storage facilities, etc.), consist in picturesque little caves whose entrances are aligned along the inner dock of the port which also allows the only vehicular and pedestrian access to the island.

From the morphological and geotechnical stand point, this area is characterized by the presence of a nearly vertical cliff, whose peculiar features are the result of a long and complex sequence of interacting natural and anthropic actions. In particular, the first 9 m, starting from the dock, are constituted by homogeneous tuff rock partly excavated by the Romans.

The tuff surface has then been grooved by the wind erosive action over the centuries, giving rise to some characteristic natural rock slabs overhanging the dock with a span of about 2 ÷ 3 m (Fig. 6). The upper portion of the cliff is characterized by the presence of some old retaining walls, dating back to the Bourbons period (18th century), made of weakly cemented tuff masonry. The latter, which are up 6 m high, provide static support to some layers of pyroclastic soils and made land resting on top of the tuff (Fig. 7). Finally, on top of the cliff there exist several masonry buildings constructed by the

Figure 5. Global view of the Roman harbour.

Figure 6. Tuff cliff, natural slabs and 18th century buildings before restoration works.

Figure 7. Masonry wall at the top of the cliff before restoration works.

Bourbons, belonging to the old "*Granili*" barracks. These barracks were partly demolished during the works done in the last century, shortly before the second world war, leaving only the parade ground which is used today as a public terrace (Fig. 8).

Figure 8. Side view of the Roman and the commercial harbours from the "*Granili*" terrace, during the restoration works.

The physical-mechanical properties of rocks and soils were estimated by in situ and laboratory investigations carried out on the port cliff and in the neighbouring areas.

The data were integrated by back analysis of previous instability phenomena which have occurred in the north-eastern area of the island, some hundred metres far from the Roman harbour. The overall results are collected in Table 1.

The restoration works were commissioned by the municipality of Ventotene, in order to ensure public safety with respect to possible falling materials resulting from two main potential causes:

i. flexural or block toppling of the natural tuff;
ii. failure of the old masonry walls.

As it was previously explained, the overall design was developed not only to achieve appropriate safety factors, for both the natural tuff cliff and the pre-existing retaining walls, but also with the purpose of preserving the complex historical landscape. Therefore a detailed survey of the harbour

Table 1. Geotechnical properties of the Roman Harbour cliff.

	γ kN/m^3	σ_c MPa	c kPa	ϕ °
Pyroclastic soil	15	–	2.5	30
Tuff	18	1.9	890	30

area was preliminarily provided by means of three-dimensional laser scanning (Fig. 9) in order to document in an objective way the conditions of the premises prior to restoration, thus securing the faithful recovery of the historical complex.

The project was carried out considering three principal requirements:

- preservation of the tuff surface, especially the rock shelves jutting up to 3 m that characterize the top section,
- representing a unique historical-landscape;
- restoration of the retaining walls of the embankment at the top of tuff formation;
- integration of the remedial works with the historical buildings built by the Bourbons above the Roman Harbour.

A special attention was paid to the yard organization, because the Roman harbour area can be considered as the *island door*, since the existing dock is the only way to access the island coming from the new commercial harbour, with a lot of tourists passing by in the spring and summer season.

For this purpose a provisional steel structure was placed all over the dock to ensure full protection during the works (Fig. 10).

Moreover the project had to take account for two additional requirements:

- plan a simple and fast execution, and therefore likely to be completed before the peak touristic period of the summer season;
- provide minimally invasive works, or, alternatively, reversible ones, to avoid that remedial works could modify the historic and landscape value of the area.

Due to the morphology of the area it was necessary to operate with unusual techniques. In particular specialized climber workers, operating for the most part in rope were employed (Fig. 11), and small size manageable equipment was used (Fig. 12).

Inspections carried out on the cliff showed the good conditions of the tuff shelves and verified that there were no evidence of cracks or discontinuities. Therefore it was decided to avoid invasive remedial works and to perform a shallow cleaning of the shelves removing soil, vegetation and altered elements corresponding to the thinner breakable

Figure 9. 3D laser scanner survey of dock, caves, cliff and masonry of the Roman harbour before the restoration works (courtesy of Idrogeo s.r.l.).

Figure 10. View of the yard area and provisional steel structure over the dock.

Figure 11. Climber workers on the cliff.

Figure 12. Drilling rig for deep mixing at the top of the cliff.

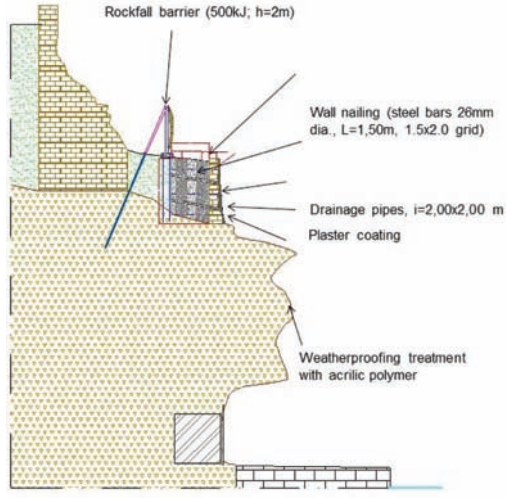

Figure 13. Schematic section of the restoration works (courtesy of Idrogeo s.r.l.).

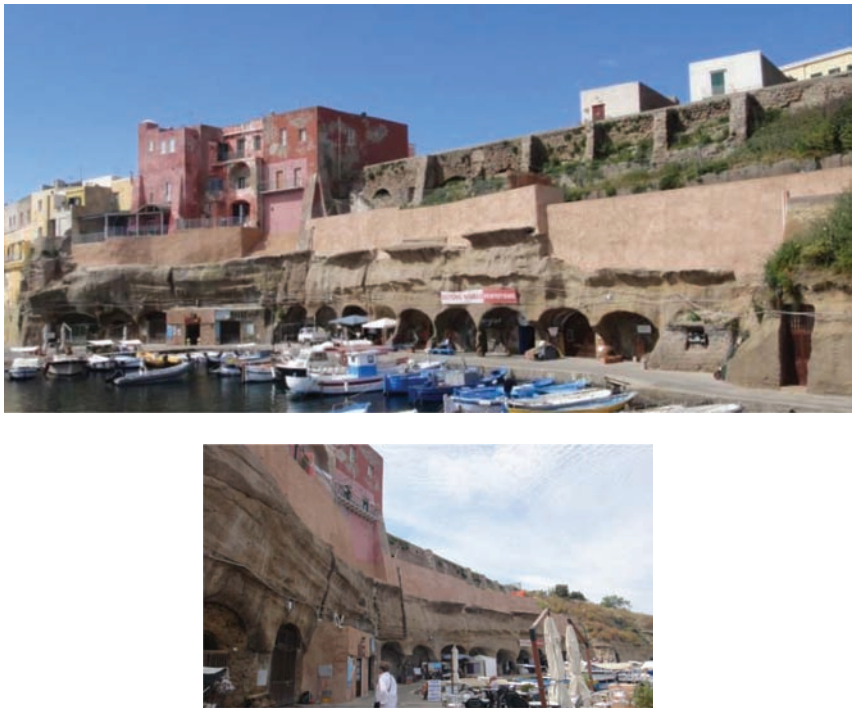

Figure 14. Roman harbour area after the restoration works.

parts on the edges. Furthermore, in order to prevent the erosive action by the atmospheric agents, the tuff surface was treated by spray application of acrylic polymer in aqueous dispersion, able to increase the abrasion resistance without altering the wall natural aspect.

One of the most critical problem was due to the inadequate strength of the old masonry retaining walls at the top of the cliff. In fact it was recognized that it was not possible to provide effective structural strengthening to the existing walls.

However it was also considered that a new structure would have altered the architectural characteristics of the harbour. It was thus decided to improve the mechanical characteristics of the by soil at the backside of the wall, in a zone with thickness ranging from 1.2 to 1.5 m. Such soil improvement was provided by deep mixing, which was carried on by using customized light equipment, achieving columns having 200 mm diameter (Papa and Ramondini, 2011 & 2012). After the grout curing, the treated soil acquired compressive strengths comparable to those of a weak concrete.

Following soil improvement, the old retaining tuff walls now act as a sort of coating, subjected only to its self weight and possible seismic actions.

However, the walls were studded with 1.5 m long steel bars, designed to anchor the masonry in the grouted soil behind the wall. On the front face of the wall a special structural plastering, armed with FRP (Fyber Reinforced Polymer) grid was installed to ensure high protection and durability against the corrosive action of the aggressive sea environment. The work section is sketched in Fig. 13.

The final arrangement has revived the original plaster coating of the Burbon walls (Fig. 14).

5 CONCLUSIONS

The case of Ventotene has been described by considering several interconnected topics: The geological nature of the island, the main historical events, the characteristics of its monuments and ruins, the geotechnical properties of the volcanic deposits, the erosive process, the typical landslides mechanisms.

Particular attention has been given to the search for equilibrated criteria and methods for the reduction of natural hazard as well as for the protection of the monuments and landscape.

By comparing the wide extension of the natural hazards with the reasonable economical resources, it was recognized that is not possible to stop the natural erosion process and to provide effective slope stabilization all over the island. It was then decided to identify the most valuable areas which could be effectively protected within economical availability. Four main projects were thus planned and designed.

It is underlined that several peculiar requirements should be met by each restoration project, in the island of Ventotene: people safety, monuments integrity, landscape conservation, fauna and flora preservation, touristic industry protection.

The restoration project of the ancient Roman harbour was then presented in some detail, providing a practical example of careful restoration works carried out by means of appropriate techniques chosen to meet the previously mentioned requirements.

ACKNOWLEDGEMENTS

The Authors would like to thank the Ventotene Municipality, and in particular the Mayor G. Assenso, for their avaiability, Mr M. Seccaroni and Dolomiti Rocce s.r.l. for their cooperation. Special gratitude is addressed to I. Caso, G. Di Fonzo, A. Ruocco and G. Zito for their contribution to the field activity.

REFERENCES

Bellucci F., Lirer L. and Rolandi G. 1999. *Geological map of Ponza, Ventotene and Santo Stefano islands*. Dipartimento di Geofisica e Vulcanologia, Università degli Studi di Napoli Federico II, 1999.

Cruden D.M. & Varnes D.J. 1996. Landslides Types and Processes. In: *Turner A.K. & Schuster R.L.* (*Eds.*) *Landslides: Investigation and Mitigation*. Transportation Research Board Special Report 247. National Academy Press, WA, 36–75.

Palma B., Calcaterra D., Parise M. 2009. Modelli geologici e meccanismi di innesco di frane da scorrimento-colata rapida nei depositi vulcanoclastici della Campania. GEAM—Geoingegneria Ambientale e Mineraria Anno XLVI, Vol. 1, pag. 21–48.

Papa R., Ramondini M. 2011. Il consolidamento dei terreni mediante Fast Deep Mixing. Proc. *XXIV Convegno Nazionale di Geotecnica*, Napoli, 22–24 June 2011.

Papa R., Ramondini M. 2012. Soil deep mixing by small equipment. *Proc. 4th International Conference on Grouting and Deep Mixing* New Orleans (USA), 15–15 February 2012.

Perrotta A., Scarpati, C.L. Giacomelli, Capozzi, A. 1996. Proximal depositional facies from a caldera forming eruption: The Parata Grande Tuff at Ventotene Island (Italy). *Journal of Vulcanology and Geothermal Researc*h, 71, 207–228.

Varnes D.J. 1978. Slope movement types and processes. In: *Special Report 176: Landslides: Analysis and Control* (Eds: Schuster, R.L. & Krizek, R.J.). Transportation and Road Research Board, National Academy of Science, Washington D.C., 11–33.

Geotechnical Engineering for the Preservation of Monuments and Historic Sites – Bilotta, Flora, Lirer & Viggiani (eds)
© 2013 Taylor & Francis Group, London, ISBN 978-1-138-00055-1

19th and 20th century coastal military installations affected by coastal erosion in the UK

E.N. Bromhead
Retired, formerly Professor of Geotechnical Engineering, Kingston University, London

M-L. Ibsen
Senior Lecturer, Kingston University, London

D. Tapete
Conservation Scientist and Research Associate, University of Florence, Italy

ABSTRACT: At four particular points in the last two centuries, Britain has believed itself to be under the threat of invasion, and has responded by building coastal fortifications, particularly along the southern and eastern coasts of England. Perhaps fortunately, they were never subject to any serious test. Sometimes, these defensive works exploited and modified earlier sites of Late Iron Age, 3rd century Roman age and from the 16th Century Tudor period, all of which lie outside the scope of this paper for reasons of brevity. In many cases, the defensive works were intended from the outset to be temporary in character, and particularly the newer structures are commonly held to be ugly, and as in the public mind they are not 'historic', they have proved to be more at risk from deliberate demolition and land redevelopment than from natural processes. The attrition rate since about 1950 from these causes has proved huge. However, the southern and eastern coasts of England are occupied by low-lying coastal marshes related to post-glacial sea level change, and thus to flooding and erosion; and by 'soft cliffs', which are low to medium height bluffs of weak rocks and strong soils, commonly subject to landslides and with appreciable rates of retreat. The natural processes are thus also responsible for some attrition of these sites and monuments. The paper describes the processes acting at a sample of sites and the nature of the defensive works lost or under threat. There are few instances of engineering works to stabilize or conserve these monuments, which (with the exception perhaps of some of the 19th century examples) are unloved, and their demise is therefore largely unlamented. Future historians and archaeologists may regret this neglect. The paper describes briefly some examples of stabilization works.

1 MILITARY BACKGROUND

1.1 *19th century*

The perceived threats of invasion of the British Isles from the end of the 18th C through the 19th C came from France, under Napoleon Buonaparte and later the 3rd Empire of Louis Napoleon in mid-century. In the first of these, ship technology was wooden construction and sail power, with smooth-bore cannon of comparatively short range, and the corresponding land-based response was to use similar guns, mounted in casemates in masonry-built fortifications, or in open–air batteries. It was long believed that one shore-based gun was the equal of three naval guns of the same calibre, as the shore-based gun was much more accurate, and ships more vulnerable. Land-based guns also benefitted in most cases from better protection from thick masonry or earth ramparts, as ships not only had weak hulls, but their masts and sails were vulnerable to damage.

As well as a number of fixed fortifications around a number of ports, usually controlling their entrances, two chains of so-called Martello Towers were constructed. These mounted a single large calibre gun with a 360° traverse on top of an approximately circular planform tower. In SE and E England, these were erected as two closely spaced chains, with the opportunity to provide covering fire. They were also erected all over the British Empire, sometimes in conjunction with polygonal earthwork forts, and in some cases to stiffen the defenses of much earlier castles. Martello Towers can also be found in the Republic of Ireland, which was then part of the United Kingdom. The threat of seaborne invasion evaporated after the sea battle of Trafalgar (1805).

The general perception of threat arose from the construction in France of iron-clad warships,

notwithstanding the joint Franco-British actions in Algeria, Greece and the Crimea. Nevertheless, as well as fixed fortifications, the Royal Navy was supplied with its own fleet of steam-powered ironclad warships, of which the first, HMS Warrior (1865) is still afloat. Once again, the threat evaporated, but this time not due to an engagement at sea, but as a result of the Franco-Prussian War of 1870, at the end of which Napoleon III was deposed. Paradoxically, he sought sanctuary with his family in England!

1.2 *20th century*

As the enemy during the 20th century was Germany, much of the focus of defense moved from the English Channel to the North Sea coasts, although following German military gains in the 1914–18 war, and especially after the Fall of France in 1940, the Channel coast again became of importance.

During the First World War of 1914–18, the Palmerston forts were retrofitted with more up to date guns and partly remodelled, but the threat of invasion by sea was rather distant, especially after the Battle of Jutland (1916). However airborne attack by airship and aircraft developed into a significant factor, for which acoustic early warning installations built of concrete were developed (Zeppelin airships and primitive biplane bombers mounted a number of attacks on London and coastal towns).

Ship technology had reached the point by mid 20th century where the relative stability of shore-based guns was no longer a factor in their effectiveness, and the ability of ships to move, and to arrive in force, made shore forts less worthwhile.

Thus, during the Second World War, 1939–45, fortifications tended to be on a smaller scale (the ubiquitous 'pillboxes'), but the further march of technology meant that attack from the air was a big threat, countered by the radar stations (radar had replaced the dead-end acoustic technology), anti-aircraft batteries and airfields. Of these, only the first was likely to be at the coastal margin. A few large gun batteries were constructed in the Dover area for cross-Channel artillery exchanges, but again, they were not immediately on the coast. Once more, the Palmerston-era forts were pressed into service.

Airbases tended to be distant from the coast, and therefore do not feature in the following account. However, early-warning radar stations were close to the coast, and some have been affected by coastal processes. On the other side, threat for the conservation of inland acoustic radar equipments can derive from ground instability, such as the sound reflector in Figure 8 situated within the Roughs landslide complex near Hythe, Folkestone (Bromhead et al., 1998), although this is a former coastal cliff.

2 GEOLOGICAL SETTING

The geology of Southern England (Figure 1) is dominated by a suite of rocks that are Jurassic or later in age, folded gently into two basins (Hampshire Basin and London Basin) separated by the Wealden Dome. Tertiary rocks are found in both basins. In general, dips are small, and there is but little manifestation of faulting except for the fold structure off the south coast and running through the Isle of Wight formed where the rocks have been deformed by movements of a deep basement fault, and bringing dips of nearly vertical in contrast to the near-ubiquitous 1° to 2° dips found elsewhere. The rocks consist of thick clay deposits, separated by weak sandstones and weak limestones, the latter including the Chalk of the upper part of the Cretaceous. All of the rocks in this sequence are readily eroded, and the recovery of sea level after the Late Glacial Maximum (LGM), reaching more or less contemporary levels about 6 ka bp, has created conditions in which coastal retreat can occur. There are few locations left where the slopes formed under periglacial conditions have survived, and they are located either inland, or where the coast is protected by spits, bars or coastal marshland.

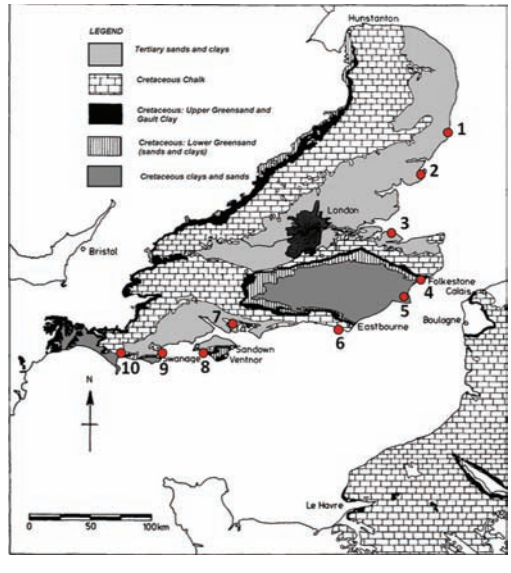

Figure 1. Geological sketch of SE England with location of the sites and coastal military heritage mentioned in this paper (clockwise): 1) Slaughden; 2) Walton on the Naze; 3) Isle of Sheppey; 4) Hythe; 5) Romney Marsh; 6) Newhaven Fort; 7) Portsmouth; 8) Isle of Wight—Military Road; 9) Studland; 10) Osmington.

3 THE FIRST TO GO—MARTELLO TOWERS

Martello Towers are described by Sutcliffe (1972), Telling (1997) and Clements (1997). After the Battle of Trafalgar (21 October 1805) it became progressively clearer that prospects for invasion were negligible. After the cessation of hostilities, the Martello Towers fell out of use: they were never comfortable billets at best, and at worst were damp and airless inside. Some were used for artillery practice, and others were demolished to recycle their content of bricks as the construction of the two chains of Martello Towers (Folkestone to Eastbourne on the south coast, and north east of London on the Essex/Suffolk coast) had overwhelmed brick production in southern England for some years (Clements, 1997).

Where the towers were constructed on low-lying land some were rapidly undermined by beach erosion. Elsewhere, as between Hythe and Sandgate, and East of Folkestone, they were built on former landslips, although there is no record of any being lost to landslide activity on the south coast. The East coast chain tended to have been located on top of low and fast eroding cliffs.

Once numerous, the majority of examples have now been lost. They have been lost to a diverse range of natural processes, but equally, because of their nature, many have been demolished when they fell from use. In some cases, the towers were built on spits that were never very permanent fixtures of the landscape, and their foundations were undermined by wave action (Figure 2). In other cases (Clements, 1997) towers were used for gunnery practice, especially to determine the effectiveness of improved guns and projectiles (Figure 3).

Figure 2. Martello Towers No 14 (foreground) and 15 (background) of the south coast chain alongside the Hythe Ranges, built on a coastal gravel spit, and protected from erosion by rock armour. (Photo © Oast House Archive and used by permission).

Figure 3. Martello Tower No 19 of the south coast chain in ruins (Photo © Oast House Archive and used by permission). This may be an example used to test gunfire.

Figure 4. Martello Tower CC* at Slaughden, Aldeburgh, Suffolk, located perilously along a tombolo (picture taken from uk-shore.com).

Coastal protection schemes sometimes included interventions on the Martello Towers (Figure 2), especially those converted to private residence with consequent civil protection issues, such as that sited at Bawdsey Cliffs, Suffolk (W*), threatened by storms and progressive removal of the shingle beach. Storm and flooding hazards are indeed non-negligible issues, which can also be emphasized by the topographic configuration of the Martello Tower with regard to sea level (Figure 4).

The SE England Martello Towers were designed to operate as a system, with adjacent examples providing gunfire support to each other, and collectively being able to triangulate cannon fire on approaching ships. Thus, the survival of isolated examples (especially when converted to dwellings), while preserving them as *monuments*, neither preserves their context nor the *site* as a whole.

Due to the short period of occupancy during their original use, and especially where not permanently garrisoned, the towers have little contemporary occupation debris in their vicinity.

4 THE NEWHAVEN FORT

A fort overlooking the port of Newhaven was originally constructed in the first Napoleonic War as a small battery. It was substantially remodelled into more or less its present form in connection with the Palmerston initiative, starting in 1864 and completed in about 1871, too late to be of use. During the Second World War it was again modified, this time to take more modern guns.

The fort shelters behind earthwork slopes, built as embankments on top of Tertiary clays and sands, in turn overlying Chalk that forms steep cliffs and makes any approach to the fort from seawards well nigh impossible. Further gun emplacements were built in the reclaimed ground at the foot of the Chalk cliff. During WWII the upper earthwork slopes became unstable. The slippage was investigated by W.H. Ward from the Building Research Station, and was addressed by hand-dug drainage and minor regrading, later reported by him (Ward, 1948) in the ISSMFE conference in Rotterdam (Figure 5). In retrospect, his attribution of the slippage to seepage erosion in a thin silty sand layer near the base of the Tertiary deposits appears now not to be correct, but his drainage remedial scheme appears to have survived the test of time.

The account by Ward (1948) mentions previous use as an Iron Age hillfort, and tracks coastal retreat through old maps and reports of early geologists, as well as development of the slippages. The construction of a harbour arm breakwater intercepted eastwards littoral drift, and thus defended the Chalk cliffs from marine attack in the 19th century, unlike the Folkestone Harbour mole extension that denuded beaches downdrift (Hutchinson et al., 1980).

When this site came into public ownership, it was converted into a museum. This entailed some modifications, e.g. safety railings, as seen on the right of Figure 6, and conversion of some spaces into displays, and for ticketing, office and catering purposes. However, the monument and its context, notwithstanding an episode of slope instability, have been largely preserved.

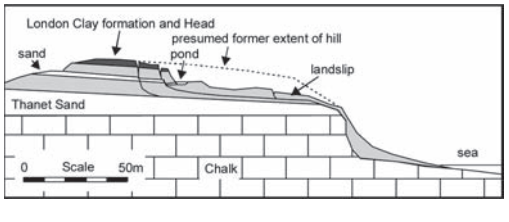

Figure 5. Cross section through maximum slip extent in seaward side of Castle Hill, Newhaven. Slip occurred in London Clay formation (after Ward, 1948).

Figure 6. Marginally stable and drained seaward slopes of the Newhaven Fort.

5 THE ISLE OF WIGHT'S MILITARY ROAD

Despite Britain's considerable wealth in the 19th century, fortifying the whole coast would have placed unsustainable demands on manpower as well as money. The compromise solution was to build military roads along which horse-drawn artillery could be deployed to meet invasion threats. One such military road traverses the SW coast of the Isle of Wight from Niton to Freshwater. This road was originally too secret to appear on early large-scale maps! In 1931 it was taken into Local Authority ownership. However, by then it had been breached by coastal landslides at various places, and some re-alignment work was carried out (Figure 7). Subsequently, coastal retreat and small-scale landsliding has again threatened the road.

Remedial work has been undertaken to the road and adjacent coastal slopes in the form of regarding and drainage, followed by road realignment at Small Chine, where the landslides follow a fault line in Wealden clays and sandstones. East of Hanover Point, the road is again threatened by coastal retreat in Wealden deposits. Here, part of the problem is the exhumation of an old river channel running parallel with the coast and filled with weak alluvial deposits. At the time of writing drainage works have been carried out and a longer term solution is under consideration. The noted politician Winston Churchill is reported to have altered the course of this stream by digging during the course of a social visit to a nearby grand house. (P. Mead, pers. comm.)

However, the major remediation works carried out on this road comprised deep bored piles in the seaward side of the road where it rises over Compton Down, and where it is threatened by encroaching landslide activity in the cliffs. The land in this area is jealously guarded by the National Trust: realignment is not possible for nature conservation reasons, and the piles are supposed to be removed at the end of their planned 50-year lifespan.

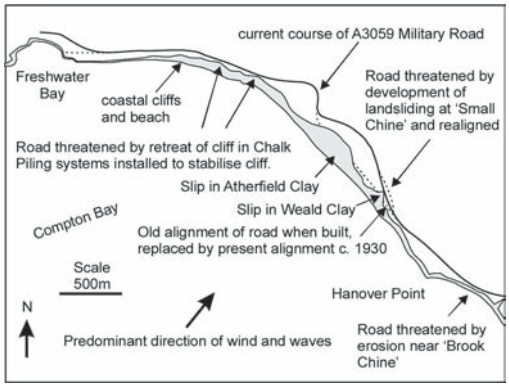

Figure 7. Isle of Wight's Military Road in the vicinity of Compton Down and Hanover Point.

Nevertheless, the public awareness of coastal and landslide hazards for the preservation of Isle of Wight's Military Road seems quite high in the local community. Recent events occurred in 2010, especially in the section near Brook, together with a still not proved impression of climate change-induced acceleration of cliff retreat (BBC, 2010), stimulated a debate and an online petition to save the Road (On the Wight, 2010a,b). Current political discussion about the types of remedial works to undertake reflects the controversy between the long-term benefits of permanent solutions (which are actually highly expensive and not feasible in times of tight finances) and temporary ones which might result only palliative.

6 ACOUSTIC EARLY-WARNING SYSTEMS AT HYTHE, SHEPPEY AND ROMNEY MARSH

Air raids into southern and eastern England using both Zeppelin airships and primitive biplane bombers were undertaken at various dates. The detector technology of the time was limited to listening for the sound of aircraft engines using large acoustic collectors. These comprised concrete structures with a shaped "mirror" surface, with a microphone or "voice pipe" at or near its focal point. Several of these were known to have been constructed, from as far north as County Durham to the south coast of England (Scarth, 1999). One, in the cliffs above Folkestone Warren, is rarely visited. A reflector at Warden Point on the Isle of Sheppey of First World War date was involved in coastal landsliding, and lies broken on the beach where it is currently being eroded away (Tapete et al., in press).

In the inter-war years further research was undertaken, including experimental installations

Figure 8. 30 foot (10 m) sound reflector at Hythe Roughs photographed in 1994.

at Hythe Roughs (located very close to the Royal Military Canal, commenced in 1804 against a feared Napoleonic invasion) as part of a research establishment comprising a 23 foot reflector (cast against a rock face), a 30 foot free-standing reflector (Figure 8) and associated infrastructure of huts and services. The 23 foot reflector toppled onto its face in a reactivated landslide in 1988, and the 30 foot reflector has recently been fenced: not so much to protect it from vandalism as to protect the vandals from falling bits of the structure.

Three other upright reflectors were built at Littlestone on Romney Marsh. These reflectors were built to various designs and have been both vandalized and affected by gravel extraction. Other types of sound detector, including flat pads, were constructed nearby (Scarth, 1999).

7 RADAR STATION AT WALTON ON THE NAZE

The development of radar technology rendered the sound reflectors obsolete at a stroke, and by 1940, a chain of large lattice mast radar stations had been erected at coastal sites. Several of these were attacked and put out of action temporarily. Soon after the end of the war they were taken down. The large foundations were left. At Walton on the Naze, Essex, the foundations took the form of mass concrete circular pads. Rapid coastal retreat (at an average rate estimated by some scholars up to 2 m/year), by a combination of small rotational slips and falls from the low cliffs in the London Clay has undermined the site of the radar station and the pillboxes that guarded it (Figures 9–10).

The retreat of the low coastal cliffs of London Clay and Head deposits at Walton on the Naze is particularly rapid, as the site is exposed to North Sea wind and waves. An earlier loss from the site, with ruins visible at extreme low water, was a

Figure 9. Pillbox at Walton on the Naze (cf. yellow square in figure 10a,b). This has survived descent down the unstable cliffs seen in the background. Coastal recession has left the bunker some distance seaward of the cliffs.

Figure 10. Comparison of aerial views from (a) Bing (© 2012 Microsoft Corporation) and (b) GoogleMaps (© 2012 Google) shows effects of high and low tides respectively, on the pillboxes at Walton on the Naze.

Roman Fort of the 3rd century Saxon Shore type (Pearson, 2002).

These WWII concrete structures have survived the passage to the beach undamaged, although their metal parts (e.g. gun port shutters) are corroding in the saltwater. Nevertheless, periodic sequences of high and low tides and consequent submersion/exposure cycles will likely lead to a progressive erosion of the concrete structures. Hence, their long-term preservation is not guaranteed.

8 PILLBOXES: OSMINGTON, SHEPPEY AND ELSEWHERE

In the early part of the 1939–45 war, numerous small concrete emplacements were constructed. Mostly, these were above ground, and designed for use by riflemen or machine gunners. Somewhat larger apertures in larger bunkers were provided for searchlights to illuminate critical sections of beach, or for anti-tank guns. Sometimes they were manned by the 'Home Guard', an organization of part-time soldiers that were initially ill equipped and poorly-organised.

Many of these constructions were to standard patterns that can be catalogued as specific types, others were more unique, and sometimes they were blended into other structures and disguised. Many of them have been thrown out of unstable cliffs subject to marine attack, such as this small structure shown in Figure 11, which is one of two presently on the beach at Osmington, Dorset. The shape of this example explains why the nickname 'pill box' was used.

Both small and medium sized coastal landslides have been responsible for casting pillboxes onto the foreshore. The second example, from the Isle of Sheppey, Kent (S shore of Thames estuary) shows 3 such buildings. All of them were originally constructed on top of the 40m high coastal slopes, and some distance inland from the edge. One bunker was carried downslope by the November 1971 rotational landslide. The pillbox that survived intact, and therefore probably most strongly reinforced of the three, was not even carried downslope by the landslide, as it was at first some 6m inland from the rear scarp of that slide. However, degradation of that rear scarp over the next few years eventually undermined it, along with another bunker that was constructed underground. Eventually, they joined the first bunker at the toe of the slope (Figures 12–13).

This complex was constructed to control the approaches to a large gun battery (Fletcher's Battery) that has been converted into part of a caravan park. The land was already owned by the military, having been used in the 1914–18 as a site for a sound detector to locate Zeppelin airships attacking

Figure 11. Small pillbox for rifleman on the beach at Osmington, Dorset. Shuttering for the concrete was corrugated iron sheeting.

Figure 12. Reinforced concrete bunker at the toe of the slope at Warden Point, Isle of Sheppey (S side, Thames Estuary). This bunker was over 6 m landward of the rear scarp on the November 1971 slip, but subsequently descended c. 45 m to the beach as the slip enlarged and undermined it (Photo 2010).

Figure 13. The reinforced concrete bunker in the foreground is that of figure 12, seen in c. 1980 shortly after it was undermined and slid from the clifftop. The bunker in the background moved with the original rotational slide.

London. The concrete sound reflector was also lost in the latter part of the 20th century due to rotational coastal landsliding and now is an almost unrecognizable mass of concrete fragments on the beach (Tapete et al., in press).

While the concrete bunkers represent *monuments*, it has become clear from exposures of archaeology in the eroding slope faces that they were not operated in isolation, but within a context of inter alia, trenches, communications (e.g. telephone wiring) and middens containing evidence of the occupants' diet. Occasionally (and not at Warden Point) live munitions are found. Thus the loss of the *site* itself may be as serious as of the specific monuments.

There are undoubtedly numerous instances of single pillboxes intended to control (for example) movement down a particular road, or access from a beach through a track, often they were set out as complexes of pillboxes with overlapping arcs of fire. Often too they were built in conjunction with

Figure 14. Reinforced concrete pillbox at Studland, Dorset, with anti-tank obstacles behind.

anti-tank obstacles usually but not always taking the form of unreinforced concrete blocks or less commonly rolled steel sections (Figure 14). Other obstacles included barbed wire and minefields, demolition charges in bridges, and a range of explosive defenses such as the flame fougasse (essentially a petroleum mine). Most of these were removed post-war for public safety, but occasionally, lost examples often in a dangerous state are found and rendered safe (the UK, like most European countries, maintains an organisation to deal with unexploded ordnance from past wars). However, it is not possible to understand the setting of individual pillboxes without an appreciation of the ancillary works.

As well as the bunkers built to defend the coasts, many were built inland forming a series of 'stop lines'. Including the inland examples, approximately 80% of those originally built have been removed.

9 SUMMARY AND CONCLUSIONS

The coastline of SE England is formed from eroding cliffs of weak rocks and strong soils of Jurassic, Cretaceous and Tertiary or later age where the land rises above sea level, and in low lying areas the coasts are occupied by reclaimed marshes and coastal spits of sand or gravel, generally associated with the post-glacial rise in sea level. All of these coastal features are subject to erosion under either steady state of particular storm conditions, with coastal spits subject to some accretion, although as a result the spits move. The dominant forms of mass movement in the coastal cliffs are compound slides with structurally-controlled basal slip surfaces (Bromhead & Ibsen, 2004) and shallow mudslides. Where coastal cliffs occur, defenses were usually constructed at the crest of the slope.

Mobile coastal features such as beaches, dunes, spits etc are likely to shift and thus undermine structures built on them.

At four critical periods in the 19th and 20th centuries, this part of the UK coastline has been perceived as under threat of invasion, and a huge range of military defenses has been built. Generally, they

have been considered ugly and intrusive, and many of them have been demolished so that the sites may be reused. Others have been vandalized. The survivors represent a small fraction of the total originally built, and natural processes are reducing even that.

Very few of the coastal fortifications built on the South and south eastern English coasts ever fired a shot in anger, and then usually in connection with air defense. With the benefit of hindsight, their construction was, in every case, completely redundant, as the perceived threat of invasion was always more apparent than real. For example, the French threat from Napoleon I was illusory given the dominance of the Royal Navy, and never more than after October 1805.

In some ways, the Palmerston Forts and defenses were even more ridiculous, as the Royal Navy was easily able to match and later counter the few ironclad vessels of the French Navy, and Napoleon III was, in any case, an Anglophile.

In the 20th century, the chance of invasion during the 1914–18 war was negligible, and seaborne raids on the coast tended to avoid defended areas. Moreover, the fixed fortifications provided no defense against airborne attack.

The 1939–45 war in Europe started badly for the UK, and a belief in the probability of invasion was widespread following the evacuation of forces from Dunkirk. However, it was probably beyond the capabilities of the Axis Powers to mount a successful invasion. As proved subsequently by war gaming, to have embarked on 'Operation Sealion' without first gaining full air superiority would have been disastrous, and even with it, given the strength of the Royal Navy would almost certainly have resulted in an equal disaster. Perhaps also an appreciation of the very uselessness of the fixed defenses leads to public neglect of their archaeological and cultural value.

Due to general indifference, this heritage is frequently abandoned and exposed to landslides and coastal processes, and its progressive disappearance is completely ignored. On the other side, it still raises people's interest, as testified by several blogs and websites. Indeed, most of the military heritage is officially listed by the heritage bodies, such as the Martello Towers, and private owners can take advantage of benefits for their maintenance and restoration.

An element to re-think about, especially for small-scale heritage like the pillboxes and acoustic installations, concerns the possibility of relocation of the elements at risk rather than expensive and enormous engineering solutions and protection schemes. For instance, the situations observed at Walton on the Naze and Isle of Sheppey might be recovered in their former configuration, relocating the still existing pillboxes on the stable ground at the top, at a safe distance from the eroding cliffs, thereby restoring the military network at least at the local scale, as an open-air museum. Interpretation initiatives and public opening might be highly feasible, not less than those currently active at Newhaven Fort. This paper has set out to describe some of the variety of fixed military defenses that are being lost to coastal instability and coastal retreat in the present day, and to give examples that may still be visited.

ACKNOWLEDGEMENTS

Images Copyright Oast House Archive are licensed under the Creative Commons Attribution-Share Alike 2.0 Generic Licence.

To view a copy of this licence, either visit http://creativecommons.org/licenses/by-sa/2.0/ or send a letter to Creative Commons, 171 Second Street, Suite 300, San Francisco, California, 94105, USA.

REFERENCES

BBC 2010. Isle of Wight Military Road faces erosion threat, by D. Blake, 20 July 2010. Online BBC News (accessed 30 October 2012).

Bromhead, E.N., Hopper, A.C., Ibsen, M-L. 1998. Landslides in the Lower Greensand Escarpment of South Kent. *Bulletin of Engineering Geology and the Environment* 57(2):131–144.

Bromhead, E.N. & Ibsen, M-L. 2004. Bedding-controlled coastal landslides in Southeast Britain between Axmouth and the Thames Estuary. *Landslides* 1(2): 131–141.

Bromhead, E.N. & Ibsen, M-L. 2006. Landslide and coast erosion damage to historic fortifications in SE Britain. *Landslides* 3(4): 341–347.

Clements, W.H. 1999. Towers of Strength: the story of the Martello towers. Leo Cooper.

Dixon, N. & Bromhead, E.N. 2002. Landsliding in London Clay Coastal Cliffs. *Quarterly Journal of Engineering Geology & Hydrogeology* 35(4): 327–343.

Hutchinson, J.N., Bromhead, E.N. & Lupini, J.F. 1980. Additional observations on the Folkestone Warren landslides. *Quarterly Journal of Engineering Geology* 13: 1–31.

On the Wight 2010a. Military Road erosion worsens, 15 February 2010. On the Wight Blog (accessed 30 October 2012).

On the Wight 2010b. Further landslide on Military Road, 23 February 2010. On the Wight Blog (accessed 30 October 2012).

Pearson, A. 2002. *The Roman Shore Forts*. Stroud: Tempus Publishing Ltd.

Scarth, R.N. 1999. Echoes from the Sky: A Story of Acoustic Defence. Hythe: Hythe Civic Society.

Sutcliffe, S. 1972. *Martello Towers.* Newton Abbot: David & Charles.

Tapete, D., Bromhead, E.N., Ibsen, M-L., Casagli, N. in press. Coastal erosion and landsliding impact on historic sites in SE Britain. In: Margottini, C., Canuti, P., Sassa, K. (eds.) *Landslide Science and Practice. Volume 6: Risk Assessment, Management and Mitigation*. Springer-Verlag.

Telling, R.M. 1997. The English Martello Towers: a concise guide. CST Books.

Ward, W.H. 1948. A coastal landslip. In: *Proc. 2nd Int. Conf. Soil Mech and Foundn Engrg*, (2) 33–38. Rotterdam.

Geotechnical Engineering for the Preservation of Monuments and Historic Sites – Bilotta, Flora, Lirer & Viggiani (eds)
© 2013 Taylor & Francis Group, London, ISBN 978-1-138-00055-1

Interpretation and modelling of the subsidence at the archaeological site of Sybaris (Southern Italy)

F. Cafaro, F. Cotecchia & V. Lenti
Politecnico di Bari, Bari, Italy

R. Pagliarulo
CNR, Istituto di Ricerca Protezione Idrogeologica. Bari, Bari, Italy

ABSTRACT: Historical subsidence in the Sibari plain is made evident by the vertical stacking of three ancient towns along the Crati river. In order to investigate the evolution and the disappearance of the archaeological site and to define the causes of the settlements affecting the area since ancient times, an interdisciplinary research, about the geological, tectonical, morphological and geotechnical aspects, has been for long carried out; recent studies have focused on a recent component of the subsidence, that is also revealed by PS-INSAR monitoring data. This paper discusses the geotechnical modeling that has been developed to interpret the source of the current settlement rates. It is related to the hydraulic boundary conditions evolving in the recent past in the plain, in particular as effect of deep water extraction and of shallow water drainage by a wellpoint system working at the archeological site since the last century. The model is based on an extensive set of geotechnical profiles and laboratory data. The calculation results are compared to the recent data collected by remote sensing and allow to forecast the possible evolution of the subsidence.

1 INTRODUCTION

The *Sybaris* case history shows how the cultural heritage may be jeopardized by geo-hydro-mechanical processes and how an appropriate coordination of advanced geological and geotechnical studies can reveal historical societal evolutions and guide the interventions to bring modern society to the knowledge of its archaeological heritage. Indeed, in the Sibari plain archaeological excavations brought about the effects of an important subsidence, causing the development of three superimposed levels of continuous habitation since VIII-VII century BC: the hellenistic towns of *Sybaris* (720-510 BC) and *Thurium* (444-285 BC) and the roman *Copia* (193 BC), currently at −3.5 m to 1.46 m a. s.l. (from 7 to 3,5 m below ground level). Sybaris (Fig. 1) was founded by the Acheans between the Crati and Coscile rivers and became the most powerful economic centre of Magna Graecia (Herodotus, Strabo, Diodorus Siculus, Livy, from 484 BC to 17 AD). But already then the plain was location of major floods, recorded in legends reporting that Sybaris was destroyed by the Crotonians in 510 BC by deviating the Crati river to flood the town. These floods were part of a long-lasting geo-environmental evolution of the plain, that brought Coscile and Crati rivers to join in historical times (Fig. 2), as reconstructed in the studies of reference in this paper.

Figure 1. The ancient theatre of Sybaris and, in the small picture, the well-point system.

In order to investigate the geological and geotechnical processes generating the burial of the archaeological site, researches have been carried in the last 20 years at the Research Institute for

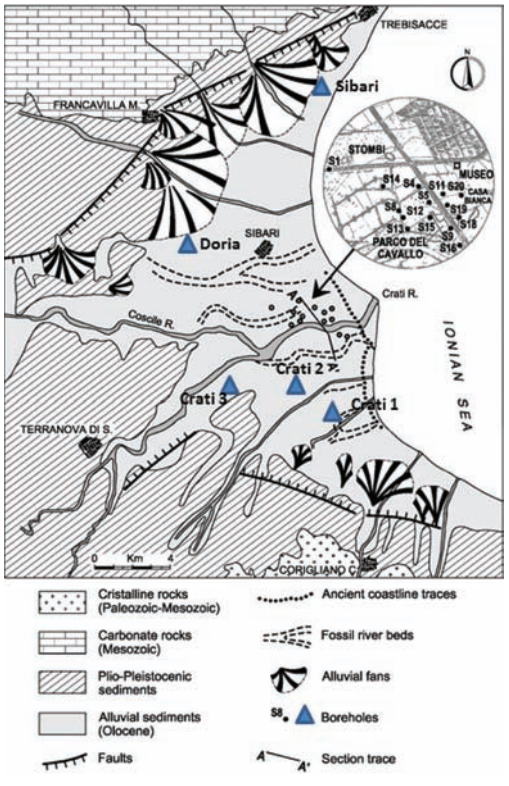

Figure 2. Geomorphological map and boreholes.

Geo-Hydrological Protection (IRPI-Bari), the Technical University of Bari and the City University of London, coordinated by Prof. V. Cotecchia within the Strategic Project for Cultural Heritage (Italian CNR—V. Cotecchia 1962, V. Cotecchia et al. 1994, Pagliarulo et al. 1995, Coop & Cotecchia 1997, Cherubini et al. 2000, Pagliarulo 2006). Recently, new analyses have been developed (POR Calabria 2000–2006), addressed to the interpretation of the causes of the current subsidence rates logged in the plain by PS-INSAR monitoring (Fig. 3, Giannico, Rocca and Ferretti, 2009), that reveals rates from 3 to 5 mm/yr, if going from Parco del Cavallo to Stombi in the archaeological area (Figs. 2 and 3). Geotechnical modeling has been developed to investigate whether these rates are due to both water withdrawal from deep aquifers, identified in previous studies, and pumping of shallow water through a well-point system active at the archeological site (Fig. 1).

This paper provides a brief background of the whole interpretation of the geological and geotechnical processes that have generated the evolution of the plain (Cotecchia et al. in prep.) and presents the study of the current settlement rates.

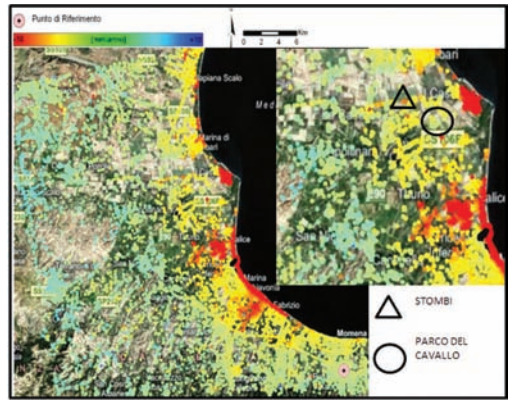

Figure 3. Remote sensing data for the Sibari Plain (Giannico, Rocca & Ferretti, 2009; modified). Copyright: Tele-Rilevamento Europa 2009.

2 GEO-STRUCTURAL SETUP AND GLACIO-EUSTATIC SUBSIDENCE COMPONENT

The Sibari Plain is bordered by the Mesozoic carbonate rocks of Pollino massif, North/North-West, and by the crystalline Sila mountains, South/ South-Est (Fig. 2). It is a graben bounded by various fault systems of different strike, the most important being NE-SW. In the upper part it is filled up by alluvial deposits, whose thickness increases from North (≅103 m) to South-East (478 m, Patacca & Scandone 2004). A series of dune ridges runs parallel to the coastline between the alluvial plain and the present beach.

The plain represents an anomaly in the regional tectonic frame of Calabria, that is characterized by strong uplift since Middle Pleistocene, triggered by deep-crustal or lithosphere-scale sources. An analysis of the spatial variations in vertical tectonic uplift across north-eastern Calabria has shown that along the Ionian coast, Pleistocene uplift formed a stepped flight of terraces whose elevation, once related to the Marine Isotope Stage (MIS 5.5) located in-land (at 115 m a.s.l.), suggests a local minor average uplift rate about 0,87 ÷ 1,1 mm/yr (Ferranti et al. 2011, Santoro et al. 2009). This becomes even lower towards the centre of the plain, such as to be negligible in the assessment of the subsidence sources in the area.

At the end of Tyrrhenian (≅125 kyr), sea level dropped down to 100 m below current sea level, triggering a major regressive erosion stage, subsequently followed by a sea level rising to current sea level (reached about 6 kyr, Cotecchia et al. 1971, Lambeck et al. 2004), with major flooding events in the plain and the formation of the alluvial

deposits. Therefore, glacio-eustatic sea level rising has caused part of the shift in elevation with respect to sea level of the sediment strata.

Lithological and chrono stratigraphical studies have been carried out on samples coming from several continuous coring boreholes drilled across the archeological area (small dots in Fig. 2). Also deep boreholes drilled in the plain during oil-search campaigns in the '50s have been taken into account (triangles in Fig. 2; see also Fig. 4).

The alluvial deposits consist of sands, silty sands, clays, sandy clays and gravels in heteropic facies, also interbedding peat levels at places (Fig. 5). The peat levels suggest the presence of swamps along the river floodplain at the time of deposition, while the presence of hydrogen sulfide and methane detected in deep boreholes indicates the chemical reduction of organic matter in brackish fossil water confined in the deepest layers (Pagliarulo, 2006). Numerous samples were subjected to ^{14}C dating, that also allowed for the assessment of the deposition environment of the sediments (Fig. 5).

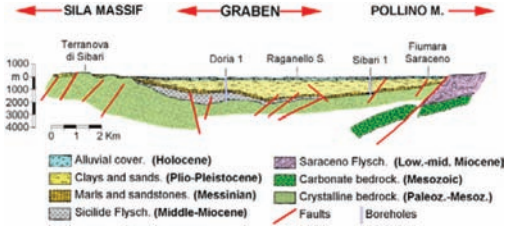

Figure 4. Schematic geological section of the plain (Cotecchia et al. 1994).

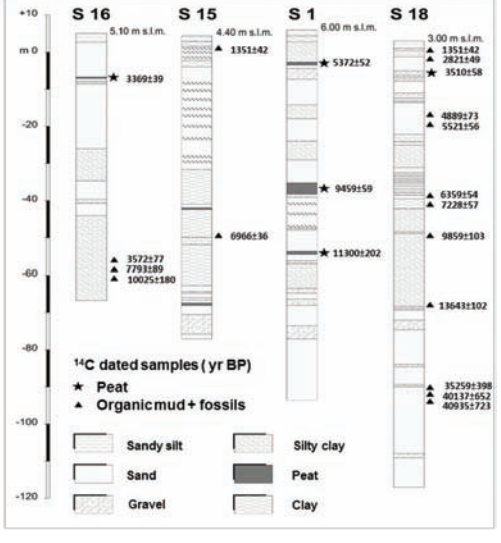

Figure 5. Schematic log of boreholes (see Fig. 1), showing position of calibrated ^{14}C ages of samples. Radiocarbon ages were calibrated by Calib Rev 5.0.1 (Stuiver et al. 2005).

Table 1. Evolution of the subsidence rate for different periods.

Age, period	Rate of subsidence
Holocene (10000 BP to present)	From 4 mm/year (average apparent rate)
Late Holocene (2670 BP to present)	1.6 mm/year (average apparent rate)
1945–1995 IGM-Parco del Cavallo	2.4 mm/year (average rate/ geotechnical)
2004–2009, PS-INSAR	3 ÷ 5 mm/year (current rate/ geotechnical)

Across the archaeological site the presence of peat levels reduces from NW (Stombi) to SE (Parco del Cavallo—Casa Bianca, Fig. 2), where a more continuous sequence of silty clay levels is found from 35 to 70 m depth (Fig. 5). These lateral variations are consistent with a transition from an alluvial to an intertidal environment. Across the whole site, sands and gravels alternate from 70 m downwards, till the top of the deep Blue Clays (Fig. 4), which occur down to about 1000 m depth.

For soil strata within 80 m depth, the average apparent subsidence rates, deduced from the ^{14}C datings in Fig. 5, reduce with reducing depth; they go from a maximum of 5,4 mm/yr for the deeper strata (of about 10000 y), to 1,6 mm/yr for the archaic habitation levels (Pagliarulo 2006, Coop & Cotecchia 1997). Topographic surveying of the IGM station at Parco del Cavallo has given evidence to a subsidence of about 12 cm in about 50 years since 1945, as such providing indication of an increase in subsidence rate at ground surface in recent modern history (≅2.4 mm/y). This rate has increased further in the last decade, according to the remote sensing data shown in Fig. 3, as summarized in Table 1. Where the Holocene subsidence rates in the table include the glacioustatic effects (apparent rates), the recent subsidence rates are necessarily the result of the sole geotechnical component of subsidence, given the negligible rates of sea level rising at present and the short period the monitoring refers to.

3 GEOTECHNICAL CHARACTERIZATION OF THE ARCHEOLOGICAL AREA

Clayey and silty samples (boreholes S1, S15, S16, Fig. 5) have been subjected to physical and mechanical testing in the laboratory (Coop &

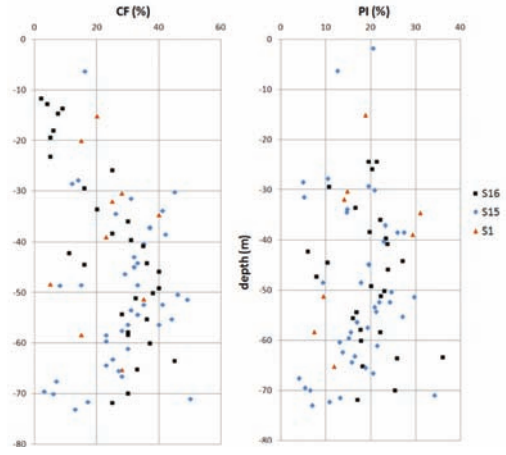

Figure 6. Clay fraction and plasticity index profiles.

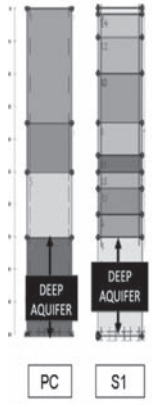

LAYER	DEPTH (m)	k (m/s)	M oed (kPa)	E(kPa)	Cv(m2/year)
1-PC	0÷35	5.0 E-8	3000	2230	473
2-PC	35÷50	1.3 E-10	5900	4380	2.4
3-PC	50÷70	1.3 E-10	8500	6310	3.5
4-PC	70÷100	10.0 E-5	25000	18600	-

LAYER	DEPTH (m)	k (m/s)	M oed (kPa)	E(kPa)	Cv(m2/year)
1-S1	0÷2	5.0 E-8	2100	1560	331.1
2-S1	2÷9	1.3 E-10	2100	1560	0.86
3-S1	9÷20	5.0 E-8	2100	1560	331.1
4-S1	20÷35	1.3 E-10	5000	3700	2.05
5-S1	35÷45	5.0 E-8	3400	2500	536.1
6-S1	45÷50	5.0 E-8	6100	4500	3.5
7-S1	50÷55	5.0 E-8	11900	8850	1876
8-S1	55÷65	5.0 E-8	15500	11500	2444
9-S1	65÷70	1.3 E-10	11900	8850	4.92
10-S1	70÷100	10.0 E-5	25000	18600	-

Figure 7. Geotechnical parameters of the *models PC* and *S1*.

Cotecchia 1995 e 1997); also, permeability tests and piezometric surveys have been carried out in situ (Cotecchia et al. in prep.).

The variation in clay fraction (CF) and plasticity index (PI) down the different boreholes is shown in Fig. 6, which confirms the presence of fine soils between 35 and 50 m depth at Parco del Cavallo (S15, S16), that are either clays of medium plasticity or highly compressible silts formed in an intertidal deposition environment, of average CF about 35%.

Silty sands and sandy silts in a clayey matrix, of CF in the range 5%–18%, are frequent above 35 m depth at Parco del Cavallo and along the whole borehole down to 70 m depth at Stombi (S1). Here, these coarser levels are interbedded with either clay or sand levels formed in alluvial conditions, all way down to the deep stratum of gravel and sands (at 70 m depth).

The 100 m depth soil deposit at Parco del Cavallo (S8, S9, S12, S15, S16, S18, Fig. 2) has been modeled as a sequence of three strata (Fig. 7, *model PC*; with average $PI_1 \leq 15\%$, $PI_2 \cong 20$–25%; $PI_3 \cong 20\%$) laying above a fourth base stratum of sands and gravels. The corresponding model at Stombi (Fig. 7, *model S1*) is formed of alternating clays (CF = 30–40%, PI = 30%), clayey silts and clayey sands (CF = 15–30%, PI = 15–20%), peat, sand with silt (CF = 0–5%, PI < 10%), above the base stratum of sands and gravels.

Fig. 8 shows the consolidation states and compression curves of clay specimens normalized for composition in the plane I_v – log σ'_v, where I_v is the void index $I_v = (e - e^*_{100})/(e^*_{100} - e^*_{1000})$, and e^*_{100} and e^*_{1000} are the void ratios of the reconstituted clay normally consolidated to σ'_v = 100 kPa and σ'_v = 1000 kPa respectively. C^*_c is the compression

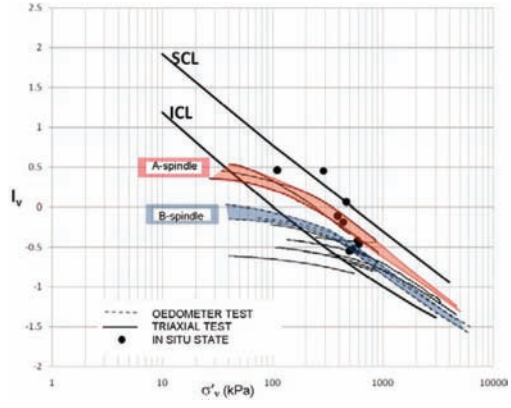

Figure 8. States and compression curves of the soils at Sybaris (Coop & Cotecchia, 1997; modified).

index of the reconstituted clay (Burland 1990), accordingly.

The data confirm that the sediments are normally consolidated. For all the tested samples, the value of the oedometric stiffness, M_{oed}, corresponding to the in situ consolidation vertical stress has been derived (M_{oed} values accounted for in the models in Fig. 7).

As recognized by Coop & Cotecchia (1995), the clays are of low sensitivity and have compression index close to the index that the same clay exhibits when reconstituted in the laboratory ($C_c = C_c^*$), due to a natural stratified meso-fabric. Consequently, it may be inferred that the C_c values of the natural samples are mainly dependent on the plasticity index, as for reconstituted clays (Schofield & Wroth 1968; Wood 1990), since no destructuring

affects the compression behavior of the natural samples.

The measured C_c values have been plotted against PI as shown in Fig. 9a and the relation reported in the figure has been considered to represent the C_c–PI relation for the Sibari clays. Based upon this relation, a C_c value has been deduced for all the strata of known PI and, here forth, the M_{oed} of the soil at the in situ consolidation stress has been also derived. To this latter purpose, a strategy has been defined to deduce from the data in Fig. 8 the compression curve of each soil stratum of given PI and given depth.

Two spindles of compression curves, A and B, have been distinguished in the I_v – log σ'_v plane, the first recognized to be representative for the clay strata shallower than 35 m depth, the other for the deeper clays.

According to this recognition, for each sample a compression curve has been selected in the plane within the appropriate spindle and the I_v – σ'_v state of the sample in situ has been deduced from the curve, based upon the σ'_v value in situ. Once known I_v, the corresponding void ratio has been deduced based on the values of C_c^* ($=C_c$ in Fig. 9a) and of e^*_{100} of the sample. This latter parameter value has been deduced according to the $e^*_{100} - e_{LL}$ relation in Fig. 9b, deduced from the compression data for the reconstituted samples shown in Fig. 8 (e_{LL} is the void ratio at the liquid limit). Based upon the e – log σ'_v curve deduced by means of this procedure, the value of M_{oed} has been calculated for all the samples of known PI and liquid limit, LL, with reference to the in situ state.

Also these M_{oed} values have been accounted for to deduce the M_{oed} values in the models in Fig. 7.

A single permeability value, $k = 5 \times 10^{-8}$ m/s, has been found to represent the silty sands with fine matrix, whereas a much lower value, $k = 1{,}3 \times 10^{-10}$ m/s, has been found to apply to the silty clay strata. The permeability of the sands and gravels at depth has been assumed to be about 10^{-5} m/s, according to the literature. All the parameter values used in the calculation of the consolidation rates in the two areas of the archaeological site, Stombi (*model S1*) and Parco del Cavallo (*model PC*), are shown in Fig. 7. Peat strata have been approximated to behave like clays, given the limited thickness of the strata and the neglection of secondary consolidation in the calculations, as discussed later.

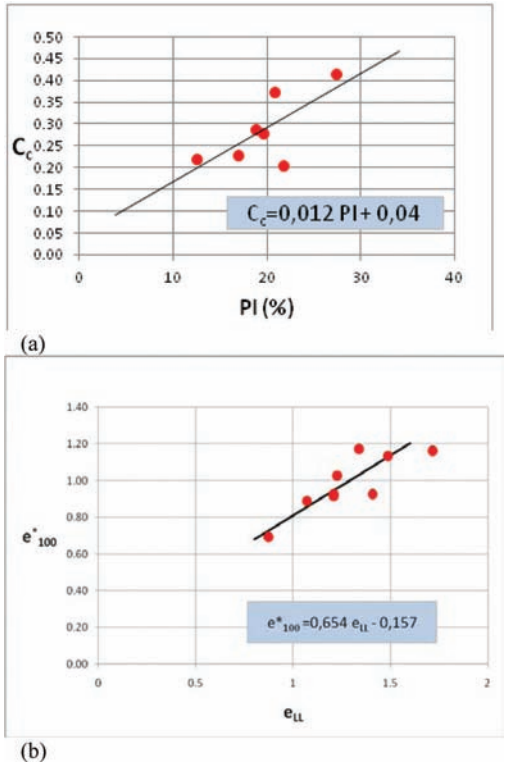

Figure 9. Relationships between compression parameters and index properties for the Sibari clays.

4 MODELLIG THE HOLOCENE SUBSIDENCE

Coop & Cotecchia (1997) studied the Holocene subsidence of most of the strata in Fig. 4 subjected to ^{14}C dating (from about 10000 yr to 1300 yr BP) and found that their elevation a.s.l. has reduced with time due to both the glacioeustatic sea level rising and a significant geotechnical subsidence, effect of the normal compression of the soils.

The authors derived the original elevation of the soil strata at deposition with respect to the original sea level, based upon the sedimentation facies of the soil samples subjected to ^{14}C dating. Here forth, based upon the current depth of the soil sample with respect to sea level and the original elevation of the soil sample with respect to the original sea level, the authors derived, for each soil sample, the depth with respect to current sea level of the sea level at the time of deposition. Then they compared this depth with the depth of the contemporary sea level that has been deduced by studies of Holocene glacioeustatism for the Ionian sea (Cotecchia et al. 1971). No difference would exist between these depths, derived via different procedures, if the soil strata had not been subjected to geotechnical subsidence. Conversely, the differences found by the authors demonstrate that geotechnical subsidence has occurred at the archaeological site, which the

authors then showed to be consequence of the primary consolidation of the soils.

The authors found the compression settlements to be very close to the discrepancies between the depths of sea level at the time of deposition of each soil stratum estimated according to the two alternative procedures recalled before. In this way the authors provided a quantitative demonstration that the Holocene subsidence of the soils at the archeological site of Sibari (Table 1) has been due to a combination of glacioeustatism and primary compression of the sediments, occurring all way down the deposit during the rising of the deposit.

Coop & Cotecchia (1997) modelled the settlements of all the dated soil strata as due to compression of the soils below, making reference to a one-dimensional model that, for the first 100 m, is close to *model PC* in Fig. 7. At larger depths, their model implements sands and gravels down to 300 m depth, followed by Subapennine Blue clays, down to 1000 m. For the clay strata in the first 100 m, they modeled the one-dimensional compression based upon C_c values that had been either measured in the compression tests in Fig. 8, or that the authors derived according to the assumption $C_c = C_c^*$ and to a relation $C_c^* - e_{LL}$ they propose as applying to the Sibari clays.

For the sand and gravel strata the authors assumed null deformability.

5 MODELLING THE RECENT SUBSIDENCE DUE TO PUMPING

Further modeling has been addressed to evaluate whether the modern subsidence at the archaeological site (Table 1, Fig. 3) is anthropogenic, being due to pumping of water both from a deep arthesian aquifer, within the base gravels and sands (Fig. 7), and at shallow depth. In particular, shallow water has been for long pumped from the well-point system set up at the archaeological site (Fig. 1).

One-dimensional strain conditions have been assumed in the modeling of the settlements due to pumping, developed with reference to either *model PC* (Fig. 7), for the central and S-E part of the site (Fig. 3), or *model S1* (Fig. 7), for the N-W part. The modeling has assumed that sediments deeper than 100 m are not significantly contributing to the recent subsidence. The consolidation settlements have been calculated through FEM analyses (PLAXIS 8.6), implementing the stratigraphic variations in the two areas being considered.

The boundary conditions in both areas have been: impermeable boundary at the bottom; constant head along the lateral boundary surface crossing the deep gravels and sands below 70 m depth, consistent with the hydraulic head of the deep aquifer; impermeable conditions along the rest of the lateral boundary; constant head along the top boundary, consistent with the shallow water conditions. As initial flow-strain regime, a permanent vertical seepage has been simulated, consistent with a water table at 2 m depth below ground level at the top (hydrostatic negative pore pressures above the water table) and at 0.5 m above ground level for the deep aquifer. Coupled consolidation has been triggered by varying the hydraulic head in both the top and bottom aquifer and has been calculated assuming an elastic constitutive law for the soils, with M_{oed} values in Fig. 7 and $\nu' = 0.3$.

In the last 50 years the changes in hydraulic head generated by local pumping along several different verticals across the plain have been chaotic in time and space. The ground settlement rates resulting from coupled consolidation along the two FEM models in Fig. 7 have been investigated in order to assess whether this process provides settlement rates, either as average with time, or at any given stage of the process, that are consistent with the rates logged in the area. Consolidation effects have been calculated for 9 different combinations of changes in hydraulic head in the two aquifers, that are: either of 1 or 2 m for the top water table and either of 1, or 2, or 3 m for the water table of the deep aquifer. Each change in hydraulic boundary conditions has been first implemented as undrained, followed by consolidation calculated as a separate stage. The initial effective stress states have been assumed to correspond to normally consolidated conditions, with $K_0 = 0.46$.

Fig. 10 reports the settlements resulting from coupled consolidation for the two models (Fig. 7) and Fig. 11 the corresponding settlement rates. Only the extreme curves of the spindle of curves resulting from all the nine simulations that have been carried out, have been plotted in the figure. The results give evidence to consolidation rates higher at Stombi (*S1*) than at Parco del Cavallo (*PC*), due to the corresponding differences in stratigraphy. In particular, as first along *S1* the total thikness of the low permeability fine soil layers is slightly lower than the corresponding one along *PC*. Furthermore, more important difference is that along *S1* the clayey strata are thin and interbedded with more permeable layers of silts and sands with fine matrix, at places including significant organic matter, whereas along *PC* a single thick sequence of firm clayey strata occurs between 35 and 70 m depth (Fig. 7). Therefore, on the whole model *S1* is more free-draining than *PC* and is also more compressible, due to the high compressibility of the silty and sandy layers that are quite loose and include fines and peat. Indeed, for any given set of changes in hydraulic boundary conditions triggering consolidation, the calculated stress-strain

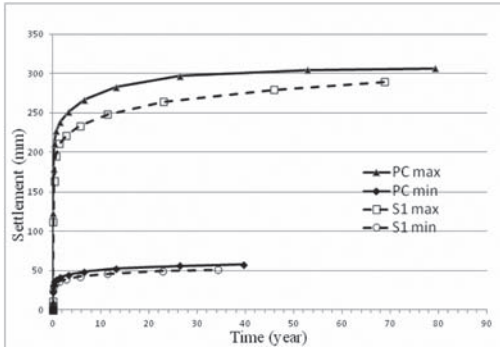

Figure 10. Numerical predictions of subsidence for the two adopted models, in the settlement *vs* time plot.

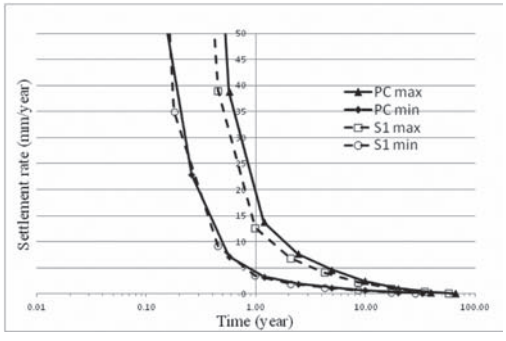

Figure 11. Numerical predictions of subsidence rate for the two adopted models, in the settlement rate *vs* time plot.

distributions have been found to evolve with time quite differently in the two models, providing the larger settlements and settlement rates at Stombi, in accordance with the gradient in subsidence from N-W to S-E across the archaeological site recorded by remote sensing and shown in Fig. 3.

For both the models, subsidence resulting from pumping develops in 30 to 40 years and gives rise to total settlements from 5 to 28 cm for *model PC* and from 6 to 31 cm for *model S1*. These total settlements are consistent with the 12 cm settlement recorded at Parco del Cavallo in about 50 years since 1945. The settlement rates calculated in the first year and half of consolidation are in the range 3–10 mm/y for *model PC* and 3–13 mm/y for *model S1*, dropping to 1–2 mm/y in the years going from the tenth to the thirtieth for both models. Therefore, also the calculated rates are consistent with the rates monitored by means of interferometry (Fig. 3).

The high variability of the calculated settlement rates with the different variations in boundary conditions is consistent with the variability in subsidence rate logged across the plain, that is not only due to variations in stratigraphy, but also to both the variability in timing of the pumping activities at the different sites and the variability in hydraulic head difference being generated. Although the hydraulic head changes assumed to trigger consolidation in both the models are low, the resulting settlements are reasonably large; in particular, the 50 year settlement logged at Parco del Cavallo occurs in the middle-lower part of the interval of calculated settlements. This result is plausible, since on one hand the calculated settlements refer to complete consolidation, that has not necessarily occurred at most pumping sites in the plain. On the other hand, the occurrence of most of the settlement in the first years of pumping implies that the calculated total settlements provide a minor overestimation of the real settlements.

With regard to the settlement rates, the highest ones, corresponding to the first year of pumping, are representative of any activation of pumping. Therefore, since it is likely that pumping has been stopped and reactivated at most sites in the plain, these initial rates can be considered frequently on going in the plain due to step-wise consolidation processes at the various pumping sites.

6 CONCLUSIONS

The geo-hydro-mechanical characterization of the archaeological site of Sibari and the back analysis of the events that have caused the burial of the most flourishing colony of Magna Grecia, makes nowadays this archaeological site as a real-scale physical model of known behavior. The design of interventions aimed at completing the archaeological excavations and bringing to light the archaic town of Sybaris can now be developed at ease.

The back analyses have demonstrated that the site subsidence during the Holocene has been caused by the compression of the sediments when buried, due to the sedimentation of either alluvial or inter-tidal sediments, whereas the recent increase in subsidence rates is due to the further consolidation caused by water withdrawal from the local aquifers. The accurate definition of the stratigraphic variabilitity across the site has provided reasons for the occurrence of spatial gradients in the subsidence rates. The results show that today the archaeological site may be location of 3 to 5 mm/y settlement rate due to water pumping started at the end of the '90s.

The Sibari case history provides evidence of the success of collaborations between geological and geotechnical expertise to model real occurrences of natural events, that have deeply influenced the history of society. In Italy, this type of interpretation

of the historical heritage could become a productive activity, since this interpretation of the past events at our archaeological sites is the appropriate background for a safe design of interventions for the preservation of our historical heritage.

ACKNOWLEDGMENTS

The authors thank Prof. V. Cotecchia for guiding the research and recall the productive collaboration of Prof. M.R. Coop to the research funded by British Council. Also, the authors thank the Calabria Basin Authority for funding the more recent project concerning the recent subsidence in the Sibari plain (POR Calabria 2000–2006; Asse 1, Misura 1.4).

REFERENCES

Burland, J.B. 1990. On the compressibility and strength of natural clays. Géotechnique 40: 3, 329–378.

Cherubini, C., Cotecchia, V., Pagliarulo. R. 2000. Subsidence in the Sybaris Plain (Italy). *In L. Carbognin, G. Gambolati G., A.I.Johnson (Eds). "Land Subsidence" –1. Proceedings of the 6th International Symposium on Land Subsidence.* Ravenna. 3–15.

Coop, M.R. & Cotecchia, F. 1995. The compression of sediments at the archeological site of Sibari. *Proceedings XI European Conference of Soil Mechanics and Foundation Engineering (ECSMFE)*, Copenaghen, Vol. 8, 19–26.

Coop, M.R. & Cotecchia, F. 1997. The geotechnical settlements of the archaeological site of Sybaris. *Proceedings International Symposium Geotechnical engineering for preservation of monuments and historic sites*. Balkema, 89–100.

Cotecchia, V. 1962. Appunti geologici sui dintorni della piana di Sibari. *Estratto dagli Annali della Facoltà di Ingegneria*. Università di Bari.

Cotecchia, V., Dai Pra, G., Magri G. 1971. Morfogenesi litorale olocenica tra Capo Spulico e Taranto nella prospettiva della protezione costiera. *Geologia Applicata e Idrogeologia*, 6. 65–78.

Cotecchia, V., Cherubini, C., Pagliarulo R. 1994. Geotecnical characteristic of outcropping deposits in the Sybaris Plain. *Proceedings 13rd International Conference of Soil Mechanics and Foundation Engineering*. New Delhi, 1, 245–250.

Lambeck, K., Antonioli, F., Purcell, F., Silenzi, S. 2004. Sea-level change along the Italian coast for the past 10,000 yr. *Quaternary Science Reviews* 23, 1567e1598.

Ferranti, L., Santoro, E., Mazzella, E., Monaco, C., Morelli, D. 2010. Active transpression in the northern Calabria, Southern Italy. *Tectonophysics*, 476 (1-2), 226–251.

Ferranti, L., Pagliarulo, R., Antonioli, F., Randisi, A. 2011. "Punishment for the sinner": Holocene episodic subsidence and steady tectonic motion at ancient Sybaris (Calabria, southern Italy). *Quaternary International,* 232, 56–70.

Pagliarulo, R. 2006. Coastal changes and the environmental evolution of the archaeological site of Sybaris (Southern Italy). *Geografia Fisica e Dinamica Quaternaria*. 29, 51–59.

Pagliarulo, R., Cotecchia, F., Coop, M.R., Cherubini, C. 1995. Studio litostratigrafico e geotecnico della Piana di Sybaris con riferimento all'evoluzione morfologica e ambientale del sito archeologico. *Geologia Applicata e Idrogeologia*. 30, 375–391.

Pagliarulo, R. & Cotecchia F. 2000. Le influenze dell'evoluzione geoambientale e della compressione dei sedimenti sulla scomparsa dell'antica Sybaris. *In G. Lolino (ed.) "Geological and geotechnical influences in the preservation of historical and cultural heritage". Proceedings Geoben 2000*. Torino, 715–722.

Patacca, E. & Scandone, P. 2004. The Plio-Pleistocenic thrust belt-foredeep system in the Southern Apennines and Sicily (Italy). *In Crescenti U., D'Offizi S., Merlino S., Sacchi L.(Eds) "Special Volume of the Italian Geological Society for the IGC 32 Florence 2004".* Roma, 93–129.

Santoro, E., Mazzella, M.E., Ferranti, L., Randisi, A., Napolitano, E., Rittner, S., Radtke, U. 2009. Raised coastal terraces along the Ionian Sea coast of northern Calabria, Italy, suggest space and time variability of tectonic uplift rates. *Quaternary International* 206, 78e101.

Schofield, A.N. & Wroth, C.P. 1968. *Critical State Soil Mechanics* (London: McGraw-Hill).

Stuiver, M., Reimer, P.J., Reimer, R.W. 2005. CALIB 5.01 [www.calib,qub.ac.uk].

Wood, D.M. 1990. Soil Behaviour and Critical State Soil Mechanics. Cambridge University Press.

Geotechnical Engineering for the Preservation of Monuments and Historic Sites – Bilotta, Flora, Lirer & Viggiani (eds)
© 2013 Taylor & Francis Group, London, ISBN 978-1-138-00055-1

Geotechnical aspects in the preservation of the *Domus Tiberiana* in Rome

G. Calabresi
University "La Sapienza" of Rome, Italy

L. Cavalera & V. Ascoli Marchetti
Geotechnical Engineers, Rome, Italy

M.G. Filetici
Italian Ministry of Culture S.S.B.A.R, Italy

ABSTRACT: The *Domus Tiberiana* is the first imperial palace of Ancient Rome. Its impressive and spectacular ruins are mainly the substructure levels since the noble part of the building, most of which was pillaged, was covered up in the 16th century to create the Farnese Gardens. In the multidisciplinary project for the conservation of the *Domus*, the contribution given by Geotechnical Engineering has proved to be particularly effective in understanding the origin of the instability, that started to occur during construction, and in suggesting the most appropriate maintenance actions.

1 INTRODUCTION

It is believed that the *Domus Tiberiana*, an impressive architectural complex, was built on the Palatine hill close to the native house of the Emperor Tiberius (14–37 AD), step-son of Augustus, incorporating the nearby houses of the late Republican period. Just as Augustus chose the Palatine for his palace, also Tiberius and all his successors did the same. The excavations carried out in 1880 demonstrated that the *Domus Tiberiana* is a structure that formed over time through successive expansions. Tradition has it that first addiction was made by Nero (54–68 AD); substantial changes were later made by Domitian (81–96 d.C), who expanded the *Domus* towards the Forum and the Velabro, and subsequently by Hadrian (117–138 AD). Throughout the 8th century AD the *Domus Tiberiana* was still so magnificent that Pope John VI chose it as his residence; he restored it but also altered its nature. Nothing was left of that restructuring because starting from the 10th century the palace was abandoned and its materials were looted to build churches and palaces for the aristocracy. During the 16th century indeed, the still standing remains of the *Domus Tiberiana* were buried to create the Farnese Gardens just on the top of the Palatine Hill under the orders of Cardinal Alessandro Farnese, nephew of Pope Paul III. The powerful prince obtained the Pope grant for his ownership of the areas, buried the *Domus* under soil and rubble, and assigned the design of the garden to architect Vignola. This is how the famous *Horti Palatini Farnesiorum* came about. The famous architect drew inspiration from the *Horti* of the ancient Romans who used to arrange their gardens in terraces with flights of steps, marble railings, statues and fountains to create magnificent walkways looking out over the landscape. This is what the gardens of the *Domus* must have looked like.

However it is still the least known complex of the Palatine Hill of which it occupies the western side extending for about 135 × 120 m^2. With its impressive remains especially on the side of the Forum where its slim arches rise for a height of about 20 m, the imperial palace is still an evocative but impenetrable place.

Actually relevant structural damages of the *Domus* standing parts appeared after the removal of a soil and debris layer of about 7 meters from the adjoining Forum area during the first great excavation campaign of modern times at the end of the 19th Century. The formation of new vertical fissures and the enlargement of the existing ones showed the rotation of the front structures towards the Forum and prompted a set of subsequent structural measures to ensure the equilibrium stability of the *Domus* present front. Nevertheless after a series of minor, local structural collapses the whole complex was closed to the public.

The project for returning this monument to the visitors enjoyment was to begin with the reconstruction

Figure 1. *Domus Tiberiana*: Northern facade towards the Roman Forum.

of the historic events that most influenced the current status of its structures, with an approach that necessarily had to be multidisciplinary. This type of approach was started by the Superintendence of Rome in 1980, but the effective collection of all multidisciplinary data has been performed by V. Ascoli Marchetti from 2004 to 2008. His studies conducted to the restoration design in large part concerning the north side looking out over the Roman Forum (Fig. 1) and the west side that looks towards the Velabro.

This paper presents the results of the geotechnical investigations carried out on soils underlying this vast archaeological area in order to establish their stratigraphy and mechanical properties and to research the origin of the structural damages.

Stability analyses of the more critical sections were performed to explain the recent movements highlighted by monitoring activities and to support the structural design of the restoration works.

2 FOUNDATION SOILS

2.1 *In situ geotechnical investigations*

The in situ investigations were carried out in different periods between 1972 and 1999. They have been summarized and arranged by the CISTeC, Scientific Committee for the Conservation of Historic and Monumental Heritage (Cistec 2003) of the University of Rome "La Sapienza", and next, starting from 2005, they have been elaborated from V. Ascoli Marchetti in his critical reviewing work (Ascoli Marchetti 2006).

Between July 2010 and February 2011, within the framework of a research contract between the National Research Council and the officer appointed for preparing urgent interventions in the archaeological areas of Rome and Ostia Antica, a rich and articulated investigation campaign was carried out which included: geomechanical measurements of the tuff masses; core borings; geotechnical laboratory tests on undisturbed samples; georadar investigations; seismic testing of the MASW type, downhole and crosshole testing; electrical resistivity tomography; microtremor measurements. (Moscatelli et al. 2011)

2.2 *Stratigraphic reconstruction*

The borings carried out in the subsequent investigation campaigns show a clear but complex lithological sequence; consisting of the following layers from the top-down.

(The numbering T1, T2, etc., indicates an entire formation within which various types of soil are present, identified by the acronyms MVA, VGU2, h, etc. in the geological profile of reference shown in Figure 2).

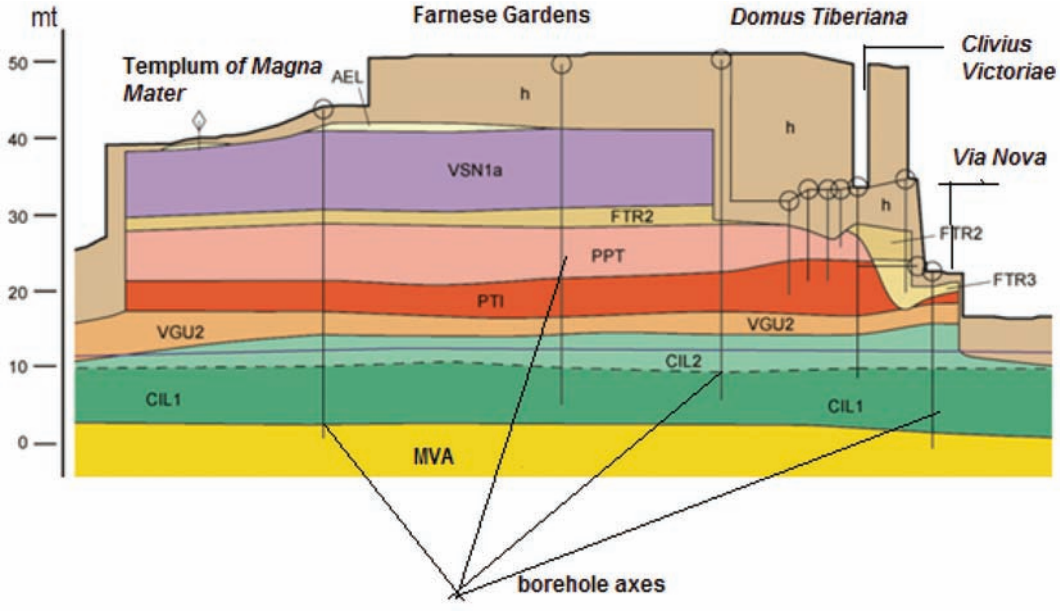

Figure 2. Geological profile orthogonal to the front in figure 1 (Moscatelli et al. 2011).

- Soil T1 (h): archaeological layer including the remains of walls and filling materials with a roof at +51 meters a.s.l. and thickness varying from a few tens of centimeters to about 10 meters, at times overlying a thin layer of compact silts (AEL).
- Soil T2: late pleistocene complex of fractured and altered volcanic tuffs (VSN1a) at the surface, to nearly compact and compact tuffs (PPT, PT1) in depth, for a total thickness of about 22 meters and a roof at +40 meters a.s.l.; they are separated by an episode of fluvial deposits of compact yellowish fine sands and tawny clayey silts (FTR2, FTR3), having thicknesses varying from 5 to 15 meters along the front of via Nova.
- Soil T3: (VGU2, CIL1, CIL2): Sicilian complex (late pleistocene) consisting of yellowish sands overlying firmly packed sands and gravel with total thickness of 16 meters and roof at +18 meters a.s.l.
- Soil T4: (MVA): plio-pleistocene complex consisting of very compact grey clayey silts with roof at +3 meters a.s.l. approximately.

The layers are characterized by a quasi sub-horizontal position even though a marked sag is visible in the deeper PT1 tuff formation, subsequently filled with fluvial deposits (FTR2, FTR3).

The water table is located in the Sicilian complex layer of sands and gravels (soil T3).

Table 1. Soil parameters.

Soil	γ (KN/m^3)	c′ (kPa)	ϕ' (°)
T1	19	10	27
T2a,T2c	22	30	40
T2b	19	30	30
T3	20	0	42
T4	20	20	27

2.3 *Mechanical characterization of soils*

The average physical and mechanical characteristics of the identified lithological units shown in Table 1 have been obtained from all in situ and laboratory tests, carried out during past and recent (2010) campaigns.

It is worth recalling the meaning attributed to the abbreviations used for the studied soils: T1, filling materials; T2a superficial tuffs; T2c deep tuffs; T2b intermediate silts; T3 sands and gravels; T4 deep and very compact clayey silts.

2.4 *Types of foundations and supporting soils*

Stratigraphic and archaeological reconstructions make it possible to define the types of foundations and their relevant supporting soils with a good approximation. (Ascoli Marchetti 2006)

Along the front facing the Forum, characterized by arches and *tabernae* brought to light by

excavation campaigns, various zones can be distinguished. From the top of the Palatine down to about 30 meters from the *Via Nova* front, the Domitian structures have direct foundations on the superficial tuff (T2a) or deeper down in the lithoid tuff bed (T2c); in the 30 meters close to the *Via Nova,* the structures built by Hadrian that were added to the Domitian preexisting ones either rest on former structures or have direct deeper foundations in the silty sandy deposits (T2b), that filled the deep tuff sag.

Along the front looking towards the Velabro, characterized by the high Farnese Bulwark supporting the overlying gardens, the ancient structures are still mostly buried.

A basement area can be distinguished lying on the deep tuff bed (T2c). This zone presents back walls belonging to ancient *tabernae* and orthogonal large brick septum walls resting directly on the tuff, which however, being in a state of ruin, no longer carry on their original buttress function in support of the back walls.

The sand and silt layer (T2b) outcrops along the slopes, above the basement zone resting on the deep tuff (T2c) and beneath the reddish more superficial tuff bed (T2a).

3 INSTABILITY CAUSES

The soil movements and the consequent structural distresses in a large part of the complex are probably due to environmental changes dating back to pre-Augustan times, when century-old trees on the steep slopes of the hill were removed: It was probably a sacred forest, the so named *lucos Vestae*, quoted also by Cicero.

The alarming phenomena of 1970 showed up a static problem that was probably present at the time when Hadrian expanded the building (2nd century AD); witness of this is the presence of a double brick lining in the back walls of the *tabernae* looking out on the *Via Nova* and the unusual pattern of the rows of *bipedalis* (double length bricks) on some walls that can be accounted for as measures taken during construction to hold back ground settlements.

Major collapses were obviously caused also by some disastrous earthquakes that occurred in the 4th and 7th centuries; subsequently, the collapse phenomena probably stopped, while continuous despoliations of the ancient buildings began, together with excavations to isolate the slopes of the Palatine Hill.

So there are distress causes that acted from the constuction time, given the difference in foundations soils among structures that were rigidly linked in the above ground portions; others that acted throughout the centuries like the masonry despoiling of the structures and the vaulted ceilings between the current level of the *Via Nova* and the hill top. Actually an important massive element of change at the basement of the structure is represented by archaeological excavations starting from the early twentieth century and the demolition of part of the Farnese Bulwark that surrounded the base of the hill. Other causes are currently at work, like the disorderly flowing from the hill top of rain waters that erode the volcanic deposits, the slope instability due to lack of counterweights downhill, the different seismic responses of structures whose foundations have uneven depths and rest on soils having different mechanical behavior.

On the Velabro front, today covered by the Farnese Bulwark and the overlying gardens, there is another vulnerable spot where the structure collapsed in the 19th century, namely where the sand layer included between the two tuff formations is subject to the slope erosion. On the one hand the exposed sand has progressively crumbled, due to rain and wind, thus depriving the overlying degraded and fractured tuff of its support; on the other hand, the sand layer made it easier tunnels and drifts digging to extract the tuff used for new buildings.

4 MONITORING AND RESTORATION

Continuous monitoring through extensometers distributed evenly on different masonry structures at various elevations has guided the complex and innovative restoration design (Filetici 2011), and the carrying out of the works.

The first monitoring operations date back to August 1971 (Joppolo 1998); the subsequent campaigns by Marnetto (1984) and by Fanelli & Cavallotti (1994) enabled the first geotechnical model to be built of the Domus complex (Calabresi & Scarpelli 1998). Geodetic monitoring continued over the time span between April 1985 and July 2012 with an interruption between July 1994 and April 2006.

Here we report the results of the settlement measurements that for the 1985–2011 period show a continuous settlement of Hadrian's structures at a rate of 0.2–0.3 millimeters per year, occurring mainly in autumn. The average settlement recorded during the above mentioned period amount to 22 mm at an average rate of about 1 mm per year.

From April 2007 to April 2009 settlement increase rate was much higher, of the order of 5 millimeters per year, then it decreased considerably and it almost stopped in the period between 2009 and 2012 after the implementation of restoration measures.

Taking account of the geotechnical and the environmental conditions the restoration of the

Hadrian's structures overlooking the Roman Forum was carried out by rebuilding the collapsed parts of the foundation and above ground structures by means of shooting portions of barrel vaults, reconstituting dividing brick walls, that have assumed the function of useful buttresses and by implementing stainless steel chains for a general improvement (Filetici 2006, Filetici et al. 2006). Adequacy of the foundations was therefore tested intervening with local repair of injuries by means of massive scaffolding and anchor bolting of the existing walls. (Croci et al. 2011).

On the Velabro front (Fig. 3), along the side where the Farnese Bulwark had collapsed during the 19th century, interventions of various kind were adopted: the reconfiguration of some buttresses to contrast the collapse of the overlying front; the regularization of the collapse front; the construction of a reinforced masonry course at the wall top integrating the portion of the still remaining boundary Nero brickwork (Carluccio 2011). The restoration project also included measures to protect the exposed sand layer from erosion by planting special anti-erosion shrubs on the hill slope.

Difficult and complex excavations are currently underway to bring to light precious Roman hypogeums and phases of republican age to date unpublished.

Figure 3. Restoration works along the Velabro front.

5 STABILITY ANALYSES

The moderate, but ongoing, settlements shown by the monitoring equipment have prompted the need of evaluating the safety margin of the *Domus* current configuration with respect to limit equilibrium conditions and the effects of the structural works envisaged by the restoration project.

The performed stability analyses refer to: a) the bearing capacity of the foundations of the reinstated septum walls, which acted as a bearing skeleton for the *Domus* expansion towards the Roman Forum made by Hadrian; b) the safety factor against sliding of the whole unit of the foundation soil and the overlying building.

The analyses involve the part of the building rising between the *Via Nova,* the road that runs along the northern slopes of the Palatine, and the *Clivius Victoriae*, a way that was laid out in ancient times to connect the Velabro area with the top of the hill.

The bearing capacity analyses were carried out at the septum walls identified by the labels M1, M2, M3, M4, M5, whereas the global stability analyases concern the most significant septum walls in terms of overlying loads and type of bedding, M3 and M5.

The analyses were performed in compliance with the safety rules currently in force (NTC 2008) following Approach 1—Combination 2, namely taking account of unvaried permanent actions, increased variable actions, decreased geotechnical parameters and final structural resistance.

For the stratigraphy reference was made to: the geological profile presented in Fig. 2, performed at septum M5; the orthogonal profile shown in Figure 4; the geotechnical investigations results. They show that the thickness of the silty layer in contact with the foundations varies in both

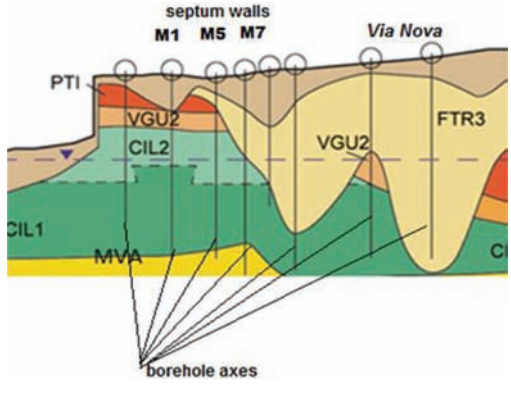

Figure 4. Detail of the geological profile parallel to the front in figure 1 (Moscatelli et al. 2011).

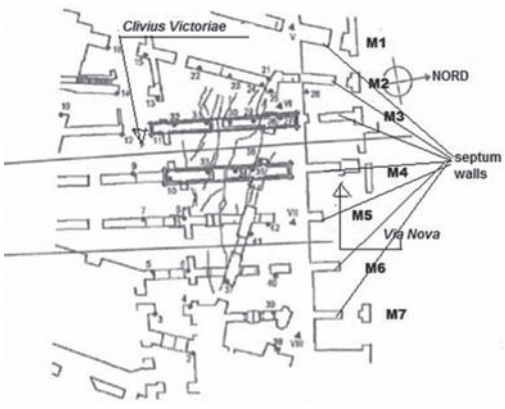

Figure 5. Layout of the foundation septum walls along the *Via Nova* (Calabresi & Scarpelli 1998).

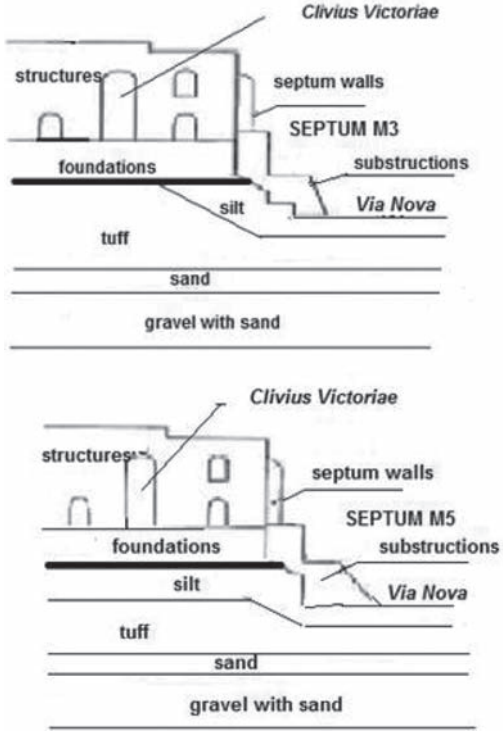

Figure 6. Stratigraphy sketch at septum walls M3 and M5 (Calabresi & Scarpelli 1998).

directions. The assumption was therefore made that there is a linear variation of the average thickness of the silt between the M1 septum and the M5 septum, from 0 to 8 meters, adopting the weighted average of the mechanical properties.

The layout of the septum walls and the diagram of the calculation stratigraphy for septum M3 and septum M5 are shown in Figures 5, 6.

The analyses which have been carried out both to verify the bearing capacity of the foundations and the overall stability of the soil-superstructure unit show that in static conditions the safety factor values are acceptable, provided that the original continuity of the foundation walls is reinstated; the same does not hold for the analyses run in seismic conditions which provide safety factor values close to one (Cavalera & Ascoli Marchetti 2011); however, recent studies on the local seismic response of the area (Pagliaroli et al. 2011) suggest seismic stress values below those envisaged by the NTC08 Rules adopted in the analyses.

6 CONCLUSIONS

All the geotechnical studies carried out in support of the structural restoration project of the *Domus Tiberiana* currently confirm the absence of extensive or significant instability phenomena. The reinforcement measures adopted or envisaged, which are based on the understanding and restoring the original static scheme of the structures, are aimed to save their full archaeological value avoiding any improper structural insertion.

The recent rather moderate settlement trend is somewhat compatible with a general subsidence of the whole alluvial area of the Tiber (Fanelli 2011).

This phenomenon entails the need for ongoing and widespread monitoring of the masonry structures in order to highlight any anomalous behavior or sudden increase of subsidence rates, well before any dangerous condition should occur.

REFERENCES

Ascoli Marchetti V. 2006. Relazione geotecnica di accompagnamento al progetto di restauro della Domus Tiberiana in Roma.

Calabresi G. & Scarpelli G. 1998. Domus Tiberiana-Studi e ricerche di geotecnica. *Area Archaeologica 95*: 379–407.

Carluccio G. 2011. Considerazioni strutturali sulla sicurezza e interventi per il miglioramento e la conservazione. In M.G: Filetici (ed.) *Domus Tiberiana. Scavi e Restauri: 1990–2011: 190–197.* Milano: Mondadori

Cavalera L. & Ascoli Marchetti V. 2011. Terreni di fondazione e analisi geotecniche. In M.G: Filetici (ed.) *Domus Tiberiana. Scavi e Restauri: 1990–2011:131–137.* Milano: Mondadori.

Cavallotti D.F. & Fanelli V. 2011. Controlli delle condizioni di equilibrio statico dell'area archeologica centrale. In M.G: Filetici (ed.) *Domus Tiberiana. Scavi e Restauri: 1990–2011: 128–130.* Milano: Mondadori.

C.I.S.Te.C. 2003. Sondaggi geotecnici ed archeologici effettuati nell'area della Domus Tiberiana nel periodo 1972–1999 (unpubl).

Croci G., Bozzetti A., Donatelli A. 2011. Il progetto di consolidamento statico e antisismico. In M.G: Filetici (ed.) *Domus Tiberiana. Scavi e Restauri: 1990–2011: 114–119.* Milano: Mondadori.

Fanelli V. & Cavallotti D.F. 1994. Osservazioni geodetiche dei movimenti plano altimetrici delle strutture prospicienti la via Sacra e controlli dei movimenti relativi e delle lesioni (Ottobre 1985–Luglio 1994) (unpubl.).

Filetici M.G. 2006. La Domus Tiberiana ed il crollo del Bastione Farnesiano: costruzioni e interventi per la sua riconsegna alla città. *Atti del VI Convego ARCo Nazionale Manutenzione e Recupero della Città storica, Mantova, 30 novembre 2 dicembre 2006.*

Filetici M.G., Calabresi G., Ascoli Marchetti V., Carluccio G. 2006. The Domus Tiberii in the Palatino hill of Rome. A complex intervention of strengthening to restore the soul of the site". *International conference on Structural Analysis of Historical Constructions, New Delhi 2006.*

Filetici M.G. 2011. Domus Tiberiana, Scavi e Restauri 1990–2011. Milano: Mondadori.

Ioppolo G. 1998. Domus Tiberiana—Sostruzioni Palatine sulla Via Nova—Rilievi e analisi del dissesto strutturale (1970–1972) (unpubl.).

Marnetto R. 1984. Domus Tiberiana al Palatino—Indagine sull'assetto strutturale del monumento nel tempo: strumentazione misure e rilievi (unpubl.).

Moscatelli M., Mancini M., Pagliaroli A., Corazza A., Simionato M., Stigliano F., Piscitelli S., Cicogna A., Cavinato G.P. 2011. Assetto geologico del sottosuolo della Domus Tiberiana. *In* M.G: Filetici (ed.) *Domus Tiberiana. Scavi e Restauri: 1990–2011:296–302.* Milano: Mondadori.

Pagliaroli A., Quadrio B., Sanò T., Sabetta F., Castenetto S., Naso G., Moscatelli M., Lanzo G., Di fiore V. 2011. Risposta sismica locale dell'area archeologica comprendente il colle Palatino, i Fori e il Colosseo. *Roma archæologia 2011-Interventi per la tutela e la fruizione del patrimonio archeologico-terzo rapporto.*

This page intentionally left blank

Geotechnical Engineering for the Preservation of Monuments and Historic Sites – Bilotta, Flora, Lirer & Viggiani (eds)
© 2013 Taylor & Francis Group, London, ISBN 978-1-138-00055-1

New underground lines in historic centres: Experiences in Naples

E. Campa, A.M. Ajmone Cat, C. Fioretti & L. Mormone
Astaldi S.p.A., Engineering Department, Rome, Italy

ABSTRACT: For some time now, Astaldi S.p.A. (AST) has been engaged in building infrastructures that interact with pre-existing sites and structures of historic and artistic importance. This article illustrates one of the experiences gained in recent years, in building new undergrounds in major historic centres. In Naples, in delicate areas of the historic centre, an underground station is under construction (Line 6, San Pasquale station), excavated in loose pyroclastites and sands beneath the water table, avoiding impacts on the surrounding buildings (e.g. Palazzo Ruffo della Scaletta, with its frescoes). The work's successful outcome is the result of an organisation careful to the collaboration between the contractor and all the local stakeholders (Municipality, Heritage Authorities, the Academic consultants, the local company for urban transportation).

1 INTRODUCTION

For some time now, Astaldi S.p.A. (AST) has been engaged in carrying out major civil works, including transportation infrastructure (railways, ports, undergrounds …), which often interact with sites and structures of historic importance—where such interaction is an element of fundamental importance in determining the possibility of and procedures for intervention. Along this "path," collaboration with the local bodies and experts plays an essential role.

In Italy, mention should be made of the cases, among others, that involved the Aurelia railway tunnel near Rome's St. Peter's Basilica, in the late 1970s; the sites along the high-speed Rome—Naples railway line in the 1990s (Corcolle, Casal del Dolce); two new piers at the Porto Torres port in Sardinia (on the site of nineteenth-century port works, built with materials from the Roman era); the new Turin station (interaction with seventeenth-century Savoy defensive tunnels by Pietro Micca), in 2011; and currently, the centre of Genoa and monumental areas in Milan.

Similar experiences recently completed in Brescia or underway in Rome (Line C) are discussed in companion papers submitted to this Symposium.

AST is operating in similar settings in Bucharest, Warsaw and Istanbul as well. The following are some aspects of an experience in progress in Naples along the underground Line L6 under construction, for the "San Pasquale" Station.

2 UNDERGROUND L6, "S. PASQUALE" STATION

2.1 *Overview*

The "San Pasquale" station, under construction in Naples along the future underground line L6, is in a particularly "sensitive" urban setting, along the Riviera di Chiaia, adjacent to the Villa Comunale public park, and up against some seventeenth- and eighteenth-century buildings of monumental importance, under the protection of the Heritage Authority. All this area is relevant from a historic—artistic, social, and commercial point of view; and the church of San Pasquale, in the heart of this setting, gives the station its name (Fig. 1).

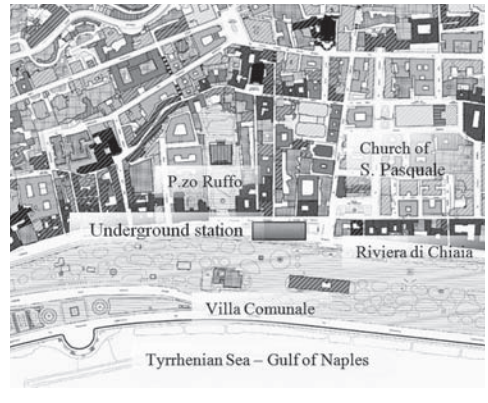

Figure 1. S. Pasquale Station. Urban setting-main interactions.

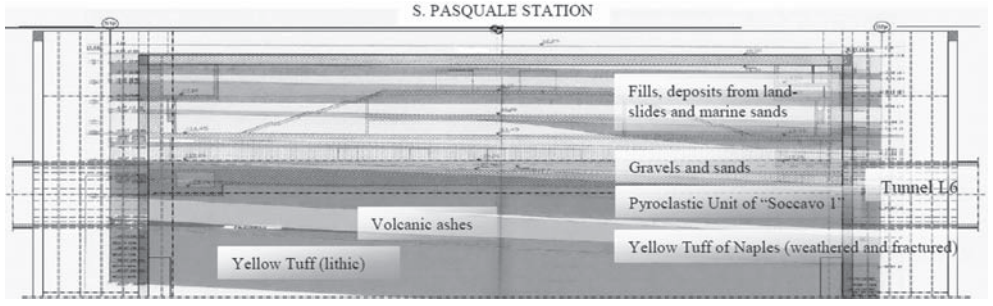

Figure 2. S. Pasquale station. Geotechnical soil profile.

Local ground conditions (Viggiani 2008) are characterized by sandy and clayey pyroclastic deposits in chaotic alternation, with variable thickness and interlayers of pumice/volcanic ashes (Fig. 2 above). The lithic substratum is in "Yellow Tuff" (weathered and fractured on top). For about 3 metres on top, these soils are the result of overfills realised by the Bourbon kings for a major urban reorganization and expansion plan of the city along the coast (from C. Vanvitelli's design, "Real Passeggio di Chiaia alla Villa Comunale", 1780).

These fills are thus subject to archaeological constraint, as are deeper deposits from 5 to 6 m in thickness (alluvial and marine deposits, mainly resulting from ancient coastal landslides, probably involving Roman buildings or remains in the modern-day Vomero Hill area).

Given the close proximity to the coast, the water table is found at max 1 m below the ground level.

The historic buildings, as well as the more recent ones, thus have very shallow foundations resting directly on such fills, which in general are poor and loose, with low density or stiffness and strength.

Some geotechnical characteristics for tuff and pozzolana (cemented layers) are shown in Table 1.

The typical characterization for granular materials according to elastic-plastic constitutive models is summarized in Table 2.

Such foundations are then quite "sensitive" to even small water table oscillations, and to the effects of vibrations or subsidence. During works, a series of issues needed to be faced. The following ones are some elements of more direct importance for the specific aspect of the interaction with the above-described historical setting.

What is described is the result of close cooperation between the Municipality of Naples, the licensing authority (with the support of a Scientific Committee), along with a Riviera Committee of Citizens for the area's protection, and Ansaldo STS, as Concessionaire, relying on the broad experience of the Metropolitana di Napoli S.p.A. and the technical assistance of specialists from Naples

Table 1. Design parameters for lithic/weakly cemented layers.

	Yellow Tuff pozzolana	Yellow Tuff of naples
γ_d [kN/m^3]	14	14
γ_{sat} [kN/m^3]	16	16
γ' [kN/m^3]	6	6
E [GPa]	2,21	6,36
c [kN/m^2]	500	500
φ [°]	27	27
ν [–]	0,3	0,3
T. strength* [kPa]	150	150
Perm.K [m/s]	3E-04	3E-05

*T: tensile strength of the Yellow Tuff of Naples (Mohr Coulomb).

Table 2. Typical design values for granular soil parameters.

	Fills and marine sands interbedded	Pyroclastic layers (undisturbed)
γ_d [kN/m^3]	16	14
γ_{sat} [kN/m^3]	18	16
γ' [kN/m^3]	8	6
E_{50}^{ref}* [MPa]	70	268
E_{oed}^{ref}* [MPa]	70	268
E_{ur}^{ref}* [MPa]	210	804
c [kN/m^2]	0	0
φ [°]	36	36
ν_{ur} [–]	0,3	0,3
p^{ref}* [kPa]	100	100
m* [–]	0	0
K_0^{nc} [–]	0,465	0,465
Perm.k [m/s]	3E-04	3E-04

* Definitions according to the constitutive elasto-plastic Hardening Soil model in Plaxis (stress dependent elastic moduli and non-linear, different loading—unloading behaviour).

University "Federico II". The specialized consortium "3S" was in charge for monitoring operations, on the behalf of the Municipality; and the temporary association "Linea 6" was tasked with designing and carrying out the civil works. Astaldi S.p.A., acting as the executor of the civil work of the San Pasquale station, in turn relied on the support of many specialists, some of them from the Second University of Naples, "SUN".

3 DESIGN REVIEW FOR THE PRESERVATION OF THE URBAN SETTING

3.1 *The guidelines*

The original station layout was placed right up against the buildings facing the Riviera di Chiaia (as shown in Fig. 3).

The initial design called for realising a perimeter of diaphragm walls of panels, conceived to be excavated with mechanical grabs, and relatively "short" (to reduce the need for excavations into the layer of tuff present as substratum in the whole area, for the purpose of containing the vibrations and duration of the works interfering with the surface).

These panels were then thought to exchange reciprocal contrast on 5 levels of metal struts.

Furthermore, to prevent water table oscillations around the perimeter, excavation within the station was initially planned to be done without lowering the water level, by means of buckets (without creating a gradient from outside to inside the perimeter), as it was for the casting of the bottom slab, planned to be made in water as well (using special fiber reinforced concrete mixes, a solution already applied elsewhere with positive results).

However, as already mentioned, it was necessary to carry out archaeological excavations at the site, proceeding by sub-horizontal layers down to about 8 m below ground level.

Originally, it was also planned that the TBM (diameter of the cutterhead, D = 8.15 m) would stop once the station had been reached. The resumption of excavations would have taken place from the opposite West side of the station, after the completion of the bottom slab and the maintenance of the TBM. This solution required significant occupation time of the work site areas at surface.

Again, due to the site's specific nature and conditions, the "traditional" excavation of diaphragm walls (e.g. with rope grabs and bentonite muds) would have required first carrying out a fill embankment along the entire work perimeter (with increased and prolonged occupation of the surrounding area); this was in order to reach, with the working levels, elevations useful for guaranteeing a suitable mud head level. Lastly, the presence in the subsoil of looser and more permeable layers or lenses would have entailed risks of loss of muds, and thus of instability of the surroundings; while the abundant sandy matrix of the aforementioned soils would have required intensive sand removal from the muds, thus impacting on the timeline and on the environment.

The design was then adjusted to the specific setting and to the aforesaid needs, by introducing some modifications as described in the following.

3.2 *Refinement of the layout of the station*

The detailed design review and refinement was based on specific studies regarding the risk of damage to the surrounding masonry structures, through accurate FEM2D-3D models for the most important and "sensitive" buildings (including

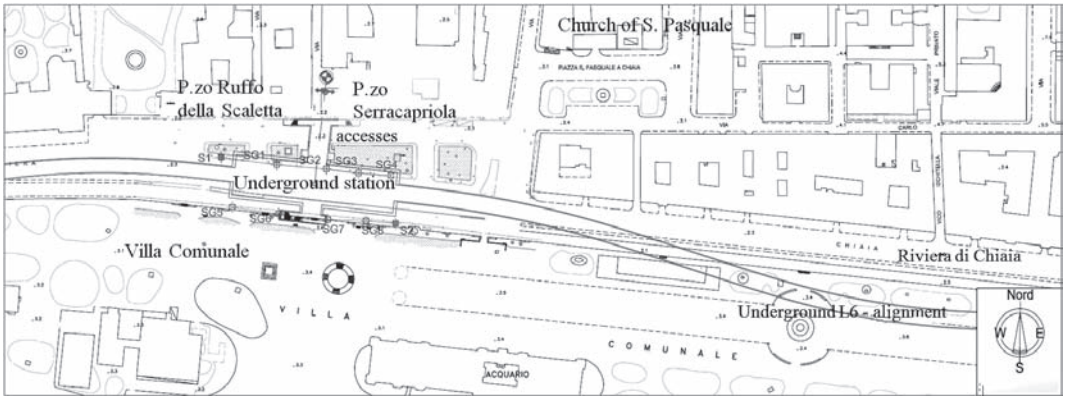

Figure 3. S. Pasquale Station, original layout and accesses.

simulations of possible impacts in different scenarios of geometry and excavation steps; Cavuoto 2011). Moreover, given the relevant risks of seepage flow from the built area towards the excavation, a 2D filtration model was also developed, to compare various scenarios; the outcomes of all these analyses made it possible to select the solutions and constructive details summarized below, which enhanced the safety of both the setting and the excavation (Fig. 4, Fig. 5; for a recent overview, Mormone & al. 2013, in press).

First of all, the station's layout was modified, shifting the accesses and the shafts away from the buildings, as well as reducing the excavation depths for the accesses itself (two levels, instead of the three initially planned).

This new layout significantly reduced the geometrical interferences also with the particularly intense traffic in the surroundings, and above all it helped to reduce the risk of impacts on the buildings nearby. Further, the entire station plan was shifted a few metres in order to safeguard an age-old magnolia tree important for the local skyline and environmental protection, with the slight consequent modifications of the underground alignment.

On the Villa Comunale side ("South" side, the old urban waterfront), the excavation for the lateral technical shafts was limited to a single level, both for safety/accessibility needs and in order to fulfill the requirements from the Authority on Cultural and Environmental Heritage and Assets (Fig. 6).

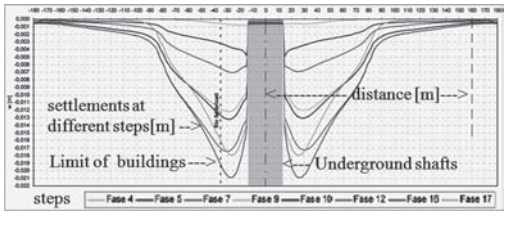

Figure 4. Evaluation of settlements induced in different phases.

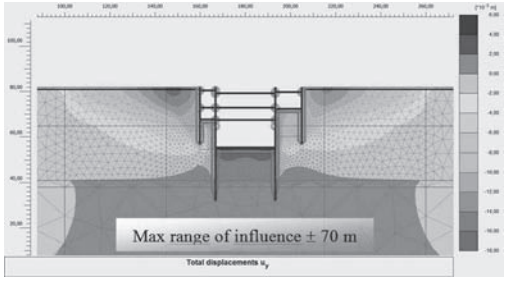

Figure 5. Numerical model and evaluation of the interactions.

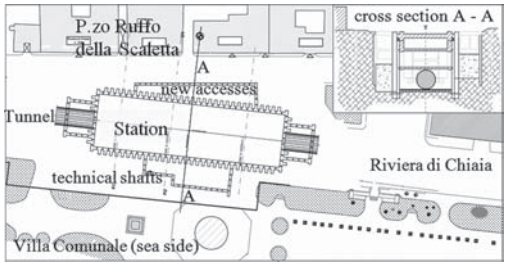

Figure 6. Final layout optimised with a refined alignment.

3.3 *Diaphragm walls and excavation phases*

The diaphragm panels were deepened at least 10 m in the tuff (well below the first initial meters, usually more fractured and heterogeneous). Moreover, the panels themselves were realized with a rigid "T" shape (1.2 m thick), excavated using hydromills. Only the panels at the corners and those for lateral shafts (1 m thick) were excavated with mechanical devices and sealed with jet grouting columns.

This solution gave the diaphragm walls greater rigidity, fostering the containment of horizontal deformation with related possible losses of volume behind, and therefore reducing the risks of damage for the adjacent buildings and the surrounding area.

Moreover, the 5 orders of struts were thus replaced with only two levels of intermediate slabs (90 cm in thickness each), excavating the bottom of the first contrast slab down to –7.1 m (beneath the ancient ground level and the strata of archaeological interest, Fig. 7), and then (after the TBM boring) excavating the subsequent slab down to –15.35 m, so as to obtain greater ease and speed of execution for the whole excavation phases (enhancing the safety through their simplification), including the surveys ordered by the Heritage Authorities (Fig. 8).

Both these two slabs were cast in one phase each on the entire station plan, always for ease and speed of completion. Therefore they could quickly take on loads, so ensuring early and diffuse contrast for all the diaphragm walls. The final functional openings were subsequently completed through the demolition of the arrangements left for at each level. In certain parts of the perimeter (e.g. access side towards the buildings, North shaft), the presence of the "stems" of the "T" panels inside the volumes to be excavated also resulted in partial demolition requirements.

Furthermore, with this configuration it was possible to "free" the route for the TBM, placing the bottom depth of the excavation at –24.6 m below g.l. (bottom slab 280 cm thick, on 85 cm lean concrete).

Thus the entire station stretch was full bored by the TBM before beginning the excavation inside,

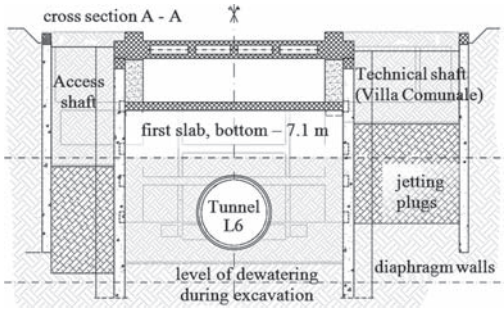

Figure 7. S. Pasquale Station. Structure during TBM operation.

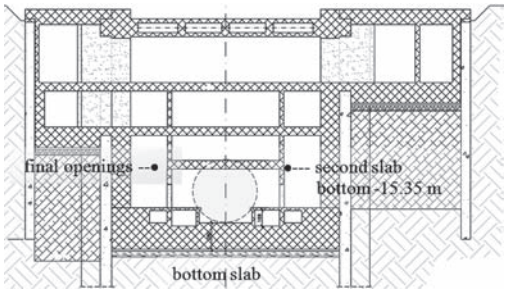

Figure 8. S. Pasquale Station. Final structural scheme.

thereby minimizing the risks of interaction with the water table and of soil losses when boring through the diaphragms. The reinforcements of the panels destined for being bored were made with reliance on the usual fibreglass bars.

Lastly, thanks to the greater stiffness of the panels, the safety and traffic restrictions that should have to be imposed in the surroundings were reduced, leaving larger paths free.

3.4 *Design solutions and operating details for the preservation of the historic setting*

Some construction refinements and details were also important for the preservation of the historic setting.

Using hydromill devices, for instance, made it possible to better seal the joints between panels, specifically since one diaphragm was "milled" in the other. And at the same time, the risk was reduced of vibrations and/or of loss of mud contrast pressure on the walls or at the bottom of the panels themselves, thus avoiding the need for grab handling in such poor and heterogeneous soils, mostly in the vicinity of the shallow foundations of buildings.

Again, to further minimize the risk of seepage and/or of losses of fine, or even of a larger instability of the diaphragm walls (especially in the first portion near to the ground level, an event which could determine heavy damages in the proximity of buildings or streets), a specific soil treatment was previously performed along the perimeter, down to depths of 6 or 10 m, using the low pressure Cutter Soil Mixing technique (C.S.M., 65 × 280 cm, 6 or 10 m depth, scheme in Fig. 9; L'Amante 2010, Mormone 2011, Mormone & al. 2013, in press).

For these shallow treatments, no use was made of jet grouting columns, in order to avoid both the risk of overpressures on the foundation side, and the need to "mill" the circular edge of such columns in the "T" shape of panels during their subsequent excavation (entailing greater costs and environmental impact for sand removal from muds). The jetting technique, on the other hand, was adopted with columns of a diameter of D 1500 mm, on a grid 105 × 90 cm, to realise: • the bottom plugs under the accesses (North side) and technical shafts (South) • some localised sealing treatments, and • the consolidation of soil in correspondence of the TBM entrance into and exit from the station (to limit to a minimum the loss of "seal" at the interface between the TBM and the diaphragms). After a relevant field test, this last intervention was operated within an "enclosure" of diaphragm panels on both sides, to prevent overpressures on building foundations and washing away from the water table. At the same time, the border structures for two West and East emergency shafts were completed.

Such shafts were needed to allow TBM maintenance, if in case, in safe conditions (Fig. 10).

3.5 *Demolition of the tunnel segmental lining during the excavation of the station*

After the TBM passage through the station area, a demolition of the installed segmental lining during the excavation for the entire station was required.

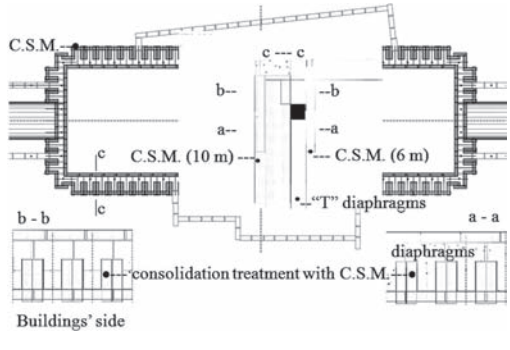

Figure 9. Primary consolidation along the border with C.S.M.

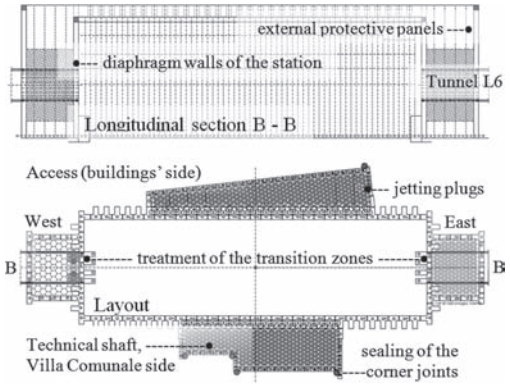

Figure 10. Jetting for gradual stiffness transition during TBM boring through the diaphragms, and plugs under the N/S shafts.

The structural features of the lining segments were calibrated for an overburden of at least one TBM cutterhead diameter (~8 m).

In the absence of this load, and still subjected to lateral confining pressures, the hollow tunnel could reach large plasticity strain conditions, and locally could even be brought into a field of structural instability during the removal of the crown segments. Thus, the related deformation could involve risks for personnel and, occurring in the absence of the bottom slab (see former Fig. 7), and induce uncontrolled decompression effects in the soil at the diaphragms' bottom.

The demolition of the segmental lining was therefore done by working in phases.

First, the tunnel was filled (isolating the stretch to be filled with end "plugs" in lightened cement mix), still preserving the minimum overburden structurally required (simplified scheme in Fig. 11).

Then, the outside excavation of the lining was performed in stages, carrying out the demolition in the crown by stretches, in parallel with the casting of the second contrast slab (former Fig. 8), and finally excavating down to the bottom (some steps are shown in Fig. 12).

3.6 *Monitoring*

Lastly, all the design and construction phases have been carried out with the aid of careful monitoring of the significant elements and components, in particular the soil response and the structural settlements, as well as the groundwater levels.

For the archiving and consultation of all the monitoring data along the L6 Line, Ansaldo prepared a specific data base and system on a GIS platform, accessible on line to authorized personnel.

Given the large volume of the diaphragm elements (about 300 m^3/each), during the phase for

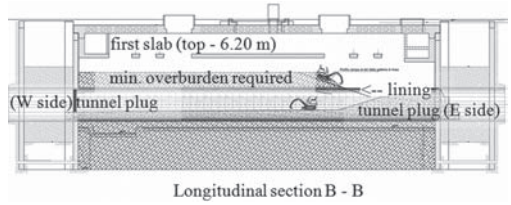

Figure 11. Filling the TBM tunnel along the station stretch.

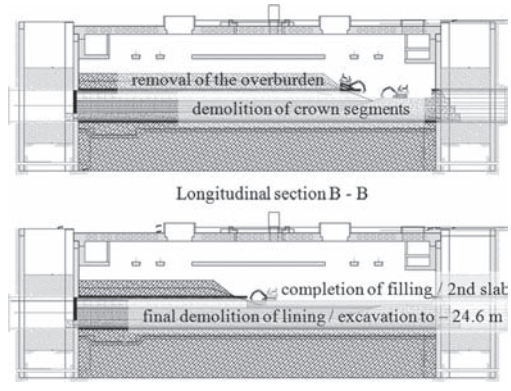

Figure 12. Demolition of segments in crown, completion of filling, casting of the second slab (–15.35 m), last excavation.

the excavation and casting of panels an inclinometric and settlements monitoring behind was planned with assestimeters and topographic levelling, in order to control the stress and strain paths around these large excavations and of the panels itself (a University degr, thesis was granted on the subject, Corbo 2009).

Then, by applying appropriate working rules, procedures and devices (including a suitable planning for the excavation sequences and configurations, timing and devices for placing the reinforcement, or the time casting of filling concrete), the final strains of the surrounding soil could be confined prevalently in the "elastic" field, obtaining high "retrieval" percentages following the concrete casting.

More generally, the inclinometric and structural monitoring with strain gauges and load cells, installed both on the reinforcements and in the concrete of the diaphragms and of the other new structures (including topographic measurements of convergence of the panels within the excavation), was continuous in all the working phases, along with the inclinometric and settlement monitoring of the soil behind (in particular in the area between the station and the buildings; L'Amante 2011).

These checks were constantly combined with an intensive and widespread topographic, structural and inclinometric monitoring of the buildings (Fig. 13).

The piezometric monitoring of the water table levels inside the station and in the surroundings outside also played an important role in each phase, particularly during the excavation, following the progressive deepening of the bottom, for both the assessments of the risks of stability and seepage of the excavation bottom, and the prevention of possible damage to the buildings (Fig. 14, Fig. 15).

Further, for the area of S. Pasquale, Astaldi S.p.A. performed a variety of preliminary permeability (Lugeon) tests, and pumping tests on four experimental wells at different depths.

Two pilot project shafts were also prepared and operated in advance for this purpose.

On this basis, AST designed and developed a specific SCADA (Supervisory Control And Data Acquisition) system to manage and monitor 8 definitive wells inside the excavation area, with pumping phases and schemes depending on the internal and external water table level (the SCADA provides its data to GIS as well).

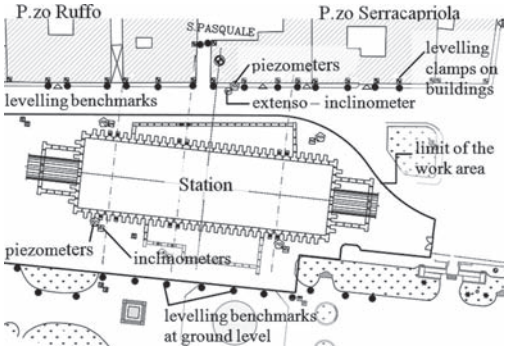

Figure 13. Some elements of the scheme of monitoring.

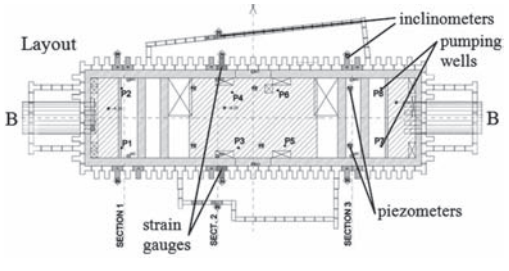

Figure 14. Piezometric and structural monitoring of the diaphragms, with the pumping wells, elev. –6.20 m (first slab).

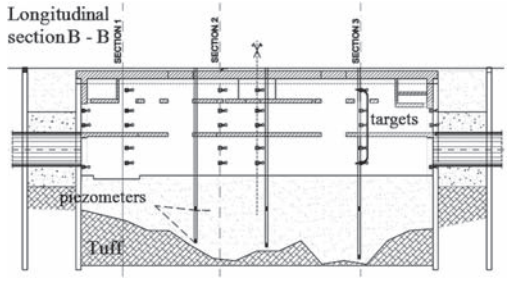

Figure 15. Piezometers and targets on the diaphragm walls for topographic monitoring.

This system is capable of acquiring, monitoring, and verifying in real time all the most significant parameters with regard to the development trends that are observed, and to corresponding pre-established alarm thresholds. The design, architecture, and initial calibration of this monitoring and management system, like the subsequent operation and maintenance, required the multidisciplinary interaction between a variety of parties, in particular between geotechnical specialists and experts in remote control systems, signal transmission and analysis, and in suitable, dedicated hardware and software systems (with contributions from AST, Boviar S.r.l., SUN). Careful "external" and general monitoring (GIS platform) and "internal" specific monitoring (SCADA) made it possible to manage the internal pumping system with no impacts on the outside environment. There were no major variations in the water table levels "outside" the diaphragm walls, particularly in the soil volume of major interest for the building foundations, while the levels inside the station at the end of excavation were lowered about 31 m beneath the initial "undisturbed" values.

A companion paper in this Symposium refers in detail to this subject (Mormone & al. 2013, in press).

Alongside the buildings, the settlements "δ" observed were contained within the established forecasts and thresholds (δaverage = 2 ÷ 3 cm); nor was any damage found on the most delicate and vulnerable buildings, and the excavation bottom was kept safe at all times.

4 PHOTO GALLERY

The pictures from Figure 16 to Figure 19 show the work area in the urban setting and some phases of the work with examples of elements of the internal monitoring and pumping out system.

Figure 16. Overview of the work area from the E side (Piazza S. Pasquale a Chiaia; Palazzo Serracapriola on the right).

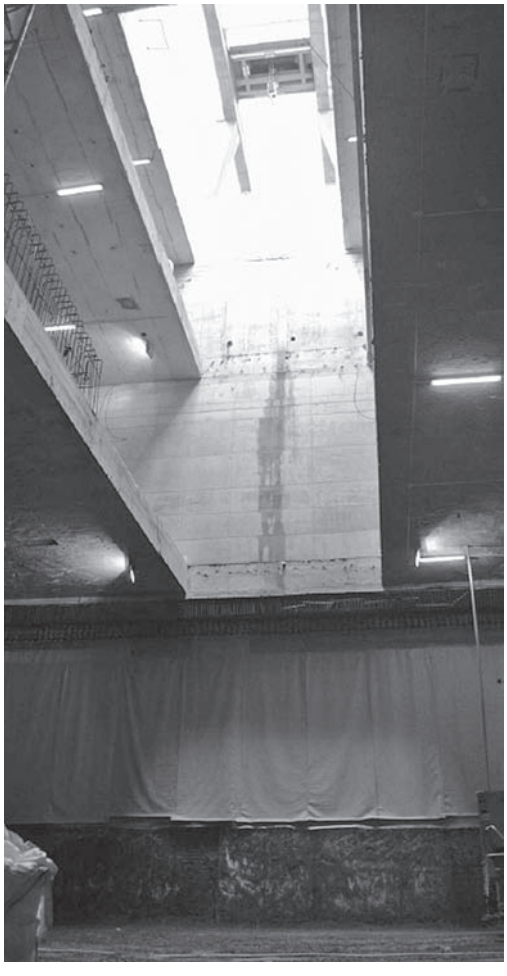

Figure 17. The crane bridge from the bottom of the station.

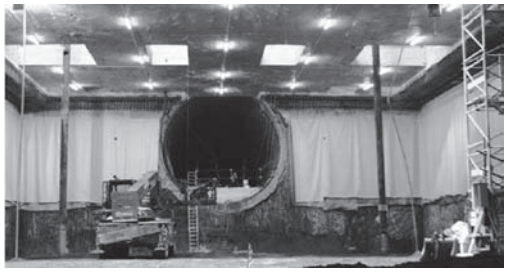

Figure 18. The L6 tunnel from the bottom of the excavation (East side of the station). Observe the two steel jackets hoisting the pumping wells P7 (right) and P8 (left) and the PVC protections of the piezometers along the monitoring Section 3.

Figure 19. Final excavation on the W side amidst some piezometers and the pumping wells P4, P2 (right) and P5 (left).

5 CONCLUSIONS

The experience described for the S. Pasquale underground station under construction in Naples (along the future L6 underground line) presents many elements similar to analogous ones in progress in other historic settings, for example in Rome.

Deep excavations over large areas, for example to build underground stations as in this case, may be realised with positive results near historic buildings and/or in densely urbanized, high-traffic areas, limiting their interactions, under the condition of positively adapting the design to the interfaces that are identified (even while the work is in progress).

The approach applied when facing situations of delicate interaction between the new works and the setting is in fact that of a detailed study of the working environment, of the excavation and consolidation sequences, and of the modes and technologies of operation.

Continuous checks, including preliminary test fields and appropriate monitoring operations in each phase, are understood as an active, integral part of the design and intervention.

An accurate reconstruction of the setting, and in particular of the prior construction and structural typologies and events, preferably including the stress/strain paths (both on the basis of documents, and through proper surveys for this purpose), is decisive.

The integration of knowledge and skills with administrations, universities and specific experts, from a search for historical sources to reliance on the most advanced available technologies, is also indispensable.

An overall engineering of the issues coordinates and capitalizes on various contributions, while combining them with construction experience. This allows appropriate solutions to be identified even in complex conditions.

REFERENCES

Cavuoto, F. 2011. Linea 6-Metropolitana di Napoli. Tratta Mergellina-Municipio. Stazione S. Pasquale. Progetto Esecutivo-Strutture-Variante Tecnica. Scavo del Pozzo di Stazione, Analisi dei Cedimenti, Relazione di Calcolo Spostamenti. Report LM67FX2B219. Metropolitana di Napoli S.p.A., Napoli Metro Eng. S.r.l., Studio Cavuoto Eng., on behalf of Ansaldo STS/Comune Napoli. Naples.

Corbo, A. 2009. Spostamenti indotti dalla realizzazione di una paratia di pannelli: misure ed analisi di un caso sperimentale. Tesi di Laurea. Tutors Prof. Flora A. & Eng. L'Amante D. Naples University "Federico II", Facoltà di Ingegneria, Dept. Eng. Idraulica, Geotecnica, Ambientale. Naples.

L'Amante, D. 2010. Comportamento di grandi opere di sostegno in area urbana. Dottorato di Ricerca in Ingegneria Geotecnica. Tutor Prof. Viggiani C., co-Tutors Prof. Flora A. & Prof. Russo G.. Granted by Naples Universities ("Federico II", "Parthenope", "Seconda Università"), Salerno Univ., "Sannio" Univ., in consortium. Naples.

Mormone, L. 2011. Linea 6-Metropolitana di Napoli. Stazione S. Pasquale. Il trattamento preventivo dei terreni, propedeutico alla realizzazione di diaframmi profondi non convenzionali. In Sabatino C. (ed.) *1° IAGIG Conf., Abstracts*: 94–96, *on behalf of Associazione Geotecnica Italiana and Ordine degli Ingegneri di Salerno*, Salerno.

Mormone, L.; Falconio, G. & Mandolini, A. 2013. Groundwater management during excavations of S. Pasquale station in Naples. In *Geotechnical engineering for the preservation of monuments and historic sites; Proc. 2° Intern. Symp., Napoli, 30–31 May 2013*. Rotterdam: Balkema (in press).

Viggiani, C. 2008. Linea 6-Metropolitana di Napoli. Tratta Mergellina-Municipio. Progetto Esecutivo-Elaborati generali. Relazione Geotecnica. Report LM67FX00010. Metropolitana di Napoli S.p.A., Metropolitana Milanese S.p.A., on behalf of Ansaldo STS/Comune Napoli. Naples.

This page intentionally left blank

Geotechnical Engineering for the Preservation of Monuments and Historic Sites – Bilotta, Flora, Lirer & Viggiani (eds)
© 2013 Taylor & Francis Group, London, ISBN 978-1-138-00055-1

The Benedictine Basilica of S. Angelo in Formis (Southern Italy): A therapy without diagnosis?

A. Cammarota, G. Russo & C. Viggiani
University of Napoli Federico II, Italy

M. Candela
Mediterranean University, Reggio Calabria, Italy

ABSTRACT: The Benedictine Basilica of S. Angelo in Formis was founded in the XI century by the Abbot Desiderio, over the ruin of a Roman temple dating back to the V century BC. It contains an outstanding cycle of frescoes with stories of Old and New Testament, probably the most important document of the medieval painting in Southern Italy. It is known that some repair works have been carried out in XVIII century; in 1930 an earthquake produced the collapse of the roof, reconstructed soon after. Starting in 1969 some fissures appeared in the central nave and gradually opened and extended to other parts of the Basilica. Following repeated alarms on the safety of the Basilica, geological survey of the area, subsoil investigations and geodetic monitoring of a number of points both inside the Basilica and outside have been carried out till present. The paper reports the results of these investigations, that confirm the occurrence of differential settlement of the monument. The attempts of interpretation of the observed movements and the possible interventions are discussed.

1 THE MONUMENT

A temple dedicated to Diana Tifatina had been erected in V century BC at the base of the South West side of the Tifata calcareous mountains in Southern Italy (De Franciscis, 1956). In AD 595 a Longobard church dedicated to the Archangel Michael was constructed over the ruins of the Roman temple, as reported in the "Regesto" of S. Angelo in Formis", in the library of the great Montecassino Abbey. In 1072 the Norman Richard the 1st, prince of Capua and count of Aversa, presented the church to the Abbott Desiderio, rector of Montecassino (Jacobitti, Abita, 1992). At the site of the ancient church Desiderio erected the present Basilica (fig. 1), whose floor is still lined with the white marble mosaic of the stylobates of the Diana temple, dating back to 150–170 BC. Capitals, columns and marbles were also reused for the construction.

The Basilica, in a simple and appealing Romanesque style, contains an outstanding cycle of frescos over the walls of its three naves. They represent stories of the Old Testament in the lateral naves, and of the New Testament (fig. 2) in the central one; a blessing Christ surrounded by the symbols of the four Evangelists is painted on the central apse (fig. 3), while the Final Judgment is painted on the opposite wall of the counterfaçade. The frescoes may be dated back to 1087, i.e. to the time of

Figure 1. The Benedictine Basilica of S. Angelo in Formis.

Figure 2. The Last Supper: Fresco in the central nave.

Figure 3. The blessing Christ. Fresco in the central apse.

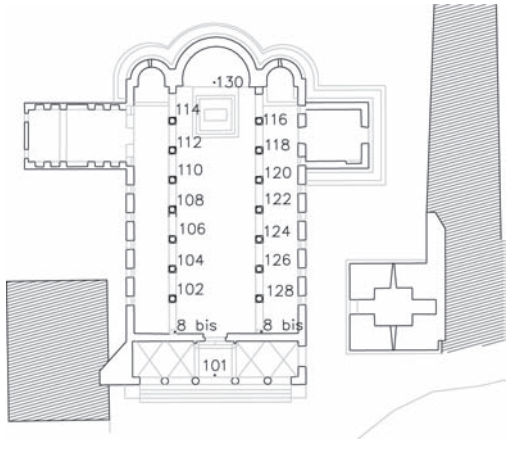

Figure 4. Plan of the Basilica.

Figure 5. Interior of the Basilica.

Figure 6. Abbott Desiderio presents the Basilica (fresco in the central apse); below: Representation of the Basilica in the Regesto of S. Angelo in Formis, in the library of the Montecassino abbey.

construction of the Basilica; they are inspired by the iconography of the byzantine art and are believed to have been painted by at least five different artists (Wettstein, 1960). After the destruction of the Montecassino Abbey during the World War II, the S. Angelo frescoes are probably the most important document of the medieval painting in Southern Italy; they have been saved in relatively good conditions, probably because they have been covered by whitewash in XVIII and XIX century.

The church has a Basilica plan divided in three naves, each one ending in a semicircular apse (fig. 4). The columns that divide the naves are made of different materials (granite, white marble and green marble) and have Corinthian capitals from the temple of Diana (fig. 5).

The façade is graced with a delicate portico or narthex of five arches, upheld by four Corinthian columns (fig. 1). The whole church epitomizes the ingenuity of Italians in reusing elements from earlier eras.

The courtyard in front of the church is retained by a front wall; this configuration is relatively recent, since there is memory of a stair bringing to the portico; furthermore older retaining structures are embedded in the fill below the courtyard. At the right there is a massive bell tower, whose base is made of white marble stones that were once part of the amphitheatre in Capua Vetere. Ancient iconography shows that the bell tower was originally on the left of the church (fig. 6) and the portico was different from the present one; both bell tower and portico probably failed for unknown reasons around 1200 and have been reconstructed, with the bell tower in a safer location.

The foundations of the lateral walls, the façade and the apses are very shallow and of the same thickness of the overlying masonry. The columns are founded over stone blocks with an height of

around 0.5 m and a square shape in plan with a side of 0.7 to 1 m. As it will be shown in the next paragraph, the apses and most of the lateral walls and columns rest on calcareous rock, while the façade, the portico and the front part of the sidewall are founded on debris or made soil.

2 THE SUBSOIL

The slope (fig. 7, 8) is composed by limestone and dolomite belonging to Trias—Cretacic, heavily fractured, somewhere brecciated and even mylonitized, interested by diffuse karst phenomena.The limestone are superimposed to Oligocene—Miocene deposits, composed by sandstones and variegated shaley clays with a chaotic structure. Limestone slipped over the Miocene formation, and such a tectonic superposition generated the fracture system affecting it. The rock formation is crossed by significant fracture lines in the North–South direction, and become thinner towards the plain.

Later on (30,000 to 35,000 years B.P.) the plain and the slopes have been covered by the grey Campanian tuff erupted by the Phlegrean volcanoes. Since then, the morphological and structural pattern of the area remained unchanged, except for the anthropic actions. Among them the retaining walls and the fill to realize, in successive stages, the courtyard of the Basilica, and the opening of stone quarries. At least three of such quarries are located within a few hundred meters from the Basilica; they have been cultivated till the 1980s with extensive use of explosives.

The water table is generally found at the boundary between the limestone, very permeable by fracturation, and the underlying complex of sandstones and clays.

Geophysical investigations allowed a detailed reconstruction of the subsoil of the zone surrounding the Basilica, which includes three horizons. The upper one is composed by made ground, for a thickness ranging from a few decimeters to some meters. Below the made ground a layer of fractured rock is found with a thickness variable between 15 and 30 m; it includes dolomite, slightly cemented dolomitic limestone and intensely fractured dolomite,

Figure 8. The Basilica in the calcareous dolomitic slope.

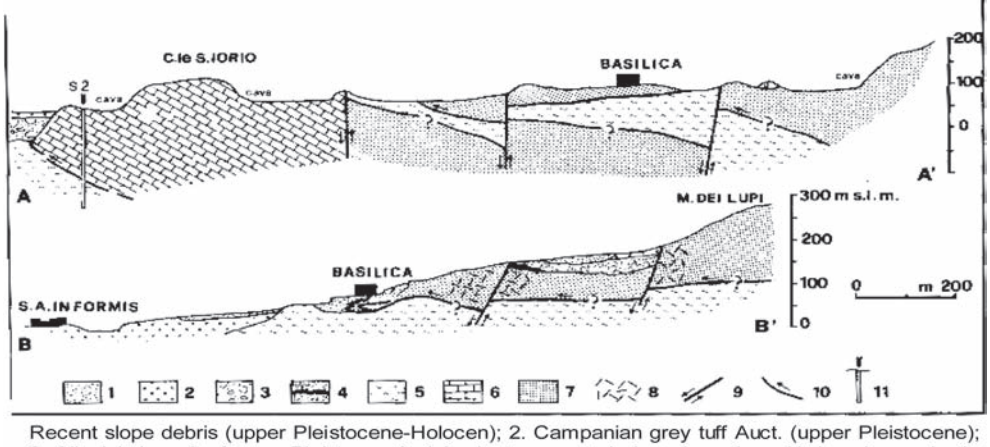

Recent slope debris (upper Pleistocene-Holocen); 2. Campanian grey tuff Auct. (upper Pleistocene); 3. Alluvial deposits (upper Pleistocene); 4.Ancient cemented slope breccias with basal pyroclastic level (lower-middle Pleistocene); 5. Sandy-clayey flysch (Caiazzo Sandstone-Tortonian); 6. Limestones (Cretaceous); 7. Dolomitic limestones and dolomite (Triassic-Jurassic); 8. rock; 9. Fault (dashed if supposed) ; 10. Thrust; 11. Boreholes

Figure 7. Geological sections of the slope. A) North–South. B) East-West (After Corniello, Santo, 1995).

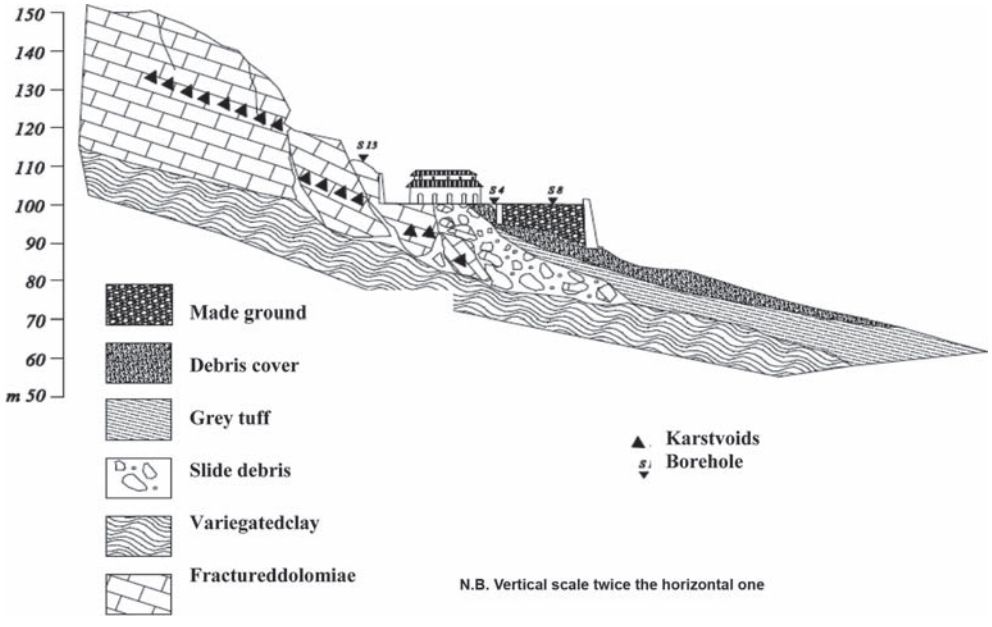

Figure 9. Schematic geological section of the area around the Basilica.

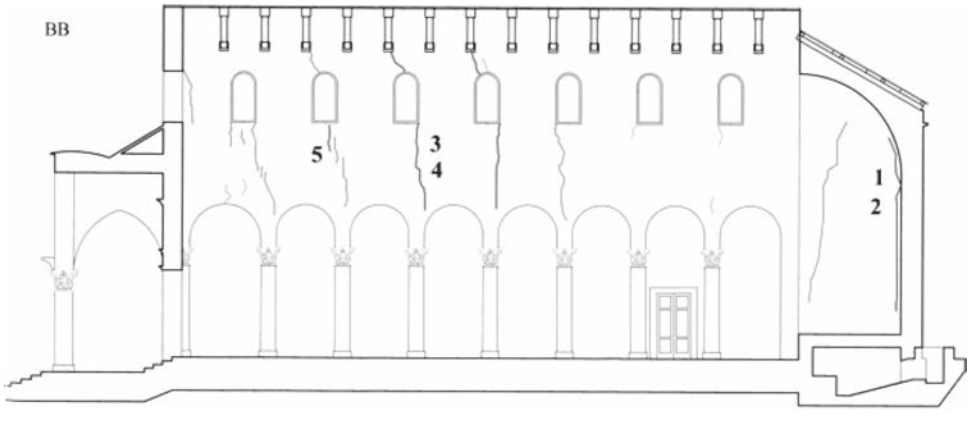

Figure 10. Pattern of the fissures in the Basilica.

besides cemented calcareous debris. Finally, the base formation of sandstones and variegated shaly clays is found.

The geological sketch in fig. 9 shows clearly that the Basilica is located across a stratigraphic discontinuity, with the apses and the backward part of the naves founded on rock, and the front on the debris cover or even on the made ground.

3 PREVIOUS DAMAGES AND REPAIRS

A stone in the right apse of the Basilica refers to repair works carried out in 1732 under the Cardinal Giuseppe Renato. Nothing is known about damages requiring such interventions; perhaps they were consequence of an earthquake occurred in the same year, with an MCS intensity equal to X

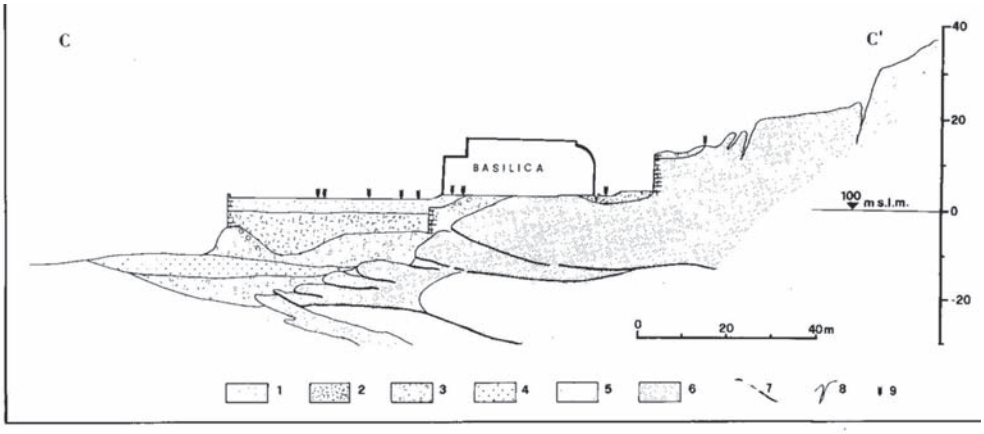

Figure 11. Detailed section of the subsoil of the Basilica (After Corniello, Santo, 1995).

in Irpinia and VIII in S. AgatadeiGoti, relatively close to the Basilica.

In 1930 a very similar earthquake produced the collapse of the wooden roof, that was reconstructed soon after.

A number of fissures had appeared in the walls above the columns and in the apse; they were repaired, and the frescoes restored "with the help of German experts". Further earthquakes of similar or higher intensity have been registered in 1962, 1970 and 1980; only the last one produced minor effects, as the displacement of some roofing tiles.

In 1969 some fissures appeared again in the walls above the columns of the central nave; in the following years the fissures gradually opened and extended to other parts of the Basilica, with a concentration in the right side of the façade and in the right nave near the façade (fig. 11). The occurrence of fissures was interpreted as the consequence of differential settlement of the foundations; an investigation of the subsoil of the monument was carried out and the opening of some fissures was monitored for about one year, in 1972/73.

At the end of the 1970s, following repeated alarms on the safety of the Basilica, some shoring was installed on the right colonnade, and a Committee formed by a geotechnical engineer, a structural engineer and a geologist was installed, with the task of interpreting the phenomena and sug gesting remedial measures.

The Committee promoted a careful geological survey of the area, some further subsoil investigations, a geodetic monitoring of a number of points both inside the Basilica and outside and some further measurements of the fissures opening. The results of investigation and monitoring are reported in two documents (Adriani*et al.*, 1980; Pellegrino, Pescatore, 1981).

The Committee inclined to think that the observed displacements and damages (that will be discussed in the next paragraphs) were essentially associated to the activity of the nearby quarries, where explosives were systematically used. Accordingly, the quarrying has been completely stopped since 1981.

Unfortunately, the fissures in the Basilica went on increasing, endangering the integrity of the frescoes; furthermore, there is a strong pressure for the removal of the internal shoring. A new cycle of investigation and monitoring has thus been started in 2012, with the aim of conceiving and implementing resolutory consolidation works.

The results of this long lasting activity are reported in the following paragraph.

4 INVESTIGATIONS AND MONITORING

4.1 *Subsoil profile and foundations*

The detailed profile of the subsoil of the Basilica, resulting from the consideration of all the site investigations carried out in different periods, including a geophysical survey, is reported in fig. 11. The geological pattern of the site is complex and articulated. There is a tectonic contact between the dolomitic limestone and the underlying Miocene flysch; the limestone layer superimposed to the flysch becomes thinner westward and is associated to and difficult to distinguish from slightly cemented calcareous debris. A layer of grey volcanic tuff is intercalated within the debris.

The groundwater table is found at the contact between the flysch and the overlying fractured limestone and debris. As mentioned above, the apses and most of the lateral walls and columns rest on fractured calcareous rock, while the front part of the sidewall, the façade and the portico are founded on debris and locally even on made soil.

4.2 *Settlement*

In the period between February 1980 and March 1981 seven geodetic surveys of the vertical displacements of some points inside and outside the Basilica have been carried out. A plan showing the location of the measuring points is reported in fig. 12. Inside the basilica, measuring points were installed on the base of each column, plus one at the entrance and one in the central apse. Points CS1 outside the basilica was located on a rock outcrop, while CS2 and CS3 on nearby constructions. During the whole observation period these latter benchmarks did not show any relative displacement to within 0.1 mm; the assumptions that they are completely stable appears hence supported. The points inside the church and the one on the wall retaining the courtyard, on the contrary, underwent measurable settlement. In the first three surveys, until April 1980, no displacements were measured; starting from the fourth one, the points on the courtyard and inside the church settled steadily up to a value of around 3.5 mm. No visible effects of the strong earthquake occurred in November 1980 was observed.

In July 2011, thirty years later, the external points CS2 and CS3 and the majority of the internal ones installed in 1980 have been recovered. A new series of periodic geodetic survey has been started. At the time of writing this paper, four further surveys have been carried out in May, September and November 2012 and in January 2013.

The results obtained in 1981/82 are reported in fig. 13. The church underwent an average settlement of the order of 1,5 mm, with a deformation in hogging rather equal on the two rows of columns. The central part of the church experienced no settlement on the right side, and a settlement of around 1 mm on the left side; the columns at the extremity on the entrance and on the apse side show a settlement of around 3.5 mm.

Assuming that CS2 has remained stable, fig. 14 reports the situation in 2012. The average settlement has increased to 30/40 mm, always with a definite trend in hogging. The central settlement increased to 30 mm on the left and to 10 mm on the right, while at the entrance the settlement equals 40 mm and at the apse 60 mm. The deflection ratio ranges from 0.7×10^{-3} on the left to 1.3×10^{3} on the right. These figures are compatible with the occurrence of fissuring (Burland, Wroth, 1975); indeed, the wall above columns at the right is definitely more damaged that the one on the left.

4.3 *Fissures opening*

Two series of measurements of the opening of fissures in the walls of the basilica were the frescoes are painted are available: the first one in 1974/75 and the second one in 1980/81. In both periods covered

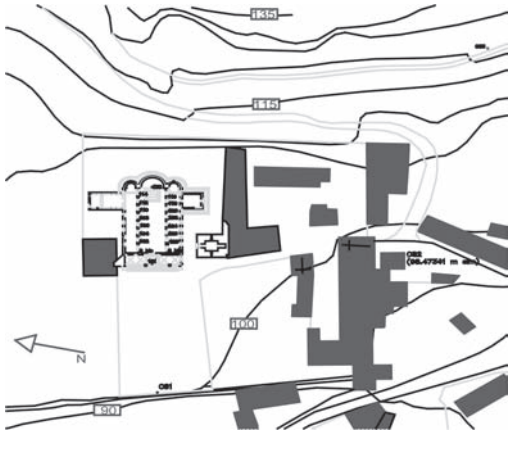

Figure 12. Location of the external benchmarks.

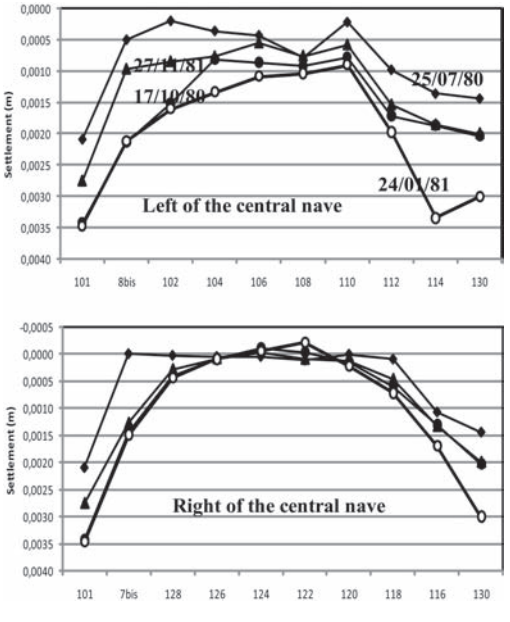

Figure 13. Settlement of the base of the columns of the central nave, 1980/81.

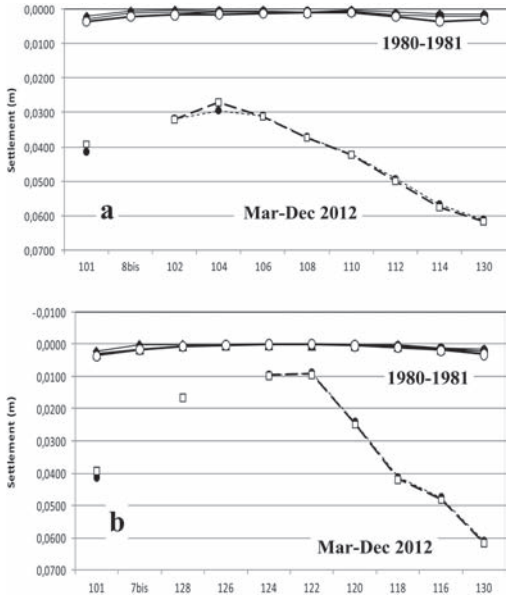

Figure 14. Settlement of the bases of the columns, 1980/2013. a) on the left and b) on the right of the central nave.

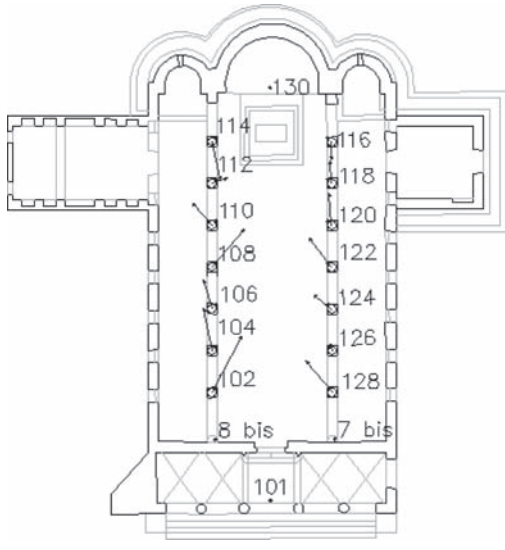

Figure 15. Offset of the columns in 1981.

by the observations an opening of the fissures has been observed.

The increase in the width of fissures was up to 0.5 mm in 1974/75 and to 0.8 mm in 1980/81. The trend of increase with time is somewhat irregular, but looking at the whole of data in both cases there is a steady increase, without any sign of a cyclical trend.

Unfortunately, the location of the measurements carried out in 1980/81 is not known and hence it is not possible to relate them with the differential settlement mentioned in § 4.3. The trend of the fissures measured in 1974/75 is compatible with a hogging deformation of the church.

4.4 *Offset of the columns*

In January 1980, in the framework of the geodetic survey, the offset of the columns has been accurately determined. The results obtained are reported in fig. 15, where the vectors shown represent the offset of the centre of the base with reference to a vertical through the centre of the top of the columns.

The measurements have been repeated until January 1981, without shoving any detectable variation.

The offsets range from 10 to 89 mm and are small enough that they could be attributed to construction defects; but the orientation of the vectors shown in fig. 15 is rather regular and seems to be due to some common origin.

4.5 *Discussion*

All the available data show definitely that the basilica is affected by a continuing settlement, with an average rate of displacement of 1.4 mm/year in 1980/81 and of 1.2 mm/year in the interval 1980/2013. The maximum settlement occurs in the zone of the apse and amounts to 60 mm in 32 years, with a rate of almost 2 mm/year, while the deflection of the right colonnade amounts to 40 mm in the same period.

If such a rate of settlement had been active since the construction of the basilica, an average settlement of almost one meter and a slightly smaller deflection would have resulted; such figures are clearly incompatible with the existence of the basilica. It is evident that the observed movements initiated relatively recently, for some unknown reason; they have a discontinuous trend in time, with no traces of cycling. Similar indications are given by the data on the opening of the fissures and on the offset of the columns.

Possible reasons that have been considered by various Authors are: (i) the extensive use of explosives in the nearby stone quarries; (ii) the effect at the surface of karst phenomena in the limestone; (iii) residual slow tectonic movements of the slope.

None of these suggestions seems totally convincing. As mentioned above, the quarrying activity has been stopped since 1980, while the movements are

continuing. There are no evident reasons why the karst phenomena should begin at a time of some decades ago. Di Nocera (2013) believes that the movements are probably connected with a tectonic activity, triggered either by recent seismic activity or by the explosions in the quarries. At the time being, no definite conclusion can be drawn from the available data; it is believed that a only careful and frequent monitoring for a period of many years will help in understanding the phenomenon.

5 POSSIBLE REMEDIAL WORKS

Notwithstanding the obscurity of the phenomena leading to the movements of the basilica and to the consequent damages to the frescoes, some intervention is badly needed to preserve the integrity of the paintings. At the time being, in the absence of a diagnosis the intervention cannot but cure the symptoms, rather than removing the cause(s).

The idea that is gradually emerging is that of correcting the differential settlement of the structure, rising the façade and the apses or making the central part to settle. This goal could be achieved acting on the subsoil, by means of techniques such as underexcavation or compensation grouting, but this approach appears not easy because of the brittle nature of the soils and of the occurrence of archaeological remains below the Basilica. Alternatively, it can be conceived an intervention on the structure itself, based on a proper use of flat jacks and cuts. In any case, the prosecution and enrichment of the monitoring is absolutely mandatory.

REFERENCES

Adriani L., Pellegrino A., Pescatore T.S. (1980) La Basilica Benedettina di S. Angelo in Formis: prima relazione. Indagini sui terreni e sulle strutture del monumento per lo studio dei dissesti. *Unpublished report, Soprintendenza ai Monumenti della Campania, Napoli.*

Corniello A., Santo A. (1995) I dissesti della Basilica Benedettina (XI secolo) di Sant'Angelo in Formis (Capua) ed il complesso assetto geologico dell'area. *Geologia Applicata e Idrogeologia, vol. XXX, I, 125-137*

De Franciscis A. (1956) *TemplumDianaeTifatinae. Soc. Di Storia Patria di Terra di Lavoro, Caserta, 60 pp.*

Di Nocera S. (2013) Personal communication.

Jacobitti G.M., Abita S. (1992) *La Basilica Benedettina di Sant'Angelo in Formis. ESI, Napoli, 97 pp.*

Pellegrino A., Pescatore T.S. (1981) *La Basilica di S. Angelo in Formis. Indagini sui terreni di fondazione ed analisi dei dissesti: relazione finale. Unpublished report, Soprintendenza per i Beni Ambientali e Architettonici della Campania, Napoli.*

Regesto di S. Angelo in Formis (1925) *Edizioni Iguanez, Montecassino.*

Wettstein J. (1960) Sant'Angelo in Formis et la peinturemédiévale en Campanie. *Geneve.*

Geotechnical Engineering for the Preservation of Monuments and Historic Sites – Bilotta, Flora, Lirer & Viggiani (eds)
© 2013 Taylor & Francis Group, London, ISBN 978-1-138-00055-1

The vineyard of the monastery of S. Martino in Napoli

M. Candela
Mediterranean University, Reggio Calabria, Italy

C. Viggiani
University of Napoli Federico II, Italy

R. Viparelli
Formerly in the Universities of Napoli and Basilicata, Italy

ABSTRACT: The Carthusian monastery of S. Martino was founded by the Angevins in 1325 and progressively enlarged and enriched. At the end of XVII century the architectural complex takes its definitive forms; in the meantime the slope of the hill is gradually converted from an impervious wooded steep crag into a succession of cultivated terraces retained by an impressive system of walls and provided with a network of drains, channels and water reservoirs. It is still known as "Vigna S. Martino" (S. Martino vineyard). The Monastery is at present the seat of the Civic Museum of the city. The underlying vineyard is bound to agricultural use and subjected to the public regulations to preserve landscape. It continues to be cultivated, but the maintenance of the system of retaining walls and hydraulic structures is abandoned, and consequently the system is steadily deteriorating, with uncontrolled water flow, concentrated erosion, collapse of some walls, landslides. The survival of this document of the past is at risk; furthermore, the densely inhabited underlying built environment is exposed to an high landslide risk. The design of the urgently needed remedial works has been recently completed, and the works are going to start; in the present paper the results of the investigations and the criteria on which the design has been based are reported.

1 INTRODUCTION

The *Tavola Strozzi* (Fig. 1) is an oil-on-wood painting of medieval Naples as seen from above and in front of the main port of the city. It is the oldest depiction of the medieval city, dating back to 1472 and very interesting for its amazing details. Many of the major landmarks of the city are quite visible: the churches (Santa Chiara, San Domenico Maggiore, San Giovanni a Carbonara among others), the castles (Maschio Angioino, Castel dell'Ovo). In the middle San Giovanni a Carbonara among others), the castles (Maschio Angioino, Castel dell'Ovo). In the middle of the picture, in a dominant position, there is the S. Martino hill with the Angevin Belforte, not yet transformed by the

Figure 1. The Tavola Strozzi, view of the city of Naples from the sea, 1470. Museo di San Martino, Naples.

Figure 2. The Monastery of S. Martino and the fortress o S. Elmo seen from downtown Napoli.

Figure 3. The Great Cloister of the Monastery of S. Martino, by Cosimo Fanzago (XVII century).

Spaniards into the fortress of Sant'Elmo, and the adjacent monastery. Below the monastery a huge retaining wall is already clearly distinguishable; on the left, a wooded steep slope.

The Carthusian monastery of S. Martino was founded by the Angevins in 1325; the construction of the Belforte started soon later in 1329. The two founded by the Angevins in 1325; the construction of the Belforte started soon later in 1329. The two monuments, both designed by Tino da Camaino from Siena, were probably conceived as an impressive symbol of the religious and military power over the city, and they still impend over the modern Naples (fig. 2). This may explain why the monastery was erected in such an uneasy location, requiring significant earth moving and retaining structures, while all other chartreuses of Southern Italy (Trivulzi, Serra S. Bruno, Capri, Padula) are located in plain areas. The monastery was progressively enriched in properties, codes and books, number of monks; in 1347 the queen Giovanna I gave to S. Martino the right of free grazing its cattle all over the kingdom.

The increased importance of the monastery is reflected by successive enlargements and improvements. A monumental subterranean tank is realized in 1578; in early 1600 Cosimo Fanzago builds around it the Great Cloister (fig. 3). At the end of 1700 the whole architectural complex takes the definitive forms that we can still admire today; the same occurs for the slope of the hill, gradually converted from an impervious wooded steep crag into a succession of cultivated terraces retained by an impressive system of walls (fig. 4) and provided with a capillary network of drains, channels and water reservoirs. It is still known as "Vigna S. Martino" (S. Martino vineyard).

At the advent of the French, the Monastery loose its religious destination and is used as military hospital from 1800 to 1831; at the unification of Italy,

Figure 4. Bird's eye view of the vineyard.

it becomes property of the State and seat of the Civic Museum of the city. The underlying vineyard, on the contrary, is at present a private property, although bound to agricultural use and subjected to the public regulations to preserve landscape.

A comparison of the map of Naples prepared by the Duke of Noja at the end of 1700 to the present situation shows that, in a period of more than two centuries, the only important variation in the S. Martino hill is the opening at the mid of 1800 of a new street on the slope (the Corso Maria Teresa,

later Corso Vittorio Emanuele). The area below the new street has been densely urbanized, while the area above it, the S. Martino vineyard, keeps unchanged. The regulations, later assimilated in the present town planning scheme, have been effective indeed in preserving this unique remain.

Since the early XIX century, while the vineyard continues to be cultivated, the maintenance of the system of retaining walls and hydraulic structures is abandoned, and consequently the system is steadily deteriorating, with uncontrolled water flow, concentrated erosion, collapse of some walls, landslides. Just to quote some of the recent events, in the winter 1996/1997 some retaining walls have collapsed; during a heavy rainstorm in September 2001 quite a number of walls have been destroyed by a significant landslide. It is evident that the same survival of this invaluable document of the past is at risk; furthermore, the densely inhabited underlying built environment is exposed to an unacceptable landslide risk.

In the early 2000s the Italian government made available some resources to investigate the situation and design the remedial works needed to stabilize the vineyard. At present the design has been completed and the works are just starting.

The present paper reports the results of the investigations and the criteria on which the design has been based.

2 GEOLOGICAL FRAMEWORK AND SUBSOIL PROPERTIES

The top of the S. Martino hill has an elevation of 250 m above sea level. At the base of the hill there is a fine grained tuff formation, deposited by the eruption of the Chiaia volcano, dated around 40,000 years BP. The subsoil of the majority of the slope, were the vineyard is located, consists of pyroclastic soils (pozzolana, pumices, ashes, lapilli), more or less cemented. At the top of the hill a layer of yellow volcanic tuff is found, deposited around 12,000 years BP after an eruption of the Phlegrean volcanoes; the yellow tuff can be seen below the fortress of S. Elmo, but it does not outcrop in the area of the Vineyard.

A broad site investigation has been performed in the early 2000s, including: 41 boreholes for a total length of 2,400 m, with retrieval of 188 undisturbed samples for laboratory testing; 39 CPT profiles, 188 SPT, 17 geophysical sections. Some in situ shear tests on blocks have also been carried out.

Although the results obtained are affected by a significant dispersion, the drained shear strength of the soils may be characterized by a friction angle ϕ' over 40° near the surface, decreasing to 37°–38° at a depth of around 20 m and an effective cohesion intercept c' increasing with depth between values of around 20 kN/m^2 near the surface to 250 kN/m^2 at a depth of around 20 m. The shear tests on blocks—all performed within a maximum depth of 1 m below the surface—gave on average a slightly lower strength ($c' = 0$–20 kN/m^2, $\phi' = 32°$–$38°$). The average unit weight equals 16–17 kN/m^3, slightly variable with the water content and typical of pyroclastic materials.

It may be seen that the soil properties are extremely favorable from the viewpoint of the stability of retaining structures. This explains why a complex of masonry retaining walls on a steep slope stayed substantially stable for some centuries, and began to show signs of degradation only after a long period, essentially because of the lack of any maintenance and the uncontrolled runoff of rainwater.

3 RETAINING WALL SYSTEM

3.1 *Existing retaining structures*

The vineyard has a surface of around 30 Ha, and contains more than 7,000 m of retaining walls with an height over 3 m. All the walls are built by tuff masonry and with different schemes: plain (fig. 5), provided with counterforts (fig. 6) or arches (fig. 7).

The thickness of the walls has been investigated by horizontal drill holes and the depth of their foundation by inclined holes and inspection

Figure 5. Plain retaining walls.

Figure 6. Counterfort retaining walls.

Figure 7. Arches retaining walls.

shafts; such investigations have been carried out at an average interval of around 15 m. Many of the walls show evident traces of degradation, such as erosion of the masonry at the outer surface with significant decrease of the structural section (fig. 8), removal of the soil at the toe uncovering the foundation (fig. 9), differential settlement and fissures at the junction of different walls. Statical problems of the retaining walls must have occurred in the past too, since counterforts have been added at many locations, as it appears from the different texture of the masonry (fig. 10). Many counterforts

Figure 8. Erosion of the masonry with reduction of the structural section.

Figure 9. Removal of soil at the toe of a wall, with uncovering of the foundation. The original level of the soil may be traced by the difference between the irregular stones of the foundation and the regular courses of upper masonry.

Figure 10. Reinforcing counterforts added to a wall after its original construction.

show signs of distress and detachment from the body of the wall (fig. 11).

Finally, as mentioned before, collapse of some walls has recently occurred (fig. 12).

Figure 11. Distress in the counterforts.

Figure 12. Collapse of a retaining wall.

3.2 *Design criteria*

The conservation of the system of retaining structures implies not only the repair of the various forms of degradation affecting them, but also their strengthening to comply with the more demanding requisites of the present seismic regulations. In general, the reconstruction of the outer facing of the walls to repair the effects of the erosion will be carried out with the same tuff masonry of the ancient walls, and cracks will be repaired by local demolition and suture. Some of the counterforts will be underpinned by micropiles, and some new counterforts will be added (fig. 13). Finally, in the most critical spots ground anchors will be used, with special care to the connection between the anchor and the masonry (fig. 14). The backfill will be protected by the infiltration of rainwater by a geomembrane.

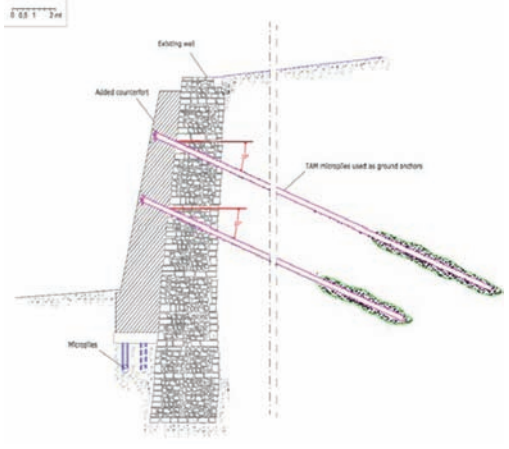

Figure 13. Reinforcement of a retaining wall with counterfort anchored and founded on micropiles.

4 DRAINAGES, CHANNELS AND RESEVOIRS NETWORK

4.1 *Present situation*

All the water raining over the area of the Monastery was formerly conveyed to an impressive system of interconnected underground reservoirs totaling a capacity of around 2,000 m^3. For instance, the monumental tank at the center of the Great Cloister, draining a surface of around 5,000 m^2, is depicted in fig. 15, evidencing the elaborated provisions for sedimentation of suspended material and the overflow and bottom effluents. Similar tanks are located in the subsoil of other cloisters and yards.

The hydraulic system was conceived with a triplfunction: (i) storage of water for domestic use of the monks, (ii) lamination of the floods following intense rainstorms and (iii) irrigation of the vineyard. The volume of water impounded in the underground tanks of the Monastery was sufficient to the yearly needs of a community of 50/100 peoples; furthermore, it equals the volume of rain in a day of rainstorm with a return period of around 100 years. When a rainstorm occurred with the reservoirs almost full, the overflows were opened and the water entered a system of ducts connecting one after the other a number of tanks located on the slope of the hill. In this way it was possible to accumulate some 20,000 m^3 per year, needed for the irrigation of the vineyard.

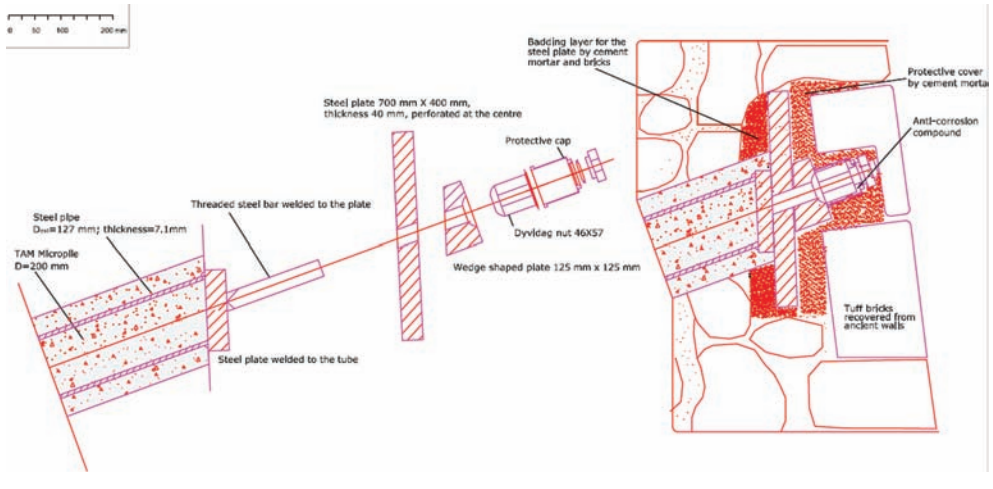

Figure 14. Connection between the ground anchor and the existing wall.

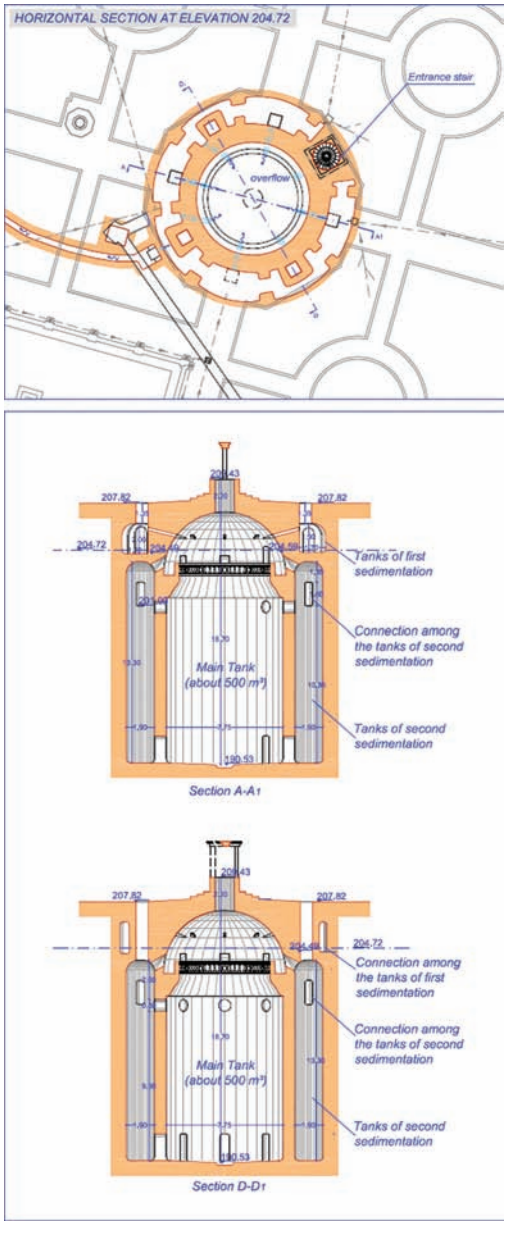

Figure 15. The monumental tank of the great cloister.

Fig 16 reports a schematic representation of the system. At present most of the ducts are closed or interrupted, and the abandoned tanks both below the monastery and on the slope are partially filled with debris and intensely fissured, leaving water leak into the ground. During intense and prolonged rainfalls the tanks fill completely and it is necessary to pump the water out. The majority of

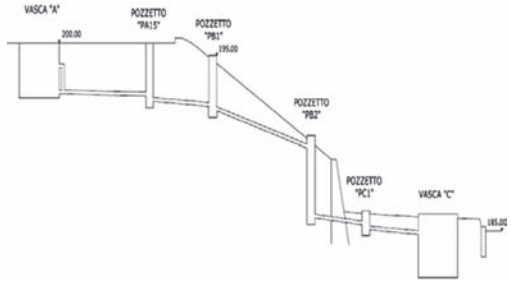

Figure 16. Scheme of the hydraulic system.

the rain water from the area of the Monastery is directly conveyed to the urban drainage system, generating frequent damages during heavy rainstorms. The vineyard is now irrigated by water from the urban aqueduct, and rain water runs on the slope and over the retaining walls producing repeated damages and collapses.

4.2 *Design criteria*

In the future, the water coming from the monastery area will be conveyed directly to the urban drainage system, that will be locally improved to cope with it. The ancient hydraulic system will keep the only function of laminating the heavy rainstorm; to this aim it will be sufficient to implement a surface drainage network, ending again in the urban sewers.

ACKNOWLEDGEMENTS

Most of the material on which this paper is based has been kindly provided by G. Pulli, architect of the Municipality of Naples. Some of the drawings have been masterly prepared by Giusy Imbriale. Their contribution is gratefully acknowledged.

The senior author is also in debt to Giovanni Santoro for the munificent presents of oranges and *friarielli* of the vineyard.

This page intentionally left blank

Geotechnical Engineering for the Preservation of Monuments and Historic Sites – Bilotta, Flora, Lirer & Viggiani (eds)
© 2013 Taylor & Francis Group, London, ISBN 978-1-138-00055-1

Site characterization by in situ and laboratory tests for the structural & architectural restoration of Saint Nicholas Church, Nicosia, Cyprus

A. Cavallaro
CNR-IBAM, Catania, Italy

L. Cessari & E. Gigliarelli
CNR-ITABC, Roma, Italy

ABSTRACT: The Bedestan (Saint Nicholas Church) is located in Cyprus, in the Turkish part of the historic heart of the city of Nicosia only a step away from the ancient Latin Cathedral of Santa Sofia, today the Selimiye mosque. It gets its name from its function of cloth and precious object market during the Ottoman period (1570–1878) following the transformation of a pre-existing Christian church. The action objectives are the enhancement of a building of great architectural value by means of action aimed at its static consolidation, conservative restoration and its requalification and re-insertion inside the historic quarter of Selimye. The development of the project is preceded by a thorough diagnostic study. In order to study the soil-structure interaction a comprehensive in situ and laboratory investigation has been carried out to obtain a soil profile. For site characterization of soil deep site investigations have been undertaken. Borings and SPT have been performed. Moreover samples were retrieved for laboratory tests.

1 INTRODUCTION

The project to study, document and restore one of the most important monuments of the fortified city of Nicosia on Cyprus, the former church of St. Nicholas, represents one of the international restorations of excellence developed by CNR since 2005 and involves a group of some thirty researchers and experts in architectural consolidation and restoration. This complex project, funded by the European Union through the United Nations development programme Partnership for the Future (UNDP-PFF), represents a particularly interesting case illustrating the problems of current restoration work that has the singular status of being halfway between an abandoned building and an architectural ruin. The complex architectural configuration of the building is a direct consequence not only of a series of alterations introduced for functional and stylistic reasons, but more frequently in the wake of calamities that led to the form and actual use of the building being modified, and for many years it served as a covered market or Bedestan. For many decades the monument was closed and was ultimately forgotten by the population after the roof fell in the 1930s. Some following interventions for the safety of the structure for a long time rendered the ancient monumental spatiality of this extraordinary architecture completely illegible. The restoration work was preceded by a long and painstaking campaign of analysis and fact-finding investigations regarding the history of the building, its state of conservation and the physical and mechanical characteristics of the materials and structures. To obtain a soil profile of site characterization for seismic response analysis in situ and laboratory investigations have been described.

2 THE HISTORY OF ST. NICHOLAS CHURCH (BEDESTAN)

The history of St. Nicholas Church (Bedestan) begins in the Byzantine Period (330–1190), with the building of a 6th Century basilica.

In the 13th Century, The Catholic Church of St. Nicholas of the English was constructed on the top of the basilica by monks of the medieval order of St. Thomas Becket, Archbishop of Canterbury, who was martyred in 1170 and canonized in 1173. These monks, who were serving in the Holy Land, were forced to leave the Holy Land, in late 12th Century, after loosing to the Arabs/Saracens and came to settle in Cyprus. They were later forced to leave Cyprus and returned to England, where the Order was later dissolved in 1538 by Hendry VIII of England.

The feudal domination of the Lusignans, stemming from French nobles, who ruled Cyprus (1192–1489), left clear traces of restructuring on

the building in a French Gothic style via arches and dome. The vaults were specially built to withstand the pressure and prevent the building from collapsing.

During Venetian Period (1489–1570), the Venetians undertook further rebuilding converting the Church into Greek Orthodox Cathedral, dedicated to Panaghia Hodegetria, (i.e. "Our Lady, who shows the way").

The Ottomans (1570–1878), transformed the religious building to suit new needs and Greek Orthodox Church was turned into a Bedestan, literally meaning closed market. As Bedestans are normally located in the city center, near the main mosque, this may have influenced the decision to adapt this building to become a covered market, due to the nearby converted Selimiye mosque (St. Sophia Cathedral), which also functioned as a "Külliye", a kind of a university of its time. The benefits of Bedestan, together with that of the nearby Büyük Han, plus many other incomes were used to finance The Külliye. The Bedestan functioned for the sale of textiles and to some extent, also as a grain store.

During the Ottoman Period, Nicosia, the capital, was subjected to the readoption of its original architectural and town planning heritage to suit the needs and customs of the new community. As far as building is covered, the old constructions, raised by one story, were provided with the typical tall windows with "balcony" on the main façade, with ornamental doors and rooms opening on to the rear enjoying a broad view of the garden and fountains. The most important aspect is without doubt the creation of public structures, such as palaces, mosques, hamams, hans, the Bedestan, and lastly the Bazar, which enveloped them, located as it is in the most important town streets and characterized by a series of crowded shops, itinerant street sellers and roofs made of reeds and matting: it is a complex urban structure that concentrates in itself all the economic, commercial and craftsmen's activities, and is inhabited exclusively by those who work there, who are divided into sectors according to the various categories. The Bazar, in the center of Nicosia, extends as far as the boundaries with the area in which the Selimiye Mosque (St. Sophia Cathedral) stands.

In the first years of the British Colonial Rule (1878–1960), a group of English residents wanted to have the possession of or to lease the ancient church of "St. Nicholas of the English", and use it under this name. This idea was however given up, since the building was owned by the Evkaf Foundation and the Islamic Law prohibits the sale of Evkaf properties. Moreover, the Islamic Law would anyway not allow a religious place of another religion to be located near mosque, i.e., The Selimiye Mosque.

The British then began restoring parts of the building which had been damaged due to natural ruin and earthquakes. Their way of restoration often did not do due justice to the building. The columns were restored to their full height.

The Bedestan was ultimately abandoned and not used any longer as a covered market. It became a ruin. The British built a new covered market just to the South of the Bedestan, in 1932.

The Bedestan (St. Nicholas Church), is located in the Selimiye Quarter, the Heart of the historic Walled City of Nicosia. The most significant monuments of Nicosia are found in the vicinity, such as the Selimiye Mosque (St. Sophia Cathedral), Haydar Paça Mosque (St. Catherine's Church), Chapter Hause, Sultan Mahmut Library, Büyük Han, Kumarcilar Han, Büyük Hamam and the Minicipal Market.

Bedestan, born as a religious complex and later turned into covered market (Bedestan); is an old church complex of Byzantine-Gothic style situated to the south of the Selimiye Mosque (St. Sophia Cathedral), combining the tall nave of a medieval church (14th century Gothic architecture) with cross-shaped Byzantine construction (6th century). The complex architectural configuration of the building is a direct consequence of a series of alterations carried out for functional and stylistic reasons, although more often as a result of catastrophic events due to which the shape and actual way of using the building were changed.

3 GEOLOGY AND SEISMICITY OF AREA

Cyprus is one of the larger Mediterranean islands with a surface area of 9251 sq. Km. It lies in the northeastern corner of the Mediterranean Sea approximately centered on latitudine 35° N and longitudine 33° E. The island is broadly divisible into four geological zones (Figure 1): Kyrenia, Troodos, Mesaoria Plain and Mamonia. These in turn give rise to four geomorphological regions, whose terrain characteristics reflect to a large extent the underlying geology.

Figure 1. The St. Nicholas Church, Bedestan.

Figure 2. Geological map of Cyprus.

The city of Nicosia (Lefkosia) is located in the Mesaoria Plain. The Mesaoria Plain is a topographically low, rather flat area which occupies the central part of the island between the Troodos Range to the south and the Kyrenia Range to the north. In its northern part, the folded Kyrenia Flysch forms a characteristics hummocky topography, whereas in the southern part a generally under formed sequence of the circum-Troodos autochthonous sedimentary succession rises towards the Troodos mountain.

The northern part of Cyprus is considered to extend from the northern flank of the Troodos Massif to the north coast of the island. From detailed field investigations and stratigraphic analysis, the northern part of Cyprus is divisible into two tectonostratigraphic terranes, a southern Circum-Troodos terrane and a northern Kyrenia terrane, which includes allochthonous rocks of the Kyrenia Range.

The Ovgos fault zone, which is a major tectonic feature, separates these two terranes, which have had a markedly different depositional and tectonic history in the Miocene, but have a somewhat similar post-Miocene history. We place the northern boundary of the Kyrenia terrane at a major east-west-striking fault that exists approximately 25 km off the north coast of Cyprus (Evans et al., 1978). Seismic reflection profiles across this fault indicate that basement reflectors dip steeply to the north and thrust faults with a southerly vergence occur in the hanging wall (Evans et al., 1978).

The fault is separated from the northern coast of Cyprus by a zone of low-angle listric faults dipping to the north.

Several geologic features in the northern part of Cyprus, which either have not been previously recognized or fully appreciated, are important to our interpretation of its tectonic framework and tectonic history:

1. the allochthonous nature of the Kyrenia Range, which consists of steeply dipping Paleozoic, Mesozoic and Cenozoic formations resting on folded Miocene flysch deposits;
2. the Ovgos fault zone, which has been structurally active throughout the Cenozoic and is a boundary that separates strongly deformed Miocene flysch deposits to the north mildly deformed Miocene shelf carbonate deposits to the south;
3. a system of transverse strike-slip faults, which are the youngest tectonic features in the northern part of Cyprus and possibly pose its greatest seismic hazard.

Cyprus falls within the second largest seismic intensity zone on earth. The island suffered from destructive earthquakes throughout the ages, and a systematic work on the available data showed that:

1. during the last century more than 750 earthquakes occurred in and around the wider region of Cyprus, 32 of which were of magnitudo greater or equal to 6.0 in the Richter scale. Twelve of these shocks caused deaths to more than a hundred people and heavy financial damages to property and infrastructure works;
2. potentially damaging earthquake have a frequency of one earthquake in every twelve years;
3. destructive earthquakes which occurred in the last past, indicate that potentially destructive earthquakes are expected to occur in the future, with a frequency of one destructive earthquake every 25–30 years;
4. there is 63% probability that an earthquake of magnitude 5.8–6.1 in the Richter scale, could occur within a distance smaller than 100 km from the towns of Cyprus in a time interval of 25 years.

Investigations on the seismic history of Cyprus have shown that 7 strong earthquakes ($M \geq 6.0$) have occurred on or near the island since 1900 and probably at least another 15 destructive earthquakes have hit the island since about 26 BC (Papazachos and Papaioannou, 1999). Figure 3 shows the seismicity of Cyprus from 1896 to 2010.

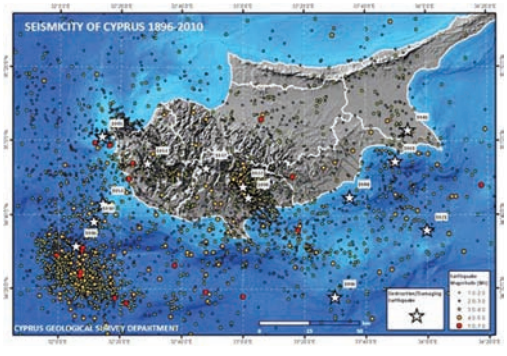

Figure 3. Seismicity of Cyprus.

4 INVESTIGATION PROGRAM AND BASIC SOIL PROPERTIES

The in situ tests were performed in the Bedestan St. Nicholas of the English Church area.

A total of six boreholes were drilled using water. Core samples were recovered. A total of 9 SPT tests were performed, and three undisturbed samples were obtained. Three vertical drill holes were BD-1, 12 m, BD-4, 16 m, and BD-6, 5 m. Three inclined boreholes were BD-2, BD-3, and BD-5 each of 4.00 m depth were drilled. Three inclined drill holes with an angle of around 15° to the vertical were drilled very close to three different foundations. BD-1, BD-2, BD-3, and BD-4 were drilled at the level of the main building. BD-5 and BD-6 were drilled at a slightly higher level (around 0.4 m) from the main level to the south side of the building.

The deepest foundation is 3.70 m deep and is located at BD-3. The foundation at BD-2 is 1.30 m. The shallowest foundation was found to be at BD-5 at a 1.00 m. The BD-5 borehole was about 0.4 m higher level.

Three undisturbed samples were obtained from BD-1, BD-2, and BD-4 all at 2.50–3.00 m. All three undisturbed samples were loose sandy silt.

The SPT N-values of the three vertical boreholes BD-1, BD-4, and BD-6 all at 1.50–1.95 m level were 12, 11, and 6 respectively. At this level the alluvium is loose. At 3.00–3.45 m level were 23, 16, and 22 respectively. At this level the alluvium is medium dense.

The following types of soil were recovered: artificial fill from 0 m to 1.5 m, dark grey gravel clay sand silt from 1.5 m to 1.95 m, dark grey clay sand silt from 1.95 m to 4.2 m, whitish clay sand silt from 4.2 m to 4.5, dark grey clay sand silt from 4.5 m to 6 m, grey gravel sand from 6 m to 7.5 m, grayish whitish coarse grained gravel sand from 7.5 m to 9 m, grayish whitish gravelly marl form 9 m to 10.2 m, whitish firm marl from 10.2 m to 10.5 m, yellowish whitish firm marl from 10.5 m to 12 m, whitish hard marl from 12 m to 13.5 m, small amount of gravel, marl from 13.5 m to 14 m, whitish stiff marl from 14 m to 15.9 m and whitish gravely marl from 15.9 m to 16 m.

Typical range of physical characteristics, index properties and strength parameters of the deposit encountered in these area are reported in Table 1.

Table 1. Mechanical characteristics for Bedestan area.

Unit	γ [kN/m^3]	W_n [%]	G_s	e	c' [kPa]	ϕ' [°]
A	16.8–18.3	12.9–21.7	2.655–2.79	0.621–0.791	0	24–26
B	20.0–21.0	10.2	2.365–2.42	0.324–0.417	30	28–30

where: A = Alluvium Unit; B = Marl Unit; c' (Cohesion) and ϕ' (Angle of shear resistance) were calculated from Direct Shear Test.

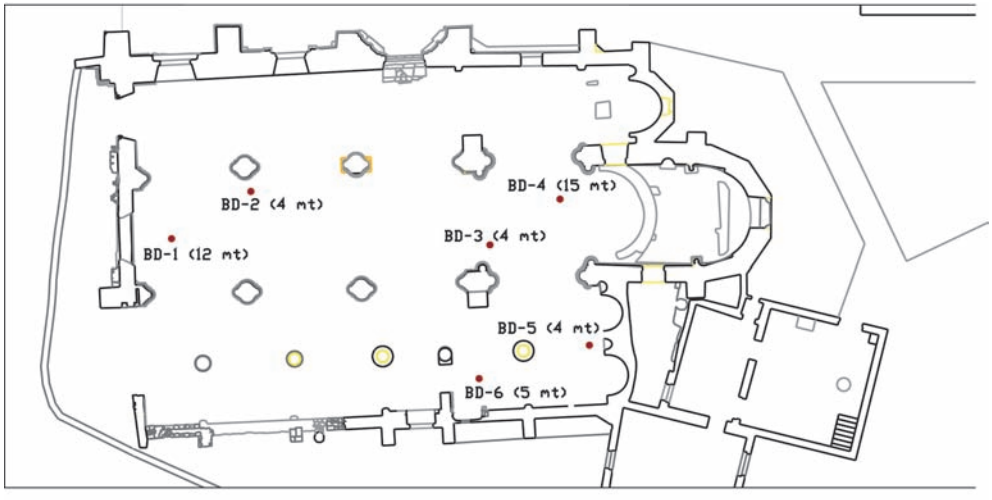

Figure 4. Lay-out of investigation program.

Mechanical (Grading) analysis was performed on the total soil samples retrieved from the boreholes of Bedestan, Nicosia. The marls contain a sand content between 0.20 and 2.22%, a silt content between 34 and 41% and a clay content between 57 and 64%. The alluviums contain a gravel content between 0.00 and 44.36%, a sand content between 2 and 34%, a silt content between 20 and 61% and a clay content between 16 and 45%.

SPT and Undisturbed samples was tested for moisture content. The alluviums contain a moisture content W_n between 12.87 and 21.69%.

Soil samples from three different boreholes are in a narrow specific gravity (G_S) range between 2.655 and 2.790.

Sixteen soil samples from three different boreholes were tested for liquid and plastic limits. Four samples are found to be non plastic. Characteristics values for the Atterberg limits are w_L = 34–83% and w_P = 22–39%, the Plasticity Index (PI) ranged between 9 to 44%, the Index of Consistence (IC) ranged between 1.10 to 1.17% while the Index of Activity (IA) ranged between 0.4 to 0.81%.

Liquid limits (w_L) versus plasticity indices (PI) are plotted in the plasticity chart in Figure 5. According to the plasticity chart results the alluviums have low to intermediate and the marls high to very high swelling potential.

The obtained results of $CaCO_3$ analysis ranged between 14.5 to 46%.

5 SHEAR MODULUS AND DAMPING RATIO

The equivalent shear modulus (G_{eq}) was determined in the laboratory by means of a Resonant Column test (RCT) performed on Shelby tube specimens by means of a Resonant Column. Moreover it was attempted to assess G_0 by means of empirical correlations, based either on standard penetration test results or on laboratory test results (Ohta and Goto, 1978; Yoshida and Motonori, 1988; Jamiolkowski et al. 1995).

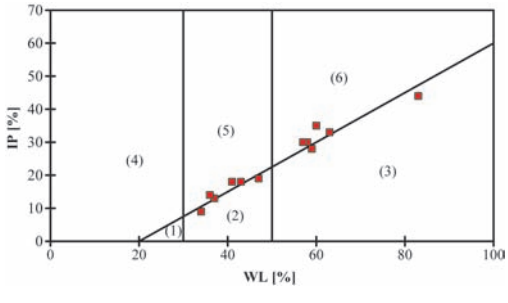

Figure 5. Casagrande plasticity chart for Bedestan area [(1): Inorganic silts with low compressibility; (2): Inorganic silts with medium compressibility and organic silts; (3): Inorganic silts with high compressibility and organic clays; (4): Inorganic clays with low plasticity; (5): Inorganic clays with medium plasticity; (6): Inorganic clays with high plasticity].

5.1 *Small strain shear modulus G_0 by laboratory tests*

Shear modulus G and damping ratio D of Bedestan deposits were obtained in the laboratory from Resonant Column tests (RCT). These tests were performed on Shelby tube specimens retrieved from Bedestan deposits. A Resonant Column/Torsional shear apparatus was used for this purpose.

G is the unload-reload shear modulus evaluated from CLTST and RCT, while G_0 is the maximum value or also "plateau" value as observed in the G-log(γ) plot. Generally G is constant until a certain strain limit is exceeded. This limit is called elastic threshold shear strain (γ_t^e) and it is believed that soils behave elastically at strains smaller than γ_t^e. The elastic stiffness at $\gamma < \gamma_t^e$ is thus the already defined G_0.

For RCTs the damping ratio was determined following the amplitude decay method and it was obtained during the decrement of free vibration.

The laboratory test conditions for cohesive soils and the obtained small strain shear modulus G_0 are listed in Table 2.

The undisturbed specimens were isotropically reconsolidated to the best estimate of the in situ mean effective stress. The size of solid cylindrical specimens are Radius = 25 mm and Height = 100 mm.

Figure 6 shows the results of RCTs normalized by dividing the shear modulus G(γ) for the initial value G_0 at very low strain.

The experimental results of specimens from Bedestan site were used to determine the empirical parameters of the equation proposed by Yokota et al. (1981) to describe the shear modulus decay with shear strain level:

$$\frac{G(\gamma)}{G_0} = \frac{1}{1+\alpha\gamma(\%)^{\beta}} \quad (1)$$

Table 2. Test condition for Bedestan area.

Test no.	H [m]	σ'_{vc} [kPa]	e	SC [%]	RCT	G_0 [MPa]
1	12.6	225	0.68	2	U	61

where: SC = Sand Content, U = Undrained (Dry Specimen), G_0 from RCT.

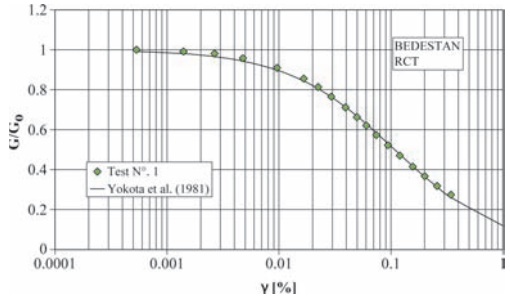

Figure 6. G/G_0-γ curves from RCTs.

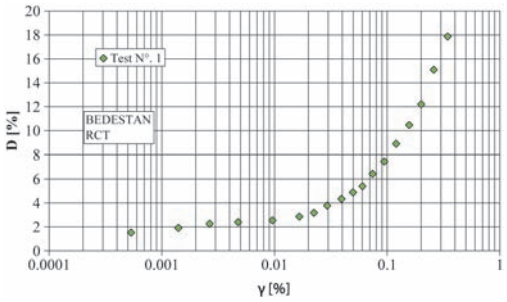

Figure 7. Damping ratio from RCTs.

in which:

$G(\gamma)$ = strain dependent shear modulus;
γ = shear strain in percent;
α, β = soil constants.

The expression (1) allows the complete shear modulus degradation to be considered with strain level.

The values of $\alpha = 7.4$ and $\beta = 0.9$ were obtained for Bedestan area.

The damping ratio values obtained from RCT is shown in Figure 7. It is possible to see that the damping ratio from RCT, at very small strains, is equal to about 2%. Greater values of D are obtained from RCT for strain levels higher than 0.01%.

As suggested by Yokota et al. (1981), the inverse variation of damping ratio with respect to the normalised shear modulus has an exponential form as that reported in Figure 8 for the area of Bedestan:

$$D(\gamma)(\%) = \eta \cdot \exp\left[-\lambda \cdot \frac{G(\gamma)}{G_0}\right] \quad (2)$$

in which:

$D(\gamma)$ = strain dependent damping ratio;
γ = shear strain;
η, λ = soil constants.

The values of $\eta = 35$ and $\lambda = 2.9$ were obtained for Bedestan area.

Equation (2) assume maximum value $D_{max} = 35\%$ for $G(\gamma)/G_0 = 0$ and minimum value $D_{min} = 1.92\%$ for $G(\gamma)/G_0 = 1$.

Therefore, equation (2) can be rewritten in the following normalised form:

$$\frac{D(\gamma)}{D(\gamma)_{max}} = \exp\left[-\lambda \cdot \frac{G(\gamma)}{G_0}\right] \quad (3)$$

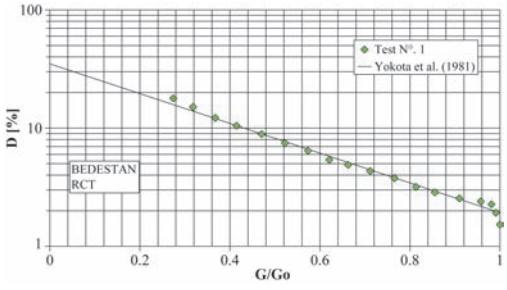

Figure 8. D-G/G_0 curves from RCTs.

5.2 *Evaluation of G_0 from empirical correlations*

It was also attempted to evaluate the small strain shear modulus by means of the following empirical correlations based on penetration tests results or laboratory results available in literature.

a) Ohta and Goto (1978):

$$V_S = 69 \cdot N_{60}^{0.17} \cdot Z^{0.2} \cdot F_A \cdot F_G \quad (4)$$

where: V_S = shear wave velocity (m/s), N_{60} = number of blow/feet from SPT with an Energy Ratio of 60%, Z = depth (m), F_G = geological factor (clays = 1.000, sands = 1.086), F_A = age factor (Holocene = 1.000, Pleistocene = 1.303)

b) Yoshida and Motonori (1988):

$$V_S = \beta \cdot (N_{SPT})^{0.25} \cdot \sigma'^{0.14}_{v0} \quad (5)$$

where: V_s = shear wave velocity (m/s), N_{SPT} = number of blows from SPT, σ'_{v0} = vertical pressure, β = geological factor (any soil = 55, fine sand = 49)

$$G_0 = \rho \cdot V_s^2 \quad (6)$$

where γ = mass density

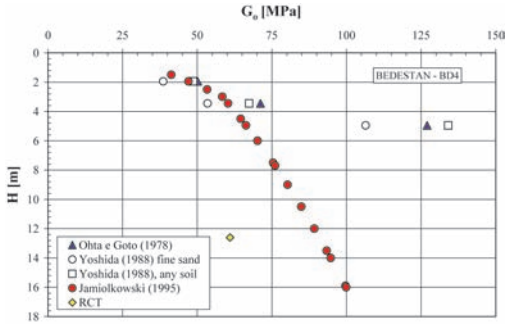

Figure 9. G_o from different empirical correlations.

c) Jamiolkowski et. al. (1995):

$$G_0 = \frac{600 \cdot \sigma'^{0.5}_m p^{0.5}_a}{e^{1.3}} \quad (7)$$

where: $\sigma'_m = (\sigma'_v + 2 \cdot \sigma'_h)/3$; $p_a = 1$ bar is a reference pressure; G_o, σ'_m and p_a are expressed in the same unit. The values for parameters which appear in equation (7) are equal to the average values that result from laboratory tests performed on quaternary Italian clays and reconstituted sands. A similar equation was proposed by Shibuya and Tanaka (1996) for Holocene clay deposits.

Equation (7) incorporates a term which expresses the void ratio.

The G_0 values obtained with the methods above indicated are plotted against depth in Figure 9. The method by Jamiolkowski et al. (1995) was applied considering a given profile of void ratio.

The empirical correlations (4) and (5) indicated the presence of dark grey clay sand silt layers at depth of about 4.5 and 6 m.

The correlation (4) and (5) show very comparable G_0 values. On the whole, equation (7) seems to provide the most accurate trend of G_0 with depth, as can be seen by Figure 9. It is worthwhile to point out that the G_0 value obtained by RCT was smaller than that by empirical correlations. Differences between G_0 value from RCT and in situ tests results are probably due to degree of disturbance of samples.

6 CONCLUSIONS

In this paper a comprehensive laboratory and in situ investigation has been carried out to obtain a soil profile in order to provide a case record of site characterization for St. Nicholas Church (Bedestan) area in the city of Nicosia on Cyprus. Available data enabled one to define the small strain shear modulus profile to describe the G and D variation with strain level. Empirical correlations inferred from laboratory and in situ test results were used to evaluate the small strain shear modulus G_0. On the whole, the G_0 values by empirical correlation are greater than those determined in the laboratory. On the basis of the experimental results obtained for St. Nicholas Church (Bedestan) area, it is possible to draw the following conclusions:

- the initial damping ratio D obtained from RCT at small strain is about 2%;
- greater values of D are obtained from RCT for strain level higher than 0.01%;
- empirical correlations between the small strain shear modulus and penetration test results were used to infer G_0 from SPT. The values of G_0 were compared to those measured in a RCT;
- differences between G_0 values from RCT and in situ tests results are probably due to degree of disturbance of samples.

REFERENCES

Evans, G., Morgan, P., Evans, W. E., Evans, T. R. & Woodside, J. M. 1978. Faulting and Halokinetics in the Northeastern Mediterranean Between Cyprus and Turkey. *Geology, 6,* pp. 392–396.

Jamiolkowski, M., Baldi, G., Bellotti, R, Ghionna, V. & Pasqualini, E. 1985. Penetration Resistence and Liquefaction of Sands. *Proceeding of the 11th International Conference on Soil Mechanics and Foundation*, San Francisco.

Jamiolkowski, M., Lo Presti, D. C. F. & Pallara, O. 1995. Role of In-Situ Testing in Geotechnical earthquake Engineering. *Proceedings of 3rd International Conference on Recent Advances in Geotechnical Earthquake Engineering and Soil Dynamic*, State of the Art 7, St. Louis, Missouri, April 2-7, 1995, vol. II: 1523–1546.

Ohta, Y. & Goto, N. 1978. Empirical Shear Wave Velocity Equations in Terms of Characteristic Soil Indexes. *Earthquake Engineering and Structural Dynamics,* Vol. 6.

Papazachos, B. C. & Papaioannou, C. A. 1999. Lithospheric Boundaries and Plate Motions in the Cyprus Area. *Tectonophysics*, 308, pp. 193–204.

Shibuya, S. & Tanaka, H. 1996. Estimate of Elastic Shear Modulus in Holocene Soil Deposits. *Soils and Foundations,* Vol. 36, N°. 4, pag. 45–55.

Terzaghi, K. & Peck, R. B. 1948. Soil Mechanics in Engineering Practice. *J. Wiley and Sons*, New York.

Yokota, K., Imai, T. & Konno, M. 1981. Dynamic Deformation Characteristics of Soils Determined by Laboratory Tests. *OYO Tec. Rep.* 3, 13–37.

Yoshida, Y. & Motonori, I. 1988. Empirical Formulas of SPT Blow-counts for Gravelly Soils. *Proceedings of ISOPT-1,* Orlando (USA).

This page intentionally left blank

Geotechnical Engineering for the Preservation of Monuments and Historic Sites – Bilotta, Flora, Lirer & Viggiani (eds)
© 2013 Taylor & Francis Group, London, ISBN 978-1-138-00055-1

Long-term mechanical behavior of wooden pile foundation in Venice

F. Ceccato & P. Simonini
DICEA, Università degli Studi di Padova, Italy

A. Lionello
Soprintendenza per i beni architettonici e per il paesaggio di Venezia e della Laguna, Italy

ABSTRACT: Many historical buildings of the historic city of Venice are founded on short and closely spaced wooden piles used to improve the shallowest layers of very soft silty clay. Some recent evidences have shown that anaerobic bacteria may, in some cases, seriously deteriorate these piles even in anoxic conditions, significantly reducing wood stiffness and strength therefore providing a possible explanation of some observed building settlements. To investigate the effect of such degradation on the overall foundation mechanical response, a series of finite element analyses has been carried out, coupling the wood decay with creeping response of surrounding clayey soil. The model is applied to simulate, along with centuries, the response of the foundations of the ancient Church of Santa Maria Maggiore, that showed important displacements of the external masonry walls.

1 INTRODUCTION

The islands, on which the historic city of Venice is founded, are formed by a layering of different soils ranging from medium-fine sands to soft silty clay, whose spatial erratic distribution in the lagoon area is a consequence of a complex depositional history (Cola & Simonini 2002).

In the case of shallow soft ground, quite common in the city area, the building construction required a significant improvement of the foundation ground, that was obtained through a sort of shallow footing made by wooden planking laying at shallow depth (referred as to *zatteroni*) or, in worst cases, by piled foundation composed by short and small diameter closely driven wooden piles.

The need for ground improvement by wooden piles was known since very old time; indeed the famous architect Palladio (1508–1580) stated that: "*if the soil is soft, as in the marshland, it is needed to realize piling with piles whose length should be 1/8 of the height of the wall and the diameter 1/12 of the length; they should be embedded one next to the other filing all the gap*"[1] (Fig. 1). Above the piles, a planking was

Figure 1. 14th century wooden piling found during archeological survey in 1999 in Venice at ex-Cinema San Marco (by Graziano Arici).

1. " (…) se il terreno sarà molle, e profonderà molto come nelle paludi; all'hora si faranno palificate: i pali delle quali saranno lunghi per l'ottava parte dell'altezza del muro, e grossi per la duodecima parte della loro lunghezza. (…) Si deono ficcare i pali si spessi, che fra quelli non ve ne possano entrare degli altri (…)"Palladio—I quattro libri dell'architettura-1570.

typically realized (*madieri*) made by oak or larch on single or multiple layers, thus forming an important element to spread the forces. After the installation of the wooden planking, blocks of white, calcareous stone of proper size were placed to reach the ground floor. Notice that the wood is constantly submerged, remaining under the minimum groundwater level.

Further instructions were given by V. Scamozzi (1548–1616), regarding the type of wood: "*it should be seasoned and peeled otherwise it would decay faster, it shouldn't be used any material that may damage the buildings by its loss of mechanical properties*"[2].

After some investigations carried out by the Authority for the Heritage Preservation of Venice (Soprintendenza), it became clear that wood may lose most of its characteristic, even in anoxic condition (Marchi et al. 2006; Gottardi et al. 2008). To deeper investigate the degradation process, its dynamics and consequences a multidisciplinary research project was sponsored by CORILA (Consortium for the Research concerning the Venice Lagoon).

In this context, this paper shows some preliminary results of the geotechnical study, whose aim is to better understand the mechanical behavior of the pile foundation over time, considering both wood deterioration and viscoplasticity of soil.

The wood deterioration model is applied to analyze the behavior of the wooden pile foundation of the church of Santa Maria Maggiore (Fig. 3), that shows a high differential settlement along its south-eastern wall.

2 WOOD BEHAVIOR

Wood is a heterogeneous, hygroscopic, cellular and anisotropic material. It is composed by cells, and the cell walls are composed of micro-fibrils of cellulose and hemicellulose, which are strong in tension, embedded in a matrix of lignin.

Mechanical properties depend on a multitude of factors such as density, water content, presence of imperfections; for this reason, constitutive modeling of wood is a very hard challenge. Giving a careful description of the mechanical behavior of wood exceeds the purpose of the research, so the material is here modeled by a simple elastic perfectly plastic model.

2. "(…) siano stagionati e maturi, il legname nuovo e bianco sotto la corteccia, per l'umidità della terra o dell'acqua, si guasta e marcisce; al legname da mettere in opera, è opportuno togliere la corteccia, il legno bianco, tenero e non stagionato, per non impiegare materiale che, nel tempo, possa portare danno alla fabbrica. (…)",V. Scamozzi—Dell'idea dell'architettura universale-1615.

Being permanently under the groundwater level does not prevent wood decay (Klaassen 2008), some evidences recently demonstrated the extremely poor state of conservation of some foundation in Venice (e.g. Gottardi et al. 2008; Biscontin et al. 2009).

Wood-degrading factors are animals, such as mollusk and crustacean, fungi and bacteria. Animals and fungi destroy rapidly the wood, but they need oxygen. On the contrary some types of bacteria can survive even in anoxic conditions and their action is particularly slow.

The evaluation of the state of wood conservation requires some chemo-physical parameters like:

– Basal Density (BD), which is the ratio between dry mass and wet volume, sometimes it is referred to the typical value of fresh wood, getting Residual Basal Density (RBD%).
– Maximum Water Content (MWC%), which is the ratio between the mass of water and the anhydrous mass of wood.
– Cellulose content (H) and lignin content (L).

It is supposed that the pile embedded into the ground, under the groundwater level, maintains the constant volume. Indeed, even severe degradation by erosion bacteria leaves intact some layers of the cell wall, which are strong enough to keep waterlogged wood in its original shape (Huisman et al 2007).

Erosion bacteria destroy cellulose very slowly, while lignin remains constant, and water replaces these large molecules. Figure 2 shows the trend

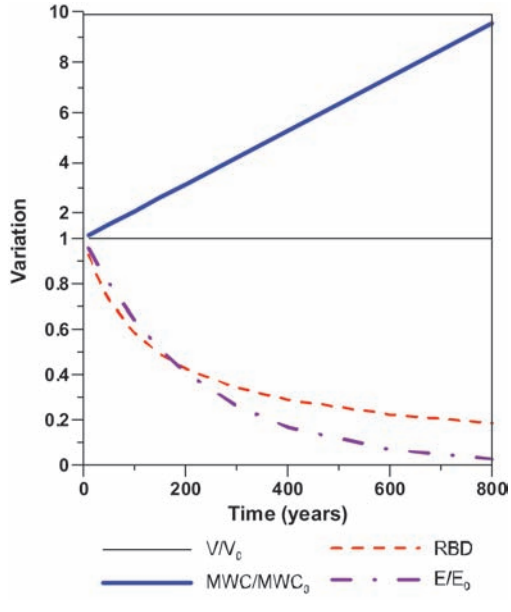

Figure 2. An hypothesis of physical and mechanical properties trend through centuries.

of the main important characteristics of wood as a function of time. Volume remains constant over time, whereas, assuming a linear variation of Maximum Water Content (MWC) with time, both BD and ratio H/L non linearly decrease, leading to the degradation of mechanical properties. To note that the real rate of degradation due to bacteria (expressed by MWC) is influenced by several environmental factors (Kretschmar et al. 2007; Klaassen 2007) and consequently it may be somewhat different from the linear trend hypothesized in this context.

Klaassen (2008) showed that MWC is the variable closely related to the variation of compression strength σ_c. The relationship between MWC and σ_c used here was calibrated by him using more than 100 pine samples, thus covering the entire range of degradation:

$$\sigma_c = 38.543 \exp(-0.6965 \cdot \mathrm{MWC}) \quad (1)$$

In order to apply the above equation to describe strength decay of other wooden species, it was transformed in dimensionless form by dividing the left term by the average σ_{c0} of the fresh wood. Hence we have:

$$\frac{\sigma_c}{\sigma_{c0}} = 1.586 \exp(-0.6965 \cdot \mathrm{MWC}) \quad (2)$$

Measurements of longitudinal elastic modulus E in ancient wood are not available; therefore it is tentatively assumed that:

$$E = E_0 \frac{\sigma_0}{\sigma_{c0}} \quad (3)$$

where E_0 is the stiffness of the fresh wood.

3 THE CHURCH OF SANTA MARIA MAGGIORE

The church (Fig. 3) and the convent of Santa Maria Maggiore are located in a suburban area of Venice, that was reclaimed at the end of 15th century. The building started in 1497 and completed in 1525. The layout is of basilican type with three naves and ionics column overlaying high plinths holding arches. There are a barrel-vaulted presbytery and two small lateral chapels (Fig. 4). The roof is made by wooden trusses over the main naves and by simply wooden struts over the lateral naves. The proportion of the church suggests that it may have been built in two different phases, but no clear evidences can confirm this hypothesis.

Figure 3. Facade of the Church of Santa Maria Maggiore.

The church and the convent have been held by the Army since 1806, and the inside artworks have been lost.

Later, after several years of abandon, the church was put in charge to the National Tobacco Authority and used as tobacco warehouse. To this purpose three new wooden floors were placed to stow more than 500 tons of tobacco, causing serious additional damage to the structures. In 1902, a first safety restoration took place and in 1961 the Authority for the Heritage Preservation was charged to carry out additional restoration works. In 1976, an earthquake destroyed the barrel vault of the apse, that was rebuilt in 1980. In 2010 the roof was retrofitted placing also ties to improve the behavior under dynamic load.

The front ad lateral walls show today diffuse cracks. In addition a relevant differential settlement between the façade and the apse (230 mm along 45 m) occurred along with the centuries (Fig. 5).

In order to investigate the cause of this relative settlement, in 2012 a geotechnical investigation campaign was carried out.The 2.40 m wide strip footing was founded on a soft silty clay soil, improved using 1.5 m long and 17 cm diameter alder piles. Soil improvement was realized according to the customary construction rule, but excluding the wooden planking, that plays an important

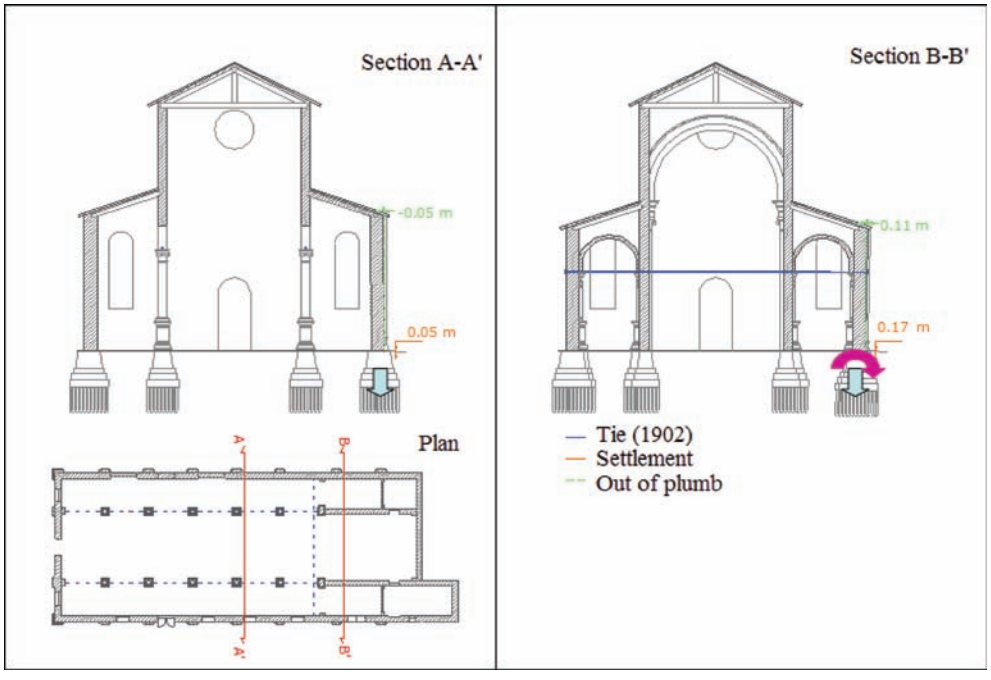

Figure 4. Plan and sections of the church of Santa Maria Maggiore.

Figure 5. South-eastern lateral wall of S.M. Maggiore.

role in spreading the vertical forces. To correctly simulate the behavior of this foundation, a proper estimation of the stress state increase from the construction beginning to date is of course necessary. The vertical stress over the piles is today constant along the lateral wall, besides the presence of arches in the nave. A careful survey showed that the 8 m-high lateral wall is not perfectly vertical, leaning out 11 cm near the apse and 5 cm to the opposite direction along the nave.

This is due to the static scheme of the church with the horizontal forces transferred by the arches partially neutralized in 1900 by the steel ties. Before this intervention, the rotation of the wall caused high stress on the outer part of the foundation leading to possible local instability.

3.1 *Geotechnical site investigation*

The soils in the Venice lagoon are very heterogeneous and characterized by the presence of a predominant silt fraction, combined with clay and/or sand. These form a chaotic interbedding of different sediments, whose basic mineralogical characteristics vary narrowly, as a result of similar geological origins and common depositional environment.

In the city area, under a filling material layer (1–4 m), the soil profile is typically composed by an upper 2–5 m thick soft clayey and silty deposit lying, between 5 and 15 m, over deeper alternating layers of fine silty sand, sandy or clayey silt.

In some zone, a stiff silty clay, referred as to *caranto,* can be found. The high OCR is the result of oxidation during the 10 000-years emergence during the last Pleistocenic glaciation (Cola et al. 2002).

At Santa Maria Maggiore the campaign of in situ tests included:

- 4 boreholes, inclined at 15° and 4.0–6.5 m long, through the foundation;
- 1 vertical boreholes down to 15 m below g.l.;
- 3 CPTu tests, driven between 6.8 m and 12.6 m depth below g.l.

From the boreholes, three undisturbed soil samples and some wood samples were collected and subjected to laboratory tests on cohesive soils and on the ancient wood.

The tests on wood have been carried out by the National Research Council (CRN-IVALSA in Florence) and the Department of Environmental Science of the University Ca' Foscari in Venice.

Figure 6 displays the CPTu profiles, suggesting a relatively homogeneous horizontal layering.

Soils have been classified from $Q_t - F_r$ data

$$Q_t = (q_t - \sigma_{v0})/\sigma'_{v0} \tag{4}$$

$$F_r = [f_s/(q_t - \sigma'_{v0}]100\% \tag{5}$$

$$q_t = q_c + u_2(1-a)[a = 0{,}83] \tag{6}$$

according to Robertson chart (1990) (Fig. 7) or through the soil behavior type index I_c, as proposed by Jefferies and Davies (1993) (Fig. 6, right column). In the above equation, q_c is the cone resistance, f_s is the lateral shear and u_2 the water pressure, σ'_{v0} and σ_{v0} are the effective and total vertical stresses.

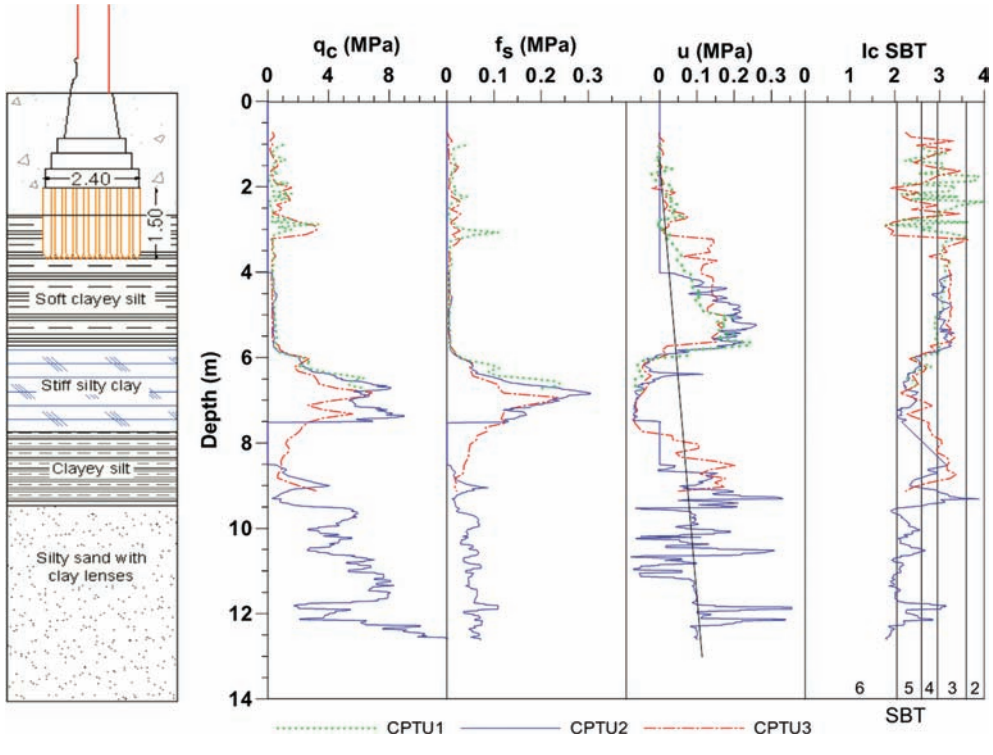

Figure 6. Soil layering and CPTu profiles.

Mechanical properties such as critical state angle (ϕ'_c), undrained shear strength (c_u) and the slope of the normal compression and critical state line (λ) were estimated as suggested by Cola & Simonini (2002) and validated on the basis of laboratory tests, consisting of oedometric tests, Rowe cell tests and triaxial compression tests.

Table 1 (below Fig. 5) summarizes the relevant geotechnical parameters assumed in the numerical analyses.

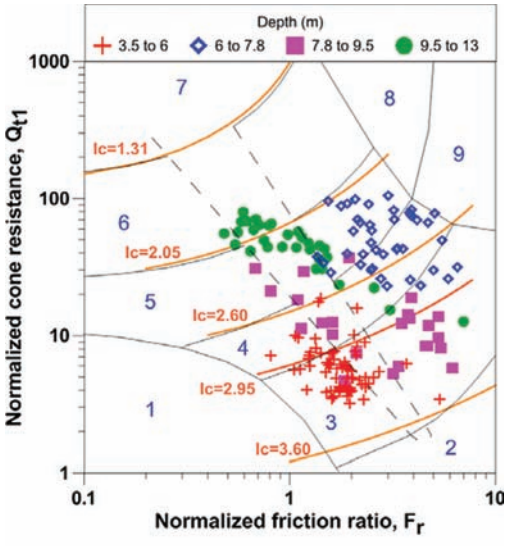

Zone	Soil Behaviour Type (SBT)
1	Sensitive fine-grained
2	Clay - organic soil
3	Clays: clay to silty clay
4	Silt mixtures: clayey silt & silty clay
5	Sand mixtures: silty sand to sandy silt
6	Sands: clean sands to silty sands
7	Dense sand to gravelly sand
8	Stiff sand to clayey sand *
9	Stiff fine grained*
	*Overconsolidated or cemented

Figure 7. Soil type from CPTu at S.M. Maggiore.

4 FINITE ELEMENT ANALYSES

To investigate the effect of wood degradation as possible cause of relative settlement measured along the lateral wall, a Finite Element approach was used. Selected material models are Soft Soil Creep model (Vermeer & Neher 1999), for the cohesive soil, and elastic perfectly plastic, with exponential decreasing mechanical properties with time, for the wood (see section 2).

The vertical stress transmitted by the wall and the stone strip footing to the pile is estimated in 90 kPa, relatively far from the limit load in undrained condition.

To perform the numerical analyses, it was tentatively assumed that the zone improved by the piles under the stone footing could be described by an equivalent continuum, as shown in Figure 8.

The improved zone was modeled by an elastic-perfectly-plastic constitutive model with a Tresca failure surface.

Elastic stiffness was calculated averaging the elastic modulus of soil and the elastic modulus of wood, through the substitution ratio $\alpha = 0$, 80 The cohesion was taken equal to the wood compressive strength and the friction angle was set to zero.

$$E_{eq} = aE_{wood} + (1-a)E_{soil} \quad (7)$$

with E_{soil} = 20 MPa; fresh wood compression strength and stiffness are σ_{c0} = 20.4 MPa and E_{0wood} = 8100 MPa respectively.

To consider the presence of defects, damage during driving and viscous effects on wood, it is necessary to apply reduction coefficients to E_0 and σ'_c namely 0.5 for defects and 0.7 for viscosity.

Wood decay was simulated by a linear MWC increase with time, from 100% to 1000%, and mechanical properties were calculated through the relationship proposed by Klaassen (Eq. 1).

After 500 years from the construction, MWC is at 800%, which is slightly higher than the value measured at S.M. Maggiore (the worst scenario was simulated).

Table 1. Input parameters for soils of the final model of S.M. Maggiore.

Layer	Soil type	Depth	λ^*	κ^*	μ^*	$\varphi(^\circ)$	γ(kN/m^3)	OCR
1	Filling	0–3.5						
2	Clayey silt NC	3.5–5.8	0.0557	0.022	0.0026	32	17	1.01
3	Silty clay OC	5.8–7.8	0.0367	0.0093	0.0003	32	21	6
4	Clayey silt	7.8–9.5	0.0862	0.007	0.0026	32	19	2
5	Silty sand	>9.5	0.055	0.009	0.003	35	19	1.05

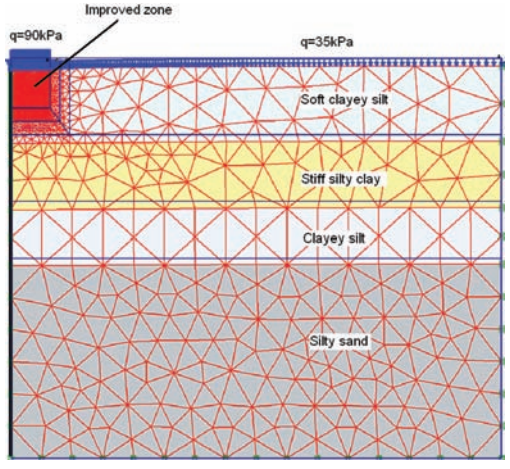

Figure 8. Finite elements model (Plaxis 2D 8.2).

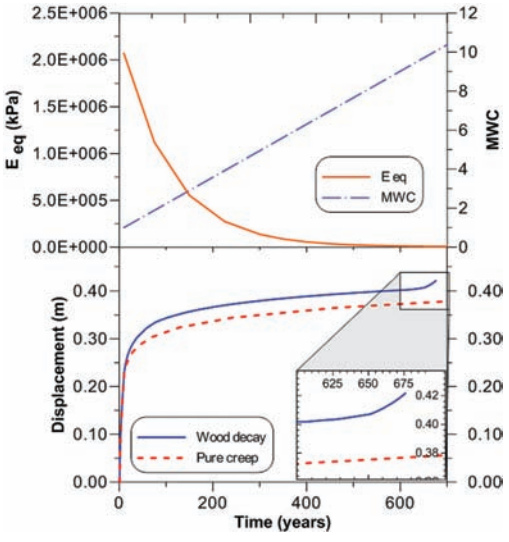

Figure 9. Time-displacement curves considering wood decay and viscoplasticity of soil.

After the calculation of initial stress, a uniformly distributed load (35 kPa) was applied at the piles' head level to simulate the weight of the filling material over the foundation.

After that, displacements were reset to zero and, over the piles, the stress was raised to 90 kPa.

The use of Soft Soil Creep model needs to specify the time phase: load phase took 3600 days, which was the estimated construction period. Afterwards, mechanical properties of the equivalent continuum were reduced to simulate the wood degradation.

Figure 9 shows the time-displacement curves, given by the numerical model, both considering and not considering wood decay. As it can be seen, a moderate or severe wood deterioration increases displacements of a few of centimeters; greater settlements occur when wood totally loses the mechanical properties (MWC > 970%, $\sigma'_c < 20$ kPa).

From the Finite Elements simulations carried out so far, it seems that wood decay cannot fully explain the high measured differential settlement along the lateral wall.

An alternative explanation of the differential settlement may be due to the possible presence of a layering discontinuity in the foundation soil below the eastern part of the wall. By carefully inspecting the results of the borehole logs, it seems that the stiff clay layer (*caranto*) between 6 m and 6.5 m below ground level suddenly vanishes in the eastern area of the church, where the ground appears to be mostly composed of antropically remolded, silty clay with shells and wooden fibers. From this point of view, the heterogeneity of soil profile may justify the relevant differential displacement depicted in Figure 5.

5 CONCLUSIONS

To the authors knowledge, this study represents the first attempt to evaluate the effect of wood degradation on the response of a wooden pile foundation.

From the study carried out so far the following preliminary conclusions can be draw:

- Most of the foundations of ancient buildings in Venice are formed by short and closely spaced wooden piles used as cohesive soil local improvement;
- The wood structure of these piles may undergo to a process of degradation, even in saturated anoxic condition, due to the bacteria action, that may increase the maximum water content with time thus reducing significantly strength and stiffness;
- This influences the overall improved-ground behavior over time, possibly leading to settlements of the above structures;
- The relationship between maximum water content variation and wood strength is highly nonlinear and can be described via an exponential equation linking water content to wood strength;
- The constitutive model for wood degradation has been used into a numerical model to simulate, via an *equivalent continuum,* the response of the ancient wooden pile foundation of the Church of Santa Maria Maggiore, whose lateral wall was subjected to significant differential settlements;
- The analyses carried out so show that wood degradation may be responsible of only of a small

part of occurred differential settlements, being probably the heterogeneity of soil layering their main cause.

Further development of the research is of course necessary to deeper investigate the dynamic and direction of the degradation process, including more information concerning the mechanical properties of wood as a function of its state of conservation. The effect of pile driving and possible presence of wooden planking above the pile heads should be investigated in more detail.

ACKNOWLEDGMENTS

The authors wish to thank CORILA and Regione Veneto for sponsoring the project, CNR-IVALSA for the information concerning ancient wood behavior, University Ca' Foscari, IUAV and all the people involved in the research project for the kind cooperation.

REFERENCES

Biscontin, G., Izzo, F., Rinaldi, E. 2009. *Il sistema delle fondazioni lignee a Venezia. Valutazione del comportamento chimico-fisico e microbiologico. Venice*: CORILA.

Cola, S., Simonini, P. 2002. Mechanical behavior of silty soils of the Venice Lagoon as a function of their grading characteristics. *Canadian Geotechnical Journal* 39: 879–893.

Gottardi, G., Lionello, A., Modena, C. 2008. Influenza delle caratteristiche di fondazione sulla stabilità dei campanili di S. Stefano e dei Frari a Venezia Metodi e strategie di progetto. *Quaderni IUAV:54 Geologia e progettazione nel centro storico di Venezia—La riqualificazione della città e dei territori*, Padova: Il Poligrafo, 79–98.

Huisman, D.J., Manders M., Kretschmar E., Klaassen R.K.W.M., Lamersdorf N. 2007. Burial conditions and wood degradation on archaeological sites in the Netherlands. *International Biodeterioration and Biodegradation*, in press, doi:10.1016/j.ibiod.2007.06.008.

Jefferies, M.G., and Davies, M.P. 1993. Use of CPTU to estimate equivalent SPT N60. *Geotechnical Testing Journal*, ASTM, 16(4): 458–468.

Klaassen, R.K.M. 2007. Water flow through wooden foundation piles: a preliminary study. *International Biodeterioration & Biodegradation* 61:61–68.

Klaassen, R.K.W.M. 2008. Bacterial decay in wooden foundation piles—Patterns and causes: A study of historical pile foundations in the Netherlands. *International Biodeterioration & Biodegradation* 61: 45–60.

Kretschmar, E.I., Keijerb, H., Nelemansb, P., Lamersdorf, N. 2007. Investigating physicochemical sediment conditions at decayed wooden pile foundation sites in Amsterdam. *International Biodeterioration & Biodegradation* 61: 85–95.

Marchi, M., Gottardi, G., Lionello, A. 2006. *Sulle fondazioni dei campanili di Venezia, in Fondazioni Superficiali e Profonde*, Benevento: Hevelius Edizioni 177–192 (atti di: V Convegno Nazionale dei Ricercatori di Ingegneria Geotecnica, Politecnico di Bari, 15–16 Settembre 2006).

Ricceri, G., Simonini, P., Cola, S. 2002. Applicability of piezocon and dilatometer to characterize the soils of the Venice Lagoon. *Geothecnical and geological engineering* 20: 89–121.

Robertson, P.K. 1990. Soil classification using the cone penetration test. *Canadian Geotechnical Journal* 27(1): 151–158.

Vermeer, P.A. & Neher, H.P. 1999. A soft soil model that accounts for creep. *Proceedings of the international symposium 'Beyond 2000 in Computational Geotechnics'*, Amsterdam, 249–261.

Geotechnical Engineering for the Preservation of Monuments and Historic Sites – Bilotta, Flora, Lirer & Viggiani (eds)
© 2013 Taylor & Francis Group, London, ISBN 978-1-138-00055-1

Cultural Heritage and physical environment: A geo-archaeological approach to the analysis of interaction and risk factors

A. Cinti
Cultural Resources Manager, Italy

L. Coppola
Geological Consultant, Formerly Professor at Università della Basilicata, Potenza, Italy

E.N. Bromhead
Geotechnical Consultant, Formerly Professor at Kingston University, London, UK

ABSTRACT: Topography, geology, climate and anthropogenic actions appear to have a significant influence on environmental processes and, consequently, a considerable impact on the conservation of the built environment. Taking into account the conditions in which architectural and archaeological heritage have come down to today, the need is clear to combine an analysis of current conditions with a historical and evolutionary approach, in order to reconstruct the changes that have affected sites and buildings. The geo-archaeological approach has to be understood as a study aimed at determining, in different ages and situations of occupation/abandonment of a site, the extent of interactions between the local physical environment and human settlements. So a study of geological-structural conditions of the slopes is associated to another one focused on historical and archaeological evidence based on a thorough analysis of structural and architectural features still on the ground, as well as of archival evidence, when available, that, in many cases, help to locate, in the time scale, significant events in the history of ancient sites and buildings. The result obtained through this approach is twofold: on the one hand, it allows full understanding of the time and manner of the abandonment of these settlements; on the other, analyzing the factors of degradation in a diachronic perspective, it allows us to identify more clearly the prevalent risk factors, and to implement appropriate risk mitigation strategies in contexts geographically contiguous or similar. This approach is able to provide much more information when an archaeological or architectural site shows traces of significant structural degradation causing, in a more or less distant past, their complete abandonment. Such situations are common across the Apennines, where neotectonics has been responsible for the process of evolution of the slopes, while the lithological and structural characteristics of the soils, within local climatic conditions, have governed the mechanisms of erosion. This paper considers three case studies: archaeological and monumental sites of three different ages, types and constructive characteristics, but linked by the fact that they were, at some point in their history, abandoned because of the conditions of geological instability and environmental degradation.

1 INTRODUCTION

The archaeological and monumental heritage of the central-southern Apennines is today degrading strongly, and the transformation of the physical environment has profoundly affected the conditions of conservation of ancient buildings. In Basilicata, in particular, the hillsides are subject to the erosional aggression of natural and anthropogenic agents causing frequent and widespread hydrogeological instabilities. Landslides, gullies and soil subsidence have, over the centuries, threatened a large number of settlements and buildings, forcing, in many cases, local communities to abandon their historic locations. An integrated approach that combines the study of archaeological remains with the analysis of the geological context offers the opportunity to examine the construction phases, occupation and abandonment of the site connecting these moments with natural phenomena. The result is a framework in which the events of the physical environment appear to be closely related to those of the local communities, in many cases, trying, with the tools at their disposal, to oppose the worsening of the conditions of structural degradation. Throughout the Apennines, neotectonic processes have led to the evolution of the slopes, with lithological and structural settings, associated

with local climatic conditions, ruling the mechanisms of erosion and the distribution of erosion areas. In the study area, the geological instability of the slopes was created by the deepening of rivers resulting from lifting of tectonic blocks and eustatic changes in the level of the Mediterranean Sea. The predominantly clay and silty-clay soils have experienced stress relief; with an increase in the piezometric level in the vicinity of the erosion escarpment. The renewed steepness of the slopes, the decay of the mechanical properties of the soil and water table fluctuations, the latter related to the amount of rainfall, were the most frequent causes of instability in the hillside. The three case studies presented in this paper take into account three sites of different historical periods (ancient, medieval and post-medieval), which have different historical and construction characteristics, as are different the natural factors that led to their abandonment.

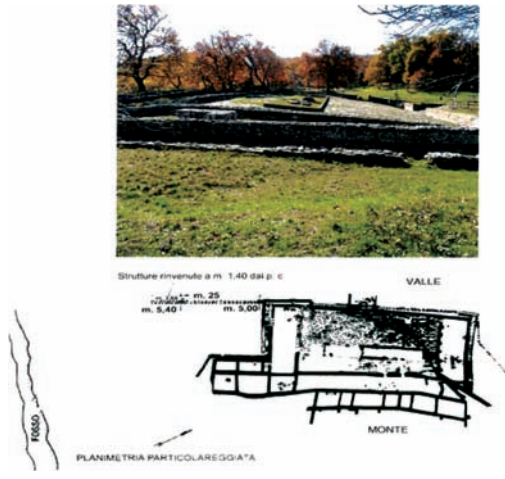

Figure 2. Plan of the sanctuary of the goddess Mephitis.

2 THE SANCTUARY OF THE GODDESS MEPHITIS

Situated in the territory of Rossano di Vaglio (Fig. 1), province of Potenza, it was built in the second half of the IV century BC on a slight slope on the eastern side of the Macchia di Rossano mountain (Fig. 2) and quickly became one of the most important religious complexes of Lucania as well as a political center, when the Samnites dominated the region. Towards the end of the third century BC the environment around the sanctuary underwent a first transformation, leading to a structural modification of the building on the west side of the parvis. This involved in a slight movement of the slope, probably due to an earthquake. The presence of some inscriptions of the second century BC on the pavement of the parvis, and the bases of the columns placed under the same floor, determine the limits of time in which the restoration was made. Among the III-II century the sanctuary was well—attended, witnessed by many inscriptions and coins found on the site; the presence of pilgrims and priests increased and led to an increased use and consumption of local natural resources; new channels were built to supply water to the place of worship; the water was allowed to flow freely along the hillside. At the end of the Republican period the entire complex was affected by a new instability caused by the movements of an ancient landslide. The conditions of the sanctuary in the first half of the first century AD required a member of the family Acerronia from Lucania to restore nearly all that was left standing, reusing materials found in situ. Many inscriptions became part of the wall on the north side, others were included in the pavement, others in the structures of the external channel with a drainage channel on the west side of the building. With the reconstruction of the pavement of the square (Fig. 3), the workers of Acerronius uplifted the level of a new cloaca, trying to harmonize it with the other channels and smaller pipes. The most challenging job, however, was conducted on the west side, where a diversion channel of the water on the southern side of the hill was built. It was, in the end, a general restoration, with new facilities on the southwestern side of the sanctuary. With these renovations, the sanctuary went back to its ancient greatness, became one of the most important religious complexes of Lucania, and, at the same time, an important political and administrative center. Unfortunately, that did not last very long: at the age of Tiberius or a little later (~79 AD) the sanctuary died when a new tilting of the existing landslide turned the whole area into a swamp. After the final abandonment, Potentia was founded nearby.

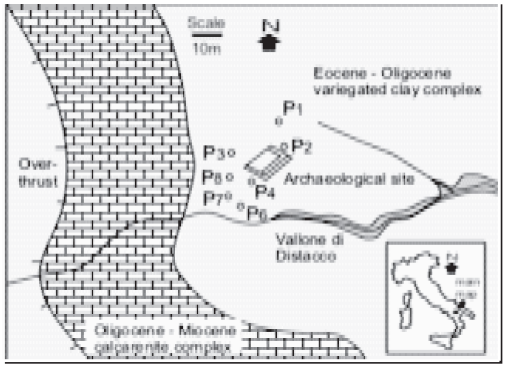

Figure 1. Geological map of the eastern side of M. Rossa Macchia di with the location of the site.

Figure 3. Gutter, embedded in the pavement of the churchyard, for the disposal of water from a fountain at the entrance of the sanctuary.

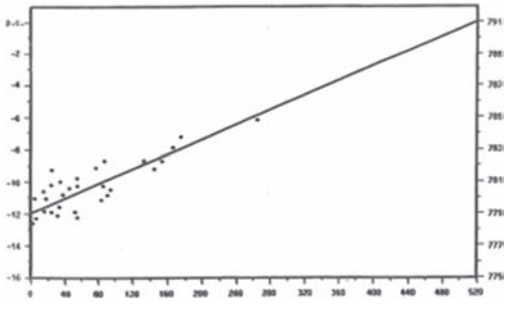

Figure 4. Diagram of regression between precipitation values and those of the piezometric variations relative to 31 months of observations (06/1993–12/1995). The portion 791 corresponds to the ground level and is a portion of the normalized slope, according to the position of the wells, referenced to mean sea level.

The lithological and morphological analysis of the slope, as well as the technical properties of the subsoil consisting of Varicolori Clays showed that, by testing the stability of the slope made by the method of Balance Limit, the sanctuary of Mount Rossano has undergone periodic disruptions due to increases in water intake located on the site. Taking as a point of reference the old sliding surface of the mass movement, reconstructed through morphological indications of the landslide body, it is evident that the conditions of instability of Varicolori Clays are reached when the water pressure in the soil corresponds to a piezometric value (level of the water table) of about –1.5 m from ground level (Fig. 4).

Furthermore, by the analysis of long-term rainfall linked with the fluctuations of the piezometric level of the aquifer in the subsurface, we get the critical value of the pressure corresponding to the value of –1.5 m from ground level (Fig. 5) and the same figure indicates that this value is achieved with 455 mm/month of rain.

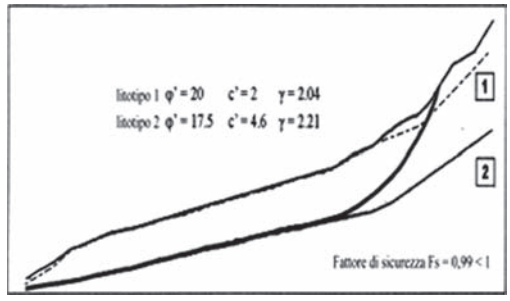

Figure 5. Check of the stability of the slope with groundwater level at –1.5 m down the ground level, a condition in which the A.V. show instability with a safety factor Fs less than 1 (Fs < 1 = 0.99).

Such precipitation can be attributed to weather events that are rather exceptional for a semi-arid Mediterranean climate such as that of southern Italy.

Although the Mediterranean climate of 2000 years ago is considered to be more humid than at present, a rainfall up to 455 mm/month is an event difficult to verify; much more likely is the fact that the value of the water of –1.5 m was achieved when the surrounding waters of the springs were channeled to the sanctuary, in order to meet the needs of a growing number of pilgrims and priests at a time when the site took its greatest importance moment. Ultimately, the contractions of the wooded areas, the cultivation of new cereal-growing areas, but especially the more localized water supply, were the factors that have interfered deeply in the environmental system causing the collapse of the structure and the final abandonment of the sanctuary and of the surrounding area.

3 THE MEDIEVAL SETTLEMENT OF UGGIANO

It is located about 5 km NW far from Ferrandina, in the province of Matera; it is shown on maps as "Ferrandina Vecchia" (Fig. 6). The walls indicate not only the importance of the settlement in antiquity (Fig. 7), but also the need to study it deeper: in fact, a considerable amount of monumental structures is now buried or converted for different purposes. The site currently reveals only the facilities of the castle; structures of considerable architectural merit and which deserve to be protected. The settlement is situated at 476 m above sea level along a stretch of land that is bordered on the east by the "Canale Lavannara"(Fig. 8), to the "Fosso del Varvaro" to the west, however, with the silt-clay badlands formation of "Coste Uggiano". The site, in fact, is known only for the presence of the castle but, as already mentioned, the hill preserves traces of a large village.

Figure 6. Medieval settlement of Uggiano.

Figure 7. Detail of the inner walls of the castle (XI century AD).

Figure 8. Overview of the channel Lavannara.

The presence of such a large settlement, although already popular in the early history, is justified by the strategic value taken during the eleventh century AD, when the Normans arrived. At that time Uggiano was already equipped with walls and fortifications. The interconnection between these elements, composed of large agglomeration and peripheral territorial entities—but not minor—it was so deeply rooted that even in contemporary chronicles seemed that the southern regions were rich in fertile and wooded areas. These considerations led JM Martin to assess how the conquest by the Normans was directed to a country absolutely not desert and underdeveloped.

The first historical evidence of the existence of Uggiano's castle date back to 1023 and in 1029, when Lupo Protospata described that two Muslims, "Rajca et Saffari obsederunt castellum Obbianum, qui Obbianenses extraneos tradentes pacificaverunt cum ipsis". It is documented, in this way, the strategic value of the settlement in which, 6 February 1068, offered refuge to Roberto Guiscardo, when he had not yet taken Montepeloso (Irsina). This suggests that the castle had not only a strategic value but, resisting the siege for so long, it also had a certain amount of food reserves, or at least the possibility of regular supplies. In fact Uggiano had some land around and other properties used as pasture. These were the lands cleared of forest by Greek monks during the seventh and eighth centuries AD. In this period on the hillside surrounding the site of Uggiano, in a predominantly semi-arid Mediterranean climate, began to spread surface instabilities produced by the intense erosion of productive soils. The deforested areas were pervaded by badland shapes with heavy consequences on the socio-economic development of the medieval settlement. The land affected by this kind of instability belong to the formation of Subapennine Clays, which is represented by the blue-gray silt and clay that are the product of a Pleistocene marine deposition in a restricted basin, called Bradanico Basin. Field surveys have also found that gully erosion is the peculiar effect of the process of slope instability. The landslides, both superficial and deep, are developed all through the incisiveness of the gully bed cause the variation of the equilibrium limit of the slope. In fact, the causes that trigger landslide fronts are due to the process of regressive erosion of waterways. The hydrographic network on the slopes, in fact, undergoes a continuous rejuvenation due to relative fast lowering of the basic level of the main watercourses that, for the most part, are channeled into pre-existing fractures (faults). However, structural and lithological characteristics (particle size and chemical-mineralogical settings) of the ground are not sufficient to explain the morphology of the badlands. In fact this kind of erosion develops through a mechanical process induced by the flow rate and the speed of concentrated runoff, i.e. through the acquisition of energy needed to overcome the limit of resistance of the lithic material when rainwater flows on slopes that already possess a certain steepness (typically 34°).

Consequently, if in morphogenesis of badlands the steepness of the slope is unquestionably a primary component and there is a limit value of the angle of slope (α_{lim}) below which the capacity of erosive factors is not very effective against soil resistance.

The model is summarized in a mathematical way as follows:

$$\alpha_{lim} = F_A - R_i$$

where:

F_A includes all the variables driving the evolutionary process, ie those causing he erosion;

R_i encompasses those forces opposing the erosion.

The angle α_{lim} can be defined as the angle of steepness of a slope giving the value limit in the genesis of gullies and at the same time can be considered as the resultant of all the physical and anthropogenic components affecting the slope, such as lithology, grain size, structural settings, sediment fracturing, local climate, exposure of the slope, runoff, rain, deforestation, plowing, etc.

In this situation, the walls of the castle Uggiano were compromised by the failure; so some buttresses were built on the eastern side of the fortress, perpendicularly to the wall, in order to incorporate the structure and to contrast the regressive erosion of the slope (Figs. 9–10). Unfortunately, by the time the castle was attacked from all sides the effort in consolidating and supporting the building was in vain. In 1492 a violent earthquake shook an area already affected by the geological collapse and becoming essentially unproductive.

For this reason the local population began a migration to more fertile areas, from the mid-fifteenth century onwards, gradually building a new village known as Ferrandina. Therefore the settlement of Uggiano did not experienced a sudden abandonment because of the earthquake, as the contemporary chronicles tell, attributing to Federico D'Aragona and the refugees from Uggiano the foundation of Ferrandina in 1492, but a slow depopulation due to changes in the environment and in the socio-economic framework.

Figures 9–10. Effects of regressive gully erosion at the base of the wall.

4 CAMPOMAGGIORE VECCHIO

In the province of Potenza, a ghost settlement (Fig. 11) located on the side facing the left bank of the Basento river. Between 8 and 10 February 1885, following three days of heavy rain, the ground on which the town was built belonging to the lithological formation of the "Flysch Rosso" and specifically to the clayey-marly member, was affected by a large and slow geological instability caused by a rotational landslide. It was the reactivation of an ancient landslide that in the past produced a noticeable terrace on a slight slope, on which in the Baroque period the settlement was recklessly refounded. The town, in fact, having been inhabited from prehistoric times until 1300 AD, went through a period of neglect, as has often happened in Basilicata, a land of constant movement of people in search of new and more fertile lands to cultivate.

In 1622 the territory of Campomaggiore, freed from the old feudal lords, was granted by king Filippo IV to Carlo Rendina with the title of Count, requiring him to inhabit the ancient feud.

The landslide was so slow and gradual that the town underwent a progressive shift, from upstream to downstream of about 200 m, partially preserving the integrity of the buildings. Only resisted the bell tower and the Church itself (Fig. 12), the Palace Rendina (Fig. 13), the cemetery and the houses, all of them, of course, suffering cracks and disarticulation of the structures so that the inhabitants were forced to abandon the site and rebuild the village about 2 km to the east on the top of a hill. Campomaggiore Vecchio today assumes a significant importance, both from a historical point of view and from the point of view of the architecture as a witness to the past way of life and building types as well as example of the interactive relationship within the local environment and the evolution of itself.

In order to clarify this aspect of the problem concerning the conservation of the architectural heritage of one of the many villages of Basilicata with the same condition of geological instability, it is necessary to take a step back to analyze the causes of the landslide, then you have to answer, first of all, these questions:

a) why an ancient site that has been stable for many centuries (from 1622) has just collapsed in February 1885?
b) why there was just one type of movement?
c) which were the real causes of the disaster?

Figure 11. Geological map of Campomaggiore Vecchio area.

Figure 12. Places of worship.

Figure 13. Palace Cutinelli-Rendina (from Campomaggiore, archeologia dell'edilizia storica di Pierfrancesco Rescio, 1997).

Referring to the causes of instability, the prolonged rain of February 1885 do not satisfy these questions. Such a meteorological event, in fact, is no exception in the historical period. Is there therefore a cause-effect relationship?

In 1673, the Count Gerardo Antonio Rendina, son of Carlo, finally acquired the entire territory of Campomaggiore. In 1741, the village was concentrated in only one place, at the behest of Don Ferrante Rendina. Whoever wanted to live in the village of Campomaggiore had the obligation to plant a vineyard for which he had to pay, after 6 years, 5 carlini for each "tomolo". However, the residents also had a chance to cut the wood of the oak forest for roof beams, but planting, for each felled oak, three fruit trees chosen by the baron. Between 1760 and 1780, Teodoro Rendina and his successors, increased the agrarian economy.

A small swamp was drained and the houses were grouped around the baronial palace thus creating a village with grid pattern, with wide streets that crossed at right angles. Everything was built in masonry. In this period at the behest of Teodoro Rendina, many inhabitants of Bitonto moved to the village of Campomaggiore and introduced in the area forestry, pastoral activities and the cultivation of the olive. Campomaggiore had 410 inhabitants in 1795 and in 1820 they doubled to 820. In 1885 there was a landslide.

Through the analysis of the stability of the slope (back-analysis) it is possible to determine the water pressure in the soil, and the rise in piezometric level in terms of failure of the slope. It is also possible to relate the amount of rainfall with the variations of the aquifer in the subsoil through piezometric observations of long period, in order to identify the content of rainfall corresponding to the water pressure driving to the rupture of the slope. The analysis of the stability (Fig. 14) supplied the values of the safety factor (Fs) always greater than 1 even in conditions of interstitial water pressure at maximum, that is the piezometric level corresponding to the ground level (Fig. 15).

The result is pretty obvious, considering that the existing landslide terrace on which the village developed after 1662, had acquired a consolidation that determined the state of rest of the clay. The ancient steepness of the slope, according to the reconstruction, had a value of $\alpha = 14°$. Referring again the same analysis with steepness of slope equal to $\alpha = 25°$, ie that of the same slope, but at the moment of activation of the landslide (1885), it was found that the hydrogeological instability, which involved Campomaggiore Vecchio, occurred under conditions of interstitial water pressure corresponding to a piezometric depth of 1 m below the ground surface (safety factor Fs = 0.95—Fig. 16). This fact indicates that the activation conditions of the landslide movement depended mainly by the changed conditions of the steepness of the slope that arose in the period between the establishment of the village in the Scarrone del Salice (1622) locality until the landslide of 1885. Thus it seems that the main cause of reactivation of existing landslide is the process of regressive erosion of rivers tributary to the Basento river.

The river, in this case, acts as the base level and with the incision of its own bed has led, over the centuries, an evolutionary process in the morphology of the slope with a gradual increase in steepness of the surface profile. By current geomorphological observations made on the slope, downstream of the landslide, on which is located Campomaggiore Vecchio is clear, with much evidence, that the most amount of the landslide develops along incisions that go up the slope from the course of Basento

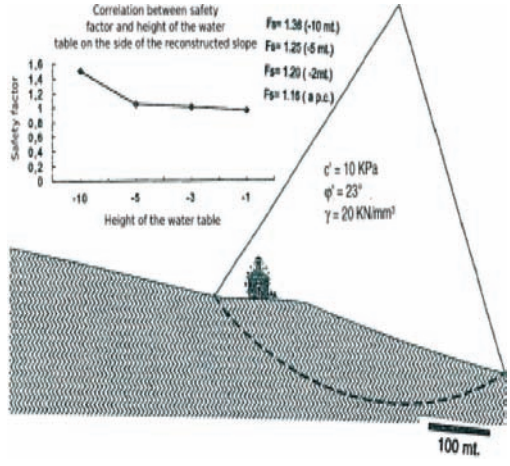

Figure 14. Check of the stability of the pre-existing landslide carried out on the side (reconstruction), before the event of 1885. The steepness of the slope $\alpha = 14°$.

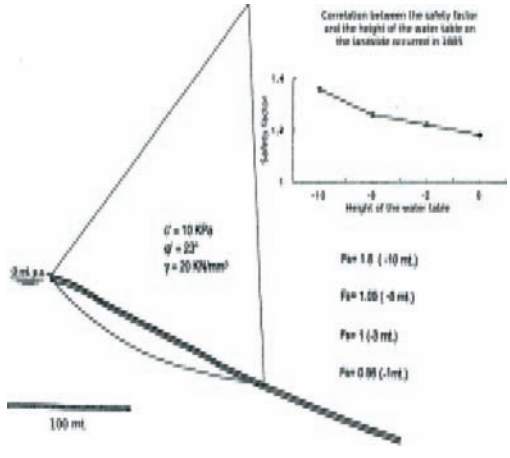

Figure 15. Check of the stability of the slope at the time of the landslide of 1885. The steepness of the slope $\alpha = 25°$.

river. At the edges of these recordings the clays of the Flysch Rosso undergo a discharge stress, decreasing the consolidation pressure. Simultaneously, the slope is the seat of a filtration process with stationary hydraulic gradient that is particularly high closer the ground surface. For this reason, the most frequent landslides occur along the incisions and evolve gradually going up the slope. It follows that the main cause of a further activation of the Campomaggiore landslide of 1885 it has been due to the process of regressive erosion of water streams.

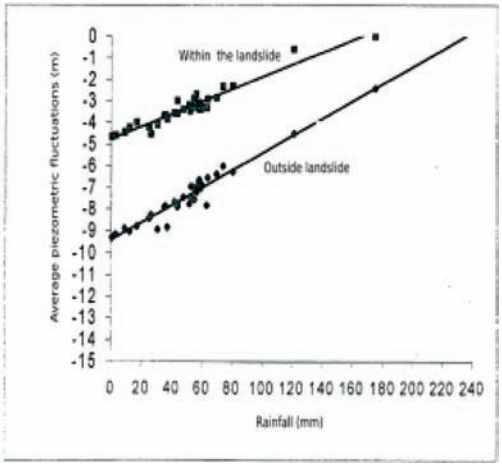

Figure 16. Correlation between meteoric inflows and fluctuations of the water table within the landslide and outside of it.

5 CONCLUSIONS

In the end, it can be concluded that the attendance of people, since ancient times, on the hills of Basilicata, consisting mainly of clay, has undoubtedly changed the ecosystem of these areas, as a result of productive processes as result of the growth of the population. More recently, the cultivation of new land, land reclamation, the contraction of the forests, moving from smaller towns and the crisis of agriculture are the causes of an acceleration in the degradation of the physical environment. The change was immediate and sometimes violent; in some cases, slow and gradual. However, the historical reconstruction of these environments and their changes as well as of the locations, changes, reorganizations and social crises of the centers of human aggregation can provide an assessment of the factors of cause and effect in the historical process of transformation of the territory. Following the path of the modifications joint is possible in this way to reconstruct the interactive relation between the two systems, natural and anthropogenic, over time and evaluate the speed of the processes of change. This knowledge can be also translated in terms of forecasting and assessing future changes affecting the architectural and archaeological heritage as a function of environmental degradation (cultural heritage) and the use of the land (the history of the natural/anthropic environment).

REFERENCES

Adamesteanu D. & Dilthey H. (1992) Macchia Rossano; il Santuario della dea Mephitis. Deputazione di Storia Patria per la Lucania. Quaderni di Archeologia e Storia Antica, Congedo Editore.

Adamesteanu D. & Lejeune M. (1971) Il santuario lucano di Macchia Rossano di Vaglio. Mem. Lincei, XVI, 2, 39–82.

Capano A. Allevamento, transumanza, tratturi in Basilicata dall'antichità all'Età contemporanea, in Lucania archeologica, V, 1–4, dicembre 1986, pp. 6–15.

Coppola L. (1993) Evoluzione tettonica e meccanismi deformativi della media valle del Basento. Boll. Soc. It., 112, 159–179, 20 ff., 1 tav. f. t.

Coppola L. (1998) Monitoraggio storico-ambientale per la tutela del patrimonio archeologico e architettonico. Atti del Convegno Internazionale "Archeologia e ambiente", Ferrara, 3–4 Aprile 1998.

Cutinelli Rendina G. Necrologia di Campomaggiore, in Lucania letteraria, 7–8, 29 marzo-8 aprile 1885, pp. 17–19, 29–30.

Del Prete M., Melidoro G. & Valentini G. (1977) Influenza dell'assetto geostrutturale sulla franosità delle formazioni pelitico-fliscioidi nella fascia orientale dell'Appennino Lucano (Campomaggiore). Geol. Appl. e Idrogeol., Vol. XII, P. II, Bari.

Ducci A. Osservazioni geologiche sul territorio di Campomaggiore Nuovo (Potenza) e sulla frana che minaccia l'abitato, in Bollettino dell'Ufficio Geologico d'Italia, LXX, 1945–46, parte I.

Filardi G. Campomaggiore. Storia di un paese lucano, I-II, Matera s.d. (ma 1985).

Francovich R. – Parenti R. (eds), Archeologia e restauro dei monumenti, [I Ciclo di Lezioni sulla Ricerca Applicata in Archeologia], Firenze 1988.

Fuchs M. (2007) An assessment of human versus climatic impacts on Holocene soil erosion in NE Peloponnese, Greece. Quaternary Reseaxch, 67, 349–356.

Iverson R.M. & Major J.J. (1987) Rainfall, groundwater flow and seasonal movement at Minor Creek landslide, NW California: physical interpretation of empirical relations. Geol. Soc. Am. Bull., 99.

Kenney T.C. & Lau K.C. (1984) Temporal changes of groundwater pressure in a natural slope on nonfissured clay. Canadian Geotechnical Journal, 20, 138–146.

Mannoni T. Caratteri costruttivi dell'Edilizia storica (Archeologia dell'Architettura), Genova 1994.

Moreno D. Dal documento al terreno. Storia e archeologia dei sistemi agro-silvo-pastorali, Bologna 1990.

Rescio P. Campomaggiore, archeologia dell'edilizia storica, 95 pp. Centro Studi per la Storia della Cultura Materiale nel Mezzogiorno.

Rescio P. I castelli della Basilícata: Problemi di archeologia e storia, in Bollettino della Biblioteca Provinciale "T. Stigliani" di Matera, 27–28, 1996, pp. 41–53.

Rescio P. Il contributo dell'archeologia allo studio dei castelli e dei centri storici minori: alcuni esempi, in Archivio Storico Pugliese, XLVIII, 1995, pp. 179–206.

Rescio P. La Chiesa di Campomaggiore Vecchio: relazione sul suo degrado e proposta di intervento conservativo, (ad uso del Comune di Campomaggiore, 18 gennaio 1997).

Rescio P. Tra castelli e cinte murarie di Puglia e Basilicata: un approccio archeologico, in la Capitanata. Rassegna di vita e studi della Provincia di Foggia, XXXII-XXXIII, 3–4,1995–96, pp. 171–208.

Geotechnical Engineering for the Preservation of Monuments and Historic Sites – Bilotta, Flora, Lirer & Viggiani (eds)
© 2013 Taylor & Francis Group, London, ISBN 978-1-138-00055-1

Settlement response of masonry constructions

M. Como
Department of Civil Engineering, University of Rome, Tor Vergata, Italy

ABSTRACT: Masonry constructions, due to the constitutive model of the masonry material, characterized by very low ratios between tensile and compression strengths, exhibit a typical static behavior in regards to the occurrence of small foundation settlements. The same settling structure controls the intensity of the reaction of the settled constraint that is unrelated on the magnitude of the settlement.

The actual degree of settling is difficult to quantify. Despite this uncertainty, the internal stress state of the structure is, on the contrary, well-defined. No equilibrium loss can occur during the settling. This is a proper aspect of the masonry structures behavior that can explain the great durability and longevity of so many historic buildings. The paper ends with a comparison between the masonry behavior and that of the standard cohesionless soils. It is so shown that these two materials present the same mechanical behavior.

1 INTRODUCTION TO MASONRY BEHAVIOR

Reinforced concrete buildings, as a rule, are seriously damaged by differential settlements occurring in their foundation. Masonry buildings, particularly the historic ones, behave, on the contrary, very differently. The majority of them experienced shifts and settlements over the centuries. Nevertheless, they remain unaltered up to the present day, after many centuries following their construction.

The old builders, were not geotechnical engineers. While the interest of the modern engineer is to prevent settlements, the old builders were prepared to allow foundations movements and consequent cracking. There is something of *singular* in the behavior of masonry structures. This is due to the mechanical masonry response, very different from that shown by usual elastic materials. The difference is due to the masonry low tensile strength and to the consequent different masonry response in tension and in compression (Heyman, 1966).

We outline the main features of this behavior. An ancient masonry construction can be regarded as an assemblage of rigid particles, stones or bricks, placed one on the other. It is unsafe to assume that mortar, that may have decayed with time, adds strength to the construction. Stability on the whole is assured by gravity forces that generate compressive stresses inside the masonry mass and, because the friction, lock together the various elements against slippage. A masonry structures can suffer cracks or detachments that may in turn generate displacement fields, called *mechanisms*, which develop without any internal opposition from the material. As soon as the pushing loads begin to exceed the action of the resistant loads along one of these mechanisms, the structure fails (fig. 1). Under a given loading path, a masonry structure can thus reach a collapse condition solely due to loss of equilibrium, that is to say, in absence of any material failure. Such a condition can therefore arise even in masonry with infinite compression strength.

Common programs of stress analysis are not at disposal for masonry structures, unlike modern steel and reinforced concrete ones. Because the strong non linear behavior of the old masonry, usual linear elastic methods, if applied, give, in fact, unsatisfactory predictions. The very low tensile strength of the masonry suggests, on the contrary, the use of unilateral models—the so called no tension models—in place of the unacceptable linear elastic ones. The simplest model that retains essentials of the masonry behavior is the Heyman rigid in compression no tension one. We recall the key assumptions introduced by Heyman (1966): the masonry is incapable of carrying tensions and has an infinite compression strength; sliding failures cannot occur.

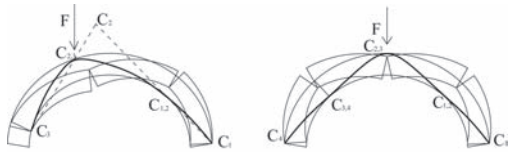

Figure 1. Failure mechanisms occurring in masonry arches.

The foregoing assumptions turn out to be very clear if we refer to the elementary resistant cell of the masonry structure, represented by two idealized rigid masonry bricks compressed one against the other by a more or less eccentric axial load and eventually loaded by a shear force (fig. 2).

The two rigid bricks of the unit resistant cell, of height h, cannot deform internally but can detach from each other (fig. 2). A *crack* occurs in the cell. The overall stress state is determined by an axial orce N applied at the section's centre, a moment M and a shear force T. Thus, the stress state acting on the unit cell can be represented by the vector

$$\sigma = \begin{bmatrix} M \\ N \\ T \end{bmatrix} \tag{1}$$

According to the assumptions, only compressive stresses are consistent. Thus, the eccentricity of the axial load N

$$e = M/N \tag{2}$$

must satisfy the inequalities

$$-h/2 \le e \le h/2 \tag{3}$$

The model prohibits sliding. Consequently, the shear force T will not be bound by any restrictions. Since shear T is uninvolved in defining the limit equilibrium between the two ideal bricks, we can consider the projection σ' of σ on the coordinate plane (N,M) as shown in figure 3. Thus the eccentric axial loading state, defined by the values of the axial force N and moment M (and which we will continue to indicate as σ for the sake of simplicity), cannot extend beyond the two limit lines represented in the plane (N,M) by the two straight lines OA and OB of figure 3

$$M = Nh/2 \qquad M = -Nh/2 \tag{4}$$

The set of *all consistent stress states* in the space (M,N,T) is thus the region included between the two π planes orthogonal to plane $T = 0$ and having intersections in the two limit lines $M = Nh/2$ and $M = -Nh/2$. In particular, the region Y of the consistent stress states in plane M,N is the region delimited by angle OAB.

A vector σ placed along either line OA or line OB represents an axial force with eccentricity respectively equal to $h/2$ or $-h/2$, as shown in the two schemes of figures 4. These peculiar stress states are denoted as σ_o^+ and σ_o^- and are expressed as

$$\sigma_o^+ = \begin{bmatrix} Nh/2 \\ N \\ T \end{bmatrix} \qquad \sigma_o^- = \begin{bmatrix} -Nh/2 \\ N \\ T \end{bmatrix} \tag{5}$$

Any deformation of the unit resistant cell will be either zero or a detachment strain and will be represented by the strain vector whose components ϕ, Δ and γ are the elementary strains on which the force components M, N and T respectively do work. No strain can occur until the eccentric axial force reaches the upper or the lower edge of the brick cell section. If the stress is σ_o^+ the corresponding detachment strain, the vector ε^+, is produced by the opening of the hinge situated at the upper edge of the section; conversely, strain ε^- corresponds to the stress σ_o^-. These strains are thus defined as

$$\varepsilon^+ = \begin{bmatrix} \phi \\ -\phi h/2 \\ 0 \end{bmatrix} \qquad \varepsilon^- = \begin{bmatrix} -\phi \\ -\phi h/2 \\ 0 \end{bmatrix} \tag{6}$$

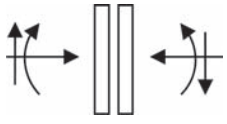

Figure 2. The unit resistant masonry cell.

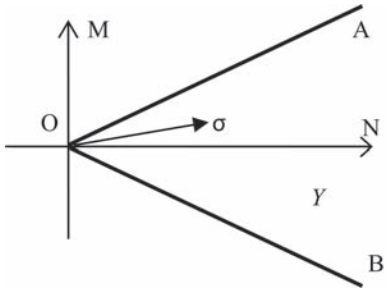

Figure 3. The region Y of the admissible stresses.

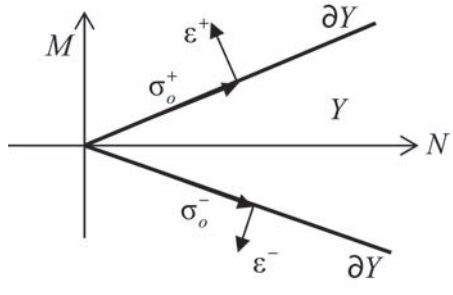

Figure 4. Admissible stress states and detachment strains.

Stresses at the limit state (+), represented by the vector σ_o^+, don't work on the corresponding detachment strain ε^+. Likewise, at the limit state (–), σ_o^- does no work on the strain ε^-:

$$\sigma_o^+ \cdot \varepsilon^+ = 0 \qquad \sigma_o^- \cdot \varepsilon^- = 0 \tag{7}$$

The detachment strain ε^+ is thus *orthogonal* to the limit line $M = Nh/2$, while the vector ε^- is orthogonal to the other limit line $M = -Nh/2$, as shown in fig. 4. Surprisingly, as for ductile steel, the masonry material obeys the associated flow rule.

The settlement response of the masonry buildings is strongly influenced by this behaviour. Contrarily to reinforced concrete or steel structures that suffer early brittle failures and severe damage, masonry settled constructions deform according mechanisms whose hinges open without any material distress. While settled reinforced concrete structures scale up damage with the settlement increasing, masonry structures follow freely the settlement progress with no equilibrium loss under constant stresses, provided geometry changes, generally confined, remain negligible. This aspect of the masonry behavior can explain the great durability and longevity of so many historic buildings.

2 SETTLED MASONRY CONSTRUCTIONS

Loads can be considered composed as

$$p = g + \lambda q \tag{8}$$

where, with a simple notation, g and q are respectively the *dead* and the *live* loads and λ is a multiplier. Live loads q, affected by the loading parameter λ, can exert a pushing action along some mechanism. As a rule, the weight g, on the contrary, represents the resistant load for a masonry structure. Consequently, the structure will certainly be *safe* under the action of its own weight g if and only if the following condition will be satisfied (Como, 1996)

$$< g, v > \; < 0, \quad \forall v \in M \tag{9}$$

where the notation $<g,v>$ indicates the work of the loads g on the displacement mechanism v; the symbol $\forall v \in M$ means that the condition $<g,v> < 0$ will be satisfied along *any* v belonging to the set of the admissible displacement mechanisms. The weight g thus will always *oppose* any deformation of a *safe* masonry structure.

Masonry constructions have been built so that their corresponding mechanisms produce vertical displacements in which lifting is always dominant. It is the geometry that ensures that the structure's weight counters the emergence of any mechanisms. Weight and geometry represent the essential elements in the strength of masonry structures.

Let us consider a masonry structure at a safe equilibrium state: it occupies the configuration C_i under the actions of loads g (fig. 5). Inequality (9) holds: it means also that the internal stresses make negative work on the strains corresponding to any mechanism v. Let us now assume that the structure becomes deformed as a consequence of a *settlement* of one of its external constraints. The structure deforms with the mechanism displacement v_s, representing the settlement.

Let C_s be the configuration taken on by the structure once the settlement has occurred. By assuming that C_s is *very near to* C_i, we can refer to the geometry of its *initial* configuration C_i when expressing equilibrium equations.

As the settlement occurs, the structure's internal equilibrium shifts from initial configuration C_i to the displaced one C_s. Changes in the internal stresses and constraint reactions will occur during the transition from C_i to C_s, so that the initial stress state σ_i is altered and becomes

$$\sigma_s \tag{10}$$

By way of example, consider the arch under its own weight that, satisfying condition (9), mobilizes a pressure line that, at any section, never touches its extrados and intrados.

This arch suffers a small increase of span due to the settlement; it deforms and takes on the mechanism configuration of fig. 6. The pressure line from its original position π_i changes into π_s and will pass through hinges of mechanism v_s. Consequently, internal stresses σ_s don't work on the deformations $\varepsilon(v_s)$ corresponding to v_s.

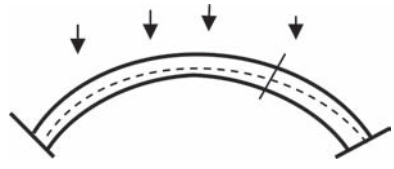

Figure 5. The safe masonry arch.

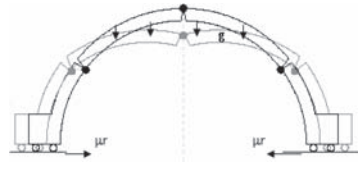

Figure 6. The released settled arch.

The same occurs for any structure that is deformed by a mechanism and adapts itself to settling. Thus, at the settlement state the following *mechanism state condition* holds

$$<\sigma_s, \varepsilon(v_s)> = 0 \tag{11}$$

We can *release* the structure by removing the settled constraint by applying the reaction $\mu_s r$. The set of all the mechanisms of the released structure is denoted by M'. The weights g and the reactions $\mu_s r$ are the applied loads acting on the released structure at the settled state. Thus, considering the released structure at the admissible settled equilibrium state, from the virtual work equation we get

$$<g, \delta u> + \mu_s <r, \delta u> = <\sigma_s, \varepsilon(\delta u)>, \forall \delta u \in M' \tag{12}$$

where δu is any virtual mechanism displacement. In condition (12) the virtual work of the weight g and of the reaction μr of the released structure equals the internal virtual work of stresses σ_s on the virtual strains $\varepsilon(\delta u)$. Condition (12) with $\delta u = v_s$, yields

$$<g, v_s> + \mu_s <r, v_s> = 0 \tag{13}$$

Loads g make positive work on the mechanism displacements v_s and the reaction $\mu_s r$ of the released constraint opposes settling, so that

$$<g, v_s> > 0 \tag{14}$$

and

$$\mu_s <r, v_s> < 0 \tag{15}$$

In spite of the occurred settlement, the work of the loads g on the mechanism δu evaluated at the displaced configuration C_s is still the same as the work at C_i assuming that displacements v_s are *small,* i.e. that the geometry changes are negligible. Thus, if at the initial state C_i, the admissibility condition (9) is satisfied, the same condition holds at the new configuration C_s. No equilibrium loss will occur during the settling. In this regard we meet the Heyman's statement (1966): "if the foundations of a stone structure are liable to small movements, such movements will never, of themselves, promote the collapse of the structure".

By assuming that the settled configuration C_s of the arch is *very near to* C_i, the geometry of the distorted arch is virtually unchanged.

Thus the conclusion is that, despite perhaps virtually alarming cracking, the deformed arch has virtually the same margin of safety as the arch in its perfect state. Moreover, if settlement becomes

$$kv_s, \quad k > 1 \tag{16}$$

the static arrangement of the structure will not change and the internal stresses will remain fixed at σ_s. Thus, if the pressure curve touches the arch extrados and intrados at the hinges corresponding to the mechanism v_s and, consequently, condition (11) is satisfied, the same condition (11) will continue to be satisfied by assuming the mechanisms kv_s, $k > 1$. In short, the structure follows freely any increase in the settlement, maintaining its configuration in admissible equilibrium. Settling develops with frozen internal stresses σ_s and constraint reactions $\mu_s r$. The actual degree of settling is difficult to quantify. Despite this uncertainty, the internal stress state of the structure is, to the contrary, *well-defined*.

We point out the limitations of the previous statements.

They are firstly contained inside the same simplifying constitutive equations of the masonry material and, particularly, in the assumed infinite compressive strength. But this hypothesis is justified by the very low level of compression stresses, as a rule present in the masonry structures.

The other limitation comes from neglecting geometry changes. Any settlement, even small, allocated in correspondence with one of the abutments, transforms the arch into a mechanism and causes the formation of three instantaneous opening hinges: thus the structure assumes the typical static determinate configuration of the three hinges arch.

Then, the subsequent gradually increasing settlement modifies the geometry of the arch so that it can reach the collapse as soon as another hinge opens, as shown in fig. 7. (Romano, 2005).

The magnitude of the settlement producing the failure depends on the initial static condition of the structure For instance, the safety state of a semicircular arch subjected to its own weight depends on its thickness/radius ratio s/R. If this ratio is not larger than about 0.1 (Heyman, 1966, Ochsendorf, 2009), the arch is not capable of sustaining even its own weight. If the value of the ratio s/R is only a little larger, the arch will be very disposed to failure during the settlement occurrence. Likewise, a masonry structure with piers strongly compressed because of their very reduced sections, can rapidly reach collapse when exposed to settlements.

Figure 7. Large displacements failure of the settled arch (A. Romano, 2005).

This not the case, as a rule, for the majority of masonry constructions. Historic constructions, particularly, have been built following rules obtained by the long experience of past. In spite of the large variety of architectural forms developed during the time, the old builders, more or less, managed always the same material so that the vast variety of masonry constructions presents the following significant common aspects:

– low compressive stresses in structural components as arches, piers, vaults, if compared with the masonry strength;
– stocky resisting sections or sufficient constraints able to avoid the occurrence of not negligible geometry changes during loading.

Consequently, the settlement state as a rule develops in the framework of the previous small displacements behavior.

3 MINIMUM THRUST STATE

Let us consider any statically admissible stress state σ in equilibrium with the given loads, for instance, the dead loads g. In the case of the arch of fig. 4 this statement means that we consider a generic pressure line σ that is funicular of the assigned loads g and is contained within the arch.

The static and the kinematical theorems of the Limit Analysis for the minimum thrust still hold in a reversed form (Como, 1996,1998). The static theorem of the minimum thrust affirms in fact that

$$\mu(\sigma) \geq \mu_s \qquad \sigma \in S \tag{17}$$

i.e. the multiplier, μ_s of the thrust r of the settled structure is *lower* than all the statically admissible multipliers $\mu(\sigma)$. This result extends the well-known property of the masonry arch that, due to settling at its springings, increases its span. The thrust acting in the settled arch is minimum because the corresponding pressure line, passing through the hinges of the settlement mechanism, has the minimum span and the maximum sag. (Heyman, 1966).

Let us examine now the settlement equilibrium from a *kinematical* point of view. New approaches to study statics of settled structures follow from this analysis.

The actual settlement mechanism v_s is a priori unknown: for instance, for the case of the arch of fig. 6, the position of the internal hinge is unknown. Let us define the *kinematical multiplier* λ of the reaction r so that the structure is in equilibrium along an assumed settlement mechanism v, i.e., so that the following condition

$$<g,v> + \lambda <r,v> = 0 \tag{18}$$

holds. Taking into account (14), reaction $\lambda r(v)$ thus opposes the development of settling v. The kinematical multiplier of reaction r is

$$\lambda(v) = -\frac{<g,v>}{<r,v>}, \quad v \in \bar{M} \tag{18}$$

With these positions it is easy to prove that

$$\lambda(v) \leq \mu_S \quad \forall v \in M' \tag{19}$$

i.e. the multiplier μ_s of the thrust r of the settled structure is *larger* than all the above defined kinematical multipliers $\lambda(v)$. Thus μ_s is *the maximum* of all kinematical multipliers $\lambda(v)$ for varying v in the set of all settlement mechanisms M'. In other words

$$\mu_S = MAX\left(-\frac{<g,v>}{<r,v>}\right) \quad v \in M' \tag{20}$$

3.1 *An example: The evaluation of the reaction of a settled pier of a masonry bridge*

Let us consider the masonry bridge sketched in figure 8. The bridge's central pier has undergone a vertical settlement. The corresponding mechanism v is traced out in the figure, where $\mu_s r$ indicates the vertical reaction of the settled central pier.

Fig. 8 shows a kinematical reaction of the pier, denoted by $\lambda(v)r$, defined by the equilibrium equation (17). The multiplier $\lambda(v)$ depends on the unknown position of the hinge B. The actual pier reaction R_c can thus be obtained as the *maximum* of all the kinematical reactions $\lambda(v)r$ by varying v in the set of all the admissible settlement mechanisms.

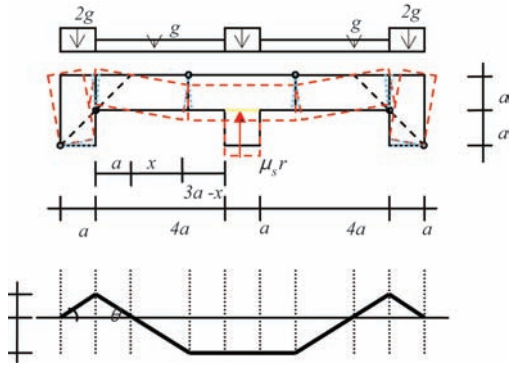

Figure 8. A masonry bridge whose central pier has settled vertically.

The work of weight g along the mechanism v is given by

$$< g,v > = 2\left[-2g\frac{a^2\theta}{2} - g\frac{a^2\theta}{2} + g\frac{x^2\theta}{2} + g(3a-x)x\theta + 2g\frac{ax\theta}{2}\right] = g(-3a^2 - x^2 + 8ax)\theta \quad (21)$$

and the work $<r,v>$ of the pier's reaction is: $-\lambda(v)\, rx\theta$. According to (18) the kinematical reaction $\lambda(v)r$ is thus given by

$$\lambda r(x) = \frac{g(-3a^2 - x^2 + 8ax)}{x} \quad 0 \le x \le 3a \quad (22)$$

and is depending on the position x of hinge B. The distance x is included in the range $0 \le x \le 3a$. When $x \to 0$, $\lambda r \to -\infty$ while $\lambda r = 4ga$ with $x = 3a$. (fig. 8). The function $\lambda(x)$ effectively reaches *a maximum* for $0 \le x \le 3a$.The value x^* at which $\lambda r(x)$ attains its maximum is thus obtained by solving the equation

$$\frac{d(\lambda r)}{dx} = g\left(\frac{3a^2}{x^2} - 1\right) = 0 \quad (23)$$

which yields (fig. 9)

$$x^* = a\sqrt{3} \approx 1.73a. \quad (24)$$

Substitution of (24) into (22) thus gives the reaction of the central pier

$$R_C = (\lambda r)_{\max} = \lambda r(x = a\sqrt{3}) = 2ga(4 - \sqrt{3}) \approx 4.54ga \quad (25)$$

The corresponding pressure line runs inside the bridge structure as shown in fig. 10. The minimum thrust can also be otherwise obtained by means the statical approach searching, among all the admissible funicular curves, the pressure line exhibiting the minimum slope at sections where girders join the central pier.

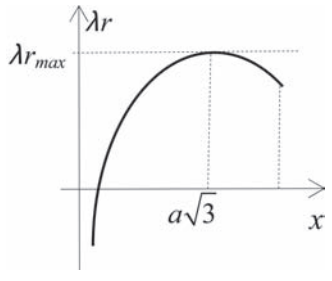

Figure 9. Finding the maximum of function $\lambda r(x)$.

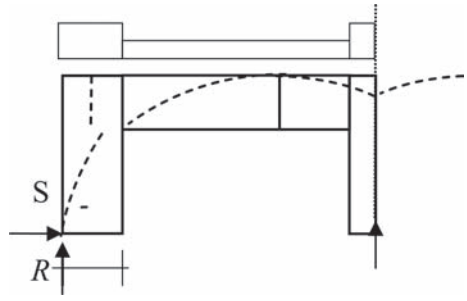

Figure 10. The pressure line inside the masonry bridge.

4 ANALOGY BETWEEN MASONRY AND COHESIONLESS SOIL BEHAVIOUR

We meet similar results in Geotechnical Engineering. Consider the limit analysis solution for a smooth vertical wall with a flat backfill of *cohesionless* material, as shown in fig. 11.

The wall undergoes an horizontal outward displacement D. It can due, for instance, to inadequate horizontal wall foundation constraint or to a sudden dynamical action. It is assumed that, caused by the weight, a large mass of soil moves as a rigid body downward and outward while deformation occurs in the narrow transition zone RS limited by two planes parallel to each other.

Making the assumption that plastic flow is associated, plastic volume expansion during simple shearing demands that the tangential velocity change $\dot{u}$ along RS of the portion RTS of the wedge must always be accompanied by a separation velocity $\dot{v}$ normal to RS

$$\dot{v} = \dot{u} \cdot tg\phi \quad (26)$$

The soil is a perfectly cohesionless plastic material with Coulomb's rule of yielding. The condition defines the yield curve in the stress space $(\sigma; \dot{\varepsilon})$;$(\tau; \dot{\gamma})$.The soil is assumed *standard or s*table, as defined in Geotechnical Engineering. (Drucker, 1959, Tamagnini, 2005).

$$\tau = \sigma \cdot tg\phi \quad (27)$$

It is assumed that the soil obeys the associated flow rule of the theory of Plasticity so that the plastic strain rate vector $\dot{\mathbf{P}}$ is normal to the yield curve, as shown in fig. 12. Comparison between

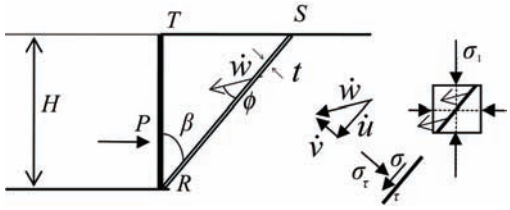

Figure 11. The sliding mass of soil.

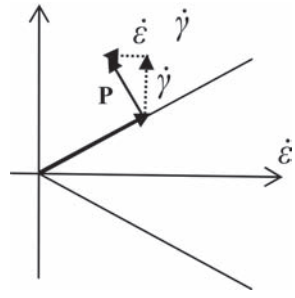

Figure 12. The normality rule for the cohesionless soil.

figures 4 and 12 shows that the cohesionless soil and the masonry material have the same flow rule.

The kinematical slip condition simply states that the relative velocity change $\dot{w}$ in the narrow transition zone bounded by two parallels planes will form the angle ϕ with the slip planes. The compatible velocity relations are shown in fig. 11 and 12.

There is no rate of dissipation of energy in the transition soil layer plastically sliding. In fact, the shear strain rate $\dot{\gamma}$ and the normal strain rate $\dot{\varepsilon}$, uniform in the layer of width t, are equal to

$$\dot{\gamma} = \dot{u}/t \qquad \dot{\varepsilon} = \dot{v}/t \tag{28}$$

so that the rate of energy dissipation during the plastic shear deformation in the thin soil layer vanishes:

$$\begin{aligned} D &= (\tau \cdot \dot{\gamma} - \sigma \cdot \dot{\varepsilon})t = (\tau \cdot \dot{u} - \sigma \cdot \dot{v}) \\ &= (\tau \cdot \dot{u} - \sigma \cdot \dot{u} \cdot tg\phi) = 0 \end{aligned} \tag{29}$$

because of (17), These results show the full correspondence occurring between the behaviors of the idealized masonry and cohesionless soil.

The rate of external work consists of two parts, the rate of work done by the soil weight moving downward and the rate of work done by the force P moving horizontally

$$\frac{1}{2}\gamma \mathrm{H}^2 \mathrm{tg}\beta \cdot V \cdot \cos(\beta+\phi) \qquad \mathrm{P} \cdot \mathrm{V} \cdot \sin(\beta+\phi) \tag{30}$$

Assuming a frictionless wall implies no energy dissipated along RT. Likewise the energy dissipation along RS is zero for the assumed cohesionless soil layer. Thus, as it is well known, equating the rate of internal and external work yields

$$P(\beta) = \frac{1}{2}\gamma \mathrm{H}^2 \mathrm{tg}\beta \cdot \mathrm{tg}^{-1}(\beta+\phi) \tag{31}$$

The failure plane is the one that gives the minimum of P(β). This minimum is attained at $\beta = (\pi/4 - \phi/2)$ and

$$P_{\min} = \frac{1}{2}\gamma H^2 \mathrm{tg}^2\left(\frac{\pi}{4} - \frac{\phi}{2}\right) \tag{32}$$

The soil mass RST, overlying the narrow transition zone RS, is in equilibrium under the weight W, the thrust P and the actions transmitted along RS. The soil is at a plastic state in this layer and can deform under constant stress. As far as the ultimate displacement D_u is not reached, the soil wedge RTS follows any increase of the outward displacement of the wall RT *maintaining constant the thrust on the wall without no equilibrium failure.* In fact, no exchange occurs from conditions of existence to those of non-existence of the admissible equilibrium state. The soil mass is thus at a settlement *mechanism state* like the masonry arch of fig. 6. The outward displacement of the wall represents the settlement just as the span increasing defines the settlement of the arch. These results can explain because the retaining walls, struck by quakes, frequently remain undamaged but only shifted forward. The research of the minimum thrust of the settled masonry construction is thus alike to the research of the minimum thrust of an ideal plastic soil on the retaining walls.

REFERENCES

Bati S.B., Paradiso M. & Tempesta G. 1997. Archi in muratura soggetti a carichi e cedimenti alle imposte. *Costruire in laterizio*: 60.

Como M. 1992. Equilibrium and Collapse of masonry bodies, *Meccanica*, *27*, 185–194. London: Kluwer Academic Publ.

Como M. 1996. On the role played by Settlements in the Statics of Masonry Structures in Carlo Viggiani (ed.), *Geotechnical Engineering for the Preservation of Monuments and Historic sites*,Proc. Intern. Symp., *Napoli*, 3–4, *October 1996*, Rotterdam:Balkema.

Como M. 1998. Minimum and maximum thrust states in Statics of ancient masonry buildings, in Anna Sinopoli (ed.) *Proc. 2nd Intern. Arch Bridge Conf., Venice*, *6–9 October 1998*. Rotterdam:Balkema.

Como M. 2010. Statica delle costruzioni storiche in muratura, Roma: Aracne e, 2013 Statics of Historic Masonry Constructions. Berlin: Springer (in printing).
Drucker C.K. 1959. A definition of stable inelastic material, Journ. Appl. Mechanics, 26,1.
Heyman J. 1966. The stone skeleton, *Intern*, *Journ. Solids Structures*, *2*, 249.
Heyman J. 1982. *The masonry arch*, Chichester: Ellis Horwood.
Heyman J. 1995. The stone skeleton, Structural Engineering of Masonry Architecture, Cambridge: Cambridge University Press.
Ochsendorf J. 2006. The masonry arch on spreading supports. *Int Journ. Struct. Eng.*—A 84 (2).
Paradiso M, Tempesta G, Galassi S. 2004. A numerical method for no-tension analysis of masonry arches. In Roca P. and Molins C. (eds.) *Arch Bridges* IV-*Advances in Assessment, Structural Design and Construction,* Barcellona:Balkema.
Rankine W.J.M. 1895. "On the Stability of Loose Earth, *Applied Mechanics*, 14th ed.
Romano A. 2005. Modeling, Analysis and Testing of Masonry Structures, *P.h.d. Thesis, Univ. of Naples Federico II, Faculty of Eng*. Napoli.
Tamagnini C. 2005. Analisi limite in Ingegneria Geotecnica, Benevento: Hevelius.

Geotechnical Engineering for the Preservation of Monuments and Historic Sites – Bilotta, Flora, Lirer & Viggiani (eds)
© 2013 Taylor & Francis Group, London, ISBN 978-1-138-00055-1

Assessment of geological and geotechnical conditions for rebuilding Avala's television tower

S. Ćorić, D. Rakić & G. Hadži-Niković
Faculty of Mining and Geology, University of Belgrade, Belgrade, Republic of Serbia

T. Janković, V. Filipović & B. Marjanović
Institute of Transportation CIP, Belgrade, Republic of Serbia

ABSTRACT: The paper presents the geotechnical conditions for the rebuilding of Avala's television tower near Belgrade, the capital of Serbia, which was destroyed due to brutal NATO bombing in1999. The total height of the tower is 204.33 m, i.e. 136.65 m is the height of the reinforced concrete construction and 67.68 m is the height of steel structure. The fundamental condition for the rebuilding was that the shape and dimensions of the new tower and its location have to be the same as for the old one. But the old tower has been constructed half a century ago, according to the standards which were valid at that time, and the new tower has to be designed according to the present building codes which are more complex than the old ones. In order to satisfy that condition, it was necessary to perform extensive geotechnical investigations. Following the obtained results, consolidation grouting has been performed, as a measure for the improvement of physical-mechanical properties of the rock mass in the foundation zone. On this basis, a shallow pad foundation, with three reinforced concrete footings, was assumed as quite satisfactory.

1 INTRODUCTION

The old Avala's television tower was built during 1961–1964. In 1965 it served as telecommunication building with numerous antennas for radio, television, post and other communications. With restaurant in gondola it was a tourist building, too. Its height was 204.33 m and it was situated near Belgrade at vacation area Avala, at ground level of 439.0 m. For many years the tower was the highest building in the Balkans, as well as a symbol of Belgrade—the capital city of Serbia. It was destroyed due to brutal NATO bombing in 1999.

After removing its ruins in 2005, ground and laboratory investigations have been performed for defining the geotechnical conditions for the new Avala's television tower, which was completed at the end of the 2009.

2 STRUCTURAL FEATURES OF AVALA'S TELEVISION TOWER

The total height of Avala's television tower is 204.33 m. It consists of two parts: the lower part is constructed of reinforced concrete and its height is 136.65 m and the upper part is constructed of steel with height 67.68 m.

Dominant load for structure is a load of wind and it was analyzed in detail. Accordingly, a study of wind load took into consideration the following effects: topography of the ground, wind velocity, return action period of wind, a coefficient of forces for reinforced concrete part and steel part of tower, a frequency of tower vibrations, a calculated deformations of tower and horizontal acceleration at the level of gondola at the height of 119 m (Dunica et al. 2009).

The calculated design was interactive (wind-structure) and iterative. The structure of the tower was analyzed as a total structure. The analysis was based on the harmonic features of the structure and the calculated load of the wind which is based on Serbian code. According to the obtained resultant forces and moments, the reinforced concrete part as well as the steel part of the structure have been dimensioned.

The reinforced concrete part of the tower consists of three inclined supporting columns, pillar and gondola which lie on it (Fig. 1). The lowest part of tower is statically indeterminate reinforced structural frame which has three inclined supporting

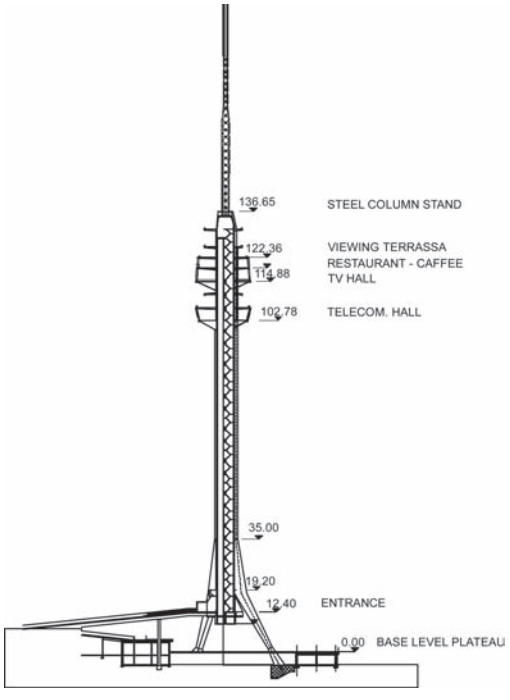

Figure 1. Avala's tower with characteristics levels.

columns with variable cross sections. At the height between 17.10 m–19.10 m the columns penetrate into reinforced concrete plate with penetration depth of 2.0 m (Fig. 1).

From level 19.10 m starts the pillar of the tower. It is statically determinate structure i.e. cantilever. The pillar has closed reinforced equilateral triangle cross section with side length of 7.0 m. The thichness of the pillar walls is 15 cm and at angles of triangle are projected circular reinforcements with diameter of 1.04 m. In the tower are two very fast lifts and spiral stairs. All stairs loadings and stair flights are built with reinforced concrete and have a thickness of 10 cm.

From the level 102.78 up to the height of 136.65 there are five stories with gondola and platforms. There are rooms of telecommunication systems and restaurant with sightseeing terrace at height 558.13 m. At the pick of the pillar, at a level of 136.65 m, there is a reinforced concrete plate with thickness of 1.50 m in which has a fixed end of vertical steel column for television antennas.

The height of steel column is 67.68 m, from 136.65 m to the top of tower at 204.33 m. It has been projected to meet specifications for antennas and to be stable for wind loading. All members of steel structure have circular cross sections according to their aerodynamic properties. They were dimensioned in order to have a required stiffness which enables usability of antennas, as well as global stability of structure.

3 SITE AND GROUND CHARACTERIZATION

Morphology, geology and engineering geological properties of the terrain are defined using data from available documentation of earlier investigations, as well as the results of the new investigations performed in 2005 (Janković et al. 2005).

At first, ground had to be cleared up, and after that we could approach to new ground investigations. The new investigations involved topographic survey, engineering geological mapping and investigation of ground conditions using pits and boreholes associated with sampling (Fig. 4). Laboratory testing of samples were performed to determine the strength and compressibility of soils and rocks. The surface geophysics was also done: electrical conductivity of the ground and refraction method of seismic surveying.

Figure 2. Avala's tower building site in 1964.

3.1 *Morphology*

Avala is low height mountain, the nearest to Belgrade, with top at 511 m. The tower site is on mountain plateau at 439 m, which was cut on nature crest at 447 m.

Figure 3. Avala's tower investigation & building site in 2005.

After NATO bombing, 1999 and breaking out Avala's tower, the plateau surface was covered by ruins and tons of concrete, steel, bomb-shell remains and other waste (Fig. 3).

3.2 *Geology*

As it can be seen in Figure 4, the terrain is built up of Upper Cretaceous flysch sediments, consisting mainly of layered sandstone and thin or thick layers of clays and sandy clays.

These sediments are more or less weathered. The thickness of the beds is highly variable, ranging from few centimeters to more than half a meter.

Sandstones are fissured by joints of very different space orientation, while claystones are very crushed and weathered so their properties are similar to clay ones. The rock is locally penetrated by veins of volcanic rocks which partially metamorphosed the flysch sedimentary rocks.

Dip direction is NS and average dip is about 35–45° to the east. Since the rock beds are very distorted and fissured, their dips and dip directions sporadically vary from these average values.

3.3 *Physical and mechanical properties of soils and rocks*

From an analysis of data, obtained from all investigation results, we can conclude that the site of earlier tower mainly consists of layered (silica cemented layers of 20–60 cm thick), fine grained, gray to green-grayish, very hard sandstones.

It was obvious that we can distinguish two zones: "upper zone", which is more weathered and weaker, and "lower zone", which is fresh and very hard.

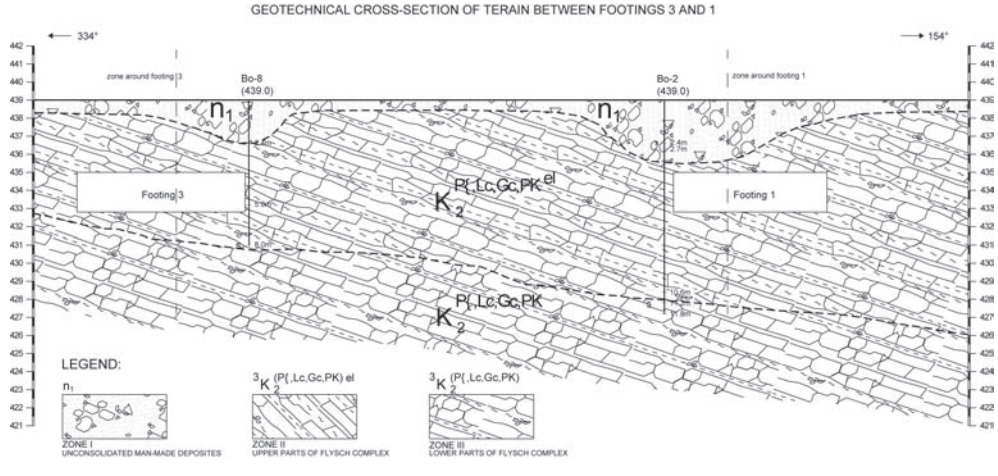

Figure 4. Geotechnical cross section.

Superficially parts of sandstones are weathered with joints filled with clayey debris. Average mechanical parameters of monolith/intact rock samples are: unit weight $\gamma = 25.5–25.8$ kN/m^3 and unaxial strength $\sigma = 53.6–90.8$ MPa.

Claystones are less spaced. Their beds are about 10–50 centimeters thick. In superficial parts claystones are strongly weathered and appear as sandy clay or silty clay with variable content of sand, silt and clay. Some average parameters of clay, obtained from laboratory testing are: unit weight $\gamma = 19.5$ kN/m^3, dry unit weight $\gamma_d = 15.4$ kN/m^3, moisture content $w = 41\%$, liquid limit $w_l = 72\%$, plastic limit $w_p = 43\%$, plasticity index $I_p = 29\%$. According to the unconfined compressive strength $q_u = 447$ kPa, the clay is classified as hard.

According to the results of differential thermal analysis and X-ray analysis, the clay belongs to the hydromicas type and corresponds to mineral illite with a small presence of kaolinite.

3.4 *Ground water and seismic conditions*

According to topography and geology of the plateau site, an insignificant amount of ground water can exist in the terrain.

It flows from surface infiltration or from higher parts of the slope. It can be drained very easily through the existing discontinuities to lower areas of the slope.

Refraction method was performed to obtain seismic waves velocities, and according the Serbian code, the following seismic parameters were determined: acceleration $a = 115$ cm/s^2, seismic intensity map for return period 500 years is 8^0 MCS, cumulative probability $F(a) = 0.99863$ and seismic coefficient $Ks = 0.025$.

4 GEOTECHNICAL CONDITIONS FOR TOWER FOUNDATION

The assessment of geotechnical conditions for Avala's new tower foundation was performed on the basic terrain geotechnical model and the relevant calculated pressure in the foundations level.

4.1 *Geotechnical model of the terrain*

Foundations of tower pillars are in flysch complex which is very non-homogenous and anisotropic. It has variable lithology and because of that, it was subjected to variable degrees of physical, chemical and mechanical alteration (Hunt, 1986).

Using data from all investigations' results, i.e. lithology, structural properties of rock masses and physical and mechanical parameters such as shear strength and deformability, three different zones can be distinguished: 1) zone of man-made non-homogenous fill, 2) zone of weathered flysch, 3) zone of fresh flysch.

Zone 1 consists of unconsolidated man-made deposits of fill which contents different materials: sandy and silty clayey debris soil, concrete, steel and other rests of bombing waste. Thickness of this, very non-homogenous zone varies on the site and is about 0.25–5.0 m. Performed surface geophysics defined the following parameters: velocity of primary waves is $V_p = 340–550$ m/s and electric resistance $\rho = 142–1346$ Ωm. It was not competent for foundation because of its poor quality.

Zone 2 consists of upper parts of flysch complex which are weathered, fissured and weak. Variable thickness, about 3.5–10.0 m, it mainly comprises low cemented and destroyed claystones and marls. In relation to zone 3, it shows reduced parameters of shear strength and deformability.

Zone 3 mainly consists of fresh sandstone parts of flysch complex. It is widely-spaced fissured, very hard and in practice undeformabile.

Values of physical and mechanical parameters of soils and rocks from zone 2 and 3 are given in Table 1. Geotechnical cross-section is presented in Fig. 3.

These values σ_{cm} were estimated on the basis of uniaxial strength of monoliths, RQD values and site inspection.

4.2 *Geotechnical conditions of the foundation subsoil of the new television tower*

The fundamental requirement for the tower rebuilding was that its location as well as the shape and dimensions of all structural elements (except footings) had to be the same as of the old one. Moreover, the old tower was designed 50 years ago, according to the standards valid at that time. However, the new tower had to be constructed according to the present codes of practice, which are more complex than the old ones. As a consequence, the foundation design of the new tower was changed: shape and dimensions of footings and a depth of foundations (Janković et al. 2009a).

Taking into consideration the geological formations and structure of the ground and geotechnical properties of particular zones of the flysch complex, a shallow pad foundation with three reinforced concrete footings was selected. The footings are rectangular in plan with dimensions of 6.0×7.3 m with variable height ranging from 2.0 m to 4.0 m (Fig. 5).

The depth of the foundation is 8.2 m from the ground level and the inner platform (439.0 m) and 2.2 m from the new exterior plateau (435.0 m).

The altered flysch zone (with depth from 5 m to 12 m) has intense non-homogeneity and lower

Table 1. Values of physical and mechanical parameters of soils and rocks from zone 2 and 3.

Rock mass parameters		Zone 2	Zone 3
γ	Unit weight (kN/m^3)	18–22	20–26
c	Cohesion (kPa)	10–30	30–250
φ	Shear resistance (^{0})	18–27	28–55
V_p	Velocity of primary waves (m/s)	1350–1650	2500–3500
ρ	Electrical resistance (Ωm)	70–155	75–233
E_d	Modulus of deformability (MPa)	904–1506	5302–8944
E_{din}	Dynamic modulus of elasticity (MPa)	3030–4434	2.284–25.107
μ	Poisson`s ratio	0.35–0.33	0.30–0.28
RQD	Rock quality description (%)	<10	10–50
σ_c	Unaxial strength of monoliths (MPa)	18–28	50–80
σ_{cm}	Unaxial strength (MPa)	1.3–2.4	7.8–14.5

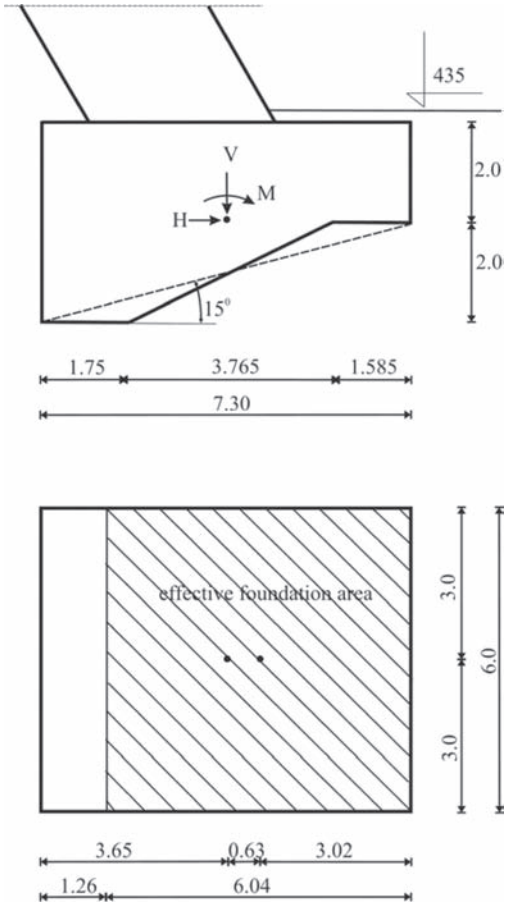

Figure 5. Reinforced concrete pad footing.

strength-deformations properties than the zone under it. As a consequence of bombing and breaking out the old tower, it has become even weaker. In order to improve these properties, in the zone of foundation, consolidation grouting has been performed. It has been carried out with 13 vertical grout boreholes for each footing i.e 39 boreholes totally. The length of each borehole was 13 m (Janković et al. 2009b).

As a consequence of total loading (dead load + live load + wind load) the resultant forces, for each footing, at the level of foundation (432.8 m) are: vertical force V = 29,830 kN, horizontal force H = 13,368 kN and the eccentricity, along the length of footing, is 0.63 m, i.e moment is M = 18,752 kNm. The effective foundation area is $A' = 6.0 \times (7.3 - 2 \times 0.63) = 36.24$ m^2.

The contact pressure is:

$$\sigma = \frac{29830}{36,24} = 823 \text{ kPa}$$

The estimated allowable pressure (Peck et al, 1974) is q_a = 3000 kPa. It should be mentioned that when the design is based on this value, the settlement of the footing should not exceed 12.7 mm.

In order to get higher values of safety factor against sliding, design engineers assumed the packed contact area between rock mass and footing with average inclination to horizontal of 15° (Bowles, 1997). The resultant forces are projected to that inclined plain and in this case the following safety factor against sliding has been obtained

$$F_s = 0.78 \times \frac{32273}{5192} = 4.8$$

where 0.78 is assumed equivalent friction coefficient between reinforced concrete footing and altered flysch rock mass.

The footing settlement has been determined as it is commonly for rock mass i.e. it was assumed that contact pressure acts on homogenous, isotropic, linear-elastic space. In such a way, following theory of elasticity and using the conservative value of deformation modulus of 904 MPa, it has been estimated settlement of cca 5 mm (Ćorić, 2008). It is interesting to note that the maximum measured settlement of the old tower footing, for the period of ten years, has been 12 mm (Bogdanović et al. 1976).

5 CONCLUSION

Extensive geotechnical investigations have been carried out for the rebuilding Avala's television tower near Belgrade, with a height of 204.33 m. According to the results, the geotechnical properties of the ground in the zone of foundation have been determined. On this basis a shallow pad foundation with three reinforced concrete footings was selected The footings are rectangular in plan with dimensions of 6.0×7.3 m and the minimum depth of foundation is 2.20 m.

The calculated contact pressure and the settlement of footings are in tolerable limits, as well as the safety factor against sliding. So it can be calculated that such type of shallow foundation is quite appropriate for new Avala's television tower (Fig. 6 and Fig. 7).

Figure 6. Photo of rebuilding Avala's tower in 2008.

Figure 7. Photo of rebuilding Avala's tower in 2009.

REFERENCES

Bogdanović, Lj. (1976). Settlments and deformation moduli of rock masses in the foundation zone of Avala's television tower (in Serbian). *Our civil engineering* No 10: 1473–1484.

Bowles, J.E. (1997). *Foundation analysis and design.* New York: Mc Grow Hill Book Company.

Ćorić, S. (2008). *Geostatic calculations (in Serbian).* Belgrade: Building and Faculty of Mining and Geology—Special issue.

Dunica, Š., Bojović, A. & Životić, B. (2009). Design of the new Avala's tower (in Serbian). *Building No 63, 3–4:* 169–172.

Hunt, R.E. (1986). *Geotechnical engineering analysis and evaluation*. New York: Mc Grow Hill Book Company.

Janković, T. (2005). *Geotechnical foundation conditions for Avala's tower* (in Serbian). Report of Institute of transportation CIP, Belgrade.

Janković, T., Marjanović, B. & Nedeljković, S. (2009a). Engineering geological and seismic foundation conditions for TV tower on Avala (in Serbian). *Building No 63, 3–4:* 161–164.

Janković, T., Marjanović, B. & Anagnosti, P. (2009b). Consolidation grouting for foundations on the New Tower on Avala (in Serbian). *Building No 63, 3–4:* 165–168.

Peck, R.B., Hansen, W.E. & Thornburn, T.H. (1974). *Foundation engineering*. New York: John Wiley & Sons.

Geotechnical Engineering for the Preservation of Monuments and Historic Sites – Bilotta, Flora, Lirer & Viggiani (eds)
© 2013 Taylor & Francis Group, London, ISBN 978-1-138-00055-1

Afghanistan, Buddhas of Bamiyan: Emergency consolidation of the cliffs and niches

C. Crippa & R. Granata
Trevi S.p.A., Cesena, Italy

C. Margottini
ISPRA, Italian Geological Survey & UNESCO Expert, Italy

ABSTRACT: The statues of the Buddhas of Bamiyan, carved around the VI century into the calcareous cliff of the Bamiyan valley, are the largest Buddhist monuments in the world. These monuments were almost destroyed by the bombing perpetrated by Talebans in March 2001. Since then, UNESCO is active in the Bamiyan area with the aim to preserve the remaining parts of the Buddha statues and to recuperate the artistic remains. The complex of Bamiyan has been inscribed in 2003 in the World Heritage List of UNESCO as "cultural landscape". Among the most urgent operations required for the structural rehabilitation of the area there was the stabilization of the rock face in the vicinities and within the niches, deteriorated both by the explosions and the natural processes. The emergency measures were also aimed to consent to the archaeologist to catalogue and remove the Buddhas' rock remains safely. The specialized engineering works were designed by Prof. C. Margottini and implemented by the Italian company Trevi Spa. The site operations, which are described in this paper, were carried out in three separate phases between 2003 and 2006.

1 INTRODUCTION

Bamiyan is located to the North West of Hindu-Kush and Himalaya mountains, in Central Afghanistan. The river valley in Bamiyan is quite large due to the confluence of different rivers, at an elevation of about 2540 m.

The archeological site was constructed between the V and IX century AD, positioned in a strategic location along the Silk Road, the trade routes that for centuries linked China and Central Asia with India and the West. Bamiyan served as an important monastic center, as well as a hub of intense commercial activity. During this period two massive Buddha images were carved out of a high cliff facing the widest part of the valley. The greatest sculpture (Western Giant Buddha, 53 m high) was carved in a niche (55 m high) on the west side of the cliff. The second one (Eastern Giant Buddha, 35 m high), was in a niche (41 m high), at the east side (Figure 1).

All along the cliff, between the two niches hosting the giant sculptures, there are hundreds of caves of various size, which were used as chapels, ambulatories and stairways. Most of this rock-carved chapels and ambulatories were decorated with a rich variety of murals.

In March 2001, the Taliban regime blew up the two giant Buddhas, which were the largest Buddhist sculptures in the world. The effects of the explosions were quite dramatic: the two statues totally collapsed, some small pieces of the niches fell down, a large portion of the East Giant Buddha Niche was close to the collapse.

UNESCO was immediately prompt to undertake an emergency intervention to secure the remains of

Figure 1. General view of the Buddhas' Cliff at Bamyan.

such wonderful cultural heritages and, thanks to the generous Government of Japan financial support, the works started in November 2003.

The present paper describes the emergency interventions performed in Bamiyan for the consolidation of niches and unstable blocks.

2 GEOLOGICAL SETTINGS

The Bamiyan Valley is located on the northern edge of the 600-km-long E-W valley along the Herat fault, one of the largest and most prominent faults in Afghanistan. The fault represents a suture zone between the Farad and Tadjik blocks occurred during the Cretaceous. Bamiyan Valley is an intramountain basin filled with debris originated from the surrounding mountain ranges.

From the late Pliocene to the end of the Pleistocene the fluvio-glacial erosion engraved the subhorizontal beds of Neogene sediments, creating the Bamyan Valley (Reineke, 2006).

The flood valley is mainly covered by fluvial sediment, landslide-slope deposits, eluvial and colluvial debris. The valley morphology is due to multiple factors such as lithological characteristics, tectonic activity, paleo-climatic events, fluvial activity along the river valley and slope evolution in the cliffs.

At the archeological site, the cliff presents a general E-W orientation, but it can be divided into two sectors: the western side (Western Giant Buddha), 820 m long, is N65°E oriented; the eastern portion (Eastern Giant Buddha) is 525 m and exhibits a N95°E orientation. The two segments are separated by a large alluvial cone area generated by two creeks still flowing into the Bamiyan river.

The Buddhas' cliff presents an average slope inclination around 80°. This morphology is probably affected also by the excavation of niches and grottos handmade to host the monastic settlement (Delmonaco e Margottini, 2009).

The cliff and niches are excavated into the so called Buddha Formation, composed by an alternation of conglomerate and siltstone (Figure 2).

Landslide deposits are widely present along the slope toe, generated by toppling of large conglomerate and siltstone blocks (from <1m^3 to over 10 m^3 in volume).

The walls and the top of the cliff are largely affected by diffuse and intense erosion phenomena: the weak structure of the soils, the absence of vegetation, the severe climatic conditions are leading factors accelerating the erosion process.

The conglomerate is the predominant material in the cliff and exhibits a moderate cohesion. Large discontinuities can be detected in the conglomerate, with a tendency to enlarge in the upper part.The siltstone exhibits a moderate apparent cohesion and two major pattern of discontinuities, that are isolating small blocks (volume generally <1 m^3).

Figure 2. Major features of the lithology in Bamyan Cliff.

The density of the conglomerate and siltstone is reported as 17.65 and 22.35 kN/m^3 respectively. The average strength, estimated by Schmidt Hammer Test is 30 MPa for conglomerate and and 34 MPa for the siltstone. Some Point Load Test were performed in a rock mechanic laboratory, on samples collected at site: the conglomerate gave an average value of 5.4 MPa, siltstone of 11.0 MPa, i.e. about 20% and 30% of the strength measured in situ by Schmidt Hammer Tests (Margottini 2009).

The strength of the conglomerate is due to the calcite chemical bonding between the gravel particles. Vice versa, investigations by SEM (scanning electronic microscope) show that the calcite content in the siltstone is negligible: the siltstone strength is due to its high density, which results in large cohesion force that completely disappear under wet condition.

3 SITE INVESTIGATION AND SURVEY

3.1 *Topographical survey*

At the beginning of the works, in 2002, a detailed topographical map, at a scale suitable for engineering purposes, was not available in the study area. In 2002 and 2003 preliminary topographic investigation were performed, under the UNESCO coordination, based on existing aerial photographs. Unfortunately, the photos do not cover the northern side of the valley where the niches are located.

Therefore the existing maps had to be integrated with direct topographic measurements and survey (by a portable GPS and laser scanner) of both

niches (Pasco, 2003). All the consolidation works were designed and carried out with the help of such new maps.

3.2 *Site study*

Engineering geological study of the site started in 2002 and lasted for the entire execution of the consolidation work. The study included site analysis with direct investigation on site. Laboratory tests were conducted in Europe on selected samples collected at site. Major constrain to field investigation was also the presence of land mines.

3.3 *Identification of most critical areas*

The explosions of March 2001, besides the demolition of the statues, reduced the stability of the shallower parts of the niches (Margottini, 2004). The field investigation and surveys allowed the identification of the most unstable sites.

In the Eastern Niche (East Giant Buddha), three minor rock falls occurred from the top of the niche. Blasting also degraded the strength of the highest right side of the niche, where a stairway is located inside the cliff and the wall between the stairs and the niche is quite thin (about 30–50 cm). The left portion, protected by the existing buttress, did not show significant displacements, with the exception of the upper part where a rock fall and some instabilities were evident.

In the Western Niche (West Giant Buddha), beside the collapse of the statue and the consequent instability of the rear of the niche, only small rock fall occurred from the top left of the niche. Probably, the 1 m thick wall between the niche and the stairway into the cliff reduced the propagation of the blasting effects and, in turn, the injury of the structure. A crack, 20–30 cm wide, was present in the corridor at the back of the head of the statue.

4 EMERGENCY CONSOLIDATION WORKS

4.1 *Local constrains*

The specialized engineering works were designed by Prof. C. Margottini and implemented by the Italian company Trevi Spa. The site operations were carried out in three separate phases between 2003 and 2006.

A first multiparty site visit was carried out in September 2003. Scope of the mission was the analysis of the existing conditions, with regard to the stability of two niches, and the definition of the methodology and the priorities for the monitoring and consolidation works.

At the same time contacts were taken with local authorities, and a preliminary verification on local available suppliers was carried out, for the identification of local resources, finding in situ lodging, etc.

Apart the technical aspects, the main difficulty in this project was the execution of works in difficult logistic condition. Afganistan is a country with poor availability of equipment and material. The summer is hot and the winter in Bamyan extremely cold. In addition, the Bamyan site is characterized by environment arduous condition, due to the presence of land mines and rocks prone to fall down from the cliff.

Due to the urgency of the required emergency intervention (since the approaching of 2003 winter season that could increase the risk of sudden collapses) and the unavailability of scaffolding, as well as the high probability of rock fall (with consequent risks for the operators and scaffolding itself), alternative approach had to be found. After a careful investigation and the evaluation of possible alternatives for implement the job, the choice fell on the use of professional climbers.

Climbers, supported by ground staff, were operating directly on the surface of the cliff, hung on a stable area at top of the cliff, in safe condition with respect to any potential rock fall (Figure 3). The climbers also were able to provide assistance to the UNESCO geologists for an accurate geological stratigraphical logging.

In order to speed up the starting of the operations, UNESCO decided to organize an air cargo for the direct transportation from Europe to Kabul of the three containers (containing indispensable equipment and material). This decision resulted being quite productive since the containers reached the site within two weeks, with a considerable saving of time with respect to the original schedule, which was considering a transportation by sea.

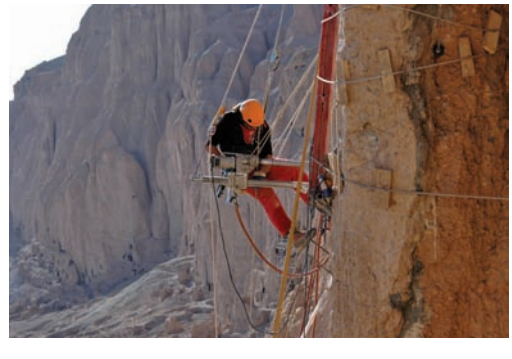

Figure 3. Drilling in progress.

4.2 *General technical approach*

The activities were developed according to the following general scheme.

1. Installation of a monitoring system, to measure in real time any possible deformation of the cliff. Sensors were designed to monitor the entire working area and were connected with an alarm system, to monitor in real time the effect of the works being executed (Figure 4).
2. Installation of temporary support infrastructures, suitable to avoid lateral deformation inside the niches and secure the blocks that were at limit equilibrium during the execution of works. Among the temporary works, wire nets were installed on the back side of both niches to allow archaeologists to work on the ground floor in safe conditions, just after the consolidation of the niche's wall.
3. Execution of the consolidation work, with professional climbers to avoid any activities below the hanging and unstable blocks, by means of a system of short and long passive nails and anchors properly grouted.
4. Minimization of visual impact of the anchor heads, with a mixture of special mortar, designed with the support of ICOMOS expert.

One of the major difficulties was the calibration of drillings with respect to the existing cavities: in the cliff are located a large number of grottos and tunnels (around 800). Therefore the drilling works had to be based on a detailed investigation, in order to define the better orientation and inclination avoiding the disturbance of the archaeological caves.

The larger diameter anchors, installed in 2003, were of pre-grouted type, to grant adequate protection against steel corrosion. Starting from 2004, only stainless steel anchors and nails were installed. In all cases, anchors and nails were grouted in site, using a special thick grout, to avoid risk of siltstone slaking. The grout was prepared with water and cement (W/C $\leq$ 0.5), added with a special admixture to completely avoid bleeding (low water-release grout). Tests performed on purpose demonstrated the grout suitability, since no difference was recorded from anchors bounded to conglomerate or siltstone.

Figure 4. Installation of monitoring system.

The anchor/nail head were finished to minimize the visual impact. All anchor and nail heads were designed to be placed slightly inside the rock. Therefore all the anchor/bolt heads and steel plates were covered with mortar of suitable color, allowing a total camouflage of the work. The composition and color of mortar was designed and developed in 2003, in cooperation with the support of ICOMS experts (International Council of Monuments and Sites). A number of tests were performed, on mixture of cement, clay/silt and water, to obtain the best chromatic effect, as well as stability and durability of the mixture. Actually it is now quite difficult to identify the areas were anchors and nails were installed.

4.3 *Installation of steel protective nets*

For a temporary stabilization of the back side of both East and West Niches, steel protective nets were installed in order to provide safety to the workers at the base. The nets were 8 × 10 grid, 2.70 mm dia. wires, double torsion and high galvanization. A total of 1500 m^2 of steel net was set: wooden distance holders, covered with non-woven fabric, were utilized to preserve as much as possible the areas where original plaster is still existing.

5 WORKS AT EASTERN GIANT BUDDHA NICHE

As said, a preliminary site visit was carried out in September 2003, aimed to the identification of potential negative evolution of the cliff and niches during the next winter 2003–2004.

The site investigation at the Eastern Niche (Figure 5) detected a very critical condition on the top right (east) side of the niche, where large fissures were widening. The abrupt rock fall could have involved large part of the upper Eastern part of the cliff and lead to the destruction of the whole niche. Emergency consolidation works were immediately designed to stabilize the most critical blocks prone to fall, in order to avoid any collapse in the coming winter season.

The intervention was also necessary to create safe working condition for the archaeologists that had to catalogue and recover the Buddha sculptures' remains from the floor of the niches.

Figure 5. Eastern Giant Buddha Niche.

The stabilization activities at the Eastern Buddha Niche started in October 2003. During the first phase (October–December 2003) and the second phase (April–June 2004) the activities were concentrated on the right side. During the final phase (September–November 2006) the works were carried out at the left side and at portion of cliff above the niche.

5.1 *Right side of the Eastern Giant Buddha Niche*

At the starting of the first phase (2003) a real time monitoring network was designed and installed to monitor the most remarkable cracks, in order to assure the proper execution of the consolidation works.

The installed monitoring system included 11 potentiometer crack gauges (0–50 mm, 4–20 mA, 0.01 mm accuracy), fitted with couplings and connecting cable, for a total length of 350 m (Figure 6). The system included also an acquisition unit Datalogger Geolog with 24 channels, a dedicated laptop computer with data management software, and alarm system. The monitoring system was re-installed at the starting of the second phase of the works (2004), to monitor the same cracks. The monitoring of the movements allowed a safe performance of the drilling and grouting works.

As temporary safety measure, to limit the possible deformations, two metallic beams (struts) were installed between the niche walls, at the elevations 2560 circa. These struts, designed at site, were ultimately adapted with the materials actually available in Afghanistan. During the second phase of the works these struts were re-installed at approx. elevation 2568 and 2570, at the area interested by the second phase of the works (Figure 7).

The temporary protection (removed on 2006) included a grid of 0.6" diameter steel ropes with a light pre-tensioning, to increase the factor of safety of the most unstable block from possible collapse. Five horizontal and two vertical steel cables were

Figure 6. Location of the 11 crack gauges.

Figure 7. Installation of temporary protection.

installed, fixed to short nails irregularly placed to avoid any stress concentration in a given line or area. At the end of the second phase of the works, UNESCO decided to leave the cables in place in order to provide additional safety to the archaeologists working at the basis of the niche.

Once the temporary protection had been installed, the consolidation works started.

The consolidation of the east side was obtained by means of passive anchors and nails. The anchors were 4 m spaced, to obtain a safety factor Fs = 2 disregarding the nailing support.

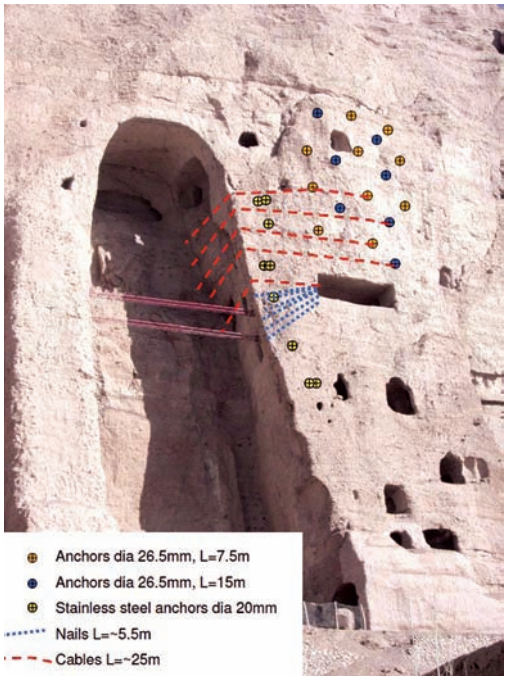

Figure 8. Eastern Giant Buddha Niche—anchors and nails installed at the right side.

The nails did not follow a regular pattern, being placed in the most suitable position to strengthen the smaller blocks. Direction and inclination of anchors and nails were defined on site, taking into consideration direction of deformation and position of rock discontinuities. In detail, at the east wall were installed (Figure 8):

- 17 passive anchors, 15.0–7.5 m long, on the external side of the niche (anchor bars VSL, dia 26.5 mm, st 835/1030, pre-injected, with external corrugated sheathing, with plates and nut).
- 6 nails, dia 16 mm, with average length of 5.5 m, from the existing balcony on the cliff to the internal wall of the niche (steel nails, dia 16 mm, FeB44K, threaded with couplers, anchor plates and nut).
- 24 short passive nails, max length 7.5 m, for a total length of 127 m, both in the niche and outside (stainless steel anchor bars VSL, dia 18.25 mm, steel st316, threaded, with couplers, anchor plates and nut).
- 2 test anchors (total length 20 m).

During the initial phase (2003), two different drilling techniques were utilized: rotopercussion (DTHH) dia. 90 mm, with air as drilling fluid, for the installation of 17 deep anchors; rotary drilling (dia. 36 mm), for the installation of nails (diamond drilling was adopted to reduce as much as possible the vibratory effects).

For the second phases of the works (2004), a special drilling rig was delivered to the site, to allow the diamond rotary drilling dia 50 mm, for the installation of anchor bars dia 18.25 mm with couplers of 20 mm dia.

The design strength of passive anchors was assumed in 200 kN, for a bound length (behind the major discontinuity) >5 m (about 40 kN/m).

Details on the design calculations of the initial intervention are reported in the following Figures 9 and 10. A major concern in the initial phases was the understanding of the adherence between grouting mix and siltstone, a very slaking material.

In these sketches we have:

- the geometrical distribution of the load and the assumptions for the calculation, based on the mechanic of the rigid body, and the related moment;
- the assumptions for calculation the moment of the anchors and the related safety factor;
- evaluation of the possibility to generate toppling according to the static loads and the uniaxial compressive strength of material.

A comparison between a standard anchor strength and the strength that had to be mobilized (as per the design calculations) was verified.

When specific site tests are not available, the adherence between the mortar and these types of rock is generally considered between 500 and 800 kPa. Assuming a value of 500 kPa, with a bond length of 5 m and a drilling diameter of 90 mm, we can consider about 700 kN for each anchor. Therefore, being the design anchor strength 200 kN, the mobilized adherence is about the 30% of the available one. In other words, the calculated adherence is 141 kPa, which it is significantly lower than the

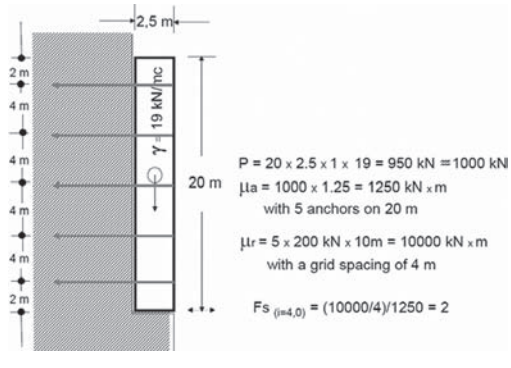

Figure 9. Anchor safety factor—verification of moments.

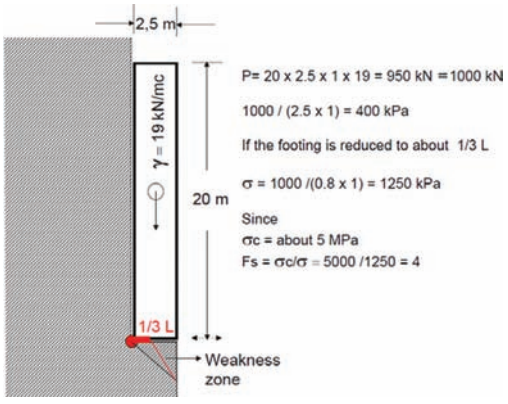

Figure 10. Verification of toppling.

designed 500 kPa. The resulting safety factor is about 3.6, which can be considered suitable, given the lack of information on the detailed geomechanical distribution of discontinuities.

The correctness of the adopted solution and the good bounding capacity of grouting mortar was later on confirmed by suitability tests, carried out in 2004 on two anchors to verify the bounding capacity both in siltstone and conglomerate. The two tests were performed on 1 m bond length, with a pulling force up to 400 kN (close to the yield capacity of steel). Up to this value no remarkable permanent elongation were detected, demonstrating the effective bounding between the anchor grout and the rock (conglomerate and siltstone, Figure 11). Again, taking into consideration the insufficient amount of information available on the actual distribution of the major fissures and of the difficulties in the homogeny of the grouting operations carried out by climbers, this result was considered as a confirmation of the designed pattern.

The technical approach and the techniques adopted were satisfactory, since the monitoring system did not record any remarkable deformation in the unstable blocks through at the working period, in spite of all the drilling and grouting operation performed on the cliff.

At the end, camouflage of the anchor heads was performed using proper mortar, to minimize the visual impact.

5.2 *Left side of the Eastern Giant Buddha Niche*

On the left side of the Eastern Giant Buddha Niche, the effects of March 2001 explosion are mainly evident at the top of the niche, probably due to the maximum concentration of stress as a consequence of the morphology of the niche, characterized by the presence of arches and pillars

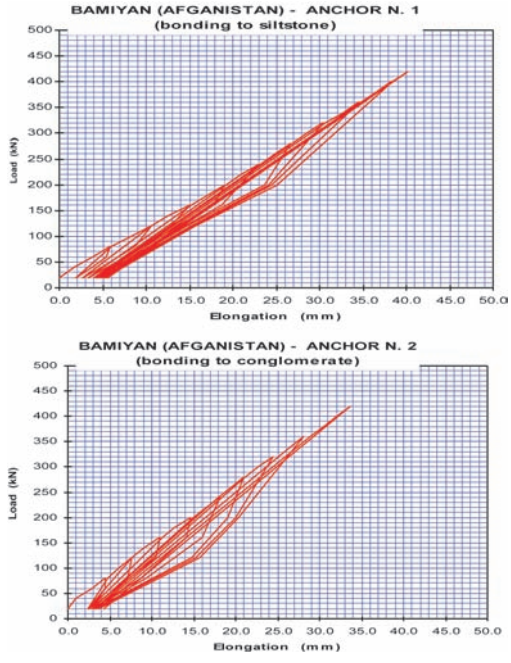

Figure 11. Anchor test in siltstone and conglomerate.

(Colombini & Margottini, 2003). In particular, a small pillar at elev. 2570 was prone to collapse (inducing deformation of the whole western part of the niche) and required consolidation works.

This intervention was carried out in 2006, starting with the installation of the monitoring system. Six (6) potentiometric crack gauges were newly installed to monitor the cracks identified as most dangerous in the area of the drilling and grouting works.

Afterward, the temporary support was set up. The two long steel beams (utilized in 2003–2004) were moved to the upper part of the niche, to provide some lateral support to the niche itself. In addition, two iron/wood beams were installed to support any possible lateral deformation of the pillar (Figure 12).

Temporary steel cables were installed on the west side of the niche (at El. 2570): 4 cables were fixed through steel bolts on the inner/outer wall of the niche, and 9 circular cables were placed embracing horizontally and vertically the rock pillar and the septum.

The emergency intervention included the installation of passive anchors and grouting works. Prior to starting the drilling works, the large cracks in the area of the pillar were thoroughly filled in and injected with cement grout. After the preliminary caulking, the main fissures were filled in with 0.96 m^3 of thick and stable grout (low water-release cement grout).

Figure 12. Installation of temporary support at the left side of the Eastern Giant Buddha Niche.

Figure 13. Eastern Giant Buddha Niche, left side, June 2004.

The drilling operations were carried out by diamond rotary system, 50 mm dia., to limit as much as possible vibratory effects to the structure, which was characterized by a very precarious stability.

A total of 12 stainless steel passive anchors were installed, dia 20 mm, each one with different length, for a total drilled length of 52.4 m. These anchors (three of them with double plate) were drilled into the pillar from two orthogonal faces, to create a steel-grid reinforcement in order to stabilize the upper gallery where a large fissure was present (Figure 13). The consolidation and grouting works provide a further protection against water infiltration, which may cause the slaking of the siltstone.

At the end, camouflage of the anchor head and fissures was carried out, using proper mortar, to minimize the visual impact (Figure 14).

5.3 *Cliff above the Eastern Giant Buddha Niche*

Three permanent stainless steel passive anchors (20 mm dia, 12.0 m long) were installed with subhorizontal inclination in the portion of rock just above the niche.

Figure 14. Eastern Giant Buddha Niche, left side, November 2006.

Figure 15. Installation of instrumented anchors on top of the Eastern Giant Buddha Niche.

Open vertical fissures, reaching downwards the upper part of the niche, were intercepted by the 3 boreholes, at depths of 8–9 m. Therefore, about 540 liters of cementitious grout were injected to seal the fissures so as to protect the niche from water infiltrations from the above during snowmelt and rainfalls.

To monitor the tensional state of the rock masses, a total of 10 strain gauges were installed. Namely, two anchors were instrumented with a series of 5 spot weldable strain gauges. The connecting cables were conveyed into small grooves to the steel boxes located into the niche, were readings can be taken utilizing the portable datalogger with LCD display (Figure 15).

6 WORKS AT WESTERN BUDDHA NICHE

The Western Niche did not suffer severe consequence as a result of the explosion that destroyed the statue (Margottini, 2006). Therefore, the emergency intervention included only the grouting of

the large fissure in the corridor behind the niche and minor consolidation works. These activities were performed during the last phase, between October and November 2006 (Figure 16).

The grouting of the large crack was performed working both from the corridor behind the statue head and from the top of the cliff. At first, the fissure was sealed and grouted in the internal part of the niche, in order to protect the niche from leaching of grout to be injected from the top. Small vent pipes were installed to avoid internal overpressure. Afterward, inclined boreholes were drilled from the top of the cliff to the fissure to be grouted. Special care had to be paid when working on top of the cliff since, although the area had already been demined, the heavy rains might have brought to the surface new mines (Figures 17 and 18). Two minor interventions were performed in two areas on the left side of the niche.

In the area at elevation 2550, three stainless steel passive anchors were installed by 50 mm coring drilling (1.6 m long, 20 mm dia.).

This area demonstrated to be relatively stable and less compromised. On the contrary, in the area at elevation 2538 five similar passive anchors were installed, with significant grout takes. As usual, at the end the camouflage of the anchor heads was crafted.

Figure 16. Western Giant Buddha Niche.

Figure 17. Western Giant Buddha Niche, March 2004.

Figure 18. Western Giant Buddha Niche, November 2006.

7 CONCLUSION

After the engineering geological studies (started in September 2002 under the UNESCO direction) and the emergency consolidation works (October–December 2003, March 2004 and October–December 2006), the cliff and niche of the Eastern Giant Buddha are now stable and the risk of collapse almost avoided.

Further works are still in progress, managed directly by UNESCO, and other will be needed in the future, especially to complete the consolidation of the back wall of both niches, but the major risk of collapses involving also the few remains not destroyed by Taliban it is now turned away.

REFERENCES

Colombini V. and Margottini C. (2003). Reducing the most critical rock fall-prone areas in the Buddhas niches in Bamiyan (Central Afghanistan). *UNESCO Report*, July 2003.

Colombini V., Crippa C., Margottini C., Tonoli G. (2009). Emergency Intervention, *The Destruction of the Giant Buddha Statues in Bamyan, Claudio Margottini Editor, Union Printing S.p.A.* February 2009.

Delmonaco G. and Margottini C. (2009). General Environmental Condition of the Bamiyan Valley, *The Destruction of the Giant Buddha Statues in Bamyan, Claudio Margottini Editor, Union Printing S.p.A.* February 2009.

Margottini C. (2004). Instability and geotechnical problems of the Buddha niches and surrounding cliff in Bamiyan valley, Central Afghanistan. *Landslides*, n.1. January.

Margottini C. (2006). Definition of 2006 activities for completing the emergency consolidation of Large Eastern Buddha and for the preservation of Large Western Buddha. *UNESCO Report*, August 2006.

Margottini C. (2009). Properties of Local Material., *The Destruction of the Giant Buddha Statues in Bamyan, Claudio Margottini Editor, Union Printing S.p.A.* February 2009.

PASCO (2003). Bamiyan mapping project. UNESCO report. Buddhas laser scanner project. *UNESCO reports*, 2003.

Reineke T. (2006). Environmental Assessment of the Bamiyan Valley in the Central Highlands of Afghanistan. *University of Aachen, Bamiyan Masterplan Campaign 2005*. Aachen, 2006.

Geotechnical Engineering for the Preservation of Monuments and Historic Sites – Bilotta, Flora, Lirer & Viggiani (eds)
© 2013 Taylor & Francis Group, London, ISBN 978-1-138-00055-1

Archaeology and geotechnical engineering

S. D'Agostino
Formerly Professor of Structural Analysis and founder of the Center of Engineering for Cultural Heritage (CIBeC), University of Naples Federico II, Italy

G. Tocco
Formerly Superintendent Archaeologist for the Provinces of Salerno, Avellino and Benevento, Italy

ABSTRACT: Archaeological sites began to be investigated with scientific methods during the XIX century; geotechnics evolved into an engineering science in the following century, with the development of soil mechanics. Both archaeologists and geotechnical engineers investigate the subsoil, though for different purposes; furthermore since the mid of the XX century the development of construction industry resulted in deeper and deeper excavations, piled foundations, urban tunneling, frequently interfering with the study and preservation of archaeological remains. For a long period, preliminary investigations to avoid irreparable damages to the archaeological heritage were very difficult, also because of the lack of specific regulations.

In 1969 the European Convention for the protection of the archaeological heritage claimed for preventive exploration before the works. In fact, England and France soon developed methods and rules to make such investigations timely and rapid, and hence compatible with the economy of industry. In Italy, where more than in any other country the subsoil preserves traces of the previous civilisations, only in 1999 a regulation prescribing archaeological investigations before the start of public works has been issued. During the construction of large infrastructures, hence, if the interference between the archaeological findings and the new structures is not avoidable, archaeology and engineering are obliged to find a meeting point. Furthermore, geotechnical engineering may play a significant role in archaeological excavations and in the safe conservation of monumental buildings and archaeological sites and parks.

It is evident that an intervention protocol for an interdisciplinary approach between archaeology and geotechnics needs to be developed, based on real experiences as the ones reported in this paper.

1 INTRODUCTION

In Italy, one of the first significant reflections on the relationship between archaeology and geotechnical engineering, as well as on the need for a synergy between the two disciplines, came at the National Conference of Italian Geotechnical Society in 1980. Giorgio Gullini, an archaeologist and great connoisseur of ancient architecture, traced with expert memory the evolution of the foundation techniques throughout the West and the Near Middle East, from the fourth millennium B.C. to the fourth century A.C. (Gullini, 1980); Arrigo Croce, one of the founders of geotechnical engineering in Italy, perfectly understood the broad scientific perspective that a shared research would open up and underlined its multifaceted values, to be followed by younger students (Croce, 1980; Viggiani, 1980).

Unfortunately this serene historic and scientific approach did not spread out in the professional world in connection with the design and execution of public works and infrastructures. A harsh contrast developed between the needs of archaeological research—made by hand excavations and accurate analysis—and the technical and economical requirements of public works—often implemented with funding scarcity and predetermined deadlines.

The conflict began to arise since the early decades of the last century, due to the rapid development of construction industry and the expansion of urban areas. In addition, new techniques as the piled foundations and the shallow urban tunnelling, widely adopted both in current construction and in infrastructure, made the conflict more frequent.

The three decades which bring us to the present days, however, have seen also many shared interests. A greater awareness of the needs of archaeological research and of the remarkable progress of geotechnical research, in particular of modern diagnostic possibilities, makes not only an agreement, but also an efficient and productive

interdisciplinary collaboration possible with all the ensuing benefits too often sacrificed to low-profile economics needs.

2 SUBSOIL EXPLORATION AND EXCAVATION

The importance for an archaeologist of the stratigraphic excavation of the soil is more than evident. Each layer features a phase of deposition of objects, documenting its sequence and obtaining a relative and absolute chronological reference. But each layer also determines a phase of soil sedimentation which, through a careful geotechnical reading, can lend important contributions to understanding the evolution of the land and the natural and human events and that have marked it. In the maintenance and preservation of archaeological sites the management of ground water is of the utmost importance to prevent uncontrolled runoff, floods and erosion processes. Such a task is often included among the responsibilities of the geologist, while it is believed to be better attributed to the geotechnical engineer, more used to a detailed analysis of shallow layers.

The planning of archaeological investigations has to be supported by geotechnical studies, to guarantee the overall stability of the area. These studies have to be extended to the large areas of significant archaeological interest, and for this reason subjected to use restrictions; but they are often omitted for economic and organizative reasons.

Many examples of this kind can be mentioned; just to stay in the Campania region, the Roman cities of the Vesuvius area, the Greek colonies on the coast or the inland areas of the Samnite cities, all only partially excavated.

The safety of the excavations is also an obvious task of geotechnical engineering, while it is usually handled by archaeologists in an empirical manner, sometimes generating serious incidents. Even if the current Italian legislation requires the presence of a qualified technician for the safety site (Decree n. 81/2008), a timely joint examination by an archaeologist and a geotechnical expert might propose a different configuration of the excavation and an implementation of appropriate measures to ensure safety.

A further field of important joint research, relevant for ancient history, is the study of the foundations of archaeological construction, especially within the ancient cities, inhabited since centuries or millennia, where the new buildings are superimposed on older settlement. In fact, considering the architecture of the Greek temples, of which outstanding examples remain in Magna Graecia and Sicily, one realizes the scarcity of valid scientific knowledge concerning the foundations of the great temples. Their complex structures are known only in a few cases, both from the viewpoint of archaeology and of engineering.

One exception is the archaeological site of Paestum. The geotechnical investigation on the foundations of the temple in the northern sanctuary of the city, the Athenaion, has been one of the preliminary analyses for the restoration of the monument. In the same site a rich documentation of the system and the consistency of the foundations of the most archaic temple of the southern sanctuary, are ensured by the excavations and surveys carried out by Krauss (1941) and the comprehensive study by Mertens (1993) on the Temple of Hera (figure 1). These and other valuable studies (Pescatore, Viggiani, 1991) are to be compared, however, to the vastness and complexity of the architecture of ancient world. A joint research effort by archaeologists and geotechnical engineers with a direct confrontation on the field, and both animated by the same cultural motivations, is therefore needed if the knowledge about the ancient world and the evolution of the anthropized areas have to reach a much higher scientific level.

A significant example is the restoration of the Domus Tiberiana in Rome (figure 2), on which archaeologists, geotechnical and structural engineers have actively collaborated (Tomei, Filetici, 2011). Today, all this is facilitated and enriched by powerful development in diagnostics applied in geotechnical engineering, as well as in archaeology.

In addition to traditional investigations these include developments in high precision geodetic surveys, the use of ground penetrating radar and

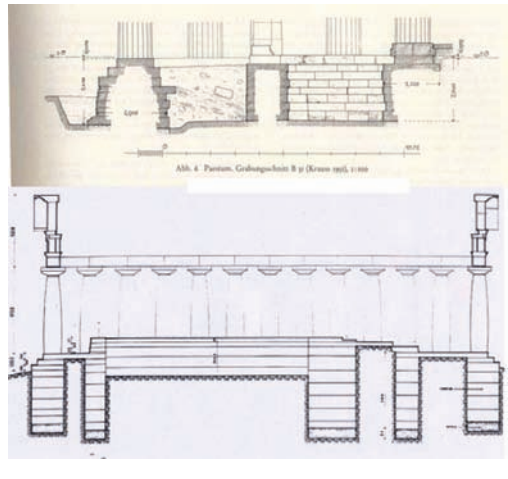

Figure 1. Paestum (SA). Foundations of the so called Basilica (above) and foundations of the temple of athena.

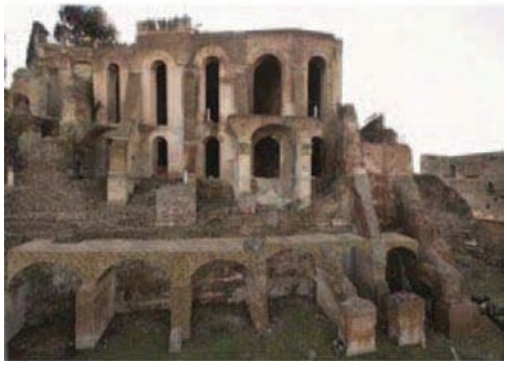

Figure 2. Roma, Domus Tiberiana.

ultrasonics as well as complex and articulated laboratory tests.

3 A PAINFUL HISTORY

During the last century in Italy, however, the relationship between archaeologists and geotechnical engineers unfortunately has not always been satisfactory due to the absence of adequate regulations as well as to the lack of a shared culture. Superintendents often did not pay particular attention to the need for geotechnical analyses, especially in the field of restoration and maintenance, and geotechnical engineers did not show sensitivity to the needs for protection. Moreover, there has been a lack of coordinated actions between the various departments of the Ministry for Cultural Heritage, in particular between the Superintendences for Archaeological and Architectural Heritage.

Not only in Italy, but also in Europe and the Near East, quite a number of famous monuments have been underpinned by micropiles without due consideration to the fact that generally more ancient archaeological sites are found in the subsoil underneath. This practice has permanently damaged areas which are certainly still rich in archaeological remains, hindering their historical knowledge (figure 3).

Massive intervention of landslides stabilisation by means of piles or other invasive techniques, which often have revealed ineffective (figure 4) and have contributed to the cementification of the land.

Concreting of many river banks brought too often to the catastrophic consequences that periodically mark the Italian territory. Sometimes reinforced concrete retaining walls have been built within archaeological sites, while the use of stone masonry would have been more proper because it

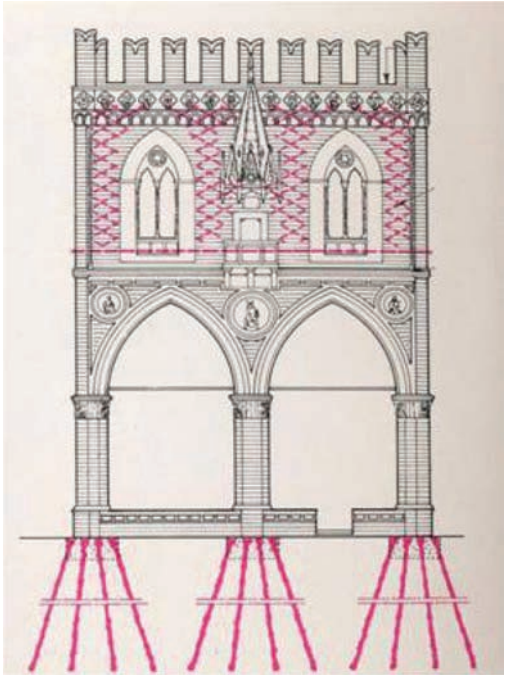

Figure 3. Bologna, loggia della mercanzia. Underpinning of the monument with micropiles.

Figure 4. Failure of a pile row supporting a landslide.

best harmonizes with the archaeological materials (Figures 5 and 6). Finally, a particular violence has been inflicted to the archaeological heritage by the vast network of infrastructures built in the second half of XX century. The designers completely ignored the occurrence of archaeological remains in the choice of the location of infrastructures as

Figure 5. Velia (SA), porta rosa. Reinforced concrete walls.

Figure 6. Velia (SA), porta rosa. Stone masonry boundary walls.

roads and railways. Even within sites where excavation was already in progress, archaeological findings, sometimes of considerable value, only rarely and incidentally came to light.

The conflict among different institutions and the absence of an interdisciplinary culture between archaeologists and geotechnical engineers have been repeatedly denounced and exemplified in detail (Calabresi, D'Agostino, 1997).

4 CONSERVATION AND SECURITY: PREVENTIVE ARCHAEOLOGY AND ENVIRONMENTAL ENGINEERING

The situation described above could not leave the world of historical culture indifferent for long. In fact, since History is the "science of humanity" and material history is a fundamental aspect of historical research, archaeological remains make up the material documents of history, and as such must be properly collected, studied, and preserved (D'Agostino *et al.*, 2009). Every destroyed archaeological site represents the destruction of an archive of mankind's material history. Thus as early as 1969, with the European Convention for the Protection of the Archaeological Heritage (London, 06.05.1969), later replaced by the Convention of Malta (01.16.1992), preventive archaeological investigations were proposed for any intervention of territorial transformation, requesting all the member states to establish appropriate standards. Some countries, such as Sweden and Portugal, soon complied with this commitment.

In France, methods and standards capable of making archaeological exploration timely and fast, and of reconciling the demands of research with those of economic development were fixed. In 1973 the "*Association pour les fouilles archéologiques*" (AFAN) was created to perform excavations under the control of state organs. During the construction of the Lyon metro it was established that the cost of excavations was to be paid by the bodies committing the works. In 2002 a new national body was created, the "*Institut National de Recherches archéolgiques préventives*" (INRAP), in which a part of the archaeologists of the AFAN merged, with the task of carrying out preventive investigations, from diagnostic to exploration, restoration and study of materials, all still at the expense of those who committed the work. It is interesting that this same preventive investigation was also foreseen for the construction of public or private housing, but in this case at the expense of the State.

In Italy, a country that more than any other bears testimony of an intense human presence in its subsoil, no provision has been made for many years to ensure preventive control in soil transformation, and the Convention of Malta has long been disregarded. Only an ever more vigilant control by the Superintendences for Archaeological Heritage has allowed for some prior interventions or, unfortunately, interventions only made during the execution of the works, in order to safeguard the archaeological heritage with preventive explorations. In a few cases, where it was not possible to reconcile the protection with the implementation of the work, the projects had to be modified but always with great difficulty.

All the while, aid was found in a field near to geotechnical engineering. The "*Fondazione Lerici*", an institute of applied geophysics active since 1955, began in 1970 to increase its activity in the application of preventive diagnostic instruments and methods of geophysical prospecting to archaeological research, allowing a substantial decrease of the time needed for preliminary surveys.

Continuing to quote applications in Campania, the exemplary case of the municipality of Pontecagnano can be mentioned. During the construction of the Salerno-Reggio Calabria highway in 1962, a great Etruscan settlement was intercepted. This discovery unfortunately allowed the recovery of only a few pieces of the ancient settlement; later on, however, through an electromagnetic prospections campaign carried out by *Fondazione Lerici* it was possible to define the entire area, identifying its greatest extent that fortunately is away from the highway layout. In the General Municipal Plan of Pontecagnano, being discussed in those years, the area was identified as archaeological and declared not to be used for housing. For the areas which held the rich necropolis, coincident with building development zones, any building permit was qualified to prior archaeological exploration. This procedure allowed the recovery of many and rich burial objects which constitute an exceptional example of the expansion of the Etruscans much to the south of Etruria; they are now exhibited in the National Archaeological Museum "*Etruschi di frontiera*" in Pontecagnano (Tocco, 2010) (figure 7).

Other extraordinary discoveries have been made during the construction of infrastructures, such as the high-speed railway, the doubling of the pipeline bringing gas from Algeria, the extension or adaptation of some internal roads such as the Vitulanese valley or the Isclero valley, the construction of the new metro line in Naples or the third lane of the Naples-Salerno and Salerno-Reggio Calabria highways. Without a specific legislation on the matter, all prior investigations have been the result of arguments, negotiations and laborious agreements. They were possible thanks to the will of the Superintendences for Archaeological Heritage and to the increasing sensitivity of the institutions or organisations committing the works.

The establishment of the so called "service conferences" (L. n. 241/1990), which brought to the same table all interested parties to review the draft design of public works, has facilitated and promoted preventive control in territory transformation, greatly contributing to the enrichment of its archaeological heritage. Just to mention a couple of examples, the extraordinary paintings that adorned the triclinium of a Roman villa discovered during the construction of the third lane of the Naples—Salerno highway near Moregine, in the territory of Pompeii (figure 8) or the outline of the urban settlement stratifications of Naples which emerged during the metro construction (figure 9), showing the coastline of the ancient Neapolis and the location of the port during the Roman period.

Out of Campania, we note the enormous importance of what has been found in preventive investigations during the doubling of the railway line Palermo-Messina in Sicily. In fact, communal tombs and graves were found with a large number of warrior skeletons laid in lines and atop the skeletons of many horses (figure 10). This allowed

Figure 7. Pontecagnano (SA). The archaeological museum "Etruscan frontier". Exhibition room.

Figure 8. Pompei (NA). Paintings from the Moregine villa.

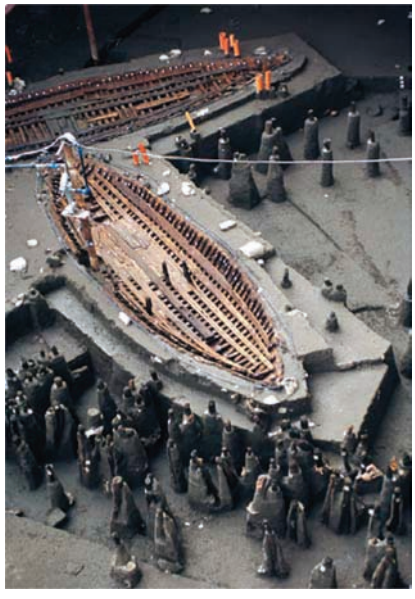

Figure 9. Napoli, piazza municipio. Ancient Roman ship.

Figure 10. Himera, Sicily. Graves of warriors.

finally the documentation of two famous battles which took place near the walls of the Greek colony of Himera in 480 and in 409 B.C., between Greeks and Carthaginians, as reported by Diodorus Siculus (VI, 165–167) and Herodotus (VII, 164–166), of which we had never had a concrete testimony (Vassallo, 2010).

With the preliminary investigations for the construction of the third lane of the Salerno-Reggio Calabria highway it was possible to identify and explore a large number of ancient settlements. In particular, in the above mentioned section on the municipality of Pontecagnano, the exploration carried out away from the highway, on the side of smaller extension of the ancient settlement, identified its urban organization and city's defence system which was made up of an embankment

Figure 11. Pontecagnano (SA). Highway Salerno-Reggio Calabria. Area of the ancient ditch.

slope bordered by a wide moat. Furthermore the outline of a very interesting sanctuary erected to put under the divine protection the northern edge of the city was brought to light. These findings give us an idea of the destructions that have probably occurred during the construction of the previous highways (Pellegrino, Rossi, 2011), (figure 11).

The experience gained in these prevention exercises during more than twenty years, despite the lack of law rules, made finally the time ripe for the adoption of a series of regulations that, starting in 1999 and even with a succession of ups and downs, have finally sanctioned the duty of preventive archaeological control of the subsoil before the implementation of public works. The General Law of Public Works (Law n. 109/1994) prescribed archaeological investigations in the framework of the preliminary project (DPR n. 554/1999, Art. 18, § 1. d). A step back was marked by the Decree n. 190/2002, concerning the construction of infrastructure, since the obligation of submitting the preliminary design to the Ministry of Cultural Heritage was limited to only the areas already declared of cultural interest (Art. 3, § 4). The Code of Cultural Heritage and Landscape (Decree n. 42/2004, Art.28, § 4) made up for this, by requiring preventive investigations at the expense of the body promoting any public work, even in the areas not yet declared of interest. The Law n. 109/2005, which (urgent provisions for the development and territorial cohesion), provided

for the preliminary verification of the archaeological interest, articulating the design of public work in three phases—preliminary, definitive and final—(Art. 2 ter, 2 quater, 2 quinquies). Unfortunately, however, the Code of public contracts for works, services and supplies (Decree n. 163/2006, Art. 95 and 96), which accelerates the time for the design procedures, rendered the verification, and hence the protection, more difficult. However, the rules for the execution and implementation of the Decree April 12, 2006, n. 163, and its modifications (DPR n. 207/2010) have more organically inserted archaeological investigations throughout the preliminary and final phases of the project. Finally, pending the publication of the guidelines laid down by law, the General Directorate of Antiquities of the Ministry of Heritage and Cultural Activity has provided the Superintendences for Archaeological Heritage the first operational guidelines relating to a preventive verification procedure of archaeological interest (Circular n. 10/2012).

In this framework a dialogue between the discipline of archaeology and the geotechnical engineering is mandatory, not only in the surface investigations phase where the tools developed in the geotechnical field are routinely applied, but even more so in the execution of excavations often performed at great depth, and in the final execution phase of these works, when conflicts arise between the safeguard of the archaeological remains and the construction of the new artefacts.

All these problems are even worst in urban areas, where the archaeologists often work in tight spaces, already intensely constructed areas, or even in areas with historical buildings affected by works of restoration or rehabilitation and which very often have fragile foundations. In these cases a legislation providing for the comparative analysis of the design both from an archaeological point of view and a geotechnical point of view would be desirable, in order to identify from the early stages non-invasive solutions, capable of safeguarding both the archaeological remains and the security of the constructions. As we have seen in the case of Paestum, particularly significant is the role of geotechnical engineers in the restoration and maintenance of large monumental complexes, for which the analysis of the soil, and of the foundation levels may be essential for the conservation of the monument itself.

Finally, further progress in the collaboration between the two disciplines may be derived from the so-called naturalistic geotechnical engineering in protected areas. In fact, avoiding extensive cementing and adopting specific plantings as well as creating support walls with traditional and regional materials, can consolidate the area on one hand and respect the natural constraints on the other (figure 12).

Figure 12. Example of naturalistic engineering.

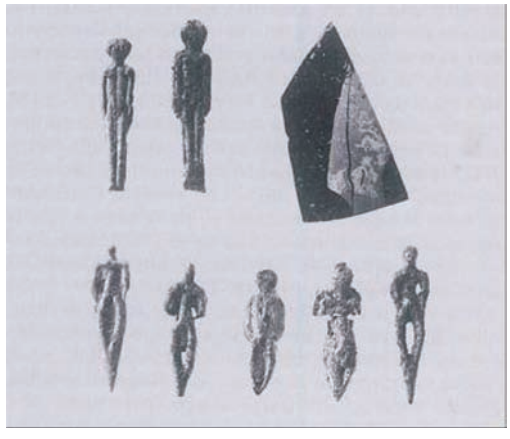

Figure 13. Pisa, piazza dei miracoli. archaeological findings.

5 A COMMON FUTURE: GOOD PRACTICE

We have seen that archeology and geotechnical engineering had in the past divergent paths; it must be stressed, however, that certain instances do exist in which the sensitivity of the planners has led to positive results.

The emblematic case of the intervention on the Tower of Pisa, which not only prevented intrusive underpinning of the monument but also brought to the discovery of many important archaeological remains in the Piazza dei Miracoli, (AA.VV., 2005 is well known (figure 13). Other interventions, carried out in full compliance with the requirements, were already presented in 1996 at the International Symposium on Geotechnical Engineering for the Preservation of Monuments and Historical Sites, such as

Ponte Milvio in Rome and Rocca dei Rettori in Benevento (Calabresi, D'Agostino, 1997). This cultural attitude has been particular followed by the University of Naples Federico II, with research focused on the knowledge and the recovery of some famous ancient monuments, such as the Cripta metropolitana (Amato *et al.*, 2000), the tunnels of Cocceio in Naples (Amato *et al*., 2001) and the Tomb of the Ogre in Tarquinia (D'Agostino *et al.,* 2010), (figure 14).

Sometimes the consequences of a dramatic seismic event require collaboration between geologists, geotechnical engineers and archaeologists. The Irpinia earthquake in 1980/81 in Campania, hit many small towns rich in history. The historical centre of Buccino, in the province of Salerno, is located on an emerging hill and built upon the Roman city of *Volcei*, keeping the ancient urban layout. It has been deeply devastated by the earthquake. In the subsequent reconstruction, the Superintendence for Archaeological Heritage understood that the City should not resort to the demolition and complete reconstruction of the damaged buildings, but instead opt for the restoration and verification of the presence of archaeological remains, prior to the consolidation of the foundations. The extremely complex work of investigation, consolidation of the existing buildings and presentation of ancient remains discovered, required a continuing collaboration between archaeologists, geotechnical engineers and structural engineers.In addition to the restoration of the historical centre, an archaeological park was created that, being developed partly in the basements and partly at the street level, offers a meaningful perception of the settlement in a continuous interweaving of past and present (figure 15). In conclusion, the historical centre of Buccino has maintained its consolidated configuration without the alterations occurred in many other towns damaged by the earthquake; at the same time, it has gained an archaeological interest that can attract a significant flow of tourists (Lagi, De Gennaro, 2003).

Figure 14. Tarquinia. Interior of the Ogre tumb.

Figure 15. Buccino (SA). Base of an Italic temple built into a place in the historical centre, visible from one side at the street level (above) and from the other side from an underground passage.

Even in the course of ordinary restoration and monumental renovation, a prior archaeological survey can achieve extraordinary discoveries with the aid of geotechnical engineering also. During a restoration intervention in the crypt of the church of S. Maria Assunta in Positano (Salerno), remains of a sumptuous Roman *maritima* villa have been found. Among them, the wall of a room decorated with an extremely important painting (figure 16). Judging from this discovery, probably only a small portion of the monument, the villa was not affected by the foundations of the church above it because buried in the eruption of the Vesuvius in 79 A.C. (Tocco, 2004). In this case the archaeological investigation, besides adding another important step in the knowledge of the distribution of Roman patrician villas along the coast of Sorrento and Amalfi, provided interesting insights into the dynamics of the eruption, showing that the pyroclastic material projected from the Vesuvius overcame the barrier of the mountains Lattari distributing itself on the coastline behind. Obviously, in order to assess the feasibility of an excavation expansion and of the preservation and enhancement of the Roman ruins, without endangering the structural safety of the Church above, the assistance of structural and geotechnical engineers was needed.

In the restoration of the Savoia royal mansion at Venaria Real, near Turin, the contribution of the geotechnical engineer was crucial to avoid underpinning with micropiles of the huge complex of the Citroniera. In fact, in this way, it was possible to

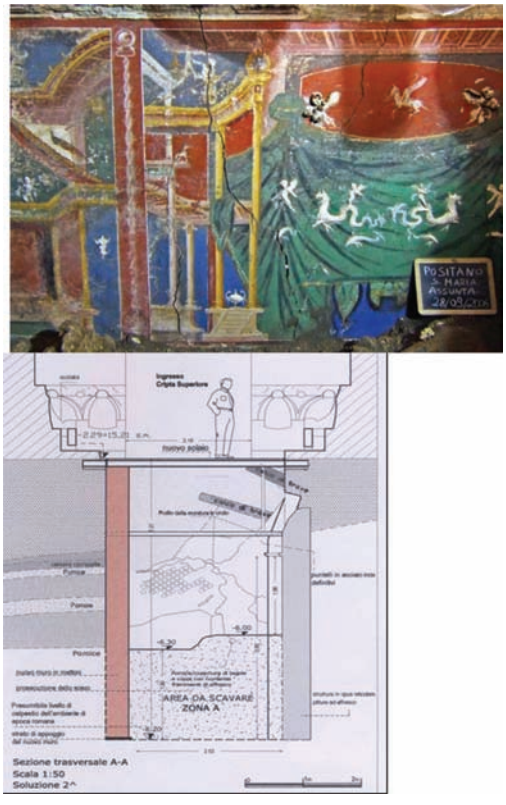

Figure 16. Positano (SA). Painted wall of a Roman villa below the church of S. Maria Assunta.

Figure 17. Venaria reale, torino. The foundation wall of the Citroniera.

Figure 18. Napoli. The hill of S. Martino in the tavola strozzi, oil on wood at the S. Martino Museum, 1470.

highlight the wall material of the massive Iuvarriane foundations resulting in the discovery of many ancient artefacts (D'Agostino, Migliore, 2007), (figure 17). The hill of San Martino (figure 18), just in the centre of the city of Napoli, has on its slope some 7 km of retaining walls, constructed by the monks to transform an impervious wooded steep crag into a succession of cultivated terraces. Most of the walls show evident traces of degradation, such as erosion of the masonry at the outer surface with significant decrease of the structural section, removal of the soil at the toe uncovering the foundation, differential settlement and fissures at the junction of different walls. The conservation of the system of retaining structures implies not only the repair of the various forms of degradation affecting them, but also their strengthening to comply with the more demanding requisites of the present seismic regulations. After a first hasty design with extensive of reinforced concrete, the reinforcing interventions have been recently redesigned in the traditional tuff that characterizes the ancient Neapolitan retaining walls (figure 19).

Figure 19. Ancient tuff masonry of the retaining walls at S. Martino.

6 CONCLUSIONS

The experiences briefly reported in the paper show that the old conflict between archeology and geotechnical engineering can be overcome by sharing the principles of preservation and safety and by cooperating to understand each other's needs. In the context of prevention, the investigation of subsurface features from both a geotechnical and archaeological point of view should be made obligatory in territorial planning, especially in the context of historical buildings. The still unresolved issue of specific legislation for preventive investigations for private works should be discussed.

The contribution of geotechnical engineering should be required in the restoration as well as in the maintenance of monuments and archaeological sites, just as a regular flux of resources for monitoring should be provided within the operating funds of the Superintendences. For safety in excavation sites, in case of deep excavations or excavations in the proximity of buildings, a preliminary verification and the assistance of a geotechnical engineer during construction should become mandatory. In the arrangement and safety of sites it is recommended the use of naturalistic engineering, which only recently geotechnical projects have tended to focus on.

Finally, because the two worlds of geotechnical engineers and archaeologists, apparently so different, have frequently met in shared activities and have achieved important results, it would be important to develop common guidelines for the education of both the archaeologists and the engineers; not only the geotechnicians, but also the structural engineers, who encounter problems very similar to those illustrated in the preservation of architecture in ruins.

REFERENCES

AA.VV. (2005) La torre restituita. *Bollettino d'Arte, Ed. speciale in 4 volumi*. Roma: Ist. Poligrafico dello Stato.

Amato, L., A. Evangelista, M.V. Nicotera, C. Viggiani (2000) The Crypta Neapolitana; a Roman tunnel of the early imperial age. More than two thousands years in the history of Architecture. *UNESCO-ICOMOS International Congress, Bethlehem.*

Amato, L., A. Evangelista, M.V. Nicotera, C. Viggiani (2001) The tunnels of Cocceius in Napoli: an example of roman engineering of the early imperial age. *AITES/ITA World Tunnel Congress. Milano*.

Calabresi, G., S. D'Agostino (1997) Monuments and historic sites: Intervention techniques, in: C. Viggiani ed., *Geotechnical Engineering for the Preservation of Monuments and Historic Sites*. Rotterdam: Balkema.

Croce, A. (1980) Geotecnica e Beni Culturali, Relazione introduttiva, XIV Convegno Nazionale di Geotecnica.

D'Agostino, S., M.R. Migliore (2007) Il restauro costruttivo del complesso Citroniera-Scuderia a Venaria Reale: gli aspetti strutturali, *Atti VI Convegno Nazionale ArCo "Quale sicurezza per il patrimonio architettonico?, Mantova 30/11–2/11 2006. Roma: Nuova Argos.*

D'Agostino, S., F. Cairoli Giuliani, M.L. Conforto, E. Guidoboni (2009) Raccomandazioni per la redazione di progetti e l'esecuzione di interventi per la conservazione del costruito archeologico. *Napoli: Cuzzolin Ed.*

D'Agostino, S., G. Lombardi, G. Russo, C. Viggiani (2010) Structural engineering and geology applied to the static problems of the Etruscan "Tomba dell'Orco" (Tarquinia,Central Italy*). Journal of Cultural Heritage,* 11, 107–112.

Gullini, G. (1980) Le fondazioni e il supporto fisico del costruito nelle culture architettoniche dell'antichità, *XIV Convegno Nazionale di Geotecnica. Firenze.*

Kerisel, J. (1997) Geotechnical problems in the Egypt of Pharaos, in C. Viggiani ed., *Geotehcnical Engineering for the preservation of Monuments and Historic Sites*. Rotterdam: Balkema.

Krauss, F., (1941) Paestum. Die griechischen Tempel, *Berlin.*

Lagi, A., R. De Gennaro (a cura di), (2003) Parco archeologico urbano dell'antica Volcei. *Napoli.*

Mertens, D. (1993) Der alte Heratempel in Paestum und die archaische Baukunst in Unteritalien, *Sonderschriften, 9, Mainz am Rhein.*

Pellegrino, C., A. Rossi (2011) Pontecagnano I.1. Città e campagna nell'agro picentino *(Scavi dell'Autostrada 2001–2006*. Fisciano.

Pescatore, T.S., C. Viggiani (1991) Geologia della piana del Sele e caratteri del sottosuolo dell'area di Paestum. *Paestum, Etude de cas de vulnérabilité du patrimoine*, PACT, n. 32.

Tocco, G. (2004) L'attività archeologica della Soprintendenza di Salerno, Avellino e Benevento nel 2003–2004, *XLIV Convegno di studi sulla Magna Grecia, pp. 560–562. Taranto.*

Tocco, G. (2011) Gli Etruschi di frontiera tra affabulazione e rigore scientifico: l'allestimento del Museo archeologico Nazionale di Pontecagnano, *in "Restituire la memoria. Modi e forme dei linguaggi museali", Atti del Convegno Internazionale—Aosta 4/5 giugno 2010, pp. 91–98*. Prato.

Tomei, M.A., M.G. Filetici (2011) Domus Tiberiana/scavi e restauri 1990–2011. *Verona: Mondatori Electa.*

Vassallo, S. (2010) Le battaglie di Himera alla luce degli scavi nella necropoli occidentale e alle fortificazioni. I luoghi, i protagonisti. *Sicilia Antiqua, vol. VII, p. 17–38. Roma: F. Serra Ed.*

Viggiani, C. (1980) Alcune osservazioni sul ruolo della Geotecnica negli interventi sui monumenti, *Convegno Nazionale di Geotecnica. Firenze.*

Geotechnical Engineering for the Preservation of Monuments and Historic Sites – Bilotta, Flora, Lirer & Viggiani (eds)
© 2013 Taylor & Francis Group, London, ISBN 978-1-138-00055-1

Long-term stability of old cathedrals in St. Petersburg

R.E. Dashko & A.V. Shidlovskaya
National Mineral Resources University (Mining), Saint-Petersburg, Russia

ABSTRACT: A number of historic cathedrals in Saint Petersburg, such as Peter and Paul Cathedral, Kazan Cathedral and St. Isaac's Cathedral, experience progressive foundation failure alongside long-term and differential settlements leading to development of cracks in their bearing structures. Similar adverse conditions of these edifices is currently related to the natural conditions of Saint Petersburg's historic centre and negative transformations of underground space components: soils, groundwater, microorganisms, gases and materials contributed from subsurface structures and services. The generalities of Cathedrals location and its bases are typical geotechnical section of Low terrace, development of swamps, peaty soils, quick sands and water and gas saturated weak soils and fissured bed clays (hard soils). The high degree of groundwater contamination with organic and inorganic pollutants generates active development of marsh and alien biocenoses. The authors propose a concept and structure of a complex programme of preventive geotechnical and geoenvironmental monitoring for cathedrals.

1 GEOTECHNICAL AND GEOENVIRONMENTAL CONDITIONS OF HISTORIC CITY CENTRE IN SAINT-PETERSBURG

Long-term stability and safety of historic buildings in downtown St. Petersburg, including old cathedrals of 18th–19th centuries, to a large extent depends on geotechnical and geoenvironmental conditions of the city's underground space, intensity of dynamic impact generated by public traffic, local climate conditions, the degree of atmospheric pollution and precipitation. The concept developed by the authors presupposes conceiving of the underground space as being a multi-component system. (Fig. 1).

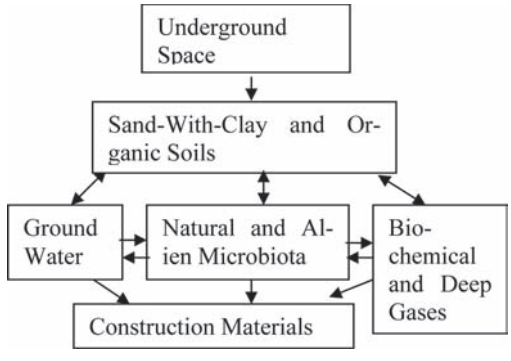

Figure 1. Underground space as a multi-component system.

In doing so, particular importance is ascribed to the influence rendered onto bearing structures by transformations of the major components of the underground environment as it is being contaminated.

The historic centre of Saint Petersburg and its cathedrals constructed in 18th–19th centuries are listed as World Cultural Heritage and have been protected by UNESCO since 1990.

The historic centre of Saint Petersburg is located in the main estuary part of the city on a low littoral terrace with absolute ground levels of 0,5 to 8 m.

The geological profile of the area features quaternary saturated sand-with-clay strata deposited during the glacial and postglacial periods of the Russian North-West. However, man-made and organic (swamp) deposits in the upper part of the profile, high occurrence of quick soils (littoral sands), thixotropic clay strata (glacial lake soils), technically reshaped moraine as well as fissured upper Wendian and lower Cambrian clays are of the highest significance for understanding the geotechnical conditions.

Thickness of Quaternary strata and location of the upper level of the bedrock clays depends on the depths to which ancient river beds cut into the bedrock clay deposits.

Geoenvironmental situation of the city's underground space is defined by a number of both natural and man-made factors. The authors' research has shown the adverse effect of swampy and peaty soils to extend down in excess of 25 m, as such soils

contribute fines of biogenic and abiogenous origin to the underlying strata. The swampy and peaty deposits contain various microflora such as bacteria, micromycetes, actinomycetes (ray fungi) *etc*, whose content, composition and quantities depend on the oxidation-reduction potential, acid-base conditions, presence of nutrient and energy substrata, underground environment temperature, as well as on the degree of decomposition of plant residues.

Maximum quantities of microorganisms are usually found in anaerobic environment at intermediate degrees of plant residue decomposition. The highest activity of microbiota is observed at pH = 6–9, ground water mineralization in excess of 1,0–1,5 g/l and when oxidized organic compounds are present. Anaerobic areas of swamps (redox potential, Eh < 0 mV) below 2 m usually contain ammonifying, sulphate-reducing, methane-generating groups over one hundred million cells per 1 g of material. The transition area (Eh from 0 mV to 50 mV) contains facultative types of denitrifying bacteria, while the weakly aerated areas develop nitrifying and Thiobacilli, producing, as it is well known, nitric and sulphuric acids, respectively. Aerobic environment is also characterized by micromycetes responsible for decomposing cellulose and lignin.

Sands in the upper areas under swamps in Saint Petersburg within the boundaries of the historic city centre are characterized by quicksand properties. Clay swampy soils formed in genetically restorative environment do not possess cementation bonds caused by Fe^{3+} compounds. Stiff moraine deposits formed in restorative environment under swamps in conditions of volumetric strains act as quasiplastic media with high lateral heave in any degree of consistency. Adsorption or adhesion of microorganism cells and their metabolic products forms films on clayey and silty soil particles, which leads to reduction of internal friction angle (down to $5–7^0$ and more) and thus predetermines plastic strains of soils. According to back analyses performed based on deep benchmarks in subsoils of certain structures, the modulus of deformatiothe moraines of restorative areas get reduced to values in excess of 3 MPa.

One of the important factors of environmental impact on underground space components and, correspondingly, on transformation of geotechnical conditions is contamination of underground environment through various sources whose action must be analysed historically.

A degree of adverse impact on underground space components is contributed by sewer leakages from dewatering systems, each millilitre of which contains up to $10^7–10^8$ microorganism cells. Those leakages provide an additional nutrient source for microbiota, because they contains compounds of nitrogen, sulphur, phosphorus, potassium, sodium, microelements, as well as such organic compounds as proteins, lipids, and carbohydrates which provide good nutrients for microorganisms. Additionally, it is necessary to consider the impact of the buried public waste depositories of 18th–19th centuries in the historic city centre, along with the effects rendered by liquidated cemeteries and burial grounds.

Permanent long-term deformations of a number of cathedrals of 18th–19th centuries are considered as a consequence of gradual deterioration of their subsoil bearing capacities brought about by a reduction of strength and the corresponding growth of deformability.

The present paper considers the geotechnical and geoenvironmental conditions in the subsoils of three Saint Petersburg cathedrals located within the boundaries of the historic city centre. Those include the first masonry city cathedral, viz. Peter and Paul, as well as Kazan and St. Isaac's Cathedrals.

2 SPECIFIC CONDITIONS OF DEFORMATION DEVELOPMENT AND GRADUAL DILAPIDATION OF PETER AND PAUL CATHEDRAL

Peter and Paul Cathedral, constructed in 1712–1733 according to a design by architect Domenico Tresini is the centrepiece of the architectural ensemble located on waterlogged Zayachiy Island (Fig. 2).

Building of Peter and Paul Cathedral on Zayachiy Island commenced with construction of foundation for the whole building right from the start. The belfry tower was constructed first, as instructed by Tsar Peter I, while construction of the cathedral as such started only four years later, viz. in 1716. As the masonry works for the walls began the belfry tower had not been finished yet and according to the archive materials its settlement was gradually developing.

Figure 2. Peter and Paul Cathedral of Saint Petersburg.

Deformations of the cathedral continued after its completion. As testified by historical records, 40 years into the cathedrals life cracks between the tower and the main buildings started to form (Трофимов, 1998). At the end of the 20th century the bearing walls of the cathedral had cracks opening from 1 to 3 mm and more. Currently repairs are being carried out to seal the cracks in the bearing structures of the cathedral.

Separate sections of the cathedral, such as the exterior walls, the colonnade and the belfry tower were constructed on different foundation types, embedded into the littoral sands and sands-with-clay characterized by presence of natural and man-made organic components. The colonnade and the belfry tower were constructed on slabs with square area of 4 m^2 and 12 m^2; the slabs were constructed of limestone and brick rubble masonry with limestone mortar. The exterior walls of the cathedral have a 4-m wide strip foundation of limestone rubblework.

Condition survey of the foundations of Peter and Paul Cathedral, conducted in the end of the 20th century revealed their unsatisfactory condition. In a number of locations the foundation had seepage of water coloured like watered down milk and containing calcium hydroxide, meaning that the mortar was being washed out and leaching of the limestone foundation slabs was ongoing. Content of alkaline-earth elements—Ca^{2+} and Mg^{2+}—in the ground water near the cathedral reaches 132 mg/l and 29 mg/l respectively (see Table 1).

Table 1. Chemical composition of ground water associated with Peter and Paul Cathedral.

		Borehole reference numbers	
Element	Unit	2501	2502
Ca^{2+}	mg/l	80.0	132.0
Mg^{2+}	mg/l	12.0	27.6
$K^+ + Na^+$	mg/l	11.5	147.2
NH_4^+	mg/l	2.6	1.9
SO_4^{2-}	mg/l	41.1	57.5
Cl^-	mg/l	35.4	226.9
HCO_3^-	mg/l	231.8	427.0
NO_3^-	mg/l	<0.45	0.5
NO_2^-	mg/l	0.022	0.032
Mineralization	mg/l	418.4	770.2
General hardness	mg-equ/l	5.8	7.6
$Fe^{2+} + Fe^{3+}$	mg/l	7.2	13.8
Permang. oxid. value	mgO_2/l	640	320
CO_2 agress	mg/l	44	132
pH*	–	74	71
Eh*	mV	–107	–94

Ground water contamination parameters are as follows: relatively high content of easily oxidizable organic matter—permanganate oxidability value reaches 64 mgO_2/l; increased chlorine content Cl^-—up to 226.9 mg/l; presence of aggressive carbonic acid CO_2 agress up to 19.8 mg/l; presence of deoxidized forms of sulphur as hydrogen sulphide; high content of fine organic suspensions (of biogenic and abiogenous origin) (see Table 1).

Negative values of oxidation-reduction potential is suggestive of anaerobic medium caused by oxidation of organic matter which results in breakages of cementation bonds in sand-with-clay strata and the corresponding strength reduction.

Mineralization of ground water is low and fluctuates, as observations suggest, within the range of 418–770.2 mg/l, which is because of the wash-through regime in the ground water on account of the island's small size and water fluctuation in the River Neva and the tributaries characterized by low mineralization, i.e. below 100 mg/l.

Sewer discharge occasions contamination and negative evolution of sand-with-clay properties rendering them as softer and less reliable in terms of bearing capacity. As mentioned above, sewer contents cause development of quick soil properties in sands on account of reduction in values of internal friction angle as colloid fractions of biogenous and abiogenous origin are adsorbed on to sand particles and marginally soluble biochemical gases, namely, methane and nitrogen, are generated.

Geotechnical definition of deformations of Peter and Paul Cathedral using strength parameters obtained from unconsolidated triaxial tests showed the load of structure ($p = 0.387$ MPa) to exceed the rated resistance of the subsoil ($R = 0.207$ MPa), defined for foundation width $b = 4$ m, toe level $h_f = 3.4$ m, cohesion $c = 0.015$ MPa and angle of internal friction for littoral sands $\varphi = 14°$. At $p > R$, subsoil is under the second stage of deformability (Gersevanov 1937, Puzyrevsky 1947, Dashko 1987), i.e. the shear stage (Gersevanov 1937, Dashko 1987), which explains the constant rate of the structure's deformations.

Calculated relative settlement differential for the bearing structures of the cathedral exceeds the reference values prescribed in the codes 6–12 times. The cracks provide an additional way for the microorganisms' deeper entry and growth in the walls and foundations of the buildings, on account of capillary rise of contaminated ground water.

Tests conducted Vlasov (2003, 2009) at Biology of Soils Department of St. Petersburg University confirmed a defining role played by microorganisms (micromycetes and bacteria) in integrity degradation of Peter and Paul Cathedral's construction materials. The samples studied revealed presence of 39 types of micromycetes,

among which the greatest diversity of species was identified for genus Penicillium (10 species). The most frequently encountered species was Cladosporium cladosporioides (81.25%) which possesses the highest corrosion activity. The predominant group also included active decomposers such as Aspergillus flavipes (28.13%) and Epococcum nigrum (34.38%). The majority of micromycetes identified in various samples of construction materials are classified as active decomposers of construction materials.

Microbiological studies conducted in 2009 identified a lower level of biological decomposers in construction materials of Peter and Paul Cathedral compared with 2003. This can be explained by the remedial measures and repairs aimed at reducing intensity of biological hazard in structures of the cathedral.

3 CONTEMPORARY STRUCTURAL CONDITION OF KAZAN CATHEDRAL

Kazan cathedral constructed in 1801–1811 according to a design by a Russian architect A.N. Voronikhin is one of the domed buildings of Saint Petersburg, with height of 71,6 m featuring unique interior granite pillars and an exterior colonnade of Pudost stone. The building has 136 exterior columns forming the outer colonnade and the portico, whereas construction of the 56 internal massive vault-bearing pillars, hewn of Serdobolsky granite, each weighing 28–30 tonnes and reaching 10,7 m in height, made the cathedral heavier and increased subsoil pressures to 0.2–0.25 MPa.

A piled foundation of Kazan Cathedral was constructed of over 18000 pine timber piles. The piles underneath the walls are 6.5-m long, reaching 8.0 m underneath the pillars. The capping structure of Kazan Cathedral is made of two courses of logs placed on top of each other in a criss-cross fashion. The underside of the capping structure is at the level of 5.0 m from the surface. The slab is constructed of granite blocks under the pillars and of limestone rubblework masonry under the walls. The raised plinth of the cathedral is lain of large block monoliths of grey Serdobolsky granite.

Kazan Cathedral is located on the bank of the River Krivusha (Griboedov Canal) in the northeast part of the Kazan Island within the boundary of the sloping part of the Neva paleovalley. The upper bedrock crusts, being the upper Kotlin Wendian clays, were found at 31–35 m and at 40 m from the ground level on the western and the eastern pats of the cathedral respectively (Fig. 3).

The profile of quaternary soils is represented by a complex mantle of saturated sand-with-clay deposits. Additionally the profile features a heavy

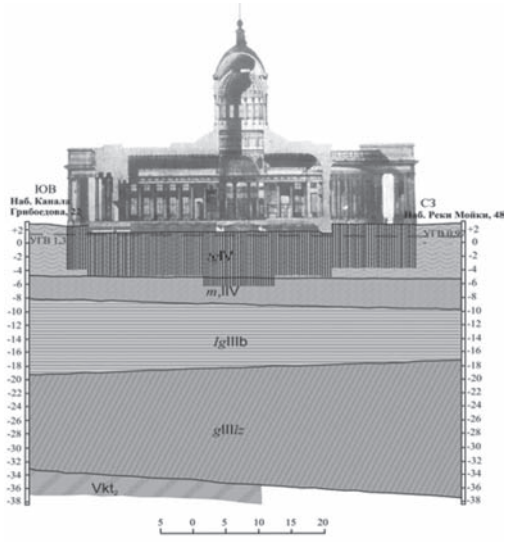

Figure 3. Geological profile of subsoil associated with Kazan Cathedral in Saint Petersburg.

Legend:

tgIV	tarmac
	made-up ground—gravelly sand, sand-with-clay with inclusions of brickwork rubble
mIV	medium density, medium-grain saturated sand
lgIII vd_3^b	light silty varved clay-with-sand
gIII vd_3^{lz}	soft silty clay-with-sand with gravel inclusions and sand lenses
Vkt_2	upper Kotlin Wendian clays

8 m stratum of made-up sands, which is related to removal of the 5-m thick stratum of swampy deposits. The piles have their toes embedded in made-up sands and littoral clays-with-sand containing natural and artificial organic matter.

Considering the proximity of Kazan Cathedral to Griboedov Canal in studying the building's current conditions one needs to bear in mind the specific technology of the canal and the quay construction, as well as preparation of the territory and quality of the construction materials. As mentioned above, the contemporary canal location is associated with a former river Glukhaya ('Krivusha'), which in 1748 was broadened and linked to the River Moika. The banks of Krivusha were low and in that particular area swampy and barely passable. The preparation of the site included removal of the swampy deposits and partially of the underlying soils, whereupon the level was raised by backfilling with high quality river sands. In the second half of the 18th century the soft soils were strengthened with organic compounds, such as ox blood and dynamic compaction.

The chemical composition of the ground water is demonstrative of contamination with sewage and oil related compounds (see Table 2).

The following contamination features can be noted: an increased degree of ammonium NH_4^+ (up to 7 mg/l), chlorine ion Cl^- (up to 785.9 mg/l), presence of sulphates SO_4^{2-} (up to 76.8 mg/l), presence of aggressive carbonic acid (CO_2 agress) (up to 15.4 mg/l) and presence of easily oxidizable organic matter—permanganate oxidability value reaches 17.6 mg O_2/l. High degree of ground water mineralization, reaching 2303.3 mg/l is a consequence of a high degree of contamination and hydrodynamic congestion. Ground water has an increased content of calcium (up to 248.5 mg/l) and magnesium (up to 126.5 mg/l), which is uncharacteristic for the ground water in the city, and is suggestive of leaching of limestone and limestone-based mortar from the foundation rubblework masonry. Ground water is diluted during floods when the water level in Griboedov Canal is above the groundwater level. Mineralization of water in Griboedov Canal does not exceed 200 mg/l. Evolution of soil properties in the upper part of the geological profile associated with Kazan Cathedral went on in reducing medium underneath swampy deposits, which resulted in soil enrichment with organic remains of biogenic and abiogenous origin and the corresponding strength reduction.

Major man-made sources of contamination of ground water and sand-with-clay subsoils of Kazan Cathedral can be divided into two main categories: long-term historical and contemporary. The former include the imperfect historical dewatering system (timber sewage collectors and septic tanks) and disposal of household waste leading to contamination of the surrounding and the underlying soil strata down to a considerable depth. The latter group of contaminating factors includes unsatisfactory condition of the active dewatering system, raw sewage discharge from outlets located on the side of Griboedov Canal (on the eastern side of the cathedral) and oil-related products from the nearby Nevsky Avenue.

Table 2. Chemical composition of ground water associated with Kazan cathedral.

Element	Unit	2003	2004
Ca^{2+}	mg/l	96.2	248.5
Mg^{2+}	mg/l	19.5	126.5
$K^+ + Na^+$	mg/l	568.1	301.3
NH_4^+	mg/l	2.0	7.0
SO_4^{2-}	mg/l	76.8	38.4
Cl^-	mg/l	785.9	775.6
HCO_3^{2-}	mg/l	451.5	811.5
Mineralization	mg/l	2001	2303,3
Permang. oxid. value	mgO_2/l	n/a	17.6
CO_2 agress	mg/l	15.4	15.2
pH	n/a	7.04	7.16

Biotic contamination of saturated subsoils leads to formation of hydrogen sulphide traces of which were identified below the ground water level. Hydrogen sulphide generation is derivative from activity of sulphate-reducing bacteria, common in the subterranean environment of Saint Petersburg. In reduction conditions, formation of hydrogen sulphide and bivalent iron is accompanied by generation of hydrotrolite $FeS*nH_2O$ in the form of black and dark grey powder which was found throughout the upper strata down to the moraine deposits of the aquiclude.

Thermal impact from a heating main running alongside the cathedral's perimeter is conducive to increased rates of physiochemical and biochemical activity, growth of microorganisms and gas-saturation of soils, which provoke gas and mud outbreaks, one of which was registered during works on a fountain construction in front of the cathedral.

Dynamic ground water regime in the subsoil leads to an additional deterioration of mechanical soil parameters. The ground water regime in the colonnade subsoil adjacent to Griboedov Canal is additionally affected by water level fluctuations in surface water flow, whereas the subsoil of the other half of the colonnade is not so affected. It needs to be noted that the highest deformation values are registered for the colonnade adjacent to Griboedov Canal. The bearing structures of Kazan Cathedral are affected by differential and long-term deformations, whereby cracks in the in cast iron column bases begin to form.

Progress of deformations of Kazan Cathedral is confirmed by surveying 29 deformation reference points mounted on the cathedral's superstructure. The highest absolute settlement values were observed on the eastern colonnade (on the side of Griboedov Canal), varying between 115 and 128 mm (based on the late 20th century surveying). Relative differential settlement between the colonnade and the main building is geodetically and numerically proved to have exceeded the permissible levels prescribed in the codes. It should be borne in mind that the eastern part of the colonnade is also affected by differential deformations.

4 GEOTECHNICAL AND GEOENVIRONMENTAL ANALYSIS OF DEFORMATIONS OF ST. ISAAC'S CATHEDRAL

Construction of St. Isaac's Cathedral commenced in 1768 according to a design by an Italian architect Antonio Rinaldi. This cathedral could have become

the finest Rinaldiesque structure ever built, however the architect had been unable to complete the work and the construction was brought to completion in 1802 by another Italian architect, V. Brenna, who reduced the building's size and dispensed with the minor domes. The resulting structure proved to be a low, squat building—quite out of concord with the celebrity looks of central Saint Petersburg, which made it necessary to rebuild the cathedral already in 1809, whereby a part of Rinaldiesque foundations was retained, as decreed by Tsar Alexander I. In 1825, with multiple amendments, a design by a French architect Auguste de Montferrand was ratified. That design envisaged to preserve foundations for the alter and the dome pillars in the western section. The new building had been designed to increase only in length, its width being retained.

Construction of the new foundations commenced with excavating a 5-m pit and driving of pine timber piles of 26 cm diameter and lengths of 6.4 m and 10.7 m. The overall number of piles reached 10762. Looking to save resources, Montferrand decided to use 13000 piles from the previous cathedral by A. Rinaldi. The lengths of piles were 10.5 m under the columns and 8.4 m elsewhere. Thus, the total number of piles used for the construction of St. Isaac's Cathedral was 24000. The piles have their toes embedded into soft littoral and lacustrine-glacial soils and are assumed as being friction piles.

Underneath the bearing structures and the corners of the building its foundation was constructed of massive granite slabs, alternating with courses of rubblework limestone masonry, the latter solution used for the foundations in the remainder of the building. A massive 2-m height of the foundation slab was raised above the ground level. In the 7.5-m thick body of the foundation 2.5-m by 2.5 m galleries were constructed. Construction of the cathedral was completed in 1841, requing further a span of 17 years to decorate the interior. The cathedral was consecrated in 1858. The overall length of the cathedral with porticoes is 102 m, its width is 92 m, and its weight amounts to 320 thousand tonnes, of which 100 thousand tonnes is the massive foundation masonry. St. Isaac's Cathedral is the heaviest building in Saint Petersburg.

Considering long-term stability of St. Isaac's Cathedral one needs to take into account geotechnical and geoenvironmental specificity of its subsoil. The Cathedral was constructed above the low littoral terrace and is located in the area of the left slope of the deep subterranean valley of the Neva River.

The geological profile and the geotechnical parameters of St. Isaac's subsoil were obtained only in 1954 (Fig. 4), when four 50-m deep boreholes were drilled. In 55 years, in 2009, those were followed by four additional boreholes along the cathedral's perimeter, two boreholes down to 50 m, and two down to 20 m. Static penetration test was also carried out during which the probe was being sunk into lacustrine-glacial and moraine deposits.

Bedrock clay on the sloping part of the subterranean valley was found in the south-west area o St. Isaac's Cathedral at the level of 44.5 m, corresponding to results of 1954 condition survey. In the northerly direction towards the thalweg the upper crust of bedrock goes down while the thickness of the quaternary sand-with-clay deposits increases proportionally reaching the level of 65 m, which means that the overall thickness of quaternary strata within the footprint of the cathedral varies within the range of 20–25 m, which is of ultimate importance for establishing conditions of settlement differential progress.

The quaternary strata include inter-moraine, glacial, lake-glacial, and lake-marine (littoral) formations, overlain by man-made deposits. The upper part of the profile features inclusions of pure peat or peated strata (Fig. 4).

The ground water level was found to be at 1.8–2.0 m from the surface. Contrastive analyses of

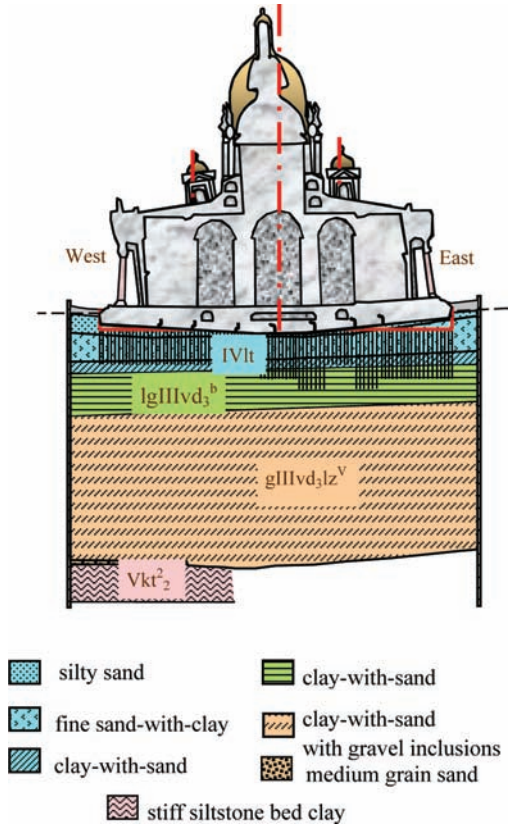

Figure 4. Geological profile of St. Isaac's subsoil.

ground water chemical compositions for 1954 and 2009 show the 55-year span to have been influential in causing a considerable and irreversible chemical changes occasioned by leakages from the dewatering circuit around the cathedral (see Table 3).

In 2005 there was a sewage leakage from the regional sewer collector laid near the south-east part of the cathedral, causing maximum values of ground water mineralization.

High contents of sulphur (81.8 mg/l), chlorides (1418 mg/l), and the permanganate oxidability value (3128 mgO_2/l) are indicative of contamination with sewage. Over the 55-year period the share of calcium ions grew considerably. Increased amounts of calcium (to 560.1 mg/l) and magnesium (up to 55.3 mg/l) in the samples, uncharacteristic for the ground water in the city, are suggestive of leaching of limestone and limestone-based mortar from the foundation slab sections located below the ground water level.

The value of oxidation-reduction potential Eh, measured directly in situ from boreholes is reduced to –100 mV, which means a reduction environment is forming due to oxidation of organic matter (see Table 3, based on 2009 testing).

Littoral sand-with-clay and lacustrine-glacial clay-with-sand in the subsoil of the cathedral are of fluid or, more rarely, fluid-to-plastic consistency, their natural moisture is within 34 to 51%. Sandy littoral deposits underneath the cathedral possess well pronounced quick soil properties. Water permeability of sands reduces to 10^{-3}–10^{-4} m/day, which is typical for clays. In such soils friction parameter is usually twice reduced.

Clay soils possess manifest thixotropic properties and low strength parameters (φ = 0–5°, c = 0.015–0.025 MPa). Soils underneath St. Isaac's Cathedral have low strength values generally specific to the city centre. Comparison of shear test results obtained in 1954 and 2009 for lacustrine-glacial and moraine deposits revealed a reduction in shear strength in excess of 30% due to increased microbe mass (MM).

Table 3. Chemical composition of ground water in subsoil of St. Isaac's Cathedral.

Analyzed components	Unit	Values
Ca^{2+}	mg/l	89.8–560.1
Mg^{2+}	mg/l	29–55.3
$K^+ + Na^+$	mg/l	10.2–816
NH_4^+	mg/l	0.10–5.0
SO_4^{2-}	mg/l	2–81.4
Cl^-	mg/l	53.2–1418
HCO_3^{2-}	mg/l	42.7–1572
NO_3^-	mg/l	0.5–2.2
Mineralization	mg/l	994–4733
Permang. oxid. value	mgO_2/l	11.5–3128
pH*	–	8.6–9.2
Eh*	mV	–108*

Subsoil of St. Isaac's Cathedral is highly contaminated with organic compounds and microbiota, arriving from a faulty sewer located along the cathedral perimeter; there is a high degree of microbiosis.

The values of MM, defined based on Bradford method is highly variable: in littoral sands of the subsoil the MM fluctuates from 39 to 70 mkg/g, in lacustrine-glacial clay-with-sand and laminated clay—from 135 to 511 mkg/g, in moraine clay-with-sand—between 56 and 85 mkg/g, in inter-moraine deposits—210–294 mkg/g, in bedrock Wendian clays—from 186 to 690 mkg/g. High values of microbe proteins are associated with the investigated clay strata—clay inclusions in laminated clays and the bedrock Wendian clays.

Microbiosis is found also in the foundation materials. Analyzed timber from depths 2.5 and 3.0 m identified 8 types of micromycetes known for their destructive effects on various substances. Micromycetes were identified only in the upper part of the profile at 2.5 m. This is because of the deep anaerobic properties in the cathedral's subsoil, in which micromycetes cannot thrive. In timber samples 8 types of microscopic destructive fungi were found, with predominance of two species of *Penicillium*.

St. Issac's Cathedral has been causing stability concerns fro many decades. Throughout the entire period of its life superficial repair works have been conducted. Surveying of basement walls conducted in 1927 identified settlement increase directed from east to west in the northern and the southern corridors. Likewise, surveying of the masonry courses underlying the four dome pillars identified settlement progress directed from north-west to south-east. In 1927, east to west deflection of the globe underneath the cross was registered to have reached 270 mm.

In 1983 a survey of the adjacent city territory revealed a settlement trough and heaving of soil around the cathedral, the highest surface level differential reaching 0.85 m.

Heaving of soil is normally observed in materials with low lithification degree and with shallow foundations. For St. Isaac's Cathedral relative depth of the capping slab

$$\frac{h_\phi}{b} \tag{1}$$

where h_ϕ-the underside of foundation slab being 5 m, b-width of foundation being 92 m) is only 0.054. In case of a shallow foundation there is intensive squeezing of soft soil in conditions of either no or low seepage related consolidation in the cathedral's subsoil.

Currently progress of differential settlement has intensified causing cracks to open in the bearing dome pillars, tilting of porticoes, deformation and dilapidation of the columns, and more recently also formation of cracks in the columns.

The settlement calculations for St. Isaac's Cathedral demonstrated the maximum settlement (S) from the structure's pressure (p_c), disregarding foundation embedment, to be 1.43 m, whereas with account of foundation embedment that value reached 0.99 m (linearly strained model). The settlement share at the stage of plastic deformation development reached 1.46 m.

Stability of the building is mostly ensured by thickness of its walls (5.0 m) and the massive 7.5 m capping slab.

In future it will be necessary to carry out further tests to establish condition of the timber piles and the consolidation degree of the soft saturated clays below the piled foundation. It is recommended to drill 25–30 m deep boreholes at the angle of 62–63°, in the north-east and the south-west of St. Isaac's Cathedral.

Geotechnical and geoenvironmental analysis of the subsoil of St. Isaac's Cathedral allows to presume a further reduction of its bearing capacity, due, among other things, to its active contamination in conditions of steadfastly adverse geoenvironmental conditions of the underground space.

5 CONCLUSION

Any predictions of long-term stability and safety of the old 18th–19th century cathedrals in complicated geotechnical and geoenvironmental conditions of Saint Petersburg's historic centre, taking into account the specific *in situ* properties, as well as the character and the degree of contamination of the underground environment must be based on permanent complex monitoring. Such monitoring must include deformation surveying, as well as monitoring of the geotechnical and the geoenvironmental factors in conditions of reconsolidating soils and increasing aggressive potential of the underground environment with respect to the masonry on foundations, basements and walls. Complex monitoring must include a system of constant long-term observation of the underground space components (soils, ground water, microorganisms, gases and the underground bearing structures of the cathedrals). Such system of monitoring has been created for each cathedral dealt with in the present paper with account of their specific geotechnical and geoenvironmental conditions, as well as of the nature and intensity of their deformations.

Results of such monitoring will be instrumental in introducing immediate alterations to restoration and reconstruction designs, as well as in ensuring long-term stability of the cathedrals. It should be noted that in reconstruction schemes for the above cathedrals special bioresistant and biostable materials must be used to resist adverse effects of the aggressive underground environment.

3-D models of the cathedrals must be built based on laser scanning, and a methodology developed for their complex geodetic survey and setting out, bearing in mind the specific nature of these monuments' deformations. This methodology should be linked to the actual conditions of soils, foundations and ground water associated with the buildings.

Additionally, specific regulations on restriction zones around the cathedrals should be drafted and ratified, within which zones no construction works may be permitted, most certainly no bulk excavations even if carried out in sparing working regimes; also, the restrictions should include dynamic impact generated by public transport, which may contribute to soil liquefaction at certain vibration amplitudes.

REFERENCES

Butikov, G.P. 1993. *St. Issac's Cathedral*. Leningrad: AO Smart.

Dashko, R.E., Aleksandrova, Yu, O. Kotukov, P.V. & Shidlovskaya, A.V. 2011. The peculiarities of engineering geological conditions of Saint-Petersburg. *Development of urban areas and geotechnical engineering-№* 13–C. 24–71.

Dashko, R.E., Aleksandrova, Yu, O. & Shidlovskaya, A.V. 2004. The role of microbiota in engineering geology: history and experimental results. In Sergeevskie chteniya volume 6: 48–52.

Dashko, R.E. 2011. Microbiota in underground space: role and consequences. *Environmental Geosciences and Engineering Survey for Territory Protection and Population safety; International conference EngeoPro-2011, Moscow, 6–8 September 2011*: 517–521. Moscow.

Dashko, R.E., Alexandrova, Yu, O. & Shidlovskaya, A.V. 2011. *Geotechnical Assesment of Bed clays as Foundation and unique constructions projects in Saint-Petersburg*. International conference EngeoPro-2011 Environmental Geosciences and Engineering Survey for Territory Protection and Population safety. Moscow, pp. 521–525.

Dashko, A.V., Shidlovskaya, A.V. Aleksandrova, Yu, O. 2010. The analyses of some architectural and historical monuments of Saint-Petersburg with geotechnical and geoenvironmental positions. Geotechnical problems of megapolis; The international conference, Moscow, 7–10 June. Saint-Petersburg: PI "Georeconstruction": 1595–1602.

Trofimov, S.V. 1998. *Peter and Paul cathedral*. Saint-Petersburg: White and black.

Geotechnical Engineering for the Preservation of Monuments and Historic Sites – Bilotta, Flora, Lirer & Viggiani (eds)
© 2013 Taylor & Francis Group, London, ISBN 978-1-138-00055-1

A study for the requalification and safety against natural hazards of the environmental and building heritage of Sant'Agata de' Goti (Italy)

F. de Silva, M. Melillo, D. Calcaterra, F. Fascia, A. Scotto di Santolo & F. Silvestri
Università di Napoli Federico II, Napoli, Italy

L. Stendardo
Università di Padova, Padova, Italy

ABSTRACT: The historical center of Sant'Agata de' Goti (Campania region, Italy) is located on a steep and narrow cliff of pyroclastic soils and rocks, overlying a thick Miocene flysch formation, which makes it particularly sensitive to both landslide and seismic hazards. The paper describes the subsoil characterization and two urban design proposals submitted to the town municipality by a multi-disciplinary research team. The first proposal deals with the environmental requalification of a cliff side, by assessing the stability of the overlooking cavities and by reshaping and consolidating the rock slope through reinforced earth and nailing. The second one includes a site-specific evaluation of seismic response, addressed to verify the seismic safety of the foundations of a masonry historical building.

1 INTRODUCTION

The progressive transformation from the protection of single monuments to that of the whole fabric of ancient cities, proclaimed by the Venice Charter (ICOMOS, 1964), brought the Geotechnical Engineering to a central role in the conservation of historical centers, for which a clearly defined limit between natural and building heritage does not exist.

The town of Sant'Agata de' Goti, located in Campania region (Italy), was built during the pre-Roman period. It was edified on a tuff cliff between two creeks, Riello and Martorano (Fig. 1), in order to give more chance to safeguard populations from attacks and invasions.

Such strategic location, however, increased the vulnerability of the center towards both landslide and seismic risk, as occurred for other small towns located on soft rock slabs or stiff soil ridges in Central-Southern Italy.

A comparative analysis of several case histories of such a kind was shown for instance by Fenelli et al. (1998), in a previous edition of this Symposium, highlighting the strong influence of the valley erosion on the slope stability and/or subsidence of the cliffs; later, Costanzo et al. (2007) evidenced that most of the high degree of seismic vulnerability of such towns results from site amplification due to both ground morphology and subsoil conditions.

Figure 1. Aerial view of Sant'Agata dei Goti.

As a result, the need for the safe fruition of the whole center and of single buildings requires both urban and architectonic plans to account for the multi-hazard complexity.

The paper summarizes the subsoil characterization of the cliff of Sant'Agata de' Goti, as reconstructed from the gathering of existing geological (§ 2.1) and geotechnical (§ 2.2) investigations, aiming at different urban design proposals which have been recently submitted to the town municipality by a multi-disciplinary research team of the University of Napoli Federico II.

In detail, they involve the stability assessment of the anthropic cavities (§ 3) and the design of an urban park along the slope facing the Martorano

creek (§ 4), as well as the seismic safety of the foundations of a historical masonry building (§ 5).

The above themes will be developed as prototype studies, highlighting the need for an interdisciplinary action strategy, which must be viewed as environmentally sustainable, in order to represent an equilibrium between the safe fruition and the conservation of the historical heritage of Sant'Agata de' Goti.

2 SUBSOIL CONDITIONS

2.1 *Geological setting*

The historical center of Sant'Agata rests on the flat summit of a N-S oriented elliptical ridge (Fig. 2a), about 170 m wide and 600 m long, delimited by subvertical cliffs as high as 50 m. Downhill, the valleys of the Riello and Martorano creeks lie to the east and west of the ridge, respectively.

The relative bedrock of Sant'Agata hill is formed by the Campanian Ignimbrite, a volcaniclastic formation erupted in the Campi Flegrei about 39,000 yrs BP (De Vivo et al. 2001), which represents the product of the main explosive episode in the Mediterranean region during the Quaternary (Barberi et al., 1978).

Following Cappelletti et al. (2003), in the Campanian Ignimbrite two main lithofacies can be recognized (Fig. 2b):

– a lowermost welded grey ash deposit (Welded Grey Ignimbrite, WGI), consisting of black scoriae dispersed in an ashy matrix, with subordinate lithics and crystals. WGI, which was feldspathized by authigenic mineralization processes, shows variable welding, both vertically and laterally;
– an uppermost yellow and lithified deposit (Lithified Yellow Tuff, LYT) made up of an ashy matrix with rounded lapilli to dispersed block pumice clasts. LYT has been affected by zeolitization processes, responsible for the typical yellow colour of the unit.

Both LYT and, to a lesser extent, WGI are affected by high-angle, intersecting joint systems, forming rock columns or slabs (Fig. 2c).

The Ignimbrite formation is covered by a few metres of pyroclastic soils and made ground (mg-Ps); at the bottom, below a thin layer of loose pyroclastic deposits, a Miocene flysch formation of significant yet uncertain thickness is present, constituted by arenaceous-clayey sediments.

Most of the buildings of the historical center are founded on the shallow cover, or directly on the LYT, which is characterized by the presence of 160 anthropic cavities detected insofar, many of which are located close to the ridge edge (Fig. 2a).

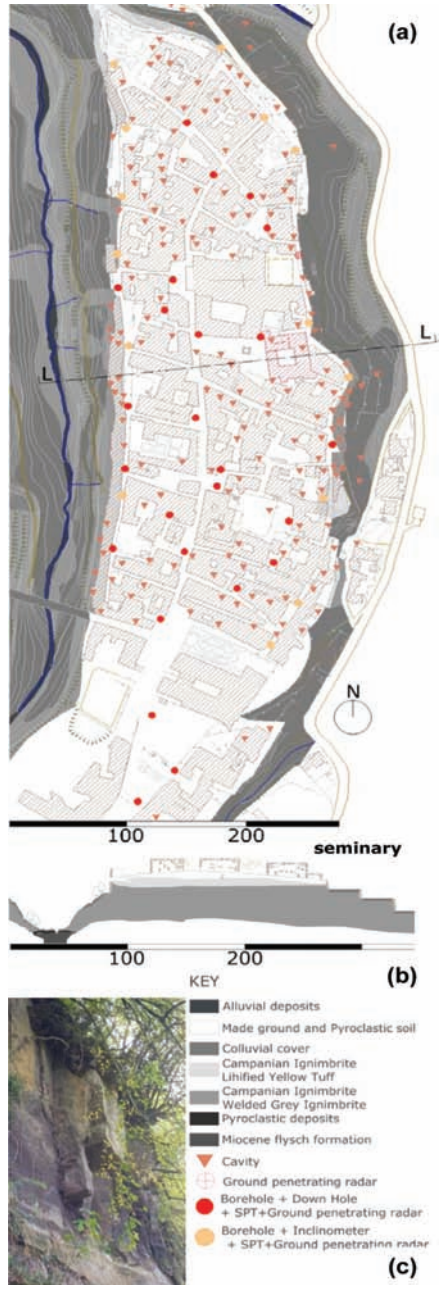

Figure 2. Geological map showing the location of site investigations (a); L-L stratigraphic section (b); picture showing the layering of the cliff (c).

Pervasive high-angle jointing, along with the continuous gully erosion, are the main predisposing factors to the instability of the tuff cliffs, which are affected by a variety of mass movements. According to Cruden & Varnes (1996), falls, topples and

slides favour the cliff retreat. Slides can occur due to the intersection of the columnar joints with low-angle (30° to 45°) minor discontinuities.

Significant seismic amplification phenomena are expected, especially along the ridge edges, due to the topographic irregularity and to the stratigraphic amplification of the seismic waves in the softer shallow soils. As a result, the interplay between seismic and landslide hazards might be considered high throughout the whole center, but it might become particularly critical along the ridge rims, where the interaction between buildings and cavities is significantly intense.

2.2 *Geotechnical and geophysical investigations*

In previous years, the subsoil of Sant'Agata dei Goti was intensely investigated in three main stages.

In 1991, a first survey was addressed to the short-term stabilization of the north-eastern part of the tuff rock cliff. In 1994, a comprehensive subsoil investigation was extended to the whole historical center: it consisted of 40 boreholes drilled down to 40 m, which never reached the Miocene formation underlying the pyroclastic rock slab. Geophysical investigations consisting of georadar measurements and Down-Hole tests with measurement of P and S wave velocity, V_P and V_S, were executed along most of the verticals; inclinometers were installed in those boreholes located close to the ridges (see Fig. 2a).

Unit weight, γ, and uniaxial compression strength, σ_c, were measured on 21 samples mostly extracted from the LYT formation, while the WGI was characterized essentially on the basis of SPT tests, due to its lower degree of cementation.

The investigation led to an overall analysis of the stability conditions of the cavities, as well as to the execution of stabilization works along the western cliff: these latter mainly consisted of rock bolts and micropiles, along with shallow covers of spritz beton mixed with tuff fragments to minimize the environmental impact.

The above works required the realization of a service road located at mid-elevation of the cliff, which later showed instability phenomena involving the colluvial covers for a depth of 5 m, as resulting from boreholes drilled within the first 10 m along the pathway. Since 2001 to 2008, these episodes required further stabilization measures, consisting of shallow drainage treatments through root canals, and structural works such as concrete gravity walls, piled slabs and a sheet pile wall.

In 2008, a further campaign addressed to town planning was carried out in several sites outside the historical center, where the Miocene formation crops out. The investigation included shallow seismic refraction surveys and MASW tests, as well as penetration and Down-Hole tests carried out in four boreholes drilled down to 30 m.

3 THE SYSTEM OF CAVITIES

The 160 hypogean quarries detected in the historical center of Sant'Agata (see Fig. 2a) were constructed for extraction purposes and utilized prevalently as storage. They were excavated in the Lithified Yellow Tuff (LYT) at shallow depths from the ground level, with a significant interaction with the superstructures (Fig. 3a), and therefore they represent a permanent risk for people and properties.

The highest degree of risk affects the western cliff, where 19 cavities directly overlook the Martorano valley (Fig. 3b). They correspond to 55 ambients, about 70% of which constituted by rooms and the remaining by stairwells (Fig. 3c) or tunnels.

In order to preliminarily assess the overall degree of instability hazard for such cavities, in this work two simplified approaches—empirical and rational—were utilized. Both methods refer to geometrical parameters of the cavity and to the rock mass characterization, based on the intact rock strength, the properties of the jointing systems and the groundwater conditions, obtained by laboratory and in situ investigations. A characteristic value of the uniaxial compression strength $\sigma_c = 3.6$ MPa was assumed on the basis of the laboratory tests, while

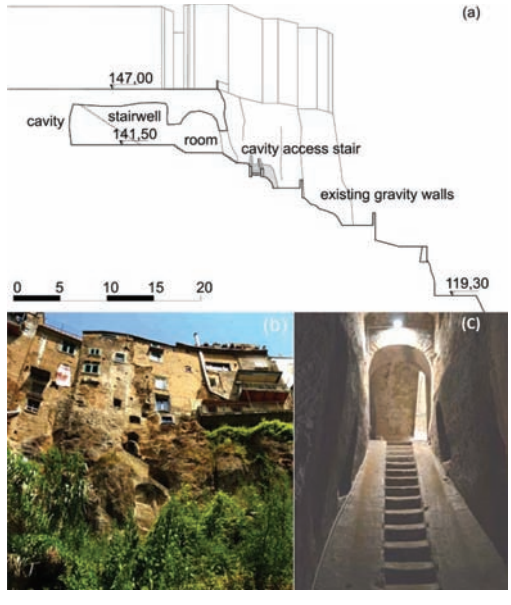

Figure 3. Typical cavity section (a, F-F in Fig. 6) and view (b) along Martorano slope; an internal stairwell (c).

the other parameters were defined from the above mentioned investigations. In applying both methods, only the collapse mechanism of the cavity roof was considered.

The empirical method by Barton et al. (1974) requires the definition of the rock mass quality, Q:

$$Q = \frac{RQD}{J_n} \cdot \frac{J_r}{J_a} \cdot \frac{J_w}{SRF} \quad (1)$$

as a product of three ground parameters, which can be thought as crude measures of:

- relative block size (RQD/J_n), being RQD the rock quality designation, and J_n the joint set number;
- inter-block shear strength (J_r/J_a), representing the roughness and friction of the joint walls with or without filling materials;
- active stresses (J_w/SRF), where J_w is a joint water reduction factor, and SRF is a stress reduction factor.

The method permits to assess the stability and support requirements of underground excavations by means of a 'Q support chart', relating the Q value to an equivalent dimension, D_e, of the excavation:

$$D_e = \frac{span}{ESR} \quad (2)$$

defined as the ratio between the excavation span, L, or height, H (in m), and the excavation support ratio, ESR, related to the intended use of the excavation and to the degree of security required. The supporting categories vary from spot to systematic bolting, with or without fiber reinforced shotcrete with variable thickness, until cast concrete lining.

A modified version of this chart is drawn in Fig 4, where the data related to the surveyed cavities have been reported. It can be observed that about 46% of the cavity ambients require reinforcement works, which can consist mainly of systematic bolting spaced 1 to 2 m and shotcrete thick 5 to 10 cm.

The rational criterion adopted to estimate the safety of the roofs was that proposed by Evangelista et al. (2002) and modified by Federico & Screpanti (2002). Each cavity was simplified into a single rectangular chamber of length L, with the vault consisting of a tuff slab of thickness t, subjected to an uniform vertical stress q, due to the self-weight and the overburden soil (Fig. 5a). The tuff was considered as a rigid-plastic material obeying to the Mohr-Coulomb failure criterion. The condition of failure can be estimated by analyzing the limit equilibrium of the vault, due to either shear sliding or flexural rotation. The above referenced analytical solutions permit to evaluate

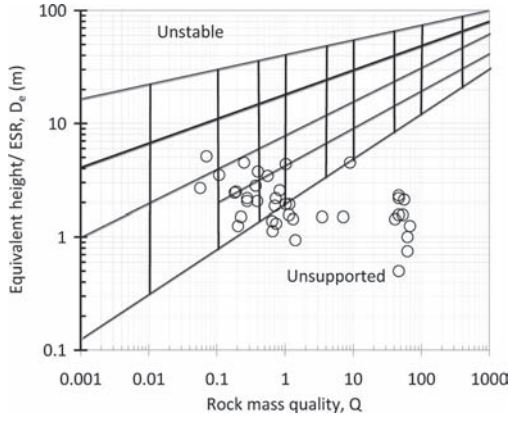

Figure 4. The Q support chart (modified from Barton et al., 1974) with the stability assessment of the cavity ambients considered in this study.

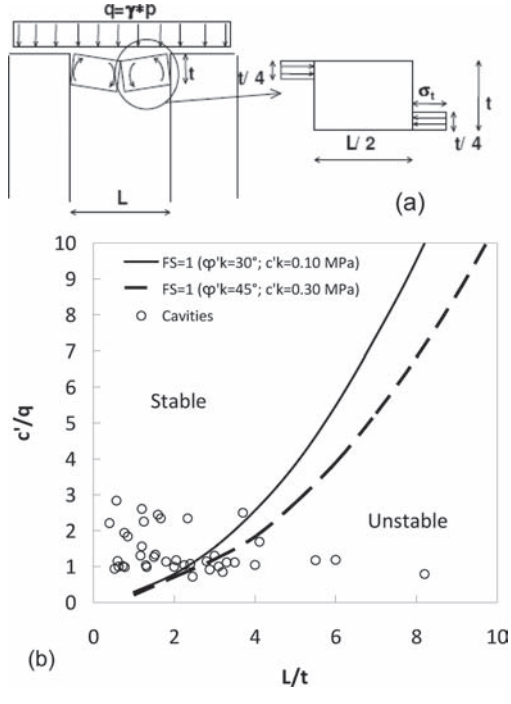

Figure 5. Limit equilibrium of cavity roof (a) and stability conditions of the ambients verified with the rational method (b).

the critical length, L_c, of the roof corresponding to the triggering of failure, and to obtain the safety factor, SF, of the cavity as the ratio between this length and that measured ($SF = L_c/L$).

The results obtained for the investigated cavities are plotted with hollow circles in Fig. 5b, in terms of slenderness of the roof slab, L/t, versus the c'/q ratio.

The curves on the graph represent the relationships between the dimensionless variables at limiting equilibrium condition ($SF = 1$) for the upper and lower bound of the characteristic strength parameters, as evaluated for the least ($c'_k = 0.3$ MPa and $\varphi'_k = 45°$, dashed line) and the most fractured rock mass ($c'_k = 0.1$ MPa and $\varphi'_k = 30°$, solid line). The above strength values resepectively imply that about 72% or 62% of the cavities are stable, with 60% of them having $SF > 1.2$.

4 ENVIRONMENTAL REQUALIFICATION OF THE CLIFF

The first project proposal is the environmental requalification of the western cliff side, facing to the Martorano creek, by reshaping the rock slope overlooking the creek valley. The basic idea is to transform it into an urban green park (Fig. 6), in which the cavities should be integrated as connective terminals with the historical center (Melillo, 2012).

The design objectives are highlighted by the park access system. The Northern gate, from the existing town gardens, should reproduce the ancient village access of Medieval age, while the Southern gate should develop along an existing climbing stair-path close to the Vittorio Emanuele III bridge. Four intermediate upper gates might be created through the cavities accessible from the western panoramic street of the historical center: they might be connected to the town through the internal stairwells and to the cliff by external stair-paths.

The design of the Northern gate, characterized by the highest altitude gap, involves intensive slope stabilization works, such as reclaiming the colluvial covers and creating slope terraces where the loose soil is present, while rock slope nailing is envisaged where the tuff crops out (Fig. 7).

The current service road will represent the downhill boundary of the park, and will be linked to the terraces through a pedestrian path. The inter-terrace gaps will be connected through stair ramps, either made with reinforced earth or directly excavated in the tuff. These works should be integrated with wicker grids along the pathways and the reinforcement of the existing walls where necessary.

5 SEISMIC SAFETY OF A HISTORICAL BUILDING

The second project proposal deals with the ancient seminar and its church, a typical brickwork three-storey building located at the eastern border of the historic centre, and again surrounded by a network of cavities. It is an isolated courtyard house, with an approximately square plan extending to about 1300 m^2 (Fig. 8). The bearing walls are made up of squared tuff blocks, except for the hypogeous basement, probably older, where the blocks are roughly cut. During the 20th century, all the floors

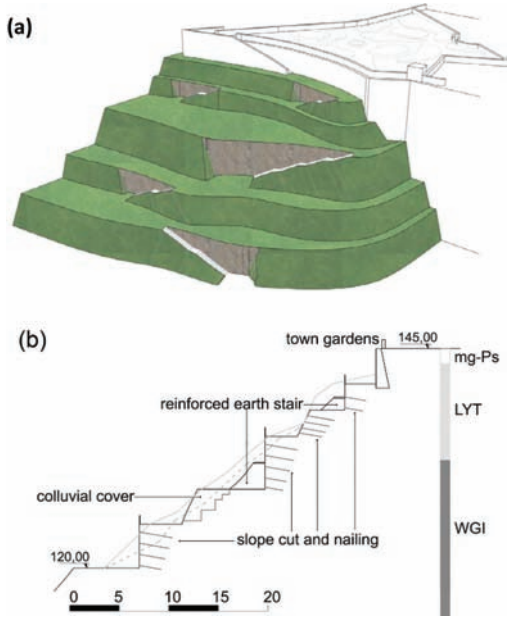

Figure 7. Assonometric view (a) and section (b), B-B in Fig. 6) of the reshaping and reinforcement of the slope.

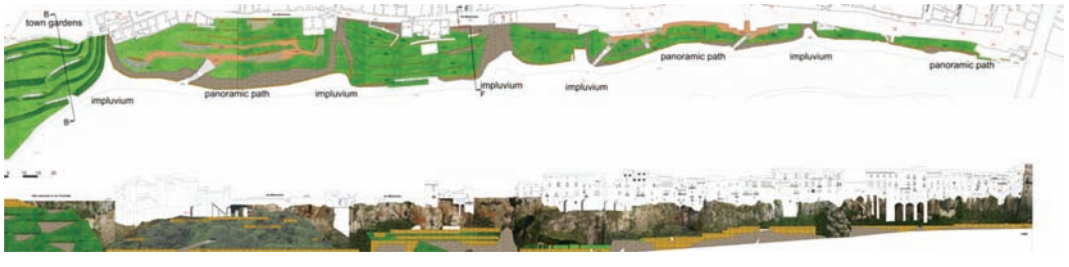

Figure 6. Plan (up) and view (down) of the design proposal for the environmental requalification of the Martorano cliff.

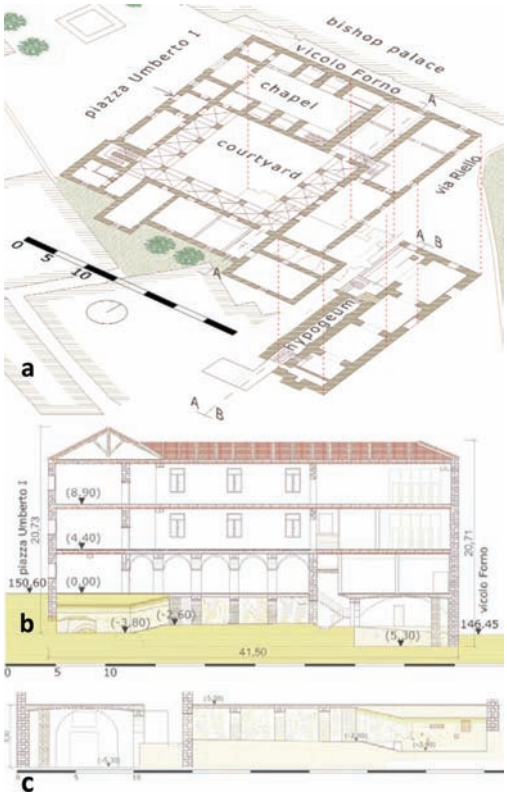

Figure 8. Plan/assonometric view (a), representative section (b), detail of the hypogeous space (c) of the seminar building.

have been rebuilt in poutrelles and perforated bricks, except for the first floor and part of the second floor, where the original brick vaults and two wooden floors have been left. The original wooden trusses support the pitched tile roof.

Since the date of its construction, 1344, to the mid-1600s, the building housed the monks of Montevergine; it was razed during the 1688 earthquake and rebuilt in its present form by the bishop S. Alfonso M. de' Liguori. Since the mid-1700's to the mid-1900's it housed the seminary and then the grammar school.

The ground floor hosts a chapel, the kitchens and further common spaces, the second floor includes the classrooms and on the third floor the dormitory for the seminarians was located. The building, forsaken in 2006, is still empty; however the town municipality is considering its reclamation, to find a new function compatible with both the architectural framework and the structural capacity, which might be for instance a specialistic school for youth.

In this study, a site-specific evaluation of seismic response (§ 5.1) was addressed to quantify the seismic actions on the building, required to assess its safety and to support future interventions for the retrofitting of structure and foundations (§ 5.2).

5.1 *Seismic response analysis*

Figure 9 shows the location of the town in the National seismic hazard map (MPS working group, 2004), drawn in terms of median peak ground acceleration, a_g, expected on a reference stiff rock outcrop with a return period of 475 yrs. A value of $a_g = 0.16$ g is returned for S. Agata de'Goti.

The disaggregation map annexed to the MPS (Spallarossa & Barani, 2007) and the Rexel code (Iervolino et al., 2009) permitted to extract a set of 7 spectrum-compatible accelerograms recorded by italian seismic stations on stiff rock outcrop, i.e. a soil class 'A' according to the National Technical Code (NTC, D.M. 14/1/2008). The record properties are listed in Tab. 1, while the single and mean response spectra at 5% structural damping are compared to the code-specified spectrum in Fig. 10.

The subsoil characterization at the building site was referred to the average layering of two nearby boreholes: the stratigraphic profile consists of 3.7 m layer of made ground and pyroclastic soil, underlain by 4.4 m of LYT and about 42 m of WGI down to the flyschoid bedrock, assumed at a depth of 50 m (Fig. 11).

The value of shear wave velocity V_S for the loose soil cover is about the average of those detected throughout the whole town center, while those pertaining to the ignimbrite layers plot closer to the upper values, being this rock mass generally more competent along the eastern ridge. For the bedrock, V_S was extrapolated from the Down-Hole tests carried out in the surrounding valleys, by increasing the measured values taking into account the change of depth (de Silva, 2012). According to the NTC criteria, the subsoil should be classified as 'stiff' (soil class B). The equivalent shear modulus, G, normalized with respect to its small strain value, G_0, and the damping ratio, D, of the pyroclastic materials were assumed as depending on the shear strain, γ, according to the curves plotted in Fig. 12, taken from literature studies on comparable materials (Vinale, 1988; Papa et al., 1988).

One-dimensional seismic response analyses were carried out with the EERA code (Bardet et al., 2000), operating in the frequency domain with an iterative algorithm based on a linear equivalent approach. Considering all the selected input motions of Fig. 10, the vertical profiles of peak acceleration, a_{max}, plotted in Fig. 13 were obtained.

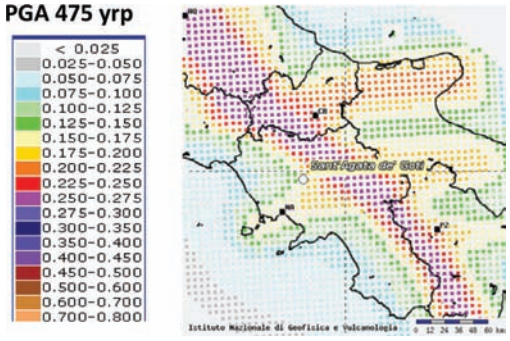

Figure 9. Sant'Agata de' Goti in the seismic hazard map of Italy (scale in PGA for 475 yrp).

Table 1. Properties of the selected records.

Earthquake	M_w	Date	Station	Epic. distance (km)	Comp.
Irpinia	6.9	23/11/1980	ALT	24	WE
Gran Sasso	5.4	09/04/2009	ANT	23	NS
Val Comino	5.9	07/05/1984	PNT	27	WE
Umbria-Marche	5.6	14/10/1997	CSC	22	NS
Friuli	5.6	11/09/1976	SRC0	26	NS
Irpinia	6.9	23/11/1980	BSC	28	NS
Val Nerina	5.8	19/09/1979	ARQ	21	NS

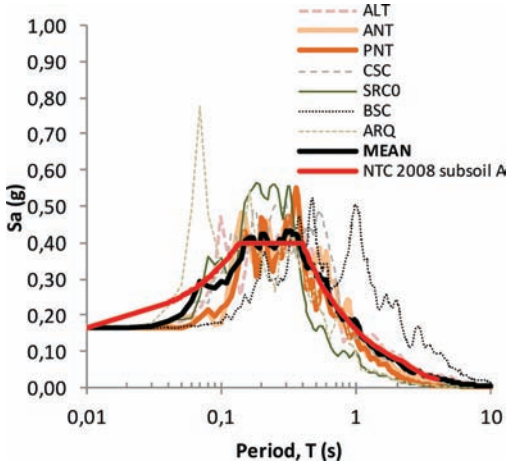

Figure 10. Single and mean spectra of the input motions vs. the NTC reference spectrum.

Although relatively stiff, the tuff layers amplify the seismic motion, which more apparently increases across the loose soil cover, attaining an average value of 0.25 g at the ground surface, higher than that specified by the NTC for a soil class 'B'.

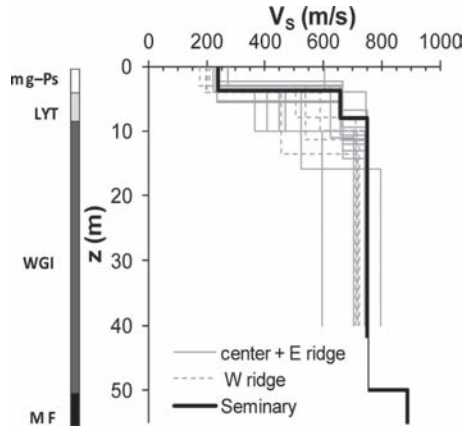

Figure 11. Layering and V_S profile at the seminary compared with the others detected throughout the historical center.

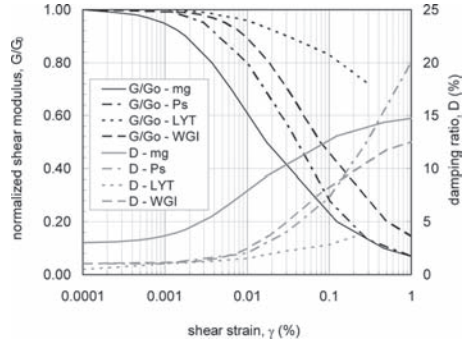

Figure 12. G-γ and D-γ curves of the different soils adopted for the seismic response analyses.

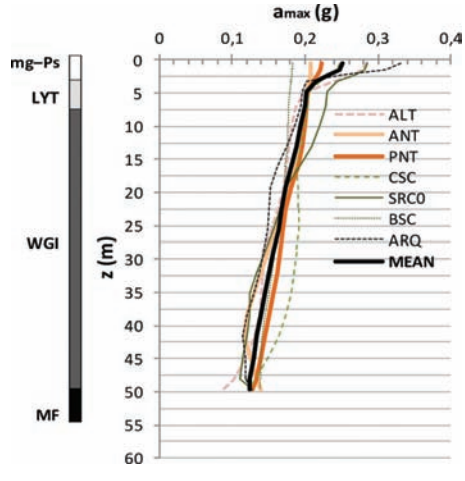

Figure 13. Peak acceleration profiles resulting from the different input motions.

As a further result of the seismic response analyses, Fig. 14 shows the average response spectrum at surface compared to the mean input spectrum and that specified by NTC for a soil class 'B'. It is worth noting that this latter underpredicts the spectral ordinates for a period T lower than about 0.4 s, while it overestimates the expected ground motion around the value of the first structural period, T_1, (0.47 s), estimated by the well-known expression:

$$T_1 = 0.05(H_b)^{3/4} \quad (3)$$

where H_b is the building height in m.

5.2 *Assessment of foundations safety*

The safety of the foundations was verified along the NS building section in Fig. 8, considered as the most representative due to the presence of the hypogeous cavity underneath and the proximity to the ridge. The building was considered as a rigid body, i.e. a conventional pseudo-static analysis was carried out. The self-weights of the tuff masonry wall and of the various structural elements (roof, trusses, archs, vaults, floor slabs) were determined on the basis of a detailed survey of the building. The overburden loads were assumed according to the standard specifications given by the D.M. 14/1/2008.

The seismic coefficients corresponding to the different foundation levels of the wall profile (Fig. 15a) were considered to vary from 0.20 for the wall strips A-B-C to 0.22 and 0.25 for the strips D and E respectively, just like the mean values of a_{max} (in g) resulting at these depths from the seismic response analyses (see Fig. 13). Due to the proximity to the steep eastern slope, the seismic demand was also amplified by the topographic coefficient $S_T = 1.4$ specified by the NTC for slope angles higher than 30°. Referring to the current trend adopted in Italy for the seismic assessment of existing buildings (DL 74 6/6/2012), the earthquake actions were also considered as scaled to 60% of their peak values.

As a result, the distribution of vertical loads (in kN/m) along the wall is pictured with different shading in Fig. 15a and plotted with a black solid line in Fig. 15b. This latter graph compares the demand to the foundation design capacity (dashed and dotted lines), reduced by a strength factor γ_R equal either to 2.3, following the design approach 2 according to the current NTC version, or to 1.2, as it is going to be assumed in a forecoming update of the same code.

The characteristic strength parameters were assumed as $\varphi_k = 36°$ and $c'_k = 1$ MPa, compatible with the mean measured uniaxial compression strength. The bearing capacity term due to the overburden soil was conservatively neglected, due to the frequent absence of cover at the foundation level in the hypogeous cavity.

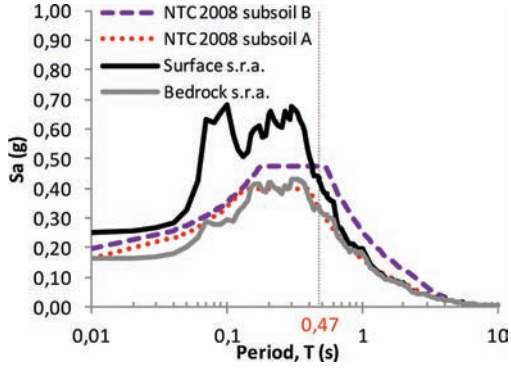

Figure 14. Mean spectra resulting at surface versus the mean reference input motion and the NTC reference (A) and stiff soil (B) spectra.

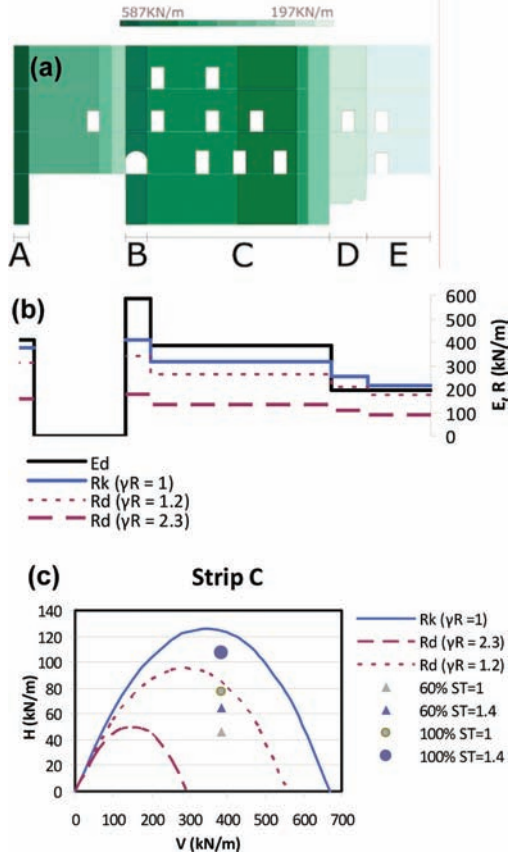

Figure 15. Representative wall of the building (a) with vertical capacity and demand distributions (b); safety assessment of the most critical foundation strip in the interaction domain (c).

The foundation capacity was computed by the conventional limit equilibrium solution accounting for correction factors for inclined load; the comparison with the vertical demand in Fig. 15b shows that the foundation is unsafe along most of the wall. The same comparison appears more encouraging if the capacity is expressed through the interaction domain (Fig. 15c), in terms of vertical (V) and horizontal components (H), as follows (Viggiani, 1999):

$$H = \psi V \left(1 - \frac{V}{V_{\max}}\right)^{\beta} \quad (4)$$

In eq. (4), V_{max} was assumed as the foundation design capacity for vertical load (i.e. without inclination correction factors); the exponent β was set equal to 0.95, as suggested by Viggiani (1999), and the initial slope ψ was computed as the characteristic coefficient of friction between soil and foundation, $\tan\varphi_k$, factorized by 1.1, as specified by the NTC. Along strip C, Fig. 15c shows that, by assuming perspectively $\gamma_R = 1.2$, the assessment is satisfied, except for the most conservative hypothesis for the seismic actions (100%, $S_T = 1.4$).

6 CONCLUSIONS AND PERSPECTIVES

This preliminary study highlighted the main aspects of the environmental risks affecting Sant'Agata de'Goti and may be very helpful to address further subsoil investigations, seismic response and stability analyses and stabilization works for the natural and building heritage.

The gathering and synthesis of data from the previous subsoil investigations point out that:

- deeper boreholes underneath the historical center are necessary to better identify and characterize the seismic bedrock, as well as further investigations such as geognostic and geophysical logs may better define the nature and extension of shallow covers along the slopes;
- further laboratory tests are necessary on both strength and cyclic stress-strain behaviour of the pyroclastic formations and colluvial covers.

The above improvements in the geotechnical characterization may be very helpful for the environmental requalification of both the slopes and the cavities, since their stabilization requires more reliable design parameters. They can also support more accurate analyses of seismic response, e.g. through 2D models, and the consequent safe design of retrofitting measures for the existing buildings, accounting for their dynamic behaviour.

In this perspective, the Authors expect that a 'road map' can be drafted since now with the town municipality, in order to improve the environmental safety and life quality of this beautiful historical center.

ACKNOWLEDGMENTS

The Authors wish to thank the town municipality and Drs. Giovanni Izzo and Maurizio Cice for the kind assistance in providing the subsoil data. Drs. Luisa Alterio and Giuseppe Tropeano are warmly acknowledged for their precious advices for the seismic analyses.

REFERENCES

Barberi, F., Innocenti, F., Lirer, L., Munno, R., Pescatore, T., Santacroce, R. 1978. The Campanian Ignimbrite: a major prehistoric eruption in the Neapolitan area (Italy). *Bulletin of Volcanology* 41(1): 1–22.

Bardet, J.P., Ichii, K., Lin, C.H. 2000. *EERA a Computer Program for Equivalent-linear Earthquake site Response Analyses of Layered Soil Deposits*. Univ. of Southern California, Dep. of Civil Eng.

Barton, N., Lien, R., Lunde, J. 1974. Engineering classification of rock masses for the design of tunnel support. *Rock Mechanics* 6 (4), 189–236.

Cappelletti, P., Cerri, G., Colella, A., de' Gennaro, M., Langella, A., Perrotta, A., Scarpati, C. 2003. Post-eruptive processes in the Campanian Ignimbrite. *Mineralogy and Petrology* 79: 79–97.

Costanzo, A., d'Onofrio, A., Lanzo, G., Pagliaroli, A., Penna, A., Puglia, R., Santucci De Magistris, F., Sica, S., Silvestri, F., Tommasi, P. 2007. Seismic response of historical centers in Italy: selected case studies. In K. Pitilakis (ed.) *Proc. IV Intern. Conf. on Earthquake Geotechnical Engineering; Thessaloniki*, Workshop on 'Geotechnical earthquake engineering related to monuments and historical centers', 319:342. Rotterdam: Balkema.

Cruden, D.M. & Varnes, D.J. 1996. Landslide types and processes. In A.K. Turner & R.L. Schuster (eds.), *Landslides: investigation and mitigation*. Nat. Res. Counc., Transp. Res. Board Sp. Rep. 247: 36–75.

de Silva, F. 2012. *Azioni sismiche e sicurezza degli edifici storici: un caso studio a S. Agata de' Goti*. M.Sc. thesis, Università di Napoli (in Italian).

De Vivo, B., Rolandi, G., Gans, P.B., Calvert, A,. Bohrson, W.A., Spera, F.J., Belkin, H.E. 2001. New constraints on the pyroclastic eruptive history of the Campanian volcanic Plain (Italy). *Mineralogy and Petrology* 73: 47–65.

DL 74 6/6/2012. *Interventi urgenti in favore delle popolazioni colpite dagli eventi sismici che hanno interessato il territorio delle province di Bologna, Modena, Ferrara, Mantova, Reggio Emilia e Rovigo, il 20 e il 29 maggio 2012*. Gazzetta Ufficiale della Repubblica Italiana, No. 131–7/6/2012.

DM 14/1/2008. *Norme Tecniche per le Costruzioni*. S.O. n. 30—Gazzetta Ufficiale della Repubblica Italiana, No. 20-4/2/2008.

Evangelista, A., Flora, A., Lirer, S., de Sanctis, F. & Lombardi, G. 2002. Studi ed interventi per la tutela di un patrimonio sotterraneo: l'esempio delle cavità di Napoli. *XXI Conv. Naz. Geotecnica, L'Aquila, I: 579–588. Bologna: Pàtron* (in italian).

Federico, F. & Screpanti, S. 2002. Analisi della stabilità di cavità sotterranee in rocce piroclastiche del sottosuolo di Roma. *XXI Conv. Naz. Geotecnica, L'Aquila, 529–536. Bologna: Pàtron* (in italian).

Fenelli, G.B., Pellegrino, A. & Picarelli, L. 1998. Stability problems of old towns built o relict plateaux on clay deposits. In C. Viggiani (ed.), *Proc. Int. Symp. on Geotechnical engineering for the preservation of monuments and historical sites*, *Napoli,* 163–173. Rotterdam: Balkema.

ICOMOS (1964). The Venice Charter (1964) - International charter for the conservation and restoration of monuments and sites. *II International Congress of Architects and Technicians of Historic Monuments, Venice.* ICOMOS, Int. Council on Monuments and Sites. internet: www.icomos.org/charters/venice_e.pdf

Iervolino, I., Galasso, C., Cosenza, E. 2009. REXEL: computer aided record selection for code-based seismic structural analysis. *Bulletin of Earthq. Eng.*, 8:339–362.

Melillo, M. 2012. *Progetto per un parco urbano a Sant'Agata de' Goti.* M.Sc. thesis, Università di Napoli (in Italian).

MPS Working Group 2004. *Redazione della mappa di pericolosità sismica prevista dall'Ordinanza PCM 3274 del 20 marzo 2003*. Final report for the Department of Civil Protection, INGV, Milano-Roma.

Papa, V., Silvestri, F., Vinale, F. 1988. Analisi delle proprietà di un tipico terreno piroclastico mediante prove dinamiche di taglio semplice. *I Conv. GNCSIG, Monselice (PD), I:265–286* (in Italian).

Spallarossa, D. & Barani, S. 2007. *Disaggregazione della pericolosità sismica in termini di M-R-ε.* Deliverable D14, Progetto DPC-INGV S1, http://esse1.mi.ingv.it/d14.html

Viggiani, C. 1999. *Fondazioni.* Benevento:Hevelius (in Italian).

Vinale, F. 1988. Caratterizzazione del sottosuolo di un'area campione di Napoli ai fini della microzonazione sismica. *Rivista Italiana di Geotecnica*, 22(3):77–100.

Geotechnical Engineering for the Preservation of Monuments and Historic Sites – Bilotta, Flora, Lirer & Viggiani (eds)
© 2013 Taylor & Francis Group, London, ISBN 978-1-138-00055-1

Study and monitoring for conservation of Sanctuary of Santa Maria Assunta at Monteortone (Abano Terme, Padova)

A. Dei Svaldi & A. Mazzucato
University IUAV of Venice, Italy

ABSTRACT: The Sanctuary of Monteortone, built at the foot of the Euganean Hills near the city of Padova (NE Italy), is one of the most significant examples of Paduan architecture, painting and sculpture of the 15th century.The Sanctuary is a Latin cross-shaped building, consisting of a nave and two aisles, supported by masonry pillars and covered with a cross-vault with pointed arches. The façade is divided into three parts by masonry pilasters, with two centrally placed round windows. The bell-tower, of the same century, rises with thick pilasters and repeated small arches.

The first reports of significant damage due to settlement and rotation of the façade and pillars (a horizontal differential displacement of about 20 cm was measured between the top and base of the pillars immediately behind the façade) date back to August 1902, when the Sanctuary was closed to the public and substantial consolidation work began. Later, in 1934 and again in 1957 and 1966, new damage was reported and required further interventions. In 1975 the church was closed because of the danger of collapse, and further restoration works were carried out on the structure and its foundations.

This paper examines the various interventions carried out during the Sanctuary's history, the effects of restorations and the results of geotechnical studies. Results of tests on structural elements and monitoring data (temperature, cracking, tilting), collected during 2004–2005, are also presented. This work, carried out in order to check the development of cracking in some structural elements, allowed the behaviour of the building to be analysed within the perspective of new restoration work.

1 INTRODUCTION

The Sanctuary of Monteortone (Figure 1), which stands at the foot of the Euganean Hills a few kilometres from Abano Terme, near Padova, is dedicated to the Conception and Nativity of the Blessed Virgin Mary, and is one of the most significant examples of 15th-century architecture, painting and sculpture in the province of Padova.

The speed with which the Sanctuary was built can be appreciated by acknowledging the faith and diligence of the Augustinian monks, who wanted to provide a prestigious setting for the icon of the Virgin, found by Pietro Falco (a man-at-arms) on the occasion of his miraculous recovery (May 1428).

According to historical reconstructions, the work was carried out by an extraordinary gathering of the faithful, who settled in Monteortone and completed the building in only seven years (1428–1435), following the precise, detailed instructions of Simone da Camerino and some of his skilled collaborators. They first raised and levelled the ground in the lee of the hill, enclosing Pietro Falco's spring in a cave, and then placed the holy icon in the *sacellum*, a small chapel behind the altar.

The Sanctuary is built to a Latin cross plan, composed of a nave and two aisles, supported by polygonal brick pillars and a vaulted ceiling. The façade is divided into three by pilasters faced with brick, with two centrally placed round windows: one large above, and the other, smaller, over the portal. The bell-tower, again of the 15th century, rises with broad pilasters and repeated small arches.

The first reports of conspicuous damage caused by settlement and rotation of the façade and internal pillars date back to August 1902, when the Sanctuary was closed to the religious community and major reinforcement work began, which continued throughout 1903. Subsequently, in 1934 and again in 1957 and 1966, new cracks were reported and required further restoration.

In 1975, the church was again closed because of the risk of collapse (the pillars immediately behind the façade were found to be about 20 cm out-of-plumb) and consolidation of the structure and foundations was undertaken.

This paper examines the various situations which arose over time, the effects of interventions, and the results of investigations of the foundation soil and structural elements. Monitoring data (temperature, cracking, tilting), covering 12 months in the period 2004–2005, are also presented. This work, organised to verify the ongoing problems still present in some structural elements, allowed analysis of the

Figure 1. Sanctuary of Monteortone.

behaviour of the building within the perspective of restoration and reinforcement.

2 STRATIGRAPHIC AND GEOTECHNICAL CHARACTERISTICS OF THE SITE

Historical information indicates that the Sanctuary was built after substantial excavation and infilling. The apse rests on the trachytic rock of the hill (historical sources refer to it as being: "well bedded in the mountain"), and the rest of the foundations are on alluvial soil.

Geotechnical study carried out at the time of the underpinning in 1973 and more recently in 2004, show that the soil layers vary greatly in thickness, in relation to the depth of the bedrock (Figure 2).

From the surface downwards, there is a highly heterogeneous, man-made layer, about 5 m thick. There are two Quaternary formations between the top layer and the bedrock. The first, about 9 m thick, is composed of clayey silt with thin layers of sandy silt, peat and clayey peat; resistance q_c of the static cone penetrometer is 0.1–0.2 MPa. The material is slightly overconsolidated (OCR = 1–1.5), compression ratio CR varies between 0.1 and 0.3, and recompression

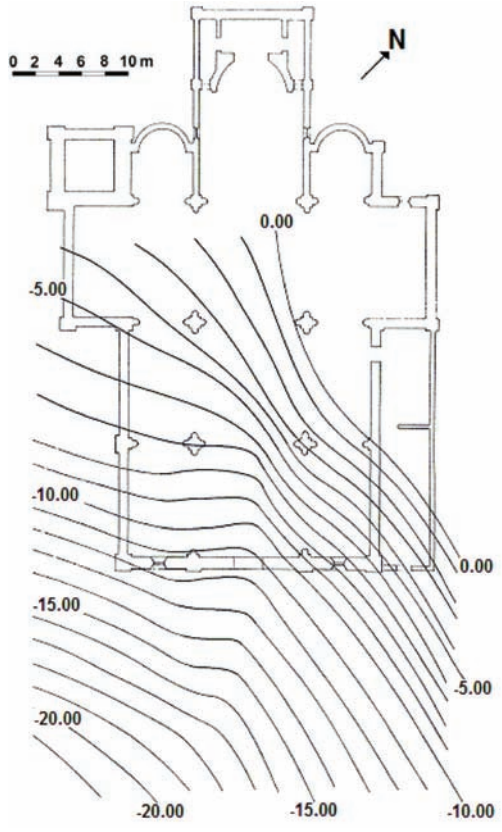

Figure 2. Plan of Sanctuary and contours of depth of bedrock. Floor of transept is at relative height of +4.80 m.

ratio RR ranges between 0.013 and 0.04; consolidation coefficient C_v is between 0.7×10^{-7} m^2/s and 1.3×10^{-7} m^2/s. The second formation, about 4 m thick, is made up of clayey and sandy silt with fragments of trachyte; resistance q_c is 0.1–0.3 MPa, occasionally reaching 0.6 MPa. The material is normal-consolidated, values being CR = 0.12, RR = 0.013 and $C_v = 1.5 \times 10^{-7}$ m^2/s (Figure 3).

In 2004 a survey of piezometric levels was made, involving 3 BAT-type piezometers placed at depths of −15.80 m (B1), −9.88 m (B2) and −6.74 m (B3) and a Casagrande piezometer at −6.20 m. With the exception of piezometer B1, installed in rock, piezometric cells were installed through a borehole down to about 50 cm from the predetermined depth and subsequently pushed into place.

Figure 4 shows piezometric measurements taken in the alluvial layers in 1975 and 2004–2005. Historical data show that, in the early 1900s, the groundwater level was at a depth of −1.00 m, about 5 m higher than that measured at the beginning of underpinning works in 1975. The measures of

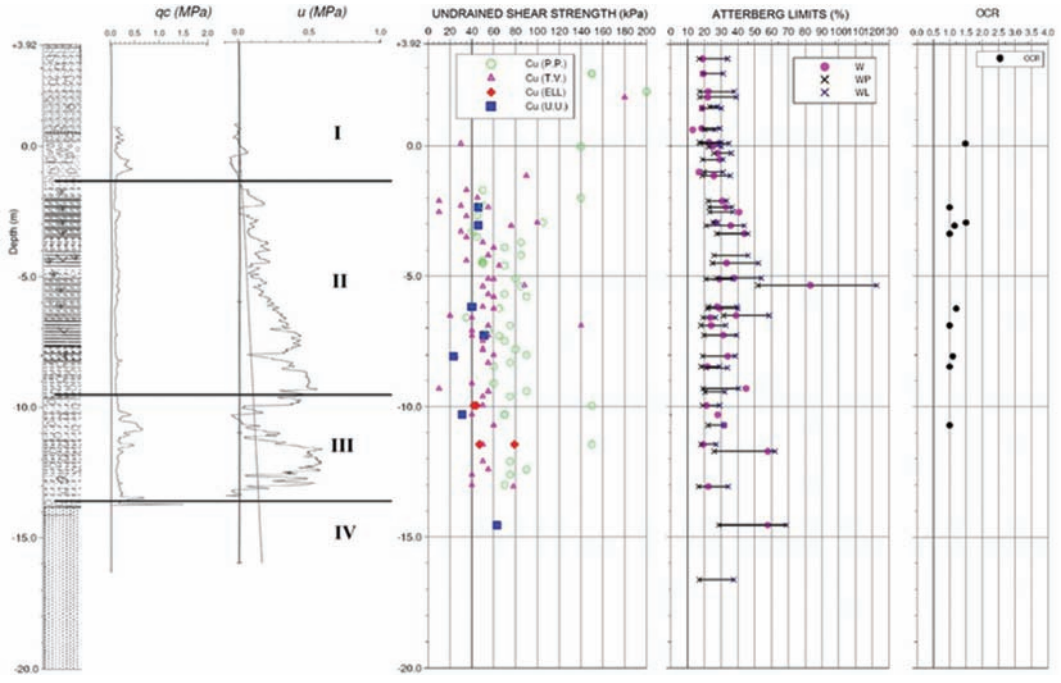

Figure 3. Soil profile and geotechnical properties (Undrained shear strength Cu (P.P.) from Pocket Penetrometer, Cu (T.V.) from Torvane, Cu (ELL) from Unconfined Compression test, Cu (U.U.) from Unconsolidated-Undrained triaxial test.).

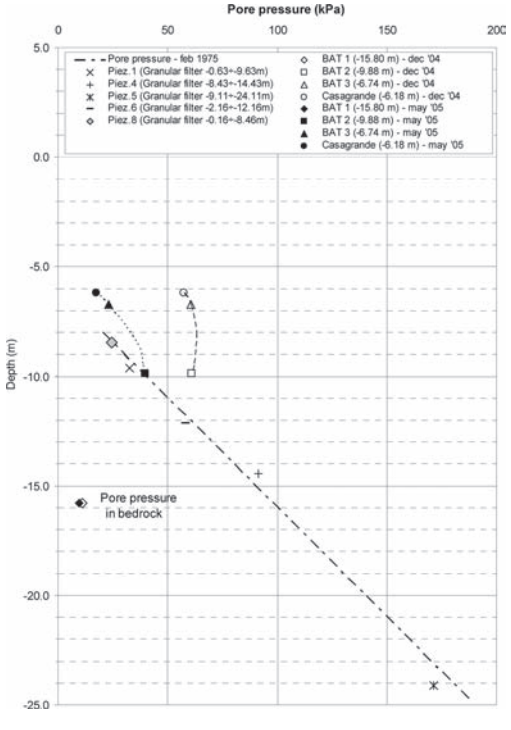

Figure 4. Pore pressure in alluvial layers.

2004–2005 show variations in groundwater level of about 4 m, due to precipitation and thermal activity which increase in spring and decrease in winter.

3 INTERVENTIONS OVER TIME

Built in the first decades of the 15th century and completed in a relatively short time, the Sanctuary of Monteortone did not undergo any major alterations in the following centuries, so that it may still be admired in its original form. However, it is interesting to note, from comparisons of prints, one by G. Giorgi in 1644 and another by S. Mandruzzato in 1792 (Figure 5a and 5b), that the flight of steps and the embankment in front of the Sanctuary were not there initially. These works, as ascertained from excavations in the parvis of the church near the façade, are composed of clay soil with boulders (about 1 m thick), brick paving resting on 20 cm of sand treated with lime, and a layer of stone, forming part of the anthropic layer.

The evolving morphology of the parvis in front of the Sanctuary may also be interpreted from careful analysis of the stratigraphy.

The stone materials, probably from the nearby hillside, were used to form the working surface on which to build the monument. The steps and the

Figure 5a. Illustration from "*Historia della B. Vergine di Monte Ortone*" (G. Giorgi, 1644).

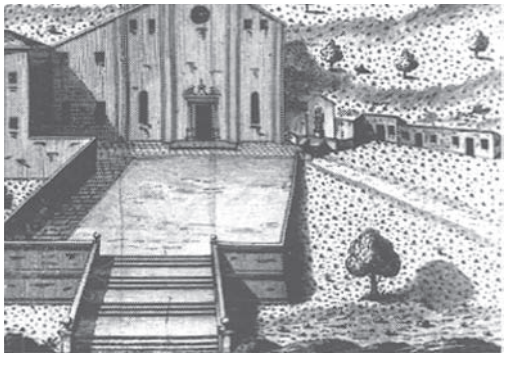

Figure 5b. Detail from "*Vista del Santuario di Monteortone*" (S. Mandruzzato, 1792).

embankment, varying in thickness from 1.20 to 2.40 m, were added later.

Historical sources therefore indicate that construction began on the bedrock and continued downhill, on soil layers of different type and thickness.

The historical evolution of the settlement of the Sanctuary, studied by finite element analysis (Figure 6, Table 1), shows settlement along the longitudinal section of the church, ranging from 26 cm (point A in Fig. 6) to 110 cm (point D) caused by the backfill (height 5 m), and further movements

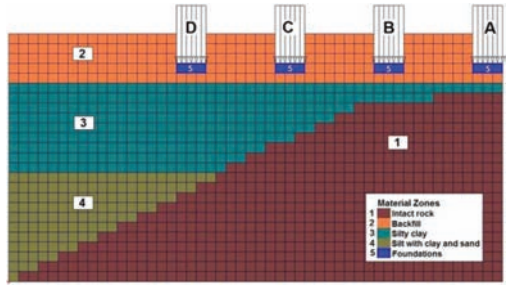

Figure 6. Finite element discretisation—longitudinal section.

Table 1. Geotechnical parameters for modified Cam-Clay and elastic models.

Layer	κ	λ	M	E (MPa)	ν
Intact rock	/	/	/	42000	0.2
Backfill	/	/	/	15	0.3
Silty clay	0.03	0.20	1.07	/	0.3
Silt with clay and sand	0.01	0.10	1.1	/	0.3

of about 20 cm (point D) of the façade, caused by the load of the foundations. Additional settlement of about 8 cm (point D) is attributed to the load of the backfill, carried out later (steps and embankment).

Another aspect, which may have contributed to the evolution of cracking in the Sanctuary since 1900, is subsidence, caused by lowering of the water-table in the Euganean Geothermal Basin through draining wells (Figure 7). In particular, there were already eight draining wells at Monteortone in 1939. The nearby Sanctuary underwent subsidence of the façade, evaluated at 25 cm (point D), due to lowering of the water-table by about 5 m from the early 1900s until underpinning in 1975. Subsequent measurements indicate that the Sanctuary did not undergo any significant settlement due to dewatering from 1975 to 2004, although the steps and embankment in front of the church settled by about 3 mm/year.

Figure 8 shows rotation θ of the foundations, from construction (1428) to 1975, obtained from numerical analysis. It also shows the inclination of pillars and church floor observed in 1975. The difference between the rotations of the floor and pillars is explained by the behavior of the structure, which probably induced substantial eccentricity of vertical loads.

Documentation examined regarding the first major restoration, carried out in the early 1900s (August 1902), does not provide sufficient detail,

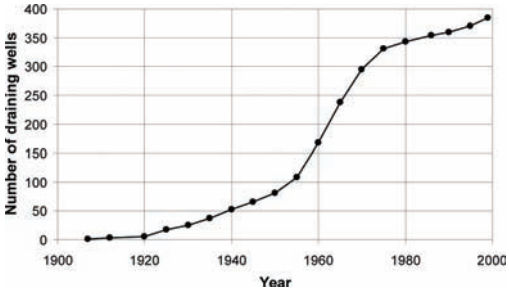

Figure 7. Trend from 1900 to 2000 of number of draining wells in Euganean Geothermal Basin.

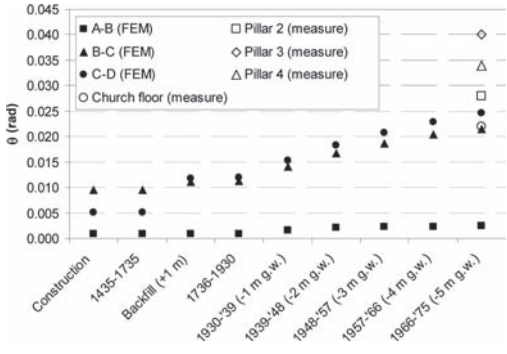

Figure 8. Rotation between the foundations from 1428 to 1975 (FEM analysis and measures).

either for understanding the extent of the cracking and its causes or for partial reconstruction of operations.

The measures adopted in this first phase of work were certainly not adequate, and a few years later the Sanctuary exhibited ongoing cracking in side walls and vaults, arousing serious concern.

In 1933, after the first thermal wells had been dug, a substantial increase in the inclination of the façade was noted, and underpinning pits were realized to a depth of 6.5 m (3 for the pilasters of the façade and 4 for the first order of pillars). The pits were made of tubes with a diameter of 1.0 m, filled with concrete.

In 1957, after further interruption of religious services, more underpinning work began with driven concrete pile elements along the side walls and façade, but not the transept, and under the first colonnade starting from the façade. New chains were also inserted in the most badly damaged spans.

Work logs show that the substructure of the foundations of the first colonnade was about 4 m below the present-day floor. They also reveal layers of peat immediately under the foundations.

In 1959, the roof was almost completely restored but, once again, in May 1962, it was necessary to repair some cracks in the ceiling of the second span of the nave. In 1966, further cracks were repaired in the vaults of the nave and aisles.

It is clear that all the operations carried out and described so far were not resolutive, since only a few years later new and radical restorations became necessary.

In 1975–76, substantial underpinning by means of small-diameter piles transferred the loads of the entire structure to the bedrock (Figure 9).

This restoration involved three phases. The first was to expose the sides of the foundations, for subsequent placing of vertical micropiles (diameter 110 mm, reinforced with steel tubes 76.1 mm in diameter and 20 mm thick, inserted in the bedrock to a depth of 8 m) and perforations in the masonry to house anchoring ties and bolts (0.6″ in diameter), poststressing of which was planned after concreting of the stripfooting. This phase also included pre-compression of piles prior to their final connection to the beams (Figure 9).

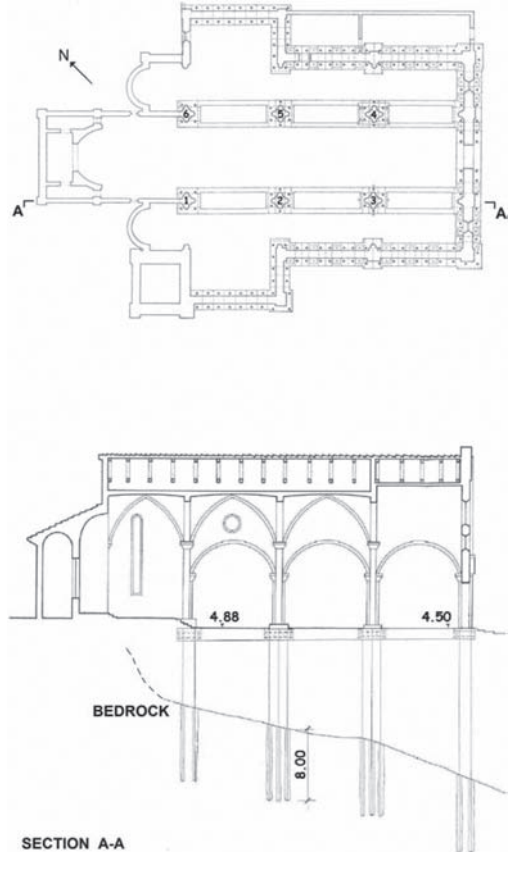

Figure 9. Plan and longitudinal section of Sanctuary. Underpinning with micropiles and concrete beams (1975–76).

The second work phase involved execution of diaphragm walls based on the rock and anchoring ties. The third phase consisted of repairing the cracks in the floors, masonry and vaults, and completing the drainage system for runoff from the hillside.

The foundations of the Sanctuary, as shown in the surveys carried out during the latest underpinning works, are in masonry and connect the bases of the columns longitudinally. The placing of small-diameter piles, laid in the bedrock and connected to the existing foundations by continuous beams, was essential for consolidation, in that not only were the most compressible soil layers bypassed by transferring their loads to the bedrock, but the whole foundation system was strengthened.

The results of inclinometric measurements in 1975 excluded the danger of possible downhill movement of the monument.

In 2004, work began on checking the causes and development of strain, still found in some structural elements.

Surveys focused on many aspects, including the composition and texture of structures, extent of stress in some significant points on side walls, mechanical characterisation and observation of the state of aggregation of walls, determination of stress on metal chains, and evaluation of the physical, chemical, petrographic and mechanical properties of mortar, bricks and stone.

A monitoring system was also installed on the main supporting structures of the Sanctuary, in order to collect data regarding:

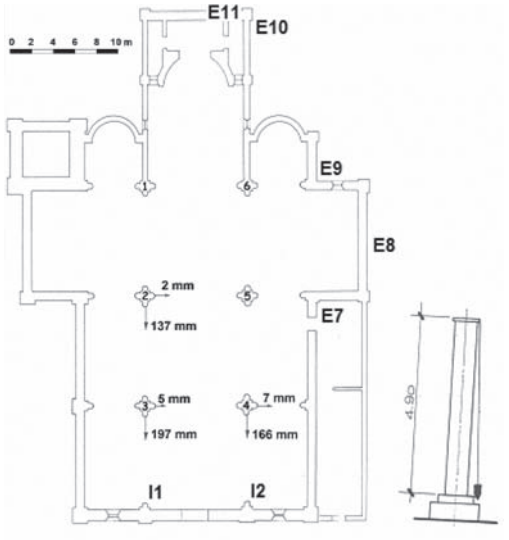

Figure 10. Out-of-plumb values measured in 1975 and location of the inclinometers (Fig. 12) and the extensometers (Fig. 13).

– temperature;
– inclination of columns;
– movement of cracks.

Figure 10 shows the out-of-plumb measured in 1975: the data were confirmed by measurements in 2004, highlighting the effectiveness of the underpinning work of 1975.

Figures 11, 12 and 13 show the trend of data collected over 12 months, from July 2004 to August 2005.

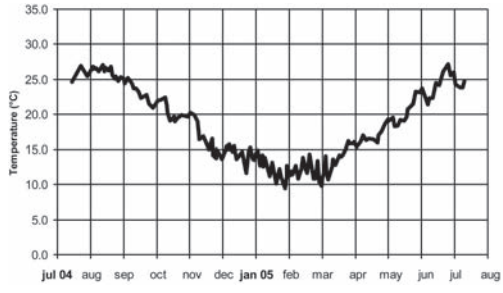

Figure 11. Temperature variations measured inside structure (daily mean).

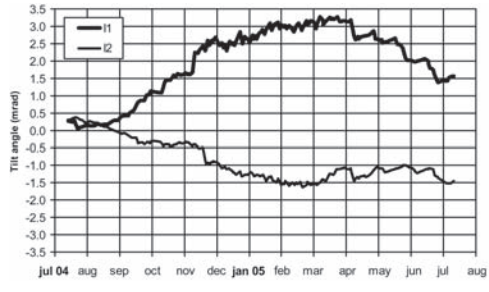

Figure 12. Evolution of inclinometer measurements on inner wall of façade (+ external rotation) – see device locations in Fig. 10.

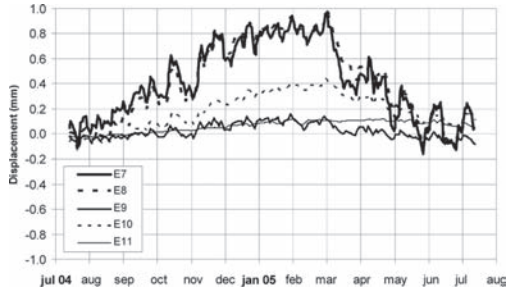

Figure 13. Evolution of cracks opening in external walls (+ opening)—see device locations in Fig. 10.

The movements measured, essentially due to variations in temperature, are relatively minor and may be considered acceptable for the structure as a whole. In structural elements where no direct effect of temperature was measured, a system of longitudinal and transversal chains was set up, with proper checking of chain tension and replacement of tap bolt, and consolidation and reinforcement of crack patterns of walls and vaults.

4 CONCLUSIONS

The Sanctuary of Monteortone, built in the lee of the hill of the same name, was originally constructed on shallow foundations set on trachyte towards the apse, and on alluvial soils consisting of silty clay and clay formations with organic material and silty sands towards the façade. The foundation structures, as shown by successive work logs, are composed of a grid connecting the various structural components in brick masonry with lime mortar of high quality and consistency.

Study on the evolution of events over time allowed us to date the phenomena which, ever since the original construction of the Sanctuary, have worried the religious community, which was constantly called upon to carry out consolidation work on its structures and foundations.

Work on the foundations was limited to partial underpinning, not always respecting stratigraphic conditions; in any case, later changes in the hydraulic conditions of the site were the result of the exploitation of the Euganean Geothermal Basin. If the cause of the sudden worsening of the cracking in the structure, with rotation of the façade, had been discovered earlier, the first foundation support work by underpinning in 1934 and later with piles in 1957, together with checking and regularization of water pumping, would have facilitated the further work carried out in 1975, without modifying the static behaviour of the foundation system.

Study of the behaviour of the foundation works shows that the Sanctuary has always been affected by soil settlements which have influenced it ever since its completion. The results also allow to verify the effectiveness of underpinning in 1975, with transfer of loads to the bedrock. These operations are efficient, and further consolidation is not required at present.

Examination of the extent of cracking and especially of the state of inclinometers and strain gauges placed on metal chains, shows the albeit limited movements of the complex structure of the Sanctuary.

The effects of temperature, in terms of both mean and actual values, are evident. In particular, daily excursions in winter, with alternating on/off phases of the heating system, give rise to cyclic behaviour, resulting in deformation, cracking and inclination of the structures inside the Sanctuary, revealing both daily and seasonal excursions. Particularly important is the role played by the system of chains, which are now degraded and becoming inefficient, although this is not the only factor responsible for the state of stress in some structural elements.

REFERENCES

Antonelli, R., Previatello, P. et al. 1995. *The geothermal Euganean field. A subsidence modelling approach.* Proc. World Geothermal Congress, Florence.

Barcaro, F.A. 1996. *Il Santuario e il Complesso Monastico di Monteortone*—Abano Terme tra storia, religiosità e arte, Studi Padovani, Vol. 1, Editoriale Programma, Padova.

Consolidamento delle fondazioni del Santuario di Monteortone, 1975. Relazione 18.043. Ing. Giovanni Rodio s.p.a.

Gottardi, G., Previatello, P., Simonini, P. 1996. *An extensive investigation of land subsidence in the Euganean Geothermal Basin, Italy*. Facoltà di Ingegneria, Istituto di Costruzioni Marittime e di Geotecnica, Università di Padova.

This page intentionally left blank

Geotechnical Engineering for the Preservation of Monuments and Historic Sites – Bilotta, Flora, Lirer & Viggiani (eds)
© 2013 Taylor & Francis Group, London, ISBN 978-1-138-00055-1

Slope dynamics, monitoring and geological conservation of the Siq of Petra (Jordan)

G. Delmonaco, C. Margottini & D. Spizzichino
ISPRA, Geological Survey of Italy, Rome, Italy

ABSTRACT: The Siq is a 1.2 km naturally formed gorge that represents the main entrance to Petra (Jordan). Discontinuities of various type (bedding, joints, faults), mainly related to stratigraphical setting, tectonic activity and geomorphological evolution of the slope can be recognized. Structural condition determines a rock-fall potential activity that may involve unstable volumes, from 0.1 m^3 up to over 500 m^3. The latter can be catastrophic according to evolution of the movement (extremely rapid) and involved rock mass volumes. Slope instability, acceleration of crack deformation and consequent increasing of rock-fall hazard conditions could threaten the safety of people walking through the Siq. UNESCO, ISPRA and Jordan local authorities have implemented a project focused on landslide hazard assessment and risk mitigation strategies as a first step for the long-term conservation of the Siq. The paper reports preliminary data on landslide inventory, geomechanical properties of materials and assessment of landslide kinematics that affect the Siq of Petra.

1 INTRODUCTION

The Siq is a 1.2 km naturally formed deep gorge in the sandstone mountains that connects the urban area of Wadi Musa with the monumental area of Petra. It represents, since Nabataean times, the main narrow entrance for some thousands tourists that access the archaeological area every day.

The Siq is formed by very steep slopes with variable height by the ground level, from few meters at the entrance to several tens of meters at the end of the path. The paper reports a preliminary analysis of an engineering geological field survey in the framework of a UNESCO project for the implementation of remote and field integrated monitoring system aimed at the detection and control of the Siq slope deformation.

The study has produced a preliminary analysis of landslide inventory and potential kinematics as well as a geomechanical analysis of the rocks through field techniques and laboratory analysis.

2 GEOLOGICAL SETTING

Petra is located on the eastern side of the Dead Sea-Wadi Araba tectonic depression, interpreted as Dead Sea rift (Bender, 1974; Mart, 1991), a transform valley (Garfunkel & Ben Avraham, 1996), a ca. 15 km-wide topographic low formed by shearing along the transform separating the Arabian and Sinai plates (Sneh, 1996; Ginat et al., 1998, Franchi et al., 2009) (Fig. 1). The local stratigraphic succession (Quennel 1951; Bender, 1974) starts with the thin (locally < 50 m in thickness) Salib Arkose arenitic formation, overlain by a thick (locally > 500 m in thickness) suite of both paralic and shallow-water (Selley 1972; Amireh et al., 2001), massive and poorly stratified Cambrian-Ordovician quartzarenites belonging to the Umm Ishrin and Disi formations (Franchi 2002; Franchi et al., 2009) (Fig. 2).

The hand-carved rock monuments of Petra are entirely cut in the sandstone of Umm Ishrin and Disi formations (Amireh et al., 2001; Franchi, 2002) moreover, many quarries in use in different historical period attest to the fact that the same sandstone was employed as construction material (Franchi et al., 2009). Lithologic and petrographic characteristics of the two formations are controlling weathering related conservation problems, affecting, as well, shear strength parameters of the rocks. The boundary between the sandstones of the Umm Ishrin formation and those of the overlying Disi formation is rather uncertain; the passage is attributed to first occurrence of whitish, thin-bedded arenites. The petrographic composition of the sandstones of the Umm Ishrin and Disi formations are quite similar, except for a considerable decrease of both iron oxides and hydroxides cements (Fig. 3). The Disi accessory minerals are the same as for the Umm Ishrin and are generally found with the same frequency (Franchi et al., 2009).

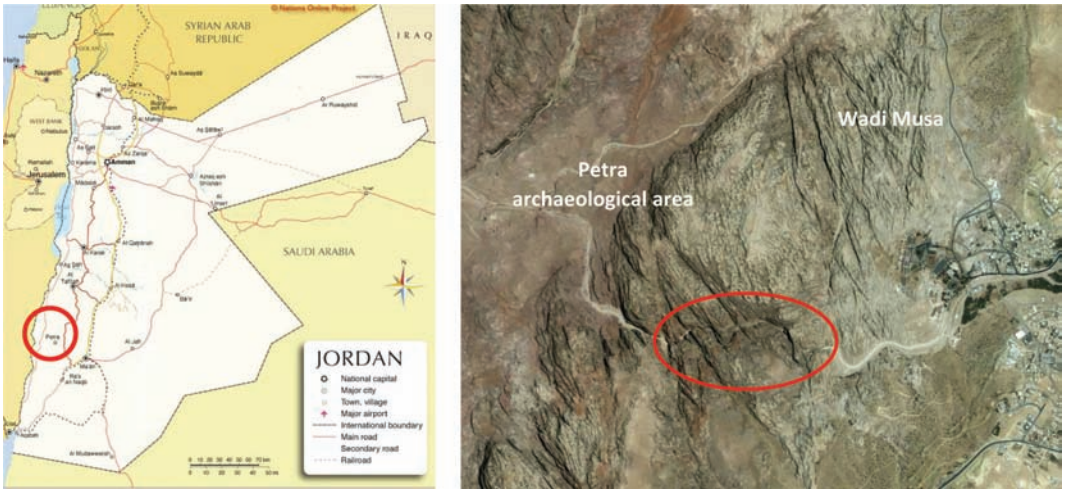

Figure 1. Location of Petra (left) and satellite image of the Siq (red circle) and Petra archaeological area.

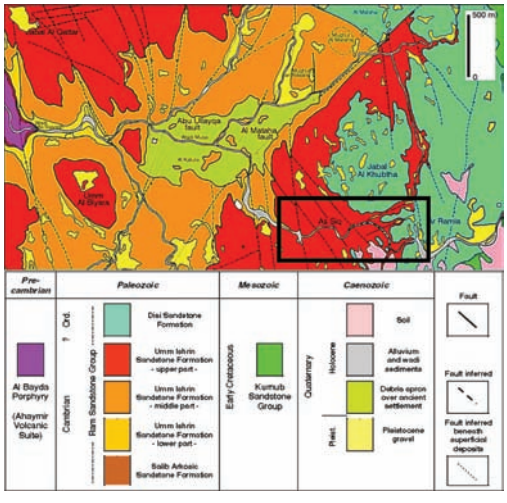

Figure 2. Simplified geological map of Petra at 1:5.000 scale, Jordan National Resources Authority (1991), (from Heinrichs, 2008, modified).

The Siq is entirely formed by the Umm Ishrin Sandstone Formation. This is mostly composed of medium-coarse grained, well-sorted quartz (in percentage as high as 80%) combined with highly variable proportions of cements consisting (Amireh, 1991) of authigenic kaolinite, hematite, goethite and subordinate poikilotropic calcite (Franchi & Pallecchi 1995; Franchi et al. 2009). The occurrence of several 10–15 cm thick arenaceous lenses/layers with amounts of hematite cement as high as 50% is a peculiarity of the Umm Ishrin formation (Franchi et al. 2009). The formation can be subdivided into three main units, according to their

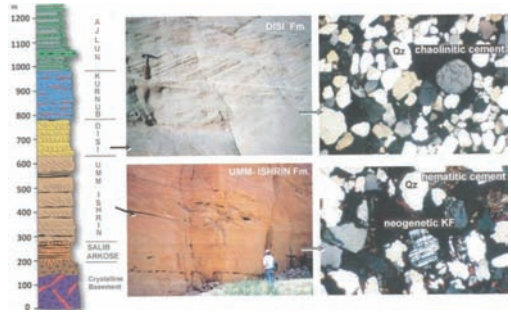

Figure 3. Litostratigraphy of the Petra-Beida area and view at the outcrop and thin section of typical sandstones from the UMM-Ishrin and Disi formation (Franchi et al., 2009).

texture, mineralogical composition and engineering classification. The Upper Sandstone, called "honeycomb sandstone", is composed of white and mauve-red, coarse to medium grained, hard and massive sandstone, capable to promote very steep slopes. It is characterized by typical cavernous weathering caused by solution of cement and consequent granular disintegration that form the typical honeycomb structures. This sandstone type is widely used as building stone in Petra due to its good engineering qualities.

The Middle Sandstone ("tear sandstone") consists of multi-coloured, medium to fine-grained, well-bedded and friable sandstone. Weathering is diffuse, especially by solution of the ferruginous and manganesiferous layers and cements that cause change or the rock face from red-brown to yellow and grey. Cross-bedding structures and presence of interbedded silty and clayey sands are quite

common. This unit, due to anisotropy of materials, sensitive to moisture change, can promote sliding of blocks especially under saturation conditions. Most of the Siq monuments of Petra are excavated in this part of the Umm Ishrin Formation. The Lower Sandstone ("smooth sandstone") is made of white, medium to coarse-grained, hard massive sandstone, mainly used as building and decorative sandstone.

3 GEOMORPHOLOGY

The geomorphology of the Siq is the result of various long and short-term factors affecting this part. The geomorphological aspect of the Siq is the result of various long and short-term factors affecting this part of the Petra territory. Active tectonics related to the Dead Sea-Wadi Araba transform system has produced steep, high rock-relieves, spaced out by fault fault-bordered narrow troughs as the "Petra Valley" (Barjous & Mikbel 1990; Franchi, et al. 2009). The Siq slopes are the result of tectonic uplift, erosion due to runoff, differential erosion and weathering of sandstone materials. The Siq has a length of ca. 1.2 km with a general E-W orientation and a meandering course. It is the natural prolongation of Wadi Musa before the Nabataeans diverted it through the Wadi Mudhlin tunnel. The difference in height between the beginning at the entrance dam and the current exit at the Treasury is 63 m, at least in the bottom part of the slopes. Actually, the difference in altitude between the path floor and the top of the slopes at the confluence with the Outer Siq is much higher (>200 m). This is due to the morphological setting of the area that presents a stepped-slope shape with a lower part, where visual survey is possible and a middle and top sectors where slope faces are only partially observable from the Siq path. The Siq is surrounded by very steep slopes formed by the upper part of the Umm Ishrin formation. The slopes, as a general rule, presents a rupestral aspect, mainly massive. Nevertheless, discontinuities of various types, are present, mainly related to stratigraphical setting (bedding, generally horizontal), tectonic activity (faults, master joints, mainly sub-vertical), geomorphological activity (from vertical to medium-inclined joints). Sub-vertical and medium-angle dipping joints intersecting horizontal bedding are quite frequent in some parts of the Siq stratification and observed during field investigation. This situation may cause potential sliding of blocks, whose dimensions are depending on local, orientation, density and persistence of joints (Fig. 4).

3.1 *Weathering*

Weathering is the main degradation process in the Petra area affecting both natural landforms and monumental heritage. The weathering effectiveness on natural landforms is underlined by a large abundance of niches, honeycomb-structures and *tafoni*, and by rounded and spheroidal rock-surfaces as well. On both monuments and natural surfaces, hardening of external rock-surfaces is a usual phenomenon. With respect to the historical and artistic heritage conservation, the principal causes of degradation depend on complex interactions of mechanical, chemical, and in part anthropogenic processes (Albouy et al., 1993; Franchi & Pallecchi 1995; Fizner & Heinrichs, 1998; Heinrichs & Fitzner 1999, 2000a,b; Paradise, 1999, 2002, 2005; Akasheh, 2000; Heinrichs, 2008). Indeed, a primary mechanism of weathering depends on the thermal stresses (i.e. thermoclastism) suffered by sandstone grains (quartz above all) for e.g. insulation changes, night drops in temperature. The loosened grains can be removed from the rock surface by e.g. gravity, wind, rain-splash, runoff. A second important cause of weathering processes-monument decay is related to salts of varying chemism, abundant all along sandstone fractures and/or faults whose origin is still matter of working hypothesis (Franchi et al., 2009). Such salts, besides producing a chemical corrosion on many sandstone cements—also owing to the presence of iron sulphate hydrate, are responsible for mechanical aloclastic processes related to cycles of salt dissolution-precipitation (i.e. Ad Dehir-Monastery).

4 LANSLIDE TYPES AND SLOPE EVOLUTION

Due to its morphological and geostructural trend, the Siq has been divided into 15 different sectors in order to provide a zoning on potential landslide types and kinematical processes affecting each single portion. Rock slope failures occurring in the Siq of Petra can be classified into one of the following categories listed below depending on the type and degree of structural control (Delmonaco et al., 2012).

4.1 *Planar failures*

The example of Fig. 5 is related to a potential sliding large volume block, located near the entrance of the Siq. Potential failure can occur along the joint with a middle-angle dipping (white arrow), also promoted by a tension crack (yellow arrow) that isolates the potentially unstable block. The presence of a tension crack, well developed until the failure surface, with an apparent opening of few tens cm, promotes the circulation of superficial

Figure 4. View of erosion, weathering and degradation processes.

Figure 5. Example of potential sliding block.

waters and development of pore pressure that may reduce the shear strength on the contact between the joint/failure surface and the block.

4.2 *Wedge failures*

Figure 6 illustrates an area where a wedge failure has been already occurred. Potential unstable volumes are as a general rule <10 m^3, though larger volumes can be involved.

Wedge failures are not so frequent in the Siq slopes, although they can develop on slope faces where main joints, oriented generally E-W, encounters secondary joints with orientation NNW-SSE (Fig. 7).

4.3 *Toppling failures*

Toppling mechanism is widespread along the whole Siq area. Figure 8 is representative of a toppling failure mode involving large volume block, located in the middle portion of the Siq.

Potential toppling is promoted by a persistent sub-vertical tension crack (white straight arrow) with an opening that locally can exceed 40–50 cm, and by circulation of water inside the crack. The pivot, i.e. the point where the block rotates towards outside, is indicated with an arrow. This zone is characterized by siltstone bedding planes

Figure 6. Example of occurred wedge failure mode.

Figure 7. Example of wedge failure mode of a medium-large blocks.

with shear strength apparently less than the upper block-forming materials.

The presence of fissures, cracks and small blocks evidence a condition of high stress of the block toe. Monitoring of displacements of unstable block vs. back stable slope, tension cracks and toe area, that will be implemented in a further stage of the project, can provide information on evolution and kinematic trends.

For example, the lowering of the block vs. the back slope and a contemporary decrease of the opening of the tension crack can indicate a trend in changing slope kinematics, from toppling failure mode to a sliding mode. This has a direct consequence on the block failure triggering that may occur on a longer time frame.

Figure 8. Example of potential toppling failure mode of a large block.

Figure 9. Example of toppling-sliding failure mode of a medium—small blocks.

4.4 *Unstable isolated blocks (toppling/sliding)*

Another typical unstable situation actually involve blocks located in the bottom part of the slope characterized by a high-angle dipping tension crack locally parallel to the slope that can isolate some 10 m^3 blocks (Fig. 9).

Figure 10. Preliminary potential landslide inventory map.

Along with predisposing structural conditions also recent change of the stream flow, such as the rapid removal of 1–2 m of debris for the restoration of the ancient Roman pavement in the Siq floor, can have caused an increasing of tensile stress in the upper part of the block with development of displacement in the crack.

All the above geomorphological processes have been collected and elaborated through a Geo database; a preliminary potential landslide inventory map has been implemented (Fig. 10). The map reports types and magnitude of the collected phenomena.

5 GEOMECHANICAL ANALYSIS

The geomechanical characteristics of the Siq slope-forming rocks have been reconstructed with geotechnical field techniques and laboratory tests on core rock samples and blocks taken in the Umm Ishrin Sandstone Formation. The whole Siq has been divided in 15 sectors parallel to the main path orientation; a rock mass classification (Hoek, 2007, Hoek and Brown, 1988 and Hoek et al., 1992) for the right and left flanks of each sector has been calculated (Figure 11).

5.1 *Field survey analysis*

A geotechnical field survey has been conducted by implementing the following activities:

Figure 11. Siq sectors divisions.

- Geo-structural analysis of the rock block (orientation and characteristics of discontinuities);
- Geomechanical scan-lines technique in order to define and estimate the main geotechnical and geomechanical indexes and parameters (i.e. RMR, GSI, Q system) of the outcropping sandstone formations;
- Burton's profilometer test for reconstructing the joint profile and roughness;
- Collection of block samples for laboratory analysis;
- Field assessment of dry unit weight on sampled blocks;
- Schmidt-hammer test on joint surfaces and intact rock block for in-situ analysis of UCS.

UCS assessment from Point Load test on sampled blocks and comparison with in-situ data.

In situ and laboratory analysis are reported in the following Table 1 and Table 2.

Table 1. Geotechnical parameters estimated from in situ techniques.

Natural unit weight (KN/m^3)	JRC	UCS (MPA) (Schmidt hammer)	$\phi°$ (Tilt test)	UCS (MPA) (Point Load test)
19.16–21.68	4–6	–	37–43	105 (hard sandstone)
–	4–6	25–35	37–43	30 (soft sandstone)
GSI	c (MPa)		$\phi°$	E_m (GPa)
72	0.4		43°	12

Table 2. Synthesis of geotechnical parameters from laboratory test.

γ_{dry} (KN/m^3)	V_p (Km/s)	V_s (Km/s)	σ_n (MPa) Triaxial tests	σ_t (MPa) Brazilian tests
20.8	2.15	1.18	22.85	2.84
ρ_{dry} (Mg/m^3)	E_{sec} (GPa)	E_{tan} (GPa)	$K(\sigma_n/\sigma_t)$	ν_{dyn}
2.12	6.45	9.46	8.04	0.28

6 GEO-STRUCTURAL ANALYSIS

The mechanical behavior of rocks under stress is generally controlled by the conditions under which deformation takes place and by the inherent rock properties. Stress condition of the Siq slope-forming rocks have promoted different types of discontinuities in the sandstone rocks.

This is due to the strain behavior (e.g. lateral unloading due to water erosion coupled with tectonic uplift) and to the typical petrographical and physical properties of the rocks (e.g. chemical and mineralogical composition, grain size, shape, thickness, homogeneity, porosity, permeability, type of cement).

The presence of brittle sandstone in the Siq area and in Petra, as a general rule, promote a block composition of rocks due to high frequency of discontinuities of various origin (i.e. faults, joints) (Fig. 12). A geomechanical characterization of discontinuities has been done along the entire Siq in order to provide structural setting of the area and define the master joints. All geomorphological processes and slope instability, acting along the Siq of Petra, are the results of different structural combination of the main joints families. The

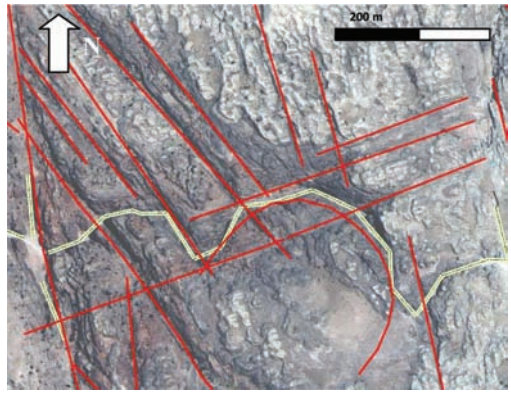

Figure 12. Sketch of the master joints and regional fault of the Siq area by aerial photo interpretation and field survey.

analysis has been performed both through satellite image photo interpretation (Fig. 12) coupled with a geomechanical and structural field survey. In our analysis, although preliminary and not exhaustive of discontinuity survey of the whole Siq, some relevant blocks and parts of the slopes of the Siq have been analysed in geo-structural terms (Delmonaco et al., 2012).

In those location a particular attention has been done to the discontinuity orientation. All data collected for blocks/slope areas in the Siq, have been analysed and represented with the geo-structural software DIPS® and reported in the Fig. 13. Generally in the Petra area straight, individual joints, with mostly vertical planes, can be followed in the field for long distances (up to 500 m).

The intensity of jointing is variable depending on distance from faults and strength of materials (i.e. higher within the siltstone sequences, lower within sandstone layers).

The trends of the joint systems in the area are controlled by, firstly, the post-Ordovician pre-Lower Cretaceous stresses which affected the Paleozoic rocks only, secondly, by the stresses which created the Dead Sea transform fault system (Miocene-recent) and, thirdly, by tectonics within the Ash Shawbak fold belt (Miocene) (Barjous, 1987).

The rose diagram shows that the major trend of joint systems ranges around a E-W directions (060–080° and 240–260°) with high slope angles (70–90°) exhibiting a trend parallel to local slope faces where the unstable blocks are located. These systems are in accordance with the dominant joint systems surveyed in the area that strike between

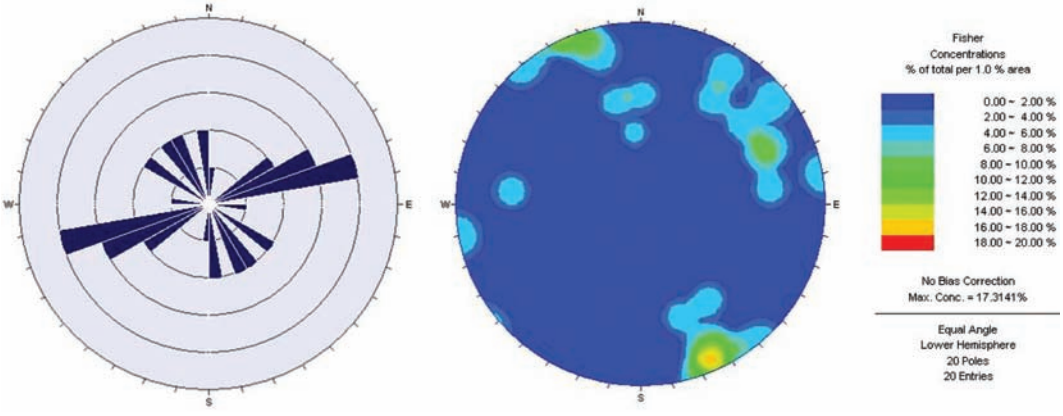

Figure 13. Rose diagram (left) and plot (right) of joints surveyed in some potential unstable blocks in the Siq.

60–70° and 160–179°. These systems are characteristic of the Umm Ishrin Sandstone and Disi Sandstone Formations (Jaser & Bargous, 1992). Also inclined joints, that represent the potential failure plane of sliding-mode blocks, are usually parallel to the main joint directions.

7 MONITORING SYSTEM PROPOSAL

According to the above results, and considering the morphological setting and slope instability processes, the following monitoring techniques will be proposed for the monitoring of the Siq in Petra:

- Satellite Squee SARTM analysis with the technique of permanent scatter. Such technique will allow the recostruction of the evolution and deformation of Petra area in the last decade (Fig. 14);
- terrestrial digital photogrammetry;
- reflectorless total station for monitoring of slope/blocks deformation (Fig. 15);
- installation of automatic extensometers, inclinometers and meteorological station with wi-fi data transmission.

During a field mission undertaken in June 2011, a manual crack gauge network system, formed by fissurimeters and manual extensometers, has been also installed on discontinuities forming the main potentially unstable blocks surveyed in the Siq. Over twenty discontinuities are actually under control; nevertheless the number of measurements taken is still insufficient to define a displacement trend.

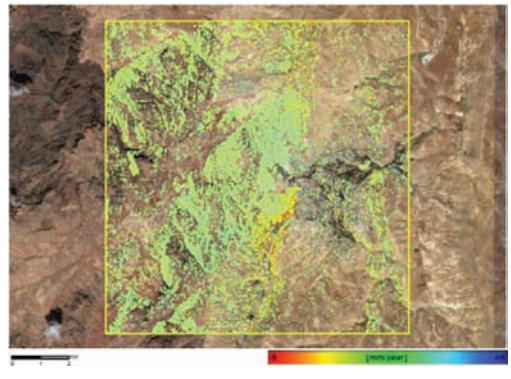

Figure 14. Preliminary results—2D view. Average velocity field (mm/year) (courtesy from TRE).

Figure 15. Selection of geodetic monitoring stations in the Siq.

8 CONCLUSIONS

According to the main geomorphological, geostructural and geotechnical evidences of the Siq of Petra slope-forming rocks, the following observations can be done:

- actual and/or potential instability processes in the Siq are the result of a combination of different predisposing factors in the area such as: lithology; presence, frequency and orientation of discontinuities vs. slope orientation;
- the potential instability processes and mechanisms observed along the Siq slopes can be referred to three main failure modes (or their combination): planar failure; wedge failure and toppling failure;
- such a instability processes differ along the Siq path both in terms of activity, namely their state (temporal evolution), distribution (spatial evolution), style (combination and repetition of different failure mechanism) and as magnitude (landslide intensity and potential volumes);
- present and/or potential instability processes in the Siq are the result of a combination of different predisposing factors such as: lithology; presence, frequency and orientation of discontinuities vs. slope orientation; physical and mechanical characteristics of slope-forming materials; morphological and hydrological dynamics; main weathering and erosion mechanisms;
- some of the main potential instability conditions detected and assessed need more accurate and specific analysis (slope scale risk analysis) in order to define landslide state in terms of intensity, potential evolution and impact;
- all detected landslide phenomena, according to the three distinct main failure mechanisms, can be classified in terms of magnitude and, hence, potential impact following three classes: large block phenomena (potential average volumes >10–15 m^3); medium block phenomena (potential average volumes between 3–5 m^3 and 10–15 m^3); small block phenomena (potential average volumes <3–5 m^3);
- a synoptical approach can consider: (a) non-structural measures (e.g. monitoring) for large blocks, (b) structural and non-structural (e.g. monitoring, consolidation, scaling) for medium-sized blocks and (c) structural interventions (e.g. scaling) for small unstable blocks, following a cost-benefit analysis.

ACKNOWLEDGMENTS

The present work is part of Rapid Assessment of the Siq of Petra project, funded by UNESCO. Authors are very grateful to dr. Anna Paolini, Director of UNESCO Amman Office and dr. Aysar Akrawi, Executive Director of Petra National Trust for their efforts on project implementation and continuous support in the field activities. We would like to express a special gratitude to Dr. Talal Akasheh (PNT-Cultech) and Dr. Bilal Khrisat (The Hashemite University) for cooperation on geological and structural field analysis. A profound gratitude to dr. Emad Hijazeen, Director of Petra Archaeological Park and eng. Tahani Sahli for support and assistance on project activities.

REFERENCES

Akasheh, T. 2000. Eine Datenbank fur Petra/A database for Petra. In: Kuehlenthal M., Fischer H. (eds.) *Petra-die Restaurierung der Grabfassaden/Petra-the restoration of the rockcut tomb facades*. ICOMOS-Hefte des Deutschen National-komitees, XXXIV. Karl M. Lipp Verlag, Munchen: 230–240.

Albouy, M., Deletie, P., Haguenauer, B., Nion S., Shreiner, D., Rewerski, J. & Seign, J. 1993. Petra, la cité rose des sables. La pathologie des grés et leur traitement dans la perspective d'une preservation et d'une restauration des monuments. In: Thiel M.-J. (ed.) *Conservation of stone and other materials*, 1, UNESCO/RILEM, E & FN Spon., London, 376–385.

Amireh, B.S. 1991. Mineral composition of Cambrian-Cretaceous Nubian Series of Jordan: provenance, tectonic setting and climatological implications. Sedim. Geol. 78: 267–283.

Amireh, B.S., Schneider, W. & Abed, A.M. 2001. Evolving fluvial-transitional-marine deposition through the Cambrian sequence of Jordan. Sedim. Geol. 89: 65–90.

Barjous, M. 1987. Structural study of the area between Petra and Al Showbak. Unpublished M.Sc. thesis, University of Jordan, Amman.

Barjous, M. & Mikbel, S. 1990. Tectonic evolution of the Gulf of Aqaba-dead Sea transform fault system. Tectonophysics 180:49–59.

Bender, F. 1974. Geology of Jordan. Gebrueder Bornstraeger. Berlin, p. 196.

Delmonaco, G., Margottini, C. & Spizzichino, D. 2012. Rock-fall hazard assessment in the Siq of Petra, Jordan. The Second World Landslide Forum, 3–9 October 2012, FAO, In: K. Sassa, P. Canuti, C. Margottini (eds.) *Landslide science and practice* Vol. 6, Inventory and hazard assessment. Springer, Heidelberg, 441–449.

Fizner, B. & Heinrichs, K. 1998. Evaluation of weathering damages on monuments carved from bedrocks in Petra/Jordan—a research project 1996–1999. Annual of the Department of Antiquities of Jordan 42: 341–360.

Franchi, R. 2002. A study of the natural environment and of the problems of conservation of the historical-artistic heritage in the area of Petra. In: Jedrkiewicz, S. (ed.): *Civilizations of the Past, Dialogue of the*

Present: Italian Research Mission in Jordan. Ambasciata d'Italia, Amman, 67–92.
Franchi, R. & Pallecchi, P. 1995. The sandstone of Petra, petrography and problems in conservation. In: Pancella, R. (ed.) *Preservation and restoration of cultural heritage*. Pancella, Losanne, 679–689.
Franchi, R., Savelli, D., Colosi, F., Drapp, P., Gabrielli, R., Moretti, E. & Peloso, D. 2009. Petra and Beida (Jordan): two adjacent archaeological sites up to an exploitation of geomorphology-related topics for a cultural and touristic development. Mem. Descr. Carta Geol. D'It. LXXXVII, 77–90.
Garfunkel, Z. & Ben Avraham, Z. 1996. The structure of the Dead Sea basin. Tectonophysics 226: 155–176.
Ginat, H., Enzel, Y. & Avni, Y. 1998. Translocated Plio-Pleistocene drainage systems along the Arava fault of the Dead Sea transform. Tectonophisics 284: 151–160.
Heinrichs, K. 2008. Diagnosis of weathering damage on rock-cut monuments in Petra. Jordan Environ Geol 56: 643–675.
Heinrichs, K. & Fitzner, B. 1999. Comprehensive characterisation and rating of weathering state of rock carved monuments in Petra/Jordan. Weathering forms, damage categories and damage index. Annu. Depart. Antiquities Jordan 43: 321–351.
Heinrichs, K. & Fitzner, B. 2000a. Deterioration of rock monuments in Petra/Jordan. In: Fassina V (ed.) *Proceedings of the 9th international congress on deterioration and conservation of stone*. Venice, 19–25 June 2000.
Heinrichs, K. & Fitzner, B. 2000b. Lithotipes of rock carved monuments in Petra/Jordan. Classification and petrographical properties. Annu. Depart. Antiquities Jordan 44: 283–312.
Hoek, E., Brown E.T. 1988. The Hoek-Brown failure criterion—a 1988 update. Proc. 15th Canadian Rock Mech. Symp. (ed. J.H. Curran), Toronto: Civil Engineering Dept., University of Toronto, pp. 31–38.
Hoek, E., Wood, D. & Shah, S. 1992. A modified Hoek-Brown criterion for jointed rock masses. Proc. Rock Characterization, Symp. Int. Soc. Rock Mech.: Eurock '92, (Edited by Hudson J.A.), London, Brit. Geotech. Soc., pp. 209–214.
Hoek, E. 2007. Practical Rock Engineering (2007 edition). http://www.rocscience.com.
Jaser, D. & Bargous, M.O. 1992. Geotechnical studies and geological mapping of ancient Petra city. Town Mapping Project, Bulletin 1, The Hashemite Kingdom of Jordan, Ministry of Energy and Mineral Resources, Natural Resources Authority, p. 62.
Mart, Y. 1991. The Dead Sea Rift: from continental rift to incipient ocean. Tectonophisics, 197: 155–179.
Paradise, T.M. 1999. Analysis of sandstone weathering of the Roman Theatre in Petra, Jordan. Annu. Depart. Antiquities Jordan 43: 353–368.
Paradise, T.M. 2002. Sandstone weathering and aspect in Petra, Jordan. Zeitung fur Geomorphologie 46(1): 1–17.
Paradise, T.M. 2005. Petra revisited: an examination of sandstone weathering research in Petra, Jordan. In: Turkington AV (ed.) *Stone decay in architectural environment.* GSA Spec. Pap. 390: 39–49.
Quennel, A.M. 1951. The geology and mineral resources of (former) Trans-Jordan. Colon. Geol. Mineral Resour. Lond. 2: 85–115.Mart, Y. 1991. The Dead Sea Rift: from continental rift to incipient ocean. Tectonophisics 197: 155–179.
Selley, R.C. 1972. Diagnosis of marine and non-marine environments from the Cambro-Ordovician sandstones of Jordan. J. Geol. Soc. 128: 135–150.
Sneh, A. 1996. The Dead Sea Rift: lateral displacement and down-faulting phases. Tectonophisics 263: 277–292.

Geotechnical Engineering for the Preservation of Monuments and Historic Sites – Bilotta, Flora, Lirer & Viggiani (eds)
© 2013 Taylor & Francis Group, London, ISBN 978-1-138-00055-1

Historic and non-historic building impact assessment methodology for major tunnelling infrastructure projects

M. Devriendt
Arup, London

E. Palmer
Consultant

R. Hill & D. Lazarus
Arup, London

ABSTRACT: Recent large tunnelling infrastructure projects in the UK have used the proposals defined by Burland (1995) to appraise impact on buildings. On recent projects such as Crossrail, a more refined approach of accounting for the heritage and structural sensitivity of a building has been introduced when appraising impact. This paper appraises the benefits and potential drawbacks of using these structured approaches to assessing impact on buildings. It focuses on the development of a robust appraisal methodology for historic buildings based on co-ordinated assessments from tunnelling, geotechnical, structural and heritage specialists.

Heritage buildings are necessarily subject to more detailed assessment in the UK due to the requirements of protection and planning. The methodology developed following Crossrail and discussed in this paper has culminated in an approach which uses heritage significance, structural form and condition of the asset alongside ground movement calculations to allow a rigorous approach to assessing potential impact. It also allows for efficient discussion of mitigation and design requirements. Recommendations for the use of this methodology as best practice during major infrastructure projects are provided.

Recent project experience is used to describe how the existing published methods can be refined and improved to achieve a more cost and time efficient assessment of impact to large numbers of buildings. In particular the use of different inspection techniques and software such as Google Street view for carrying out virtual walkover surveys and classifying buildings into different generic categories is explored. This enables the use of screening methods to be applied to specific cases such as some load bearing masonry and some framed buildings that are not necessarily appropriate to idealise as an elastic beam in accordance with the proposed methodology described by Burland (1995). Recommendations for the effective use of GIS and database systems alongside assessments are provided.

1 INTRODUCTION

1.1 *Background*

For large tunnelling infrastructure projects it is common to use a phased methodology for assessing buildings affected by ground movement from the works. The methodology proposed by Burland (1995) has been used extensively in the UK comprising three increasingly refined phases of assessment. The first phase of these assessments comprises a simple screening assessment considering greenfield movements and identifying buildings where the settlement is greater than 10 mm or 1:500 gradient. For buildings that exceed either of these criteria, a Phase 2 assessment is carried out. For the Phase 2 assessment the building façade or walls are represented by a simple elastic deep beam and equations are used to calculate the tensile strain based upon the imposed greenfield vertical and horizontal ground movements. If the imposed tensile strain exceeds 0.15% or there is concern over sensitive elements of the building requiring further investigation, a detailed Phase 3 assessment is carried out. The structure of the building is considered further for the detailed assessment and greater consideration may be given to the effects of soil-structure interaction. Assessments generally in accordance with this methodology have been used successfully in London on projects such as the Jubilee Line Extension, Channel Tunnel Rail Link and Crossrail.

1.2 *Recent developments*

Given the number of buildings required to be assessed on large tunnelling projects, generic methods for screening out buildings at less risk of damage have been developed, such as the method proposed by Harris and Franzius (2006). These methods include carrying out analysis by idealising a building facade or wall as an elastic deep beam from Phase 2 assessments as proposed by Burland (1995). Transects normal to the running tunnel alignment are considered at discrete spacings of say 100 m. A range of building geometries are then assessed at these transect positions enveloping the potential dimensions of buildings that may exist. The highest tensile strains are reported for each transect and compared against strain levels proposed by Burland (1995) delineating boundaries between damage category. In particular a tensile strain of 0.15% delineating the boundary between Slight and Moderate is considered. Tensile strains in excess of this level would warrant further consideration of the actual building geometry relative to the construction works, more refined assessment and potentially mitigation measures.

For assessment of heritage listed buildings on Crossrail a further refinement was proposed to the process defined by Burland (1995). This refinement described by Mason and Hansraj (2005) included assessing the sensitivity of significant features of the building to ground movements.

This paper describes further developments that can be applied for these screening methods and includes suggested improvements for heritage building assessments. The methods described in this paper generally follow the methodology proposed by Mason and Hansraj (2005), but has been supplemented on recent large tunnelling infrastructure building assessment commissions by considering the existing condition of buildings. The proposals described in this paper therefore represent ones that have been applied in practice and have demonstrated improvements relative to conventionally published methods.

2 GENERIC PHASE 2 ASSESSMENT

2.1 *Introduction*

The Harris and Franzius (2006) generic method provides a useful technique for screening out buildings rapidly. The elastic deep beam model proposed by Burland (1995) for Phase 2 assessments has been calibrated against case studies considering load bearing masonry structures and framed structures, see Burland & Wroth (1974) and Boscardin & Cording (1989).

Whilst the correlation between the proposed elastic deep beam model and the case studies provides a generally accepted method for carrying out screening assessments, there is a risk that some structures are more susceptible to damage impairing their serviceability or possibly causing more significant damage than the correlation proposes. Examples may include the following types of structures:

- swimming pools;
- structures housing sensitive telecommunication, radar or electrical equipment;
- structures founded on deep foundations with sensitive services such as cast iron pipes entrering the building;
- structures housing cantilever stone stairs (see Figure 1);
- structures housing sensitive mechanical equipment such as escalator trusses or turbines;
- structures on mixed foundations, eg. those that have been redeveloped but retained their original facade; and
- warehouse facilities with movement sensitive high racking facilities.

Charles and Skinner (2004) provide some quoted values from literature relating to acceptability to movement of some of these types of structures.

There is also concern that extrapolating the deep elastic beam analogy becomes tenuous with some modern frame structures with panelised or glazed facades.

As a result there is a risk that screening assessments carried out as part of a Phase 2 assessment adopting a deep elastic beam model may not reflect actual building behaviour and may not be conservative.

It is therefore proposed that generic Phase 2 assessments, such as that proposed by Harris and Franzius (2006) should be supplemented by some level of building specific inspection to provide confidence that the results are appropriate.

Figure 1. Cantilever stone staircase.

This will be of particular value in cases where the building has a high damage category from the Phase 2 assessment and/or is a building of heritage significance.

This process requires the judgement of an appropriately qualified and experienced structural engineer and ultimately may require a physical inspection of the property. There are, however, a number of progressive steps that allow a more rapid assessment of a large number of structures that will be more appropriate at different stages of a project.

2.2 *Building inspections*

2.2.1 *General*

There are various forms of building inspection that can be carried out to assist both the Phase 2 and 3 assessment processes.

For the Phase 2 assessment, the inspections can allow buildings to be identified into generic classes to facilitate the screening process. For example, those structures that are load bearing masonry and do not have features that are particularly sensitive to ground movements may form a given classification and fit into the generic assessment carried out in accordance with Harris & Franzius (2006). However, it may not be appropriate to classify certain framed structures in this manner and an alternative criteria for screening such as differential displacement from column to column may be proposed. An inspection will also allow those structures that are sensitive to movement to be identified for a more detailed Phase 3 assessment.

The various forms of inspection used to assist Phase 2 and 3 assessments can be broadly categorised into virtual walkovers, external and internal inspections.

2.2.2 *Virtual walkovers*

Recent improvements in the availability of satellite imagery via web-based viewers and photography mapping at street level offered by companies such as Google allow 'virtual walkovers' to be carried out. They allow rapid visual assessment of a large number of buildings from the safety of the office anywhere in the country/world. They can determine the number of storeys, cladding type and possibly structural form, potential existence of basement and age. The level of information provided by this method can also be limited. For instance, the condition can rarely be judged with any degree of accuracy, the image may be outdated (eg. building extended or even demolished), trees or vehicles may obstruct the image, and dating may not be conclusive. However, they often provide an opportunity to identify those structures that cannot be idealised as an elastic deep beam and require specific Phase 2 assessment against alternative criteria.

2.2.3 *External inspection*

This allows quick assessment of a relatively large number of buildings. It enables better judgement of age (for example from age plaques if present) and provides an opportunity to assess external condition or structural alterations/abnormalities. Where observations can be made from publicly accessible areas no time is lost in gaining property access. The number of buildings that can be assessed is however potentially limited by travel time to and between buildings. The ability to carry out visual inspections should consider the weather and personal safety (risks of theft, abuse, traffic). The value of external inspections is restricted in that internal condition/alterations cannot be judged. They are also limited in that age and structural form may be inconclusive (eg. retained facade).

2.2.4 *Internal inspection*

This allows better understanding of the structural form and condition both internally and externally. They provide an opportunity to identify possible alterations that are not evident externally. This type of survey is clearly restricted by the length of time taken to arrange access, travel to and inspect the structure.

The foundation type will rarely be determined by a visual inspection alone, although there is good guidance as to what would be expected for buildings of particular age and form. Dependent on the age of the property, record drawings or other archival information may exist. However for many listed buildings, records are not available. Again judgement is required giving consideration to the building's age, size, form of construction and geographical features (eg. warehouses sited next to a river are often founded on timber piles).

In summary, whilst visual inspections of buildings or inspections by appropriately qualified and experienced engineers still make an important contribution to assessing the impact of construction works on existing structures, 'virtual walkovers' allow significant savings in time relative to carrying out conventional building inspection surveys. It is suggested that much of the assessment work carried out as part of a Phase 2 assessment can be efficiently carried out by virtual surveys supplemented by a small proportion of targeted inspections by engineers.

3 PHASE 3 HERITAGE ASSESSMENT

3.1 *Introduction*

The structural, condition and heritage sensitivity methodology described in this paper is broadly in keeping with the methodology proposed by Mason and Hansraj (2005), however, it has been

further developed from experience of carrying out assessments on a recent large tunneling infrastructure project in the UK. The method has been developed in consultation with English Heritage and relevant local authorities for impact assessments.

The methodology treats each listed building as an individual case and considers the ground movements calculated at the structure's founding level. The nature of each building in terms of: a.) structural sensitivity; b.) heritage sensitivity; and c.) condition and evidence of previous repair, alteration and movement is taken into account during the scoring process. Scoring is split into these three assessment categories, ensuring that buildings which may have particular sensitivities have been accounted for.

A score is assigned to each of the above components and considered alongside the calculated building damage category obtained from the ground movement and structural impact assessment when appraising whether mitigation is necessary.

3.2 *Structural sensitivity background*

The assessment of the structural sensitivity of the listed buildings is based generally on the approach adopted for Crossrail, as outlined in Mason and Hansraj (2005). There is no formal standard which codifies this approach: it identifies a number of factors which may be accepted as being of significance in the building's response to ground movement (including the building's condition) and are then reviewed in conjunction with the magnitude of such movement.

It is likely that a significant proportion of structures will not adhere to the 'elastic deep beam' approximation. In reality structural features such as door and window openings, or recesses in plan create inherent stiff or weak areas that along with pre-existing cracks (discussed in 3.3) will affect how the structure will perform. Junctions between different parts of a building, often constructed at different periods are also significant. Examples of such factors are given in Table 1.

Differences in ground movement across a building footprint are more important than magnitude alone (eg. a building could settle uniformly by 50 mm and show no damage, whereas a relatively limited differential settlement could have significant impact on sensitive structural or heritage features such as decorative plaster or masonry with fine joints (see Fig. 2). Similarly, calculated settlements resulting in tilt will have varying impacts on structures of varying height and floor plan.

The building is given a structural sensitivity score, based on the inspection of the building and the calculated movements and damage category.

Table 1. Structural and heritage scoring matrix for listed buildings.

Score	STRUCTURE Sensitivity of the structure to ground movements and interaction with adjacent buildings	HERITAGE FEATURES Sensitivity to calculated movement of particular features within the building	CONDITION Factors which may affect the sensitivity of structural or heritage features
0	Masonry buildings with lime mortar and regular openings, not abutted by other buildings, and therefore similar to the buildings on which the original Burland assessment was based.	No particular sensitive features.	Good—not affecting the sensitivity of structural or heritage features.
1	Buildings not complying with categories 0 or 2, but still with some sensitive structural features in the zone of settlement eg.: cantilever stone staircases, long walls without joints or openings, existing cracks where further movements are likely to concentrate, mixed foundations.	Brittle finishes, e.g. faience or tight-jointed stonework, which are susceptible to small structural movements and difficult to repair invisibly.	Poor—may change the behaviour of a building in cases of movement. Poor condition of heritage features and finishes. Evidence of previous movement.
2	Buildings which, by their structural form, will tend to concentrate all their movements in one location (eg.: a long wall without joints and with a single opening).	Finishes which if damaged will have a significant effect on the heritage value of the building, e.g. Delicate frescos, ornate plasterwork ceilings.	Very poor—parlous condition of heritage features and finishes, severe existing damage to structure including evidence of ongoing movement. Essentially buildings where even very small movements could lead to significant damage.

Figure 2. Detail of terracotta facade and fine joints.

3.3 *Condition sensitivity background*

The general condition is reviewed from a structural inspection of the property and is graded as being good, poor or very poor. Pre-existing cracks may tend to act as points of weakness in a structure and be the focus for further cracking from future movement. Depending on the crack orientation and calculated movement, existing cracks may open further or close up. The poor condition may also be in areas of particular heritage interest. The condition is then related to the damage assessment score, to enable a judgement to be made as to whether the particular condition or specific defects of a certain building will make it more sensitive to the calculated movement.

The building is subsequently given a condition score, combining the ground movement damage assessment calculation with the observations on condition. The poorer the condition a building is, the higher its sensitivity is likely to be. However, if a building is in poor condition but structurally sound, and in an area where ground movement is calculated to be minimal, then its sensitivity due to condition will be low, and the works will not be expected to produce further deterioration.

3.4 *Heritage sensitivity background*

The proposed Phase 3 listed building assessment process is generally based on the approach proposed by Mason & Hansraj (2005). Refinements have been proposed to take account of improvements developed during the application of the approach on recent impact assessment work on a large tunneling infrastructure project.

It is accepted within UK heritage policy and legislation that it is often the 'special interest' of a historic building which is the reason for its designation. Therefore, the proposed approach identifies each feature, ensuring that the assessment relates directly to the special interest of each building, and the risk of damage to that interest and therefore to the heritage significance of the building.

It is proposed that the heritage assessment should be carried out at the same time and in conjunction with the ground movement impact assessment. This allows for a realistic heritage sensitivity score to be allocated without the need for re-assessment upon review of the ground movements.

An individual, building-specific appraisal, with external and internal visual survey of the building is carried out and this is complemented by a desk based study. Scoring is based on the building's structural form, sensitive features, fixtures and finishes, and the ground movement assessment results.

For example, a building may have a very significant façade, but this façade in its composition may not be sensitive to the calculated ground movements. Conversely, another building may have internal plasterwork of special interest within the context of that building, but of no great quality; this plasterwork however is likely to be more sensitive to the calculated ground movements and therefore incur a higher sensitivity score.

3.5 *Combining to produce overall building score*

The matrix in Table 1 is a tool, to be used in conjunction with the results of the various assessments. The scores are used to guide judgments for the individual buildings.

However the structural, heritage and condition assessment is not purely a scoring process, more an integrated review of the available information.

The scores from the building damage, structural sensitivity, condition, and heritage sensitivity assessments are combined to produce an overall score for each building. The overall scoring process is described diagrammatically in Figure 3.

Where the combined score is 3 or greater, consideration is given to whether mitigation measures would be appropriate. If the potential for damage is considered to be unacceptably high then judgment must be made as to whether mitigation is possible and appropriate. When considering mitigation, account must also be taken for the potential negative impact it may have. For instance it is possible for the mitigation measures (underpinning, strengthening, grouting etc.) to result in greater damage to the building fabric than the settlement from the construction works. The assessor must also be aware of scenarios where small movements are calculated, but non-zero scores are attributed to the structural

and heritage sensitivity and condition elements of the scoring. In such situations it may be preferable to avoid pre-emptive mitigation and repair any damage if it occurs using appropriate materials and techniques after the ground and structural movements have taken place.

However, the ability to repair the building and particularly to restore heritage features back to their original condition must be borne in mind if adopting this approach. Consideration must be given to the ease and cost of repair including any consequential losses that may arise from carrying out the repair work.

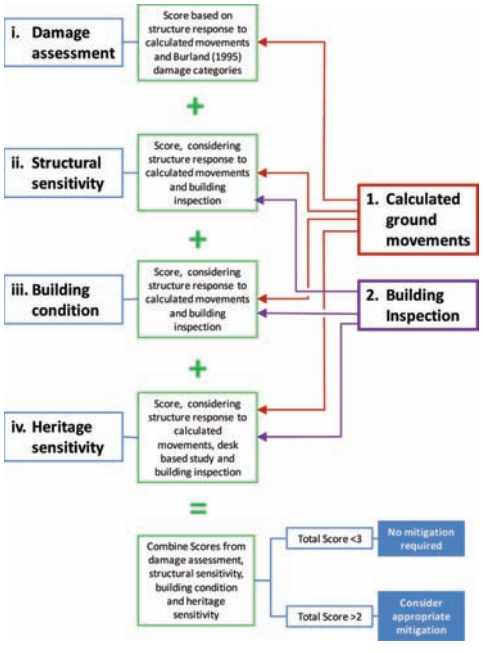

Figure 3. Overall listed building assessment process.

4 USE OF DATABASE AND GIS BASED SYSTEMS

For tunnelling infrastructure schemes affecting many buildings or other 3rd party properties, efficiencies can be gained and errors minimised by managing the inputs and outputs of the various phases of assessment by using databases. Consideration should be given to the fields of data that the database is required to store at the outset. Viewing of the data within the database is commonly carried out by linking the database to a Geographical Information System (GIS). Further efficiencies can be gained by creating project deliverables from these systems. Typically drawings including settlement contours, building type (heritage listing) and building damage categories can be readily generated with an appropriate mapping background, see Figure 4. In addition, if a classification system has been used to assist the damage assessment

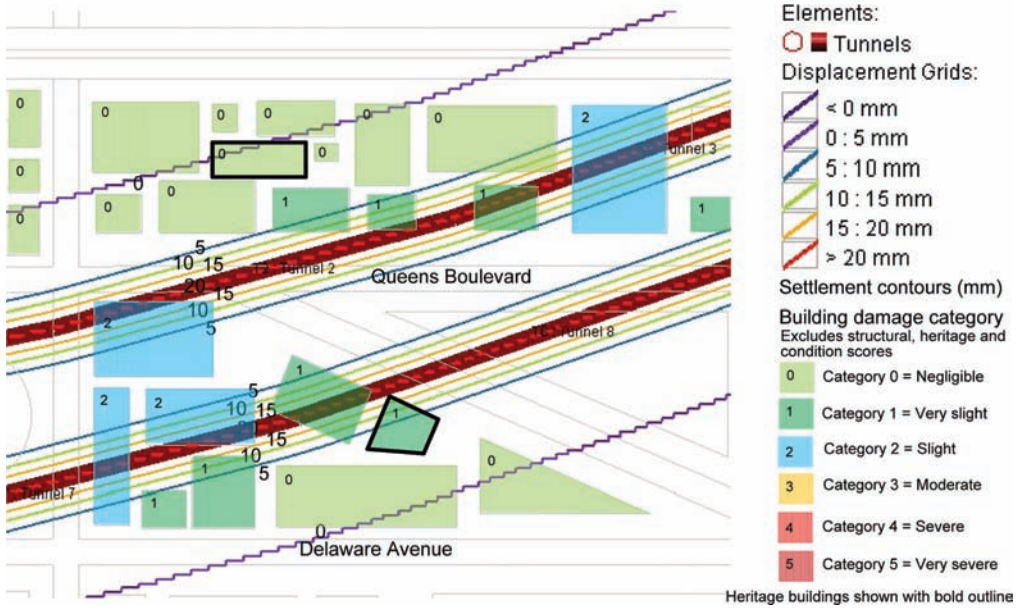

Figure 4. Example damage assessment plan produced by GIS.

process as outlined in Section 2.2, further layers can be developed to show how the buildings have been assessed and categorised. The contents of the database can be used to identify classifications of building damage and sections of impact assessment reports can be automatically generated.

A relatively sophisticated geospatial database that offered significant time saving and benefit when carrying out the impact assessment work on the Crossrail project is described by May and Budden (2010). The use of these types of system, particularly when linked with specifically designed ground movement and impact assessment software such as OASYS Xdisp that has specific features to interface with CAD and GIS software, enable savings to be made, see Devriendt et al. (2012). This is particularly the case when the tunnel alignment for a project changes in an iterative manner. The time and cost savings associated with updating deliverables as a consequence of alignment change from these systems offers great benefit relative to the more labour intensive working methods that were common practice 10 to 15 years ago.

5 CONCLUSIONS

This paper has identified recent developments based on project based experience for an appropriate methodology to assess the impact from ground movements on historic and non-historic buildings as part of large underground construction projects.

For both Phase 2 and Phase 3 assessments, it is recommended that a progressive strategy is employed for carrying out surveys comprising both desktop based 'virtual surveys', external and internal surveys. This should be carried out alongside the phased process of damage assessment. It is recommended that for historic building assessment, the nature of each building should be assessed in terms of structural sensitivity, heritage sensitivity and condition including evidence of previous repair, alteration. This approach gives a robust assessment of the risk to the significance of historic buildings, in line with UK policy and legislation regarding designated heritage assets.

When the input and output parameters from the above assessments is structured in an appropriate manner, the use of GIS software and databases can offer significant time savings when carrying out work on large infrastructure projects.

REFERENCES

Boscardin, M.D. & Cording, E.J. *Building Response to Excavation-Induced Settlement*, ASCE Journal of Geotechnical Engineering, Vol. 115, No.1, pp. 1–21, 1989.

Burland, J.B. & Wroth, C.P. *Settlement of buildings and associated damage*. Proceedings of a Conference on Settlement of Structures, Pentech Press, London, England, pp. 611–654, 1974.

Burland, J.B. 1995. *Assessment of risk of damage to buildings due to tunnelling and excavation.* Proceedings of 1st International Conference on Earthquake Geotechnical Engineering, IS—Tokyo.

Charles, J. & Skinner, H. 2004. *Settlement and tilt of low rise buildings.* Geotechnical Engineering 157. pp. 65–75.

Devriendt, M. Watterson, E. & Gates, J. 2012. *Automatic cost saving.* Ground Engineering, June 2012, p. 18.

Harris, D.I. & Franzius J.N. 2006. *Settlement assessment of running tunnels—a generic approach.* Geotechnical Aspects of Underground Construction in Soft Ground, pp. 225–230.

Mason, J. & Hansraj, M. 2005. Crossrail Line 1. *Assessment of settlement impacts on the built heritage.* Technical report, Crossrail reference 1E0317-G0E00-00001.

May, I. & Budden, R. 2010. *Award for Innovation and Best Practice (Private Sector). Association for Geographic Information* AGI) awards 2010: http://www.atkinsglobal.com/~/media/Files/A/Atkins-Global/Attachments/sectors/information-communications/library-docs/technical-papers/agipri-1.pdf.

This page intentionally left blank

Geotechnical Engineering for the Preservation of Monuments and Historic Sites – Bilotta, Flora, Lirer & Viggiani (eds)
© 2013 Taylor & Francis Group, London, ISBN 978-1-138-00055-1

Dynamic identification and seismic behaviour of the Ghirlandina tower in Modena (Italy)

A. Di Tommaso
Università di Bologna, Italy

R. Lancellotta, D. Sabia & D. Costanzo
Politecnico di Torino, Italy

F. Focacci
Università eCampus, Italy

F. Romaro
Università IUAV di Venezia, Italy

ABSTRACT: This paper presents a simplified vulnerability assessment method for masonry towers taking into account the soil-structure interaction. The soil-structure interaction model is based on *in situ* investigations, defining a detailed soil profile and the relevant mechanical parameters, aimed at capturing the expected behaviour during seismic events. In particular an upper and lower soil stiffness, appropriate for low and high intensity seismic events have been considered, and a validation of upper values was also performed throughout an identification analysis, based on vibration records of the tower. Limit analysis method was then applied to identify the collapse mechanisms geometry, under the assumption that masonry is a no-tension material. This implies that at the limit of overturning, a part of the masonry will remain attached to the base and a stress-free diagonal surface of fracture will form.

1 INTRODUCTION

The Ghirlandina tower and the Cathedral of Modena are part of the UNESCO site of Piazza Grande; during the last decade there has been an increased interest towards the potential seismic vulnerability of the tower, by also considering its interaction with the Cathedral.

The Ghirlandina tower is a square based (side: 10,8 m) structure, 87 m high, with a hollow cross section, thicker on the corners because of the presence of four masonry pillars as shown in Figure 1. In the inner part, an open stair runs along the tower from the base to the higher part where the belfry and the spire roof complete the structure (Figure 4).

The tower is characterized by a tall and slender spire built on its top and preciously decorated (ghirlandina), defining its slender architectural appearance.

The masonry diaphragms built in the tower are: the vault on the first floor, the floor of the Torresani cell and the vault above the belfry (the deck instead is a timber structure). At ground level, two masonry arches connect the tower with the adjacent cathedral.

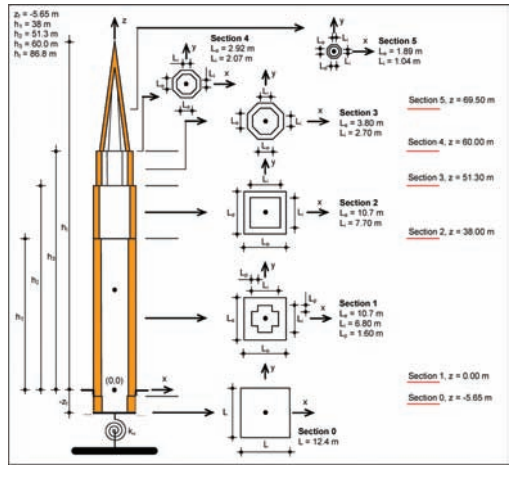

Figure 1. Geometrical model of the tower.

The tower's verticality has been corrected several times during different phases of construction: it is in fact possible to observe, along the façades, segments of variable leaning as signs of corrections

for tilting problems. The tower today presents a visible leaning, in particular on the S-W corner where the masonry arches connect the tower to the cathedral.

The construction of a tower is a great structural effort, and its leaning in fact hides some problems related to the interaction with the foundation soil, that are sometimes not so evident at first glance. It's important to remember that during the first stage of construction the tower could not have been so far from a bearing capacity collapse, due to a lack of soil strength, and could have safely survived thanks to some delay or interruption in the building process. Therefore, it is of paramount interest to get a full description of the tower's history and to highlight the construction stages and rest periods that allowed the foundation soil to improve its strength, during the consolidation process under constant external load, and that allowed the tower to be successfully finished (see Labate, 2009; Dieghi, 2009; Lancellotta, 2012).

At the same time, the danger of a leaning instability as related to the lack of stiffness of the soil as well as the seismic vulnerability are of paramount interest. Moving from these arguments, the aim of this paper is to provide a picture of the subsoil conditions (namely soil profile and relevant mechanical parameters), that have a major role in defining the seismic behaviour by taking into account the influence of soil-structure interaction, and to highlight the most relevant potential collapse mechanisms arising from expected seismic actions.

2 GEOTECHNICAL ASPECTS

Since 1980 the town council of Modena has promoted studies and investigations related to the subsidence of the Modena alluvial plain (Russo, 1985; Cancelli, 1986; Cancelli, Pellegrini, 1984; Pellegrini, Zavatti, 1980; Righi, 1980). In addition to these studies, it is relevant to outline that the Modena alluvial plain is characterized by a unique abundance of archaeological sites, and that the related interest in these promoted research on the Quaternary sedimentation of the Modena plain (Cremaschi, Gasperi, 1989; Fazzini, Gasperi, 1996; Lugli *et al.,* 2004). More recently, the increased interest towards the potential seismic vulnerability of the tower claimed for the assessment of a detailed soil profile and the relevant mechanical parameters. In this respect, a rather comprehensive site investigation was planned in September 2007 and December 2008 as described in details by Lancellotta (2009, 2012), so that at present we are able to summarize the relevant aspects as follows.

The soil profile down to the investigated depth of 80 m (Fig. 2) is composed of a first horizon of

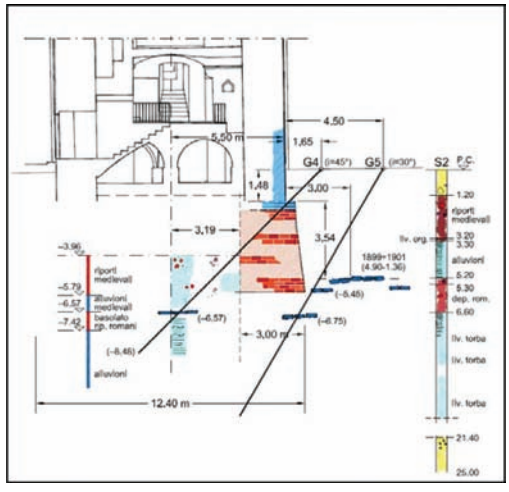

Figure 2. Details of soil profile and foundation of Ghirlandina tower (Lancellotta 2009).

medium to high plasticity inorganic clays, with an abundance of *laminae* of sands and peat, only a few millimetres thick. The upper portion of this horizon, whose thickness ranges from 5 to 7 meters, is known as Modena Unit and is linked to the flooding events (of post-Roman age) produced by minor streams (T. Fossa-Cerca).

The subsequent underlying horizons, ranging in depth from 22 to 54 m (Figure 3), represent the result of a complete transgressive-regressive cycle: the fine-grained sediments, belonging to the horizon known as Niviano Unit, were deposited during the penultimate interglacial cycle, and the superimposed coarse-grained materials, belonging to the Vignola Unit, are linked to transport activities of the Secchia River.

A second horizon of coarse-grained materials is encountered at depths ranging from 54 to 63 m, and thereafter a fine-grained materials horizon is found down to a depth of 78 m, here again characterized by a diffuse presence of *laminae* of sand.

The soil profile, shown in Figure 3, has been complemented with the results of cross-hole tests, because of their non-invasive character. This allows for preservation of the initial structure of soil deposits as well as the influence of all diagenetic phenomena contributing to a stiffer mechanical response, and for this reason the cross-hole test represents one of the most reliable methods of determining the shear modulus at small strain amplitude.

In addition, when defining the seismic design spectrum, the results referred to in Figure 3 contributed to classify the subsoil into class C, according to EC8 and Italian (NTC 2008) Codes.

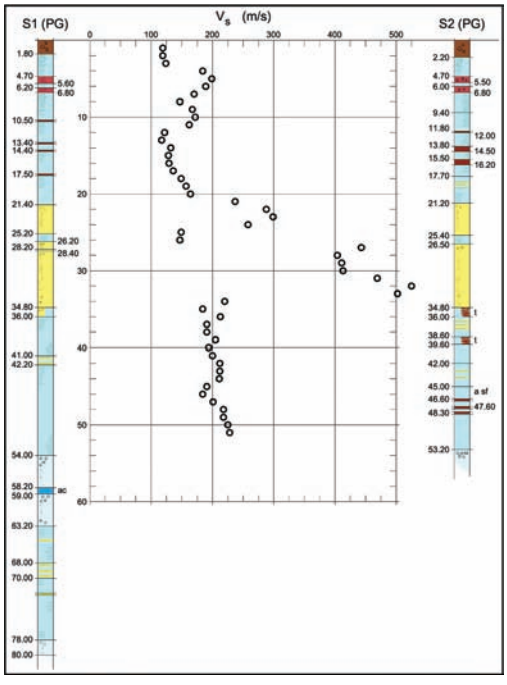

Figure 3. Cross-hole tests (Lancellotta, 2009).

3 SOIL-STRUCTURE INTERACTION

Seismic analysis is strongly dependent on the soil response, and in order to model it we rely on the so-called macro-element approach (Desideri, Viggiani 1994; Hambly, 1985; Marchi *et al.*, 2011; Heyman 1992; Lancellotta, 1993; Marchi, 2008; Nova, Montrasio, 1995). This approach is aimed at representing the soil response in terms of generalized forces and related displacement components, i.e. a formulation suitable for soil-structure interaction, moving from advanced hardening plasticity, in order to account for the irreversible and non-linear soil behaviour. As a consequence of such non-linearity, in the present analysis two assumptions regarding the rotational stiffness were used.

1. Moving from the shear wave velocity equal to v_s = 125 *m/s*, a small-strain shear modulus has been deduced:

$$G_o = \rho v_S^2 = 28\ MPa \tag{1}$$

This value refers to free field conditions, so that it has been corrected in order to account for the stress level induced by the tower ($G_o = 44\ MPa$) by considering a soil element at a depth of 3*b*/2, as suggested by the stress path method (Lambe and Withman, 1969).

Finally, taking into account the strain level, the operational value was estimated to be equal to G_{ep} = 7.26 *MPa*. The corresponding elasto-plastic rotational stiffness being (Gazetas, 1991)

$$K_\alpha = \frac{3.6Gb^3}{1-\upsilon} = 1715.96 \cdot G = 1245788\ t \cdot m \tag{2}$$

where 2*b* = 12.40 m is the foundation width and *v* is the Poisson ratio.

This value was further increased in order to account for the foundation depth the related coefficient being (Gazetas, 1991):

$$f_D = \left\{1 + 1.26\frac{d}{b}\left[1 + \frac{d}{b}\left(\frac{D}{d}\right)^{0.2}\sqrt{\frac{b}{l}}\right]\right\} = 3.19 \tag{3}$$

where:

2*b* and 2*l* are the foundation sides;

D is the founding depth;

d is the fraction of *D* that contributes to the constraint (here assumed equal to *D*).

By using this coefficient and considering that *d*/*b* = 5.65/6.2 = 0.91; *d*/*D* = 1 (see Figure 2) a corrected stiffness was obtained equal to:

$$K_\alpha = \frac{3.6Gb^3}{1-\upsilon} \cdot 3.19 = 3.97 \cdot 10^6\ t \cdot m \tag{4}$$

that, is appropriate for a strong seismic motion because of the considered strain level.

2. In addition, an upper bound value was estimated by using the elastic shear modulus, moving from the assumption that soil behaviour could still be dominated by an elastic response due to creep hardening:

$$K_\alpha = \frac{3.6Gb^3}{1-\upsilon} \cdot 3.19 = 24 \cdot 10^6\ t \cdot m \tag{5}$$

This value is appropriate for a low intensity seismic events.

4 IDENTIFICATION ANALYSIS AND PARAMETERS OPTIMIZATION

Although the above values of the rotational stiffness have been obtained by using a rational procedure, it is rather difficult to validate them, by considering the 3D nature of the problem, as well as the effectiveness of the soil contact along the vertical sides of the embedded foundation. In this respect, a rather significant contribution comes from an

experimental identification analysis, performed in the presence of ambient vibration.

This was done by collecting time histories of the components of the motion being measured along the coordinate axes x, y and z by means of accelerometers, located as shown in Figure 4.

Then, in order to extract from these measurements modal frequencies, shapes and damping parameters of the structure, a Stochastic Subspace Identification Method (Van Overschee, De Moor, 1996) was used. Moreover the emphasis was on the assessment of mode shapes, that are considered more relevant than the frequencies itself. (also see Aoki *et al.*, 2007, 2008 for Model-Updating techniques).

As an example of mode shapes, in Figure 5 the deformation modes as detected on the plane (z, y) parallel to the Cathedral nave and on its orthogonal plane (x, y), are shown, the associated frequencies being 0.74 Hz and 0.85 Hz.

Both of them are of relevance, because the first one outlines the rotation at the tower basis due to soil deformability, whereas the second one depends on the presence of the arches connecting the Tower and the Cathedral.

In Figure 6 the first two modal shapes related to vibrations along the tower axis are also shown, the related frequencies being now 4.51 Hz and 9.81 Hz, and here again the displacements at the tower basis outline the contribution of soil deformability.

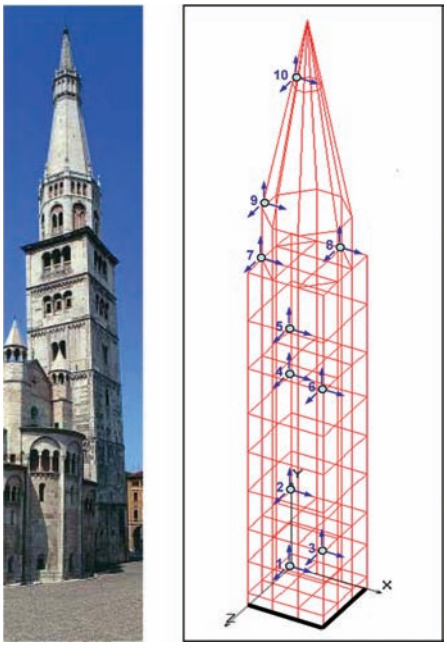

Figure 4. The Ghirlandina tower and the position of accelerometers used for identification analyses.

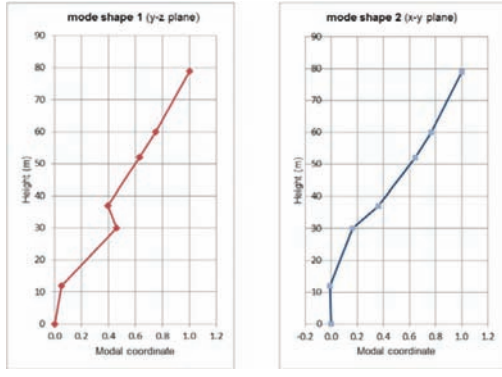

Figure 5. Mode shape as measured on the (z, y) and the (x, y) plane.

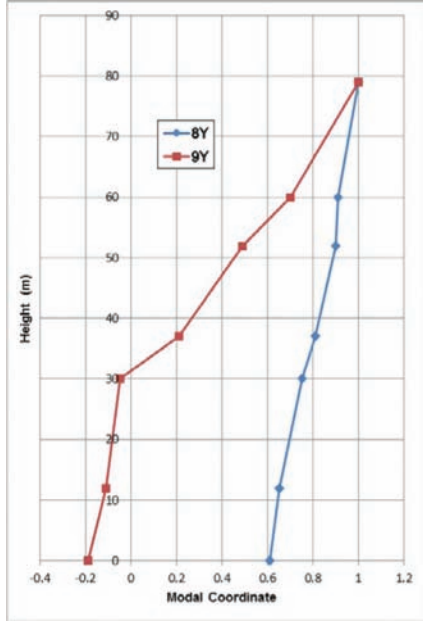

Figure 6. Mode shapes associated to longitudinal vibrations.

The main conclusion reached is that the soil structure interaction cannot be neglected, in contrast to most of published identification analyses that usually assume the structure with rigid constraint at its base.

Note that these latter results (i.e. longitudinal mode shapes and related frequencies) are particularly relevant because they allow to make an estimate of the lower bounds of both the soil and the structure stiffness in a simple but effective manner.

Let first assume the tower as a rigid body resting on a deformable soil, then frequency and the soil stiffness will be linked through the relation:

$$f = \frac{1}{2\pi}\sqrt{\frac{K_{yy,\,lower}}{M}} \tag{6}$$

being K_{yy} the axial stiffness of the soil-foundation system and M the tower mass. Since $M = 8525 \cdot 10^3\ kg$ and the measured frequency is $f = 4.51\ Hz$ one gets

$$K_{yy,\,lower} = 6.84\ GN/m$$

On the contrary, by assuming the soil as a rigid constraint while the tower is being represented with beam elements and lumped masses, a lower bound of the masonry modulus can be estimated, this being equal to:

$$E_{m,\,lower} = 1.7\ GPa$$

Obviously, soil and masonry deformability both contribute to the dynamic response of the structure, so that an optimization analysis has been performed, by considering bending and axial modes, as it is shown in Figures 7 to 11.

From these results we can deduce that the first modes (both bending and longitudinal ones) are sensitive to soil stiffness, whereas the higher modes depend on masonry deformability and, as it is shown in Figure 12, we can optimize the response of the soil-structure system by using the masonry modulus E_m ranging from 3 to 4 GPa and the following values of the axial and rotational soil stiffness

$$K_{yy} = 7.8\ GN/m$$

$$K_{\alpha} = 240\ GN \cdot m/rad$$

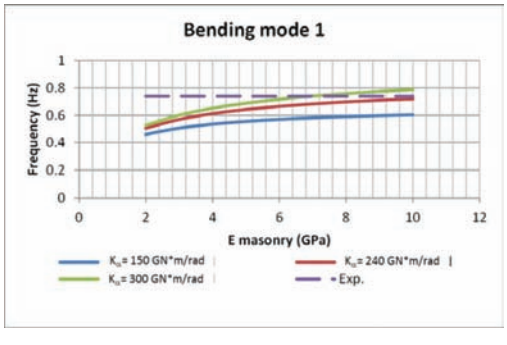

Figure 7. Frequency dependence on masonry and soil stiffness.

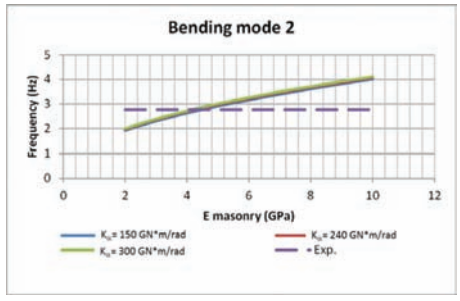

Figure 8. Frequency dependence on masonry and soil stiffness.

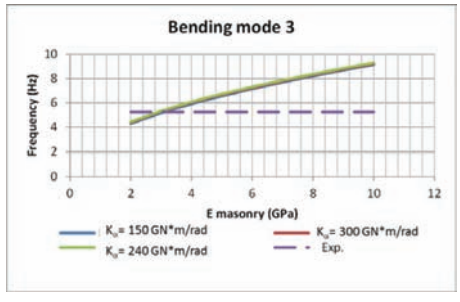

Figure 9. Frequency dependence on masonry and soil stiffness.

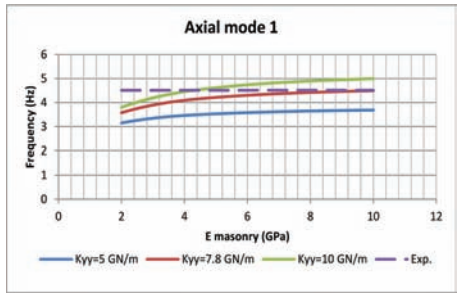

Figure 10. Frequency dependence on masonry and soil stiffness.

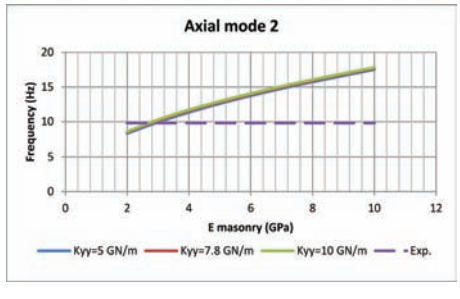

Figure 11. Frequency dependence on masonry and soil stiffness.

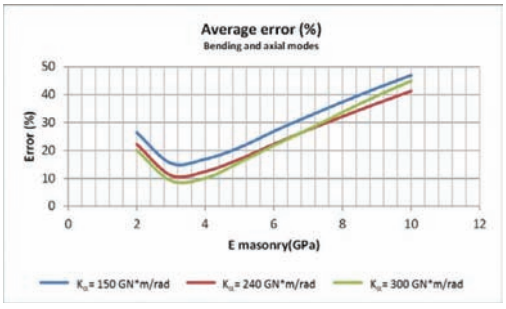

Figure 12. Average errors.

Note that the latter value is in agreement with the upper bound mentioned in the previous section, so that it can be considered as representative of an elastic response, to be used with reference to serviceability limit states or in presence of low intensity seismic events.

5 SEISMIC DEMAND AND SPECTRAL ACCELERATION

According to the soil rotational stiffness $K_{\alpha 1} = 3.97 \cdot 10^6$ *t·m* (high intensity seismic events) and $K_{\alpha 2} = 24 \cdot 10^6$ *t·m* (low intensity seismic events) and considering the model represented in Figure 1 in which the tower is considered as a rigid body, the following periods and frequencies can be evaluated:

$$K_{\alpha 1} \rightarrow T_1 = 3.44 \text{ s} \rightarrow f_1 = 0.29 \text{ Hz}$$
$$K_{\alpha 2} \rightarrow T_2 = 1.40 \text{ s} \rightarrow f_2 = 0.72 \text{ Hz}$$

Accordingly, the following values of spectral accelerations can be expected (Figure 13):

$$S_1 = S_d(T_1) = 0.025 \text{ g}$$
$$S_2 = S_e(T_2) = 0.07 \text{ g}$$

where $S_d(T)$ is the SLV design spectrum and $S_e(T)$ is the SLD design spectrum as defined by the Italian Code (NTC 2008).

Both SLD and SLV refer to a return period of 475 years, but the probability target is respectively of 63% and 10%, so that SLV introduces a structural factor $q = 2$, while for $S_e(T)$ $q = 1$.

6 SEISMIC CAPACITY

Seismic capacity of the tower was calculated according to Italian code prescriptions (NTC 2008) following the collapse mechanisms approach. Mechanisms involving an "opening" of the structure along the existing vertical cracks were not included because in order to guarantee a unitary behaviour of the tower a preventive intervention with tie-rods holding together opposite walls was made.

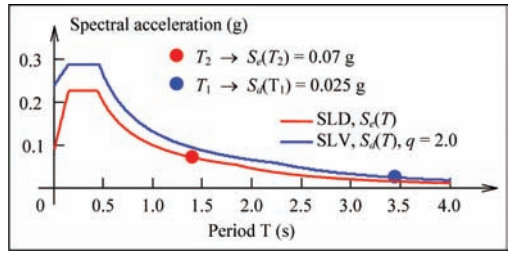

Figure 13. Spectral accelerations.

The collapse mechanisms are identified by the geometry of the overturning block and by the position of hinges. In this analysis an overturning block defined by a diagonal fracture surface is considered.

The simplified geometrical model shown in Figure 1 is considered. The main discontinuities of the cross section are included in the model, windows and openings are ignored and a hollow base cross-section is assumed.

Masonry compressive strength, considering the results of sonic test and the heterogeneity of calculated velocities, is assumed as 3 *MPa*.

Leaning of the tower (1 degree) has also been taken into account considering the effective position of the centre of mass.

6.1 *Overturning block geometry*

In the case of a tower structure, the overturning of the upper part on the base usually represents the weakest mechanism.

The most unfavorable hinge position can be easily determined; instead the identification of the overturning block geometry is a more complex task.

A simplified geometry with a straight horizontal fracture surface is inconsistent with the evidence of real collapse mechanisms, which occurred during past earthquakes.

The presence of a diagonal fracture surface is justified by the fact that masonry is a unilateral material able to resist high compressive stresses but with feeble tensile strength. As a consequence, at the limit of overturning, a part of the masonry will remain attached to the base and a stress-free diagonal fracture surface will form (Heyman 1992, Ochsendorf *et al.,* 2004). In the present paper the fracture line is identified by the position of the neutral axes of the cross sections. According to simple elastic theory, when the line of thrust falls outside the section kern a stress-free zone will develop. Considering a masonry tower and simplifying the problem into a

plane problem (Figure 15), a differential equation is searched whose solution is the curve of fracture $z = z(l)$, z being a vertical reference axis with the origin at the base.

A tower of height h_t, is considered; on the tower the dead load and a horizontal load distributed proportionally to the mass are applied. The horizontal load is considered high enough to produce the cross section partialization between $z = 0$ and $z = h_{fp}$. The following assumptions are made:

- null masonry tensile strength,
- elastic behaviour of masonry in compression,
- only the masonry in compression is involved in the collapse mechanism,
- cross-section is constant where the fracture develops.

Hence, the fracture will form in each cross-section when the line of thrust reaches the edge of the section kern.

The distance of the section kern from the external edge, in case of hollow squared cross-sections must be preliminarily calculated as:

$$U(l) = L_g(l) - \frac{\rho^2(l)}{L_e - l - L_g(l)} \tag{7}$$

where:

$$\rho^2(l) = \sqrt{\frac{J(l)}{A(l)}}$$

$\rho(l)$ being the radius of gyration of the uncracked section, $L_g(l)$ is the distance of the section centroid to the compressed edge; $A(l)$ and $J(l)$ are respectively the area of the compressed part of the cross section and its moment of inertia, being L_i and L_e defined in Figure 15.

Distance from the edge, normalized with respect to the uncracked length of the section is:

$$d(l) = \frac{U(l)}{L_e - l} \tag{8}$$

The equation of the fracture is determined based on the equilibrium conditions of an elementary slice of the tower in the fractured zone (figure 14). It is identified by the differential equation (Romaro 2011):

$$\frac{dz}{dl} = W(l, z(l)) \cdot \frac{d(U(l))}{[U(l) - L_g(l)] \cdot A(l)\gamma_m + H(l,z)} \tag{9}$$

where $W(l,z(l)) = W_0(h_{fp}) + W_c(l,z(l))$ is the weight of the tower above the abscissa z, γ_m is the masonry density, $L_g(l)$ is the distance of the section centroid to the compressed edge; $A(l)$ and $J(l)$ are

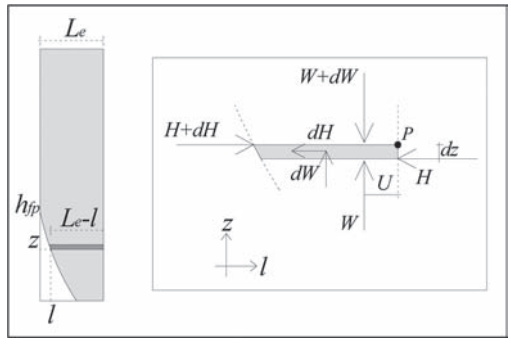

Figure 14. Elementary slice of the tower in the fractured zone.

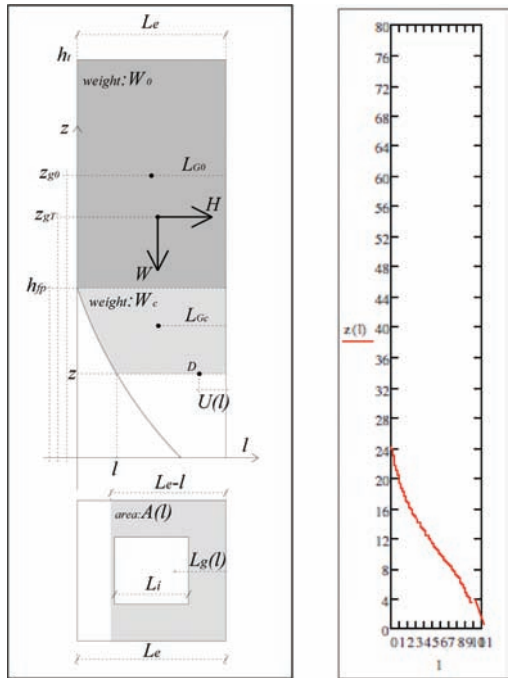

Figure 15. Geometrical model of the tower and fracture line under assumption of infinite masonry compressive strength.

respectively the area of the compressed part of the cross section and its moment of inertia, being L_i and L_e defined in Figure 15.

Hence $H(l, z)$ can be defined as:

$$H(l, z(l)) = \frac{W(l, z(l)) \cdot [L_{Gt}(l, z(l)) - U(l) \cdot (L_e - l)]}{z_{Gt}(l, z(l))} \tag{10}$$

where $L_{Gt}(l,z(l))$ and $z_{Gt}(l,z(l))$ are the coordinates of the overturning block centroid.

The fracture line is the solution of differential equation (7) with boundary condition $z(0) = h_{fp}$.

This equation was solved via a numerical *ODE solver* that uses the *Runge-Kutta* method, obtaining a family of fracture curves $z(l)$ varying with parameter h_{fp}. In a first solution step, the algorithm performs a do-loop on the h_{fp} parameter until the fracture curve reaches the external edge of the section that corresponds to an assumption of infinite masonry compressive strength. In a second step the curve of fracture has been determined by imposing the attainment of the ultimate resisting moment at the base section considering a finite value of masonry compressive strength, which defines the final h_{fp} in the iterative scheme.

Once h_{fp} has been determined with the corresponding fracture line, a collapse multiplier $\lambda = 0.127$ can be obtained as the ratio between the horizontal force and the dead load of the overturning part.

According to the Italian Code (NTC 2008) to a horizontal load multiplier a corresponding spectral acceleration activating the mechanism can be associated, as shown in Figure 16. Seismic capacity for the tower was than compared to the seismic demand, defined in paragraph 5.

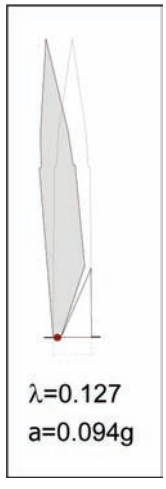

Figure 16. Collapse multiplier and acceleration values.

7 REMARKS

This paper was aimed at presenting a simplified but effective vulnerability assessment for masonry towers, by considering two major aspects: the influence of soil-structure interaction and the influence of the masonry tower as a no-tension material.

The obtained results support the conclusion that the structure-soil interaction strongly affects the seismic demand, depending on the soil stiffness.

In particular, the influence of soil non-linear behaviour was taken into account, by selecting an upper and a lower value of soil stiffness, representative of small strain and large strain response, appropriate for low and high intensity seismic events.

Due to this relevance, a major effort was made in order to validate the selected values of soil stiffness by using an experimental identification technique.

According to experimental evidence, in the case of a tower structure, the overturning of the upper part on the base usually represents the weakest mechanism. The presence of a diagonal fracture surface is justified by the fact that masonry is an unilateral material able to resist high compressive stresses but with feeble tensile strength. As a consequence at the limit of overturning, a part of the masonry will remain attached to the base and a stress-free diagonal fracture surface will form.

Further efforts will be devoted in the future to explore overturning mechanism at the foundation level, by considering all possible factors (frictional resistance along the sides as well as passive resistance on the front wall of the foundation block) contributing to the capacity of the soil-foundation system.

REFERENCES

Aoki, T., Sabia, D., Rivella, D. & Komiyama, T. (2007). Structural caracterization of a stone arch bridge by experimental tests and numerical model updating. International Journal of Architectural Heritage, vol. 1, p. 227–250, ISSN: 1558-3058.

Aoki, T., Sabia, D. & Rivella, D. (2008). Influence of experimental data and FE model on updating results of a brick chimney. Advances in Engineering Software, vol. 39, p. 327–335, ISSN: 0965-9978.

Dieghi, C. (2009). Fonti e studi per la storia della Ghirlandina, in *La Torre Ghirlandina. Un progetto per la conservazione*, Vol. 1, 48–66, Sossella ed.

Cancelli, A. (1986). Aspetti geotecnici della subsidenza. Ambiente: Protezione e Risanamento. Atti 2° *Corso di Aggiornamento per tecnici di igiene ambientale*. Modena. Ed. Pitagora, Bologna.

Cancelli, A., e Pellegrini, M. (1984). Problemi geologici e geotecnici connessi al territorio della città di Modena. *Atti 2° Congr. Naz. ASS.I.R.C.CO*., Ferrara, 53–64.

Cremaschi, M. & Gasperi, G. (1989). L'alluvione alto medioevale di Mutina (Modena) in rapporto alle variazioni ambientali oloceniche. Mem. Soc. Geol. It., 42, 179–190.

Desideri, A. & Viggiani, C. (1994). Some remarks on the stability of towers. Symp. On Developments in *Geotechnical Engineering*, Bankok.

Di Tommaso, A., Focacci, F. & Romaro F. (2009). Analisi strutturale statica e dinamica della Torre Ghirlandina. In *La Torre Ghirlandina. Un progetto per la conservazione*. Vol. 1, p. 164–177, Sossella ed.

Fazzini, P. & Gasperi, G. (1996). Il sottosuolo della città di Modena. Accad. Naz. Sci. Lett. Arti di Modena, Miscellanea Geologica, 15, 41–54.

Gazetas, G. (1991). Foundation vibrations. Ch. 15 in Foundation Engineering Handbook, Van Nostrand Reinhold, N.Y.

Hambly, E.C. (1985). Soil buckling and the leaning instability of tall structures. *The Structural Engineer*, 63, 3, 77–85.

Heyman, J. (1992). Leaning towers. *Meccanica*, 27, 153–159.

Labate, D. (2009) Il contributo dell'archeologia alla lettura di un monumento, in *La Torre Ghirlandina. Un progetto per la conservazione*, Vol. 1, 66–78, Sossella ed.

Lambe, T.W. & Whitman, R.V. (1969). Soil Mechanics. Wiley, 553 pp.

Lancellotta ,R. (1993). The stability of a rigid column with non linear restraint. *Géotechnique*, 33, 2, 331–332.

Lancellotta, R. (2009). Aspetti geotecnici nella conservazione della Torre Ghirlandina. In *La Torre Ghirlandina. Un progetto per la conservazione*. Vol. 1, p. 178–194, Sossella ed.

Lancellotta, R. (2012). La torre Ghirlandina: una storia di interazione struttura-terreno. XI Croce Lecture to be published on Rivista Italiana di Geotecnica.

Lugli, S., Marchetti Dori, S., Fontana, D. & Panini, F. (2004). Composizione dei sedimenti sabbiosi della pianura modenese. Il Quaternario, *Italian Journal of Quaternary Sciences*, 17, 379–389.

Marchi, M., Butterfield, R., Gottardi, G. & Lancellotta, R. (2011). Stability and strength analysis of leaning towers. *Géotechnique*, 61, 12, 1069–1079.

Nova, R. & Montrasio L. (1995). Un'analisi di stabilità del campanile di Pisa. *Rivista Italiana di Geotecnica*, 2, 83–93.

NTC 2008 DM 14 gennaio 2008. Norme Tecniche per le costruzioni. Circolare 2 febbraio 2009, n. 617. Istruzioni per l'applicazione delle Nuove norme tecniche per le costruzioni di cui al decreto ministeriale 14 gennaio 2008.

Ochsendorf, J.A., Hernando, J.I. & Huerta, S. (2004). Collapse of masonry buttresses. *Journal of architectural engineering*, vol. 10, n.3.

Pellegrini, M. & Zavatti A. (1980). Il sistema acquifero sotterraneo fra i fiumi Enza, Panaro e Po: alimentazione delle falde e scambi tra falde, correlazioni idrochimiche. *Quad. Ist. Ric. Sulle Acque*, CNR, 51, 205–217.

Righi, P.V. (1980). Rilevamenti geotecnici nel sottosuolo del Palazzo Nazionale di Modena. *Atti XIV Conv. Naz. Geotecnica*, Firenze, 1, 257–266.

Romaro, F., (2011) A study on seismic behaviour of masonry towers. Ghirlandina tower in Modena. Ph. D thesis, University of Trento.

Russo, P. (1985). L'abbassamento del suolo nella zona di Modena (1950–1982). Tecnica Sanitaria, XXIII, 293–3.

Van Overschee, P. & De Moor, B.: Subspace Identification for Linear Systems, Kluwer Academic Publishers, ISBN 0-7923-9717-7, 1996.

This page intentionally left blank

Geotechnical Engineering for the Preservation of Monuments and Historic Sites – Bilotta, Flora, Lirer & Viggiani (eds)
© 2013 Taylor & Francis Group, London, ISBN 978-1-138-00055-1

Performance evaluation of bending strength to predict durability of ornamental gneiss from Santo Antônio de Pádua, RJ, BR

J.L.E. Dias Filho, P.C.A. Maia, G.C. Xavier & P.A.M. Fernandes
Laboratory of Civil Engineering, State University do Norte Fluminense 'Darcy Ribeiro', Campos dos Goytacazes, Rio de Janeiro, Brazil

ABSTRACT: The durability of geotechnical materials is an important field of research in geotechnical engineering at present. Thus, while one material can be considered appropriate under certain weathering conditions, others cannot. The aim of this paper was to evaluate the behavior of ornamental gneiss from Santo Antônio de Pádua (Rio de Janeiro, Brazil) subjected to accelerated degradation using accelerated degradation tests. The behavior of the rock material was analyzed by testing its bending strength using prismatic specimens of different thicknesses. The results indicate a significant reduction in resistance in samples of lower thickness in the material degraded naturally in the field or accelerated in the laboratory when compared with the intact rock material. This behavior confirms that surface change is minimal, but which can change in places with higher energy degradation. Thus, the results support the need to determine the durability characteristics of the stone material considering the weathering characteristics from a particular region.

1 INTRODUTION

The study on the durability properties of building materials is an important field of research in Civil Construction. Assessing the long-term behavior of materials defines their useful lifetime and use due to their intrinsic characteristics and exogenous environment.

Taking into consideration that engineering projects are usually developed to last, the concern is the continued efficiency of these materials over time, raising questions about their performance and durability. Thus, the methods for assessing degradation must be improved and suitable equipment developed to facilitate the study of durability of building materials.

In this sense, the aim of this study was to assess the durability of rocks, particularly those used in building facades, considering the variations of wear energy caused by different exogenous environments. Thus, these materials were chosen because of their intrinsic characteristics, which are normally susceptible to degradation, and for being frequently used in civil construction.

The rock type studied is a mylonitic gneiss from Santo Antônio de Pádua (Rio de Janeiro, Brazil) commercially called as "Pedra Olho do Pombo" (Augen gneiss)—OP. Two different types of test specimens were used to study tensile strength.

The study material was chosen because of its wide availability in the region of Santo Antônio de Pádua where it is mined. Due to its worldwide and national commercialization, further studies on natural degradation in different climates are needed.

Some studies on durability and behavior analysis of rock alteration from the region, used in civil construction as ornaments, are found in Maia, Sayão, Nunes & Antunes (2001), Maia, Sayão, Nunes & Antunes (2002), Salles & Maia (2004), Maia & Salles (2002), Ribeiro, Correia, Seidl & Almeida (2006), ABIROCHAS (2012) and Dias Filho, Maia, Xavier & Fernandes (2012).

Accelerated degradation tests, conducted at UENF, were used to study the material behavior over time. The testing procedure was chosen in accordance with the major weathering characteristics of the region. Table 1 shows examples of studies on durability and procedures that analyze the behavior and alteration of rocks. The last study used the accelerated degradation test to predict the durability of material weight loss.

The tests to evaluate durability are chosen in accordance with the research objective and the type of material studied. Experience and research determine the testing procedures of choice. In this sense, the classification of the main tests proposed to evaluate degradation of geotechnical materials was used (Figure 1).

Table 1. Tests used in some studies to evaluate rock degradation.

Reference	Material	Analysis	Note
Philipp & Benedetti (2005)	Marble	AMSLER and Impact Resistance Test	High wear, brightness loss and roughened surface formation
Renner & Pulz (2005)	Granite	Petrography, Physical Indices, Impact Resistance Test and AMSLER	Excellent application on structures, floors and tiles
Latham, Lienhart & Dupray (2006)	Granite	Physical Indices, Los Angeles Abrasion e Micro Deval	Durability guide with different researches in the field and in the laboratory
Ribeiro, Correia, Moraes & Caranasios (2008)	Granite	Physical Indices, Exposure Salt Spray, Chemical Attack and Sulfates	Physical alterations of materials, color and changes in mechanical strength
Costa, Neto, Galembeck, Silva & Simão (2010)	Gneiss	Petrography, Physical Indices and Continuous Leaching	The material has good application in coatings
Dias Filho, Maia, Xavier & Fernandes (2012)	Gneiss	Physical Indices, Continuous Leaching and Slake Durability Test	Durability study using special laboratory equipment

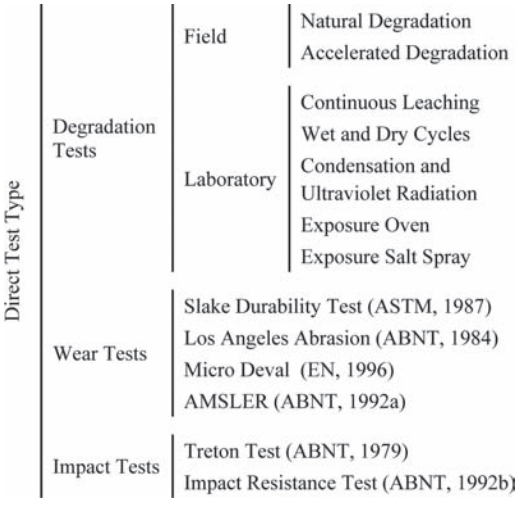

Figure 1. Classification of the main tests used to evaluate degradation of geotechnical material.

Figure 2. Augen gneiss used as flooring.

The beauty of the gneisses from the region favors its use as ornaments. Due to major events in Brazil, the World Cup 2014 and the Olympic Games in 2016, this rock material has been used in many different types of construction such as facades of houses, walls, buildings, as well as flooring and furniture, as shown in Figure 2.

2 MATERIAL AND METHODS

2.1 *Study material*

The rock material analyzed came from a quarry in "Serra do Bonfim", located in Santo Antonio de Pádua city, in the northern region of the State of Rio de Janeiro. Note that the rock studied is used for ornamental purposes and it is commercially called "Pedra Olho do Pombo" (Augen gneiss). It is a medium-grained mylonitic gneiss with white orthoclase porphyroblasts and rich in quartz, present throughout the "Serra do Bonfim" alignment. The commercial name originated from these characteristics because the minerals on the gneiss surface remind us of a pigeon's eye. Dias Filho, Maia, Xavier & Fernandes (2012) and Salles & Maia (2003) conducted some studies to classify the physical and mechanical characteristics of the rock material from this region.

2.2 *Methods*

Figure 1 shows the methods used to evaluate rock alteration. It is important to highlight that the amount of material needed to evaluate the intact and degraded conditions must be significant.

This study compared the wear of the intact material, the material degraded in the field and in the laboratory, as shown in the flowchart below (Fig. 3). This method is based on characterization and durability studies by Salles & Maia (2004) and Dias Filho, Maia, Xavier & Fernandes (2012).

2.3 *Experimental data*

The material parameters considered in the present study was bending strength σ in accordance with the International Society for Rock Mechanics (ISRM, 1981). For this test, two supports were placed on each side of the specimen and the load was applied on the central part of the specimen, as shown in Figure 3.

Field degradation was done by exposing the rock to natural weathering conditions and three samples were obtained at time intervals of 90, 180 and 270 days to evaluate the degradation of the material (Fig. 4).

The prismatic test specimens were produced in different sizes (Fig. 5). One is the standardized size, whereas the other is five times thinner.

The material degraded in the laboratory using continuous leaching was evaluated at four time intervals: 12, 18, 34 and 70 days (Fig. 6).

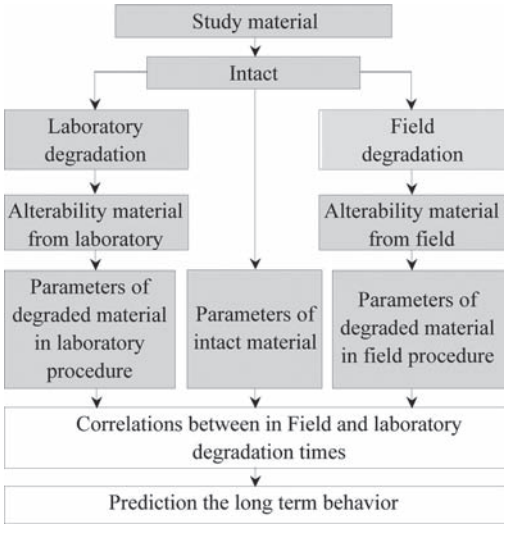

Figure 3. Method to evaluate rock degradation.

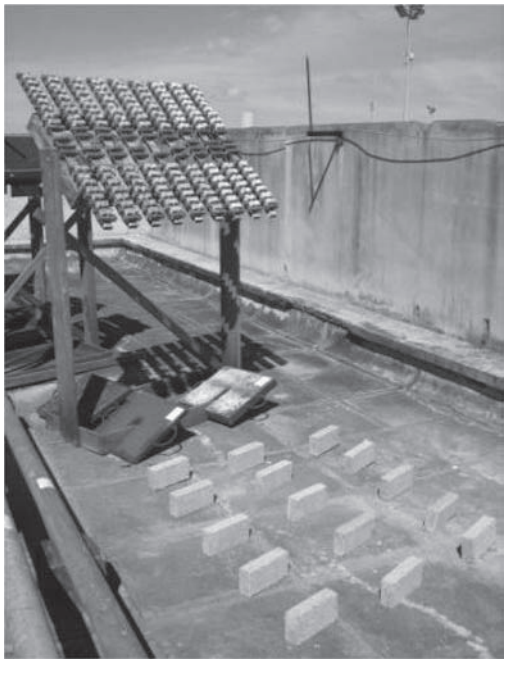

Figure 4. Location of exposure of samples to natural degradation in the field.

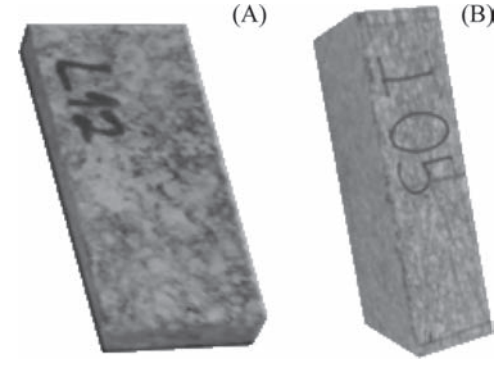

Figure 5. Samples used and size: Thinner sample (A), standardized sample (B).

Figure 6. Equipment used to study degradation and its internal view with various specimens for accelerated degradation.

3 RESULTS AND DISCUSSIONS

For the quantitative analysis, the changes in the parameters studied are evaluated with the type or rate of alteration using the alteration indexes (Farjallat, 1972). The alteration indexes compare a particular characteristic of the material in the initial state, intact, and the same characteristic in the degraded state.

Thus, the bending strength index $I\sigma$ can be defined by the equation 4.1:

$$I\sigma = \frac{|\sigma_o - \sigma|}{\sigma_o} \times 100\% \quad (1)$$

where σ_0 is an intact rock parameter and σ is an altered rock parameter. The index value I varies from zero, for the material intact, to a maximum value, always less than 100%, for the most altered material.

Table 2 shows the summary of results obtained in the mechanical tests.

Figure 7 shows the variation of $I\sigma$ of the degradation time obtained in the field, while Figure 8 shows the variation of $I\sigma$ of the degradation time obtained in equipment used to study degradation.

The results show that increasing the index $I\sigma$ indicates a decrease in bending strength of degraded materials.

It is noted that the trend in stabilization was not found for the materials degraded in the field, whereas in the laboratory a curve begins to level off after approximately 40 days of degradation. According to the results in Maia & Salles (2002), longer exposure time, exceeding 800 days of exposure, is needed for the samples in the field.

To predict the long-term behavior of materials, the correlation between the degradation time in field and accelerated degradation in the laboratory must be determined. Thus, the degradation time in the laboratory and in the field can be determined with the coincident values of $I\sigma$ for both samples.

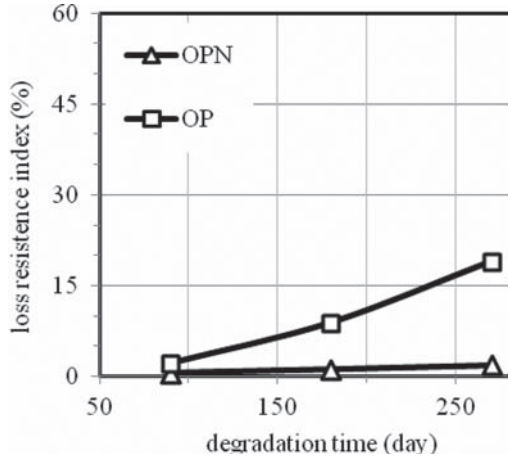

Figure 7. Bending strength performance in the field.

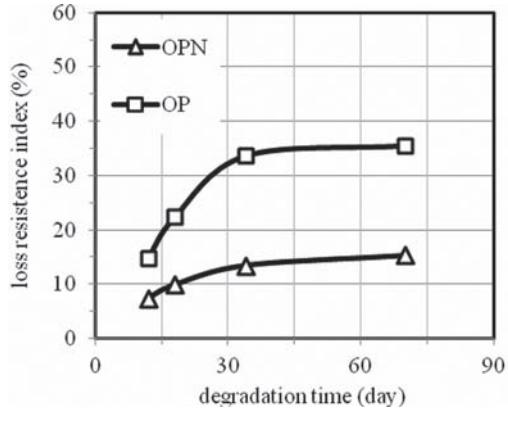

Figure 8. Bending strength performance in the laboratory.

Table 2. Behavior of bending strength over time.

Degradation time		OPN*	OP**
Intact	0	15.32	9.97
Natural (day)	90	15.23	9.76
	180	15.14	9.09
	270	15.02	7.04
Laboratory (day)	12	14.19	8.50
	18	13.81	7.75
	34	13.26	6.62
	70	12.47	6.43

*OPN—standardized sample of Olho do Pombo.
**OP—thinner sample of Olho do Pombo.

Due to the low exposure time of the samples, it was not possible to correlate satisfactorily the materials studied. It can be observed that the final bending strength indexes in the field of OP coincide with the initial levels of OP in the laboratory. In other words, we could only analyze part of the graph. As for the situation of the OPN sample, no samples in the field underwent sufficient degradation to compare them with the test specimens degraded in the laboratory. The results in the study of Maia & Salles (2002) of two gneisses found in the region and their results are a good indication of the final result that the present study will obtain with the samples that are exposed to weathering on the terrace at the University.

4 CONCLUSION

The results indicate that the thickness of the test specimens used in the bending strength tests significantly influence the results of the tests. The thinner the sample, the greater is the index of bending resistance.

The equipment used to study degradation made it possible to simulate variations in material behavior prompted to bending. From the data it was not possible to determine correlations between degradation time in the field and accelerated degradation time in the laboratory. According to Maia & Salles (2002), a linear relationship is expected between the degradation time in the field and the laboratory, irrespective of the material studied. Thus, once this relationship is defined, the alteration processes in the laboratory can simulate the variation trend of the mechanical properties of rocks due to alteration in the field. According to project specifications, the loss in material strength during the time it is applied or its useful lifetime can be determined.

It is noteworthy that the relationship between the degradation times in the field and laboratory are only valid for the weathering conditions of the place of natural exposure used in the research.

ACKNOWLEDGEMENTS

The authors thank "Serraria Olho do Pombo", UENF and CAPES for supporting this research.

REFERENCES

ABNT—"Brazilian Association of Technical Standards" 1979. Determination of Shock Resistance. *Test Designation: ABNT—NBR 964/79.*

ABNT—"Brazilian Association of Technical Standards" 1984. Aggregates: Determination of Los Angeles abrasion. *Test Designation: ABNT—NBR 6465/84.*

ABNT—"Brazilian Association of Technical Standards" 1992a. Rock for coating—Petrography Analysis. *Standard title: ABNT—NBR 12768/92.*

ABNT—"Brazilian Association of Technical Standards" 1992b. Rock for coating—Determination of bending resistance. *Test Designation: ABNT—NBR 12763/92.*

ABIROCHAS—"Brazilian Association of Ornamental Rocks" 2012. Ornamental Stones Catalog. Available: <http://www. abirochas.com>. *Accessed February, 2012.*

ASTM—American Society for Testing Materials 1987. Slake Durability of Shales and Similar Weak Rocks. Reproved 1992. *Test Designation: D 4644/87.*

Costa, A.P.L; Neto, J.A.N; Galembeck, T.M.B; Silva, Z.C.G. & Simão, J.A. 2010. "Ornamental rocks: alterability of gneisses Enderbíticos in Test Leaching Through Continuous Soxhlet extractor". *Holos, Ano, 26, Vol. 3–p. 10.*

Dias Filho, J.L.E; Maia, P.C.A; Xavier, G. de C. & Fernandes, P.A.M. 2012. "Study of the Wear Energy Effect in the Durability Predicting of Ornamental Gneiss from Pádua-RJ." *XVI Brazilian Congress of Soil Mechanics and Geotechnical Engineering, Porto de Galinhas/PE 14–18 September 2012. p. 7.*

EN—Europäische Norm 1996. Tests for Mechanical and Physical Properties of Aggregates. Part 1: Determination of the Resistance to Wear (Micro-Deval). *Test Designation: EN 1097–1.*

Farjallat, J.E.S. 1972. "Reporting on the Theme: Disaggregation of Rocks and Problems Related to their Applicability". 4th Week Paulista Applied Geology, *São Paulo, vol. II A, pp. 19–53.*

ISRM—International Society for Rock Mechanics. 1981. *Rock Characterization Testing and Monitoring*—ISRM Suggested Methods, Ed. E.T. *Brow, Pergamon Press, Oxford, pp. 1–212.*

Latham, J.P; Lienhart, D. & Dupray, S. 2006. Rock quality, durability and service life prediction of armourstone. *Science Direct. Engineering Geology. 87: 122–140.*

Maia, P.C. A & Salles, R.O. 2006. "Experimental Durability Study of the Ornamental Rocks Through Laboratory Special Procedures". *XIII Brazilian Congress of Soil Mechanics and Geotechnical Engineering, Curitiba/PR 27–31 August 2006. p. 6.*

Maia, P.C.A; Sayão, A.S.F.J; Nunes, A.L.L.S & Antunes, F.S. 2001. "Experimental Evaluation of Change Armourstone". *Soil and Rocks, vol. 24, no. 2, pp. 129–139.*

Maia, P.C.A; Sayão, A.S.F.J; Nunes, A.L.L.S & Antunes, F.S. 2002. "The Basalt Rocks Alterability—Petrography and Physical Characterization". *Soil and Rocks, vol. 25, no. 3, pp. 207–225.*

Philipp, R.P. & Benedetti, V.D. 2005. "Analysis and Assessment of Problems at the Summit of the Metropolitan Cathedral of Porto Alegre, RS: Problems Project Execution and/or unsuitable material?" *I Congress International of Ornamental Rocks, Guarapari-ES, p. 6.*

Renner, L.C. & Pulz, G.M. 2005. "Comparison and Interpretation of Technology Test for granitoids Jaguari and Santa Rita, Southwest Region Shield-Subriograndense". *I Congress International of Rocks, Guarapari-ES, p. 5.*

Ribeiro, R.C.C; Correia, J.C.G; Seidl, P.R. & Almeida, S.L.M. 2006. "Tailings Utilization the Ornamental rocks in Asphalt Mixes". *Mineral Technology Series, Rio de Janeiro, n° 00, p. 23.*

Ribeiro, R.C. da C; Correia, J.C.G; Moraes, J.M. & Caranassios, A. 2008. "Study of the alterability the silicate rocks for Ornamental Application". *Center for Mineral Technology—Rio de Janeiro: CETEM/MCT. p. 48.*

Salles, R.O & MAIA, P.C.A. 2004. "Experimental Evaluation of Alterability of Ornamental Rocks from North of the State of Rio de Janeiro". *1st Brazilian Symposium on Geotechnical Young. São Carlos/SP, 2004. p. 6.*

This page intentionally left blank

Geotechnical Engineering for the Preservation of Monuments and Historic Sites – Bilotta, Flora, Lirer & Viggiani (eds)
© 2013 Taylor & Francis Group, London, ISBN 978-1-138-00055-1

The role of the geotechnical engineer in archaeological work: The Greek experience

D. Egglezos
Civil Engineer, Athens, Greece

D. Moullou
Archaeologist, Directorate of Prehistoric and Classical Antiquities, Hellenic Ministry of Education and Religious Affairs, Culture and Sports, Athens, Greece

M. Ioannidou
Civil Engineer, Hon. Director of Acropolis Restoration Service, Athens, Greece

ABSTRACT: The present paper, taking for granted that the study and the protection of cultural heritage is an interdisciplinary task, deals with the role of the geotechnical engineer in this field. Through characteristic case studies, covering a wide spectrum of archaeological works in Greece, this paper aims to highlight the necessity of the participation of a geotechnical engineer in the aforementioned interdisciplinary team. These examples can well clarify the contribution of the geotechnical engineer as an indispensable/sine qua non link in the interdisciplinary team charged for the monuments study and protection, and assist to the enhancement of its role in heritage preservation.

1 INTRODUCTION

"The conservation and restoration of monuments must have recourse to all the sciences and techniques which can contribute to the study and safeguarding of the architectural heritage". Venice Charter, Article 2, (1964).

In 1964, the interdisciplinary cooperation for interventions on monuments was not obvious. Today, the interdisciplinary composition of a research team, not only for the conservation and restoration of monuments, but also for the undertaking of any serious archaeological work is considered self-evident, due to increased understanding of the interaction of different fields of research and to the growing acceptance of its complexity. During the past decades, scholarly research has brought to light problems previously unknown. Earlier errors, for which one person bore the sole responsibility, must not be repeated.

Thus, in Greece, for the conduction of any restoration project as well as for other archaeological works, such as excavations or surveys, law requires a multi-disciplinary team. (Greek Law 3028/2002 on the Protection of Antiquities and Cultural Heritage in General, article 36, paragraph 3 and 8 and article 40 paragraph 4). However, from article 40, paragraph 4 of the above law, it is evident that the field of structural engineering is recognized as the main domain of civil engineering involved in the preservation of monuments. Geotechnical engineering and its contribution to the safeguarding of monuments and historic sites is under-estimated, not only in the aforementioned law, but also in practice.

2 SCOPE

This paper, considering the study and the protection of cultural heritage a priori an interdisciplinary task, aims to highlight the necessity of the participation of a geotechnical engineer in the interdisciplinary team.

The main argument is that many common problems faced during the course of the archaeological work are of purely—or mainly—geotechnical nature.

This paper will discuss the role of the geotechnical engineer in maximising the usefulness and the value of results in the study and protection of monuments and sites through the presentation of case studies covering a wide spectrum of archaeological works, such as a) the preservation of monumental structures serving a pure geotechnical purpose (e.g., ancient retaining walls) or have a geotechnical role e.g. foundations, buttresses (including the proper mechanical description and

modeling of the structural members from stone geomaterials and their interfaces) b) stabilization of subsoil foundation and/or of the monument itself c) stabilization of rock masses that threaten visitors, personnel or the monuments themselves d) interpretation of the current or the historical state of the monument through well documented back analyses e) support of archaeological excavations for minimization of geotechnical failures that can lead to severe accidents f) monitoring design for the observation of the monument's state. It should be noted that this paper focuses only on cases that involve studies on the monuments themselves and not on protective interventions arising from the impact of new infrastructure/s constructed nearby.

3 WORKS FOR THE PROTECTION OF MONUMENTS

The above works include "works on immovable monuments and in particular conservation, consolidation, restoration, anastlylosis, interment, installation of protective sheds, landscape designing ... that aim at the preservation of their material existence and authenticity, their enhancement and protection in general" (as defined by Law 3028/2002, 40.1).

In the following paragraphs the role of the geotechnical engineer will be discussed in relevance to characteristic case studies of works for the protection of monuments mentioned.

3.1 *Conservation*

A typical contribution of the geotechnical engineer to the conservation of a monument is the design of drainage systems for the mitigation of the unfavorable water action on the monument's structural members (usually stone blocks).

Indicatively, the cases of two ancient retaining walls are mentioned, where the design of superficial drainage trenches has been proposed for the adduction of rainwater. The monuments in concern are the great retaining wall at the Amphiaraeion in Oropos (Egglezos, 2012) and the Kronion retaining wall in Olympia (Svolopoulos, 2013). In these cases, the drainage not only allows for the decrease of hydrostatic pressure upon the wall but also inhibits the weathering of the stones made of soft geomaterial (marly limestone).

Another case where an interaction between geotechnical engineer and conservators took place is for the protection of a faint relief carved into the face of a limestone wall of a natural rock grotto at the northern foot of the Pnyx hill at Athens, (Sanctuary of Pan). In this case a system of drainage holes has been proposed for collecting the attacking rainwater far from the wall carving and guiding the water in preset places (Fig. 1).

3.2 *Consolidation*

The stabilization of instable rock blocks in the near area of an archaeological area involves typically a geotechnical engineer. This intervention usually has three targets: the protection of the monumental structures, the safety of people in the area (working staff, visitors etc) and the preservation of the authenticity of the natural environment. As prominent cases in Greece, the stabilization of the rock in the Acropolis hill and the steep rocky slopes of the Delphi area are presented.

The stabilization of the Acropolis rock slopes concerned the implementation of strong passive anchors (10–16 m long) for the consolidation of rock masses of significant volume, in extensive areas of the slopes, limiting drastically the threatening action of rock falls (reported as a systematic problem in the history of the site) for the existing settlement around the sacred rock and the protection of numerous visitors and occupied persons in the anastylosis works. In addition small-scale interventions took place in certain areas of the rock hill with high weathering. In these latter cases, the intervention comprised the application of small length dowels (ca 1 m long), the application of proper grout (as a careful hand operation) for the restitution of the continuity of the discrete weathered small size rock blocs, and the opening of drain holes for the relief of the rock from the weathering action of the water run off (Fig. 2a, b).

In the case of Delphi rock falls occurred from ancient times, as a result of the high seismic action and the unfavorable climate conditions in the mountain areas of central Greece. The rock falls constitute major risks for the prominent monumental assets of the area as well as for the people (visitors, employees). In the past, various temporary measures (mainly of

Figure 1. Rainwater causes severe problems on the carved relief of the Sanctuary of Pan.

Figure 2a, b. Detail of the Acropolis rock hill, before (a) and after (b) the intervention.

empirical nature) have been applied (fences, masonry walls, trenches, drainage interventions, etc). Recently the Greek State recognized the necessity for a targeted and scientifically designed intervention for a rather permanent confrontation of the problem. Within this context a geotechnical study was proclaimed for 2013, comprising the design of extensive drainage systems, extensive anchoring of the steep slopes and installation of catch fences.

These aforementioned cases are very typical for a plethora of monuments in Greece, since impressive mountain sites with excellent view were usually selected for the construction of monumental structures of sacred or profane character.

3.3 *Restoration—anastylosis*

The restoration of a monument usually poses emphatically the geotechnical nature of the required intervention. This is very clear particularly in cases of monumental structures with a pure geotechnical role. In this paragraph the intervention on ancient retaining walls is discussed. As an example the classical retaining walls at the Amphiareion of Oropos (Fig. 3) and at the Kroneion hill at Olympia are presented (Fig. 4).

In the above cases the structural failures of the walls (rotation of the wall, dislocation, disorganization and significant fractures of the stone blocks) are attributed mainly to the excess earth pressures (especially under seismic action) behind the walls and the corrosive action of rainwater.

Figure 3. The great retaining wall of the Amphiaraeion of Oropos.

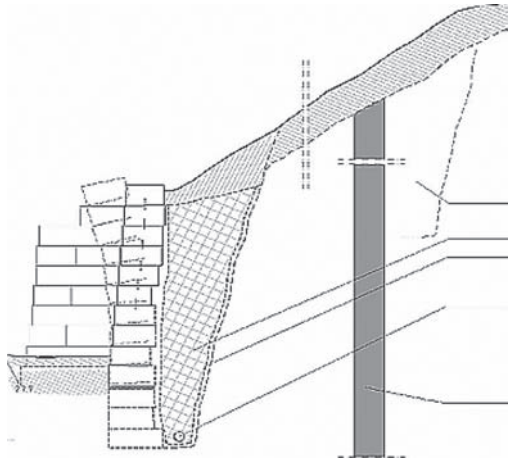

Figure 4. The proposed solution for the protection of the ancient retaining wall of Kronion hill in Olympia. The design is based on the construction of a pile diaphragm in a short distance from the back wall face.

The solution of the reconstruction of the structure in its initial form alone is inefficient for the longevity of the monument, since the factors causing the problems remain and continue to act.

For these two cases a geotechnical intervention has been proposed (Egglezos, 2012 and Svolopoulos 2013 respectively) as a passive measure, fully compatible to the restoration principles, in order to relieve the wall from the devastating effect of the earth pressures and the water action.

The design is based on the construction of a pile diaphragm in a short distance from the back wall face. Additionally, the design comprises the improvement of the back filling soil with selected granular soil and the construction of an effective

drainage system. This solution not only relieves the soil pressure but also may be useful for the general stability of the upward slope. It is worth mentioning that the analyses for the design of the measures are based on back analyses for interpretation of the current state of the walls, assuring the reliability of the design (Fig. 4). The classical N-E tower of the fort of Aegosthena, situated in Boeotia Prefecture, north of Attica, is another example of a geotechnically oriented restoration practice. The main structural failure of the tower wall—settlement and dislocation of the stone blocks—is attributed to the compressibility of the artificial foundation soil (Toumbakari, 2011).

In this case an under pinning foundation with micro-piles, penetrating the lower rock layer was proposed for the effective carrying of the structural load to the underneath rock (Fig. 5).

Besides the monument itself, the restoration practice includes the installation of a worksite (Ioannidou & Oikonomopoulos, 2003). As a characteristic case the crane serving for the dismantling of the West Colonnade of the Parthenon is referred. In this case the involvement of the geotechnical engineer concerns the design of the crane foundation (Egglezos, 2011). For the design, the following factors had to be taken into consideration: the strict requirements of the crane constructor for particularly limited absolute and differential subsidence along and across the foundation, the design against sliding and overturning of the foundation (due mainly to the action of wind and earthquake on the crane, and the eccentric loads from the crane service), the differentiation of geotechnical conditions along and across the crane foundation (half of the crane is base on pure limestone, while the other half is based on an ancient artificial soil prism with the soil in a rather loose state), and the effect of the crane to the ancient wall for the retaining of the ancient artificial soil prism, the expected time-consuming restoration procedure (dismantling, on the ground conservation and repositioning of the structural members). The foundation (two parallel foundation beams upon the rock and mat foundation upon the filling) has been constructed successfully (Fig. 6) and the restoration works are in full progress (Ioannidou, 2011).

The contribution of the geotechnical engineer may be extended to the theoretical study of the monumental structure itself. This is prominent in the case of dry masonry structures where the nature of (stone) geomaterials and the discrete plot of the structural members is similar to that of a rock mass fractured from a set of discontinuities. The case of the Opisthodomos columns (Parthenon) is a characteristic example for the contribution of the geotechnical engineer to the theoretical interpretation of the columns response. The results of a full-scale experimental project, comprising the staged horizontal loading of the columns capital and the relevant measurement of the capital drift and the base subsidence, were used for the proper modeling of the structure and the calibration of the material properties (Egglezos and Toumbakari, 2011). The key element of the modeling was the

Figure 5. The N-E tower of Aegosthena. The main structural failure of the tower wall—settlement and dislocation of the stone blocks—is attributed to the compressibility of the artificial foundation soil.

Figure 6. The crane serving for the restoration of the West Colonnade of the Parthenon.

estimation of reliable interface properties between the column drums and the assignment of proper values in the structural springs accounting for the response of the Parthenon foundation. This modeling can be the basis for soil-foundation-structure interaction analyses aiming at the prediction of the monument's response and the reliable evaluation of any restoration measures' performance.

Monitoring is an invaluable tool for the continuous observation of the monumental response (Ioannidou, 2012). Although this is not an exclusive geotechnical issue, there are cases where the nature of the observed parameters makes the design and the interpretation of the monitoring system pertaining mostly to a geotechnical "view". The case of the reburial of the Arrephoreion foundation walls (Egglezos, 2013) highlights clearly this statement. In this case the potential effect (horizontal thrust) of the reburial to the exterior circuit wall in contact, posed the need for systematic monitoring of this effect. Within this context an optical fiber in the reburial soil was installed for accurate recording of the upper part of the exterior wall's displacement. Additionally a pressure sensor was installed in the base of the wall for the recording of any change in the horizontal pressures upon the wall. These systems combined with more traditional methods (topographic measurements for settlements of the reburial surface and any displacements in the wall face) allow for a continuous observation of the reburial performance and may function as an alarm system in case of emergency.

Another worth mentioning application of monitoring is the instrumentation of the Acropolis site with an array of accelerographs for the recording of the seismic motion (Kalogeras and Egglezos, 2013). The contribution of a geotechnical engineer lies on the selection of the proper sites for the instruments' installation and the interpretation of the results for the assessment of the Acropolis broader area response under seismic motion.

Finally, the installation of series of optical fibers sensors in the outer face of the S-E area of the Acropolis South Circuit Wall (Egglezos, 2010) allows for the high accuracy recording of any strain and displacement in this area and the understanding of the nature of the action provoking them, as well.

3.4 *Interment*

The selection of reburial for rescue purposes is a method frequently applied in restoration practice. The reburial is a frequently chosen protection measure for monuments that suffer from weathering conditions. It is evident that buried parts of monuments are preserved in much better condition than the revealed ones. The reburial design seems logical to be served by a geotechnical engineer (since parameters like the selection and the synthesis of the backfill, the potential geostructural effect of the backfill on the monument to be reburied pertain mostly to the geotechnical field of science). However, reburial is considered to be a simple-non demanding-intervention, thus frequently in archaeological works the responsibility for carrying out the design and the construction is undertaken by other specialties (architects, archaeologists etc).

The following example highlights a case where the necessity for a geotechnical approach for the reburial design was not acknowledged from the beginning. The remains of the Arrephorion foundation-walls in the north side of the Acropolis hill had to be reburied since the weathering effect of the environment was devastating for the sensitive stone blocks of the walls (of soft marly limestone). The main discussion for the reburial was focused on the architectural features of the completed work, the use or not of the existing material from the ancient artificial filling etc. Although these issues are-of course-an important part for the reburial approach, the main problem was the fact that the north wall of the monument is in full contact with a part of the circuit wall of Acropolis (and it was the geotechnical "eye" to highlight this issue) (Fig. 7). The typical reburial for that (north) side could exercise a significant thrust in the (ca 5 m height) circuit wall (having in mind that there is no interlocking of the circuit wall and the foundation walls of the Arrephoreion). In this case the design of the reburial had to be more sophisticated and the decrease of horizontal thrust was a critical factor of the design. The geotechnical design—after the examination of comparative scenarios—opted for the construction of a reinforced earth block from selected granular material and geogrids (Egglezos, 2013).

This self-supporting construction satisfies the criterion for minimization of horizontal thrusts (for both static and seismic conditions). The construction of the reburial was completed successfully in

Figure 7. The foundations of Arrephorion. View from the W. The north wall of the monument is in contact with a part of the circuit wall of the Acropolis hill.

May 2007. Henceforth, the response of the system reburial-monument is observed systematically through various monitoring applications. The recordings of the monitoring applications are consistent to the expected response from the design and to the results of rigorous 2-D elastoplastic analyses.

4 ARCHAEOLOGICAL RESEARCH IN SITU

Archaeological research in situ can be defined as "the exploration of the ground, the subsoil, the seabed or the bed of lakes or rivers for the purpose of locating or discovering ancient monuments, whether such research constitutes excavation on land or underwater, surface research or scientific research carried out by geophysical or other methods" (Law 3028/2002 article 35).

The role of a geotechnical engineer during an excavation process might seem insignificant at first. However his/her participation in the research team could be literally life saving! Very often the depth of the excavation and the properties of the soil pose significant stability issues. Without proper stabilization measures, the excavation/trench faces may collapse and cause severe accidents to the working personnel. Additionally, the in situ support of excavation layers or walls, in order to dig deeper without destroying the upper stratum, is a common issue in an excavation process. A characteristic example is the case of the excavation of the Arrephorion on the Athenian Acropolis where the support of inner soil prisms with in situ ancient stones based upon them was required (Fig. 8). Another common problem faced by the archaeologists and can be solved by a geotechnical engineer is the stabilization of newly uncovered walls that need immediate support measures.

Figure 8. The Arrephorion excavation trench. In situ support of a revealed ancient wall.

Geotechnical investigation can be very useful to a research carried out by geophysical methods. Geophysics has been always a complementary assisting science to archaeological research. It is used to model the invisible subsurface elements of a monument or a research area. Recently, geophysics has been applied in harmony with investigation methods of the geotechnical sector in the case of the great retaining wall of the Amphiaraeion in Oropos. In this project a complementary application of two modern geophysical methods (Electrical Resistivity Tomography—ERT and Ground Penetrating Radar—GPR) has revealed all monument's hidden characteristics related to its geometrical shape, foundations, existing geological formations and a significant amount of valuable information to be used into a next validation phase (Dimitriadis, 2012). The geophysical analysis depended strongly on the geotechnical information that was used mostly to calibrate the results. In general, geophysical subsurface models are unconstrained theoretical solutions of the subsurface parameters that need to be calibrated to specific boundary conditions in order to be reliable and useable.

5 OTHER ARCHAEOLOGICAL RESEARCH

The science of geotechnical engineering can assist the archaeological and historical research in interpreting the current or the historical state of a monument, through well documented back analyses.

A characteristic example is the back-analysis carried out for the interpretation of a serious structural failure observed in an area of the Acropolis North Circuit Wall (Egglezos and Moullou 2011). The failure occurred, according to the available historical and archaeological evidence, at the end of the 18th or beginning of the 19th century (the failure took place between 1751–1753 and 1819) and it includes a) the collapse of the upper part of the Wall in the area examined (the crown of the Wall that had been constructed of architectural members of the entablature of the Old Temple of Athena), b) significant out-ward lean from the vertical (7 cm) of the remaining lower part (the part beneath the crown that collapsed), c) rotation of approximately 1° d) systematic cracking of the outward face of the wall.

The damage was primarily attributed to a strong earthquake motion, since a) earth pressure under static conditions could not cause such a failure and b) war activities are not reported for the period of interest.

For the correct problem description information was drawn from a wide range of scientific specialties (historical/archaeological, architectural, seismological and geotechnical—geological).

Figure 9. Part of the acropolis north circuit wall. The collapse of the upper part of the wall (cornices and metopes) and the systematic cracking of its outward face are clearly visible.

The analyses for the interpretation of the failure comprised: 2-D FE elastoplastic analysis, simplified (pseudostatic) spectral dynamic analysis and a rigorous 2-D time history analysis. For the analysis, the principles of rock mechanics were applied for simulation of the dry-masonry construction.

The results were very satisfactory. The permanent displacement of the current crown of the wall, the rotation of the structure, the collapse of the entablature members (form Γ) and the systematic net of fractures at the outward side of the wall are consistently predicted (Fig. 9).

Therefore, the assumption that the damage was caused by an earthquake was also verified, limiting the termini of the event between 1785 and 1805.

6 DISCUSSION

The role of the geotechnical engineer in the protection of cultural heritage—at least in Greece—is not fully acknowledged both in practical and in institutional level.

However, from the cases discussed in the above paragraphs it is evident that the participation of a geotechnical engineer in the interdisciplinary team catering for the study and the protection of monuments and sites maximizes the usefulness and the value of results, while his/her presence during an archaeological in situ research may be of vital importance for the safety of the persons involved and of great benefit for the research's methodological approach.

The authors' experience has shown that there is a prominent need for the participation of a geotechnical engineer in every scientific team and/or committee institutionally established for the study, the restoration and the protection of monuments and sites, so as the optimum result is attained.

REFERENCES

Dimitriadis, K. 2012. *Geophysical Analysis of the Great Retaining Wall of Amphiareion Archaeological site in Kalamos*. Athens: Geoservice (in Greek).

Egglezos, D. 2010. The use of modern technological applications for restoring the circuit Walls of the Acropolis. In *Acropolis Restoration News* 10: 53–57.

Egglezos, D. 2011. *Transportation and foundation of Potain Crane from the north to the West side of Parthenon. Geostatic calculations*, Athens: Hydroment (in Greek).

Egglezos, D. 2012. Assessment of geoseismic displacements of the "Great Retaining Wall" of the Amphiaraeion in Oropos. Proposal for stabilization measures. *Proceedings of the 3rd National Restoration Conference*, Athens: Etepam (in Greek).

Egglezos, D. & Moullou, D. 2011. Back—analysis sheds light on the history of the Acropolis Wall: The interpretation of a permanent structural failure. In *Proceedings of the XV European Conference on Soil Mechanics and Geotechnical Engineering.*: 1841–1846.

Egglezos, D. & Toumbakari, E.E. 2011. In-situ tests on the Parthenon columns for the assessment of their foundation conditions In *Proceedings of the XV European Conference on Soil Mechanics and Geotechnical Engineering*: 1847–1852.

Ioannidou, M. & Oikonomopoulos, S. 2003. General principles for the organization of the worksite of the restoration of the monuments in *Restoration of the Athenian Acropolis (1975*–2003), *Quaderni ARCo*: 142–146.

Ioannidou, M. 2011. 2010–2011: The progress of restoration on the Acropolis. In *Acropolis Restoration News* 11: 2–9.

Ioannidou, M. 2012. Research and Technology. In Ch. Bouras, M. Ioannidou, I. Jenkins eds, *Acropolis Restored,* British Museum Research Publication (187): 11–20.

Kalogeras, I.S. & Egglezos, D. 2013. Strong motion record processing for the Athenian Acropolis seismic response assessment. In *Proceedings of the 2nd Intern. Symposium Geotechnical engineering for the preservation of Monuments and Historic Sites* (present volume).

Svolopoulos, D. (ed) 2013. *Study for the restoration of the retaining wall of the Treasures in the Sanctuary of Olympia,* Athens: Hellenic Ministry of Education and Religious Affairs, Culture and Sports (in Greek).

Toumbakari, E.E. 2011. *Study for the restoration of N-E Tower of the ancient fort of Aegosthena*. Athens: Hellenic Ministry of Education and Religious Affairs, Culture and Sports (in Greek).

This page intentionally left blank

Geotechnical Engineering for the Preservation of Monuments and Historic Sites – Bilotta, Flora, Lirer & Viggiani (eds)
© 2013 Taylor & Francis Group, London, ISBN 978-1-138-00055-1

Re-burial of the Arrephorion on the Athenian Acropolis: An in situ rescue intervention against degradation

D.N. Egglezos
Civil Engineer, Researcher

ABSTRACT: The case of the Arrephorion on the Athenian Acropolis is a characteristic example of a rescue intervention using the method of reburial. The main reason the backfilling of the Arrephorion was considered necessary was the continuous degradation of its remains from the physical and chemical action of the environment. It was decided that the most suitable method of backfilling in this case was to introduce reinforced soil. With this method the Restoration Principles according to the Chart of Venice are met, while minimal horizontal thrust on the foundation walls and the part of the Circuit Wall in contact and constant physiochemical conditions are assured. The method of backfilling has been very successful as shown from the systematic monitoring of its performance, after 6 years of its completion. The reburial performance is also verified through rigorous 2-D pseudostatic elastoplastic analyses with soil-structure interaction.

1 INTRODUCTION

1.1 *General*

The case of the House of the Arrephoroi on the Athenian Acropolis is a characteristic example of a rescue intervention using the method of reburial.

Object of the geotechnical study was the backfilling of the foundation walls of the Arrephorion and the shapeless marble fragments that had piled up and were found in the removal of earth (anc. backfill) from the monument (Fig. 1).

Figure 1. Inner view of the Arrephorion central hall, before the rescue backfilling. On the right, part of the circuit wall can be seen.

1.2 *The monument*

The Arrephorion (House of the Arrephoroi), on the north side of the Acropolis next to the Circuit Wall (Fig. 1), was a cult building dedicated to the goddess Athena, dating from the 5th century B.C. The preserved parts of the building include the foundation walls, which form two underground halls. The dimensions of the central hall (Hall 1) are 8.30×4.30 m^2 and the maximum height of the foundation 4.90 m. The smaller hall, that is the porch (Hall 2), measures 8.30×2.30 m^2 and the maximum height of the foundation wall is 3.00 m (Fig. 2). The foundation walls, which are rectangular blocks of poros-stone (brittle marl limestone from Piraeus), range between 1.40 and 2.00 m in thickness.

Figure 2. Plan view of the Arrephorion.

2 SCOPE OF THE INTERVENTION

2.1 *The need for intervention*

The main reason the backfilling of the Arrephorion was considered necessary was the continuous damage to the structural components of the monument from the physical and chemical action of the environment. The course of this damage is clear from photographic evidence.

2.2 *The goals of the intervention*

The backfilling of the foundation walls of the Arrephorion has the following goals:

- Protection of the structural components of the foundation walls of the Arrephorion from the adverse mechanical and physicochemical action of the environment.
- Protection of the amorphous marble fragments in the porch by burying them.
- Protection of the interior foundation walls, which are founded on ancient introduced fill within the central hall.
- Relief of the section of the north Circuit Wall of the Acropolis, which is in contact with the north foundation wall of the central hall, from charging actions of the fill under static or seismic conditions.

A prerequisite for accomplishing the above goals is to insure—as possible—the necessary mechanical and physiochemical conditions (temperature—moisture) within the fill.

3 THE BACKFILLING DESIGN

3.1 *Restrictions for the backfilling design—the principles of the intervention*

The backfilling of monuments is considered an intervention on ancient monuments and therefore requires special attention. In making the geotechnical study for backfilling, the general principles of the Charter of Venice were borne in mind. In accordance with these principles, the study had the following restrictions:

- A priori prohibition of the use of permanently incorporated contemporary material such as concrete or metal.
- Differentiation of the modern intervention to the existing ancient structure.
- Reversibility of the backfilling (the fill must be easily removable without damage to the monument)
- Preservation of the existing structural function of the members of the monument.
- Minimizing changes in the appearance of the monument: the fill must not alter the technological and constructional characteristics of the masonry as evidence of the technology of the past.
- The backfill should restore the level of the ancient artificial ground.
- Bearing capacity: the backfill must be able to bear securely self-weight or the accidental loads.
- Minimizing the load on the structural members of the monument: the backfill must be introduced in such as way that its charging action on the building blocks of the monument is minimized.
- Longevity of the backfill: The method of backfilling must insure that the work has the maximum longevity.

The architectural study (Fig. 3) was conducted by the architect of the Acropolis Restoration Service V. Manidaki (Manidaki 2006).

3.2 *Selection of method for backfilling*

After comparative analyses, it was decided that the most suitable method of backfilling in the case of the Arrephorion is to introduce reinforced soil into the central hall, and in the porch simple fill of shapeless marble fragments and supplemented by suitable well graded selected granular soil (Fig. 4).

Around the edges of the monument smooth slopes of well compacted granular soil were formed.

With the method chosen for backfilling, the following advantages are assured:

- Minimal horizontal thrust on the foundation walls and the part of the Circuit Wall in contact.
- Facility in future removal.
- Durability of the work (at least 120 years).
- Full analytical documentation and evaluation.
- Short time needed for doing the work.
- Facility in implementation of construction.
- Reasonable cost of the operation.

4 GEOTECHNICAL STUDY

4.1 *Geotechnical calculations*

The geotechnical study for the backfilling comprises the following calculations:

1. Calculations of external stability.
2. Calculations of internal stability: The thickness of the soil layers of selected gravel, the required tensile strength of the geogrid for each layer, the geometric characteristics of the reinforcement and its positioning are designated.

The calculations were made for the most unfavorable geometry (Fig. 4).

Examined in addition, in the framework of the geotechnical planning of the work, were subjects such as, sufficient drainage of the underground

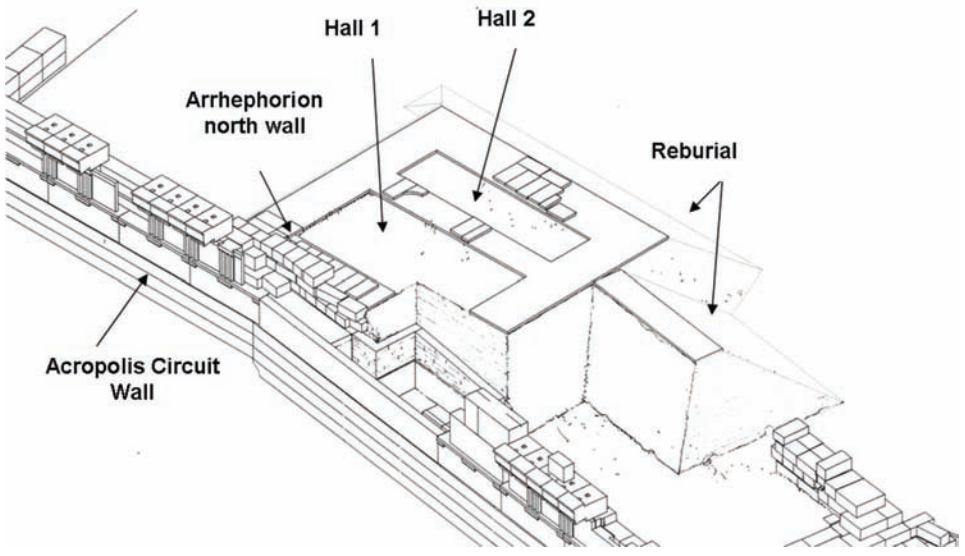

Figure 3. Architectural design of the reburial (V. Manidaki).

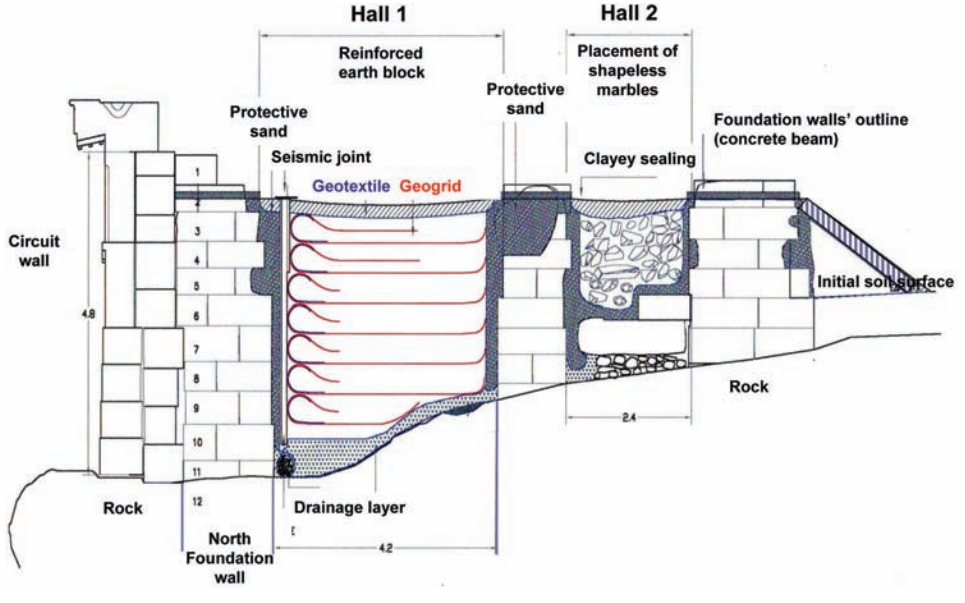

Figure 4. Reburial geotechnical design (Drawing V. Manidaki).

areas and surface protection from rainwater seepage. The calculations were performed for both static and seismic conditions.

4.2 *Seismic actions*

The seismic actions (accelerations) for the design of the re-burial and the displacement performance of the complex system Monument-backfilling-foundation bedrock are specified according to the provisions of the EC-8 since it consists of a new structure with potential impact to the monument. On the other hand the verification of the complex interaction of the system Reburial-Monument-Foundation Rock is examined through displacement performance 2-D elastoplastic analyses for two scenarios of seismic

actions according to: i) the seismic actions used for the reburial design (for comparison to the design results) and ii) a more realistic approach based on the processing of the available historical seismicity data (Papazachos 2002) and the results of the Acropolis Seismic Hazard Analysis (Stavrakakis et al. 2009). This latter scenario is justified from the fact that the analysis is focused mainly to the monument and no to the backfilling performance.

4.2.1 *Provisions of the EC-8*

Specifically, the design of the reinforced earth block is based on the provisions to the EC-8. According to this code the design accelerations in the examined area is defined as follows:

$$a_h = a_{gr}\, S\, S_T\, I_F = 0.16 \times 1.0 \times 1.20 \times 1.40 = 0.27$$
$$a_v = \tfrac{1}{2}\, a_h = 0.135$$

where, a_h and a_v the horizontal and the vertical component of the design acceleration, a_{gr} is the bedrock acceleration, S refers to the soil site effect (soil class A), S_T refers to the topographic effect since the monument lies in the crown of the acropolis rockhill, and I_F the importance factor for monuments (increasing thus the earthquake return period from 50 to 200 years). The above conservative approach is justified from the fact that the backfilling is a NEW Construction interacting to the monument.

If the Importance Factor is not taken into account (e.g. for the conduction of performance analysis) the accelerations are getting the following values:

$$a_h = a_{gr}\, S\, S_T = 0.16 \times 1.0 \times 1.20 = 0.19$$
$$a_v = \tfrac{1}{2}\, a_h = 0.095$$

4.2.2 *Seismic actions according to the Acropolis Seismic Hazard Analysis*

According to the Acropolis Seismic Hazard Analysis the following set of accelerations are proposed:

PGA = 0.14 g (T_R = 72 yrs), PGA = 0.22 g (T_R = 475 yrs), PGA = 0.30 g (T_R = 949 yrs)

4.2.3 *Seismic actions according to historical seismicity data*

The seismic actions are defined according to historical seismicity data (referring mostly to the macroseismic intensity) and empirical macroseismic relations for the estimation of the peak ground acceleration-PGA, in relation to the magnitude, the focal distance and the geotechnical conditions of the site (Scarlatoudis 2003).

In Table 1 the most significant historical seismic events that have affected the Athens area (and consequently the Acropolis Rockhill) and the expected PGA are summarized.

Table 1. Main historical seismicity of Acropolis.

Year	Epicenter	Distance (Km)	Magnitude (ML)	Intensity (MMI)	PGA* (mg)
426 BC	Atalanti	140	< 6.0	?	?
1705	Oropos	35	< 6.0	VI?	45–85
1785	Oropos	40	< 6.0	VI?	40–70
1805	Oropos	40	?	VI?	40–70
1837	Saronic G.	58	6.4	?	?
1853	Thebes	53	6.0	VIII	?
1894	Atalanti	100	6.9	?	30–60
1914	Chalkis	47	6.2	?	?
1928	Corinth	77	6.3	VI?	20–40
1938	Oropos	37	6.1	?	40–78
1981	Alkyonides	77	6.7	VI?	30–60
1999	Parnitha	20	5.9	VI	65–125

*Scarlatoudis et al. (2003), M.O – M.O + 1 std.

From the macroseismic processing of the available historical the PGA in the Acropolis area ranges in the band $0.06 \le PGA \le 0.125$ g (mean value plus a 1 std).

4.2.4 *Seismic design of the reinforced earth block*

The design of the reinforced earth block is based on the provisions of the Greek National Seismic Code (EAK-2003), for artificial embankments of limited height (H < 15 m).

According to §5.4.1 of EAK-2003 the seismic acceleration for embankment design is specified as: $a_{dh} = \tfrac{1}{2}\, [a_h/2 + a_h\, \beta(T)/2], = 0.5 \times [0.135 + 0.135 \times 2.50] = 0.24$.

where $\beta(T)$ refers to the spectral coefficient. For an assumed Vs = 400 m/s of the reinforced soil from well compacted and selected granular materials and soil class A for the rocky ground, $\beta(T) = 2.50$.

4.2.5 *Seismic actions for the conduction of 2-D soil—structure interaction pseudostatic analyses*

For the two scenarios mentioned above, the set of seismic actions are the following:

1. According to EC-8 (for comparative reasons) $a_h = 0.27$, $a_v = 0.135$.
2. According to the Seismic Hazard Analysis and Historical seismicity data (the effective acceleration (not the PGA) and the topographic effect are taken in account): $a_h = 0.18$, $a_v = 0.09$.

4.3 *External stability*

The external stability concerns the calculation for a) the general stability of the system reburial-monument-foundation soil, b) the sliding of the soil block

and c) the overturning of the soil block and d) the bearing capacity of the ground under the soil block. Only the sliding case is examined since the rock slope has been stabilized as part of the Acropolis restoration project, the high quality of the limestone bedrock (Koukis et al. 1976) assures the efficient bearing capacity of the reburial and the overturning of the block is not likely to occur since the base width of the block is greater than its height.

For the sliding analysis of the reinforced soil block upon the separation geotextile on its base the following parameters were used: friction angle between soil block and geotextile $\delta = 30°$ and (conservatively) slope of base of the soil block $\beta = 20°$. From the analysis a sufficient safety factor $FS_{ds} = 1.60$ was taken. The permanent displacement of the block under seismic action was calculated with use of empirical relations (Ambraseys and Menu 1988) and is shown analytically in the paragraph 4.3.1.

4.3.1 *Seismic displacement of the reinforced soil block*

The calculation of the permanent displacement of the reinforced soil block, u due to the design seismic action, was calculated according to Ambraseys and Menu (1988), as follows:

$$\log u(cm) = 0.90 + \log\left[\left(1 - \frac{a_y}{a_{\max}}\right)^{2.53}\left(\frac{a_y}{a_{\max}}\right)^{-1.09}\right] \quad (1)$$

where $a_{max} = 0.27$ g, $\sigma_{\log u}$ = the standard deviation, the critical acceleration $a_y = \tan(\delta - \beta). = 0.176$ g.

From the implementation of the above equation: logu = – 0.125. Taking a conservative design value $\log u_d = \log u + 2\,\sigma_{\log u} = 0.475$, a permanent displacement u_d (cm) = 2.98 cm resulted.

Furthermore, an equal movement from the foundation wall to the reinforced soil block should be taken in account (EAK2000 § 4.1.7.2).

For the permissible axial load of the geogrid a longtime creep deformation of about 2% is expected (that is a displacement of about 4 cm). From the previous results a seismic joint with minimum width b = 10 cm is required. This joint has to be filled by a highly deformable synthetic material (e.g. polysterene sheet).

However, considering an additional movement in the crown of the reinforced backfill due to seismic shaking (that is if the reinforced embankment does not response as a solid body), the joint was chosen to be increased by 50% in the upper part of the filling and spread over two levels: i) from the crest of the backfill and depth to 2 m, joint width b = 15 cm, and ii) for the part 2 m depth from the crest of the backfill to the fill base, joint width b = 10 cm.

4.4 *Internal stability*

The reburial is based on general geotechnical design principles (Bowles 1996, Abramson 2001 etc) and on methods for design of reinforced soil embankments (Koerner 1998, Leshchinsky 1989 and 1995). From the internal stability calculations, the required tensile strength of each reinforcement layer, the geometric characteristics of the reinforcement and the layout are determined.

The calculations showed a requirement for maximum length L = 4.3 m and a maximum tensile strength equal to 33.3 kN.

For the calculations the following were taken into consideration:

4.4.1 *Safety factors*

- Total safety factor for degradation of the geogrid axial strength, ΠRF = 2.40
- Safety factor for the pull-out resistance of the anchored grid: $F_{s,\,po} = 1.50$
- Interaction coefficient of geogrid and soil backfill in pull-out state: $C_i = 0.95$
- Interaction coefficient for sliding of the backfill soil upon the foundation geotechnical unit: $C_{DS} = 0.90$
- Safety factor for the shear strength of the granular backfill material: $FS_{ss} = 1.30$, [$\tan(\phi_d) = \tan(\phi_{max})/1.30$]
- Design life of the backfill t = 120 years

4.4.2 *Geotechnical parameters of shear strength*

Granular backfill soil material (by assumption):

$c' = 0$, $\phi' = 38°$

4.4.3 *Geometric data*

The calculation was realized for the most unfavorable section of the reburial region (Fig. 4):

- reinforced embankment height h = 5.00 m
- slope inclination: i = the 90° (vertical)
- crest slope inclination: $\beta = 0°$ (horizontal crest)
- distance between reinforcement: $s_v = 0.50$ m (so as not secondary reinforcement is required)

4.4.4 *Loads of the backfill*

- vertical load from seal coating and crowding: q = 10 kPa
- Seismic loads: $a_h = 0.24$, $a_v = 0.12$ (as explained in paragraph 4.2)

4.4.5 *Calculation results*

The calculations were performed with appropriate software (Forslope 1.2, 2004). These results were verified with simpler computational methods, as proposed by Koerner (Koerner 1998) for the calculation of embankments with reinforcement geogrid. The axial strength computations showed that

a FORTRAC 80/30 type geogrid (or equivalent) covers design requirements safely.

4.5 *2-D elastoplastic soil-structure performance analyses*

In order to examine the complex interaction between the backfilling block of reinforced earth, the rocky base, the foundation wall (and the circuit wall in contact), the performance of the seismic joint during the design earthquake and the effect of the loose protective sand material inserted between the foundation walls and the backfilling block, more rigorous analyses were performed.

Specifically, 2-D elastoplastic analyses, with finite and/or discrete elements, for plain strain conditions, with pseudostatic application of the seismic action and in proper number of stages so as to simulate efficiently the geostatic/geoseismic history of the monument, were conducted for the following cases:

- Performance analysis of the backfilling block of reinforced earth, with the maximum earthquake action according to paragraph 4.2, since the block is a new protective construction.
- Performance analysis for the foundation wall and the circuit wall in contact. In this area the cornice members of the circuit wall crown create a structure of low stability in horizontal action (the collapse of cornices in the adjacent area of the circuit wall from seismic action is well documented: see Egglezos & Moullou, 2011). The seismic action comes from historical seismicity data, since the analysis is focused to the monument itself and not to the protective intervention.
- Comparative analyses for the performance of a proposed—but not applied—backfilling with a new replacement of the excavated ancient geomaterials (for the two seismic levels mentioned above).

The above mentioned methodology has been applied successfully by the author for the assessment of permanent displacements of modern and historical retaining structures in various—and complex—cases of geotechnical conditions, due to earthquake action (Egglezos 2008, Egglezos & Moullou 2011, Egglezos 2012).

The geometry for the analyses is presented in the section of figure 4. The geotechnical mechanical and natural parameters of the geomaterials involved in the analyses (Egglezos & Moullou, 2011) are shown in Table 2.

The main findings resulted from the analyses are summarized as follows:

For the increased seismic action (a_h = 0.27 g, a_v = 0.135 g)

Table 2. Geotechnical properties of geomaterials.

Geomaterial	c (kPa)	ϕ (°)	E (MPa)	v	γ (κN/m^3)
Marl stones	50	30	460	0.2	24
Limestone	–	–	7000	0.2	26
Backfill	1	40	100	0.3	20
Sand	0	30	10	0.3	18
Polysterene	200	–	1	0.1	0.2
Anc. Backfill	1	36	100	0.3	22
Interface*	0	25	–	–	–

* of marl-stone blocks.

- The permanent displacement of the backfilling block of reinforced earth (fig. 5) is very limited (22.9 mm in the crown) and practically the block does not apply any thrust upon the foundation walls. The displacement resulted from the 2-D analyses is in good agreement with that arising from the empirical formulae (29.8 mm) that were applied for the design of the reinforced block.
- The horizontal pressure upon the foundation wall for the backfilling of reinforced earth (fig. 6) is ought mainly to the densification of the interjected loose sand (ranging from top to bottom: 0 to 19 kPa).
- The horizontal pressure upon the foundation wall for backfilling from the ancient geomaterials (fig. 7), ranges from top to bottom: 0 to 137 kPa. In this latter case the stress state of the wall stones is much more intense than in the case of backfilling from reinforced earth.
- The cornice displacement in both cases (reinforced earth and the replacement of ancient geomaterials) is approximately 88 mm. This displacement is mainly attributed to the inertial force developing to the cornice members and the full mobilization of the structural stones interface shear strength.

For the historical seismic action (a_h = 0.18 g, a_v = 0.09 g)

- The permanent displacement of the backfilling block of reinforced earth, is practically negligible (2.3 mm).
- The horizontal pressure upon the foundation wall (for the backfilling of reinforced earth) is attributed too, to the densification of the interjected loose sand but it is much lower comparing to that arising from the increased seismic action (ranging from top to bottom: 0 to 9 kPa).
- The horizontal pressure upon the foundation wall (for the backfilling from the ancient geomaterials) ranges from top to bottom: 0 to 82 kPa. In this latter case the stress state of the wall stones is also much more intense than in the previous one.
- The cornice displacement in the case of reinforced earth is about 9 mm, while in the case

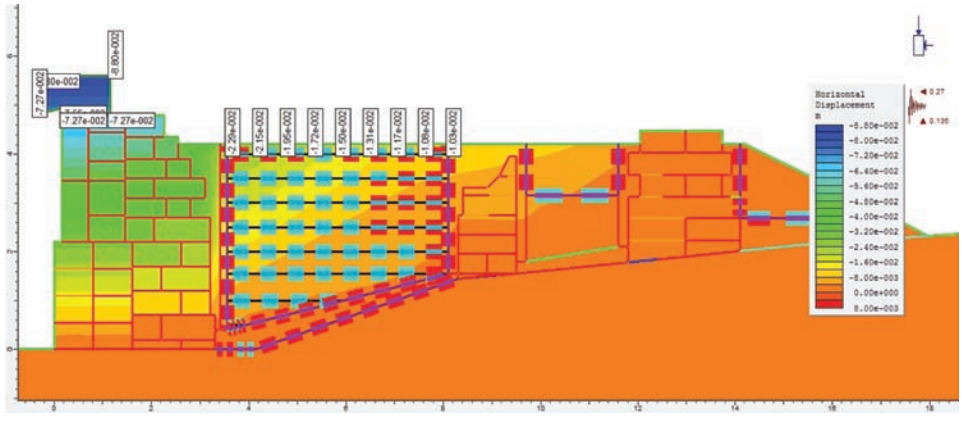

Figure 5. Displacement of the reinforced earth block for the design earthquake.

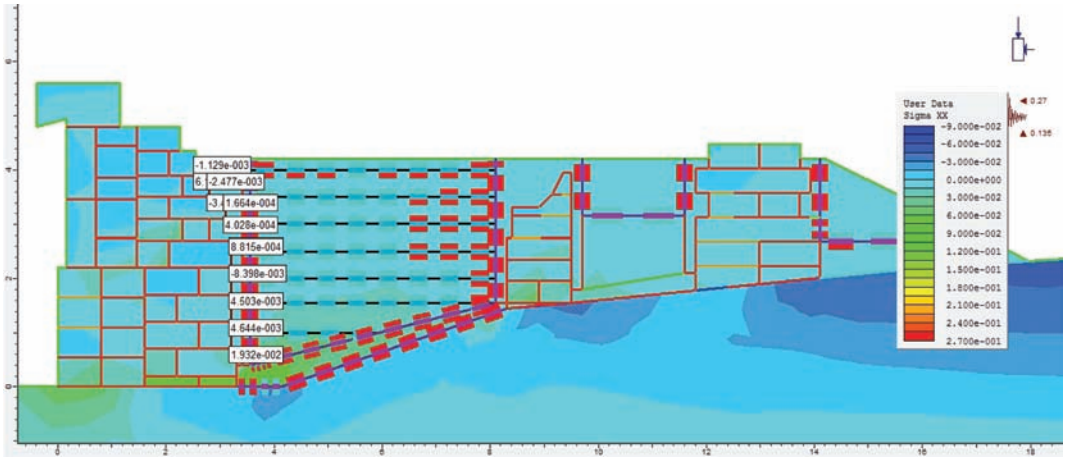

Figure 6. Horizontal pressure on the foundation wall for the design earthquake—reinforced earth block.

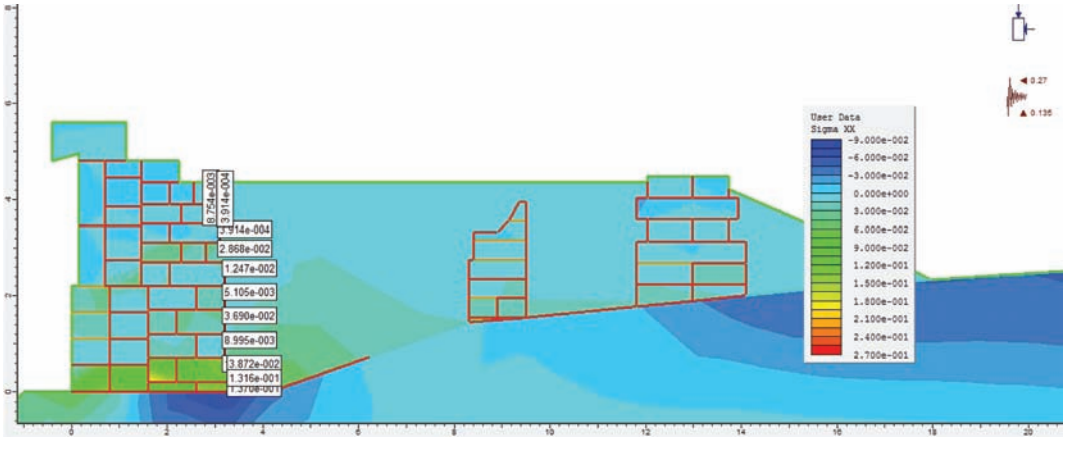

Figure 7. Horizontal pressure on the foundation wall for the design earthquake—replacement of the ancient backfill.

of anew replacement of ancient geomaterials is 19 mm. In both cases the displacement is low and the danger for overturning is minimal.

The results of the analyses are also consistent to the current situation of the monument and verify the successful design of the rescue re-burial.

Indeed, the calculated relative displacement of the north to the central wall of the Arrephorion (fig. 8), in the level of the installed optical fibre sensor (~1 m below the back filling surface) is in agreement to the optical fibre measurements (0.15–0.36 mm calculated vs 0.10÷0.36 mm measured).

In addition, the calculated horizontal pressure at the position of the installed pressure sensor (fig. 9) in the inner side of the north wall (~3 m below the back filling surface) is very close to the measured value (7 kPa calculated vs 8 ÷ 9 kPa measured). Finally, the high accuracy topographic measurements for horizontal displacements that were performed in the cornice of the circuit wall (±1–2 mm) are consistent to the practically negligible calculated value (0.06 mm), especially if the topographic error is taken into account.

The resulted displacement of the reinforced block, the cornices of the circuit wall and the relevant horizontal pressures on the inner side of the foundation walls (for the two seismic levels and geostatic conditions) are summarized in Tables 3 and 4.

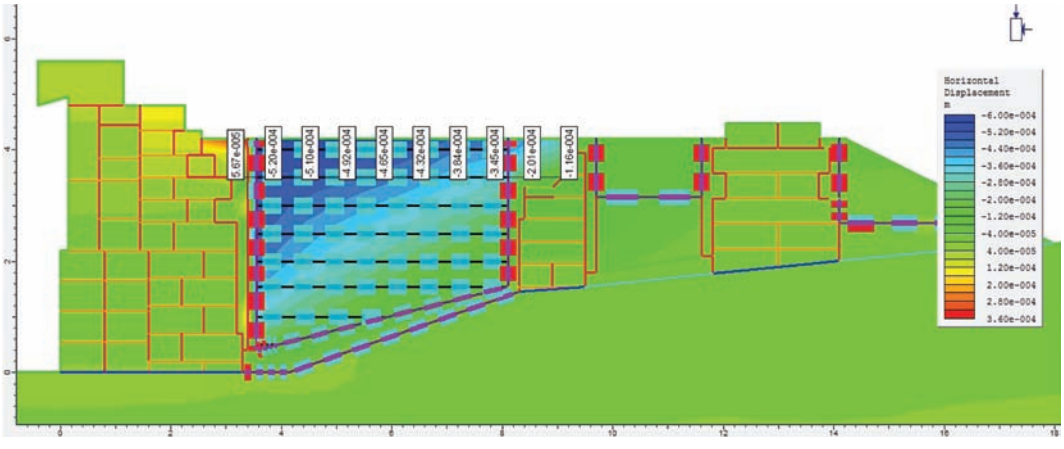

Figure 8. Calculated displacement between the north and the central wall for geostatic conditions—reinforced earth block.

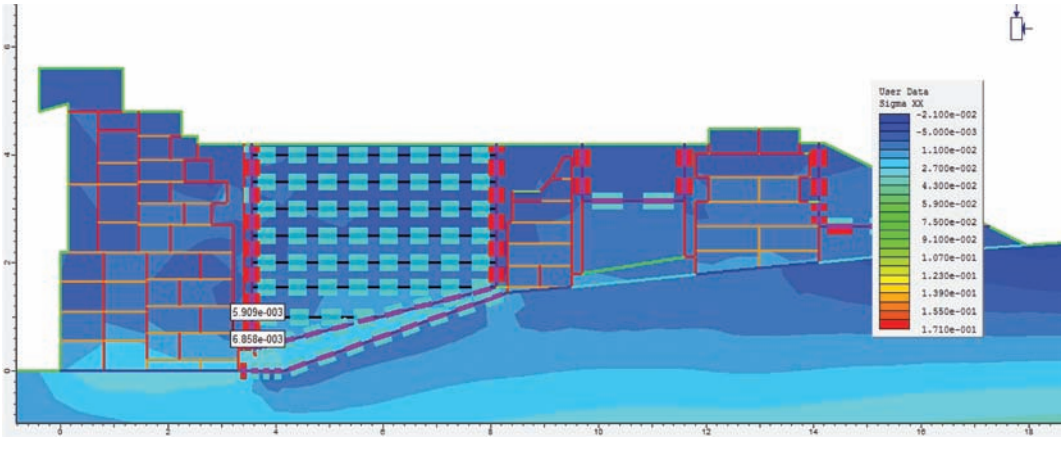

Figure 9. Calculated pressure at the base of the north wall for geostatic conditions—reinforced earth block.

Table 3. Calculated displacements and max horizontal pressure of the reinforced earth block.

Acc. (g)	Cornice displ. (mm)	Block displ. (mm)	Max. Horiz. Pressure (Kpa)
0.27	88.0	22.9	19.3
0.18	9.4	2.3	8.7
0.0*	0.06	0.5	7.0

*Geostatic state.

Table 4. Calculated displacements and max horizontal pressure of the replacement of the ancient backfill.

Acc. (g)	Cornice displacement (mm)	Max horizontal pressure (Kpa)
0.27	87.0	137.0
0.18	18.8	81.7
0.0*	0.2	23.9

*Geostatic state.

5 THE INTERVENTION

5.1 *Restrictions for the backfilling design—the principles of the intervention*

Briefly, in the framework of making the backfilling and giving functional shape to the wider environs of the area, between September 2006 and April 2007, the following works were completed:

- detailed geometric documentation of the monument with 3D laser scanning (fig. 10).
- a leveling base layer of selected gravel.
- a drainage layer in the base of the monument.
- a reinforced embankment with successive layers of compacted select gravel 25 cm. thick and geogrid. The layers of geogrid are set at intervals of 50 cm.
- sealing layer of surface material of low permeability.
- filling of the porch with the amorphous marble.
- around the Arrephorion a perimetric fill was formed with a smooth slope.
- construction of a drain around the edge at the foot of the slopes of the fill (to carry off rainwater).

During the work, in addition to continuous macroscopic monitoring, there was incessant quality control, with sufficient laboratory and field tests. The view of the monument after the completion of the intervention is depicted in Figure 11.

5.2 *Monitoring*

Backfill monitoring was made possible by placing: a) pile witnesses for the topographical monitoring of settlements at point b) optical fiber sensor for monitoring potential movements of the north wall in relation to the central wall c) a pressure sensor at the base of the north wall and d) targets for high accuracy topographic measurements concerning potential displacements of the Circuit Wall.

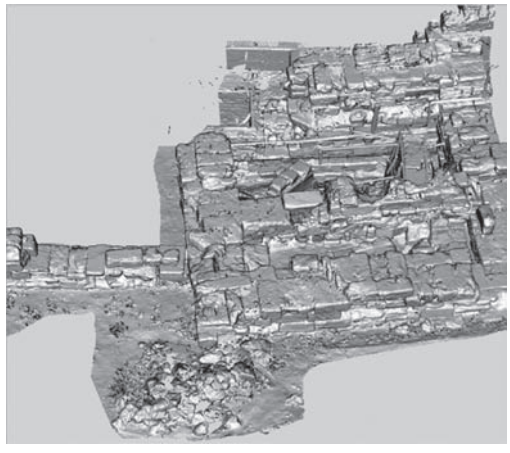

Figure 10. Geometric documentation of the monument with 3-D laser scanning (L. Grammaticopoulos, I. Kalisperakis).

Figure 11. View of the monument after the completion of the intervention.

6 SYNOPSIS-CONCLUSIONS

The reburial of Arrephorion is a characteristic case of interdisciplinary approach with the geotechnical engineer having the central role. Indeed the final design is based on archaeological, architectural, conservation and topographic data.

The design of the reburial—reinforced soil block—was based strictly on the provisions of the EC-8. The construction of the reburial was completed successfully on May 2007. Henceforth the

monument is in a state of continuous monitoring for the evaluation of the intervention performance (referring to settlement of the soil block, displacement of the circuit wall in contact, displacement between the north and the central foundation wall of the monument and lateral pressure observation on the inner side of the north foundation wall).

The reliability of the design and the construction was verified (post construction) through 2-D elastoplastic analyses. The results of these analyses are consistent to the measurements of the monitoring systems and consequently the modeling is considered efficient for the estimation of seismic displacement performance of the monument under strong seismic actions.

The basic conclusion is that the analytical and constructional approach that was applied for the reburial of the Arrephorion, is an integral methodology for reburial interventions and can be applied effectively in relevant cases.

REFERENCES

Abramson L.W., Lee T.S., Sharma S. & Boyce G.M. 2001. *Slope Stability and Stabilization Methods*. John Wiley & Sons.

Ambraseys, N.N. & Menu, J.M. 1988. Earthquake-induced ground displacements. *Earthquake Engineering and Structural Dynamics* 16, 985–1006.

Bowles E.J. 1996. *Foundation analysis and design*, Mc Graw Hill—International editions.

EAK 2003, Hellenic Seismic Code.

EC-8. Eurocode 8 2011. European Seismic Code.

Egglezos D. 2006. *Geotechnical study for the reburial of the House of Arrephoroi*, Athens: Hellenic Ministry of Culture, Acropolis Restoration Service (in Greek).

Egglezos D. 2008. Exact application of National Antiseismic Code for seismically sensitive soils-Conclusions from the design of Lefkas Marine quay wall. In *Proceedings of 3rd Greek Earthquake Engineering and Technical Seismology Conference* Athens.

Egglezos D., Moullou D. & Mavromati D. 2008. Geostructural analysis of the Athenian Acropolis Wall based on terrestrial laser scanning data, *In Proceedings of 21th ISPRS,* Beijing, China.

Egglezos D., Moullou D. Back-analysis sheds light on the history of the Acropolis Wall: The interpretation of a permanent structural failure. In *Proceedings of the XV ECSMGE*, Athens, Greece, 1841–1846.

Forslope 1.2 2004. *Software Code for design of reinforced walls and embankments,* Germany: HUESKER SYNTHETICS.

Koerner R.M. 1998. *Designing with Geosynthetics*, N.J, USA: Prentice Hall.

Koukis G., Andronopoulos A. 1976. *Geological—Geotechnical Study of the Athenian Acropolis area*, Athens: Institute of Geology and Mineral Exploration.

Leshchinsky D. & Boedeker R.H. 1989. Geosynthetic reinforced earth structures, *Journal of Geotechnical Engineering*, ASCE, 115(10), 1459–1478.

Leshchinsky D., Ling H.I. & Hanks G. 1995. Unified Design Approach to Geosynthetic-Reinforced Slopes and Segmental Walls. *Geosynthetics International*, Vol. 2, No. 5, 845–881.

Manidaki V, 2006. *Architectural study for the reburial of the House of Arrephoroi*, Athens: Hellenic Ministry of Culture, Acropolis Restoration Service.

Papazachos V. & Papazachou K. 2002. *Earthquakes of Greece* (in Greek), Thessaloniki: Ziti Publ.

Skarlatoudis A.A., Papazachos C.B., Margaris B.N., Theodulidis N., Papaioannou Ch., Kalogeras I., Scordilis E.M. & Karakostas V. 2003. Empirical Peak Ground-Motion Predictive Relations for Shallow Earthquakes in Greece, *Bulletin of the Seismological Society of America*, 93, 6 (2003), 2591–2603.

Stavrakakis G. 2009. *Seismic Hazard Analysis at the Athenian Acropolis*, (in Greek) Athens: NOA.

Geotechnical Engineering for the Preservation of Monuments and Historic Sites – Bilotta, Flora, Lirer & Viggiani (eds)
© 2013 Taylor & Francis Group, London, ISBN 978-1-138-00055-1

Egyptian experience in the preservation of monuments and historic structures. A case study: Hibis Temple, El-Kharga—Egypt

M.K. El-Ghamrawy
Al-Azhar University, Cairo, Egypt

M.A. Sakr
Tanta University, Tanta, Egypt

S.A. Gad
Al-Azhar University, Cairo, Egypt

ABSTRACT: This paper is about applying a State-Of-The-Art technology on a very ancient structure. It gives an example of how modern technology can efficiently serve in the preservation of history and heritage of civilization. A description of the structure and its location is given followed by the method used to help its preservation.

1 INTRODUCTION

This paper presents the details of a salvation project which belongs contemporarily to engineering and archeology. In order to respect the historical integrity, the structure was held and strengthened in the final configuration assumed after many historic earthquakes.

2 THE STRUCTURE AND LOCATION

The structure is an ancient Egyptian temple called Hibis Temple. It is at El-Kharga which was an oasis in the western desert of Egypt; now it is a modern city and capital of the "New Valley Governorate". El-Kharga is about 700 km south (south-west) of Cairo and reachable by highways, airplane and—partly—by train. Figure 1 shows the historic map of Egypt and Figure 2 the location of Hibis Temple at the outskirts of El-Kharga Oasis, western desert of Egypt.

Figure 1. Historic map of Egypt.

Figure 2. Location of Hibis Temple at the outskirts of El-Kharga Oasis, western desert of Egypt.

3 A GLIMPSE INTO EGYPTIAN HISTORY

The unwritten mankind history in Egypt dates back hundreds of thousands of years before Christ (BC) with many artifacts allover Egypt during different eras. Especially so is the Old Stone Age (Paleolithic) from ~ 100000 BC to ~ 10000 BC and the Middle Stone Age (Mesolithic) until ~ 5000 BC. As far as Egyptology is concerned it started to take shape

enabling scholars to properly study this history chronologically around 6000 years BC and during the New Stone Age (Neolithic). The traditional written history of ancient Egypt is divided into 30 dynasties from ~ 3150 BC to 332 BC. They are dynasty 1 to 30. (Dynasty 31 is also recorded and now Egyptologists are adding dynasties preceding dynasty 1).

These 30 dynasties are further divided into three main Kingdoms separated by unstable periods in the history of Egypt. The three Kingdoms are "The Old" (~3150 BC: ~2200 BC), "The Middle" (~2134 BC to ~1786 BC) and "The New" (~1552 BC: ~1069 BC). This is followed by the Ptolemaic period from Alexander the Great—332 BC—ending with the famous Cleopatra in the year 30 BC. Afterwards the Romans invaded and ruled Egypt for about seven centuries.

4 THE TEMPLE

The temple of Hibis is the most important monument in the entire western desert of Egypt. It is unique in its time of construction, the wealth and abundance of drawings and inscriptions and unsurpassed combinations and representations of gods, goddesses and deities of ancient Egypt. The location of the present temple is—most likely-a holy site of previous temples that may date back to the Old to and Middle Kingdoms of Egypt. Work in the present temple started during the 26th dynasty (672 BC–525 BC).

In the days of its construction the temple occupied a dominant and majestic high location over a hill in the middle of the old city of Hebet (the plough in the ancient Egyptian language) just to the north of the present city of El-Kharga.

Only a few monuments still remain of this old city. Above the ruins of the 26th dynasty temple King Dara of the 27th dynasty (~525 BC ~404 BC) constructed the present temple around 522 BC. Additional structures were added to the temple during the reign of Hekr of the 29th dynasty ~393 BC, Nekhtnebu I ~380 BC and Nekhtnebu II ~360 BC. During the Ptolemaic dynasty Ptolemy II (Philadelphious) ~284 BC erected an external portal. After the death of Nero in Rome 68 AD four emperors ruled during one year. During the reign of one of them Galba a portal was added to the Hibis temple complex nearer to the landing stage on the lake. Figure 3 shows a general layout of the Temple.

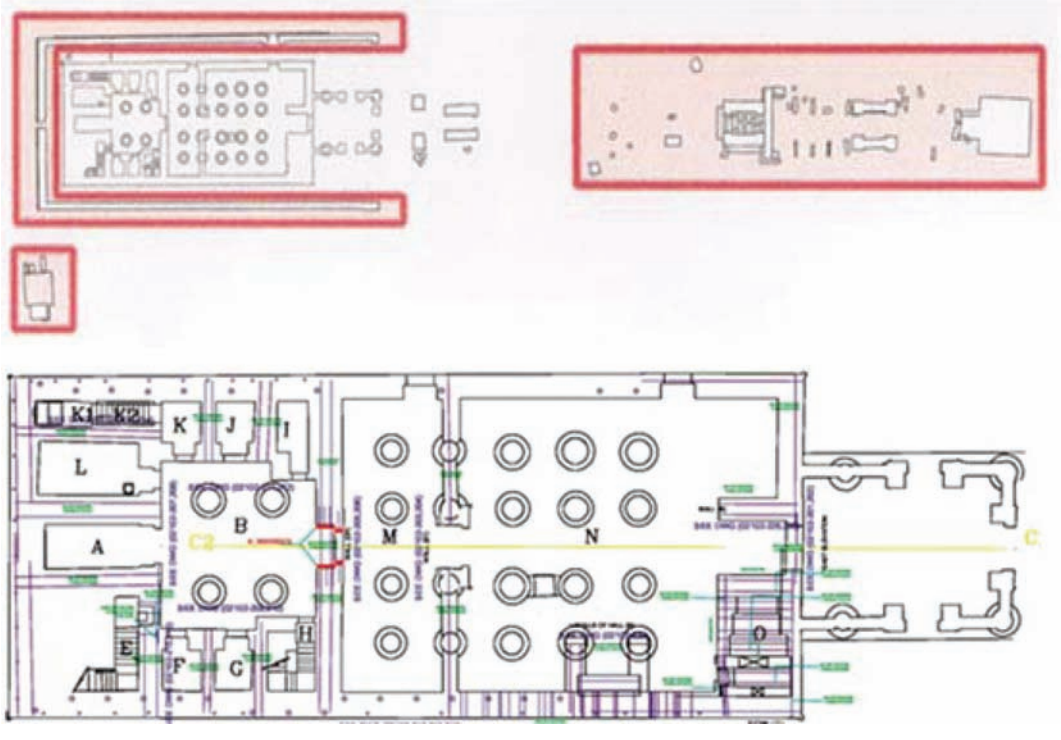

Figure 3. General layout of the temple.

The temple axis is from east to west. At present the temple and its complex consist of the following, (Figures 4 through 8):

- Landing stage on the lake.
- Avenue of the sphinxes which is crossed in locations of the added portals.
- Three portals; the Roman one nearer to the landing stage, then towards the temple, the Ptolemaic one and the original one by Dara near the temple.
- Bases of two obelisks west of Dara's portal.
- A portico by Nekhtnebu I ~ 380 BC and Nekhtnebu II ~ 360 BC. With eight floral columns separated by curtain walls. It contains religious and kings scenes.
- First (east most i.e., latest) hypostyle by Nekhtnebu II ~ 360 BC. It contains 12 columns on exceptionally solid slabs to sustain the large imposed loads by the columns and roofs.
- Second hypostyle by Hekr ~ 393 BC, Nekhtnebonu I ~ 380 BC and Nekhtnebu II ~ 360 BC. It contains eight columns and has extraordinary drawings and inscriptions some of which are only found in this place.
- Third—and original—hypostyle by Dara. It has four columns and contains very important scenes on wall inscriptions.

Figure 4. Landing stage in the lake.

Figure 5. Roman portal.

Figure 6. Pteolomic portal.

Figure 7. Original portal.

Figure 8. Birth room.

- The sanctuary (sanctum Santorum) is on the west side of the temple along its axis and contains outstanding and unique scenes.

There are also eight side rooms, a basement and four rooms on the roof. The temple was surrounded by a wall and there is a birth room outside the walls of the temple.

5 GODS AND GODDESSES IN THE TEMPLE

The 26th dynasty temple was probably constructed for the god Menes. However the present temple is dedicated to Amun Ra, his wife Mut and their son Khonsu. The three form a famous trinity among the many trinities in ancient Egyptian Theology.

Other deities are honoured in the temple such as Atum, Shu, Tefnut, Osiris, Isis, Horus, Set, Jhoty, Geb, Nut, Niet, Nephtis and others. Some of them are foreign to Egypt.

There are scenes and inscriptions in this temple which are unique in showing rare representation and combinations of deities. A situation that places the temple of Hibis as one of the most important monuments in Egypt.

6 CONDITION OF THE TEMPLE

Signs of collapse such as settlements and cracks started to appear as can be seen in figures 9 through 12.

Figure 9. Temple wall separation due to settlement cracks.

Figure 10. Damage caused by external wall leaning.

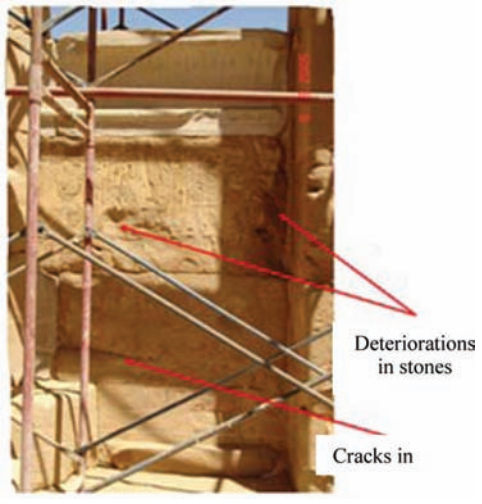

Figure 11. Temple stone cracks and deteriorations.

Figure 12. Signs of damage.

Figure 13. Inner gateway paintings before salvation.

The Temple structure condition gave an impression that the damage was due to ground deformation.

The soil investigation revealed that these signs of damage were due to the swelling pressure of soil underneath the Temple foundation due to the presence of a shallow ground water table.

7 SUBSURFACE INVESTIGATION

A field investigation program including ten soil boreholes in the vicinity of the Temple structure and geophysical surveys was carried out. The purpose of this investigation program is to characterize the subsurface material and determine the engineering properties of soil. In addition to the borings, the exploration program included three types of geophysical testing (downhole geophysical testing, soil resistivity and surface ground penetrating radar).

Based on the seismic study, the soil profile in the structure area could be broadly divided into five layers. Figure 14 shows a sample of the resulted soil profiles from this study. From this study these five layers are: (1) The first layer with a thickness varying from 0.1 m to 3.7 m and seismic wave velocity varies between 267 m/sec to 399 m/sec.; (2) The second layer with a thickness between 2.2 m and 7.7 m. The seismic wave velocity for this layer varies from 429 m/sec to 840 m/sec.; (3) The third layer has a thickness varying from zero up to 8.5 m with a seismic wave velocity between 1176 m/sec and 2353 m/sec.; (4) The fourth layer has a thickness between 1.5 m and 11.0 m and a seismic wave velocity between 1665 m/sec and 2667 m/sec.; (5) The last layer has a thickness varying from 3.1 m to 19.0 m with a seismic wave velocity between 2105 m/sec and 3125 m/sec. This last layer is followed by an extended layer with a seismic wave velocity between 2500 m/sec and 2857 m/sec.

Combining the seismic study with the results obtained from boreholes, the soil profile in the structure area can be classified as composed by a succession of layers of clayey silt to silty clayey sand varying in both vertical and horizontal directions.

These layers have a swelling pressure value between 350 and 625 kPa. From laboratory soil tests, the dry density was found to be ranging between 17.7 and 18.4 kN/m^3 and the water content between 20 and 24%.

The soil resistivity study indicated that down to a depth of up to 40 m the soil has low resistivity varies between 1.08 Ohm-m and 23.9 Ohm-m. However, the resistivity values between the depths of 4 and 10 m are higher reaching a value of 35.6 Ohm-m. For the soil below the depth of 40 m, the soil resistivity increases to more than 51.1 Ohm-m. This indicates that there is no ground water up to this depth. The water found in the site can be only due to surface infiltration.

The surface ground penetrating radar (GPR) study indicated that there are boulder stones at a depth around 3 m. These boulders can be a part of the structure foundation as shown in figures 15 and 16. This study indicated also a thin stone layer of thickness variable between 0.3 m and 0.6 m inside the temple. The GPR study showed that the foundation depth of the original portal was found at a depth larger than 3 m (Figure 15). Figure 16 shows the foundation depth of Pteolomic and original portals as resulted from the GPR investigation. From this

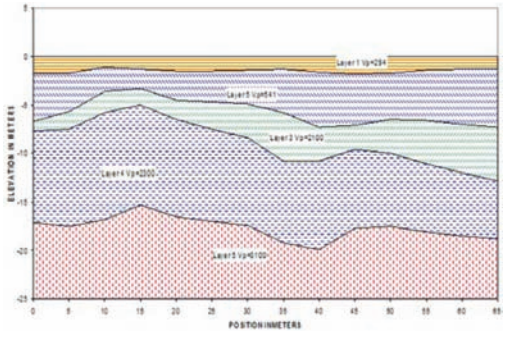

Figure 14. Sample of the soil profiles resulting from seismic study.

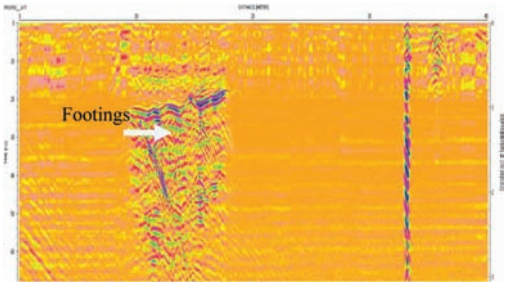

Figure 15. Foundation depth of original portal resulting from the GPR investigation.

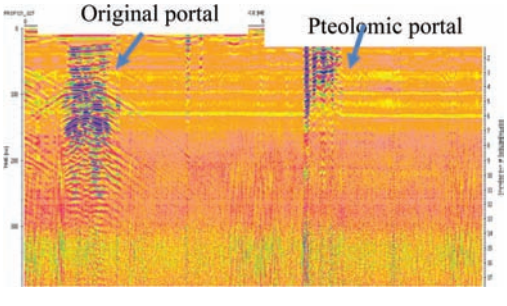

Figure 16. Foundation depth of Pteolomic and original portals resulting from the GPR investigation.

Figure 17. The temple structure before salvation work.

GPR study also, the landing stage in the lake foundation was found at a depth of around 2 m.

Finally it was decided that major restoration project is essential to salvage the temple since deterioration will continue unless drastic measures are taken to remove the essential causes of damage which are the foundation soils and the percolated surficial ground water. Figure 17 shows the Temple structure before salvation work.

8 SALVATION PROJECT

The salvation project is engineering and archeological. Its main general elements are:

8.1 *The engineering part*

The engineering salvation part was planned to overcome the problem of soil swelling pressure and to control the ground deformation due to surface water infiltration underneath the Temple structure foundation especially from the surrounding cultivated land. This is done as follows:

a) Surrounding the temple complex with a diaphragm wall as a barrier to prevent seepage of ground water to the foundation soil underneath the temple foundation.
b) Drilling piles filled with lime around the temple to control the swelling potential of the foundation soils.
c) Anchoring rocks together to reinforce the structure and prevent collapse for a long time to come. Anchoring blocks and pieces of the masonry structure together was done by a British Company with an international reputation for strengthening structures using a unique patented reinforcement system together with the latest state of the art software and engineering expertise. They have worked on nearly all the landmark structures in the UK including Windsor Castle after the fire where they reinforced the Brunswick Tower and secured all the new roof trusses in the State Banqueting Hall. The advantages of this anchoring system are: custom designed by engineers; cementitious and sympathetic to the structure; highly durable designed to last the life span of the structure; controlled grout flow and finally invisible when installed reversible. The anchoring system has to be finished by grouting under pressure passes through a series of grout holes lined by a fabric sock. The excess milk of the grout and bonding agent passes through the fabric sock both fixing and providing a mechanical and chemical bond to the parent material.

Figure 18. Surrounding the temple complex with a diaphragm wall for water control.

Figure 19. To overcome any water that might enter under this barrier a series of lime piles were formed through the entire temple to absorb any other water penetration.

Figure 20 shows the anchoring system with grouting under pressure to reinforce the temple walls and figures 21 and 22 the position of anchors. Each anchor position was carefully designed to satisfy the engineering require-

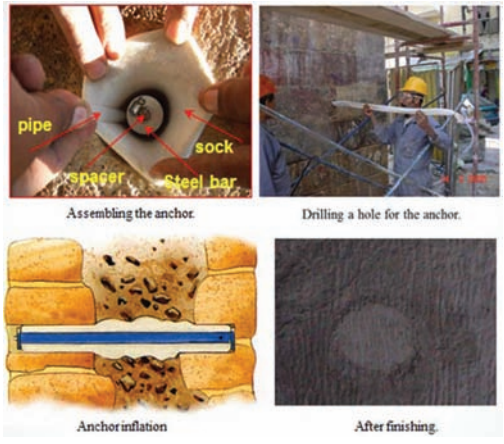

Figure 20. Steps for anchor assembly, drilling, inserting and finishing.

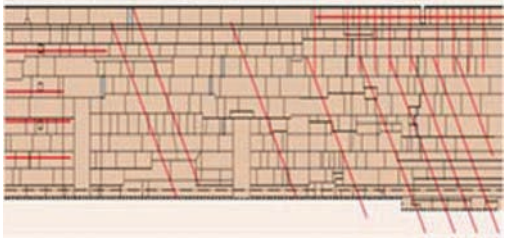

Figure 21. View of typical anchor arrangement to stabilize the outer walls of the temple.

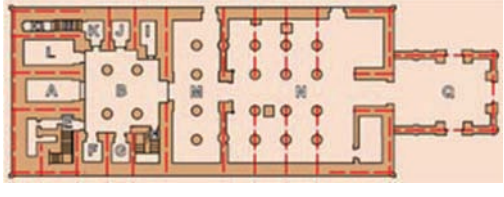

Figure 22. Position of anchors. (---)

ments, but they were also extremely sensitive to the delicate hieroglyphs adorning the temple.

d) Controlling the subsurface water by collecting the extra water with traps and a sub drainage system of perforated pipes and screen of deep gravel piles (Figure 23).

8.2 *The archeological part*

The archeological salvation part aimed to reach a proper and accurate architectural documentation. From this architectural documentation, the damages could be determined. This is was done in two steps as follows:

a) Inspecting all masonry work in the temple, portals, landing stage, birth room and fence and substituting the damaged pieces from the original quarry and placing fallen pieces in their right positions.
b) Carrying out a thorough restoration work for all the inscriptions and paintings.

Figure 24 shows a sample elevation from the original 1941 Metropolitan Museum of Art's

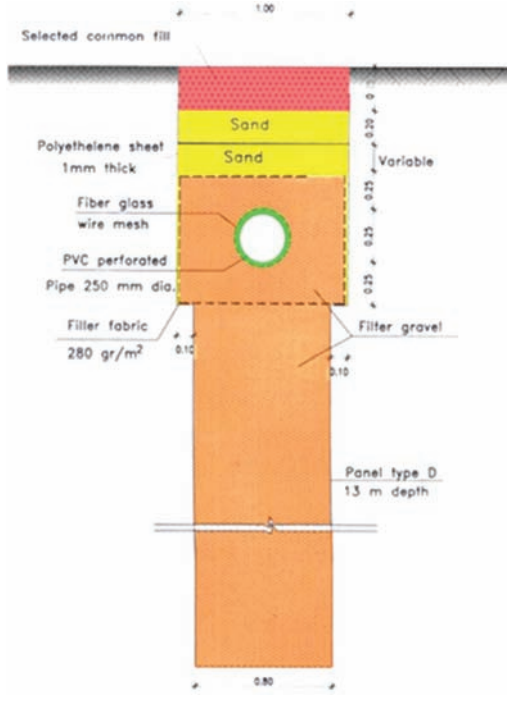

Figure 23. Controlling the subsurface water.

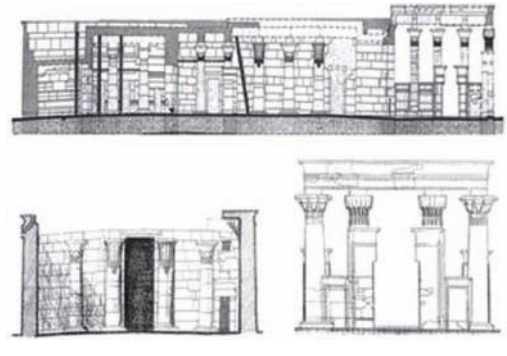

Figure 24. Architectural documentation.

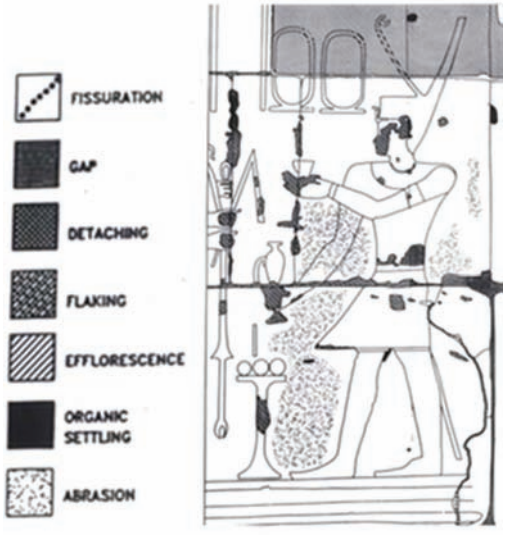

Figure 25. Determination of damages on the architectural documentation.

publication and figure 25 shows a sample of the localization of damages on the architectural documentation.

9 CONCLUSIONS

Figure 26 shows the Photograph of the building after engineering and archeological repairs were completed.

The structure performance after the application of these remedial measures was quite satisfactory, and accordingly the Temple was re-opened (Figure 27).

The structure was not repaired as new but was held and strengthened in the final configuration that it had assumed following many historic earthquakes. This repair regime is adopted to respect the historical integrity and make visible the history of the structure.

This same engineering technologies were and are still being used in restoring monuments and historical buildings that are considered world heritage. These monuments and historical buildings are from the 10th century AD to date.

10 FINAL REMARKS

Fled (1964) stated that the structure must be considered as a living thing being affected by external causes and tending to compensate internally to

Figure 26. The Hibis Temple at El-Kharga Oasis, western desert of Egypt after preservation.

Figure 27. Re—opening the Hibis Temple after preservation.

localized overstress, more readily when the action is slowly applied. Thus, no one can accurately predict the actual behavior of a structure because tolerance of structures to settlement is affected by the combination of type of structure, soil and foundation type and surrounding changes.

Finally, we can say that; extra expenditure over the foundation during construction may save a great amount of money spent on repairs in the future.

REFERENCES

Al-Ramli, A.H. and Al-Ghamrawy, M.K. (2000). Hibis Temple salvation. *A technical report submitted to the High Supreme council of Antiquities, Egypt*.

Fled, J. (1964). Tolerance of structures to settlements. *Proceedings of the conference on design of foundations to control settlement, SMFE, ASCE, pp 555–569, Illinois, USA.*

Ramadan, E.H. and Hosain, M.H. (2000). Hibis Temple site investigation—*A geotechnical report. Faculty of Engineering, Assuit University, Egypt*.

Sakr, M.A.M., Lotfy, H.A. and Abd El-Rahman, M.M. (2000). Foundation settlement causing structure distress—case study. *Proceedings of the 4th IGEC, pp (673–684), Cairo, Egypt*.

Geotechnical Engineering for the Preservation of Monuments and Historic Sites – Bilotta, Flora, Lirer & Viggiani (eds)
© 2013 Taylor & Francis Group, London, ISBN 978-1-138-00055-1

Diagnostic of the colonial structure "Palacio del Segundo Cabo" in Havana, Cuba

S. Figueredo & Y. Gámez
INVESCONS, Havana, Cuba

R. Lorenzo, J. de la Rosa & R.P. da Cunha
University of Brasilia, Brasilia, Brazil

ABSTRACT: The "Palacio del Segundo Cabo", was built at the end of 1790 in Havana, Cuba and has undergone several modifications. In recent years he has begun to have sharp deterioration in its structure. An investigation was conducted to determine the causes of the observed damages. The work was focused on analyzing the characteristics of the materials, monitoring and determining the structure of settlements occurred in the 222 years of existence. It was found that the main cause of the damage is related to the heterogeneity of the soil and foundation support. As a result the authors recommend using a micropile underpinning. The assumptions were validated by an analysis of the behavior of the structure based on the finite element method.

1 INTRODUCTION

Important building were constructed in Havana during 1770, among the main plans was a civic center where the political and administrative activities of the colony gathered together. The Plaza de Armas, as the square was finally named, would house important buildings, among which were the infantry barracks, the customs, a municipal house with the Governor General's residence, and the Post Office Management, which a few years later became the Palacio del Segundo Cabo.

The Palacio del Segundo Cabo is a monumental building with Protection Grade I and, because of its antiquity and majesty is one of the main buildings of Old Havana. The edifice is located on the corner of Tacon and O'rreily Sts and in its 222 years of existence has hosted dissimilar institutions undergoing major expansions, structural modifications and changes of use. Among the most important are the following:

- 1790–1828. Post Office Management.
- 1828–1900. Office of the General Sub-Inspection of the Army.
- 1902–1911. Senate headquarters.
- 1929. Supreme Court headquarters.
- 1956–1960. Academies of History of Cuba, Geography, Fine Arts and Spanish Language.
- 1960–1963. Academy of Sciences of Cuba.

Figure 1. Perspective of Palacio del Segundo Cabo in 1790.

- 1963–1965. Office of the deputy ministry of economy of the Ministry of Culture.
- 1970–2005. Cuban Book Institute.

Since its early decades some damage has appeared throughout the structure, resulting in imbalances that have been intensifying in recent years, something that prompted the Office of Consulting & Design of the National Applied Research, INVESCONS to conduct an investigation. The work was conducted in 2011 and it was focused on the identification of major cracks and weaknesses in the structure, the characterization of materials involved and the evaluation of the causes of the deterioration. The work also focused on the structural security taking into account the existing damage from the existing to finally establish strategies for a complete repair.

2 DEVELOPMENT

In order to achieve the proposed objectives of the research, a group of tasks was carried out as part of a methodological approach that brings together the following activities:

- Study of the historical background, typologies and the employed construction techniques.
- Performing architectural, structural and pathological surveys, to reproduce the geometry of the studied phenomenon with a high degree of accuracy.
- Location, classification and quantification of damages.
- Diagnostic and physical mechanic characterization of the materials to establish the parameters of constitutive models to be used to simulates their actual behavior.
- Implementation of instrumentation systems for measuring the activity of the cracks and validation of numerical models.
- Analysis and evaluation of the structural behavior to validate the hypothesis and define the engineering solutions for the total repair of the property.

2.1 *Surveying*

A Geometric leveling was carried out to determine the difference of levels on the perimeter of the building, taking as reference the lines of the facade's decorative elements and an arbitrary coordinate system. The results indicated differences between 0.038 m and 0.154 m, and the most significant were located on the facade on Tacon St, as shown in Figure 2.

It is considered that the slopes may have been caused by two fundamental elements, imperfections during its construction and the settlements of the structure due to its own weight.

Taking into account the geometric dimensions of the building and the geotechnical characteristics of the materials on which it rests, it is estimated that these settlements could occur during the construction of the building.

In the same way, the subsidence of each facade was determined, with values ranging from 30 to 130 mm, with the highest values on Tacon St once again.

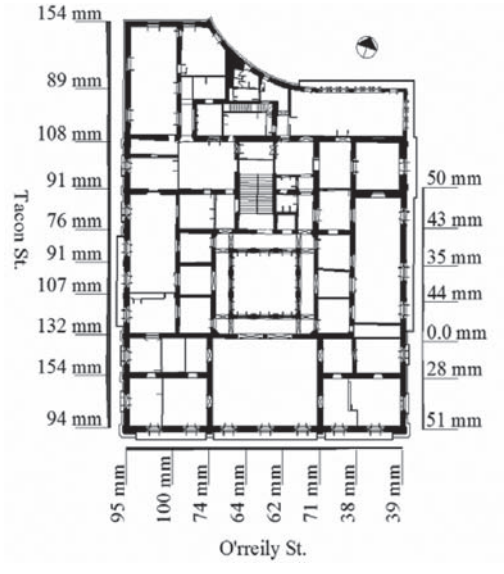

Figure 2. Results of the geometric leveling on the ground floor.

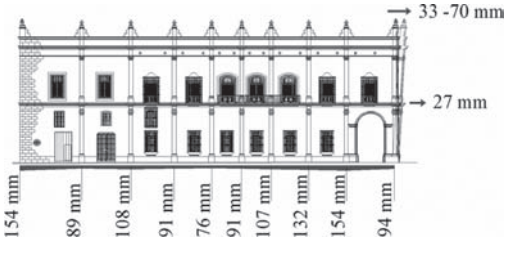

Figure 3. Subsidence on O'rreily St seen from Tacon St.

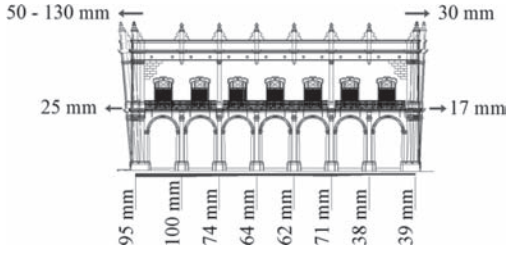

Figure 4. Subsidence of facades of Tacon St and the East side, seen from O'rreily St.

2.2 *Structures survey*

The original structure consists of load-bearing walls built of stones and rough stones with thicknesses ranging from 700 to 900 mm in the perimeter walls and between 500 and 800 mm in the interiors. The most common modifications are summarized in closing spaces, construction of partition walls made of bricks and the replacement of floors and roofs made of wooden beams with reinforced siporex type slabs. However, major structural changes took place in the early twentieth century in order

Figure 5. Palacio del Segundo Cabo after its restoration at the beginning of the twentieth century.

to convert the building into the headquarters of the National Senate. At that time, the first two bays on the first floor were drastically changed and a dome was built in the center of the main hall.

2.3 *Pathological survey*

Based on the survey prepared by the participants in the first workshop given by the Association "Sisto-Mastrodicasa" along with the San Geronimo University in Havana, an update was made to locate, classify and quantify the damages in the palace, so that problems can be identified to create an inventory of damage in each case.

The detected damages in the structure are largely of structural origin, and then some damages as result of the degradation of the materials. For a better understanding the injuries are classified according to their origin into three categories:

– Pathologies of the materials
  These damages are caused by the degradation of the constituent materials. The factors affecting them are mainly due to the environment and aging. These injuries usually do not have structural implications but in the aesthetic and they are seen through cracks, places where the plaster or panel has come off, efflorescence, corrosion of pipes and metal elements, presence of termites and rot in the wood elements of the mezzanines, etc.

– Nonstructural pathologies
  They are related to the environment and human activity on the structure causing damages and its deterioration. In general terms there are damp patches, the presence of microorganisms and plants, leaks, etc.

– Structural pathologies
  These pathologies are associated with the structural behavior and were detected in virtually all load bearing walls of the building and arches. These damages are manifested through cracks and fissures in walls and arches and facade's collapse.

The most important crack cover a great part of the building, originating from the facade of Tacon St, through the one of the East side, as shown in Figure 6.

It is again the facade of Tacon St the one with the greatest damage, concentrated mainly in the extended area made during its construction and close to O'rreily's portal, as shown in Figure. 7.

In this facade major cracks go through the entire wall, in some cases with apertures of 30 mm evidencing previous repairs as is the case represented as (1) in Figure 7. Most of these cracks are mainly associated to the movement of the structure, collapses and the effect of overloading.

2.4 *Instrumentation and monitoring of the structure*

A monitoring system was created which continuously registered the movement of cracks and the environmental temperature through vibrant wires sensors.

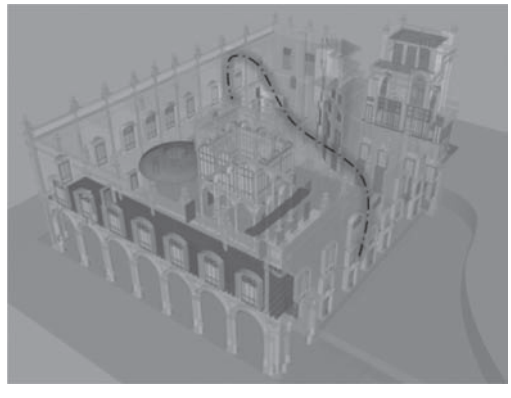

Figure 6. Scheme of the main crack.

Figure 7. Pathological survey. Facade of Tacon St. crack's detail (1).

Figure 8. Installed sensors and measurement system used.

This sensor allowed the assessment of the cracking activity in the building, which has later been served as a basis to calibrate the numerical models.

It was found that all sensors showed a significant relationship between the temperature and the movement of the cracks. The results corroborated the instrumented cracking activity. 70% of the 13 installed sensors showed a slight tendency to remain stable or closed, while 30% tended to continue the opening process. The latter sensors were located in the main cracks represented in figure 6.

3 MODELING THE PROBLEM

To assess the structural behavior of the Palacio del Segundo Cabo and the possible causes behind the pathological phenomena in the structure and its influence on structural safety, the authors use mathematical simulation tools based on the Finite Element Method. The interpretation of results corroborates the hypotheses based on their correlation with the fissure system in the facility.

Also the behavior of the recommended solutions to new conditions can be predicted.

The finite element models are adjusted using the data obtained from the work field. Because of this, the involve aspects in the modeling process (geometry, applied loads, materials and support conditions) are well calibrated.

As a result a three-dimensional model of the structure and another of the soil are created to estimate the settlements occurred in each of the load phases of the building. The combination of both models guaranteed the analysis of soil-structure interaction with the possibility of taking into account the influence of the foundation movements in the structural behavior.

3.1 *Geometry modeling*

Taking into account the surveys conducted by GEOCUBA (GeoCuba, 2009) and structural surveys made by the authors of this work, the latter created a three-dimensional model of the structure using bi-dimensional elements Shell style. With the use of the digital model the authors reproduced with great accuracy the geometry of the building.

The foundation is very variable, both from the geometrical point of view and the materials used in its construction. In the model this is taken into account since the foundation width varies between 1.10 m and 1.30 m. The foundation depth varies from 1.40 m to almost 1.60 m on Tacon Street. It ranges between 2.95 m and 3.25 on O'rreily Street and between 3.75 m and 4.00 m for the eastern façade. On the north side it is between 1.40 m and 2.50 m and the extended area constructed in the early twentieth century directly rests on the wall of the moat.

3.2 *Materials modeling*

The characterization of the materials of a structure of this type is very complex. Ashlars walls have a very large variability throughout the structure; therefore different areas were identified based on drilling resistance and 7 samples taken in the walls.

The mechanical property values are taken from tests performed to samples of the ashlars and studies conducted to similar buildings on Lombillo (2010). It is considered that ashlars have a perfect elasto-plastic behavior. The mechanical properties of the ashlars wall are show in Table 1.

As for the different soil layers, they are considered to have a behavior based on the Mohr-Coulomb criteria and the properties used are those obtained by the Geological Engineer Study, conducted by the UIC—Havana of the National Body of Applied Researches. This study identified the following geological-engineer elements.

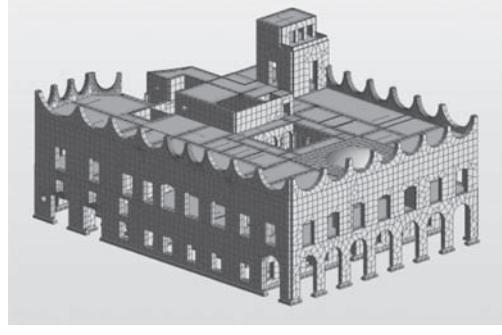

Figure 9. Geometric pattern.

Table 1. Mechanical properties adopted for the walls.

γ_d (kN/m^3)	σ_u (MPa)	E_{sec} (MPa)	σ_e (MPa)	ν
16.00	1.56	3488	0.50	0.33

γ_d: specific weight.
σ_u: ultimate compression strength.
E_{sec}: secant modulus of deformation.
σ_e: stress elastic limit.

Table 2. Physical-mechanical properties of soils involved in the behavior of the foundations.

Description	γ_d (kN/m^3)	c_u (kPa)	ϕ (°)	E (kPa)	R_c (MPa)
Heterogeneous filling	17.00	0	25	4500	–
Calcareous gravel	18.00	0	28	12500	–
Organogeneous limestone	16.68	80	31	160000	9.74
Clayey sand	20.00	50	25	5000	–
Plastic clay	17.00	80	0	3000	–

c_u: undrained shear resistance.
φ: internal friction angle.
E: modulus of deformation.
Rc: simple compression strength.

- Element # 1: Heterogeneous fill with low to medium compactness, consisting of a sandy material with shells, glass, pottery and coal. There are also calcareous gravels with irregular shape and size and limestone fragments, sometimes it is muddy. The gravel is dark brown to yellowish brown, sometimes it is dark gray to black, sometimes gray-white to yellow with red intercalations. Its thickness varies from 1.95 m to 4.00 m.
- Element # 2: Sandy and muddy calcareous gravel wrapped in a muddy and clayey matrix of low to high compactness and colored in yellowish to bluish white. Fragments ranging from 1–2 cm, although in some places they are 7 cm with angular shape. The power of this element varies from 2.40 m to 3.95 m.
- Element # 3: Organogeneous limestone in yellowish white color with red, orange and green streaks, soft resistance, porous, with cavities up to 2 cm deep and stained with brown clay. It is seen from between 4.80 m and 6.80 m minimum depth and between 1.70 m and 3.50 m thick.
- Element # 4: Half-compact clayey sand with small limestone fragments in yellowish white color. It only appears in Cove 2, of 7.00 m to 8.75 m followed by limestone with 1.75 m thick. The fact of been below the limestone with so little thickness no physical nor mechanical properties were determined.
- Element # 5: Plastic clay with firm to hard consistency, yellowish brown color with yellow, red and green streaks. This material appears in all vertical coves of 7.35 m from 9.60 m.

The water table was found in all the coves drilled to a depth between 3.55 m and 4.90 m, while the water level in the moat of the *Castillo de la Real Fuerza* is approximately 4.00 m above the ground level.

3.3 *Loads modeling*

All the different load states and combinations for which the structure has passed through have been considered. The authors have also analyzed the loads proposed in the project based on the new use of the facilities.

It was considered the following five load steps:

- Weight of the structure (PP).
- Permanent load of filling. (Roof = 35 cm, First Floor = 30 cm, Ground floor = 15 cm) (CP).
- Use loading (Roof with rainwater downpipes; Mezzanines estimated depending on use) (CU).
- Daily thermal variation load (CT).
- Differential settlements (CD).

Environmental loads are not taken into account in the analysis as the authors considered it has a negligible influence on this type of rigid structure.

3.4 *Load combinations*

The following table defines the most unfavorable combinations that may arise during the life of the structure:

3.5 *Modeling the boundary conditions*

In the structural model it is considered that the union among the different walls is continuous.

The slabs are modeled to work supported on two edges and to be articulated at their junctions with the walls.

The support of the walls on the ground has been considered as articulated because of the under-designed foundation underneath, which is unable to transmit moments to the soil.

Table 3. Most critical load combinations.

#	Loads combination	Limits
1	1.2 PP + 1.2 CP	ULS
2	1.2 PP + 1.2 CP + 1.6 CU	ULS
3	1.0 PP + 1.0 CP + 1.0 CU	ULS
4	1.2 PP + 1.2 CT	ULS
5	1.0 PP + 1.0 CD	SLS

In the soil model, the assumed boundaries were placed at a reasonable distance from the foundation to avoid any influence in its behavior.

4 SETTLEMENTS ESTIMATION

Authors estimated settlements for three phases of analysis, whose results are shown below:

– First stage

The stresses generated in the soil by the weight and all permanents loads of the building. Under this state there are settlements that reach between 3 and 13 cm. It is considered that these depressions are not the cause of the damage observed in the building, as the materials of the ground and the foundation have the property of accommodating very quickly, almost instantly. For this reason the authors state that some adjustment must have occurred during the construction of the building and its magnitudes are consistent with the results of the geometric leveling previously done.

– Second phase

Based on the state of stresses imposed in the first phase other stresses generated by the temporal loads have acted on the ground, during the various uses to which the building has been subjected. This analysis allows the calculation of the absolute and differential settlements that caused the current state of the building, which are estimated at a magnitude ranging between 0.16 and 0.64 cm. Clearly, the magnitudes are very small, but the influence of these movements in the behavior of the superstructure causes tension states which exceed the tensile strength of the wall.

– Third phase

Because of the new use of the facilities, new temporary loads will arise. The stresses generated by these last ones at the foundation base are imposed to the ground.

The behavior is similar to the second phase, therefore it is considered that no significant changes in the behavior of the foundations should be introduced.

It is considered that these differential settlements are due to the great heterogeneity existing in both the foundation structure and the soil support.

5 INTERPRETATION OF THE RESULTS

Based on these studies, the authors elaborated several hypotheses regarding the main causes that led to cracks appearing in the building.

The stresses states generated in each load combinations may be calculated with the use of numerical modelling.

As a result it could be infered the direction of the fissures and thus verified if they match those in the facilities. This would confirm the hypotheses regarding the causes of the appearance of cracks or fissures.

Hypothesis 1. The main cracks in the facade on Tacon St (1) (Fig. 7) are generated by the combination of two deteriorating effects: the application and distribution of the loads and the occurrence of small quantities of displacement as a result of the effect of live loads of long duration.

The formation of this crack is complex, it had to be analyzed in two steps to find the causes of it.

The main stresses appearing in the facade when analyzing the complete combination of gravity loads, which is permanents loads plus live loads, cause main tensile stresses coinciding with the area where the crack appears on the parapet.

The values of these tensile stresses are capable of exceeding the strength of the material the wall it is made of.

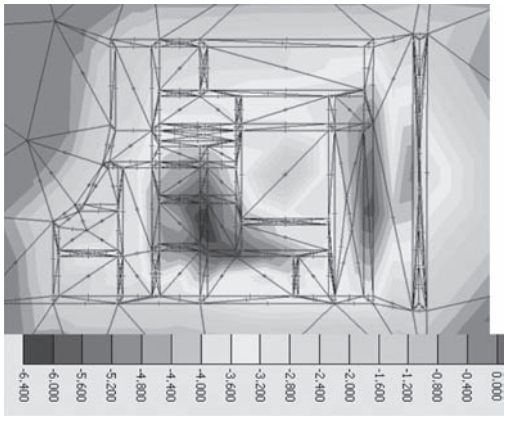

Figure 10. Estimated settlements for long term use loads. (Units 10^{-3} m).

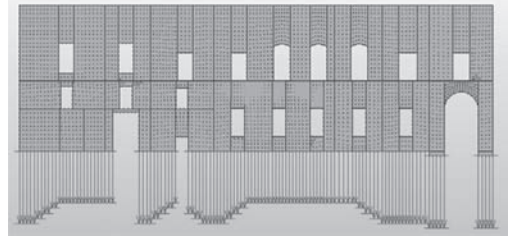

Figure 11. Differential settlements imposed to the structure.

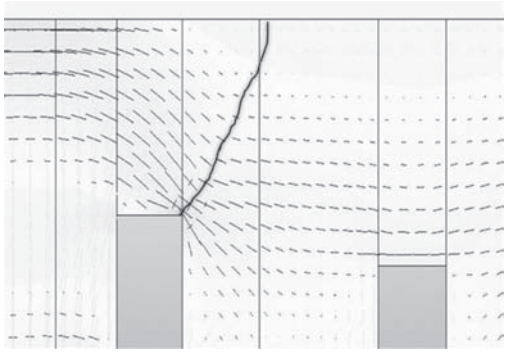

Figure 12. Main tensile stresses on Tacon St caused by differential settlements.

The development of the crack to the corner of the window has been caused by another phenomenon. In assessing the response of the structure to the differential settlements that have been calculated for the live load, tensile stress states arise in the area near the window with a direction that could cause cracks like this one until it joins the fissures created by the effect of load distribution.

Regarding this crack it could be concluded that it has been caused by two phenomena, i.e., the change in the loads direction and differential settlements. Hence, corroborating the stated hypothesis.

6 RESEARCH FINDINGS

6.1 *Regarding the structural pathologies*

- The causes that have led to the state of cracking of the structure (walls) are directly linked to three factors.
- The heterogeneity of the foundation and the supporting soil.
- The application procedure and distribution of the loads on floors and roof.
- The inadequate geometry of the arches and lack of rigidity in the supports.
- The cracks are associated mainly to three causes.
- High slenderness of the walls.
- Lack of bracing in the elements of the mezzanine and the roof.
- Pressure of the arcs.

6.2 *Regarding the structural behaviour*

- Despite deterioration levels of the structure and the eccentricity of the load due to the slenderness of the walls, the building meets the safety requirements in the ultimate limit state for the evaluated load combinations.
- In general terms, there is a perfect relationship between the variation of the temperature and the opening and closing cycles of the cracks and fissures.
- The activity of the implemented cracks were corroborated. 70% of the sensors showed a slight tendency to remain stable or closed, while 30% tended to continue opening.

7 RESEARCH RECOMMENDATIONS

The rehabilitation work should be focused on:

- Remove the heterogeneity of the foundation and the supporting soil by improving it with an underpinning.
- Strengthen the structure of the arcs through tensioners that eliminate the horizontal thrusts they generate.
- Restitution of the structural continuity in the cracked walls with metal staples.
- Implement conventional treatments with injections to the remaining cracks in walls and arches.

8 MITIGATION STRATEGIES

Key aspects are focused on underpinning the foundation with micropiles based on the following criteria:

- Respect the original dimensions of the structure.
- Eliminate the causes of deterioration.
- Structural efficiency.
- Optimal structural safety-cost relation.
- Proper execution of the solution.
- Geotechnical design of the micropiles.

The geotechnical design of micropiles has been addressed by several researchers, among which Lizzi (1985) and Bustamante (1986) stand out. These authors developed calculation methods that are widely used. It is also common to consider the design methods developed for piles.

From the physical point of view, the ultimate bearing capacity of a micropile will depend on two key factors: the friction generated between the ground and the shaft and the sinking of the tip. However, the influence of the tip is usually neglected due to its small diameter and above all because in many cases it can not develop due to its slenderness.

Its behaviour is similar to the piles and therefore has the same design uncertainties. When determining the load capacity through different methods a great variability is achieved, so that their design needs to be adjusted by loading tests on the job site.

Table 4. Load capacity for nominal diameter of 100 mm.

Design methods	∅* (mm)	α	∅** (mm)	G.S.F ***	Q_u (t)	Q_t (t)
α, β	100	1.5	150	3	38.0	12.6
C-ϕ, λ, β	100	1.5	150	3	20.1	6.7
Caquot-Kerisel	100	1.5	150	3	120.0	40.2
Lizzi (1985)	100	1.5	150	3	63.6	21.2
Bustamante (1996)	100	1.5	150	2	25.0	12.4
M.E.F	100	1.5	150	1.6	34.0	21.0
Working load (t)						15.00

* Nominal diameter.
** Calculation diameter.
*** Global safety factor.
Q_t: design load capacity.
Q_u: ultimate load capacy.

The execution technique of the micropiles itself generates a difference between the diameter of the perforation (nominal diameter) and the diameter of the micropiles performed after the injection (calculation diameter). This calculation diameter is estimated through a coefficient that takes into account the type of soil and increase of the nominal diameter.

The following table summarizes the results of the geotechnical design of micropiles by different methods. It is considered a nominal diameter or drill diameters of 100 mm.

The value of working capacity does not take into account the Caquot-Kerisel method (Caquot-Kerisel, 1953) as it was considered abnormal. This is in agree with the results presented in Lyamin et. al. (2007) about the higher values obtained by this method.

8.1 *Structural design of micropiles*

The structural reinforcement of the micropiles is carried out with a metal pipe of TM-70 60.3 × 5.5 mm placed inside the bore. The adhesion between the micropiles and the head is assured with bars welded to the head pipe.

8.1.1 *Distribution of micropiles*

Based on the structural analysis, the solicitations of the foundation for the load combination PP + CP + CU were determined and based on these values there were established four working ranges for the micropiles distribution. In each of the walls part of the supporting system of the building was established.

It was adopted a length of 10.50 m for micropiles in order to reduce the amount of perforations.

Micropiles will be place in quincunx, it means, alternately on both sides of the wall, as an underpinning recuperation process.

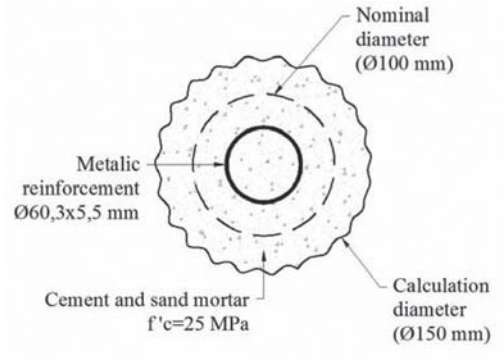

Figure 13. Schematic section of the micropiles.

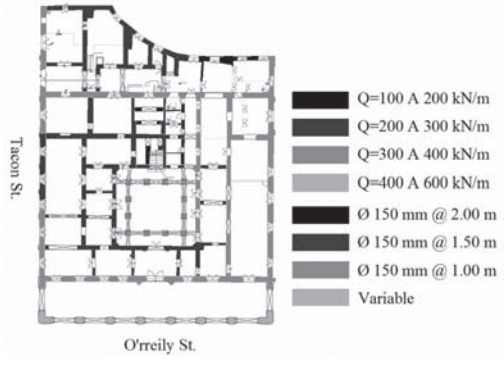

Figure 14. Load distribution in the foundation level and micropiles spacing.

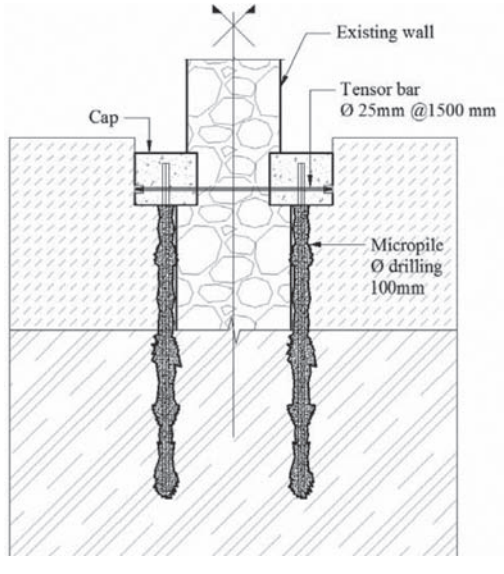

Figure 15. Underpin scheme.

The load transfer between the wall and the micropiles is expected to be through a transition element or head with a level of rigidity to ensure uniform function of the micropiles. The heads are interconnected by means of a metal tensor that goes through the wall and confines it in such a way that the load on the wall can be distributed to the heads and on to the micropiles.

9 CONCLUSIONS

The evaluations of old story building needs the combinations of different techniques as instrumentations, numerical analysis and construction technology. In this study the analysis of different possibilities and hypothesis of the actual state of deterioration of a century building was done.

The current conditions of the Palacio del Segundo Cabo urges its underpinning with 429 micropiles of 100 mm nominal diameter and 10.50 m depth to ensure the elimination of the heterogeneity of the foundation and supporting soil.

ACKNOWLEDGEMENTS

The authors acknowledge the fruitful cooperation between Cujae and Brasília Universities in regard to studying numerical models to be applied to problems similar to the one referenced herein, and also thank the Ministry from Cuba to allow the study, analysis and presentation of this case history.

REFERENCES

Bustamante, M. 1986. A method for calculating the anchors and injected micropiles. CEDEX No. 174. May-June and July-August, 3–23.

Caquot, A. & Kerisel, J. (1953). Sur le terme de surface dans le calcul des fondations en milieu pulverent. Proc. 3rd Int. Conf. Soil Mech. Found. Engng, Zurich 1, 336–337.

GeoCuba. 2009. Levantamiento Topográfico del Palacio del 2do. Cabo. Havana. p. 20.

Group of authors. 2010. *We save the salvageable* Associazione Sisto Mastrodicasa and Office of the Historian of Havana City. Havana, p. 25.

Lizzi, F. 1985. Paliradice (root piles) and reticulated paliradice, Micropiling Cap. 4 and 5 of underpinning. Ed S. Thorburn and J.F. HUTCHINSON Surrey University Press Glascow and London. pp. 84–151 and 152–159.

Lombillo, I. 2010. Theoretical and experimental research on slightly destructive testing (MDT) used for in situ mechanical characterization of the structures of built heritage. Director: Luis M. Villegas. Doctoral Thesis, University of Cantabria. Santander.

Lyamin, A.V. et. al. (2007). Two and three-dimensional bearing capacity of footings in sand. Géotechnique, 57, No. 8, 647–662.

Roman, M. 2003. Micropiles. Use in Underpinning. Conference on Underpinning Course II, Inclusions, Injections and Jet-Grouting STMR organized by the School of Civil Engineering of Valencia.

Salas, J., Jimenez, A., Just Alpañes, J.L. & Serrano, A.A. 1981. Geotechnical and foundation. Tomo I to III. 2nd Edition. Editorial Rueda. Madrid.

This page intentionally left blank

Geotechnical Engineering for the Preservation of Monuments and Historic Sites – Bilotta, Flora, Lirer & Viggiani (eds)
© 2013 Taylor & Francis Group, London, ISBN 978-1-138-00055-1

Softening and swelling mechanism affecting south slope of Civita di Bagnoregio (VT)

F. Garbin
Geoplanning Servizi per il territorio S.r.l., Rome, Italy

C. Margottini
ISPRA Institute for Environmental Protection and Research, Geological Survey of Italy, Rome, Italy

R. Brancaleoni
Geoplanning Servizi per il territorio S.r.l., Rome, Italy

A. Sonnessa
Surveylab, Università Sapienza, Dicea, Rome, Italy

ABSTRACT: Civita di Bagnoregio is a small village in Central Italy, located on the top of a hill and affected by landslides that are progressively reducing the urban area. The access consists of a pedestrian bridge that connects Bagnoregio municipality to the village. The south slope beneath the bridge, is involved by frequent instability phenomena. This work describes the analysis carried out and it aimed at the definitions of geological and geotechnical mechanism affecting the above mentioned slope. A geotechnical survey has been carried out. These surveys showed the presence of a superficial layer, resulting from the softening and swelling of underlying clay-silty strongly overconsolidated, responsible for the superficial landslide phenomena. A slope stability and a 3D laser scanner model has been carried out. The analysis demonstrates that a correct design for the landscape preservation and consolidation of unstable towns needs an understanding of triggering mechanism and geotechnical properties of the involved soils.

1 INTRODUCTION

Scope of the present work is to obtain a geological and geotechnical characterization of an area, located in south side of Civita di Bagnoreggio where there is the access to the town, through the interpretation of surveys and laboratory tests. From the results is possible to obtain a geological and geotechnical model that can help to adopt technical solutions to reduce and mitigate the geomorphological hazard. The area studied is affected by a progressive erosion that, in the last 400 years, has profoundly modified the morphology, erasing a thickness of about 40 m.

Figure 1. The site of Civita di Bagnoregio.

2 SITE DESCRIPTION

2.1 *The village*

Civita di Bagnoregio (Fig. 1) is a small village whose origin dates back to Etruscan civilisation founded in Central Italy before roman empire (about VII century BC). It is located about 100 km north of Rome in the boundary between volcanic deposit of Vulsino lake and the Tiber river fluvial valley. Civita, likely for military reason, is located on the top of a hill more than 200 m respect to the Est-West level of two rivers that border the cliff in the North and Sud sides. Major flourishing of the municipality was in the middle age until 1695 when

a disastrous earthquake destroyed most of the town and administrative and religious representatives moved to the nearby village of Bagnoregio.

2.2 *Geology and geomorphology of the area*

The Civita di Bagnoregio cliff is composed by a top layer about 20–25 m of jointed ignimbrite, underlain by a intensively stratified pyroclastic formation; both volcanic layers are originated in Quaternary and they rest on the Plio-Pleistocene bedrock composed mainly of a clayey succession with a small sand levels on top, which form the valley in the major area. The clay thickness can be estimated in some hundred meters, while the outcropping portion is about 150–200 m from northern to southern part of the valley respectively (Fig. 2). Due to this particular geology and morphological features, Civita di Bagnoregio village has suffered frequently of several slope instability phenomena (Bandis et al., 2000): the mainly landslides mechanism in the clayey layer are mudflows, debris-flows and rotational slides, while the common landslide typologies in the upper volcanic portion are rock-falls, toppling and block-slides, due to a retrogressive mechanism of erosion.

Historical phenomena have been reported since the XV Century, in total about 130 phenomena has been identified with a constant rate of events occurred in the last centuries (Fig. 3).

In the last decade some landslides have affected the northern border of the cliff of Civita. Some cases are showed. The rock-fall in February 1992 caused a scarp retrogression of 2 m and a crown surface of about 40 m; the displaced blocks covered, in the cliff foot, a pre-existing rock-fall accumulation. Moreover, along the cliff border of new formation, in correspondence of Piazza del Vescovado, an opened joint, sub-parallel to the scarp direction, was observed. The rock-fall in August 1993 interested an area located 20 m West of the previous landslide with a scarp length of about 60 m. The fall involved both massive tuffs and part of the stratified pyroclastic materials, producing an average cliff retrogression of 6 m. Such failure represents the prosecution of the existing joint in Piazza del Vescovado, prolonged in West direction, under the damaged building (Fig. 4). This joint is isolating a huge rock slide, that need an immediate intervention.

This discontinuity is monitored since 1992 and in the last decade present a stable situation. The materials fall are accumulated in the pre-existing valley below, reaching, with some isolated blocks, the bottom valley of the Northern torrent Cireneo at a distance of about 300 m from the cliff. The debris-flow in December 1996 has mobilized the materials of the 1993 landslide, a small rock-fall occurred in August 1998 and another a rock-fall of about 1000 m^3 occurred in April 1999 involving the stratified pyroclastic complex.

2.3 *Slope instability mechanisms*

Landslide mechanism can be explicated by a causes combination that, starting from the valley erosion caused by water-courses, has affected later

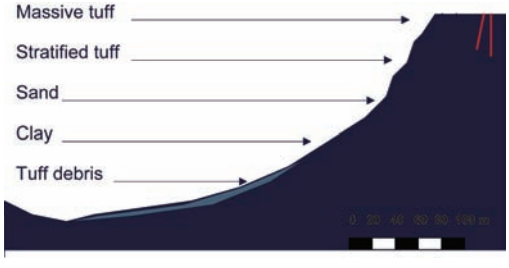

Figure 2. Geological profile of the study area.

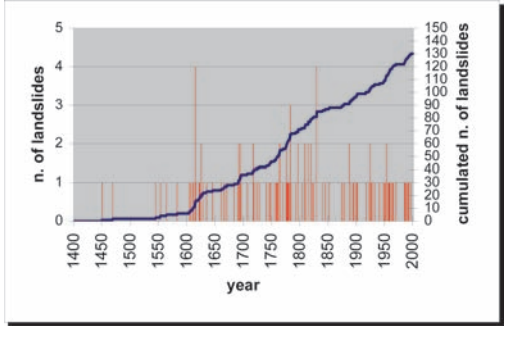

Figure 3. Historical landslide detected for the Civita di Bagnoregio site in 1400–2000 A.D. period.

Figure 4. View of the northern side of the cliff and displaying recent phenomena and the of the joints (dotts) isolating an important rock slide (red).

the slopes and, then, the cliff. Such causes can be summarized as follows:

- deepening of valley bottom due to runoff;
- decaying of the clay mechanical properties due to weathering (swelling and softening) up to an average depth of 5–10 m. In the first 0.5–1.0 m this phenomenon is more evident;
- occurrence of mudflows interesting 0.5–1.0 m depth, after heavy rainfall, with a continuous erosion of materials and exposition of underlain layers to weathering;
- intense superficial erosion due to weathering (some centimeters/year);
- deformation of the clayey bedrock due to the decay of geotechnical parameters and induction of deformation processes in the overlying tuff rocks;
- opening of pre-existing joints in the basal stratified pyroclastic formation, due to the significant increasing of deviatory stress associated with lateral unloading and clay deformation;
- opening of pre-existing fractures in the upper massive ignimbrite due to thermoclastic and cryoclastic phenomena as well as the pore pressure increase along the joints;
- increasing of deformations in the upper part of the cliff with a progressive failure mechanism from the pre-existing joints of upper tuffs to the stratified pyroclastic materials; in the latter the straining process produces rotational failures in correspondence of plastic layers;
- rock-falls in the upper portion of the cliff, in correspondence of massive tuffs.

The back analysis of historical event clearly identify crioclastic triggering factors for the 1992 rock fall, termoclastic mechanism for the 1993 rock slide (Delmonaco and Margottini, 2004), high precipitation for the 1996 debris flow. In any case, the entire process of continues slope movements can be summarized in a mix of rock fall, debris flow, superficial erosion, weathering and increasing of deviatory stress associated with lateral unloading and clay deformation.

The acceleration of geomorphological processes in the Northern cliff can be associated, likely, with a large events that occurred in other side of the valley, dated about 1114 A.D. (Fig. 5). This event, clearly visible on the field, moved the river closer to Civita, producing an higher energy relief on this part of the valley.

Due to the above processes and landslides the town was defined by B. Tecchi, a famous Italian writer, the dying town. Today it is probably one of the best Italian site to study geomorphological processes and stabilization measures, checking the efficacies of method proposed in really short time: in other word it is a perfect geotechnical laboratory.

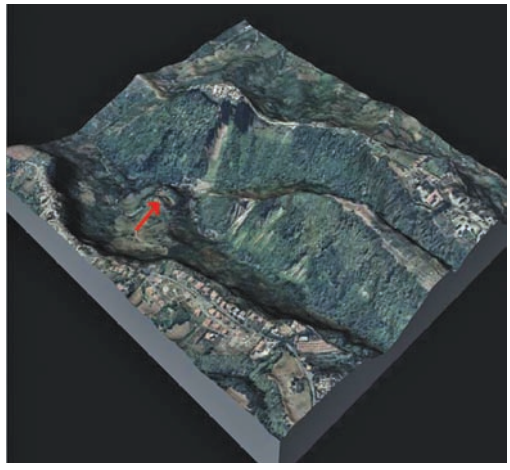

Figure 5. DEM of the area with superimposed an aerial photograph. In the left side it is possible to notice the toe of the large slide that, in 1114 A.D. moved the river from the natural linear behaviour towards the Civita cliff, Northern sector.

3 LANDSLIDES ON THE SOUTH SIDE MORPHOLOGICAL SADDLE, CONNECTING CIVITA TO THE MAINLAND

The main instability present along the slopes of the south side, subject of this study, is a phenomenon that has characterized the past evolution of this side and that was reactivated substantially in December 2008 and in March 2010 by heavy and prolonged rains reaching the current quiescent configuration as evidenced by the photographic survey follows. (Fig. 6)

Below is reported the photographic survey of the second reactivation (March 2010) and the present situation (December/January 2011) (Fig. 7).

In particular (Fig. 8), along the slopes in the south part it is present a translational mechanism type involutes in casting with speed from slow to moderate (m/year am/month) and intensity, in terms of volumes mobilized, from small to medium (from thousands to tens of thousands of m^3). With regard to the activities of these phenomena can classify them as inactive (a phenomenon that has moved the last time before the last seasonal cycle) and, within this category, identify further as quiescent.

3.1 *Saddle evolution along time*

The narrow saddle connecting Civita di Bagnoregio to the mainland was continuosly affected by soil erosion and landslides as consequence of the decay of clay materials. As a matter of fact, the following

Figure 6. Earth flows along the south slope—December 2008.

Figure 7. Reactivation flows along the south slope—March 2010 and the present.

figure (Fig. 9) is giving a reconstruction of paleo environment in the last millennium. Data are coming from a varity of sources such as archaeological, paintings and topographic measurements (Margottini, 1990).

Many historical depictions and photos are clarly showing the evolution of the saddle, as well as the

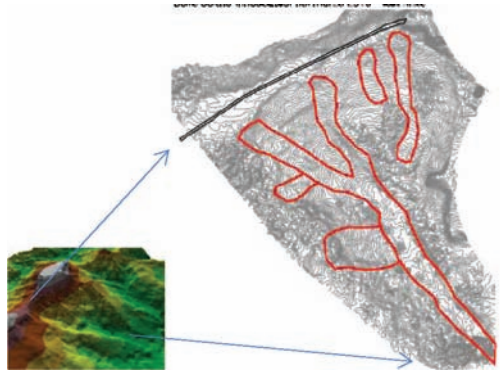

Figure 8. Earth flow instability along the south slope—March 2010.

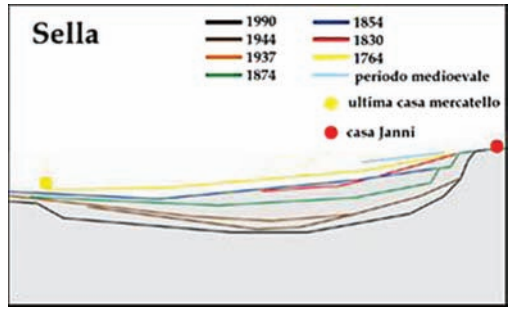

Figure 9. Evolution of the acces to Civita di Bagnoregio from medioeval time till present. Civita is on the right (Margottini, 1990, redrawn).

photos testifying the consolidation works developed along time (Fig. 10).

The instability conditions in the area (Fig. 11) are predominantly traceable to the following causes.

- The Plio-Pleistocene clays of Civita di Bagnoregio belong to the range of overconsolidated clays because in the past have been subjected to a lithostatic load greater than the current due to the weight of the overlying eroded tuff. The clay height increases towards the bottom. Such clays, especially in the most superficial parts, are subject to phenomena of swelling and softening. These phenomena produce in time the loss of resistance acquired with the preconsolidation and their behave, in term of shear strength, became that of a normal consolidated clay.
- Therefore there is a progressive loss of shear strength of soils, mainly in cohesion component, due to the pore pressure/interstitial related to the circ-lation of water, especially in the surface layer with a thickness ranging from 1.0 to 2.0 m.

Figure 10. Civita di Bagnoregio access morphological saddle: anti-erosional works in 1948.

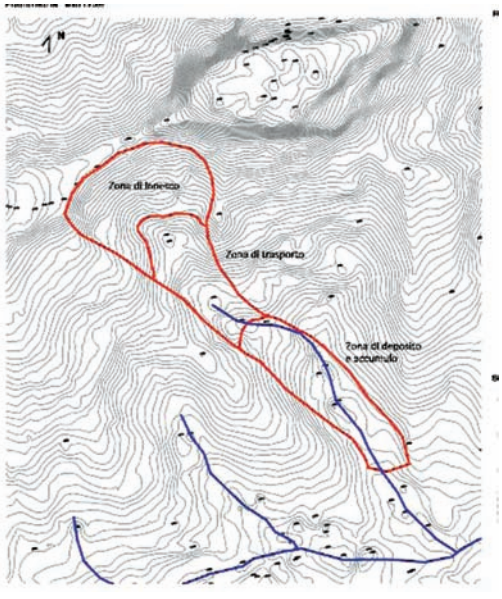

Figure 11. Geomorphological zoning of the southern part of the saddle, in terms of source, transportation and accumulation for triggered earth flow.

- Absence of a controlled drainage network, which produces a general infiltration of water in the cluster and a runoff concentrated in some sectors of the slope toward the higher part of the valley.

4 SURVEYS

4.1 *Laser 3D*

On 14 December 2012 was carried out by the Survey Lab staff, Spin Off of the Department of Civil Engineering, Construction and Environmental Engineering of "Sapienza" university—Area of Geodesy and Geomatics, a detailed survey of the landslide in south part of Civita di Bagnoregio.

As noted during the inspection, the side affected by instability looks just vegetated in the upper part, with a forest cover that increase going towards the valley. The gradient of the slope and the characteristics of the soil permit a relief with traditional topographic instrumentation. In particular, a digital model of the surface (DSM) has been extracted from the digital map, which form the basis for the detailed design of the safety measures. The survey was carried out by integrating the use of a Terrestrial Laser Scanner for three-dimensional reconstruction of the slope and methodology of GNSS (Global Navigation Satellite System) for placement in the existing maps. The use of laser scanner has allowed to obviate in part to the presence of vegetation; in fact the ability to acquire a large number of points (in the order of 106) with a minimum error on the determination of the position (a few cm to 100 m distance) permit to discriminate between ground points and vegetation points. From the point cloud data obtained was then eliminated, where possible, vegetation to reconstruct the exact morphology of the slope. The positioning of the relief in local mapping was performed using GNSS receivers geodetic mode RTK (Real Time Kinematic). From digital surface model was extracted digital mapping of detail contour, with spacing of 1 m, set within the frame of reference UTM-WGS84, with quotas related to sea level (Fig. 12).

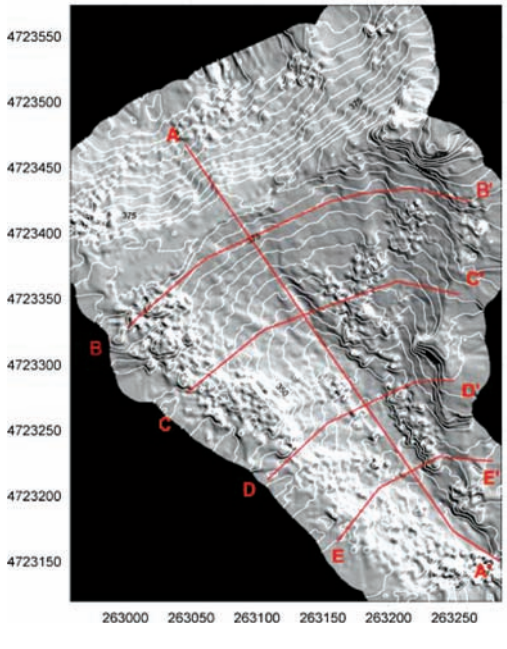

Figure 12. Digital elevation model of the area of the south side with overlapping contours (spacing 5 m) and showing the position of the sections produced.

4.2 *Soil investigation*

In December 2011, a new surveys campaign was performed on the area of intervention. The mainly aim was know the thickness, physical and mechanical properties of the material involved in the landslide of 2008 and of 2010.

The location of the surveys (Fig. 13 and 14) was chosen for the better layer representativeness in terms of geotechnical parameters, compatibly to the places accessibility.

The choice of the investigation was influenced by the presence of trees, slope steepness and instability that did not allow the use of heavier equipment.

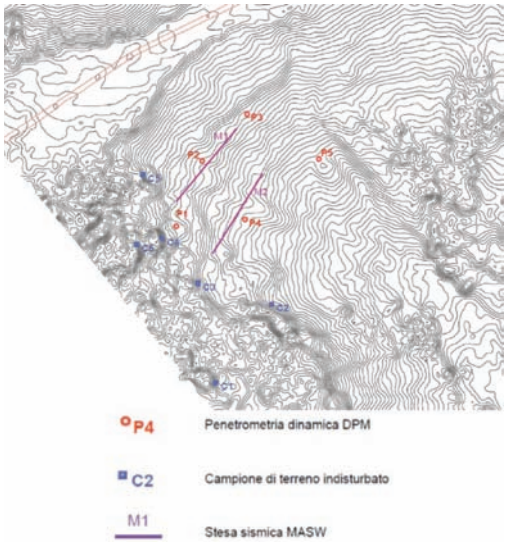

Figure 13. Geognostic surveys location—December 2011.

Figure 14. DPM penetration tests: site not easily accessible.

The surveys campaign included the following tests:

- 5 DPM penetration tests;
- 6 samples taken manually from trial pits for laboratory testing;
- 2 MASW.

Important informations concerning the thickness of potentially mobilizable can be deduced from the five penetration tests. All penetration tests show a trend rather homogeneous, it is possible to distinguish the superficial layer, resulting from the softening and swelling of underlying clay-silty strongly overconsolidated, is ranging from 1 to 2 meters (tests P1, P2, P4) to a maximum of 3 meters (P3 and P5) (Fig. 15).

As regards the seismic profiles (Fig. 16) the first variation of the waves speed is observed for a seismo layer attested to the depth included between 2 and 3 meters in agreement with the results of the penetration tests. By the two seismic profiles are clearly specified the presence of a portion of superficial layers with a low consistency resting on a more rigid layer to a 15 m depth. It is evident the presence of two inconsistent layer who can represent slide planes (Fig. 17).

Samples were taken at different stratigraphic altitudes in order to characterize the yielding levels. Sampling was done with a Shelby sampler, ϕ 100 mm and L 200 mm.

On samples were performed the main laboratory tests to estimate the geomechanical parameters with direct and anular shear tests. The following table shows the main parameters (Fig. 18). From samples taken can be seen the low effective cohesion value of the superficial layer, this shows the effect of swelling and swelling of this layer and the

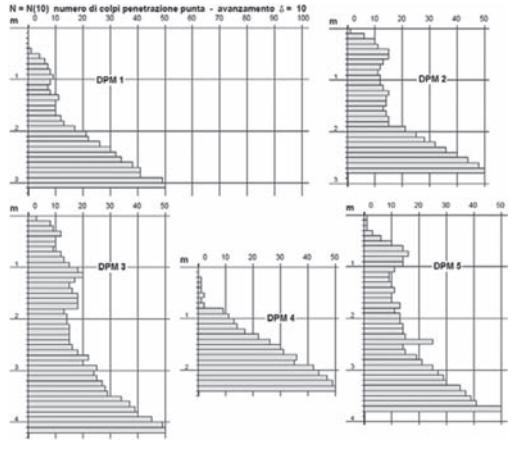

Figure 15. DPM elaboration.

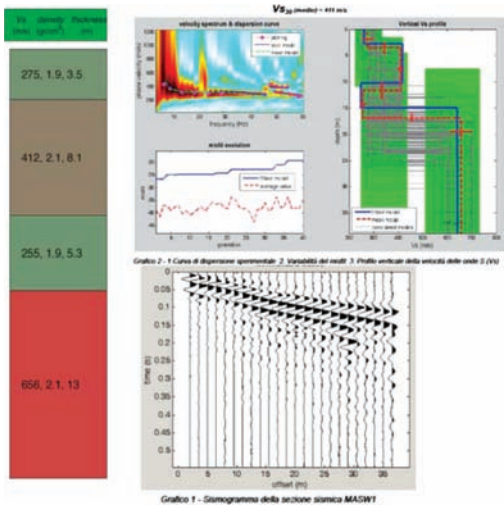

Figure 16. Seismic parameters elaboration derived from MASW test.

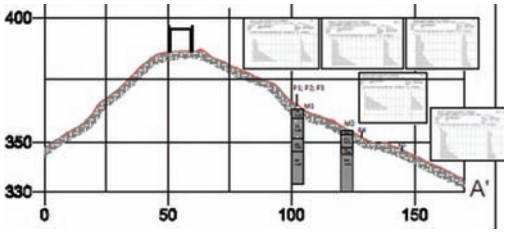

Figure 17. Geotechnical section along the southern side from penetrometric tests and MASW.

Certificato n°	Sond. & Camp.	Prof. (m)	W %	γ_{nat} kN/m³	γ_s kN/m³	e	L.L. %	I.P.	c' kPa	ϕ' °	c'_r kPa	ϕ'_r °
5906	S – C 1	00.20 –	26,7	18,91	27,28	0,828	53	26	2	22	0	22
5907	S – C 2	00.20 –	23,6	14,37	25,59	1,201	43	18	0	29	–	–
5908	S – C 3	00.20 –	24,9	19,06	26,06	0,708	42	18	6	25	0	24
5909	S – C 4	00.20 –	23,3	15,64	26,47	1,087	52	26	8	24	0	24
5910	S – C 5	00.20 –	33,2	16,07	26,61	1,206	56	27	2	27	0	26
5911	S – C 6	00.20 –	24,3	19,47	26,67	0,703	45	26	4	25	0	21

Figure 18. Geotechnical parameters summary.

high grade of erosion suffered. Moreover the coincidence between the effective angle and the residual angle says that this layer is in a quiescent state due to a remobilization (landslides) in the past.

5 CONCLUSION

The study performed has allowed the reconstruction of the morphology before and after the landslide, the identification of potential slide plane, the parametric characterization of layers and the substrate.

From surveys carried out and from the geotechnical characterization was verified, visually and analytically, the state of evident degradation that characterizes the study area and has been possible reconstructed the local geological and geotechnical model.

The causes of decay are numerous and include increased erosion superficial, the changing of rainfall resulting from climate changes (heavy rainfall concentrated in short periods of time), decreased water retention by the soil that prevents the infiltration of natural waters of precipitation. For the resolution of these problems can be necessary to create an integrated intervention, a multi-disciplinary, can substantially mitigate the impact of dynamic geomorphological and climatic conditions which have led to the state of the general deterioration of the area.

Thanks to the specific field and laboratory investigations which were carried out it was possible to develop a working plan that offers long-term solutions, to eliminate the hydrogeological conditions that characterize the area of the southern slope below the access bridge into the town of Civita di Bagnoregio.

ACKNOWLEDGEMENT

A special tanks goes to L. Tramonti. freelancer engineering.

REFERENCES

Bandis S., Colombini V., Delmonaco G., Margottini C. 2000. New typology of low environmental impact consolidation for rock fall prone cliffs through interventions from the underground. In Bromhead E, Dixon N., Ibsen M.L. (eds.) Landslides in research, theory and practice. *Proceedings of the 8th International Symposium on landslides, Cardiff 26–30 June 2000*. Rotterdam, Balkema.

Bianco B., Benigni D. 1985. Il drenaggio profondo per il consolidamento delle aree in frana. Rodio.

Bozzano F., Floris M., Gaeta M., Martino S., Scarascia Mugnozza G. 2005. Assetto geologico ed evoluzione per frana di rupi vulcaniche nel Lazio settentrionale. *Bollettino della Società Geologica Italiana,* 2, 35–51.

Caporioloni R. 1854. Archivio vescovile di Bagnoregio.

Casagli N., Delmonaco G., Focardi P., Margottini C., Serafini S. 2000. Analisi dei fenomeni di dissesto a Civita di Bagnoregio ed interventi di stabilizzazione. Convegno Geoben 2000 Torino 7–9 giugno 2000.

Cevolani F., Del Gizzo M., Quattrocchi F., Serafini S. 1990. Caratteristiche geotecniche delle argille di base nell'area di Civita di Bagnoregio. In Margottini C. & Serafini S. (eds.) *Civita di Bagnoregio—Osservazioni geologiche e monitoraggio storico dell'ambiente*. Roma.

Dawson E.M., Roth W.H., Drescher A. 1999. Slope stability analysis by strength reduction. *Geotecnique,* 49 n. 6, 835–840.

Delmonaco G., Falconi L., Margottini C., Puglisi C., Spizzichino D. 2004. A project of stabilisation for the mitigation of Cavon Grande Landslide in Civita di Bagnoregio (Italy). IX International Sympsium on Landslides, 28 June–2 July, 2004 Rio de Janeiro (Brazil).

Delmonaco G., Margottini C. 2004. Meteorological factors influencing slope stability. In Casale R. & Margottini C. (eds.) *Natural disasters and sustainable development*, Springer-Verlag, Berline Heidelberg.

Delmonaco G., Margottini C, Spizzichino D. 2009. Low-impact interventions for the preservation of Cultural Heritage: the dying town of Civita di Bagnoregio (Central Italy) and the killer landslide In: *Prohitec proceedings*, Rome 21–24 June 2009.

ENEA. 2001. Il consolidamento della rupe e delle pendici di Civita di Bagnoregio: indagini pregresse e proposte di intervento, Linee guida per la salvaguardia dei beni culturali dai rischi naturali.

Fell R. 1994. Landslide risk assessment and acceptable risk. *Can. Geotech. J*., 31, 261–272.

Focardi P. 1992. Civita di Bagnoregio: caratterizzazione geotecnica dei terreni. Atti del Convegno sul dissesto idrogeologico e centri abitati instabili. S. Martino al Cimino, 1990; Viterbo, 1991. ENEA, Associazione CIVITA, O.N.G., 120–126.

Iacurto O., Priori A. 1995. Caratterizzazione geomeccanica delle ignimbrite compatte di Civita di Bagnoregio (VT) in situazioni di dissesto idrogeologico. *Geologia Tecnica ed Ambientale,* 2, 35–51.

Itasca Consulting Group 2000. FLAC, fast lagrangian analysis of continua, version 4.0. *Itasca Consulting Group*, Minneapolis, Minnesota, USA.

Mancini M., Girotti O., Cavinato G.P. 2004. Il Pliocene e il Quaternario della Media Valle del Tevere (Appennino Centrale). *Geologica Romana,* 37, 175–236.

Margottini C. (1990). Evoluzione morfologica dell'area di Civita Bagnoregio in tempi storici. Estratto da "Civita di Bagnoregio" ENEA, Ass.Progetto Civita, pag. 23–28, 57–70.

Margottini C., Serafini S. (eds) (1990). Civita di Bagnoregio. Osservazioni geologiche e monitoraggio storico dell'ambiente. ENEA e Associazione Progetto Civita. TER, Roma. p. 174.

Napoleoni Q. 1991. Civita di Bagnoregio: un esempio di recupero. *L'Ingegnere, Ingegneria Ambientale e Territoriale*. Vol. 5–8, pp. 99–111.

Geotechnical Engineering for the Preservation of Monuments and Historic Sites – Bilotta, Flora, Lirer & Viggiani (eds)
© 2013 Taylor & Francis Group, London, ISBN 978-1-138-00055-1

Evaluation of the soil disturbance due to the installation of prefabricated vertical drains: An analytical approach applied to case histories

A. Ghandeharioon
Faculty of Science and Engineering, Department of Civil Engineering, Laval University, Quebec City, Quebec, Canada

ABSTRACT: Prefabricated vertical drains (PVDs) are among the most effective methods to control the water table and excess pore water pressure developed as a result of seepage or seismic event. Preservation of historic sites demands techniques that promptly reduce the excess pore pressure within the soil at the site and increase the shear strength. Installation of mandrel-driven PVDs and the disturbance created in soft cohesive soils were investigated in this research with a new elliptical cavity expansion theory (CET). The elliptical CET formulated is based on modified Cam clay model for undrained analysis, and accounts for the rate of mandrel penetration. Time dependent internal pressure in the cavity developed, corresponding stresses and excess pore pressure in the soil were evaluated during driving the mandrel. The pattern of distribution calculated for the excess pore pressure was verified using data obtained from large-scale laboratory tests. A more realistic elliptical smear zone around mandrels that are commonly used in the field was introduced while the disturbed soil surrounding the mandrel was characterized by the plastic shear strain normalized by the rigidity index. This analytical formulation was subsequently applied to practical situations. Case histories from the Muar clay region in Malaysia, and the Sunshine Motorway in Australia were studied to characterize the smear zone associated with the installation of PVDs. The ratio of plastic shear strain to the rigidity index was found to be useful for estimating the extent of the smear zone in the field because the basic soil parameters can be readily obtained without sophisticated large-scale testing.

1 INTRODUCTION

Conservation of historic sites requires methods to rapidly decrease the raised water table and minimize the excess pore water pressure within the soil at the site while avoiding excessive cost. For fine grained soils, prefabricated vertical drains (PVDs) are one the quickest techniques known for dissipating excess pore pressure and increasing the shear strength. This procedure reduces the drainage path in the soil, and hence accelerates gain in the shear strength of the layer by dissipating excess pore pressure generated due to seepage or earthquake.

Installing mandrel-driven PVDs and driving a pile or cone have similarities that resulted in using the cavity expansion theory (CET) for simulating the installation. According to Ghandeharioon (2010), CET is amongst the most successful techniques of modeling penetration in geomaterials, where the changes in stresses and pore pressure along with displacements encountered from the expansion of cavities are studied. The theory has been extensively applied in the areas of in-situ soil testing, deep foundations, tunnels and underground excavations.

The pressuremeter and cone penetrometer are among the most commonly used in-situ soil testing devices. The mechanical action created by these devices is similar to the expansion of a cavity, and hence the cavity expansion theory has been used in the interpretation of the measured data to obtain the soil properties (e.g., Wroth 1984, Clarke 1995, Yu and Mitchell 1998). Moreover, the shaft friction and end bearing capacity of driven piles in soils can be studied by CET. This analysis is a large-strain problem which involves high nonlinear nature of the material and geometry. Measurements of the radial displacements of the soil near the pile mid-depth taken from field data presented by Cooke and Price (1978) and the model tests of Randolph et al. (1979) show that the radial movement of the soil can be predicted by cylindrical cavity expansion theory. As discussed by Yu (2000), the installation of a pile can also reasonably be modeled by CET. Furthermore, since tunneling and underground

excavations involve reducing the in-situ stresses along the excavated circumference through removal of geomaterials from their primary location, they can be simulated by unloading cavities from a state of in-situ stress (e.g., Pender 1980, Ogawa and Lo 1987, Mair and Taylor 1993).

In this paper a new elliptical cavity expansion theory is developed to investigate mandrel penetration and its resulting disturbance in soft clays. The theory introduced studies the installation of PVDs under an undrained condition. The formulation accounts for the rate of mandrel penetration and the time factor for predicting the internal pressure in the cavity, the corresponding stresses, and excess pore pressure in the soil while driving the mandrel. The excess pore pressure in the soil predicted by this new elliptical CET was validated with the results of large-scale laboratory tests. A more realistic elliptical smear zone based on the elliptical CET is also expressed. Moreover, the theory was applied to case histories from the Muar clay region in Malaysia, and Sunshine Motorway in Australia. Although these sites were not necessarily historic sites, the concept of plastic shear strain normalized by the rigidity index of soil was used to predict the size of the smear zone under the field condition.

2 FORMULATION OF THE ELLIPTICAL CAVITY EXPANSION THEORY

2.1 *Assumptions considered in the theory*

The new cavity expansion theory developed assumes that driving a mandrel, which commonly has a rectangular or rhomboidal cross section, into soil creates an elliptical cavity that expands concentrically along the horizontal plane. The analysis is performed under an undrained condition. While the interface between the mandrel and saturated soft clay is assumed frictionless, the shape of the anchor is not considered in the analysis. The soil is taken homogeneous and it is assumed that Hook's elasticity law governs the elastic behavior of the saturated clay. The modified Cam clay model is considered for the plastic behavior of the cohesive soil. A planar view of an elliptical cavity (in polar coordinates) with an initial semimajor axis of a_0 and a semiminor axis of b_0 is presented in Figure 1. σ_0 is the initial internal pressure of the cavity, and also the uniform pressure acting on the soil boundaries at infinity. As the mandrel is driven into the ground the cavity pressure increases to P_i and the semimajor and semiminor axes of cavity expand to a_1 and b_1, respectively. Consequently, as this elliptical cavity expands the soil is assumed to have in-plane displacements.

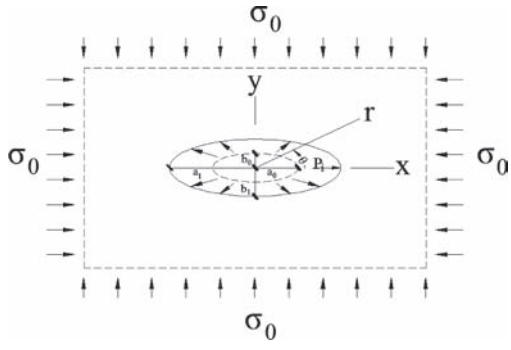

Figure 1. Planar view of the expansion of an elliptical cavity in an infinite soft cohesive soil, illustrated in polar coordinates.

2.2 *Elastic phase of cavity expansion*

The equations of equilibrium in polar coordinates, when body forces are absent, can be stated in terms of total stresses as:

$$\frac{\partial \Delta\sigma_r}{\partial r} + \frac{1}{r}\frac{\partial \Delta\tau_{r\theta}}{\partial \theta} + \frac{\Delta\sigma_r - \Delta\sigma_\theta}{r} = 0 \tag{1}$$

$$\frac{1}{r}\frac{\partial \Delta\sigma_\theta}{\partial \theta} + \frac{\partial \Delta\tau_{r\theta}}{\partial r} + 2\frac{\Delta\tau_{r\theta}}{r} = 0 \tag{2}$$

where, $\Delta\sigma_r$, $\Delta\sigma_\theta$ and $\Delta\tau_{r\theta}$ are variations in total radial stress, total tangential stress, and shear stress, respectively.

The effective stress governs any change in soil volume, and the strength and strains are only functions of the variations in effective stresses. In terms of effective stresses, Equations (1) and (2) become:

$$\frac{\partial \Delta u}{\partial r} + \frac{\partial \Delta\sigma'_r}{\partial r} + \frac{1}{r}\frac{\partial \Delta\tau_{r\theta}}{\partial \theta} + \frac{\Delta\sigma'_r - \Delta\sigma'_\theta}{r} = 0 \tag{3}$$

$$\frac{1}{r}\frac{\partial \Delta u}{\partial \theta} + \frac{1}{r}\frac{\partial \Delta\sigma'_\theta}{\partial \theta} + \frac{\partial \Delta\tau_{r\theta}}{\partial r} + 2\frac{\Delta\tau_{r\theta}}{r} = 0 \tag{4}$$

where, Δu is the excess pore water pressure.

In an undrained plane strain condition, one may show that:

$$\Delta\sigma'_r = -\Delta\sigma'_\theta, \quad \Delta\sigma'_z = 0, \quad \varepsilon_z = 0 \tag{5}$$

where, $\Delta\sigma'_z$ is the changes in effective vertical stress and ε_z is the vertical strain.

Hence, it yields:

$$\varepsilon_r = -\varepsilon_\theta = \frac{1}{2G}\Delta\sigma'_r, \quad \gamma_{r\theta} = \frac{1}{2G}\Delta\tau_{r\theta} \quad \text{with} \quad G = \frac{E}{2(1+\nu)} \tag{6}$$

where, ε_r, ε_θ and $\gamma_{r\theta}$ are the radial, tangential and shear strain, respectively. E and v are, respectively, the Young's modulus and the Poisson's ratio. G is the shear modulus of soil.

The strain-displacement relationships in the polar coordinates are:

$$\varepsilon_r = \frac{\partial U}{\partial r} \tag{7}$$

$$\varepsilon_\theta = \frac{U}{r} + \frac{\partial V}{r\partial \theta} \tag{8}$$

$$\gamma_{r\theta} = \frac{\partial U}{r\partial \theta} + \frac{\partial V}{\partial r} - \frac{V}{r} \tag{9}$$

where, U and V are the components of displacement in a radial and tangential direction, respectively.

By substituting the set of Equation (6) into Equations (3) and (4), with reference to Equation (5) and Equations (7–9), the equilibrium condition in polar coordinates can be expressed as:

$$\frac{\partial \Delta u}{\partial r} + \frac{2G}{r^2}\left(\frac{\partial^2 U}{\partial \theta^2} + U\right) + \frac{2G}{r}\frac{\partial U}{\partial r} = 0 \tag{10}$$

$$\frac{1}{r}\frac{\partial \Delta u}{\partial \theta} + \frac{2G}{r^2}\left(\frac{\partial U}{\partial \theta} + \int U\, d\theta + f(r)\right) - 8G\int \frac{\partial^2 U}{\partial r^2} d\theta$$
$$-2Gr\int \frac{\partial^3 U}{\partial r^3} d\theta - 2G\frac{d^2 f}{dr^2} - \frac{2G}{r}\left(\int \frac{\partial U}{\partial r} d\theta + \frac{df}{dr}\right) = 0 \tag{11}$$

This system of differential equations is solved by considering the applicable boundary conditions and the loading pattern in the developed cavity to yield (Ghandeharioon 2010):

$$U = \left(\frac{P_i - \sigma_0}{2G}\right)\left(\frac{r_1^2}{r}\right), V = \tau_{r\theta} = 0, \quad \Delta u = 0 \tag{12}$$

$$\Delta\sigma_r = \Delta\sigma'_r = -\Delta\sigma'_\theta = -\Delta\sigma_\theta = -(P_i - \sigma_0)\left(\frac{r_1}{r}\right)^2 \tag{13}$$

where, r is the position of a soil element measured from the center of the cavity and r_1 is the radius of an elliptical cavity.

The pressure-expansion relationship in the elastic phase is developed as:

$$r_1 = \frac{2G}{2G - (P_i - \sigma_0)} r_0 \tag{14}$$

in which, $r_0(\theta) = a_0 b_0 / \sqrt{b_0^2 + (a_0^2 - b_0^2)\sin^2\theta}$ is the initial radius of the elliptical cavity.

For a constant mandrel driving rate of V_v, the soil elements in contact with the frictionless tip of the drain shoe move radially at a rate of $V_r = V_v \tan(\frac{\beta}{2})$, where β is the apex angle of the drain shoe. Therefore, the instantaneous internal pressure of the cavity can be derived as:

$$P_i = \frac{2V_r(t - t_c)}{r_0 + V_r(t - t_c)} G + \sigma_0 \tag{15}$$

where, t_c and t are, respectively, the time required to establish contact between the drain shoe and the soil elements at the wall of the cavity, and the time increment, measured from when the drain shoe first entered the horizontal plane under consideration.

2.3 *Plastic phase of cavity expansion*

As the mandrel penetrates the soil, internal pressure in the cavity increases and as a result, the deviator stress (q) of every soil particle increases. The total stress parameters used in this research to analyze the cavity expansion in the context of critical state, in the plane strain condition, are:

$$p = (\sigma_r + \sigma_\theta)/2, \; q = \sqrt{3}(\sigma_r - \sigma_\theta)/2 \tag{16}$$

The constant deformation in soil establishes a link between q, p' and the initial state of effective stress, p'_0. Based on Cao et al. (2001), the effective stress path in the p':q plane in the modified Cam clay context under an undrained condition is given by:

$$q = Mp'\sqrt{n_p (p'/p'_0)^{-\frac{1}{\Lambda}} - 1} \tag{17}$$

where, M is the slope of the critical state line in the p':q plane. $n_p = p'_{y_0}/p'_0$ and $\Lambda = 1 - \kappa/\lambda$ are the isotropic overconsolidation ratio and plastic volumetric strain ratio, respectively. p'_{y_0} is the maximum isotropic preconsolidation stress. κ is the slope of elastic swelling line and λ is the slope of the normal compression line in the $\ln p'$:υ plane where υ is the specific volume.

Using Equation (17), the minimum internal pressure required to yield the soil elements adjacent to the wall of the cavity is determined as:

$$P_{i_{\min}} = -p_0 - Mp'_0\sqrt{(n_p - 1)/3} \tag{18}$$

The instant at which the wall of cavity yields is calculated to be:

$$t = \left[\frac{2\sqrt{3}G}{2\sqrt{3}G + Mp'_0\sqrt{n_p - 1}} - 1\right]\frac{r_0}{V_r} + t_c \tag{19}$$

Once the mandrel is driven in further the pressure in the cavity increases from the value identified by Equation (18), and the plastic region extends into the elastic area. In view of the simulated loading pattern and Equation (12), integrating Equations (1) and (2) along a particle path starting at the elastic-plastic boundary results in:

$$\sigma_r = \sigma_{r_p} - \frac{2}{\sqrt{3}}\int_{r_p}^{r} q\frac{dr}{r} \tag{20}$$

where, σ_{r_p} is the total radial stress at the elastic-plastic boundary.

As shown by Cao et al. (2001), a closed form solution of the total stresses may be derived by taking the deviator stress in the plastic zone equal to the deviator stress at failure (q_f). By incorporating the logarithmic strains to justify the large-strain effects, the internal pressure in cavity is expressed as:

$$P_i = -p_0 - Mp_0'\sqrt{\frac{n_p-1}{3}} - \frac{q_f}{\sqrt{3}}\ln\frac{\sqrt{3}G\left(r_0^2 - r_1^2\right)}{r_1^2 q_f} \tag{21}$$

in which, $q_f = Mp_0'(n_p/2)^{\lambda}$.

By taking a constant installation rate for the mandrel, the correlation between r_1, t, q and p' can then be established by:

$$\frac{1}{r_1} = \left\{1 - \exp\left(\frac{q}{2\sqrt{3}G} - \sqrt{3}\frac{\kappa\Lambda}{\upsilon M}\left[\zeta - \tan^{-1}\left(\frac{\eta}{M}\right) + \tan^{-1}\sqrt{n_p-1}\right]\right)\right\} \times \frac{1}{V_r(t-t_c)} \tag{22}$$

where, $\zeta = \frac{1}{2}\ln\frac{(\eta+M)\left(\sqrt{n_p-1}-1\right)}{(\eta-M)\left(\sqrt{n_p-1}+1\right)}$ and $\eta = \frac{q}{p'}$

Equation (21) along with Equations (22) and (17) demonstrate the link between the internal pressure, the penetration rate, and time.

According to Ghandeharioon (2010), the relationship between radial distance and its associated deviator stress can be determined by:

$$\ln\left(1 - \frac{r_1^2 - r_0^2}{r^2}\right) = \frac{q}{\sqrt{3}G} - 2\sqrt{3}\frac{\kappa\Lambda}{\upsilon M}\left[\zeta - \tan^{-1}\left(\frac{\eta}{M}\right) + \tan^{-1}\sqrt{n_p-1}\right] \tag{23}$$

The principle of effective stress denotes that the excess pore water pressure is the difference between changes in the states of total and effective stresses:

$$\Delta u = \Delta p - \Delta p' \tag{24}$$

Based on Equations (23) and (17), q and p can be calculated at any soil element inside the plastic region. Equation (20) is then used to derive the state of total stress at that particular position, while noting that $p = \sigma_r - q/\sqrt{3}$. Finally, by using Equation (24), the value of excess pore pressure can be determined at the location being considered.

2.4 *Critical state phase of cavity expansion*

Driving the mandrel further will ultimately lead to the soil being at critical state at the wall of the cavity. Thus, the internal pressure will approach its maximum value at:

$$P_{i_{\max}} = -p_0 - Mp_0'\sqrt{\frac{n_p-1}{3}} - \frac{Mp_0'}{\sqrt{3}}\left(\frac{n_p}{2}\right)^{\Lambda}\ln\left[-\left(\frac{2}{n_p}\right)^{\Lambda}\frac{\sqrt{3}G}{Mp_0'}\right] \tag{25}$$

The deviator stress of a particular soil element can then be related to its radial distance from the center of the cavity by:

$$\frac{r_1}{r} = \sqrt{1 - \exp\left(\frac{q}{\sqrt{3}G} - 2\sqrt{3}\frac{\kappa\Lambda}{\upsilon M}\left[\zeta - \tan^{-1}\left(\frac{\eta}{M}\right) + \tan^{-1}\sqrt{n_p-1}\right]\right)} \tag{26}$$

Full details of the analytical derivations are presented by Ghandeharioon (2010).

3 VERIFICATION OF THE PROPOSED THEORY

In this research, large-scale laboratory experiments that incorporate a specially designed consolidometer and a novel machine for driving mandrels at a predesired rate are conducted to study the installation of mandrel-driven PVDs, and to validate the formulated elliptical CET. The test apparatus (including a large-scale consolidometer, fast-response pore pressure transducers and a mandrel driving machine), the test materials that consist of reconstituted soft clay and a prefabricated vertical drain, and the test

procedure are discussed in Ghandeharioon (2012). The pore water pressure is measured in the consolidometer at various locations during installation of the PVD under different stresses (20 kPa, 32.5 kPa and 50 kPa) applied to the surface of the soil to simulate different depths at the field. While these tests facilitated study of smear effect and disturbed soil around the drain, they were also used to verify the finite element simulation of the mandrel installation in Ghandeharioon et al. (2012). Figure 2 shows the comparison between the distribution pattern for excess pore pressure with radial distance from the center of the cavity predicted by both the developed elliptical CET and conventional cylindrical CET, and measured in the laboratory. It is evident that the elliptical CET formulated in this research evaluates the pore pressure during installation of commonly used mandrels more accurately than the conventional cylindrical CET.

By incorporating the results of laboratory tests on soil permeability, with regard to distance to the drain,

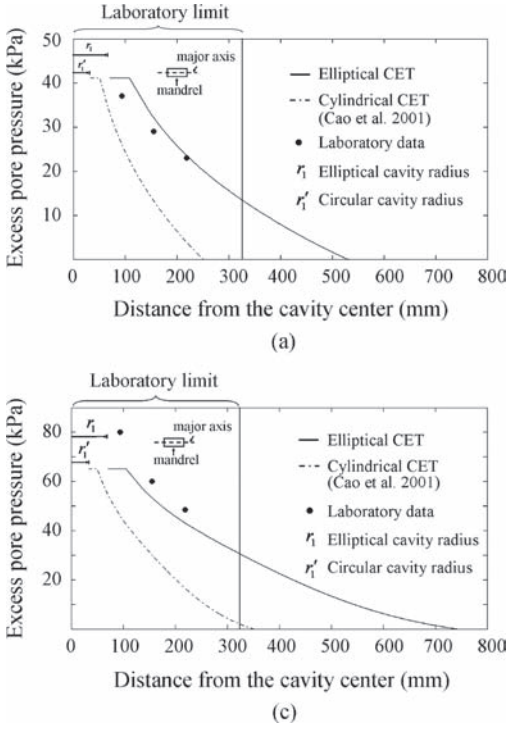

Figure 2. The distribution pattern predicted for excess pore pressure with radial distance using the developed elliptical CET and the conventional cylindrical CET along the major axis of the mandrel 0.26 m below the soil surface, and measured in laboratory when base of the drain shoe passed the horizontal plane under consideration, under a stress of (a) 20 kPa, (b) 32.5 kPa, and (c) 50 kPa.

conducted in this research and previously reported by Sathananthan and Indraratna (2006), Hird and Moseley (2000) and Indraratna and Redana (1998), it is found that an elliptical smear zone is created around the drains that are installed by common-field mandrels. Moreover, it is proposed that the plastic shear strain (γ_q^p) normalized by the rigidity index (I_r) can be adopted to characterize the disturbed soil surrounding the mandrel-driven PVDs. Normalized plastic shear strain is as large as 0.86%–1.05% at the boundary of soil that is in critical state, depending on the properties of the soft clay. The smear zone, within which the horizontal coefficient of permeability varies rapidly with the radial distance from the center of the mandrel, extends to where this ratio is about 0.10%–0.17%. The magnitude of normalized plastic shear strain varies between 0.01% and 0.05% at the boundary of the marginally disturbed zone, that region where the horizontal permeability changes slightly with distance. The plastic zone of soil experiences generation of Δu during the installation of mandrel and covers the area where the plastic shear strain is larger than zero. Finally, there is an outermost elastic zone with zero plastic shear strain, and no change in the total pore pressure before and after the mandrel penetrates the soil. Also, based on the numerical modeling of the mandrel installation in Ghandeharioon (2013), it is found that the normalized plastic shear strain associated with the boundary of the smear zone is almost constant for a given type of soil when the driving rate for a mandrel is specified, regardless of the in-situ effective stresses, and therefore this parameter can be used to evaluate the extent of smear zone in soil deposits under the field condition.

4 CASE HISTORY 1: MUAR CLAY REGION, MALAYSIA

The west coast of Peninsular Malaysia is a coastal plane of marine clay up to 20 m thick with an average lateral extent of about 25 km. A relatively stiff but brittle thin crust is on top of the very soft silty clay layer, below which the natural water content is as high as 100% and usually exceeds the liquid limit. The plasticity index is typically between 40% and 50%. While in Southeast Asia soft clays are normally consolidated in general, they may exhibit light overconsolidation as a result of surface desiccation and weathering. According to Indraratna et al. (1994), the unit weight of the clay in relation to depth at the site was fairly consistent between 15 and 16 kN/m^3, except at the top crust layer where the unit weight approached 17 kN/m^3. The coefficient of permeability ranged between 1×10^{-9} and 2×10^{-9} m/s with increasing depth within the soft clay deposit. Mandrels with cross section of 125 mm × 45 mm

were used for installing the vertical drains in this region. An attempt has been made in this research to predict the extent of smear zone in the case history of the Muar clay region using the analytical technique developed.

The concept of plastic shear strain normalized by the rigidity index of soil is utilized to obtain the size of smear zone, and evaluate it with regard to the data published previously. Table 1 shows the properties of a soft silty clay layer being analyzed for characterizing the smear zone associated with the installation of mandrel-driven PVDs.

Based on the elliptical CET, the variation of normalized plastic shear strain with radial distance in the case studied is derived and shown in Figure 3. As illustrated, the radius of the smear zone (r_{smear}) is assessed to be 3.07 times the equivalent radius of the mandrel ($r_m(\theta)$), where $\gamma_q^p / I_r = 0.135\%$ is the average value that corresponds to the boundary of the smear zone. This estimation of the smear zone is close to the assessment performed by Indraratna and Redana (2000), as depicted in Figure 4.

Table 1. The Cam clay properties for the soft silty clay layer at the Muar clay region in Malaysia (after Indraratna and Redana 2000).

Depth (m)	Soil type	κ	λ	M	υ_{CS}	n_p
8–18	Soft silty clay	0.035	0.35	1.07	2.61	1.47

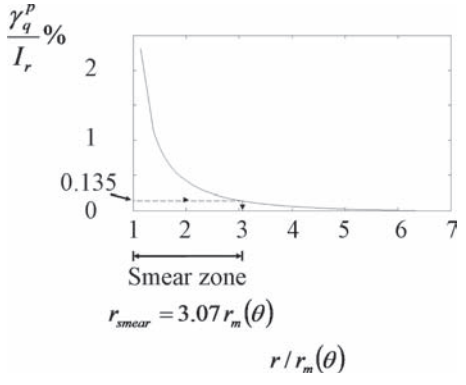

Figure 3. The variation of plastic shear strain normalized by the rigidity index in relation to the radial distance used for evaluating the extent of smear zone in the case history of the Muar clay region in Malaysia.

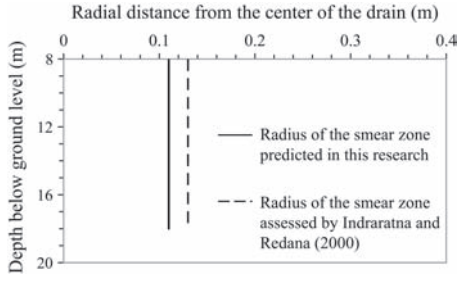

Figure 4. The extent of the smear zone in the case history of the Muar clay region in Malaysia.

5 CASE HISTORY 2: SUNSHINE MOTORWAY, AUSTRALIA

The subsoil at Sunshine Motorway site consists mainly of very soft saturated marine clays. Vertical drains were installed in the region by using mandrels of 125 mm × 45 mm in cross section. Site investigation revealed that the subsoil condition is relatively uniform throughout the site, consisting of sensitive silty clay approximately 10 m to 11 m thick with unit weight of 14–16 kN/m^3, overlying a layer of sand about 6 m thick (Queensland Department of Main Roads 1991). While this layer of sand is followed by a thin layer of soft clay extended to a depth of 18 m, another layer of sand is encountered below 18 m from surface. The liquid limit varies from 30% to 90%, and the moisture content is between 50% and 120% at different locations. Moreover, the ratio of the compression index changes from 0.15 to 0.50. According to Queensland Department of Main Roads (1991), the ratio of recompression was estimated to be about 10 times smaller than the ratio of the compression index. The coefficient of horizontal permeability (k_h) was found to be approximately two times the coefficient of vertical permeability (k_v) for all soil layers, based on the results of the oedometer tests on vertical and horizontal samples. The analytical technique developed in this research using modified Cam clay parameters for the analysis of the installation of PVDs in soft clay deposits is used to evaluate the smear effects for the case history of the Sunshine Motorway in Australia. The normalized plastic shear strain associated with the boundary of the smear zone is studied to assess the extent of smear zone in soil deposits under the field condition. Table 2 presents the properties of the soft silty clay layer 11 m thick

Table 2. The Cam clay properties for the silty clay in the case history of the Sunshine Motorway in Australia (after Sathananthan et al. 2008).

Depth (m)	Soil type	κ	λ	e_0	M	ν	n_p
2.5–5	Soft silty clay	0.20	2.02	2.2	1.20	0.3	1.20
5–11	Silty clay	0.05	0.53	1.8	1.18	0.3	1.20

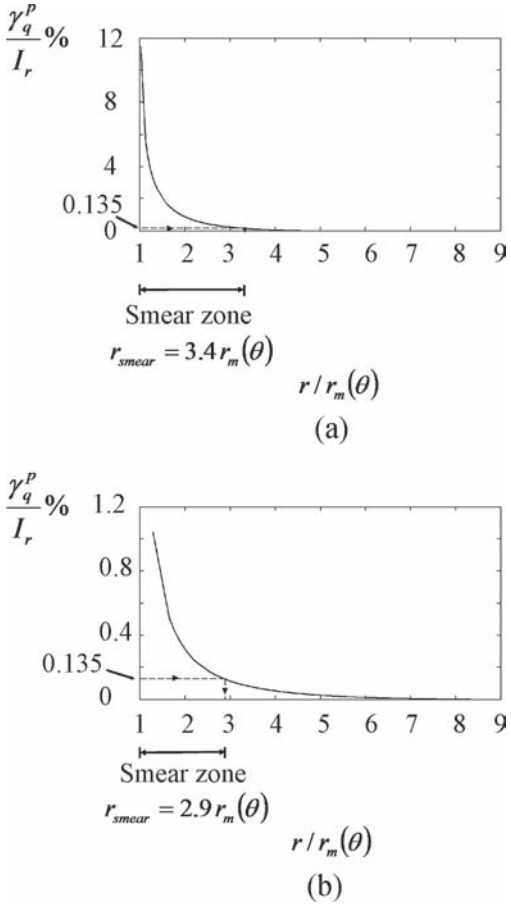

Figure 5. Variations of plastic shear strain normalized by the rigidity index in relation to the radial distance used for assessing the boundary of the smear zone in the case history of the Sunshine Motorway in Australia in (a) soft silty clay located 2.5–5 m below ground level and (b) silty clay located 5–11 m below ground level.

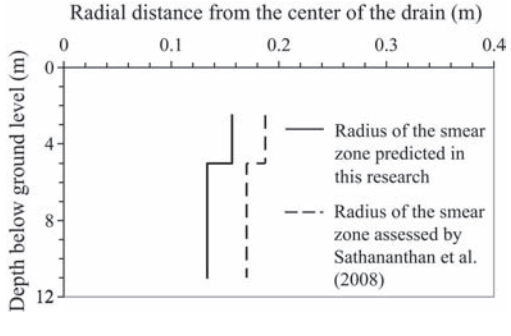

Figure 6. Variation of the extent of the smear zone with depth in the case history of the Sunshine Motorway in Australia.

being analyzed for investigating the smear zone. Variations of the normalized plastic shear strain with radial distance in this case history are calculated and demonstrated in Figure 5. As stated earlier, Ghandeharioon (2013) showed that the normalized plastic shear strain associated with the boundary of the smear zone is almost constant for a given type of soil under a specified rate of mandrel driving, regardless of the in-situ effective stresses. Therefore, $\gamma_q^p / I_r = 0.135\%$ was considered as the average of the range that corresponds to the boundary of the smear zone for the layer of soft silty clay as well as the layer of silty clay. The radius of the smear zone was evaluated to be 3.4 $r_m(\theta)$ in soft silty clay located 2.5–5 m below ground level and assessed to decrease to 2.9 $r_m(\theta)$ in the silty clay located 5–11 m below ground level (Figure 5). As illustrated in Figure 6, this finding is close to the results presented by Sathananthan et al. (2008).

6 CONCLUSIONS

An analytical theory was developed to investigate the installation of mandrel-driven prefabricated vertical drains that are commonly used as an effective technique to control the excess pore water pressure at the sites.

A new elliptical cavity expansion theory that incorporates the modified Cam clay parameters was established to study the installation of PVDs into soft clay deposits. The developed elliptical CET accounts for the rate of mandrel penetration and the time factor for predicting the internal pressure in the cavity, corresponding stresses and excess pore pressure in the soil while driving the mandrel.

The theory identifies a critical zone, a plastic zone, and an elastic zone around drains. The pattern of distribution calculated for excess pore pressure around vertical drains is verified by the results obtained from large-scale laboratory tests. While a more realistic elliptical smear zone based on the elliptical CET was expressed, the disturbed soil surrounding the mandrel was characterized by the plastic shear strain normalized by the rigidity index of the soil.

The analytical method developed was subsequently applied to case histories from the Muar clay region in Malaysia, and the Sunshine Motorway in Australia.

The predictions obtained for the size of the smear zone were compared with the data published previously. There was agreement between the results. It is found that the method identified in this research can be applied for assessing the extent of the smear zone in the field.

ACKNOWLEDGEMENTS

This research was supported by a scholarship from the Cooperative Research Center (CRC Australia) for Railway Innovation awarded to the author for his Ph.D. studies at University of Wollongong, Australia. Their support is acknowledged.

REFERENCES

Cao, L.F., Teh, C.I. & Chang, M.F. (2001). Undrained cavity expansion in modified Cam clay I: Theoretical analysis, *Geotechnique,* 51(4): 232–334.

Clarke, B.G. 1995. *Pressuremeter in geotechnical design*. London: Chapman and Hall.

Cooke, R.W. & Price, G. 1978. "Trains and displacements around friction piles. Building Research Station CP 28/78, October.

Ghandeharioon, A. 2010. Analytical and numerical study of soil disturbance associated with the installation of mandrel-driven prefabricated vertical drains, Ph.D. Thesis, School of Civil, Mining & Environmental Engineering, Faculty of Engineering, Univ. of Wollongong, Wollongong, Australia.

Ghandeharioon, A. 2012. Large-scale laboratory assessment of smear effects in soft soils stabilized by prefabricated vertical drains. *Proceedings of the 65th Canadian Geotechnical Conference: GeoManitoba—Building on the past*, Canadian Geotechnical Society, Canada.

Ghandeharioon, A. 2013. Finite element analysis of the installation of prefabricated vertical drains in soft soils. *Proceedings of the International Symposium on Design and Practice of Geosynthetic-Reinforced Soil Structures*, University of Bologna, Bologna, Italy.

Ghandeharioon, A., Indraratna, B. & Rujikiatkamjorn, C. 2012. Laboratory and finite element investigation of soil disturbance associated with the installation of mandrel-driven prefabricated vertical drains, *Journal of Geotechnical and Geoenvironmental Engineering,* 138(3): 295–308.

Hird, C.C. & Moseley, V.J. 2000. Model study of seepage in smear zones around vertical drains in layered soil, *Geotechnique*, 50(1): 89–97.

Indraratna, B. Balasubramaniam, A.S. & Ratnayake, P. 1994. Performance of embankment stabilized with vertical drains on soft clay. *Journal of Geotechnical Engineering, ASCE*, 120(2): 257–273.

Indraratna, B. & Redana, I.W. 1998. Laboratory determination of smear zone due to vertical drain installation. *Journal of Geotechnical and Geoenvironmental Engineering*, 124(2): 180–184.

Indraratna, B. & Redana, I.W. (2000). Numerical modelling of vertical drains with smear and well resistance installed in soft clay. *Canadian Geotechnical Journal*, 37: 132–145.

Mair, R.J. & Taylor, R.N. 1993. Prediction of clay behaviour around tunnels using plasticity solutions. *Predictive Soil Mechanic:* 449–463. London: Thomas Telford.

Ogawa, T. & Lo, K.Y. 1987. Effect of dilatancy and yield criteria on displacements around tunnels. Canadian Geotechnical Journal, 24: 100–113.

Pender, M. 1980. Elastic solutions for a deep circular tunnel. *Geotechnique*, 30(2): 216–222.

Queensland Department of Main Roads. 1991. Sunshine Motorway stage 2-Area 2 geotechnical investigation. *Materials and Geotechnical Services Branch*, R1765.

Randolph, M.F., Carter, J.P. & Wroth, C.P. 1979. Driven piles in clay—the effect of installation and subsequent consolidation. *Geotechnique*, 29(4): 361–393.

Sathananthan, I. & Indraratna, B. 2006. Laboratory evaluation of smear zone and correlation between permeability and moisture content, *Journal of Geotechnical and Geoenvironmental Engineering*, 132(7): 942–945.

Sathananthan, I., Indraratna, B. & Rujikiatkamjorn, C. 2008. Evaluation of smear zone extent surrounding mandrel driven vertical drains using the cavity expansion theory. *International Journal of Geomechanics*, 8(6): 355–365.

Wroth, C.P. 1984. The interpretation of in-situ soil tests. *Geotechnique*, 34: 449–489.

Yu, H.S. 2000. *Cavity expansion methods in geomechanics*, The Netherlands: Kluwer Academic Publishers.

Yu, H.S. & Mitchell, J.K. 1998. Analysis of cone resistance: review of methods. *Journal of Geotechnical and Geoenvironmental Engineering, ASCE*, 124(2): 140–149.

Geotechnical Engineering for the Preservation of Monuments and Historic Sites – Bilotta, Flora, Lirer & Viggiani (eds)
© 2013 Taylor & Francis Group, London, ISBN 978-1-138-00055-1

Preservation and monitoring of the Frari bell tower in Venice

G. Gottardi & M. Marchi
DICAM, University of Bologna, Bologna, Italy

A. Lionello
Ministry for Cultural Heritage and Activities, Italy

P.P. Rossi
R.TEKNOS SrL, Bergamo, Italy

ABSTRACT: The Frari bell tower, the second tallest in Venice after San Marco, has always been affected by structural problems since its construction in XIV century, mainly because of the slow but continuous differential settlement between the tower itself and the adjacent masonry structures of the basilica. In the last decade, within a comprehensive scheme of structural rehabilitation carried out by the Italian "Ministero per i Beni e le Attività Culturali" (Italian Ministry for Cultural Heritage and Activities), a rather innovative intervention of soil fracturing was carried out in order to improve the mechanical characteristics of the silty clay layer underlying the tower. Once the aim of improving the stability of the soil-foundation system had been achieved, a new solution was then required to reduce the damaging structural interaction induced by the foundation movements: a structural joint between the bell tower and the basilica was eventually carried out in order to improve the system deformability. The paper presents a well-documented history of such a complex and delicate intervention, since the preliminary accurate site investigation, highlighting not only the approach aimed at improving the overall safety without altering the original structure and modifying the current stress distribution but also the fundamental methodology, adopted throughout, of a flexible and modular design, constantly driven by the outcome of an extensive real-time monitoring system of the soil-structure interaction.

1 THE FRARI BELL TOWER: A HISTORY OF INTERVENTIONS

Built between 1361 and 1396, the Frari bell-tower (Figure 1) was originally conceived as a fully independent structure, 9.5 m wide at the ground level, 65 m tall and weighing about 57 MN. The internal ramp staircase up to the belfry is supported by a double structure of thick brick masonry.

During the reconstruction of the Basilica, started in 1340 and finished in the second half of the 15th century, the bell-tower was included into the masonry walls, at the south-east corner of both transept and left aisle (see plan of Figure 1). This new configuration is at the origin of the subsequent problems that have always affected the structure. In 1432 the St Peter's chapel was constructed adjacent to the basilica and the bell-tower, even if structurally independent. The first documented signs of deterioration of the structures are dated back to the end of the 16th century.

Between the end of 19th century and the first decade of the 20th, three main strengthening interventions, widely documented by projects, surveys and site sketches, were carried out (Lionello, 2008). In fact, the bell tower settlement had caused, along the centuries, major damages both to the St Peter's chapel and to the vaults of the left aisle of the church, requiring urgent repair interventions on the masonry walls and at the level of the foundations. In the first years of the 20th century the tower showed a differential settlement of already about 0.40 m with respect to the basilica and an out of plumb toward south-east of 0.765 m at a height of 42.5 m (resulting in an inclination of about 1°). Only after these repair works the structures of the bell-tower and the St Peter's chapel were connected each other at the foundation level, with a solid relieving arch made by three brick layers, and at the superstructure level, by metal ties.

In 1904, following the great concern after the sudden collapse of the worldwide famous St Mark bell tower, an extensive investigation was carried out on many Venetian structures considered at stake. In the Frari case, the surveys revealed inadequate foundations with respect to the bulk of the

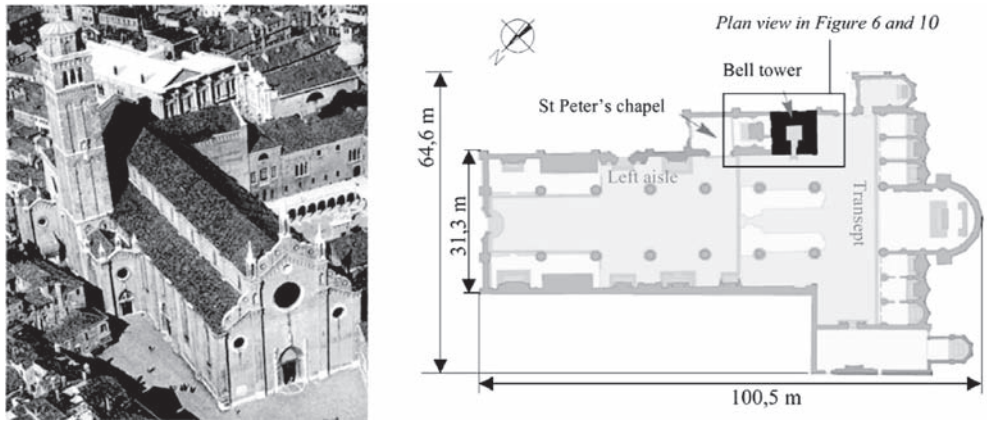

Figure 1. Left: A view of the Frari square (*Campo dei Frari*) and its monuments: the bell tower, the basilica and the cloister. Right: A plan of the basilica with the bell tower and the St Peter's chapel.

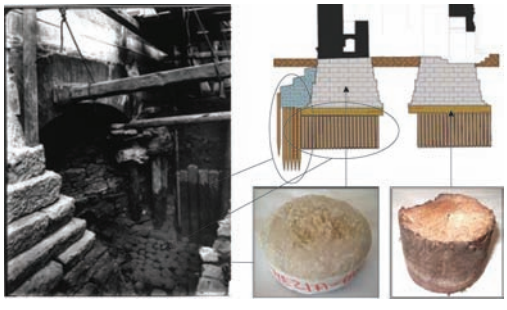

Figure 2. Left: Picture of the strengthening intervention on the bell tower foundations, dated back 1904 (Photo archive of the "*Soprintendenza per i beni architettonici e paesaggistici di Venezia e laguna*"). Right: Schematic drawing of the foundation enlargement with pictures of samples extracted during the recent survey (Marchi *et al*., 2006).

bell tower, this being therefore the main cause of the tower settlements. For this reason, a strengthening intervention on the bell tower raft foundations was carried out, consisting of widening its base, starting from the south side (toward which the tower was essentially leaning, see Figure 2). At the time, the intervention was designed according to the traditional Venetian soil strengthening technique, with the insertion of closely spaced timber piles (made from larch, length 3.80 m, transverse dimensions 0.20×0.20 m and essentially touching each other), covered by a 2.00 m wide concrete bed, parallel to the side of the bell tower. All the masonry walls were also treated with cement mortar to restore the cohesion of the brick masonry and improve its strength. Such raft foundation enlargement would have been most probably extended also to the other sides; as a matter of fact, however, for emergency reasons that gave priority to other interventions, it was never executed (Lionello *et al*., 2004).

2 INVESTIGATIONS AND MONITORING BEFORE THE INTERVENTION

At the beginning of the 1990's, subsequent to an extensive survey concerning the general safety conditions of Venice bell towers—planned and implemented by the local *Architectural Heritage Office* of the *Italian Ministry for Cultural Heritage and Activities*—a rather detailed diagnostic investigation of the Frari bell tower started, including photogrammetric survey, crack-pattern survey carried out with the aid of climbing technicians, endoscopies, single and double flat-jack tests on the masonry walls, sonic tests on steel ties, monitoring of the main cracks by means of extensometers and positioning of clinometers for the detection of rotations of the bell tower, as well as preliminary geotechnical investigations of the foundation soil. In 2000, a further survey aimed at detecting the differential settlements of the bell tower, by comparison with 1902 situation, revealed downward movements as large as 49.8 mm in the east corner, 61.3 mm in the south corner and 92.3 mm in the west corner of the bell tower base (Lionello *et al.,* 2004). Such pattern, together with the photogrammetric survey of the 1990's, indicated that the bell tower was tilting in the opposite direction with respect to the "historical" trend, essentially moving back toward its vertical position (Figure 3).

Emergency interventions were provided to the structures more affected by the deformation processes. In particular, the installation of a timber prop system was required to support the stone

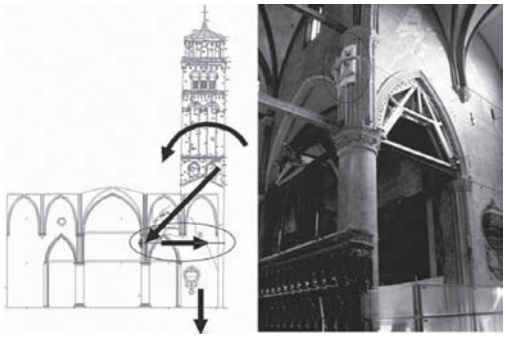

Figure 3. Left: Possible evolution of the bell tower displacements and interaction with the adjacent basilica structures (from Lionello *et al.,* 2004). Right: A picture of the temporary intervention by a steel cable to support part of the horizontal thrust acting on the adjacent column of the Frari basilica.

arch that connects the bell tower to the adjacent pillar of the basilica (Figure 3). A monthly survey carried out from 2000 to 2004 confirmed the displacement trend, recording an average settlement of 1 mm/year in the west corner of the tower.

2.1 *Measurement of the state of stress*

Flat-jack testing technique was used to measure the existing state of stress on the masonry structures of the bell tower and of the adjacent basilica (Figure 4). At the base of the bell tower an average value of 1.92 MPa was measured on the outer side, while on the inner part a mean value of 1.44 MPa was estimated (Figure 5). Inside the bell tower, flat-jack tests were carried out on both sides of an inclined oblique crack which runs along the southwest side of the tower. The similar stress values measured at two different levels, clearly show that the crack, even if passing through the entire thickness of the wall, does not induce particular stress concentration on the structure. Very high values of compressive stress were measured at the top of the column sustaining the propped arch: 1.76 MPa on the outer side and 3.20 and 3.04 MPa on the inner side (Figure 5). A detailed analysis was also carried out on the wall above the propped vault and the results indicated the presence of a thrust line going from the bell tower to the structures of the basilica (shown in Figure 3), in correspondence of the upper area of the above-mentioned column, with stress values ranging from 0.56 MPa to 0.95 MPa. The presence of this thrust line is confirmed by the results of the numerical model, also included in Figure 5. Flat jack tests with two parallel jacks were used to determine the deformability characteristics of the masonry.

Figure 4. Flat-jack test for measuring the state of stress at the base of the bell tower (left) and at the top of the adjacent column of the Frari basilica (right).

2.2 *Geotechnical investigations*

A rather detailed geotechnical investigation was carried out in May 2003 (tests "x"/A in Figure 6) and, on that basis, the subsequent ground improvement intervention by soil fracturing was planned. The investigations of such A-phase consisted of: 4 piezocone tests, 2 vertical and 5 inclined continuous coring boreholes, 4 continuous borings into the foundation block, together with the extraction of several undisturbed soil and foundation block samples for the subsequent execution of the laboratory tests, which enabled the stratigraphy, the subsoil properties and the geometry of the foundation block to be defined with some detail (Gottardi *et al*., 2008). A section of the thus reconstructed peculiar bell tower foundation along the SE-NW direction is provided in Figure 7 (see also for clarity the sketch of Figure 2b). As usual in Venice (Marchi *et al*., 2006), the Frari bell tower foundation is made up of Istrian limestone squared blocks and short timber compaction piles (1.70–2.20 m long), with an interposed larch boarding 0.40–0.50 m thick.

The soil profile under the tower, shown in Figure 7, consists of:

- Unit A, between ground level and a depth of about 3.2 m: anthropic fill;
- Unit B, between 3.2 m and about 6.7 m: dark grey, soft, silty clay, with occasional organic material, normally consolidated or slightly overconsolidated, with organic inclusions and shells In Figure 8 the relevant main geotechnical characteristics, as deduced from laboratory and in situ tests, are reported;
- Unit C, between 6.7 m and 14 m: grey medium-fine sand, non plastic, from dense to very dense;
- Between 14 m and the maximum investigated depth: alternation of soft clayey silt and medium-fine dense sand.

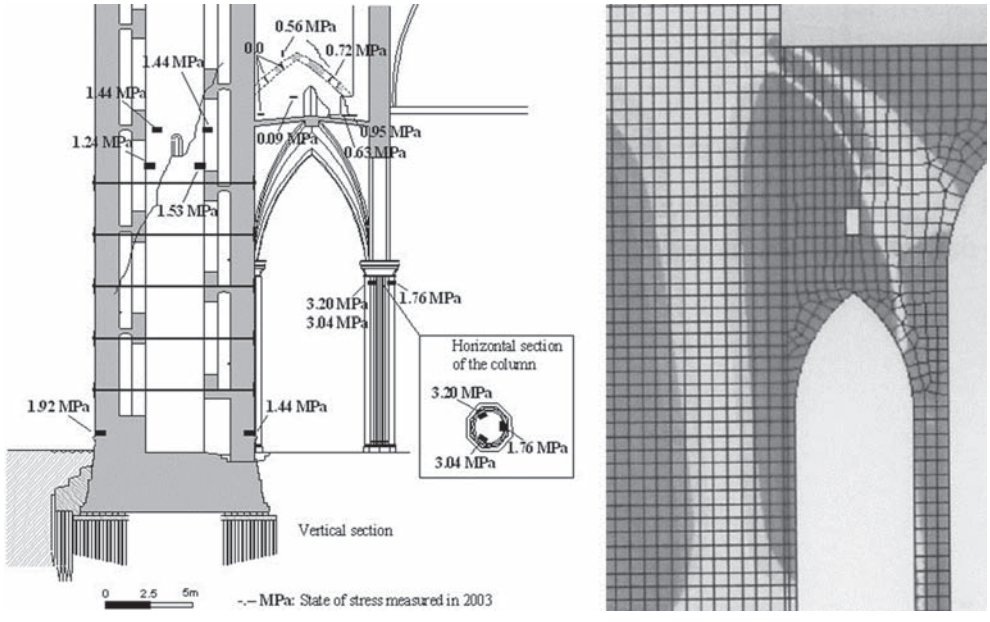

Figure 5. Left: Values of the state of stress measured by flat-jack test in the structures of the Frari basilica and of the bell tower. Right: Comparison with the outcome of the numerical model (Lionello, 2008).

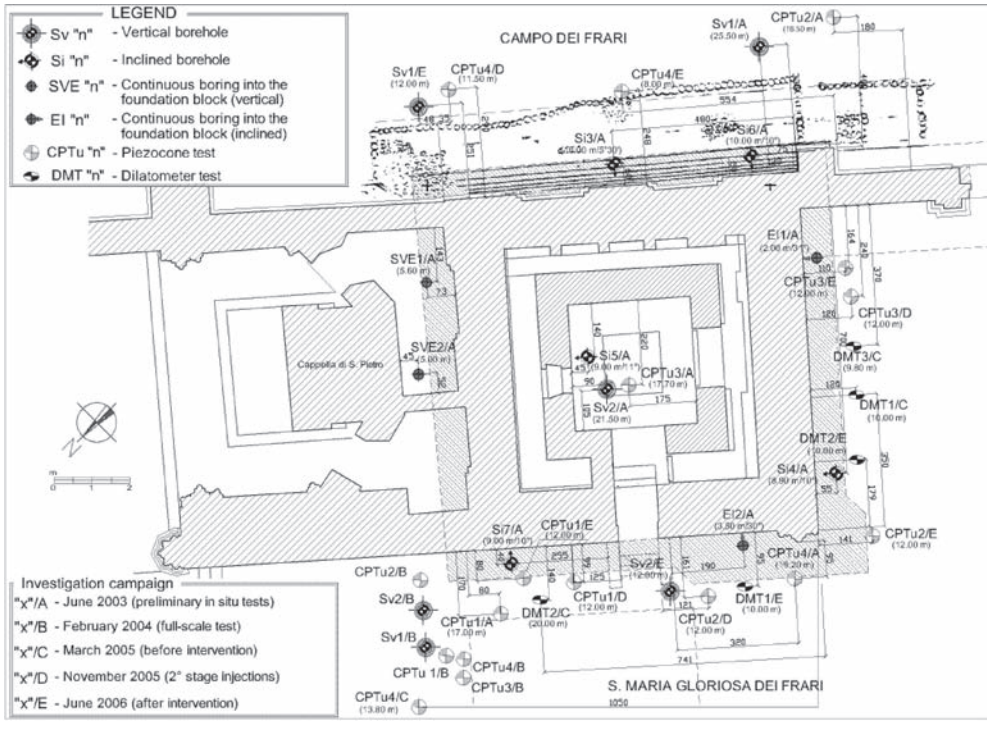

Figure 6. Plan of the Frari bell tower with the location of the geotechnical in-situ investigations at various stages of the intervention (Lionello, 2008).

Finally, the good conditions of the foundation enlargement built on the external side of the bell tower were confirmed. A careful evaluation of settlement trend with time excluded that the movements of the tower could be entirely ascribed to secondary settlements in confined conditions. Hence, the reasons of the continuous foundation problems were also attributed to a slow lateral plastic flow under high stress gradients within the soft silty clay layer, squeezed between the pile ends and the underlying sand.

2.3 *Monitoring system*

After the end of the diagnostic investigations, a comprehensive monitoring system was installed to analyze the deformation behaviour and the structural conditions of the bell tower and the adjacent portion of the basilica during all the phases of the strengthening interventions, consisting of:

- crack-gauges and long-base extensometers installed on the main cracks of the masonry walls;
- strain-gauges to measure the deformation of the steel cable installed in the bell-tower;
- thermal gauges to measure the temperature of the internal and external air, as well as inside the masonry at different distances from the outer wall;
- geotechnical instrumentation, including electrical piezometers, multibase extensometers and biaxial inclinometers;
- direct pendulum equipped with automatic telecoordinometer, for the measurement of the absolute horizontal movements of the top of the tower. The scheme of this most valuable device for the analysis of the movements of a high structure is provided in Figure 9.

All the instruments were connected to an automatic data acquisition system that enabled to follow in real time the effect of the works on the structures, thus enabling to introduce possible suitable modifications to the intervention design. In addition, it was considered of vital importance to measure the vertical movements of the bell tower and of the adjacent portion of the basilica. A high-precision and accurate manual leveling system with several measuring points was thus installed and periodical surveys were carried out and intensified during the most significant phases of the works.

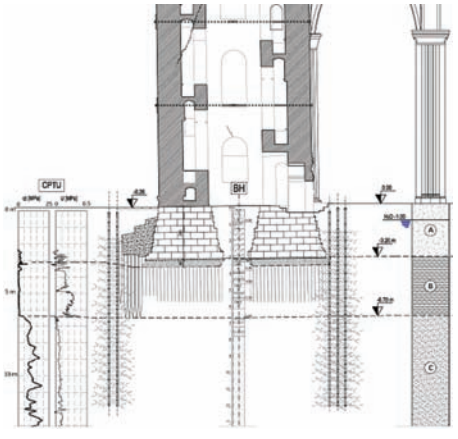

Figure 7. Schematic section of the tower foundation and of the relevant subsoil (SE-NW direction in Fig. 6), with the in-situ test logs, the strengthening intervention of 1904 (left) and the TAMs of the new fracture grouting intervention (Marchi *et al*., 2012).

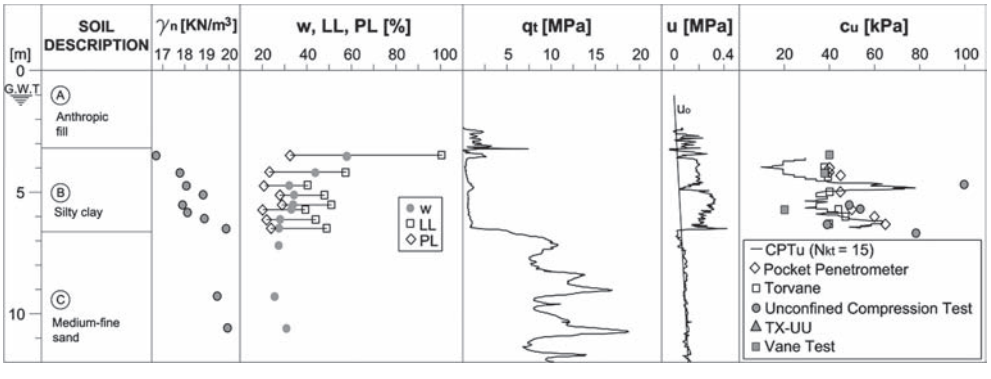

Figure 8. Upper soil profile with the relevant main geotechnical characteristics, as deduced from laboratory and in situ tests.

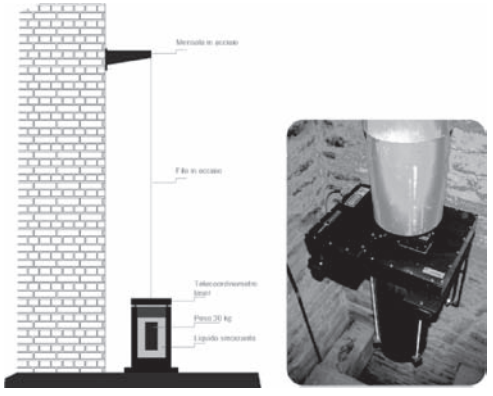

Figure 9. Left: Scheme of the direct pendulum installed in the Frari bell tower. Right: View of the telecoordinometer.

3 THE INTERVENTION

The slow, but continuous, constant rate, differential settlement of the bell tower has soon become cause of major concern for the present and future stability, not only of the bell tower but, above all, of the structurally connected basilica. From the results of the diagnostic investigations and the following numerical simulations (Lionello *et al.,* 2004), it clearly emerged that the interacting structures of the bell tower and the basilica cannot bear further differential settlements without serious consequences.

It followed the need of a strengthening intervention, at the level of the foundations, aimed at reducing the differential settlements of the bell tower. A rather innovative intervention of careful soil fracturing was eventually designed, in order to improve the mechanical characteristics of the soft silty clay. Once the aim of improving the stability of the soil-foundation system had been achieved, a new solution was required to reduce the damaging interaction between the masonry structures, activated by the foundation settlements. A structural joint between the bell tower and the basilica was finally executed in order to improve the system deformability.

In order to guarantee the safety of the whole basilica and bell tower, a gradual strengthening intervention was designed, with a strict and constant control during the execution of the works, a rather typical and well implemented example of the so-called "Observational Method".

3.1 *Phase 1: Provisional strengthening intervention*

A preliminary intervention was required by the concern of deformations induced on the column of the basilica by the thrust of the bell tower. A provisional intervention was then carried out in order to increase the safety level of this specific and most delicate component of the basilica. A steel cable was thus positioned connecting the stone ashlars just above the capital of the column to the bell tower structure at a height of 14.40 m (round circle in Figure 3), aimed at supporting part of the horizontal thrust acting on the column. Two strain-gauges were installed on the steel cable and the relevant tension constantly monitored during the whole intervention period.

3.2 *Phase 2: Soil strengthening*

The principles on which the soil strengthening intervention was based were (Lionello, 2008):

- making compatible the remaining settlements of the complex basilica and bell tower;
- preserving as much as possible the original foundation structure and the current stress distribution;
- avoiding a rigid foundation system for the bell tower;
- enabling a flexible and modular intervention, in constant agreement with the outcome of an extensive real time monitoring.

In order to evaluate the feasibility of the soil fracturing intervention (Mori & Tamura 1987, Panah & Yanagisawa 1989, Raabe & Esters 1990, Andersen *et al.* 1994, Alfaro & Wong 2001, Soga *et al*., 2005) and calibrate the design parameters (injection pressures, injection rate, grout mixture, etc.), a full-scale test site with geotechnical monitoring devices (piezometers and multibase extensometers) was carried out on the northern corner of the bell tower, inside the basilica. The test gave the expected results and the soil fracturing intervention was then carried out by means of eighty-eight 12 m-deep sleeve steel pipes (so-called "tubes à manchettes", i.e. TAMs) installed all around the perimeter of the bell tower (Figure 10). Such special injection pipes had equally spaced (0.5 m) valves, selectively injectable by means of a double packer device. They were aligned along two rows, according to local geometric constraints, except for the west side where a third row was subsequently added The inner row was placed as close as possible to the foundation side; the other two rows were spaced of about 50 cm (Figure 10). A cement-bentonite grout was injected from each valve in three main separate stages (cycles). A fourth cycle was designed to enhance the intervention on the clay layer only and for the 55 pipes that had registered a lower injection pressure in the previous stages. The selected grout was made up of water, cement, bentonite and calcareous fill, with

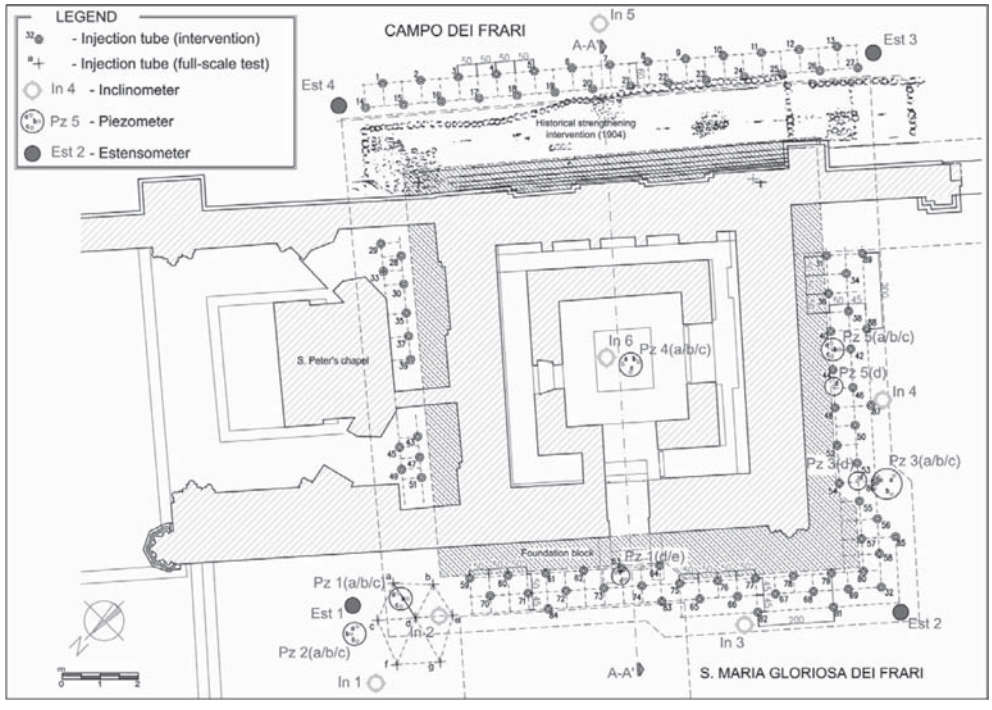

Figure 10. Plan of the Frari bell tower with TAMs lay-out and location of geotechnical monitoring devices (Lionello, 2008).

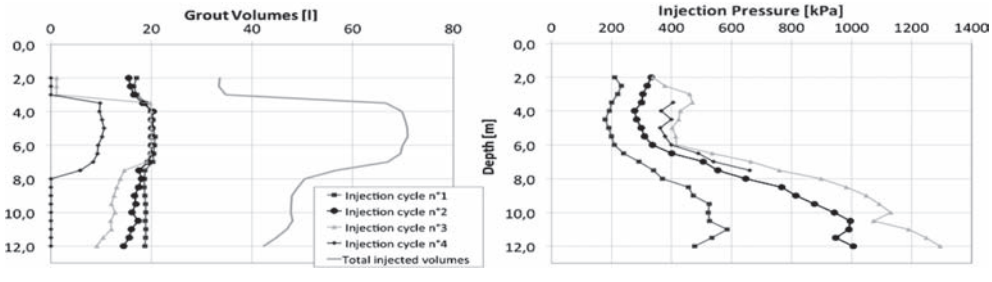

Figure 11. a) Average (for the overall 88 pipes) volumes injected from each valve, at selected depths, for the 1st, 2nd, 3rd and 4th cycle. b) Average injection pressures *vs*. depth, for each cycle, as measured at the manometer (Marchi *et al*., 2012).

a water/cement ratio of about 1.5 and a cement/bentonite ratio of about 14, thus producing a very low viscosity grout (1.5×10^{-2} Pa × s).

During the intervention the flow rate was fixed (about 6 l/min); the resulting valve opening pressure and the following steady-state injection pressure were recorded. In the final cycle, a flow rate about half than the previous cycles was used. Injected volumes are shown in Figure 11a. Grout volumes of 20 l/valve were injected each cycle in clay, variable volumes between 14 and 20 l/valve in sand. In the 1st cycle all valves could be opened. In the 2nd cycle a few valves could not be opened in sand. In the 3rd and 4th cycles more restrictive criteria were adopted: a pre-fixed limit to the opening pressure of 500 kPa in clay and of 2500 kPa in sand, where therefore many more valves could not be opened. Figure 11a shows the total volumes injected in each cycle from each valve depth, divided by the total number of existing pipes (i.e. 88). Notice that the total amount of grout injected in clay is clearly greater than in sand. At the end of the intervention, a total of about 100 m^3 of grout was injected.

Figure 11b reports the average steady-state injection pressures (P_i) vs. depth for each cycle, as measured at the manometer. P_i is clearly greater in sand and tends to increase almost linearly with depth. Injection pressures vary between about 200–500 kPa in the first cycle to about 400–1200 kPa and more in the final cycle. In particular, the low injection pressures (P_i) recorded in the third cycle between 2.00 and 3.00 m depth are not significant since they result from only 5 pipes. In addition, P_i recorded in the fourth cycle, resulting from a reduced and selected number of pipes (55), turned out to be lower than that in the third cycle; this could be also due to the lower injection flow rate used in the final cycle, as already noticed in previous experiments. However, the clearly noticeable general increase of pressures with injection cycles reflects a corresponding increase of the soil minor principal stress during the intervention, as intended (Gottardi *et al.*, 2008; Marchi *et al.*, 2012).

3.3 *Phase 3: Structural joint*

Once completed the intervention on the foundation soil and whilst continuing to monitor the bell tower behaviour, the relevant structural interaction with the most damaged arches, vaults and columns of the basilica had to be tackled.

Such interaction implied in fact:

- a substantial compression stress increment on the column, much greater than the contribution of the dead weight of walls, vaults and roofs;
- the formation of a large flexural stress on the column itself, due to the eccentricity of the vertical load and to the horizontal thrust component;
- the corresponding reduction of the vertical stress along the bell tower walls.

In view of the restoration and preservation intervention it was therefore opted, instead of opposing the current forces acting on the structures, to reduce their stress distribution (Lionello, 2011). About two years after the end of strengthening works on the foundation soil, it was decided to insert a gap between the bell tower and the adjacent church by creating a structural joint that would allow the relative movements and prevent the mutual stress transmission. It was assumed that it could be thus reduced the compression stresses flowing above the arch and transmitting substantial elevated forces to the column of the basilica (Figure 12a).

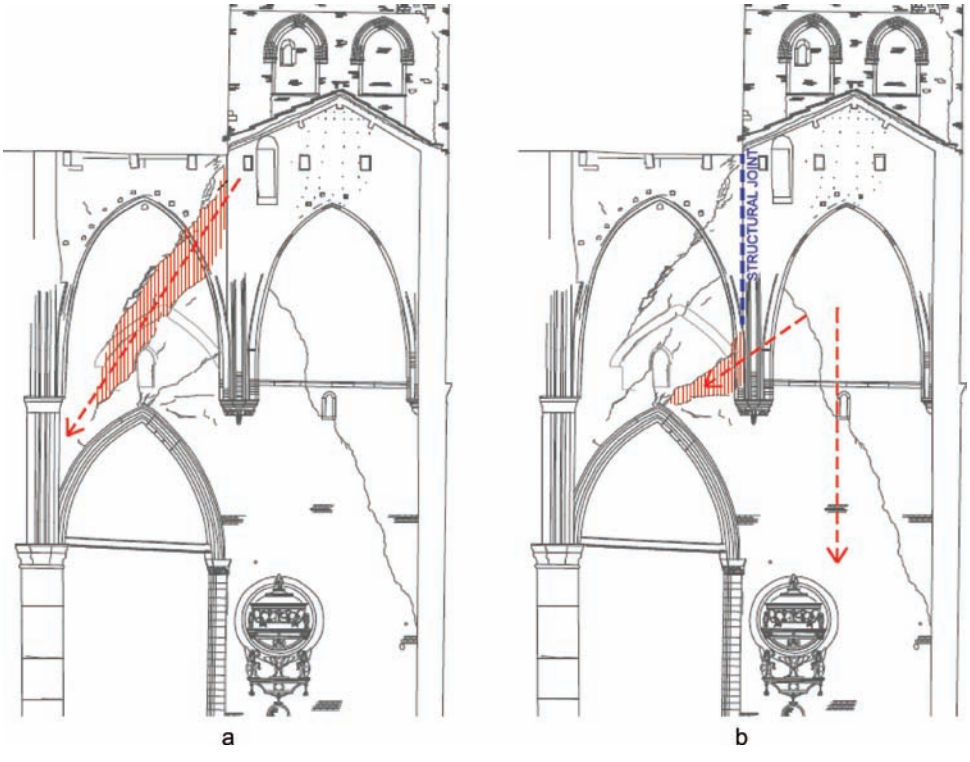

Figure 12. Direction of the thrust between the bell tower and the basilica: a) before the structural joint execution, b) after the structural joint execution.

Such structural joint was created at the beginning of June 2008 in the position shown in Figure 12b and, in order to preserve the basilica architecture, it was carried out only above the vaults where, on the other hand, mechanical interaction was greater. During the intervention, it could be confirmed that the existing structural link had been executed only after the construction, probably together with the interventions of early twentieth century, when it was wrongly pursued the connection of the bell tower to the basilica structures.

The effect of this intervention was a marked change of direction of the thrust applied by the bell tower to the adjacent column, as shown in Figure 12b and predicted by numerical models.

The execution of the structural joint was very slow and lasted about 6 months. During this period a detailed analysis of the information obtained by the monitoring system enabled to carry out the different steps of the intervention with a continuous check of the structural response, thus avoiding to induce damages to the bell tower and to the supporting structures of the basilica.

4 INVESTIGATIONS AND MONITORING DURING AND AFTER THE INTERVENTION

4.1 *Soil investigations and monitoring*

As reported in Section 2.3, the geotechnical instrumentation installed throughout the area of the intervention enabled to carefully check the effects of the soil fracturing (Lionello, 2008). As an example, in Figure 13 the records of most of the electric piezometers installed within the silty clay layer are provided: the pore pressure peaks induced by adjacent grout injections are clearly visible as well as the subsequent relatively quick consolidation rate, which enabled to drive the operations under constant control and safety conditions.

As designed, the injections led to soil fracturing: evident and diffuse cement lenses in the soil were found in undisturbed continuous core sampling carried out at the end of the intervention. Specific additional in situ geotechnical investigations (piezocone and dilatometer tests) were planned and carried out to assess its effect on the mechanical properties of soil (Gottardi *et al*., 2008). The global effect of the injections could be assessed by comparing the results of in situ tests performed at different stages of the intervention. The soil strength improvement is clearly noticeable in Figure 14 by the increase of the average cone tip resistance from all CPTu tests carried out before the intervention, after the second injection cycle and at the end of the injections (respectively CPTu"n"/A, /D and /E in Figure 6). Peaks of the tip resistance are due to the diffuse presence of grout lenses, the relevant average increase among them being more effective though. Analogous data on the dilatometer modulus are also available (Gottardi *et al*., 2008). The relevant stiffness increase was further confirmed by laboratory oedometer tests, which provided a modulus increase of about 100% at 50 kPa and about 20% at 400 kPa (Lionello, 2008).

However, more comprehensive information for the analysis of the structure behaviour during the soil fracturing works come from the direct pendulum records and precision leveling surveys. In Figure 15, the movement trend along two orthogo-

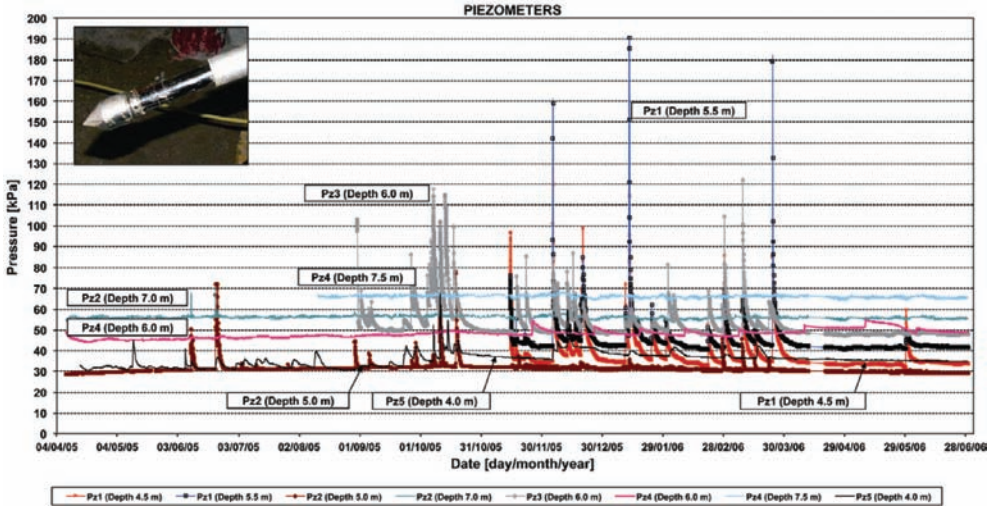

Figure 13. Records of most electric piezometers installed within the silty clay layer (after Lionello, 2008).

nal components from direct pendulum are shown. The period of observation is from December 2003 (date of installation of the monitoring system) to the end of December 2011. During the soil fracturing intervention (from April 2005 to March 2006, grey shadow 1), the monitoring system was also useful to define the rate of the intervention phases as well as to support decisions on the parameters of the grouting procedures (injection pressure, flow rate, etc). A significant movement of the bell tower during this intervention phase was observed, the component in x direction (toward the apse) being about 9.0 mm and in y direction (toward the basilica) about 5.0 mm. After the end of the soil fracturing, the rate of the bell tower movements showed a quick reduction, reaching a lower value than observed before the intervention. Movements of cracks in the stone arch which connects the bell tower to the basilica also showed a marked increase during soil fracturing and a rapid decrease after.

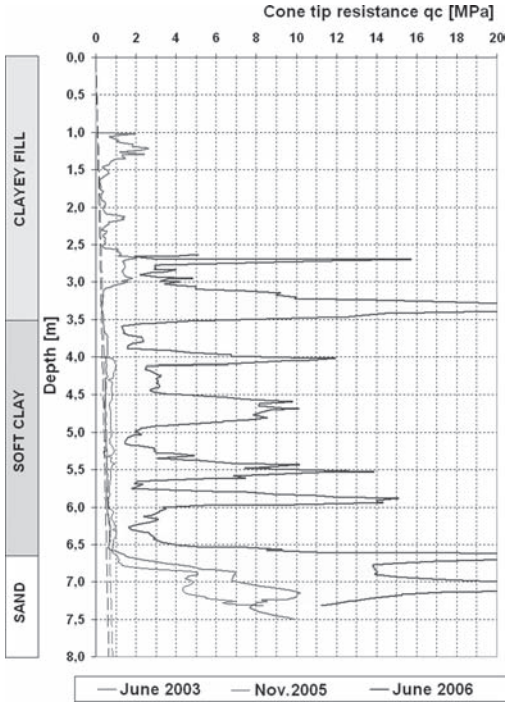

Figure 14. Comparison of cone tip resistance logs from piezocone tests carried out before, during and after the intervention (Gottardi *et al.*, 2008).

In Figure 16 the settlement trend of several benchmarks from precision leveling is provided. A more pronounced vertical movement of the bell tower west and south corners (points 5 and 6) is clearly observed during the soil fracturing intervention (time interval highlighted in grey), but all measuring points display a similar rate increase during the intervention and a significant reduction immediately after, also with respect to original rates before, consistently with design expectations. Such observation is confirmed by the differential settlement trend (Figure 16) along main alignments and, above all, between the critical column of the basilica and the adjacent bell tower corner (points 1 and 5): 1.01 mm/year before, 5.04 mm/year during and 0.27 mm/year after the intervention.

The settlement values are also in very good agreement with the measures obtained by the direct pendulum in the period from December

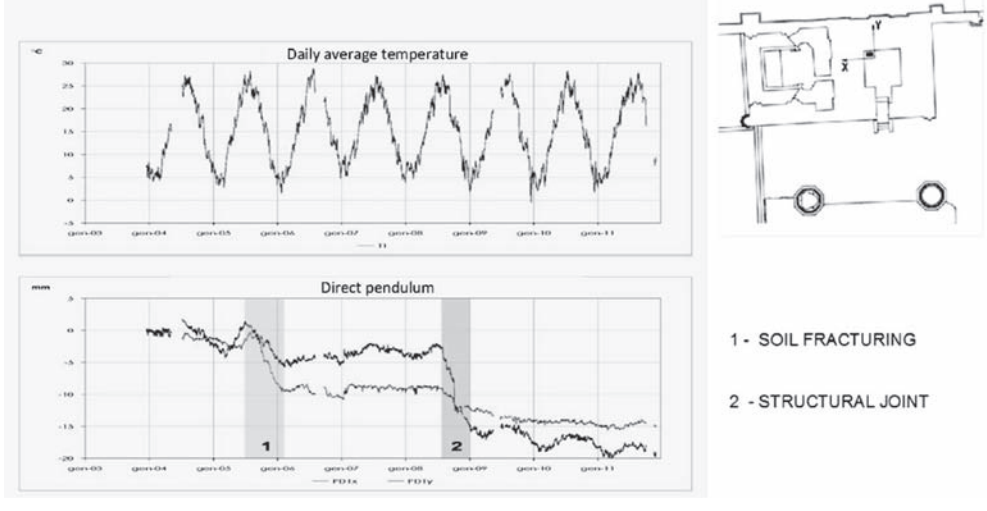

Figure 15. Complete history of the displacement components measured by the direct pendulum with the indication of the intervention phases (1. soil fracturing and 2. structural joint execution) (Rossi & Rossi, 2012).

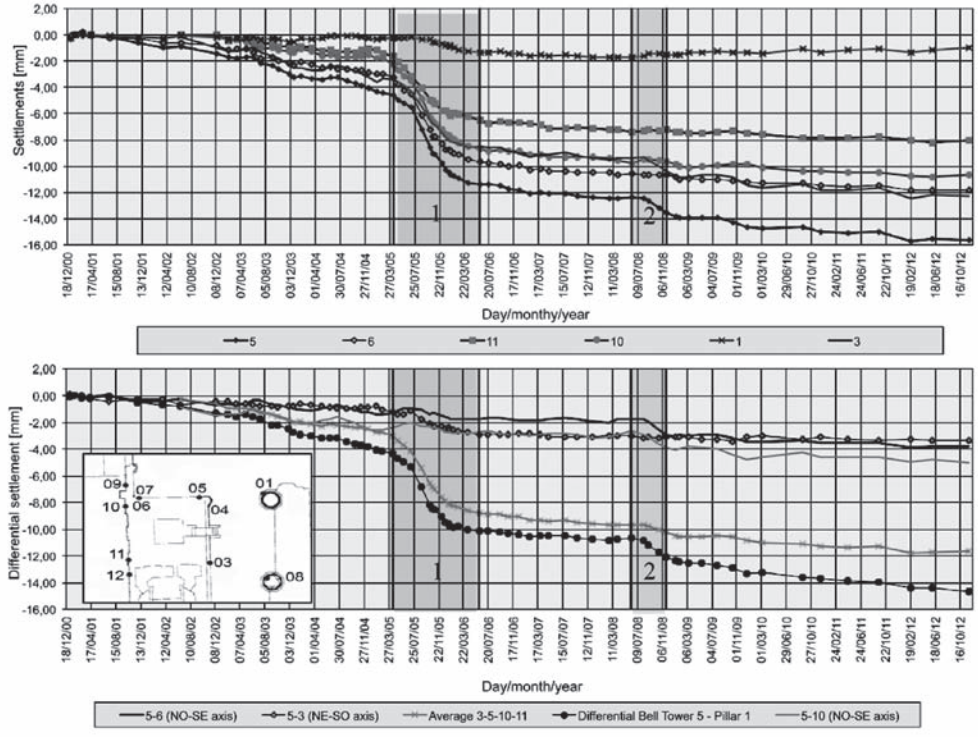

Figure 16. Settlements (top) and differential settlements (bottom) of several benchmarks from precision leveling (courtesy of FOART srl, Parma).

2003 to March 2007 (Figure 17). Along the alignment of points 3 and 4, the differential settlements at the base of the bell tower (2.16 mm) multiplied for the ratio between the height and the base of the tower (4.70) turns out to be 10.15 mm, very close to the x component measured by the direct pendulum (10.00 mm). Along the alignment of points 5 and 10, the differential settlements at the base of the bell-tower (0.95 mm), multiplied for the same ratio, is equal to 4.46 mm, which is again very close to the y component measured by the direct pendulum (4.00 mm).

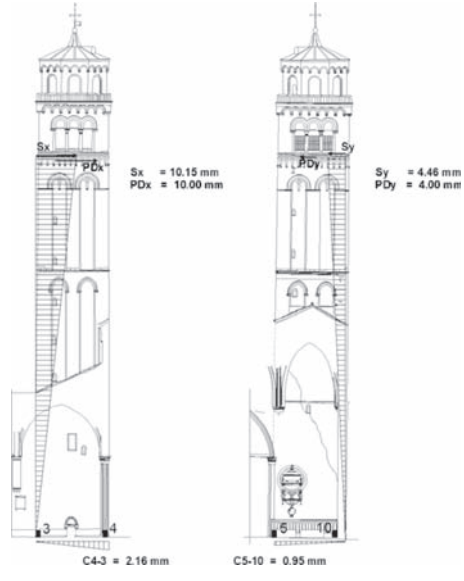

Figure 17. Comparison between the movements at the top of the Frari bell tower induced by the differential settlements of the foundations and those measured by the direct pendulum.

4.2 *Structure investigations and monitoring*

In order to follow with special care the deformation behaviour during the execution of the structural joint, new crack-gauges as well as new long-base extensometers were installed. Futhermore, in order to check the thrust modification between the bell tower and the basilica, special flat-jacks were installed in the positions indicated in Figure 18: on the right the stress values measured before the execution of the structural joint, while on the left the stress changes after the intervention are shown. It can be observed a significant decrease of the state

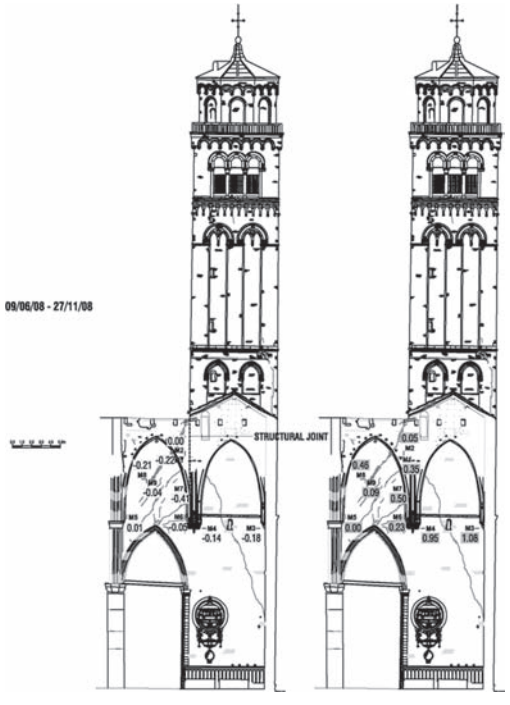

Figure 18. Measurements of the state of stress before the structural joint execution (on the right) and variation of the states of stress induced by the structural joint execution (on the left).

of stress in the upper part of the wall between the bell tower and the basilica, which is a clear experimental confirmation of the assumptions on the thrust reduction applied by the bell tower.

In particular, the positive effects of the structural joint can be summarised as follows:

1. a substantial reduction of the load acting on the column of the basilica, estimated as about 800 kN (–17%);
2. a corresponding increase at the base of the bell tower;
3. a restoration of the original conditions when the two structures were statically more independent.

An interesting indication of the bell tower response to such structural modification can come again from the measurements of the direct pendulum (Figure 15, second shadowed time interval). It can be observed a more evident effect along the y direction, i.e. consistently with the newly introduced lack of support.

It can be also helpful to analyse the movements of the masonry structures along the existing cracks together with the displacements provided by the direct pendulum and the settlements coming from precise levelling, especially when comparing the situation before (Figure 19) and after (Figure 20) the structural joint intervention. In the time interval—about two years—between the soil fracturing and the structural joint, the tower has settled less than one millimeter (see surveying records at the top left of Figure 19), with a modest inclination toward the external side.

After the end of the structural joint execution and the complete removal of the temporary steel cables and of the timber prop system, the deformation behaviour has been constantly observed. The displacement components of the bell tower, measured by the direct pendulum, are more substantial and in the opposite direction, toward the basilica. They appear to be now only partly related to the differential settlements of the foundation, the remaining part being due to deformation processes of the bell tower masonry. Despite such substantial modification of the load distribution, however, which has inevitably produced a new increase (up to 0.65 mm/year) of the differential settlement between the bell tower corner and the column (which has even showed a temporary upward

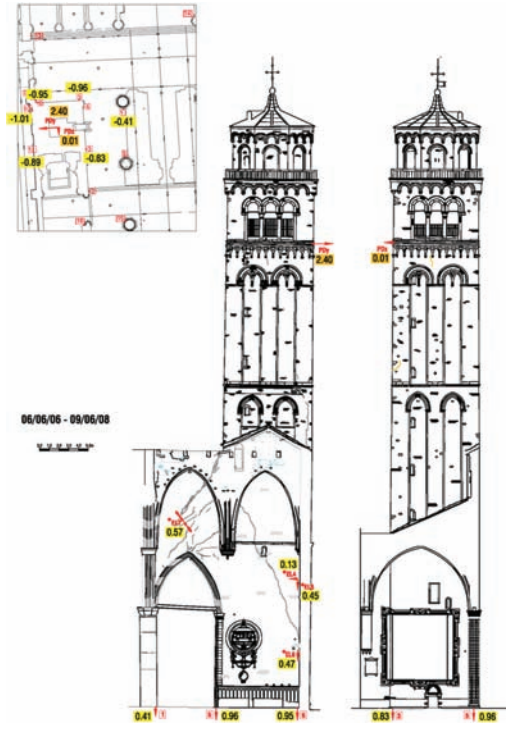

Figure 19. Analysis of the deformations measured during a period of two years, between the soil fracturing intervention and the structural joint execution.

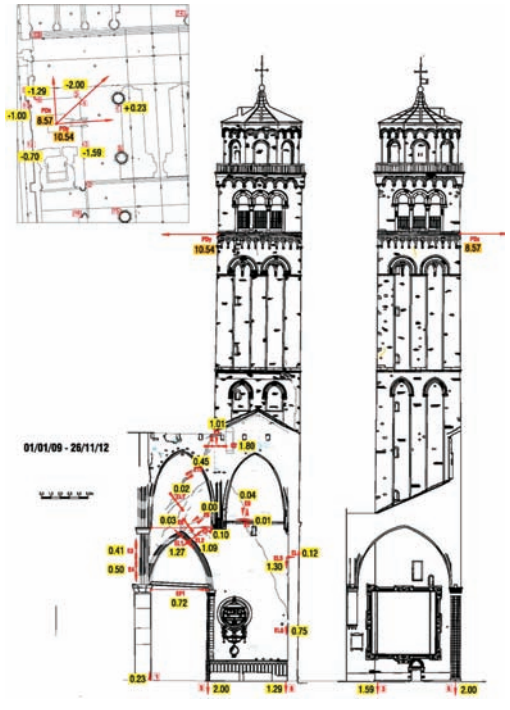

Figure 20. Analysis of the deformations measured during a period of three years, after the structural joint execution.

relative movement, benchmark 1 in Figure 16), the average—and still rather uniform—settlement of the bell tower in this period has proved to be less than 0.40 mm/year. When compared to the rate of about 1 mm/year before the soil fracturing intervention, it appears to confirm its overall effectiveness.

It is finally of extreme interest to compare the readings of two adjacent benchmarks located inside the bell tower, one at the foundation level (+1.00) and the second—installed more recently—anchored in the soil, at -6.00 just below the tip of timber piles: in the last 3 years, they provide a differential settlement of 0.95 mm which corresponds to about 90% of the overall foundation settlement. This new evidence would suggest that the progressive and already established (rather unexpected in these terms, though) decay of timber piles can count for most of residual movements of the bell tower.

Careful monitoring of settlement rates in the near future will enable to fully understand the ongoing mechanisms and predict possible trends. However, the current reduced static interaction can accommodate further movements of the bell tower without inducing excessive stresses on the structures of the adjacent basilica. The separation of the two structures has proved to be positive also in relation to seismic effects, if after recent shakes of May 2012 no specific consequence has been recorded in the isolated structure, while new cracks have appeared in the nearby St. Peter Chapel, still interested by structural links, which will have to be carefully removed.

5 CONCLUSIONS

The Frari bell tower has been affected since its construction by a slow but constant differential settlement between the tower itself and the adjacent masonry structures of the basilica. More recently a growing concern for the stability of the structures involved provided the impetus for the development of modern remedial measures, first in foundation and then on the elevation structure.

A ground modification intervention by soil fracturing was then carried out in order to improve the mechanical characteristics of the clayey layer underlying the tower. Once the aim of improving the stability of the soil-foundation system had been achieved, a new solution was required to reduce the damaging interaction between the masonry structures, activated by the foundation settlements. A structural joint between the bell tower and the basilica was finally executed in order to improve the system deformability.

As regards the intervention on the foundations, innovative criteria and methodologies have been used, so far devoted to rehabilitation and strengthening works on the upper structures. The material preservation of the foundation has been fully guaranteed, without any direct interventions on the relevant structures, by the insertion into the surrounding soil of injection pipes for soil fracturing. Through the articulated and extensive real-time monitoring system, purposely implemented, it has been possible to focus on the intervention areas, calibrating and minimizing the amount of injected grout. The technology used has proved to be especially flexible and it will enable further injection cycles in the future, if required.

In the design of the intervention, any possible action producing a stiffness increase of the elevated structures, thus altering the overall structural behaviour, has been carefully prevented; the monitoring carried out after the works has confirmed the good compatibility of the strengthening intervention on the bell tower with the mechanical characteristics of the adjacent basilica.

REFERENCES

Alfaro, M.C. & Wong, R.C.K. 2001. Laboratory studies on fracturing of low-permeability soils. *Canadian Geotech-nical Journal*, 38: 303–315.

Andersen, K.H., Rawlings, C.G., Lunne, T.A. & By, T.H. 1994. Estimation of hydraulics fracture pressure in clay. *Canadian Geotechnical Journal*, 31: 817–828.

Gottardi G., Cavallari L., & Marchi M. 2008. Soil fracturing of soft silty clays for the reinforcement of a bell tower foundation. In *2nd International Workshop on Geotechnics of Soft Soils—Focus On Ground Improvement, University of Strathclyde, Glasgow, Scotland, 3–5 September 2008.* London: Taylor & Francis Group.

Lionello, A., Cavaggioni, I., Marchi, G., Gottardi, G., Ragazzini, A., Modena, C., Casarin, F., Rossi, P.P. & Rossi, C. 2007. Monitoraggio e controllo del consolidamento della fondazione del campanile dei Frari a Venezia. In *Previsione e controllo del comportamento delle opere; XXIII Convegno Nazionale di Geotecnica, Abano Terme, 16–18 Maggio 2007.* Bologna: Patron Ed. (In italian).

Lionello, A., Cavaggioni, I., Rossi, P.P., Rossi, C., Modena, C., Casarin, F., Marchi, G., Gottardi, G. & Ragazzini A. 2004. strengthening intervention on the Frari basilica, Venice. In *Possibilities of numerical and experimental techniques, IV International Seminar on Structural Analysis of Historical Constructions (SAHC), Padova, 10–13 Novembre 2004.* Balkema.

Lionello, A. (ed.) 2008. *Il campanile di Santa Maria Gloriosa dei Frari in Venezia—conoscenza, consolidamento e restauro*. Milano: Electa (in Italian).

Lionello, A. (ed.) 2011.*Tecniche costruttive, dissesti e consolidamenti dei campanili di Venezia.* Venezia: Corbo e Fiore Eds. (in Italian).

Marchi, M., Gottardi, G., Lionello A. 2006. Sulle fondazioni dei campanili di Venezia. *Fondazioni Superficiali e Profonde, V Convegno Nazionale dei Ricercatori di Ingegneria Geotecnica, Bari, 15–16 Settembre 2006.* Benevento: Hevelius Ed. (in Italian).

Marchi M., Gottardi G., Ragazzini A. & Marchi G. 2012. On the sand response of fracture grouting on a bell tower foundation. *Int. Conf. on Ground Improvement and Ground Control (ICGI), 30 Oct. – 2 Nov. 2012, University of Wollongong, Australia*. ISBN: 978-981-07-1896-1.

Mori, A. & Tamura, M. 1987. Hydrofracturing pressure of co-hesive soils. *Soils and Foundations*, 27(1): 14–22.

Panah, A.K. & Yanagisawa, E. 1989. Laboratory studies on hydraulic fracturing criteria in soil. *Soils and foundations*, 29(4): 14–22.

Raabe, E.W. & Esters, K. 1990. Soil fracturing techniques for terminating settlements and restoring levels of buildings and structures. In M.P. Moseley (ed.), *Ground Improve-ment*: 175–192. Glasgow: Blackie A & P.

Rossi, P.P. & Rossi, C. 2012. Monitoring of two great venetian cathedrals: San Marco and Santa Maria Gloriosa dei Frari. *Proc. of the Int. workshop on Monitoring of Great Historical Structures. Florence, January 2012.*

Soga, K., Ng, M.Y.A., & Gafar K. 2005. Soil fractures in grouting. *Proc. of the 11th International Congress on Computer Methods and Advances in Geomechanics, Turin, Italy*, pp. 397–406.

Geotechnical Engineering for the Preservation of Monuments and Historic Sites – Bilotta, Flora, Lirer & Viggiani (eds)
© 2013 Taylor & Francis Group, London, ISBN 978-1-138-00055-1

Collapse of a backfilled wall at the Castle Wespenstein

I. Herle, J. Männer & E. Schwiteilo
Institut für Geotechnik, Technische Universität Dresden, Dresden, Germany

J. Wehr
Keller Holding, Germany

ABSTRACT: The Castle Wespenstein is located in Thuringia, Germany, and was built around 1250. Due to a fire in the 17th century, most of the roofs were damaged and a large area of the castle was abandoned. The rubble was deposited behind the walls which were not supposed to carry any earth pressure. In spite of that, the vast majority of the walls remained stable over the centuries. In one particular section, a sudden collapse of the backfilled wall took place in 2010. This contribution gives an overview of the wall and backfill mechanical properties. A geotechnical analysis of the wall and backfill system is performed and options for the rehabilitation are discussed.

1 INTRODUCTION

The town of Gräfenthal with the Castle Wespenstein is located in the south of Thuringia, Germany. The castle was founded around 1250 on a shale rock in order to protect the trade route Leipzig-Coburg-Nuremberg and to collect the toll. Since 1621, the castle was a residence of the Duke of Saxony-Altenburg including an office of the bailiff. In 1686 a big fire destroyed the castle roof and the upper floors. The collected rubble was deposited in the preserved lower two floors. Several years later (no specific data available), a part of the wall corresponding to the second floor collapsed, perhaps due to the vault pressure. In 1897, this collapsed part of the wall was repaired. On the top of the rubble corresponding to the second floor, a so-called bailiff's garden was created.

At the wall base, a vault reaching the rock cliff is situated. This vault was probably built as a part of the foundation to bridge a gap in the rock. In the right part of the wall, a cross vault room is located. A stone staircase from this room is buried by the rubble. In the left part of the wall, there is a breakthrough to the bailiff's garden.

The south-west wall of the castle, approximately 10 m high and 11 m long, served as a retaining wall for the rubble over more than a century. In November 2010 a partial collapse of the wall took place, see Figure 1. The upper edge of the slide is almost vertical, the inclination of the backfill (rubble) underneath is about 35° (maximum 50°).

In the bottom part, the wall thickness of 2.1 m can be recognized. The wall crest has the thickness of 0.75 m. One can expect a change in the wall

Figure 1. View of the collapsed south-east wall of the Castle Wespenstein.

Figure 2. Masonry composed of shale stones and lime mortar.

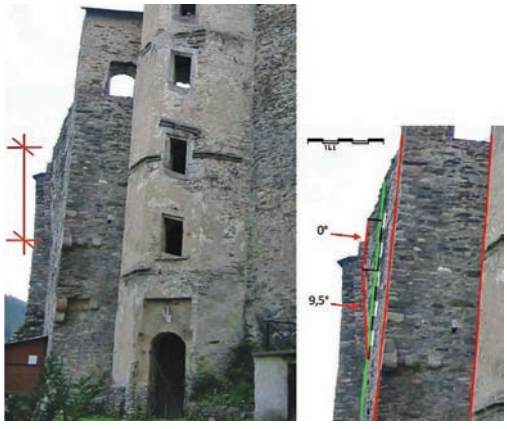

Figure 3. Estimation of the wall tilting prior to the collapse.

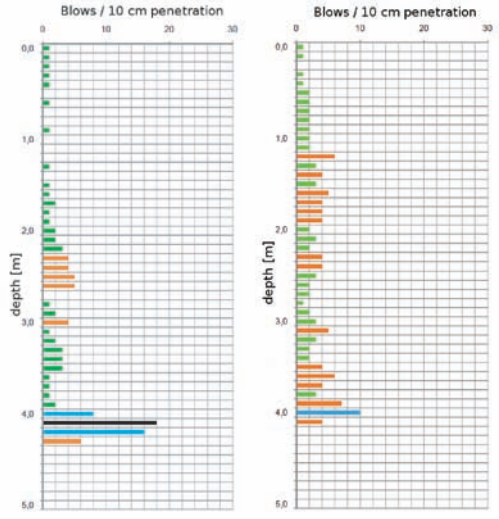

Figure 4. Heavy dynamic penetration at 0.5 m (left) and 3.0 m (right), respectively, behind the wall crest (Klehm, 2005).

thickness between the first and the second floor which arised during the repair works in 1897. The wall is composed of shale stones with a lime mortar (Figure 2). Old photographs reveal that the wall was in a bad condition already prior to the collapse. Cracks, bulging and spalling phenomena could be observed. A wall tilting of 9.5° in the upper part can be estimated from Figure 3.

2 FIELD AND LABORATORY INVESTIGATIONS

The characterization of the wall and backfill properties is based on field and laboratory tests.

In 2005, heavy dynamic penetration was done behind the wall from the surface of the bailiff's garden (Klehm, 2005). The penetration resistance increased with the distance from the wall crest, see Figure 4, suggesting a loose backfill zone close to the wall. After the failure, dynamic sounding with a light penetration device was performed. It reached the cross vault at the depth of approximately 4 m. No cavities could be found in all but one soundings.

The rubble backfill material corresponds roughly to the wall material and contains not only stones of different sizes but also pieces of mortar. The grain (rock) density was measured in the laboratory as 2.72 g/cm^3. The density of the mortar was determined by immersion. Furthermore, approximate values of the maximum and minimum densities of the rubble were measured as 1.53 g/cm^3 and 1.03 g/cm^3, respectively. Taking into account the penetration results, in situ density of 1.18 g/cm^3 can be assumed for the wet backfill.

Regarding the wall density, the volume fraction of 70% was estimated for the stones and of 25% for the mortar (with 5% of extra voids). This results in the dry unit weight of 22.1 kN/m^3 for the masonry.

The shear strength was investigated in shear box tests. The shear box device with the square cross section 30 × 30 cm was used. The specimens were prepared by hand reaching a higher density than the estimated one in situ. Normal stresses varied between 50 and 100 kPa. The shear strength calculation was based on the results of three specimens at different normal stresses. The scatter of the obtained results served as a basis for the parameter variation during the analyses.

2.1 *Wall stones aligned with shear direction*

The alignment of the large stones parallel with the shear direction (Figure 5) yields the lowest shear strength of the rubble material.

The friction angle of 43° was measured. A low value of cohesion (4 kPa) resulted probably from the linearization of the shear strength envelope. Neglecting the cohesion, a friction angle of 44.7° is representative for the relevant stress range. A test series for flooded specimens yielded slightly higher values of the shear strength. This result can be attributed to the densification of the material due to the flooding.

2.2 *Wall stones aligned perpendicular to shear direction*

The alignment of the large stones perpendicular to the shear direction (Figure 6) yields the highest

Figure 5. Shear box specimen with the large stones aligned with the shear direction.

Figure 6. Shear box specimen with the large stones aligned perpendicular to the shear direction.

shear strength of the rubble material. The friction angle of 70° and the cohesion of 60 kPa were measured. A pronounced breakage of the large stones could be observed after the dismantling of the shear box.

2.3 *Shear strength between two large stones*

Two large stones were selected and fixed in the shear box apparatus. The location of their contact surface corresponded to the location of the shear plane enforced by the apparatus. Friction angle of 42° was measured together with cohesion of 19 kPa. The latter value suggests that the strength envelope is strongly non-linear. Additionaly, the sliding resistance of two stones sliding over each other without an additional normal (Figure 7) load

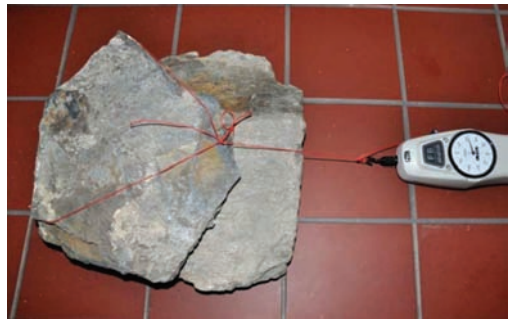

Figure 7. Determination of the friction angle between two stones.

was measured. The friction angle of 40° was calculated for this setup.

3 FAILURE ANALYSIS

The check of the bottom (thick) part of the wall reveals its sufficient stability for any possible design situation. Thus, the analysis of the wall failure is performed with respect to the contact pressure and overturning and sliding stability, respectively, for the up-per part of the wall. Although the failure was clearly three-dimensional, the analysis considers the plane strain condition which is on the conservative (safe) side. The earth pressure calculation is based on the standard DIN 4085.

The allowable pressure for the masonry follows from the standard DIN 1053-1. Taking into account the compression strength for the mortar of 1 N/mm^2 (based on the chemical analysis and the related strength database provided by Prof. H. Siedel from the TU Dresden) and for the shale of 50–100 MN/m^2, one obtains the allowable pressure for the masonry of $\sigma_0 = 0.7$ MN/m^2.

3.1 *Wall geometry I*

The first geometry corresponds to the idealized state after the wall repair in 1897, see Fig. 8. The unknown factors are the surface load and the water pressure which could evolve due to an insufficient drainage of the backfill.

Regarding the ultimate limit state, the wall is sufficiently stable without any surface and water load. The critical surface load would be 8.5 kPa which is too high for any realistic surcharge. The critical ground-water surface 2.5 m above the cross vault could produce overturning instability and a non-allowable contact pressure. However, the permeability of the back-fill is rather high, as it was observed in the shear box tests. Thus, such a high water level is also unrealistic. A surface load

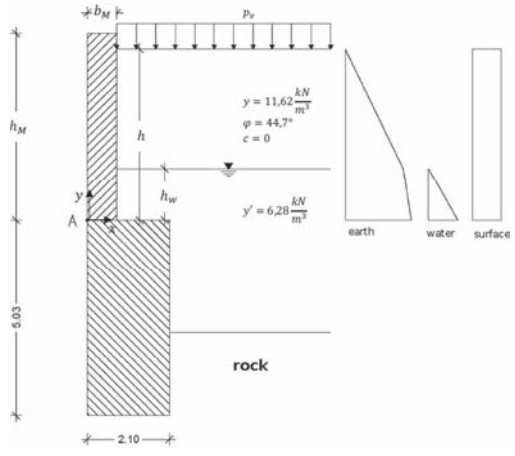

Figure 8. Geometry I.

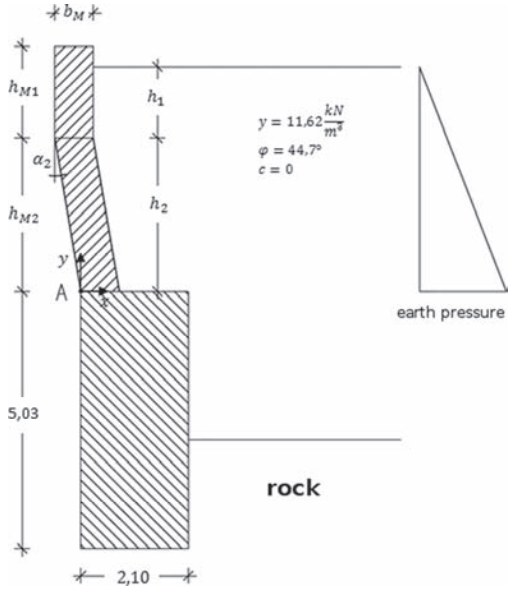

Figure 9. Geometry II.

of 5 kPa would require the water height of 2.25 m which is still too much. Consequently, the wall in the initial state was sufficiently stable.

Alternatively, it can be assumed that water could not penetrate downwards fast enough and thus a water table was created at the ground surface, with a saturated zone extending down to a certain depth (analogy of a surface crack filled with water). Taking into account a surface load of 5 kPa, a water depth of 1 m could destabilize the wall. One can still doubt if the water pressure of 10 kPa at the surface could arise along the wall. Nevertheless, even smaller water pressures could bring the wall close to the ultimate limit state. This would have been linked with excessive deformations, explaining the tilting and bulging of the upper wall part prior to the failure.

Moreover, a historical survey showed that there were two big trees behind the wall in the bailiff's garden in the past. They could certainly contribute to the saturation zone and, additionally, produce a root pressure on the wall. Thus, it can be assumed that the wall was repeatedly close to the ultimate limit state. This produced substantial deformations of the upper part of the wall and progressively worsened the situation.

3.2 *Wall geometry II*

The deformed shape of the wall, deduced from the old photographs, can be considered as a second possible geometry for the analysis, see Figure 9.

Considering $h_2 = 3$ m and $\alpha_2 = 9°$, the proofs for the overturning stability and the allowable pressure of the wall are not fulfilled. Theoretically, the stability could be increased either by a higher shear strength of the backfill or by 3-D effects or by the backfill cohesion producing a crack between the wall and the backfill. However, considering the geometry from Figure 9, the stability is not sufficient even for the wall without any backfill! Nevertheless, the situation is slightly more complex since the earth pressure in the bottom part of the inclined wall has a stabilization effect. The most optimistic combination of all mentioned factors yields a critical inclination of the wall of 5.5°.

Obviously, an exact determination of the wall geometry from the old photographs is not possible. The geometry effect on the stability is dominant and even small deviations can substantially change the stability. Even if the wall was initially stable, it was not far away from the ultimate limit state. This produced an accumulation of the wall deformations with time, reaching the critical value of the inclination at the moment of the failure.

3.3 *FEM analysis*

In order to check the pressure distribution in the masonry, a 2D finite element analysis with the software PLAXIS was performed.

The masonry was modelled with the linear-elastic perfectly-plastic model. Young's modulus and Poisson's ratio of the masonry were assumed as

$$E = 3000\ \sigma_0 = 2.1 \cdot 10^3 \text{ MPa} \quad \text{and} \quad \nu = 0.2$$

Young's modulus and Poisson's ratio of the backfill were assumed as

$$E = 1 \text{ MPa} \quad \text{and} \quad \nu = 0.25$$

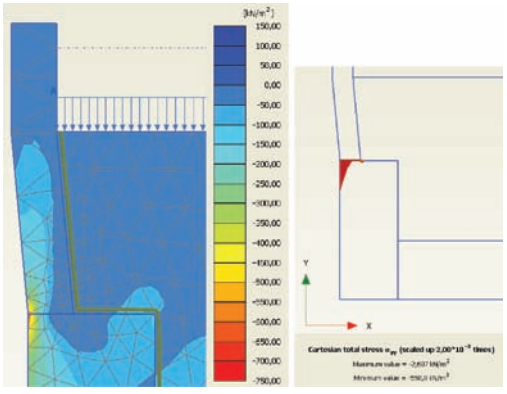

Figure 10. Example of the FEM calculation as a check of the maximum compressive stresses in the masonry.

The stiffness of the backfill was determined from the load-deformation behaviour in the large shear box prior to the shearing phase.

The reason for choosing the elastoplastic model for the masonry was to prevent tensile stresses in the material. In the compression range, the behaviour should remain elastic. Thus, a very high (fictitious) friction angle of 85° was selected for the masonry, which guaranteed elastic behaviour in the compression range.

In Figure 10, the geometry setup with a reduced backfill height due to a crack between the wall and the rubble is shown. The inclination of the upper part of the wall amount 5.4°. For this case, the maximum pressure in the masonry is slightly below the maximum allowable pressure. This inclination coincides well with the limit tilting obtained from the classical analysis described in Section 3.2.

4 WALL REHABILITATION

One can imagine three different options for the wall repair:

1. The upper part of the wall will not be repaired and a permanent slope will be created (Figure 11).
2. The upper part of the wall will not be repaired and a permanent slope will be created. Additionally, a roof above the slope will be constructed (Figure 12) in order to keep the bailiff's garden in operation.
3. The upper part of the wall will be newly built to preserve the original form of the castle (Figure 13).

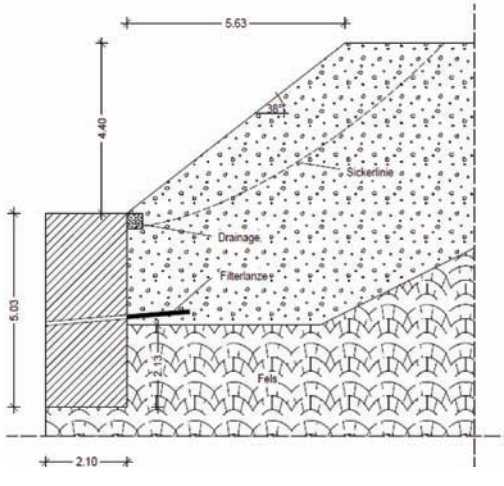

Figure 11. Repair option I.

The selection of an appropriate version depends mainly on the available budget and the philosophy on the monument preservation.

5 CONCLUSIONS

A sudden collapse of historical backfilled walls can happen after many years of their service. In the presented case, the wall at the Castle Wespenstein

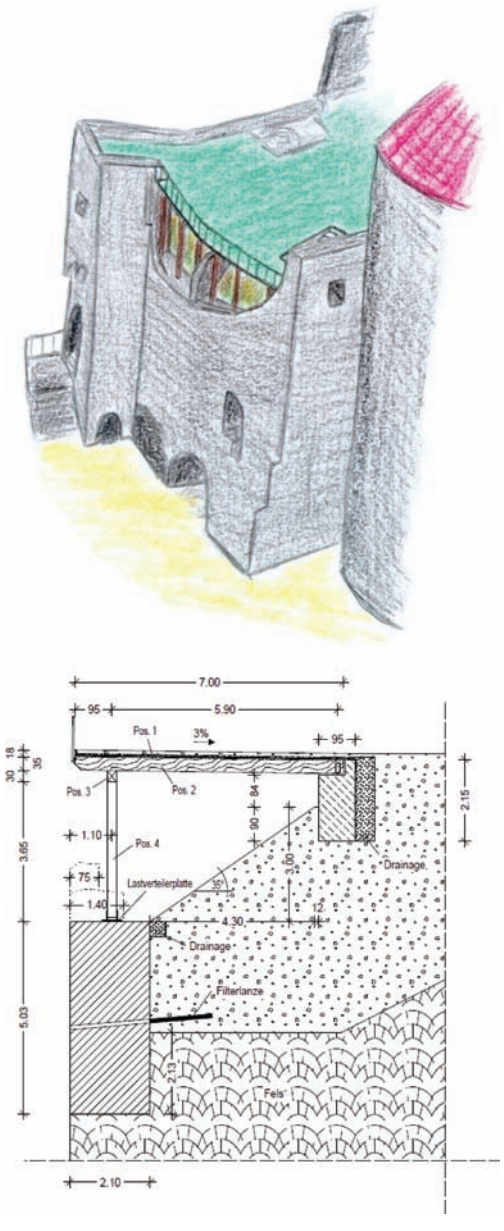

Figure 12. Repair option II.

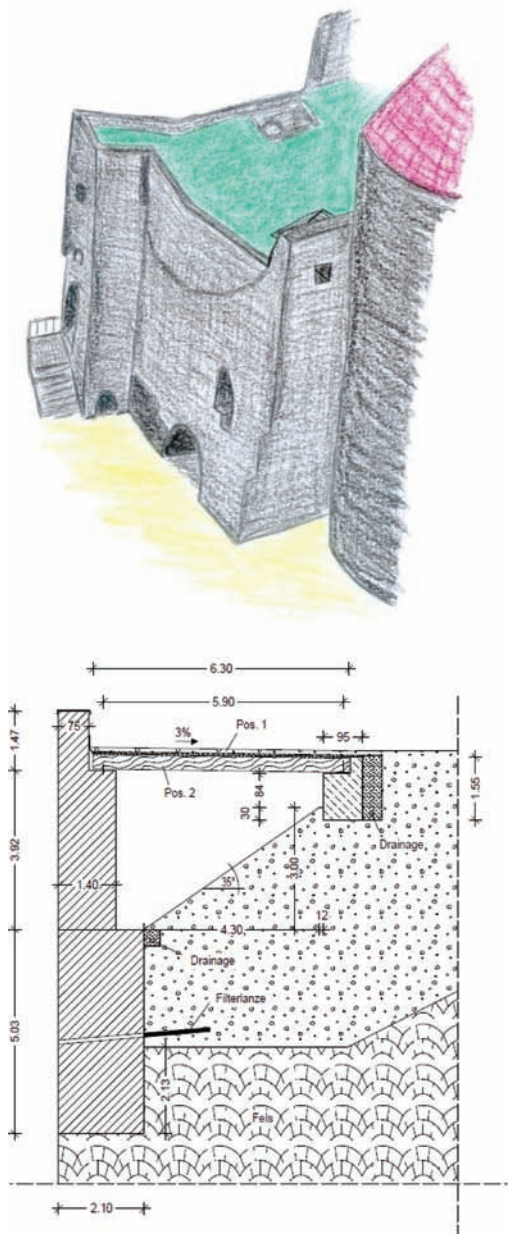

Figure 13. Repair option III.

was close to the limit equilibrium for a longer time and progressively approached the failure. Gradual changes in the wall geometry as well as an additional small water pressure could be identified as the responsible trigger mechanisms.

There are different alternatives for the wall rehabilitation. The final decision depends on the available funding and the philosophy of the cultural preservation.

REFERENCES

Klehm, T. (2005). Bautechnische Sanierung historischer Stützmauer im Schloss Wespenstein. Diploma thesis, Fach- hochschule Erfurt.

Männer, J. (2012). Untersuchungen zum Versagen einer Stützwand. Diploma thesis, Technische Universität Dresden.

Geotechnical Engineering for the Preservation of Monuments and Historic Sites – Bilotta, Flora, Lirer & Viggiani (eds)
© 2013 Taylor & Francis Group, London, ISBN 978-1-138-00055-1

Geotechnical problems on historical buildings from Transylvania

N.M. Ilieş & A. Popa
Faculty of Civil Engineering, Technical University of Cluj-Napoca, Romania

ABSTRACT: The paper will present the analysis of the degradations that occurred on an important historical load-bearing structures from Transylvania, together with the causes of their appearance on construction and with the proposed solutions. There will be presented also the requested investigations for the soil, the analysis of the causes which leaded to the appearance of the degradation. The proposed solution for the rehabilitation is analyzed, based on methods for strengthening the foundations and solutions to improve the soil and the foundation's body.

1 INTRODUCTION

Starting from the particular aspects that an historical monument presents, the intervention works have to be compatible to the monument's importance, its cultural value, but also with the type, the degradation and degradation causes. The main element vulnerable to the external factors is the foundation system. Its quality is influenced by the building material's quality, but also by the manner in which external factors influence the behavior of the fourth structural element: the foundation ground. This is the reason why any significant analysis of degradations on historical buildings, first, has to take into account two subsystems: the foundation ground and the foundation system, and, secondly, the compound effect between those two subsystems and the superstructure.

Foundations degradation is considered to be the generator of general degradation in historical structures; an analysis of the causes leading to the foundation damage is absolutely necessary in order to approve the most efficient solution for foundation/foundation ground consolidation works.

Very important for the behaviour of the foundation ground is the water or the ground water table. This is one of the factors causing a great number of degradations.

This paper presents the analysis of degradations, occurred on an historical structure, the causes and the proposed methods to solve them. It also presents the necessary investigations of the supporting soil and its degradation causes. The conservation and the consolidation methods of foundations are analyzed, as well as the improvement solution, employed for the ground and foundation elements.

Sic Reformed Church is a monument of national value, included on the national list of historical monuments with the number CJ-II-mA-07759, originally dating from the XIIIth century, suffering a large number of changes over time, encompassing Gothic elements, murals, original banks, historical organ. Foundations degradation cannot be clearly separated from the overall behavior of structural walls. The cause of degradation is closely linked to the behavior of the foundation and the foundation soil. One major inconsistency revealed to all foundations is their placing in the seasonal variations of moisture area, for foundations supported by active clays. It can also highlight the lack of compliance of the foundation system directly to land sliding. The two conditions give rise in time to structural damage. The paper will present the solution proposed for consolidation.

2 SIC CHURCH CONSOLIDATION

2.1 *General presentation of the church*

The construction period of the Sic Reformed Church is unknown, but certainly it dates from the second half of the thirteenth century, based on the stylistic architectural elements. At the entrance, on the east wall, it is inscribed the date of 1241. Over time, the church has undergone several interventions. During 1435–1517, it was partially rebuilt in late Gothic style, with gothic elements. Murals are dated in the second half of the fourteenth century, respectively sixteenth century. Most remarkable are the interventions of the years 1740–1780, which completely changed the image of exterior and interior of the church: the church and tower were re-coated, the western gable was built, banks and ceilings were made by Lőrinc Umling.

The pulpit is made in 1793 by Adam Horvath of Chidea. Another major intervention is the one from 1946–1947, led by architect Karoly Kos, when a nave was built on the north side of the church. It also changed the church and tower roof shape, the church regaining his basilica character.

Nowadays, the building is a basilica church type, with extended choir apse, which is closing three sides of the octagon, with buttresses outside. An asymmetric western tower was built on the south side of the church, even beyond the southern façade plan (the tower was built during interventions in the second half of the twentieth century). In the years 1946–47, on the right triumphal arch side, on the north side, a transept, two spans wide, was built. The pillars between these two spans were demolished (pulpit was moved to the opposite side) and like this the opening was increased and closed with a brick arch, erected just across the triumphal arch key. The main galleries of the nave and transept, are supported by a timber structure and have painted planks parapets. From Umling Lőrinc's works, remained only the banks, the ceiling was replaced with plywood boxes, painted with oil paint. The church sits on a hill and it is surrounded by a low enclosure wall, Figure 1.

2.2 *Foundation soil investigation, structural technical state and consolidation solutions*

2.2.1 *Soil geotechnical investigations*

The site belongs to the structural unit of the Transylvanian Depression and it is located in the southern area of contact between Somes Plateau and Somes Plain. The landscape looks like a hilly plateau.

The platform, on which the church stands up, is conducted as a mixed structure (cut and fill) having a slope of approx. 30% on the southern, southeastern and eastern side. On the southern side, approximately at the middle of the slope, a terrace was erected, having 10 to 15 m width. Total height of slope (up to the village market) is 15–20 m, with a variable height on the North-West side. On the North and North-West side, the location is limited by a road that descends from the church platform up to the village market.

Figure 1. Calvin reformed church of Sic, Jud. Cluj.

Investigated area is characterized in terms of subbasement lithology by deposits of clayey marl, sandstone, salt, tuffs etc. The superior layers consist of a succession of clay, yellowish with altered tuff horizons.

Based on nine geotechnical drillings, the following sequence of layers was established:

- Clayey filling material and building demolishment materials,
- Marly gray clay, with brown clay nests,
- Greenish gray tuff, altered,
- Hard clay, brown,
- Altered tuff, greenish, gray (sandy gravel),
- Clay, brown, with sandstone fragments with silica,
- Greenish gray tuff, altered,
- Clay, gray—yellow, hard.

Considering the drillings performed on site, the following appreciations can be made:

- Throughout the site there is a cross stratification with a succession of layers of clay gray—brown—yellow, separated by layers of altered tuff, gray—green,
- Separating layers of tuff have the thickness of 0.30 to 0.40 m and they are found on 1 to 2 levels at: 0.50–1.00 m, 1.50 to 3.00 m, 3.30–4.15 m and 4.60 to 4.70 m. They occur only in the Western part of the site (the choir area) and they have a slope similar with the natural terrain,
- Tuff fragments were identified in the packages of gray clay, brown clay and yellow clay, in all drilling performed,
- It was found a nonhomogeneous filling package (including construction materials) of a thickness up to 1.20 m.

Based on heavy dynamic penetration test (HDPT) realized on the site, some conclusions were established:

- Filling materials packages are very loose,
- Package of gray clay (1.60 to 2.10 m) is loose (e = 1.0 to 1.1) and contractile, within the group of less active clays, also within the compressible soils,
- Sandy gravel layer is a loose layer (e = 0.92),
- After the depth of 2.10 m it was found a package of tuff, hard,
- At depths of ~4.00, 4.20 and 6.50 m appeared possible sliding surfaces,
- There is the possibility of the presence of slip surfaces in altered tuff package, at 1.50 m, 2.70 m, 6.10 m deep,
- All packages of striped clay (gray, yellow, and brown) are contractile soils, the category of active/less active soils. The most active clays

appear in the western side of the site. Packages of clays appear in some drillings having a loose state and medium density.

When the investigations were performed, the groundwater table was not intercepted, on the corresponding drilling depth.

Moderate continental climate zone requires, according to Romanian norms, lowering the foundation bottom below the maximum freezing depth. For this studied site the freezing depth is 0.80 to 0.90 m

2.2.2 *Structure of the church and previous interventions*

The main structure of the walls is made from stone masonry and lime mortar. In some areas, further parts of the church have brick masonry (the Northern portico, the Southern portico, the transept); the tower is also made from bricks masonry, rebuilt during repairs.

In the central apse choir, the walls were reinforced with four buttresses (b = 70 cm). The walls have different thicknesses and this varies in different parts of the church. In the tower, the wall thickness is 1.22 to 1.25 m and the wall thickness reduces with the height of the tower. At porticoes, the wall thickness is 35–50 cm, in the nave is 65 cm and in the sacristy the wall thickness is 51 to 72 cm, Figure 2.

Floors have a variety of compliance. The tower's floor is made out of timber and the floors of the two balconies of the church (West and North) have also timber structure. Over the central nave, there is a plywood ceiling, suspended by strings from the structure of the roof. The lateral naves are also covered with timber slabs.

The timber roof support is made of softwood (fir or spruce). The lateral naves and the vestry roofs are covered in one slope. The main nave, the transept and the choir have timber beams, bounded by ropes, which represents the ceiling beams. The roof is galvanized.

The presence of a significant degradation required the execution of a support with timber framework. In 2004, a wooded framework was raised, in order to strengthen the brick arch, in the axis D between 5 and 7.

To strengthen structural walls, following demolition of masonry walls from axis D between axis 5 and 7, a reinforced concrete belt over the apse and choir was constructed, continuing on the rest of the nave. During the interventions from the years 1946–47, the apse vault was reinforced by concrete covering, about 1–6 cm thick.

The foundations are made of stone masonry. The foundation thickness is the same as the walls of the building –0.80 up to 1.00 m. The foundation depth, determined on the basis of excavations, was 1.27 to 1.60 m. When the excavations were carried out, the presence of some consolidation works was revealed.

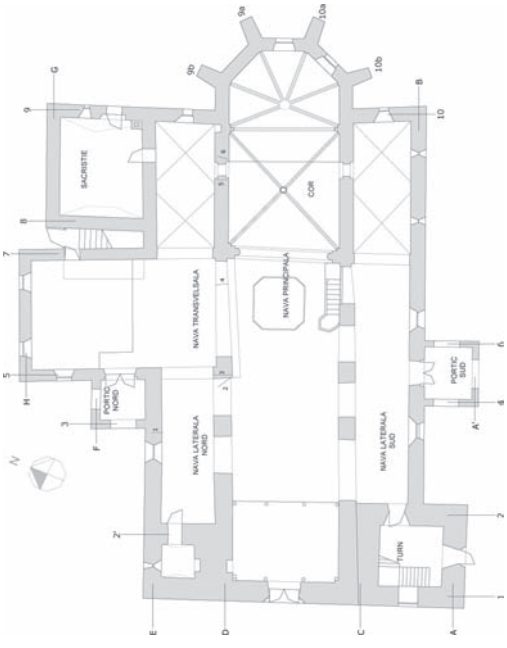

Figure 2. The church plan.

One intervention exposed the consolidation of the foundations for the buttress in the side of the axis 10b and 10 (south side nave). The employed concrete covering layer has a width of 50 cm and reaches the foundation bottom (1.37 m). This concrete covering was probably placed in order to strengthen the Western wall (axis 10) of South side nave.

A second intervention seems to be the initial foundation consolidation, on the North-Western side (axis 10), set as a doubling of the original foundation, by stone masonry.

A third intervention observed was done on the Eastern side of the main nave (entrance). It was executed as a simple concrete foundation, covering on the axis 1 foundation, with the width of 0.60 m and a depth of 0.40 m.

The technical condition of the church can be appreciated as 'bad', having degradations of structural elements.

2.2.3 *Foundations and structure degradations*

The degradation of foundations can't be shown separately from the behavior of the whole superstructure, structural walls. The cause of the degradation of the walls is closely linked to the behavior of the foundation and the foundation soil. It can be highlighted major non-conformities of all foundations, namely placing foundations in the seasonal variations of moisture (<2.00 m), bearing in the contractile soil (active) and without any constructive requirements.

Even if the ground water table was not intercepted in the drillings performed, it is evidenced a state of over moistening at all exterior walls of the building, Figure 3.

Major structural degradation can be mentioned: the emergence of major vertical cracks in the Eastern wall of the choir, vertical cracks in walls with windows, Figure 4, corner cracks between the walls and ceiling, vertical cracks in the door lintels, transverse cracks in stone masonry arches, inclined cracks in the door vault of the north side nave etc.

All vertical cracks appear in the chorus—sacristy—transept (East and West). They appear as fragmentation cracks of stone masonry walls; even the area, reinforced with buttresses, suffered fragmentation by vertical cracks.

Correlating the degradation with the subsoil stratification, it can be concluded that the degradation occurred as a result of a phenomenon of sliding of the clayey layer (contraction), on the altered tuffs package arranged, on several levels. The most active seems to be the upper level, which has led to the emergence of plastic sliding flow (specific also to active clays). This phenomenon is evidenced also by the decompression of an electricity column anchor, in the N-E area of the site, Figure 5.

Between the main nave and lateral naves, tower and Northern lateral nave, vertical cracks appeared due to several factors: the various stages of completion

Figure 3. Over moistening walls state-exterior, interior.

Figure 4. Buttresses and walls cracks, outside and inside view.

Figure 5. Electricity column tie rod decompressed.

of the different church parts, the lack of structural links between the walls, the different soil compressibility characteristics, specific to the moment when the construction started, the transmission of different loads values to the foundation ground etc.

On axis 1, of the Northern nave, the walls have suffered, in time, a settlement towards the corner E1, coupled with an inclination of the wall outward. In the E5 wall area, some cracks appeared as well (vertical and inclined), leading to the conclusion of a probable subsidence of the E5 axis wall, affecting the vault, the walls and vault of axis D, Figure 6.

There is a state of serious deterioration of the Northern portico, Figure 7, added in time, with a weak structural conformation, which suffered multiple subsidences. Multiple vertical cracks (with dislocation of masonry) are observed in the vault of the Northern portico. These are very dangerous because they can lead to the collapse of the opening.

On the exterior portico walls, a high concentration of loads in the corner can be seen, this led to the settlement and appearance of degradation of each side and in the vault.

Settlement of the B axis walls towards 2B corner appeared due to the high load sent by the tower (further construction). This supplementary construction led to further settlement of all foundations of the adjacent walls.

2.2.4 *Solutions to strengthen the foundation and structural elements*

Based on the severity and frequency of the existing degradation on the construction, the following interventions are proposed for execution:

In order to strengthen the choir—sacristy—apse area, against the phenomenon of sliding, on N-E and S-E direction, and to transmit loads to the bearing layer, a system of micro piles, tied at the top with a concrete belt was proposed.

This system will strengthen the apse wall, representing also a building and foundations consolidation, Figure 8.

Figure 6. Cracks between the Northern lateral nave and the main nave.

Figure 7. Degradation of the Northern portico.

By the consolidation concept of a micro piles row, the building is anchored in bearing foundation layer. The connection in the choir area is realized through a belt disposed below ground level, around the micro piles, which are embedded in the soil, at a minimum depth of 6.00 m and disposed around the buttresses.

For the walls of the axis 1, it is proposed to strengthen the foundation as in Figure 9.

For porticoes, the foundations will be checked during execution and the necessary embedding will be ensured. In the case of technical and financial disadvantage, poor foundations will be demolished and it will be rebuilt, ensuring interlacing with the foundations of the lateral naves walls.

This solution is indicated for the Northern portico, for a foundation depth of 1.10 m, which will connect the new foundation with the neighboring foundations, in order that differences between near levels to not exceed 50 cm. For the Southern portico, if demolition and rebuilding is not considered necessary, it is required to check and ensure the necessary foundation depth.

The cracks strengthening, along apses walls, sacristy and nave sides, (axis 9 to 10—buttresses) can be made with steel bars, placed in horizontal joints. Their placement into walls is realized by two-component adhesive based on cement, injected,

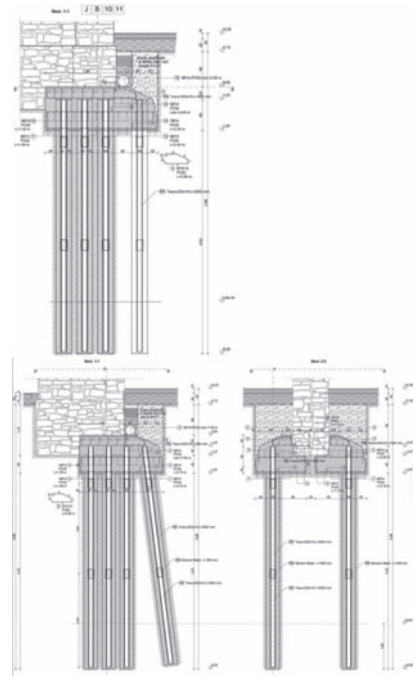

Figure 8. Intervention proposal in the choir—sacristy—apse area (SC IROD SRL, 2009).

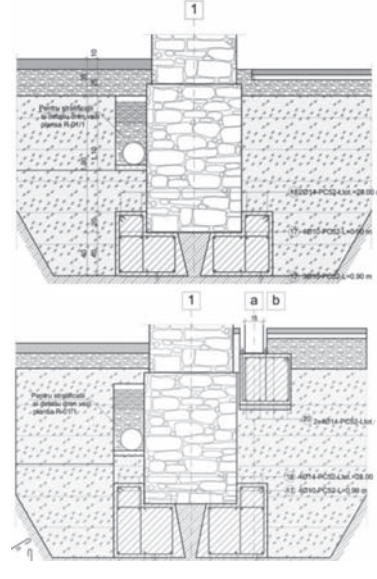

Figure 9. Foundation strengthening by concrete covering (SC IROD SRL, 2009).

thixotropic and without contractions. The solution is suitable for all the degradations of the walls: to strengthen weakened lintels, for the vertical cracks, to strengthen weakened brick vault.

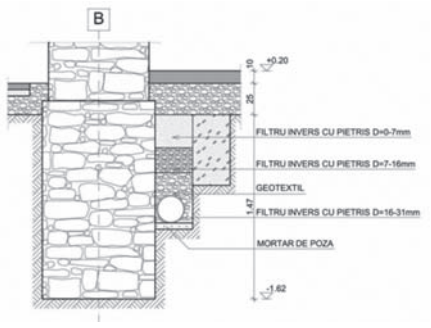

Figure 10. Foundation ventilation system (SC IROD SRL, 2009).

In the Northern portico area, emergency demolition of the vault and lintel and rebuilding may be required. Consolidation is no longer possible because of the serious degradation that occurred.

In order to eliminate the dampness phenomenon, which occurs in all exterior walls, considering the importance of building, one corresponding drainage systems is used. The system utilized consists in a ventilated space inside of a screen made of: primer with granules of 2–3 mm, waterproofing mortar, porous, having 2 cm thickness and finishing – 2 mm. For all interventions is to be used only breathe through primer paint, Figure 10. Breathable plaster execution will be on a height that exceeds the over moistening area with approximately 50 cm. The system will run on both sides, plastered, without expanding on the manual plastered protected areas.

It is also necessary to achieve a ventilation drain (ditch) around the building, Figure 10, in order to ensure the ventilation of the foundations, even if it is necessary to remove all architectural, non-breathable, details. It will remove non breathable sidewalks, it will repair/replace rainwater drainage systems, drains, and it will introduce breathable layers under the church floor.

In order to remove water from the site, the execution or repair works on the dewatering and disposal system of rain water should be compulsory. It is not acceptable to eliminate the water on the slope, but through channels, at a large distance from the slopes.

All these interventions were a part of the technical project, accepted to consolidate the church and the site. There were also proposed monitoring systems for the walls and site (inclinometers), but unfortunately the repair works are still in standby.

3 CONCLUSIONS

Because of the historic conditions, the buildings were placed on locations where the supporting soil had hidden vices. These vices led, in time, to the modification of the physical–mechanical characteristics of the foundation supporting soil layers. Some works performed on the site affected the supporting soil.

These factors indicate the appearance of degradations in the structural elements of the historic buildings, including the foundations and foundation soil.

The intervention over the foundation structures demands, first of all, detailed analyses of the supporting soil and its evolution in time, as well as the analysis of the geotechnical characteristics.

Construction degradation is a slow process of structural and operational performance changes. Analysis of a historical building involves several aspects: overall composition of the building, the nature of the foundation soil, the overall stability of the site, the transmission of dead loads and horizontal loads to the foundation soil, the quality of the materials, the construction techniques, the maintenance level, the effect of interventions over time etc.

Works involving the structure will be compatible with historic buildings: the importance of building the cultural value, the type and the extent of damage and the damage causes etc.

In all cases, it will adopt solutions that will ensure the maintenance and preservation of physical integrity, with minimal alterations, following historic buildings specific criteria: effectiveness, compatibility, durability, reversibility.

Works to be performed at the Church of Sic have the purpose of bringing the construction to a state of normal service, safely. Bringing it in a state of normal service, fits a current trend to revitalize historic buildings and saving them from a progressive degradation.

REFERENCES

Ilies, N.M. 2009. *Causes of degradation in historical buildings and solutions for consolidation,* PhD Thesis, Cluj-Napoca: Technical University of Cluj-Napoca.

Popa, A. & Ilies, N.M. 2008. *Technical expertise regarding the bearing structure of the reformed Church CJ-II-m-A-07759 and the enclosure wall, Sic, department of Cluj*, Cluj-Napoca.

Popa, A. & Ilies, N.M. 2009. *Foundations consolidations*, Cluj-Napoca: UT Press.

S.C. IROD M. S.R.L. 2009. *Technical project and execution details—Vol. II. Load bearing structure. Structural and architectural rehabilitation of the Reformed Church CJ-II-m-A-07759 and the enclosure wall, Sic, department of Cluj*, Cluj Napoca.

SR EN 1997–1. 2006. Eurocode 7: Geotechnical design—Part 1: General rules.

SR EN 1997–1/NB. 2007. Eurocode 7: Geotechnical design—Part 1: General rules. National Annex.

Stanciu, A. & Lungu, I. 2006. *Foundations.* Bucharest: Editura Tehnica.

Geotechnical Engineering for the Preservation of Monuments and Historic Sites – Bilotta, Flora, Lirer & Viggiani (eds)
© 2013 Taylor & Francis Group, London, ISBN 978-1-138-00055-1

Research and advanced technology in the restoration of the monuments of the Athenian Acropolis

M. Ioannidou
Civil Engineer, Director Emerita of the Acropolis Restoration Service, Athens, Greece

ABSTRACT: The use of temporary technology for the restoration of the monuments along with traditional techniques and methods, is included among the principles of the Chapter of Venice, of the first internationally accepted theoretical framework of principles for interventions on the monuments. In recent years, new perceptions stemming from globalization require the use of modern technology for the protection of the monuments. Advanced technology is utilized more and more during the research and performance phase of the program of protection. The primary concern is to repair their structure and form and to display the historical and artist values they embody.

1 INTRODUCTION

Advanced technology in study, research, and in the execution of the works, has been a basic characteristic of the interventions on the Acropolis monuments. This was so from the very beginning in 1975 and the founding of ESMA the Committee for the Conservation of the Acropolis Monuments. Particularly after 2000 and the establishment of the Acropolis Restoration Service (YSMA), by the Ministry of Culture and Tourism, advanced technology supported the development and acceleration of the extensive restoration program and led to innovative scholarly and technical methods and to technological applications. (Fig. 1)

Interventions on the monuments that began in 1975 were considered at that time inevitable; serious structural damage was caused mainly by the

Figure 1. The Acropolis from the west during the restoration works of 2001–2010.

choices of the older restoration, while problems of surface erosion stemmed from the atmospheric pollution. During the course of the works the original character of the interventions, at first purely rescue, was de facto expanded; the identification of the marble architectural members that lay scattered on the rock, their resetting in the monuments from which they come and the correction of the faulty placing of marble members in the previous interventions led to a broader *anastelosis*, extended to a greater part of the monuments, thus increasing their comprehensibility and their educational value. This theoretical framework was the basis for the methodology that was followed in the restoration work (Bouras 1994, Ioannidou and Lebidaki 2011).

2 METHODOLOGY OF THE INTERVENTION

During the course of the intervention, the marble blocks of the monuments, previously restored, had to be dismantled (Fig. 2). The dismantling was extended to sections that had not been restored in the past but showed signs of deterioration. The rusted joining elements of the previous restoration were removed and the filling material (cement mortar in the restored areas or, rarely lead) was taken out.

White cement and titanium reinforcements are used for the structural restoration of the architectural members; threaded titanium rods are inserted into holes in the marble mass and secured by an inorganic mortar made of white cement (Fig. 3). Titanium is selected for joining fragments of architectural members (Zambas et al., 1986). It is a relatively light metal, of satisfactory strength and with features (the coefficient of thermal expansion and the modulus of elasticity) that allow it to work well with marble. The main characteristic for which it was chosen for connecting the fragments, however, is its excellent resistance to all forms of corrosion.

Figure 2. Dismantling the column capital of the Propylaea west hall.

Fragments that do not belong together, that is to say, that do not come from the same architectural member, were never joined together.

Where necessary, the missing parts of members were added in new marble so that they have regained their original form and structural independence (Fig. 4).

The fillings in new marble are usually limited and the criterion for the decision is always the stability of the member and the monument, and the structural and aesthetic self-autonomy of the areas being restored. The aim is not to rebuild the monument, but to preserve the character of the ruin and whatever bears witness to its course through history. The additions to the blocks are of Pentelic marble, from the Dionysos quarries. The joining surface of the additions are cut with the use of a traditional device for copying named *pontadoros* or with an electric pantograph. Both methods ensure that the additions agree precisely with the broken surface of the ancient block being filled in.

Figure 3. Mending joining fragments of an architrave block of the north side of the Parthenon with titanium rods.

Figure 4. Fitting a new marble filling to a column capital of the north colonnade of the Parthenon.

Figure 5. Parthenon; resetting of an architrave of the north colonnade.

Figure 6. Resetting of the titanium clamps in the ancient cuttings.

Then, the eroded surface of the monuments undergoes conservation, a work comprising the consolidation of disintegrating surfaces, the filling of cracks with injected mortar and the removal of soot deposit and black crust.

When the architectural members have been repaired, they are set again in their original positions which are found after research. In exceptional cases where this is not possible, the architectural members are set in the positions they held in the previous restoration (Fig. 5).

They are connected with titanium elements (clamps and dowels) which are secured in the ancient cuttings and sockets with inorganic mortar according to the ancient system of joining (Fig. 6).

During the resetting of members, geometrical deformations of the area that was dismantled are partially corrected to the extent allowed by the remaining distortions of the members that were not dismantled, in order to achieve as much as possible the original form.

Finally, in order to avoid irreversible damage, the architectural sculptures were moved to the Acropolis Museum. They are replaced on the monuments by accurate copies in artificial stone, finished especially for tone and texture.

3 COMPLETED AND IN PROGRESS RESTORATION WORKS

A big restoration project started in 2001, funded by the Hellenic State and the European Community, with restoration works to the Parthenon, the masterpiece of ancient Greek architecture, the little Ionic temple of Athena Nike and the Propylaia, the monumental entrance to the sanctuary on the Rock (Fig. 7).

This project comprising also the recording and inventorying of the thousands of ancients stones scattered on the Acropolis plateau as well as the monitoring and consolidating of the circuit walls around the Acropolis slopes, was brought to

completion in 2010. The restoration of the Erechtheion, the elegant ionic temple, was completed in 1987 (Fig. 8).

During the last decade—from 2001 to 2010 – more than 1094 blocks of the monuments with a weight of 2.675 tons have been dismantled, mended and restored, 686 blocks were joined from fragments, 905 fillings were made from new marble while 158 blocks were carved from new marble. For this enormous project almost 530 cubic meters of new marble were used.

A new restoration program, funded by the Hel-lenic State and the European Community, started in 2011. This project comprises restoration works to areas of the Acropolis monuments which appear structural problems or can be restored with architectural members that lay scattered on the Acropolis rock, and their original position is recognised after research, such as the intervention on the restored corners of the west side of the Parthenon (Fig. 9), and the restoration of the south wing of the Propylaia (Ioannidou 2011).

Figure 7. Parthenon *opisthonaos*; view of west frieze. The original blocks of the west frieze are replaced by copies of artificial stone.

Figure 8. Erechtheum; the east prostasis after restoration (1979–1987).

Figure 9. The restoration of the west side of the Parthenon began in 2011.

4 CONTRIBUTION OF RESEARCH TO THE RESTORATION

During the restoration works, thanks to research, much new information has come to light about the archaeology, history and architecture of the Acropolis monuments, while in these fields the monuments are—and will continue to be—the focus of study by leading scholars. The new information has not simply increased our knowledge and added to the relevant bibliography; it has contributed to the compiling of studies that are basic to the interventions being carried out. Yet, theoretical, scholarly and technical problems have been encountered during the application of these studies (Ioannidou, 2012). To resolve those problems, research has been carried out by the scholarly personnel of the works, either alone or in collaboration with a large range of scholarly foundations in Greece and abroad, such as the National Technical University of Athens, the Aristotle University of Thessaloniki, the University of Crete, the University of Patras, the Foundation for Research and Technology—Hellas (FORTH), the National Observatory of Athens, the Nuclear and Research Center "Democritos", the British Museum, l' Université X de Paris, the Mie University of Tokyo, and the ETH Universität and others (Ioannidou et al., 2010).

Within the framework of the academic and scholarly research undertaken in the recent years, the most important could be resumed as follows:

4.1 *Joining ancients fragments*

A field of investigation is the joining of ancient fragments dismantled from the monuments or

Figure 10. Ceilings of the west hall and the east stoa of the Propylaea after restoraton.

Figure 11. Parthenon, north side after restoration.

scattered on the Rock and the forming of architectural members from fragments belonging together. This work, together with recognition of the original position of the created members, allows greater areas of the monuments to be restored.

A representative example is the restoration of the ceilings of the Propylaia with coffered slabs and beams, over a surface that is almost double than that of the previous restoration. (Fig. 10).

The intervention in the Propylaia provided the opportunity for a systematic research of the more than 1.000 fragments that came both from dismantling and from the ceiling fragments that lay scattered on the ground and that had not been used in the previous restoration. The fragments were grouped and separated with the help of a computer according to their various characteristics such as the dimensions, the quality of work on the surface of the fragments, the quality of the marble, the geological layering, existence of interior marble discontinuities (*kommoi*), colour and texture, the traces left from the earlier intervention on the coffers. The method, using also optical drawings of the break surfaces, was especially successful for joining fragments and recreating coffered slabs. The research led to fragments belonging together that with small additions of new marble, formed architectural members of the ceilings (coffered slabs and beams) that could be restored in their original position or in similar positions in the ceilings (Ioannidou, 2007).

4.2 *Resetting architectural members*

Research carried out on certain areas of the monuments restored in the past, led to their rearrangement by resetting the architectural members in their correct positions, on the basis of new evidence found after their dismantling. The criteria for the research were; measurements of the dimensions of the blocks to millimetre precision; the quality of the marble; the geological layering; the existence of interior marble discontinuities (*kommoi*); colour and texture; the quality of work on the surface of the fragments, as well as deterioration features on the marble surface; special architectural and construction details.

Among the representative examples of the above work should be mentioned the rearrangement of the 6 blocks of the south and 23 blocks from the north walls of the Erechtheion; the rearrangement of the walls blocks of the temple of Athena Nike; the restoration of the north colonnade of the Parthenon. There, the dismantling of the area restored in the past (from the 4th to the 11th columns) provided the opportunity for a systematic research on the dismantled blocks, which led to the resetting the drums in their original positions (Fig. 11).

4.3 *Structural restoration of the monuments*

Another field of investigation is the stability of the restored areas of the monuments and those *in situ* against static or dynamic loads. Research is carried out on the structural restoration of architectural members joined from ancient fragments. This research led to the development of an original calculating method for joining marble pieces with titanium rods, according to the strain applied to the members (Ioannidou, 2003). The titanium reinforcements, are calculated so as to take on tensile force in a direction at right angles to the surfaces of fracture. The basic criterion for calculating the reinforcements is that they can safely take on the functional loads and in a near limit situation the reinforcements in the joining should fail rather than the marble itself (Ioannidou, 2008) (Fig. 12). During recent years, special emphasis has been attached to the methodology of restoring the monolithic aspect of the large bending members of the monuments (beams and architrave blocks). This methodology is developing continuously, from the standpoint of both calculation and process of application in the worksite (Ioannidou and Paschalidis, 2003).

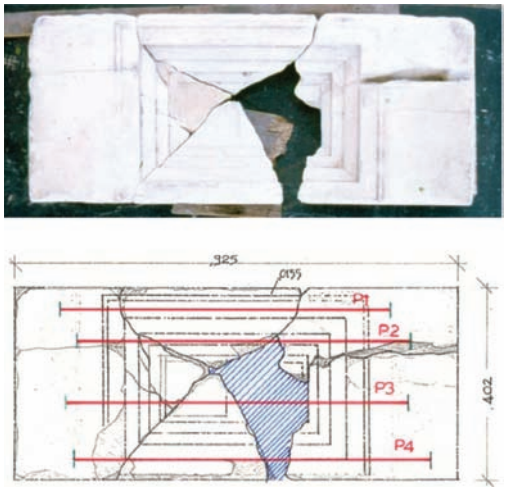

Figure 12. Propylaia, structural restoration of a coffered slab of the ceiling with titanium rods.

4.4 *Research on the materials of the restoration and the structural efficiency of the restored areas*

During recent years, investigation is carried out of the natural and mechanical properties of the building materials of the monuments and the materials used in restoration, such as ancient and new marble, ancient iron, titanium, special mortars.

The behaviour of the parts reinforced by titanium has been studied in bending trials and pull-out tests.

The behaviour of beams mended with titanium rods is also being studied in three-point bending tests. These tests are particularly important for the restoration of large bending members (beams, epistyles).

5 INNOVATIVE APPLICATIONS WITH ADVANCED TECHNOLOGY

During the course of the works a lot of innovative applications were developed in order to resolve theoretical, scholarly and technical problems have been encountered. Among them are;

– The repair in situ of the cracks in columns of the Parthenon Opisthonaos caused by thermal fracture in antiquity. In order to avoid dismantling them and to retain their authentic structure, the cracks in the drums were injected with a hydraulic grout especially prepared for this purpose.
– An innovative application is the method applied for the conservation and cleaning of the sculptured surface of the blocks of the Parthenon west frieze, dismantled in 1992, in order to repair the damage it had suffered during its long history on the monument. The cleaning of the blocks from the soot deposit and the black crust that had covered them was a most sensitive and delicate operation, since the historical layers of the surface of the sculpture had to be preserved. The cleaning method chosen was the laser in an entirely original application, using simultaneously two wave-lengths, infrared and ultraviolet (Fig. 13).

By means of this system, the frieze blocks were safely cleaned without affecting the underlying layer. In addition the historical layers of the surfaces of the frieze were preserved, with an excellent aesthetical result; information about the original workmanship and traces of ancient colour were also revealed. After their cleaning the blocks of the frieze are exhibited in the Acropolis Museum, replaced on the monuments by exact copies of artificial stone, finished especially for tone and texture (Papakonstantinou, 2012).

Figure 13. The Parthenon west frieze Block VIII, detail during cleaning.

Figure 14. Erechtheum, south porch, laser cleaning of the coffers.

– Special emphasis was given during this past year, to the conservation and cleaning of the ceiling of the Porch of the Caryatids in the Erechtheion using this laser system (Fig. 14). In the course of cleaning were revealed traces of painted decoration and traces of ancient paint. Apart from the application of non-destructive methods of analysis for the study and analysis of these traces, research on the Egyptian blue is being carried out in collaboration with the British Museum.

6 THE INSTALLATION OF THE WORKSITES

Worksite organisation for the Acropolis restoration works in the archaeological areas adjacent to the monuments as well as the visitors themselves, caused special difficulties. Access and the transportation of technical equipment and materials (massive loads of marble, etc.) required special study and the development of innovative solutions, since vehicles cannot be moved on the Acropolis Rock. Special care is taken with the form and extent of the hoisting system used, so that it is adaptable to the particular aesthetic and environmental requirements of the sensitive area of each monument, which is surrounded by ancient remains and at the same time must cope daily with hordes of visitors (Ioannidou and Oikonomopoulos, 2003). During the works important technical knowledge was developed about the hoisting systems that are used for dismantling and reassembling the monuments. To a great extent this technological knowledge is based on ideas and hoisting systems already known and employed in antiquity for building the monuments (Fig. 15).

Developments and achievements of modern technology, however, are utilized in the motive power of the systems and in the choice of material.

Figure 15. The ancient crane used for the construction of the Parthenon. Drawing M. Korres.

Figure 16. Parthenon; dismantling a block from the west pediment using a special grab.

Thus we have metal systems of cranes and scaffolding, which are moved by electricity with low speeds and can obtain great precision.

The tools employed in the *anastelosis* are about the same as those used by the ancient technicians for building the monuments. Innovative constructions, however, using the ultimate in modern technology were developed in order to accelerate the works, while retaining their well known high quality.

As representative examples should be mentioned: grabs for lifting architectural members (Fig. 16), special pointing devices used for the construction of the missing parts of the marble blocks. Notable among these is the cutting machine, devised for carving the flutes of the column drums of new marble that can cut to millimetre precision. Its use has greatly accelerated the work of restoration of the north colonnade of the Parthenon. The final phase of carving the flutes is to be done by hand by the experienced marble technicians of the service.

7 DOCUMENTATION OF THE RESTORATION WORKS

One of the basic features of the Acropolis restoration is the scholastic documentation, graphic, photographic, cinematographic etc., which has been carried out from the very beginning of the work and accompanies all its phases.

For processing and direct use of the documentation a single–digital data base has been developed and the material produced each day at the work–sites is thus preserved (Mallouchou-Tufano and Alexopoulos, 2007).

In recent years special emphasis has been placed on using techniques of advanced technology for documenting and graphic mapping of the monuments, the fortification walls and the rock itself.

Among the applications of recent years an attempt was made to utilise photogrammetry, the science that uses information about natural objects and the environment drawn from the procedure of recording, measuring and interpreting photographic images.

The development of photogrammetry during the past years, with the application of digital techniques, has made it possible to produce orthophotomosaics and three-dimensional models with texture of high quality and precision. With correct processing and composition of significant numbers of photographs, this method allows the production of orthophotomosaics that combine the geometrical accuracy of the plan with the optical—quality information of the photograph (Fig. 17).

A large programm of geometric documentation was accomplished during recent years including the mapping of the relief of the Acropolis with full topographical and photogrammetric survey of the circuit walls and a plan of the Acropolis and the three-dimensional (3-D) scanning of the Erechtheion and the fortification walls for their full length, interior and exterior. The data of the above documentation are exported to the internet (www.ysma.gr). (Fig. 18, 19). A new programm of geometric documentation including photogrammetric surveys of areas of the Parthenon, the Propylaia and the temple of the temple of Athena Nike is carried out this period.

8 MONITORING THE MONUMENTS

In the frame of documentation special emphasis was placed in recent years also on monitoring with instruments and recording of the Acropolis monuments and of the Acropolis circuit walls, a monument of great significance with continuous repairs from antiquity onwards that have contributed to

Figure 17. Parthenon; orthophotomosaic of the entablature and pediment of the west side. Study D. Mauromati.

Figure 19. Erechtheum. 3-D models of the Caryatids.

Figure 18. Orthophotomosaic of the Acropolis rock.

Figure 20. The south wall of the Acropolis.

its preservation to the present time. The purpose was to document and to monitor structural faults, cracks and distortions of the walls and the monuments, as well as the effects of seismic activity, using the most advanced methods of electronical recording, so as to study their static efficiency, to draw up studies and to carry out interventions on them of a rescue nature. (Egglezos and Moullou 2011) (Fig. 20).

Among the applications of recent years, in the context of monitoring the walls and monuments, the most important are:

- Geophysical prospection: electrical tomography carried out in order to determine the contours of the south side of the Wall. It was not possible to determine precise geometric contours, but an area with a high amount of dampness were located.
- Installation of a network of seven accelerographs at specific points of the rock and the Parthenon. The purpose of developing this network, being carried out collaboration with the Geodynamic Institute of the National Observatory of Athens, is to record seismic action and the response of the hill and the monuments to these.
- Installation of a system of optical fibers to detect deformations, temperature and pressure at specific points on the wall and the monuments.
- Highly accurate measurements of topographical targets on the wall. The measurements are for the purpose of monitoring micro-movements at specific points of the wall with a topographical instrument of high accuracy.

9 DISCUSSION

The completion of the great anastelosis programme, launched in 2001, brings to an end a highly productive period in the Acropolis restoration story. A new programm, including interventions in other parts of the monuments that show structural problems, is carried out this period, co-funded by the Hellenic State and the European Community. In the new phase of the works the driving forces will be the knowledge and experience gained in the preceding years, together with the creative spirit and enthusiasm that has characterised the period that has ended.

The current restoration project on the Acropolis bears, as always, the stamp of its time. It responds to the contemporary social demands for a more direct comprehension, enjoyment and experience of the heritage from our ancestors. At the same time it reflects the advanced scientific and technological level and know-how not only of contemporary Greece but of the whole European Community. The Acropolis restoration project is a European project not because it is partially financed by the European Union, but because it affects monuments that constitute the cradle of European thought, feeling and culture.

REFERENCES

Bouras, Ch. 1994. Restoration work on the Parthenon, and changing attitudes towards the conservation of monuments, in P. Tournikiotis (ed.), *The Parthenon and its Impact in Modern Times, Athens*: 310–339.

Egglezos, D. & Moullou, D. 2011. Back—analysis sheds light on the history of the Acropolis Wall: The interpretation of a permanent structural failure. *In Proceedings of the XV European Conference on Soil Mechanics and Geotechnical Engineering.*

Ioannidou, M. 2003. The structural restoration. *In Restoration of the Athenian Acropolis (1975–2003),* Quaderni ARCo, Rome: 150–155.

Ioannidou, M. & Paschalidis, B. 2003. Joining the beams of the Propylaia with titanium reinforcements: a new approach, *Proceedings of the Fifth International Meeting for the Restoration of the Acropolis Monuments,* 4–6 October 2002: 291–300.

Ioannidou, M. & Oikonomopoulos, S. 2003. General principles for the organization of the work-sites for restoration of the monuments. Hoisting technology in the Acropolis restoration *works. In-Restoration of the Athenian Acropolis (1975–2003)*. Quaderni ARCo, Rome: 142–144.

Ioannidou, M. 2007. The Restoration of the Propylaia of the Athenian Acropolis. Athens.

Ioannidou, M. 2008. Principles and methodology of intervention for structural restoration. *Proceedings of the XXI International Symposium CIPA 2007 AntiCIPAting the future of the cultural past,* Athens: 376–381.

Ioannidou, M., Alexopoulos, Y., Egglezos, D., Mavromati, D. & Moullou, D. 2010. Modern technology in the restoration of the Acropolis monuments. *Proceedings of a one day conference. In Acropolis Restoration News 10*, Athens.

Ioannidou, M. 2011. 2010–2011. The progress of restoration on the Acropolis. *In Acropolis Restoration News 11:* 2–9.

Ioannidou, M. & Lebidaki, E. (eds) 2011. *The Restoration of the Monuments of the Athenian Acropolis.* 2nd edition, Athens.

Ioannidou, M. 2012. Research and Technology. *In Acropolis Restored*, British Museum Research Publication, no 187, Bouras, Ch., Ioannidou, M. & Ienkins I. (eds), London: 11–20.

Mallouchou-Tufano, F. & Alexopoulos, Y. 2007. Digital management of the documentation of the Acropolis restoration, *Proceedings of the XXI International Symposium CIPA 2007 AntiCIPAting the future of the cultural past,* Athens: 475–479.

Papakonstantinou, E. 2012. Surface Conservation. *In Acropolis Restored*, British Museum Research Publication, no 187, Bouras, Ch., Ioannidou, M. & Jenkins I. (eds), London: 57–64.

Zambas, K., Ioannidou, M. & Papanikolaou, A. 1986. The use of titanium reinforcement for the restoration of marble architectural members of the Acropolis monuments. *Case Studies in the Conservation of Stone and Wall Buildings,* IIC Congress, Bologna: 138–141.

Geotechnical Engineering for the Preservation of Monuments and Historic Sites – Bilotta, Flora, Lirer & Viggiani (eds)
© 2013 Taylor & Francis Group, London, ISBN 978-1-138-00055-1

Estimation of moisture condition with salinity in the ground behind the Dunhuang Mogao Grottoes using the electrical resistivity method

M. Ito, K. Koizumi, K. Oda & T. Miyawaki
Graduate School of Engineering, Osaka University, Osaka, Japan

C. Piao
Hytec Geotechnical Consultant Co., Ltd., Osaka, Japan

C. Tanimoto
International Institute for Advanced Studies, Kyoto, Japan

Y. Iwasaki
Geo Research Institute, Osaka, Japan

X. Wang, Q. Guo & S. Yang
Dunhuang Academy, Dunhuang, China

ABSTRACT: There is moisture movement under the ground as a factor contributing to salt damage at the arid regions. Some parts of wall paintings of the Dunhuang Mogao Grottoes, which is a World Heritage site, have been seriously damaged by the crystallization of salts. This damage is likely to have been caused by short-term factors such as rainwater and flooding, and a long-term factor, namely, groundwater movement. In order to preserve the grottoes, it is important to know the relationship between underground moisture and salts. The purpose of this study is to understand the moisture content and salinity in conglomerate layers behind the Mogao Grottoes by the electrical resistivity method. The resistivity characteristics of the field sample focused on water saturation with salinity were determined by laboratory tests. By obtaining the distribution of water saturation from the resistivity distribution in the ground, the moisture content in the ground was estimated. The result indicates that reasonable quantity of moisture exists behind the Mogao Grottoes.

1 INTRODUCTION

1.1 *Study area*

The Dunhuang Mogao grottoes are located in Dunhuang City which is an arid region in China. Dunhuang City itself is located around 1,900 km west of Beijing. The average annual temperature is 9° C and the average annual rainfall is 39.9 mm, respectively. Figure 1 shows the location of Dunhuang.

The Dunhuang Mogao grottoes are located 25 km southeast of Dunhuang City and the Daquan River flows in front of the grottoes (Figure 2).

The Mogao grottoes are a group of caves that were excavated into the western cross section of the cliff, which itself resulted from erosion by the Daquan River.

The grottoes were excavated over about 1000 years, from 366 A.D., and extend about 40 m in height and 2 km in north–south length. Figure 3 shows a part of the Mogao Grottoes. Presently, 492 caves, 2,400 painted sculptures and 45,000 m^2 of mural are preserved; additionally, the grottoes were registered as a World Heritage site in 1987.

Figure 1. Location of Dunhuang.

Figure 2. The Daquan River in front of the Mogao grottoes.

Figure 3. The Mogao grottoes.

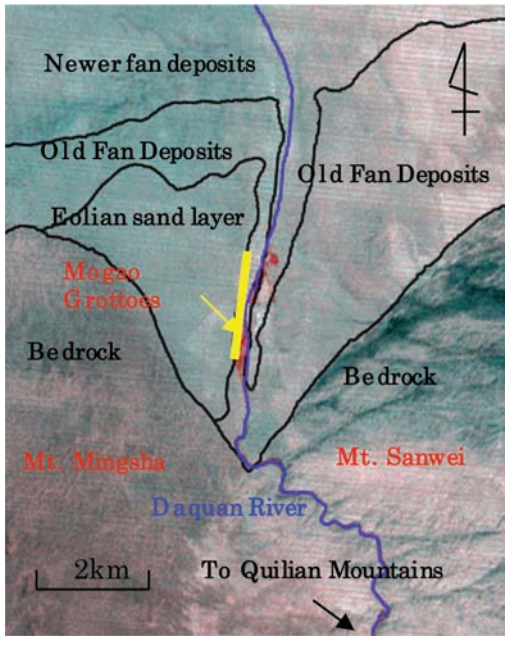

Figure 4. Geology of the Mogao grottoes.

1.2 *Geological information*

Mingsha Mountain, which is formed by windblown sand, is located to the southwest of the Mogao grottoes; Sanwei Mountain is in the southeast in the grottoes. These mountains are 1,600–1,700 m in height. The Qilian Mountains, which exceed 5,000 m in height, is located to the southern side of these mountains, and Dunhuang is located in an oasis that receives meltwater from glaciers on the ridges. In Dunhuang, a vast alluvial fan has formed in the vicinity of the river and displays two main types of deposit: old fan deposits that are distributed in the south, and newer fan deposits that are distributed on the north (downstream) side of the river. The Mogao grottoes were cut into the western cross section of a cliff that resulted from the erosion of the old fan deposits by the Daquan River. The grottoes were basically formed by the reasonable consolidated conglomerate layer which can be excavated by human-beings. (Kuchitsu, N. 1992) Currently, the water of the Daquan River that flows in front of the grottoes is dammed by the south dam, although water flow can be observed in the upstream reaches. Near the caves, snow, ice, and surface water cannot be confirmed, except during winter, early spring (i.e., during thawing), and periods of rainfall. Figure 4 presents an overview of the geology around the grottoes.

As illustrated in Figure 5, the present cliff is divided into five layers: Q_2 A–D and Q_3. The upper

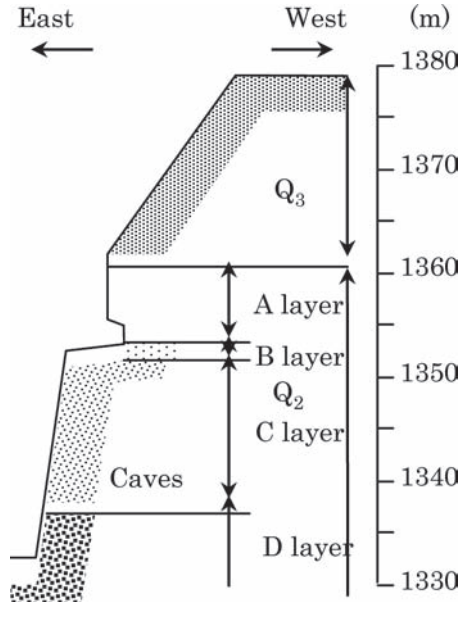

Figure 5. A cross-sectional schematic of the Mogao grottoes (Adachi, K. 2001).

layer (Q_3) consists of unconsolidated conglomerate and forms the upper portion of the grottoes. The lower layer (Q_2) is formed by conglomerate consisting of old fan deposits. Most of the caves

are within the Q_2 C and Q_2 D layers, although a few are within the Q_2 B layer.

1.3 *Degradation and preservation of the Mogao Grottoes*

Examples of famous stone ruins include the Sphinx of Egypt, Angkor Wat in Cambodia, and Machu Picchu in Peru. The Dunhuang Mogao grottoes can also be included in this category. The Mogao grottoes are better preserved than other stone ruins because of the dry climate in Dunhuang, yet infrequent heavy rains and floods over a long period have gradually eroded the grottoes. The Research Institute on Cultural Relics of Dunhuang (currently Dunhuang Academy) was established in 1944. The walls of the cliff face have been reinforced by artificial walls, and doors have been emplaced at the entrance to the caves for dust protection. Trees were planted in front of the caves to act as shields to windblown sand, and sand prevention fences have also been emplaced extensively on the Mingsha Mountain, which extends from the cliff toward the southwest. Such measures are designed mostly to offer resistance to windblown sand. Conversely, specific measures to mitigate salt damage (Figure 6) on the surface of the murals inside the caves have not been implemented yet.

Recrystallization of salt can be observed owing to the particular desert conditions surrounding the Mogao grottoes (Figure 7), and likely occurs as a result of evaporation of fluid that became loaded with salt when the surrounding rock reacted with fluids such as rainwater. Such processes cause salt damage in the caves, resulting in the deterioration or collapse of murals as a result of recrystallization of the salt. Salt damage is observed mostly on the ceiling of a cave in the upper layer and is confirmed at the bottom of side wall of a cave in the lower layer. The movement of water (rainwater and floodwater in the upper and lower layers, respectively) may dissolve salt within the ground. Salt damage has occurred in more than 70 caves in the grottoes and is an issue that must be addressed in order to preserve the grottoes.

Figure 6. Salt damage on cave wall.

Figure 7. Salt recrystallization.

1.4 *Purpose of the research*

To prevent salt damage to the walls of the caves, it is necessary to understand the movement of water and salt in the ground around the Mogao grottoes. Moisture behavior in the area can be classed as short term (e.g., rain, flood) or long term (e.g., groundwater). In order to elucidate the mechanisms of the salt damage, this study is intended to estimate moisture conditions, especially salinity, in the ground behind the Mogao grottoes. First, electrical resistivity distribution within the cliff of the grottoes is measured in the field by electrical survey. However, because there is abundant salt in the ground, it is difficult to estimate moisture conditions based on the resistivity distribution without considering salts. Therefore, the characteristics of the electrical resistivity distribution are examined by laboratory experiments focusing on relationship between the degree of water saturation and the salt content by using filed samples. Finally, the moisture conditions of the ground are estimated by converting the resistivity distribution into distribution of water saturation using the results of the laboratory experiments.

2 SALT CONTENT OF THE GROUND AROUND THE MOGAO GROTTOES

2.1 *Preface*

Typically the continental interior desert contains relatively large amount of salts in the ground. It's eluviation due to rainfall is extremely small. Salts in the soil accumulate at the ground surface when

the amount of potential evaporation is larger than precipitation. In addition, land water, such as rivers, contains large amount of salts. The recrystallization of land water salts due to evaporation is also important. Dunhuang, which is in the eastern Taklamakan Desert, has same behavior. (Kitano, Y. 1994) Salt damages at the Mogao Grottoes and salts contained in the ground are strongly related. Using electrical resistivity method, an estimation of moisture condition is obtained by considering the influence of salts contained in the ground. In this chapter, the salts contained in the soil are quantitatively clarified by the electrical conductivity (EC) and total dissolved solid (TDS) around the Mogao Grottoes obtained by field measurements.

2.2 *Method and item of measurement*

EC (electrical conductivity), measured in field survey, indicates the salt concentration of the soil easily. The definition of EC is as follows. If a 1 m × 1 m × 1 m solid cube of material has sheet contacts on two opposite faces, and these contacts have 1 V potential difference, and the electric current is 1 A, the cube's EC is 1 $S \cdot m^{-1}$. The S unit is the Siemens, which is the reciprocal of resistance. In brief, EC is the inverse of resistivity, and the TDS is the total amount of material dissolved or suspended in water. (Miyazaki, T. & Nishimura, T. 2011)

In the field survey, multi-pocket tester (PCST35, Takemuradenkiseisakusho) was used for convenience. The measuring method was a 1:5 solution method with a container that comes with the tester. This method measures the pH, EC and TDS of the supernatant water which is added about five times to the mass of soil samples. In addition, because precise mass spectrometer cannot be used in the field, the samples and the amount of water added to the samples was measured by using the scale that is marked on the side of the container. Therefore, each sample was measured, the average value was used. Although adding distilled water is better, it was difficult to use on-site. So irrigation water, tap water and mineral water were measured because they were easy to get. Table 1 shows each pH, EC, resistivity and TDS, of irrigation water, tap water and mineral water. Mineral water is the closest to neutral, and has the lowest EC and TDS; therefore mineral water was used as water added to the samples. In the actual measurement, the pH, EC and TDS of the mineral water were measured for each bottle. It should be noted that EC of the irrigation water in the Mogao grottoes is nearly equal to the drainage water of irrigated land in the Uzbekistan Syr Darya region where the farmland has salinization problem. (Miyazaki, T. & Nishimura, T. 2011)

Table 1. Each water pH, EC, resistivity, TDS.

	pH	EC (μS/cm)	Resistivity (Ω · m)	TDS (ppm)
Irrigation water	8.03	3180.0	3.14	2250.0
Tap water	7.87	1202.0	8.32	854.0
Mineral water	6.83	26.1	383.14	18.5

2.3 *PH, EC, resistivity and TDS, in the ground behind the Mogao Grottoes*

Table 2 shows each pH, EC, resistivity and TDS in the ground on the cliff of the Mogao grottoes. Usually cultivated fields need EC less than 300 μS/cm. A field requires salt removal when EC of the field is more than 2000 μS/cm. Considering this, we know that the soil in the ground behind the Mogao grottoes contains a large amount of salts. EC and TDS of the soil at the surface is larger than those in the position of 30 cm from the ground surface. It may be because of the salt accumulation due to evaporation. In Dunhuang, the annual rainfall is about 39 mm, and rain fall is concentrated in the rainy season. Rainwater penetrates the ground and spreads downward while dissolving the salts in the ground. In dry season, water penetration stops. After that, the soil suction is reduced by evaporation at the ground surface. The water is soaked up toward the surface again by capillary action. Finally, moisture evaporates near the surface, and salts are recrystallized. EC and TDS of the soil that is deposited on the bottom of the 20 m depth vertical borehole are about 1.5 times larger than those at the surface. The depth corresponds to the depth of the caves. This may suggest that the ground around the caves contains larger amount of salt than near the surface. Although, it is necessary to consider several other possibilities such as sample contamination from surface soil fallen down from the borehole wall.

Table 2. Each soil sample pH, EC, resistivity, TDS.

	pH	EC (μS/cm)	Resistivity (Ω · m)	TDS (ppm)
Ground surface	7.96	2535.0	3.94	1800.0
30 cm depth from the surface	8.39	1394.0	7.17	987.0
30 cm depth from the surface (another point)	8.38	1722.0	5.81	1225.0
Bottom of 20 m depth borehole	8.92	4125.0	2.42	2905.0

3 ELECTRICAL RESISTIVITY DISTRIBUTION

Electrical resistivity was measured at the top of the cliff of the Mogao grottoes. A borehole was located at a point 150 m west of the Nine-story Pagoda that is the landmark feature of the grottoes. The borehole reached a depth of 150 m. The two-pole method was carried out. Figure 8 presents the measurement results, and Figure 9 illustrates a cross-sectional view showing Line 100 gake and Line V 100. It is clear that the electrical resistivity is higher for shallow ground than for deep ground. In particular, a lower resistivity zone of about 45 Ω · m exists at 50–100 m depth; additionally, the higher resistivity zone in the vicinity of 120 m depth appears to be a localized phenomenon. A lower resistivity zone can be seen over the caves in Line 100 gake. Accurate measurement of resistivity was impossible in the section between Line V 100 and Line 100 gake because the steel wires for the environmental stations were buried in the ground. The results of this measurement indicated that a lower resistivity zone, which may affect the caves, is present at the back of the Mogao grottoes.

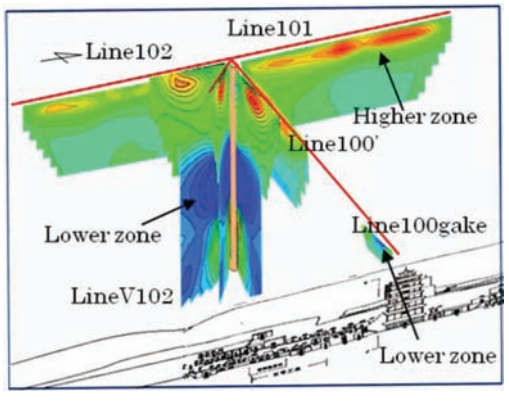

Figure 8. Results of measurement.

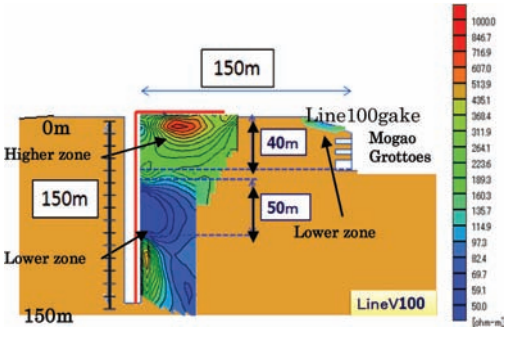

Figure 9. Cross-sectional view.

4 CHARACTERISTICS OF ELECTRICAL RESISTIVITY OF LOCAL SAMPLES

In this study, moisture conditions in the ground behind the Mogao grottoes are estimated from electrical resistivity distribution measured by field survey. In general, electrical resistivity changes under the influence of various elements; therefore, it is important to interpret the resistivity distribution by laboratory tests. In this section, we discuss the relationship between electrical resistivity and water saturation using field samples.

4.1 *Methods*

Experiments were conducted in the laboratory to elucidate the relationships between electrical resistivity and water saturation of field samples under changing salt concentration. The samples are conglomerates which were collected near the Mogao grottoes. First, salts contained in the samples were leached by filtering with distilled water. Then, salts were impregnated by injecting aqueous solution that dissolved the certain quantitative saturated salt into the samples leached salts. While gradually drying samples, resistivity and weight measurements of the samples were repeated several times. Table 3 shows impregnated salts based on the ratio of NaCl to the dry weight. The experiment was conducted based on four patterns: Case A calculated the average value of all samples; twice amount of Case A in Case B; Case C gives the maximum value of all samples; and Case D provides the upper limit, i.e., the maximum amount of salt that was detected in aqueous solution in pore water. Figure 10 illustrates the electrode device used in the electrical resistivity measurements.

4.2 *Results and discussion*

The measurement results are shown in Figure 11; the black-framed inset of Figure 11 is shown in Figure 12. Electrical resistivity increased gradually with increasing degree of saturation, increasing rapidly when the degree of saturation became less than 10%. The resistivity changes were small in the range of high water saturation; however, with increases in salt impregnation, the lower resistivity

Table 3. Salt impregnation amounts of the test pattern.

Pattern name	Conversion ratio of NaCl
Case A	0.756×10^{-3}
Case B	1.50×10^{-3}
Case C	3.14×10^{-3}
Case D	16.7×10^{-3}

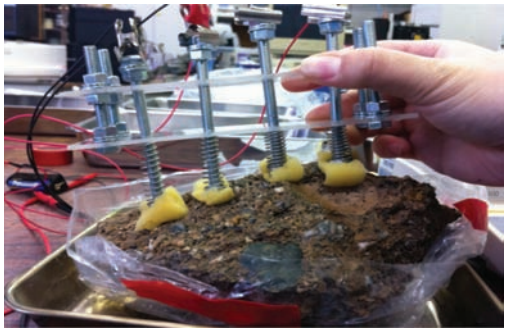

Figure 10. An electrode device.

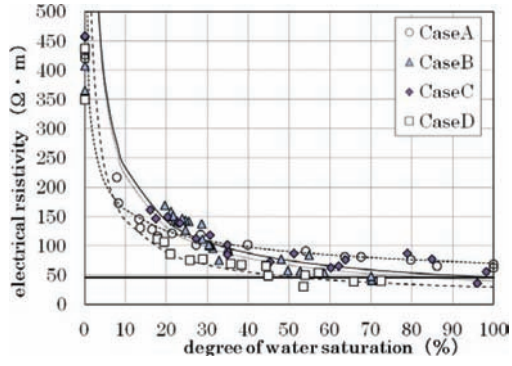

Figure 11. Measurement results.

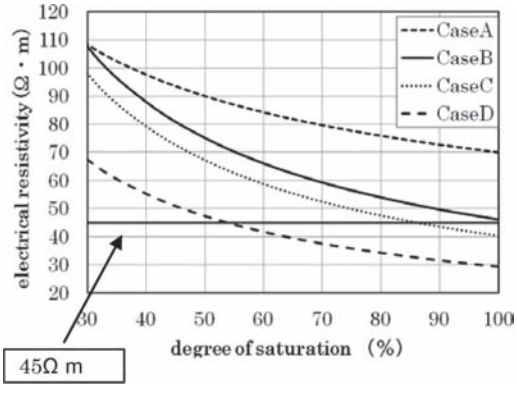

Figure 12. Inset: Lower resistivity zone.

is indicated. For resistivity of 45 Ω · m (i.e., the lowest resistivity obtained in field measurements), Case B exhibited saturation of 100%, Case C a saturation of 85%, and Case D a saturation of 55%. The lowest resistivity zone, in the ground behind the Mogao grottoes, exhibited resistivity of 45 Ω · m; therefore, the possibility that the degree of saturation is at least 55% (i.e., conversion ratio of NaCl is 16.7×10^{-3}) was confirmed.

5 MOISTURE CONDITONS BEHIND THE GROTTOES

This section estimates moisture conditions in the area behind the Mogao grottoes based on the results of Sections 3 and 4. The resistivity distribution in the field survey was converted into two types of water saturation distributions using the results of laboratory experiments.

Figure 13 illustrates the distribution of water saturation. Figure 13(a) shows the distribution of water saturation reflecting the ground environment of Case B, while Figure 13(b) shows the distribution of water saturation reflecting the ground environment of Case D; it is clear that the degree of water saturation is higher in Case B than in Case D. These figures cover the same range of resistivity distribution, and the difference in the amount of salt is reflected in the distribution of water saturation. Moreover, for 50–100 m depth, the degree of saturation is 100% for Case B and 55% for Case D. Near the top of the caves, the degree of saturation is 60.1% for Case B and 46.6% for Case D.

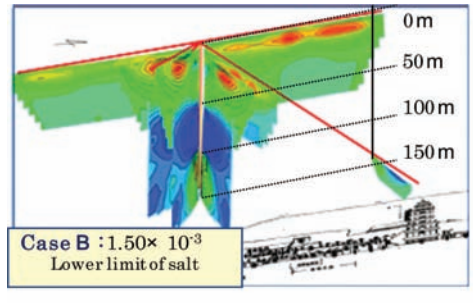

(a) If Case B: Lower limit of salt

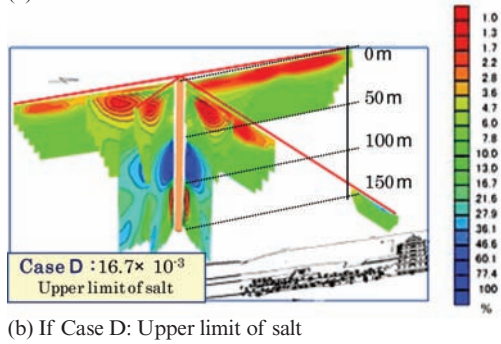

(b) If Case D: Upper limit of salt

Figure 13. Distribution of water saturation.

6 CONCLUSIONS

The resistivity distribution behind the Mogao grottoes was measured by the field surveys, and lower resistivity zones were confirmed at 50–100 m depth and on the top of the caves. In subsequent laboratory experiments, the resistivity characteristics of the field samples with respect to changing water and salt concentrations were identified, and the resistivity distribution derived from the field survey was converted into a distribution of water saturation using the results of laboratory experiments. The results indicated that deep ground is subject to relatively high water saturation compared to shallow ground. The degree of saturation was more than 55% when electrical resistivity was 45 Ω·m, which was the lowest resistivity measured in the field; therefore, the low resistivity in the surrounding ground is likely to indicate at least 55% water saturation. In conclusion, water saturation is relatively high at 50–100 m depth and above the caves, indicating that moisture behind the Mogao grottoes would be exerting an influence on the caves. Our next research should be clarified how to control the moisture movement to the caves through the on-site monitoring.

ACKNOWLEDGEMENTS

This study was funded by an Overseas (A) type (22254003) Grant-in-Aid for Scientific Research, for which I wish to express my gratitude here.

REFERENCES

Adachi, K. 2001. Study of water distribution by resistivity measurement Dunhuang Mogao Grottoes. *56th Annual meeting of J.S.C.E.* 642–643.

Kitano, Y. 1994. The Chemical Composition of Land Waters in the Dunhuang Area and of Evaporites in Various Desert Areas of China. *Sience for Conservation.* No. 33, 1–26.

Kuchitsu, N. & Duan, X. 1992. Geological environment of the Dunhuang Mogao-Grottoes, Gansu Province China. *Science for Conservation*. No. 31, 79–80.

Miyazaki, T. & Nishimura, T. 2011. Soil physical experimentation. *University of Tokyo Press.* 95–96,103.

Tanimoto, Y. 2007. The state of water and salts in the Dunhuang Mogao Grottoes. *36th Symposium on Rock Mechanics*. 141–146.

This page intentionally left blank

Geotechnical Engineering for the Preservation of Monuments and Historic Sites – Bilotta, Flora, Lirer & Viggiani (eds)
© 2013 Taylor & Francis Group, London, ISBN 978-1-138-00055-1

Dismantling for reconstitution of N1 Tower of Prasat Suor Prat, Angkor Thom, Cambodia

Y. Iwasaki
Geo Research Institute, Osaka, Japan

Y. Akazawa
Japan Cultural Heritage Consultancy Co., Tokyo, Japan

M. Fukuda
Taisei Geo-Tech Co. Ltd., Kumamoto, Japan

J. Nakazawa
Tokyo Engineering Consultants Co. Ltd., Tokyo, Japan

K. Nakagawa
Osaka City University, Osaka, Japan

I. Shimoda & T. Nakagawa
Waseda University, Tokyo, Japan

ABSTRACT: Prasat Suor Prat, an independent masonry tower, was dismantled before restoration work by JSA (Japanese Government Team for Safeguarding Angkor) to study possible mechanism that had caused inclination of the towers and horizontal spreading of stair stones. Dismantling upper structures as well as foundation mound were performed. Archaeological trench had revealed the mechanism of deformation of the structure as well as foundation. To avoid the possible defects, strengthening soil ground was selected rather than adapting the same methodology of only dense compaction of sand as done in ancient Angkor.

1 ANGKOR AREA

Angkor locates at a wide plain that expands between the Kulen Mountain in the north and the Ton le Sap lake in the south as shown in Fig. 1. The width of the plain is about 50 km with gentle inclination of 1/1000 from the north to south.

Angkor monuments distribute within the vast area of the plain. The famous monuments of Angkor Wat as well as Angkor Thom locate in the middle of the plain. Water is provided in the plain not only from rain fall but also from Kulen Mountain by Siem Reap River. In the middle of the plain, great man made reservoirs called as "Barai" were constructed to supply water in dry season. At present the West Barai is still in use with a dimension of 8 km by 2.5 km as shown in Fig. 1.

JSA (Japanese Government Team for Safeguarding Angkor) had performed the first deep geological boring in the area that revealed underground condition in 1994.

Figure 1. Angkor plain, Cambodia.

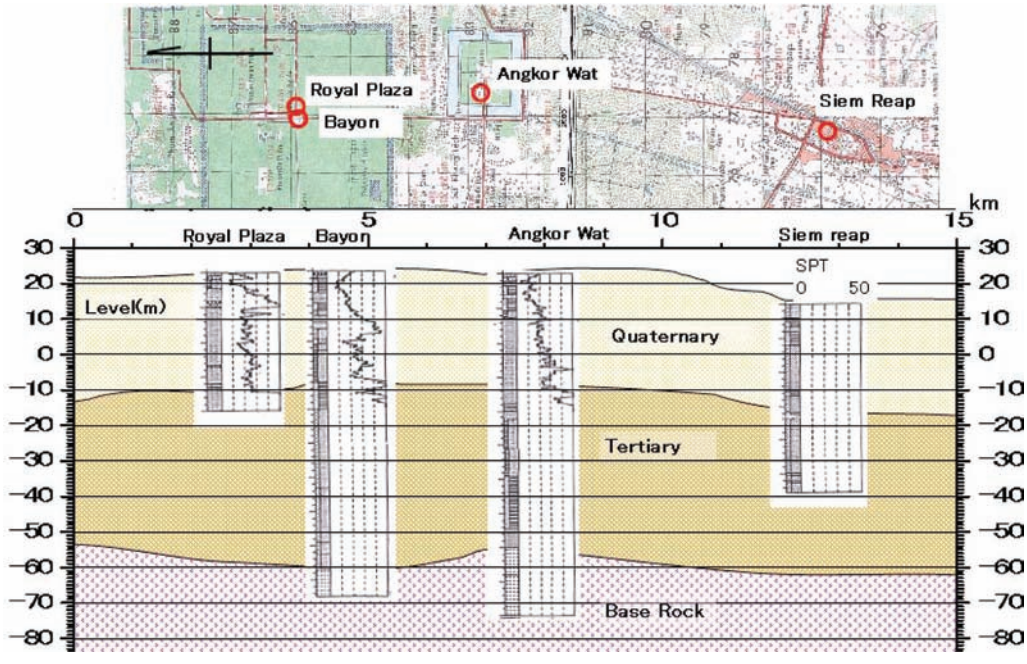

Figure 2. Underground section along Angkor Thom and Angkor Wat in north to south direction.

Fig. 2 shows a north-south section of the boring logs at the Angkor Thom to Angkor Wat. The upper 40 m of the ground surface is Quaternary deposits of silty fine sand with several clayey rich layers. In general SPT (standard penetration Test) N-value increases with depth except at the top surface. N-value at the top surface is 20 and decreases to 10 at the depth of 5 m. The boring at this point was carried out in March 1995 of dry season. The cone penetration test that was performed in rainy season at the same site revealed that the cone resistance decreased to zero at the surface and increased with depth down to about 5 m. The top surface of 5 m is affected by the seasonal change of water level.

Water condition in the ground gives crucial effects upon mechanical characteristics of surface ground in Angkor and forms one of the characteristic elements of cultural heritage.

2 PRASAT SUOR PRAT

Prasat Suor Prat (Tower of Rope Dancer) is a group of 12 independent towers along the west side in the Royal Plaza as shown in Photo 1.

2.1 *N1 Tower*

One of the 12 towers named as N1 that is inclined about 5 degrees towards northwards was selected by JSA for safeguarding work as shown in Photo 2. The tower consists from a main tower with a front room called antechamber. The main tower is three story masonry structures with laterite brocks with 10 m in width at foundation and about 20 m in height. The inside of the tower is hollow structure with four open windows at every wall. Fig. 3 shows vertical section and plan view of the N1 tower nearby the north pond. The differential settlement of the foundation was measured about 40 cm at the north and west corner lower than that of the south and east corner Akazawa (2005a).

Fig. 3 also shows contour lines of equi-settlement relative to the south-east corner of the foundation.

The open window of the west wall is deformed as shown in Photo 3.

The widths of the bottom of the window are wider than those of the top for all four walls and the measured results are shown in Table 1. The laterite blocks of the side face of the foundation were found widened about 6–8%. One of the characteristics of the deformation of the foundation of N1 Tower is horizontal spreading. Fig. 3 shows two major trends of deformation in the foundation system of inclination towards the North pond and horizontal spreading.

2.2 *Inclinations of N1 Tower*

The horizontal line of side face stones of foundation mound was inclined to northwards. The levels

Photo 1. Prasat Suor Prat.

Photo 2. N1 Tower, Prasat Suor Prat.

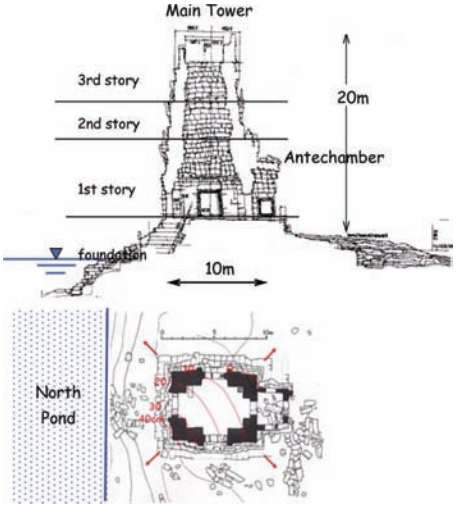

Figure 3. Vertical section and plan for N1 Tower.

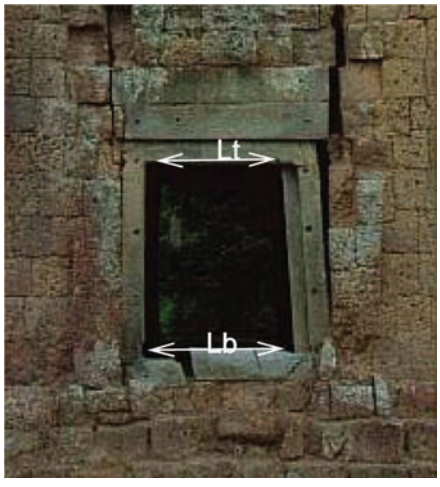

Photo 3. Deformed frame of open window at west side.

Table 1. Width of open window at top and bottom.

	Width of opening			
	Top	Bottom	Difference	Expanded rate
	Lt	Lb	ΔL = Lb – Lt	ΔL/Lt
Side	cm	cm	cm	(%)
East	170.3	182.0	12.0	7.1
West	171.3	185.0	14.0	8.2
North	168.0	178.0	10.0	6.0
South	124.0	131.7	7.7	6.2

of upper surface of the top (L1), the second (L2), and the third (L3) lines in Fig. 4 were measured at several points and plotted in Fig. 5.

The inclinations of these side stones of the foundation mound were found about 0.4 m per 10 m in horizontal distance. The inclination of the foundation as well as upper structure suggested that the inclination might have been caused by rather foundation system than only upper structure.

2.3 *Inclinations of other Towers*

Prasat Suor Prat consists of 12 towers. Fig. 6 shows inclination of these towers of Prasat Suor Prat in Royal Plaza whose position is shown in Fig. 7.

It should be noted that N1 and S1 show higher inclinations than others and both of them stood nearby north and south ponds.

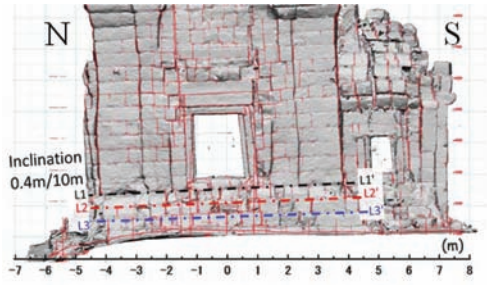

Figure 4. West side view of N1 Tower.

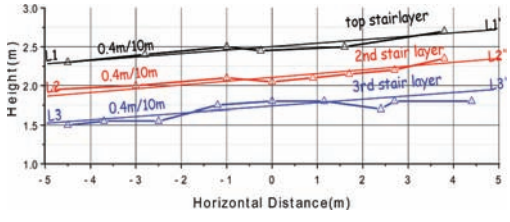

Figure 5. Inclination of top surface face stones.

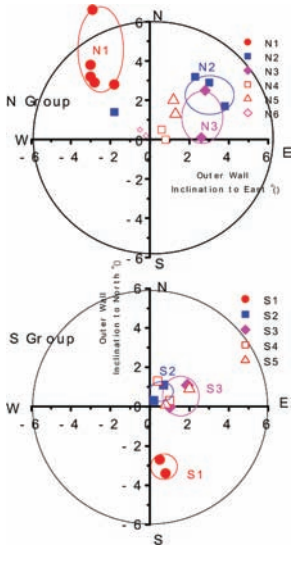

Figure 6. Inclination of Prasat Suor Prat.

2.4 *Result of restoration of N3 Tower*

In 1960', N3 Tower of Prasat Suor Prat had been found badly inclined.

French team had performed restoration work for the N3 Tower. Stones of the upper structure had been dismantled without treating the foundation system. After the restoration work, the N3 Tower had been found inclined again within a few years.

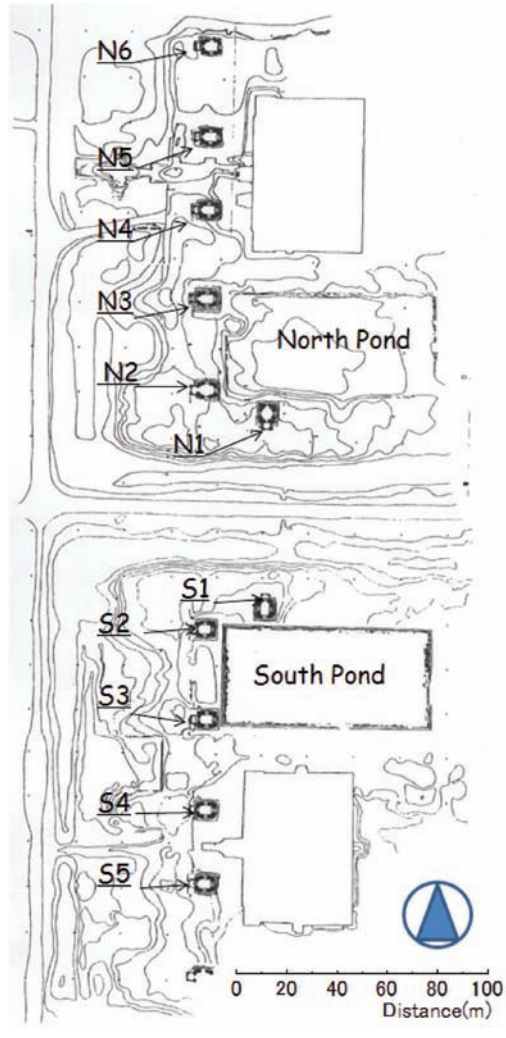

Figure 7. Location of Prasat Suor Prat.

When JSA began the restoration work of N1 Tower of Prasat Suor Prat, the question of insufficient result of restoration work of N3 was discussed and it was decided to study foundation system by dismantling and solve mechanical instability that had caused inclination of the upper and foundation structures.

3 DISMANTLING OF FOUNDATION

Dismantling of N1 Tower of Prasat Sour Prat was carried out before reconstruction of the Tower.

After the laterite blocks of the upper structure were dismantled, the foundation structures were

further dismantled. The soil mound was excavated down to reach natural ground layer (Nagatomo et al., 2005).

Photo 4 shows the Trenched site of N1 Tower of Prasat Suor Prat, where west-north face was exposed.

3.1 *Inclination of step stone and soil mound*

Fig. 8 shows archaeological section of trenches of N1 Tower along N-S direction. The upper structures consist from Main Tower and Antechamber. The bottom level of the upper structures was the same level of top level of side step stones. As already stated, the top level of step stones had inclined to northwards with settlement of 0.4 m for horizontal length of 10 m as shown in Fig. 4 and also indicated in Fig. 8.

Photo 4. Dismantling of foundation mound.

We had expected the same inclination of compacted soil layers in the foundation mound.

However, amazingly, we found the manmade layers of soil mound formed almost horizontal lines of compacted sand layers as shown in Fig. 8. It was mysterious for us to understand until the excavation reached to the much lower level.

3.2 *Slip down movement of side face of foundation platform*

When the trench was further deepened, the section in the north side of the foundation mound showed a small local bearing failure at the northern edge of the compacted fill in Fig. 8, which had resulted in sliding of retaining slope of north side face. The bottom element of side stones had settled by about ΔH_2 = 0.5 m from the original level. The bearing failure took place for the bottom of the step stones. It should be noticed that the bottom of the step stones settled about 0.5 m, however, the highest block of the step stones was found settled only ΔH_1 = 0.2 m as shown in Fig. 8.

3.3 *Systematic streaks on the trenched surface of foundation mound*

As shown in Photo 5, many streak lines were found on the trenched section of platform and foundation mound. Based upon the photos of sections, the streaks were read with their angles from vertical line. The angles were grouped into every five degrees of angles and plotted their distributions.

Fig. 9 shows the distribution patterns of the angles of streak line from the vertical line for an

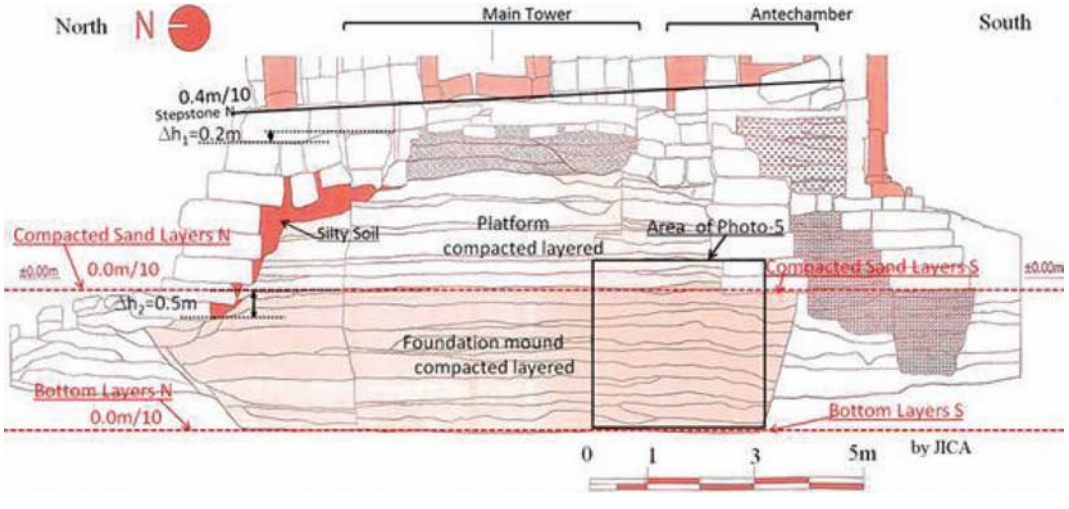

Figure 8. Archaeological trench section in NS direction.

Photo 5. Streak lines on the trenched N-S section.

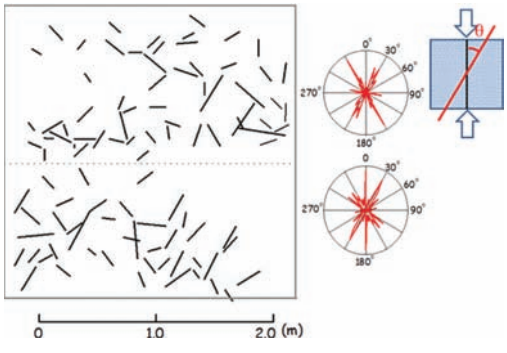

Figure 9. Pattern and distribution of streak angles.

example. The strong tendency of the angle of 30 degrees from the vertical direction was obtained, which suggests the streak lines correspond to shear surface under yielding condition.

The angle between the direction of failure surface and principal stress direction under the Mohr-Coulomb criteria is expressed by the following equation (1) with as the angle of internal friction of the material.

$$\theta = 45 \pm \phi/2 \quad (1)$$

The laboratory triaxial test for unsaturated sample showed that the internal friction showed is $\phi = 30$ degree, which results in $\theta = 30$ and 60 degrees.

The coincidence between the estimated angle of shear failure line from the laboratory test and field observation, the streak lines is very likely the shear failure line that have occurred in the soil mound under the vertical load of the upper masonry structures.

It is very likely that the compacted soil layers had reached shear yielding due to rather heavy load of the upper structure.

4 NUMERICAL SIMULATION

An FEM model was used to simulate the stress states in the manmade mound of Prasat Suor Prat to understand the geomechanical aspects of the Angkor structures.

4.1 *Properties of geotechnical material in Angkor*

Test sample of compacted sand was prepared to perform triaxial tests under unsaturated condition. Total stress parameters was obtained as $c = 23$–42 kPa, $\varphi = 27$–36.3 degree.

Fig. 10 shows mesh model for N1 Tower. There is the north pond at the left side of N1 Tower. The water level shown in Fig. 10 corresponds to the highest level just for a reference. In the FEM analysis, no water level was introduced in the analysis.

4.2 *Results of FEM simulation*

The material properties used in the FEM analysis under plain strain condition was listed in Table 2.

Vertical load from the upper structure was estimated as about 400 kPa. Fig. 11 shows the induced plastic zones for two different loads of 100 kPa and 400 kPa for stepwise constructing condition of the upper structures. Plastic zones were found developed within the manmade soil mound as the load increased. Both plastic zones of yielding of shear as well as volumetric stresses were initially found at the stage of 100 kPa and further developed at the final load of 400 kPa. Fig. 12 shows shear strain

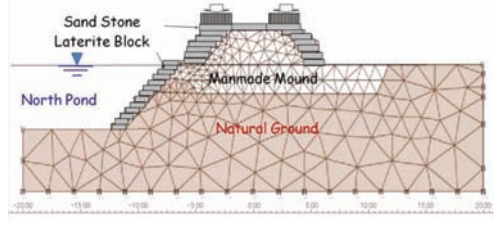

Figure 10. FEM mesh for modeling N1 Tower.

Table 2. Soil parameters.

	Density	Young's modulus	Cohesion	Friction angle
	kN/m^3	kN/m^2	kN/m^2	degree
Sandstone	24	400,000	50,000	
Laterite	24	200,000	30,000	
Compacted fill	18	800	20	30
Natural soil	17	250	20	30

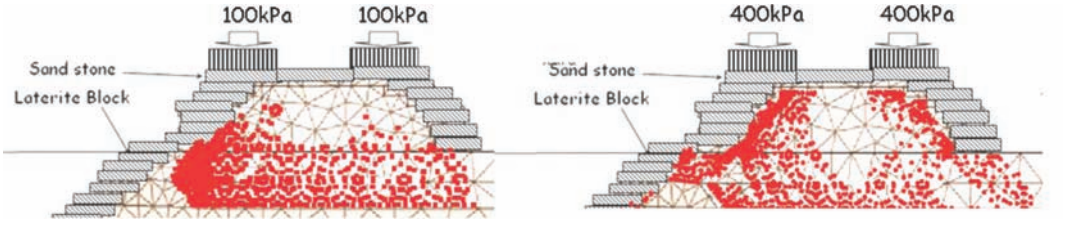

Figure 11. Increase of plastic zones due to load steps.

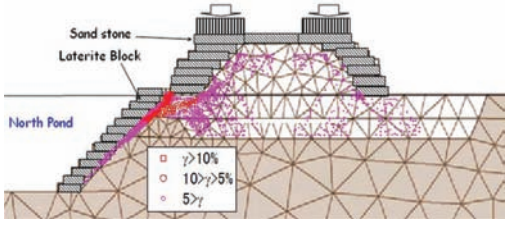

Figure 12. Distribution of large shear strain.

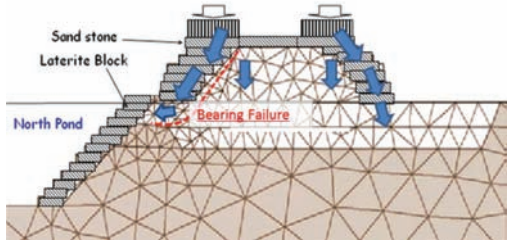

Figure 13. Stress flow by the load of the upper structure.

distribution in the soil mound. The pattern of shear strain in Fig. 12 shows the same tendency with what was found in the field as shown in Fig. 8.

The soil ground beneath the bottom of the upper part of the step stones was under large shear strain and corresponds well to the slid state as shown in the trenched section as shown in Fig. 8.

5 GEOTECHNICAL PROBLEM OF N1 TOWER, PRASAT SUOR PRAT

Based upon the discussions in the preceding sections, several geotechnical points were identified to have cause problems in foundation system.

1. Widened width between columns and horizontal spreading of foundation systems.
2. Local failure of the bottom of the side face stone of northern side that had caused slid down of not only northern but adjacent of western and eastern sides.
3. Shear yielding of soil mound by vertical compression stress took place.

It should be noted that strains in north pond side exceeds more than $\gamma > 10\%$, on the other hand, those in south side shows less than $\gamma < 5\%$. The difference was caused by the lateral confinement of the foundation system. The north side of the foundation situated at the embankment of the North Pond and has no confinement. The south side is surrounded by compacted fill that constrains the horizontal movement of the foundation system. Fig. 13 shows stress flow of the upper load to the foundation system.

The load on the face stones is partially transferred to manmade mound through stepping outward configuration with depth. However, still the large stress transferred into the soil beneath the side stone and resulted in bearing failure.

The above problems were caused by large loading of the upper structure upon the step stones and the special configuration of the foundation system of Khmer structure as discussed in the following chapter.

6 CHARACTERISTIC ELEMENT OF FOUNDATION SYSTEM OF KHMER STRUCTURE

The masonry structures in ancient Khmer have some common and special characteristics.

Photo 6 shows Northern Library at Bayon before restoration work by JSA. The Northern Library was partially dismantled and the trenched section was shown in Fig. 14. Platform for the upper structure is a soil mound with 5 m in height. The platform has a retaining system that consists from densely compacted sand layer, retained with laterite blocks inside and sand stones at outer surface. Clay sand soil is used at the side and upper boundary of platform between laterite blocks to prevent water infiltration.

In Fig. 14, stress flow is also shown. Loads from the upper structures are transferred to the foundation stones that are supported by compacted sand

Photo 6. South side of Northern Library, Bayon, Angkor Thom, before restoration.

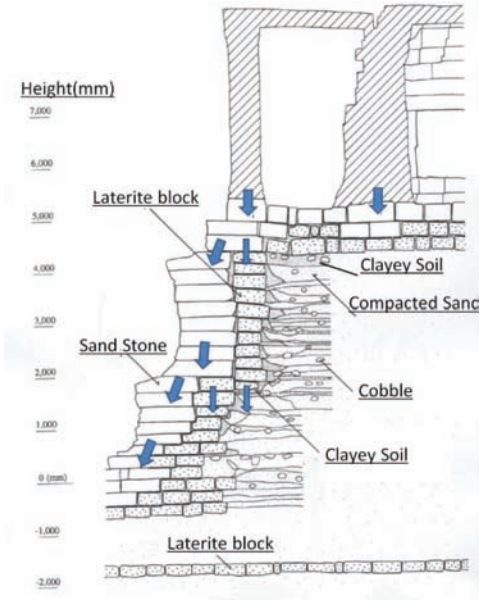

Figure 14. WE-section of Northern Library, Bayon.

in the central part or by laterite block and sand stone at the edge side. Stress flow at the middle of the retaining wall, vertical load is divided into three parts of sandstone, laterite block, and compacted sand mound.

Since the stress flow is always directing rather outwards than vertical, horizontal deformation is very likely to take place without confinements.

For the foundation system, several characteristic elements are identified as follows,

1. Foundation trench; the original ground is excavated with a depth of about 3 m and replaced with dense compacted sand. Pavement of laterite blocks are found within the compacted sand layers (see Fig. 14).

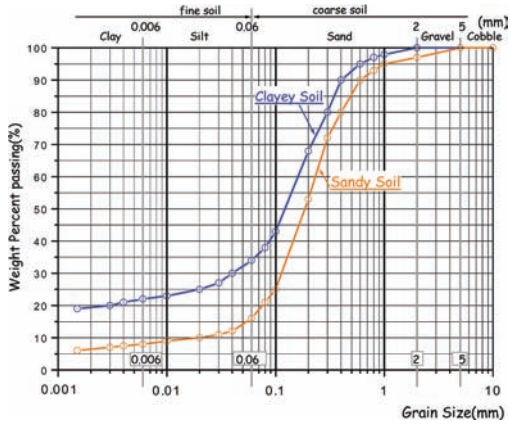

Figure 15. Grain size characteristics of soil materials.

2. Retaining wall; high embankments of more than 5 m in height have retaining structure that consists of sand stone and laterite inside with clayey soils are densely compacted sand with retaining wall by stone blocks.
3. Compacted soil mound; main body of high soil mound consists of densely compacted sand layers whose surface is covered with sand stone and laterite block. At the top surface beneath the pavements of sand stone and laterite blocks, clayey sand layer exists for preventing seepage from the surface. Clayey soil is also found at the side face boundaries between laterite blocks and compacted sand mound.
4. Soil materials; As explained, Khmer used these two different kinds of soils whose grain size distribution is shown in Fig. 15. Sandy soil contains only 15% of fine contents and clayey soil contains about 35% of fine contents.

These characteristics of foundation system and the soil materials compose the characteristic elements of the authenticity of ancient Khmer masonry structure.

7 RECONSTITUTION OF N1 TOWER, PRASAT SUOR PRAT

The main principle of restoration of cultural heritage is to keep and maintain the authenticity of the cultural heritage.

At the same time, when some deficiency is discovered, it is recommended to modify or improve based upon the minimal intervention, which is stated as "Intervention should be kept to the minimum level that meets structural requirements in order to ensure the least harm to heritage values."

7.1 *Soil material and improvement*

Sand material shows very large bearing capacity under unsaturated condition but becomes weaken under saturated states. JSA has developed a method of soil mixed with slaked lime during the restoration work for Northern Library at Bayon in 1996. The improved method uses the soil material with same grain size distribution as to maintain the important element of soil material used by ancient Khmer culture.

For the restoration work of N1 Tower, Prasat Suor Prat, the slaked lime was adapted to avoid the yielding of soil mound under the heavy upper masonry structure (Fukuda, 2005). Another deficiency that comes from no constraint of the north side of the platform by the North Pond is also prevented by introducing soil mixed with slaked lime when the strength is increased after aging.

7.2 *Geotextile*

The reconstitution of the upper masonry structure is expected to complete before the time of enough aging of slaked lime since the chemical process is rather slow.

Geotextile was provided within the soil mound to cover and to give enough constraint in the earlier young stage of aging of the soil mound against rather heavy load from the upper structures during reconstitution (Akazawa, 2005b).

8 CONCLUSIONS

Dismantling of a tower of Prasat Suor Prat, Angkor Thom, Cambodia was described.

The apparent inclined upper tower and foundation platform suggested the differential settlement of soil mound of the platform. However, it was identified caused by only slipping down of side stair stones of along north, west, and east sides of the platform.

Characteristic elements of the authenticity of the foundation system were discussed and the following items were identified.

1. Foundation trench.
2. Retaining wall.
3. Compacted soil mound.
4. Soil materials.

Reconstitution of N1 Tower was planned to improve the deficiency of the foundation system with minimal modification to keep the authenticity of the cultural heritage of the ancient Khmer.

REFERENCES

Akazawa, Y. (2005a) "Damage Conditions before Repair and Modifications in later Years," Report on the Conservation and Restoration Work of Prasat Suor Prat Tower, 44–57, Tokyo, JSA.

Akazawa, Y. (2005b) "Reconstruction of the Foundation and Platform", Report on the Conservation and Restoration Work of Prasat Suor Prat Tower, 269–298, Tokyo, JSA.

Fukuda, M. (2005) "Geotechnology, Geology, and Environment," Report on the Conservation and Restoration Work of Prasat Suor Prat Tower, 127–155, Tokyo, JSA.

ISO13822:2010 (2010) Annex I (informative) Heritage structures, I.9.2 Minimal intervention, 9, Paris, ISO.

Nagatomo, T., Kong, V. and HENG, P. (2005) "Archaeological Surveys," Report on the Conservation and Restoration Work of Prasat Suor Prat Tower, 58–120, Tokyo, JSA.

This page intentionally left blank

Geotechnical Engineering for the Preservation of Monuments and Historic Sites – Bilotta, Flora, Lirer & Viggiani (eds)
© 2013 Taylor & Francis Group, London, ISBN 978-1-138-00055-1

A variegated embankment dam in a historical territory*

R. Jappelli
Formerly: Universities of Napoli, Palermo and Roma Tor Vergata, Italy

… a piè del Casentino
traversa un'acqua c'ha nome l'Archiano,
che sovra l'Ermo nasce in Apennino.
Purg. V, 94–96

To the memory of Giulio Supino

ABSTRACT: A story is told of a dam completed in 1995 on a tributary of Arno River for the defence of the City of Florence, struck by the disastrous flood in 1966. The harsh conflicting dilemma between the construction requirements and the Mugello landscape integrity was composed in progress of the earthwork by a quasi-permanent "knowledge yard" searching for the continuous adjustment of the dam body to the situations prevailing in a territory rich of monuments dating back to the Medici Family under the quarrying constraints progressively imposed by local authorities. Overall safety and compliance along the interzone boundaries were guaranteed by suitable computations and technical precautions, in full respect of the originary design criteria. The case demonstrates that progress encourages the construction of embankment dams even in territories heavily constrained by monuments, provided the available materials entrusted with separated functions be appropriately distributed in the dam body and their safe compatibility ensured.

1 INTRODUCTION

The word construction designates the building act and also the resulting artefact. With reference to the technical professions, the term includes all kind of artefacts men have created to make possible their survival on and in the ground.

The notions aimed to ensure *firmitas* and *venustas* to the constructions are disseminated in different disciplines confined in the area of Civil Engineering. However, the diversity of constructions demands distinct competences. For a summary, constructions and related disciplines are classified in civil, railway, highway, hydraulic, and so on, according to the finality (residence, transportation, production, distribution, selling, and more). Should one refer to the building material, further great differences are noticed (timber, metal, conglomerate, masonry, earth, …); therefore, a different criterion exists, that is the classification per material, independently of its use. To this aim, one has found convenient to assemble the same notions under disciplines headed by the prevailing building materials. The fast accumulation of knowledge explains also the advent of mixed disciplines, such as the construction of bridges, where the influence of both the classification criteria can be perceived.

In the realm of geotechnical constructions, the earth removed from its natural site is used as building material after mechanical preparation: the most important applications of earth construction is in embankment dams, that are *almost pure geotechnical constructions* (Penman,1986). The embankment conforms to foundation soils and rocks, where other types of constructions fail; moreover, earth fills can be adjusted to contact with different materials, like conglomerates, in an agreeable equilibrium with the landscape (Fig. 1).

A story is told in the paper of a large variegated embankment dam that was built in a territory rich of historic monuments, where the fitting to progressively imposed constraints was possible, thanks to the versatility of solutions due to technical and scientific advancement in Dam Engineering. The proposed case is representative of the situation of a number of Italian construction yards, where the materials cannot be quarried from the sites selected at the design stage, so that the *as built* artefact, even though conforming the features of the *planned* one, can appreciable differ from the former.

*From a paper by the A. in the Magazine L'Acqua 6, 2012.

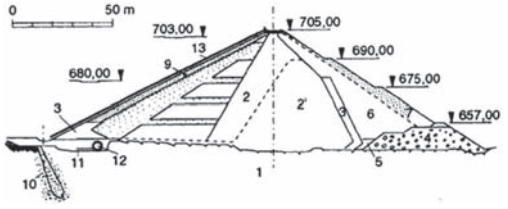

Figure 1. A zoned earth dam: 1 foundation, altered granite; 2, 2' core, more or less altered granite; 3, 5, 9, 11 drains, filters: crushed and selected granite; 4 downstream toe granite in selected blocks; 6 downstream transition, granite tout venant; 7 revetment: selected granite; 8 upstream shell: granite, tout venant; 10 grouting courtain; 12 adit; 13 upstream facing.

2 A WATER RESERVOIR FOR FLORENCE

The story of the Bilancino dam on a tributary of the Arno River, goes back to 1966, when the City of Florence was flooded by its water (Supino, 1974) (Apollonio et al., 1986) (Baldovin, 1988). The artefact dams the Sieve at a site about 60 km upstream the City of Florence. The reservoir ($V = 62 \times 10^6$ m^3) has a dominant role in the realm of the measures for the hydraulic defence of the historical City and offers also a hydro-potable service. The dam ($H = 42$ m; $V = 2 \times 10^6$ m^3) is a markedly zoned embankment with central core; the crest length is 720 m, its width 8,00 m (Baldovin, 1991).

The idea of such an important enterprise was proposed with far-sightedness by the late eminent Professor of Hydraulics Giulio Supino, whose contribution is gratefully acknowledged.

The formal interdictions of the municipalities to the quarrying activity supervened while the work was in progress; the event involved the necessity of using for the dam body materials of different sources provided that it satisfied the original design criteria. After the first dissent (Fig. 2) an agreement of the population was reached at the construction stage through a thorough debate; the acquired experience convinced the Regione Toscana to integrate the plans with some measures aimed at a proper environmental and recreational improvement with special care for the reservoir's shores.

3 THE MUGELLO

The Mugello's landscape (Fig. 3) is dotted with small towns, historic villas, religious buildings, farm houses, mills and other historic artefacts (Becattini et al., 1985). The magnificence of the Medici's Villas (Fig. 4), the elegant features of some masonry bridges (Fig. 5), the fascination of the native house of one of the greatest Italian

a

b

Figure 2. The former dissent a) of Mugello's inhabitants has gradually changed into consent and expectation b) for the benefits of Bilancino dam (Apollonio et al., 1986).

Figure 3. The Tuscan landscape in a detail of the painting *Viaggio dei Magi* by Benozzo Gozzoli (Sereni, 1993).

painters (Fig. 6), the simple architecture of the farmer houses spread over the countryside, are representative of the situation (Fig. 7).

The disastrous flood that struck Florence in 1966 is well described by modern authors (ITCOLD, 1997); however, two older unforgettable extreme events, are recorded in the Italian literature.

The first is told by Dante in the splendid verses describing the death of Bonconte da Montefeltro after the Campaldino Battle (1289):

Indi la valle, come 'l dì fu spento,
da Pratomagno al gran giogo coperse

a

b

Figure 4. The Villas: a) Cafaggiolo (Barberino) was built by Michelozzo for Cosimo dei Medici (Becattini et al., 1985); b) the entrance of Le Maschere on the right bank of the Bilancino reservoir, after the anastilosis.

a

b

Figure 5. The Bridges: a) Ragnaia on the River Ensa at Vicchio is said *Cimabue Bridge*, where the famous painter would have met the young Giotto; b) the two span medi-aeval bridge on the T. Sorcella nearby Villa del Monte, Barberino (Becattini et al., 1985).

di nebbia; e 'l ciel di sopra fece intento,
sì che 'l pregno aere in acqua si converse;
la pioggia cadde, e a' fossati venne
di lei ciò che la terra non sofferse;

Figure 6. The native home of the famous painter Giotto at Vicchio (Becattini et al., 1985).

a

b

Figure 7. Rural constructions: a) a farmhouse between Vaglia and San Piero a Sieve (Vallecchi, 1966); b) an old barn in the reservoir's area (Apollonio et al., 1986).

e come ai rivi grandi si convenne,
ver' lo fiume real tanto veloce
si ruinò, che nulla la ritenne.

(Purg. V, 115 e segg.)

The second event (1333) is handed down through the vivid narrative by Clini (Apollonio et al., 1986):

«Era il giorno d'Ognissanti di detto anno, quando sui monti di Firenze e del Mugello oscuratosi a un tratto il cielo cominciò a diluviare una continua dirottissima pioggia accompagnata da fulmini e tuoni sì fragorosi che assordavano 1'aere e metteano in tutti grande spavento. In Firenze e più nei popolati castelli della campagna era un continuo gridar misericordia, uno spaventoso suonar di campane, un correre di casa in casa, un confondersi tumultuosamente: le grida delle desolate genti vinceano il romore de' tuoni e lo strepito delle acque. Seguitando queste a sformatamente diluviare per quattro interi giorni e quattro intere notti; crebbero in guisa i fiumi che la Sieve allagò in Mugello tutti i campi adiacenti, atterrando case, sommergendo mulini e trascinando seco uomini, masserizie ed armenti, sicché dalle falde della Calvana sino a Dicomano parea la vallata ritornata ampio lago come a' tempi degl'antichi liguri ed etruschi. Immenso fu il danno intorno a Borgo San Lorenzo, ove era la Sieve cavalcata da un antico ponte di legno: questo sparì fra i gorghi dell'irato fiume, che ingrossato viepiù per 1'acque di tanti torrenti e fossi che quinci e quindi scendono da' monti, giunse al Pontassieve ed entrò nell' Arno che minaccioso e fremente dopo aver sommerso il Casentino, il pian d'Arezzo e di Figline, cacciando ogni cosa davanti a sé, venne recando a Firenze desolazione e sterminio».

Historic floods occurred in 1269, 1333, 1547, 1557 in Valdarno and in Florence are mentioned by the scientist Evangelista Torricelli in the following excerpt out of the *Replica del Torricelli ad una risposta di Don Famiano Michelini* alla sua *Scrittura sopra la bonificazione della Chiana*, Scienziati del Seicento, tomo II, Ricciardi Ed., 1980, p. 299:

«… Ricordiamoci solamente la rovina delle terre di Valdarno e la strage delle porte di Firenze, quando il fiume, non come cittadino, ma come nemico venne ad assaltare la propria città. …»

4 THE PLANNED EMBANKMENT

The design cross section of the embankment (Fig. 8) was markedly zoned and reflects a local situation offering materials with a great variety of mechanical properties. The dam body was defined after extensive geotechnical research within a wide radius aiming at the optimization of the use of local materials as for properties and available volumes. Zoning, compatibility at the boundaries and placing prescriptions were accurately established. The withdrawal of the materials suitable for the construction of the different zones of the planned embankment was intended from existing or newly granted quarries.

5 THE SUPERVENED CONSTRAINTS

When the work was in progress the situation revealed itself different because one or other of the following

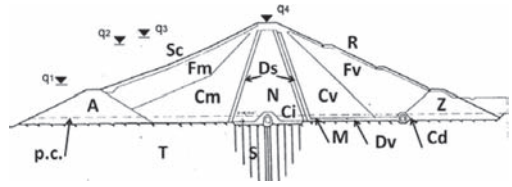

Figure 8. The as planned dam body, materials and *primary sources* (Fig. 11): A cofferdam, limestone, *Ponte Nuovo (7)*; Ci adit; Cd drain outlet; Cm, Cv upper and downstream transitions, sand and gravel, *reservoir's area (10)*; Ds vertical drain and filters, aggregates, plant; Dv horizontal blanket, aggregate *plant;* Fm upstream shell, limestone, *Ponte Nuovo (7)*; Fv downstream shell, marly limestone, *Carlone (2)*; M leakage deviator; N core, silt, *Scarperia (9)*; p.c. originary ground level; R revetment, sand and gravel, *reservoir's area (10)*; S grouting curtain; Sc rockfill, limestone, *Covigliaio (3)*; Z downstream heel, marly limestone, *Paterno (6)*; T foundation soil; sandstone, siltstone, claystone in rytmical sequence (Macigno del Mugello); q_1 reservoir's min level 234,50 ms.l.m; q_2 normal level 252,00, q_3 max level 254,50, q4 embankment crest level 259,00.

reasons: exhaustion of materials, that were in the meantime assigned to different works; expiry of the operation or interdiction of extending the activity of the existing quarries; non-concession of the quarrying activity in new areas. It was soon necessary to take cognizance that the local authorities were reluctant to deliver the concessions; moreover, the non-availability of the materials revealed itself along with the progression of the work, that was necessarily carried out on a *learn as you* go basis.

While the work was in progress, design research was extended farther with new investigations, difficulty of access, new affairs and steps arising under different hypotheses, boundaries and constrains.

6 THE EVOLUTION

In an ever changing world of regulations, the interest of the actual case is in the versatility of the modern earth constructions technique. Adjustability gives the opportunity of introducing new materials without altering the main general features and the zoning of the dam body in full respect of the compatibility criteria, other than the mere introduction of some safety measures at the new contacts between internal zones and at the external boundaries.

To clear up the situation is sufficient to compare the *planned* (Fig. 8) to the *as build* artefact (Fig. 9).

It can be noticed that the original materials are left only in a small part of the as built body and precisely the lowest portion of the transitions (Cm, Cv) and the drains (Ds, Dv); the remaining materials have been supplied by sites different

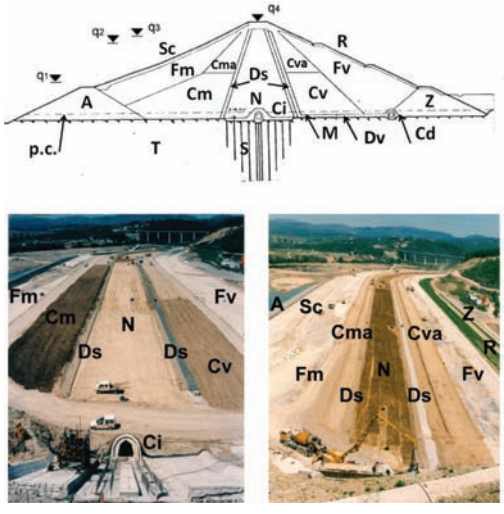

Figure 9. The as build dam body with the work in progress at two different elevations; ( ) *the actual quarries R* (Fig. 11): A cofferdam, limestone, *Sasso di Castro (8)*; Ci adit; Cd drain outlet; Cm, Cv upper and downstream transitions, sand and gravel, *reservoir's area (10)*; Ds vertical drain and filters, aggregates, *plant*; Dv horizontal blanket, aggregates *plant*, Fm upstream shell, limestone, *Tana (11)*; Fv downstream shell, marly limestone, *Tana (11)*; M leakage deviator; N core, silt, *reservoir's area (10)*; p.c. originary ground level; R revetment, sand and gravel, *reservoir's area (10)*; S grouting curtain; Sc rockfill, limestone, *Covigliaio (3)*; Z downstream heel, marly limestone, *Tana (11)*; T foundation soil; sandstone, siltstone, claystone in rytmical sequence (Macigno del Mugello); q_1 reservoir's min level 234,50 ms.l.m; q_2 normal level 252,00, q_3 max level 254,50, q_4 embankment crest level 259,00.

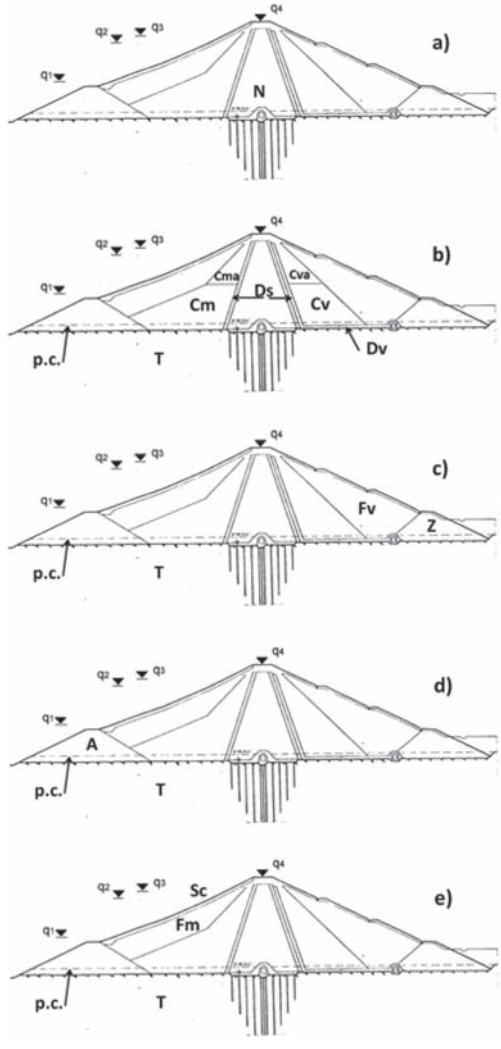

Figure 10. The progressive adjustments a) … e) of the cross section consequent to the severe constraints imposed to quarrying activity (fig. 11): a) N: 9 → 4 → 12 → **10,** homogeneization; Cm, Cv: **10**; Cma, Cva: 5 → **10** washing; Ds, Dv: plant treatment and/or conforming; Fv, Z: 2 → 6→**11**; A: 7 → **8**; Fm: 7→8 →1→**11**; Sc: **3**.

from the original. As a consequence each part of the dam body has an own story, marked by constrains, investigations, revisitation of computation and prescriptions as summarized with the sketches inserted between the design and the final solutions for the cross sections (Fig. 10).

The evolution is illustrated with some details as follows with reference to a map (Fig. 11), where the main monuments M are allocated among the sites R considered in the materials quest.

6.1 *Core N*

According to the design solution the core was made of sandy silt from the site (9) close to Scarperia. After a long negotiation, the Municipality forbidden the opening of a quarry in the area. Therefore, the materials from the localities (4) and (12), were considered, again without success. After other vain attempts, the solution of improving the materials available in the reservoir's area was reconsidered. That recent alluvial material was discarded at design stage on account of its marked heterogeneity; at the construction stage, after extensive experiments, an acceptable homogenization was achieved by means of special precautions in earth moving after recovery from an artificially arranged borrow area.

6.2 *Transitions Cm, Cma; Cv, Cva*

At the design stage the alluvial sands and gravels existing in the reservoir's area intended for the wide transition zones, were found almost fully exploited

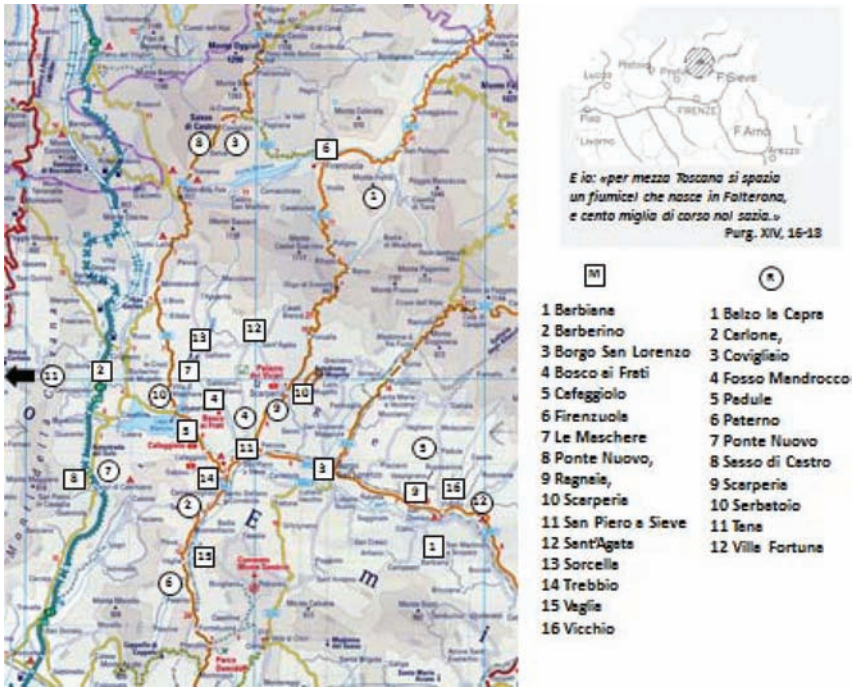

Figure 11. The sites (R) considered in the search for materials among the sites (M) of historic or artistic interest in Mugello.

for different previous uses. The leftover were rich of a fine fraction; in order to satisfy to design requisites it was necessary a treatment in a screening and washing plant (Cma, Cva). The non-selected sands and gravels (Cm,Cv) were set aside for those portions of the transitions not subjected to drawdown; a bond of selected alluvials was placed at the boundary. Moreover, the grain size distribution of the drains (Ds, Dv) was conformed to the situation.

6.3 *Downstream shell Fv*

The planned material was the marly limestone from Carlone (2), a quarry, where soon the operation was interdicted; the interdiction was extended to similar materials in the area. To solve the problem the most convenient supply was localized at Tana (11), where a quarry with a concession for large quantities was in operation. The quality was even better that the required and no further corrections were necessary.

6.4 *Cofferdam*

After the prohibition of the competent municipality, the cofferdam for the river diversion that was designed to be incorporate in the dam body, was not possible to build with the limestones available at Ponte Nuovo (7) near Croci di Calenzano.

In order not to slow down the river's diversion the contractor resorted to the diabasis available at Sasso di Castro (8), where a quarry with a concession for hardly sufficient quantities was in operation. Diabase in dam construction is not usual and required some supplementary investigation. Soon, however, this source was lacking as well for discontinuation of the quarrying activity.

6.5 *Upstream shell Fm*

The interdiction of the widening of the quarrying activity in the area of Ponte Nuovo (7) stimulated the search for alternate solutions: the diabase of Sasso di Castro (8), the sandstone of Balzo la Capra (1), the limestone of Tana (11), the last already considered for the downstream shell. Decision was for this last material, after slight improvement of the grain size distribution. In order to ensure the continuity of the placing work, small quantity of diabase from the site (8) was used in the upstream shell before the closure.

7 THE AS BUILT EMBANKMENT

The *as built* dam body resulting by the substitutions carried on when the work was in progress is markedly zoned; even though, the combination of

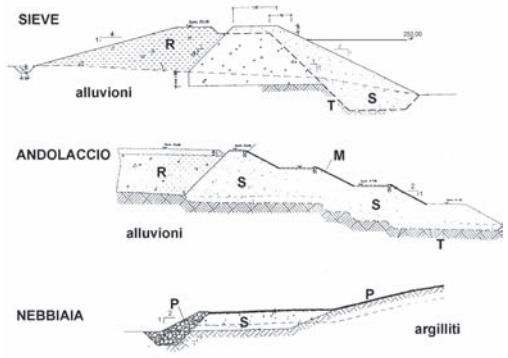

Figure 12. Recovering the reservoir's slopes with poor materials: R stabilizing recharge; S drain, sand and gravel; T transition with geotextils; P protection with blocs.

Figure 13. The Bilancino embankment dam from the left shoulder with the reservoir and its maximum level.

all the numerous variants did not change the type and the geometry of the dam, that was built in full compliance with the design safety requirements and the peculiar features of the landscape; but the situation created non negligible obstacles to the work, that was not interrupted, thanks merely to continuous experiments and an alive computation yard in front of the ever changing prescriptions on materials quality and placement conditions.

The main mass and/or boundary measures that have been introduced in order to keep unaltered the safety level declared at the design stage were the following: selections in the quarries; the *artificial* quarry in the reservoir's area; mechanical preparation; ploughing and scraping; grain size corrections; washing; placement constraints; at the new internal boundaries the contacts were improved by transition materials; the surveillance was also necessary to reinforce with special checks.

It is worth also mentioning that in recovering and stabilizing the reservoir's slopes the available poorest materials were used (Fig. 12).

8 FINAL REMARKS

The design of Bilancino Dam on the River Sieve an Arno tributary near Florence (Fig. 13), has been severely restrained by the opposition of local authorities to the quarrying activity.

The transformations of the dam body have been imposed by exhaustion of the originally planned materials, constraints in quarrying, such as concession discontinuance, interdiction of extending the activity, lack of concessions for new areas. The complexity of the situation was greatly increased by the fragmentation and the contradictory strategies of the municipalities over the territory.

The spreading non propension of local authorities to new quarrying concessions was ascertained necessarily on a *learn as you go* or even *wait and see* basis. As a consequence, the design research during construction was progressively extended at increasing distance from the dam site, with access obstacles, new affairs, and new uncertainty, that proposed itself again for each new quarrying site.

Hence, every spot of the embankment has its own story dotted with constrains, investigations, computations, prescriptions, evolving between the original and the final frameworks.

The difficulties of such an important enterprise of building an earth embankment ($V = 2 \times 10^6$ m^3) in an area rich of peculiar monuments spread over the territory, were overcome thanks to the great versatility and conformability attained by the art of earth dam construction; satisfactory solutions were invented step by step leaving unaltered the general features of the dam body with full respect of the design safety mass and the internal and external boundary requisites (Jappelli, Di Maio, 1990) (Jappelli, et al., 2004).

In order to adjust and fit the design to the ever-changing environmental and administrative local situations, a number of provisions were necessary: a convenient dosage between mass and contact measures to compensate adequately the possible lowering of the safety level declared in design documents; an intense, permanent and prompt design activity; imagination addressed to a wise and cautious engagement of the unforeseen, that is a rate of the small non declared safety margin (robustness, redundancy) existing in every design; the continuous surveillance exercised by the work conduction; the prompt cooperation of the contractor; endurance and strictness, that were not lacking, from the Toscana Region, National Dam Office inspectors and consultants accompanying the steps of a permanent design.

The Bilancino story and other embankment dam constructions in Italy should stimulate the invention of new design strategies considering explicitly among the limit states the critical events consequent to the sudden deficiency of some materials, on which design was based. Such a strategy would require that research activities during construction evolve in parallel and not in series, according to a flow chart far more intricate than the conventional one. Finally, the opportunity should be evaluated to increase somewhat the hidden or perhaps undeclared margin of safety in order to count on a wider reserve to be consumed.

In spite of the difficulties, the case demonstrates that a wise integrated management can produce useful infrastructures without altering the features of a landscape rich of historic monuments and that a large earth construction is not a calamity but an occasion, perhaps unrepeatable, of an agreeable recreation of the territorial features (Figs. 14, 15).

The originally dissentient Tuscan population was tolerant with the gradual exploration of every inch of its territory for the creation of a consistent water capacity intended to the hydraulic protection and to the hydro-potable supply of the City of Florence.

Bilancino dam and related reservoir are by now part of the Mugello landscape, which the Toscana Region has contributed to enrich with other recreational initiatives, matching the formerly suspicious residents and strengthening the social bond in one of the most beautiful lands of Italy.

With reference to the intrinsic complexity of the subsoil of the by now old Vermilion embankment dam in Central California, Karl Terzaghi remarked the necessity *to check on the design assumption during construction and to modify some details of the original design in accordance with the findings. As a result of this procedure the finished structure is as safe and satisfactory as if all the essential properties of the site had been known in advance of construction* (Terzaghi, Leps, 1958).

Figure 14. Herons populate already the Bilancino reservoir.

Figure 15. The Mugello landscape around the Bilancino reservoir.

REFERENCES

Apollonio G., Mannori D., Mugnai A. 1986, Bilancino, una storia che viene da lontano, C.R.I., Firenze, Vallecchi.

Baldovin G. 1988, Bilancino Dam: a reservoir for Florence, Idrotecnica, 2.

Baldovin G. 1991, Notizie sul Bilancino, A.I.I. e ITCOLD, Lincei, Roma.

Becattini M., Granchi A. 1985, Alto Mugello e Val di Sieve, G. & G., Firenze.

ITCOLD 1997, Venice and Florence: a complex dialogue with water, Symposium.

Jappelli R., Di Maio S. 1990, Ricerca progettuale in corso d'opera sul tema materiali, Visita C.I.G.D. al Bilancino.

Jappelli R., Federico F., Marchetti A. 2004, Sull'efficienza dei dispositivi di tenuta delle dighe, XXII AGI.

Penman A.M.D. 1986, On the embankment dam, *Geotechnique*, 36.3.

Sereni E. 1993, Storia del Paesaggio Agrario Italiano, Laterza.

Soliart, 1980, I Medici a Firenze.

Supino G. 1974, La sistemazione del bacino dell'Arno, Com. De Marchi, Vol. II.

Terzaghi K., Leps T.M. 1958, Design and Performance of Vermilion Dam, California, *Journal of the Soil Mechanics and Foundations Div*., ASCE.

Ufficio Commissario Bilancino, 1997, Un invaso per Firenze, un lago per il Mugello, Giunta Regionale Toscana.

Vallecchi 1966, La casa colonica in Toscana.

Geotechnical Engineering for the Preservation of Monuments and Historic Sites – Bilotta, Flora, Lirer & Viggiani (eds)
© 2013 Taylor & Francis Group, London, ISBN 978-1-138-00055-1

Safety and/or security of monuments? An apparent dilemma

R. Jappelli
Formerly: Universities of Napoli, Palermo and Roma Tor Vergata, Italy

ABSTRACT: The Italian word *sicurezza*, the German *Sicherheit* and the Spanish *seguridad* include meanings that in English are distinct in *safety* and *security* and in French in *sécurité* and *sûreté*. The inherent ambiguity, reflecting the engineering measures of *defense* and *protection*, deserves consideration in every technical activity. The topic is relevant to the *safeguard* and possibly to the *secureguard* of important monuments acted upon by enormous tourist pressure. The paper accounts for the reasons that were considered in 1989, when the public access to the Tower of Pisa was temporarily interdicted. Safety (structural, geotechnical, seismic, …) was obviously given attention, but the unpopular decision was mainly supported by considerations of security. Nowadays the world over famous monument has reached the definitive stabilization, thanks to the excellent work carried on by some eminent Colleagues. *Safety* and *security* can hardly be separated in engineering responsibility and should be considered as different aspects of the same problem.

1 INTRODUCTION

In a world threated by all sort of hazards, including those triggered by the counteracting remedies, *protection* and *defence* of objects (men, constructions, natural areas, …) are growing and primary needs.

The very general demand of protection and defence is associated with an increased safety and security claim. This growing expectation can be satisfied by the adoption of suitable measures aiming at the compliance with sets of rules related to the human approach in handling goods, food, materials, utensils and any other mean supporting everyday life. However, the act of complying to or adjusting object's properties yields merely partial solutions, because unfortunately fully reliable means to turn the actual into fully secure objects are not available.

As a matter of fact man has not been able so far to invent a direct mean of *measuring* the hazardous situations with an appropriate index including the varieties and the boundless number of undesired events, that threaten safety and security in the form of *incidents* or *accidents*.

The traditional hypotheses the modern engineer should responsibly integrate by checking and controlling the undesired events, even though of uncertain intensity, occurrence, and evolution. Such events are so transformed into actions that the literature is inclined to distinguish in natural (ageing, floods, earthquakes, …) and anthropic (carelessness, sabotage, terrorism, vandalism, …) (Laqueur, 1987), (Fig. 1). A careful reader could have noticed that in the former sentences some words have been used rather freely as it happens in some documents issued in the main current European languages; this is the case e.g. of the words *incident* and *accident*, *protection* and *defence*, *measure* and *measurement*, *check* and *control*, *safety* and *security*, and possibly others.

Figure 1. Terroristic attack to the *Georgophili*, Florence 1993.

However, in a scientific or technical wording the terms should be given as far as possible precise meanings in order to control misinterpretations and/or ambiguities in the awkward transfer of concepts from one language to another (Jappelli, 2012c).

This well-known general problem deserves special attention should a monument be the object of the analysis.

2 THE MONUMENT

Monuments (monument, Monument, monument, monumento) and monumental buildings are noticeable artefacts, that for some intrinsic property or due to an acquired quality, men consider unrepeatable evidence of the past. Such evidence can be given by historical significance, destination, construction materials, primacy over the landscape, impressive characters like dimensions, compactness, slenderness or else. The broad definition embraces single constructions, ensembles of constructions, peculiar cliffs or slopes, rupestrian cemeteries, old quarries; it includes building foundations and the underlying ground.

Monuments and monumental buildings share the characters of monumentality, a term used to designate at the same time architectural beauty, proportions, harmony related to the landscape and robustness, warranting long lasting survival and/or solemnity derived by a peculiar geometry in a lonely site (Fig. 2); the past possibly occurred deep transformations should also be considered among the singularities. An ensemble of buildings may be remarkable for historical reasons or special events (Fig. 3); monumentality could also be ascribed to some unedifyed sites (Fig. 4).

Figure 2. With its massive structure dominating the lonely landscape of Apulia, Casteldelmonte is one of the magnificent monuments of the Swabian period (1270) in Southern Italy (De Agostini, 1955).

Figure 3. An overall view of Pompei in the area of *Via dell'Abbondanza* (De Agostini, 1969).

Figure 4. The monumental cliff of Pantalica with the cavities of the Neolithic rupestrian cemetery.

Italy holds a large portion of the world monumental patrimony covering a wide assortment of different ages; the peculiar characters as for variety and beauty have been depicted by famous painters (Fig. 5).

The opportunity that for whatsoever purpose the Monument (M) be considered composed with three constituents Structures (S), Foundation (F), Ground (G) bound in an unique physical system has been recommended elsewhere (Jappelli, 2005). However, another important character of a (M), that is the peculiar fascination attracting large masses of visitors (Jappelli, 2012a) should not be disregarded; the intensity of this attraction power has greatly increased with time, thanks to the touristic call; it is hardly the case to mention the Coliseum supporting a flux of almost 5000 visitors per day and the Tower of Pisa, even though the anthropic action is very differently distributed in the body of the two monuments.

Figure 5. Detail or the San Sebastiano painting by Andrea Mantegna (1431–1506) in a landscape offering the image of a monument in precarious equilibrium on top of a cliff.

Modern plans related to an important (M) should not neglect such an anthropic component, which is acquiring an increasing weight on different aspects of the safety and security problems. Therefore, and with reference to the object of the paper, it seems appropriate to integrate symbolically the former system with a lively component (A):

$$(M) = (S) + (F) + (G) + (A)$$

Moreover, the mentioned irresistible attraction has far-reaching impact on the relationship of the (M) itself with the environment (E); the interaction reveals itself with the wear of the artefact and reciprocally the vulnerability of the visitors in case of emergency. Therefore, the environment (E) should be conveniently imagined made in turn of a physical or natural (N) and an anthropic component (A):

$$(E) = (N) + (A)$$

3 SAFETY AND SECURITY

In the common language the words *safety* and *security* both imply that something can be regarded as free from danger and are frequently interchangeable; *safe* however is rather applied to a person or thing that is out of an escaped danger or passed beyond, the reach of danger as in the expressions *the ship is safe in port* (Fig. 6) and *food safety from the farm to the* table (Lindner, 2007); *secure* is

Figure 6. Ships searching for *safety* in a port.

applied to that, about which there is no need to fear or *worry as to feel secure about the future* or *the foundation of the house does not seem very secure*. The same shade of meaning, actually associated to complementary aspects of the problem, seem to exist in the French words secure and sure; but this is not the case in other languages, as *sicurezza*, *seguridad*, *Sicherheit* are more comprehensive words.

Safety and security are said *public* when the situation warrants for a peaceful course of people activity.

Unfortunately, a convincement has taken root in the public opinion; that is an attractive safety criterion, according to which the old buildings could be considered safe, just because they have successfully supported since long time very severe actions. Experience and theory show consistently that this criterion is fallacious, because buildings (like men) are not always ageing in good health and consequently safety decreases inexorably with time. As a matter of fact human artefacts are involved in an enduring process of transformation, that initiates with the occasional collapse of fragments and proceeds until the construction takes up gradually the title of *ruin*, *remain*, *remnant*, *maceria*, *vestige*, *trace*, …; the building survives possibly in a state of *dust* (Jappelli 2012a).

The *incident* (incident; incidente, Vorfall; incidente) is an event due to natural or artificial causes during the life of an object; should the happening be undesired or unexpected, the incident turns into an *accident* (accident; accident; accidente; accidente).

The accidental fall of the cornice (Fig. 7) or similar architectural details is undoubtedly caused by an insufficient local *safety* of a building.

However, such incidents or accidents rise at the same time a problem of *security* referred to occasional pedestrians; this last problem the public opinion inclines to catch better than the first in the erroneous convincement that a full *security* could be attained, e.g. by strengthening the surveillance or with similar *measures*. More precisely, a second

Figure 7. The cornice on the verge of failure from the top of the Politeama Theatre in Palermo, 1993.

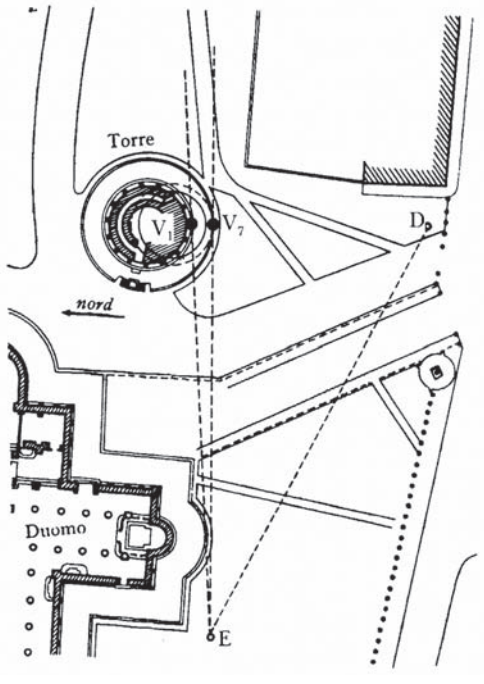

Figure 8. Geodetic survey of the inclination of the Tower of Pisa (Viggiani, Squeglia, 2005).

fundamental fallacy that in a number of situations mere checks or monitoring measures would solve the problem is very common.

The topic arises growing concern for the future of the patrimony of monuments and mobilizes engineers, architects, and restorers. Therefore, the culture of security around some important monuments, the safety of which is difficult to assess, demands great care, as a consequence of the endless ever increasing flux of visitors. In some old constructions tourists are densely compacted in narrow spaces, not at all fit for emergency; in those situations *safety* and *security* are not independent and cannot be easily separated; all the more with the decrease of safety (structural, geotechnical, seismic,…) it is right to pay increasing attention to the related *security*, that is diminishing as well.

As a consequence, in the realm of security a variegated culture is spreading with the concourse of a number of different disciplines inspired by the common interest for the *protection* of the population against hazards of different kind due to natural and human actions, as well as for the *defence* of the environment. The figures of people of an urban agglomerate that should be secured or dispersed in case of emergency are very different; the following can be considered in their order of magnitude: from a lift 10; from a small boat 10^2; from an important monument 10^3; from a large ship 10^4; from a city struck by an earthquake or from a stadium 10^5; from Vesuvio's slopes 10^6; and so on.

Confusion may also arise in some languages, as in Italian, between the terms *measure* and *measurement*. The well-known word measurement (mesure; Messung; misura; medida) indicates an experimental determination of a physical property of an entity, as taught by Physics (Perucca, 1959); with reference to the monuments the measurements under way on the Tower of Pisa (Fig. 8) are exemplary (Viggiani, Squeglia, 2005). *Measure* (mesure; Massnahme; provvedimento; proveimiento) denotes currently an action or procedure intended as a means to an end, a remedy, an intervention.

4 A HOLISTIC APPROACH

In the writers opinion the two aspects of safety and security could fall in a unique definition, provided one considers the living matter (A) part of the Monument (M) and includes the human (anthropic) actions among the possible undesired events.

In the oversimplified sketch (Fig. 9) the monument (M) is immersed in the environment (E); in both systems the physical and human constituents are included. In order to imagine the interaction

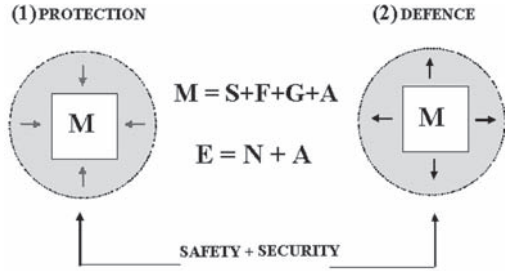

Figure 9. Safeguard and *Secureguard* demand Protection and Defence: S-Structure; F-Foundation; G-Ground; N-Natural; A-Anthropic.

between the two systems, let us separate the actions of (E) on (M) from the actions of the latter on the former.

The distinction between safety and security invites to the consideration of different aspects of the related remedial measures; these can be best specified by the attribution of different meanings to the words *protection* and *defence*, that are almost synonymous in the common language.

The control of the possible effects of the actions exerted by (E) on (M) may require some measures on (M) itself; such measures one could appropriately designate with the general term *protection*.

In the jargon of the historians of Architecture the word *protection* (protection; Schutz; protezione; proteccion) refers to the bastions invented in XV and XVI centuries *to improve the protection of the city walls against the fire-arms that made inefficacious the middle age forts* (Pisano, Capecchi, 2010).

The same word indicates in general the measures devised to counteract the undesired actions directed against an object, e. g. building or man. Protection can be accomplished with measures aimed to counteract the actions before these hit the object or with measures on the object itself.

Examples of the first type of total or partial human protection are armours, veils (Fig. 10), umbrellas and similar; constructions can be protected by cofferdams, facings, shields (Fig. 11), prescriptive measures and similar. Protective measures, even though often *post mortem*, are entrusted to some authorities entitled to provide help to people liable to be struck by calamities.

It is important to remark that in the common language the tendency exists to restrict to the sphere of security the remedies aimed at *protection*, that is to the *human* component (A) of the (M).

Should interdiction of the public access be applied to a monument such a protective measure would be hardly perceived in terms of an increase of *safety*, because the human is but a very small

Figure 10. The veiled Jesus Christ by Giuseppe Sammartino (1753) guarded in the Sansevero Chapel, Naples, is a splendid example of *protection*.

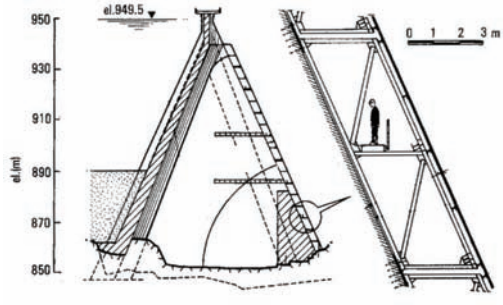

Figure 11. The recently installed thermic shield on the downstream face of Ancipa dam (Ruggeri, Adami, 2011).

fraction of the own weight; however, such an extreme protection plays a great role in increasing *security*. The example of the Tower of Pisa (see par. 5) is significant.

Let us now consider the reciprocal problem of the effects of (M) on (E); these effects, e.g. originated by materials that could be harmful for the

environment (E), are not necessarily symmetrical of the effects of the last on the former.

The measures *controlling* the effects of (M) on (E) could be best designated by the term *defence* (defense; Verteidigung; difesa; defensa) as in the expression *soil defence* or *soil conservation*.

The full *safety* and *security* of a (M) can only be achieved with the concourse of (1) *protection* measures towards the action exerted by (E) on (M) and (2) *defence* of the (E) against the actions transmitted by the (M).

Hence, *safety* and *security* around a monument are tightly interconnected in a system in which Structure, Foundation and Ground coexist permanently with the human component represented by visitors and janitors. In such a complex a number of processes evolve with different laws; measures aimed at the control of the undesired effects can be successful, provided the various components of the system and its interactions be regarded and evaluated in close relationship with the environment, from which should not be separated, other than for the convenience of study and analysis.

Such an overall approach complies with the modern demand of a broader conception of national security, one that takes into account such environmental concerns as resources, pollution and populations.

5 THE TOWER OF PISA

Twenty-two years ago the pro-tempore Ministry of Public Works appointed an "ad hoc" Committee[1] with the task of investigating the actual *sicurezza* of the Tower of Pisa and the efficiency of the emergency measures with possible suggestions for different solutions. The C. was confronted with the *frontal question whether the Tower of Pisa is safe or not* (Jappelli et al., 1999).

The Committee laid its considerations on analysis of previous records and on direct observation; the conclusions of a thorough debate were the following.

The general and local margin left from the main ultimate limit state of the ensemble *Structure*, *Foundation*, *Ground* was judged very limited.

An ultimate limit state in the Structure, while the Ground is still in service, so to say, was given major importance. Among the other reasons of concern, the persistent trend of the increase of the rate of movement; the evident high sensitivity of the Monument to a number of external actions, such as wind, soundings, ground water level oscillations; the enduring high level of uncertainty in identification of the parameters controlling safety and the definition of their critical values; the presumably high state of stress and the ascertained local deterioration of the masonry; the inadequacy of the existing monitoring system; the concern that permanent safety measures could be taken only on a long term basis.

Concern was expressed by the C. members about the efficiency of a provisional framework (*girello*) predisposed on the site with the purpose of supporting temporarily the (M) in case of a dangerous increment of the inclination.

However, after a naïve confession of the local responsible, the C. was led to acknowledge that the assemblage of the existing structural elements of the *girello* (Fig. 12) had been never attempted and that the related instructions were not immediately available. Moreover, the C. expressed perplexity on account of the possible iatrogeneous effects of such a trestle on the ornamental parts of the Monument and on the masonry itself.

The continuous intense flux of visitors was found *uncontrolled*; the possible undesirable consequences of an emergency occurring among people distributed along the narrow spiral staircase (300 steps) from the entrance up to the longed-far bell chamber crowning the Monument at the 8th level, can hardly be imagined. In case of emergency the evacuation would have taken considerable time in a

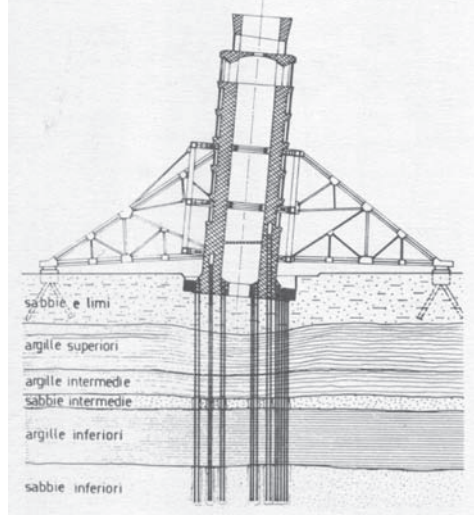

Figure 12. The *girello*, a provisional trestle devised for a temporarily support of the Tower of Pisa in case of emergency (Diamanti, 1980).

1. The Committee operated during the year 1989; members were: Calzona R., Giangreco E., Guerrieri F, Jappelli R., Pozzati P., Scarselli M., Selleri F.; Secretary was appointed Del Monte M.; coordination was entrusted to the A.

climate of panic among the visitors thronging the narrow passage (1×2 m^2) (Fig. 13) with increasing density toward the exit; the panic would presumably grow on account of the communication difficulty among people from different parts of the world, just as occurred on the occasion of a recent shipwreck (Jappelli, 2012b). It should be added that at the time the Monument was not endowed with whatsoever emergency plan, nor the janitor and the accompanying persons were aware of what to do, should a situation of danger suddenly emerge.

The state of mind of the visitors leaving the fascinating stairway of the Tower can be best described by the following sentences by two eminent architects:

... Seven sections of an upward spiral flow into seven rings that can be scanned by a progressive, round-angle line of vision; that is how a unique and overwhelmingly original phenomenon of the history of architecture occurs; a visual device consisting of a fixed and single upward route which offers users the opportunity to open up seven, not overlooks, but exceptional gyroscopic views in levels rising up to 50 metres..."

(C.L. Ragghianti)

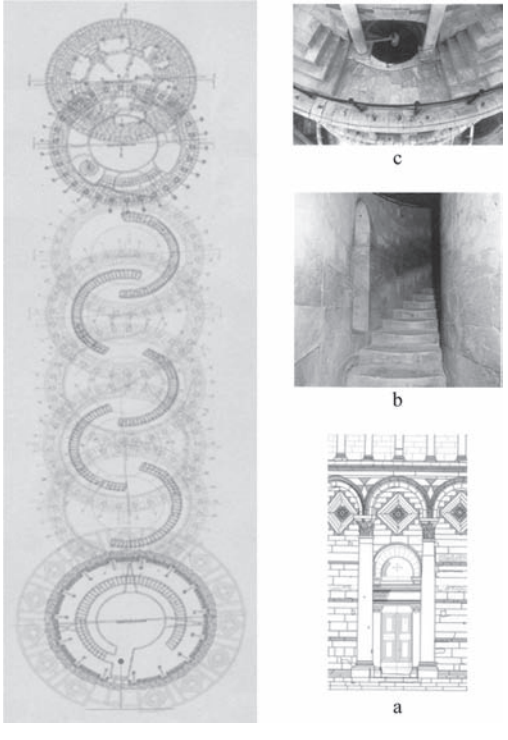

Figure 13. The one-way spiral staircase offering the visitors the opportunity of a splendid gyroscopic view from the eight levels of the Tower of Pisa up to the height of 50 m; a) entrance; b) staircase; c) exit at the 7th level.

... Our light palpitations will grow for the puzzling fatigue that the stairs force on us and for the precipice opening up deeper and deeper at our feet, with no shelter at all for any of the slanting storeys. And as we start moving up again from one storey to the next within the spiral staircase that now urge «us to be quick, now steep and wearying, almost stops us and makes us lose sight of that glimmer of the sky from the door we are not completely sure if that step giving way under our feet or that raising against us are not actually due to the whole building suddenly giving way…"once al the top and after enjoying the view, we turn and move out of the soft and safe lawn, heaving a secret sigh of relief even if looking back with a hint of longing .."

(P. Sanpaolesi)

Hence, among the reasons carefully considered in 1989, supporting the decision of interdicting temporally the access to the Tower, the public *security* was dominant over the structural and geotechnical *safety*. In its final report the C. concluded that the situation was not sufficiently *sicura* (safe+secure) and suggested that the Tower of Pisa be closed to the public, at least until adequate transitory safeguarding and possibly *securguarding* measures could be taken.

The opinion expressed by the C. was submitted to the advice of the Superior Council of Public Works. In its full session of November 28, 1989 the Council agreed unanimously with the proposal (CONSULP, 1989). As a consequence, the Ministry signed a decree, that appeared on the issue of December 6, 1989 of the Official Gazette of the Italian Republic under the title: *Interdiction of the access of the public to the Tower of Pisa* (Min. LL.PP.,1989).

Even though an encouraging consensus was expressed by authorities in the fields of History of Architecture and more generally Human Sciences, the public opinion and particularly the local community were understandably shocked by the measure, as it appeared drastic and perhaps not opportune.

The press was not mild with the members of the C. indicated as responsible of a very unpopular measure. In fact, they experienced the feeling that Arthur Casagrande depicted with the following sentence at the time he was member of the Committee for drafting the Boston Building Code:

If someone would want to write a book on how not to make friends, he might well suggest, as one of the most successful methods, serving on a committee...

(Casagrande, 1958)

It is worth mentioning also that the C. was not given the opportunity to undertake any specific investigation; nor the travel expenses were refunded.

However, the interdiction opened the way to the later step of activity, that in the following decade was very successfully completed (Jamiolkowski, 2012).

In the meanwhile, research on the specific subject of the safety of leaning towers was not discontinued (Como, 1993) (Federico, 1996); (Federico Ferlisi, 1999a, 1999b) (Jappelli, Federico, 1995).

6 CONCLUSIVE REMARKS

Ten years after the *Reconsignement of the Tower to the City of Pisa*, the Council of Public Works, the Council of Cultural Activities and the Committee for the Surveillance of the Monument celebrated the event in a Meeting held on May 18, 2012, with the contributions of the Authors of the brilliant enterprise.

The great success of the stabilizing measures as well as the reassuring perspectives for the status of one of the most famous monuments of the world were evident. In the well documented reports of the renowned colleagues (MBAC, 2005) the fundamental reasons why in 1989 the access to the Tower of Pisa was temporally interdicted, are fully confirmed.

The experts engaged for the actual ensuring measures of the Tower of Pisa ended up their work with the courageous assessment that the so far achieved stabilization is *definitive*. This sounds like a declaration that the actual inclination does not require further *control*, but a mere *check*; this means that from now on the world over known geometry of the Monument is permanent or that the inclination doesn't increase nor decrease "too much".

For their brilliant results the Colleagues deserve the best compliments of the international community.

The achieved control of the margin of safety relieves the problem of the *safeguard*, but has positive effects also in the realm of security, even though a satisfactory answer to the question of *securguard* is left to future generations, as for other famous monuments (Fig. 14). Obviously, the awkward question proposed to the 1989 Committee concerning the actual degree of safety against the main known limit states, is also waiting for a quantitative answer.

The successfully achieved stabilization of the geometry, to which the Tower of Pisa owe its fame, demonstrate once again that *safety* and *security* must be laid on an unitarian base comprehensive of the lively component in both the strictly associated spheres of *protection* and *defence*, which are merely different aspects of the responsibility of architects and engineers.

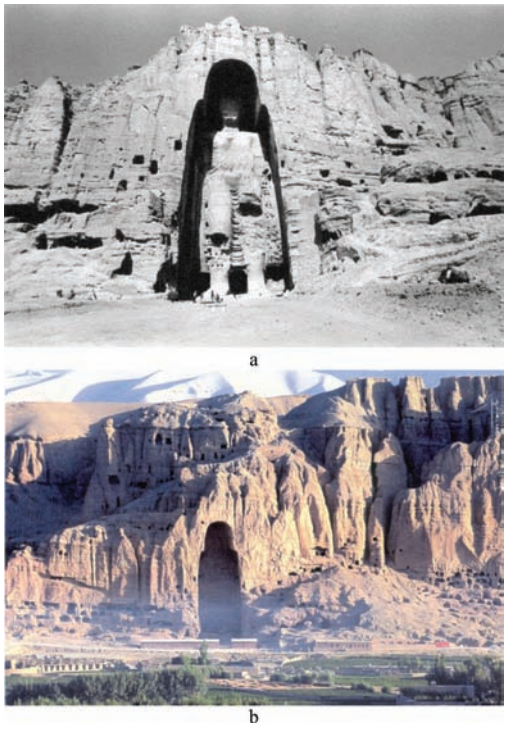

Figure 14. The monumental statue of Budda destroyed by iconoclasts at Bamyan, Afghanistan, in March 2001: a) *ante mortem*; b) *post mortem*.

It is worth mentioning that success achieved by the experts in the old-new branch of *Pisology* was firmly laid on and well supported by a long run platform of experience. The act of conforming present measures to past performance was the foundation that gave the opportunity to the Greek *imperial spirits* of building up the present from the past and to impose their seal on the world's heritage:

But Greece and her foundations are
Built below the tide of war,
Based on the crystalline sea
Of thought and its eternity;
Her citizens, imperial spirits,
Rule the present from the past,
On all this world of men inherits
Their seal is set.

P.B. Shelley[2]

The case of Pisa should stimulate Europe to attain an unitarian view in preserving its historical unrepeatable patrimony of culture and monu-

2. Semichorus of Greek captive women, Hellas, 1821.

ments. However, such a noble goal is still far ahead as demonstrated by the fact that in the prospect of the separation of Greece hardly some isolated voices were raised so far to claim that such an event would be for the future United States of Europe a loss in terms of culture and democracy well heavier than could appear from the current dissertations on mere economical ground.

REFERENCES

Casagrande A., 1958, Preface to the Draft for a revision of Part 29 of the Boston Building Code. Journ. Boston Soc. Civ. Engineers, January.

Como M., 1993, Plastic and visco-plastic stability of leaning towers, Int. Conf. "Physics Mathematics and Structural Engineering", C.N.R., Elba, Italy, pp. 187–210, June.

CONSULP, Ass. Gen., 28 novembre 1989, Voto n. 593, Torre di Pisa, Relazione del C.T.S. sullo stato di sicurezza del monumento.

Diamanti L., 1980, Pali trivellati di piccolo diametro, XIV AGI, I, pp. 153–162.

Federico F., 1996, Perturbation factors of the stability of leaning towers. 2nd. Int. Conf. on "Multi-purpose High-Rise Towers and Tall Buildings", Singapore, July.

Federico F., Ferlisi S., 1999a, Time evolution of stability of leaning towers. Sixth Int. Conf. STREMAH 99, Structural Studies, Repairs and Maintenance of Historical Buildings, Dresden.

Federico F., Ferlisi S., 1999b, Effects of a counterweight on tilt evolution of leaning towers, Sixth Int. Conf. STREMAH 99.

Istituto Geografico De Agostini, 1955, Castelli d'Italia.

Istituto Geografico De Agostini, 1969, I documentari, 15.

Jamiolkowski M., 2012, Il Comitato di Salvaguardia della Torre di Pisa, Incontro, La Torre di Pisa a dieci anni dalla conclusione dei lavori, Cons. Sup. LL. PP., maggio.

Jappelli R., Calzona R., Giangreco E., Gurrieri F., Pozzati P., Scarselli M., Selleri F., 1999, Interdiction of the Access to the Tower of Pisa, Workshop on the Tower of Pisa, Pisa, July 8, 9.

Jappelli R., 2005, Le système sol-monument; propositions pour une approche intégrale, Revue Française de Géotechnique, n. 113, 4.

Jappelli R., 2012a, Engineering the ruins of constructions, Lagrangianum 2008, in "Models and Methods in Civil Engineering", vol. 61, pp. 97–122, Fremond a. Maceri Eds, Springer.

Jappelli R., 2012b, About the Giglio tragedy, L'Acqua, 1.

Jappelli R., 2012c, Operating reservoirs of words, L'Acqua 3.

Jappelli R., Federico F., 1995, Remarks on geotechnical safeguarding measures for leaning towers. Proc. 1st Int. Congress "Science and Technology for the Safeguard of Cultural Heritage in the Mediterranean Basin" Catania, Siracusa, Nov.

Lane E.W., 1935, Security from Under-Seepage Masonry Dams on Earth Foundations, Trans. ASCE, vol. 100, pp. 1235–1351.

Laqueur W., 1987, Reflections on terrorism. Dialogue 3.

Lindner Line Friis, 2007, Food Safety: European Policies and International Perspectives, in Broadsheet, ICCR Foundation, Annual Report, p. 7.

MIN. LL.PP., 1989, Interdizione dell'accesso del pubblico alla Torre di Pisa, D.M. n. 92, 1 dic., G.U., Suppl. Ord. n. 285, 6 dic.

MBAC, 2005, Volume Speciale, La Torre restituita: gli studi e gli interventi che hanno consentito la stabilizzazione della Torre di Pisa, Ist. Pol. e Zecca dello Stato.

Perucca E., 1959, Fisica Generale e Sperimentale, UTET.

Pisano R., Capecchi D., 2010, Il ruolo della Meccanica ne Le Fortificazioni di Bernardo Lorini, III AISI, Tomo II, pp. 797–807.

Ruggeri G., Adami S., 2011, Lo sviluppo dell'energia elettrica in Italia, L'Acqua 6.

Terzaghi K., 1922, Sicherung von Bauwerken gegen Grundbruch, Wasserkraft, München.

Viggiani C., Squeglia N., 2005, Studi ed Interventi del Comitato Internazionale: Aspetti geotecnici, MBAC, Vol. Speciale, La Torre Restituita, Ist. Pol. e Zecca dello Stato.

This page intentionally left blank

Geotechnical Engineering for the Preservation of Monuments and Historic Sites – Bilotta, Flora, Lirer & Viggiani (eds)
© 2013 Taylor & Francis Group, London, ISBN 978-1-138-00055-1

Strong motion record processing for the Athenian Acropolis seismic response assessment

I.S. Kalogeras
Institute of Geodynamics, National Observatory of Athens, Athens, Greece

D. Egglezos
Civil Engineer

ABSTRACT: Although extensive restoration works took place at Athens' Acropolis during the last decades, it was only 2006 that Institute of Geodynamics, National Observatory of Athens (NOAIG) and Acropolis Restoration Service (YSMA) cooperated towards the seismic instrumentation of the site aiming to study the response of the monuments against an earthquake.

A brief description of the installation phase is presented here, showing the techniques used to overcome the difficulties and the special characteristics of the archaeological site. Characteristic records from various earthquakes are processed, showing the complex properties of the hill and the monuments. Although no strong earthquake occurred in near field during the up-to-now operation of the array, specific records are processed and presented. Furthermore, some comments are presented for the Tohoku 2011 and Van 2011 earthquake records. The ambient noise monitoring via PQLX software can also lead to some useful results concerning structural properties of the Parthenon and local characteristics of the artificial fillings installation. Selected strong motion records are used for the monument response analysis within the frame of an earthquake resistant design. 2-D nonlinear analyses along a characteristic section of the Acropolis were also performed for a preliminary calibration of the dynamic properties of the geomaterials.

1 INTRODUCTION

It is well known that the broader Aegean area is characterized by high seismicity that affects the variety of building stock. The construction type is classified as an important issue concerning the extent of damage, amongst other parameters, that also contribute even further (e.g. seismic source properties, propagation path of seismic waves, local soil conditions).

The archaeological sites and their monuments comprise a special case of structures, since they were built in the past, with the technological knowledge of their age, and also because they have suffered a number of strong earthquakes, as well as human interventions.

The Acropolis of Athens was the greatest and finest sanctuary of ancient Athens during its Golden Era (5th century BC), dedicated to city's patron, the goddess Athena. The Acropolis of Athens is a complex of monuments (comprising the Parthenon, the Propylaia, the Erechtheion, the Temple of Athena Nike etc.) and it was included in the World Heritage List since 1987.

After the liberation from the Ottoman occupation and the establishment of the Greek State excavation and restoration works took place. The most important of them were that under the responsibility of N. Balanos during the early 20th century and the most recent one after the establishment of the Committee for the Conservation of the Acropolis Monuments (ESMA) in 1975 and of the Acropolis Restoration Service (YSMA) in 1999. Some efforts were made for the monitoring of strong ground motions after the strong earthquake of February 24, 1981 (M6.7), which affected the Athens urban complex and some of Acropolis monuments; nevertheless, none of them was successful and no record was obtained even during the Athens earthquake (September 7th, 1999 M5.9).

Taking into account the fore-mentioned aspects, the Institute of Geodynamics of the National Observatory of Athens (NOAIG) and the Acropolis Restoration Service (YSMA) started a collaboration in 2006, with the installation and the permanent operation of a free-field accelerograph, followed by the deployment of an accelerographic array of 6 more instruments in 2009.

A brief description of the installation phase is presented here, showing the special characteristics of the archaeological site. Moreover, specific records obtained during the array operation were processed and are commented in the paper, together with the ambient noise monitoring, to assess the effect of subsoil amplification at the installation site.

2 TECTONICS AND SEISMICITY

Attiki region, in central Greece, is considered as an area of low seismicity. Strong Earthquake sources are located mainly to the west (eastern Corinth Gulf) and to the north (Thiva basin, Evoikos Gulf, Oropos area) and are associated to an extensional N-S tectonic field. Athens suffered from historical and instrumental earthquakes from these areas, the most recent of which was the one of September 7th, 1999 M5.9 caused 143 deaths, about 800 injuries and about 40 collapsed buildings (Elenas, 2003). The tectonic field and the seismicity is described by various authors (Galanopoulos 1971, Ambraseys & Jackson 1997, Papazachos & Papazachou 2003, Rondoyianni et al., 2000).

A comprehensive review on the long-term seismicity of Athens was presented by Ambraseys (2010) in Academy of Athens. Near the historical center of Athens, within a radius of 10 km only small, shallow normal faults exist, which are not capable to produce any earthquake. All the known active faults are more than 10 km away from the center of Athens and are of short length, implying that the earthquakes originated by them are only felt in Athens, with no damage at all. So, it seems from the systematic historical studies and the recent earthquakes that the seismic hazard in the center of Athens is rather low. However, Ganas et al. (2005) concluded that events with M_s between 6.4 and 6.6 are to be expected from possible movements of the Attiki mapped faults.

Table 1 summarizes the main historical and instrumental earthquakes that affected the Acropolis and the monuments taking into account the literature search (Galanopoulos 1960, Papazachos & Papazachou 2003) and using attenuation relations (Skarlatoudis et al., 2003) to estimate PGA.

Acropolis was constructed on a small Late Cretaceous limestone hill of about 150 m in height, which lays on the marls and sandstone of Athenian schist series (Andronopoulos & Koukis 1976). Limestone is exposed on the hill and all the monuments were built on this rock. The hill surface was leveled with artificial fill and a Circuit Wall surrounded as fortification of the site. The artificial fill thickness varies with a maximum of 10–18 m towards the south wall and of 3–6 m towards the north wall. Figure 1 shows a geological map of the hill (Higgins & Higgins 1996).

Table 1. Earthquakes that affected Acropolis.

Year	Site	Distance km	M	PGA* cm/s^2	Effect
426 BC	Atalanti	140	?	?	Parthenon
1705	Oropos	35	> = 6.0	45	South wall
1785	Oropos	40	> = 6.0	40	North wall**
1805	Oropos	40	?	40	Parthenon, North wall**
1874	Athens (?)	?	?	60(?)	North wall
1894	Atalanti	100	6.9	30	Parthenon
1938	Oropos	37	6.1	40	South wall
1981	Korinthos	77	6.7	30	Parthenon
1999	Athens	20	5.9	65	Propylaia

* Estimated.
** Egglezos and Moullou, 2011.

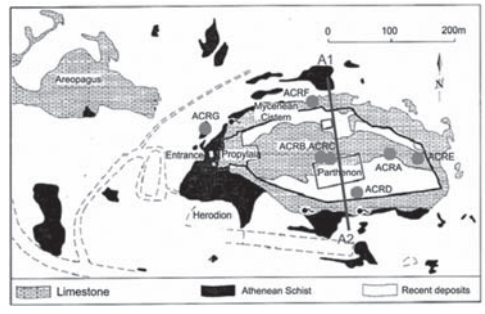

Figure 1. Geological map of the Acropolis hill (revised from Higgins & Higgins 1996), showing the main topology names, the accelerograph installation sites (grey circles) and the section A1A2 of Figure 12.

3 ARRAY DESCRIPTION

After the YSMA expressed interest, the NOAIG established a digital 3-component accelerograph on the Acropolis hill (emergence of limestone) with a 12 bit resolution. The accelerograph (ACRA) was connected on the internet through the Public Administration Network "Syzefxis" so that its management (monitoring the condition of the instrument and receiving data), could be carried out at distance by the central installations of the NOAIG at the Thission. This resulted in the first seismic events recorded on the Acropolis hill. The earthquakes of Andravida Achaia (8/6/2008, M6.5, distance 195 km, PGA = 0.006 cm/s^2) and of Mantoudio Euboia (14/10/2008, M5.6, distance 100 km, PGA = 0.004 cm/s^2), were specifically

recorded. Although the values of the greatest seismic movement were particularly low, it is worth noting that an accelerographic instrument of low resolution was triggered by earthquakes of moderate size at a great distance.

Since 2008, NOAIG installed six digital 3-component accelerographs of the latest technology with a 24 bit resolution, within the project "Development of a Network of Accelerographs in the Acropolis Area". Six sites were chosen for installation in order to cover various local characteristics: a site (ACRG) on the Athenian schist (geological bedrock), a site (ACRF) on the limestone at the base of the north Wall, a site (ACRE) on the east side of the hill (on limestone next to the Wall), a site (ACRD) on the south side of the hill (where there is the thickest artificial fill), a site (ACRB) at the base of one of the columns of the Parthenon north colonnade and a position (ACRC) on the architrave of the same Parthenon column. Figure 1 shows the installation sites noted by grey circles. Detailed description of the array deployment can be found in Kalogeras et al. (2010).

Various factors were kept in mind for the installation of each instrument, mainly to keep to a minimum interference with the monument and the public, and to protect the equipment from the difficult weather conditions that prevail (for example, protection against lightening strikes, supply of 12VDC to the instrument sites, etc.).

At each location, the equipment was placed on a small foundation base and comprises the accelerograph, the fused 12VDC box, the timing unit (GPS), the lightning protector and the antenna for wireless network connection and data transmission.

The equivalent connections of the antennae, as well as the electrical current of 220VAC with surge protector and battery charger were placed at selected sites. The orientation of all the accelerographs is X(+)N0°,Y(+)N90°. In certain cases techniques were employed to limit the wiring used (for example passing electrical power along with data on Ethernet cabling, PoE), while special care was devoted to the wireless equipment (limiting the signal, security in sending the signal, etc.).

Two computer systems were installed outside of Acropolis site, in the YSMA office and in NOAIG premises, to function as servers and were designed to have direct contact with the instrument at each installation position. The systems attend to a) monitor the condition of each instrument and setup the instrument, b) gather data in real time from each instrument, c) store the data, d) have the capacity to forward the data of the instruments to other research agents, e) send warning signals to various recipients (e.g. station out of operation, loss of power, loss of internet connection, memory remaining etc.).

4 AMBIENT NOISE MONITORING

The continuous streaming of the modern Acropolis accelerographic array provides the ability to monitor the long-term seismic noise at each site, by using the PASSCAL Quick Look eXtra (PQLX) software tool (McNamara & Boaz 2011) based on the McNamara & Buland (2004) approach. With this method the power spectral densities (PSDs) and their corresponding probability density functions (PDFs) can be estimated at each installation site using the continuous waveform data, without removing earthquakes, system transients or instrumental glitches. The method was applied for the ambient noise levels in Greece as recorded by the Hellenic Unified Seismic Network (Evangelidis & Melis 2012). The same method was also applied for the 66 continuously recording stations of the strong motion network of NOAIG. The instrument response is removed from each PSD in order for the segment to be compared with the low—or high-noise model (NLNM and NHNM) defined by Peterson (1993). The PDFs monitoring provides the array performance and the level and source of noise at each site. The main source of noise at high frequencies (7–16 Hz, 0.07–0.14 s) is the cultural noise, which can be observed during working hours near populated areas. Acropolis hill is characterized by high cultural noise mainly due to the monument restoration works (motion of heavy machinery, crane operation, transport of heavy monument members etc.), but to the high tourist traffic as well. More over, since the installations are true free-field, the weather conditions may produce diurnal and seasonal noise variations.

Figure 2 presents the ambient noise monitoring for 2 years of operation of the Acropolis accelerographic array. The black line is the new high-noise model NHNM defined by Peterson (1993). The dark grey shadowed area marks the area between

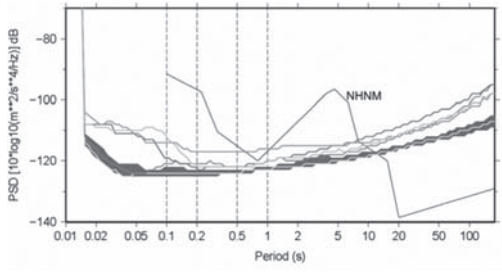

Figure 2. Ambient noise monitoring for 2 years of Acropolis array operation. The cultural noise exists within the range of 0.07 and 0.014 s, quite higher for Acropolis site compared to the minimum of the NOAIG strong motion array (dark grey shadowed area).

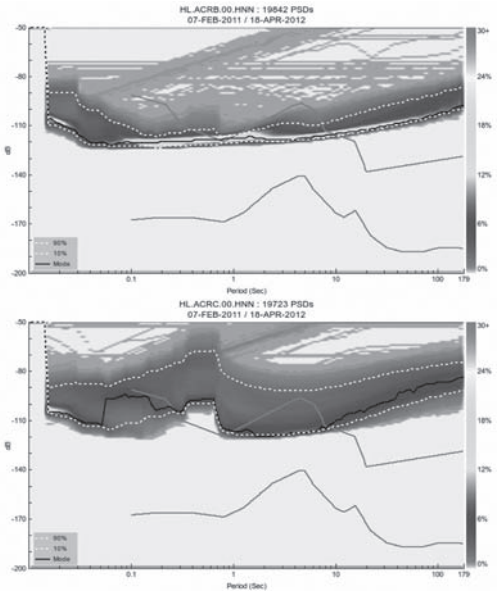

Figure 3. PDFs of PSDs for the N-S horizontal component of ACRB (top) and ACRC (bottom). The two individual grey lines stand for the NHNM (upper) and NLNM (lower) respectively (Peterson 1993), while the black line represent the mode for each PDF.

the minimum 10th and 90th percentiles of all NOAIG 66 strong motion stations. ACRE shows the lowest noise level for all the Acropolis stations.

Figure 3 shows the PDFs of PSDs for the N-S horizontal component of ACRB (top) and ACRC (bottom). The black lines represent the mode for each PDF. The grey lines are the new low- (NLNM) and high- (NHNM) noise model defined by Peterson (1993). The dashed lines mark the area between the minimul 10th and 90th percentiles of all NOAIG 66 continuously recording strong motion stations.

There is significant difference in the level of noise between the two sites within the periods of 0.04 and 1 sec.

Since the two instruments record noise from the same sources, this difference probably represents the response of the monument itself. The same difference is apparent in noise recordings of E-W horizontal component of ACRB and ACRC.

5 SPECIFIC RECORDS PROCESSING

During the period of array operation no near-field significant earthquake occurred. However, due to the operational characteristics of the 6 modern accelerographs (continuous recording and real time transmission), a number of earthquakes with different characteristics are recorded and processed. For indicative reasons specific records are presented here.

5.1 *Recordings from weak local earthquakes with shallow depths*

These earthquakes have a focal depth less than 30 km, a local magnitude M_l of the order of 3.0 to 3.5 and an epicentral distance R between 20 and 50 km. The PGAs recorded are low of the order of some cm/s^2. Figure 4 shows an example of records from an earthquake of this kind, occurred on December 8th, 2011 M_l = 3.4, R = 21 km, epicenter at Elefsina, to the NW of Acropolis. The effect of local site characteristics in the modulation of the record is apparent. The lower PGAs were recorded by the instruments at the basement of Parthenon (ACRB E-W, 0.7 cm/s^2) and at the outcrop of the limestone near the East Wall (ACRE E-W, 1.3 cm/s^2), while the highest PGAs were recorded by the instruments at the artificial fill material close to the South Wall (ACRD N-S, 3.3 cm/s^2), at the emergence of Athenian schist (ACRG E-W, 2.8 cm/s^2) and at the Parthenon architrave (ACRC N-S, 1.9 cm/s^2).

For almost all the records of this set of earthquakes, a magnification by a factor of 3 between the PGAs recorded by ACRB at the Parthenon basement and by ACRC at the Parthenon architrave was noted. Furthermore, the spectral accelerations of the Figure 4 records were calculated for a damping factor $\zeta = 5\%$.

The peak of ACRC horizontal components (Parthenon architrave) are apparent at a period around 0.5 s showing the effect of the structure, since the Parthenon columns have a height of about 18 m.

The higher spectral acceleration refer to the E-W component of ACRD (artificial earth filling) and appears at a period around 0.07 s showing probably the effect of soil conditions.

5.2 *Recordings from moderate regional earthquakes with shallow depths*

These earthquakes have a focal depth pf the order of 30 km, a moment magnitude M_w of the order of 5.0 to 5.5 and an epicentral distance R of about 250 km. The PGAs recorded are also low, of the order of some hundredths of cm/s^2. Figure 6 shows an example of records from an earthquake of this kind, which occurred on January 27th, 2012 (M_w = 5.4, h = 31 km, R = 247 km, epicenter to the SE of Acropolis, at Cretan Sea. In these case the PGAs vary around 0.03 cm/s^2 at all stations, except for the records of ACRC (N-S) at which PGA is calculated to 0.3 cm/s^2, ten times higher compared to the one of ACRB.

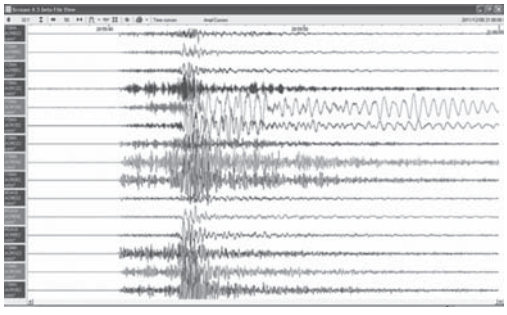

Figure 4. Records from the earthquake of December 8th, 2011 $M_l = 3.4$, R = 21 km. From top to bottom the 3 components (Z, N-S, E-W) of ACRB, ACRC, ACRD, ACRE and ACRG are shown.

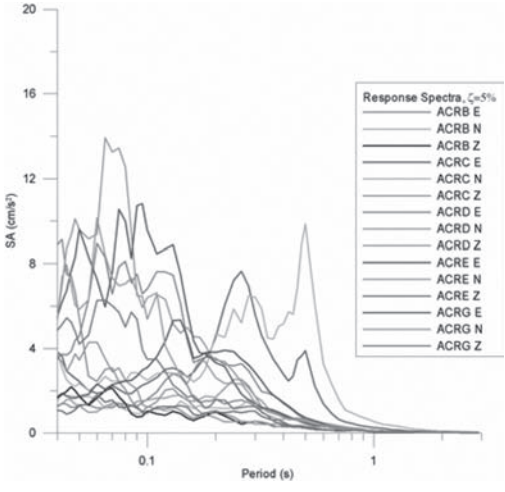

Figure 5. Response spectra ($\zeta = 5\%$) of the records in Figure 4.

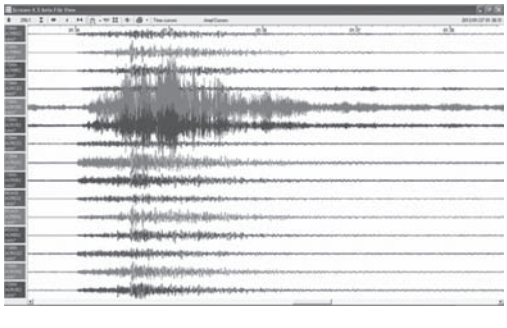

Figure 6. Records from the earthquake of January 27th, 2012 ($M_w = 5.4$, h = 31 km, R = 247 km). From top to bottom the 3 components (Z, N-S, E-W) of ACRB, ACRC, ACRD, ACRE and ACRG are shown.

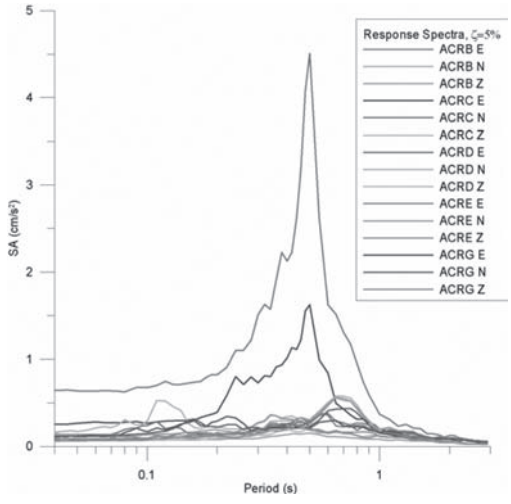

Figure 7. Response spectra of the records in Figure 6. The peaks at higher periods refer to the horizontal components at ACRC (Parthenon architrave), with a dominant peak at 0.5 s.

The response spectra at ACRB, ACRD, ACRE and ACRF show a low peak around 0.1 s, while a dominant peak at 0.5 s is shown by ACRC horizontal components (Fig. 7).

For this set of records it seems that the site amplification does not play a significant role, which it was present for the case of local events, and only the characteristics of the Parthenon architrave have an effect on the accelerographic records.

5.3 *Recordings from strong regional earthquakes with intermediate depth*

The strong earthquakes that occur along the subduction zone of southern Aegean have an intermediate focal depth of 60 to 130 km. Due to their intermediate depths and the large magnitudes, they are felt at long distances especially for high-rise buildings; however, the hot asthenospheric wedge dominating the back-arc region of the Aegean Sea area is resulted into high attenuation of the seismic energy (e.g. Hashida et al., 1988). A typical earthquake of such a kind, recorded by the Acropolis array during the up to now operation, occurred on April 1st, 2011 with $M_w = 6.2$ and a focal depth of 63 km. The epicenter was at a distance of about 360 km SE of Acropolis, near the island of Kasos. Figure 8 shows the records from this earthquake. Again, no site amplification affected the recordings, except for the ACRC at the Parthenon architrave. Recorded PGAs vary between 0.6 cm/s^2 and 0.9 cm/s^2 while the PGA at ACRC (N-S) reached 3.0 cm/s^2, more than 4 times the corresponding PGA at ACRB (N-S).

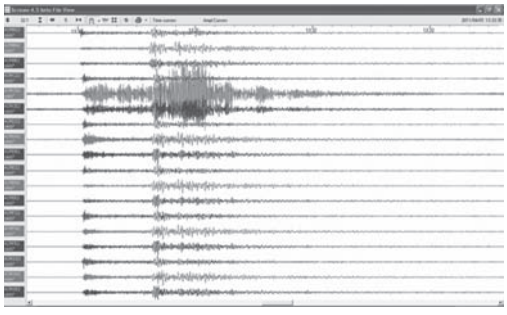

Figure 8. Records from the earthquake of April 1st, 2011 M_w = 6.2, R = 360km. From top to bottom the 3 components (Z, N-S, E-W) of ACRB, ACRC, ACRD, ACRE, ACRF and ACRG are shown.

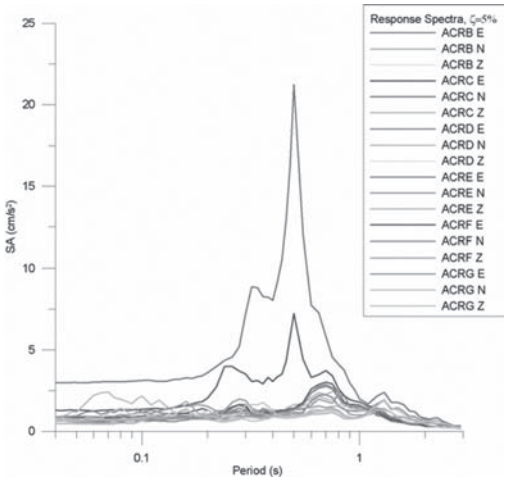

Figure 9. Response spectra of the records in Figure 8. The peaks at higher periods refer to the horizontal components at ACRC (Parthenon architrave), with a dominant peak at 0.5 s.

A dominant peak of spectral acceleration at 0.5 s was observed in the response spectra ($\zeta = 5\%$) of the records at ACRC site (Fig. 9). Moreover, the spectral acceleration for the same components is amplified by a factor of about 8 compared to the response spectra of the other sites (which are quite higher than the respective spectral accelerations of Figures 5 and 7), probably due to a combination of both the earthquake and the monument characteristics.

5.4 *Recordings from strong long-distance earthquakes*

On March 11th, 2011 the Tohoku, Japan earthquake M_w = 9.0 occurred. The epicentral distance from Athens is about 9500 km. Figure 10 (top) shows the record from an STS-2 broadband seismometer installed at NOAIG premises (ATH, HHZ) as well as the record from an accelerograph (NOAC HNZ) of the same type as of the Acropolis array co-located with the seismometer, after it was de-convolved for the instrument response. The Seismic Analysis Code (SAC)—a general purpose interactive program for the study of the time-series data (Goldstein et al. 2003, Goldstein & Snoke 2005)—was used to remove the digitizer interference and to obtain the pure motion and to integrate the acceleration to get velocity). All the phases recorded by the seismometer are also present in the de-convolved accelerographic record, showing the good quality of the strong motion instrumentation and the broadband content recorded. Since NOAIG premises are founded on the same type of Late Cretaceous limestone as Acropolis is and the two sites are close to each other (about 1 km in distance), the recordings from Acropolis accelerographic array were also de-convolved. Figure 10 (bottom) compares NOAC HNZ and

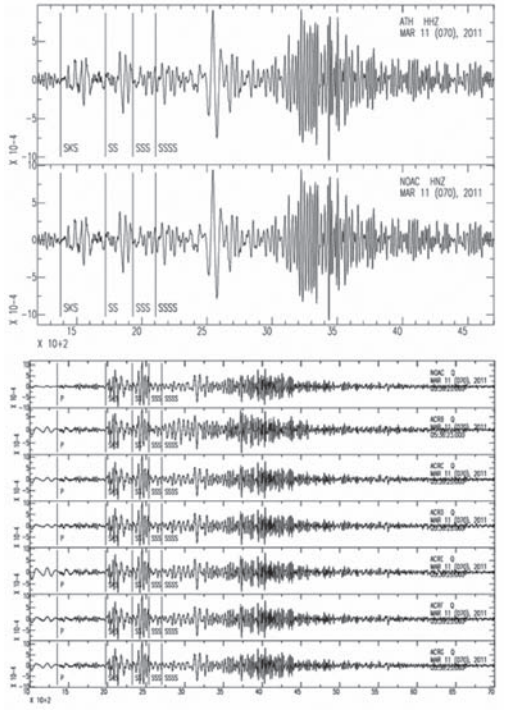

Figure 10. Comparison of the Tohoku, Japan 2011 earthquake records between the ATH HHZ seismometer after de-convolution (top) and between the de-convolved strong motion records of NOAC-HNZ and of the adjacent Acropolis array (bottom).

Acropolis array de-convolved records, showing the similarity of the waves recorded at the same arrival time.

The Van (Turkey) strong earthquake ($M_w = 7.2$) occurred on October 23rd, 2011 with an epicentral distance of about 1700 km from Athens. The Acropolis array recorded the earthquake with PGA varying between 0.09 cm/s^2 (ACRE) and 0.20 cm/s^2 (ACRD), meaning a magnification of 2 due to artificial fill material. Figure 11 shows the recordings at four sites. ACRC has been omitted due to high noise content at the time of the earthquake.

5.5 *Response interpretation for the Parthenon (ACRB, ACRC) records*

For engineering purposes, it was tried to deduce the Parthenon architrave response (maximum acceleration of the architrave) with respect to that at the Parthenon basement (ACRB). PGAs at the architrave are compared to the spectral acceleration (SA) of the basement records. The SA(T) from the ACRB response spectrum (where the period T is the fundamental period of seismic event in ACRB for the weak local events or the fundamental period in ACRC for all the other seismic events) is compared to the PGA of ACRC. The response spectrum of ACRB seismic motions refers to the response of a SDOF system for damping ratio $\xi = 1$–1.5%. It was found that for the weak local earthquake records the dominant period of the earthquake record plays the most significant role for the response estimation of ACRC, while for both the regional events with shallow depths and regional events with intermediate depths the fundamental period of architrave was prevailing (0.48–0.5 s). The resulting acceleration values range between ± 15% compared to the recorded ones.

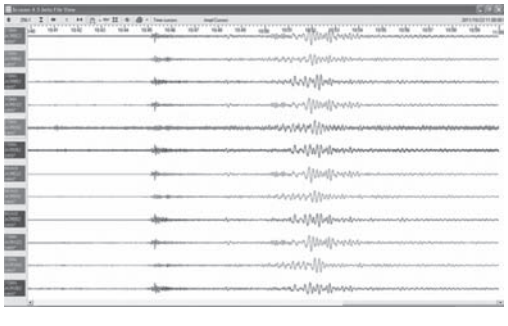

Figure 11. Van, Turkey earthquake as recorded by four stations of the Acropolis array. From top to bottom the three components (Z, N-S, E-W) of ACRB, ACRD, ACRE and ACRG are shown.

6 2-D DYNAMIC RESPONSE ANALYSES

In this section the results of preliminary 2-D dynamic response analyses of the Acropolis rockhill are presented. The execution of 2-D dynamic response analyses of the broader area subsoil model of the Acropolis rockhill aims to reliably predict the seismic motion along the free surface of the sacred rock (terrace and slopes). These analytically resulting motions could be used as the base seismic action for the calculation of the dynamic response of the monuments standing upon the Acropolis terrace, with the seismic action applied either as time history of acceleration, or spectral values for modal or even simplified pseudo-static analyses. Within this context, the analytical results of the 2-D dynamic response analyses of the Acropolis were compared with the recordings of the Acropolis accelerographic array for different seismic scenarios, aiming at calibrating the dynamic properties of the geomaterials encountered in the rockhill, and at evaluating the modeling applied for the analyses.

The analyses were conducted along the middle cross-section of the rockhill, in the N-S direction (Figs. 1, 12), the layering of which was defined according to the existing geological data (Andronopoulos & Koukis 1976). The software code QUAKE/W (Geoslope International Ltd 2004) was used for the preliminary 2-D FE analysis. An unstructured mesh was applied with typical mean dimensions of 5 m × 10m (height × base) for the discretization of the model. The vertical boundaries of the model were set free to vibrate along the horizontal direction and were restricted to vertical movement. The bedrock limits were set far away from the limestone hill lateral limits (the bedrock base is about 40 times greater than that of the limestone hill), in order to avoid trapping effects of the seismic waves. On the other hand, the boundary conditions in the schist lower horizontal limits and (at sufficient depth from the limestone hill-base) restrict fully any vertical or horizontal movement.

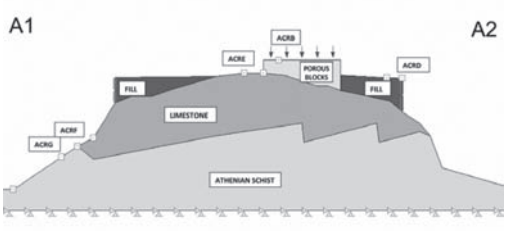

Figure 12. Characteristic section of the Acropolis hill (N-S), for the conduction of dynamic response analyses (A1A2 section noted in Figure 1).

A number of 8 seismic scenarios were used for the analyses, considering the horizontal N-S recordings of the Acropolis accelerographic array. These scenarios included both near and far field seismic events, in order to represent impartially the effect of frequency content and directivity.

The rocky materials (Athenian schist bedrock, limestone of the Acropolis rock, and the huge Parthenon foundation from marly limestone blocks) were modeled as homogeneous linear materials with elastic stiffness and viscous damping. The artificial fill for the construction of the Acropolis terrace was modeled as an equivalent linear material with shear modulus and damping ratio dependent on the cyclic shear strain. The reduction curves for shear modulus (G/G_{max} vs γ) and damping ratio (ξ vs γ) were taken from well established literature data for gravel (Rollins et al., 1998). Finally, the circuit wall was modeled as a structural beam element.

The bedrock input seismic motion resulted from the processing of the horizontal component recordings in the schist surface (ACRG) and/or the foot of the limestone rock (ACRF) in the north side of the rockhill. The processing refers to an iterative set of dynamic analyses, in order to let the recordings in the locations of the fore mentioned instruments to practically coincide with the analytical results.The dynamic properties of the geomaterials were assigned according to the relevant literature (NEHRP, 2005) for geological formations of similar nature. These properties are shown in the Table 2.

The Parthenon foundation (where the ACRB instrument has been installed) was constructed from porous-stone blocks with dry masonry structure.

For this reason a (notional) relative high damping ratio (40%) has been applied, in order to account for the expected high absorption of seismic energy. In other words, this notional value of 40% (with no physical meaning) is a rather tricky attempt to incorporate the SFSI effect of the Parthenon's superstructure and foundation.

Table 2. Dynamic properties of geomaterials.

Material	VS (m/s)	Gmax (kPa)	ν	ξ (%)	γ (kN/m³)
Limestone	1500	6,08E + 06	0,25	10	26
Schist	700	1,20E + 06	0,25	5	25
Backfill	350	2,45E + 05	0,30	1,5*	20
Porous stone	600	8,64E + 05	0,30	40**	24

*Initial value (ξ_{min}).
**Notional value to account for the Parthenon foundation structure.

The analytical results were compared to the ACRG, ACRF, ACRB, ACRE and ACRD recordings, while the accelerations on the architrave of the North Colonnade of the Parthenon (ACRC) were calculated from the response spectrum of the seismic motion on the base (ACRB instrument).

The comparison of the analytical results to the recordings is presented in Table 3.

From the analyses, the following conclusions result:

– Given the uncertainties about the geomaterials properties and the exact geotechnical modeling, as well as the simplifications in the analytical model, there is a satisfactory agreement of analytical results and recordings for the majority of the analyzed sites. The ratio of the resulted to the recorded PGA ranges from 0.50 to 4.80 for all the examined cases, with mean value equal to 1.57, 1.87 and 1.00 for all, the near-field and the far-field seismic events respectively. The comparison made apparent that the analytical results overpredict systematically the recordings in the ACRB and ACRE locations with a prediction ratio (predicted vs measured value) ranging from 1.1 to 3.6 (mean value equal to 2.2) for ACRB and from 1.0 to 4.8 (mean value equal to 2.2) for ACRE.
– In the case of ACRD location (thick artificial fill material) where a direct comparison of analytical results and recordings took place, the prediction ratio ranges from 0.45 to 1.45 (mean value equal to 0.97) denoting satisfactory agreement of the results and the recordings. A more detailed modeling of the fill material properties (e.g. a stress dependent shear modulus) may contribute to an increased accuracy of the results.

Table 3. Comparison of recordings and analytical predictions (PGA)*.

Earthquake		ACRB		ACRD		ACRE	
				Rec.	Pred.		
M	R (km)	Rec.	Pred.	(cm/s² × 10³)		Rec.	Pred.
3.0	45	25	60	76	83	41	56
3.4	21	568	1800	–	2800	372	1800
5.1	118	362	380	1072	450	331	370
3.1	53	60	220	284	410	57	210
6.2	363	703	750	727	780	740	800
3.1	53	60	190	284	220	57	180
3.5	45	288	530	895	770	278	470
3.4	21	738	2000	3313	3700	913	2000
5.3	244	105	120	140	135	120	120

*Input base motion for the analyses has been derived from ACRF and ACRG recordings.

– In the case of the instruments installed upon the free-hill surface limestone sites (ACRB and ACRE), the PGA is systematically overestimated. This is attributed mainly to a) the interaction of the overlaying monumental structure (North Colonnade) for the ACRB site (but a rigorous 3-D analysis could finally clarify this behavior) and b) the expected different dynamic properties in zones of limestone differing significantly in weathering, and the actual location of ACRE in the rockhill (far for the section used for the 2-D analyses).
– The response of the architrave (ACRC site) is mainly governed, at least for the low amplitude seismic events used in the 2-D analyses, from the frequency content (the fundamental period) of the earthquake and not from the characteristic period of the site. As it was explained previously (section 5.5), the spectral acceleration of the underneath installed ACRB instrument, for the fundamental period of the ACRB recording and a rational value for the minimum damping ratio ($\xi_{min} \approx 1$–1.5%) may well compared to the maximum acceleration of ACRC recording. This observation may be used for prediction of the acceleration in the monument structure.
– The modeling applied for the dynamic response analyses, though its simplicity, seems promising for the prediction of the superficial seismic motion in the Acropolis rockhill. However, a more detailed geometrical model of the geotechnical layering and the measurement of dynamic properties (e.g. from the results of a properly focused geotechnical investigation) could be exploited for a more effective modeling of 2-D analyses and may significantly improve the accuracy of the results.

7 DISCUSSION

The accelerographic array deployed at Acropolis site during the last years, is an application of modern technological systems to support the monitoring and mitigation of earthquake hazard during works of restoration of the monuments. Especially valuable is the continuous operational reliability of the array towards the processing of possible strong earthquake records that could affect the monuments together with their geotechnical documentation. The available information could be included in a multidisciplinary system (e.g. a Geographical Information System integrated to a Decision Support System) for security limits legislations that would help the engineering and archaeological work on the site.

Modern tools (like the ambient noise monitoring (PQLX software) based on the characteristics and the operation of modern accelerographs (broad frequency content, continuous recording) are very helpful towards the description of installation site characteristics. Finally, the recordings of the array may contribute invaluably to the proper dynamic modeling of the Acropolis rockhill and its monuments, and allow the safe design of measures aiming to the mitigation of seismic hazard.

REFERENCES

Ambraseys, N. 2010. On the long-term seismicity of the city of Athens. *Proc. Academy of Athens* Vol. A.: 81–136.

Ambraseys, N.N. & Jackson, A. 1997. Seismicity and strain in the Gulf of Corinth (Greece) since 1694. *J. Earth. Eng.* 1: 433–474.

Andronopoulos B. & Koukis G. 1976. *Engineering geology study in the Acropolis area*. Athens: Institute of Geology and Mineral Exploration.

Egglezos D. & Moullou D. 2011. Back—analysis sheds light on the history of the Acropolis Wall: The interpretation of a permanent structural failure, *Proc. XVth European Conference on Soil Mechanics & Geotechnical Engineering, Hellenic Society for Soil Mechanics and Geotechnical Engineering, Athens,* Vol. A: 1841–1846.

Elenas, A. 2003. Athens earthquake of 7 September 1999: Intensity measures and observed damage. *J. Earthq. Technology, Technical Note* 40(1): 77–97.

Evangelidis, C. & Melis, N. 2012. Ambient noise level in Greece as recorded at the Hellenic Unified Seismic Network. *Bull. Seism. Soc. Am.* 102 (6): 2507–2517.

Galanopoulos, A.G. 1960. *A catalogue of shocks with Io > VI or M > 5 for the years 1801–1958*. Athens: Seism. Lab. Univ.

Galanopoulos, A.G. 1971. Minimum and maximum magnitude threshold in the area of Attica, Greece. *Annali di Geofisica* XXXIV (1): 29–54.

Ganas, A., Pavlides, S. & Karastathis, V. 2005. DEM-based morphometry of range-front escarpments in Attica, central Greece, and its relation to fault slip rates. *Geomorphology* 65: 301–319.

Goldstein, P., Dodge, D., Firpo, M. & Lee Minner. 2003. SAC2000: Signal processing and analysis tools for seismologists and engineers. *Invited contribution to "The IASPEI International Handbook of Earthquake and Engineering Seismology"*, Edited by WHK Lee, H. Kanamori, P.C. Jennings, & C. Kisslinger, Academic Press, London.

Goldstein, P. & Snoke, A. 2005, "*SAC Availability for the IRIS Community*", Incorporated Institutions for Seismology Data Management Center Electronic Newsletter.

Hashida, T., Stavrakakis, G. & Shimazaki, K. 1988. Three-dimensional seismic attenuation structure beneath the Aegean region and its tectonic implication. *Tectonophysics*, 145: 43–54.

Higgins, M. & Higgins, R. 1996. *A geological companion to Greece and the Aegean.* London: Gerald Duckworh & Co Ltd.

Kalogeras, I., Stavrakakis, G., Melis, N., Loukatos, D. & Boukouras, K. 2010. The deployment of an accelerographic array on the Acropolis hill area: Implementation and future prospects. *The Acropolis Restoration News, Proc. One-day conference "Modern Technologies in the restoration of the Acropolis", Athens, 19 March 2010.* Athens: YSMA.

McNamara, D. E., & Boaz, R.I. 2011. PQLX: A Seismic Data Quality Control System Description, Applications, and Users Manual, *U.S. Geol. Surv. Open-File Rept.* 2010–1292: 52 pp.

McNamara, D.E. & Buland, R.P. 2004. Ambient Noise Levels in the Continental United States. *Bull. Seism. Soc. Am.*, 94 (4): 1517–1527.

Papazachos, B.C. & Papazachou, K. 2003. *The earthquakes of Greece*. Thessaloniki: Ziti.

Pacific Engineering Analysis. 2005. NEHRP site class (Vs(30 m)) amplification factors from site response simulations: 1–48.

Peterson, J. 1993. Observation and modeling of seismic background noise. *U.S. Geol. Surv. Open-File Rept.* 93–322: 94 pp.

Rollins, K., Evans, M., Diehl, N.B. & Daily, W.D. 1998. Shear modulus and damping relations for gravel. *J. Geotechn. and Geoenvironm. Engineering,* ASCE 124(5): 396–405.

Rondoyanni, Th., Mettos, A., Galanakis, D. & Georgiou, Ch. 2000, The Athens earthquake of September 7, 1999: its setting and effects. *Ann. Geol. Pays Hellen.* 38(B): 131–144.

Skarlatoudis A.A., Papazachos C.B., Margaris B.N., Theodulidis N., Papaioannou Ch., Kalogeras I., Scordilis M.E. & Karakostas V. 2003, Empirical Peak Ground-Motion Predictive Relations for Shallow earthquakes in Greece. *Bull. Seism. Soc. Am.* 93(6): 2591–2603.

Geotechnical Engineering for the Preservation of Monuments and Historic Sites – Bilotta, Flora, Lirer & Viggiani (eds)
© 2013 Taylor & Francis Group, London, ISBN 978-1-138-00055-1

Settlements due to tail gap of shield tunnelling

D. Kolymbas
Division of Geotechnical and Tunnel Engineering, University Innsbruck, Austria

ABSTRACT: Surface settlements due to tail gap of tunnel boring machines cannot be reversed by compensation grouting of the gap, even if the volume-loss is overcompensated. This phenomenon can be explained in terms of soil mechanics if we take into account the dilatancy-contractancy behaviour of sand at loading reversals.

1 INTRODUCTION

Rapid growth in urban development has resulted in an increased demand of tunnels. For obvious practical reasons such as accessibility, serviceability and economy, tunnels are often constructed at shallow depths through soft soil or weak rock (Rowe & Lo 1983) and this is of particular importance if historical buildings and monuments are affected. The point is that deformations of the ground induced by tunnelling can hardly be estimated.

Think, e.g., of the bother and fear in view of the recent construction of a tunnel very near to the famous church Sagrada Familia in Barcelona.

This was finally completed without any complaint. About 80% of soft ground tunnels recently completed or currently under construction are excavated using tunnel boring machines (TBM) (Eisenstein 2003). In this category, the earth pressure balance or slurry TBM with controlled face pressure are the most widely used ones, as they offer superior ground control capabilities.

Recent technical developments in shield tunnelling technique caused a decrease of ground deformation due to tunnelling, however the deformations of the ground surface are still noteworthy.

The causes of settlements are various and interact with each other. The interaction between TBM and the ground belongs to the most complex soil-structure interaction problems in geotechnical engineering. Attempts are made to model this complexity by analytical, laboratory or numerical modelling. Although these techniques are still of limited use for practical purposes, they help to understand the key features of these tunnelling techniques.

The objective of this publication is to investigate soil behaviour due to shield tunnelling. Special focus is put on effects due to the volumetric behaviour of soil, which are neglected in the majority of former research. This investigation is done by means of small scale laboratory models and numerical analyses (Mähr 2006).

2 ANALYTICAL SOLUTION

The author Kolymbas (1998) proposed the following equation to estimate the vertical displacement distribution above the crown (see figure 1):

$$u_z = u_{z0}\left(\frac{r_0}{r}\right)^d \tag{1}$$

with u_{z0} being the vertical displacement at the crown. u_{z0} can be estimated by the following consideration. We start with the following kinematic relation:

$$u_{z0} = \varepsilon_{\vartheta 0} r_0 = (\varepsilon_{v0} - \varepsilon_{r0}) r_0, \tag{2}$$

where ε_{r0} equals the radial strain at the crown and $\varepsilon_{\vartheta 0}$ the tangential strain at the crown. The parameter d is obtained from (2) as

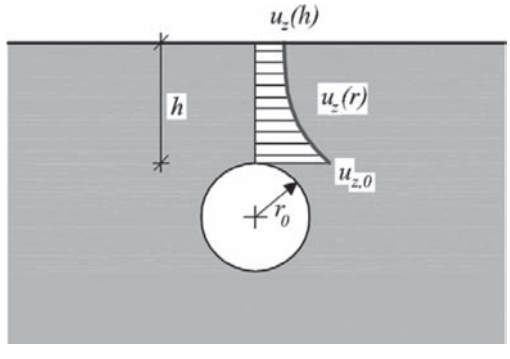

Figure 1. Distribution of the vertical displacement u_z above the crown, according to Kolymbas (1998).

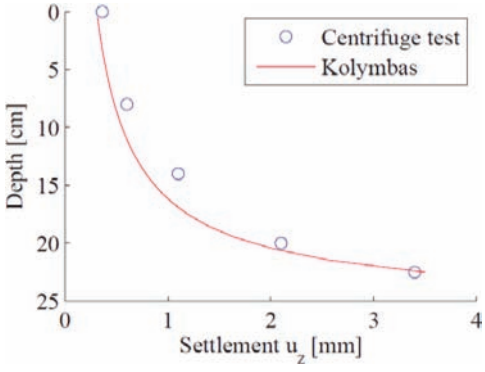

Figure 2. Observed and predicted vertical displacements above centerline from centrifuge tests with non-cohesive soil, König (1994).

$$d = -\frac{\varepsilon_{r0}}{\varepsilon_{\vartheta 0}}. \tag{3}$$

The volumetric strain at the crown equals $\varepsilon_v = \varepsilon_{\vartheta 0} + \varepsilon_{r0} = \varepsilon_{r0} \tan\psi$, where ψ is the dilatancy angle. Thus, the radial strain can be calculated using ψ:

$$\varepsilon_{r0} = \frac{\varepsilon_{\vartheta 0}}{\tan\psi - 1}. \tag{4}$$

By combining (3) and (4) the parameter d is obtained as

$$d = \frac{1}{1 - \tan\psi}. \tag{5}$$

Figure 2 shows the predicted and observed vertical displacements of centrifuge tests conducted by König (1994). The analytical solution obtained with an estimated angle of dilatancy $\psi = 10°$ is in good agreement with the observations. Clearly, for $r = r_0 + h$ eqn. (1) yields the settlement of the ground surface.

3 CONSTITUTIVE MODEL

A suitable constitutive model is crucial for numerical modelling of mechanical behaviour of sand. As granular materials are in many aspects different from other materials, advanced constitutive relations are necessary. Hypoplasticity is a nonlinear, tensorial equation of the rate type. It can be represented in the following form:

$$\overset{\circ}{T} = \mathcal{L} : \mathrm{D} + \mathrm{N} \| \mathrm{D} \| \tag{6}$$

$\mathcal{L}$ and $\mathbf{N}$ are constitutive tensors. $\boldsymbol{D}$ is the symmetric part of the velocity gradient. In contrast to Hypoelasticity (Truesdell 1955), (6) is incrementally nonlinear in stretching $\boldsymbol{D}$ (Kolymbas 1978). $\overset{\circ}{\mathrm{T}}$ is the objective ZAREMBA-JAUMANN stress rate of the Cauchy stress tensor $\boldsymbol{T}$:

$$\overset{\circ}{\mathrm{T}} = \dot{\mathrm{T}} + \mathrm{W} \cdot \mathrm{T} - \mathrm{T} \cdot \mathrm{W} \tag{7}$$

where $\mathbf{W}$ denotes the spin tensor (Truesdell et al. 1992).

For the analyses in this section standard Hypoplasticity, version of von Wolffersdorff (1996), was used. $\mathcal{L}$ and $\mathbf{N}$ are functions of the Cauchy stress and the void ratio and read:

$$\mathcal{L} := f_b f_c \frac{1}{\hat{\mathbf{T}} : \hat{\mathbf{T}}} (F^2 \mathcal{I} + a^2 \hat{\mathbf{T}} \hat{\mathbf{T}}) \tag{8}$$

$$N := f_d f_b f_e \frac{Fa}{\hat{\mathbf{T}} : \hat{\mathbf{T}}} (\hat{\mathbf{T}} + \hat{\mathbf{T}}^*), \tag{9}$$

$$\text{with } \hat{\mathbf{T}} := \mathrm{T}/\mathrm{tr}\mathrm{T}, \qquad \hat{\mathbf{T}}^* := \hat{\mathbf{T}} - \frac{1}{3}\mathbf{1}, \tag{10}$$

$$a = \frac{\sqrt{3}(3 - \sin\varphi_c)}{2\sqrt{2}\sin\varphi_c} \tag{11}$$

$$F := \sqrt{\frac{1}{8}\tan^2\psi + \frac{2 - \tan^2\psi}{2 + \sqrt{2}\tan\psi\cos 3\vartheta}} - \frac{1}{2\sqrt{2}\tan\psi}, \tag{12}$$

$$\tan\psi := \sqrt{3}\,\| \hat{\mathbf{T}}^* \|, \tag{13}$$

$$\cos 3\theta := -\sqrt{6}\frac{tr(\hat{\mathbf{T}}^* \cdot \hat{\mathbf{T}}^* \cdot \hat{\mathbf{T}}^*)}{(\hat{\mathbf{T}}^* :)^{\frac{3}{2}}} \tag{14}$$

$$\mathcal{L} := f_b f_e \frac{1}{\hat{\mathbf{T}} : \hat{\mathbf{T}}} (F^2 \mathcal{I} + a^2 \hat{\mathbf{T}} \hat{\mathbf{T}}) \tag{15}$$

$$N := f_d f_b f_e \frac{Fa}{\hat{\mathbf{T}} : \hat{\mathbf{T}}} (\hat{\mathbf{T}} + \hat{\mathbf{T}}^*), \tag{16}$$

$$\text{with } \hat{\mathbf{T}} := \mathrm{T}/\mathrm{tr}\mathrm{T}, \qquad \hat{\mathbf{T}}^* := \hat{\mathbf{T}} - \frac{1}{3}\mathbf{1}, \tag{17}$$

$$a = \frac{\sqrt{3}(3 - \sin\varphi_c)}{2\sqrt{2}\sin\varphi_c} \tag{18}$$

$$F := \sqrt{\frac{1}{8}\tan^2\psi + \frac{2 - \tan^2\psi}{2 + \sqrt{2}\tan\psi\cos 3\vartheta}} - \frac{1}{2\sqrt{2}\tan\psi}, \tag{19}$$

$$\tan\psi := \sqrt{3}\,\| \hat{\mathbf{T}}^* \|, \tag{20}$$

$$\cos 3\theta := -\sqrt{6}\frac{tr(\hat{\mathbf{T}}^* \cdot \hat{\mathbf{T}}^* \cdot \hat{\mathbf{T}}^*)^{\frac{3}{2}}}{(\hat{\mathbf{T}}^* :)} \tag{21}$$

The scalar factors f_d, f_e and f_b are functions of the void ratio e and the mean pressure $p_s := -\mathrm{tr}\,\mathbf{T}/3$ and comprise the dependence on the mean pressure (barotropy) and the density (pyknotropy):

$$f_d := \left(\frac{e - e_d}{e_c - e_d}\right)^{\alpha},$$

$$f_e := \left(\frac{e_c}{e}\right)^{\beta},$$

$$f_b := \left(\frac{e_{i0}}{e_{c0}}\right)^{\beta} \frac{h_s}{n} \frac{1 + e_i}{e_i} \left(\frac{-\mathrm{tr}\hat{\mathbf{T}}}{h_s}\right)^{1-n} \left[3 + a^2 - a\sqrt{3}\left(\frac{e_{i0} - e_{d0}}{e_{c0} - e_{d0}}\right)^{\alpha}\right]^{-1}.$$

e_i, e_c and e_d are the maximum, critical and minimum void ratios (characteristic void ratios) and depend on the mean pressure $-tr\mathbf{T}$. Bauer (1996) proposed the following relation:

$$\frac{e_i}{e_{i0}} = \frac{e_c}{e_{c0}} = \frac{e_d}{e_{d0}} := \exp -\left(\frac{-tr\,\mathbf{T}}{h_s}\right)^n. \tag{22}$$

e_{i0}, e_{c0} and e_{d0} are the void ratios for a stress-free state. This particular formulation enables the definition of a pressure dependent density index:

$$r_e := \frac{e_c - e}{e_c - e_d}. \tag{23}$$

$r_e = 1$ represents the densest and $r_e = 0$ the critical state.

Triaxial and oedometer tests with Hochstetten sand from the vicinity of Karlsruhe (von Wolffersdorff 1996) were used for the determination of the material parameters of the hypoplastic model (Herle & Gudehus 1999). The initial relative density based on the void ratio has been chosen as

$$I_e = \frac{e - e_{\min}}{e_{\max} - e_{\min}} = 0.5.$$

For comparison, a numerical analysis has also been conducted with the 'classical' elastoplastic model of Mohr-Coulomb. The parameters of the Mohr-Coulomb model were adjusted as a best fit to the results of triaxial experiments at $\sigma_0 = 0.1$ MPa, obtaining Young's modulus $E_0 = 22$ MPa, friction angle $\varphi = 33°$, Poisson's ratio $\nu = 0.3$ and an angle of dilatancy $\psi = 30°$. The Young's modulus E was varied with depth z according to a pressure-dependent law proposed by Ohde (1938), with α set to 0.7:

$$E(z) = E_0\left(\frac{\sigma_z(z)}{\sigma_0}\right)^{\alpha} \tag{24}$$

Table 1. Parameters of the Mohr-Coulomb model for Hochstetten sand.

ϕ[°]	E_0 [MPa]	ν	ψ[°]
33	58	0.3	30

Table 2. Parameters of the hypoplastic model for Hochstetten sand.

ϕ_c[°]	h_s [MPa]	n	e_{d0}	e_{c0}	e_{i0}	α	β
33	1000	0.25	0.55	0.95	1.05	0.25	1.50

The elasto-plastic and hypoplastic parameters are summarised in Tabs. 1 and 2.

The analyses have been carried out with the FE program ABAQUS. Mohr-Coulomb law is a standard part of this FE-package. For this purpose the UMAT from Fellin & Ostermann (2002a) has been used, which provides a consistent tangent operator including error control.[1]

Three calculations with Mohr-Coulomb model with varying dilatancy angle ψ have been performed, to analyse its influence on the results.

4 BEHAVIOUR OF SOIL AT CYCLIC LOADING

We first consider the stress path of a soil element above the crown (figure 3 and figure 4), since it is assumed, that the stress path in this area has the biggest impact on settlements. Lee & Rowe (1991) investigated this stress path by means of a 3D FE-analysis. They concluded, that the trend of the stress path is similar to that of triaxial compression for a soil element ahead of the tunnel face. Once the face advances beyond the point of interest, the stress path quickly changes to one closer to triaxial extension. This stress path can be simulated by means of laboratory tests, i.e. triaxial or biaxial (= plane deformation). Figure 5 and figure 6 show some typical results.

In Kolymbas et al. (2002) is pointed out, that one should pay attention to the dilatancy behaviour of

1. The UMAT is available on http://www.geotechnik.uibk.ac.at.

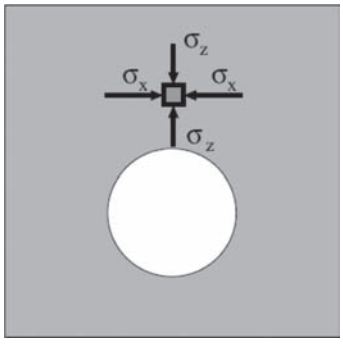

Figure 3. Definition of stress variables.

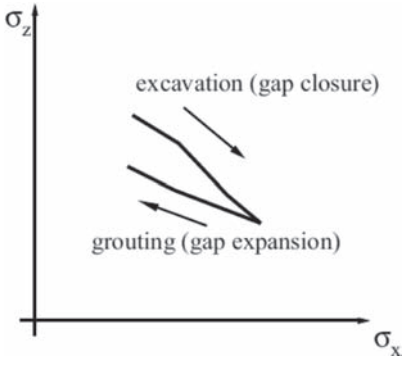

Figure 4. Stress path above the crown due to tunnel excavation and subsequent tail gap grouting Kolymbas et al. (2002).

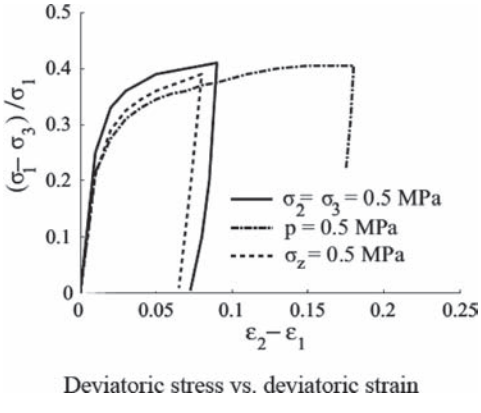

Figure 5. Triaxial experiments under different stress paths with Hostun Sand (Lanier et al. 1991).

sand (and soil in general). During (triaxial) loading, dense sand exhibits first contractancy and later dilatancy. As known, dilatancy is the increase of volume (and, consequently, also of void ratio) that

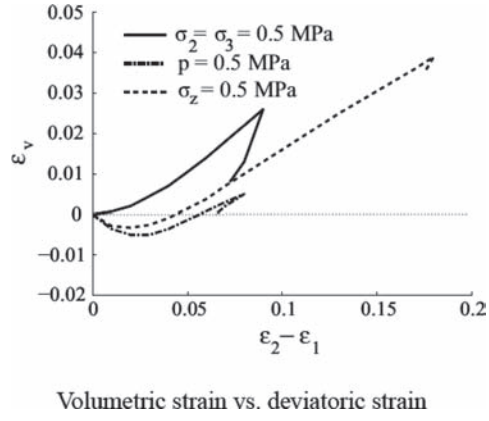

Figure 6. Triaxial experiments under different stress paths with Hostun Sand (Lanier et al. 1991). Note the pronounced contractancy upon unloading.

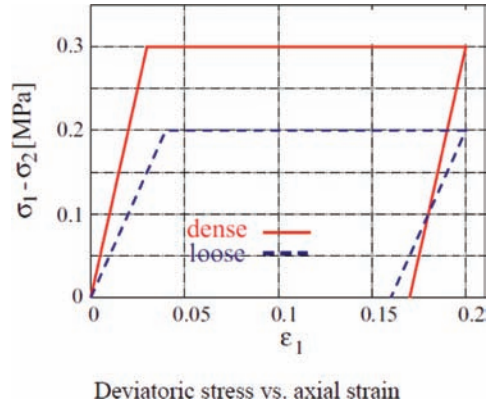

Figure 7. Simulation of triaxial test results with the Mohr-Coulomb constitutive model.

occurs during shearing. Of paramount importance is what happens at reversals of the deformation, i.e. at loading-unloading transitions. Unloading is characterised by a much higher stiffness. Considering the evolution of volumetric strain, it is observed that the previous dilatancy is reversed to contractancy, the rate of which is much higher than the one of dilatancy (figure 6). This fact implies the following result: A loading-unloading cycle leaves behind a compaction of the soil (Kolymbas et al. 2002).

Interestingly, the previously described fundamental behaviour of soil at cyclic loading is not modelled by most of the constitutive equations implemented in standard FE codes. E.g., the Mohr-Coulomb elasto-plastic constitutive equation predicts dilatancy at loading and also immediately after the reversal from loading to unloading (see figure 7 and figure 8), which is fundamentally

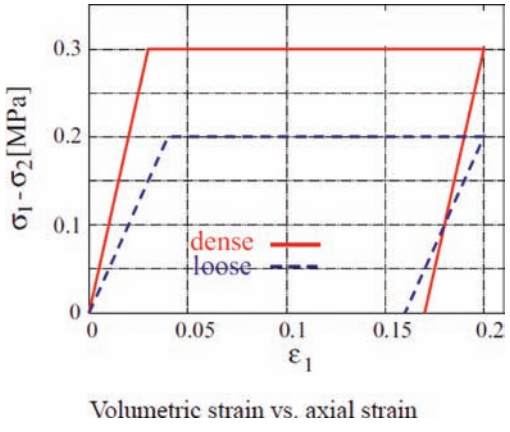

Figure 8. Simulation of triaxial test results with the Mohr-Coulomb constitutive model.

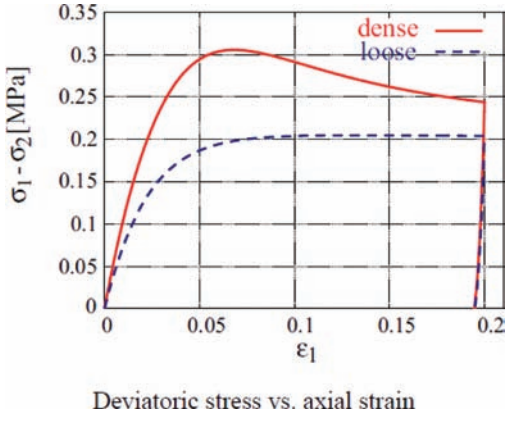

Figure 9. Simulation of triaxial test results with hypoplasticity.

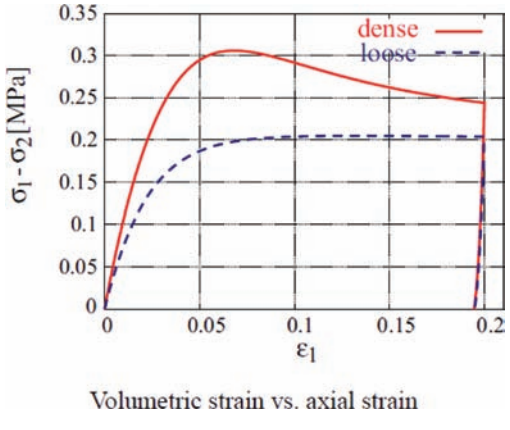

Figure 10. Simulation of triaxial test results with hypoplasticity.

wrong. As a result, the Mohr-Coulomb constitutive law is unable to simulate the behaviour of soil in a shield tunnelling problem (Mähr & Herle 2004). In contrast, the hypoplastic constitutive equation reproduces this effect realistically (figure 9 and figure 10).

5 BOUNDARY CONDITIONS

To test the appropriateness of several constitutive models for shield tunnelling analyses, a simple FE-model has been investigated. This model is not intended to simulate the entire soil-shield interaction nor to predict the behaviour of the lining, but merely to show the importance of a realistic constitutive law for the considered problem of gap grouting.

The boundary conditions and the mesh have been chosen as illustrated in figure 11. The sequence of the applied deformation is shown in figure 12

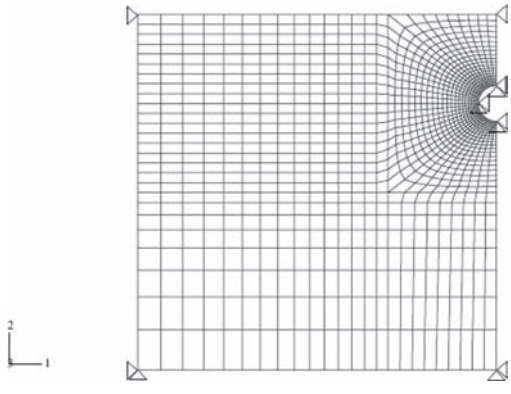

Figure 11. Boundary conditions.

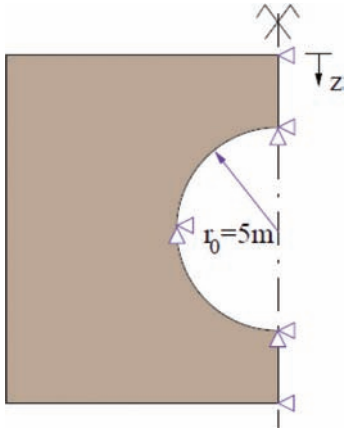

Figure 12. Displacements applied to the tunnel contour line (a) Initial configuration.

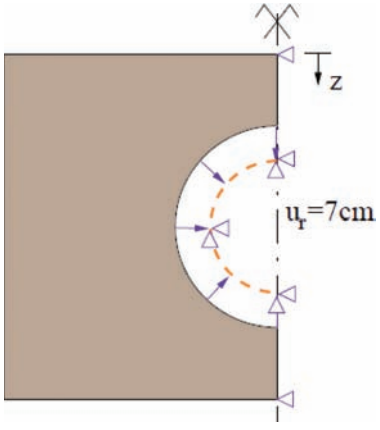

Figure 13. Displacements applied to the tunnel contour line (b) convergence.

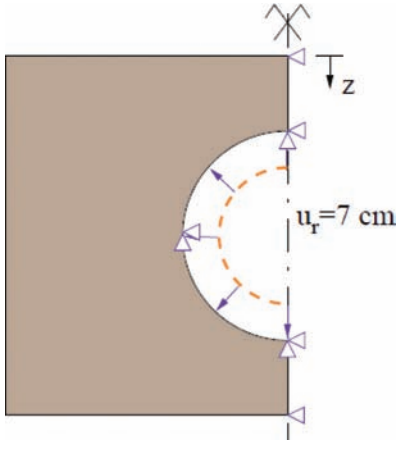

Figure 14. Displacements applied to the tunnel contour line (c) expansion.

to figure 14. We start from a circular tunnel with 5 m radius (figure 12) and apply a convergence of 7 cm (figure 13) to simulate the excavation. In the second step the tunnel cavity is expanded (say, by compensation grouting) to its original size as displayed in figure 14.

5.1 *Results of the numerical simulations*

5.1.1 *Hypoplasticity*

Figure 15 shows the evolution of the settlement trough. One can clearly see that the trough is not annihilated by the cavity expansion (i.e. compensation grouting)—in agreement with field observations (Jancsecz et al. 2001). This behaviour is also

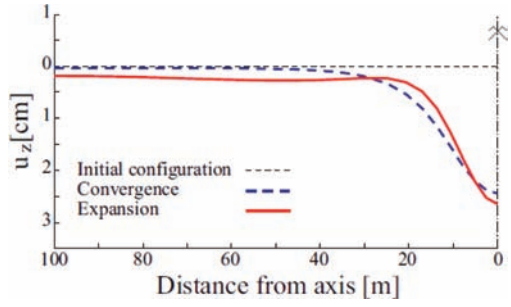

Figure 15. Evolution of the settlement trough, hypoplasticity.

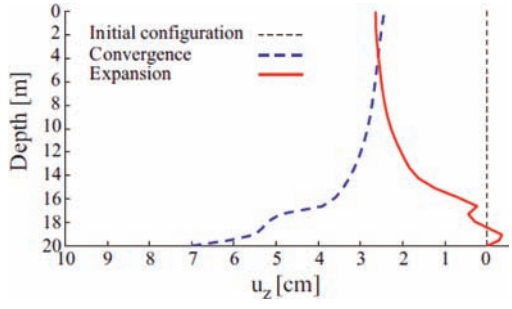

Figure 16. Evolution of vertical displacements u_z along the vertical symmetry axis, hypoplasticity.

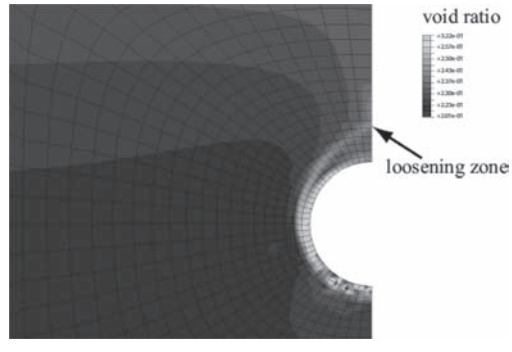

Figure 17. Distribution of void ratio, numerically obtained with hypoplasticity.

reflected in the evolution of vertical displacements along the vertical symmetry axis in figure 16. There, a loosening zone about 2 m above the crown can be identified. It is below the soil arch created during the tunnel convergence. This loosening zone is also shown in a contour plot of void ratios at the end of the convergence-expansion cycle (figure 17). The volume of settlement trough still increases during gap expansion (see figure 20), due to densification of the soil sideways to the tunnel.

5.1.2 *Mohr-Coulomb*

In contrast to the settlement troughs calculated with hypoplasticity, the volume of settlement trough obtained with the Mohr-Coulomb model (see figure 18) is nearly annihilated by the cavity expansion. Moreover, about 30 m beside the symmetry axis a heave can be observed. This is also depicted in figure 20, where the volume of settlement trough is plotted against tunnel convergence.

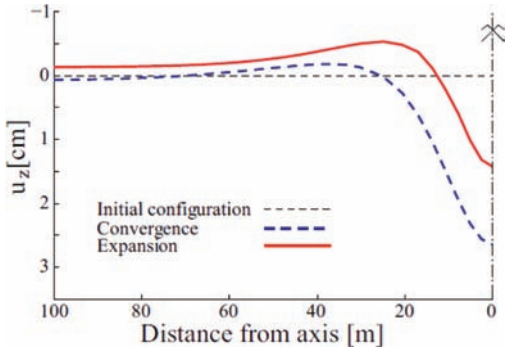

Figure 18. Evolution of the settlement trough, Mohr-Coulomb.

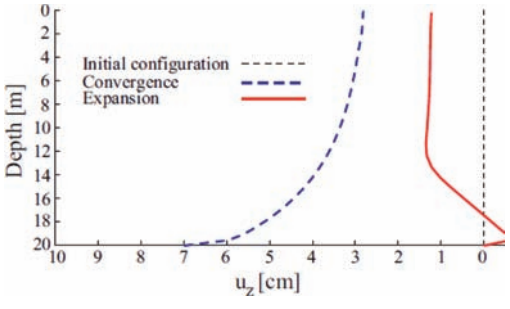

Figure 19. Evolution of vertical displacements u_z along the vertical symmetry axis, Mohr-Coulomb law $\psi = 30°$.

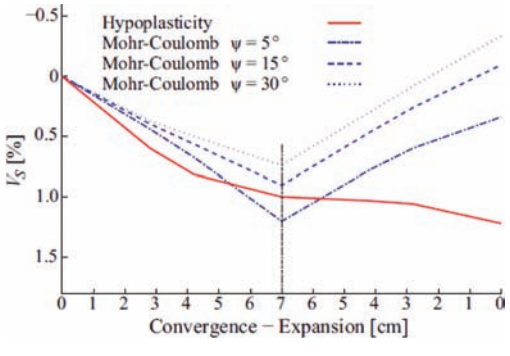

Figure 20. Evolution of volume of settlement trough V_S with the change of the cavity radius.

While the volume of settlement trough computed with the hypoplastic material law is still increasing during gap expansion, the volume of settlement trough computed with Mohr-Coulomb decreases during expansion. In fact—depending on the angle of dilatancy—one even gets a net volume increase.

6 MODEL TESTS

While there are a lot of model tests regarding shield tunnelling in clay, only few can be found for sand or gravel, and there is no model known to the author that takes tail gap grouting into account. The model test presented in this publication has been developed by Mähr (2006) to simulate shield tunnelling in sand. The main emphasis is put on the influence of tail gap grouting on soil displacements.

The test apparatus consists of a container of 100 cm width, 40 cm depth and 100 cm height and a cylinder of 40 cm length and a diameter of 17 cm (see figure 21). The front wall of the container is made of glass (1) to enable taking photographs, the 2 cm thick side walls and the 3 cm thick back wall are made of chip boards (2). The frame is made of L-sections from aluminum.

The width of the container has been chosen according to the following consideration: to reduce the influence of the side walls, the settlements at the side walls, which are placed 50 cm from the axis, must be negligible. The settlement trough $u_z(x)$ is assessed using the equation

$$u_z = u_{z,max} e^{-x^2/2i^2}. \tag{25}$$

The parameter i of the GAUSS-curve can be empirically estimated as:

$$i = \frac{D}{2}\left(\frac{H}{D}\right)^{0.8} = \frac{17.0\ cm}{2}\left(\frac{42.5\ cm}{17.0\ cm}\right)^{0.8} \approx 17.7\ cm. \tag{26}$$

Thus, the settlements in a distance of $3i = 3 \cdot 17.7\ cm = 53.1\ cm$ equals 1% of the maximum settlement above the crown and, consequently, the influence of the side walls of the box can be neglected.

A cylinder with variable diameter from 16 cm to 17 cm is placed in the centre line of the container at a height of 58 cm. It is supported by thin aluminium beams (see figure 21, (3)), which allow vertical movements of the cylinder axis.[2] The cylinder

2. As shield and tunnel are only supported by the surrounding soil in reality, a compliant bearing has been chosen.

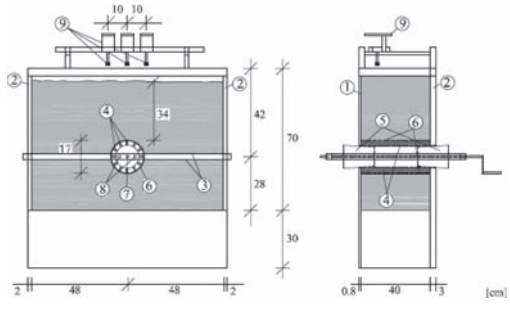

Figure 21. Sketch of the model container: (1) Glass panel; (2) chip boards; (3) aluminium beams; (4) cylinder segments (sheet metal and 3 cm high plastic beams); (5) aluminium frustums; (6) rubber membrane; (7) screw thread; (8) support rods to hinder twisting of the frustum; (9) infrared sensors.

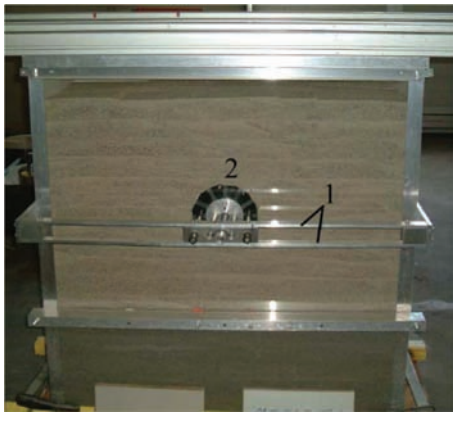

Figure 22. Test apparatus with (1) aluminium beams and (2) cylinder.

Figure 23. The cylinder consists of (1) two frustums, 12 segments composed of (2) plastic beams and (3) metal sheets, (4) rubber membrane, (5) screw thread and (6) rods against twisting.

consists of 12 segments (4), which are supported by two aluminium frustums (5). A rubber membrane coats the cylinder (6). The segments are made from sheet metal and 3 cm high plastic beams. The frustums are guided by a screw thread (7), whereby the frustums can be moved along the tunnel axis. Two additional rods (8) save the frustums against twisting. The movement of the frustum along the screw threads leads to a gradual decrease or increase of the cylinder diameter (figure 24).

After the sand is built in, shield tunnelling is modelled in two steps. In a first step the cylinder is contracted by ΔD to simulate face loss and shield loss (figure 25). In the second step the cylinder is dilated by the same amount to simulate tail gap grouting.

All tests have been carried out under normal gravitational conditions (so called 1 *g* tests).

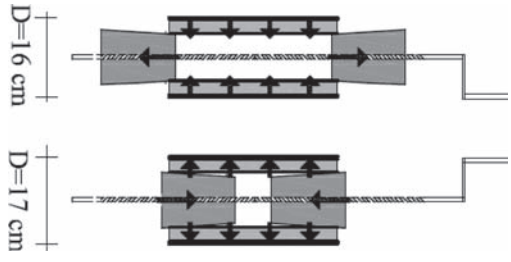

Figure 24. (1) Frustums are moved outward and the segments move towards the axis. The diameter decreases. (2) Frustums are moved inward and the segments outward. The diameter increases.

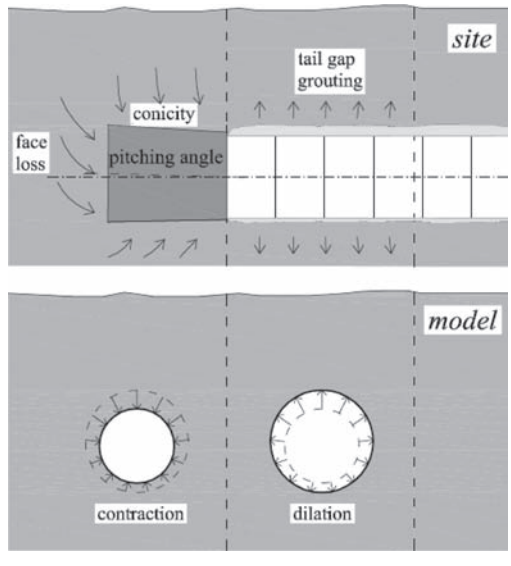

Figure 25. Shield tunnelling modelled in 2 steps: Face loss and shield loss is simulated by contraction of the cylinder, tail gap grouting by dilation of the cylinder.

Due to the stress dependence (barotropy) of soil behaviour, these tests have limited applicability: The main problem of 1 *g* tests is the high dilatancy, high friction angle and the low stiffness of the soil at low pressures. To overcome this shortcoming, test series using Soiltron have been carried out. Soiltron is soil enriched with light and soft additives and behaves in the model test as prototype soil under higher stresses (Laudahn 2004). The results from these tests may be found in Mähr (2006).

Apart from the limitations of barotropy[3] the so-called particle size effect is a further limitation of geometrically scaled tests. As the grain size of the model soil is in the range of natural soils, the shear bands, which generally have an approximate thickness of 10 times the mean particle size, will have the same thickness in the model as in reality. The particle size effect is reported by ETH Zürich (2003) to play a minor role, if the relevant dimension of the model (e.g. the diameter $D = 170$ mm) is >30 d_{50} of the soil model (here, the mean diameter is $d_{50} = 0.58$ mm), which is the case in this work.

6.1 *Results*

6.1.1 *"Loose" initial state*

The qualitative behaviour of soil in the FE model is examined by a comparison of FE analyses and laboratory tests with similar initial densities. The initial density indices I_e of the model test series **OR0.66**[4] are in the range from 0.52 to 0.57.

Their qualitative soil behaviour corresponds to the class of tests with "loose" initial state. The tests are compared to a FE analysis with an initial relative density index of $I_e = 0.55$.

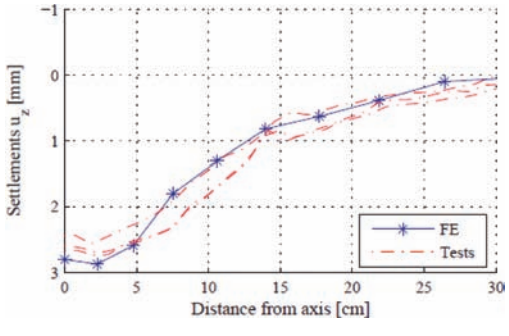

Figure 26. Settlement troughs from FE analysis with $I_e = 0.55$ and test results of tests with "loose" initial state (test series OR0.66): (a) Settlement after contraction of cylinder.

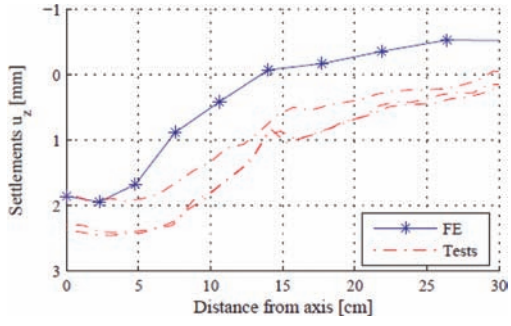

Figure 27. Settlement troughs from FE analysis with $I_e = 0.55$ and test results of tests with "loose" initial state (test series OR0.66) (b) settlement after dilation of cylinder.

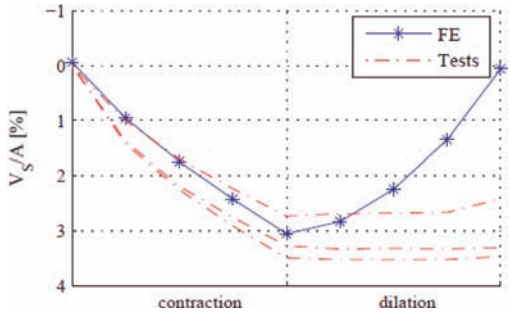

Figure 28. Volume of settlement trough from FE analysis $I_e = 0.55$ and test series OR0.66.

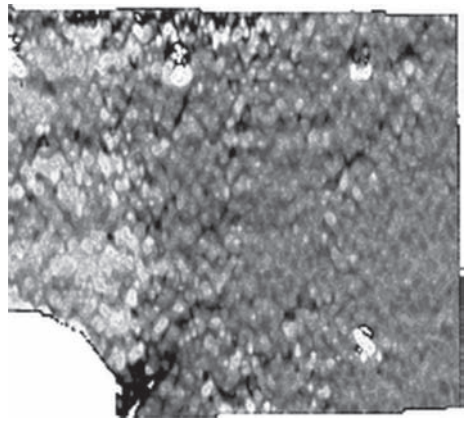

Figure 29. ε_{zz} after contraction: (a) Test OR066-3.

The settlement trough of the FE analysis after contraction shows good agreement with the test results, and so does the graph of the volume of the settlement trough (figure 33 and figure 35). Only at the end of dilation the reduction of the settlement trough is overestimated (figure 34).

3. The stress dependence of soil behaviour is termed barotropy.
4. Ottendork-Okrilla sand; built in with a rake; diameter change of 0.66 cm.

Figure 30. ε_{zz} after contraction: (b) FE analysis, $I_e = 0.55$.

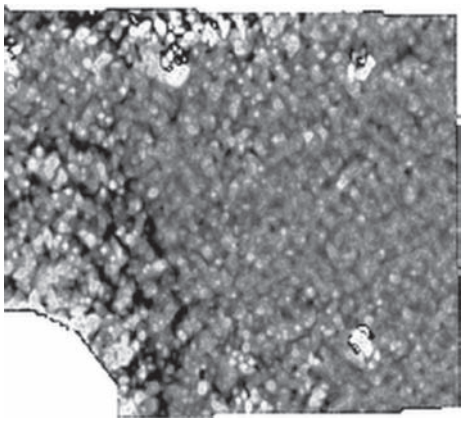

Figure 31. ε_v after dilation: (a) Test OR066-3.

Figure 32. ε_v after dilation: (b) FE analysis, $I_e = 0.55$.

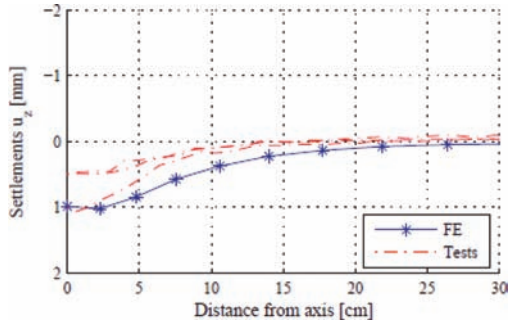

Figure 33. Settlement troughs from FE analysis with $I_e = 0.75$ and test results of tests with "dense" initial state (test series OT0.66): (a) Settlement after contraction of cylinder.

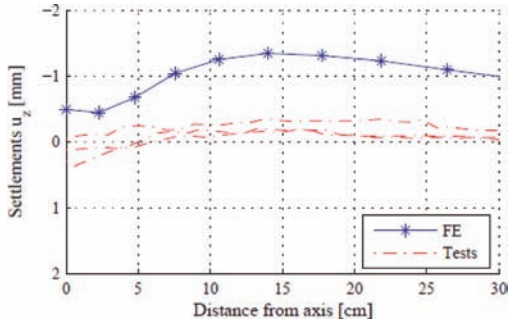

Figure 34. Settlement troughs from FE analysis with $I_e = 0.75$ and test results of tests with "dense" initial state (test series OT0.66): (b) settlement after dilation of cylinder.

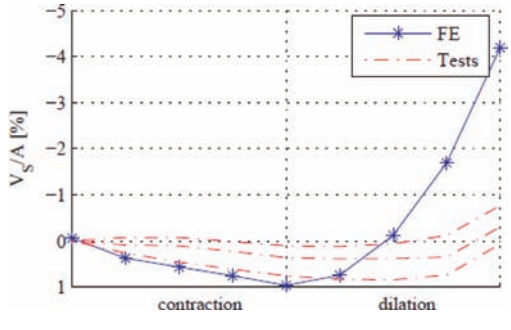

Figure 35. Volume V_S of settlement trough from FE analysis with and test $I_e = 0.75$ series OT0.66.

The vertical strain ε_{zz} after contraction is plotted in figure 30. This plot matches the test results fairly good (figure 29). The volumetric strain after dilation (figure 32) show some discrepancy to the test results (figure 31). Contrary to the model tests no densified

areas (shown by the black areas in figure 31) can be found in the results of the FE analysis. This behaviour may result from the low stress level. Note that the material parameters were calibrated for a stress range from 500–1500 kPa (Laudahn, 2004).

6.2 *"Dense" initial state*

The model test series **OT0.66** may be considered as "dense" initial state tests. All tests of this series were built in with an initial relative density index of 0.75. Their results are compared to a FE analysis with an initial relative density index of $I_e = 0.75$.

Again, the settlement trough of the FE analysis shows good agreement with the test results after contraction (figure 33). But the upheaval at the end of dilation (figure 34) is overestimated and thus the resulting volume of settlement trough is not realistic (figure 35).

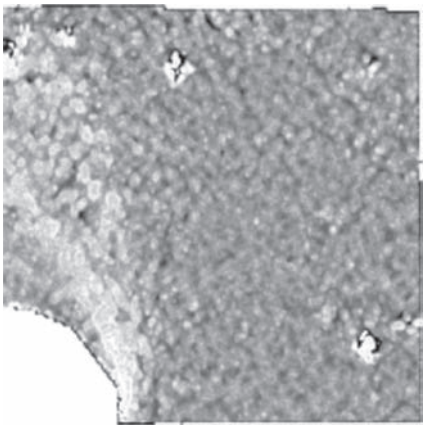

Figure 36. ε_v after contraction: (a) Test OT066-2.

Figure 37. ε_v after contraction: (b) FE analysis.

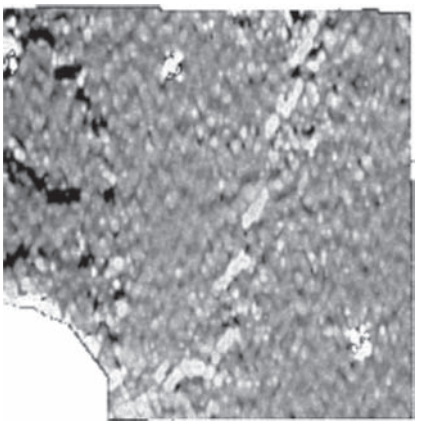

Figure 38. $\varepsilon_{zz,inc}$ after dilation: (a) Test OT066-2.

Figure 39. $\varepsilon_{zz,inc}$ after dilation: (b) FE analysis.

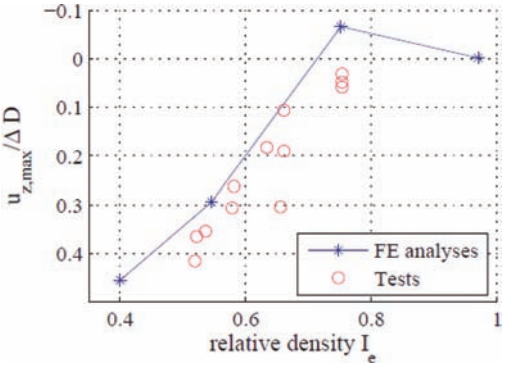

Figure 40. Comparison of FE analyses with tests *after dilation*: (a) Maximum settlements.

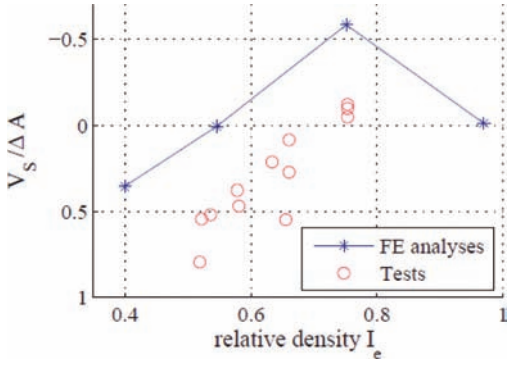

Figure 41. Comparison of FE analyses with tests *after dilation*: (b) Volume V_S of settlement trough.

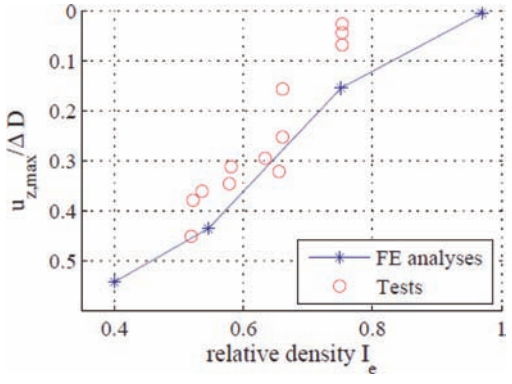

Figure 42. Comparison of FE analyses with tests *after contraction*: (c) Maximum settlements.

The volumetric strain of FE analysis and model test after contraction is plotted in figure 36 and figure 37. The arching effect observed in the test is reproduced by the FE-calculation, even the size of the arch equals the one from the model test.

The white spots in figure 40 border a block that is moving upwards at the end of dilation. The origin of this block formation is also shown in the FE-analysis (figure 41).

6.3 *Summary of FE-calculations with laboratory conditions*

Beneath the above described FE analysis, further calculations with varying densities have been carried out.

The calculated maximum settlements and the volume V_S of the settlement trough after contraction show very good agreement to the ones from the laboratory tests (figure 42 and figure 43). Remember that the material parameters are not fitted, they are taken from Laudahn (2004).

While the maximum settlements after dilation show quite a good agreement to the ones from the tests (figure 40), the heave due to tunnel dilation is overestimated and thus the volume V_S of settlement trough is underestimated by the FE analyses (figure 41).

As discussed above, this may result from the low stress level and the fact that the material parameters are not fitted to this conditions.

6.3.1 *Influence of stress level*

All laboratory tests and FE analyses have been carried out under normal gravitational conditions, so called 1 *g* tests. Due to stress dependence (barotropy), these tests and analyses have limited applicability. Thus, FE analyses with prototype stresses have been carried out. The earth pressure coefficient for the initial state has been set to $K = 0.46$. In this

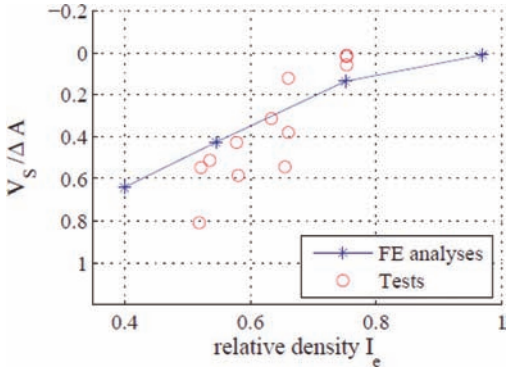

Figure 43. Comparison of FE analyses with tests *after contraction*: (d) Volume V_S of settlement trough.

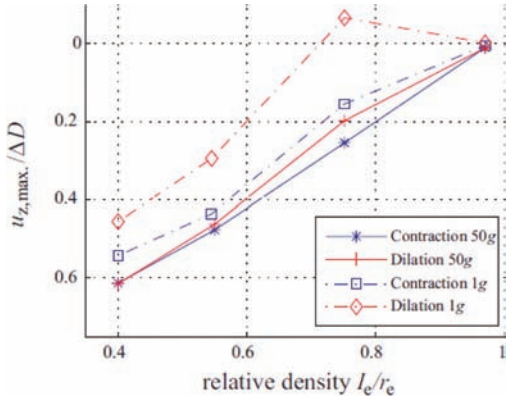

Figure 44. (a) Volume of settlement trough V_S vs. relative density I_e (1 *g* analyses) and relative stress dependent density r_e (50 *g* analyses).

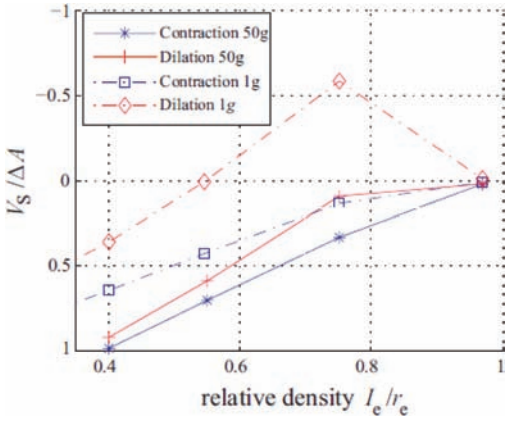

Figure 45. (b) Settlement above crown vs. relative density I_e (1 *g* analyses) and relative stress dependent density r_e (50 *g* analyses).

parametric study the stress dependent density has been used to define the initial density, which has been varied as follows: r_e = [0.4; 0.55; 0.75; 0.97].

Due to higher stresses the soil behaves softer and thus the settlements from prototype analyses (50 *g*) are larger than the ones from the model analyses (1 *g*) (figure 44).

Moreover the upheaval of the surface due to dilation of the cylinder is smaller in the prototype analyses than in the model analyses.

This results from the lower angle of dilatancy at higher stresses.

Thus, "dense" soil behaviour is not likely to occur at tunnel sites. One may conclude that non-cohesive soils behave at stress levels of shallow tunnel sites like the model tests with "loose" initial state.

6.3.2 *Influence of earth pressure coefficient K*

The influence of the earth pressure coefficient K is studied by a number of analyses with various initial lateral earth pressure coefficients. Figure 46 and figure 47 show that form and extent of the settlement trough depends on K. The higher the lateral pressure is, the smaller are the settlements after the contraction (figure 48). Due to the lateral restrain the settlement trough from analyses with high K values are wider than the ones with low K values. As a result the volumes V_S of the settlement trough after contraction from high K are nearly the same, as from low K (figure 49).

Furthermore the earth pressure coefficient K has considerable influence on the soil behaviour at dilation of the cylinder (i.e. tail gap grouting). While the surface is more or less unaffected at low earth pressure $K = 0.46$ (figure 46), the settlements

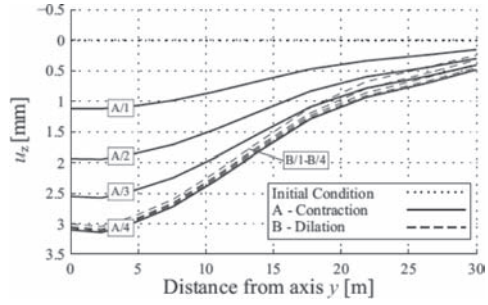

Figure 46. Settlement troughs for (a) $K = 0.46$.

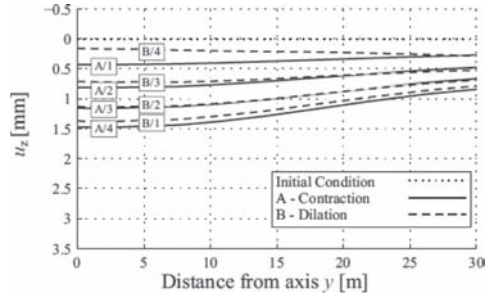

Figure 47. Settlement troughs for (b) $K = 2.0$.

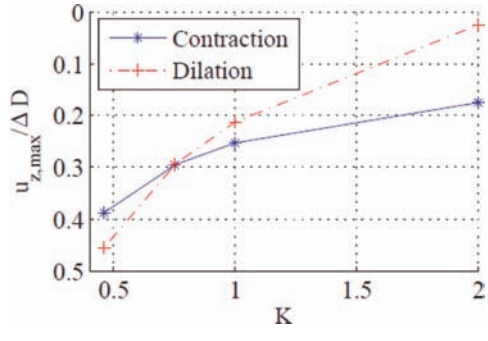

Figure 48. Influence of K on (a) maximum settlements.

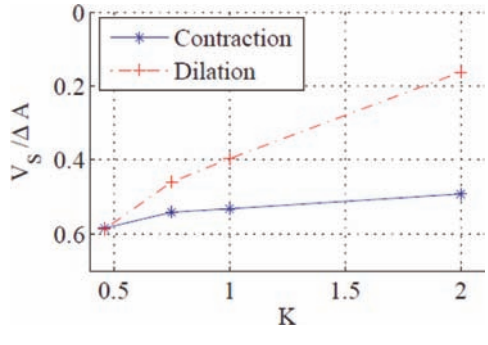

Figure 49. Influence of K on volume V_S of (b) settlement trough.

are nearly reversed at high lateral earth pressure coefficient $K = 2.0$ (figure 47).

7 CONCLUSIONS

Tunnelling near historic buildings can affect them due to deformation of the ground. Since this deformation can hardly be estimated, we should try to control and limit it. One of the principal tools is tail gap grouting. The settlement due to tail gap closure, however, can not be completely revoked with grouting from the very beginning—apart from excessive grouting. This is due to the contractancy of soil at loading-unloading cycles and has been simulated with finite elements and the hypoplastic constitutive equation. The comparison of the settlement trough obtained using elasto-plasticity and the one obtained with hypoplasticity points out to the advantage of using realistic constitutive laws such as hypoplasticity. In FE models of shield tunnelling with advanced boundary conditions (e.g. Kasper & Meschke (2004) or Komiya (2003)) loading-unloading cycles are produced. Thus, the use of a realistic constitutive model is of major importance.

The FE analyses showed, that

- Hypoplasticity is an appropriate tool to model cyclic dilation/contraction of a cylinder and thus to model shield tunnelling,
- non-cohesive soils behave at stress levels of shallow tunnel sites like the model tests with "loose" initial state. Hence, tail gap grouting is not successful for such soils.
- the earth pressure coefficient K influences magnitude and extend of the settlement curve. The higher K, the wider is the settlement trough and the smaller are the maximum settlements. Thus, a higher K value means a flatter settlement curve and minor danger for adjacent buildings.

REFERENCES

Bauer, E. (1996). Calibration of a comprehensive hypoplastic model for granular materials. *Soils and Foundations*, 360 (1):0 169–183.

ETH Zürich, Institute of Geotechnical Engineering Modelling in geotechnics (2003). Technical report, http://geotec4.ethz.ch/mig/.

Eisenstein, Z. (2003). Geotechnical challanges in soft ground tunnelling—examples from significant projects. In Vanicek et al., editor, *Proc. XIII ECSMGE*, volume 3, 779–782, Prague.

Fellin, W. & A. Ostermann (2002a). Consistent tangent operators for constitutive rate equations. *International Journal for Numerical and Analytical Methods in Geomechanics*, 26:0 1213–1233.

Herle, I. (1997). Hypoplastizität und Granulometrie einfacher Korngerüste. Institut für Bodenmechanik und Felsmechanik, University of Karlsruhe. *Heft 142*.

Herle, I. & G. Gudehus (1999). Determination of parameters of a hypoplastic constitutive model from properties of grain assemblies. *Mechanics of Cohesive frictional materials*, 40(5):0 461–486.

Jancsecz, S., W. Frietzsche, J. Breuer & K.R. Ulrichs (2001). *Tunnelbau 2001*, volume 25, chapter III. Minimierung von Senkungen beim Schildvortrieb am Beispiel der U-Bahn Düsseldorf, Glückauf, Essen, 165–214.

Kasper, T. & G. Meschke (2004). A 3D finite element simulation model for TBM tunnelling in soft ground. *Int. J. Numer. Anal. Meth. Geomech.*, 28:0 1441–1460.

König, D. (1994). *Beanspruchung von Tunnel—und Schachtausbauten in kohäsionslosem Lockergestein unter Berücksichtigung der Verformungen im Boden*. PhD publication, University of Bochum.

Kolymbas, D. (1978). Ein nichtlineares visko-plastisches Stoffgesetz für Böden., Institut für Bodenmechanik und Felsmechanik, University Fridericiana, Karsruhe. *Heft 77*.

Kolymbas, D. (1998). *Geotechnik—Tunnelbau und Tunnelmechanik*. Springer, August 1998.

Kolymbas, D., M. Mähr & I. Herle (2002). Tail gap grouting. In *Proceedings of ACUUS 2002—Urban Underground space: a Resource for Cities*, Turin.

Komiya, K. (2003). Finite element modelling of TBM excavation and advancement processes in soft ground. In E. Onate and D.R.J. Owen, editors, *VII International Conference on Computational Plasticity*.

Lanier, J., C. Di Prisco & R. Nova (1991). Induced anisotropy in hostun sand: experiments and theoretical analysis. *Rev. Franc. Geotech.*, 0 (57):0 59–74, October 1991.

Laudahn, A. (2004). *An Approach to 1g Modelling in Geotechnical Engineering with Soiltron*. PhD publication, Institute of Geotechnical and Tunnelling Engineering, University of Innsbruck.

Lee, K.M. & R.K. Rowe (1991). An analysis of three-dimensional ground movements: the thunder bay tunnel. *Canadian Geotechnic Journal*, 28:0 25–41.

Mähr M. & I. Herle (2004). Volume loss and soil dilatancy. *Rivista Geotechnica Italiana*, 0 (4):0 32–40.

Mähr, M. (2005). Ground movements induced by shield tunnelling in non-cohesive soils.

Nübel, K. (2002). Experimental and Numerical Investigation of Shear Localization in Granular Material., Institut für Bodenmechanik und Felsmechanik, University Fridericiana, Karsruhe. *Heft 156*.

Ohde, J. (1938). Zur Theorie der Druckverteilung im Baugrund. *Bauingenieur*, 20:0 451–459, 1938.

Rowe, R.K. & K.Y. Lo (1983). A method of estimating surface settlement above tunnels constructed in soft ground. *Canadian Geotechnical Journal*, 20:0 11–20.

Truesdell, C. (1955). Hypoelasticity. *Journal of rational mechanics and analysis*, 4:0 83–133.

Truesdell, C. & W. Noll (1992). *The Non-Linear Field Theories of Mechanics*. Springer.

von Wolffersdorff, P.-A. (1996). A hypoplastic relation for granular materials with a predifined limit state surface. *Mechanics of Cohesive-Frictional Materials*, 251–271.

Geotechnical Engineering for the Preservation of Monuments and Historic Sites – Bilotta, Flora, Lirer & Viggiani (eds)
© 2013 Taylor & Francis Group, London, ISBN 978-1-138-00055-1

An innovative approach for reducing the seismic risk of existing buildings and historic sites

D. Lombardi, A. Flora, S. Lirer & F. Silvestri
University of Napoli Federico II, Italy

ABSTRACT: The seismic risk is one of biggest challenges for civil engineers, and a number of mitigation strategies have been developed in time with reference to existing or new buildings. Nowadays, refined techniques based either on structural reinforcement or seismic isolation exist to protect new and existing structures from seismic shaking. This paper presents some results of a research activity in progress at the University of Napoli Federico II (Italy), aimed to check the effectiveness of an innovative approach for reducing the seismic risk by using soft grouting mixtures installed at an optimum depth in the foundation soil. The basic idea is that a thin grouted layer, with a dynamic impedance much smaller than that of the surrounding soil, will filter most of the seismic ground motion, with very little energy being transmitted to the overlying soil. The effectiveness of the insertion of a soft grouted layer in the range of frequency affecting the response of squat buildings was numerically tested via a parametric analyses, with reference to a simplified one-dimensional scheme.

1 INTRODUCTION

The safety of existing buildings against natural hazards is one of the major issues in geotechnical and structural engineering research, still far from being satisfactorily solved. In the case of historical buildings, further difficulties in approaching the problem are due to the tight constraints imposed by the cultural value of the construction to be preserved: in taking care of valuable monuments and buildings, no matter the resources required, the preservation of their overall integrity should be granted (ICOMOS, 1964). Even though the definition of integrity itself is not straightforward (Viggiani, 2013), the ideal strategy in the design of protection interventions should be that of solving the problem without modifying the original structure, or affecting it the least possible.

In other words, the optimum risk mitigation approach for valuable buildings and monuments should either imply the lowering of the site-specific hazard and/or the reduction of vulnerability; the former option corresponds to limiting the effects of the external action (i.e. the 'demand'), the latter to increasing the 'capacity' of the structure. Indeed, the first strategy is possible and currently pursued when facing those natural hazards (like slope instability) for which the probability of happening of a critical natural mechanism can be reduced by designing stabilization interventions; on the other hand, it might be observed that there is nothing that the technical community can do to reduce the seismic hazard. As a consequence, it is widely accepted that the mitigation of seismic risk cannot be carried out but reducing the building vulnerability through structural reinforcement. While this is nowadays relatively simple for new and existing ordinary buildings, it is very difficult to accomplish for historical building and monuments, for which integrity is of concern.

As it is formulated, it seems a problem which allows no completely satisfactory solution. This paper presents a research activity in progress, conceived to overcome this lack of solution.

2 AN INNOVATIVE APPROACH

In the performance-based design approach, the two key elements for a seismic safety assessment of a building (Fig. 1a) are the seismic demand and the capacity curve. This latter is often referred to as a 'pushover curve' (Fig. 1b), relating the base shear force, V_b, to a reference horizontal displacement, Δ, for instance at the top of the building (see Fig. 1a).

The seismic demand for the pseudo-static analysis of a rigid system can be typically defined in terms of a seismic coefficient (proportional to the design peak ground acceleration, a_{max}); for deformable systems, the most conventional way to express it is by using the spectral acceleration, $S_a(T)$, the spectral displacement, $S_d(T)$, or both (Fig. 1b). For a structure with a given fundamental period,

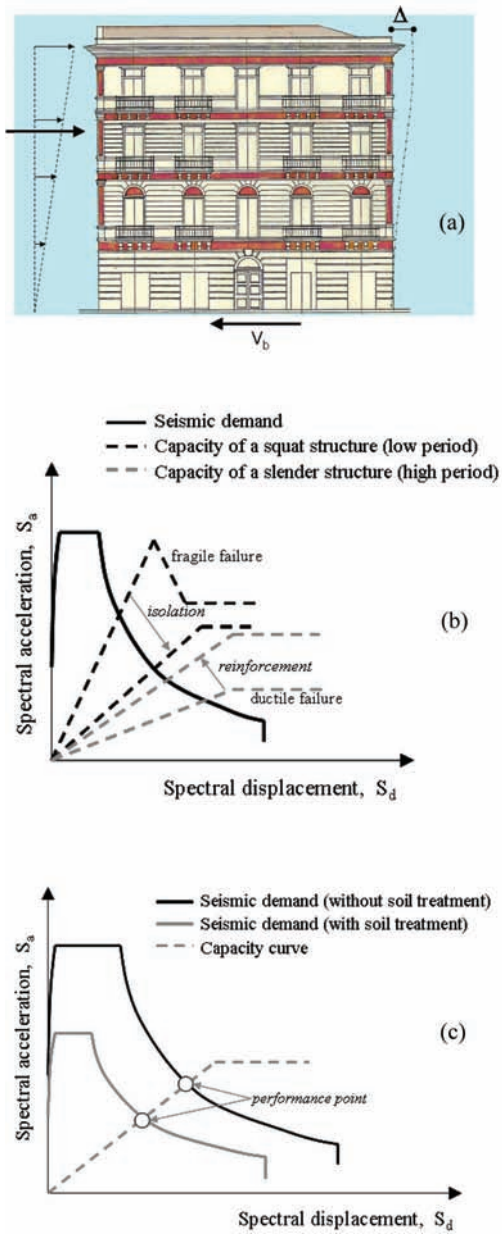

Figure 1. Seismic safety assessment procedure.

T, these latter can be viewed as proportional to the above defined shear force and displacement, respectively.

These latter can be thought as depending on the regional seismic hazard, the seismic site response and the system ductility. The safety assessment can be therefore expressed by comparing demand and capacity, individuating a 'performance point' at the intersection of the curves (Fig. 1c).

If the safety of the building is not guaranteed, its vulnerability can be mitigated by changing either the capacity curve or the seismic demand. While a reinforcement can be viewed as modifying the pushover curve by increasing both the stiffness and the strength of the building, the base isolation techniques reduce the fragility and increase the ductility in the structural capacity (Fig. 1b). In the case of old constructions, it would be desirable not to modify the capacity curve of the building, but to change the seismic demand.

A research programme, coupling both theoretical and experimental activities, is in progress at the University of Napoli Federico II (Italy) (Lombardi et al., 2012); the aim is to explore the possibility of mitigating seismic risk of historical buildings by reducing the seismic demand in the range of periods most typical for old masonry structures (Fig. 1c). Since neither the building ductility can be increased nor a base isolation system can be adopted, the approach involves the optimized design of a soil treatment in depth with the aim of artificially changing the seismic site response in the range of periods of interest.

The basic idea is to install a grouted layer at a suitable depth, by injecting a soft material with a dynamic impedance η ($= \rho \cdot V_S$, where ρ is the material density and V_S the shear wave velocity) much lower than that of the surrounding soil. As for base isolation systems, most of the seismically induced effects should concentrate into the treated layer, with very little energy being transmitted to the overlying soil and structure. Literature indications on this topic are few, and-if any-referring to shallow soil treatments (e.g. Chouw and Schmid, 1992; d'Onofrio et al., 1999; Kellezi, 2001). Recently, some authors approached the topic in a similar way, using soft layers beneath the structure (Wood, 2007; Kirtas and Pitilakis, 2009; Alterio, 2012).

The relevant-and not trivial-issues to be addressed are:

- the choice of the best suited grout to be injected
- the depth and the geometrical configuration of the grouted layer.

In particular, the grouted material should be soft and fluid enough to be easily and continuously injected at depth, while the curtain should be deep enough to prevent measurable static settlements and to exclude a reduction of the foundation safety. This latter requirement can be guaranteed by grouting at depths high enough that no interaction must be expected with the structure to be protected; on the other hand, the grouting depth should be not too high to make the installation procedure not affordable or the attenuation of seismic energy not

effective. Unless the structure is extremely large or founded on piles (which is hardly the case for historic buildings and monuments), a good working balance between the two requirements might be a depth of the order of 15–30 m. Whatever the choice, specific seismic response analyses must be carried out case by case, in order to verify the effectiveness on the attenuation of the seismic actions at surface.

In the following, preliminary simplified numerical analyses will be presented and the results discussed to assess the beneficial effect of the proposed grouted curtains. Since no particular building structure is considered, the overall effect of the proposed intervention on the free-field seismic response will be quantified through the spectral intensity SI (Housner, 1952), often called 'Housner intensity', defined as:

$$SI(\xi) = \int_{T_1}^{T_2} S_v(\xi, T)\,d(T) \quad (1)$$

where $S_v(\xi,T)$ is the spectral velocity for a given structural damping ratio ξ and $[T_1,T_2]$ is a reference range of the structural period. The integral quantity SI, which has the dimensions of a displacement, is often adopted as a synthetic ground motion parameter able to capture the combined effect of amplitude and frequency content on the structural damage (Kramer, 1996).

The integration extremes T_1 and T_2 originally proposed by Housner (1952) were respectively 0.1 and 2.5 s, in order to include most of the fundamental periods of civil structures. In this paper, the integration interval was set to focus the attention on squat masonry structures. Consistently with the indications of National Technical Code (NTC, D.M. 14.I.2008), the natural period T_B (s) of a masonry building of height H_B (m) can be estimated through the simplified formula:

$$T_B = 0.05 \cdot H_B^{3/4} \quad (2)$$

In this pilot study, buildings with height H_B = 3–20 m are considered of interest; for such H_B values, eq. (2) yields a fundamental period T_B in the range 0.1–0.5 s, thus assumed as integration extremes in eq. (1).

2 NUMERICAL ANALYSES

2.1 *Geometry and material properties*

In this parametric analysis, a homogeneous fine-grained subsoil was considered, with a thickness H = 60 m (Fig. 2a), a unit weight $\gamma = 20$ kN/m^3 and a shear wave velocity V_S = 300 m/s, corresponding to a medium consistency clay. The natural period, T_S, of the deposit is therefore $T_S = 4H/V_s = 0.8$ s.

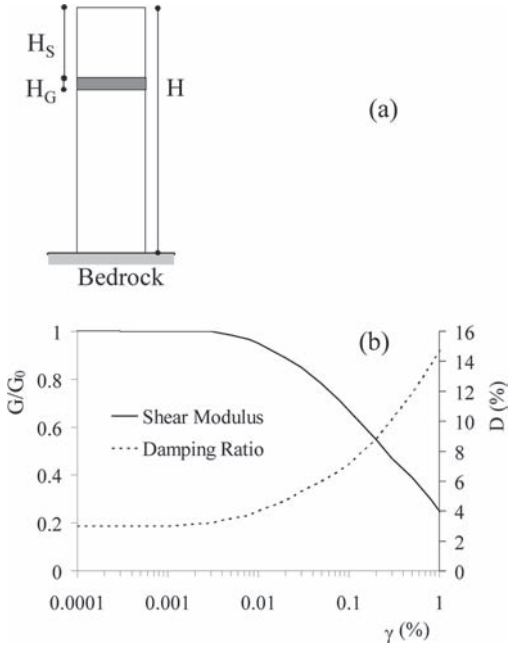

Figure 2. Subsoil model: layering (a), $G(\gamma)/G_0$ and $D(\gamma)$ curves for the natural clay (b).

The clay layer overlies a bedrock, with a thickness of 60 m, at the bottom of which a reference seismic motion with variable frequency content was applied, as described in the next section. To explore the effects of the possible variability of the reference input motion amplitude, two different hypotheses have been considered for the constitutive model of the clay:

i. linear behaviour, characterized by $G = G_0$, where G_0 was calculated as $G_0 = \rho \cdot V_S^2$;
ii. non-linear behaviour, with the shear modulus, G, and the damping ratio, D, depending on the shear strain level as shown in Fig. 2b.

A layer of grouted material with thickness H_G = 1m was then placed at a depth H_S = 20 m (Fig. 2a). The same density as the soil and two extremely different shear wave velocities, V_g, were assumed for such layer, in order to simulate either a stiff (V_g = 1000 m/s) or a very soft grouting (V_g = 20 m/s). Both results can be obtained with low pressure grouting (Lirer et al., 2006; Lombardi et al., 2013).

To evaluate the dependency of the results on the grouting stiffness only, in both cases the material was assumed as linear and the damping ratio set to zero.

Table 1 summarizes the main properties of the natural soil, the bedrock and the grouted layer.

2.2 *Input motions*

The numerical analyses of 1D seismic response were carried out using the code EERA, operating in the frequency domain with linear equivalent approach (Bardet et al., 2000). Simplified input motions were applied at the bedrock in terms of acceleration (a) by means of the seismic Ricker wavelet model (Ryan, 1994). This model can be expressed in term of displacements u as (see Fig. 3):

$$u(t) = u_{\max} \cdot \left(1 - 2\pi^2 f^2 \left(t - t_c\right)^2\right) \cdot e^{-\pi^2 f^2 (t - t_c)^2} \qquad (3)$$

In eq. (3), the parameter f is the dominant frequency, inversely proportional to the peak time, t_c, which also quantifies the wavelet duration. Three different dominant frequencies (f = 1, 3, 5 Hz) were considered, while the peak acceleration (a_{max}) was kept constant and equal to 0.5 g (Tab. 2).

2.3 *Results of the parametric analyses*

The seismic response analyses carried out are summarized in Tab. 3. The behaviour of the natural subsoil (without the grouted layer) was assumed as the reference case.

Table 1. Main properties of the materials.

Material	γ [kN/m³]	ρ [kg/m³]	V_S, V_g [m/s]	η [kg/m²s]	D_0 [%]
Natural soil	20	2040	300	$6.12 \cdot 10^5$	3
Grouted layer	20	2040	1000	$2.04 \cdot 10^6$	0
			20	$4.08 \cdot 10^4$	
Bedrock	20	2040	1000	$2.04 \cdot 10^6$	0

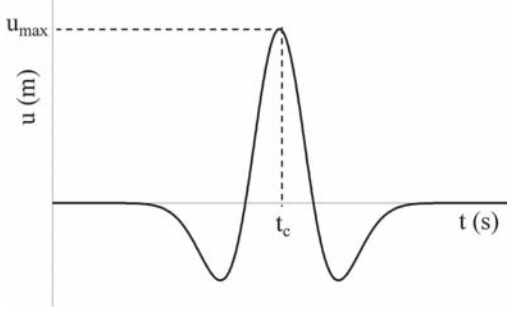

Figure 3. Ricker wavelet in term of displacement (u).

Table 2. Ricker wavelets adopted in the analyses.

Ricker wavelet	f (Hz)	u_{max} (m)	t_c (s)	a_{max} (g)
1	1	0.0828	1.5	0.5
2	3	0.0092	0.5	0.5
3	5	0.0033	0.3	0.5

Table 3. Summary of the parametric analyses.

Layering	Case	f (Hz)	V_g (m/s)
Natural soil	S1, S1*	1	0
	S3,.S3*	3	
	S5, S5*	5	
With grouted layer	T-1000-1	1	1000
	T-1000-3	3	
	T-1000-5	5	
	T-20-1 T-20-1*	1	20
	T-20-3 T-20-3*	3	
	T-20-5 T-20-5*	5	

* Case with linear soil behaviour.

The results of two analyses are plotted in Figs. 4 (S1, T 20 1) and 5 (S3, T20 3) in terms of acceleration and displacement time histories at ground level.

As in the examples shown in the figures, in all cases (see Tab. 4 and Fig. 6) the soft grouted layer was found to increase the duration of the shaking but reducing, even strongly, the peak ground acceleration. On the contrary, the effect was not always the same in terms of maximum surface displacements (see Tab. 4 and Fig. 6): in most cases, the introduction of the soft grouted layer did not reduce significantly the peak value, with the exception of the linear analysis T-20-1*, for which the dominant frequency of the Ricker wavelet (1 Hz) was close to the natural frequency of the deposit (1.25 Hz). In this latter case, the peak displacement at ground level was seen to slightly increase. It can be noted (Tab. 4) that the stiff grout layer has no influence on the seismic response: these analyses will not be therefore considered in the following.

The numerical results are also plotted in Fig. 7, in terms of peak acceleration a_{max} (Fig. 7a) and maximum displacement u_{max} (Fig. 7b), in each layer. For each seismic input considered, the peak acceleration profile strongly decreases across the soft grouted layer, keeping reduced values up to ground surface. At the same time, the peak displacement increments are concentrated within the grouted layer.

The effectiveness of the soft grouted layer and the role of soil non-linearity in attenuating the seismic inertial actions can be better inferred by ana-

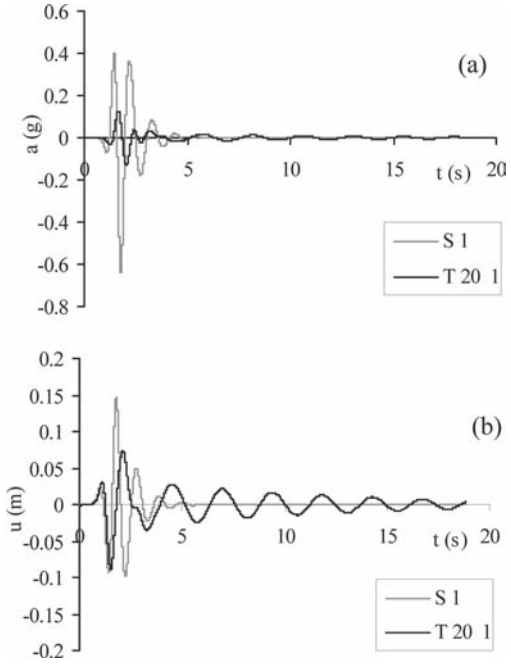

Figure 4. Time histories of acceleration (a) and displacement (b) at the ground surface for natural and treated soil under a 1 Hz input motion.

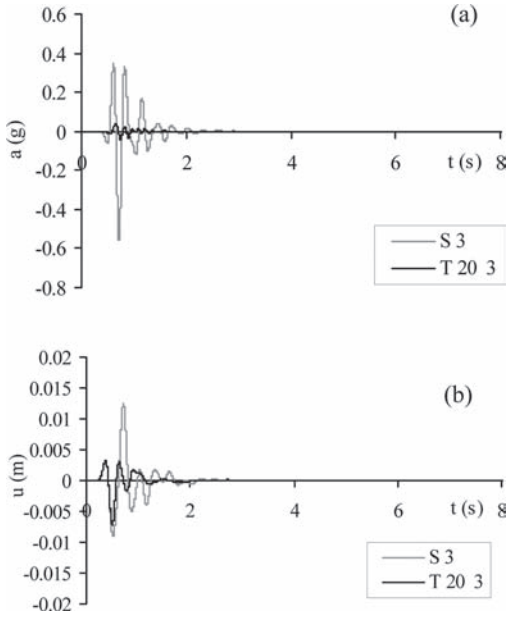

Figure 5. Time histories of acceleration (a) and displacement (b) at the ground surface for natural and treated soil under a 3 Hz input motion.

Table 4. Summary of the numerical results.

Layering	Case	Peak acceleration a_{max} (g)	Peak displacement u_{max} (m)
Natural soil	S1	0.639	0.146
	S1*	0.898	0.133
	S3	0.558	0.012
	S3*	0.649	0.014
	S5	0.505	0.004
	S5*	0.582	0.004
With grouted layer	T-1000-1-	0.631	0.145
	T-1000-3-	0.568	0.013
	T-1000-5-	0.505	0.004
	T-20-1	0.130	0.090
	T-20-1*	0.377	0.146
	T-20-3	0.036	0.007
	T-20-3*	0.066	0.007
	T-20-5	0.052	0.003
	T-20-5*	0.145	0.003

* Case with linear soil behaviour.

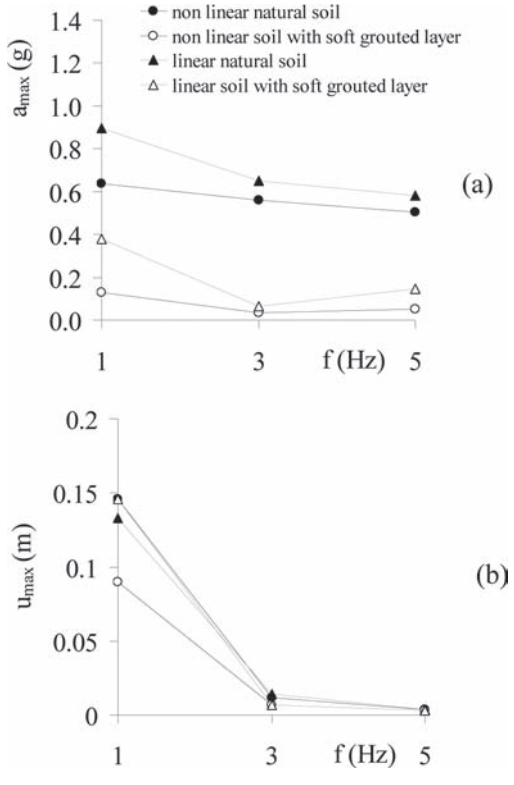

Figure 6. Results in terms of peak acceleration (a) and displacement (b) at the ground level.

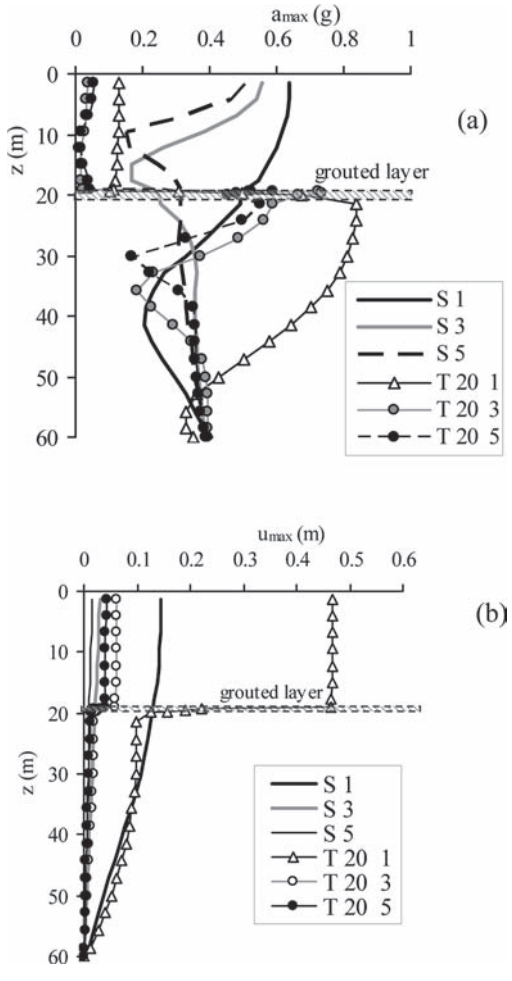

Figure 7. Vertical profiles of peak acceleration (a) and peak displacement relative to the bedrock (b) computed without (S1, S3, S5) and with (T 20 1, T 20 3, T20 5) the grouted soft layer.

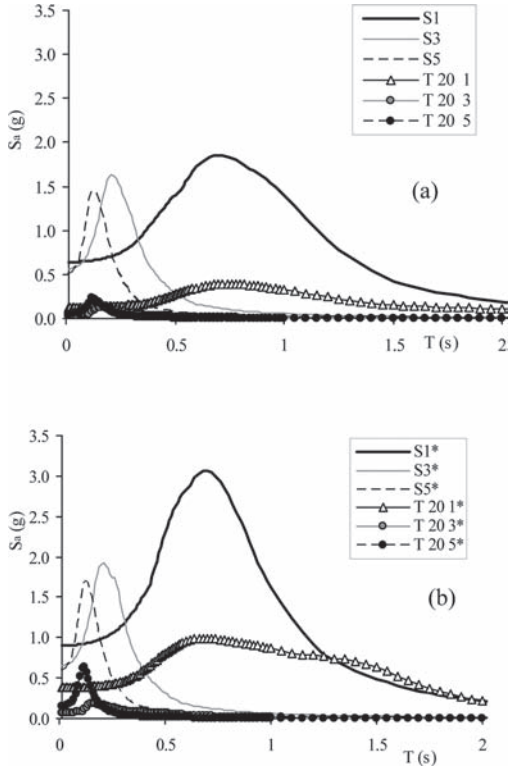

Figure 8. Acceleration response spectra at surface from non-linear (a) and linear (b) analyses without (S1*, S3*, S5*) and with (T 20 1*, T 20 3*, T20 5*) the soft grouted layer.

lysing the acceleration response spectra $S_a(T, \xi)$, calculated assuming—as usual—a structural damping $\xi = 5\%$.

The spectral accelerations at surface resulting from the non-linear and linear analyses are plotted in Figs. 8a and 8b, respectively. It can be observed that, for all the input motions, the soft layer significantly modifies the seismic response at surface, reducing the peak values of the spectral acceleration.

For the range of periods considered as significant in this work ($0.1 < T < 0.5$ s), both Figs. 8a and 8b indicate that the grouting intervention is effective in reducing the inertial forces on structures.

In the case of non-linear analysis (Fig. 8a) of untreated soil shaken by the 1 Hz Ricker wavelet (S1), the maximum spectral amplification corresponds to a SDOF (single degree of freedom oscillator) with a natural period close to that of the soil deposit (double resonance mechanism). For such a case, the insertion of the grouted layer (T 20 1) induces a beneficial effect by reducing the maximum spectral acceleration to about 20%.

Similar qualitative considerations can also be taken for the spectral accelerations predicted under the hypothesis of linear soil behaviour (Fig. 8b). The quantitative differences are related to the stiffer response of the clay soil, which in these cases induces larger amplifications. For the cases S1* and T 20 1*, the crossing point of the spectra, individuating the onset of a worse response with the grouted layer, is shifted at a period equal to 1.3 s, corresponding to a structure as high as 75 m.

From this latter example, it can be concluded that the insertion of a soft layer cannot be viewed as an universal mitigation solution, but it needs to be accurately tuned on the basis of the expected dynamic coupling between the expected ground motion and the structure to be protected.

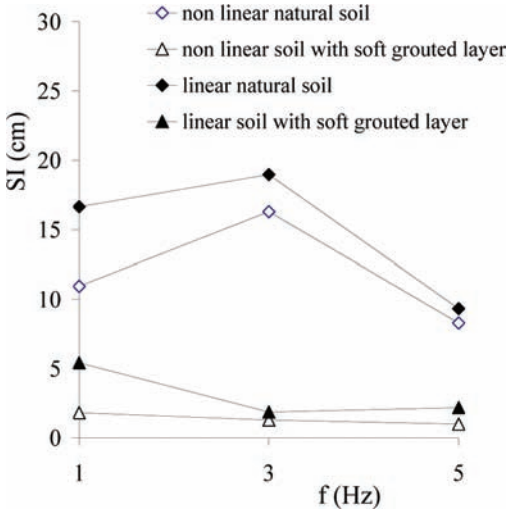

Figure 9. Spectral intensity SI values (eq. 1) obtained at surface versus the dominant input frequency.

The above observations can be further synthesized in terms of spectral intensity, SI (eq. 1), plotted in Fig. 9 against the input frequency, for all the analyses carried out with and without the soft grout layer. For every input dominant frequency adopted (1, 3, 5 Hz), the soft grouted layer reduces the effects at ground level in the range of periods T typical for old squat masonry structures.

3 CONCLUDING REMARKS

In this pilot study, the insertion of a soft grouted layer, with a dynamic impedance much smaller than that of the surrounding soil, was observed to reduce the peak ground acceleration and, as a consequence, the pseudo-static equivalent force acting on an ideally rigid body at surface.

The proposed deep ground treatment was also verified to be effective for the attenuation of spectral intensity in the range of periods pertaining to medium-stiff constructions, including masonry buildings. On the other hand, the insertion of a soft grouted layer may increase the spectral acceleration for large periods, corresponding to slender structures such as, for instance, tall towers.

This approach appears therefore a valid alternative to other more conventional and invasive solutions, such as the structural reinforcement and base isolation, and can result suited for the historical constructions for which integrity has to be preserved.

Since the effectiveness of the grouting depends on the dynamic coupling of the input motion with the subsoil and the building response, further analyses considering different mechanical properties of both the natural soil and the grouted layer are required, in order to support preliminary design criteria to tune the properties of the soft grouting and the optimal installation depth. Also, 2D or 3D geometrical configurations need to be analysed to get more conclusive considerations on the feasibility of such interventions.

ACKNOWLEDGMENTS

This work is part of a Research Project funded by ReLUIS (*Italian University Network of Seismic Engineering Laboratories*) Consortium.

REFERENCES

Alterio, L. 2012. Seismic vulnerability reduction of monumental building by soils treatments, PhD thesis on Construction Engineering, Università di Napoli.

Bardet, J.P., Ichii, K., Lin, C.H. 2000. *EERA a Computer Program for Equivalent-linear Earthquake site Response Analyses of Layered Soil Deposits*. Univ. of Southern California, Dep. of Civil Eng.

Chouw, N. & Schmid, G. 1992. Building isolation using the transmitting behaviour of a soil layer. *Proc. 10th World Conference on Earthquake Engineering*, Madrid. 4:2519–2524.

DM 14/1/2008. *Norme Tecniche per le Costruzioni*. S.O. n. 30-Gazzetta Ufficiale della Repubblica Italiana, No. 20-4/2/2008.

d'Onofrio, A., Mancuso, C., Silvestri, F. 1999. Reduction of seismic vulnerability by geomaterial attenuation procedures. *II Int. Symp. on Earthquake Geotechnical Engineering, Lisboa*, 2:725–730. Balkema, Rotterdam.

Housner, G.W. 1952. Spectrum intensity of strong-motion earthquakes. *Proc.. Symp. on Earthquakes and Blast Effects on Structures*, EERI, Univ. of California at Los Angeles, Earthquake Engineering Research Institute, Oakland, Calif., 26–36.

ICOMOS 1964. The Venice Charter (1964). International charter for the conservation and restoration of monuments and sites. *II International Congress of Architects and Technicians of Historic Monuments, Venice.* ICOMOS, Int. Council on Monuments and Sites. internet: www.icomos.org/charters/venice_e.pdf.

Lirer, S., Flora, A., Verdolotti, L., Lavorgna, M. & Iannace, S. (2006): Permeation grouting of fine grained pyroclastic soils and rocks. *Ground Improvement*, Vol. 10, pp. 135–177, Thomas Telford Ed.

Lombardi, D., Flora, A., Lirer, S. 2012. A new approach for reducing seismic hazard on existing buildings by unusual deep soil grouting. *Int. Conf. on Ground Improvement and Ground Control* (ICGI 2012), University of Wollongong, Australia. Spec. Pub. in Ground Improvement.

Lombardi, D., Flora, A., Lirer, S., Silvestri F. 2013. Soil Grouting for the seismic protection of existing buildings. *Ground Improvement*, Thomas Telford Ed. *In press.*

Kellezi, L. 2011. Dynamic behavior of a softer layer overlying hard soil/bedrock and vibration reduction. *GEO-Danish Geotechnical Institute,* Lyngby.
Kirtas, E. & Pitilakis, K. 2009. Subsoil interventions effect on structural seismic response. Part II: parametric investigation. *Soil Dynamics and Earthquake Engineering*, 13(3): 328–344.
Kramer, S.L. 1996. *Geotechnical Earthquake Engineering.* Prentice Hall, p. 653.
Ryan, H. 1994. *Ricker, Ormsby, Klauder, Butterworth—A choice of wavelets*. CSEG.
Viggiani, C. 2013. CH Volume, This conference.
Wood, D.M. 2007. Modelling of dynamic soil problems. *Proc. 4th International Conference on Earthquake Geotechnical Engineering*, Thessaloniki. 6: 131–149.

Geotechnical Engineering for the Preservation of Monuments and Historic Sites – Bilotta, Flora, Lirer & Viggiani (eds)
© 2013 Taylor & Francis Group, London, ISBN 978-1-138-00055-1

Preservation of historic structures and monuments using minimally invasive Screw-Piles and Helical Anchors—two cases

A.J. Lutenegger
University of Massachusetts, Amherst, USA

D. Robson
Subsurface Technologies, Ltd., Alnwick, Northumberland, UK

P. Mohan
GP Structural Ltd., Henley-in-Arden, Warwickshire, UK

ABSTRACT: The fabric of most historically significant structures and monuments is often delicate and sensitive to invasive methods of preservation. This often requires special consideration to geotechnical practices used for preservation through common methods. The technology associated with the use of Screw-Piles and Helical Anchors for historic preservation of structures allows for an alternative approach that can be minimally invasive while at the same time providing long-tern structural solutions in the case of potentially unstable conditions. This technology can also be attractive for seismic retrofitting of historic structures which is often of great importance and can be applied to buildings, bridges, retaining walls and many other structures. Installation of Screw-Piles and Helical Anchors generally proceeds without loss of ground and often requires only minimal ground disturbance and almost no vibration. In the case of underpinning, some excavation may be required but this can usually be performed without damage to the existing structure. The technology of Screw-Piles and Helical Anchors is described through the presentation of two cases in the UK that are used to illustrate where this approach was used to successfully stabilize two historically important masonry structures. The advantages and limitations of the technology are discussed as they pertain to preservation of historic structures and monuments.

1 INTRODUCTION

Historic structures, like all structures, can undergo settlements over time which are produced from several sources. Settlement can occur as a result of the slow long-term consolidation process that occurs if a structure has been built on soft soils such as clays or organic soils. Alternatively, settlements can occur if subsurface changes have occurred at a site for example by lowering the water table leading to desiccation and shrinking of the soil or removing support from under or adjacent to a structure by recent excavations. No matter the cause, the result of settlements is generally structural distress that must be addressed before additional problems arise or for that matter a partial or complete failure occurs. Structural intervention to provide an engineering solution in these cases generally involves some form of underpinning although other methods, such as soil extraction which was successfully used to stabilize the bell tower at Pisa (Burland et al. 2003).

The foundation restoration of historic structures can present some unique challenges to the engineer to devise appropriate remedial support techniques. These challenges often include such issues as: unknown existing foundation conditions, unknown or unexpected soil and groundwater conditions, heavy loads, limited access, sensitive status of the historic fabric of the structure (Ciancia et al. 2006), but can also include: maintaining adequate support during restoration, sensitivity to specific construction activities such as vibration or noise, and the desire to create the least amount of intrusion to the structure or disrupt the current use of the structure. Historic structures can be particularly sensitive to structural intervention to stabilize the foundation as in some cases the structural connection between the foundation and the overlying structure may also be weakened over time.

A number of examples may be cited in which foundation repairs have been made to historic masonry structures using a wide variety of techniques, including, drilled micropiles,

jacked minipiles, jet grouting, chemical grouting and conventional piles (e.g., Dooff et al. 1995; Avellan & Lange 1997; Chartres 1997; Rodriguez Ortiz & Monteverde 1997).

Screw-Piles have also previously been used to underpin or repair the existing foundations of historic structures. Crocker (2005) suggested the possibility of helical piers in historic settings Sherwood (2006) described the use of 83 screw-piles to support new classrooms in Salisbury, UK. Screw-Piles were selected to reduce ground disturbance to a minimum since the site was located adjacent to the Salisbury Cathedral Close. Lutenegger and Kempker (2008) described the use of screw-piles to reinforce the foundations of four masonry structures in the U.S. built between 1854 and 1906 representing historical structures from 100 to 150 years old.

Two case histories are presented in this paper and illustrate the application of Helical Screw-Piles for the preservation of two historic masonry structures in the UK. The cases represent a range of soil conditions and demonstrate that Screw-Piles present a unique approach for engineers who are faced with foundation stability problems in historic settings.

2 SCREW-PILE TECHNOLOGY

Screw-Pile foundations are a product of mid 19th century Victorian engineering (Lutenegger 2011). Most historians give credit to the introduction of Screw-Piles as viable foundations to Alexander Mitchell, a Scottish self-taught engineer and contractor who initially developed iron Screw-Piles for use as foundations for offshore lighthouse around the coasts of England. Mitchell (1848) described the mechanics of the functionality of Screw-Piles as:

> "Whether this broad spiral flange, or "Ground Screw," as it may be termed, be applied … to support a superincumbent weight, or be employed … to resist an upward strain, its holding power entirely depends upon the area of its disc, the nature of the ground into which it is inserted, and the depth to which it is forced beneath the surface."

All of the Screw-Piles used by Mitchell between about 1836 and 1870 were fabricated by a combination of cast-iron plates and wrought-iron shafts, both of which could be readily manufactured in England during this time period. In nearly every case of Screw-Pile installation before about 1900, the Screw-piles were installed by manual labor using a large capstan attached to the top of the shaft and turned by as many as 40 men. No vertical load was applied to assist the installation, the pitch of the screw blade was sufficient to produce advance of the crew with rotation of the shaft.

During the mid to late 19th century, Screw-Piles were used throughout the world to provide support for offshore and onshore lighthouses, ocean front piers, bridges, slope stabilization and underpinning. Duckham (1889) described the use of Screw-Pile foundations to underpin the town hall at Great Yarmouth, UK, which had undergone several inches of settlement as a result of consolidation of very soft underlying soils.

Modern Screw-Piles have a variety of geometries and applications and include both single helical and multi-helix configurations on both square shafts and round shafts. With the advent of modern hydraulics in the construction industry which largely took off after the 2nd World War, Screw-Piles can now be installed with ease using a variety of commonly available construction equipment.

All Screw-Piles and Helical Anchors consist of a central steel square or round shaft with one or more helical blades welded to the shaft. The blade takes the form of one full revolution of a spiral around the shaft. In the industry, Screw-Piles have a variety of names, such as Helical Pier, Screw Anchor, or Helical Pile but they are all generally fabricated as one of three general configurations. They may consist of a bare shaft with a single helical element, a bare shaft with a multi-helix lead section or a helical lead section (single—or multi-helix) followed by a cement grout column which surrounds the extension sections behind the lead. Grouted shaft Screw-Piles may be used to provide additional load capacity, working in combination with the lead helical section, or they may be used to simply transfer the load to the lead helical section, as in the case of short Screw-Piles end-bearing on rock or other hard material. The grout column also provides additional stiffness to reduce buckling which may be a concern when the lead section passes through very soft material and rests on a hard base.

After installation the Screw-Pile is attached to an existing foundation using a structural bracket that can be bolted to the existing foundation and then attaches to the shaft of the Screw-Pile. In some cases, strengthening of the existing foundations, which often consist of stone or other masonry in historic setting, may be necessary using a thread bar or a grouted bar before installing the Screw-Pile support system. This may be particularly important given the age of most of the structures that predate the use of concrete for foundations.

3 FOUNDATION REPAIR USING SCREW-PILES

The approach for using Screw-Piles for foundation underpinning typically starts by making a small excavation to expose the base of the existing foundation. The Screw-Pile is then installed adjacent to the foundation using a hydraulic torque motor to the required design depth or a sufficient depth as determined by the installation torque to develop sufficient load capacity. A foundation bracket is then attached to the shaft of the pile and to the existing foundation to provide a structural connection between the two and provide for load transfer.

If appropriate, given the condition of the structure and the degree of distress, a small amount of lifting may also be performed using hydraulic jacking system to provide vertical adjustment to the structure and preloading of the screw-pile. This load is then locked off and the final position of the foundation bracket is achieved. If needed, the existing foundation may also be reinforced using either thread bars or grouted bars inserted into the existing foundation blocks or a small section of reinforced concrete may be cast in place and tied to the existing foundation.

The underpinning sequence is illustrated in Figure 1. Note that Figure 1 illustrates that the Screw-Pile can include a grout column around the central shaft as previously described or it may be installed without a grout column, depending on the soil conditions and the design of the pile for bearing capacity. The depth of the excavation and the degree of undercutting on the existing foundation depends on the condition of the foundation. In many cases, it is only necessary to excavate a small enough space to allow room for the new foundation bracket to be installed. In other cases, if the existing foundation needs repaired to improve the internal structural integrity, it may be necessary to create a larger excavation for more work room.

Depending on the project, the Screw-Piles may be installed vertically, as shown in Figure 1, or the site conditions may require a slight batter to the installation.

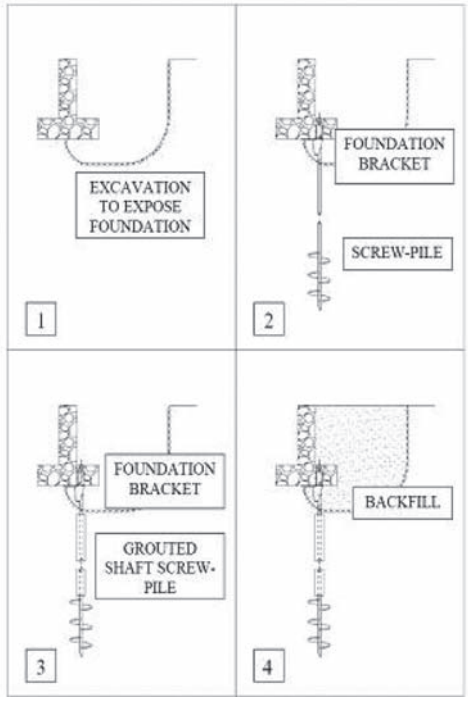

Figure 1. Sequence of underpinning existing foundations with Screw-Piles.

Figure 2. Forest Lodge.

4 CASE-1: FOREST LODGE, HULNE PARK, ALNWICK, NORTHUMBERLAND, UK

Forest Lodge is the gate house into Hulne Park, which is part of the Duke of Northumberland's estate in Northumberland, UK. The Lodge was built in 1853 of local stone, Figure 2. Over the years, the north wing of the gate house had experienced excessive settlement.

4.1 *Site conditions*

In order to investigate the ground conditions at the site, a trial sounding was performed using a Screw-Pile. After first creating a small excavation to foundation level, about 1.5 m below exiting grade, helical screw pile was installed to test the load bearing capacity of the soil and evaluate

the depth of installation that would be required to achieve support. Based on this trial sounding, it was found that the soil was very poor, probably fill, until bedrock was encountered at 7.5 m below ground level.

4.2 *Repair*

It was decided that the building could be stabilised by installation of a series of grouted shaft Screw-Piles (Helical Pulldown™ Micro Piles) down to bedrock along three walls of the building. The piles would be terminated with structural foundation lifting brackets, bolted to the foundation stones, in order to transfer the live load of the building to the piles. No attempt would be made to lift the building, due to the fragile state of the vaulted cellar. Capacity of the piles was based on end bearing on rock, not installation torque. A total of fourteen Screw-Piles were installed to support the structure.

Due to a bathroom extension against the west wall of the structure, access to the outside of that wall was not possible. This meant that the work had to be split into two stages. Initially, the west wall foundation was exposed from inside the cellar with removal of spoil out through the window, as shown in Figures 3 and 4. Five Screw-Piles were installed, from inside the cellar using portable hand-held equipment. The piles were preloaded prior to undermining the foundation and pouring a reinforced concrete haunch.

Once the inside work of installing the Screw-Piles and foundation brackets was completed, the two outside walls were exposed down to foundation level and nine Screw-Piles were installed around the perimeter, Figure 5. Two battered Screw-Piles were also installed to counteract any lateral movement and turning moments. The nine external Screw-Piles were also preloaded prior to undermining the foundation and pouring a reinforced concrete haunch, which also encapsulated the two battered piles.

Figure 3. Installation of Screw-Piles inside the cellar of Forest Lodge.

Figure 4. Screw-Pile installation using portable hand equipment inside.

Figure 5. Installation of Screw-Piles and foundation bracket on exterior of Forest Lodge.

Figure 6 shows a pile being loaded with a small hydraulic jack.

All of the Screw-Piles for Forest Lodge consisted of a 38.1 mm square shaft double-helix lead section with helical plates of 250 and 305 mm diameter.

Figure 6. Preloading of Screw-Pile (note grout bucket at right).

Figure 7. Installing Screw-Piles at Forest Lodge.

Figure 8. Corner of Forest Lodge gate house after installation of Screw-Piles and foundation brackets.

Soil displacement plates were used on square shaft extension sections to produce a 100 mm diameter grout column behind the lead section. Grout take was high due to rocky nature of the underlying fill.

Installation torque was low until bedrock was encountered at depths ranging from 6 to 8 m below existing foundations so that they would act in end bearing. A total of fourteen Screw-Piles with grouted shafts were installed to support the structure.

This case represents a good example of using Screw-Piles as end-bearing elements on bedrock. In these cases, the installation torque is only useful in evaluating the soil conditions above the rock and identifying when bedrock has been encountered.

Once bedrock is encountered the torque may be initially high but then typically drops off as the Screw-Pile "spins out" on the rock. Figures 7 and 8 show the progress of the work outside the walls.

A small mini-excavator was used on the outside of the structure as shown.

Note that in this case the Contractor elected to remove all of the soil along the exterior perimeter of the structure because of the close spacing used for the Screw-Piles and foundation brackets.

The work was successfully completed over a period of about 8 days, including cleanup.

5 CASE-2: BAPTISTRY OF ST. MARY'S CHURCH, NEW ROAD, GREENHAM, THATCHAM, BERKSHIRE, UK

The stone church at St. Mary's in Greenham was built in 1876 on the site of a former Chapel which was demolished. The Baptistry was added in 1895. In 2009 the Baptistry had experienced significant movement and the south-west corner had settled and rotated outwards at the top. This resulted in considerable cracking of the exterior stone and considerable cracking of the plaster on the vaulted ceilings inside the Baptistry. It was initially thought that some of the movement may have been caused by desiccation and shrinking of the underlying soils.

5.1 *Site conditions*

A subsurface investigation conducted at the site consisted of a single test boring to a depth of 5 m and two test pits adjacent to the Baptistry to determine soil conditions and existing foundations. The site consisted of about 1.5 m of made ground (fill) overlying firm to stiff low plasticity clay. At the time of the investigation no water table was encountered. The exposed foundations in the test pits typically showed a concrete footing supporting four courses of brickwork which supported the stonework of the Baptistry. The concrete footings only extended to a

depth of about 0.9 m at the buttresses and about 0.4 m along the main wall. The concrete underling the main wall was of very poor quality.

5.2 *Repair*

The repair consisted of installation of nine helical screw-piles adjacent to the foundation to transfer the load from the upper soils to the deeper very stiff soils that would not be affected by additional desiccation. It was decided to use a grouted shaft helical pile for the work. A square-shaft helical screw-pile with a lead section configuration consisting of a triple-helix with helical plates of 200, 250 and 305 mm diameter was selected. A 127 mm grout shaft was created behind the lead section using steel soil displacement plates, as previously described. Piles were installed adjacent to both the buttresses and the wall. Similar to the Forest Lodge project, the following construction sequence was used:

1. A small excavation was created to expose the existing foundation at selected pile locations;
2. A helical screw-[pile was installed consisting of a lead section, extension section, soil displacement plates and Portland Cement Grout;
3. A structural foundation bracket was attached to the existing foundation;
4. The helical pile was preloaded by using a small hydraulic jack between the foundation bracket and pile;
5. The preload was mechanically locked off; and
6. The excavation was backfilled and the ground surface was restored.

This sequence is illustrated in Figures 9 to 14.

The depth of the helical piles ranged from 6.5 to 11 m below grade and was based on achieving a minimum installation torque resistance in the stiff clayey soils. The installation torque for

Figure 9. Excavation to expose existing foundations at St. Mary's.

Figure 10. Installation of triple-helix Screw-Pile adjacent to foundation.

Figure 11. Mini-excavator installing Screw-Pile along wall between buttresses.

Figure 12. Small excavations around corner of St. Mary's Baptistry with foundation bracket installed.

Figure 13. Excavations for Screw-Piles along wall and next to buttresses.

Figure 14. Completed backfill after installation of Screw-Piles and foundation brackets.

each pile was recorded continuously every 0.3 m for on site quality assurance and to insure proper installation.

6 ADVANTAGES OF SCREW-PILES FOR STRUCTURAL REPAIR/RESTORATION

The use of Screw-Piles for the structural restoration and underpinning of historic structures has a number of advantages over traditional stabilization techniques. One of the highest priorities for this type of work is preserving the historic fabric of the existing structure during construction activities. Potential advantages include:

6.1 *Minimal disruption to existing structure*

Installation of Screw-Piles is generally minimally invasive work involving slow rotation using a high torque hydraulic torque head. There are no soil cuttings to dispose of from installation of the Screw-Piles. Soil from the excavation to expose the existing foundation may be carefully stockpiled and used as backfill at the completion of the repair work. In many cases, the structure may still be used while the repair work is in progress.

6.2 *Minimal construction vibration*

There are essentially no vibrations produced by the hydraulic plant during installation of the Screw-Piles. This may be particularly important in situations where the existing structure may be sensitive to construction vibrations. Most Screw-Piles for restoration work may be installed with light duty construction equipment such as mini-excavator or skid steer or portable hand held equipment.

6.3 *Installation in high groundwater*

The installation of Screw-Piles is unaffected by high ground water condition since no excavation is required below the foundation level. Of course is water is above the foundation level, temporary drainage may be required as in most other replacement methods.

6.4 *Construction in confined space*

As demonstrated by the description the work at Forest Lodge, Screw-Piles may be installed in areas of limited access or low head room. The portable equipment can easily be managed by a single operator. Short extension section may be use inside to install the Screw-Piles to the required depth.

The power unit used to operate the portable torque motor can be placed outside and hydraulic hosed can be routed through a window or small opening in the structure.

6.5 *Field verification of capacity for QC*

During installation the hydraulic torque is usually monitored to provide a record of the installation torque. This attribute of Screw-Piles allows for field verification of the soil conditions at each pile location and for verification of load capacity. This is particularly important in regard to historic structures where the soil conditions under the structure are often unknown and difficult to determine, especially at interior locations. The installation torque record provides an excellent quality control tool and should be included in the specifications for every Screw-Pile as a part of every project.

6.6 *Rapid installation and construction*

In most soil conditions, Screw-Piles may be installed very quickly. A typical installation time

using conventional construction equipment such as a skid steer or mini excavator is about 1/2 hour for a 10 m length of pile. Only a small amount of additional time is needed when using a grouted shaft Screw-Pile.

6.7 *Flexibility of geometry*

As illustrated with the two cases presented, Screw-Piles are available in a variety of configuration, including single and multi-helix lead sections with a variety of diameters. This allows considerable flexibility for the designer to select an appropriate geometry for a specific project to match soil and structural conditions. Increasing the helix diameter and/or number of helices or modifying the installation length to achieve the required load capacity is generally very easy. In cases where increased bending stiffness is needed to support eccentric loading, the use of the grouted shaft is appropriate. Even when a grouted shaft is used, the additional equipment needed to mix and place the grout is minimal. In both cases described, the square-shaft of the helical pile extension sections were encapsulated with Portland Cement Grout to increase the pile stiffness.

6.8 *Immediate load transfer*

In most soils Screw-Piles allow for load transfer to essentially take place as soon as the pile has been installed. This can be important in some cases where emergency repairs are needed before additional damage can occur. In the case of grouted shaft Screw-Piles, sufficient time, usually 5 to 7 days may be required for the grout to attain sufficient strength before being loaded. The load capacity of Screw-Piles normally increases with time due to aging effects of the soil.

7 CONCLUSIONS

The two cases described illustrate the successful use of helical Screw-Pile and anchors to provide a cost-effective alternative to underpinning and stabilizing foundations of historic structures with minimal invasion to the existing structure. Screw-Piles offer a number of advantages to other perhaps more traditional foundation repair methods and should be considered provided that the site conditions and access to the structure will allow proper installation. Sites with excessive boulders or cobbles would not typically be considered good candidates for using helical Screw-Piles.

REFERENCES

Avellan, K. and Lange, K. 1997. St.-John's Church, Tartu, Estonia—Underpinning of Tower. *Geotechnical Engineering for the Preservation of Monuments and Historic Sites*: 521–525.

Burland, J.B., Jamiolkowski, M. and Viggiani, C. 2003. The Stabilization of the Leaning Tower of Pisa. *Soils and Foundations*, 43(5): 63–80.

Chartres, F.R.D. 1997. Monitoring the Installation of Piles Beneath the Round Tower, Windsor Castle, U.K. *Geotechnical Engineering for the Preservation of Monuments and Historic Sites*: 349–356.

Ciancia, A.J., Biesiadecki, G.L. and Ladd, B.E. 2006. Challenges of Underpinning Two Historic Landmark Buildings. *Practice Periodical on Structural Design and Construction*, ASCE, 11(3): 142–148.

Crocker, E.E. 2005. Non-invasive Underpinning Technologies in Historic Settings. *Proceedings of the 4th International Seminar on Structural Analysis of Historical Constructions*: 821–828.

Drooff, E.R., Furth, A.J. and Scarborough, J.A. 1995. Jet Grouting to Support Historic Structures. *Foundation Upgrading and Repair for Infrastructure Improvement*, ASCE: 42–55.

Duckham, F.E. 1889. Underpinning Great Yarmouth Town Hall. *Minutes of the Proceedings of the Institution of Civil Engineers*, 98: 372–374.

Lutenegger, A.J. 2011. Historical Development of Screw-Pile Foundations: 1936–1900. *International Journal for History of Engineering and Technology*, 81(1): 108–128.

Lutenegger, A.J. and Kempker, J. 2008. Preservation of Historic Structures Suing Screw-Pile Foundations. *Proceedings of the 6th International Conference on Structural Analysis of Historic Structures*, 2: 1079–1086.

Mitchell, A. 1848. On Submarine Foundations; particularly Screw-Pile and Moorings, *Civil Engineer and Architects Journal*, 12: 108–149.

Pilla, D.R. 2010. Evaluating Historic Structures for Adaptive Re-use. *Structure Magazine*, September: 14–16.

Rodriguez Ortiz, J.M. and Monteverde, P.R. 1997. A Review of Recent Spanish Interventions in Monuments. *Geotechnical Engineering for the Preservation of Monuments and Historic Sites*: 499–508.

Sherwood, T., 2003. Screw Piling in Salisbury. *New Steel Construction*, 11(6): 2 pp.

Geotechnical Engineering for the Preservation of Monuments and Historic Sites – Bilotta, Flora, Lirer & Viggiani (eds)
© 2013 Taylor & Francis Group, London, ISBN 978-1-138-00055-1

Seismic risk assessment of San Gimignano towers: Geotechnical aspects and soil-structure interaction

C. Madiai, S. Renzi & G. Vannucchi
Università di Firenze, Dipartimento di Ingegneria Civile e Ambientale, Firenze, Italy

ABSTRACT: San Gimignano, the 'City of the Beautiful Towers' is located on the top of a hill in 'Val d'Elsa', about 60 km south of Florence (Italy). It was founded by the Etruscans in the 3rd century BC and in the Middle Ages it was a relay point along the Via Francigena for pilgrims on their way to Rome. From 1199 to 1353 AC the city saw its period of greatest splendour. As symbols of the wealth and power of the strongest major families, seventy-two tower houses were built in that period. Fourteen of these have survived to now and they represent a priceless heritage. Because of their significance, an important multidisciplinary research project (named RiSEM) has been founded by the Regional Government with the aim of developing new investigation techniques for seismic risk assessment of monumental buildings. The present paper provides a synthetic report of the main aspects concerning the definition of the geotechnical model and the seismic soil-structure interaction analyses performed. The first part of the report, after some brief historical notes, describes the site conditions, including morphological, stratigraphic and geotechnical subsoil characterization from a recent survey. The results of the geotechnical investigations (two boreholes with taking of undisturbed samples, down hole and laboratory tests, both in static and dynamic conditions) are presented and discussed. In the second part, a general overview of the soil-structure system and a description of the main features of its components are given. The local seismic response analyses of the site and the soil-structure FEM analyses performed on the "Torre Grossa" using the computer program SASSI2000 (Lysmer et al., 1999) are also described. Real strong motion recordings were selected according to the local seismic hazard and used in the analyses. The numerical modelling results obtained both in time and frequency domain are presented and discussed in the paper.

1 INTRODUCTION

As unfortunately shown also by recent events in Emilia Romagna (Central Italy), the damage and the collapses caused to monumental heritage by earthquakes (sometimes not even of great intensity) not only involve huge losses, often of inestimable value, but they also cause additional extensive damage in terms of a reduction of the tourist resources of a territory and the disappearance of elements from the social connective cloth of a community. It is then necessary for the scientific community to be activated in trying to develop tools and techniques that are an aid in the conservation of these buildings, allowing analysis of their safety under seismic conditions.

The RiSEM research project (standing for seismic risk in monumental buildings), funded by the Regione Toscana Government and involving researchers from the University of Florence and Siena, as set up born with the aim of developing, proposing and validating survey techniques, analysis and diagnosis which allow sufficiently rapid and relatively low cost evaluation of the seismic risk of monumental heritage of relevance, and possibly the proposal of methodologies that can be used to analyse whole urban agglomerations of historical interest.

The comparison of seismic risk associated with different monuments or buildings in general, can be used to plan, on a regional scale, the priority and urgency of safeguarding measures to be put in place in the medium to long term.

The project focuses on San Gimignano as the city represents a case that is both unique in the world and marked by strong typological homogeneity: the presence of several elements with "analogous" dynamic behaviour (the towers) also ensures that the situation identified represents a "test bed" for the development of new techniques of investigation and analysis.

San Gimignano, the 'City of the Beautiful Towers' is located on the top of a hill in 'Val d'Elsa', about 60 km south of Florence (Italy). It was founded by the Etruscans in the 3rd century BC and in the Middle Ages it was a relay point along the Via Francigena for pilgrims on their way to Rome. From 1199 to 1353 AC the city saw its

period of greatest splendour. As symbols of the wealth and power of the strongest major families, seventy-two tower houses were built in that period. Fourteen of these have survived to now and they represent a priceless heritage (Fig. 1).

San Gimignano is thus a "pilot project" for the development of methodologies that might be extended later on, not only to buildings of historical and monumental interest in the same municipality, but also to other realities in the region and throughout Italy.

The first step in the project regards the knowledge of the geological and geotechnical environment, through which it is possible to evaluate the potential effects induced by a seismic shaking in free field conditions. This step aims to define the local seismic hazard, i.e. the assessment of the local seismic response and of the seismic soil-structure interaction. This phase obviously then concerns the monuments under study. A survey of the towers was carried out with different methodologies: direct survey, topographical and satellite survey, use of scanner. Reliable plans, sections and elevations on large scale of different towers, not available till now, were drawn up. This was to enable acquisition of geometric and material information on the shape and structure of the towers and on their transformation over time. In parallel, archaeological and documentary investigations were carried out to correlate the knowledge provided by direct investigation on the buildings.

Finally, a further survey was performed consisting in interferometric measurements "over distance" using the radar technique. Displacements induced by external causes (for example, the action of the wind) of a large number of points along the structure were measured, enabling assessment of the dynamic characteristics of the towers. Further investigations were carried out using the penetrating radar technique (GPR), in order to characterize the masonry texture of the towers and to detect the presence of underground cavities.

Figure 1. Ancient view of San Gimignano (original wood engraving drawn by P. Benoist, engraved by A. Sargent, 1877).

All the information previously collected allow the definition of numerical models of the towers. Such models are used to quantify the actual level of the seismic risk on the towers by means of FEM techniques.

The present paper provides a synthetic report, in the current state of the research, of the main aspects concerning definition of the geotechnical model and the performed seismic soil-structure interaction analyses. The first part of the paper describes the site conditions, including morphological, stratigraphic and geotechnical subsoil characterization from a recent survey. It presents and discusses the results of the geotechnical investigations (two boreholes with taking of undisturbed samples, down-hole and laboratory tests, both in static and dynamic conditions).

The second part of the paper presents the first results of one-dimensional seismic response analysis in free field conditions and of dynamic soil-structure interaction analysis performed on one of the towers, the "Torre Grossa". Real strong motion recordings were selected according to the local seismic hazard and assumed as input for the ground response analyses. The dynamic soil-structure interaction analysis presented is still at a preliminary stage in which the tower was assimilated to an equivalent Single Degree of Freedom (SDF) system supported on a set of frequency-dependent strings and dashpots accounting for the stiffness and compliant damping of the soil-foundation system. Period lengthening and effective damping of the analyzed SSI system was compared to the corresponding values of the fixed-base structure period and to the period assessed by means of vibrodyne and radar interferometric techniques.

2 SITE CONDITIONS AND GEOTECHNICAL CHARACTERIZATION

San Gimignano is located on the Plio-Pleistocene hills, carved by tributaries of the Elsa river, that characterize the river basin of the Val d'Elsa (Tuscany, Central Italy). The elevation is about between 344 m and 223 m above the sea level.

The steepness of the area differs widely from area to area, with slopes between 5% and 10% of the alluvial valley escarpment to more than 55% on the slopes carved by the most important rivers.

To define in detail the geologic and geomorphologic features of the area, a in depth geological survey was carried out and three main outcropping geological formations were identified (Albarello et al., 2012): 1) Calcareous Tufa (Pleistocene) characterized by different continental lithofacies and consisting of white calcareous silt or fine-grained sand intercalated with

up to 1 metre thick micritic limestone. Such formation frequently shows internal parallel stratification and lamination; 2) Blue Clays (Pliocene), a marine formation consisting of two main lithofacies: sandy silts and clays and sands, very fine-grained, only locally cemented; 3) Breccia of Grotti (Miocene), a continental rock formation of clast-supported gravels and debris of carbonate rocks. Clasts range in size from a few centimetres to several decimetres and are sometimes weathered; sandy matrix consists mainly of medium-coarse-grained sand.

Alluvial deposits and debris landslide, widely graded particle size, outcrop locally in several areas.

Figures 2 and 3 show respectively the map of the main outcropping geological units and the lithologic cross section thorough the centre of San Gimignano.

The geotechnical model to perform local seismic response and soil-structure interaction numerical analyses was defined by means of available data and results of two soundings with taking of undisturbed samples, Down-Hole and laboratory tests specifically performed within the RiSEM research project.

Boreholes were carried out in the centre of San Gimignano (elevation about 324 m a.s.l.), near the towers named "Torre Grossa" (borehole S1) and

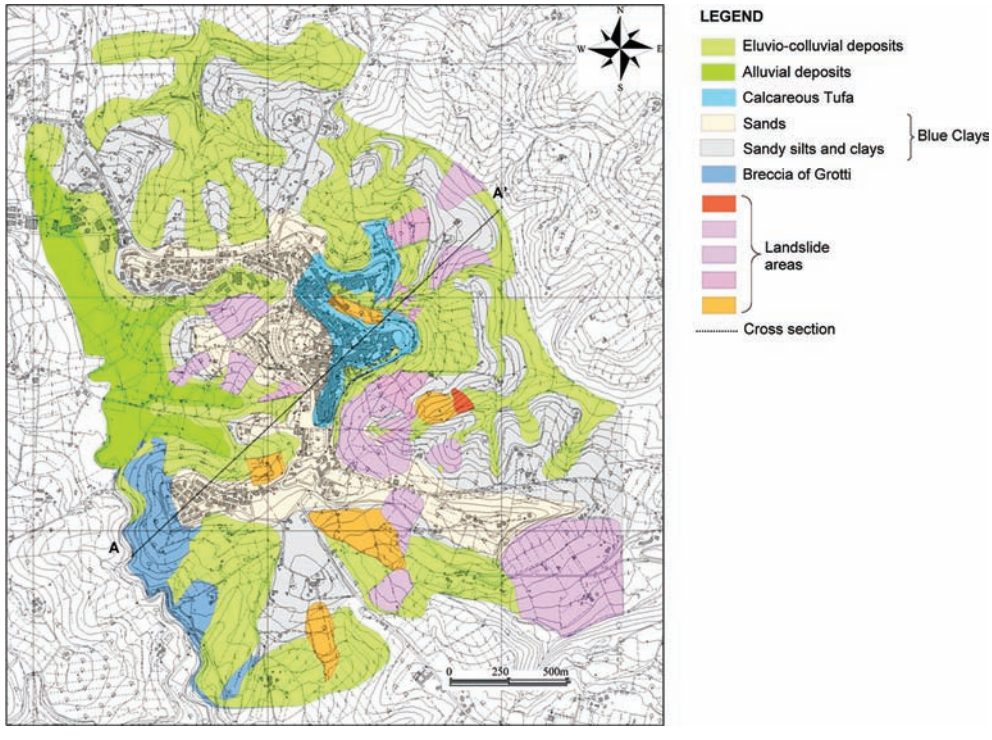

Figure 2. Geological map (from Albarello et al., 2012).

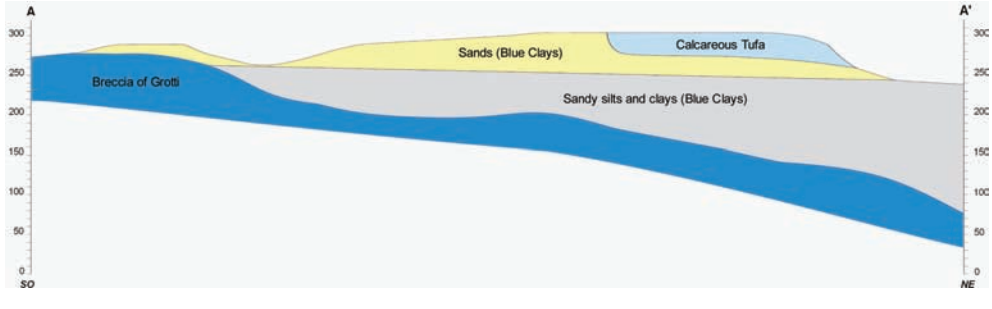

Figure 3. Geological cross section through the centre of San Gimignano (from Albarello et al., 2012).

"Torri Gemelle" (or "Torri Salvucci") (borehole S2) (Fig. 4). Both reached a depth of 30 m below ground level. SPT were performed in borehole S1 at about 2.4 m (N_{SPT} = 24), 11.30 m (N_{SPT} = 24), 18.30 m (N_{SPT} = 22). The soil profiles recognized at the two sites examined are in agreement with available data from previous surveys (Malesani & Becattelli 1990). Specifically, below a man-made filling (few decimetres thickness in S1 and about 3.5 m in S2), calcareous materials of continental origin (Calcareous Tufa) were encountered in the most superficial part in both soundings, consisting of layers of soft rocks (cemented calcareous silts similar to Travertine) alternating with layers of mixtures of loose silty, sandy and gravelly soils. These lithologic units appear to be very heterogeneous and characterized by high porosity. More in depth, i.e. closer to the top of the marine formation (sands and sandy silts and clays), alternating layers of sands, gravels and calcareous silts with variable density and containing layers of cemented soil a few inches thick were observed. The materials of marine origin (Blue Clays) were encountered at a depth of about 22 m and 24 m in S1 and S2 boreholes respectively.

Both boreholes were equipped to perform Down-Hole tests. S-wave and P-wave velocities measured at "Torre Grossa" (DH S1) and "Torri Gemelle" sites (DH S2) are shown in Figure 5. As can be observed, V_S values are slightly lower than 200 m/s at the ground level and range from 300 to 400 m/s at depths greater than 2 m from g.l. up to the top of the marine sands. Above 24 m in depth and up to the end of the borehole V_S increases from 400 m/s to about 600 m/s.

Two undisturbed samples were collected in borehole S1 at a depth of 1.85 m (S1-C1) and 27.65 m (S1-C2) respectively; one undisturbed sample was taken in borehole S2 at a depth of 27.45 m (S2-C1) from ground level.

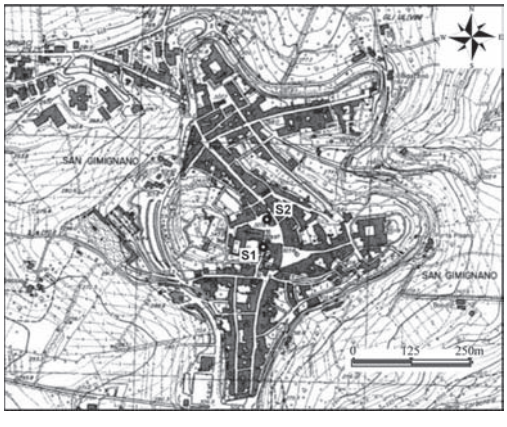

Figure 4. Location of boreholes S1 and S2.

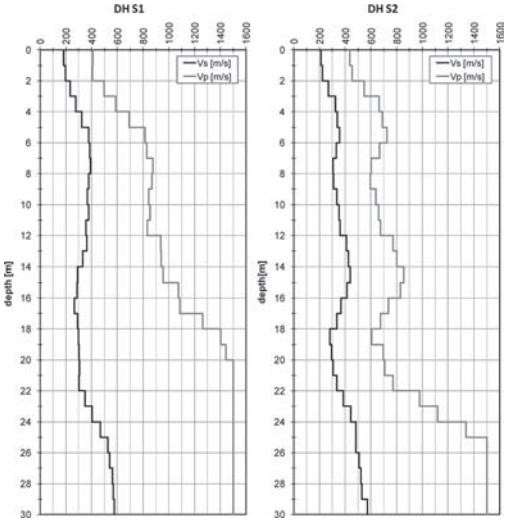

Figure 5. V_S profiles from DH tests at the two sites.

Samples were investigated in dynamic conditions using Resonant Column (RC) tests. The main index properties and physical parameters of the three samples are summarized in Table 1. Figure 6 shows the experimental values of shear modulus reduction G/G_0 and damping ratio D versus shear strain γ from RC tests.

To perform numerical analyses at the "Torre Grossa" (S1) site, the geotechnical model was mainly defined according to the above described experimental data and with reference to the relations suggested in the literature for similar materials where data was lacking.

In particular: i) the depth of the bedrock, represented by the Breccia of Grotti formation, was assumed at 150 m from ground level with a V_S = 1200 m/s; ii) for soil overlying the bedrock, V_S profile was defined to a depth of 30 m from g.l. based on the results of the DH test in the borehole S1. A power law in the form $V_S(z) = V_0 \cdot z^x$ with V_0 = 170 m/s and x = 0.25 was assumed from –30 m to the top of the bedrock; iii) four different relations for shear modulus reduction and damping ratio versus shear strain were taken to characterize as many lithotypes in the soil profile: the relations from RC tests on the samples S1-C1 and S1-C2 were attributed respectively to loose silty-clayey sands of Calcareous Tufa formation (soil type 1) and to very dense clayey sands of Blue Clay formation (soil type 4); the relations of $G/G_0(\gamma)$ and $D(\gamma)$ proposed by Pergalani et al. (1999) for 'Travertine' were assumed for the layers cemented and very porous calcareous silts (soil type 2) and the relations suggested by Rollins (1988) were attributed to the layers mostly consisting of gravels (soil type 3).

Table 1. Main index properties and physical parameters of the samples from boreholes S1 and S2.

Sample	w_L [%]	w_P [%]	w [%]	Unit weight [kN/m^3]	Density of solids [Mg/m^3]
S1-C1	46	19	30.4	19.3	2.70
S1-C2	32	19	22.8	20.2	2.70
S2-C1	41	13	16.5	21.5	2.68

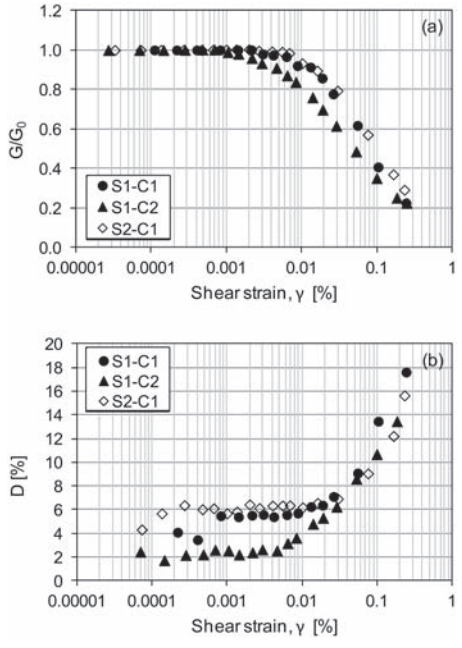

Figure 6. Shear modulus reduction (a) and damping ratio (b) versus shear strain from RC tests.

3 LOCAL SEISMIC RESPONSE ANALYSIS

With the aim of obtaining strain compatible moduli and damping to be assigned as input to SASSI2000 computer program (Lysmer et al., 1999) for performing seismic soil-structure interaction analyses, one-dimensional ground response analyses in free field conditions were first carried out at the S1 site, beneath the "Torre Grossa", by means of EERA program (Bardet et al., 2000).

The main details of the geotechnical model, defined following the criteria described in the previous section, are summarized in Table 2.

3.1 *Selection of the input motion*

The reference input motion for the numerical analyses was selected according to the seismic local hazard of the site (Montaldo & Meletti 2007).

It consists of a set of seven real strong motion accelerometric records matching the pseudo-acceleration target spectrum expected on outcropping rock at San Gimignano according to the suggestion of the Italian seismic code (Ministero delle Infrastrutture 2008) for a return period of 475 years (Fig. 7). Upper and lower tolerance for fitting were fixed at 20% and 10% respectively in a period range 0.1–2 s (Fig. 7).

The value of the target spectral acceleration at period T = 0 (that is the expected PGA at San Gimignano in the fixed return period) is 0.141 g.

Recordings were selected by means of REXEL computer program (v. 3.4 beta) (Iervolino et al., 2010) within the ITalian ACcelerometric Archive ITACA (Working Group ITACA 2008).

The selection was carried out in a such a way that the signals were scaled with a factor between 0.5 and 2 as suggested in the literature.

Table 2. Main properties of the layers at the S1 site for ground response analysis.

Soil type	Depth [m]	Unit weight [kN/m^3]	V_S [m/s]
1	0–2.9	19	185
2	2.9–5.5	20	324
3	5.5–6.4	20	383
2	6.4–8.1	20	401
3	8.1–10.6	20	365
1	10.6–14.2	19	360
1	14.2–15.0	19	295
3	15.0–16.0	20	253
1	16.0–18.0	19	281
3	18.0–19.5	20	309
1	19.5–22.0	19	300
1	22.0–24.0	19	358
4	24.0–24.8	20	500
4	24.8–26.5	20	534
4	26.5–30.0	20	585
4	30.0–150.0	20	600–900
bedrock		22	1200

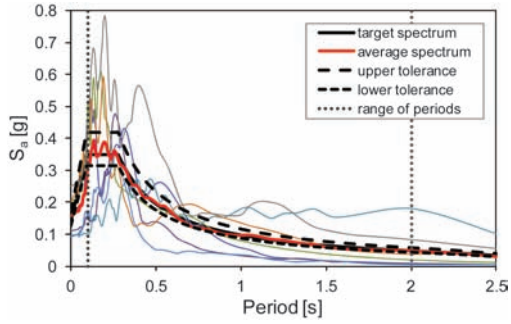

Figure 7. Spectra of the 7 selected recordings, average spectrum and target spectrum assumed in the selection.

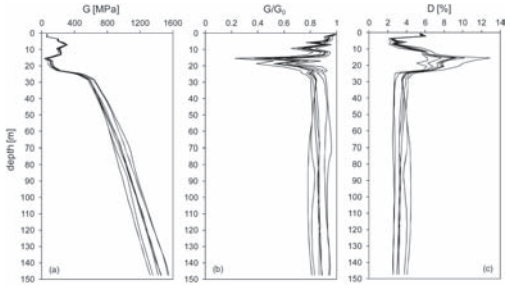

Figure 8. G, G/G_0 and D profiles from ground response analysis.

Figure 7 shows the pseudo-acceleration spectra of the seven recordings adopted as input motions in the numerical analyses. In the same Figure 7 the average spectrum of the selected signals is compared with the target spectrum assumed in the selection.

3.2 *1D-analysis results*

As already mentioned, 1D local seismic response analyses were performed in order to define the subsoil model as required by SASSI2000 computer program for the subsequent seismic soil-structure interaction analyses. Specifically, the values of strain compatible moduli, G, and damping ratio, D, for each layer in soil profile were selected among all the output results from EERA computer program.

The vertical profiles of G and D obtained from ground response analyses and used to define the input data of SASSI2000 are represented in Figure 8 (8a and 8c respectively) together with the vertical profile of G/G_0 (Figure 8b).

4 SEISMIC SOIL-STRUCTURE INTERACTION

The Torre Grossa (Fig. 9) has been thoroughly investigated within the framework of a research contract called "San Gimignano Project" (Bartoli & Mennucci 2000) in which the static and dynamic behaviour of the masonry tower has been evaluated using a 3D FEM program (ANSYS), as well as with respect to a series of "in situ" measures.

The outer perimeter of the horizontal cross section is a 9.5×9.5 metre square. The sustaining infilled walls ("*a sacco*" is the Italian term) have an outer face in stone masonry (20 cm), and an inner layer of brick masonry (25 cm). The internal filling is made up of heterogeneous material. The walls vary in thickness, from 2.6 m (at the base) to 1.6 m (at the top).

The tower has an overall height of about 60 m (Fig. 10).

Figure 9. View of the "Torre Grossa".

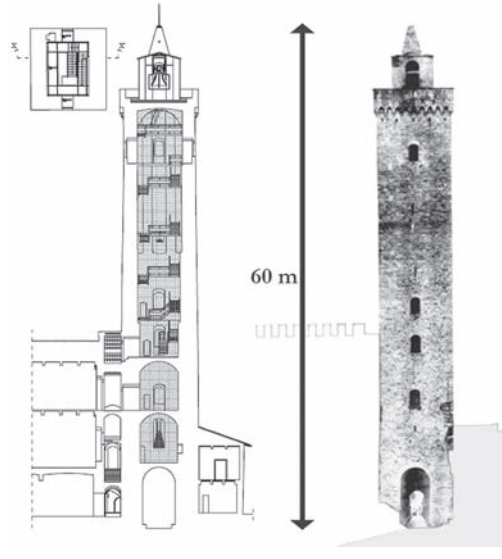

Figure 10. Section (a) and view (b) of the "Torre Grossa" (from Bartoli et al. 2006).

The results obtained from the static identification have been used to set up the mechanical properties of the model (Tordini 2005, Bartoli et al., 2006) (Table 3).

The SSI effects were investigated in this study by means of SASSI2000 computer program (Lysmer et al., 1999).

The problem was broken down into a series of subsystems which were solved separately then reassembled using the principle of superposition, requiring as assumption soil and structural linear behaviour (substructuring approach).

The SASSI site model was constructed from the strain-compatible soil properties obtained from the free-field EERA deconvolution analyses described in the previous chapter.

In the SASSI model, the structure above the grade was modelled using 3D lump mass stick model.

The basemat and excavated soil volume were modelled using 3D brick elements, which were connected to the stick model above the grade by a series of rigid links (Fig. 11).

The analyses were performed in the following steps:

1. idealization of the tower as a SDF system;
2. estimate of SSI effects, in terms of modified fundamental period $\tilde{T}$.

The classical approach for elasto-dynamic analysis of Soil-Structure Interaction aims to replace the current structure with an equivalent Single Degree of Freedom (SDF) system supported on a set of frequency-dependent springs and dashpots accounting for the stiffness and damping of the compliant soil-foundation system (Chopra 2007).

The resulting equivalent SDF system is characterized by an equivalent height, h_{eq}, equivalent mass, m_{eq}, and equivalent stiffness, k_{eq}, with 5% viscous damping ratio.

Foundation was modeled by means of 3D brick finite elements, with a base length ranging from 10 m at ground level to 13 m at the soil-foundation interface located –3 m from g.l. (Fig. 11).

For the numerical analyses the deposit was subdivided into different sublayers. Each of these was identified by its thickness, unit weight, strain compatible compressional (V_P) and shear wave velocity (V_S) inferred from the result of 1D ground response analyses (Fig. 8) and associated damping ratio.

Table 3. Material properties (Bartoli et al. 2006).

Material	Elastic modulus E [kPa]	Unit weight γ [kN/m³]
Outer stone masonry	1.1×10^8	24.0
Internal filling	1.6×10^6	20.0
Inner brick masonry	3.0×10^6	18.0

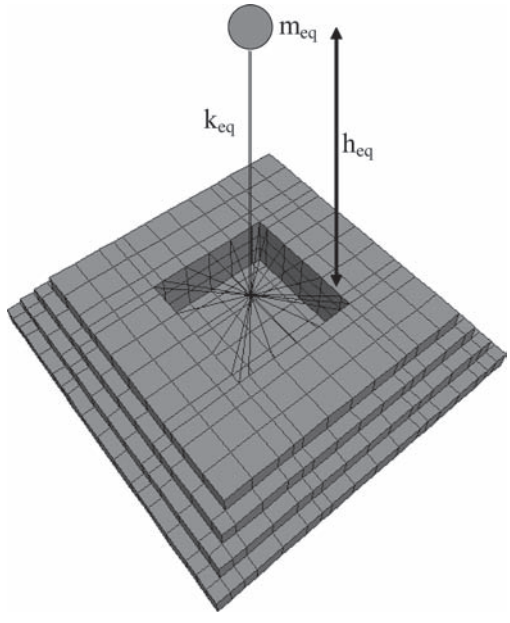

Figure 11. SASSI model: 3D FEM foundation and SDF system scheme.

The shallow foundations of adjacent buildings were modeled as a 1.5 m layer having the mechanical properties of the tower's outer stone masonry.

Soil-foundation interaction was assumed only at their common nodes.

5 DISCUSSION AND CONCLUSIONS

The present paper provides a synthetic report of the main aspects concerning the definition of the geotechnical model and the preliminary seismic Soil-Structure Interaction analyses performed on the main tower (called "Torre Grossa") of San Gimignano.

Results obtained from the numerical SSI analysis carried out in the present work are summarized in Table 4 and compared to those from previous different dynamic analyses.

In order to compare the results, the limitations and advantages of each method of analysis must be taken into account. They are briefly summarized below.

The fixed-base 3D analysis (Bartoli et al., 2006) was performed by modelling the entire current superstructure, but disregarding the foundation and the soil-foundation interface.

The base of the tower was assumed fixed at the ground level. Such assumption tends to

Table 4. Fundamental vibration frequencies in N-S direction.

Case	f_0 [Hz]
Fixed-base (numerical 3D analysis)	1.3310
Vibrodyne (experimental analysis)	1.3306
Radar (experimental analysis)	1.3200
SSI (numerical 3D analysis—this study)	1.3070

overestimate the rigidity of the tower and, as a consequence, to overestimate the fundamental frequency of vibration.

On the other hand, both experimental methods, vibrodyne (Bartoli et al., 2006) and radar measurements (RiSEM Research Project 2012, unpubl.), provide the current dynamic characteristics of the tower, as well as the influence of the soil-foundation interface. However, these methods are limited by very low strain levels and are not suitable for accurate assessment of the fundamental period of vibration at higher levels of deformation, such as those induced by the earthquakes expected at the site.

Finally, the preliminary Soil-Structure Interaction (SSI) analysis performed has the advantage of better approximating the conditions induced on the structure by actual earthquake motions, with higher strain level in the soil layers. The major limit of the present analysis is the idealization of the superstructure as a Single Degree of Freedom system, which is suitable for reproducing the dynamic characteristics of the tower itself, but does not allow to evaluate stress and deformation of the masonry. Such additional analyses will be examined in the framework of the RiSEM Research Project, by modelling complete SSI systems.

Comparison of the results from the previous Fixed-Base and the herein proposed simplified SSI analyses show a little difference (around 2%) in estimating the fundamental period of vibration of the tower. This is mainly due to the medium-high rigidity of the soil in the historical centre of San Gimignano which reduces compliance of the soil-foundation interface.

However, despite the differences in the results from the two approaches being negligible, the application of such a complex method adopted in the present work and of the forthcoming implementation of the SSI model are justified by the significance of the monumental buildings under investigation. The assessment of seismic vulnerability of such historical buildings which are unique, due to their intrinsic geometric and material complexity, in fact requires such sophisticated analysis and cannot be performed with reference to a standard structural analysis.

REFERENCES

Albarello, D., Coltorti, M., Fantozzi, P.L., Firuzabadi, D., Lunedei, E., Pieruccini, P. and Sandrelli F. 2012. Level II seismic microzoning in the San Gimignano area (Central Italy). *7th European Congress on Regional Geoscientific Cartography and Information system. Bologna 12–15 June 2012.*

Bardet, J.P., Ichii, K. and Lin, C.H. 2000. EERA a computer program for equivalent-linear earthquake site response analyses of layered soil deposits. *University of Southern California, Department of Civil Engineer*.

Bartoli, G., Betti, M., Spinelli, P. and Tordini, B. 2006. An "innovative" procedure for assessing the seismic capacity of historical tall buildings: the "Torre Grossa" masonry tower. In: P.B. Lourenço, P. Roca, C. Modena and S. Agrawal (Eds.), *Structural Analysis of Historical Constructions, New Delhi*, ISBN 972-8692-27-7.

Bartoli, G. and Mennucci, A. 2000. Progetto S. Gimignano, la Torre Grossa: indagini conoscitive e diagnostica. *Convegno "La diagnostica per la salvaguardia dei beni culturali", S. Gimignano, Teatro Comunale, 6–7 Dicembre 1999.*

Chopra, A. 2007. Dynamics of structures—Theory and applications to earthquake engineering, 3rd ed. *Prentice Hall, Englewood Cliffs (Eds), New Jersey*: 305–336.

Iervolino, I., Galasso, C. and Cosenza, E. 2010. REXEL: computer aided record selection for code-based seismic structural analysis. *Bulletin of Earthquake Engineering.* 8: 339–362.

Lysmer, J., Ostadan, F. and Chin, C. 1999. SASSI2000 Theoretical manual—Revision 1. *Geotechnical Engineering Division, Civil Engineering Department—University of California, Berkeley.*

Malesani, P. and Becattelli, S. 1990. Relazione geologica e geologico-tecnica sulle caratteristiche fisiche e fisico-meccaniche dei terreni incontrati nel sondaggio geognostico posizionato in Piazza della Cisterna. *Comune di San Gimignano*.

Ministero delle Infrastrutture 2008. Nuove norme tecniche per le costruzioni. D.M. 14 Gennaio 2008. G.U. del 4/2/2008. Suppl. ord. n. 30.

Montaldo, V. and Meletti, C. 2007. Valutazione del valore della ordinata spettrale a 1sec e ad altri periodi di interesse ingegneristico. *Progetto DPC-INGV S1, Deliverable D3* (http://esse1.mi.ingv.it/d3.html).

Pergalani, F., Romeo, R., Luzi, L., Petrini, V., Pugliese, A. and Sanò, T. 1999. Seismic microzoning of the area struck by Umbria–Marche (Central Italy) Ms 5.9 earthquake of 26 September 1997. *Soil Dynamics and Earthquake Engineering*. 18(4): 279–296.

Rollins, K.M., Evans, M.D., Diehl, N.B. and Daily, W.D. 1998. Shear modulus and damping relationships for gravels. *ASCE (American Society of Civil Engineers) Journal of Geotechnical and Geoenvironmental Engineering*. 124(5): 396–405.

Tordini, B. 2005. La Torre Grossa di San Gimignano: modellazione strutturale e valutazione della sicurezza sotto l'azione sismica. *Bachelor Thesis, University of Florence.*

Working Group ITACA 2008. Data Base of the Italian strong motion data (http://itaca.mi.ingv.it).

Geotechnical Engineering for the Preservation of Monuments and Historic Sites – Bilotta, Flora, Lirer & Viggiani (eds)
© 2013 Taylor & Francis Group, London, ISBN 978-1-138-00055-1

Analytical modelling of the creep-rotation rate for leaning towers

M. Marchi, I. Fabbi & G. Gottardi
DICAM, University of Bologna, Italy

R. Butterfield
School of Civil Engineering and the Environment, University of Southampton, UK

R. Lancellotta
Department of Structural, Geotechnical and Building Engineering, Politecnico di Torino, Italy

ABSTRACT: The role of geotechnical engineering in the preservation of historical towers is particularly relevant, not only for the definition of possible failure mechanisms of the soil-foundation system, but also for the prediction of the rotational rate of the structure with time (creep rate). This paper describes how the rotational creep process, based on a well-known creep model for a material volume element, can be extended to the "macro-element" model through a formal analogy, and thereby formulated in terms of generalised variables. The model needs to be calibrated against displacement-time data of real towers; much effort has therefore been devoted to collecting rotation records of historical towers. In this contribution, the creep rotational rate prediction has been developed for one of them: the Asinelli Tower in Bologna. The analysis shows that a reliable risk assessment of these structures is possible, provided that the evolution of the tower rotation is available accompanied by accurate monitoring of the current tilting rate. The use of modern monitoring systems is strongly recommended.

1 INTRODUCTION

Historical towers are exposed to many hazards: long-term creep deformations of the foundation soil, earthquakes, weathering, etc. Creep is one of the many causes of decreasing stability of such towers and our understanding of the process needs to be improved. In fact, the progressive increase of tilting due to creep may not only drive the soil foundation system to failure, but may also produce high compressive stresses in the masonry walls with consequent, prior, structural failure. For this reason the development of a reliable time-displacement law for tower foundations would significantly improve the evaluation of the overall safety of these vulnerable historical monuments.

2 SOIL—STRUCTURE INTERACTION FOR LEANING TOWERS

The two major failure modes of tower foundations are: (a) bearing capacity failure, due to lack of strength of the supporting soil; and (b) instability of equilibrium, due to lack of foundation stiffness. The long-term process that may lead towers to such failure conditions is, essentially, the foundation creep (rotational in particular). Leaning tower foundations are subjected to combined loads and the bearing capacity prediction must be developed for the relevant load path of a tower (constant vertical weight and increasing moment). Most of traditional bearing capacity formulations apply to general shear failures, unlikely to occur for ancient towers in long-term conditions. Hence, stability of equilibrium failure is the most probable collapse mechanism of the foundation.

An analysis of the stability of equilibrium, a typical structural problem of slender structures, can be developed by considering the tower to be a rigid bar resting on a support at which the deformability of the system is concentrated. The problem is sketched in Figure 1, where W is the weight of the tower, h the height of the center of gravity at which the weight of the tower is applied, θ the rotation of the structure axis from the vertical position and θ_0 its initial imperfection in verticality. The equilibrium condition for small rotations requires the resisting moment generated by the foundation (M_r, also called rotational stiffness of the tower) to be equal the external moment (M_e) due to the geometrical configuration of the tower. Then, the main issue of the analysis is the definition of the rotational stiffness of the soil foundation system, which deeply affects the outcome of the analysis. Various ways of modelling the soil foundation system

(spring, finite elements and strain hardening plasticity models) are shown in Figure 2.

The simplified elastic models with single degree of freedom (Figure 1) can be useful in order to develop simplified preliminary analyses (Lancellotta, 1993), but the real essence of the problem can be captured only taking into account the non linear, irreversible and time-dependent behavior of soil. In this respect, an effective practical alternative to the more widely used numerical modelling is provided by strain-hardening plasticity models, the so-called 'macro-element' or 'force-resultant' models. Recent developments in the latter field provide a powerful framework, in which an advanced foundation analysis can be performed that enables significant non-linear behavior of the soils to be directly incorporated in the soil-structure interactions analysis of leaning towers.

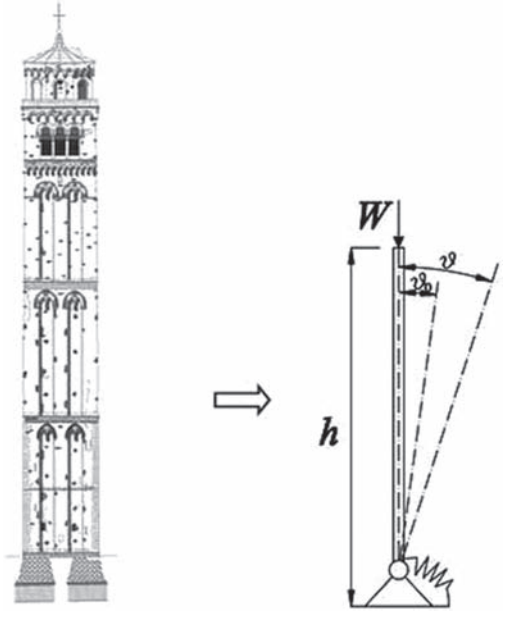

Figure 1. Modelling of a real tower as rigid bar column with flexible support: W is the weight of the tower, h the height of the center of gravity, θ is the total rotation and θ_0 the initial inclination of the column from vertical position.

3 STRAIN-HARDENING PLASTICITY MODELS IN TOWER MODELLING

Historical tower foundations are usually shallow, therefore they can be analysed by modern strain-hardening plasticity models. Such models, developed in relation to the overall soil—footing system, enable us to define both the strength and the stiffness of the foundations (Butterfield, 1978, Nova & Montrasio, 1991, Gottardi *et al.,* 1999, Houlsby & Cassidy, 2002, Randolph *et al.,* 2005). The model formulation is based on a formal analogy with the elementary volume element: external resultant forces (V, M, H) and displacements (w, θ, u) of the foundation are considered as generalised stress and strain variables (Figure 3) and their behaviour is governed by a constitutive law based on the theory of hardening elasto-plasticity. Then, for any given load path the displacements of the foundation can be calculated. Como (1993), Desideri & Viggiani (1994), Nova & Montrasio (1995) and Federico *et al.* (2001) investigated the potentials of these models applied to the analysis of towers. Recently, Marchi *et al.* (2011) gave a comprehensive methodology for the unified approach of all soil—structure interaction problems for leaning towers. The general outcome of such an analysis is shown in Figure 4a, where stability of equilibrium and brittle bearing capacity failures are compared in the M–θ plane.

For the bearing capacity analysis, in case of brittle bearing capacity failure, the knowledge of the failure envelope of the foundation in the (V – M/B) plane is sufficient to define the relevant ultimate moment (M_{ult}) for the load path of a tower of weight W ($V = W$ and M increasing with θ). M_{ult} locates, in the M–θ plane, the critical value of rotation (θ_f) at

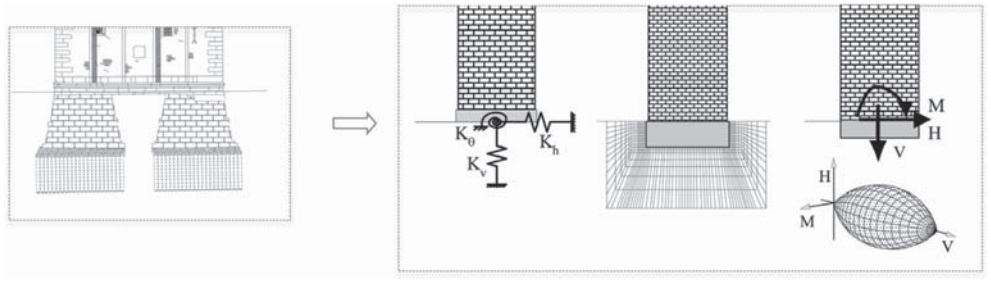

Figure 2. Various ways of modelling the soil foundation system: Springs, finite elements and strain hardening plasticity models (modified from Randolph *et al.*, 2005).

which bearing capacity failure will occur (point B in Figure 4a). If punching failure is expected, the most likely outcome for ancient towers in long-term conditions, no specific outer failure envelope exists and stability of equilibrium failure is the only possible collapse mechanism of the foundation. The stability of equilibrium analysis, assuming an elasto-plastic—and consequently load-path dependent—soil model, is best presented in the M–θ plane. Plotting M_e and M_r together, as first suggested by Cheney *et al.* (1991), the equilibrium condition ($M_e = M_r$) is satisfied when the line (M_e) intersects the curve (M_r), defining the stable and unstable equilibrium conditions (respectively point E_0 and point E_1 in Figure 4b). The stability of equilibrium can then be assessed following a non-hardening creep model. In this simplified interpretation, the shape of the M_r curve is not affected by creep deformation and it merely translates along the θ axis (progressive tilting due to creep is analogous to an increase of initial rotation θ_0). Instability failure occurs at E in Figure 4a, when M_r and M_e paths become tangent.

Combining the bearing capacity and the stability of equilibrium failure predictions, as shown in Figure 4a, enables the most probable failure mechanism to be identify.

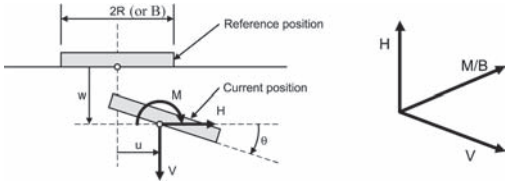

Figure 3. Generalised stresses and strains for a shallow strip footing and sigh convention (after Butterfield *et al.*, 1997).

4 CREEP IN STRAIN-HARDENING PLASTICITY MODELS AND STABILITY PREDICTION

The long-term process that may lead towers to failure conditions is, essentially, the foundation creep (rotational in particular). Creep phenomena were first considered in conjunction with a strain hardening plasticity model by Marchi *et al.* (2011). The analysis is based on an extension of Bjerrum's (1967) Rankine Lecture interpretation of creep-hardening for the volume element. Time now becomes an additional hardening parameter of the model ('Time-hardening') so that displacements (i.e. from w to w' and from θ to θ' in Figure 5) develop also at constant load following a specific time-displacement law. The consequent simple new alternative interpretation, also in the M–θ plane, of the progressive deterioration of stability generated by rotational creep, is shown in Figure 4b.

The relevant rotational stiffness to be considered for equilibrium of the tower is the rotational unload–reload stiffness of the soil—foundation system. The predicted value of θ at which the tower collapses (the critical equilibrium condition) is given by point E_1 in Figure 4b. Notice that such a condition provides a much larger value of critical rotation than would result from Chenney's non-hardening creep model (point E_2 in Figure 4b). However, since the creep rate tends to rapidly increase as failure is approached, the lifetime increase of the tower provided by the alternative analyses will turn out to be much less than it would appear from Figure 4b. Thus, the definition of a reliable rotation rate becomes crucial.

4.1 *Rotational creep rate prediction for towers*

A rotational creep function governing the rate at which post-construction rotation increases (triggered

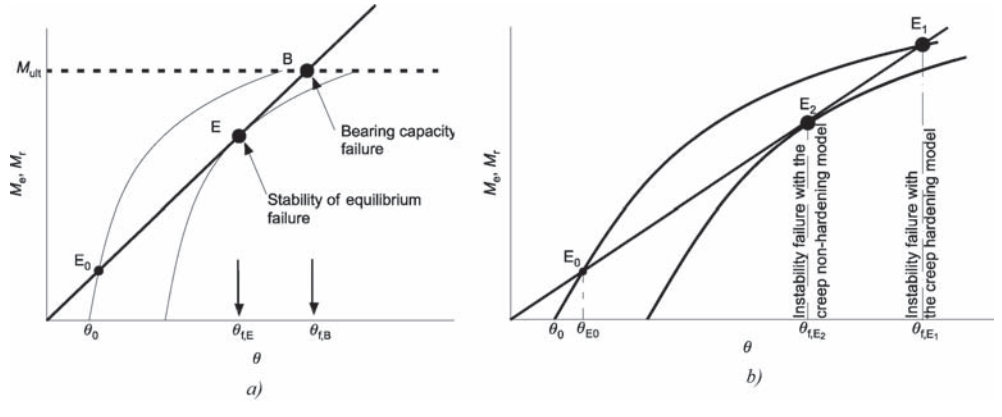

Figure 4. (a) Stability of equilibrium against brittle bearing capacity failure in the M–θ plane. (b) Stability of equilibrium failure prediction via conventional non-hardening and hardening rotational creep models for a tower (from Marchi *et al.*, 2011).

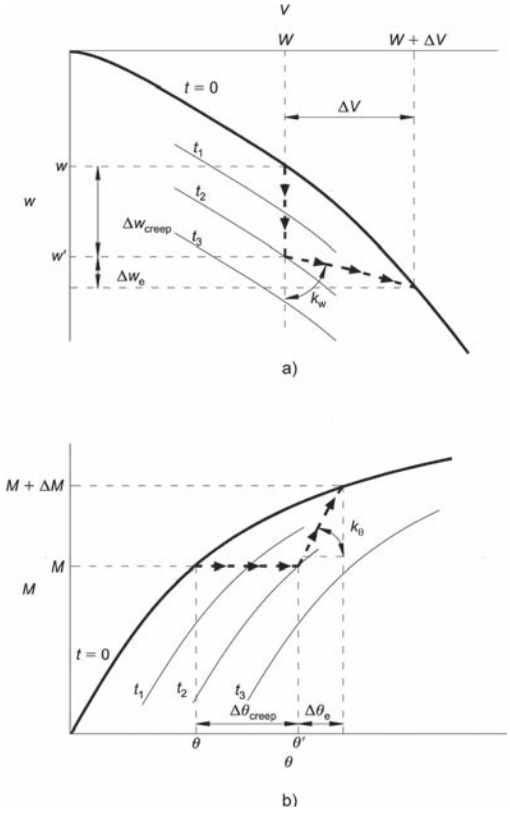

Figure 5. (a) Vertical creep-hardening and (b) rotational creep-hardening for shallow foundations.

by θ_0) was first explored by Marchi *et al.,* 2011, using a logarithmic expression, to be completely calibrated against historical tower displacements. A different prediction can be achieved introducing a direct connection with the soil behavior, hence using the already well established analogy between the macro-element and the volume element. Let us consider the semi-empirical model developed by Tavenas *et al.* (1978) for the volume element, based on the results of creep tests at constant deviatoric stress in a tri-axial apparatus. Assuming that such model, formulated in terms of stresses (p', q) and strains (ε_v, ε_q) for the volume element, applies to the generalized stresses (V, M) and strains (w, θ) of the foundation, the hardening due to the deviatoric creep component can be quantified by the following equations:

$$\dot{\theta} = \frac{d\theta}{dt} = A \exp(\alpha M) \left(\frac{t_i}{t} \right)^m \tag{1}$$

where θ is the viscous rotation of the foundation (consolidation is not included), A, α and m are creep parameters of the model and t_i the reference time.

In the development of the model for the volume element such parameters have been first introduced by Singh e Mitchell (1968) for the interpretation of creep triaxial tests of cohesive soils. Then, assuming the validity of the suggested analogy, the meaning of the parameter m is the rotation rate reduction with time:

$$m = \frac{\Delta \log \dot{\theta}}{\Delta \log t} \tag{2}$$

A is the intercept of the reference time (t_i) curve in the [$Log(d\theta/dt) - M$] plane, hence quantifies the strain rate at null moment:

$$A = \frac{d\theta}{dt}(t = t_i, M = 0) \tag{3}$$

α controls the effect of the moment on the tower rotation rate:

$$\alpha = \frac{\Delta \log \dot{\theta}}{\Delta M} \tag{4}$$

Obtaining the parameters A and m is not a simple matter since, for towers, it is not possible to register rotations at constant moment. This problem can be only partially avoided, assuming null moment increment in a short time lag. Further explanation of the parameter calibration is given in the final Section of this paper, in relation to the Asinelli Tower analysis.

The integration of Equation 1 has been developed assuming the rotation increments due to the elastic unloading-reloading stiffness of the foundation and to the initial load conditions negligible. Such an integration, assuming $\theta = \theta_0$ for $t = 0$ and introducing the progressive increase of external moment with the rotation ($M = Wh\theta$), gives:

$$\theta(t) = -\frac{1}{\alpha W h} \ln \left[\exp(-\alpha W h \theta_0) - \alpha W h A \frac{t_i^m}{1-m} t^{1-m} \right] \tag{5}$$

Note that the initial imperfection θ_0 is usually unknown for any tower, since it represents the eccentricity of the center of gravity generated during the construction of the structure. It can be estimated to be about 0.5–1°, but the sensitivity of the model to the variability of such parameter should be further investigated.

The term of the natural logarithm in Equation 5 has to satisfy the following condition:

$$0 < \left[\exp(-\alpha W h \theta_0) - \alpha W h A \frac{t_i^m}{1-m} t^{1-m} \right] < 1 \qquad (6)$$

In this case Equation 5 gives a continuous increase of θ with time. Its trend is shown in Figure 6a for W = 100 [MN], h = 10 [m], t_i = 1 [years], m = 0,8 [–], A = 0.1 [1/years], α = 0.00035 [1/yearsMNm] and θ_0 = 1°. With reference to the experimental evidences of creep tests performed at constant stress in a triaxial apparatus (Augustensen *et al.*, 2004), the process described by Equation 5, shown in Figure 6a and b, can be divided in three phases: a primary or transient creep, a secondary or stationary creep and a tertiary or acceleration creep. Each one of these phases is characterized by different strain rates: decreasing, constant and rapidly increasing, respectively. It should be noted that tertiary creep might eventually lead to soil failure, known as creep failure or creep rupture. Practical experience suggests that creep failure may happen only at high deviatoric stress levels in soft clays and undrained conditions and in heavily overconsolidated clays and drained shear (Mitchell & Soga, 2005).

From Equation 5 the time at which rotation becomes infinite can be calculated:

$$\bar{t} = \left[\frac{(1-m)\exp(-\alpha W h \theta_0)}{\alpha W h A t_i^m} \right]^{\frac{1}{1-m}} \qquad (7)$$

Although $\bar{t}$ cannot be assigned a physical meaning analogous to the *time to failure* of cohesive soils (long term failure). In fact, large rotations cannot be accommodated by a tower foundation without causing a stability of equilibrium failure. More significant is the point at which rotation rate starts to increase: the inflexion point of the curve θ (t) (flex point in Figure 6a and b). This point could be related to a physical change of the soil-foundation system; for example, as suggested in Marchi *et al.* (2011), a possible assumption is that the tertiary phase starts when the inclination of the tower becomes large enough for the unloaded edge of its base to begin losing contact with the ground. Then, the effective area of the foundation will reduce progressively with increasing rotation.

In the final section Equation 5 is applied to the case history of the Asinelli Tower in Bologna.

5 THE GARISENDA AND ASINELLI TOWERS IN BOLOGNA

The Garisenda (48 m) and Asinelli (97 m) Towers, town symbols typically referred as the Two Towers, are the two most well-known medieval towers of Bologna (Figure 7).

Therefore, the preservation of these monuments now represents an important challenge. Both were constructed at the beginning of the XII century, but the exact construction period and which was the former to be constructed are still unknown. It has been conjectured that the Asinelli was constructed because the immediate inclination of the adjacent Garisenda did not allow it to get to the intended height (Giordano, 2000). It was then assumed that the Garisenda construction started in 1100, while the Asinelli in 1110. Between the 12th and the 13th century, the number of masonry towers in the city was incredibly high, possibly 80 towers and tower houses from recent studies. In the subsequent centuries, many towers were demolished or simply collapsed. At present, only about 20 towers are still standing (Fanti, 1989). The Two Towers have been studied and partially monitored since the beginning of the 20th century by the local authorities. All the information collected during the last century and documented in various reports, has been recently summed up in a comprehensive report (Traversa,

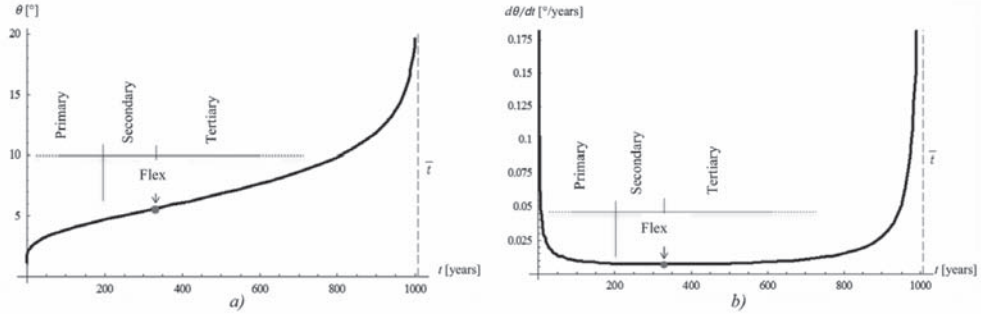

Figure 6. Trend of Equation 5 (a) and its derivative (b) for generic values of the parameters.

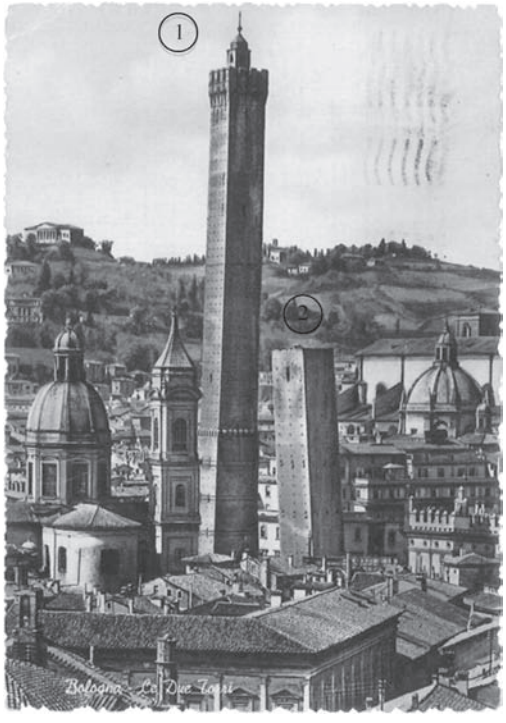

Figure 7. The Asinelli (1) and Garisenda (2) Towers of Bologna, also known as "The Two Towers", in a postcard of the last century.

Table 1. Asinelli Tower historical rotations.

	Out of plumb over 35 m	Tilt θ	
Year	m	°	rad
1110 Presumed start of construction	Unknown	Unk.	Unk.
Between 1400 and 1477	0.59	0.97	0.017
1912	0.90	1.45	0.025
1985	0.94	1.55	0.027
2009	1.01	1.62	0.028

Table 2. Garisenda Tower historical rotations.

	Out of plumb over 48 m	Tilt θ	
Year	m	°	rad
1110 Presumed start of construction	Unknown	Unk.	Unk.
1868	2.52(Est)	3.00	0.052
1902	3.22	3.83	0.067
1999	3.40	4.05	0.071

2011). The soil profile underlying the Two Towers consists of about 4.2 m of anthropic fill, followed by alternation of clayey silt and silty clay, up to the maximum investigated depth (48 m).

The Asinelli Tower center of gravity is about 47 m high above the foundation level. Its foundation comprises selenite blocks down to 1.5 m depth, followed by a solid conglomerate made with lime and well-graded cobbles, down to 7 m. The squared foundation has a width of about 10 m, hence it stretches out less than 1 m all around the outer boundary of the tower structure at ground level, where the base width is about 8,15 m. In addition, from one single boring it was hypothesized, but never confirmed, that wooden piles had been installed under the tower foundation. The tower weight is about 73 MN.

Originally, the Garisenda Tower was 60 m high. In 1353 it was partially demolished to 48 m high, because of its dangerous leaning, acquiring its present stocky aspect. At present, the center of gravity of the Garisenda Tower is about 25 m above the foundational level. The geometry of the Garisenda Tower foundation was investigated in 1999 using the georadar technique and afterwards, in 2000, with inclined boreholes. The width of the squared selenite base is 7.4 m at the ground level, constant for 2 m depth; between 2 m and 5.5–6 m (depth of the foundation base) the foundation enlargement is about 0.5 m, all around the perimeter. The tower weight is about 42 MN.

For Garisenda and Asinelli towers, few records of historical inclination exist. Direct and indirect measurements of rotations, collected over the centuries, are reported in Tables 1 and 2.

A monitoring of the differential settlement at the base of the Asinelli tower started in 1972; 18 years later, in 1990, Garisenda tower monitoring also started. Such readings are still ongoing and suggest that, in the last century, the Asinelli tower differential settlement increased with a rate of about 0.3 mm/year. In the same period of time, a slightly higher rate of about 0.4 mm/year has been calculated for the Garisenda (Traversa, 2011).

6 CREEP-RATE PREDICTION FOR THE ASINELLI TOWER

The records of the historical rotations of the Asinelli tower from its initial construction to the present day are shown in Figure 8. The continuous

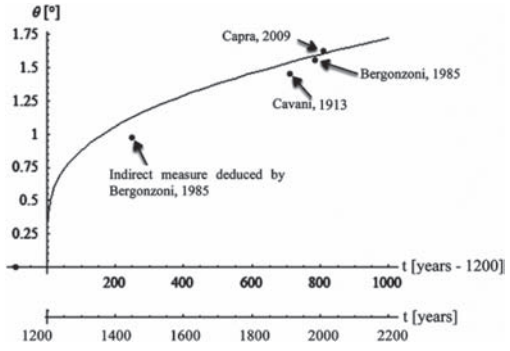

Figure 8. Asinelli tower historical rotations (see Table 1) compared with creep rate prediction from Equation 5.

line in this figure shows the evolution of the inclination predicted by Equation (5). The tower characteristics involved in the calculation are $W = 73$ [MN] and $h = 47$ [m]. The unknown initial imperfection of the system has been set at $\theta_0 = 0{,}1°$. The parameters calculation, following their definition of Section 4, gives $m = 0{,}75$ [-], $A = 0.05$ [1/years], $t_i = 90$ [years] and $\alpha = 0.00012$ [1/yearsMNm]. In addition, the start of construction was set at 1200.

The model predicts a rate of rotation close to the average assessed for the tower in the 20th century (about 1.7×10^{-3} degrees per year). If this rate stays constant the tower should remain stable for a very long time. It is interesting to note that a rotation of around 4° would be required for this tower to enter the tertiary creep phase whereas, from a first estimation, about 6° would be required for the Garisenda tower. However, a longer and accurate monitoring of the tower rotation rate is required in order to develop more reliable predictions.

7 CONCLUSIONS

This paper describes how the rotational creep process can be included in a framework of a strain-hardening plasticity model for shallow footings (i.e. the so-called 'macro-element' models). The suggested formulation is based on a well-known creep model for a material volume element, extended via a formal analogy to the tower foundation as a "macro-element", hence describable in terms of generalized variables. Such an analysis has been applied in the paper to the case history of the Asinelli Tower in Bologna. The parameters calculation and calibration is based on historical rotations of the tower. Consequently the outcome of the analysis is highly influenced by the reliability of such data, limiting, in particular the precision of an estimate of the current tilting rate of the tower. For this reason a collection of measurements of inclination and rotation rate is being undertaken to compile case-histories for a number of ancient Italian towers. The analysis clearly shows that creep can be a main cause of the progressive deterioration of stability for real towers. In fact, the progressive increase of tilting not only tends to drive the foundation towards stability of equilibrium failure, but also produces high compressive stresses in the masonry that may cause premature structural failure. A reasonably reliable risk assessment of such structures can only be made after obtaining a time-series of accurate measurements of their current tilting rate.

REFERENCES

Augustensen, A., Liingaard, M. & e Lade, P.V. (2004). Evaluation of Time—Dependent Behavior of Soils. *International Journal of Geomechanics, ASCE*, Vol. 4(3), pp. 137–156.

Bergonzoni, F. (1985). Un'istantanea del Quattrocento: quanto pendeva la torre degli Asinelli nel sec. XV. *Strenna Storica Bolognese*. pp. 47–54 (in Italian).

Bjerrum, L. (1967). Engineering geology of Norwegian normally consolidated marine clays as related to the settlements of buildings. *Geotechnique*, Vol. 17(2), pp. 83–119.

Butterfield, R. (1978). Another look at the rigid surface footing on sand. *King's College Lecture*, London.

Butterfield, R., Gottardi, G. & Houlsby, G.T. (1997). Standardised sign conventions and notation for generally loaded foundations. *Géotechnique*, Vol. 47(4), pp. 1051–1052.

Cavani, F. (1913). *Sulla pendenza e sulla stabilità della Torre Asinelli*. Collegio degli Ingegneri ed Architetti di Bologna (in Italian).

Cheney, J., Abghari, A. & e Kutter, B.L. (1991). Stability of leaning towers. *Journal ASCE-GED*, Vol. CXVII(2), pp. 297–318.

Como, M. (1993). Plastic and visco-plastic stability of leaning towers. P*roceedings of the international symposium 'Fisica Matematica e Ingegneria delle Strutture: rapporti e compatibilita', Isola d'Elba*, pp. 191–214.

Desideri, A. & Viggiani, C. (1994). Some remarks on the stability of towers. *Proceedings of the symposium on developments in geotechnical engineering, Bangkok,* pp. 457–468.

Fanti, M. (1989). Quante furono le torri di Bologna?, in: *Le Torri di Bologna—Quando, come e perchè,* edited by Roversi, G. Grafis Ed., Bologna, Italy, pp. 55–83 (in Italian).

Federico, F., Ferlisi, S. & Jappelli, R. (2001). Safety evolution of masonry leaning towers on deformable soils. *Proc. 15th Int. Conf. Soil Mech. Geotech. Engng, Istanbul* 1, 679–682.

Giordano, F. (*ed.*) (2000). La torre Garisenda. *Bologna: Costa Ed. (in Italian)*.

Gottardi, G., Houlsby, G.T. & Butterfield, R. (1999). The plastic response of circular footings on sand under general planar loading. *Géotechnique*, 49(4), 453–470.

Houlsby, G.T. & Cassidy, M.J. (2002). A plasticity model for the behaviour of footings on sand under combined loading. *Geotechnique* 52, No. 2, 117–129.

Lancellotta, R. (1993). Stability of a rigid column with non-linear restraint. *Geotechnique* 43, No. 2, 331–332, doi: 10.1680/geot.1993.43.2.331.

Marchi M., Butterfield, R., Gottardi, G. & Lancellotta, R. (2011). Stability and strength analysis of leaning towers. *Géotechnique*, 61(12), 1069–1079.

Mitchell, J.K. & Soga, K. (2005). Fundamentals of soil behavior (3rd edn). *John Wiley & Sons.* p. 577 ISBN 13: 978-0-471-46302-7.

Nova, R. & Montrasio, L. (1991). Settlements of shallow foundations on sand. *Geotechnique* 41, No. 2, 243–256, doi: 10.1680/geot.1991.41.2.243.

Nova, R. & Montrasio, L. (1995). Un'analisi di stabilità del capanile di Pisa. *Rivista Italiana di Geotecnica*, 2, 83–93 (In Italian).

Randolph, M.F., Cassidy, M.J., Gourvenec, S. & Erbrich, C. (2005). Challenges of offshore geotechnical engineering. *Proc. XVI Int. Conf. Soil Mech. Geotech. Eng., ICSMGE, Osaka, Japan*, vol. 1, 123–176.

Singh, A. & Mitchell J.K. (1968). General stress-strain-time function for soils. *J. Soil Mech. Found. Div.*, Vol. 94(1), pp. 21–46.

Tavenas, F., Leroueil S., La Rochelle P. & Roy M. (1978). Creep behavior of an undisturbed lightly overconsolidated clay. *Canadian Geotechnical Journal*, Vol. 15(3), pp. 402–423.

Traversa, F. (2011). Risultati dell'analisi della documentazione relativa agli studi di caratterizzazione del sottosuolo delle torri Asinelli e Garisenda di Bologna. *Technical report. ISPRA—Istituto Superiore per la Protezione e la Ricerca Ambientale, Dipartimento Difesa del Suolo (in Italian).*

Geotechnical Engineering for the Preservation of Monuments and Historic Sites – Bilotta, Flora, Lirer & Viggiani (eds)
© 2013 Taylor & Francis Group, London, ISBN 978-1-138-00055-1

Geotechnical and geophysical characterization of Moai statues—Rapa Nui Easter Island (Chile)

C. Margottini & D. Spizzichino
ISPRA, Italian Institute for Environmental Protection and Research, Rome, Italy

L. Orlando, M. Marsella, B. Renzi & A. Sonnessa
Università La Sapienza DITS, Roma, Italy

O. Pandolfi
YourLIFE, Empowerment Community Network

P. Soddu
Civil Protection Department, Italy

ABSTRACT: Major cultural heritage of Easter Island are the MOAI statues, carved on local tuff from Ranu Raraku quarry. Most statues are presently affected by extensive weathering caused by marine spray and climate factors that produce alteration of tuff primary minerals. A geomechanical and geophysical survey and sampling of rock materials forming the statues has been developed. Geodetic surveying activity was implemented aimed at 3D reconstruction of the Moai statues geometry. Data indicated that the Moai are mainly formed by *palagonite* tuff rock and though low seismic velocities were not detected (due to their saturation degree) the material can be classified as soft rock. The main target of the interdisciplinary study, has been a research program finalized to the comprehension of rock strength and deformation parameters as well as the weathering mechanisms and processes in order to provide to local authorities a scientific and technical support for the conservation of Rapa Nui heritage and identity.

1 INTRODUCTION

The activities of the present work, carried out during the scientific survey "Rapa Nui-Moai in the world" must be seen as part of an international project "*Moai in the world*" developed between 2008–2010.

The project has as its primary purpose the spread in Europe and in the world of Cultural Heritage the archaeological identity of Easter Island (Rapa Nui), of which the Moai Statues represent the maximum expression (Figure 1).

At the same time, the project aims to promote long-term strategies for the collection of scientific and technical data oriented to the definition of criteria for the conservation of artefacts rises-to archaeological value, as the Moai Statues, located in remote areas and subject to degradation due to weathering. The investigations, carried out during the field survey were also used to identify the most suitable statue to be potentially transported for exhibition purposes. A geological survey and sampling of materials has been carried out through thin section analysis for reconstructing mineral composition and X-ray diffractometry analysis. Geomechanical parameters have been defined through field and laboratory tests conducted on Ranu Raraku quarry tuff samples. The geophysical surveys (georadar and seismic tomography) were collected in order to characterize the inner geometry and the 3D P-wave distribution of stratified tuff, respectively. The geodetic surveying activity was aimed at the

Figure 1. Moai statues of Easter Island.

three dimensional (3D) reconstruction of the Moai statues and to precisely locate the seismic and georadar sensors positioned on their statues surface.

2 HISTORICAL AND ARCAELOGICAL SETTING OF RAPA NUI ISLAND

Cultural Heritage represent the identity of a given territory in a specific historic period (Bobrowsky, 2004), geology and geomorphology play a fundamental rule for the realization at the beginning and for their conservation after. Eastern Island it's a perfect link of cultural heritage, geology, landscape and archaeological setting. The first who see the Easter Island was probably the pirate Edward Davis, aboard of his battle Bachelors Delight in 1687 AD. The first-recorded European contact with the island was on April 5 (Easter Sunday) 1722 AD, when Dutch navigator Jacob Roggeveen visited the island for a week and estimated a population of 2,000 to 3,000 inhabitants (Sharp, 1970). Four years later, in 1774 AD, British explorer, James Cook, visited Easter Island; he reported that some statues had fallen over. The British ship HMS Blossom arrived in 1825 and reported seeing no standing statues.

2.1 *The Mystery of the MAOI statues*

About 887 statues are actually in the island (about 400 of them incomplete and partially buried in the Ranu Raraku quarry); the origin, the function and scope of such monolithic block creation, is not yet entirely clear, the only certainty is that they are one of the main archaeological attractions of the island.

Though Moai are whole-body statues, they are commonly referred to as "Easter Island heads". This is partly because of the disproportionate size of most Moai heads and partly because the only Moai standing on the island were the statues on the slopes of Rano Raraku, many of which are buried to their shoulders.

Some of the "heads" at Rano Raraku have been recently excavated and their bodies seen, and observed to have markings that had been protected from erosion by their burial (EISP, 2012).

The most accepted hypothesis is that the statues were carved by the Polynesian colonizers of the island, mostly between circa 1250 CE and 1500 CE (Fisher, 2005). In addition to representing deceased ancestors, the Moai, once they were erected on *Ahu*, may also have been regarded as the embodiment of powerful living or former chiefs and important lineage status symbols.

Completed statues were moved to *Ahu* mostly on the coast, then erected, sometimes with red stone cylinders (*pukao*) on their heads. Moai must have been extremely expensive to craft and transport; not only would the actual carving of each statue require effort and resources, but the finished product was then hauled to its final location and erected.

Figure 2. Panoramic view of Ranu Raraku quarry.

The quarries in Rano Raraku appear to have been abandoned abruptly, with a litter of stone tools, many completed Moai outside the quarry awaiting transport and almost as many incomplete statues still in situ as were installed on *Ahu*. In the nineteenth century, this led to conjecture that the island was the remnant of a sunken continent and that most completed Moai were under the sea. That idea has long been debunked, and now it is understood that:

- some statues were rock carvings and never intended to be completed;
- some were incomplete because, when inclusions were encountered, the carvers would abandon a partial statue and start a new one (Routledge, 1919);
- some completed statues at Rano Raraku were placed there permanently and not parked temporarily awaiting removal (Routledge, 1919);
- some were indeed incomplete when the statue-building era came to an end.

3 GEOLOGICAL SETTING OF THE ISLAND

Easter Island forms part of the Easter Line, a continuous latitudinal chain of volcanic seamounts and islands in the Pacific Sea (27° Lat. S). The island's roughly triangular shape (length: 24 km, surface: 166 km^2) derives from the merging of lava flows produced in the Upper Pleistocene by three main volcanoes, Rano Kau, Terevaka and Poike. The Rano Kau volcano is made up of numerous basaltic lava flows and has been reduced in size by faulting and marine erosion (Fig. 3).

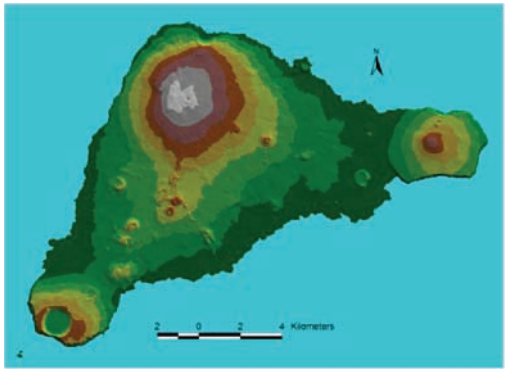

Figure 3. Digital elevation model of Easter Island. Scale 1:100.000.

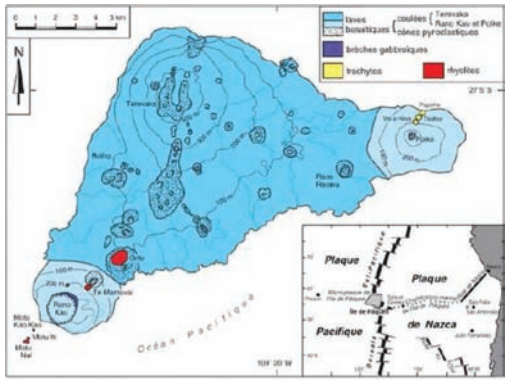

Figure 4. Geological sketch map of Eater Island (modified after Baker et al., 1974).

Its crater (1.4 km wide) is a small caldera that collapsed after a late, large explosive phase, as attested by the presence of *breccia* deposits around the eastern rim of the crater. This breccias comprises gabbroic blocks dispersed in a completely altered white matrix. A late aa-type lava flow of benmoreite composition extends to the east of the crater. The three small islets ("motu"), to the south of Rano Kau are composed of whitish and obsidian rhyolite (Vouvè et al., 1994). Te Mamavai is a parasite pyroclastic cone adjacent to a small dome of white rhyolite and spherulitic obsidian. Another exposure of obsidian occurs on the upper slope of Rano Kau, north of the crater. The Orito dome is probably related to Rano Kau; it essentially consists of whitish banded rhyolitic lava interlayered with obsidian layers (Sawada et al., 2001). Terevaka is the largest and highest (507 m a.s.l.) volcano of the island. It consists essentially of basaltic lava that flowed mainly southwards and of more than 50 pyroclastic cones. Rano Raraku is composed of layered deposits of coherent hyaloclastic tuff probably erupted from a shallow submarine vent (Hagen et al., 1990). The statues have been carved on its flanks. Poike, which forms the eastern part of the island, is a basaltic volcano made up of numerous basaltic lava flows (up to 30 flows have been identified in the eastern cliff) with a small central crater (Fig. 4).

The volcano has been cut by faulting and is limited by vertical cliffs. Most of the outcropping materials are basalt flows (hawaiite), intermediate lavas, pyroclastic layers and palagonitic tuff. The tuff constitutes the forming material of moai statues, all carved in the quarry of Ranu Raraku.

4 ROCK MECHANIC SURVEY AND LABORATORY TEST CHARACTERISATION OF PALAGONITIC TUFF

Different survey techniques and instrument have been adopted and implemented for the characterization of MOAI statues materials. Main purpose of different investigations was to fully understand the mechanical proprieties of tuff from the quarry of Ranu Raraku, which have been used for the most of Easter Island's Moai statues. Such properties are of basic importance to future protection and conservation polices and strategies. To define the mechanical properties of Moai's rock the following investigation have been performed:

1. collection of bibliographical references. Main available information regards weathering processes and only few information are dealing with rock mechanic parameters, including density;
2. development of field survey investigation such as point load test, Schmidt hammer test, roughness profile, in situ density. The performed test allow a preliminary estimation of Uniaxial Compressive Strenght (UCS), weathering degree and general mechanical proprieties of the statue;
3. rock mechanic laboratory test on selected samples, kindly authorized by Consejo Des Monumentos Nationals to bring in specific laboratory in Italy.

This samples are likely very similar to the material constituting the Moai. The test includes UCS in a standard compression test machine, Brazilian test for definition of tensile strength, petro-geophysical properties, physical properties. The test suggests an UCS of about 5–15 MPa (Fig. 5) and density ranging from 14 to 15 KN/m^3.

The tensile strength obtained from the Brazilian test execution (Figs. 6 and 7) varying from 1 to 2 MPa. Adopting K (ratio between σ_n and σ_t) equal to 8 (from similar material), the corresponding σ_n has been estimated between 8 and 16 MPa in accordance with Point Load test.

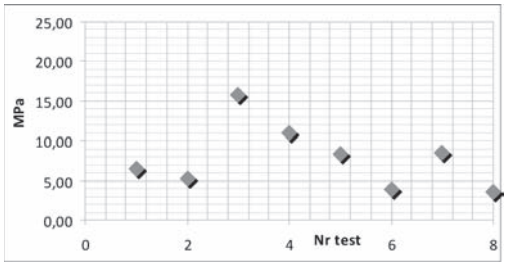

Figure 5. Point load test output.

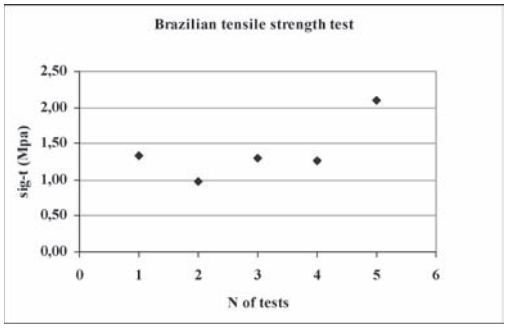

Figure 6. Brazilian test output.

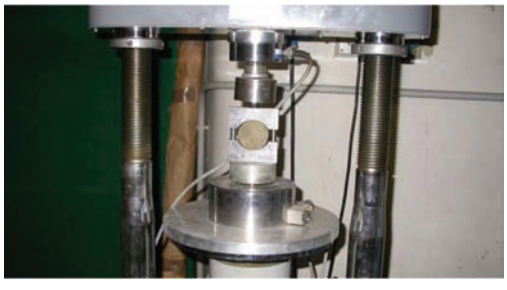

Figure 7. Brazilian test execution.

The material could be classified as a rock with a very low resistance (Deere & Miller, 1966).

The parameters seems to change from statue to another statue depending mainly from: clasts dimensions, granulometric homogeneity and index of weathering. Since the tests are destructive tests, they are conducted on samples collected directly on quarry formation and not belonging to the Statues.

5 GEODETIC SURVEY

The geodetic surveying activity was aimed at the three-dimensional (3D) reconstruction of the Moai statues identified on the island by the experts participating to the project in agreement with the local authorities. The surveyed statues were selected mainly considering their sizes and representative conservation conditions in addition, to being in a convenient location for future transportation operations. The surrounding areas were also surveyed in order to obtain Digital Terrain Models to make possible the accurate re-positioning/location of the statues at the end of the operations. Topographic surveys (Fig. 8), were also conducted jointly with the geophysical measures to precisely locate the seismic and georadar sensors on the Moai statues. The collected data were used to obtain 3D coordinates of the objects and of the ground in Local Reference Systems established on each sites. GNSS measurements were performed in order to obtain georeferenced data in the UTM-WGS84 reference system.

Surveying activities were performed using the following high precision topographical instruments: two laser scanners for measuring the 3D models (Riegl Laser Scanner Z210i for long range surveys and ZF Laser Scanner Imager 5003 for short range surveys), an automatic Total Station (Topcon Total Station Imaging Scanning GPT-9001A IS 03) for establishing the reference networks and measuring 3D coordinates of the seismic and georadar sensors and GNSS receivers (Topcon GR3) for data georeferentiation (Fig. 9).

Figure 8. Laser scanner acquisition for the three dimensional reconstruction of the Moai statues.

Figure 9. GPS survey for geo-referencing the Moai site.

Laser scanning is an automatic process which surveys a real object contact-free and completely, obtaining its location, size, orientation and form. It is able of collecting 3D coordinates, namely a cloud of up to 800 million spatial points, at a very high spatial and geometric accuracy (Fig. 10).

This allows to obtain very accurate 3D surface models for archiving uses or for further quantitative analyses.

The geometrical model can be associated to other information, such as high resolution digital RGB images or intensity images which help to describe the appearance and to understand the conservation conditions of the surface (Figs. 11 and 12).

Table 1 contains the main technical characteristics of the laser scanning instruments used for the surveys.

The total geodetic activity conducted on the Rapa Nui Island is summarized in the table 2, including both the surveys useful for the Moai 3D models reconstruction and those linked to the geophysical measures. The figures 11 and 12 show the detailed results obtained from the collected data.

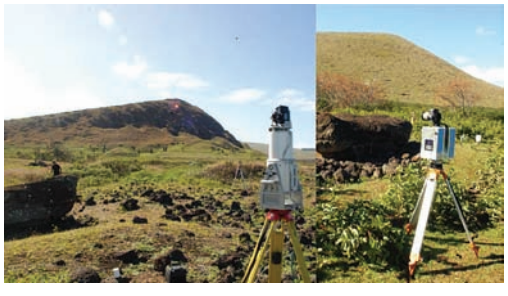

Figure 10. Riegl and ZF laser scanning stations used to obtain the 3D model of the Moai statues and surrounding areas.

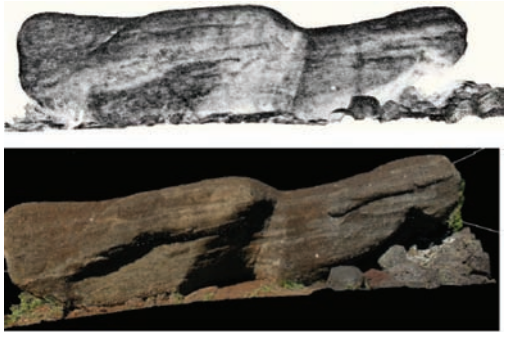

Figure 11. Lateral view of the 3D model of Moai 3 with the superimposition of RGB image.

Figure 12. Different view of the 3D model of Moai to estimate size and volume.

Table 1. Main characteristics of the laser scanning instruments.

Setting	Riegel LS Z210i	ZF LS 5006
Field of view	vertical: 90° horizontal: 360°	vertical: 90° horizontal: 360°
Maximum range	External calibrated mount	External calibrated mount
Resolution range	5 mm	1 mm
Resolution	0.002°	0.0018° ± 0.007°
Beam divergence	0,25 mrad	0,22 mrad
Data acquisition	12.000 pixel/s	500.000 pixel/s

6 GEOPHYSICAL DATA ACQUISITION, PROCESSING AND ANALYSIS

Seismic tomography and ground penetrating radar were combined to determine weakness zones and the degree of alteration in the rock of the statues (Orlando & Renzi, 2012). Stratified argillaceous tuff rock subjected to weathering for long periods and type of degradation was investigated. Argillification and unsaturated condition of rock leads to ambiguity in interpreting the seismic and georadar data individually, but the jointly data interpretation removes this ambiguity. There were surveyed 2 statue with seismic tomography and four with Georadar.

6.1 *Georadar*

The GPR data were collected using an instrument (manufactured by the IDS® corporation) equipped with a 900 MHz antenna frequency. A distance-triggering device, based on an electro-mechanical odometer, was used to ensure constant trace spacing. The GPR transects were collected at the back of the statues along parallel profiles directed from the bottom of the statues to the head (Fig. 13). The statues were investigated by the implementation of

Table 2. Summary of the surveying activities conducted on Rapa Nui Island.

Date	Site	GPS survey	RIEGEL laser survey	ZF laser survey	Topographic survey
18/07/08	Moai 1	2 stations	3 close-range lateral view 1 panoramic view	4 close range view	Georadar profiles (G. Lombardi)
19/07/08	Moai 2	–	–	2 close range view for surface analysis	Seismic sensors Georadar profiles (G. Lombardi)
19/07/08	Tongariki	2 stations	1 front view of moai settlement 2 front and back view of 1 statue	–	–
20/07/08	Laboratory	Data checking and analysis			
21/07/08	Moai 2	2 stations	4 close range lateral view 1 panoramic view		Local reference system for laser survey
21/07/08	Moai 3	–	–	–	Seismic sensors Georadar profiles
22/07/08	Moai 3	2 station	4 close range lateral view 1 Panoramic view	4 close range lateral view	Local reference system for laser survey
23/07/08	Tongariki	2 station	2 front and back view	–	Local reference system for laser survey

Figure 13. The GPR transects along the Moai 2 statues.

longitudinal and perpendicular profiles through the following schema: longitudinal profiles with length equal to 5 m and 0.3 m spaced; perpendicular profiles with length equal to 2 m and 0.5 spaced.

The data were acquired in a time window of 100 ns with a sample number of 1024 and a trace spacing of 0.01 m. We used a standard processing scheme to increase signal-noise ratio, which consists of static corrections for the zero time setting, a time band-pass filter to remove frequency out of the signal band, and application of exponential gain to recover the energy damping inferred by wave propagation. At the end, the topography extracted from the laser scanner survey was included in the profiles.

The longitudinal georadar profiles of Moai, acquired in the middle of the rear surface, show that profiles investigated the statues throughout their thickness, sometimes highlighting the opposite

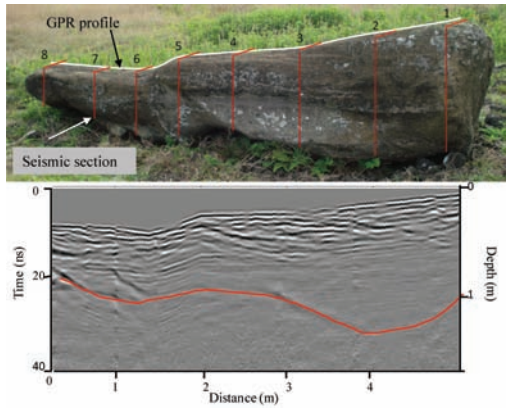

Figure 14. Moai 1. On the top the photo image and on the bottom the interpreted longitudinal central GPR profile.

surface of the statue as shown in the interpreted GPR sections (Fig. 14). The front side of the Moai was not detected at all because of the complexity of the their geometries, which were not all illuminated by the GPR energy. The GPR profiles detected many reflective surfaces with complex geometries. A good signal-noise ratio was observed in the window 0–15 ns and a very low ratio is in the remaining part. We linked the high back-scattered zones to the dry-weathered rock and strongly attenuated ones to the water saturated rock due to water seepage from the ground. Data acquisition in different Moai show different degree

of signal attenuation with the depth interpreted as a different index of statues quality.

6.2 *Seismic tomography*

The seismic survey was performed using the instrument GEODE of EG&GGeometrics with A/D conversion at 24-bit. The instrument was equipped with 24 channels. The sensors were accelerometers with center frequency at 7 kHz and the source was a hammer, 200 gr in weight (Fig. 15).

The instrument was equipped with two triggers to increase the accuracy of the start time of the shot. The first trigger was an electrical bridge positioned on the source; it started the recording a few milliseconds earlier than the actual moment of the shot; the second trigger was a piezoelectric sensor mounted on the hammer and connected to the first channel. This channel was used to record the real zero-time of the shot, and was used as the reference for picking the receiver delay times. The statues were preserved by using medical patches to couple both the sensors and the source plate. The sensors were randomly scattered on circles more or less parallel to the base of the statue and extended from the bottom of the statue to its head. The shots were placed in the middle of the sensors. All the shots were repeated for each set of sensor positions. The statues were investigated with 8 sections, and the acquisition geometry was designed for 2 and 3D data inversion. Because of the irregular geometry of the Moai, the shots and receivers of each section are not all positioned in a plane (x,y); moreover the interpolating plane is not parallel to any reference axis. To reduce error in the calculation of ray-path distance, the 2D data were inverted taking into account the x, y, z coordinates of the shots and sensors, not the projection the x and y on a plane. In this way we were able to take into account the effective distance of the shot-receiver in the data inversion. Shot and receiver points were surveyed for a total station with an accuracy of ±5 mm. The sensors and shots were respectively around 30 cm and 50 cm apart, and the distance between the sections was around 60 cm. A total of 231 and 168 shots were fired. Figure 16 show an example of the 8 sections where the sensors and receivers were arranged, numbered in ascending order starting from the base to the top of the two statues. Unfortunately, due to their position, it was not possible to place sensors and shots on the face of the statues that touched the ground, and this reduced the ray-path coverage of the part of the statues touching the ground. For 2D data inversion we used the ray-paths related to each section more or less perpendicular to the main axis of the statue; in the 3D data inversion all the ray-paths were used (Fig. 16).

The standard deviation of the misfit of the forward models varies from 0.07058 to 0.11209, with mean of 0.08839. Seismic tomography has allowed us to highlight some differences in the elastic characteristics between the most superficial zone of the statues and the inner core. There is a significant difference between the minimum and maximum velocities in the statues due to the fact that the medium is considered homogeneous, although, in reality, it is an inhomogeneous single block of tuff because of the different types of environmental change the monolith has suffered over the centu-

Figure 15. Seismic tomography equipment for data acquisition.

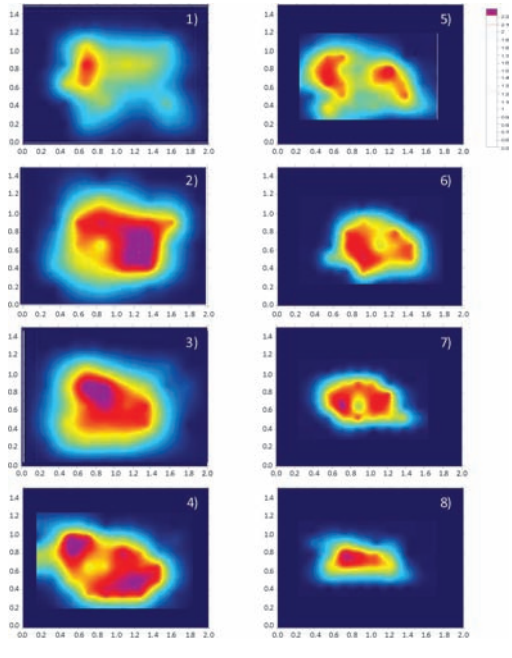

Figure 16. 2D data inversion of Moai statues starting from the bottom (1) to the top (8).

ries. The statue has been exposed to the climate, and its preservation state has also been determined by the influence of coastal and marine spray. Thus, the deterioration of the material of the outer area of the statue is very evident in the tomography results. A comparison of the 2 and 3D data inversion shows remarkable similarities to both the velocity values and their distribution. They show an outer zone characterized by a lower velocity (1.0–1.5 km/s) around 20–30 cm thick and a core with a maximum velocity of 2.5 km/s (Fig. 17).

We can advance the hypothesis that the low velocities of the outer ring, corresponding to poor elastic properties, are due to the weathered zone being attacked by atmospheric agents, while the high velocities of the inner part, corresponding to good elastic properties, create ambiguity in the data interpretation as they could be due to water saturation and the compacting of the rock. We found variation of the range of seismic velocities between the surveyed Moai. The range variations are linked to the different preservation condition of the Moai.

6.3 *Geophysical survey conclusion*

The analysis remove the ambiguity by making a joint interpretation of seismic and georadar data. In fact, the high attenuation of the georadar signal in the inner part of the statue leads us to assume that the high velocities are due to water saturation rather than to the compacting of rock. Joint data interpretation reveals the high seismic velocities of the inner part of the statues to be related to water content, not better rock quality, evident because of the high attenuation of the georadar signal. Instead the weathered zone is characterized by a high signal-noise ratio of georadar data and low P-wave seismic velocities. On comparing, the seismic and GPR data sets of two statues we found that the seismic velocity and the signal attenuation of the georadar section differed, in line with the degree of rock alteration. The experience shows that the joint interpretation of seismic and georadar data overcomes ambiguity in seismic velocity interpretation in argillified massive rock, defines the thickness of the weathered layer, and links seismic velocity to the degree of Moai preservation, all of which are useful for a preliminary classification of Moai health.

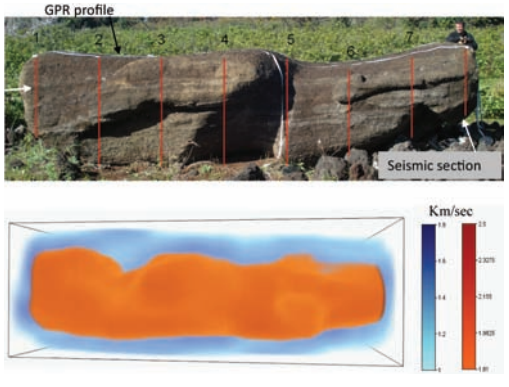

Figure 17. Moai 2. Picture of the statue (on the top) and 3D seismic thomograph (on the bottom). The seismic velocities are mapped with a threshold of 1.8 km/s.

7 CONCLUSION

The main goals of the present work is a better understanding of rock strength and deformation parameters as well as the weathering mechanisms and processes affecting the material forming the Moai statues. From geotechnical point of view the rock can be classified as a anisotropic soft rock (palagonite tuff). The strata are composed by coarse, medium and fine grain-size lapilli interbedded with coarse ash. The statues are lying/face-down on the ground and the rock is saturated to different degrees on passing from the surface in contact with the ground to that fully exposed to the elements. All this leads to a very complex reference model for both seismic tomography and GPR data. In fact, the high seismic velocity could not be interpreted univocally because in the study case it could be linked to both compact and water argillified saturated rock. Georadar penetration is influenced by clay and water content and both are a bad index of rock quality. Combine 3D laser scanning techniques and geophysical survey, we tested the ability of seismic tomography and georadar data to remove this ambiguity in the Moai statue characterization Seismic tomography data inversion showed that the statues are characterized by an outer ring, about 10–20 cm thick, where the velocities are lower than in the inner part. The GPR surveys gave signals of up to 15–20 ns, the signal being strongly attenuated. We linked the attenuation to argillification and water saturation. The combining of the seismic and georadar interpretation led us to interpret the outer ring, the weathered layer, as having low seismic velocities, while the inner zones, which are saturated argillified tuff, are characterized by high velocities. Such interdisciplinary analysis and approach also allows to estimate the thickness of the weathered layer, and links seismic velocity to the degree of Moai preservation.

REFERENCES

Baker P.E., Buckley F., Holland J.G. (1974). Petrology and geochemistry of Easter Island. Contrib. Mineral. Petrol., 44, 85–100.

Bobrowsky P. (2004). Impact of geology on our cultural heritage, plenary lecture, Abstract Volume, Part—I, 32nd IGC, Florence, Aug 20–28, 2004, p. 68.

Brooks N. (2007). Adaptation to Climate Change: Rhetoric and Reality. Proceeding SHIFT07—Shift in Thinking Perspectives of Vulnerability and Hazard Assessment. Potsdam, Germany. October 04–05, 2007.

Canuti P. & C. Margottini, N. Casagli, G. Delmonaco, L. Falconi, R. Fanti, A. Ferretti, G. Lollino, C. Puglisi, D. Spizzichino, D. Tarchi. (2008). Monitoring, geomorphological evolution and slope stability of Inca citadel of Machu Picchu: results from Italian INTERFRASI project. In Canuti and Sassa (eds), Landslides—Disaster risk reduction, Proceedings 1st World Landslide Forum. Tokyo, Springer-Verlag, November 2008.

Canuti P., Margottini C., Fanti R., Bromhead E. (2008). Cultural Heritage and Landslides: research for risk prevention and conservation. In Canuti and Sassa (eds), Landslides—Disaster risk reduction, Proceedings 1st World Landslide Forum. Tokyo, Springer-Verlag, November 2008.

Canuti P. & Margottini C., R. Mucho, N. Casagli, G. Delmonaco, A. Ferretti, G. Lollino, C. Puglisi, D. Tarchi. Preliminary remarks on monitoring, geomorphological evolution and slope stability of Inca citadel of Machu Picchu. In Sassa K., editor. Proceedings of International Consortium on Landslides general Assembly of Washington, October 2005.

Deere D.U., Miller R.P. (1966). Engineering classification and index proprieties for intact rock. Tech. rept. No. AFWL-TR-65-116, Air Force Weapons lab., Kirtland Air Force base, new Mexico.

Delmonaco G., Margottini C., Spizzichino D. (2005). Slope-structure stability modeling for the rock hewn church of Bet Aba Libanos in Lalibela (Ethiopia): preliminary results. In Sassa K., editor. Proceedings of International Consortium on Landslides general Assembly of Washington, October 2005.

Delmonaco G., Falconi L., Margottini C., Puglisi C., Spizzichino D.: The dying town of Civita di Bagnoregio. Proceedings of World Conference on Landslides, Rio the Janeiro 28 June–1 July 2004. Balkema.

Déruelle B., Figueroa A.O., Joron J., Schilling D.M., Silva P.C., Hervé A.F., Demaiffe D. (2002). Le volcanisme de l'île de Pâques (Chili). Géologie de la France, 2002, n° 2, 53–67, 6 fig., 2 tabl.

Di Castri F., Nereo Rotelli M., Pandolfi O. (2005). Empowerment. Da Rapa Nui ad ovunque nel mondo. Carrara.

EISP—Easter Island Statue project. (2012). http://www.eisp.org/3879/

Fischer S.R. (2005). The island at the end of the world. Reaktion Books. ISBN 1-86189-282-9.

Fitzner B. Documentation and evaluation of stone damage to monuments. In Kwiatkowski D. and Lofvendahl R. (ed): Proceedings of the 10th International Congress on deterioration and conservation of stone, 27 June–2 July 2004, Stockolm, Vol. II, 667–690, ICOMOS, Sweden, 2004.

Hagen R.A., Baker N.A., Naar D.F., Hey R.N. (1990). A SeaMARC II survey of recent submarine volcanism near Easter Island. Marine Geophys. Res., 12, 297–315. Pisa University.

Margottini C. (2005). Engineering geology problem for the conservation of the Kogurio mural tomb (North Korea). UNESCO Internal report.

Margottini C. (2006). Aksum Stalae 2 re-erection project. Environmental impact assessment. UNESCO Interrnal Report.

Margottini C. (ed.) (2009). Rock engineering aspects related to the consolidation of the Maaloula cliff, over the Monastery of Santa Tekla (Syria). Report to the Directorate-General for Antiquities and Museums, Damascus, Syria.

Margottini C. (2009). Editor. The destruction of Giant Buddha Statues in Bamiyan (Central Afghanistan). Unesco's emergency intervention for the recovering and rehabilitation of cliff and niches. ISBN 978–448–0375–5, Viterbo 2009.

Margottini C., Pandolfi O. (eds) (2008). Rapa Nui 2008—Results from scientific activity. Fondazioen Marenostrum Internal report.

Margottini C., Marsella M., Orlando L., Pandolfi O., Renzi B., Sonnessa A., Soddu P., Spizzichino D. (2012). Low impact investigation techniques for Cultural Heritage conservation: case study of Moai statues—Rapa Nui Easter Island (Chile). Proceeding of 34th IGC.

Orlando L. and Renzi B. (2012). Non-destructive testing for the characterization of Moai Statue (Easter Island, Chile). Archaeological Prospection, in press.

Routledge K. (1919). The Mystery of Easter Island ISBN 0-932813-48-8 page 181.

Sassa K, Fukuoka H, Kamai T, Shuzui H. (2001). Landslide risk at Inca's World Heritage in Machu Picchu, Peru. Proceedings UNESCO/IGCP Symposium on Landslide Risk Mitigation and Protection of Cultural and Natural Heritage, Tokyo, 1–14.

Sassa K, Fukuoka H, Shuzui H, Hoshino M. (2002). Landslide risk evaluation in Machu Picchu World Heritage, Cusco, Peru. Proceedings UNESCO/IGCP Symposium on Landslide Risk Mitigation and Protection of Cultural and Natural Heritage, Kyoto, 1–20.

Sawada M., Koezuka T., Kohdzuma Y. Inoue S., Bahamondez M. (2001). In-Situ weathering tests of conservation materials applied to volcanic tuff samples from Ahu Tongariki, Easter Island. In Stevenson C.M., Lee G., Morin F.J. (editors) "Pacific 2000", Proceedings of the fifth international conference on Easter Island and the Pacific. Hawai'I preparatory Academy, Kamuela, Hawai'I, August 7–12, 2000.

Sharp A. (ed.), The Journal of Jacob Roggeveen (Oxford 1970).

Steven R Fischer. The island at the end of the world. Reaktion Books 2005. ISBN 1-86189-282-9.

Valentino P. (1999). Strategie innovative per uno sviluppo economico locale fondato sui beni culturali. In "La storia al futuro—Beni culturali, specializzazione del territorio e nuova occupazione", a cura di P. Valentino, A. Musacchio, F. Perego. Giunti editori.

Vouvé J., Aurouze J., Lacazedieu G., Malaurent Ph., Vidal P., Vouvé F. (1994). Deterioration phenomena of lavas abd tuffs under subtropical and temperate conditions: field and laboratory study using multisequential methodology. In E. Charola (Editor), "Lavas and volcanic tuff". Proceedings of the ICCROM International meeting. Easter Island, Chile, October 25–31, 1990.

World Bank (1994). Cultural Heritage in Environmental Assessment. Environmental Assessment Sourcebook, Update, n. 8 (prepared by J. Taboroff). The World Bank, Environment Dept., pp. 8.

This page intentionally left blank

Geotechnical Engineering for the Preservation of Monuments and Historic Sites – Bilotta, Flora, Lirer & Viggiani (eds)
© 2013 Taylor & Francis Group, London, ISBN 978-1-138-00055-1

Landslide risk and monitoring system for conservation of Vardzia monastery, Georgia

C. Margottini & D. Spizzichino
ISPRA, Italian Institute for Environmental Protection and Research, Rome, Italy

A. Sonnessa
Università La Sapienza DITS, SurveyLab, Roma, Italy

ABSTRACT: The present paper reports preliminary results of a feasibility project developed in cooperation with National Agency for Cultural Heritage Preservation of Georgia, aimed at envisaging the stability conditions of the slope-forming rocks of the Vardzia Monastery (rupestrian city cave in the south-western Georgia) and finalized to the implementation of a low impact monitoring systems together with long term mitigation/conservation policies. A field analysis was conducted to reconstruct geometry of the rock cliff, characteristics of discontinuities, main failure modes of potential unstable blocks, magnitude of phenomena and geomechanical parameters. Instability processes are the result of different combination of causative factors such as: lithology, frequency and orientation of discontinuities versus slope orientation, physical and mechanical characteristics of slope-forming materials, morphological and hydrological dynamics. The adoption of different survey techniques (e.g. 3D laser scanner, Ground Base Radar Interferometry) adopted together could be the best solution in the interdisciplinary field of Cultural Heritage preservation policies.

1 INTRODUCTION

The rock-cut city of Vardzia is a cave monastery site in south-western Georgia, excavated from the slopes of the Erusheti mountain on the left bank of the Mtkvari River. The main period of construction was the second half of the twelfth century. The caves stretch along the cliff for some eight hundred meters and in up to fifty meters. The monastery consists of more than six hundred hidden rooms spread over thirteen floors, inside of which it has been possible to protect the monastery from the Mongol domination (Fig. 1). The main lower site was carved from the cliff's central stratum of volcanic and pyroclastic rocks (Gillespie and Styles, 1999) at an elevation of thirteen hundred meters above sea level. The cave city included a church, a royal hall and a complex irrigation system. The earthquake that struck Samstkhe in 1283 AD, destroyed about two thirds of the city cave and the irrigation system, exposing the majority of the rooms to view outside. The site was largely abandoned after the Ottoman took over in sixteenth century. Now part of a state heritage reserve has been submitted for future inscription on the UNESCO World Heritage List. At present the site is affected by frequent landslides and slope instability processes for the entire vulcanite tuff façade of the slope, mainly rock slides along the main discontinuities systems. Due to this phenomena the National Agency for Cultural Heritage Preservation of Georgia has promoted, with the support of ISPRA, a landslide hazard assessment for the entire area through rock mechanics characterization, geotechnical engineering survey, geostructural and kinematics analysis, slope stability model, 3D laser scanner elaboration and a real time monitoring system (GBR interferometry) for the identification of deformation path of the most hazardous areas.

2 VARDZIA ROCK-CUT MONASTERY

2.1 *Historical and archaeological setting*

Vardzia historical-architectural museum reserve, occupies the western part of Aspindza district (historical lower Javakheti) and is stretched along the 30 km-long beautiful section of the Kura river gorge located at Georgian Turkish State border. In the reserve, abandoned villages, ancient settlements, fortress, churches and monasteries, steles, epigraphy monuments, samples of monumental painting, irrigation and water supply systems, bathhouses, caravansaries, rock-cut city monasteries

Figure 1. Panoramic view of rock cut city of Vardzia monastery.

and residential quarters, can be encountered. The town-monastery of Vardzia is absolutely unique example of rock-cut architecture not only at national level, but worldwide as well.

With its huge scale, is an outstanding and incomparable example of Georgian medieval art. The majestic complex was founded by order of King George III and enlarged by his daughter Queen Tamara (1184–1213 AD). Organized along the cliffy rock wall on seven levels for a height of 50 meters and a length of about 800 meters, it consists of several hundred rooms with aqueducts, subterranean tunnels and vertical connections between the various storey. Soviet-era excavations have shown that the area of Vardzia was inhabited during the Bronze Age and indicated the reach of Trialeti culture (*Vardzia Historical-Architectural Museum-Reserve*, 2012). Cave settlements such as Uplistsikhe are known along the Mtkvari River from at least the fifth century BC, while rock cut architecture in the context of Georgian Christianity is known from Zedazeni and Garedzhi from the sixth century AD, and more locally from Vanis Kvabebi, Cholta and Margastani from the eighth century (Gaprindashvili, 1975). A number of documentary sources supplement the knowledge derived from the site's physical fabric. The collection of chronicles known as the History of Georgia refers to Tamar erecting a church to house the icon of the Virgin of Vardzia after receiving divine help in her campaigns, before transferring the monastery from Upper or Zeda Vardzia. Tamar is said to have departed from Vardzia during her campaign against the Muslims, and her ensuing victory at Basian is celebrated in the Hymns in Honor of the Virgin of Vardzia by Ioane Shavteli. The History of Georgia also relates how Vardzia escaped the Mongol invaders in the 1290s (Rapp et al., 2003). The Persian Safavid chronicler Hasan Bey Rumlu describes Vardzia as a "wonder", "impregnable as the wall of Alexander the Great", before recounting its sack by the Persians under Shah Tahmasp I in 1551; a near-contemporary note in the Vardzia Gospel tells of its repatriation from a Persian bazaar. After the arrival of the Ottomans in 1578, the monks departed and the site was largely abandoned (Gaprindashvili, 1975).

The monastery is divided into an eastern and a western part by the Church of the Dormition (Fig. 2).

In the eastern part of the complex there are seventy-nine separate cave dwellings, in eight tiers and with a total of 242 rooms, including six chapels, "Tamar's Room", a meeting room, reception chamber, pharmacy, and twenty-five wine cellars; 185 wine jars sunk into the floor document the importance of viticulture to the monastic economy (Rapp et al., 2003). In the western part, between the bell tower and the main church, there are a further forty houses, in thirteen tiers and with a total of 165 rooms, including six chapels, a refectory with a bakery, other ovens for baking bread, and a forge. Beyond the bell tower the complex rises to nineteen tiers, with steps leading to a cemetery (Rapp et al., 2003). Infrastructure includes access tunnels, water facilities, and provision for defense (UNESCO and ICOMOS, 2012). Since 1985 the site has formed part of the Vardzia Historical–Architectural Museum-Reserve, which includes forty-six architectural sites, twelve archaeological sites, and twenty-one sites of monumental art. In 1999 Vardzia-Khertvisi was submitted for inscription on the UNESCO World Heritage List as a Cultural Site. In 2007 Vardzia-Khertvisi was resubmitted as a mixed Cultural and Natural Site. From 2012, the conservation of the wall paintings in the Church of the Dormition (attributed to the painter Master Giorgi) was carried out by the Cultural Institute of Art in conjunction with the National Agency for Cultural Heritage Preservation of Georgia and Tbilisi State Academy of Arts (UNESCO and ICOMOS, 2012).

Figure 2. Particular of wall paintings inside the Church of the Dormition.

Figure 3. Aerospace image of the site.

3 TOPOGRAPHICAL SETTINGS AND GEODETIC SURVEY THROUGH LASER SCANNER TECHNIQUES

3.1 *Local topography*

The rock-cut monastery city of Vardzia is located in the south-western Georgia, near Akhaltsikhe close to the Turkish border, faces southwards onto the Mtkhvari river valley. As a preliminary data base, topographical map has been collected and elaborated through a GIS platform in order to implement a geo data base to store all the information useful for future analyses (Fig. 3).

In order to carried out a site-scale specific analysis and to support the monitoring system activities and outcomes, a detailed geodetic survey through 3D Laser Scanning techniques have been performed and implemented during May 2012 field mission. The geodetic surveying activity was aimed at the three-dimensional (3D) reconstruction of the Vardzia cave monastery, and collection of all data useful to future potential stability analysis of the cave complex.

All 3D data of the objects were collected in a Local Reference Frame by means of a terrestrial high-resolution laser scanner, and then georeferenced by using high-precision dual frequency geodetic GNSS receivers (Margottini et al., 2009).

Laser scanning is an automatic process which surveys a real object contact-free and completely obtaining its location, size, orientation and shape in a reference system coincident with the instrument. It is able of collecting 3D coordinates, namely a cloud of up to 800 million points, at a very high spatial and geometric accuracy. This allows to obtain accurate 3D surface models for archiving uses or for further quantitative analyses.

Thousands of points are scanned per second. Also the intensity of the reflected laser pulse is often recorded, providing an indication of the reflection characteristics of the surface and enabling the creation of quasi images. The basis of the 3D laser mapping system technology is a scanning laser range-finder. The distance from sensor to arbitrary points on the object surface is calculated from the pulse travel time.

Table 1. Main technical characteristics of the laser scanning instrument used for the survey activity.

	Riegel laser scanner Z210i
Field of view	Vertical: 90°
	Horizontal: 360°
Maximum range	1000 m
Digital camera	External calibrated mount
Resolution range	5 mm
Resolution	0.002°
Beam divergence	0.25 mrad
Data acquisition rate	12.000 pixel/s

Depending on the inter-visibility between the instrument and the object to survey, multiple scans are required for complex shapes that can't be acquired from a single scan position.

The geometrical model can be associated to other information, such as high resolution digital RGB images acquired with a built-in calibrated camera or intensity images which help to describe the appearance and to understand the conservation conditions of the surface. From the above, it is quit clear the actual and future potentiality of such techniques in the field of conservation and protection of Cultural Heritage.

Surveying activities were performed using a topographical Riegl Z210i laser scanner for measuring the 3D coordinates of the models and acquiring the RGB information linked to the point clouds.

Several scans were acquired in order to exactly reconstruct the topography of the site (Fig. 4); ten scans were collected from two different scan positions, with an average spatial resolution ranging from 10×10 cm up to some meters, depending on the distance between the laser and the object.

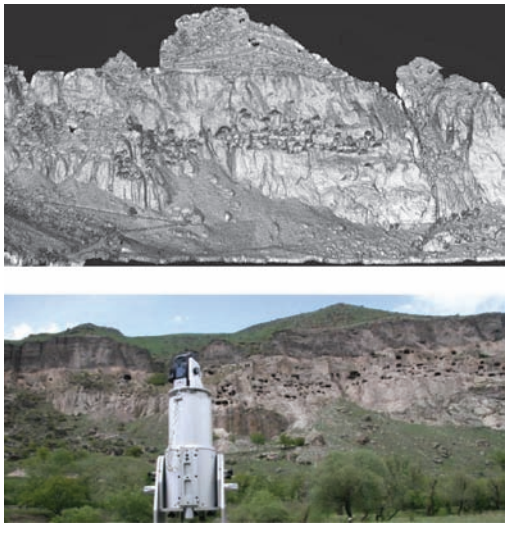

Figure 4. 3D model of the cave monastery of Vardzia from laser scanning techniques.

Purpose-built targets were used to link the scans together. Collected data were used to build up a high-resolution 3D model of the cave monastery, in order to provide an useful tool for helping the Georgian Authorities and the scientific community in the protection and conservation of the site.

4 GEOLOGICAL AND GEOMORPHOLOGICAL SETTING

4.1 *Local geology*

The Vardzia monastery is entirely cut and carved in volcanic and pyroclastic rocks (Gillespie and Styles, 1999) formations (Upper moitsen—lower moitsen) see figure 5 (Gudjabidze et al., 2003). From lithologic point of you a representative detailed cross section of the slope have been carried out and implemented during last field mission (figure 6). The entire slope is the final results of several volcaniclastic and pyroclastic falls in time and space, characterized by different explosion dynamics and chemical lava compositions.

Concerning the structural setting, at the slope scale, is possible to define two main settings, the first (sub vertical) due to volcaniclastic cooling phase and a second one (locally parallel to the slope face) mainly due to lateral detensioning caused by opening of the valley by the river.

The spacing became stitched proceeding towards the inside of rock mass. Probably both layers number 1 and number 4 can be further divided

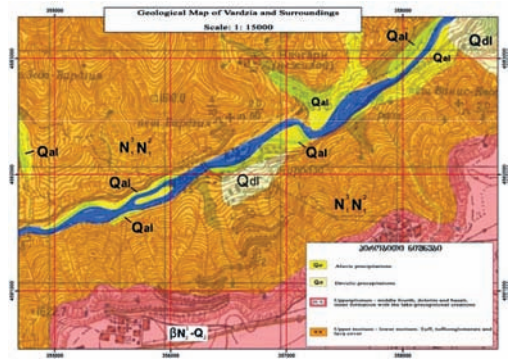

Figure 5. Geological map of Vardzia at 1:15.000 scale.

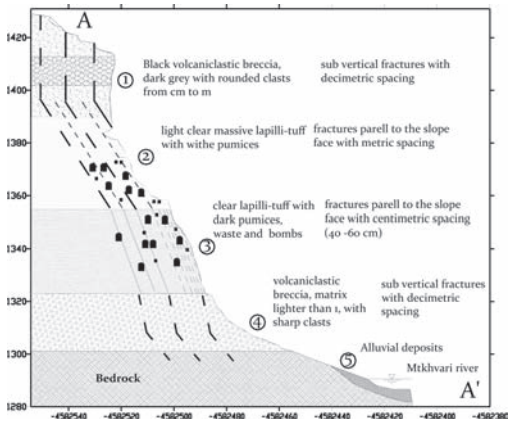

Figure 6. Litostratigraphy cross section of the cliff.

into sub-layers. The structural setting of layers 2 continues its persistence also within the layer 1.

The boundary between the different volcaniclastic levels are not always cleared marked but they are all sub parallel according to the stile of depositions. Further analysis would be needed (thin section and x-difrattometry analysis), in order to classify the different type of rocks from petrographical point of view.

4.2 *Local geomorphology*

Vardzia it's one of the main example of the so called Cultural Landscape (Margottini et al., 2009) in which the human activities (e.g. excavation, construction and implementation of the cave monastery, painting) and natural, geological and geomorphological processes are strictly connected and interdependent. Often, type of rock material (soft rock easy to cut), geomorphological processes (e.g. landslide, erosion and weathering), beauty and impressive landscape, inaccessibility, have been the

main input in the history of humanity concerning the choice for the realization of city, monument, religion structures, defense works. The geomorphological aspect of the Vardzia monastery is the result of various long and short-term factors (natural and human), that affected this part of the Georgia region. Active tectonics related to the Caucasian System jointly with the volcanic activity have a big influence to the actual morphology of the surrounding territory. Vardzia slopes are the final result of tectonic, different volcaniclastic and pyroclastic falls and erosion and deposition cycles of the Mtkhvari river. The entire cliffy rock wall has a length of about 800 meters for a height of 130 meters with a general E-W orientation. The slopes, as a general rule, presents a rupestrian aspect, mainly stratified and alternatively massive. Nevertheless, discontinuities of various types are present, mainly related to: cooling phase after volcanic activity (vertical); tectonic activity (faults, minor joints, mainly sub-vertical) geomorphological activity (lateral detensioning caused by opening of the valley by the river from vertical to inclined joints). Sub-vertical and high-angle dipping joints intersecting horizontal bedding (layers of different pyroclastics falls) are quite frequent in some parts of the area and observed during field investigation (Ershov et al., 199). This situation may cause potential falls, sliding and topples of blocks, whose types, dimensions and kinematics are depending on local orientation, mechanical property of pyroclastics layer, spacing and persistence of joints.

4.3 *Landslide types and slope evolution*

Following the general scheme of the cross section defined in the figure 6 and with the aim to provide a preliminary assessment according to landslide type and processes affecting the entire cliff rock (from the top to the bottom), most rock slope failures can be classified into one of the following categories listed below (Cruden et al., 1996, and Cruden DM, 1991), depending by structural combination of the main joint's families.

In the level 1 (Fig. 6) the main rock slope failures are:

a. Rock falls, topples or wedge failure often due to the lack of support of the underlying layer affected by planar sliding (Fig. 7);
b. Large roto-translational rock slide involving both layers 1 and 2 and 3 (Fig. 8).

In the level 2 the main rock slope failure are mainly due to:

a. wedge failure and rock fall (Fig. 9);
b. high and low angle planar rock slide along the main structural settings (Fig. 10).

Figure 7. Rock falls in the upper part of the layer 1.

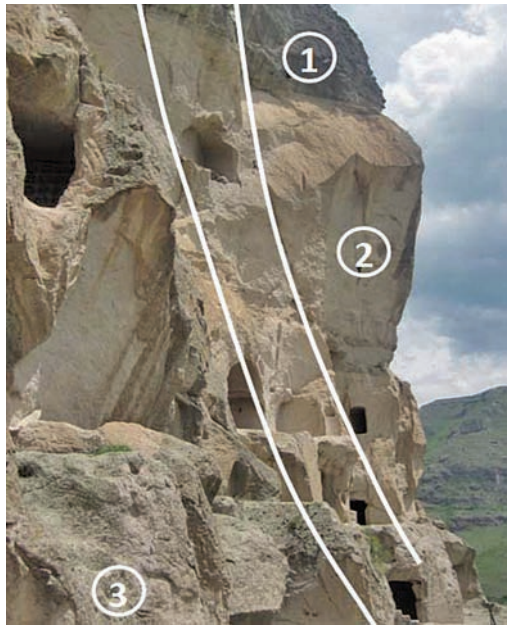

Figure 8. Large roto-translational rock slide involving both layers 1, 2 and 3.

Figure 9. Wedge failure at the contact between layer 1 (on top) and layer 2.

Figure 10. High and low angle planar rock slide.

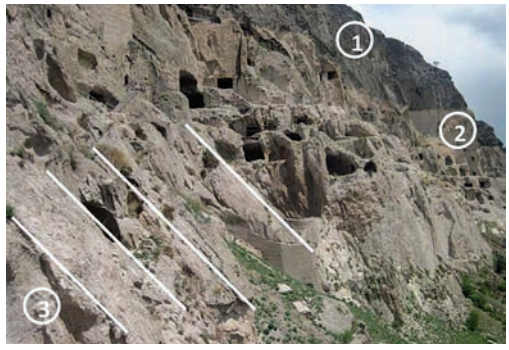

Figure 11. Planar sliding along the mains structural setting.

In the level 3 the main potential rock slope failures are:

a. planar sliding along the main structural settings (figure 11);
b. topples.

Furthermore widespread superficial erosion shape has been recognized an mapped along the slope. They are manly due to superficial water circulation and minor stream network able to create small depositional fan delta at the toe of the slope and, depending from the slope angle, alternation of erosion, transportation and deposition zone of debris. The site is then affected by many examples of slope instabilities such as rock fall, topple and rock slide, with volumes ranging from few cubic meters till thousands (WP/WLI 1993). Many phenomena also occurred in recent years, such as in May 1968 when a huge protective wall was constructed just above the main Church, till the very recent rock slide of spring 2011.

4.4 *Geotechnical and geo-mechanical parameters from field survey*

Geo-mechanical characteristics of the Vardzia slope-forming rocks outcropping in the study area (mainly volcaniclastic and pyroclastic rocks), have been reconstructed through geotechnical field techniques and laboratory tests (executed in Italy), on rock blocks (core samples and blocks collected in the area) of the local formations (Hoek, 2007). The following activities have been carried out during 2011 and 2012 field survey:

– field survey implementation through Rock Mass Classification techniques, in order to define and reconstruct the main geotechnical and geomechanical parameters and Index (e.g. RMR, GSI, Qsystem);
– strength and deformation parameters are collected starting from scientific and technical literature (Burton, 1973, and ISRM) as well as from local technical report;
– geo-structural analysis (orientation and characteristics of discontinuities);
– sampling of blocks in the field for the laboratory tests;
– schmidt-hammer test on joint surfaces and intact rock block for in-situ analysis of UCS;
– laboratory Point Load test to provide UCS data from sampled blocks and compare them with in-situ data (ISRM 1978, 1981).

Table 2. Main geomechanical parameters.

Lithology	Natural unit weight (KN/m^3)	UCS from schmidt-hammer test (MPa)	ϕ° Tilt test	UCS from Point Load test (Mpa)
Layer 1				
Black volcanic breccia	18.9	19	–	14.8
Layer 2				
Light massive tuff	17.5	17	22°–32°	9.6
Layer 3				
Clear tuff with dark pumices	15.1	15	22°–32°	10.8

The preliminary site engineering geology investigation for reconstruction of the strength of slope-forming materials and geo-structural characteristics of the joints, have provided the following results.

The rock of the site is quite weak (Lembo Fazio et al., 1984), as usual in areas where human being realised important settlement. Uniaxial Compressive strength is ranging between 10–15 MPa, with density from 15 till 19 KN/m^3 according to the different layers.

4.5 *Geo-structural analysis*

The mechanical behaviour of rocks is generally controlled by the conditions under which deformation takes place and by the inherent rock properties (Turner et al., 1996). Stress condition of Vardzia monastery slope-forming rocks have promoted different types of discontinuities in the volcaniclastic igneous rocks (Mitchell et al., 1999). This is due to the strain behaviour (e.g. lateral unloading due to water erosion coupled with tectonic stress and cooling of the pyroclastics falls) and to the typical petrographical and physical properties of the soft rocks (e.g. chemical and mineralogical composition, grain size, shape, thickness, homogeneity, porosity, permeability, type of cement). The presence of brittle volcanic and pyroclastic rocks in the area, as a general rule, promote a block composition of rocks due to high frequency of discontinuities of above mentioned various origin (Gamkrelidze, 1986). A geo-mechanical characterisation of discontinuities has been done along the entire study area in order to provide structural setting of the area and define the master joints. All geomorphological processes and slope instability, acting along the area, are the results of different structural combination of the main joints families (Spizzichino et al., 2009). In our analysis, although preliminary and not exhaustive of discontinuity surveyed of the whole area, some relevant blocks and parts of the slopes have been analysed in geo-structural terms. In those location a particular attention has been done to the discontinuity orientation. All data collected for blocks/slope areas have been analysed and represented with the geo-structural software DIPS®. The intensity of jointing is variable depending on distance from master joints and strength of materials (i.e. lower within the black volcanic *breccia* sequences, higher within clear white tuff and lapilli-tuff). The plot of joints shows that the major trend of joint systems ranges around NW-SE direction (140°–165°) with high slope angle 70°. The main result of possible kinematics are reported in the figure 12.

A preliminary kinematic analysis focused on verifying of possible ruptured modes in the study area has been carried out, with particular attention to slides, rock fall and toppling phenomena. The main results are shown in the plots of figure 12.

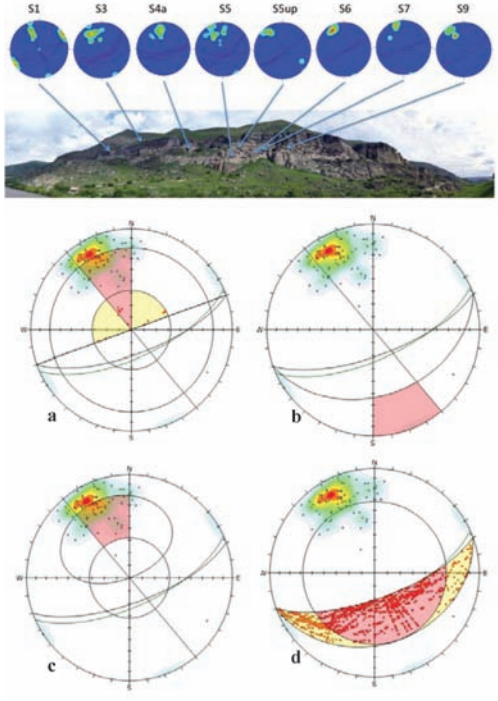

Figure 12. Plot of joints surveyed in the Vardzia monastery study area and kinematics analysis: a) direct toppling; b) flexural toppling; c) planar sliding; d) wedge failure.

5 MONITORING SYSTEM PROPOSAL AND IMPLEMENTATION

According to the above results, considering the morphological setting (big portion of a slope ca. 10^5 m^2) and slope instability processes (different typologies in size, magnitude and probability of occurrence), a new advanced simple and flexible monitoring system has been implemented in order to obtain: measurements, processing and remote control in real time; possibility of transforming the monitoring system in a warning system. The system has been chosen for its versatility and adopted for the monitoring of the entire cliff of Vardzia.: it considers the application of an advanced ground based radar interferometry, developed by IDS from Pisa (Italy) named IBIS (Fig. 13). The radar equipment allows the monitoring displacement area's, with a resolution of mm, in the direction of the instrument.

The radar system is a Stepped-Frequency Continuous Wave (SF-CW) coherent radar with SAR and interferometric capabilities, dedicated to the remote monitoring of terrain (e.g. landslides, unstable slopes, glaciers) or structures (e.g. dam, bridge). The acquisition station has been realized with the incredible support of National Agency for Cultural Heritage Preservation of Georgia and the pre-acquisition and start up activities have been finalised and calibrated during the last field mission.

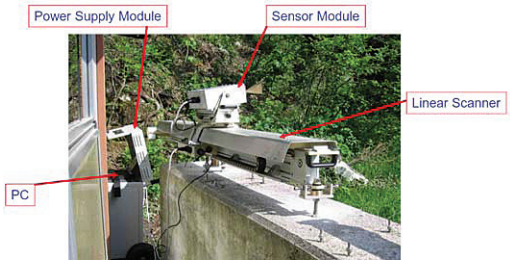

Figure 13. IBIS-L radar monitoring system HW description.

Figure 14. Remote sensing monitoring system realised in Vardzia.

The above mentioned techniques (SF-CW) allows the resolution of the scenario along range direction independently from the distance (IBIS Range Resolution up to 0.75 m). The SAR technique also allows the resolution of the scenario along cross-range direction independently (in the angular value) from the distance (IBIS Cross-Range Resolution up to 4.3 mrad). The differential interferometry technique (Ground Based Radar) enables the measure of the displacement of the objects resolved through coupling SF-CW analysis.

5.1 *Preliminary outcome May–October 2012*

The system has been installed during the May 2012 field mission. During the period May—October 2012 the system has been initialized and tested. The radar configuration adopted is reported in the following table, the "selection mask" contains about 50.000 points.

The DTM has been used as 3D model for the visualization of the main parameters (displacement and velocity) collected, stored and implemented by the monitoring systems in real time (figure15).

The monitoring system is actually close to the end of the first 6 months of acquisition and the preliminary results are quite stable and comfortable.

Table 3. Main parameters of radar configuration.

Distance from the slope	(m)	350–500
Antenna beam width	(deg)	> 70
Number of points	–	50.000
Range resolution	(m)	0.5
Cross range resolution	(mrad)	4.3
Scanning time	(min)	5

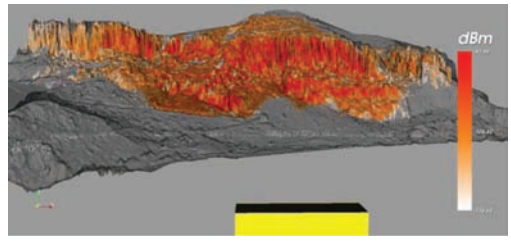

Figure 15. Radar amplitude map.

With the exception of some individual control points (mainly due to noise factors related to vegetation) the investigated area is stable and under control (Fig. 16).

In the next 6 months the verify and control of the main outcome of the monitoring systems will be carried out directly on site and along the cliff in order to calibrate and correct the results and define the most active zone of the area in which downscale the landslide hazard and risk assessment.

6 CONCLUSION

The main geomorphological, geo-structural and geotechnical evidences obtained after two distinct field missions (October 2011 and May 2012) suggest the following observations and recommendations:

1. the potential instability processes and mechanisms observed for the entire rock cliff can be referred to different failure modes (or their combination): rock fall; planar rock slide; roto-translational rock slide; wedge and toppling failure;
2. such instability processes differ along the whole cliff both in terms of activity, namely their state (temporal evolution), distribution (spatial evolution), style (combination and repetition of different failure mechanism) and magnitude (landslide intensity and potential volumes);
3. actual and/or potential instability processes in Vardzia monastery are the result of a combination of different predisposing factors such as: lithology; presence, frequency and orientation

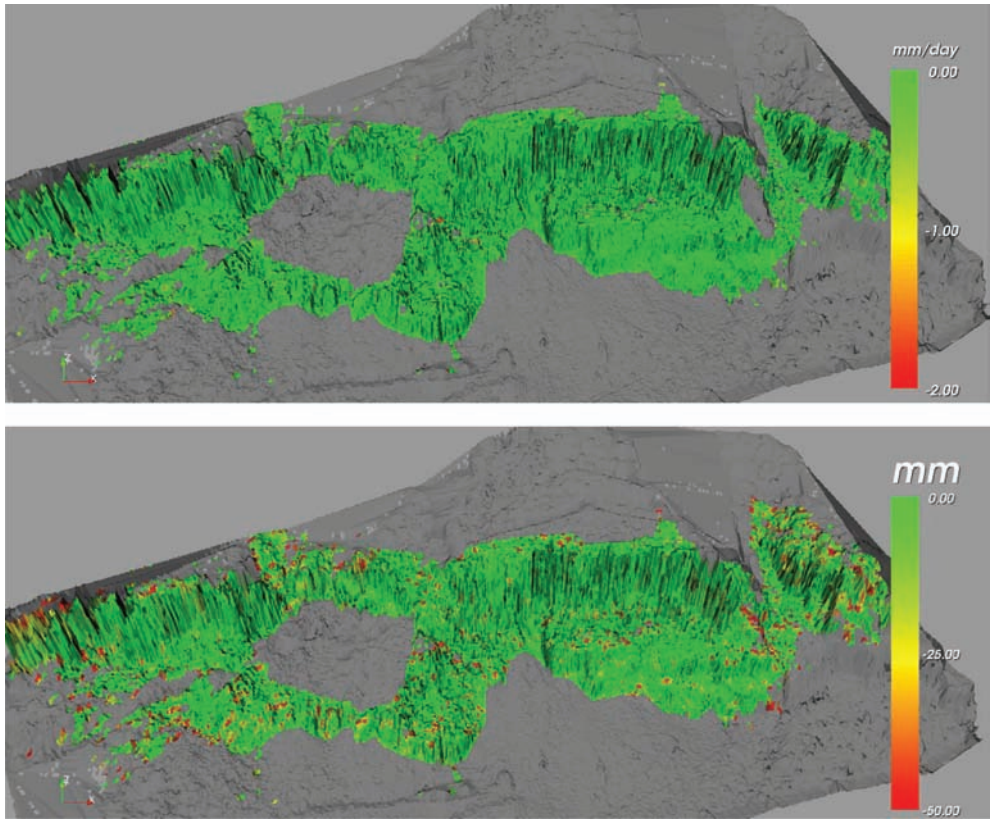

Figure 16. Velocity and displace map: Whole 5-month period average.

of discontinuities vs. slope orientation; physical and mechanical characteristics of slope-forming materials; morphological and hydrological dynamics;

4. some of the main potential instability conditions detected and assessed need more accurate and specific analysis (slope scale risk analysis) in order to define landslide state in terms of intensity, potential evolution and impact;
5. the adoption of different survey techniques (e.g. 3D laser scanner, engineering geology, geotechnical field survey, GBR Interferometry) coupled together is the best strategy in the interdisciplinary filed of Cultural Heritage protection and conservation policies;
6. the adopted monitoring system is the most suitable for the specific condition of the site and actually the unique technical solution able to take into account all the above mention peculiarity of the site giving displacement information in real time;
7. Preliminary outcomes of the systems will be used for the implementation of feasibility project addressed to landslide risk analysis as fundamental management tool of a master plan for sustainable future tourist exploitation of the site.

ACKNOWLEDGMENTS

Authors are very grateful to all the National Agency for Cultural Heritage Preservation of Georgia staff members for their support and continuous help.

REFERENCES

Barton, N.R. 1973. Review of a new shear-strength criterion for rock joints. Engineering Geology, 7, 287–332.

Cruden, D.M. 1991. A Simple Definition of a Landslide. Bulletin of the International Association of Engineering Geology, No. 43, pp. 27–29.

Cruden, D.M. & Varnes, D.J. 1996. Landslide types and processes. In: A.K. Turner, R.L. Schuster (eds.) Landslides investigation and mitigation (Special report 247, pp. 36–75). Transportation Research Board, Washington, D.C.

Ershov, A.V., Brunet, M.F., Korotaev, M.V., Nikishin, A.M. & Bolotov S.N. 1999. Late Cenozoic burial history and dynamics of the Northern Caucasusmolasse basin: implication for foreland basin modeling. Tectonophysics, 313, 219–241.

"Evaluations of Cultural Properties by ICOMOS (2001)". UNESCO. pp. 18–21. Retrieved 1 May 2012.

Gamkrelidze, I.P. 1986. Geodynamic evolution of the Caucasian and adjacent areas in Alpine time. In: L.P. Zoneshain (Editor), Tectonics of the Eurasian Fold Belts. Tectonophysics, 127, 261–277.

Gaprindashvili, G. 1975. (in English, Russian, Georgian). Ancient Monuments of Georgia: Vardzia. Aurora Art Publishers, Leningrad. pp. 7–25. ISBN 978-1-135-68320-7.

Gillespie, M.R. & Styles, M.T. 1999. BGS ROCK Classification Scheme Volume 1 Classification of Igneous Rocks. British Geological Survey Research Reports, (2nd edition) RR 99-06.

Gudjabidze, G.E., Gamkrelidze, I.P. 2003. Geological Map of Georgia, 1:500.000. Georgian State Department of Geology and National Oil Company "Saqnavtobi".

Hoek, E. 2007. Practical Rock Engineering (2007 edition). http://www.rocscience.com

ISRM—Commission On Classification Of Rocks And Rock Masses (1981)—Basic Geotechnical Description of Rock Masses. Int. Journ. Rock Mech. Min. Sci. & Geomech. Abstracts, 18, 85–110.

ISRM—Commission On Standardization of Laboratory and Field Tests (1978)—Suggested methods for the quantitative description of discontinuities in rock masses. Int. Journ. Rock Mech. Min. Sci. & Geomech. Abstracts, 15, n.6, 319–368.

Lembo Fazio, A., Manfredini, G., Ribacchi, R. & Sciotti M. 1984. Slope failures and cliff instability in the Orvieto hill. 4th Int. Symp. on Landslides, Toronto, 2, 115–120.

Margottini, C. & Spizzichino, D. The management of cultural and environmental heritage sites: a pivot for conservation and enhancement. Proceedings of the first International Symposium on Danxia Landform. The 2nd collection. Danxiashan, Guadong (China), 26–28 May, 2009.

Margottini, C., Marsella, M., Orlando, L., Pandolfi, O., Soddu, P., Sonnessa, A., Spizzichino, D., Delmonaco, G., Cardareli G. & De Donno G. 2009. Low impact investigation techniques for parameterization and conservation of Cultural Heritage: the case study of Moai statues at Easter Island (Chile). Geoitalia 2009—sesto forum italiano di scienze della terra, Rimini 09–11 settembre.

Mitchell, J. & Westaway, R. 1999. Chronology of Neogene and Quaternary uplift and magmatism in the Caucasus: constraints from K-Ar dating of volcanism in Armenia. Tectonophysics, 304, 157–186.

Rapp, Stephen H. 2003. Studies in Medieval Georgian Historiography: Early Texts And Eurasian Contexts, passim. Peeters Publishers, ISBN 90-429-1318-5. Retrieved on 26 April 2009.

Spizzichino, D. Delmonaco, G. & Margottini, C. 2009. Geo-structural modelling for potential large rock slide in Machu Picchu—European Geosciences Union 2009 General Assembly, Vienna Austria, 19–24 April.

Turner, A.K. & Schuster, R.L. 1996. Landslides investigation and mitigation (Special report 247), Transportation Research Board: Washington, D.C., p. 673.

"Vardzia-Khertvisi". UNESCO. Retrieved 1 May 2012.

"Vardzia Monastery complex". National Agency for Cultural Heritage Preservation of Georgia. Retrieved 4 May 2012.

"Vardzia Historical-Architectural Museum-Reserve". National Agency for Cultural Heritage Preservation of Georgia. Retrieved 1 May 2012. ISBN 978-9941-0-3547-0.

WP/ WLI. 1993. A suggested method for describing the activity of a landslide. Bulletin of the International Association of Engineering Geology, No. 47, 53–57.

Geotechnical Engineering for the Preservation of Monuments and Historic Sites – Bilotta, Flora, Lirer & Viggiani (eds)
© 2013 Taylor & Francis Group, London, ISBN 978-1-138-00055-1

Strength and structure of the roofed mud-walls of Toji Temple

M. Mimura
Kyoto University, Kyoto, Japan

M. Yoshimura & T. Terao
Soil and Rock Engineering Co. Ltd., Toyonaka, Japan

ABSTRACT: Toji Temple was constructed as a governmental temple to pray the public peace in 796, 2-years after the transfer of the capital to Kyoto in 794. It is the general head-temple of the Shingon Buddhism and has become the world heritage since 1994. The mud wall that surrounds the precincts is restored for the first time in about 400 years. Kyoto City Archaeological Research Institute has conducted the investigation. The authors have taken charge of the geotechnical investigation particularly for the strength and structure of the rammed earth inside the wall that has remain through partial collapse and restoration. The strength characteristics in terms of the converted cohesion by using a needle penetration test apparatus that has been utilized at the archaeological sites as a non-destructive method. It is found that the rammed earth has the feature which changes with constructed ages and definite layered structure.

1 INTRODUCTION

Toji Temple was constructed in Kyoto as a governmental temple to pray the public peace in 796, 2-years after the transfer of the capital to Kyoto in 794. It is the general head-temple of the Shingon Buddhism and has become the world heritage since 1994. The five-storied pagoda that is a national heritage is a symbol of Kyoto (Figure 1). The precincts of the temple are surrounded by the roofed mud-walls as is shown in Figure 2. There is a report that the walls were burned down by a spreading fire and repaired in 1000. The walls were again destroyed according to the earthquake in 1596, after that, restored completely in 17th century followed by minor restoration such as replacement of the damaged tiles of the roof. Full-scale repair for the first time in about 400 years has been conducted associated with archaeological investigation since 2010 because of the occurrence of serious damages of the mud walls. The roofed mud walls that surround the precincts of the temple have hence been disassembled in restoration.

Figure 1. Five-storied pagoda in Toji Temple (national heritage).

Figure 2. Side view of the roofed mud wall of Toji Temple.

The cross-section of the roofed mud wall is schematically shown in Figure 3. The support pillars stand on the cornerstones to prop the tiled roofs. A rammed earth mounds exist in the trapezoidal room surrounded by these pillars between which the mortar walls are equipped. The inner earth mound is thought to be constructed as a gravity type structure so that the mud wall might not collapse by external forces while it is free from propping the heavy tiled roof.

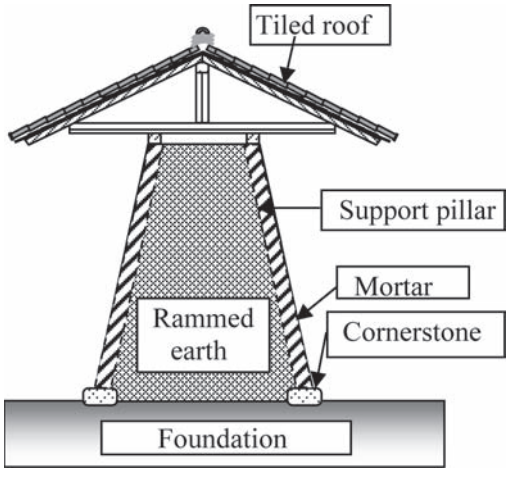

Figure 3. Schematic cross-section of the roofed mud wall of Toji Temple.

A series of in situ experiments using a needle penetration testing apparatus is carried out to know the strength properties of the rammed earth mound that is directly connected with the stability of the mud wall. Converted values of unconfined compression strength can be calculated from the index measured by this experiment without damage mostly to the target. Characteristics of the restored structure as well as the construction procedure of the rammed earth mound are clarified in the present paper based on the experimental results using the needle penetration testing apparatus.

2 RAMMED EARTH MOUND

A mud-wall is constructed by ramming the soil put into the room both sides of which are restrained with wooden boards. This method as well as the produced structure is called "Hanchiku". A "Hanchiku" structures can be found for mud-walls, tumulus mounds etc. One of the most elaborate "Hanchiku" is found at Takamatsuzuka Tumulus, Asuka Village, Japan. Figure 4 shows an example of "Hanchiku" derived from the mound of Takamatsuzuka Tumulus. The profiles of wet density were measured for all samples derived from the tumulus mound with a radio isotope densimeter. The measured results of wet density are also demonstrated in the same figure. The definite horizontal structures of thin layers caused by compaction during construction of the mound can be seen. The results of the radio isotope densimeter show that the density at the rammed surface tends to be higher whereas the measurement at the bottom plane of the individual strewed soil becomes lower due to the dispersion of compaction energy. As a result, the

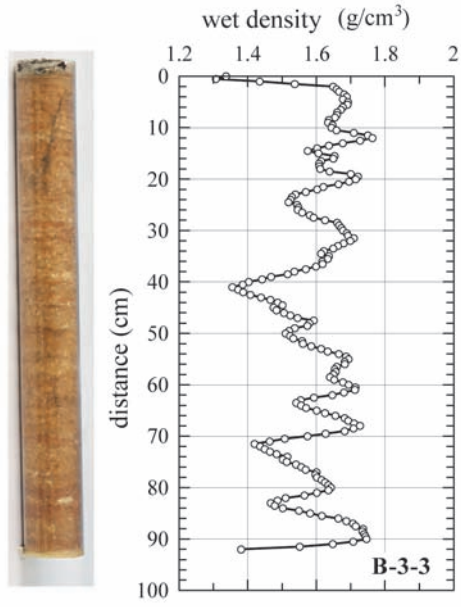

Figure 4. Sample of the rammed earth, "Hanchiku" from the mound of Takamatsuzuka Tumulus and the profile of wet density measured by a radio isotope densimeter.

density profile of the rammed earth sample exhibits a wavy profile reflecting the individual thickness of the rammed earth. From the measurement of wet density of "Han-chiku", the mound of Takamatsuzuka Tumulus was constructed by ramming the strewed soils with the thickness of 5 cm. It is natural that elaborate structure with sufficiently thin rammed stratum gives the high strength. Mimura and Yoshimura (2011) showed that the mound of Takamatsuzuka Tumulus had very high strength as an artificial soil mound rammed by human power.

3 IN SITU TEST

3.1 *Needle penetration test*

In situ tests are very useful for detecting the mechanical parameters in terms of the strength index without the effect of disturbance. Penetration tests such as the standard penetration test (SPT) and cone penetration test (CPT) are normally adopted for construction projects. Those tests are carried out associated with destruction of the ground due to penetration because the strength is generally defined as the stress at failure. In the sense, for historical relics which are forbidden to be damaged or destroyed, in situ tests which might damage the relics cannot be used. The needle penetration test

was hence adopted as the one with the least impact against tumulus mounds (Mimura and Ishizaki, 2006, Mimura and Yoshimura, 2008). A schematic structure of the needle penetration testing apparatus is shown in Figure 5. When the frontal needle is manually penetrated into the target soil, the penetration force, P, can be calculated from the deformation at the spindle caused by the compression of the spring. Once P is derived, the ratio $\Delta = P/L$ is calculated. Here, L is defined either as the penetration depth at peak penetration force or the maximum penetration depth (10 mm). On the basis of the calibration between Δ and the unconfined compression strength, q_u (kN/m^2), the in situ measurement with the needle penetration test can give the unconfined compression strength, q_u for the target soil (Yoshimura et.al., 2012).

Figure 6 shows the schematic plan view of the precincts of Toji Temple. A series of needle penetration tests is conducted at the points in the east wall shown in Figure 6. Among the trenches 4 sections are selected, namely the trench No. 9, 10, 11 and 12.

3.2 *Results and discussion*

It is necessary to introduce the relation between the Christian Era and the Japanese division of period for discussion of the mound structure that has a specific characteristics related to the period of restoration. Figure 7 shows the relation between the Christian Era and the Japanese division of period. The Japanese division of period is used on the occasion of the discussion in this section.

Figure 8 shows the contour of the converted unconfined compression strength on the north wall of the trench No. 9 based on the needle penetration testing results and the archaeological evaluation for the division of the period. First of all, the area of high strength is distributed along the circumferential part of the mud wall with the increase in strength with depth. On the contrary, the inside of the mud wall exhibits relatively small strength particularly between the elevation of 23.4 m and 24.1 m. It should be noted that the difference between the circumferential and inner part is very serious, namely more than 1 MN/m^2 of strength is measured along the circumferential part is observed while 100 kN/m^2 is found at the inner part. The clearly layered part exists above the elevation of 24.1 m overlain by the definitely weak topmost part. It is interesting that the strength

Figure 5. Schematic structure of needle penetration testing apparatus.

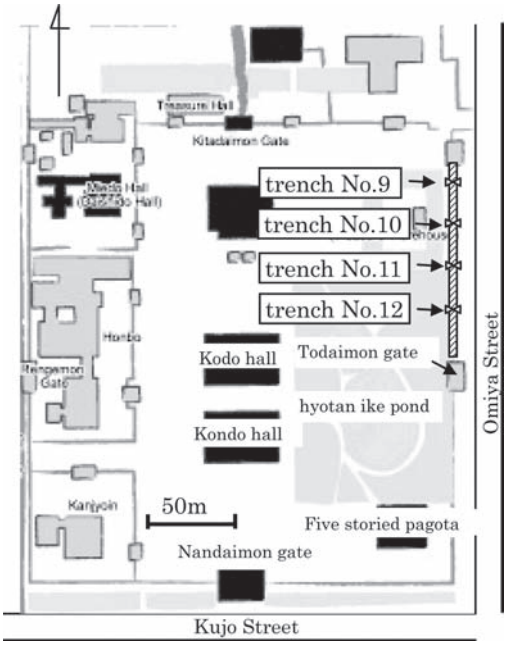

Figure 6. Schematic plan view of the precincts of Toji Temple and the location of the in situ needle penetration tests.

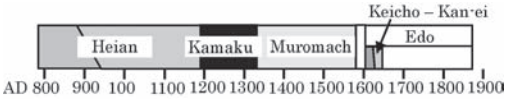

Figure 7. Relation between the Christian Era and the Japanese division of period.

characteristics coincide to the period of restoration. The mud wall above the elevation of 23.4 m is constructed for restoration in 17th century after the destruction due to 1596 Tensho Earthquake. The lower part of the restored mud wall is found to be constructed firmly. The outside is particularly built firmly to keep sufficient stability to suppress the deformation toward the outside of the mud wall. The trace of compaction is found even inside the mud wall at the elevation of 24.1 m to 25.1 m to have enough bearing capacity for the overlying earth mound. From these results, the authors guess that the outer mud wall was constructed by ramming soils under the restrained condition with boards followed by strewing soils inside. Only the required part is clearly rammed to gain sufficient strength to support the overlying earth mound. The rammed earth before the Muromachi Period (1338 to 1573) remains in chronological order below the elevation of 23.4 m.

Figure 9 shows the contour of the converted unconfined compression strength on the south

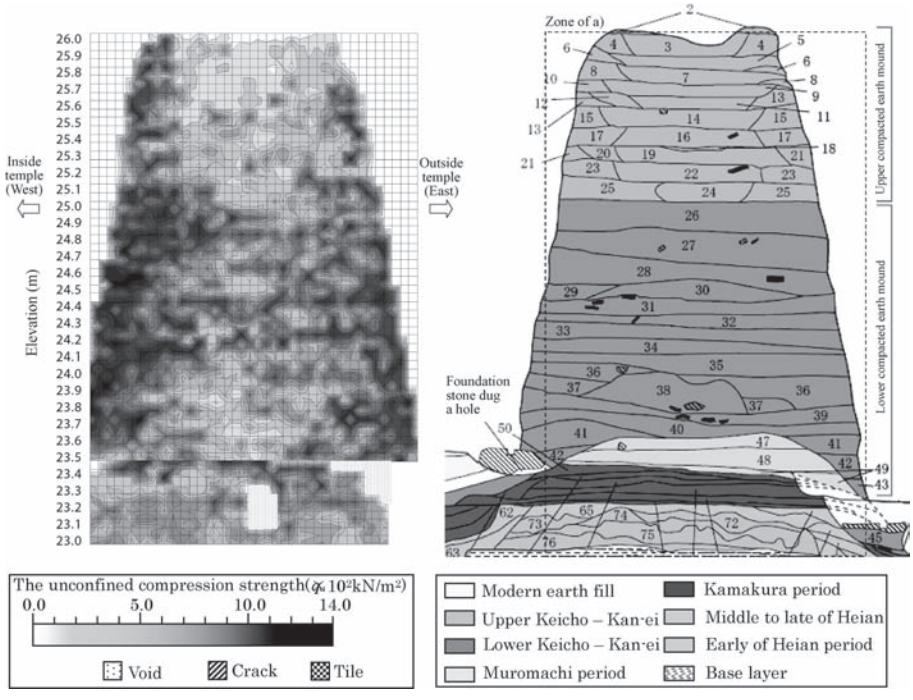

Figure 8. Distribution of the converted unconfined compression strength and the period of restoration for the north wall of the trench No. 9.

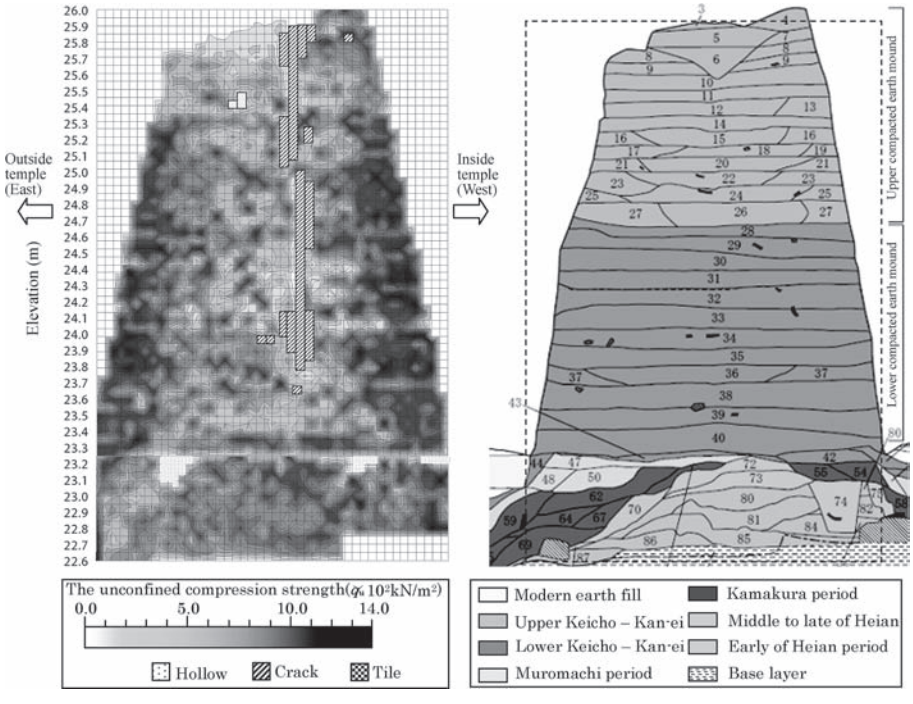

Figure 9. Distribution of the converted unconfined compression strength and the period of restoration for the south wall of the trench No. 10.

wall of the trench No. 10 based on the needle penetration testing results and the archaeological evaluation for the division of the period. The mode of strength distribution is same in the case of the trench No. 9. The inner less rammed earth is covered by the outer firmly rammed earth and the wall No. 10 and No. 9 are found to have equivalent intensity. The domain shown with the slash is crack and it is no information from the needle penetration test. The converted unconfined compression strengths in the vicinity of the crack become smaller (around 100 to 300 kN/m^2) because the structure in the vicinity of the crack is damaged. A due attention should be paid to the fact that a definite level layered structure in terms of the contour of the strength because of the ramming effect.

Figure 10 shows the contour of the converted unconfined compression strength on the south wall of the trench No. 11 based on the needle penetration testing results and the archaeological evaluation for the division of the period. The general characteristics of the strength distribution are very similar to the above-mentioned walls, namely the inner rammed earth with smaller intensity is covered by the outer firmly rammed earth. In the topmost block, intensity of the inside of the mud wall is small as what are seen on the other walls, while the level layered structure with larger intensity can be observed. We have to pay attention to that the layered part with larger intensity coincides to that is constructed with the layers with small thickness. Sufficient compaction was achieved for the thin layers without dispersion of ramming energy even if the applied rammed energy is the same. The level layered structure can also be seen in all the sections mostly. This structure has been formed caused by careful compaction work.

Figure 11 shows the contour of the converted unconfined compression strength on the north wall of the trench No. 12 based on the needle penetration testing results and the archaeological evaluation for the division of the period. The dotted domain denotes the data deficit because of the concavity due to collapse. The mode of strength distribution is very similar to that is seen in the other walls. The top part of the mud wall is found to be constructed with insufficient compaction, whereas the underlying part has a definite layered structure with relatively high intensity due to careful compaction because it has to support the overlying earth block. At the elevation of 23.2 m to 23.7 m, there remains the convex earth block evaluated to be constructed in the Muromachi Period (1338 to 1573). It is pointed out that the corresponding domain with smaller strength can be seen in the strength contour. As is same as the other walls, the strength characteristics coincide to the period of restoration.

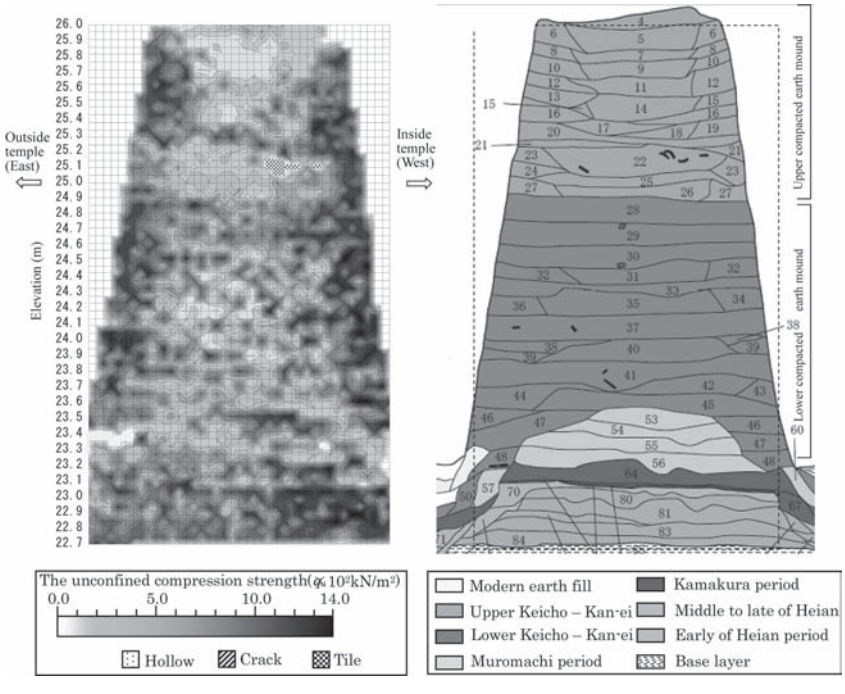

Figure 10. Distribution of the converted unconfined compression strength and the period of restoration for the south wall of the trench No. 11.

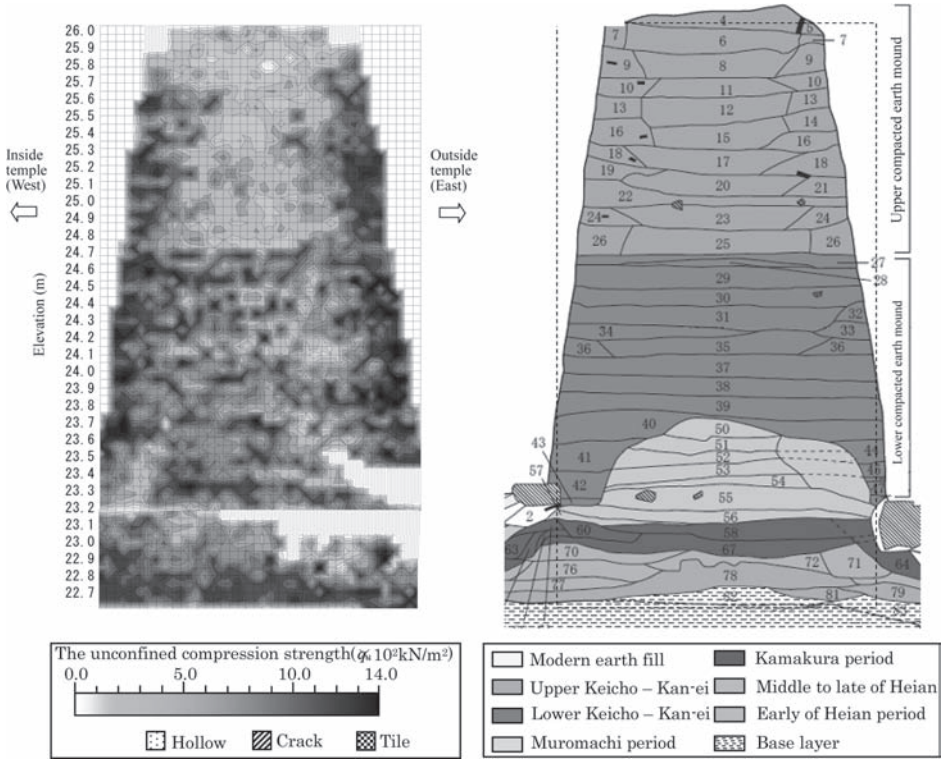

Figure 11. Distribution of the converted unconfined compression strength and the period of restoration for the north wall of the trench No. 12.

From the experimental results through a series of the needle penetration tests together with the archaeological investigation, the rammed earth mound inside the roofed mud wall of Toji Temple is found to have a definite level layered with compaction. Larger strength is observed at the circumferential part of the mound covering the weaker inner earth. It is also very interesting that the distribution of strength is found to coincide to the period of restoration.

4 CONCLUSIONS

The roofed mud wall that surrounds the precincts of Toji Temple is restored for the first time in about 400 years. A series of needle penetration tests were conducted on the different 4 cross-sections of the rammed earth mound in the roofed mud wall using the opportunity for the roofed mud wall to be disassembled for restoration. The derived strengths for the rammed mound converted from the measurement by the needle penetration tests showed very large values enough to support the earth mound as well as the superstructures. It is noteworthy that the strength of the circumferential part of the rammed earth mound close to the surface is larger than that of the inside of the mound whereas the definite layered structure with relatively high strength partly appears. On the basis of this finding together with our visual observation for the structure of the rammed earth mound, the outer part of the earth mound is conjectured to be more carefully rammed compared to the inside in order to secure higher stability.

REFERENCES

Mimura, M. & Ishizaki, T. 2006. Current status of Takamatsuzuka Tumulus and its geotechnical properties, Japanese Geotechnical Journal, 1(4), pp. 157–168 (in Japanese).

Mimura, M. & Yoshimura, M. 2008. Geotechnical properties of Takamatsuzuka Tumulus and its stability. *Proc. Int. Symp. on Conservation and Restoration of Cultural Property*, pp. 83–92.

Mimura, M. & Yoshimura, M. 2011. Geotechnical characteristics and stability of Takamatsuzuka Tumulus. *Proc. 14th Asian Regional Conf.*, *SMGE*, Paper No. 283.

Yoshimura, M., Terao. T. & Mimura, M. 2012. Geoarchaeological approach to evaluate the in-situ strength of earth mound. *Proc. 4th Central Asian Geotechnical Symp. on Geo-Engineering for Construction and Conservation of Cultural Heritage and Historical Sites.*

Geotechnical Engineering for the Preservation of Monuments and Historic Sites – Bilotta, Flora, Lirer & Viggiani (eds)
© 2013 Taylor & Francis Group, London, ISBN 978-1-138-00055-1

Spatial-temporal analysis of the subsidence in the city of Bologna

G. Modoni, G. Darini, R.L. Spacagna, M. Saroli, G. Russo & P. Croce
DICeM, Department of Civil and Mechanical Engineering, University of Cassino and Southern Lazio, Italy

ABSTRACT: The land subsidence induced by groundwater withdrawal is particularly troublesome, primarily because settlements develop with relatively fast rates but, moreover, because it often affects densely populated areas where exposure to risk is particularly high. In the second half of the last century, several cities of northern Italy suffered subsidence determined by an intensive exploitation of groundwater. One of the cases worthy of major attention is the city of Bologna, which holds a significant heritage of historical buildings and monuments and where settlement as high as 4 m have been recorded. This paper reports a study on the spatial distribution of the phenomenon and its evolution with time. The data recorded by a number of sequential topographical campaigns and, more recently, with satellite surveys, cover a period of more than 60 years (from 1943 to 2005) and an area of 272.25 km^2. The spatial analyses, performed with the support of a Geographical Information System, have revealed a progressive development of settlements with different time histories over the territory. The distribution of total and differential settlements is consistent with the characteristics of the subsoil, the groundwater withdrawal activity and the effects noticed on buildings.

1 INTRODUCTION

The deformation of the ground surface can be determined by different natural causes such as tectonic activity, self weight consolidation of recently deposited materials, chemico-physical transformations, volcanic activity, long term variation of the groundwater regime due to climatic changes. The incidence of these factors become particularly problematic when modifications occur in relatively short times so as to interact with the human activities or, moreover, when alterations of the natural equilibrium are compounded by anthropogenic causes. Rapid growth of population, intensive urbanization and industrialization are typical factors capable of determining deep transformations to the territory. The consequences of these processes may be particularly severe when they occur in areas particularly valuable from environmental or historical viewpoint, but also because the economic investment made to promote the development itself contribute to increase the exposure to the risk associated with the produced modifications.

Land subsidence is one of the most troublesome phenomenon which may occur when intensive extraction of groundwater is carried out in lowland areas. It may turn into a reduced functionality of buildings and infrastructures, which may reach collapse in the most severe situations, but also into changes of the natural or artificial water courses, retreat of coastlines, flooding and inundation.

The importance of the phenomenon on densely populated areas can be seen from the following list of studies retrieved from the literature:

- Mexico city (Marsal & Mazari 1962; Zeevaert 1983);
- Santa Clara valley (Poland 1958);
- Houston (Lockwood 1954);
- London (Wilson & Grace 1942);
- Japan cities (Yamamoto 1995).

The equilibrium becomes particularly delicate when subsidence affects areas where historical, cultural and monumental sites are settled. The historic centers of ancient Italian cities are acknowledged among the most relevant evidences of the contemporary civilization, not only for the presence of buildings and churches, representing authentic masterpieces from artistic and architectural viewpoints, but moreover because they have the fundamental role of preserving and passing to the new generations the memory and the culture of populations. In the present paper the attention has been focused on the city of Bologna, affected in the second half of the last century by extensive subsidence phenomena consequent to the exploitation of groundwater. The work, carried out by collecting the results of sequential topographical campaigns, is aimed to analyze the evolution with time and the spatial distribution of the phenomenon.

2 THE CASE STUDY

The city of Bologna, was settled before 1000 b.C in the southern part of the Po valley, at the foot of the Italian Apennines. It has always been an important

centre, before under Etruscans (Velzna), then under Celts (Bona) and Romans. In the Middle Ages it became one of the most populated European cities. Famous for hosting the oldest university in the world, founded in 1088, Bologna has one of the largest and well-preserved historical centres in Italy, also due to the restoration and conservation policy started at the end of the last century. It has always represented an important cultural and artistic mark in the Italian landscape, thanks to a homogenous combination of monuments and architectural masterpieces including medieval towers, porticos, antique buildings and churches. The Hippodamian plant of the city, founded on the original setting of the Roman "Castrum", is a noteworthy example from the urban viewpoint.

Since its first settlement, the city was affected by a long term deformation of the ground, induced by the self weight consolidation of the thick alluvial deposits of the Po valley. However, settlement proceeding with rates of few millimetres per year were not a serious cause of concern. In the decades after 1950, similarly to what happened to other cities of northern Italy (e.g. Milano, Venezia, Ravenna), a rapid deformation of the ground occurred in the town and the surrounding areas, developing in some cases with rates of dozens centimetres per year (Carminati & Martinelli 2002).

The Figure 1, which reports the ground deformation recorded all over the Emilia Romagna region during the period 1992–2000 (Provincia di Bologna 2012), shows a clear concentration of the phenomenon near the city of Bologna.

Damages produced by differential settlements were then noticed on several buildings of the historical centre. A noticeable attention was concentrated on the buildings of Zamboni street, a major urban artery located in the north-east side of the historical centre (Fig. 2). Displacements surveyed along this road between 1979 and 1983 (Alessi 1985) give the profiles evolution reported in Figure 3.

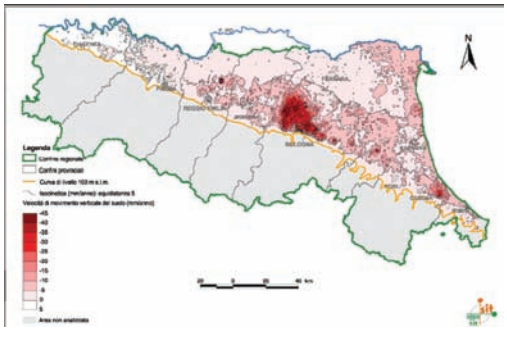

Figure 1. Map of settlements recorded during the period 1992–2000 (Provincia di Bologna 2012).

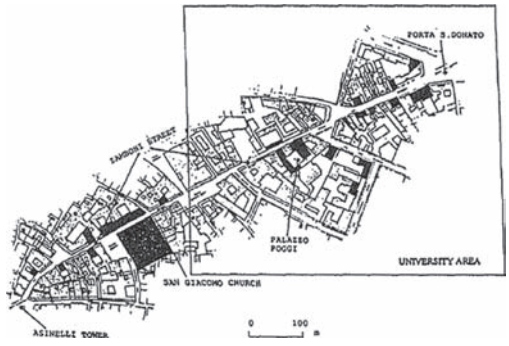

Figure 2. Map of damages buildings detected along via Zamboni (Capra & Folloni 1991).

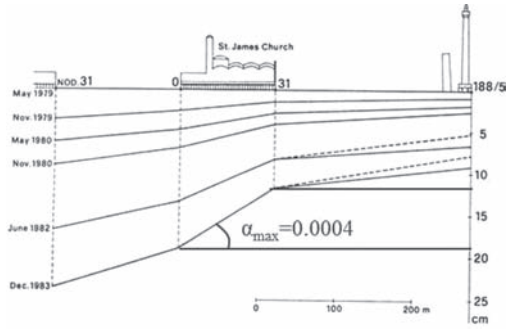

Figure 3. Settlements between the 2 towers and the University (Alessi 1985).

This new situation induced the local governmental institutions and agencies to undertake serious investigations campaigns aimed at discovering the causes of such unexpected phenomenon. Many studies have then been promoted to survey the ground deformation in the area, by means of increasingly more precise geometrical levelling networks: Pieri & Russo (1977), Pieri & Russo (1984), Pieri & Russo (1985), Arca & Beretta (1985), Folloni et al. (1996); Bondesan et al. (1997). In 2005 a campaign of satellite records was undertaken to monitor the vertical movement of the territory (Stramondo et al., 2007).

The goal of the present research is to find a mechanical explanation of the phenomenon by a quantification of the different variables (Darini et al., 2008, Modoni et al., 2012). To this aim, measures of different variables and results of numerical analyses have been merged in the same Geographical Information System, to create a comprehensive database where information of different nature can be combined.

In the present paper attention is confined to the analysis of settlements. For this investigation, an area of 272.25 km^2 has been delimited (Fig. 4), including the city centre and the upper plain area,

Figure 4. Plain view of the studied area.

Figure 5. Sea level in the lower Pliocene (Ricceri, 2007).

where a grid of points has been ideally superposed. The variables have been computed in each node of this grid by using a geostatistical interpolation method (Chilès & Delfiner 1999).

2.1 *Geological and hydrogeological layout*

From a geological viewpoint the Po Valley can be considered as the product of the foreland basin evolution process (Carminati & Martinelli 2002) formed at the link between the padanian-adriatic sector and the external portion of the thrust belt formed by the up-lifting tectonic units of the Upper Miocene—Quaternary (Bartolini et al., 1996).

After the middle Plio-Quaternary age, when the Po Valley formed the north-west extension of the Adriatic Sea (Fig. 5), a gradual eastward movement of the shoreline occurred thanks to a progressive deposition of marine sands and continental fine grained sediments. In the southern part, this sedimentation process is tightly interconnected with the erosion of the Apennines (Amorosi et al., 1996) resulting into two big alluvial fans, formed respectively by the Reno and Savena rivers and including predominantly gravelly and sandy materials.

The province of Bologna extends over an area of about 3702.5 km^2 and can be subdivided into the following distinct geomorphologic contexts:

- *flood plain*, consisting of alluvial materials transported by rivers and deposited in the plain mostly during floods;
- *foothill plain*, morphological connection between the hill and the alluvial plain, characterized by decreasing topographical gradients, and containing coarser materials deposited by the two major rivers (Reno and Savena);
- *hill*, characterized by a parallel to dendritic drainage system;
- *mountain*, consisting of geological units formed from chaotic complex of clay with the presence of sub-horizontal flaps of more resistant lithological units.

The investigated area can be substantially divided in the northern floodplain of continental origin and to southern chain of the Apennines. It is crossed by two rivers, Reno and Savena, flowing with torrential regime from the upper mountains to the plain.

The hydrogeological setting (RER and ENI-AGIP 1998) shows a recurrent superposition of permeable (aquifers) and semi-permeable or impermeable strata (aquitards). Three aquifer groups (named A, B and C) are classically distinguished, each of them consisting of an alternation of coarse and fine grained strata of relatively limited thickness and extension (Fig. 6). They are separated each other by thicker and widely extended layers of fine grained strata.

The upper aquifer group A, reaching depths of about 300 metres, is strongly dominated by the presence of the two alluvial fans of Reno and Savena rivers which are the most important groundwater supplies (Elmi 1984, Fava et al., 2005). These alluvial fans are present also in the upper part of the aquifer group B near the foot of Apennines. Coarse grained materials of marine origin can be found in the lower strata of aquifer group B and in Group C.

The groundwater circulation in the upper layers is mostly fed by the dispersion of the two rivers, while a secondary more limited contribution coming from remote sources can be found in the lowland area.

The withdrawal of water from wells is mostly achieved from the upper aquifer unit A, with a more limited portion extracted from the lower group B; the hydro-chemical characterization of groundwater shows the presence fossil water in the deeper group C.

The physical and mechanical characteristics of the subsoil in the whole area have been investigated by collecting the available results of fields and laboratory tests performed at different locations and depths.

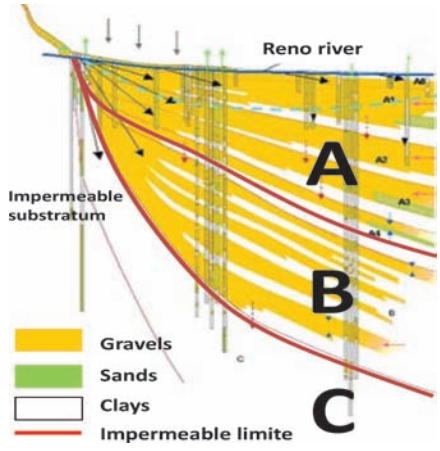

Figure 6. Longitudinal section along the Reno river (RER and ENI-AGIP 1998).

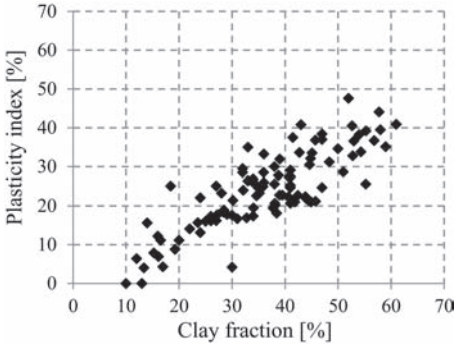

Figure 7. Activity of the finer soils. (Darini, 2007).

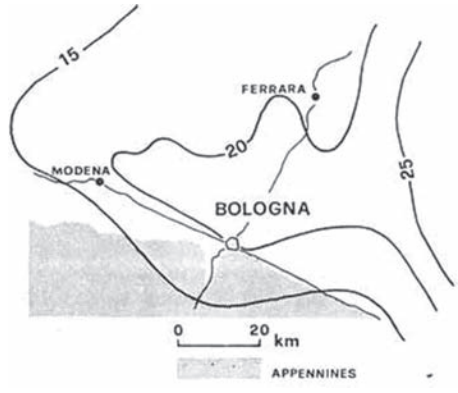

Figure 8. Contour lines (cm) of equal subsidence in the period 1897–1957 (Pieri & Russo 1984).

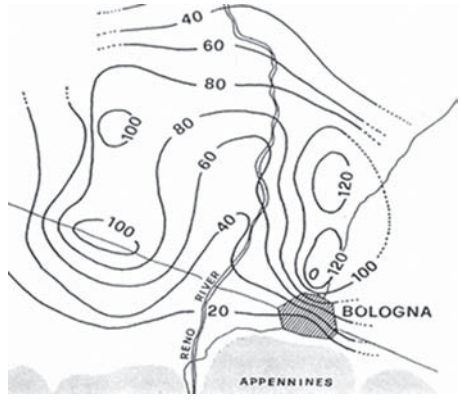

Figure 9. Contour lines (centimetres) of equal subsidence in the period 1943/1950–1970/1973 (Pieri & Russo 1984).

The grain size distributions of fine grained soils are randomly distributed over the considered area. The predominant soil fraction is made of silt (ranging between 40 and 60%) with a slightly lower content of clays (from 10 to 50%) and a small percentage of sand (from 0 to 20%). A normal activity of the clay fraction can be seen from the chart shown in Figure 7, together with a mineralogical homogeneity of the deposits. Limited differences can be seen on the dots representing samples cored at shallow (<50 m from the ground level) and deep (<300 m from g.l.) boreholes.

3 GROUND DEFORMATION

The Po Valley is known to be affected by a natural subsidence phenomenon, determined by tectonic movements and sediment compaction. In the Bologna area, this natural long-term subsidence is estimated to progress with rates ranging from 1.5 to 2 mm/year. In fact, the comparison between the levels of some benchmarks measured in the period 1897–1902 and 1947–1957 (Pieri & Russo 1977, Pieri & Russo 1984) reveal settlements ranging from 10.7 cm to 20.9 cm (Fig. 8).

Even though some works carried out in Roman times to reclaim land and reduce the swampy areas situated at the northern part of the Via Emilia (Bertoni et al., 1973) produced some limited movement of the ground surface, the subsidence in the city of Bologna area has been noticed in relatively recent times, together with the intensive exploitation of groundwater sources.

This subsidence has become increasingly pronounced after 1950, as brought out by the geometrical levelling carried out around 1943–1950 and some repetitions performed by I.G.M.I. (Italian Geographical Military Institute) in the period 1970–1973 (Fig. 9). The map derived from Pieri & Russo

(1984) show a concentration of settlements in two areas surrounding the Reno river (with settlements greater than 1 m), whereas less pronounced values are noticed along the course of the river.

Being aware of the uncertainty related to a limited number of benchmarks (measures from 1950 are available only on about 20 benchmarks), this map has been used in the present study, by digitalizing the curves in the Geographical Information System, to extend the analysis of subsidence to the period 1943–1973.

One of the consulted database (Fig. 10) is released by the *Autorità di Bacino del Fiume Reno*, which contains information for the period 1950–1997 and represents the first attempt to perform an extensive monitoring the subsidence phenomenon in *Emilia Romagna*. In the area of Bologna this database gathers about 200 benchmark coming from three different geometrical leveling networks previously installed by various public authorities (*Autorità di Bacino del fiume Reno, Istituto Geografico Militare Italiano, Ministry of Public Works*).

The second database (Fig. 11) was acquired by *ARPA Emilia Romagna*, in cooperation with the municipality of Bologna, and provides the localization of the 527 benchmarks and subsidence of the ground, relative to the period between 1983 and 1999. During this period more comprehensive and refined analysis could be performed on the investigated area thanks to a much higher spatial density of this network compared with the previous one (in the city center benchmarks were located at mutual distances lower than 250 m).

Subsequently, after the development of the differential interferometry synthetic aperture radar techniques DInSAR (Hanssen, 2001), a more detailed monitoring was performed for the period 1999–2005 (ARPA Emilia Romagna). It is however pointed out that a relatively limited number of benchmarks (approximately 118 mostly located along the Via Emilia and A13 motorway) were necessary to calibrate the DInSAR measurement (Fig. 12).

Figure 10. Monitoring network of the *Autorità di Bacino Reno* (period 1950–1997).

Figure 11. Monitoring network of the *ARPA Emilia Romagna* (period 1983–1999).

Figure 12. Network used by the *ARPA Emilia Romagna* to calibrate DInSAR measurement (2005).

3.1 *Analysis of settlements*

All previous information have been combined in the Geographical Information System to compute the ground level positions and the progressive development of settlements on the studied area.

The interpolation over the studied area of the measures taken at singular points has been accomplished by performing a series of geostatistical analysis. By this method, the spatial variability of the studied quantities is evaluated considering the latter as "regionalized variables", i.e. random realizations of a space function (Matheron 1971). An experimental variogram is first plotted where the squared increments between each couple of measures are related to the distances (h) between sampling points (Fig. 13) A fitting curve (theoretical variogram) is then chosen among various possible functions. The estimate of values in unmonitored positions

is computed with a linear interpolator (Kriging), assigning a weight to each of the measured values function of the theoretical variogram. This function is found minimizing the variance of the estimation error.

Setting a zero for subsidence in the period before 1943–1950, a sequence of map has been created to reproduce with contour lines the settlements obtained in the different periods (Fig. 14).

A similar pattern of subsidence is repetitively shown by all plots with larger concentrations of settlements occurring around the alluvial fan of the Reno river.

Explanation to this result can be given considering that the largest part of groundwater is extracted for civil purpose in the upper part of the Reno river (Vassena, 2003). Interception of such a large amount of water coming from the mountains prevents the feeding of water bearing strata in the lower plain and causes a significant lowering of the hydraulic heads. Although the drop of water head is maximum in the alluvial fan, where the most active wells are located, the subsidence is not particularly high in this zone due to the predominance of coarse grained materials in the subsoil strata.

The maximum observed settlements occur in the surrounding zone, where thicker strata of fine grained soils are present. Finally, the development of settlement with time for two points representative of different locations (Fig. 14) is plotted in Figure 15.

Both curves show the maximum rate in the period between 1970 and 1980, i.e. when groundwater extraction reached its peak. However, it is worth observing that the curve representative of the situation in the city centre shows an almost stable phenomenon. On the contrary, a further increase of settlements must be expected in the surrounding area, being the rates computed in 2005 still significantly high.

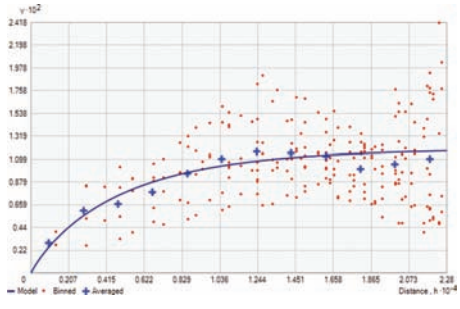

Figure 13. Experimental and theoretical variograms for settlements in the period (1983–1987).

3.2 *Damage on buildings*

As shown by literature, damage of buildings, ranging from the formation of small fissures to complete collapse, can be correlated with the development of angular distortion (e.g. Skempton & Mc Donald 1956) or tensile strain (Burland & Wroth 1974). Limiting values depends on the type of structure (open framed structures may tolerate higher defor-

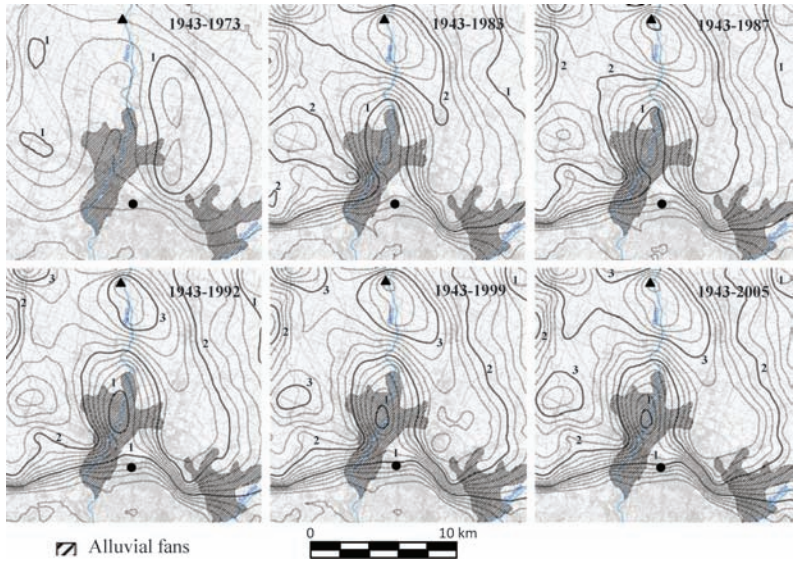

Figure 14. Settlements cumulated in different periods from 1943.

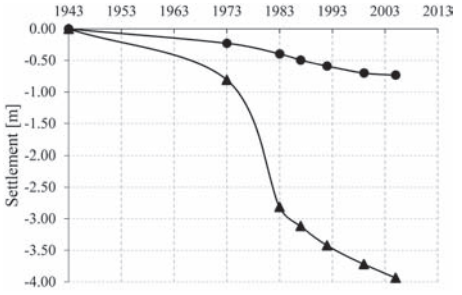

Figure 15. Settlements time histories for two positions of the city and surrounding area.

mation compared with load bearing walls) and on the deformation mode (sagging or hogging). Irrespective of the assumed criterion, angular distortion ranging between 0.5 and $1 * 10^{-3}$. have been observed to produce cracks in continuous walls (Sowers 1962; Burland & Wroth 1974).

The angular distortion is correctly computed as the ratio between maximum differential settlement and distance of two contiguous points, provided rigid tilting of the structure is discounted. Being the decoupling of tilting and distortion meaningless at the very large scale of the present work, rotation has been herein assumed as indicator of the damage on buildings.

The analysis has been restricted to the historical centre of the city, superposing an ideal grid of points (nodes are positioned at a mutual distance $\Delta = 60$ m). and computing settlements at each node (i, j) with the previously described geostatistical method. Rotation in each node $\alpha_{i,j}$ has been then computed with the following relation:

$$\alpha_{i,j} = \sqrt{\left(\frac{w_{i+1,j} - w_{i-1,j}}{2\Delta}\right)^2 + \left(\frac{w_{i,j+1} - w_{i,j-1}}{2\Delta}\right)^2} \qquad (1)$$

Calculation of these values over the studied area (Fig. 16a) show that the largest rotations occur in the central part of the city. Focusing the attention on Zamboni street, the road where noticeable cracks were recorded (Figs. 2 and 3), it is worth noting that the curvature (either concavity or convexity) of the deformed ground (given by the gradient of rotation) is maximum along the direction of this road. The maximum rotation computed in this area for the period 1943–2005 is equal to about 0.002, which five times larger than the one (0.0004) calculated by Alessi (1985) for the period May 1979–Dec 1983 (Fig. 3). The settlement profiles traced along this road with the present analysis (Fig. 16b) are fully consistent with the profiles (reported in the same plot with a shaded area) derived by Alessi (1985).

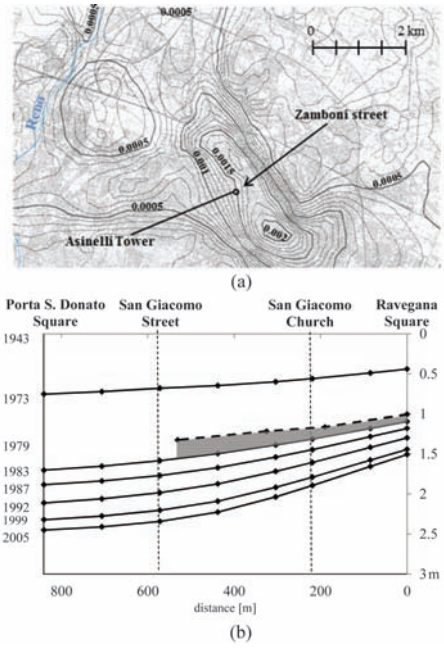

Figure 16. Map of rotations computed for the period 1943–2005 in the historical centre of Bologna (a) and settlement profiles along Zamboni road (b).

4 CONCLUSION

The settlements induced in the area of Bologna by an intensive groundwater extraction carried out in the second part of the last century have been quantified by combining information reported in the literature with results of topographical investigations and satellite records. The patterns reconstructed for different time lengths (from 1943 to 2005) show a recurrent situation with larger settlements (up to a maximum cumulated values of 4 m) in the area surrounding the alluvial fan of Reno river, i.e. the countryside part of the city. Nevertheless, high cumulated settlements have been recorded in the central part of the city. Additionally, relative large rotations have been computed in this area consistently with the damages observed on the buildings of Zamboni street. The rotation computed for the period 1943–2005 is about five time larger than the one observed by previous authors during the period 1979–1983. Luckily, the evolution of subsidence with time shows an almost stable condition for the historical centre, while relative fast rates are observed in the outer part of the city. It is finally worth considering that the computed distribution of settlement is fully consistent with the causes determining the phenomenon combined with the mechanical characteristics of the subsoil. In fact, the largest observed settlements

have been recorded where the water table lowering induced by groundwater extraction matches with the compressibility of fine grained materials.

REFERENCES

Alessi, R. 1985. La subsidenza nel centro storico della città di Bologna. Il grado di dissesto dei fabbricati nella zona di via Zamboni. *Inarcos, n. 456.* Bologna (Italy).

Amorosi, A., Farina, M., Severi, P., Preti, D., Caporale, L., Di Dio, G. 1996. Genetically related alluvial deposits across active fault zones: an example of alluvial fan-terrace correlation from the upper quaternari of the southern Po Basin, Italy, *Sedimentary Geology, 102,* 275–295.

Arca, S., Beretta, G.P. 1985. Prima sintesi geodetico-geologica sui movimenti verticali del suolo nell'Italia Settentrionale (1897–1957). *Bollettino di Geodesia e scienze affini, n. 2.*

Bartolini, C., Caputo, R., Pieri, M. 1996. Pliocene–Quaternary sedimentation in the Northern Apennine Foredeep and related denudation, *Geological Magazine, 133(3),* 255–273.

Bertoni, W., Carbognin, L., Gatto, P., Mozzi, G. 1973. Note interpretative preliminari sulle cause della subsidenza in atto a Ravenna. *C.N.R., Lab. per lo Studio della Dinamica delle Grandi Masse, Tech. Rep. 65*, Venezia.

Bondesan, M., Gatti, M., Russo, P. 1997. Movimenti verticali del suolo nella Pianura Padana orientale desumibili dai dati I.G.M. fino a tutto il 1990. *Bollettino di Geodesia e scienze affini, n. 2.*

Burland, J.B., Wroth, C.P. 1974. Settlement of buildings and associated damage. *Proc. of Conf. on Settlement of Structures*, Cambridge, UK, 1974, 611–654.

Capra, A., Folloni, G. 1991. Subsidence Controls in the Town of Bologna. *Proceedings of the Fourth International Symposium on Land Subsidence.* IAHS Publ. no. 200.

Carminati, E., Martinelli, G. 2002. Subsidence rates in the Po Plain, northern Italy: the relative impact of natural and anthropogenic causation. *Engineering Geology, 66,* 241–255.

Chilès, J.P., Delfiner, P. 1999. Geostatistics: Modeling Spatial Uncertainty. Wiley, New York.

Darini, G. 2007. Land subsidence due to groundwater withdrawal: the case of Bologna. *PhD Thesis. Università degli Studi di Cassino.*

Darini, G., Modoni, G., Saroli, M., Croce, P. 2008. Land subsidence induced by groundwater extraction: the case of Bologna, *Proc. of IEMSs 2008: International Congress on Environmental Modelling and Software,* Barcelona 10–13 Luglio 2008, pp. 1386–1393, ISBN 978-84-7653-074-0.

Elmi, C., Bergonzoni, A., Massa, T., Montaletti, V., Barattella, P.L., Ronchi, A. 1984. Il territorio di pianura del Comune di Bologna: aspetti geologici e geotecnica, *Giornale di Geologia, 46(2),* 127–152.

Folloni, G., Radiconi, F., Russo, P. 1996. La subsidenza del territorio bolognese dal 1983 al 1983. *Inarcos, n. 571.* Bologna (Italy).

Fava, A., Farina, M., Marcaccio, M. 2005. Le caratteristiche degli acquiferi della Regione Emilia-Romagna. *Report 2003. RER-APAT.* Grafiche Pioppi Settembre 2005.

Hanssen, R., 2001. Radar Interferometry. Data Interpretation and Error Analysis, Kluwer Academic Publishers.

Lockwood, M.G. 1954. Ground subsides in Houston areas, *Civ. Eng.* 24, No. 6, pp. 48–50.

Matheron, G. 1971. The Theory of Regionalized Variables and Its Application—Spatial Variabilities of Soil and Landforms. *Fontainebleau, Les Cahiers du Centre de Morphologie Mathematique 8.*

Marsal, R.J., Mazari M. 1962. El subsuelo de la Ciudad de Mexico, The subsoil of Mexico city, *Universidad Autonoma de Mexico, Facultad de Ingenieria*, 2nd ed. p. 614.

Modoni, G., Darini, G., Spacagna, R.L., Saroli, M., Russo, G., Croce, P. 2012. Quantitative interpretation of the land subsidence induced by groundwater withdrawal. *Engineering Geology*, submitted for publication.

Pieri, L., Russo, P. 1977. Studio del fenomeno di abbassamento del suolo in atto nella zona di Bologna. *Bollettino di Geodesia e scienze affini, n. 3.*

Pieri, L., Russo, P. 1984. The survey of soil vertical movements in the region of Bologna. *Proceedings of the Third International Symposium on Land Subsidence.* Venezia (Italy).

Pieri, L., Russo, P. 1985. Situazione attuale delle ricerche sull'abbassamento del suolo nel territorio bolognese. *Inarcos, 456*.

Poland, J.F. (1958). Land subsidence due to groundwater development, *ASCE Journal of Irrigation and Drainage Div*., 84, paper 1774, p. 11.

Provincia di Bologna, 2012. http://www.provincia.bologna.it/ambiente/Engine/RAServePG.php/P/256511030707/T/Subsidenza

Regione Emilia Romagna and ENI-AGIP. 1998. Riserve idriche sotterranee della Regione Emilia-Romagna. *S.EL.CA. (Firenze)*.

Ricceri, G. 2007. Il futuro di Venezia tra subsidenza ed eustatismo. *Rivista Italiana di Geotecnica, 3.* Patron Editore (Bo).

Skempton, A.W., Mac Donald, D.H. The allowable settlements of buildings, *ICE Proceedings: Engineering Divisions*, Volume 5, Issue 6, 01 December 1956, pp. 727–768.

Sowers, G.F. 1962. Shallow Foundations. *Foundation Engineering, G.A. Leonards (ed.), McGraw-Hill Book Co., New York, NY, USA* pp. 525–632.

Stramondo, S., Saroli, M., Tolomei, C., Moro, M., Doumaz, F., Pesci, A., Loddo, F., Baldi, P., Boschi, E. 2007. Surface movements in Bologna (Po Plain—Italy) detected by multitemporal DInSAR. *Remote Sensing of Environment*, XX.

Vassena, C. 2003, Sviluppo e applicazione di modelli di flusso delle acque sotterranee nella conoide alluvionale del fiume Reno*, PhD Thesis*, *Università degli Studi di Milano.*

Wilson, G., Grace, H. 1942*, The settlement of London due to* underdrainage of the London clay, *Journ. Inst. Civil Engrs*., London, 19, pp. 100–127.

Yamamoto, S. 1995. Recent trend of land subsidence in Japan. In Land Subsidence, (Eds. Barends F.B.J., Brouwer F.J.J. and Schroder F.H.), *IAHS, Publication* n. 234, pp. 487–492.

Zeevaert, L. 1983. Foundation Engineering for difficult subsoil conditions. *Van Nostrand Reinhold Company Inc*. (USA).

Geotechnical Engineering for the Preservation of Monuments and Historic Sites – Bilotta, Flora, Lirer & Viggiani (eds)
© 2013 Taylor & Francis Group, London, ISBN 978-1-138-00055-1

Repair works at Saint Claire Convent in Chinchón (Madrid, Spain)

P.R. Monteverde & J.M. Avila-Jalvo
UPM, Universidad Politécnica de Madrid, Spain

ABSTRACT: The Chinchón Saint Claire Convent is a Count Foundation of 1653. Some repair works were made around 1965, but some important cracks were remained. This paper describes the soil study made to know, its properties, the reason of these movements and its consequences to the convent and the repair works done. A high swelling phenomenon has been detected. The convent is on a high plasticity clayey soil with soil sandy insertions. The soil water has a high content of sulphates. In addition, some sewer system piping was broken around the convent and frequently flooded the convent crypt. A micropiles underpinning was made and the water leaked has lead to the sewer system to avoid the crypt flooding, also a drainage system has been made and the ground around the church has been paved.

1 INTRODUCTION

The Chinchón Saint Claire Convent is a Count Foundation of 1653, but the works was beginning in 1597 with a plan of Nicolás de Vergara, the Young, Master Builder of Toledo Cathedral. In this building the best stone masters of the El Escorial Convent worked. The construction style is a Herrera style.

The building has a one nave church, with a barrel vault; the convent has also an interesting cloister. Below the transept church, a crypt exists. The external walls are built with a type of stone and brick masonry, known as Toledan bond. In the Figure 1 can see the construction type.

The convent is found in the village entrance, is an isolated building, although near the apse it exits a street that connects with the city. The urban sewer system is very old and has some leaks.

Some repair works was made around 1965, as some braces in the main vault, but some important cracks were remained, overall in the church external side and also the crypt, sited bellow the apse. In 2008, a new work phase was done to complete the works intervention. This paper describes this intervention from 2008 to now.

A detail of the walls state is possible see in the Fig. 2, some cracks and movements are found in the dome walls.

In the Figure 3 can see the church plant and some points of vertical movement control and

Figure 1. Lateral church Façade of Saint Claire convent. The walls are a type of stone and brick masonry.

Figure 2. Dome walls state. It can see some cracks and their deformation.

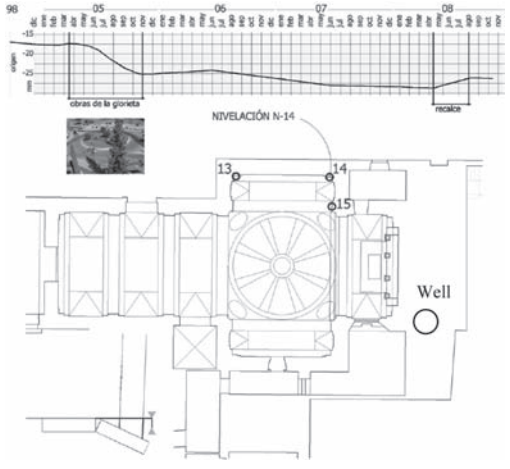

Figure 3. The church plant. The numbers are the points of the movement control and their graphic.

their graphic. From 2004, December until 2008, November, the active movements had been measured. The movement was active, nevertheless the braces placed in 1965. In the graphic can see the maximum movements happen during an urban works made near the convent entrance access (year 05, on left in the graphic) and also during the micropiles underpinning works (year 08, on right in the graphic) (Figure 3). The controlled points are sited in the external wall church.

2 GEOTECHNIQUE STUDY

A soil study was made to know its properties and the performance reason, and its relation with the building cracks to define the adequate repair works. Eight test drilling and four dynamic penetration test were made. In addition some soil moisture specimens were taken to look for the water leaks. Some samples had been taken to make different test, also had been made some SPT test.

The soil is clayey, overall high plasticity clay, with a little stratum of sandy clay and different coloration clays with sandy intercalation. The soil description is:

2.1 *Anthrop filler soil*

This stratum has not any resistance and its thickness is changeable, from 0 to 1,70 m, it only appears in four of eight bores. Its moisture content is done between 10% and 44,4%. The maxima values are found in the 8th bore, next to the convent point of water leak problem, sited near of the well (Figure 3).

2.2 *Sandy clay soil*

A sandy high plasticity clay soil of a variable thickness from 1 to 4,5 m is found. Its swelling pressure is 100 kN/m^2; it is a little value to affect the main foundation walls but it is enough to affect the slab pavement support. Only a part of the convent foundation is sited on it. The more representative values are found in the Table 1. The mean characteristic undrained shear strength, c_u, is 120 kN/m^2.

2.3 *Greenish clay soil*

Bellow a greenish high plasticity clay soil with whitish intercalations exists. This stratum is found from 3 to 5 m deep. Its thickness oscillates between 5 and 7 m. The major swelling pressure is 267 kN/m^2 in a sample obtained to 3 m deep. The foundation of the convent zone more damaged is sited on this stratum or on its influence zone. This swelling value affects to the foundation walls and the crypt walls, also to the micropiles underpinning. The mean undrained shear strength is 116 kN/m^2. The more representative values are found in the Table 2. Also, the moisture oscillation is important, as it can see with de rate w_{nat}/LP (Table 2) with values from 0,49 to 1,14.

2.4 *Clayey sand with gravel soil*

The clayey sand with gravel soil is a stratum intercalates between two strata of clays and drives the

Table 1. Sandy clay soil characteristics values.

	N_{SPT}	c_u kN/m^2	w_{nat} %	Ph kN/m^2	LL %	LP %	IP %	w_{nat}/LP
Max	43	146	30		67	34	33	1,23
Min	12	105	13		45	23	22	0,63
Med	29	120	23	100	55	27	27	0,843

Table 2. Greenish high plasticity clay soil with whitish intercalations characteristic values.

	N_{SPT}	c_u kN/m^2	γ_d kN/m^3	Ph kN/m^2	ϕ' °	c' kN/m^2
Max	40	135	18,9	267		
Min	10	78	13,4	10		
Med	25	116	15,6	50,1	27	26

	w_{nat} %	LL %	LP %	IP %	w_{nat}/LP
Max	51	90	45	49	1,14
Min	10	28	19	9	0,49
Med	27	59	30	29	0,90

Table 3. The sandy clay with gravel soil characteristics values.

	N_{SPT}	w_{nat} %	LL %	LP %	IP %
Max	55	28			
Min	38	8			
Med	45	15	46	26	20

Table 4. Orangey to brownish clay soil characteristic values.

	N_{SPT}	c_u kN/m^2	w_{nat} %	γ_d kN/m^3	Ph kN/m^2
Max		155	37	16,5	
Min			22	14,9	
Med	19	145	26	15,7	92

water. It is found in a variable deep between 7 and 15 m. The micropiles must support bellow this stratum because of the water movement. The more representative values are found in the Table 3. The water level is found at 7,40 m, but next the water escape area the water level is 5,25 m, driving by this stratum.

2.5 *Orangey to brownish clay soil*

An Orangey to brownish high plasticity clay soil is the deepest stratum obtained; it does not found in everything drillings. The more representative values are found in the Table 4.

In short, a high swelling phenomenon has been detected. The swelling pressure oscillates between 10 and 267 kN/m^2, the largest swelling values are found in the foundation influence zone. The high value specimen is obtained to 3 m deep. The swelling active zone is increased to the water leaks.

The foundation convent is on a high plasticity clayey soil with soil sandy insertions. The soil water has a high content of sulphates. In addition, the soil moisture is higher than normal because there are some water leaks. The sewer system piping was broken around the convent and frequently flooded the crypt.

3 MICROPILES UNDERPINNING

A micropiles underpinning solution has been considerer to repair the convent by the swelling phenomenon effect. The micropiles pass through the high plasticity clay with a plastic cover to protect the micropiles of the swelling soil movements. The plastic cover is found in the 3–4 first meters where it is found the sandy clay soil and the greenish clay soil, the swelling active zone. In the Figure 4 can see the micropiles situation.

Only the north wall is underpinning because is the more damage and joints exist. It is the only wall with an appreciated lean and the main cracks are found here. The other convent walls have less swelling problems because the water leaks are driven to the north wall by the soil strata and the active zone is deeper here. Also, the rest of the convent building helps to the wall stability. By contrast the north wall is an external wall without bracing help.

The micropiles have 18 meters long to arrive just the orangey to brownish clay soil, due to the water quantity obtained in the clay sandy with gravel soil stratum.

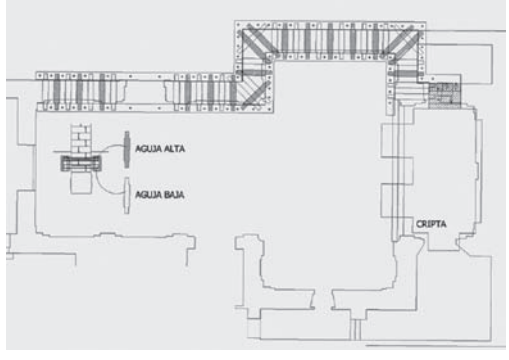

Figure 4. The church plant with the north wall area of micropiles underpinning.

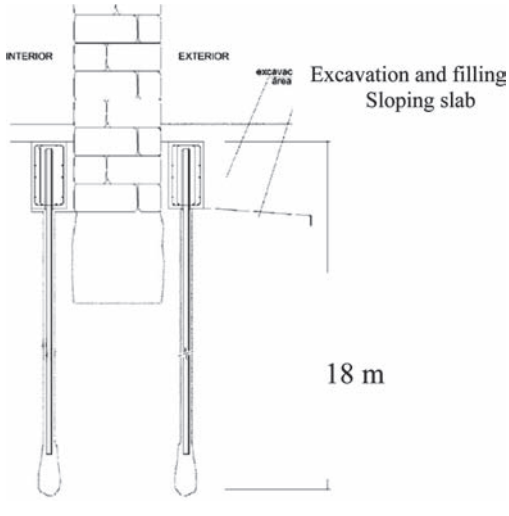

Figure 5. Micropiles placed in both sides of the foundation wall.

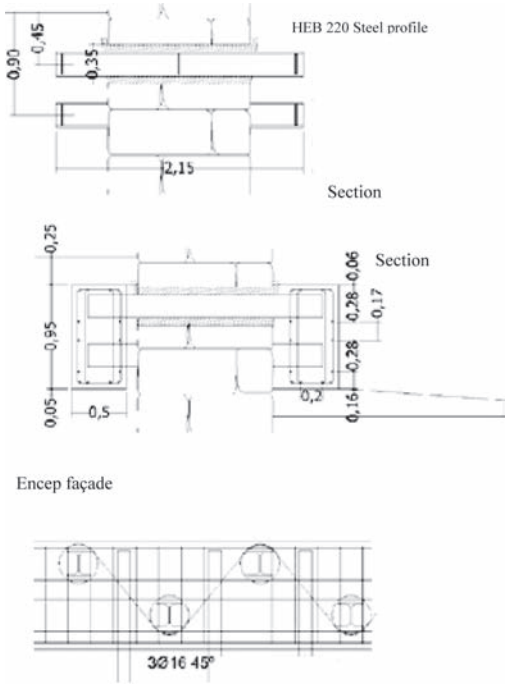

Figure 6. Detail of the HEB 220 steel profiles. It can see their position and the reinforced beam to connect with de ancient foundation. The concrete beams are C25.

The connection between the ancient foundation and micropiles is realized by a beam with 1,25 meters edge; the connection long is 0,85 m. Also, it exist a sloping slab to avoid the water entrance to foundation. The plan design can see in the Figure 5.

To connect the ancient foundation wall to the mi-cropiles, both lateral beams are united by two HEB 220 steel profiles, oxide protected, and sited alternately on the top and in the bottom. In the Figures 6 and 7, it is possible see a detail. The drills are 350 mm. The concrete is C50 and the liquid consistency with sulphate resistant additive.

When the beam has been concreted, it exits a foundation reinforced working jointly.

4 URBAN SEWER SYSTEM EFFECT

In the convent east side, it is found an entrance across a courtyard, there it exists a well. Its level water is around 5,25 m deep, only a little bellow the foundation crypt. In the Figure 3 can see the well position.

The street level, in this side, is higher up than the convent approximately 4 m. The urban sewer system leaks water, it is found in the upper street.

Figure 7. The HEB 220 steel profiles sited to connect the micropiles and the foundation wall.

When it had a water leak, the convent crypt was flooded. The water escape increases the high swelling phenomenon and its effect catches up the walls and crypt foundation. The walls are cracked just the upper side.

The effect is greater in the church north side because the slope of soil strata drives the water towards that side. In addition it is an exterior side without pavement to protect from the rain water. Also that wall has an appreciated lean, due to the wall movements. The rest of the convent is situated in the south and west sides protecting the church from the water entrance and the instability movements. The micropiles underpinning is only realized in that side for that reason, as it can see in the Figure 4.

A drainage system was done to collect the water leaks before it can get up the crypt.

5 OTHER WORKS

After the underpinning intervention, the following works have been realized:

- A new exterior pave of lime concrete to avoid the rain water reaches the walls foundation.
- Also a new interior *pave* of marble and limestone.
- The cracks repair, *cleanliness* and restructure of damaged walls and vaults. The main cracks are sited in the vaults and in the top of the walls. The roof and the walls dome were demolished to work up the vaults (Figures 2, 8 to 11).
- The lateral walls dome demolition and its reconstruction.
- The structure roof *and* its tiles cover repair.

The initial and final state can see in the Figures 8, and 12.

Figure 8. Initial state. It can see the convent walls state and the dome cracks.

Figure 9. Initial state. It can see a detail of the convent dome walls state and its cracks.

Figure 10. Initial state. It can see a detail of the internal dome wall.

Figure 11. Initial state. It can see the vault state.

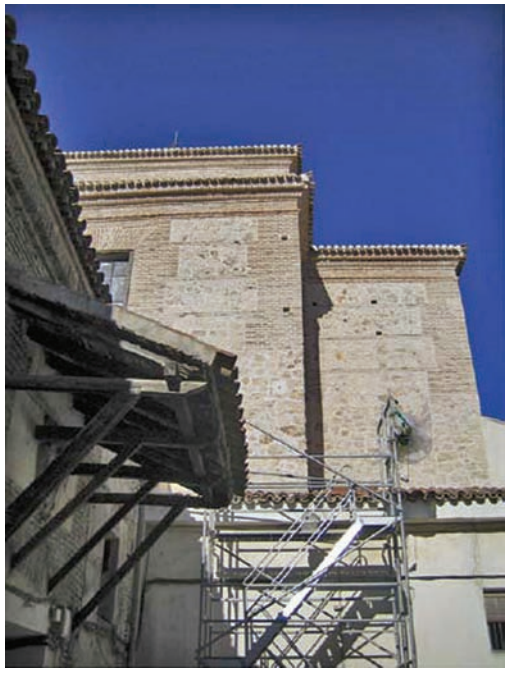

Figure 12. Final state. It can see the wall and dome repaired.

6 CONCLUSION

The Saint Claire Convent is a Foundation of 1653. Its walls have some active cracks although it had an intervention around 1965.

The convent is on a high plasticity clayey soil with sandy soil insertions. It has a swelling pressure between 100 and 267 kN/m^2. The last value is high to move the church walls, specially the north wall. Also, the soil water has a high content of sulphate and the sewer system piping was broken around the convent and frequently flooded the crypt.

A micropiles underpinning solution has been considerer to repair the convent by the swelling phenomena effect.

The micropiles pass through the high plasticity clay with a plastic cover to protect the micropiles. The plastic cover is found in the 3–4 first meters.

To connect the ancient foundation wall to micropiles, both lateral beams are united by two HEB 220 steel profiles.

Also, a drainage system was done to collect the water leaks.

REFERENCE

Avila, J.M. 2006. Proyecto de Rehabilitación del Convento de las Clarisas de Chinchón (Madrid).

Geotechnical Engineering for the Preservation of Monuments and Historic Sites – Bilotta, Flora, Lirer & Viggiani (eds)
© 2013 Taylor & Francis Group, London, ISBN 978-1-138-00055-1

Groundwater management during excavations of S. Pasquale station in Naples

L. Mormone
ASTALDI s.p.a., Rome, Italy

G. Falconio
IGA s.r.l., Naples, Italy

A. Mandolini
Department of Civil Engineering, Design, Architecture and Environment, Second University of Naples, Italy

ABSTRACT: The path of underground Line 6 runs beneath Riviera di Chiaia, the old waterfront of Naples. Once lapped by the sea, this land was reclaimed in the nineteenth century to create the Villa Comunale garden, where many remarkable and notable buildings dating back to the seventeenth century are located, overlooking the Gulf of Naples from Castel dell'Ovo to the Posillipo hill. Design and construction of the S. Pasquale station, strategically located in the heart of the main shopping area of Via V. Colonna, Via de' Mille, and Via Filangieri and in front of Pignatelli Museum, focused on major geotechnical problems: the presence of groundwater controlled by the sea; the particular geological site conditions with sandy and alluvial deposits and significantly fractured underlying tuff; the preservation of the historical buildings which cannot sustain even small displacements. This paper illustrates the main phases of the project: preliminary experiments of full scale pumping and "dewatering"; setting up the soil and excavation model for the best accuracy and predictions of soil response; design of an enhanced pumping and control system to conform to all the specific design requirements; model recalibration and parameter verification by back analysis of data collected from monitoring. The excavation of the S. Pasquale station was supported by a reliable, cost-effective and integrated devices groundwater monitoring system with a "holistic approach", capable not only of recording and remotely transmitting the data of all the measured parameters, but also of optimizing their real-time processing and giving decision-makers a constantly clear overview of the ongoing process, in order to promptly evaluate any relevant risk and the most appropriate remedial actions to be undertaken. The paper also describes the dedicated SCADA (Supervisory Control And Data Acquisition) system that was adopted and proved to be a precious tool for data integration, analysis and the continuative management of soil groundwater, in order to guarantee the safety of valuable buildings and of the people involved, and to avoid local collapse during excavations.

1 INTRODUCTION

1.1 *S. Pasquale station*

Naples Underground Line 6 was conceived in the late 1990s as a project to convert into a new light underground line the old unfinished Fast Cable Line (LTR), that was to connect the district of Fuorigrotta and Chiaia to Ponticelli on the occasion of the "Italy 1990" FIFA World Cup. This connection has been fully redesigned and re-engineered according to the most modern underground systems; the existing works have been completely transformed and the three partially executed stops have been converted into actual stations, with access halls and security checkpoints. The route, which is now totally underground, has also been completely changed and adapted to the users' new demands and the city's mobility needs; it has thus become an integral and fundamental part of the municipal transportation plan. Line 6 travels from Piazzale Tecchio to Piazza Municipio for a total of 5.6 km, with four stations (Mostra, Augusto, Lala, Mergellina) today in operation, and another four stations (Arco Mirelli, S. Pasquale, Chiaia, Municipio) and 3.3 km of TBM tunnel to be completed. The Mergellina—Municipio section currently under construction is without a doubt the most challenging part from an engineering standpoint, since it stretches across an urban network (figure 1) characterized by valuable historical buildings, mainly in groundwater and loose soils.

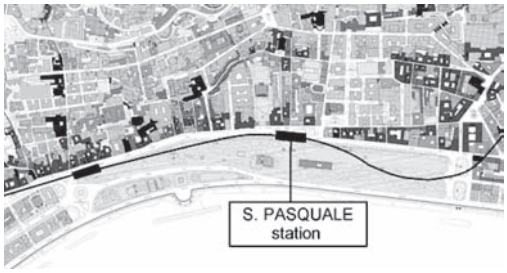

Figure 1. The urban fabric of Riviera di Chiaia interfering with Naples underground Line 6.

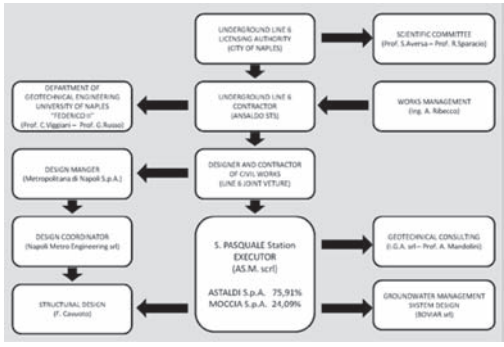

Figure 2. Key players involved in the design and construction of the S. Pasquale station.

In this section, proceeding from Torretta towards Via S. Pasquale, a series of very interesting buildings stand out, such as *Palazzo Mirelli di Teora, Palazzo Guevara di Bovino, the Church of San Giuseppe a Chiaia, Palazzo Battiloro, Palazzo Caravita di Sirignano (1535), Villa Acton* (now home to the Diego Aragona Pignatelli Cortés museum), *Palazzo Ruffo della Scaletta* and *Palazzo Serracapriola.* Continuing towards Piazza Vittoria are *Palazzo Ischitella, Palazzo Caracciolo di S. Teodoro, Palazzo Ravaschieri (1605), and Palazzo Calabritto.*

Precisely because of its location in a valuable and socially sensitive metropolitan context, and also in response to the demands addressed by the Riviera civic committee (especially for S. Pasquale station), the licensing authority City of Naples, the contractor Ansaldo STS, and the associated enterprises executing Line 6, have relied on the collaboration of a large number of other key players (figure 2), for the resolution of issues related to special geotechnical and hydrogeological conditions of the construction site: a Scientific Committee, the Department of Geotechnical and Environmental Engineering at University of Naples "Federico II", and a lot of experienced professionals.

Astaldi S.p.A., a leader in infrastructure construction with established experience in the design and implementation of underground railways in cities of historical importance, as executor of the civil works of the S. Pasquale station has played an active part in the process, coordinating and synthesizing the contributions of all those involved, guiding and directing the design choices and promoting a series of technical variations, all aimed at optimizing execution of the work in conditions of maximum safety for the preservation of the adjacent buildings.

In particular, the work referred to in this article was the result of the interaction of different disciplines, requiring expertise in geotechnical, hydraulic, and also structural engineering, as well as in hardware systems design and software programming in the field of monitoring and data acquisition.

2 DESCRIPTION OF THE WORK

2.1 *Morphology, geology and hydrogeology*

S. Pasquale station falls almost at the centre of the zone of formation of the two calderas connected to the creation of the Campania Ignimbrite and Neapolitan yellow tuff. The current appearance of Chiaia and S. Pasquale basins took shape on a pre-existing paleo-morphology, covered by the Neapolitan Yellow Tuff and then filled by recent material (eruptive and marine) in the more depressed parts (figure 3).

Looking at S. Pasquale site (figure 4), it is characterized by carryover sand to a depth of about 20–21 m from ground level, followed by a thin layer of deposited volcanic ashes and pumice that are interblended in a layer of sand defined as "deposits from beach and dunes". In the upper 6–8 m of deposits, significant quantities of pottery fragments from the collapse of the Roman Imperial period have been found during the geo-archaeology surveys, which resulted in the need for hand digging investigation under the supervision of the competent Archaeological Authority. Further down, the stratigraphy acquires features of greater regularity and uniformity and is characterized by the presence of pyroclastics (two Soccavo eruptions) at a depth of 32–33 m; a paleo-ground separates the pyroclastics within the pozzolana of the Yellow Neapolitan Tuff, in contact with the top of the tuff surface, which has a somewhat irregular pattern. The SPT tests have confirmed the high degree of densification for the loose material, beyond a certain dispersion of data typical of this type of test.

In the area of the Riviera di Chiaia and of the adjacent areas located upstream overlooking the

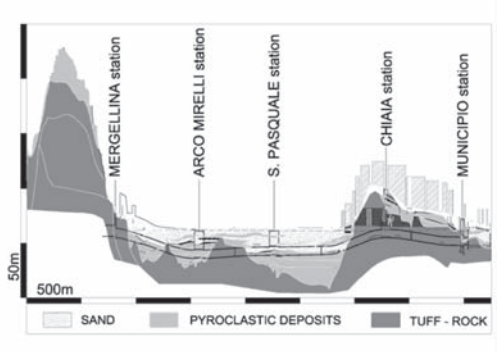

Figure 3. Geological section of the Mergellina-Municipio stretch of Line 6.

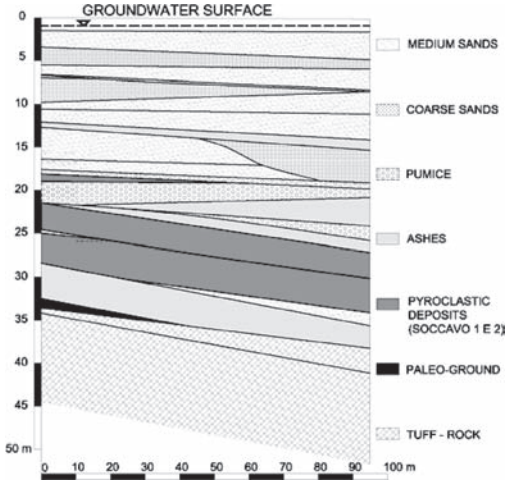

Figure 4. Geotechnical section of the S. Pasquale station.

sea (particularly for S. Pasquale and Arco Mirelli stations), the underground water circulation is affected by the complexity of the geometric relationships between the different volcanic elements and their lithological and particle size variability (with different permeability), by the presence of sea water below the continental water and of two morphological "minimums" in the Neapolitan Yellow Tuff. The one located between S. Pasquale a Chiaia and Piazza Vittoria (ridge of Monte Echia) is the deepest, filled with loose material of pyroclastic and marine origin. This configuration results in the formation of a preferential drainage into that area in the NNW-SSE direction: only one shallow groundwater layer flows into the Chiaia Basin. The piezometric and tuff bedrock surfaces were reconstructed using data extracted from the literature and by the installation of piezometers appropriately placed along the route of the subway line.

2.2 *Design issues*

The main body of the S. Pasquale station has a box-shape rectangular plan 24.10 × 85.50 m^2, and the maximum excavation depth to be performed under the roof slab is approximately 28 m (27 m under water level); the T-section perimeter panels in reinforced concrete reach a depth of about 50 m below ground level, ending up in the tuff. During the excavation phase, the diaphragms are contrasted by the construction of the boundary walls and of two more slabs in "top-down". The station has two exits adjacent to the main body, one of which is located in the Villa Comunale and the other on the opposite side toward the curtain of buildings between Piazza S. Pasquale and Via Bausan. The first station is an irregularly shaped shaft about 12 meters deep, while the other one consists of a smaller shaft with ramps and some underlying technical rooms, which will be realized with excavations to a maximum depth of 15 m from ground level.

Design and construction of the S. Pasquale station had to cope with the particular geological and hydro-geological conditions described above, with the presence of groundwater layer in proximity to the sea, of loose alluvium and of deep fragmented tuff, but mainly with the need to preserve historic buildings especially vulnerable to even small displacements. The bottom of the station is located in the lower part of the bank of pyroclastics and next to the pozzolana of yellow tuff. The thickness of the loose material between the bottom of the excavation and the top of the tuff is highly variable, ranging between 5 and 18 m.

The method of execution of the S. Pasquale station was revised several times—in part due also to the changes made to the route and profile of the line—in order to reduce to a minimum the two most important aspects related to the excavation close to monumental buildings: reducing the risk of "piping" of the pyroclastic layer, and reducing the effects of subsidence for the preservation of buildings. During the different design phases, three different solutions were taken into consideration for excavation in the presence of a high water head:

1. Excavation in water.
2. Dry excavation, after realization of a bottom plug in jet-grouting.
3. Dry excavation with dewatering of the filtering flows inside the shaft.

The first solution provided for the excavation between the diaphragms and the subsequent cast-

ing of the bottom slab in the water, with underwater diving activities without pumping out groundwater and maintaining the hydrostatic levels inside and outside of the station shaft undisturbed, to eliminate the hydrostatic thrust on the diaphragm walls and the concern over the possible effects of piping in the absence of filtrations. Subsequently, since the profile of the underground was deepened to ensure larger covering of the gallery, it was soon appropriate to clamp the diaphragm walls to the bedrock of the underlying tuff bank at highly variable depths of about 35 meters (even though it was strongly fractured), to constrain the bulkhead at the foot and provide less permeability with respect to seepage from the bottom. Consequently, the first solution with underwater excavation was definitely abandoned, also since the activities were going to be carried out in turbid waters with the presence of pyroclastic soil clay, and this would have limited the control of the operations and the proper outcome of the work. The assessments about the uplift strength on a jet-grouting plug in the loose soil above the tuff, in order to waterproof the bottom of the shaft, indicated that its weight would have been insufficient. Consequently, the preferred solution was the dewatering of the filtering flow, while the results of the analysis carried out on the top of the tuff (maximum and minimum known level) showed very high gradients of water in the areas included beneath the bottom of the excavation, because of the differences in permeability between loose soil and tuff, with the consequent risk of piping in the pyroclastic substrate above the rock-bank averaging 10 meters thick. This risk of piping could be eliminated by the installation of vertical drains in loose soils, so as to make them on the whole more permeable and maintain the groundwater surface constantly free at the excavation bottom. The latter solution, although ensuring dewatering in safety since in case of shutdown of the pumps the only consequence would have been the flooding of the working area, would have entailed major operational difficulties in the management of the pumping system while excavating.

Therefore, given the need to carry out the excavation in the best dry working conditions, during the final design Astaldi S.p.A. proposed as an alternative the use of deep wells in tuff to pump the filtering water, appropriately designed and sized to lower significantly pore water pressures in the soils overlying the bedrock and to guarantee broadly precautionary safety factors for the piping. Clearly, this solution relies on the proper and continuous operation of the pumps for the safety of the works. The interruption of their functioning, in fact, could cause piping in a very short time, for which it has proved indispensable to devise a system of maximum reliability in terms of efficiency and operation. The various steps of the design which have made it possible to define the more suitable pumping and management of the groundwater system, are the following:

1. Design and construction of an experimental field for the execution of single-well pumping tests and dewatering test of the station (pumping without soil removal);
2. Implementation of a numerical model aimed at back-analyzing the experimental results in terms of dewatering and water seepage;
3. Design and implementation of the pumping wells (using the best estimate of all relevant parameters) and a remote control and monitoring system to manage the groundwater inside the shaft during excavation;
4. Estimation of failure and induced effects, and back analysis for the verification and calibration of the fixed parameters and estimated safety factors.

3 GROUNDWATER MANAGEMENT AND CONTROL

3.1 *Pumping and dewatering tests*

Given the particular site conditions and the presence of historical buildings, it was first necessary to carry out a series of studies and verifications on site, in order to validate the variant proposal and to design a groundwater remote control and monitoring system, ensuring the prescribed safety requirements during the excavation phase. In fact, the station shaft's proximity to the sea and buildings, and the considerable uncertainties that always govern the seepage phenomenon in highly heterogeneous soil such as that affected by the station, with the related risk of occurrence of instability phenomena (piping), suggested arranging an experimental field in order to simulate the dewatering of the S. Pasquale station. This is in order to verify the design hypotheses regarding the number and final placement of the pumping wells and to properly select both the system to pump out the filtration water coming in, and the piezometric system monitoring the inside of the station. The purpose of the tests was to define the optimal configuration of the pumping out system, necessary for excavating in no longer saturated conditions of the S. Pasquale station. In particular, 4 pilot wells were installed in the western portion of the site for the dewatering, in a position compatible with the archaeological constraints and the surveying activities in progress at the time by the Superintendency, by drilling holes 600 mm in diameter with a final lining DN400. Five internal piezometric verticals were put in place (figure 5), one consisting

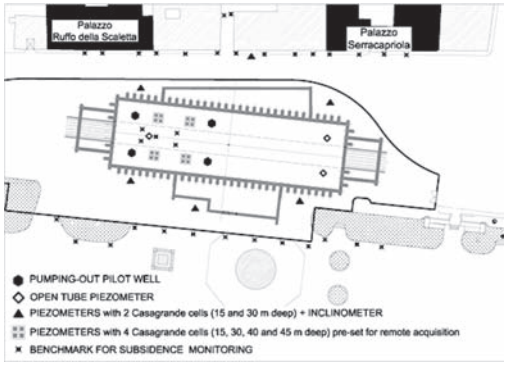

Figure 5. Plan of the S. Pasquale station with installations for experimental dewatering and monitoring.

of an open tube piezometer and the other four each equipped with four Casagrande cells respectively at 15, 30, 40 and 45 m below ground level (16 piezometric in total), for the measurement of the hydraulic gradients. During the experiment, changes in piezometric level were measured inside and outside the excavation shaft, using piezometers installed for this purpose in loose soil and in tuff, as well as the displacements of a number of benchmarks and levelling clamps. Experiments started on 18 May 2010 and lasted for about 2 months and consisted of preliminary tests on a single well (emptying, steps, and long-duration), and a dewatering test of the whole box-shaped station, with a total duration of 40 days. Examination of the results showed that no significant effects were produced in terms of piezometric changes at the external piezometers and of displacements (on the order of few millimetres on both sides).

3.2 *Numerical model and wells-field design*

The analysis and the interpretation of this type of boundary value problem are highly complex (three-dimensional, soil heterogeneity, non-stationary hydraulic conditions imposed during the tests). Although the modern calculation tools available today are able to make qualitative (sometimes also quantitative) predictions of the role played by different factors on the observed behaviour, it is almost impossible to simultaneously take all of them into account within a unitary approach aimed to reproduce measured performance. In accordance with the current trend in the field of both research and practical applications, an "adequate" model (which is a model aimed at providing a limited amount of information able to satisfy the pre-established objectives) was preferred over an "exact" model, which proposes grasping all the different aspects of a problem.

Based on these considerations, in order to obtained an interpretative model aimed at optimizing the design choices in terms of number of wells needed to lower the groundwater in the excavation area and reducing the effects caused to the outside, 2D numerical analyses were implemented. They were calibrated through the choice of the right values to be assigned to the numerical model's most appropriate fundamental parameters. Since the main purpose was also to calibrate a numerical procedure, capable of best reproducing the effects observed over time in terms of variations in piezometric level by pumping out a fixed water flow rate, it was preferred to refer to the 2D longitudinal plane section (figure 6). This is more suited to the placement of the pumping-out wells (placed symmetrically along the longitudinal axis), thus being able to impose changes in conditions on the surrounding area by means of a flow rate by unit of width.

The recorded data were taken as a reference to calibrate the numerical model and the main parameters of the problem in question, in order to reproduce, in a satisfactory manner by using dedicated specialist software (PLAXIS 2D version 9.0 and PLAXFLOW version 1.0), the measures collected during the experimentation: variations of piezometric levels over time and vertical displacements. In particular, the adopted underground model involved the presence of two strata (loose soil and Neapolitan yellow tuff) which were essentially assigned the physical and mechanical properties taken from the final design. With specific reference to permeability, information collected during the preliminary tests (on the individual wells) was used.

After a trial-and-error procedure, it was possible to establish that the best results in terms of variations of piezometric level over time were obtained by assigning the following values for the loose soil permeability K_s and the Neapolitan yellow tuff permeability K_t: $K_s = 3 \times 10^{-4}$ m/s and

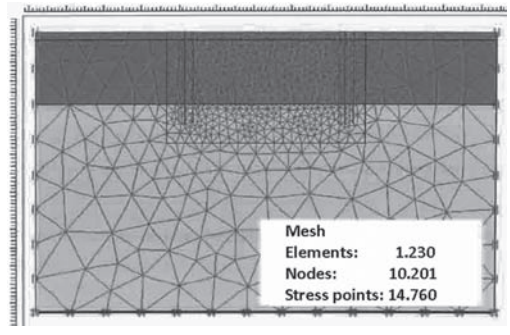

Figure 6. Schematization of 2D section.

$K_t = 3 \times 10^{-5}$ m/s. At the same time, to reproduce the observed values of the average settlements measured by the benchmarks, it was necessary to adopt a soil stiffness about 3 times greater than those assumed at the design stage (E = 137 MPa instead of E = 40–50 MPa), confirming the fact that the soil experiences small strains. With these values of the fundamental parameters, the numerical model yielded results quite close to those measured in the field, especially in the final phase of the test tending towards stationary conditions (figure 7), and therefore deemed satisfactory to be able to proceed to the subsequent design phase.

The calibrated model was then used to identify the most suitable configuration to be adopted to pump out the groundwater and to attain the excavation level at a depth of 28 m. Different configurations of the pumping system were taken into consideration, with a number of wells varying depending on some constraints (such as the requirements of the manoeuvrability of the dumping machines during the excavation and the encumbrance of the TBM tunnel crossing the station). As a result of the analyses, the scheme in figure 8 (with eight wells positioned along two longitudinal axes) was selected because they provide the best redundancy and reliability (including auxiliary wells) and the most suitable placement. For sizing the wells' filters, some grain size analyses were carried out in the stratum of the water table above the tuff, after which the adoption of a Johnson filter with 0.7 mm thick slots, surrounded by gravel drainage, was suggested.

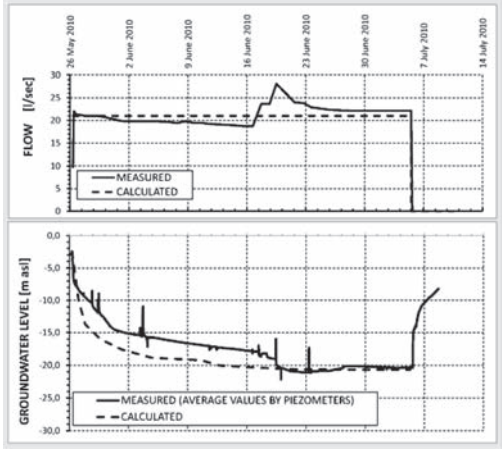

Figure 7. Back-analysis of measured data during dewatering.

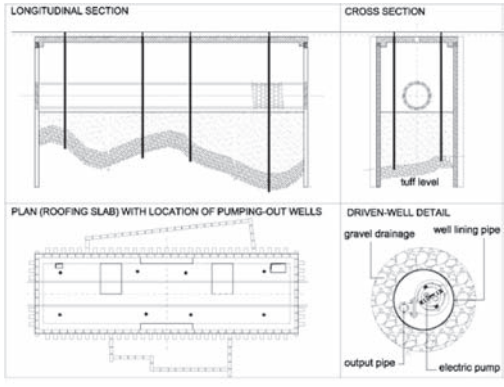

Figure 8. Pumping wells design.

3.3 *Groundwater management and monitoring system*

Monitoring the construction of the S. Pasquale station is part of a broader and more complex control plan, designed for the building work of the entire Mergellina—Municipio stretch of Line 6, coordinated by the general contractor Ansaldo STS with the involvement of the executors and of a specialized enterprise, and managed on a GIS platform accessible on a website. In the specific case of the S. Pasquale station, the need for a detailed control of induced displacements required: benchmarks at the ground level along the entire work site perimeter, wall clamps on the exterior facades of the historic buildings adjacent to the construction site, inclinometers inside and behind the diaphragms panels (placed on three cross sections of control), and optical surveys within the work area for convergence measurements during the excavation. The monitoring of groundwater levels in the surrounding area was entrusted to six piezometric verticals, each consisting of two Casagrande cells placed at different levels: one at a depth of about 15 m below ground level and another above the tuff roof. The number of instruments to be installed was established based on criteria of redundancy, to verify the congruence between the different measurements and in view of possible damage or temporary unavailability of some during the works.

Due to the above-mentioned considerations about the specific problems of the site and the vulnerability of the adjacent historical buildings, Astaldi S.p.A. decided to integrate the entire monitoring with a real-time monitoring system of the groundwater inside the excavation area based on: 8 pumping-out wells, 12 monitoring piezometers and 4 flow rate measurers. The aforementioned control fields are associated with the "general"

variables connected with the physical magnitudes of interest:

– Measurements of the hydric and alarm (on/off) levels, magnitudes associated with the pumps' operation (power absorbed, number of revolutions, hours of operation).
– Groundwater levels.
– Flow rate measurements.

The installation of each well is specifically designed to be able to house all the instrumentation needed to control its operation. Therefore, within the lining is the output pipe in flanged stainless steel (to facilitate the operations of removing and replacing the electric pump in the event of scheduled maintenance or of failure), and a guidance pipe to house two more sensors: an electric piezometer and an optical sensor. The former was entrusted with measuring the hydric level in the well, on which the automatic regulation of the pump with regard to pre-set levels depends, with control of the minimum (to protect the pump) and of the maximum (as alarm threshold). The second sensor, on the other hand, was prepared as an additional second-level alarm level, in the event of failure of the electric piezometer. For piezometric monitoring, six control verticals were designed, each consisting of two electric piezometers (for a total of 12 measurers) placed between two wells respectively above the tuff and about 2 m beneath the excavation bottom, for the measurement of any hydraulic gradients in the pyroclastic soil.

The flow rate values were acquired by 4 electromagnetic measurers with output in current; eight traditional mechanical litre counters with reel, placed on each output pipe, complete the system, allowing for datum check. The value of the output flow rates, in fact, although not closely connected with the safety requirements, is still an essential element to the system's calibration in the choice of the best operating configuration, and above all as a feedback for verifying the reliability of the prediction model and of the used permeability values.

SCADA software, with various overview windows (main control, configuration, data management, alarm management), acts as interface populated by the data originating from second-level software installed on the PLC at the side of the field and manages the remote peripherals through TCPIP and Modbus RTU communication. It was entrusted with the system's strategic functions, capable of allowing the user to constantly regulate and monitor all the process variables, also recorded on a specific database for the historical analysis of the data.

To make the system maximum as flexibile as possible and to manage the variable flow rates while deepening the excavation, an inverter was used: it ensures, in fact, broad regulation of the pumping units, adjusting the machines' characteristic curves to the system's needs. The inverters, which interact with the software and are able to bring all the variables under process control, were thus entrusted with acquiring all the data from each well, and with transmission to the PLC, where the piezometric and flow-rate measurements also converge. In accordance with the same criteria of operating versatility, also with a view to any system failures, 3 modes of operation were provided for, programmable with independent on/off cycles using a timer:

– Automatic: With closed-cycle control on hydric level pre-set in the well.
– Manual: With manually pre-set impeller speed control.
– Local: With direct control from panel—inverter.

In terms of system reliability, auxiliary communication cables were put in place and all the devices were equipped with double electric power supply. In fact, the system, powered by an electrical substation, was equipped with an auxiliary current generator; the PLC and the server with SCADA were provided with UPS. Lastly, the system was equipped with spare parts for the immediate replacement of the main components in the event of failure: 1 PC auxiliary, 1 PLC, 1 inverter, and 2 pumps. Figure 9 shows the system's layout.

3.4 *Induced effects analysis and back analysis*

In order to estimate the effects and changes in terms of state of stress and/or strain of the adja-

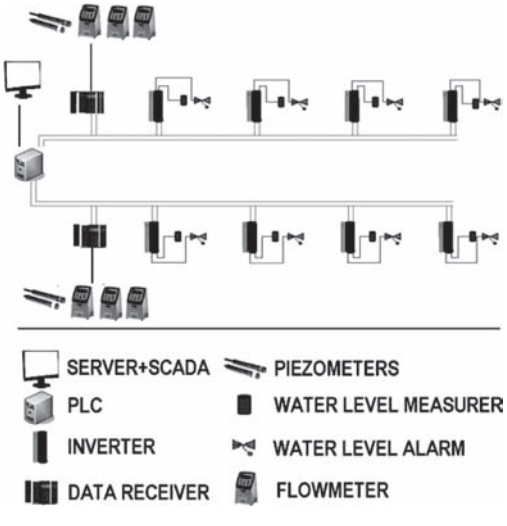

Figure 9. System layout (courtesy of Boviar s.r.l.).

cent historic and most highly prized buildings, some detailed structural analyses were also carried out. Looking at one of the oldest and most "sensitive" buildings, in figure 10 the results of the structural analysis performed by prof. R. Sparacio are reported with reference to Palazzo Ruffo della Scaletta (built in the seventeenth century and also known as Palazzo Carafa di Belvedere). All the structural analyses were aimed at estimating the maximum differential settlement unable to cause damage to bearing walls.

Unlike what was set out for the dewatering analysis, in the estimate of the effects induced to the surrounding area and on the buildings in terms of subsidence, we referred necessarily to the cross section. The geometric model used in the numerical analyses that were conducted is represented in figure 11. The soil and the diaphragm walls of the main excavation and of the two lateral shafts were schematized using a grid of 15-node triangular elements.

The plane decks, on the other hand, were modelled using node to node anchors, which are elements with an elastic-linear behaviour and that are characterized solely through axial stiffness EA/L.

On the other hand, to describe the mechanical behaviour of the soil and diaphragms, it was decided to adopt:

– An elastic-plastic constitutive model with Hardening Soil Model, for loose soil over the roof of the Neapolitan Yellow Tuff;

Figure 10. Maximum stresses on the façade wall of Palazzo Ruffo della Scaletta with a differential settlement of 60 mm from the structural FE analysis (courtesy of Prof. R. Sparacio).

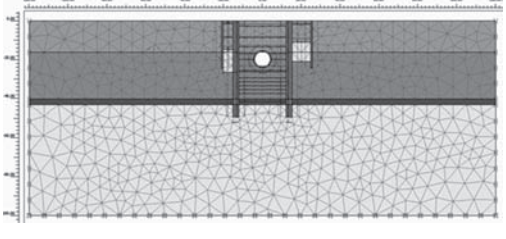

Figure 11. PLAXIS model used for the numerical analyses.

SOIL	h (m)	γ (kN/m^3)	γ_{sat} (kN/m^3)	c (kN/m^2)	φ (°)	E (kN/m^2)	k_1 (m/s)	k_2 (m/s)
DEPOSITS	16,2	16	18	0	36	$70x10^3$	$3,0x10^{-4}$	$1,5x10^{-4}$
PYROCLASTIC	24,0	14	16	0	36	$268x10^3$	$3,0x10^{-4}$	$1,5x10^{-4}$
POZZOLANA	3,0	14	16	500	27	$2210x10^3$	$3,0x10^{-4}$	$1,5x10^{-4}$
YELLOW TUFF	-	14	16	500	27	$6360x10^3$	$3,0x10^{-5}$	$1,5x10^{-5}$

Figure 12. Physical and mechanical characteristics of the soils.

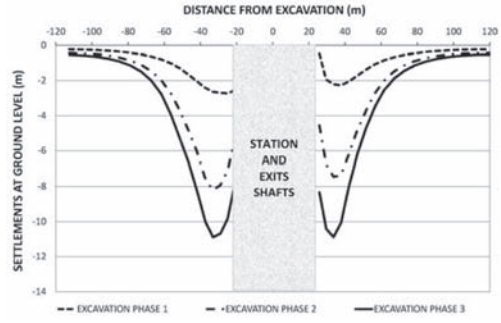

Figure 13. Numerical analysis results in terms of average building settlement.

– A perfectly plastic elastic constitutive model with Mohr-Coulomb failure criteria for the Neapolitan Yellow Tuff and for the jet-grouting plugs made at the bottom of the wells;
– A Linear Elastic constitutive model for the reinforced concrete diaphragms.

Figure 12 reports the main physical and mechanical properties assigned to the four soil types; permeability values ("k") were initially taken as equal to those derived from the dewatering test field, and then gradually updated based on the values of the flow rates pumped out, as measured during the excavation phase.

The results of the prediction analyses in terms of vertical displacements caused by pumping and by the excavation are represented in figure 13.

After the completion of the excavation of the main station shaft, the values of flow rate pumped out reached a maximum of 29 l/s, with groundwater levels of about 31 m below the initial value. Measured piezometric changes for the external piezometers were of the order of 1 m; the measured maximum vertical displacements were on the order of 20 mm, giving rise to small angular distortion.

4 CONCLUSIONS

The Mergellina—Municipio section of Line 6 of the Naples underground runs along the Riviera di Chiaia in saturated loose soil, between the Villa

Comunale and a curtain of considerably valuable historical buildings from the seventeenth and eighteenth centuries.

In such an important setting, Astaldi S.p.A. played a major role in the design and execution of the S. Pasquale station, providing its long-established know-how in realizing undergrounds in historic centres, with the collaboration of authoritative experts and the synergy of a number of different disciplines, while implementing a system to manage and control the groundwater within the excavation, through a long and complex process of experimentation, modelling, analysis, design, realization, and verification of the data acquired in the field.

The results of this system were entirely satisfactory, allowing the station to be excavated in absolute safety, in terms of reliability of the system and of precautionary safety factors against piping, to the benefit of the preservation of the buildings overlooking the work site, in particular Villa Acton, Palazzo Ruffo della Scaletta and Palazzo Serracapriola. The displacements observed at the end of excavation were small enough, within the range of predictions, and compatible with the structural characteristics of the affected buildings.

REFERENCES

Falconio, G. 2010. Linea 6—Stazione S. Pasquale—Relazione sull'interpretazione delle prove di svuotamento del pozzo di stazione.

Falconio, G. 2011. Linea 6—Stazione S. Pasquale—Verifiche degli stati limite idraulici.

Viggiani, C. 2008. Linea 6—tratta Mergellina–Municipio—Relazione geotecnica.

This page intentionally left blank

Geotechnical Engineering for the Preservation of Monuments and Historic Sites – Bilotta, Flora, Lirer & Viggiani (eds)
© 2013 Taylor & Francis Group, London, ISBN 978-1-138-00055-1

Offshore soil investigations on the bottom of Ohrid Lake and authentic reconstruction of timber piles settlement

D. Nikolovski, B. Veljanovski & A. Stojkovska
SPG—Geoing, Skopje, Republic of Macedonia

ABSTRACT: In 2008, the activities for construction of museum complex started on wider scale at the archeological site on the peninsula Gradishte Ohrid Lake, by patronage of the Board for cultural heritage of the Republic of Macedonia. The works are to create an authentic reconstruction of prehistoric palafitte settlement on timber piles, located in the place called "Bay of the bones", which dates from the late bronze age and beginning of iron age, in the period of 1500–700 BC. The aim of such activities was to build a Museum on water that would be unique to the Balkans by its form, construction and cultural heritage. In the first phase, an offshore investigations with CPTu tests was conducted for the means of this construction, for definition of the geotechnical characteristics of the soil in the bottom of the lake, as well as defining of the depth on the base rock material. In accordance with the results from the geotechnical investigations, the timber piles construction is designed and executed, on the same place in the lake where prehistoric artifacts were found. In this paper the geotechnical investigations, technical characteristics and details of the authentic reconstruction of the timber pile construction are detailed.

1 INTRODUCTION

The Ohrid Lake was formed by tectonic forces, 2–4 million years ago, therefore it is considered to be the oldest lake in Europe and one of the oldest in the world, along with the Baikal Lake in Kafkaesque and the African Lake Tanganyika. In Ohrid Lake more than 146 endemic species and fauna are found, mostly because of its age, and the fact that it is surrounded by hills and mountains. As a result, in 1980, UNESCO proclaimed it as site of cultural and natural values of the global partimony. Still, this natural system does not only abound in endemic species and fauna, but also at the bottom of the lake exceptional archaeological values from the old prehistoric period, such as pile settlements, have been preserved.

Pile settlements, as a way of living for people in the past, were especially characteristic of the period of Prehistory, in the Neolithic, Eolithic, Bronze and Iron Age. They were built and used, generally, for the protection of the prehistoric man from the attacks by wild animals as well as by other tribes. This also allowed them to obtain food either by water or by land. These pile settlements, in Europe can be mostly found in Switzerland, Northern Italy, Germany, Austria etc., originating from various chronological periods. Pile settlements in Macedonia were first mentioned by the antique Greek historian Herodotus (B, 16) who described the Prasiade Lake, nowadays known as the Dojran Lake. Apart from the remains of prehistoric pile settlements found on the territory of the Dojran Lake after the archaeological research conducted in the last years of the 20th century, such remains have also been found on the territory of the Prespa Lake and Ohrid Lake in Macedonia.

The only settlement of this kind which has been reconstructed, and which can be found on the coast of the Ohrid Lake, in the Bay of the Bones, will be the topic of this research.

2 GENERAL CHARACTERISTICS OF BAY OF THE BONES PILES SETTLEMENT

For the first time in Macedonia, in the years between 1997–2005 and 2007–2008, underwater archeological researches were carried out in the Ohrid Lake next to the Gradiste peninsula, more specifically in the Bay of the Bones. These detailed researches at the aforemetioned location, resulted in the discovery of a prehistoric pile dwelling settlement, where about 6000 remains of timber piles with a diameter of 13.0–30.0 cm, comprising a surface of 8500 m^2, were registered. These piles, grouped in such a way, constituted the foundation of a joint wooden platform. According to the archaeological researches, it is assumed that 20 prehistoric residential facilities built from similar

Figure 1. Remains of wooden objects at bottom of Ohrid Lake.

Figure 2. Remains of timber piles at bottom of Ohrid Lake.

material had been located above this platform. Regarding the authentic construction execution, it is important to mention that these piles were registered at a depth of 3.0–5.0 m, while the nearest piles are found 12.0 m from the coast of the lake, which is oriented South from the Gradiste peninsula. The survey of the bottom of the lake registered a large density of fragmented and whole ceramic pots, stone artifacts, animal bones and many other objects used as tools.

Based on the results obtained from these detailed researches, and in accordance with the archaelogical analysis of the objects taken out from the bottom of the Ohrid Lake, it can be said with absolute certainty that this pile settlement dates back to the late Bronze Age and the beginning of the Iron Age, that is the period between 1500 and 700 B.C. Due to these reasons, this object has raised considerable interest among the members of this professional field. As a result it was decided to start the construction of a museum on water, the only one of this kind on Balkans, under the auspices of the Macedonian Ministry of Cultural Heritage.

3 GEOTECHNICAL INVESTIGATIONS

The specific location of the pile settlement's construction in the waters of the Ohrid Lake imposed the need of uncommon geotechnical investigations. It was decided to conduct offshore soil investigations through the CPTu test, keeping in mind the difficulties in handling the standard drilling equipment in a limited space, as well as the inability to obtain an undisturbed soil sample from the bottom of the lake. Undoubtedly, as a result of these reasons, the CPT test has been an essential part of offshore soil investigations in the last 40 years.

The position and dimensions of the platform, generally required the conduction of the tests at 6 investigation points, all in 20–40 m distance from the shore of the Ohrid Lake. Taking into consideration its distance from the shore of the lake, the conduction of the offshore tests was adapted to shallow waters (<30 m), by placing the equipment on a floating barge with a central core in the middle. The tests were provided using an electric piezocone CPTu, type ENVI Memocone.

Despite the fact that the tests were carried out in shallow waters, care was taken for the equipment to be well anchored to the bottom of the lake in order to prevent any horizontal displacements and inclination. In this way the free standing casing protrudes trough an anchored barge, with the hydraulic jacking system mounted on a stable casing (Figure 4).

Because of the nature of the constructions itself, it was very important to determine the soil profile of the lake bottom, which is without doubt one of the biggest advantages of this type of *in situ* testing. The tests were carried out to varying depths, until the power of the penetrometer of 200 kN was reached which indicates the appearance of

Figure 3. Layout with disposition of investigation points.

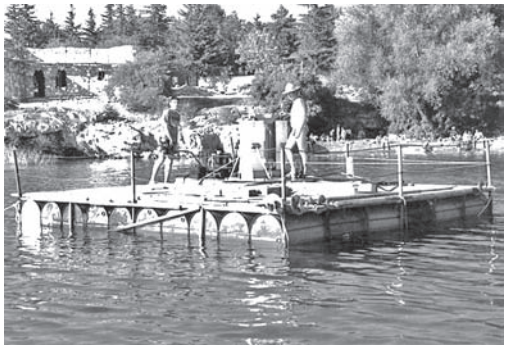

Figure 4. Offshore investigations with CPTu.

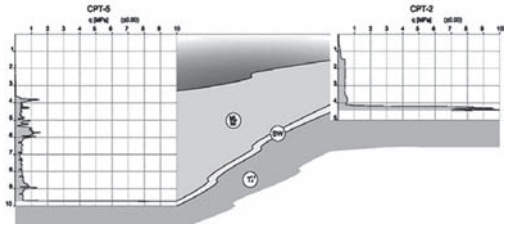

Figure 5. Offshore investigations with CPTu.

the base rock material, limestone. The base rock material is registered at a varying depth from the surface of the lake, and with an inclination of n ≅ 1:2.8, with orientation from the shore to the lake (Figure 5).

The identification of the soil materials will be done according to *Robertson* (1990) normalized charts, which offer a three-dimensional system for soil classification. The advantage of this popular method for classifying soil materials to others is that it uses all three series of data from the CPTu test (q_t, f_s, U_2) which is essential for this kind of offshore investigations. The normalization of the CPTu data, will be done according to the equations (1) to (3) below (Wroth, 1988). Considering that the piezocone used in the tests, only measures the pore pressures behind the cone U_2, the normalization of the sleeve friction f_s to f_t will not be done.

$$Q_t = \frac{q_t - \sigma_{vo}}{\alpha'_{vo}} \qquad \text{norm. cone resistance} \qquad (1)$$

$$F_r = \frac{f_s}{q_t - \sigma_{vo}} \qquad \text{norm. friction resistance} \qquad (2)$$

$$B_q = \frac{\Delta U}{q_t - \sigma_{vo}} \qquad \text{pore pressure ratio} \qquad (3)$$

Analyzing the obtained data values from all 6 conducted tests, it can be concluded that the registered data values, according to all three parameters, indicate materials of a similar kind in a quasi—homogenous zone up until the registering of the base rock material. As a result, the series of values of a characteristic CPTu test will be shown and analyzed below (Figure 6).

According the diagrams, the series of values are generally concentrated around zones 1, 3 and 4, interpreted as sensitive fine grained soils and silty-clay mixtures, which overlaps with the other examinations and analogoue experiences, for this micro-locality. Smaller number of values refer to other zones in both diagrams, which is completely expected and pointed out by *Robertson* in his researches. Based on the conducted tests, a classification was done according to the consistent condition of the soil material, in accordance with

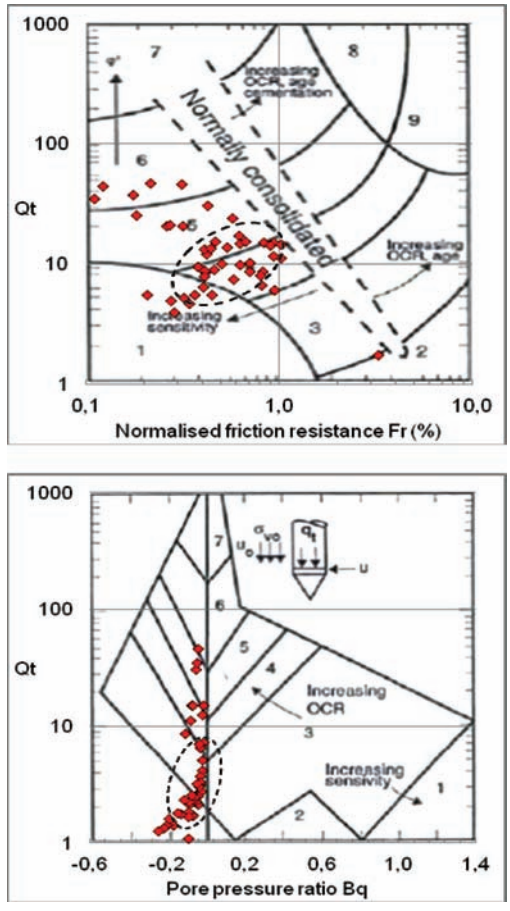

Figure 6. Charts of soil classification from CPTu test, by *Robertson (1998)*.

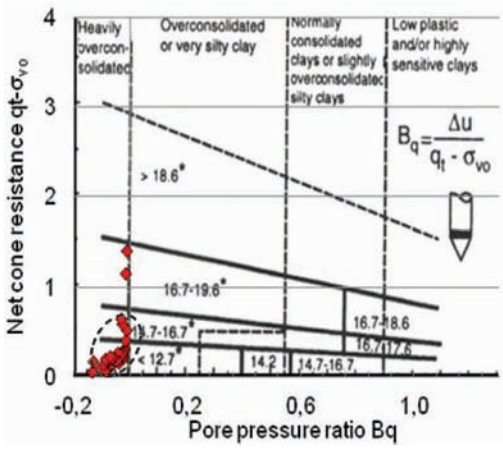

Figure 7. Chart of soil classification from CPTu test, by *Larsson & Mulabdic*.

Larsson and *Mulabdic's* method, based on piezocone tests of sensitive fine grained soils. A preliminary conclusion can be made with this method about the bulk weight of the tested material, which in this case ranges between $\gamma = 12.7 \div 14.7$ kN/m^3 (Figure 7).

From the conducted tests and analyses, and with the purpose of choosing a suitable construction system, it can be said that the soil under the surface of the future platform on which the timber piles needed for the authentic reconstruction of the settlement are to be placed, has extremely weak geotechnical characteristics to a depth of 4.2–10.0 m.

4 AUTHENTIC RECONSTRUCTION OF THE TIMBER PILE SETTLEMENT

4.1 *Materials for execution of the pile settlement*

According to the requirements imposed by the Institute for Protection of Cultural Heritage, the complete reconstruction of the settlement was to be authentic. This entailed use of the equivalent materials used in its original construction. The underwater archaeological investigations determined the use of piles made of oak wood, with a diameter of 15–30 cm.

Considering the extreme atmospheric influences, constant influences of water, as well as the fluctuation of the water level during the period of exploitation of the piles and the above-water platform, it was necessary to subject these materials to impregnation. Thus it was decided to use a method of impregnation of the wood, by a procedure including the use of vacuum and pressure in special closed devices—autoclaves. It is important to mention that particular care was taken in the choice of means for this process, in order for it not to contaminate the environment and not to be toxic for the wildlife in the surrounding where it takes place.

4.2 *Execution and technical characteristics of the construction*

In coordination with the Institute for Protection of Monuments of Culture, it was decided the platform of the pile settlement to be positioned near the site where the remains of timber piles and other archeological artifacts were found. The dimensions of the reconstructed platform, on which the museum is set, are 25 × 42 m and it is placed on 1012 timber piles. These are placed in 25 rows at an average axial distance of 1.0 m, with a diameter of 20 cm, in coordination with the main project for execution of the construction. According to the geotechnical investigations and the lithologic structure of the terrain, it was determined to drive the piles into the base rock material, as end bearing piles, in order to avoid the possibility of differential settlements of the platform. Possible flooding was taken into consideration in determining the length of the piles, besides the lithologic structure of the terrain. The piles are positioned 2.0 m above the surface of the lake in order to avoid flooding of the platform due to fluctuation of the water level or waves. Therefore, piles with length of 6.0–12.0 m were chosen, which were supposed to be driven into the base rock material and which were to penetrate it to a minimum depth of 0.5 m. The depth of penetration is depending on the conditions extent to which it had degraded in the upper parts. Piles placed in this way, with a varying depth, adapted to the field conditions, were hydraulically driven through the soil material with height of 1.2–5.7 m (Figure 8).

Additional type RTS vibratory equipment was used for overcoming the friction resistance on the surface of the piles, in the process of their driving through the soil material at the bottom of the lake. In the upper part these piles will be connected to wooden beams, also made of oak, in order to ensure greater rigidity of the entire construction system, in case of horizontal or vertical load.

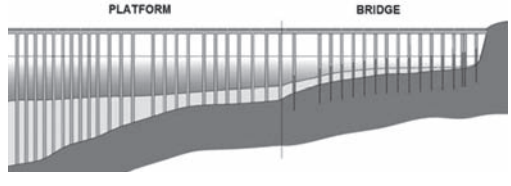

Figure 8. Cross section of the timber pile settlement.

Figure 9. Preview of the authentic reconstruction of timber pile settlement.

The length and position of the bridge which provides a passage between the shore and the platform, was chosen based on the remains of piles nearest to the shore of the lake as well as on their schematic positioning, also determined with the underwater investigations. In accordance with this, the wooden bridge with a length of 19.0 m was anchored in the shore in order to prevent any horizontal movements of the platform. In the execution of the bridge, 68 piles were placed in 17 rows at a distance of 1.0 m.

The execution and the driving of the piles from the reconstructed pile settlement, took place in specific conditions, in the waters of the Ohrid Lake. For this purpose, a floating barge was brought and mounted by means of a special transport. The dimensions of the platform are 7.5 × 17.0 m, and its capacity allows for unobstructed functioning of the machinery with a weight of 25–30 t.

5 CONCLUSIONS

Macedonia is great mine of cultural and historic inheritance, therefore projects of this type should become common activities in government's projects for promoting tourism and cultural legacy. The Museum on water represents an authentic reconstruction of a settlement from the Iron and Bronze ages, and it is a tourist attraction for Macedonia but also for many visitors from abroad. All the materials used in this construction, as well as the means used in the process of testing and research are from natural material, in order to preserve the natural environment and not to harm the existing flora and fauna.

The role of geotechnical engineering in preservating this historical monument took major part in the whole project. The investigations as well as the planning, designing took essential part in the authentic reconstruciton of the whole project.

Just a few meters from the shore is the passage, not only for a simple settlement, but a passage for a real time travel experience of tourists from all over the world that will find themselves right in the prehistoric times.

ACKNOWLEDGEMENT

The authors would like to direct special thanks, to National Office for protection of historical monuments and cultural heritage—Ohrid, R. Macedonia, for their valuable help during providing the reasrches and writing of this paper.

REFERENCES

Bahchevandziev, K. and Gj. Gruevski (2009). Methods of improving the quality and impregnation of oak tree exposed on extreme atmospheric influences, (in Macedonian).

Gjorgjevski, H., S. Suvaka, B. Veljanovski, D. Nikolovski, and A. Stojkovska (2009). Main Project for authentic reconstruction of palafitte settlement on timber piles "Bay of the Bones" (in Macedonian).

Kuzman, P., E. Kochkovska, and M. Sekulovski (2010). Museum on water, Bay of the Bones, reconstruction of pile dwelling settlement.

Poulsen, R., B.N. Nielsen, and L. Bo Ibsen (2011). Field cone penetration tests, with various penetration rates-Tests results.

Robertson, P.K. and J.J.M. Powell (1997). Cone Penetration Testing in geotechnical practice.

Robertson, P.K. K.L. Cabal 5th edition (2012). Guide to cone penetration testing.

Sachetto, M. and A. Trevisan (2005). CPTs executed in dificult conditions using CPTWD and its future developements.

Terzaghi, K., R.B. Peck, and G. Mesri (1996). Soil mechanics in engineering practice.

This page intentionally left blank

Geotechnical Engineering for the Preservation of Monuments and Historic Sites – Bilotta, Flora, Lirer & Viggiani (eds)
© 2013 Taylor & Francis Group, London, ISBN 978-1-138-00055-1

Groundwater development and management in Siem Reap, Cambodia: Impacts of groundwater pumping on Angkor Wat

M. Nishigaki
Okayama University, Okayama, Japan

S. Takahashi & M.Takahashi
Nippon Koei Co., Ltd., Tsukuba, Japan

Y. Maruo
Japan International Cooperation Authority, Tokyo, Japan

ABSTRACT: Reliable and clean water is essential for sustainable development. Siem Reap city is the center of the tourism for Angkor Wat, and the population and tourist has rapidly increased over the last decade. However, the present water supply system cannot fulfill the water demand. Groundwater can be expected to meet the increasing municipal and industrial use of water. However, there are great concerns about land subsidence over the Angkor Wat due to excessive pumping of groundwater. This study describes the existing production wells, located 7.5 km far from Angkor Wat and addresses the influence on Angkor Wat from the existing and further groundwater development in the Siem Reap region. In order to predict the aquifer response to groundwater development, a three-dimensional groundwater flow model is constructed, and its application is presented to demonstrate how to use the simulation for groundwater development and management in this region.

1 INTRODUCTION

The great issue in stabilizing the Cambodian people's life in the Siem Reap region is to enhance the tourism of Angkor Wat, the world heritage. Because of this, water resources of quality and quantity have been needed to meet the increasing water demand for municipal use due to urbanization and tourism. JICA (Japan International Cooperation Agency) succeeded in developing groundwater, located around 7 km far from Angkor Wat, and clean water has been supplied to Siem Reap city, the local capital and the center of the tourism of Angkor Wat, since 2006. In the feasibility study of JICA's water supply project, the optimal spatial distribution of pumping was computed near the Siem Reap airport, bounded to allowable drawdown around the heritage area. The pumping strategy results were then verified using a transient groundwater simulation. Recently, additional water resources have been explored for the further water demand of growing tourism industries in this region. Groundwater can be useful water resources especially for a country whose economy is not matured enough. However, there are great concerns about land subsidence over the Angkor Wat due to excessive pumping of groundwater.

This study is made to address the influences on Angkor Wat from water resources development in the Siem Reap region. and aims at pointing out the following necessities;

- to collect hydrological data by continuing to monitor groundwater levels and ground displacements.
- to construct a numerical model which can precisely evaluate ground displacements over the Ankor Wat heritage area, simultaneously simulating recharge and discharge in the groundwater basin.
- to determine the spatial distribution of the allowable volume of groundwater pumping in future by using the numerical model.
- to establish an administrative system which instructs appropriate groundwater use to avoid the various problems induced by disorderly groundwater pumping.

2 THE STUDY AREA

2.1 *Present natural environment*

The study area is the Siem Reap region, located north of Tonle Sap Lake in the northwest of

Cambodia. The length in the west-east direction is 35 km and that in the north-south direction is 40 km, and the area covers a total of 1,400 km^2. In the study area, there are Angkor Heritages, West Baray, Siem Reap city, and the Siem Reap river, originating the Kulen hills and flowing into Tonle Sap Lake (Figure 1). The area of Tonle Sap Lake varies between the dry and rainy season, and its water level rises from 1.5 m to 10 m (Kummu, 2008, JICA, 2000).

The Siem Reap region belongs to the tropical monsoon climate. The rainy season is May to October, while the dry season is November to April. The average annual rainfall of Siem Reap city is 1,465 mm from 1988 to 2008, and around 90% of the annual rainfall concentrated in the rainy season.

The aquifer widely extends under the alluvial fan and can be easily accessible as the groundwater table lies between 0 and 5 m below ground surface. Based on the simultaneous well observations, groundwater-flow directs southward and finally reaches to Tonle Sap Lake corresponding to the geological feature. Figure 2 shows generalized groundwater flow directions in this region and the eight observation wells installed by JICA in 2000.

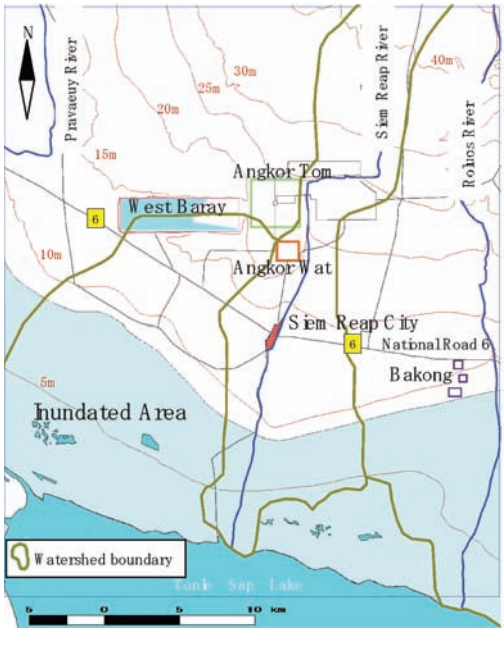

Figure 1. Siem Reap city, Angkor heritages, rivers, hydrological boundary, and inundated area in the rainy season.

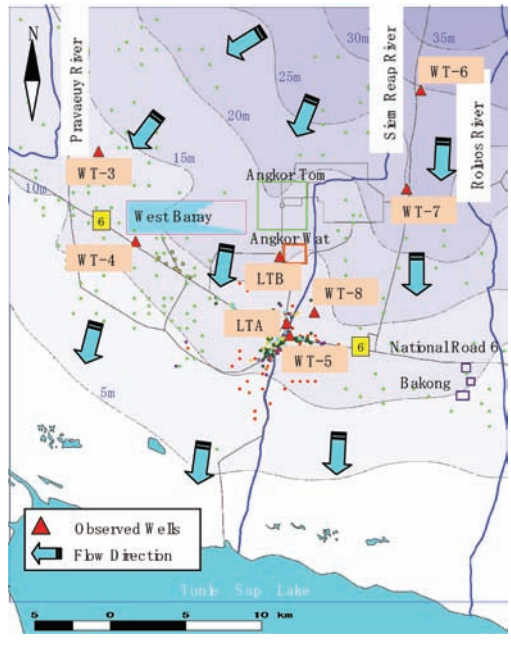

Figure 2. Groundwater levels in July and generalized groundwater flow directions.

2.2 *The rapid increase in water demand and recent groundwater development*

Siem Reap city is the capital of this region, and its population is around 200 thousands in 2009. Around 2 million tourists visit Siem Reap city for sightseeing of Angkor Heritages. The high growth rates in its population and tourist numbers have been experienced over the last decade.

There are four possible water resources, including Tonle Sap Lake, the Siem Reap river, West Baray reservoir, and groundwater. The aquifer consists of sand deposits of Quaternary age and generally contains groundwater under unconfined conditions. Most of residents withdraw groundwater from shallow dug wells and hand-pump wells, but the water is not suitable for drinking and domestic use because of its high concentration of iron. However, the aquifer is capable of yielding water of quality and quantity if new pumping wells are installed in appropriate places and depths. Thus, groundwater was selected as the best resource because of less construction cost for the related facilities and good water quality in the first feasibility study of JICA's water supply project (JICA, 2000).

After the completion of the feasibility Study, the new eight production wells and drinking water treatment plant were constructed near the Angkor airport under the Japanese grand aid of 1,537 million yen. The Siem Reap Water Supply Authority

(SRWSA) started their operation in 2006 and has produced 9,000 m^3/day at full capacity since 2008. This water supply system has contributed to the improvement of drinking water supply in Siem Reap city. However, Siem Reap city's water demand has increased rapidly since 2000, and this water treatment plants are not enough to fulfill the demand. In addition, many luxury hotels have been constructed since 2000, the number of the hotels counted around 70 in 2008. Such hotels installed their own wells and pumped a large volume of water. This disorderly groundwater pumping may cause the regional decline of groundwater, resulting in harming the Angkor heritage.

To solve the current shortage of municipal and industrial water of Siem Reap city and prevent the Ankor heritage from possible land subsidence, the second feasibility study on the water supply system was implemented by JICA from 2009 to 2011, and Tonle Sap Lake was selected as additional water resources (JICA, 2011).

3 GROUNDWATER SIMULATION

3.1 *Numerical simulation of the groundwater flow*

A quasi-three dimensional groundwater flow model, MODFLOW (McDonald & Harbaugh, 1988), was used for the groundwater-flow simulation.

3.1.1 *Model discretization*

The study area was discretized with 100 m size cells around Siem Reap city and the Ankor heritage area because groundwater flow is simulated using a finite difference method (Figure 3).

3.1.2 *Boundary*

On the north side, a general head-boundary head was used to simulate flow from the Kulen hills. On the south side, a constant head boundary and a quasi-high hydraulic conductivity zone was used to simulate groundwater-flow into Tonle Sap Lake. On the east and west side, constant head boundaries were set along the rivers, the Roluos river and a branch of the Puok river.

3.1.3 *Aquifers*

Based on 11 geological profiles interpreted with 8 drilling cores and sounding tests, the aquifer system consists of three layers, the upper unconfined aquifer and the lower confined layer, and the bedrock.

3.1.4 *Geo-hydrological parameters*

Hydrological parameters were obtained from the pumping tests and the spatial distribution was determined through the calibration as follows:

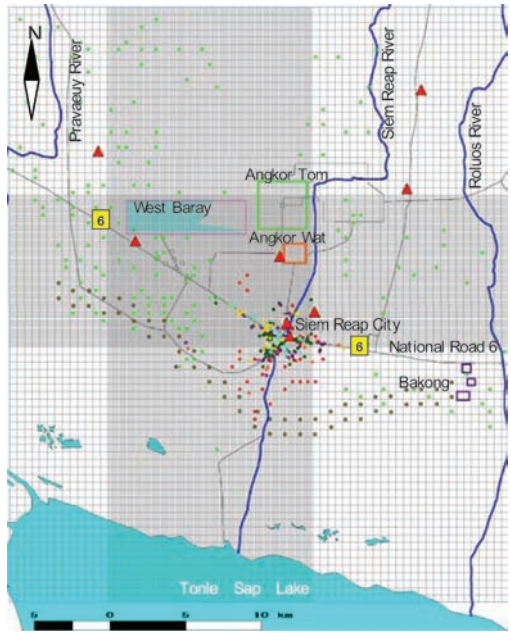

Figure 3. Discretization of the study area for the groundwater simulation model.

Layer 1 (the upper unconfined aquifer):
Hydraulic conductivity around the existing SRWSA production wells is 8.0×10^{-3} cm/sec. Those in the other location are lower than 4.0×10^{-2} cm/sec. Storativity is around 0.1.

Layer 2 (the lower confined layer):
Hydraulic conductivity is 1.0 to 2.0×10^{-6} cm/sec, and storativity is 2.0×10^{-3}.

3.1.5 *Deep percolation*

Deep percolation for each land use type was estimated from a water balance around the root zone. For example, the components of the water balance in a paddy field are precipitation, net irrigation requirement, evapotranspiration, soil moisture content, and surface runoff.

3.1.6 *The Siem Reap river and discharge from drains*

Flow between the aquifer and the Siem Reap river is formulated as a function of the groundwater table and the water level of the river in the model. The river bottom elevation and width were obtained from the longitudinal survey results. The water stage of the river varies seasonally and rises from 0.5 m to 4.0 m around the Siem Reap city.

Especially in the rainy season, considerable discharge seems to come from the previous river

course of the Siem Reap river, and natural and artificial drains on the low lands along the lake shore. The discharge from such drains was estimated from the relationship between the groundwater level and the drain bottom.

3.2 *Groundwater withdrawal from the existing wells*

3.2.1 *Domestic use of the residents*

The groundwater withdrawal for domestic use of the residents was estimated based on the village population, assuming the water use of one person is 100 liter per day. The village populations were obtained from the survey in 1999.

The population in Siem Reap city has increased around double from 10,379 in 1999 to 17,392 in 2009. According to the increase in population, the withdrawal from 1998 to 2008 was estimated.

3.2.2 *Water uses of the hotels, guest houses and factories*

The detail well inventory survey in Siem Reap city was made by JICA. The survey targets were 280 commercial and public facilities including 75 hotels, 115 guesthouses, 10 factories, and 4 schools.

Figure 4 shows the locations of the target wells and SRWSA's water service area. Based on this survey, groundwater withdrawal from 1998 to 2009 was estimated. The withdrawal has increased 6.8 times from 710 m^3/day in 1998 to 4,850 m^3/day in 2009 (Figure 5).

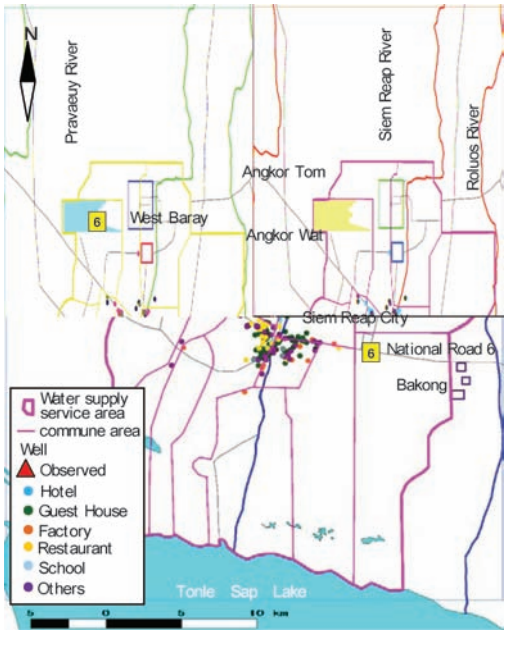

Figure 4. Commercial and public facilities and SRWSA's water supply service area.

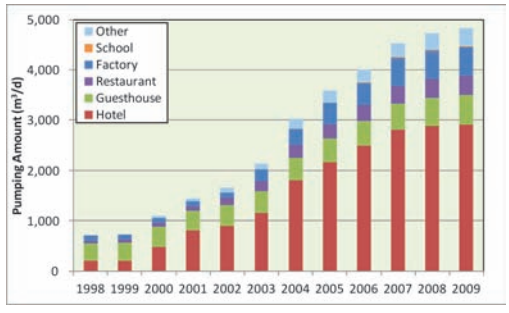

Figure 5. Groundwater withdrawal of commercial and public facilities in Siem Reap city.

3.2.3 *Withdrawal of the new French water supply system*

SRWSA installed two pumping wells near Siem Reap city, producing 1,440 m^3/day and renewed the previous water supply system, called the new French water supply system. These production wells were operated from 1999 to 2005 until the eight SPWSA production wells started operating.

3.3 *Model calibration*

The simulation model was calibrated for both steady and transient conditions until the appropriate distribution of various hydrological parameters was determined. The groundwater levels for the period from 1998 January to 2009 January were selected for the calibration, minimizing the differences between the simulated and observed groundwater levels.

3.4 *Model application for the future water supply scenarios*

The calibrated model was used to simulate possible effects on groundwater tables caused by replacing the current withdrawal from the private and commercial wells with the managed withdrawal from the existing SRWSA and possible production wells in the future. These model simulations were presented to demonstrate model performance and to show how the model might be used for water resource management in the Siem Reap region. The predicting model simulation was based on a daily basis using the historical rainfall series in the recent 10 years from 1998 to 2007, including the dry and rainy year occurring once in 10 years.

3.4.1 *Scenario description*

Alternative scenarios were prepared for the future water supply in the Sieam Reap region.

Scenario 1: Continuing present water supply with groundwater.

In this scenario, the present groundwater withdrawal and water demand will not change until the target year 2030 (Figure 6).

In order to predict the influence due to full-time pumping by the existing SRWSA production wells with 9,000 m^3/day, a transient simulation was performed for the 21 years period from 2009 to 2030.

Scenario 2: Further groundwater development.

Due to the rapid urbanization and a surge of tourism in the Siem Reap region, the water demand has increased markedly and this trend seems to continue.

In this scenario, further groundwater development will be implemented to meet the increasing water demand. The future water demand was predicted using the growth rate of various water users.

The growth rate in water use for the hotels assumed 5%, and those for the other water uses such as domestic use of the residents are also assumed 5% until 2030. In the mean time, the water supply system will be expanded in a staged wised manner. The first and second expansions assumed to be made in 2017 and 2022. The expansion capacity in water is 32,400 m^3/day for each, and that amount water will be pumped with the existing and additional production wells. As shown in Figure 7, the water supply capacities are 9,000 m^3/day from 2009 to 2016, 41,400 m^3/day from 2017 to 2021, and 73,400 m^3/day from 2022 to 2030. This stage-wised plan can fulfill the water demand from 2017.

A total of 53 production wells are needed, assuming one well produce 1,200 m^3/day, and they will be installed along the lake shore above 10 m to avoid any influence on the Angkor heritage (Figure 8).

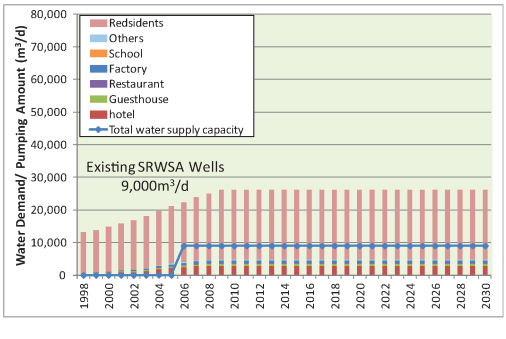

Figure 6. Water demand and water supply plan of scenario 1.

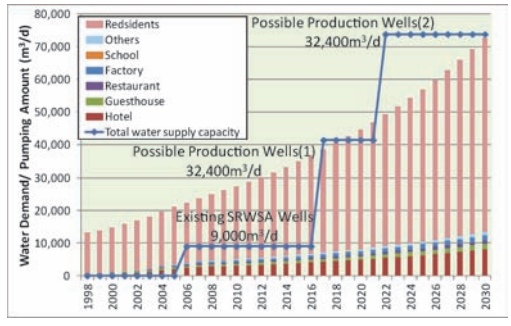

Figure 7. Water demand and stage-wised water supply plan.

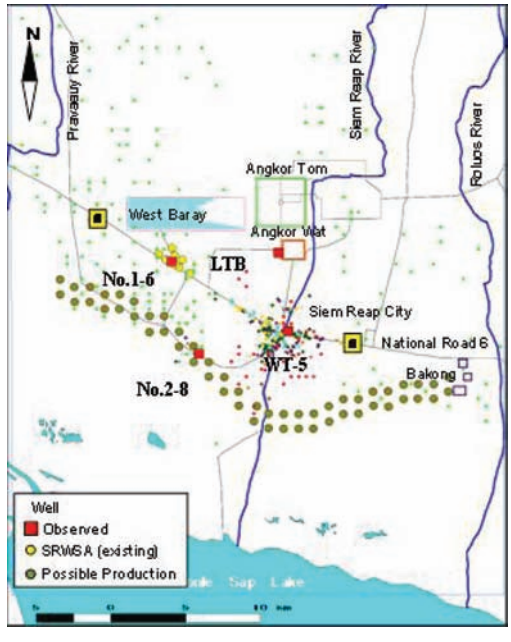

Figure 8. Possible locations of additional production wells in scenario 2.

3.4.2 *Simulation results*

The simulated groundwater table fluctuations at selected locations for Scenario 1 and Scenario 2 are shown in Figure 9. LTB is in front of Ankor Wat, No. 1–6 is at the center of the existing SRWSA productions wells, WT5 is near the center of Siem Reap city, No. 2–8 is in the possible production wells of Scenario 2.

In general, groundwater table fluctuate, corresponding to amount of rain which change seasonally and yearly. At No. 1–6, before the SRWSA production wells start pumping, the lowest water level is 12.9 m in July 1998. After starting pumping

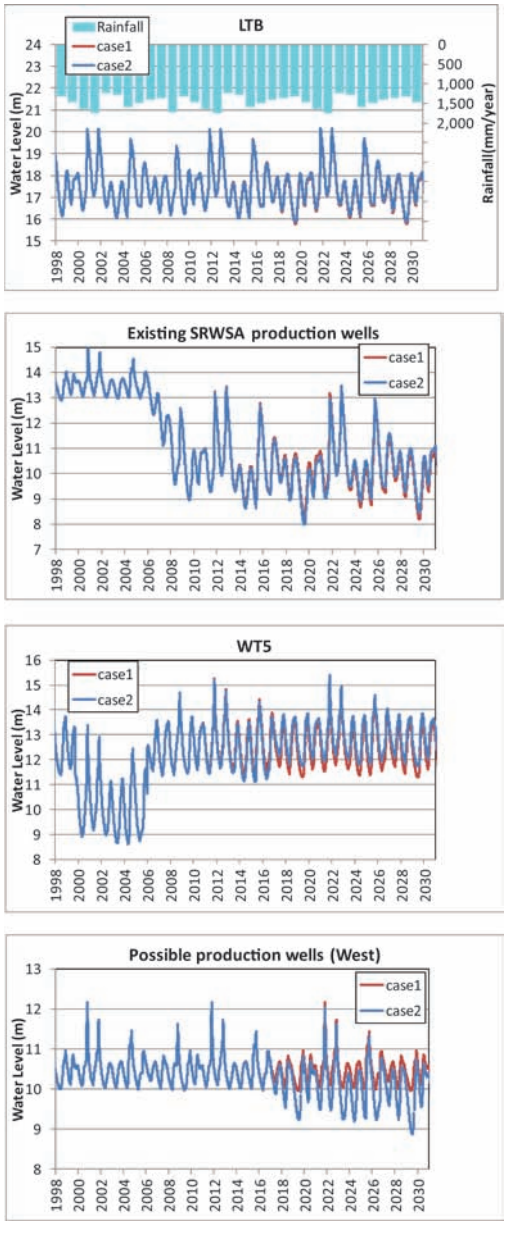

Figure 9. Groundwater table fluctuations at selected locations.

in 2006, the groundwater table recedes year by year but reaches to a certain level and does not recede below the lowest level in July 2019.

The lowest levels are 8.0 m in Scenario 1 and 8.2 m in Scenario 2. At LTB, the groundwater table in July 1998 is 16.1 m.

After the production wells started pumping, the groundwater tables begin to gradually recede and reach a certain level. The lowest levels are 15.8 m for Scenario 1 and 15.9 for Scenario 2 in July 2019.

At WT-5, the groundwater-table fluctuation shows the different manner to the other locations. The groundwater level declines from 11.5 m to 8.6 m, corresponding to the production well operation of the new French water supply system.

The pumping of 1,440 m^3/day started in 1999 and stopped in 2005. Then the SRWSA production wells with 9,000 m^3/day starts to supply water to Siem Reap city. According to the water supply plan, private and commercial wells in Siem Reap city stop their withdrawal equivalent to that amount, and so the groundwater level gradually rises.

The spatial distributions of the drawdown from July 1998 to July 2029 for Scenario 1 and Scenario 2 are shown in Figure 10 and Figure 11, respectively.

In both scenarios, the drawdown in the existing SRWSA production wells reaches to around 5 m, while that around Angkor Wat heritage area less than 0.3 m (Figure 10 and 11). In Scenario 2, around the production wells field along the lake shore, the drawdown is around 3.0 m. All the private, commercial wells except for the existing SRWSA and 53 possible production wells will be stopped pumping in this scenario, and thus the groundwater level

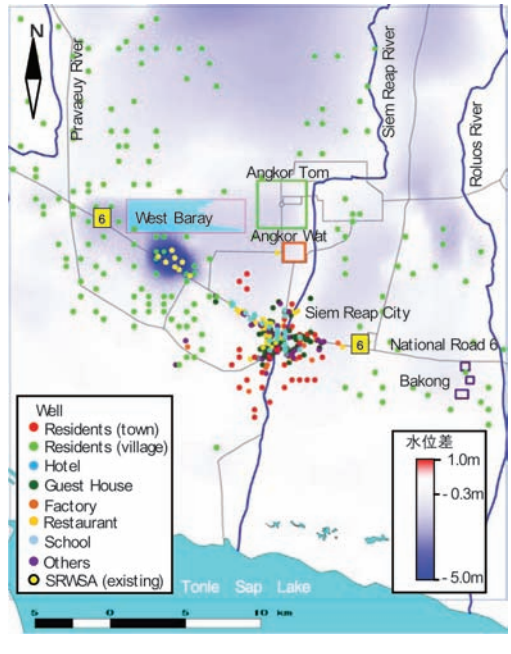

Figure 10. Predicted spatial distribution of drawdown from July 1998 to July 2029 for scenario 1.

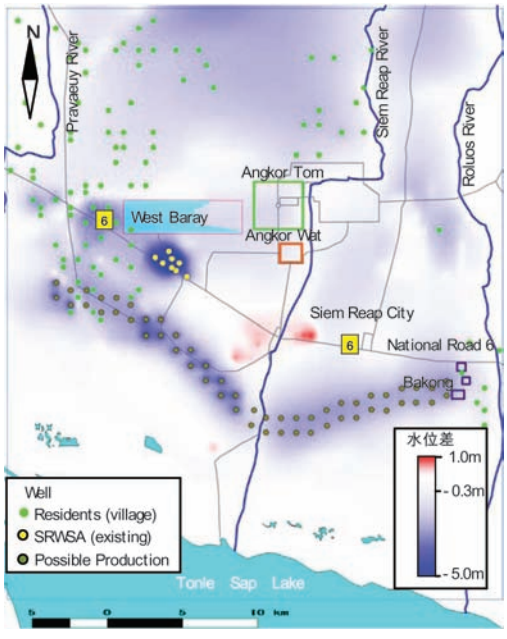

Figure 11. Predicted spatial distribution of drawdown from July 1998 to July 2029 for scenario 2.

will rise in the center of Siem Reap city. The rise reaches to 1.0 m at the east side of the city where the hotels pumps a certain amount of groundwater at present.

4 CONCLUSION

The groundwater simulations reveal that the influences of the existing SRWSA production wells and possible production wells will be limited in and around their well fields and does not extend to Angkor Wat. The drawdown around Angkor Wat is less than 0.3 m. Therefore, it is considered that these pumping plans will not cause land subsidence around the Angkor Wat because the groundwater is explored far from Angkor Wat. However, the groundwater simulation should be verified using future monitoring data such as groundwater level and ground displacement obtained by continuing the observation. Also the groundwater simulation model should be revised with additional information of the aquifer such as hydraulic conductivity and geological profiles and hydrological factors in the surface such as land-cover characteristics in order to obtain more reliable and precise prediction.

The groundwater withdrawal of commercial and public facilities in Siem Reap city has increased around seven times from 1998 to 2009.

The current amount is 4,850 m^3/day and the future amount in 2030 is predicted 13,500 m^3/day in this study. In the mean time, the simulation shows the aquifer underlying this region can physically produce 73,000 m^3/day, eight times of the current withdrawal of 9,000 m^3/day. However, all the production wells are located far from the Angkor Wat. The groundwater exploration should be avoided near the Angkor heritage, and an administrative system which instructs appropriate groundwater should be established.

REFERENCES

JICA 2000. The study on water supply on water supply system for Siem Reap region in Cambodia.

JICA 2011. The preparatory study on the Siem Reap water supply expansion project in the Kingdom of Cambodia.

Kumm, M. 2009. Water management in Angkor: Human impacts on hydrology and sediment transportation. *Journal of Environment Management 90:* 1413–1421.

McDonald, M.G. & Harbaugh, A.W. 1988. A three-dimensional finite-difference groundwater model. *U.S Geological Survey. Open File Report* 83–875.

This page intentionally left blank

Geotechnical Engineering for the Preservation of Monuments and Historic Sites – Bilotta, Flora, Lirer & Viggiani (eds)
© 2013 Taylor & Francis Group, London, ISBN 978-1-138-00055-1

Unsaturated sand in the stability of the cuesta of the Temple of Hera (Agrigento)

N. Nocilla, L. Ercoli & M. Zimbardo
University of Palermo, Italy

A. Nocilla
University of Brescia, Italy

P. Meli
Soprintendenza BB.CC.AA. di Agrigento, Italy

G. Grado, G. Parello & G. Presti
Parco Archeologico e Paesaggistico della Valle dei Templi di Agrigento, Italy

ABSTRACT: In the *Valle dei Templi* in Agrigento seven Doric temples stand lengthwise the crest of a rigid calcarenite cuesta over a layer of carbonate sand which lies along a thick stratum of clays. The environment is highly prone to landslides since topplings of calcarenite blocks often occur. The rock slopes are moving back and the slope edge draw near to the foundation of the Temple of Hera Lacinia contributing to increase their perilous condition. To assess the role of unsaturated sands in the instability processes, after the compositional and textural analysis of the material, direct shear tests and oedometer tests have been carried out on sand samples initially at the natural state, with low or very low values of natural water content, and finally at higher values of the saturation degree.

The mechanical behaviour of sands seems one of the main causes of the instability influenced by the presence of an open metastable structure, which develops through bonding mechanisms generated via suctions and/or through cementing material such as clay or salts.

1 INTRODUCTION

The *Valle dei Templi* in Agrigento (ancient Akragas) is one of the most outstanding examples of art and architecture in Magna Graecia. The Valley, which has been added in the UNESCO Heritage Site List, includes remains of seven temples, all in Doric style, that stand on the crest of a cuesta made of calcarenite overlaying a thin layer of sand, which overlies a stratum of clays. The environment is highly prone to landslides as highlighted by several previous studies that evidence both the role played by the discontinuity pattern in calcarenite and the role of the clays and sands in land forming processes (Croce et al., 1980, Cotecchia 1996). Cotecchia's work has also evidenced the role of earthquakes in the evolution of the territory, particularly from the point of view of the "human" landscape.

In 1976, on the E-NE slope close to the Temple of Hera Lacinia, a huge reactivated landslide occurred. This landslide, known and previously mentioned by Cavallari in his writing in 1883, involved the whole outcropping stratigraphy, from the deep clays up to the calcarenite bench (Musso & Ercoli 1988, Cotecchia et al., 1995). According to Cotecchia et al., the intense rainfall, which occurred just before the event, is the main cause of the landslide reactivation. This seems to be confirmed by the Royal Commission, presided over by the Prince Lanza di Scalea in 1883: although in the stratigraphy no sand layer is identiied, the stability of the cuesta, the Temple and its access route is influenced by the "softening" of the basal clay stratum and by the condition of the rock "calcareous tuff made of shells fragments" ("tufo calcare conchilifero") under the stratum, which "tends to disintegrate under mechanical and chemical actions". The Royal Commission indicated the erosion, caused by rainfalls and wind actions, as the origin of the instability and consequently arranged structural operations in order to limit erosion and further instabilities.

Nowadays, the mechanical behaviour of the sand layer seems to have a key role in the understanding of the mechanisms of instability. Several year long in situ observations and a laboratory experimental programme enabled the authors of the present

paper to ascribe the problems of instability to the mechanical behaviour of the sand layers.

Several studies (Fredlund & Rahardjio 1993, Fredlund & Xing 1994) have highlighted that the "rock like" behaviour of partially saturated sands is caused by low water contents and consequentially by elevate suctions that might arise in such materials.

Relatively large suctions and strengths can arise in uncemented coarse-grained soils with very low water contents after the application of high compressive stress, as recently studied by Atkinson & Nocilla (2003). In their work the application of high compressive stress was one convenient method for achieving the required suction and a metastable structure. The presence of a metastable structure is caused naturally by various geologic and geomorphologic processes and it is a prerequisite to the formation of a collapsible deposit (Dudley 1970). In this perspective the sands of Agrigento have the suitable characteristics for studies on the presence of a metastable structure on the mechanical behaviour of coarse grained soils.

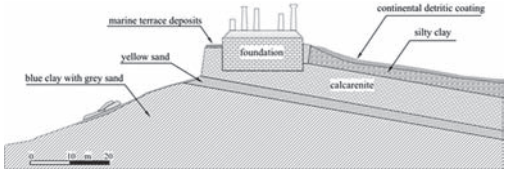

Figure 1. Stratigraphic section.

Figure 2. The sand layer and the overlying calcarenite.

2 INSTABILITY PROCESSES

The Valley of Temples stands on the southern limb of an asymmetrical gently sloping syncline made of calcarenitic benches and interbedded sand, sandy clay and clay of the Pleistocenic age. The northern limb is steeper than the southern and the axis is oriented towards W-NW/E-SE.

In spite of the occasional typical badlands surface configuration on the southern limb, the clay slopes exhibit a rather uniform profile. According to the stratigraphy furnished by the *Parco Archeologico e Paesaggistico della Valle dei Templi di Agrigento,* the blue clay, which contains grey and slightly silty sands, are offlapped by a few meters thick layer of yellow sand, which underlies an abrupt calcarenite plate about 10 m thick (Figs. 1, 2).

In the geological scheme by Ruggieri (1961) this plate is the III level of calcarenite. On the top of the calcarenite plate, there are: another layer of silty clay, a thin layer of marine terrace deposits and finally, a few meter thick detritic coating of continental origin.

Over the centuries, the landscape has acquired the typical geomorphological setting of cuestas, which is due, as indicated by many authors, to selective erosion, therefore a considerable undermining of the calcarenite plate has taken place. Several serious instability processes have been affecting foundation soils in the archaeological area where landslides often occur. When the instability reaches the upper slopes, the calcarenite rocks are subject to topplings (Figs. 3, 4).

Figure 3. An incipient toppling.

Figure 4. Aerial photo of the Temple of Hera: Note the fallen blocks and the fractured cliff face.

This instability affects the morphology of the site, where the rock slopes are moving back.

The situation of the south-east cuesta edge is particularly interesting: the well preserved Doric temple, the Temple of Hera Lacinia, is located on its top, as shown in Figure 4.

The cliff faces of the cuesta edge are exposed towards south, aligned with the direction of the stratum, and by faces oriented towards E-NE, which is approximately the corresponding dip direction.

At the end of the nineteenth century, as referred to by Cavallari (op. cit.) and the Royal Commission records presided over by the Prince Lanza di Scalea (op. cit), it was already known that the deep foot erosion of the sand layer was coming to light again and was aggravating the condition of both the natural cliffs and the coating walls increasing the concerns for the safety of the Temple foundations. Several works aiming at improving the stability such as stone ashlars or brickwork "fillings" had been carried out in the past (Cavallari, op. cit.).

For instance, a retaining wall was built on the south side and in proximity of the SW and SE corners of the cliff where the Temple is based.

This "substructure" of supporting buttresses, as shown in Figure 5, was built taking into account a potential excess of flowing water, hence the construction of a catch-water and a drainage system situated along the back side of the retaining wall, between the Temple's basement and the cuesta edge, reinforced by further underpinning.

According to the stratighraphic section supplied by the *Parco*, the foundation of the temple of Hera is still an original Greek manufacture, set 6 m deep at most in the calcarenite bench.

As shown in Figure 6, an exploratory excavation gave access to the observation of the bare foundations, formed by large *isodomum* blocks, separated from debris soils with an impressive French drain,

Figure 5. Old photograph showing the underlying retaining structure beneath the western cliff of the Temple.

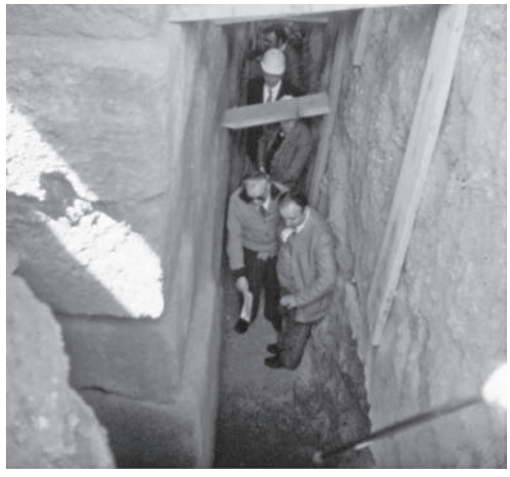

Figure 6. The Temple foundations.

which is situated all around the foundation wall and under the Temple's floor.

The study presented in this paper focuses on the 3 m sand layer situated underneath the Temple starting from 2 to 6 m below foundations.

In the area of the Temple, the groundwater table located 20 ÷ 25 m underneath the topographic surface in correspondence of the upper calcarenite plate, descends progressively along the slope until it reaches almost ground level, in proximity of the bottom of the valley.

3 CLASSIFICATION AND PETROGRAPHIC CHARACTERIZATION

The experimental programme and the numerical modelling have been carried out in the laboratories of the DICAAM Department of the University of Palermo and DICATAM Department of the University of Brescia.

A preliminary observation *in situ* revealed the presence of a sand which apparently seems a weakly cemented locked sand. Because of their consistency, an electric saw was used to take parallelepipedal samples of several cubic decimeters. The shape and the dimension of the samples have been chosen accordingly to match the standard sample packing used for mechanical testing.

The particle size distribution resulting from the tested soil revealed a fine and medium sand characterized by a quite high uniformity coefficient (Fig. 7).

As for the sand properties, the particle density is 26.47 kN/m^3, the bulk density is 15 kN/m^3, the porosity is between 45%–54% with an average value of $n_{average}$ = 49%, the degree of saturation in situ is much lower than 100%, between 6% and 9%.

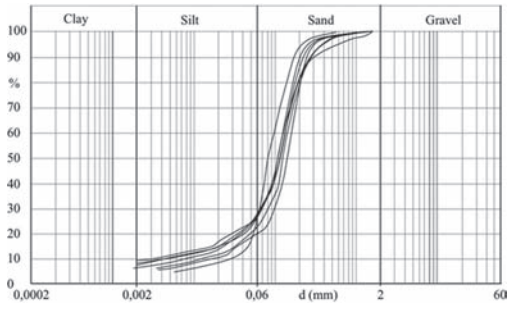

Figure 7. Particle size distribution of the analysed sands.

The slaking test provides a very low value of the durability index (Id < 50%). However, although the soil does not present neither the typical low porosity of dense sands nor the typical values of the durability index of the weakly cemented sands, the consistency of this soil and its ability to be moulded indicates non-zero values of strength that seem to be caused by the high values of negative superficial stresses between grains, resulting from the reduced water content.

The textural and petrographic characterisation of the sands has been performed by means of the observation of four thin sections in transmitted light (Fig. 8).

According to Zimbardo et al. (2011), the pores can be classified as *macropores* when their size is a multiple of the modal size of the grains, *mesopores* when they have about the same size of the modal size of the grains, and *micropores* when the size is lower than the modal size of the grains or like the smallest grains.

The soil fabric of the present case study can be described as a sponge type (lithotype B), with the area of all *macropores* much smaller than the *mesopores*.

Although the intraparticle pores contribution to the total porosity is very high, an amount of these pores (less than 10% of the total porosity) are close and not destroyable during saturation or mechanical tests. For this reason, the interparticles pores, in spite of their low amount, have a bigger impact on "collapsibility".

The composition of clasts is rather uniform. In more detail the clasts are made of quartz, fragments of mollusca shells, foraminifera and plates of echinoderms, algal micrite and microsparite. The relative abundance of each type of clasts is variable. As shown in the thin section of Figure 8 two irregular areas are detectable: the A area, where quartz clasts prevail and the B area, where bioclasts prevail. As for the quartzose clasts, they are generally composed by monocrystalline grains. Composition percentages are listed in detail in Table 1.

As for the particle size distribution, the quartz grain dimensions are between 25–500 μm, with a

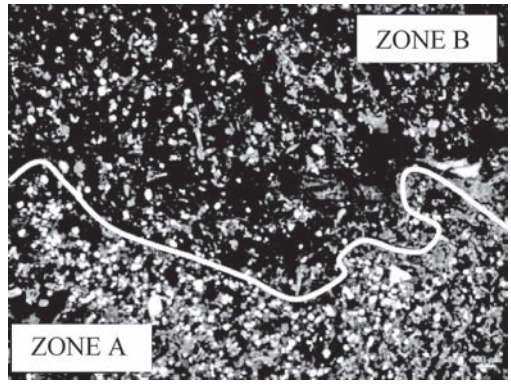

Figure 8. Thin section (7x magnification, cross polarized light) and relative composition of zones A and B.

Table 1. Composition of zones A and B.

Composition	A	B
Quartz	50%	30%
Bioclasts	20%	55%
Micrite microsparite	20%	55%

modal value of 130 μm; the dimensions of fragments of mollusca shells and foraminifera exoscheletons are between 100–600 μm; the micrite grain dimensions are between 80–230 μm; the microsparite grain dimensions are between 130–260 μm and the dimensions of the plates of echinoderm are about 320 μm. Only as much as 0,5% of both quartz and microsparite grains have dimensions bigger than 500 μm. Fragments of fossils of 900 μm are also present.

Roundness is low in most cases. Sphericity is variable. The grain contacts are of flat type or concave-convex and tangential type, with a predominance of flat contacts. However, the presence of pelitic and silty coats that cover grains often prevent their direct contact (Fig. 9).

The presence of particles of such a nature aroused special interest. In the literature regarding the mechanical behaviour of partially saturated soils (Collins & Mc Gown 1974, Alonso et al., 1987), the presence of these kind of particles is considered of fundamental importance because, together with the type of grain contacts and pore geometry, it affects the way in which water wraps solid particles (Kezdi 1974) and the continuity, distribution and interaction among solid, liquid and gaseous phases in the material (Wroth & Houlsby 1985).

Hence, it affects the presence and the intensity of suction forces resulting from the presence of menisci.

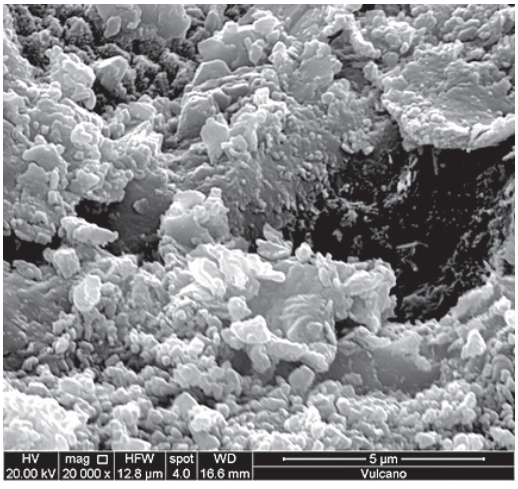

Figure 9. SEM photograph: Tabular silty particle aggregates are present (see lighter zones).

According to the classification suggested by the aforementioned authors, the sand layer considered in this paper can be included in a class of soils with a continuous gaseous phase ad a discontinuous liquid phase. This condition is typical of natural soils, common in dry areas where the degree of saturation is very low (S << 100%).

According to many authors (Barden et al., 1973, Clemence & Finbarr 1981, Rogers 1995) bonding mechanisms in collapsible soil can be classified in three main types: by capillarity or matric suction forces, clay and silty particles at coarser particle contacts and cementing agents such as carbonates and oxides. According to the durability test results obtained on the investigated sand, the bonding mechanism seems to be able to be attributed only to capillarity or matric suction forces. Although fabric lacks a simple quantitative descriptor (Alonso 1993 as cited by Pereira & Fredlund 2000) it is widely recognised as important in explaining collapse behaviour. In order to ensure realistic assessments about the mechanical behaviour of this sand, the nature of weak connectors (the coating pelitic and silty particles) present will be investigated in future research together with their mineralogical nature.

4 MECHANICAL CHARACTERIZATION

The testing programme consisted of 8 direct shear and 3 oedometer tests. Direct shear tests have been carried out under 8 different vertical loads, from 25 kPa to 300 kPa, as shown in Figure 10. The direct shear tests have been performed with a non–standard procedure: samples have been set up and initially loaded for a period of 24 hours at their natural water content. Very low values of the natural water content ($1{,}8\% < w_N < 3\%$) and a degree of saturation between 6% and 9% have been detected.

After the initial 24 hours, samples have been flooded and wetted at a constant load for additional 24 hours. As a last stage, standard shear tests have been carried out.

Regarding the oedometer tests, samples have been consolidated under vertical load at a natural water content below 3%. In correspondence of 3 different vertical stresses, respectively of 1.54 MPa, 3.22 MPa and 7.26 MPa, the three samples have been flooded and wetted.

After settlement completion, a new step of load has been applied. Settlements caused by each load have been recorded by the displacement transducer.

During the direct shear tests, a particular attention was required when applying vertical stresses, before and after cell flooding and the consequential sample wetting. A vertical strain occurs rapidly after wetting and, even in the case of low vertical applied stresses, it can reach the 1% of the initial sample thickness in few minutes. This percentage tends to increase with the increasing of the applied vertical stress. In Figure 10 experimental values of the void indexes variations (Δe) for different values of normal applied stress (σ_n), after cell flooding are shown and the equation of the best-fit line presented. In the same diagram, labels with degree of saturation values at the beginning and at the end of each test show that the final degree of saturation is always lower than 100% after the flooding of the cell. The water content increases but never saturates samples completely.

As for the oedometer tests, in Figure 11, the void ratio against the vertical applied load has been plotted and the vertical stress corresponding to the cell flooding and sample wetting has been highlighted.

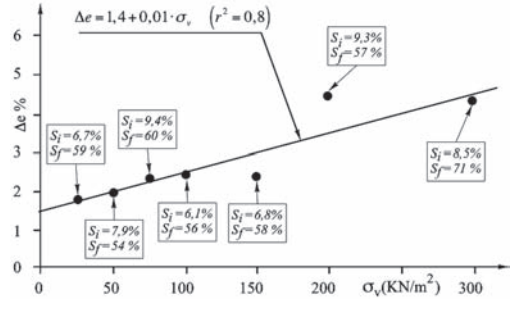

Figure 10. Quick variations of void indexes (Δe) for different values of normal applied stress, after cell flooding.

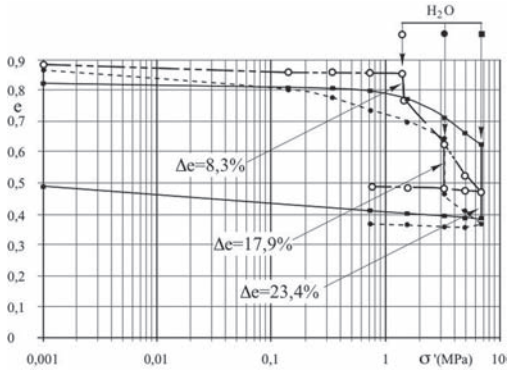

Figure 11. Compression paths during oedometer tests.

Accordingly to the illustrated compression paths, quick settlement with increasing intensity occurs when the flooding is applied in correspondence of the given vertical stress. When the unloading is applied, the irreversibility of the compression is evident: this is due to the structural "collapse", resulting from the erasing of the suction forces. These suction forces have a "structural" role (Kavvedas 2000), which is comparable to weak cementation or to grain locking for those material for which, if a collapse occurs, a fabric destruction is identified similarly to what described by Gens et al. in 1995.

Similar collapse phenomena, caused by wetting of the material, have been observed in Aeolian fine sand deposits in South Africa (Jennings 1965) or Naples volcanic tuff (Feola et al., 2004, Evangelista et al., 2004).

In conclusion, two separate settlement developments have been observed respectively during the two phases: a first phase of the test carried out on samples at their natural water content, and a second phase conducted after wetting. The two recognizable compression paths are separated by the quick settlement, which corresponds to the collapse originated by the wetting phase. According to these results, the artificial wetting of the soil is clearly unable to erase completely the suction forces of menisci, similarly to what occurs in natural soils after a rainfall, no matter how intense. Residual suctions guarantee non-zero strength even in presence of elevate and irreversible strains.

5 THE MODELLING PROCESS

In order to perform the stability and safety analysis, a modelling process has been carried out for the site under investigation. Although a more sophisticated analysis involving a more complex partially saturated soil characterization is advisable, at this level of the research, a simple Mohr-Columb strength failure criterion has been considered appropriate and the numerical analysis has been carried out in a plane deformation state using the finite element program Plaxis, once defining and quantifying the geometry of the boundary value problem under investigation.

The foundation soil section consists of an 8 m thick layer of calcarenite overlying a 3 m thick stratum of sand, situated over the clayey deposit. The above assumptions, although simplified, allow a first understanding of the essential elements of the mechanical behaviour of this case study.

Figure 12 also illustrates the mechanical parameters obtained from the experimental tests on the sand and successively used in the model. Regarding the clay deposit and the layer of calcarenite parameters, labels with values are also reported. The values have been obtained from the literature review and from previous research studies. In detail, Musso & Jappelli (1980) and Croce et al. (1969) reports provided the values of clay parameters and Evangelista & Pellegrino (1990) the values of calcarenite parameters. After determining the initial stress state resulting from the stratigraphic sequence shown in Figure 1, the changes in stress states have been calculated.

Changes in stresses have been estimated considering the partial destructuration of sands, resulting from the increased natural water content only.

The increment in the degree of saturation in sands is due to the permeability deriving both from calcarenite porosity and from the subvertical discontinuities in the calcarenite stratum.

Along the crest of the calcarenite cuesta, all around the temple, discontinuities have a spacing of 4–5 m so that, in the modelling process, the quick strain which occurs in sands after wetting, has been taken into account in two different analyses: the first in which the sand strains occur for 5 m from the cuesta edge, and the second for which strains occur for 10 m from the same edge. In this first phase of the analysis the vertical contact stresses between the sand layer and the calcarenite cuesta have been

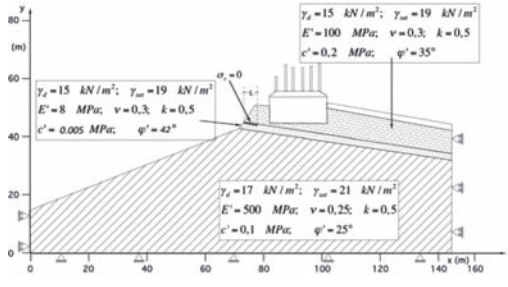

Figure 12. Geometry of the boundary value problem under investigation.

considered equal to zero. In other words, a condition hardly reachable in reality has been simulated in order to perform the sand layer settlement according to the laboratory test results. A lithostatic initial stress state and a value of 0.5 coefficient of earth pressure at-rest have been chosen by the authors: shear stress contours are illustrated in Figure 13a. It is worth noticing that, in uncemented soil, the volume change associated with "collapse" is confined to the wetted zone (Fredlund & Gan 1995). Hence, two simulations corresponding to different saturation conditions of sand have been performed (Figs. 13b, 13c). The two analyses highlight the change in stress states with the inwards progression of the wetting of the sand. In the first case (L = 5 m), the ratio between the mobilised shear strength to the available shear strength tends to unity in the wetted zone. In the second case (L = 10 m) in accordance to the extension of how much the wetting process has moved inwards, this ratio remains below the unity and the safety conditions are improved, if tensile stresses that might cause plastic points in the calcarenite cuesta are not considered. The analyses illustrated in Figure 14a, for the L = 5 m case and in Figure 14b,

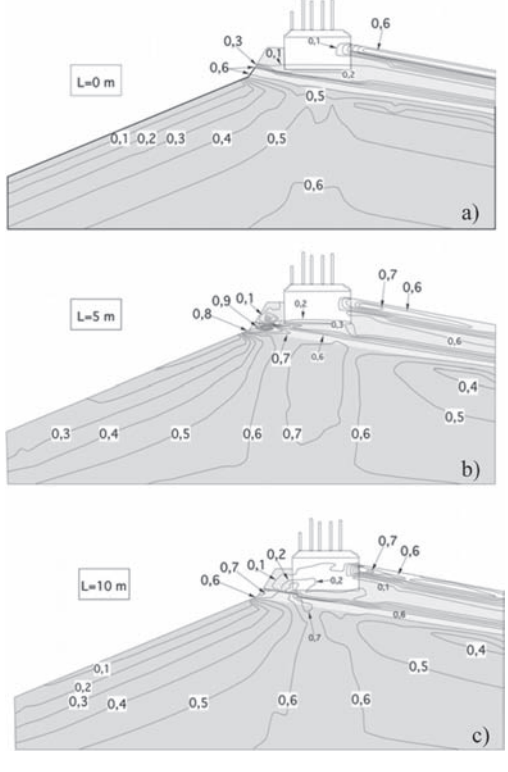

Figure 13. Relative shear stress contours in a) Lithostatic state, sand at the natural water content b) Wetted sand zone 5 m long c) Wetted sand zone 10 m long.

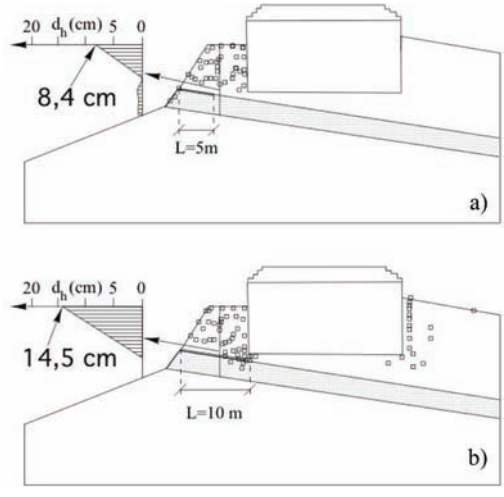

Figure 14. Plastic points and horizontal displacements d_h for a) Wetted sand zone 5 m long b) Wetted sand zone 10 m long.

for the L = 10 m case, pinpoints the following: plastic points might occur in the calcarenite cuesta in both cases, resulting from tensile stress states, which might also arise on the right of the Temple for L = 10 m (Fig. 14b). Figures 14 include horizontal displacements in the vertical section comprehensive of both the sand and the calcarenite layer.

As highlighted, displacements can reach the value of 10 cm and more: this result, together with what previously detected about the destructuration process of sands, indicates that toppling failures might arise in the calcarenite cuesta. Summarising, at the top of the calcarenite cuesta, displacements, which are decreasing in depth towards the contact with the underlying sands, might occur as typical in toppling movements. As a result of this background, the subvertical discontinuities in the calcarenite cuesta might be connected to the deformation mechanisms in the sand layer and in the underlying clay deposit and not only to the uplift phenomena, as reported by several authors so far.

6 CONCLUSIONS

The behaviour of the investigated sand has been recognized by the authors of the paper as typical of collapsible soils of which an essential requirement is that an open metastable structure develops through bonding mechanisms. To achieve this open structure, bonding between particles or grains of sufficient strength must occur which, when weakened by the addition of water, allows particles

to slide over one another, resulting in collapse. According to the durability test results obtained on the investigated sand, the bonding mechanism seems to be able to be attributed only to capillarity or matric suction forces. In order to ensure realistic assessments about the mechanical behaviour of this sand, the nature of the weak connectors present will be further investigated.

The direct shear and the oedometer test experimental results during consolidation show that vertical strains occur rapidly after wetting and that, even with low vertical applied stresses, the settlement can reach the 1% of the initial sample thickness in few minutes under constant load. Settlements occur because of the suction stresses reduction after flooding. These suction forces have a "structural" role. The volume reduction progressively increases with the increasing of the external applied stress. In the *in situ* calcarenite, the primary permeability and, above all, the presence of subvertical discontinuities, allow elevate amount of water to flow in the case of high intensity rainfall phenomena. As a consequence, an important increment of the water content takes place in the underlying sand layer, which usually has a very low degree of saturation. Although the full saturation is not reached, the suction stresses decrease and a structural settlement occurs.

As indicated by many authors, the geomorphological landscape evolution has been attributed to a considerable undermining of the calcarenite, in which sands participated because of their aptitude to Aeolic erosion and splash erosion only.

The present study introduces sand collapse, resulting from the suction stress reductions, as the main cause of the toppling failures that might arise in the calcarenite cuesta, where the subvertical discontinuities might keep on developing. As highlighted by the numerical analyses, further instability phenomena might arise because of the plastic conditions, due to tensile stresses, reached in the sand layer and in the calcarenite bench.

In the sand layer, the plastic strain accumulation, can be a contributory to its elevate aptitude to erosion, the more so since the erosion occurs even in areas protected by vegetation, which mitigate the wind and splash erosion impacts. What kind of role deeper sand layers situated in the deeper clay deposit might have had in the instability phenomena of the past and in the slope stability in general, still needs clarification. In this far from encouraging context a monitoring of the instability processes in relation to sand decay is of the upmost importance and presently being scheduled be the *Ente Parco Archeologico e Paesaggistico della Valle dei Templi* in charge of monitoring the stability of the temples since decades.

ACKNOWLEDGEMENT

The authors are grateful to Prof. ssa M. Santamaria and to Ing. F. Di Franco for scanning electron microscope.

REFERENCES

Alonso E.E., Gens A., Hight D.W. 1987. Special problem soils. General Report. In: *Proc 9th Eur Conf on Soil Mechanics and Foundation Engineering*, Dublin, Ireland 3:1087–1146.

Atkinson J., Nocilla A. 2003. Suction and strength in heavily compressed carbonate sand. 2003 *Géotechnique* 53, no. 9, 831–832.

Barden L., McGown A., Collins, K. 1973. The collapse mechanism in partly saturated soil. *Engineering Geology*, 7, 49–60.

Cavallari C. 1883. Rapporto dell'Ing. topografo Cristoforo Cavallari sui Danni avvenuti al muro di sostegno della strada di accesso al Tempio di Giunone Lacinia e visita alle antichità di Girgenti, in data 19genn. E 30 apr., *Archivio centr. dello Stato,* II vers, II serie, busta 147 fasc. 1713.

Clemence S.P., Finbarr A.O. 1981. Design considerations for collapsible soils. *Journal of Geotechnical Engineering*, 107(3), 305–317.

Collins K., McGown A. 1974. The form and function of microfabric features in a variety of natural soils. *Géotechnique*, Volume 24, Issue 2, pages 223–254

Cotecchia V., D'Ecclesiis G., Polemio M. 1995. La dinamica dei versanti della Valle dei Templi di Agrigento. *Geologia applicata e idrogeologia* Bari, volume XX—parte I.

Cotecchia V. 1996. Geotechnical degradation of the archaelogical site of Agrigento. *Arrigo Croce memorial Symposium*, Balkema.

Croce A., Jappelli R., Pellegrino A., Viggiani C. 1969. Compressibity and strength of stiff intact clays. *Proc. VII Int. Conf.on Soil Mechanics and Foundation Engineering, Mexico City*.

Croce A., De Miro E., Fenelli G.B., Jappelli R., Liguori V., Morandi R., Nocilla N., Pace E., Pellegrino A., Rossi Doria P. 1980. La Città di Agrigento e la Valle dei Templi. *Questioni di stabilità del territorio e di conservazione dei monumenti XIV Conv. Naz. di Geotecnica*.

Dudley, J.H. 1970. Review of collapsing soils. *Journal of Soil Mechanics and Foundation Division, ASCE*, 96(3), 925–947.

Evangelista, A., Pellegrino, A. 1990. Caratteristiche geotecniche di alcune rocce tenere italiane. *Le rocce tenere: terzo ciclo di conferenze di meccanica e ingegneria delle rocce*.

Evangelista A., Nicotera M.V., Aversa S. 2004. Un'apparecchiatura di taglio a suzione controllata per lo studio delle condizioni di innesco dei fenomeni franosi nelle coltri piroclastiche, *XXII Convegno Nazionale di Geotecnica, Palermo 22–24 settembre 2004*.

Feola A., Lombardi G., Pellegrino A., Viggiani C. 2004. I dissesti di Via Settembrini a Napoli a seguito dell'evento piovoso del 15 settembre 2001. *XXII Convegno Nazionale di Geotecnica, Palermo 22–24 settembre 2004.*

Fredlund D.G., Rahardjo H. 1993. Soil mechanics for unsutered soils. Wiley and Sons, Toronto.
Fredlund D.G., Xing A. 1994. Equation for the soil water characteristic curve. *Can. Geotech. J*. 31, 3.
Fredlund D.G., Gan J.K.M. 1995. The collapse mechanism of a soil subjected to one-dimensional loading and wetting. In *Proceedings of NATO Advance Workshop on Genesis and Properties of Collapsible Soils* (eds Derbyshire, E., Dijkstra, T. and Smalley, I.J.). Loughborough, April 1994, pp. 173–205.
Gens, A., Alonso E.E., Suriol J., Lloret A. 1995. Effect of structure on the volumetric behavior of a compacted soil. *Proc. 1st Int.Conf on Unsatured soil. NSAT97*. Alonso, Delage eds. Paris.
Lanza Di Scalea F. 1883. Verbali della Commissione per la conservazione e i restauri delle antichità agrigentine 11, 12 e 17 ott, *Archivio centr. dello Stato,* II vers, II serie, busta 147 fasc. 1713.
Jennings J.E. 1965. Theory and practice of construction on partly satured soils as applied to South African conditions. *Proc. Int. Conf. expansive Clay Soil. Texas A.M. Press.*
Kavvadas M.J. 2000. Modelling the soil behaviour—Selection of soil parameters. *The Geotechnics of Hard Soils—Soft Rocks—Balkema,* Rotterdam.
Kézdi A. 1974. Handbook of soil Mechanics—Soil physics, Elsevier Amsterdam, Oxford, New York.
Musso A., Jappelli R. 1980. Indagini relative al movimento franoso del Dicembre 1976 che ha interessato la Valle dei Templi di Agrigento. *Rapporto di ricerca ex istituto di geotecnica e arte mineraria dell'Università di Palermo.*
Musso A., Ercoli L., 1988. Monuments and landslides in the Agrigento Valley. Proc. Int. Symp. IAEG The engineering geology of ancient works, monuments and historical sites. Balkema ed.
Pereira, J.H.F., Fredlund, D.G. 2000. Volume change behaviour of collapsible compacted gneiss soil. *Journal of Geotechnical and Geoenvironmental Engineering*, 126(10), 907–916.
Rogers, D.D.F. 1995. Types and distribution of collapsible soils. *In Proceeding of NATO Advance Workshop on Genesis and Properties of Collapsible Soils* (eds Derbyshire, E., Dijkstra, T. and Smalley, I.J.). Loughborough, April 1994, pp. 1–17.
Ruggeri G. 1961. Commenti ad una recente nota sul Pliocene in Sicilia. *Rivista Mineraria Siciliana* n° 70–71.
Wroth, C.P., Houlsby G.T. 1985. Soil mechanics: property characterization and analysis procedure.
Zimbardo M., Nocilla N., Ercoli L. 2011. Petrographic and textural characteristics and mechanical behaviour of Sicilian calcarenites. *Proceedings of the 15th European Conference on Soil Mechanics and Geotechnical Engineering (geotechnics of hard soils/soft rocks*). A. Anagnostopoulos al. (Eds.)

This page intentionally left blank

Geotechnical Engineering for the Preservation of Monuments and Historic Sites – Bilotta, Flora, Lirer & Viggiani (eds)
© 2013 Taylor & Francis Group, London, ISBN 978-1-138-00055-1

Slope consolidation of Monteagudo de las Vicarías castle (Soria)

C.S. Oteo
Prof. Dr. Eng. C. C. & P. A. G. I., S. L. Madrid, Madrid, Spain

P. de la Fuente
Prof. Dr. Eng. C. C. & P. Polytechnical University of Madrid, Madrid, Spain

ABSTRACT: This paper describes the consolidation work on the slope of Monteagudo de las Vicarías Castle, located in the province of Soria (Spain), carried out between September 2004 and March 2005. The tasks were carried out as emergency works, under the management of technicians from the Regional Government of Castilla y León, according to the directives provided by the geotechnical-structural studies, in order to resolve issues related to the castle resting on a calcareous crust, under which a clay layer was being eroded. This paper explains the most important antecedents in relation to the consolidation work on the slope and provides a summary of the work carried out to reinforce the foundations of the Castle and the structure of the Honour Tower. Moreover, it includes the results of the instrumentation installed and controlled during—and after—the reinforcement works.

1 ANTECEDENTS PRIOR SURVEYS AND STUDIES

Under commission by the Council for Education and Culture by the Regional Government of Castilla y León (Spain), in May 2002, the Fundación Agustín de Betancourt made a report on the geotechnical factors for restoration of the Monteagudo de las Vicarías Castle (Soria). That document, prepared by the authors of this paper, gathered the available information, analysed the situation of the monumental complex from the geotechnical point of view, and established a proposal of situations aimed at consolidating the slope. In April 2004, the Council for Culture and Tourism of the Government of Castilla y León authorised execution of the emergency works of Consolidation of the slope of the Monteagudo de las Vicarías Castle (Soria), by the company CONDISA.

Monteagudo de las Vicarías Castle, a gothic construction from the 15th Century, is located in the town with the same name, in the south east of the province of Soria (Center of the Spain). The castle has a pentagonal ground plan and covers an area of about 800 m^2 on a hill crowned by limestone (Fig. 1). Diverse shaped towers are included in the complex, particularly the Honour Tower, that is octagonal shaped.

Although some elements of the castle have been restored in recent times, over the last 15–20 years there has been major deterioration of the Honour Tower, shown by vertical cracks that indicate movement of the tower toward the steep slope on which the monumental complex stands.

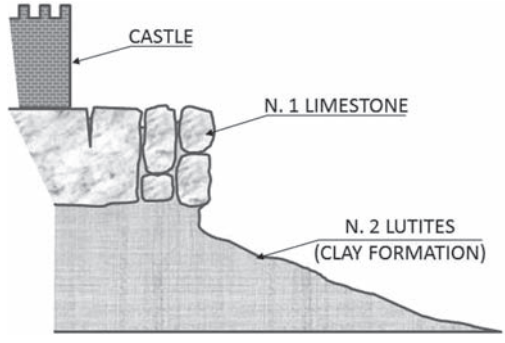

Figure 1. Geological profile of the zone.

Based on the descriptions recorded in the prior test drilling, the following levels are distinguished within the hill on which the castle stands (Fig. 1):

- Level 1: comprised of marly limestone, of small interspersed amounts of clayey material. The average thickness of this level is 2.50 metres.
- Level 2: it is a formation of lemonites and/or lutites. The upper part of the level (between 1.5 and 2.0 metres) has a greater content of the sandy fraction and the calcareous component. It is not a rocky formation, but rather a ground that is lightly cemented by carbonates and is liable to water erosion.

An anthropic level of 0.5 metres has been identified within the castle, comprised of grey silty sand. The existence of filling at some points on the slope was also observed. During performance of the prior test drilling, the presence of a water table was not detected. The Lefranc trials showed that Level 2 of lutites was practically impermeable. Level 1 of limestone had a permeability of about 10^{-3} cm/sec. The calcareous crust on Level 1 had an unconfined compressive strength exceeding 35000 KN/m^2, with a dry bulk density of 24.6–24.8 KN/m^3. It was a practically horizontal level in which fissures and vertical diaclasses appeared, that tended to conform the limestone in nearly isolated blocks (Fig. 1).

On Level 2 of lutites, the fine content generally exceeded 96%, with medium-high plasticity, with a liquid limit between 40–65 and a plasticity index between 15 and 30. The dry density was located between 14.8 and 19.0 KN/m^3 and the natural humidity between 16% and 29%. In the unconfined compression strength, q_u, obtained extreme values of 110 KN/m^2 and 469 KN/m^2, although generally q_u was higher than 200–300 kN/m^2, that allowed that level to be classified as "soil" and one might add the qualifier of cohesive, with medium-high strength. No erosion factor trials were carried out in the laboratory but "in situ" signs were noted of the action of water on that "lutite" or clay, facilitated by its plasticity and slight degree of expansiveness. This was also shown by the soft natural slope it had.

Fig. 2 is an old panoramic view (1933) of the castle and the limestone slope. The most affected element of the monumental complex is the Honour Tower. Several vertical cracks are noted in the tower. Some of those cracks affected the tower itself, and others are located at the adjoining walls. These cracks appear to indicate movement of the tower, or part of it, toward the slope.

Figure 2. Monteagudo de las Vicarias Castle. (Carrascosa, 1933).

A masonry wall was added to the foot of the Tower in previous times, that is now very deteriorated (Fig. 3 and Fig. 4).

That wall is prior to 1950, subsequently having been repaired. As a possible cause of breakage of the wall, one may state the existence of vertical fractures in the calcareous formation.

The alterations due to changes in water content, temperature, etc., are introduced in the fissures.

Due this influence, hydrostatic thrust of the water in these fractures configure isolated blocks of limestone rocks, of metric size that, not being well supported on the lutite level either, as the contact between formations was eroded, eventually came loose from the calcareous formation. Some of these blocks of rock were smaller and were already nearly isolated due to the environmental splitting up. The movement of those blocks of rock in the rocky mass—due to erosion of the lutite or underlying clay—undoubtedly contributed to breakage of the wall, the design of which must not have foreseen major horizontal thrusts (such as those of water). Notwithstanding the reasons stated, at the foot of the wall, resting directly on the zone nearest to the surface, that is altered by the lutites,

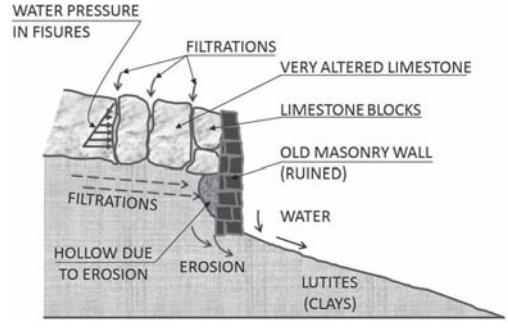

Figure 3. The wall in their initial situation and the enviromental erosion.

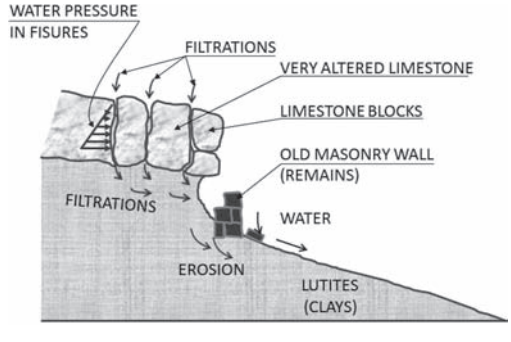

Figure 4. The old mansonry wall: Actual position.

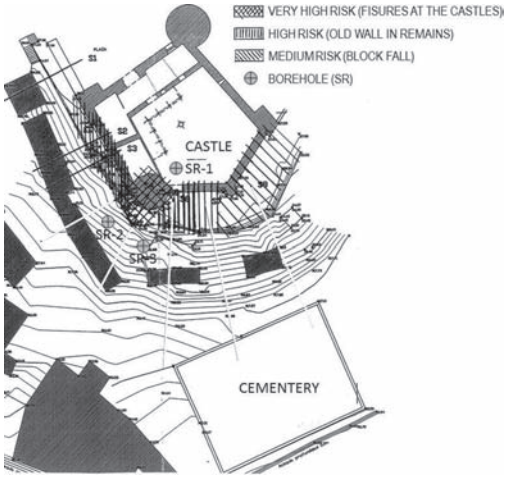

Figure 5. Risk at the different castle zones.

it may have suffered some movement, partially due to deformation of the ground, but also due to circulation of water over time, that is highly intense in the limestone-lutite contact. These movements, even when small, were sufficient to break the wall (Fig. 4).

The alteration of the limestone formation and formation of blocks that gradually became independent within the perimeter of the calcareous crown, contributed decisively to the movement of part of the area supporting the Honour Tower, a movement shown by the vertical cracks that exist on its faces and the cracks that are visible where the tower meets the adjoining walls.

Fig. 5 shows the ground plan of the zone and the existing risk classification, according to the problems detected.

2 CONSOLIDATION WORK ON THE SLOPE

From a geotechnical point of view, the deterioration of the monumental complex and, particularly, of the Tower, that was caused by the movements originated when large blocks of limestone came apart on the perimeter of the calcareous complex crowning the hill on which the castle stands.

The solutions aimed at stabilising the Tower and castle walls must avoid progress of the vertical cracks in the calcareous formation, as well as erosion in the limestone-lutite contact. The most adequate solution was considered to be to build a wall on the perimeter of the limestone slope in order to avoid horizontal movement of the blocks, for which the foundations should be very well laid (using micropiles, in order for them not to be affected by surface erosion of the clay). Moreover, in the more massive rock zones, it was necessary to prevent their movement, previously pinning that rock with bolts in resin or injected with grout. The bolts would allow the joints to be stitched together and confine the rocky mass, avoiding progression of the vertical fractures on the perimeter of the calcareous formation. The wall was to contribute avoiding the fractures increase in size and to protect the foot of the limestone from erosion. Figs. 6 and 7 provides a scheme of that solution.

Once the instrumentation described in the following section was laid out, the consolidation work of the tower and stabilisation of the wall were as follows:

a. Reinforcing of the Tower, for which six binding levels were established, by cables of Ø 12 mm, according to the schemes in Figures 8 and 9. The cables, initially tensed to 95 kN, transmit a tension on the vertexes of the octagon that define the section of the tower.
b. Withdrawal of blocks, execution of accesses and the working platform in the area for intervention, affected by the wall consolidation works.
c. Consolidation of the tower base by injection using T.A.M. technics (Fig. 10).

Consolidation of the base of the Tower was performed by cement mortar injections performed by drilling openings Ø 150 mm, inserting PVC pipes and performing the injection under pressure through the sleeves (T.A.M.). The injection was performed from the platform located at the south east of the Tower. From

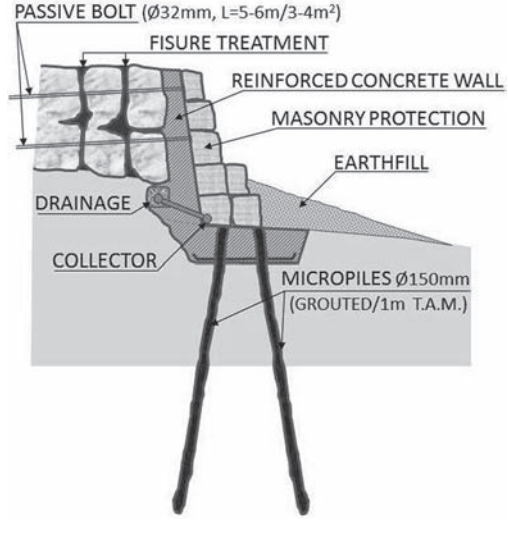

Figure 6. Solution lay-out.

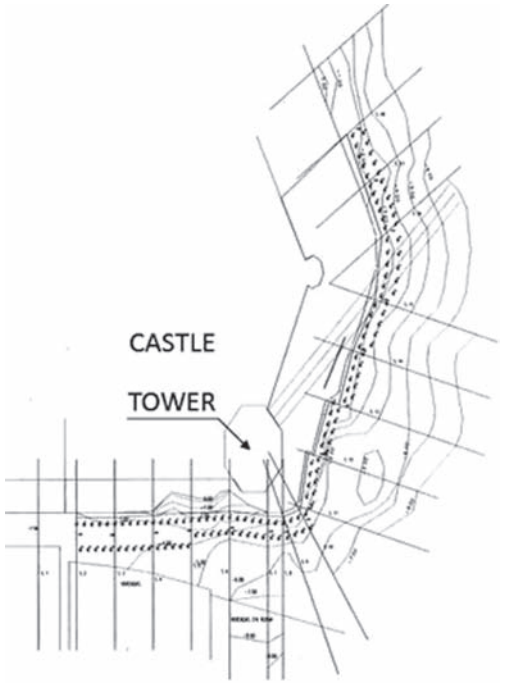

Figure 7. Micropiles carried out.

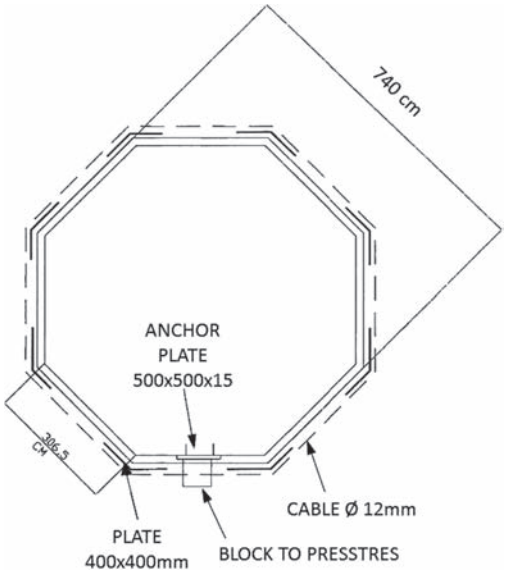

Figure 8. Honour Tower: lateral and surface reinforcement.

that platform, the injections were executed in fan shape, on the ground plan, under the north half of the tower, with the layout and slopes recorded in Fig. 10. That layout was the only

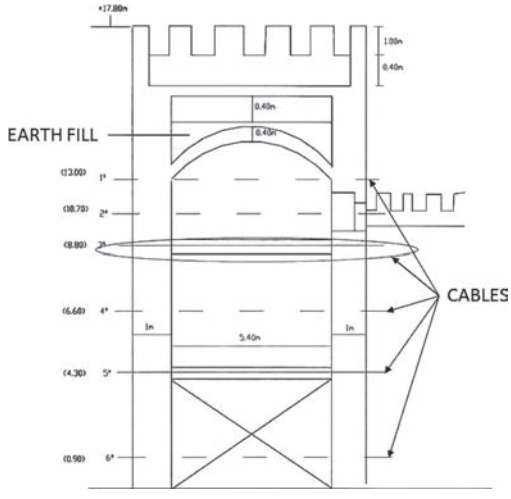

Figure 9. Situation of the reinforcement cables at six levels (initial load: 95 kN).

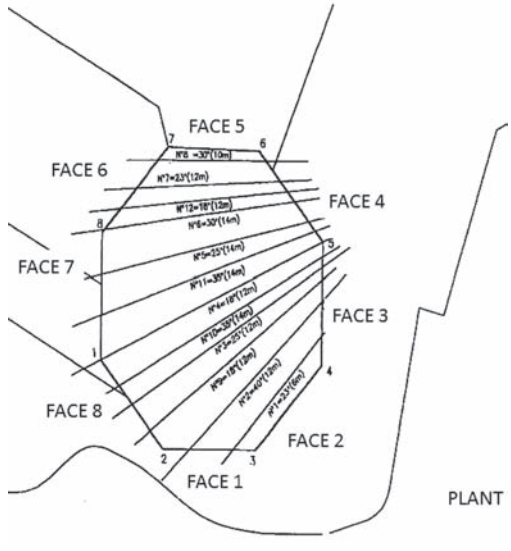

Figure 10. T.A.M. Grouting for consolidation of tower basis.

feasible one due to machinery access to the area only being possible to that exterior zone of the tower. A total of 12 test drills were bored, with a length between 6 and 14 metres and a diameter of 150 mm.

d. Stabilisation of the castle walls, the construction phases of the operating system are here listed (Fig. 6):

1. Construction of a horizontal platform 3 metres wide from which the micropiles were executed

in pairs, at a slope of nearly 1(H):4(V) (Figs. 6 and 7), with a length of 12–14 metres, with a diameter of 150 mm, with a tubular reinforcement with a section of 11.66 cm^2, grouted metre by metre through sleeve tubes in the lower part. The two references cited were taken into account to define these micropiles (Oteo, 2012 and Oteo et al., 2005).

2. Construction of a reinforced concrete wall, 0.5 metres thick, formwork against the ground and supported on a footing that was tied into the micropiles. The rear face of the wall erected at the foot of the limestone formation was fitted with a porous pipe of 100 mm in diameter, that was provided an exit through the wall every 5–6 m, leading to a general collection drain.
3. Placement of two bolts of 5–6 m lengt (Fig. 6), in a gird of 3–4 m^2 each, in resin or injected with cement grout. The existing cracks in the limestone formation were previously filled with grout (Fig. 6).
4. Construction of a masonry lining to obtain adequate aesthetic conditions (Fig. 6).

e. Concrete floor. In the zone between the castle walls and the concrete wall executed on the slope, a floor was laid of HA 220 concrete, in order to prevent water from entering the limestone level, in addition to regularising the surface.

   A grid of 15 × 15 cm of 10 mm diameter bars was placed over the floor area. Styrofoam plugs of 1 cm were placed at the meeting between the floor and the castle wall, around the entire perimeter.

f. Conditioning the flooring of the castle courtyard. The castle courtyard was laid out and compacted with a layer of crushed rock with a maximum size of 20 mm, except for a width of approximately two metres by the wall. In order to collect the run-off water, a hopper of 25 × 25 cm was built. Geotextile was placed under the existing crushed rock in the hopper area to reinforce the drainage function.

3 INSTRUMENTATION AND AUSCULTATION

3.1 *Typology*

Prior to commencement of the consolidation work on the monumental complex, an instrumentation plan was drawn up, which is described below (Fig. 11).

The auscultation system used was manual, using topographic and electric equipment, in addition to supervision "in situ".

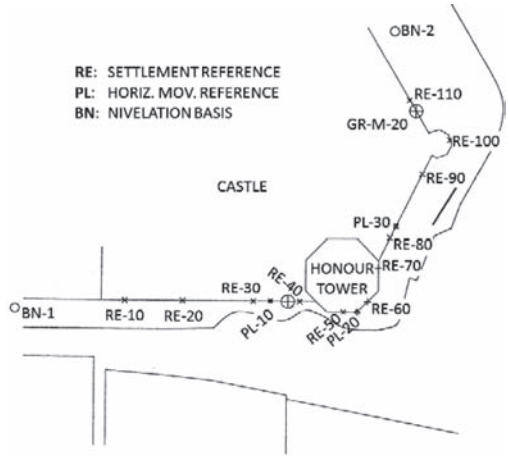

Figure 11. Plant of the castle with references to measure movements.

Thus, correct monitoring and control of movements or evolution of fissures was achieved. Periodic reading campaigns were carried out by technical personnel, by topographic readings and electrical readings. The topography recorded subsidence and inclines and the electric apparatuses deformations in the cable of the tower footing, and opening of the existing cracks and fissures. The data obtained was uploaded to the computer and subsequently interpreted. The following were recorded: vertical movements, inclination of walls, evolution of movements in fissures and cracks and deformations in the reinforcement cables (Fig. 11).

3.2 *Vertical movements*

On starting the consolidation work, 11 feet rules were placed and in two deep levelling phases. Those bases had a depth of 11 m each one. The topographical measurements were taken using a digital level and an invar sight. Fig. 12 shows the evolution of the vertical movement measured in diverse points (defined in Fig. 11). The subsidence ranged from 0 to 6 mm. After the reinforcement work was completed, those movements were totally stabilised.

3.3 *Inclinations*

Base plates were installed on three points of the castle walls, fitted with screws, to which the optic plumb-line was fitted. Thus, data gathering was faster as the plumb-line was always placed at the same point. That point was deemed to be fixed and immobile, so a fixed point on the ground did not become necessary. Targets were placed at the top,

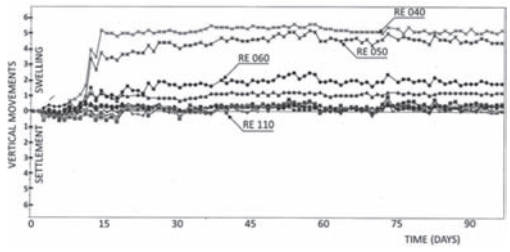

Figure 12. Measured settlements.

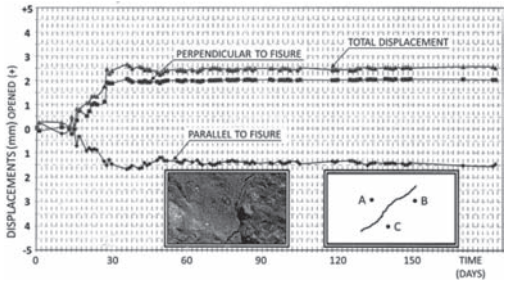

Figure 13. Displacements at a fisure in the Honour Tower.

of 10×10 cm, millimetre scaled. The daily reading indicated possible variations in the inclination of the walls.

3.4 *Fissures and cracks*

Metal discs were then placed on diverse walls of the castle, fixed to the surface using an adhesive with high adherent power, formed by a set of three points, or failing that, a couple of discs.

For the triple set, two of the discs were located on one side of the crack and placed on a straight line parallel to it, and the third point was placed on the other side of the crack, attempting to form an equilateral triangle. Thanks to this triple point system, it was possible to calculate the displacement in the direction of the fissure, the displacement perpendicular to the direction of the fissure, and the total displacement of the fissure.

Where the morphology of the crack and/or the surface of the rock did not allow placement of triple points, two points were fixed (one on each side of the fissure) thus obtaining a direct measure that would show the perpendicular displacement in the direction of the fissure, which allowed one to note whether the crack opened or closed. Some of the results of those controls may be seen in Fig. 13: the maximum opening of a vertical fissure in the Keep managed to increase by 2.5 mm during the reinforcement tasks, then having been stabilised.

3.5 *Deformation of the reinforcement cables*

Two vibrating cord extensometers were set on the two reinforcement cables of the Tower (Fig. 14). That kind of vibrating cord extensometers allowed measurement of the deformations produced in the material on which they are installed, in this case on the steel cables. Based on the data of the elasticity module of the steel and the deformation recorded, the tension value to which the steel cable was subject was obtained, as well as the traction stress and increase in length of the cable.

Two measures were taken daily, one at the beginning of the morning and another at the end of the afternoon. The measures were intensified during winter months, taking three per day, in order to check that the records were those matching the temperature increase.

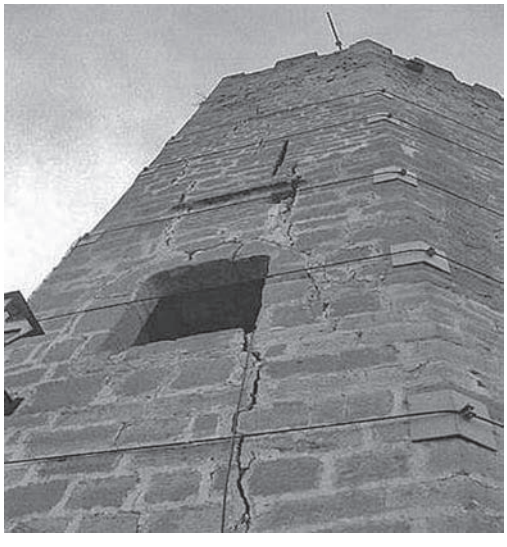

Figure 14. Honour tower reinforcement.

3.6 *Risk thresholds*

The risk thresholds established for each one of the readings were of three types:

- Normal: the data was within the reasonable range of the work (Maximum settlement of 5 mm).
- Precaution: taking readings and controlling the work must be intensified, even reducing the rate. One must possibly reconsider the execution phase (Maximum settlement between 5 and 10 mm).
- Danger: the site personnel and technicians in charge must be informed. Execution of the

works may even be halted, so that, after the relevant queries, measurements may be recommenced or another type taken, according to the cases (Maximum settlement exceeding 10 mm, drop exceeding 10 mm).

The danger threshold was not reached at any moment during the work, although precaution was reached during the consolidation phase of the tower by micropiles, and as of the month of December for subsidence. That level was also reached on the vibrating cord extensometers, due to the low temperatures.

4 CONCLUSIONS

The work to rehabilitate the Tower and the slope of Monteagudo de las Vicarías Castle (Soria), were carried out between mid 2004 and March 2005. Diverse phases of execution were established, there being an overlap between some of them.

The first work to be carried out was taking references and set up the instrumentation equipment at the beginning of September. That allowed good control of the different tasks to consolidate the slope, as well as determining to what extend these affected the castle. In a first phase, the reinforcement of the Tower was installed, using steel cables tensed to 95 kN at six levels (Figs. 8, 9 and 14).

In a second phase, the slope was cleared, removing blocks, and in the third, the work platform was set up.

The fourth phase is that of consolidation of the base of the wall around the castle. A total of 12 micropiles were drilled, laid out in a fan under the tower, with a variable angle, and thus, the length was also variable, but always exceeding the base of the tower ground plan. The injection was performed using sleeves at low pressure.

The fifth phase was the execution of the micropiles for the wall footing. These micropiles were drilled practically vertical, reaching a depth between 12 and 14 metres. Their injection was carried out though sleeves at low pressure, ensuring the injection metre by metre. During these two phases (4 and 5) the majority of the movements reproduced in Figures 13 and 14 took place.

In the sixth phase, the micropile footing, the concrete wall and drainage were executed. The drainage was of two types: one lengthwise, on the back face of the wall, and another perpendicular to the wall. Once the micropiles were executed, the footing was concreted and then the concrete wall with the relevant drainage. The cavity detected under the footing was also filled in.

Once the wall was completed, filling was carried out with lime grout, of the existing cracks in the rear face of the wall, in the castle esplanade, that was the seventh phase. Then the eighth phase was carried out, consisting of setting pins into the wall. Two offset rows of pins were inserted, with a separation of 3 linear meters between them, on the same line of pins. Each pin had a length of 9 metres and an incline between 10º and 15º.

In the ninth phase, the concrete flooring was laid on the castle esplanade.

Conditioning the courtyard was made by placing crushed rock throughout, except in a two metre trench beside the castle walls and a hopper to collect the run-off water, constituting the last phase.

Movements were monitored from the moment of ending the work, until several months afterward, checking its stabilisation.

ACKNOWLEDGEMENTS

The authors wish to express their gratitude to the Architect Mr Fernando Cobos and the Technical Architect Mr Valentín Cobo, from the Government of Castilla y León (Regional Authority of Spain), for their support during the development of these reinforcements works. Also, the cooperation by some companies (INCOSA, ENDOSA, EIS and CONDISA), charged with the geotechnical, control and instrumentation works, is acknowledged.

REFERENCES

Carrascosa, J. 1933. Photographic File. Nº 1301. Internet.

Oteo, C. 2012. "Inclusiones en recalces: De las inyecciones a los micropilotes". Recalces con micropilotes y otras técnicas especiales. SEMSIG-AETESS, Madrid, pp. 55–79.

Oteo, C., de la Fuente, P. and Botello, A. 2005. "Sobre los esfuerzos en pilotajes para estabilizar taludes". VI Simposio Nacional sobre laderas y Taludes inestables". Univ. Pol. de Barcelona y Univ. Pol. de Valencia. Vol. I. pp. 373–380.

This page intentionally left blank

Geotechnical Engineering for the Preservation of Monuments and Historic Sites – Bilotta, Flora, Lirer & Viggiani (eds)
© 2013 Taylor & Francis Group, London, ISBN 978-1-138-00055-1

Load transfer in micropile underpinning of old foundations

J.M. Rodríguez Ortiz
Polytechnical University of Madrid, Madrid, Spain

ABSTRACT: The problem of the amount of load that can be transferred to new inclusions, as micropiles, from a settling foundation has been rarely addressed. The final load depends on the nature of the ground, the history and velocity of settlements, the stiffness of the inclusions and the time of the strengthening as related to the time for completion of the settlements or to reach a near collapse condition. Several cases are analysed through creep models, showing the difficulties for assessing a reliable design load when studying the use of micropiles as an underpinning tool.

1 INTRODUCTION

There is no clear criterion on the design load of micropiles when used as reinforcement of foundations subjected to progressive or non-stabilized settlement.

A frequent solution is to assume the full load of the foundation to be taken by the micropiles. Some authors however suggest, quite arbitrarily, to absorb the 50% of the total load. In very heavy foundations, as is the case of columns of cathedrals, the underpinning hardly exceeds 10% of the existing loads.

These poorly supported approaches tacitly assume that the transfer of load to the micropiles can be achieved without dangerous displacements. The settlements associated to the drilling and installation of the micropiles are equally ignored.

2 THE PATTERNS OF SETTLEMENT

Obviously the reinforcement or underpinning is only needed when the structure suffers a non stabilized settlement, close or above the limits for impending cracking or distortion.

Damages, by themselves, are not a sign of an active process of instability. A monitoring is necessary in order to assess the evolution of the settlements and to predict whether a dangerous threshold can be trespassed in a moderate time period or not.

In granular soils the settlements occur very quickly, thus the underpinning is of little help. In cohesive soils, however, a consolidation process can be triggered and it is necessary to estimate the future settlements until stabilisation as well as the associated damages to the structure. The decision on underpinning depends of the level of risk and the time to proceed.

In made fills and collapsible soils the sudden settlements caused by saturation or flooding can be close to the maximum expected movements and their magnitude can only increase a little under new cycles of saturation. The underpinning is less effective in these cases that other measures of protecting the foundations against accidental saturation.

The underpinning is justified in evolutive soils as degrading organic fills, saline soils with risk of leaching or karstification, etc. In normal cases the intervention is only advisable when the speed of the settlements is very slow (a value below 1 mm/month seems allowable) or the structure can yet accept some additional settlement, as expected from the installation and loading of the underpinning. Otherwise is necessary to unload and shore the parts to be acted upon.

It must be said that micropiles are a very risky solution in the case of made fills or loose soils as very often water is added to help the boring of masonry or concrete and even to perform the drilling to insert the micropile. The drilling water and even the cement slurry used to protect the tubes and filling their inner hole induce collapse in a ground of bad quality. A solution can be to help the boring by compressed air and drilling in the dry but this is rarely the adopted method, sometimes by cost reasons and more frequently due to the lack of the necessary equipment. In addition to the settlements derived from the micropiles installation, the main attention must be paid to the time-settlement process of the structure itself.

Figure 1. Cistercian footing of the Sta. Maria de Huerta Monastery (XIth c.), before underpinning. Observe the tie-beams.

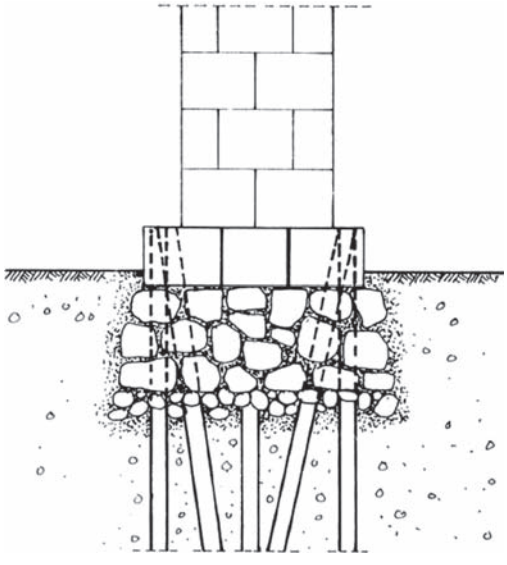

Figure 2. Scheme of an ancient foundation reinforced by micropiles.

In a very simplified manner the following patterns (fig. 3) are normally encountered in historical buildings:

- A decreasing velocity process, usually associated to a consolidating ground (case A).
- A near-constant velocity, at least during the monitoring period. Several causes can be called upon in this case. Sometimes it reflects the initial stage of a quasi-parabolic behaviour (case B).
- An increasing velocity. This is typical of leaning towers or walls suffering softening or plastic yielding in their supporting soils (case C).

This paper is not the place to discuss the numerous causes which can activate instability in long

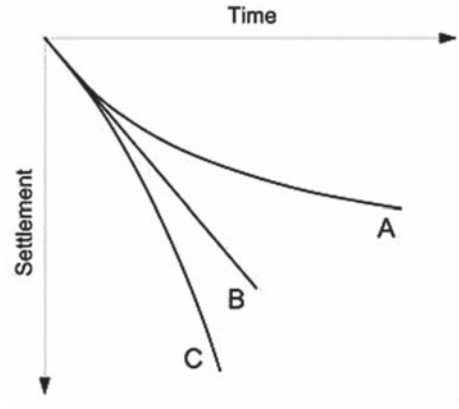

Figure 3. Time-settlement relationships according to different processes.

time stable structures. The effects of water table lowering, nearby excavations, leaks of sewage or water mains, suppression or development of vegetation, decay of old foundations, chemical attack, improper structural interventions, increase of loads, etc. are well known.

The strengthening of the foundation can modify the velocity of settlement or, hopefully, to stop it. However is difficult to design the right underpinning without a good knowledge of the history of settlements and a proper identification of the type of process under way.

A clear case of settlement activation is the application of additional loads to the structure or changing the load distribution due to structural interventions. In these cases the increasing of loads can be estimated and the underpinning can be preventively designed to cope with the new state of loading.

3 THE TRANSFER OF LOAD

If a structure stands, even in a delicate condition, it is obvious that the ground below it bears the foundation pressures with a safety factor close to 1. The transfer of load to any underpinning element cannot be performed without additional settlements which could be harmful to the structure.

In other cases the process is approaching stabilisation and the remaining settlements are too small to mobilize a significant part of the strength of the inclusions. It is not rare the case of underpinning stable structures, with minimum settlements, only by showing a worrying pattern of cracks or distortions. Obviously the intervention has little sense, and it can only worsen the problem.

One can conclude that the time of installation of the inclusions, i.e., the expected settlements

before stabilisation (patterns A and B), determine the load that the foundation can transfer. For patterns of C type, suggesting a possible collapse of the structure, the inclusions should be designed for the complete load of the structure, provided a safe intervention can be granted (see above).

An interesting contribution to the subject for the case of a consolidating ground has been made by Georgiadis & Anagnostopoulos (1997).Their model follows the hydromechanical approach of Terzaghi for computing the load share between the soil skeleton and some inclusions, piles or micropiles, installed at a certain point of the consolidation process. The settlements after underpinning are given by

$$\Delta s = u_t \, A/(K_s + K_p)$$

u_t being the excess pore pressure at the moment of the underpinning, A = the loaded area and K_s and K_p the spring constants relative to the soil and the inclusions. Obviously the residual settlements will be very small at the end stage of the process, independently of the stiffness of the underpinning.

Estephan (2003) quotes the case of the Stone Bridge in Bordeaux, built in 1880–1921 on wooden piles not reaching the firm level.

In order to slow down the settlements (about 15 mm/year) each footing was underpinned in 1992–94 by 8 micropiles. After 6 years the micropiles had only absorbed between 5 and 20% of the total load, but the settlements have stabilised at a rate below 0.5 mm/year. This behaviour changes in the case of preventive underpinnings. The micropiles may absorb between the 60 and 85% of the load, the rest being transferred to the ground (Hand & Ye, 2006).

It is interesting to remark that the additional settlements induced by the load transfer can be avoided by loading the micropiles before their connection to the old foundation. This prestressing is highly desirable in structures close to the threshold of severe damage, but is very complicated when the number of micropiles is high. In some cases the elastic shortening of the micropiles has been eliminated by including inside the tube a threaded bar, anchored at the micropile end section and tensioned by tightening a nut at the pile cap.

The nut is loosen after connecting the micropile to the foundation. This is useful in the case of long and slender micropiles.As refers to the stiffness of the micropiles, it is greatest when they are short and reach a rocky non-deforming substratum, but it can be very small in the case of floating micropiles, a non suitable solution. A quasi-parabolic behaviour is not always the result of a consolidation process. It can reflect a strain-hardening process of elasto-plastic nature,

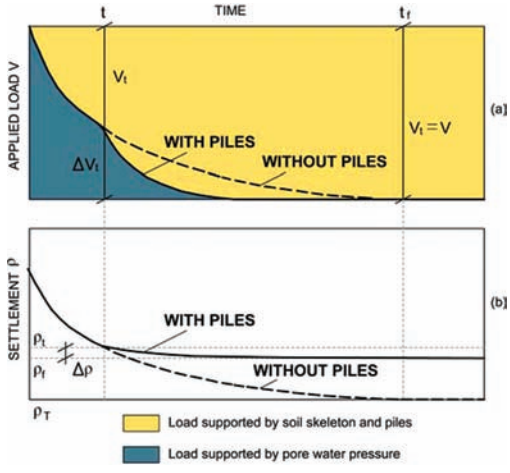

Figure 4. The hydromechanical model of Georgiadis & Anagnostopoulos (1997) for load transfer between the soil and the inclusions.

very common in old monuments where the ground has been loaded for centuries. It can also correspond to a long term creep behaviour, typical of foundations charged close to the bearing capacity of the ground.

It is worth to say that the overconsolidation can only be detected in samples taken below the foundations, not in external borings, as is frequently the case, due to space difficulties as well as the natural fear to endanger the structure.

In order to exclude hydrodynamic effects, as the dissipation of excess pore pressures, we have simulate the parabolic behaviour by means of a classic creep model with a power law of the type

$$\varepsilon^f = \frac{1}{E} D^{-1} \sigma A (t - t_0)^m$$

where A and m are material parameters.

We have concentrated in this paper upon the very common case of a parabolic decreasing settlement, as it occurs very often in reactivated foundation movements in ancient buildings. Figure 5 shows the time-settlement relationship for a strip or continuous footing under a load of 400 kN/m.

The adjusted creep parameters were $A = 1 \times 10^{-5}$ and m = 0.4, with equal values for the deviatoric and volumetric parts of the creep deformation.

The four near-horizontal curves refer to the installation at four different times of underpinning micropiles (2 per meter, with an effective length of 10 m). Although three different sections or micropiles were initially tested (see table below), the absorbed load was very similar, within a range of 5%.

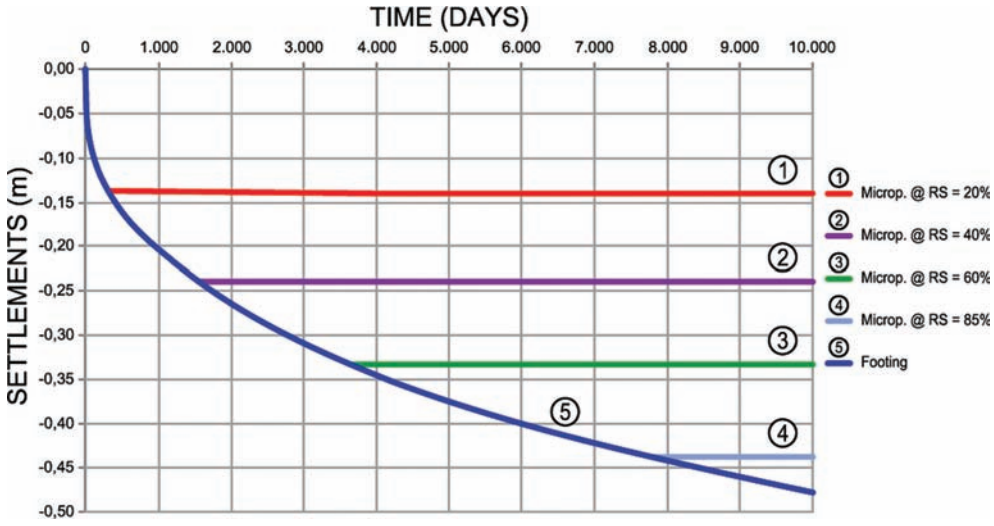

Figure 5. Time-settlement relationships for a strip footing with instant stoppage at the micropiles installation with different values of the relative settlements (RS).

Table 1. Properties of the micropiles.

Micropiles (diameter × thickness) (mm × mm)	Steel area (cm^2)
88,9 × 4,5	11,9
114,3 × 6,3	21,4
140 × 12,5	50,0

Thus a unique steel area is considered in Table 1.

The relative settlement (RS) is the percentage of the final settlement at 10.000 days.

Figure 6 shows the load transfer between footing and micropiles when only the 20% of the final settlement has occurred at the time of the underpinning. Figure 7 corresponds to a relative settlement of 60%.

As it could be expected a complete transfer of load never occurs, which justifies a design for a percentage of the total load.

Only in cases of total contact loss, as could arise by self compacting, collapsible or soluble soils, a full transfer must be taken into account.

As a summary, fig. 8 shows the percentage of load absorbed by the micropiles related to the time of installation. The curve shown is a narrow mean for EA stiffness between 250 MN and 1050 MN. As it can be observed the relationship is practically linear, but the effect of the micropiles is very small when applied at the end stages of settlement.

In any case, however, the "stoppage" effect is very clear, irrespective of the micropiles stiffness

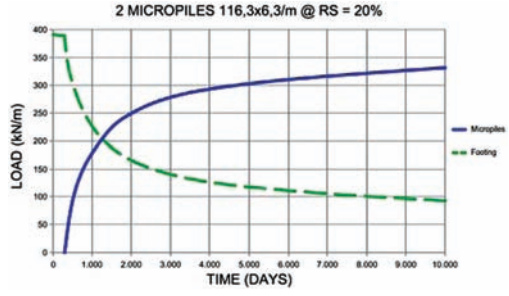

Figure 6. Load transfer between footing and micropiles when installed at 20% of relative settlement.

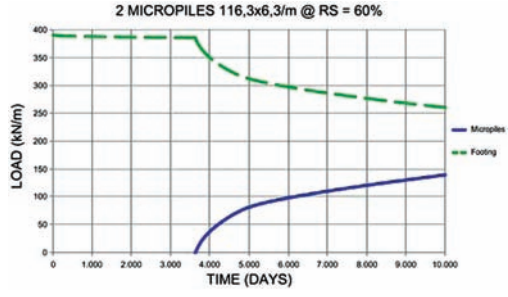

Figure 7. Load transfer between footing and micropiles when installed at 60% of relative settlement.

ant their time of installation. In the case of figure 5, the settlements undergone by the micropiles vary from 4 mm when installed at a relative settlement of 20% to 1 mm for RS = 85%.

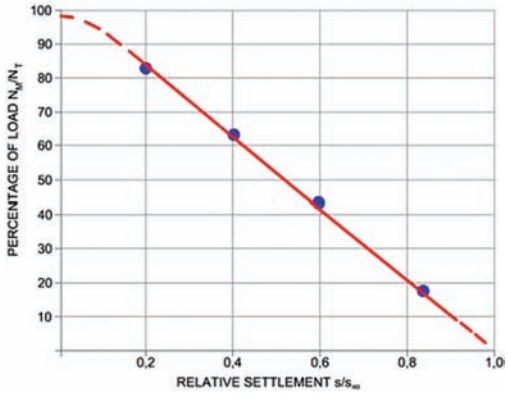

Figure 8. Percentage of the total load absorbed by the micropiles as related to the relative settlement at the time of installation.

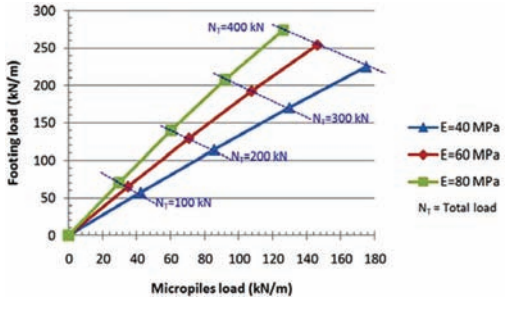

Figure 9. Load share between footing and micropiles when installed in advance.

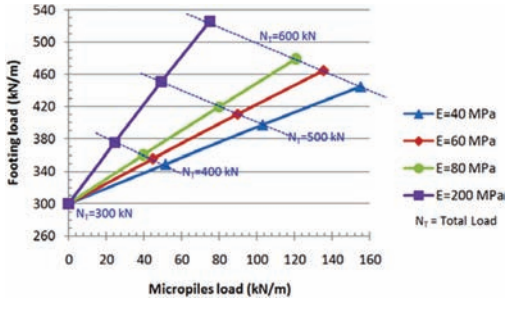

Figure 10. Load share between footing and micropiles when installed at a load of 300 kN.

The load share varies, as it can be expected, according to the relative stiffness of the micropiles and the ground.

For the same case of fig. 5, but with 4 micropiles per metre in order to avoid bearing failure of the footing, the figure 9 shows this share for micropiles installed at advance, before any load be applied, for three different moduli of deformation of the ground. Figure 10 shows the results for the case of underpinning when the footing is partially loaded. A stiffer type of ground has been added for a broader picture.

4 CONCLUSIONS

After adjusting a creep model to the parabolic settlement history of a foundation, the effect of an underpinning with micropiles has been analysed. The stoppage effect of end bearing micropiles is evident, although the transfer of load from the original footing depends on the time of installation as well as the relative stiffness between the ground and the micropiles.

A significant absorption of load is only developed when the micropiles are installed in early stages of deformation. Therefore the design load of the micropiles for advanced stages of settlement rarely needs to exceed 50% of the total load. Obviously this conclusion does not apply to foundations with a trend towards increasing settlements.

REFERENCES

Babu, G.L.S. et al. 2004. Bearing capacity improvement using micropiles. A case study. GeoSupport 2004. Geot. Sp. Publ. nº 124. GeoInstitute, ASCE, Ed. Turner & Mayne. 692–699.

Estephan, R. 2003. Contributions aux méthodes de calcul des groupes et des réseaux de micropieux. Thèse de Doctorat en Géotechnique. Ecole Nat. des Ponts et Ch., Paris.

Georgiadis, M. & Anagnostopoulos, C. 1997. Design of underpinning piles to control monument settlement. *Proc. Int. Symp. Geot. Eng. Preservation of Monuments and historical sites*. Napoli. Ed. C. Viggiani, 453–456.

Han, J. & Ye, S-L. 2006. A field study on the behaviour of a foundation underpinned by micropiles. *Canadian Geot. J.*, 43, 30–42.

Konovalov, P.A. 1998. Bases and foundations of buildings under reconstruction. Balkema. 239 p.

Makarchian, M. & Poulos, H.G. 1997. An experimental study of foundation upgrading by piles. Proc. 14th Int. Conf. SMFE, Hamburg, 2, 835–838.

This page intentionally left blank

Geotechnical Engineering for the Preservation of Monuments and Historic Sites – Bilotta, Flora, Lirer & Viggiani (eds)
© 2013 Taylor & Francis Group, London, ISBN 978-1-138-00055-1

Construction of the Line C San Giovanni station in Rome

E. Romani & N. Miniero
Metro C S.c.p.A., Rome, Italy

ABSTRACT: The construction of Rome's Line C San Giovanni station required adopting building techniques suitable for responding to the numerous problems concerning geology, archaeology, public utilities and surrounding buildings. The procedures for building this station were strongly constrained by what emerged unexpectedly at the start of the work sites: the presence of archaeological findings down to a depth of 18 m below ground level.

These findings required an overall revision of the Line C's design in the historic centre of the city of Rome, starting from the San Giovanni station, to safeguard archaeologically sensitive strata.

1 GENERAL INSTRUCTIONS

Line C is Rome's third underground line; once completed, it will cross the city from northwest to southeast, almost doubling the extent of the currently existing underground network.

Metro C S.c.p.A is the General Contractor, consisting of Astaldi (representative), Vianini Lavori, Ansaldo STS and CMB, which deals with the construction of Line C in all its phases: design, archaeological surveys, tunnel drilling, excavation and construction of stations, building of trains, and start-up.

The part currently under construction, from Monte Compatri—Pantano to San Giovanni, extends for 18.5 km, and consists of 22 stations and 12 ventilation shafts.

One work of many that required adopting particular building techniques suitable for responding to the problems due to geological/geotechnical, archaeological, and territorial nature, with a high density of buildings and underground utilities, is certainly the San Giovanni station.

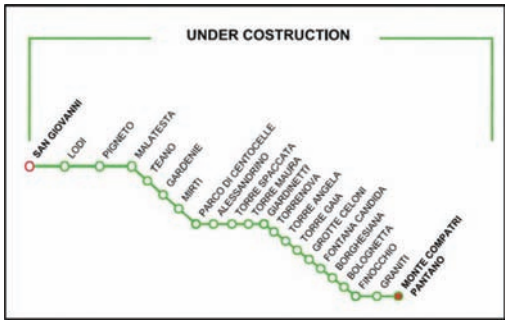

Figure 1. Layout of Line C.

Figure 2. San Giovanni—the work site.

The station is located in the difficult urban setting of the Appio—Latino neighbourhood, and extends along Via La Spezia next to the existing San Giovanni station of Rome's Line A subway.

It measures 140 m per 22 m and reaches a depth of 35 m below ground level.

The structure, with its 7 floors, is adjacent to the existing Line A station allowing passenger interchange between Line A and Line C.

2 GROUND CONDITIONS

The encountered geological/geotechnical units are a transition from the volcanic units of the eastern periphery of the city towards the fluvial or marine units of the historic centre of Rome (the Tiber's ancient riverbed).

Starting from ground level, the first layer consists of made ground [R], with thickness reaching 13–16 metres. It is a heterogeneous material with

sandy-silty matrix mainly of pyroclastic nature. These materials offer fair shear resistance in effective tensions accompanied by modest cohesion.

This is followed by a strata of recent alluvial deposits [LSO] that have filled deep cuts with often variable thicknesses, reaching the level of about 17 metres at San Giovanni station. In terms of granulometry, it consists mainly of silty sands and clayey silt, blackish in colour, from low to medium stiff.

The succession of the units composing the Pleistocene deposits is represented, proceeding from top to bottom, by an initial unit [ST] consisting of an alternation of white or yellow silty sand and clayey sandy silt [STa], with carbonate concretions and localised levels on travertine concretions, with a high degree of thickening and of medium to high dense, followed by a unit consisting of clayey silt and silty clay [AR] of grey or yellowish colour due to oxidation, very stiff.

The lower unit of Pleistocene sediments is composed by medium to coarse sand with gravel [SG], very dense, with the roof localised at +6 ÷ 11 m below sea level.

This stratum of sand with gravel rests directly upon the Pliocene formation of very stiff grey-light blue silty clay and clayey silt [APL], with the top at the depth of 44 metres from ground level. In the first 5/6 metres of the unit top, the strata consists of some levels of fine sand, very dense, alternating with consistent clayey silt of different thickness no more than a decimetre thick; continuing downward, the facies becomes purely silty/clayey and highly stiff.

Site investigations show a relatively complex piezometric regime in accordance with the stratigraphic situation, in which erosion phenomena have partially or totally removed the sandy and clayey layers of the Pleistocene formation. The buffering effect into this formation does not always appear effective.

Generally, the measurements obtained by Casagrande piezometers or open wells, installed at different depths into various formations, or by drainage tests, demonstrate that the alluvial deposits and the made ground are the site of an unconfined aquifer with piezometric level at the absolute depth of 25.00 ÷ 28.15 m below sea level.

The measurements indicate the westward flow of the acquifer.

The deep unit, formed of sand and gravel, is the site of an artesian aquifer, supported by the formation of basal Pliocene clays and plugged from the roof by the clayey levels of the Pleistocene formations, whose piezometric level is at a maximum depth of +17.20 ÷ 17.66 m below sea level.

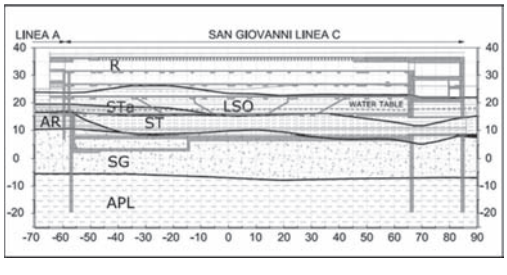

Figure 3. Geotechnical profile.

3 PRE-EXISTING STRUCTURES

The presence of a considerable made ground layer makes the buildings adjacent to the station particularly sensitive during the excavation phase. These buildings were constructed in the early twentieth century; their bearing structures are in masonry, and their shallow foundations are not sunk into the deeper and more consistent strata.

Moreover, around the mid 1950s, some of the buildings surrounding the station were elevated with additional reinforced concrete structures, without upgrading the existing foundations

The buildings, with masonry bearing structure, floors made with steel beams coupled to hollow flooring blocks, Roman-style stairways, and presumably shaft foundations, present a more or less widespread cracking phenomena.

The station's diaphragm walls, far deeper than the buildings' bottom level, are positioned at a distance varying between 1.80 and 3.00 m from the buildings' façade.

The presence of major cracking phenomena due to settling of the bottom level, interaction with the station's excavation and with the line tunnels running for about 100 m along Via La Spezia, have required introducing jet grouting into the executive design, for building L3—Scuola Carducci.

Among the pre-existing structures, mention must be made of the existing Line A San Giovanni station. This structure, placed at the centre of Piazzale

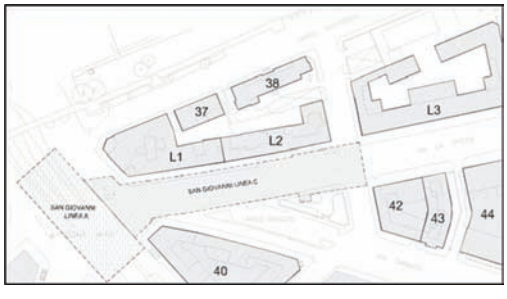

Figure 4. The builds surrounding the San Giovanni station.

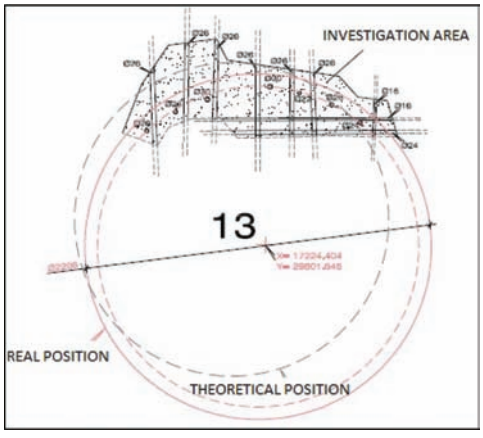

Figure 5. 3-D reconstruction of the piles' diameter.

Appio, stands between diaphragm walls 80 cm thick; rectangular in design, it measures 75 × 30 m, and lies at a depth of 22 m below ground level.

The interior bearing structures are in reinforced concrete beams, steel columns, and brick/cement slabs connected to the perimeter partitions by pockets and/or grouting. The columns are based upon piles ø2000 in diameter, sunk into the layer of sands and gravels.

Right beneath the entrance level, the existing station, designed in the 1970s, has a floor completely dedicated to the future passage of Line C.

The existing station was the object of a highly in-depth study to reveal the geometry of its structures, the reinforcement of the main structural elements, as well as the length and position of the foundation piles.

The length of these elements was assessed by echometric tests performed from the underplatform area, while the topographical position was surveyed by partially demolishing the upper concrete cover of the foundation slab, and reconstructing the pile's surface starting from the rods in the reinforcement cage.

4 ARCHAEOLOGY

The design choices regarding this station's construction were strongly constrained not only by the pre-existing structures and the geological/geotechnical landscape discussed above, but also by what emerged during the archaeological surveys performed once the work site was begun: an unexpected presence of archaeological layers distributed in landfill down to depths of between 14 and 18 m, with a water table level at about 8 m below ground level.

Following the results of the archaeological surveys, carried out before building the station's diaphragm walls and executing the jet grouting bottom plug, the archaeological Superintendence of the Municipality of Rome imposed the following construction constraints:

1. impossibility of performing consolidations from ground level without prior archaeological excavation;
2. need to carry out all the excavations by archaeological procedure down to "virgin" ground.

These obligations required an overall review of the Line C design in the historic centre of the city of Rome, starting right from the San Giovanni station, to safeguard the archaeologically sensitive strata.

The results of the archaeological surveys were reported in a document named "*Prontuario*" ("handbook"), written together with the archaeological Superintendence of the Municipality of Rome. This document illustrates the excavation procedures and the cataloguing of the findings, so as to ensure respect of performance times, but at the same time guarantee all the requirements of historical and scientific nature.

5 DESIGN CHOICES

The archaeological findings obliged Metro C to change the design of the line that runs from San Giovanni to Malatesta and abandon the level left available in the Line A station.

In detail, a plano-altimetric variation of the Line was required starting from the Lodi station, right before San Giovanni; the TBM tunnels were deepened beneath the archaeological strata, and traditionally excavated tunnels were introduced in order to pass beneath the existing station.

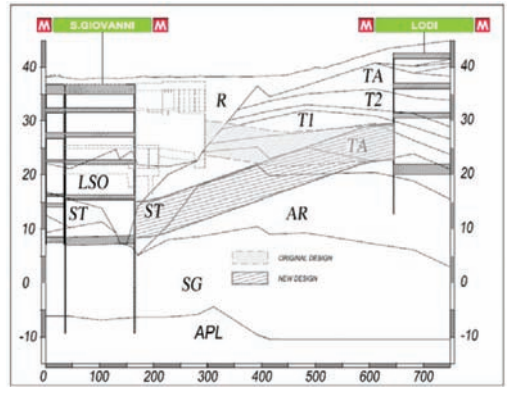

Figure 6. Geotechnical profile of Line C—comparison between the original design and the new design.

6 DIAPHRAGM WALLS AND DAM EFFECT

The new station configuration, with an excavation bottom brushing up against the strata of sands and gravel, along with the impossibility of making a bottom plug, required lengthening the diaphragm walls down to the waterproof stratum of Pliocene clays, thus reaching 56 m below ground level.

Moreover, given the buildings' proximity and having entrusted the lateral waterproofing and the stability of the excavation bottom entirely to the diaphragm walls, the hydromill technique was chosen, in order to guarantee verticality and watertight joints by means of concrete milling.

Given the nature of the adjacent buildings' foundation terrain, and the considerable size of the station body, it was deemed necessary to perform a hydrogeology study of the area in order to assess any barrier effect that the station's diaphragm walls, sunk into the consistent blue clays, could create in the water table's flow.

By modelling the underground water resources, it was possible to consider the aquifer's actual geological and hydrogeological features, thus solving the filtration problem by seeking the solution to the equations governing the phenomenon.

The more than 100 probes done in an area of about 30 km^2 around the San Giovanni station site (Ventriglia, 1971-Ventriglia, 2002-Line C from 1995 to 2008) made it possible to reconstruct the roof surfaces of the formations already identified in the geological and hydrogeological characterization phase of the site, which presents a rather complex situation given the presence of numerous lateral passages between the formations.

The hydrogeology of the area in question was synthesized considering the existence of two separate water tables with points in which they appear to come into contact. This is actually a single water table moving from the Alban Hills towards the Tiber, but the presence of impermeable Pleistocene layers determines a loss of hydraulic load, with a consequent variation of the piezometric level between the surface landfills and the layer of sands and gravels.

After establishing that the calibrated model adhered to the actual situation, new work was inserted for the purpose of observing and quantifying the dam effect produced on the flow in the aquifer. The results obtained are:

1. for the surface stratum, the maximum overflow value upstream is about 10 cm, while the depression downstream reaches values of about 12 cm;
2. for the deep stratum, the maximum overflow value upstream and the depression downstream is about 10 cm.

In addition to these values, it was assessed that the extent of the area influenced by the damming is circumscribed around the work in an area of about 0.1 km^2 north-east of the station (flow upstream) and 2.5 km^2 south-west of the station (flow downstream).

The effect the work has on the stratum's arrangement takes place largely in the first 100 days, after which the differences in piezometry attenuate until becoming stable about 10 years after the work is constructed.

7 STATION EXCAVATION

The study of the new execution phases, strongly constrained by the archaeology, in the desire not to lose the benefits of the "top-down" method, with the execution of descending slabs functioning as a strut to support the perimeter partitions, led to defining the following succession in construction which, for each slab, calls for:

1. excavation with archaeological method down to about 1.00 m beneath the slab's inner face;
2. execution of a perimeter concrete edging resting upon pockets created in the diaphragms and hung on the covering slab using Dywidag bars;
3. deepening of the excavation with archaeological method for an additional 2.00 m;
4. execution of the slab with self-bearing prefabricated structures, and subsequent casting.

These phases, by eliminating the excavation on the inner face of the slabs cast against the earth, typical of the "top-down" method, allow the excavation to be deepened by horizontal levels, thus preserving the ancient structures.

For the self-supporting structures in the casting phase, mixed reticular precast beams were chosen, having spans of up to 20 m, along with ribbed girders, also self-supporting, with spans of up to 8 m and with a finished slab thickness of 40 cm.

Figure 7. Construction of hall floor slab in S. Giovanni station.

Figure 8. Archeological findings in the San Giovanni station.

8 INTERACTION WITH EXISTING LINE A

The interaction with the existing station of Line A entailed a series of design and construction choices.

The deepening of the excavation of the Line C station also generated problems of carrying capacity for the Line A diaphragm partitions, since, given that there are no internal linings, the partitions transmit the vertical loads to the ground's deep strata. To avoid this problem, it was deemed necessary to consolidate by jet grouting the stratum of sands and gravels at the foot of the diaphragm walls for the station's entire horizontal extent. This expedient makes it possible to build the Line C diaphragm walls adjacent to the Line A ones without altering the balance of the existing station.

To guarantee the transmission of the vertical loads over the long term, also after the execution of the tunnels passing beneath Line A, it became necessary to link the two structures with a reinforced concrete wall made by underpinning, connected to 5 Line C diaphragms and by means of grouting, to the Line A partition.

Moreover, given the need to cross beneath the existing station by means of a traditionally excavated tunnel abutting the foundation piles, it was necessary to assess the reduction of these elements' lateral resistance. Since these were large-diameter piles (Ø2000) sunk into the extremely rigid stratum of sands and gravels, it was evaluated whether the carrying capacity at the end is preponderant with respect to the lateral carrying capacity. Moreover, the presence of a continuous foundation slab 40 cm thick guarantees a reduction in any displacement that may be generated.

Lastly, the two under-crossing tunnels cut the longitudinal diaphragm walls of the existing station, thus generating a reduced vertical carrying capacity for these diaphragms. To avoid the problem, a wall beam was made, about 40 m long, connected to the Line A diaphragm walls at the existing station's platform level.

This structure, resting upon 3 plinths with preloaded micro piles, has the function of transferring all the vertical loads of the longitudinal alignment of the partitions to the deep layers of ground beneath the line tunnels.

As the traffic of Line A and/or the station could not be interrupted while the tunnels were being built, a track support system, for both directions, was provided for within the platform level, built with a continuous metal deck with two spans 20 m in length, resting on micro piles.

In compliance with the regulations in force, having altered the existing station's foundation structure, as described above, it became necessary to verify seismic safety and to perform the consequent adjustment work.

9 MONITORING SYSTEM

A wide monitoring activity has been carried out in order to verify the stability of supporting structures during construction and also the design assumptions to allow adjustment and optimization of the constructed processes.

For these reasons, the monitoring system has interested different topics:

I. Water-table monitoring, by means of piezometers installed outside (Casagrande cells) and inside (electric piezometers under final excavation level) excavation;
II. Ground movement monitoring, by means of several in-place inclinometers, multi-base assestimeters and precise levelling points;
III. Building monitoring, by means of automated total stations that give real-time three dimensional displacements and remotely logged biaxial electrolevel tiltmeters;
IV. Monitoring of structures, by means of inclinometers for measurement of horizontal displacements, extensometers for the determination of the stress-strain of the structures and strain gauges on steel struts.

The monitoring design has fixed thresholds and limiting values for all the instruments, which may trigger responses ranging from more frequent readings to modifications of construction procedures and, in the extreme, to implementation of a specified contingency plan.

In such a delicate setting, given the particular nature of the hydro geological picture and the preexisting structures, the monitoring has mainly the function of supporting the designer in the assumptions that are made.

The water table levels measured by the piezometers installed outside the partitions have shown a substantial stability of the water table. While the internal electrical piezometers have revealed the stability of the excavation bottom and the watertight joints of the diaphragms down to the foot of the partition.

In the structural monitoring, the inclinometers in the diaphragm walls are particularly important, given the nature of the terrain, possible irregular warping might generate displacements and distortions of the adjacent buildings.

Figure 10 compares the design displacement values to the measured displacement of a diaphragm wall during the construction phase.

Should irregular warping of the diaphragms occur during the works' development, the observational method implemented for the monitoring, calls for a back-analysis that makes it possible to calibrate the calculation model based on the results of the measured values, also proceeding to modify the executive phases should the evolution of the phenomenon be incompatible with the designed structure. For example, this procedure, already implemented in other Line C stations, has sometimes led to the introduction of excavation by sampling for building the foundation slab, in such a way as to exploit the three-dimensional nature of the problem and consequently limit the partition's warping.

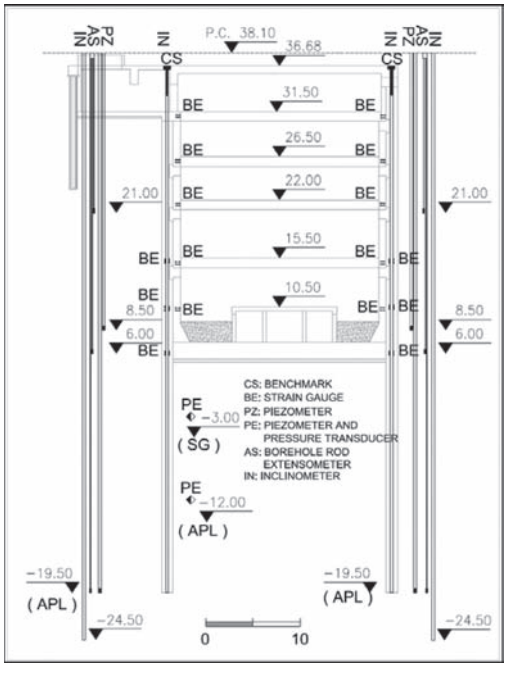

Figure 9. Monitoring instruments in a cross section.

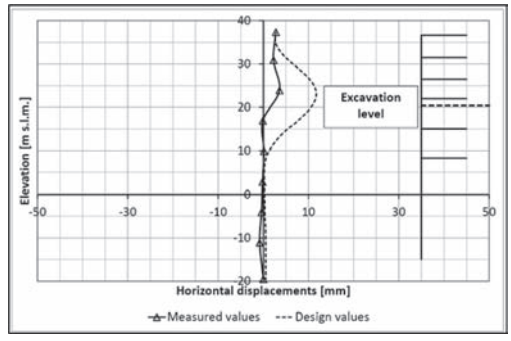

Figure 10. Inclinometers—comparison between design values and measured values.

Special attention was also dedicated to drawing up the monitoring project of the existing station which, given the non-conventional working operations to be performed, may undergo stresses not compatible with the structures. In this regard, 3 total stations within the various levels, as well as electric inclinometers capable of measuring any distortion, were installed.

During the construction of the under-crossing tunnels, electrolevel tilt meters will be installed on the line A tracks to continuously check any settling of the metal decks' foundation plinths.

10 CONCLUSIONS

The work on the San Giovanni station has currently reached about 20 m below ground level, with the construction of the fourth underground slab including the top slab.

As emerged during the archaeological surveys, at the time of the excavations ancient structures were discovered, whose removal certainly slowed the works at the site. The versatility of the construction system chosen with modular prefabricated structures and the presence of 3 alignments of construction rings along the station's longitudinal extent at any rate allowed the works not to be halted, by performing the station construction activities in parallel with the archaeological digging.

The execution phases and the construction choices thus made it possible to perform the archaeological excavation without provisional propping and without timbering for the casting of underground slabs, guaranteeing the complete execution of a slab, the laying of beams, girders, and completion casting, in about 45 natural days, as planned.

Geotechnical Engineering for the Preservation of Monuments and Historic Sites – Bilotta, Flora, Lirer & Viggiani (eds)
© 2013 Taylor & Francis Group, London, ISBN 978-1-138-00055-1

Permanence and preservation of the Metztitlán convent in Hidalgo, Mexico

E. Santoyo-Villa
TGC Geotecnia, Mexico City, Mexico

E. Ovando-Shelley
Instituto de Ingeniería, Universidad Nacional Autónoma de México, Mexico City, Mexico

ABSTRACT: This paper describes the case of the Metztitlan convent, built in the XVIth century some 136 km north of Mexico City. We postulate that the survival of both the convent and the village nearby are threatened by an ongoing geological instability condition associated to a massive ancient landslide. We describe the general geological and geotechnical setting, the damages produced in the convent and the cracking patterns in the ground. We also analyze the measures that have been taken up to now to stabilize the slopes surrounding the convent. Based on the results of geotechnical data, precision topographic levellings and inclinometric data, we suggest that some of these measures have had beneficial effects but others have been ineffectual. In the Authors' view, the case of the Metztitlan convent must remain open and we suggest some new measures to ensure its survival.

1 INTRODUCTION

The Agustinian convent of Metztitlán is located some 136 km north of Mexico City on a hill at the bottom of a deep gorge. Construction of the convent began in the XVIth century, just a few years after the fall of the Aztec empire to the Spaniards. It comprises a large basilical church with its cloister on the east side, surrounding a large patio and smaller structures positioned along its east side. The photo in Figure 1 provides a view of the convent.

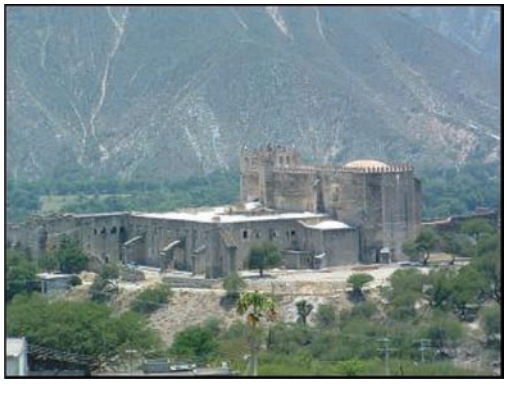

Figure 1. View of the Metztitlán Convent seen from the apse.

A small river, the Tlaxomotl Brook, winds its way at the lowest part of the gorge along the east side of the convent. The basilica has been tilting towards the southwest and the eastern portion of the cloister tilts eastwardly towards the Tlaxomotl Brook, inclination vectors in the garden area are directed towards the west.

The basilica and the cloister are severely cracked and fissured; cracks have also appeared in the ground. From the cracking patterns in the structures and in the ground, at least two failure mechanisms have been identified: low rate movements, probably creep, towards the south or southwest combined with instability of slopes along the brook in the east side.

It has also been established that inclination rates and damage increased after low income dwellings were built in the forties on higher lands north of the convent. There were no sewage pipes at the time and uncontrolled flows from septic tanks towards the convent gradually increased humidity in the subsoil. Seepage continued after installing water and sewage pipes in the forties.

The amount of water seeping into the subsoil increased as did the number of dwellings.

Hurricanes strike periodically the region which is mainly dry under normal conditions, being 170 km from the coast. In 1992, intense storms brought about the collapse of many low income dwellings,

of an evangelic temple and of the latrines in the north-east side of the convent (Lugo-Hubpt et al., 1993). Large storms enhance erosion of the east side slopes due to the action of water flowing in the Tlaxomotl Brook at the bottom of the east side slope. The passage of Hurricane Gilbert in 1996 produced the collapse of other dwellings and small, local slope failures along the right hand side of the brook.

2 GEOLOGICAL AND GEOTECHNICAL ENVIRONMENT

Several ancient landslides have been identified in the region surrounding Metztitlan. The geological process that brings about instability in the region has been described elsewhere (Suter, 2004). Local geological data suggest that the convent lies over one of these landslides that is precariously stable nowadays. The displaced mass at the site dips at an angle of more than 20° towards the south as seen in Figures 2 and 3.

The village of Metztitlan spreads in and around the lower lands south west from the convent, surrounded by the same Tlaxómotl Brook along its east bound and by a smaller brook in the west. Both are dry most of the time and may occasionally drag large boulders during eventual storms that erode the slope feet. The east side is especially vulnerable to erosion induced by boulders and large rock fragments carried by the Tlaxomotl Brook during such storms. Local instability followed the passing of Hurricane Gilbert in 1996 as well as the destruction of several structures built on the east slopes in 1992 (Lugo-Hubp et al, 1993, 1996). The convent latrines also collapsed at that time.

The main soil strata are exposed along the slopes in the east side, above the Tlaxomotl Brook. The upper most stratum contains transported clayey materials, 10 to 20 m thick that overlie fenobasaltic lavas with thicknesses varying from 1 to 2 m, as shown in Figure 4. The lavas rest on top of soft claystones and marls that belong to the Méndez Formation (Mooser, 1993). Additional stratigraphic details and relevant soil properties were obtained from the results of SPT tests performed in 1994 (Pliego, 1997).

Towards the north, the Tlaxomotl Brook joins the Metztitlán River, along a steep gorge. Alluvia deposited by the river form very fertile deposits but the gorge slopes are very dry. Interpretation of satellite images, like the one shown in Figure 5 suggests that the Village of Metztitlán lies on the lower part of a block which may have moved during a massive slide (Suter, 2004). Some of the geotechnical soundings performed in 2007 tend to support this hypothesis. Indeed, lacustrine clays found in those soundings may have originated in the medium Pleistocene, (some 200,000 years from now) and may have formed the bed of an ancient lake which may have been some 600 m above Metztitlan's present elevation. In the authors' view, the slopes

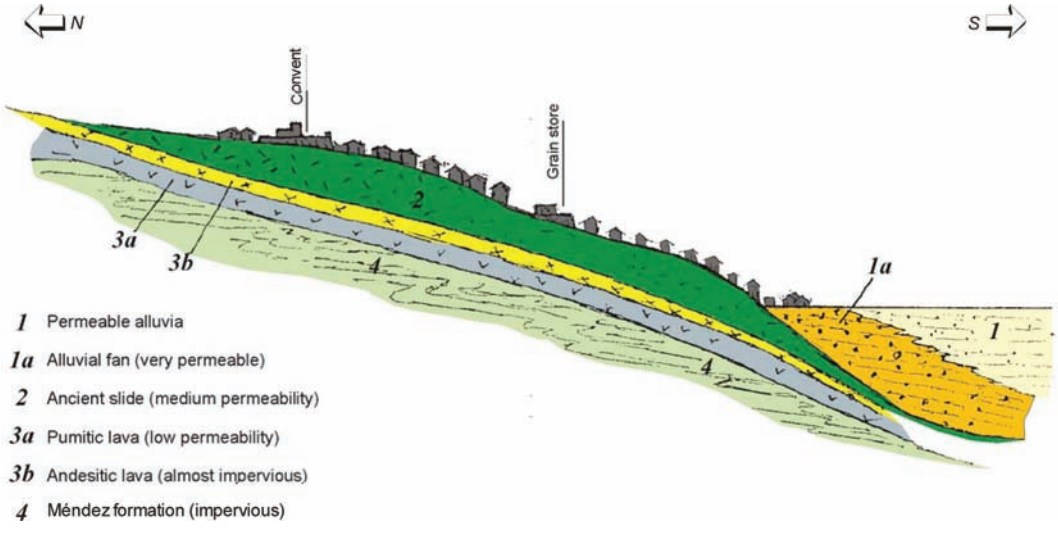

Figure 2. Stratigraphic model, north-south section.

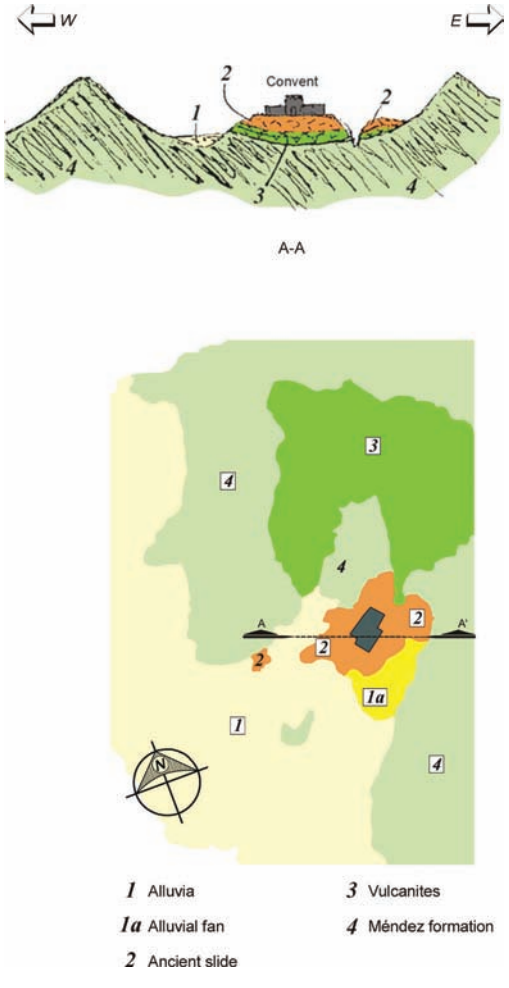

Figure 3. Stratigraphic model east-west section and plan.

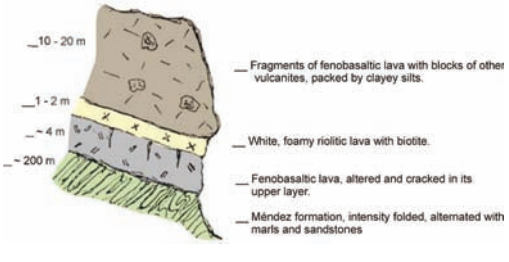

Figure 4. Stratigraphy along the Tlaxomotl Brook.

along this huge block (inclined 14 to 22°, Figures 2 and 3) were stable until water seepage from the dwelling gradually set in.

Figure 5. Slides along the Metztitlan gorge.

3 GEOTECHNICAL DIAGNOSIS

A large number of ancient fissures and cracks in the temple structure and in the floors were recorded in 1992, many of which are currently active. Two-families of fissures in the ground align along parallel curves, as indicated in Figure 6. The most harmful and notorious fissures have developed northwest of the convent. They induce eastward ground movements and are marked with numbers 1 and 2 in Figure 6. Another family of fissures in the south west induces ground movements towards the west. It is also reasonable to expect that ground is also moving southwardly but this has not been yet been confirmed. It is the Authors' opinion that these fissures and ground movements were triggered by water seeping into the subsoil.

Regarding the structural damages to the convent, the ceiling of one of the store rooms in the east side was propped with a concrete column.

4 PROPOSALS FOR SOLUTION

The speed at which damage was accumulating in 1992 led to identifying actions to mitigate the effects of soil wetting. From the mere observation of the site it was suggested that instability of the slopes surrounding the convent could be controlled with an anchored concrete retaining wall. Lacking information about the geotechnical conditions at the site, i.e. stratigraphy and soil properties, the validity of this solution was never assessed (TGC, 1992a; TGC, 1992b).

Local and federal authorities undertook a demolition programme: all the damaged dwellings were

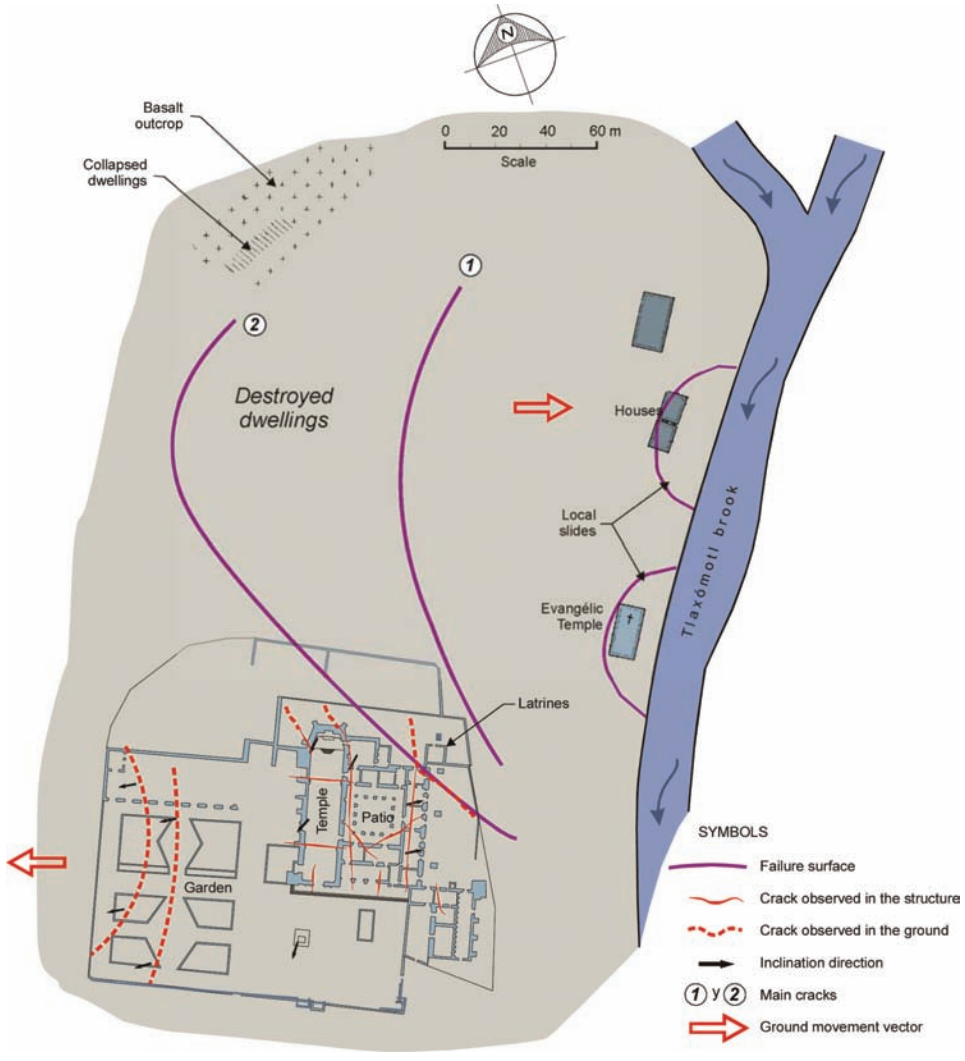

Figure 6. Failure surfaces and cracks.

torn down and construction of new houses above the elevation of the convent and along the slopes of the Tlaxomotol Brook was prohibited. Also, both the sewage and water supply networks were cancelled.

Electro-osmosis was also considered as a possible means for reducing the humidity of the clays and the upper most clay stone layer (TGC, 1993). Water collected with this procedure would be removed with small size pumps. Assessing this procedure required field trials which, however, were never performed.

Geotechnical studies were finally commissioned, starting in 1994 (Pliego et al, 1992 y 2003). They comprised geotechnical soundings, mainly SPT tests, laboratory tests and the installation of two stations with open head piezometers, 15 to 24 m deep. No water table was present at the site, according to piezometric data. The soundings showed that the subsoil comprises two clay strata with a layer of basaltic lava interspersed between them. The lower clays overlie claystones (the Mendez formation in Figure 4). A detailed structural evaluation of the temple and the structures surrounding the cloister was also performed in 2003 (Sánchez Martínez, 2003).

These studies did not consider vegetating and reforesting the slopes and the higher grounds that surround the convent, a useful and beneficial complementary measure.

5 SOLUTION USED

The solution that was finally implemented was conceived as a means of strengthening the east side boundaries of the convent with a line of 41 cast in situ concrete shafts, 1.2 m diameter, capable of bearing the horizontal thrust exerted by the unstable soil mass. The first four experimental piles were installed in 1994, five more piles were placed in 1995 and the remaining 32 piles were commissioned between 1996 and 1997 (the location of the piles is seen in Figure 7). Pile tips were driven about 1 m into the basalt at depths that ranged between 8.4 and 27.5 m, separated horizontally 4.0 to 5.5 m; the five piles on the apse's east side are separated 2.0 m.

Lateral bearing capacity was later increased by means of two 41 t anchors inclined 45°. Figure 7 only shows four of the anchors that were installed south of the convent. The sketch in Figure 8 illustrates the distribution of the piles along the east side of the monument. As seen there, pile tips reach the basalt. It is interesting to note that the basalt upper surface is rather irregular and that the elevations of its upper layes differ in more than 20 m, a fact that tends to support the hypothesis that this mass was displaced by an ancient slide.

Undrained unconsolidated triaxial tests (UU tests) performed on block samples retrieved from a location some 1500 m from the convent were used to obtain shear strength parameters of the upper clays. Shearing resistance can drop substantially when the material is wetted: apparent friction angle (in terms of total stresses) from the UU envelope can drop from 42° at the natural water content of about 20% to about 12° when wetted to a water content of nearly 27%.

These data were the used to estimate the piles' lateral bearing capacity. For partly saturated soils tested with their natural water content the bearing capacity can be as high as 300 t, using Brom's lateral capacity theory (Broms, 1964). Assuming

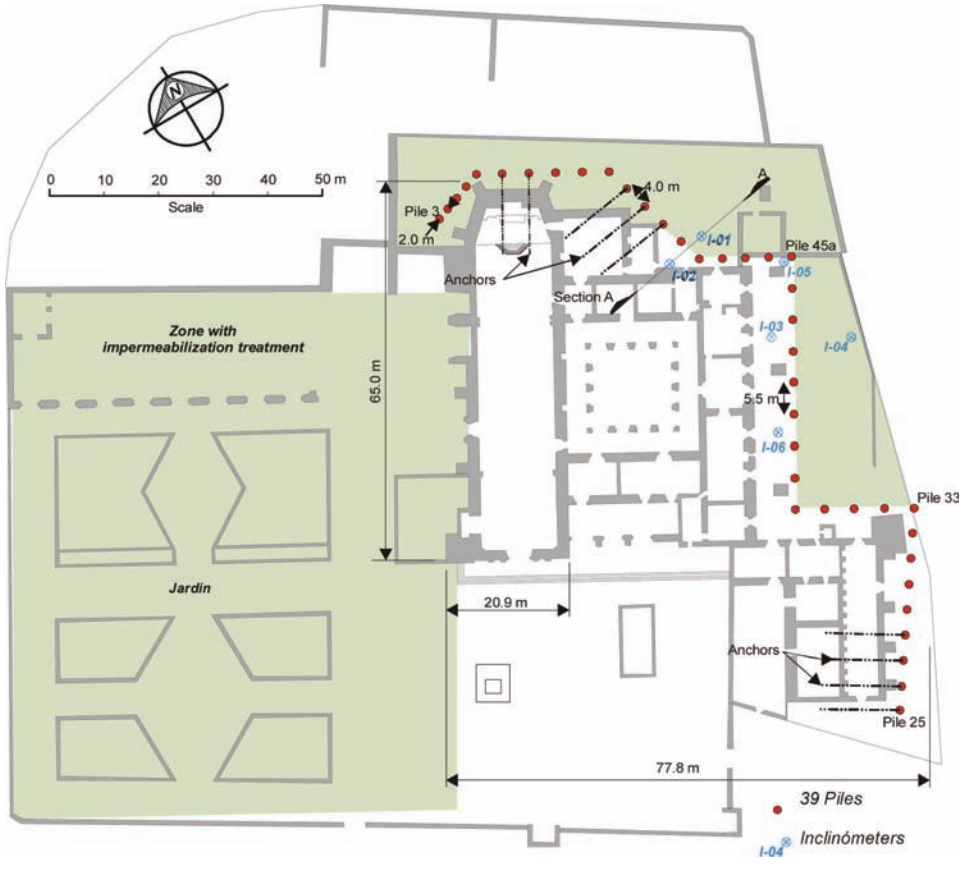

Figure 7. Location of instruments and piles.

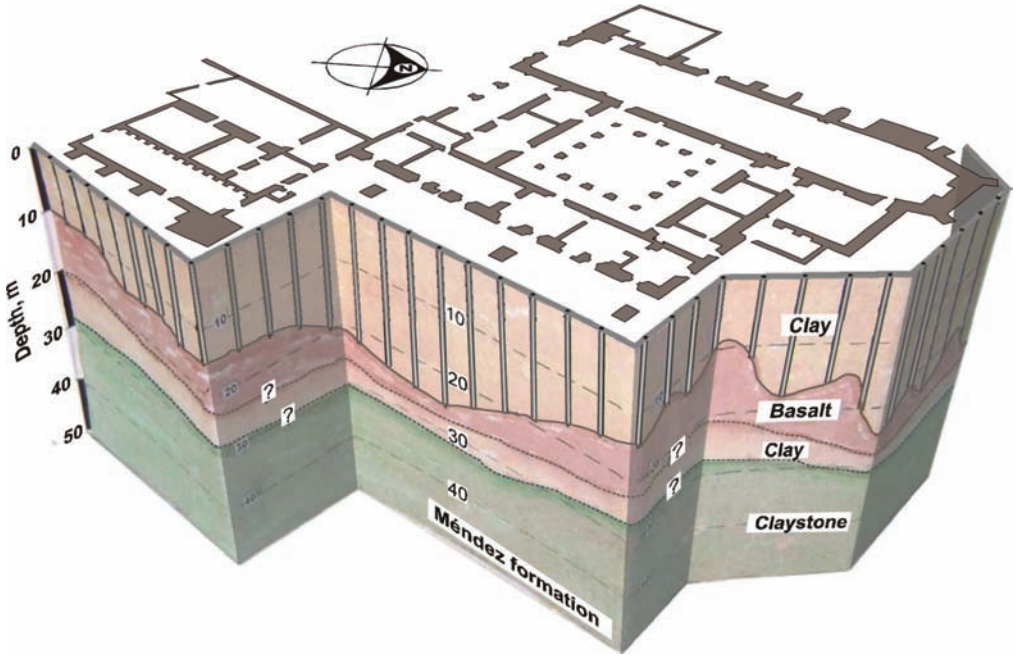

Figure 8. Strata below the convent.

that each pair of anchors will take 55 t of lateral thrust, the combined capacity of the 34 piles installed at the convent's east side, along 200 m approximately, is about 60 t per metre run. If sliding occurs at the interface between the upper clays and the basalt, the thrust exerted on the anchored piles is 15 t per metre run which means that the overall factor of safety is 4.0. Should the upper clays get wet, the factor of safety would reduce substantially but it would still be acceptable.

6 OBSERVED BEHAVIOUR

Six inclinometer casings were installed along the convent's northeast side. Location of the inclinometers is given in Figure 7. Inclinometers I-1 and I-2 were installed on either side of the line of piles at a depth of 40 and 49 m, in the northeast side of the convent. Referring to Figure 7, inclinometers I-3 and I-4 are next to the kitchen and the two remaining inclinometers, I-5 and I-6 are aligned along the line of piles (Pliego, 2003 y 2007). Two wells for observing the phreatic level and two piezometric stations were also installed.

Inclinations in the temple and the cloister were measured with a portable electronic device (Digitilt). Cracks in walls and evolution of openings and closures were monitored closely and precision topographic levellings were also carried out. An impermeable HDP geomembrane was installed in the garden area and in the atrium to prevent water from seeping into the subsoil (Pliego, 2003).

Contour lines given in Figure 9 are settlement rates with respect to an arbitrary reference. Data to produce this graph were obtained from the results of topographic levellings performed over a ten year period, from December 1997 to December 2007. As seen there, settlement rates in the cloister vary between 1 and 2 mm/year and rates inside the temple are even smaller. Outside the built area settlement rates are higher, reaching 6 mm/year northeast of the convent and 4 mm/year in the south atrium.

We show the stratigraphy along section A-A' (see Figure 7 for its location) in Figure 10, including data collected from readings in inclinometer tubes I-1 and I-2, taken between April 2008 and December 2007 (Pliego, 2007). Readings in tube I-1 indicate a uniform lateral displacement of 6 cm down to a depth of about 27 m, directed outside the line of piles, towards the northwest. It should be noted that deformations mainly take place in the clays that underlie the basalt. Deformations measured with inclinometer tube I-2 indicate movements towards the southeast that reached 3.1 cm down to a depth of 40 m. These movements also take place mainly in the lower clays. Both inclinometer tubes show anomalous readings between 20 and 26 m for which the Authors have no explanation.

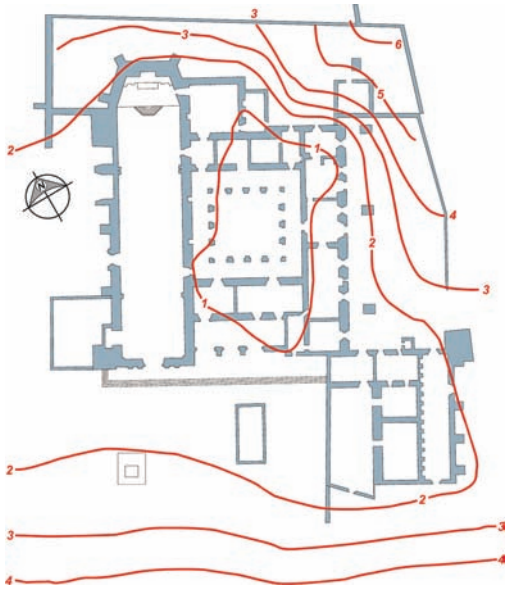

Figure 9. Rate of settlement contours in mm/year.

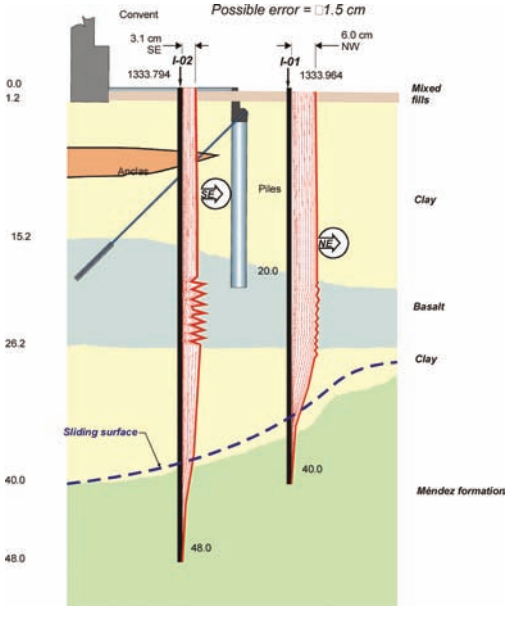

Figure 10. Strata and below the convent and deformations measured with inclinometers. An anchored pile is also shown.

We were only able to analyze readings taken between December 2003 and December 2007 in inclinometer tubes I-3 and I-4. Inclinometer tube I-3 recorded a deformation of 1 cm towards the south, down to a depth of 26 m and in tube I-4 the deformation was 2.5 directed towards the east. In both tubes deformations occurred in the clays that underlie the basalt. We were not able to obtain data from the other two inclinometer tubes. Overall, we estimated that the magnitude of the error that may be present in the inclinometric readings is of the oreder of +/– 1.5 cm.

7 DISCUSSION OF INCLINOMETER DATA

Horizontal deformations recorded at the two pairs of tubes (I-1 and I-2 and also I-3 and I-4) show that the line of anchored piles did reduce the magnitude of deformations next to the convent. Deformation vectors inside and outside the line of piles are nearly orthogonal for both pairs of tubes, a fact that must be reviewed in the light of further instrumental observations and even with 3-D numerical analyses.

It should also be noted that deformations measured in tubes I-3 and I-4 barely exceed the precision range for these instruments. Data available from the third pair of inclinometric tubes, I-5 and I-6, span over a rather short period of time (2003–2007) and accumulated deformations recorded in them are smaller than the precision range. Consequently, data extracted from them over this period is not reliable. The authors have not been able to obtain data spanning over a longer period of time.

Inclinometric data show that a potential sliding surface can develop or has developed at the clays that underlie the basalt, as illustrated in Figure 10. Another potential failure surface can develop at the upper layers of the claystones belonging to the Mendez formation because their properties can degrade more drastically upon wetting.

8 FINAL COMMENTS, CONCLUSIONS

The information made available to the authors shows that the Convent of Metztitlan is being subjected to the effects of lateral displacement of the soil mass over which it was built. The moving mass has induced the apparition of cracks in the cloister and in temple's apse, as well as large fissures in the ground (see Figure 6). Cracking and fissuring are the result of a natural instability process that was enhanced by anthropic actions induced by wetting of the subsoil. The sliding mechanism is complex and according to our analyses, it comprises three components. Presently the most active mechanism develops northeast of the convent and is caused by the instability of slopes along the Tlaxomotl Brook which in turn is produced by the erosive action of torrential currents in the brook at the feet of the

slopes. The other two mechanisms are also significant. They induce movements towards the west and towards the south and are associated to seepage from domestic water supply and sewage pipes, and to creep in the whole of the displaced mass.

Several projects for stabilizing the slopes along the Tlaxomotl Brookl have been proposed. An anchored concrete wall was initially put forth that appears to be an ineffectual solution in the light of the discussions presented here.

Dwellings were gradually built northeast of the convent, mainly on grounds higher than the convent. Water leaking from the municipal supply network, from septic tanks and later, from a very inefficient sewage network increased the humidity of the subsoil and was a major contributor to the observed movements. These dwellings were demolished in 1992 and it is our opinion that this was an adequate measure that reduced significantly the amount of water penetrating into the subsoil and, as a consequence, deformation rates reduced. Flow and water removal with electosmosis was also considered before demolishing those dwellings, a proposal that was never tested in situ and that can still be applied.

The authorities accepted a stabilization project based on using 41 concrete piles, 1.2 m in diameter, complemented with 41 t tension anchors. These piles bear 85% of the horizontal thrust imposed on them by the sliding soil mass and the remaining 15% is taken by the anchors.

An impermeable high density poliethilene membrane was also installed in the atrium garden. The effect of this membrane must be revised since it is possible that it will interrupt the natural evapotranspiration cycle below it and may favour condensation of water beneath it. This may increase the humidity of the subsoil, inducing additional deformations.

Inclinometric measurements show that the sliding surface is located in the lower layers of the lacustrine clays that underlie the basalt. This means that the line of anchored piles will not stabilize the moving mass under the convent. More topographic and inclinometric measurements are certainly needed to ratify this assertion.

The case of the Metztitlan Convent must remain open and its behaviour must continue to be observed instrumentally. It is almost certain that new measures will need to be taken to ensure its survival, such as drilling horizontal drains in the clays that underlie the basalt and in the upper layers of the clay stones of the Mendez Formation. The electrosmotic treatment should also be tested in a trial area next to the convent.

The slopes surrounding the village and the convent should also be instrumented with inclinometers and periodic precision levellings should also be made to measure displacements, displacement rates and also displacement vectors. Shear strength parameters must also be determined precisely. Ring shear tests must be used to determine peak and residual strength parameters, under static and dynamic loading conditions. The latter is a key factor since we have postulated that both the convent and the village lie on top of a massive ancient slide.

REFERENCES

Broms, B. (1964). Lateral resistance of piles in cohesive soils. *Journal of the Soil Mechanics an Foundation Division*, ASCE, New York, v 90, SM2, 27–63.

Lugo-Hubp, J., J.J. Zamorano & G. Gallegos. (1993), Deslizamiento de tierras activo en Metztitlan, Hgo. *Geofisica Internacional*. v. 32, No. 1, 153–166.

Lugo-Hubp, J., T. García-Arizaga, J.J. Zamorano, & O. Salas. (1996), Landslide in Metztitlan (Stateof Hidalgo) México—Causes and effects. *Annals of Geomorphology*, Berlin-Stuttgart, v. 103. 323–343.

Mooser, F. (1993), Personal communication.

Pliego, L., S. Alarcón, & R. Vargas. (1992), *Informe geotécnico correspondiente al estudio preliminarde estabilidad de la ladera oriente del Convento de los Santos Reyes y de la Tercena en la poblaciónde Metztitlán en el Estado de Hidalgo*. Technical report, Colinas de Buen, consultants, Mexico City.

Pliego, L. (2003), *Informe sobre el Comportamiento del ex-Convento Agustino de los Santos Reyesen Metztitlán, Estado de Hidalgo*. Technical report, Colinas de Buen, consultants, Mexico City.

Pliego, L. (2007), *Plano de mediciones de los inclinómetros. Ex-Convento Agustino de los Santos Reyes en Metztitlán, Estado de Hidalgo*. Technical report, Colinas de Buen, consultants, Mexico City.

Sánchez Martínez, J.L. (2003), *Informe sobre la revisión estructural del estado fisico de la bóveda del Refectorio y Ante-refectorio; en el ex—Convento Agustino de los Santos Reyes en Metztitlán Estado de Hidalgo*. Technical report, Colinas de Buen, consultants, Mexico City.

Suter, M. (2004), A neotectonic-geomorphologic investigation of the prehistoric rock avalanchedamming Laguna de Metztitlán. *Revista Mexicana de Ciencias Geológicas*, v. 21, No. 3, 397–411.

TGC Geotecnia. (1992), *Reconocimiento del ex-Convento y La Tercena de Metztitlán*. Technical Report 1279, TGC Geotecnia, geotechnical consultants, Mexico City.

TGC Geotecnia. (1992), *Medidas correctivas urgentes para las zonas inestables del oriente del ex-Convento y La Tercena en Metztitlán, Hidalgo*. Technical Report 1312, TGC Geotecnia, geotechnical consultants, Mexico City.

TGC Geotecnia. (1993), *Inspección al Convento y La Tercena de Metztitlán. Hidalgo*. Technical Report 1448, TGC Geotecnia, geotechnical consultants, Mexico City.

Geotechnical Engineering for the Preservation of Monuments and Historic Sites – Bilotta, Flora, Lirer & Viggiani (eds)
© 2013 Taylor & Francis Group, London, ISBN 978-1-138-00055-1

The Fontanelle Cemetery: Between legend and reality

A. Scotto di Santolo, L. Evangelista & A. Evangelista
University of Naples Federico II, Italy

ABSTRACT: The paper reports the history of the "Cimitero delle Fontanelle" (literally: cemetery of the small fountains), one of the most fascinating among the cavities of the subsoil of Naples. During its four centuries of life this cave has experienced a number of events, until it found in the modern age its final destination as a place of warship and became part of the cultural heritage of the city. After touching historical, urban and social aspects, an evaluation of the stability condition of the cavity is attempted. The state of stress in the tuff, in which the excavation has been carried out when the present cemetery was an underground tuff quarry, is analyzed by means of a 3D finite difference code, taking into account the various stages of excavation and subsequent partial filling. The results obtained show that there are some stability problem for the roof of the cavity; further investigations on the shape of the pillars, partially hidden by the fill, and on the mechanical properties of the tuff are needed for a more satisfactory evaluation.

1 INTRODUCTION

The sacred remains of the queens of the Mediterraneum (Athens, Syracuse, Rome and their colonies), rich in history and culture, are also characterized by a subsoil crossed by an intricate network of tunnels, shafts and tanks. The subsoil of Naples does not escape this feature; it is characterized by the widespread presence of the Neapolitan Yellow Tuff (NYT), a soft rock of volcanic origin through which the system of cavities has been excavated in the centuries (Melisurgo 1889; Puntillo 1994).

Though being not particularly beautiful neither rich or famous, one of the most fascinating among the Neapolitan cavities is the so called Fontanelle Cemetery (Esposito 1992), Figure 1.

It is an ancient tuff quarry, destined to become an ossuary in the XVIII century and progressively turned into a Christian worship place of the Neapolitan lower class.This paper aims to report not only the geomorphological and geotechnical aspects of the Cemetery, but also the historical, social and environmental ones, in order to highlight the tight connections between the past of the cavity and the history of the city.

Figure 1. Picture of Fontanelle Cemetery, Naples, Italy.

2 MORPHOLOGICAL ENVIRONMENT

The city is located at the southern border of an upland plain of volcanic origin known as *Terra di Lavoro*, formed around 35,000 years ago as the results of a gigantic eruptive explosion, Figure 2. The territory of the ancient city of Naples may be ideally split into two areas with rather different morphology. The western area exhibits a hilly and articulated morphology, while the eastern one is gently sloping towards the sea from north to south. This gentle slope, called "Pendino", is the seat of the historical centre; here Naples, unique in the world, after almost three millennia still bears the original structure of the former Greek city. This structure is characterized by three greek "plateiai", later Roman "decumani", 6 m wide and oriented in the east-west direction, intersected at right angle in the north-south direction by the "stenopoi", or "cardi", only 3 m wide.

The eastern and western parts of the city are split by a road running in north-south direction, on the line of the present Via Toledo, Via Santa Teresa degliScalzi and CorsoAmedeo di Savoia. The road connects the coast to Capodimonte, a piece of the Terra di Lavoro separated from the upland plane by the canyon of the Vallone San Rocco. CorsoAmedeo di Savoia overpasses

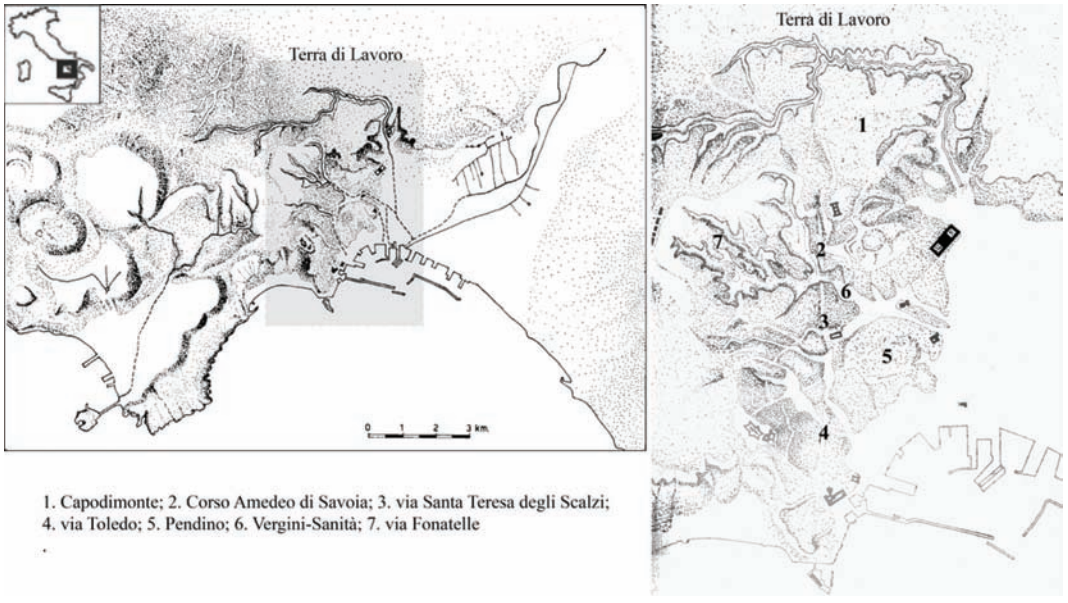

Figure 2. Morphological setting of Naples, Italy and location of the Fontanelle Cemetery (modified from Scherillo, 1967).

with a bridge the densely populated district of Vergini—Sanità.

The backbone of the hills is the NYT, covered by pyroclastic soils (pozzolana and pumices) that are easily eroded by rain water; deep gorges have been hence excavated in the slopes. The materials eroded were transported by mud and debris flows, the so called "lava dei Vergini", through the valley of Vergini, at present densely urbanized. So frequent was this event, that the lower classes had invented the practice of "passalava": a porter who carried the lords across the roads invaded by the mud and debris, in order not to let them get dirty. Disastrous floods are known to have occurred in 1435 (the so called "diluvio della Conocchia), 1566 and 1569. Such aneroding action going on through the centuries exposed the underlying tuff on the sides of the valleys, creating the optimal conditions for quarrying it as a construction material. As a matter of fact, the bridge over the Sanità and all the houses where built with the stones extracted from the hills where the tuff outcrops. There are at least seven large underground quarries left along Corso Amedeo di Savoia, with volumes up to 372.000 m^3. The same road, via Fontanelle, where the cemetery is located, is an old water course; on its sidesseveral quarrieshave provided the building materials for the constructions in the city and are today addressed to different uses. It is to mention that the Neapolitan laws of XVII century forbade quarrying the tuff inside the city, so that the quarries were concentrated just out of the walls, right in this zone (Rosi 1994).

All these cavities are rather large, with a total volume of the order of six millions of cubic meters. Many of them were later used for Pagan and Christian worshipping (Puntillo 1994; Esposito 2007). Each cavity has its own complex story, but that of Fontanelle is particularly suggestive.

3 THE HISTORY OF FONTANELLE CEMETERY

The ancient tuff quarry named "Cimitero delle Fontanelle" is located near the church of Maria Santissima del Carmine, at the boundary of the densely populated district of Vergini—Sanità, just outside the ancient Greek—Roman necropolis, Fig. 2. This area was chosen for the pagan—and later Christian—cemeteries. The cavity in question has no particular architectural features, nor its size (width and height) is worthy of special note. Its particularity is that it was used for different purposes and, since its excavation, experienced several changes.

The origin of the quarry may be traced back to the XVI century, and its expansion to the XVII century. At that time, the city was scourged in rapid succession by popular rebellions, famines, earthquakes, eruptions of the Vesuvius and epidemics. Being our cavity located in an isolated place, outside

the walls of the city but close to them, it was used to collect the corpses of the victims. It is said that in 1656, after a deadly plague, the walls that closed the cave were broken and 250,000 corpses (other sources quote a figure of 300,000) out of a population of 400,000 inhabitants where accumulated. The canon Andrea de Iorio reports that, at the end of XVIII century, all well-to-do persons wanted to be buried in churches where, however, there was not more space left. It happened so that the grave diggers pretended to adhere to the request of burial in the church and then, late at night, the corpse was put in a sack and "they went to put it back in the quarry of the Fontanelle, which was no longer in use".

In 1764 the architect Carlo Praus confirms this practice by stating that that the quarry was used to bury the bodies of the lower class. But due to a sudden flood into the cave, the corpses were dragged outside and ended up to clogging the great sewer running beneath Via Toledo. Later the bones were reassembled in the cavity, a wall and an alter were built and the place began the charnel house of the neighbouring districts. Still in 1834 the bones removed from the burial of the churches were laid in this ossuary. In 1872 some faithful people, led by father Gaetano Barbati, arranged the thousands of bones in neat stacks in various distinct areas, and from then on a spontaneous and strong popular devotion arose for those unidentified dead. Some skulls were adopted by the faithful, placed in special glass and wood cases and treated so that they might come in a dream and predict the future. Only the identity of two people, Filippo Carafa Count of Cerreto and his wife, is known. It seems that the stones cut from the quarry was indeed used for the construction of the mansions of Prince Carafa.

The ossuary was closed in 1969, by order of the Archbishop of Naples, due to religious deviations that were believed to take place there. Despite this, in the following years the devotion for these corpses increased; the devotes identified in them the souls of the Purgatory that needed care and attention.

The cavity was reopened only in 2010, after some consolidation interventions carried out in 2002.

The ossuary of the Fontanelle emblematically represents the horror of the plague and death. The figuration and remind of those dramas take the value of tools for a reflection on the disrupting effects of the disasters caused by the human sin, on the pain and on the death.

4 STRUCTURAL DESCRIPTION OF THE CAVITY

The Fontanelle Cemetery is a chamber and pillar cavity with two direct access; the roof is supported by 9 isolated pillars (P1 to P9) and 4 further vertical elements or septums (SE1 to SE4) protruding from the walls (Fig. 3).

The portal is made of piperno stone; at the entrance there is a very wide area, the roof of which is supported by three isolated pillars (P1, P4 and P8) and three septums (SE1, SE2 and SE3).

The overall shape in plan is rectangular, elongated in a north-south direction and consisting of three naves (Fig. 3). The intermediate one is called "navata degli Appestati" (nave of the plague stricken persons) and the second one is the "navata dei Preti" (nave of the priests). Entering on the right, there is a third secondary aisle with an inclination of 45° respect to the other ones and a smaller span, called "navata dei Pezzentelli"(nave of the small beggars). The overall width of the two main naves is 40 meters and the length 105 m, with a total area of more than 3.000 square meters.

The height of the "navata dei Preti" is 7 m, while the "navata degli Appestati" is 10 m high. The

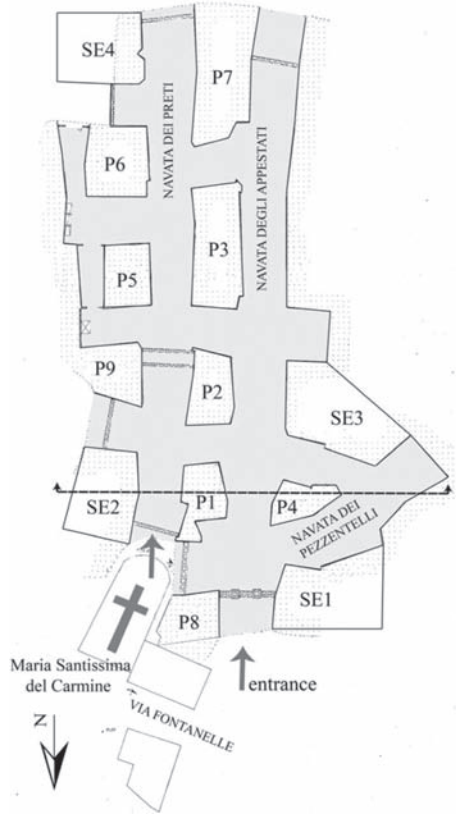

Figure 3. Plan view of the Fontanelle Cemetery with its numbers of structural elements (9 isolated pillars and 4 septum) and the trace of a representative cross section.

cover above the roof (tuff plus pyroclastic soils) ranges between 8 and 10 m. In the entrance and in the central chamber the height of the roof rises up to 12.0 m, while the cover is 30 m thick.

The naves sections have a trapezoidal shape with a flat roof and walls inclined of 10°–15° to the vertical; the pillars, consequently, have a structural section decreasing with depth.

The material below the present floor level (72 m a.s.l.) is composed by an inter-bedding of anthropic fill and cineritic levels of different grain size and alluvial origin. The floor of the ancient quarry lies at an average depth of 9.0 m from the actual walking level. It is therefore believed that the pillars, for a substantial stretch, are buried in the filling material.

An intense fracturation is present in the central part of the roof at the entrance, with a prevailing northwest-southeast orientation; for its persistence, this is probably the main discontinuity family. There is probably a second discontinuity system in the east-west direction; it appears in the points where there are variations of height of the cavity. A few vertical discontinuities have been found in the navata dei Pezzentelli, at the intersection between the roof and the pillar.

A systematic survey of the discontinuities is not available, and accordingly they have been considered only marginally in the following analyses.

5 POSSIBLE MODALITY OF EXCAVATION OF THE CAVITY

Even if the cavity has been interested by several inspections, a systematic and exhaustive campaign of geological, geotechnical and structural investigations has never been performed. Due to the complexity of the problem, a number of uncertainties remain concerning the hidden geometry of the cave, the profile of soils and rocks, the structural characterization of the rock above the roof and the mechanical properties of the materials.

One of the major uncertainties is connected to the hidden geometry below the present floor, that is closely related to the unknown details of the excavation technique. It is well-known, however, that in Central and Southern Italy the extraction of the tuff was often carried out underground to preserve the ground level and to use the soil in situ for rural activities (Minardi 1999; Padovan 2009). The most widespread technique was the "chamber and pillars" one: the quarries have generally a regular layout in plan, with mutually orthogonal directions of excavation to create a mesh of isolated pillars. A number of vertical shafts, communicating with the outer surface, allowed the ventilation and the evacuation of the quarried material.

Figure 4 shows a picture of the pillar P4, in which there are clear traces of steps cut into the tuff to allow the quarrymento leave the cavity through a shaft. The treads could be also made by a folded iron bar cemented into the rock.

It is to remind that, in the XVII century, the transportation of large rock boulders outside the cavity was not easy. For this reason the building stones were cut in the quarries, leaving the debris of this activity inside.

The possible excavation technique of the Fontanelle Cemetery, therefore, seems to follow these phases: (1) excavation of a vertical shaft in the pozzolana till to the top of the NYT and then at least 8 m inside the tuff; (2) underground horizontal excavation leaving above a tuff slab of 8 m thickness to act as a roof structure and to preserve the pozzolana in situ; in this way the roof is bounded to the lateral walls of the cavity.

The excavation went on gradually deepening the floor of the chambers, until a height of around 20 m of the cavity is achieved, and leaving the pillars in proper position.

With this modality of excavation, the bottom of the cavity reached an average level of 60 m a.s.l. (Old Level, OP) and 9 pillars and 4 septums were left to support the roof structure.

A period of inactivity inside the cavity follows. On the bottom of the excavation a mixture of tuff cuttings, debris and mud transported by the floods gradually accumulated, where human remains were buried or simply abandoned by the gravediggers. This material has been regularized and levelled to the present ground floor level has risen, at an elevation of 72 m a.s.l. (Present Floor Level PFL).

The present entrance and ticket office is at an elevation of 75 m a.s.l. According to this reconstruction of the sequence of events, currently in the cavity the exposed height of the pillars is on average 9 m, while the remaining part, of which the shape is unknown, is buried in the fill for an average length of 11 m.

Figure 4. Picture of the pillar P4 on which the traces of the ladders, used by the quarrymen, are visible.

6 SIMPLIFIED ANALYSIS OF THE CAVITY

The state of stress around an underground cavern and its static conditions may be evaluated following different approaches wit different accuracy.

To evaluate the vertical stress acting on the pillars, the so-called 'area of influence' method may be adopted (Evangelista et al., 2002). The stress in the pillars is evaluated through equilibrium conditions between the vertical load in the pillar and the weight of the roof and the cover materials, corresponding to their area of influence, defined by geometric conditions. The weight is determined by taking into account the external morphology of the soil and assigning for the tuff rock and the covering soil a unit weight equivalent respectively equal to 14 kN/m^3 and 15 kN/m^3. The values of the average vertical compression stress on the pillars σ_v, determined at the present planking level as a function of the height h_p, are reported in Table 1. In the same Table, the value of the base area of the section, A_p, the relative influence area, A_i, as well the thickness of the cover soils, S, are reported for each pillars.

The safety factor, FS, can be estimated as the ratio between the uniaxial compression strength σ_c, assumed equally to 3 MPa for the intact rock (Evangelista et al., 1998; Aversa & Evangelista 1998), and the average vertical stress σ_v in the pillar. It has been found that FS is nearly unity for pillar 4, and takes relatively low values for pillars 2 and 7; all the remaining pillars appears to be safe with ample margin.

The method of the areas of influence is generally conservative. No account has been taken of any defect or major variation of the section of the pillars, which may increase the stress level. Moreover, a significant scale effect is known to occur for the strength of the rock mass compared to that determined on core samples (Paparo Filomarino & Pellegrino 1980). For all these factors, the reported evaluations are to be considered as a first approximation. Simple analyses of the safety of the roof have been carried out under plane strain conditions and adopting a limiting equilibrium methods; mechanisms of partial or total collapse have been considered. The coefficient of safety against failure of the roof is calculated as the ratio between the existing span and the critical span evaluated by the limit equilibrium approach (Evangelista et al., 2000). In the case of Fontanelle cemetery the total collapse of the roof may be excluded, while the detachment and fall of blocks of tuff is possible and could endanger the stability of the whole cave.

Table 1. Stability condition of the pillars.

Pillar #	A_p m^2	A_i m^2	h_p m	S m	σ_v kPa	FS 1
P1	107.6	384.9	11.0	13.0	852.0	3.5
P2	101.4	389.6	7.0	17.0	1079.0	2.8
P3	197.8	540.0	7.0	23.0	1040.0	2.9
P4	68.37	493.7	12.0	25.0	2876.0	1.0
P5	97.67	267.0	7.0	13.5	631.0	4.7
P6	151.4	321.9	7.0	14.0	545.0	5.5
P7	253.7	643.5	7.0	27.0	1124.0	2.7
P8	88.55	232.5	8.0	6.0	328.0	8.6
P9	101.8	275.7	7.0	10.0	505.0	6.0
SE1	204.0	516.0	12.0	15.0	737.0	4.0
SE2	208.0	649.0	7. 0	6.0	378.0	7.9
SE3	262.7	516.7	12.0	25.0	905.0	3.3
SE4	180.0	591.0	7. 0	12.0	689.0	4.3

7 3D NUMERICAL ANALYSIS

The availability of efficient and low cost software and hardware encourages the designers and researchers to perform numerical calculations with complex constitutive laws. In spite of it, however, a sufficiently accurate evaluation of the stress and deformation field around existing underground cavities is far from an easy task. The reliability of the prediction depends entirely on the accuracy of the input data used in the model: the hidden geometry, the mechanical properties of the in situ rocks, the initial state of stress, the sequence of mining processes and so on. Due to the difficulty of getting a reliable evaluation of all these data, in this paper a three-dimensional finite difference method was adopted in a simplified way. The analyses have been performed by the code FLAC3D (Version 5, Itasca, 2012).

In the analyses of the cavity the geometry of the cavity has been simplified assuming that the pillars have their lateral surfaces inclined ±15° to the vertical from the roof to the present fill level (PFL), while they are vertical till the base (OL).

The soil profile, starting from the top of the hill, is composed by pyroclastic soil ("pozzolana") overlying pyroclastic soft rocks (NYT). Over the floor of the cavity a fill as described above has been considered. The materials have not yet been deeply investigated, especially for the debris that is indeed very peculiar. The mechanical properties adopted in the calculations are the average values available in the literature for Neapolitan materials (Evangelista et al., 1998; Picarelli et al., 2006), and are reported in Table 2.

Due to the lack of sufficient information about the discontinuities in the tuff, the properties of the intact material have been assumed for the rock mass. The materials were modelled as elastic-perfectly plastic, using the Mohr-Coulomb failure criterion.

Table 2. Mechanical properties of materials adopted.

Material	γ kN/m³	E kPa	ν 1	ϕ °	c kPa	σ_t kPa
Pozzolana	15.0	1.96e+5	0.30	33	15.0	4.9
Tuff	14.0	9.81e+6	0.17	29	80.0	9.8
Debris	13.0	9.81e+4	0.37	25	0.7	0.1

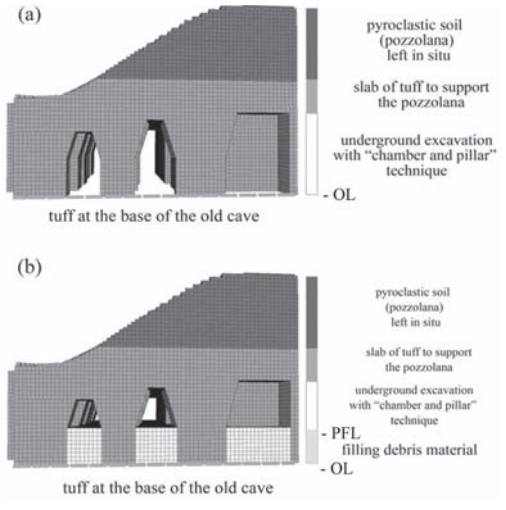

Figure 5. Numerical models adopted; materials in situ and the possible sequence of excavations: (a) ancient cavity; (b) actual cavity.

The finite difference mesh adopted is shown in Figure 5. The mesh relates to the different possible configuration assumed by the cavity during its life:

a. the ancient cavity at the end of the mining works;
b. the present configuration after the slow filling with debris material.

The elements are square bricks of 100 cm and u-wedge (of the same dimensions) for the inclined walls of the portals, for a total of about 300,000 elements.

The boundary conditions are: at lateral boundaries the horizontal displacements prevented at the lateral boundaries, no displacement at the bottom. These hypotheses have almost negligible effects in our case, since a very low value of the Poisson's ratio has been assumed.

The analyses don't take into account the consolidation work, carried out in 2002, and which affected the roof in the entrance to the cavity and the last septum (SE4) in the nave of the Priests (Navata del Preti in Figure 4).

8 RESULTS

The numerical analyses have been carried out in three phases:

1. evaluation of the initial state of stress in the hill ($k_o = 1 - \text{sen}\varphi$) before the underground opening;
2. excavation of the tuff up to the old level (OL) in steps of 20 m in longitudinal and transverse directions;
3. filling up to the present ground floor (PFL at 72 m a.s.l.) in three steps.

The results reported are expressed in terms of the vertical stresses, maximum shear stress and plastic zones in the horizontal section at OL and PFL and in the vertical section reported in Figure 3.

Figure 6 shows the vertical stress at the end of the three stages analyzed, at the section shown in Figure 3. It may be observed that the pillars are more loaded at the end of the phase 2 than after the refilling by the debris material, due to the presence of shear stresses at the interface between them.

The contours of the vertical stress in the pillars at the end of the phase 3 (present configuration) is reported in Figure 7 with a plan view of the 3D model at the PFL. It appears that the weight of the cover material is unevenly distributed on each pillar and septum; the structural elements that support the greater thickness of coverage result the most heavily loaded.

In Figure 8 the history of the vertical stress during the three phases analyzed are reported for the pillars P1, P2, P3 and P4 at the PFL. The load on the pillars grows from phase one to three with a delay depending on the mining procedure adopted.

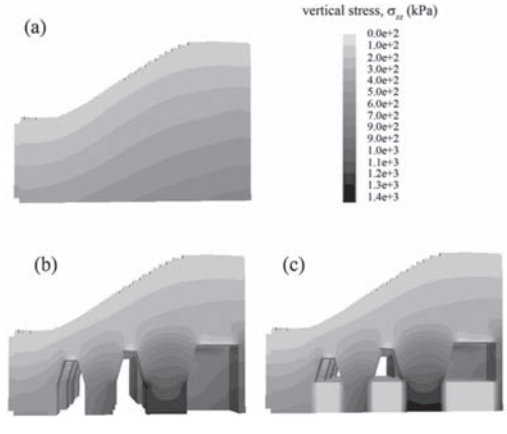

Figure 6. Vertical stress at the end of the three phases analyzed: (a) initial state; (b) after excavation up to the OL; (c) after filling up to PFL.

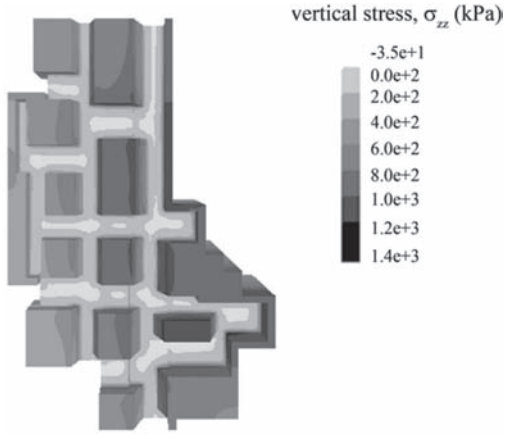

Figure 7. Plan view of the vertical stresses at the end of the phase 3 from the PFL.

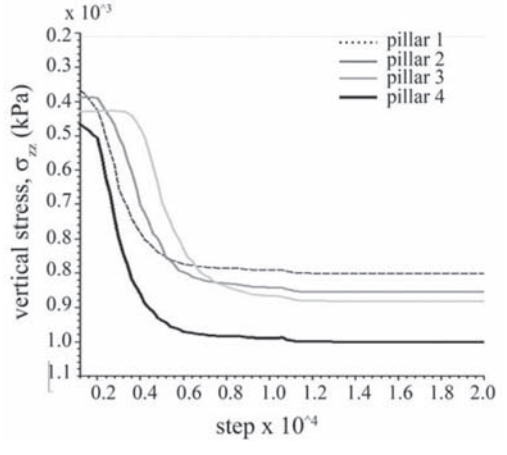

Figure 8. Histories of the vertical stresses at the base (PFL) of pillars.

Pillar 4 is more loaded than the other ones, due to its greater height and area of influence.

In Figure 9 the contours of the maximum shear stress in the cross-section of Figure 3 are reported. The maximum value occurs in the pillars P4 at the PPL, but it doesn't reach the failure condition.

The computed vertical stress in the pillars are lower than those obtained previously with the simplified analyses and reported in Table 1. These results are confirmed by the shear stress distribution around the pillars after the filling of the cavity with debris materials (Fig. 9).

No dangerous stress state occur in the pyroclastic material that covers the tuff.

Figure 10 (a) reports the distribution of the plastic zones resulting from the computation;

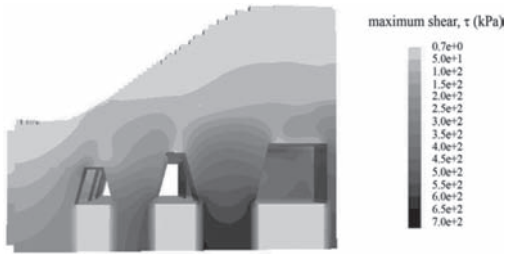

Figure 9. Maximum shear stress at the end of the phase 3.

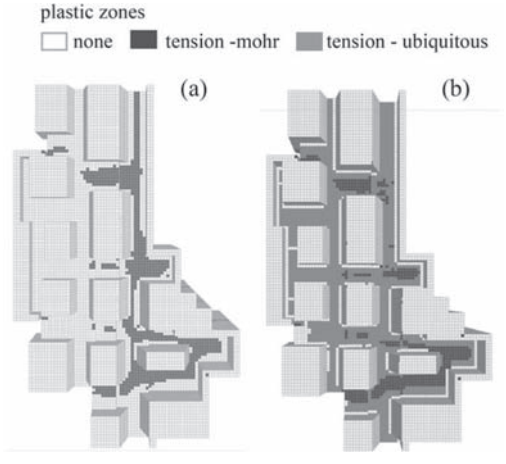

Figure 10. Plan view of the plastic zones: (a) Mohr-coulomb and (b) ubiquitous joint model for the TGN.

they are concentrated on the roof. The portions of the cavity mainly affected by tension failure are the "navata degli Appestati" and the "navata dei Pezzentelli"; in these galleries, the roof is interested by tensile vertical stress higher than the tensile strength of the tuff. This is in agreement with the distribution of the vertical stress on the roof, already reported in Figure 7, and with the in situ observations that show the presence of transverse cracks in the roof.

As said before, in the above analyses the influence of the fracture orientation and fracture persistence on the strength of the rock mass and its response to caving has been totally neglected.

An attempt to take it into account has been carried out, by modelling the rock mass with the ubiquitous joint technique.

Ubiquitous joint model is adopted here to account for the presence of weak plane. Yielding may occur either in the intact rock mass or along the weak planes, depending on the stress state, the

orientation of the weak planes and the material properties of the weak planes.

For the material properties of the joints the cohesion along the joints has been assumed equal to 265kPa, the tensile strength to 2kPa and the friction angle to 19°. Based on a preliminary analysis of the available data, the dip direction and dip of the weak planes are assumed respectively equal to 85° and 45°.

A comparison of the results obtained with this model with those previously reported shows that the state of vertical stress in the pillars is practically unaffected by the different models.

Substantial difference, on the contrary, have been found for the plastic zones in the roof. With the ubiquitous joint model, in fact, the tension failure condition spreads over the whole roof (Fig. 10b).

9 CONCLUDING REMARKS

The paper reports the story of one the most fascinating cavities of the subsoil of Naples, the Fontanelle Cemetery, which during 400 years of life experienced a series of events until it finds, in the modern age, its role as a place of worship for the population of the neighbouring districts.

The paper mixes historical, urban and social aspect, as well as technical results on the stability conditions of the cave.

A numerical study is presented to evaluate the stress state conditions around the cavity, carried out by the finite difference code FLAC3D Version 5 (Itasca, 2012). Through these numerical analyses, it was tried to reproduce the present state of stress of the structural components, taking into account the sequence of the excavations and the subsequent filling up of the cavity with human rests and debris of mud, till the present ground level.

The comparison between elasto-plastic numerical 3D analyses and a 2D rigid-plastic limit analysis confirms that the latter is conservative. The simple procedures, however, keep their validity if coupled to sound 'Engineering judgments'. Two different failure criteria (Mohr Coulomb and ubiquitous joint) have been also adopted to evaluate the influence of weakness plane.

Due to the lack of an accurate and updated mechanical characterization of the materials, the results obtained represent but a rough estimate, which highlights however the occurrence of a critical situation in the cavity roof. It is believed, therefore, that the cavity should be subjected to furthermore complete and reliable investigations and analyses.

ACKNOWLEDGEMENTS

This work has been made possible thanks to the data supplied by C.U.G.RI., Naples.

REFERENCES

Aversa, S. & Evangelista, A. 1998. The mechanical behaviour of pyroclastic rock: yield strength and destructuration effects. *Rock Mechanics and Rock Engineering*, Vol. 31, No. 1, pp. 25–42.

Esposito, C. 1992. *Il cimitero delle Fontanelle*. Napoli: Oxiana.

Esposito, C. 2007. *Gli Ipogei Greci della Sanità.* Napoli: Oxiana.

Evangelista, A., Aversa, S., Pescatore, T.S. & Pinto, F. 2000. Soft rocks in the Southern Italy and the role of volcanic tuffs in the urbanization of Naples. *Proc. of the II Int. Symp. on "The Geotechnics of Hard Soils and Soft Rocks", Napoli, Vol. 3:* 1243–1267. Rotterdam: Balkema.

Evangelista, A., Feola, A., Flora, A., Lirer, S. & Maiorano, R.M.S. 2000. Numerical analysis of roof failure mechanism in soft rocks. *GeoEng2000, Melbourne*.

Evengelista, A., La Pegna, U. & Pellegrino, A. 1980. Problemi geotecnici nella città di Napoli per la presenza di cavità nella formazione del tufo. *Atti del XIV Convegno Nazionale di Geotecnica, Firenze.* Bologna: Pàtron.

Evangelista, A. & Pellegrino, A. 1990. Caratteristiche geotecniche di alcune rocce tenere italiane. *Terzo ciclo di conferenze di Meccanica ed ingegneria delle Rocce (MIR), Torino*, Vol. 2, pp. 1–32.

Evangelista, A., Flora, A., Lirer, S., de Sanctis, F. & Lombardi, G. 2002. Studi ed interventi per la tutela di un patrimonio sotterraneo: l'esempio delle cavità di Napoli. *Atti del XXI Convegno Nazionale di Geotecnica*, *L'Aquila,* pp. 579–588. Bologna: Pàtron.

Itasca, 2012. FLAC-3D Fast Lagrange Analysis of Continua Version 5. User's Guide. Itasca Consulting Group, Minneapolis, USA.

Marrone, R. 1996. *Le strade di Napoli.* Newton & Compton.

Melisurgo G. 1889. *Napoli sotterranea*. Reprinted by ESI, Napoli, 1997.

Minardi, M. 1999. *Cave e Cavamonti*. Ed. del Grifo.

Padovan, G. 2009. Archeologia del sottosuolo. Manuale per la conoscenza del mondo ipogeo. Milano: Mursia.

Paparo Filomarino, M. & Pellegrino, A. 1980. L'effetto dimensione nel Tufo Giallo Napoletano. *Atti del XIV Convegno Nazionale di Geotecnica*, *Firenze.* Bologna: Pàtron.

Picarelli, L., Evangelista, A., Rolandi, G., Paone, A., Nicotera, M.V., Olivares, L., Scotto di Santolo, A., Lampitiello, S., Rolandi, M. 2006. Mechanical properties of pyroclasticsoils in Campania Region. *Proc. Int. Workshop on Characterisation & Engineering Properties of Natural Soils, November- 1 December 2006,* pp. 2331–2383. London: Taylor & Francis.

Puntillo, E. 1994. *Grotte e caverne di Napoli*. Newton & Compton.

Rosi, M. 1994. *Napoli entro Le Mura*. Napoli Tascabile.

Geotechnical Engineering for the Preservation of Monuments and Historic Sites – Bilotta, Flora, Lirer & Viggiani (eds)
© 2013 Taylor & Francis Group, London, ISBN 978-1-138-00055-1

A class C prediction of the settlements induced in a historical masonry structure by the excavation of shallow twin tunnels

M. Sebastianelli, G. de Felice & M. Malena
University of Roma Tre, Rome, Italy

A. Amorosi
Politecnico di Bari, Bari, Italy

D. Boldini
University of Bologna, Bologna, Italy

G. Di Mucci
Metro C S.p.c.A, Rome, Italy

ABSTRACT: In this paper a class C prediction of the possible damage induced in an existing old masonry structure by the construction of two parallel shallow tunnels is discussed and compared to the behaviour observed during the excavation stages. The structure under study is the ancient Felice Aqueduct in Rome, recently underpassed by the tunnels of the future underground line known as Metro C. The local geotechnical profile is mainly characterised by a sequence of relatively stiff soil and weak rock strata of volcanic origin, all subjected to an extensive investigation carried out by means of in-situ and laboratory tests. The structure itself has been properly characterised in terms of sub and above-surface geometry and mechanical properties of its block and mortar components. The back predictions were carried out by means of the FE code Abaqus, assuming plane strain conditions for the soil and plane stress ones for the structure. The masonry structure is schematised as an anisotropic elasto-plastic medium, whose elastic properties and yield criterion are derived via homogenization starting form a block structure with periodic texture. The macroscopic model is shown to retain memory of the mechanical characteristics of the joints and of the shape of the blocks. The soil strata are modelled by means of a linear elastic-perfectly plastic model, calibrated against the available experimental results. In the analyses a realistic construction sequence is simulated imposing volume losses consistent with those observed in situ: the resulting settlement profiles as predicted at different elevations of the Aqueduct are in good agreement with those monitored during the real excavations. The adopted approach proves to be valuable for the class of problems under study and, as such, is amenable to be used in future as a class A predictive tool for similar soil-structure interaction processes.

1 INTRODUCTION

Tunnel excavation in urban areas, nowadays more and more frequent due to the development of underground infrastructure networks, is always associated to ground movements and settlements at the ground surface. In this respect possible damage to above—and sub-surface structures, especially if ancient and historically-valuable, represent one of the principal risk associated to tunnelling operations.

In this paper a real case history is selected to evaluate the performance of a comprehensive numerical model to predict the interaction among tunnel construction, ground movements and structure response. Reference is made to the Felice Aqueduct in Rome, a masonry historical construction of the XVI Century, recently underpassed by two tunnels for the new C line subway. During the tunnel excavation, which was performed by a EPB machine in a sequence of relatively stiff soil and weak rock strata of volcanic origin, vertical settlements were measured at the ground surface and in the structure by an extensive monitoring system.

The numerical model is characterised by an advanced constitutive law for the masonry and an effective simulation of the tunnel excavation (i.e., capable of reproducing the typical Gaussian subsidence profile at the ground surface in free-field conditions). In order to mimic the real geometric conditions at the site with the two-dimensional Finite Element discretisation, plane strain and plane stress conditions were assumed respectively for the soil and the structure.

The calibration of soil and masonry constitutive parameters was performed against results of in situ and laboratory tests, while the simulation of tunnel excavation was forced to induce volume losses consistent with those back-calculated from the available in situ measurements.

In the following the case history and the numerical model are described in detail. In the last part of the paper numerical results are presented and compared with available monitoring data.

2 THE CASE STUDY: THE AQUEDUCT FELICE

2.1 *An historical overview*

The Felice Aqueduct in Rome (Fig. 1) is an historical construction built by Pope Sisto V in 1585 on the ruins of Circo Variano, a buried amphitheatre dating back to the III Century B.C.

The structure is made of a sequence of arches having 2.3 m span and 9.3 m height. In early XX Century, some of the original arches were replaced by five larger arches, characterized by 5.5 m span and 8.0 m height separated by rectangular piers 1.5 m × 2.3 m large. The original structure is made of combined tuff and brick masonry, while the more recent additions are made of brick masonry.

The underneath Circo Variano, a 8 m thick structure which extends completely below ground level, is made out of poorly bonded tuff blocks, whose continuity is interrupted by a sequence of little openings in its upper portion.

2.2 *Geotechnical conditions*

The subsoil in the area was investigated by means of 8 boreholes which showed the presence of six different layers: made ground (R), Villa Senni tuff (VS), a highly dense silty sand, alternate levels of cemented (T1/T2) and partly cemented (TA) tuffs and a cohesive stratum of stiff silty clay (ST-AR). Apart from the latter, all the above materials are characterised by relatively large permeability coefficients.

Four piezometers were installed at different depths along two verticals, showing the existence of a permanent vertical flow from the upper layers across the silt and clayey one, leading to the pore water pressure profile shown in Figure 2.

Figure 1. Frontal view of the Felice Aqueduct.

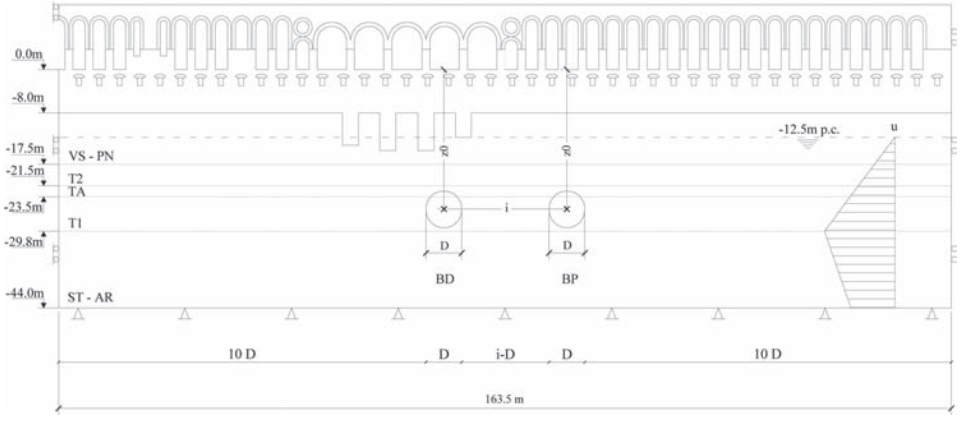

Figure 2. Schematisation of the Felice Aqueduct and of the geotechnical conditions.

A set of laboratory tests were carried out to identify the shear strength parameters of tuff (T1, T2 and TA) and ST-AR strata. Forty SPT tests were also performed to complete the characterisation of the subsoil in terms of shear strength and stiffness.

The profile of the very small strain stiffness was obtained by performing a specific Cross-Hole test; the average G_0 values for each stratum were further elaborated to obtain the corresponding G values appropriate to the strain level expected for the class of problem under study ($0.01\% \leq \varepsilon_s \leq 0.1\%$), with reference to stiffness decay curves taken from the literature (Vucetic & Dobry, 1991).

The selected parameters γ, K_0, E', υ', c', ϕ' for each soil layers are summarised in Table 1.

2.3 *Masonry characteristics*

Masonry characteristics were investigated by means of sub-and above-surface in-situ tests.

In particular the stratigraphy was identified by conducting drills at structure and foundation levels. In addition flat jacks were carried out to provide Young's modulus and Poisson ratio for both blocks and mortar.

The selected parameters a, b, t, E_b, E_m and c for each masonry type are summarised in Table 2, where a, b and t are the block dimensions and the joint thickness, respectively.

For both the masonry types, the unit weight of volume γ is equal to 18 kN/m^3, while Poisson ratios are $\nu_b = 0.23$ and $\nu_m = 0.3$, for bricks and mortar respectively. The friction angle ϕ is set equal to 31°.

Table 1. Geotechnical properties of soil layers at the construction site.

	γ (kN/m^3)	K_0 (–)	E' (MPa)	υ' (–)	c' (kPa)	ϕ' (°)
R	17.0	0.50	40.0	0.3	10.0	31
VS	17.5	0.40	83.2	0.3	12.5	37
T2	16.0	0.40	300.0	0.3	40.0	35
TA	16.0	0.60	200.0	0.3	27.0	25
T1	16.0	0.40	300.0	0.3	40.0	35
ST-AR	19.5	0.60	145.0	0.3	15.0	25

Table 2. Mechanical parameters of masonry components.

	a (cm)	b (cm)	t (cm)	E_b (MPa)	E_m (MPa)	c (kPa)
Bricks	5	30	1.5	2000	600	25
Tuff	4	25	1.0	1500	300	10

2.4 *The Metro C tunnel excavation*

The new C line of Rome subway will have a total length equal to 25.5 km with 30 stations and will link the North-West part with the South-East part of the city. The study presented in this work deals with the undercrossing of the Felice Aqueduct by the twin tunnels of the subway.

The excavation was carried out with an Earth Pressure Balance (EPB) machine. In relation to the fair geotechnical conditions at the site, no pressure was applied at the tunnel face during excavation.

The tunnel lining is composed by cast-in-place concrete rings, erected at the tail of the shield. Each lining ring, having 1.4 m wide, is made of 7 concrete segments with a thickness of 30 cm.

The two tunnels have a diameter $D = 6.7$ m, inter-axis $i = 22.8$ m and their axes are located at a depth $z_0 = 25.8$ m from the ground surface.

The tunnel excavation under the Felice Aqueduct was carried in April 2011. The odd line (BD) was excavated first, followed after 10 days by the even one (BP).

2.5 *Monitoring system*

The contractor monitored vertical displacements in the structure and at the ground level during the tunnel undercrossing. The equipment used is formed by monitoring benchmarks at the base of the structure (Figure 3—section D) and targets on it (Figure 3—sections A-B-C).

3 THE NUMERICAL MODEL

3.1 *Geometry, Finite Element discretisation and initial conditions*

The whole system consisting of the Felice Aqueduct, the Circo Variano and the soil layers, including the two tunnels to be excavated, was modelled using the 2D Finite Element Abaqus.

The domain is characterized by a height of 44 m and a width of 163.5 m; the latter dimension being evaluated considering a distance of 10 diameters from each of the two tunnels, in order to minimise boundary effects.

The coordinate system is defined such that x is the distance from the left boundary in the horizontal direction and z is the depth below the ground surface.

The FE mesh is composed by 8-node quadrangular plane strain elements for the soil and 4-node quadrangular plane stress elements for the masonry. This assumption is considered necessary when modelling the problem in two-dimension, as plane strain elements, if assumed for the wall, would induce a non realistic enhancement of its

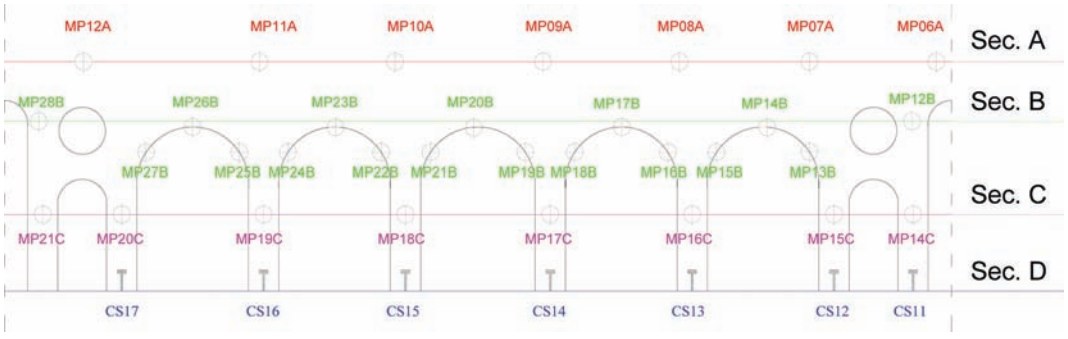

Figure 3. Monitoring system of the Felice Aqueduct.

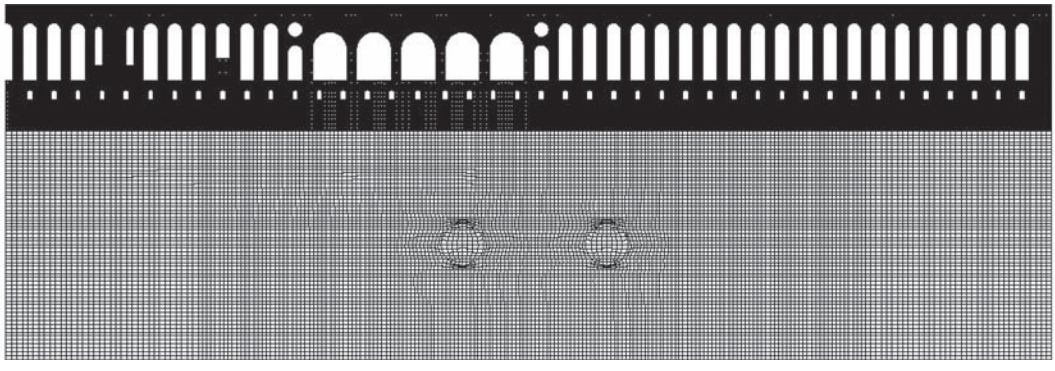

Figure 4. Finite Element discretisation.

stiffness. The latter hypothesis also holds for the underground Circo Variano structure, given its far larger stiffness as compared to that of the surrounding soil.

The whole Finite Element discretisation is shown in figure 4. Some details of the FE discretisation adopted for the Felice Aqueduct and Circo Variano are provided in Figure 5.

3.2 *Analysis stages and modelling of excavation*

The first stage of the numerical analyses consisted in the activation of gravity, first in the soil layers and then in the masonry structure. For the latter, due to the complexity of the geometry, gravity was activated in several steps considering subsequent layers from the bottom to the top of the structure.

Tunnel excavation was simulated using a displacement-controlled technique (Rowe et al., 1983): first the soil elements inside the tunnel section were deactivated while all the tunnel boundary nodes were constrained in terms of displacements, then a vertical displacement field was applied at the nodes of the upper tunnel half-section and

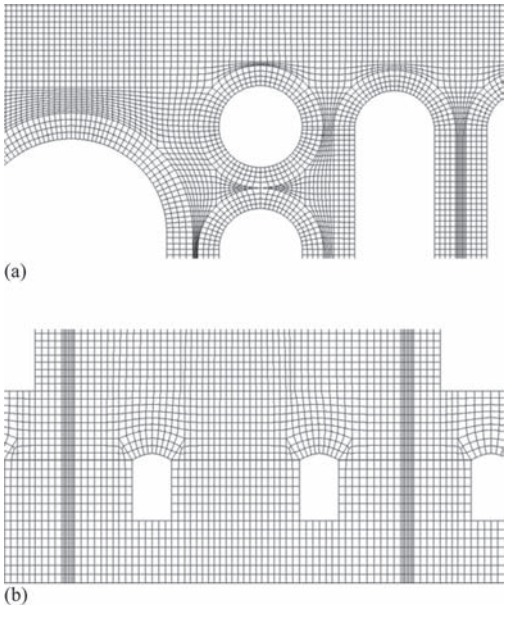

Figure 5. Details of the Finite Element discretisation: (a) Felice Aqueduct, (b) Circo Variano.

increased until the required subsidence volume at the surface was reached.

This procedure was adopted in sequence for both tunnels. The subsidence volumes considered in the numerical analyses, back-calculated from the monitoring ground displacement data, were $V_S = 0.49\%$ and $V_S = 0.48\%$ for the BD and BP tunnels, respectively. These values were obtained imposing maximum vertical displacements of 25 and 26 mm at the tunnel crown, which were compatible with available gap of the adopted tunnel boring machine.

3.3 *Constitutive models*

The constitutive models for both soil and masonry are formulated in the framework of classical rate-independent plasticity.

A linear elastic-perfectly plastic constitutive model is selected for the soil, characterised by a Mohr-Coulomb yield criterion and a null dilatancy angle. Although relatively simple, this constitutive assumption seems to be appropriate for the case at hand.

A linear elastic-perfectly plastic constitutive model was considered for masonry as well, where however anisotropy in both elastic properties and strength envelop are taken into account. The model is formulated in the framework of homogenization theory of periodic media, referring to brick masonry made of elastic bricks with cohesive and frictional joints. In such a case, a closed-form approximated expression for the elastic strain energy is provided in de Felice et al. (2010), that takes the form:

$$W(\varepsilon^e) = \frac{1}{2}\left[\frac{E_x}{1-\nu_{xz}\nu_{zx}}\left(\varepsilon^e_{xx}\right)^2 + \frac{E_z}{1-\nu_{xz}\nu_{zx}}\left(\varepsilon^e_{zz}\right)^2 + \frac{2\nu_{xz}E_z}{1-\nu_{xz}\nu_{zx}}\varepsilon^e_{xx}\varepsilon^e_{zz} + 4G\left(\varepsilon^e_{xz}\right)^2\right] \tag{1}$$

where x and z are the horizontal and the vertical direction, respectively. The coefficients in (1) depend on the elastic Lamè coefficients of the blocks (λ'_b, μ_b), on the normal K_n and tangential K_t stiffness of the joints, as well as on the height a and the width b of the bricks as follows:

$$\frac{1}{E_x} = \frac{4a}{4abK_n + b^2K_t} + \frac{1}{4\mu_b} + \frac{1}{4\left(\lambda'_b + \mu_b\right)} \tag{2}$$

$$\frac{1}{E_z} = \frac{1}{aK_n} + \frac{1}{4\mu_b} + \frac{1}{4\left(\lambda'_b + \mu_b\right)} \tag{3}$$

$$\frac{1}{G} = \frac{1}{aK_t} + \frac{4a}{4abK_t + b^2K_n} + \frac{1}{\mu_b} \tag{4}$$

$$\frac{\nu_{xz}}{E_x} = \frac{\nu_{zx}}{E_z} = \frac{\lambda'_b}{4\mu_b\left(\lambda'_b + \mu_b\right)} \tag{5}$$

The elastic domain is defined in the context of multi-surface perfect plasticity as:

$$E_\sigma = \{\sigma \mid f^\alpha(\sigma) := \mathrm{n}^\alpha : \sigma - c^\alpha \le 0 \;\forall\; \alpha \in [1,..,m]\} \tag{6}$$

where $f^\alpha(\sigma)$ are m independent planes, intersecting in a non smooth way, which define the yield surface. The expression for the yield surface of block masonry is provided in de Buhan & de Felice (1997) on the basis of the yield design homogenisation method. In particular, if the bricks are assumed as infinitely resistant bodies and the joints as interfaces, with cohesion c and friction angle ϕ, the yield surface comprises $m = 4$ planes which can be written in terms of stress components in the Oxz reference adopted for the joints as follows:

$$\begin{aligned} f^1 &:= \mu\sigma_{xx} + tg(\phi)\sigma_{zz} + (1 + tg(\phi)\mu)\sigma_{xz} \\ &\quad - c - c\mu/tg(\phi) \le 0 \\ f^2 &:= \mu\sigma_{xx} + tg(\phi)\sigma_{zz} - (1 + tg(\phi)\mu)\sigma_{xz} \\ &\quad - c - c\mu/tg(\phi) \le 0 \\ f^3 &:= \sigma_{zz} + 1/tg(\phi)\sigma_{xz} - c/tg(\phi) \le 0 \\ f^4 &:= \sigma_{zz} - 1/tg(\phi)\sigma_{xz} - c/tg(\phi) \le 0 \end{aligned} \tag{7}$$

where $\mu = 2a/b$ is the aspect ratio height-to-width of the bricks.

The evolution of plastic strain $\boldsymbol{\varepsilon}^p$ is controlled by the associated flow rule expressed as:

$$\dot{\varepsilon}^p = \sum_{\alpha=1}^{m} \dot{\gamma}^\alpha \frac{\partial f^\alpha(\sigma)}{\partial \sigma} \tag{8}$$

where $\dot{\gamma}^\alpha$ are the m multipliers, subjected to the Kuhn-Tucker conditions for $\alpha \in [1,..,m]$:

$$\dot{\gamma}^\alpha \ge 0 \qquad f^\alpha(\sigma) \le 0 \qquad \dot{\gamma}^\alpha f^\alpha(\sigma) \equiv 0 \tag{9}$$

and to the consistency condition $\dot{\gamma}^\alpha \dot{f}^\alpha(\sigma) \equiv 0$ (the summation convention is not enforced).

The assumption of associated flow rule allowed the model to be integrated at the Gauss point level by means of a very efficient numerical procedure based on quadratic minimization.

The selected parameters for each soil layers are the ones summarised in Table 1, while those adopted for the masonry structure are reported in Table 2.

4 NUMERICAL RESULTS AND COMPARISON WITH MONITORING DATA

In this section a comparison between the numerical results and the monitoring data collected during tunnel construction is presented.

The vertical displacements recorded at two of the monitoring sections (sections A and D in Figure 3) are reported in Figure 6. It can be observed that, despite some little differences and localised phenomena, the numerical outcomes compare well with the monitoring data.

Settlement curves are characterized by a reduction in the extent and in the maximum settlement from the base (section D) to the top of the Aqueduct (section A); this should be related to the effect of the structure stiffness.

The heave observed in the numerical results at the sides of the structure can be ascribed to the dilatant response of the masonry model and seems in accordance to a similar trend displayed by the monitoring data.

The contours of the principal tensile plastic strains resulting from the numerical analysis are shown in Figure 7. It is worth observing that no plastic strains take place in the Aqueduct, while small tensile ones only occur in the upper portion of the Circo Variano, being characterised by an order of magnitude of 10^{-4}.

Plastic strains are concentrated at the base of the Aqueduct central piers and in the adjacent small openings of Circo Variano. They appear to be localised in the zones of maximum deflection of the predicted subsidence curves. Their inclination of about 45° can be associated to the prevailing shear-type damage mechanism occurring in the structure, as opposed to bending.

The interpretation of the numerical results indicates clearly that the Circo Variano, thanks to its massive structure, played a key role in the overall response of the Felice Aqueduct, preserving it against any excavation-related damage.

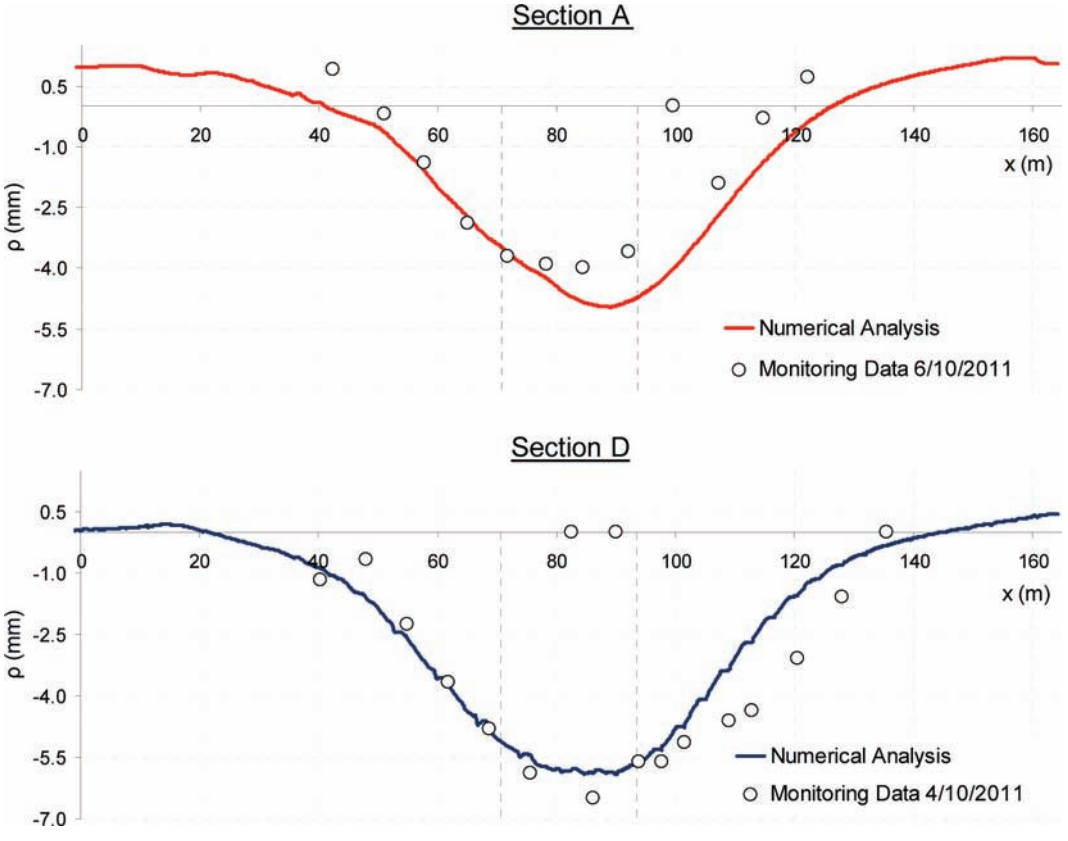

Figure 6. Settlement curves: Comparison between numerical results and monitoring data.

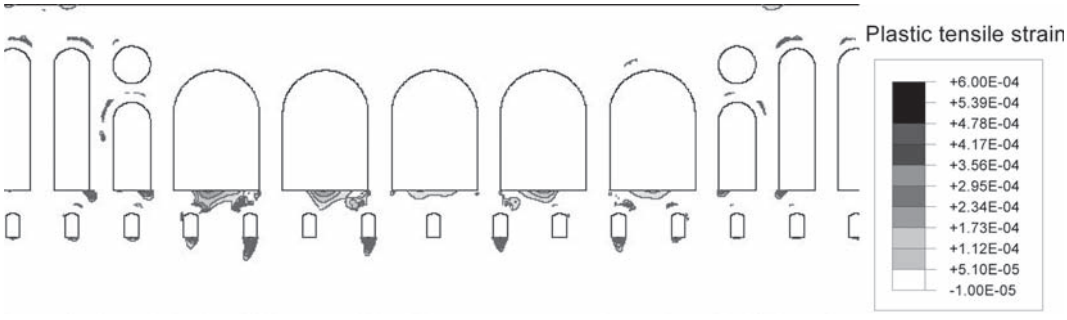

Figure 7. Distribution of principal tensile plastic strain.

5 CONCLUSIONS

In this paper a class C numerical prediction of the settlements induced in a historical masonry structure by the excavation of shallow twin tunnels is presented.

The satisfactory comparison with available monitoring data proved the soundness of the numerical model in terms of adopted constitutive laws, simulation of tunnelling sequence and Finite Element discretisation. It makes the approach being amenable for future use as a class A predictive tool for similar soil-structure interaction processes.

It is worth of remarking the novelty and potentiality of the presented approach, in which all the important ingredients of the problem (i.e., the tunnels, the soil layers and the structure) are incorporated in a unique model without the need of cumbersome, or sometime obscure, links between the "geotechnical" and the "structural" responses.

In addition, the masonry constitutive law allows the evaluation of plastic strain initiation and accumulation within the structure and the estimation of the induced damage using a realistic (i.e., inelastic and anisotropic) material model.

REFERENCES

de Buhan, P. & de Felice, G. 1997. A homogenisation approach to the ultimate strength of brick masonry. *Journal of the Mechanics and Physics of Solids* 45(7): 1085–1104.

de Felice, G., Amorosi, A. & Malena, M. 2010. Elastoplastic analysis of block structures through a homogeneization method. *International Journal for Numerical and Analytical Methods in Geomechanics* 34: 221–247.

Rowe, R.K., Lo, K.Y. & Kack, G.J. 1983. A method of estimating surface settlement tunnels constructed in soft ground. *Canadian Geotechnical Journal* 20: 11–22.

Vucetic, M. & Dobry, R. 1991. Effects of the soil plasticity on cyclic response. *Journal of Geotechnical Engineering Division (ASCE)* 117(1): 89–107.

This page intentionally left blank

Geotechnical Engineering for the Preservation of Monuments and Historic Sites – Bilotta, Flora, Lirer & Viggiani (eds)
© 2013 Taylor & Francis Group, London, ISBN 978-1-138-00055-1

Soil structure interaction on the dynamic behavior of two historic masonry structures

S. Sica, F. Ceroni & M.R. Pecce
University of Sannio, Benevento, Italy

ABSTRACT: The interaction between soil and structure (SSI) is a typical issue of structural and geotechnical engineering, still open regarding its practical implications. Further investigation is actually required to develop simplified but reliable methods to account for SSI in routine structural analyses.

A multidisciplinary approach for assessing the seismic vulnerability of heritage masonry buildings is described throughout the paper. The procedure is applied to two specific case studies that represent very common typology of masonry buildings in Italy: Bosco-Lucarelli Palace in Benevento and the Bell Tower of the Carmine Church in Naples. The seismic vulnerability of the two monuments was assessed after the following steps: (a) historical investigation about the structure and the surrounding area, (b) detailed geometrical survey, (c) identification of materials by means of surveys and literature indications, (d) dynamic *in-situ* tests, (e) foundation soil characterization, (f) dynamic identification of the structure by means of a refined Finite Element (FE) model. Finally, the effect of soil-structure interaction on the dynamic behavior (namely, fundamental frequencies and vibration modes) of the two structures is discussed.

1 INTRODUCTION

1.1 *Problem statement*

The structural behavior of monuments and, in general, of existing masonry buildings is a complex issue to deal with, due to the unavoidable uncertainties regarding geometry, typologies and mechanical properties of structural materials, effects of age and past loading history, presence of architectonical and structural interventions with different techniques or materials, interaction with surrounding buildings and foundations, foundation soil properties. Thus, for an existing masonry building, a complete knowledge is needed before starting any study of its structural safety or designing any retrofitting intervention.

A complete knowledge needs detailed *in-situ* inquiries according to a multidisciplinary approach implementing both traditional and innovative investigation techniques. The mechanical properties of masonry blocks and mortar joints are usually assessed by means of destructive *in-situ* tests. For monuments a significant effort has been spent in the last years to use non-destructive testing techniques in order to preserve monument integrity and limit destructive tests to only a few points.

Investigation techniques based on *in-situ* dynamic tests carried out through ambient or forced vibrations represent an innovative and useful tool to observe different aspects of historical buildings thanks to the study of their dynamic response in terms of frequencies and modal shapes (Brincker et al., 2001, De Sortis, 2005).

Firstly, based on the comparisons of experimental evidence (mainly consisting of principal modal shapes and related frequencies) and predictions given by linear dynamic models, the values of elastic properties and unit weight of masonry can be easily assessed, taking into account the overall assembly of stones/bricks and mortar (Bennati et al., 2005).

Moreover, dynamic *in-situ* tests can be aimed at studying the response of the structure under seismic actions and investigating the interaction of the examined building with adjacent constructions or with the foundation soil. This latter aspect is rarely considered in common structural modeling because type and dimensions of the foundations or properties of the subsoil are often unknown. When the foundation soil is soft, the hypothesis of a fixed-base condition for the superstructure is no longer valid and the effect of Soil-Structure-Interaction (SSI) should be accounted for. If dynamic *in-situ* monitoring is carried out, the role of SSI should be properly accounted for, because the recordings acquired in different parts of a building may contain the effect of coupling between soil and structure.

As well known, SSI produces two important effects from the structural viewpoint: (i) elongation of the fundamental vibration period of the coupled system compared to the fixed-base scheme; (ii) increase in damping due to the energy dissipation through the foundation soil (radiation damping).

Because of these effects, SSI is usually considered beneficial for the structural analysis since it is expected to reduce the seismic action on the building.

In this paper, for a noble palace (Bosco-Lucarelli Palace), located in Benevento (Italy) and the Bell Tower of the Carmine Church in Naples, the outcomes obtained by *in-situ* dynamic monitoring are compared to the results of numerical modal analyses performed by a refined three-dimensional Finite Element (FE) model.

Parametric analyses have been carried out to check the sensitivity of the dynamic response of the buildings to masonry and soil stiffness.

1.2 *State of the art on simplified approaches for evaluating SSI*

Historic masonry buildings usually have shallow foundations built by enlarging the bearing walls for 1 ÷ 2 m below the ground level. For shallow foundations the kinematic aspect of dynamic SSI is negligible and only the inertial counterpart of the phenomenon is worth considering (Kramer, 1996).

When the foundation subsoil is not a rock (i.e., conventionally, a geomaterial with a shear wave velocity $V_s > 800$ m/s) the structure cannot be modelled with a fixed base, but it is necessary to take into account the interaction with the foundation soil (SSI).

Traditionally, the importance of soil-structure interaction phenomena can be estimated by means of some synthetic parameters, such as:

a. the relative stiffness between the foundation soil and the structure, expressed by Ciampoli & Pinto (1995) through the parameter σ:

$$\sigma = \frac{V_s}{h f_{fix}} \tag{1}$$

where f_{fix} is the frequency of the fixed-base structure, h is the height of the structure, V_s is the shear wave velocity in the foundation soil, assumed as a halfspace;

b. the ratio $\frac{h}{r}$, where r is the radius of the circular foundation equivalent to a shallow foundation with any shape, provided that this latter is characterized by a shape coefficient (i.e., the ratio between the longer and shorter side of the foundation) lower than 4:1 (Roesset, 1980). The criterion of equivalence is imported in some seismic codes, such as the NEHRP (1997).

It can be intuitively seen that the higher the parameters $1/\sigma$ and h/r, the more relevant the SSI effect.

c. a third parameter, ϕ, combining the first two ones (Veletsos, 1977):

$$\phi = \frac{1}{\sigma} \cdot \left(\frac{h}{r} \right)^{0.25} \tag{2}$$

which can be used for the evaluation of the threshold above which the SSI effects are negligible for the dynamic behaviour of the structure and its design. Literature studies (Veletsos, 1977) indicate that for $\phi \leq 0.125$ the effect of SSI can be neglected.

In order to evaluate the effect induced by SSI on the fundamental vibration period of the structure, it is usually referred to the scheme of a single degree of freedom (SDOF) system.

This is defined by a mass m placed at a height h and connected to the ground by means of concentrated translational and rotational springs (for sake of simplicity any torsional effect is neglected), defined by complex functions known as "dynamic impedances". If the foundation structure is stiffer than the foundation soil, the springs can be considered uncoupled each other.

According to this approach, the period of the coupled system, T_{comb}, can be evaluated using the formula proposed by Veletsos & Meek (1974):

$$T_{comb} = T_{fix} \cdot \sqrt{1 + \frac{k}{k_u} + \frac{k \cdot h^2}{k_\theta}} \tag{3}$$

where T_{fix} represents the period of the fixed-base structure, k is the stiffness of the fixed-base structure modelled as a SDOF, k_u and k_θ are the translational and rotational spring stiffness, respectively.

In general, k_u and k_θ depend on the frequency ω of the input motion and can be expressed multiplying the static stiffness, K_u or K_θ, by a frequency-dependent coefficient, α_u or α_θ, (Gazetas, 1991):

$$k_u = \alpha_u(\omega) \cdot K_u \tag{4a}$$

$$k_\theta = \alpha_\theta(\omega) \cdot K_\theta \tag{4b}$$

For the estimation of parameters in Eqs. 4a–b, Gazetas (1991) provided different analytical expressions and/or charts, depending on the shear stiffness, G, and the Poisson coefficient, ν, of the soil, the geometrical characteristics of the foundation and the frequency, ω, of the input motion.

Afterwards, Mylonakis et al. (2006) presented a state-of-the-art about different formulas proposed in literature for the evaluation of SSI, taking into

account: 1) the shape of the foundation (circular, strip, rectangular/square foundation); 2) the soil model (homogeneous halfspace, soil layer over rock); 3) the foundation embedment (foundation placed on the limit surface of the halfspace or embedded in it).

The solutions found in the literature are always obtained under the hypothesis of linear elastic behaviour of the foundation soil.

Anyway, in presence of strong seismic actions, soil does not show a linear elastic behaviour anymore; hence, the elastic parameters to be assigned to soil should be accurately set. For example, FEMA 273 and following codes suggest estimating SSI effects by means of upper—and lower-bound criteria, assigning to soil, in the first case, the small strain stiffness G_0, and, in the second case, the stiffness G_{eq}, compatible with the level of deformation that can be induced by the earthquake.

Similarly, in presence of seismic actions at the ultimate limit state, the structure will undergo plastic deformation and the stiffness ratio between the structure and the soil will be certainly modified.

In a very few papers, SSI is analysed taking into account the main aspects of soil behaviour under cyclic and dynamic loads (Cremer et al., 2001–2002; di Prisco et al., 2006; Jeremic et al., 2004–2009) or the non-linearity of the structure materials (Ciampoli & Pinto, 1995). However, the computational effort and difficulties in the calibration of the parameters required by the constitutive models do not encourage the use of such approaches in the current design practice and in the individuation of cases in which SSI should be taken into account.

1.3 *The dynamic monitoring of buildings*

To identify the natural vibration modes of a structure, different methods have been proposed in recent years. They may be divided in parametric and non-parametric methods (Michel et al., 2008).

In the former group, the main parameters of the structural model are iteratively updated to fit the recorded data; in the latter, the structural model is ignored and only signal processing by Operational Modal Analysis (OMA) is adopted (Brincker et al., 2001).

The most known OMA is the Peak Picking Method (PPM), where Fourier transforms of the recordings are carried out and frequency peaks are detected on the Fourier amplitude spectra.

If the mode shapes of the structure are well separated, the PPM may provide reliable indications on the dynamic parameters of the structure.

2 THE CASE STUDY OF A NOBLE PALACE

2.1 *Main features of the structure and foundation soils*

'Palazzo Bosco Lucarelli' is an old noble palace (Figure 1a) located in Benevento (Italy). Research in the archives of City Hall and in public libraries allowed collecting information about the different construction phases of the building thanks to historical reports, maps, urban plans and, for the XX century, photos.

The original nucleus of the current building probably was built in the XI century; subsequently, some documents of XIII and XIV centuries confirm the presence of a construction with an adjacent church in the same site of the current palace. This building is located in a zone of high seismicity in the core of Apennines and was severely damaged during a strong earthquake in 1702. After then, it was rebuilt and enlarged to assume the present 'palace' structure with an internal closed court. At the beginning of the XX century, the current first and second floors were probably added.

Nowadays, the largest dimensions in plan are 33.5 m and 26.3 m (Figure 1c) and the total height is 18.2 m (see a vertical section of the building in Figure 1b). The walls are made of different masonry materials and textures: calcareous and tuff natural stones at the underground and ground floors, clay bricks at upper floors.

The thickness of masonry walls ranges between 0.6 m and 1.0 m with greatest values attained at the ground floor. The current floors are made by standard steel profiles IPE 200 (spaced 0.85 m) interspersed with brick tiles and covered by a concrete deck 100 mm thick. At the ground floor, in the entrance hall some rooms are covered by the original masonry vaults. The roof is made by a steel truss externally covered by a profiled steel sheet and brick tiles.

The foundation soil has been characterized by means of two boreholes, in one of which a downhole test was carried out. In the first 15 meters from the ground level, the subsoil (Figure 2) is made by a sequence of layers of sandy silt and silty sand. At higher depth, a conglomerate formation with variable degree of cementation and weathering is present for about 45 meters. Finally, at a depth of about 60 meters a stiff blue-gray clay deposit is found, representing the seismic bedrock, as assumed in previous studies on the seismic response of Benevento subsoil (Marcellini et al., 1995a-b; Santucci et al., 2004; Improta et al., 2005). As a result, the shear wave velocity in the soil volume influenced by the building varies between 400 and 1200 m/s.

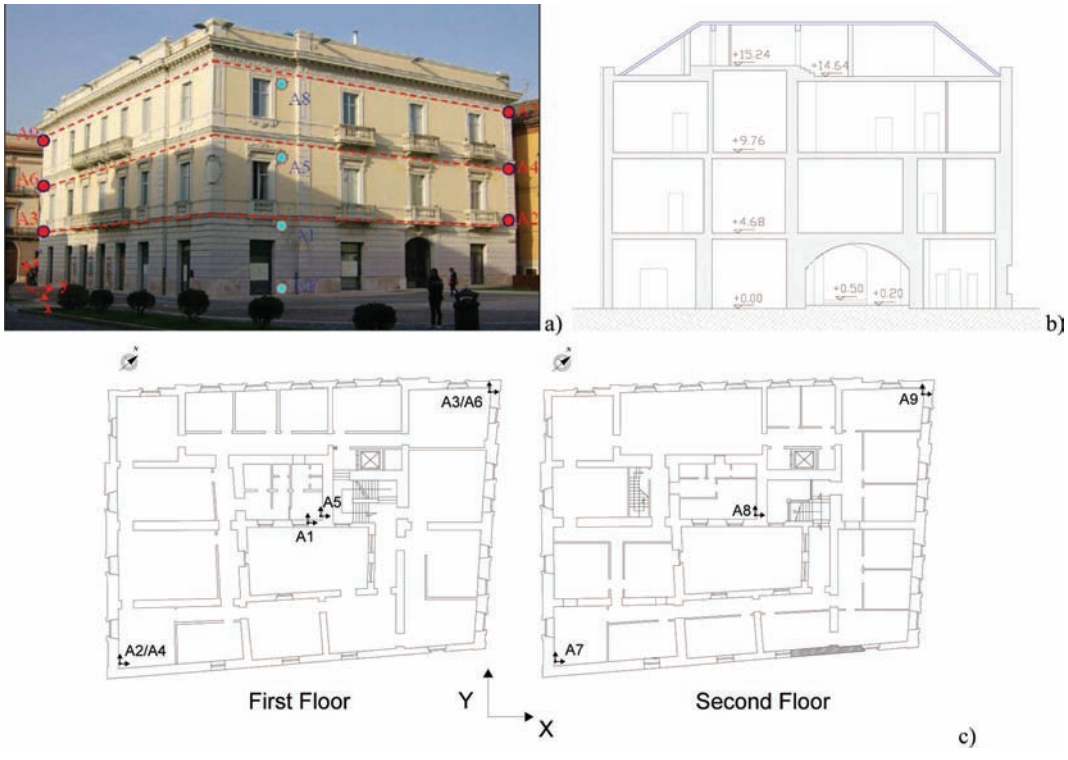

Figure 1. Palace Bosco-Lucarelli: a) North-West and South-West wings of the building and instrument location; b) Longitudinal section Y-Y; c) Ground floor plan.

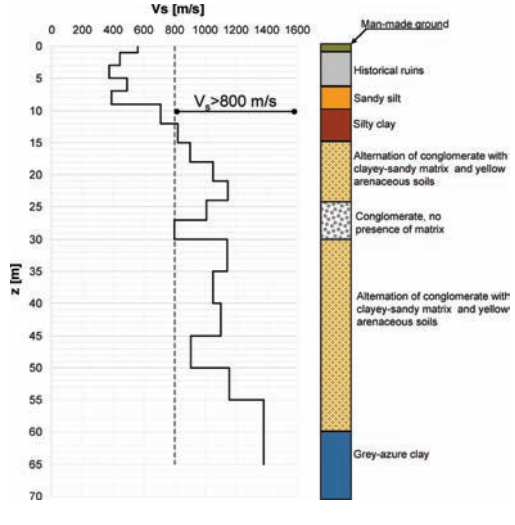

Figure 2. Shear wave velocity profile measured by DH test.

2.1.1 *Dynamic identification and structural modeling*

In 2008 a dynamic monitoring system was installed on Bosco-Lucarelli Palace by the Italian Department of Civil Protection to perform a continuous monitoring of the structure. The system is aimed at providing real-time information on the dynamic motions due to both exceptional events as earthquakes and other low-energy sources such as traffic, wind, and human activities.

The monitoring system is made of nine couples of uni-axial accelerometers placed at the three floors of the building and a triaxial accelerometer located at the ground floor (see Figure 1a and 1c). Each couple of sensors is oriented along the X and Y directions, as shown in Fig. 1b–c. The sensors have been aligned as accurately as possible along three vertical arrays: one corresponds approximately to the centre of the building and the other two to the external edges. The central vertical array is made of sensors A1-A5-A8, while the two external edges of sensors A3-A6-A9, and A2-A4-A7. The sensors A1-A2-A3 are placed at about 100 mm from the first floor intrados, the couples A4-A5-A6 at about

100 mm from the second floor extrados, and the couples A7-A8-A9 at about 100 mm from the third floor extrados.

Different sets of accelerometric recordings are available. These recordings were caused by ambient noise and impulsive sources activated on-purpose. During the installation and the trial stage of the monitoring system, two different impulsive sources were activated, represented by: (1) the fall of a concrete block (1 m^3) on a truck placed close to the building; (2) the rapid braking of the truck along the Y direction of the building.

The Peak Picking Method was used in order to identify the main eingenfrequencies of the building based on the experimental accelerometric recordings. In Figures 3 the acceleration spectra of the recordings at sensors A3-A6-A9 (external edge array), induced by the concrete block fall, are reported. Table 1 shows the mean values of the experimental frequencies obtained by means of different recording sets; it is worth to notice that the frequency in the Y direction of the building (shorter side, see Figure 1b) is slightly lower (about 10% less) than that related to the X direction.

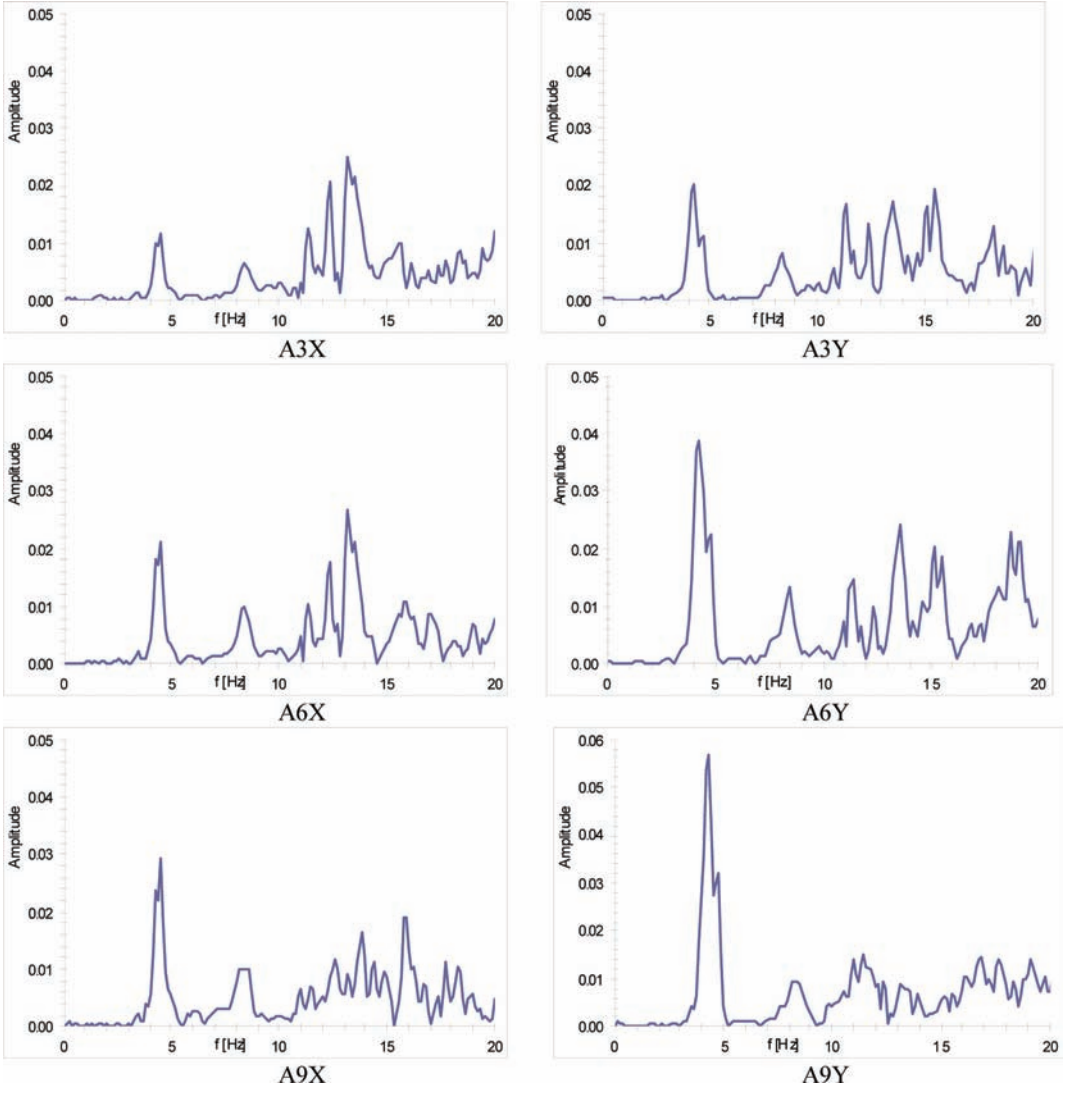

Figure 3. Fourier spectra of the acceleration recorded at sensors A3-A6-A9 (external edge array), induced by the concrete block fall.

Table 1. Numerical vs. experimental values of frequencies for Bosco-Lucarelli Palace.

	Experimental		Theoretical $E_G = 1500$ MPa $E_{1-2} = 1200$ MPa	
Mode	f_{exp} [hz]	T_{exp} [s]	$f_{th,fix}$ [hz]	$T_{th,fix}$ [s]
1 (Transl. Y)	4.3	0.233	3.75	0.267
2 (Transl. X)	4.7	0.213	4.19	0.239

This can be indicative of a greater deformability of the building in the Y direction. To corroborate this assumption, it can be observed that along the Y direction the building has a lower amount of masonry walls, often not continuous, than in the orthogonal X direction (see the ground floor plan in Figure 1b). Moreover, the small coefficients of variation of the peak frequencies, defined as the ratio between the mean value of the frequencies measured by the nine accelerometers in each direction and the standard deviation, (max CoV = 2.7%) highlight their reliability.

A three-dimensional model of the structure was realized by means of 'brick' finite elements in the DIANA software (DIANA, 2002) basing on the detailed geometrical survey; checks under gravity loads, modal analysis and non-linear static analysis were carried out (Ceroni et al., 2012).

On the basis of the *in-situ* surveys and Italian code indications (NTC 2008; Document 617, 2008), the following unit weights have been assumed: $\gamma_G = 24$ kN/m^3 for underground and ground floors made of "*chopped stones with a good texture*" and $\gamma_{1-2} = 20$ kN/m^3 for the first and second floor made of "*Clay bricks with lime mortar*". Different values were considered for the Young's modulus, included within the ranges provided by the Italian code for the two masonry types indentified in the building (1500–2000 MPa for masonry of the ground floor and 1200–1800 MPa for the upper levels).

For the modal analyses, the following assumptions were made: a coefficient of participation for variable loads of 0.6 in quasi-permanent loading combination, the underground floor was neglected, the basement was assumed completely restrained. Under these hypotheses, the total weight of the structure is 88900 kN and the first two modes of vibration have been clearly evidenced. Both modes are characterized by participating mass ratio of 75% and by translational deformed shape: the first along Y direction and the second along X direction. By means of the comparison with the experimental frequencies, the values of the Young's modulus have been identified ($E_G = 1500$ MPa for the ground floor; $E_{1-2} = 1200$ MPa for the first and second floors).

In Table 1 the computed periods of vibration for these values of masonry Young's modulus are reported. As it has been highlighted by the experimental results too, the first frequency (direction Y) is about 10% lower than the second one. Moreover, also the experimental recordings have shown that only the first two frequencies were well identified by all sensors in both X and Y directions. The higher frequencies may not be identified because of the low rate of participating mass joined to these modes. The data listed in Table 1 have been obtained without considering any interaction between the building and the foundation soil; the influence of such mechanism on the dynamic behavior of the structure will be discussed in the following.

2.1.2 *Soil-foundation-structure interaction with concentrated springs at the base*

Since the frequency-dependent functions (α_u or α_θ) in Eqs. 4a-b exert a negligible contribute to the dynamic foundation impedances of the Palace, only the static stiffness was accounted for. Different soil-foundation geometrical schemes can be retrieved from literature. The following ones were considered:

1. rectangular foundation resting on the limit surface of an elastic halfspace;
2. rectangular foundation embedded in an elastic halfspace;
3. equivalent circular foundation resting on a deformable soil layer (with finite thickness H) on rock.

For the sake of brevity, the analytical expressions of the static stiffness K_u and K_θ are omitted, referring to specific works (Gazetas; 1991; Mylonakis et al., 2006). In the following, the approach featured by the introduction of concentrated translational and rotational springs at the base is applied, in order to consider soil-foundation-structure interaction and estimate the actual period of the structure (T_{comb}).

In Figures 4a-b-c the ratio between the period of the structure with SSI, T_{comb}, and the fixed base period, T_{fix}, is plotted against the previously introduced parameters $1/\sigma$, V_s, and ϕ. The period of the structure with SSI is calculated from Eq. (3).

For the foundations of the building, an enlargement of the walls at the base of the underground floor with an embedment of 1.5 m has been assumed. For the sub-system soil-foundation of Bosco-Lucarelli Palace, the three schemes introduced above have been considered. The case 3) of an equivalent circular foundation resting on a deformable soil layer on rock better represents the subsoil conditions under the palace, where the first

10–15 meters are more deformable compared to the deeper layers.

The variability range for soil shear wave velocity, V_s, considered in all the plots reported in Figures 4 is 300 ÷ 1500 m/s. The lower limit corresponds to a reduced soil shear modulus G equal to 1/4 of the initial value G_0 (corresponding to an average value of V_s in the first 15 meters, i.e. $V_s = 600$ m/s) in case of significant nonlinear effects, while the upper limit represents the case of an ideal rock.

Due to the combined effect of translational and rotational spring, in all models an increment of the period of the structure, T_{comb}, is clearly observed (Fig. 4a), with the increase of $1/\sigma$ (Wolf, 1985; Ciampoli & Pinto, 1995; Stewart et al., 1999). The three curves give comparable values; it is observed that for $V_s = 600$ m/s, corresponding to $1/\sigma = 0.075$, the increment of period, compared to the fixed base condition, varies between 12 and 18%, depending on the assumed model.

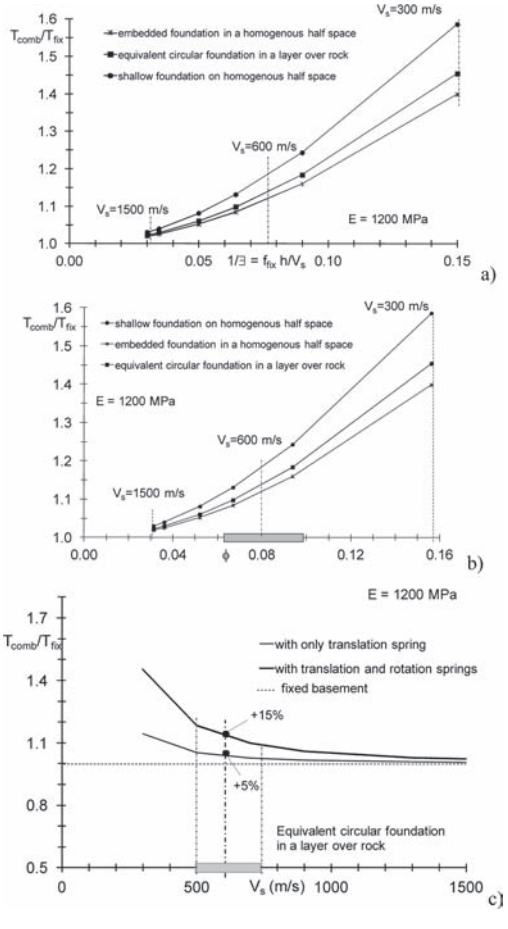

Figure 4. Variation of period of the structure with SSI in presence of concentrated springs: a) vs. $1/\sigma$; b) vs. ϕ; c) vs. V_s.

In Figure 4b the increment of the structural period considering SSI effects is plotted against the parameter ϕ. An uncertainty of ±120 m/s (±20%) on the "operative" value of V_s within the significant volume of the building was considered as not linked to the uncertainty of V_s measurements by Down Hole test, but to the necessity to select a mean stiffness value to characterize the entire volume of soil interacting with the building. As a result, the parameter ϕ ranges between 0.065 and 0.095, with an increment of the period of the structure between 5% and 25%, depending on the model assumed for the foundation. Therefore, the increments of the period can be not negligible also for values of ϕ below the limit $\phi = 0.125$ suggested by Ciampoli & Pinto (1995).

In Figure 4c the variability of the period of the structure with SSI compared to the fixed base solution is reported as function of V_s, differentiating the contribution to the global deformability of the translation spring from the combined effect of both translation and rotational springs. Note that in presence of the translation spring only, Eq. 3 has been used without taking into account the rotational term. In this analysis the scheme of equivalent circular foundation placed on a deformable layer over rock has been considered, since, as stated above, it better represents the case of Bosco-Lucarelli Palace foundation. Under this hypothesis and for the estimated average soil velocity $V_s = 600$ m/s, the increment in period is 5% due to the effect of the translational spring only, and 15% in presence of both springs. Considering an uncertainty of ±20% on the value of V_s, it has been observed an increment of period between 10 and 20%, accounting for the effect of both concentrated base springs. The increment rises to 45% if the lower limit of velocity $V_s = 300$ m/s is considered.

3 THE CASE STUDY OF A BELL TOWER

3.1 *Main features of the structure*

The second structure considered in this study is the Bell Tower of the Carmine Church in Naples (Fig. 5a). The current structure from XVII century is founded on the basement of a former bell tower from XIV century. The plan of the ground level is rectangular with maximum dimensions of about 8.0 m × 9.7 m (Fig. 5b). The rectangular cross section is retained up to 41 m (Fig. 5a–c) with masonry walls made by yellow tuff. The upper part has an octagonal cross section (Fig. 5d) with walls made by clay bricks up to about 57 m. A spire completes the structure up to a height of about 70 m.

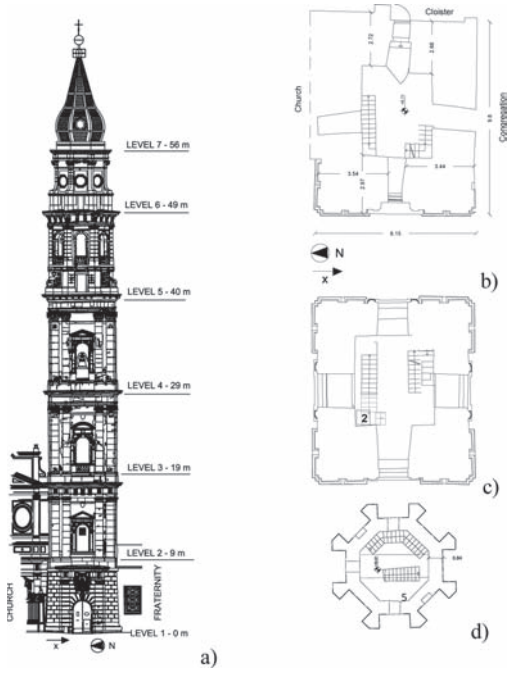

Figure 5. Bell Tower of Carmine Church: a) principal façade; b) ground floor plan; c) cross section at 19 m; d) octagonal cross section at 49 m.

The thickness of the walls is variable between 4 m and 1 m with decreasing thickness along the height. Even if the Bell Tower is located between other constructions, any structural connection can be excluded (Ceroni et al., 2009); a light interaction with the adjacent church in X direction can be assumed due to contact constraints up to the height of 19 m, beyond which the Bell Tower is completely free (Figs. 5a-b).

3.2 *Dynamic identification and structural modeling*

The *in-situ* dynamic characterization of the structure (Ceroni et al., 2009) was performed by recording environmental noise for 32 hours. Extra vibrations were also produced by localized impulses given by an instrumented hammer in order to clarify uncertainty related to low acceleration levels. Six pairs of uniaxial accelerometer sensors were positioned horizontally at each floor, from level 2 to 7 (see Figure 5a), according to various measurement schemes. The sensors were placed at each level in a corner of the cross section (see an example in Figure 5c and 5d). The identification of the first natural frequencies was based on the examination of the power spectra of measured accelerations.

The first four modal shapes are flexural and the fifth is torsional, even if the latter resulted not very well identified. For the 1st and the 3rd modal shapes, displacements occur along the X direction, while for the 2nd and 4th modal shapes, displacements are along the Y axis: the modal shapes along the two directions appear uncoupled and are associated to similar values of frequencies (slightly greater in the Y direction). The experimental 1st and 2nd modal shapes show no change in curvature sign along the tower, while for the 3rd and 4th modal shape there is a point where the curvature sign changes, confirming the expected behaviour of a cantilever.

In Figures 6 the acceleration spectra of the recordings measured by sensors in X and Y directions are reported evidencing peaks at about 0.7 and 2.3 Hz. On the basis of a detailed geometric survey, the structure has been modeled by means of DIANA software in order to carry out verifications under gravity loads, linear modal analysis and non linear static analysis (Ceroni et al., 2010). 3D brick finite elements were adopted up to the height of 57 m, while the spire has been modeled with shell elements. The unit weight of masonry has been assumed equal to 12 kN/m^3 for tuff in the first 9 m, 11 kN/m^3 from 9 to 40 m, and 16 kN/m^3 for the bricks.

The total weight of the building is 33700 kN considering the permanent loads only, since the structure is not open to the public. Several constrain conditions were considered in the linear modal analyses (Ceroni et al., 2010) in order to check the effects of the surrounding buildings: a) a cantilever scheme fixed only at the basement, b) a cantilever scheme with lateral restrains that take into account the effect of the adjacent buildings along the first 19 m, and c) a cantilever scheme with also the surrounding buildings partially modelled too.

In order to assess the values of elastic modulus, several analyses were performed (Ceroni et al., 2010). The elastic moduli of the materials and the constraint degree were back-figured by minimizing the differences between experimental and numerical eigenfrequencies and mode shape components. The values of Young's modulus were finally estimated as 900 MPa and 1200 MPa respectively for tuff and clay masonry; these values fall in the ranges suggested by national codes (NTC 2008; Document 617, 2009). In Table 2 the numerical values of frequencies for the three considered schemes are reported.

For all schemes the first two vibration modes are the principal ones, as expected due to the cantilever behavior; in particular they are both characterized by a participating mass ratio of about 85%. The first modal shape is translational in X direction,

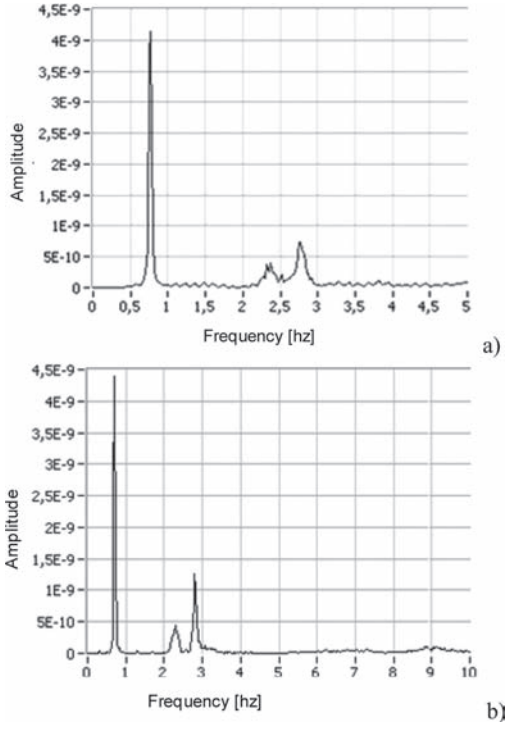

Figure 6. Power spectrum of the Tower: a) Y direction; b) X direction.

Table 2. Numerical vs. experimental frequencies for the Bell Tower.

	Experimental		Theoretical $T_{th,fix}$ [s]		
Mode	f_{exp} [hz]	T_{exp} [s]	*(a)*	*(b)*	*(c)*
1-X	0.69	1.45	2.13	1.45	1.61
2-Y	0.76	1.32	1.79	1.30	1.49

parallel to the shorter side, and the second one is translational in Y direction, parallel to the longer side (see Figure 5b–c). Very low mass percentages are involved in the third and fourth modes for all schemes.

The best fitting with experimental values is given by the configuration (b) with lateral restraints, even if the experimental vibration modes are better represented by the simple cantilever scheme (a); finally, the scheme with the partial modeling of the lateral buildings simulates quite well both the experimental frequencies and vibration modes.

3.2.2 *Soil-foundation-structure interaction with concentrated springs at the base*

For the foundation system at the base of the tower, an enlargement of the walls at the base and an embedment of 1.5 m have been assumed. The soil model assumed for the calculation of the seismic impedances and period according to Eq. 5 is a shallow foundation on a homogeneous halfspace.

In order to carry out parametric analysis to be compared to those performed for Bosco-Lucarelli Palace, the range of velocity considered is the same (V_s = 300–1500 m/s), also because detailed information about the foundation soil in this case are not available. Only the scheme of simple cantilever (a) has been considered to evaluate the SSI effects.

In Figures 7a, b, c the period of the structure with SSI, compared to the fixed base period related to the cantilever scheme (a), is reported as a function of the previously introduced parameters $1/\sigma$, ϕ and V_s. In Figure 7a the variability of Bell Tower's period

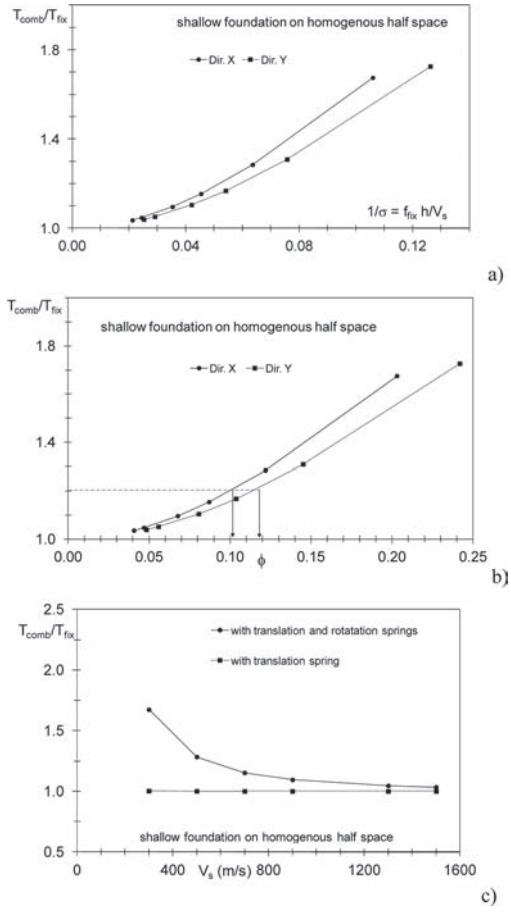

Figure 7. a) Variation of period vs. a) $1/\sigma$; b) ϕ; c) V_s.

with the parameter $1/\sigma$ is shown for both principal directions of the structure. It is observed that in Y direction, characterized by a period 15% lower than that in X direction, the period of the structure is slightly more sensitive to variation of V_s.

In Figure 7b the variability of the period with parameter ϕ shows that a period increment of 20% in both directions corresponds to an increase of ϕ from 0.10 to 0.12. These values are slightly higher than the one (ϕ = 0.095) estimated for Bosco-Lucarelli Palace to obtain the same increment of period.

Finally, Figure 7c shows that for the case of the Bell Tower the translational spring has a negligible effect on the structure period, even for low shear wave velocity (V_s = 300 m/s), due to high deformability of the structure itself. On the contrary, a relevant effect is obtained accounting for the rotational spring, with an increment in period ranging from 5% to about 70%, depending on shear wave velocity of the soil. Moreover, it is observed that the variability of the period with V_s is higher for the Bell Tower than for the Palace where, for the same lower limit (300 m/s) the maximum increment of period was 45%. This different influence of the rotational spring for the Bell Tower is due to the significant height of the structure, which has to be squared in Eq. 3.

4 CONCLUSIONS

The structural analysis of historical masonry buildings is a complex matter, as each construction is an individual case study, being designed and erected with site-specific practice and subsoil conditions. The properties of the masonry are often uncertain due to various types of stones, assembling technique, age and style of construction, details, etc. Extensive *in-situ* tests usually need to be carried out in order to define the main structural and geotechnical parameters and to develop reliable numerical models.

Dynamic *in-situ* monitoring represents an innovative, effective and not invasive procedure to assess: 1) the overall dynamic behavior of the structure (modal shape and eingenfrequencies); 2) the elastic and mass properties of the masonry; 3) mechanisms of interaction with the foundation soil and/or surrounding buildings.

Starting from the interpretation of experimental data of dynamic *in situ* tests with OMA techniques, the first two vibration modes have been identified with enough reliability for the case-studies herein presented. These values have been used as target to perform several parametric analyses aimed at investigating the influence of both masonry and foundation soil stiffness on the eingenfrequencies of the building. The obtained results point out that SSI can have a relevant influence on the dynamic behavior of masonry structures (especially for the Bell Tower) and its effect cannot be neglected in implementing the models to identify the mechanical characteristics of structures and related constraints.

In future research work, the dynamic response of Bosco-Lucarelli Palace will be better investigated by: (i) integrating the dynamic monitoring system with further instruments on the building (to detect modal shapes and damping) and outside it to detect soil response in free-field conditions; (ii) refining the 3D FE model with the foundation soil modeled as a continuum.

REFERENCES

Bennati, S., Nardini, L. & Salvatore, W. (2005). Dynamical behaviour of a masonry medieval tower subjected to bell's action. Part I: bell's action measurement and modelling, Journal of Structural Engineering, ASCE, 131(11), 1647–1655.

Brincker, R., Zhang, L.M. & Andersen, P. 2001. Modal identification of output only systems using Frequency Domain Decomposition. *Smart Materials Structures*, 10: 441–445.

Ceroni, F., Pecce, M. & Manfredi, G. 2010. Seismic Assessment of the Bell Tower of Santa Maria del Carmine: problems and solutions, *Journal of Earthquake Engineering*, 14(1): 30–56.

Ceroni, F., Pecce, M., Sica, S. & Garofano, A. 2012. Assessment of Seismic Vulnerability of a Historical Masonry Building, Buildings, special issue: Earthquake Resistant Buildings, 2: 332–358; doi:10.3390/buildings2030332.

Ceroni, F., Pecce, M., Voto, S. & Manfredi, G. 2009. Historical, architectural and structural assessment of the Bell Tower of Santa Maria del Carmine, *International Journal of Architectural Heritage*: Conservation, Analysis, and Restoration, Francis Taylor, 3(3): 169–194.

Ciampoli, M. & Pinto, P.E. 1995. Effects of Soil-Structure Interaction on inelastic seismic response on bridge piers, *J. of Structural Engineering*, 121(5): 806–814.

Cremer, C., Pecker, A. & Davenne, L. 2001. Cyclic macro-element for soil-structure interaction: material and geometrical non-linearities, *Int. J. for Numerical and Analytical Methods in Geomechanics*, 25(13): 1257–1284.

Cremer, C., Pecker, A. & Davenne, L. 2002. Modelling of nonlinear dynamic behaviour of a shallow strip foundation with macro-element, *J. of Earthquake Engineering*, 6(2): 175–211.

De Sortis, A., Antonacci, E. & Vestroni, F. 2005. Dynamic identification of a masonry building using forced vibration test. *Engineering Structures*, Elsevier; 27: 155–165.

di Prisco, C., Massimino, M.R., Maugeri, M. & Nicolosi M. 2006. Cyclic numerical analyses of Noto Cathedral: soil-structure interaction modelling, *Rivista Italiana di Geotecnica*, 2: 49–64.

DIANA finite elements analysis, 2002 (release 9.1). User's manual, Element Library, Material Library, TNO Building and Construction Research, Dep. of Computational Mechanics, A.A. Delft, Netherlands.

Document 617, 2008 *Istruzioni per l'applicazione delle "Nuove norme tecniche per le costruzioni di cui al D.M. 14 gennaio 2008;* Ministero dei Lavori Pubblici, Roma, 02/02/2009 (in Italian).

Eurocode 8, 2004. *Design provisions for earthquake of structures—Part 1–4: strengthening and repair of buildings*, European Prestandards, ENV 1998–1–4, Comite European de Normalization, Brussels.

Gazetas, G. 1991. Formulas and charts for impedances of surface and embedded foundations, *J. of Geotechnical Engineering*, 117(9): 1363–1381.

Gazetas, G. & Mylonakis, G. 1998. Seismic soil-structure interaction: new evidences and emerging issues, *Geotech. Spec. Publ.*, ASCE, 1119–1174.

Improta, L., Di Giulio, G. & Rovelli, A. 2005. Variations of local seismic response in Benevento (Southern Italy) using earthquakes and ambient noise recordings. J. Seismol. 9: 191–210.

Jeremic, B., Jie, G., Preisig, M. & Tafazzoli, N. 2009. Time Domain Simulation of Soil–Foundation–Structure Interaction in non–Uniform *Soils, Earthquake Engineering and Structural Dynamics*, 38(5): 699–718.

Jeremic, B., Kunnath, S. & Xiong, F. 2004. Influence of soil-foundation—structure interaction on seismic response of the I-880 viaduct, *Eng. Structures*, 26: 391–402.

Jennings, P.C. & Bielak, J. 1973. Dynamics of building-soil interaction, *Bull. Seism. SOC. Am*. 63: 9–48.

Kausel, E., Roesset, J.M. & Christian, J.T. 1976. Nonlinear behaviour in soil-structure interaction. *J. Geotech. Eng. Div.*, 102 (GT12): 1159–1178.

Kramer, S., 1996 *Geotechnical earthquake engineering*. Englewood Cliffs, NJ: Prentice-Hall.

Marcellini, A., Iannaccone, G., Romeo, R., Silvestri, F., Bard, P.Y., Improta, L., Meneroud, J.P., Mouroux, P., Mancuso, C., Rippa, F., Simonelli, A., Soddu, P., Tento, A. & Vinale, F. 1995a. Benevento Seismic Risk Project: seismotectonic and geothecnical background. Proceedings of the Fifth International Conference on Seismic Zonation, October 17–19, Nice, France, vol. I: 802–809.

Marcellini, A., Bard, P.Y., Iannaccone, G., Meneroud, J.P., Mouroux, P., Romeo, R., Silvestri, F., Duval, A., Martin, C. & Tento, A. 1995b. The Benevento Seismic Risk Project: the microzonation. Proceedings of the Fifth International Conference on Seismic Zonation, October 17–19, Nice, France, vol. I: 810–814.

Michel, C., Gueguen, P. & Bard, P.Y. 2008. Dynamic parameters of structures extracted from ambient vibration measurements: an aid for the seismic vulnerability assessment of existing buildings in moderate seismic hazard regions. *Soil Dynamics and Earthquake Engineering*, 28: 593–604.

Min.LL.PP, DM 14 gennaio, *Norme Tecniche per le Costruzioni* (NTC), G.U.R.I., 29, 2008.

Mylonakis, G., Nikolaou, S. & Gazetas, G. 2006. Footings under seismic loading: analysis and design issues with emphasis on bridge foundations, *Soil Dynamics and Earthquake Engineering*, 26: 824–853.

NEHRP, 1997. *Recommended provisions for seismic regulations for new buildings and other structures*, BSSC.

Roesset, J.M. 1980. The use of simple models in soil-structure interaction, *Civil Engineering and Nuclear Power*, ASCE 10/3: 1–25.

Santucci de Magistris, d'Onofrio, Sica S. 2004. Studies on the seismic zonation of the city of Benevento. In: Pecce, M., Manfredi, G., Zollo, A. (Eds.), The Many Facets of Seismic Risk, CRdC-AMRA, 125–133.

Stewart, J.P., Fenves, G.L. & Seed R.B. 1999. Seismic soil-structure interaction in buildings. I: Analytical methods, *J. of Geotechnical and Geoenvironmental Engineering*, 125(1): 26–37.

Veletsos, A.S. 1977. *Dynamic behaviour of building-foundation systems*, W.J. Hall, Structural and Geotechnical Mechanics, Prentice-Hall, New Jersey, 333–361.

Veletsos, A.S. & Meek, J.W. 1974. Dynamic behaviour of building-foundation systems, *J. Earthquake Engrg. Struct. Dyn.*, 3(2): 121–138.

Wolf, J.P. 1985. *Dynamic Soil–structure Interaction*, Prentice-Hall, New Jersey.

This page intentionally left blank

Geotechnical Engineering for the Preservation of Monuments and Historic Sites – Bilotta, Flora, Lirer & Viggiani (eds)
© 2013 Taylor & Francis Group, London, ISBN 978-1-138-00055-1

New Lanark Walls: Examples of sustainable design for a World Heritage Site

M.J. Smith
Jacobs Engineering Group Incorporation (Jacobs), Glasgow, Scotland

ABSTRACT: New Lanark Village is a World Heritage Site and Conservation site comprising a beautifully restored 18th century cotton mill village in Southern Scotland, close to the Falls of Clyde. Founded by David Dale in 1785, the village became famous as a model industrial community under the enlightened management of Dale's son-in-law, Robert Owen, from 1800–1825. Owen transformed life in New Lanark with ideas and opportunities which were at least a hundred years ahead of their time. Child labour and corporal punishment were abolished, and villagers were provided with decent homes, schools and evening classes, free health care, and affordable food. Failure of one of the old masonry wall led tp immediate remedial works to maintain the World Hertitage status while providing a safe environment.

1 INTRODUCTION

Jacobs has been working with New Lanark Trust for a number of years. However, in 2007 a competitive tender was let for a condition survey of the 250 year old retaining walls and rock slopes around the village. Jacobs won this contract and its Ground Engineering team in Glasgow carried out a detailed inspection of the walls and slopes which involved roped access inspections and assessments. Conditions survey and remedial options reports were submitted, which included colour coded risk rated wall diagrams to assist the client. This helped the client apply for funding for remedial works.

While the client was applying for funding, a failure occurred in one wall next to residential buildings. Emergency works were completed for stabilisation of the wall and rock slope below. This made up Phase I of the works. The successful completion of this emergency work led to Phases II and III for all of the main walls in the village, as well as stabilising the 'Aviary', the walls around the village War Memorial, and re-building the bell tower.

This paper describes the various stages of the design and construction through condition survey, emergency stabilisation to completion of a third phase of repairs. The success of the project is based on the use of sustainable innovative designs to improve stability while protecting and maintaining the historic appearance of the repaired elements and the excellent relationship with the client and Government bodies like Historic Scotland who have had a major input. In order to retain the historic appearance designs have included buried invisible rear mass concrete walls, buried cut off walls to remove the need to excavation and underpinning of accommodation blocks and bringing back to 'life' the 'Avery'.

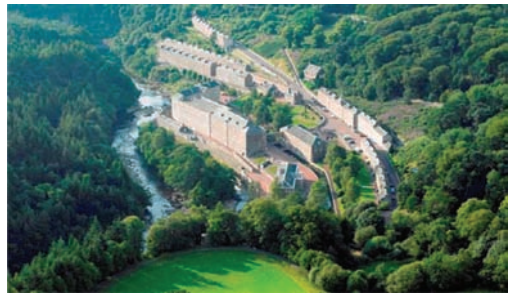

Photo 1. The New Lanark UNESCO World Heritage Site on the River Clyde. (Photograph provided by New Lanark Trust).

2 BACKGROUND

New Lanark, now a UNESCO World Heritage Site, was founded in 1785 by Scottish merchant David Dale as a cotton spinning settlement, powered by water from the adjacent River Clyde. The village, which at one time had a population of 2,500, was one of the largest cotton mill complexes in the country. The village was built on a steep site on the edge of the Clyde valley in order to capture the power of the river. However, this location presented its initial development with challenges; not least the provision of a stable and functional site which was able to house and educate its workforce.

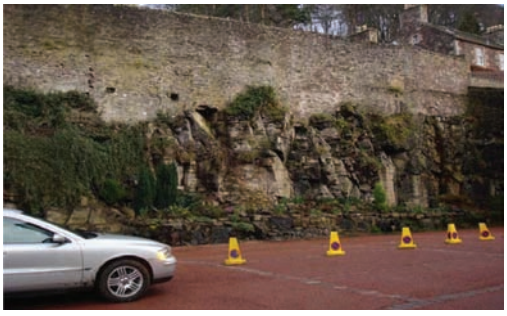

Photo 2. An example of one of the old masonry walls and rock slopes.

Figure 1. Retaining walls surveyed, together with rock slopes.

This was managed by the construction of large three-storey terraced residential buildings directly on bedrock, with quarried stone from the local area, together with retaining walls up to 6 m high to stabilise soil and fill slopes, some of the retaining walls sitting directly onto bedrock. Over the centuries a number of the old masonry retaining walls, many of which date from the 1790's, have shown evidence of wear are tear and although they have survived a number are in relatively poor condition. In addition to the walls themselves, the existing exposed rock slopes onto which the walls sit also exhibit potential instability in light of the centuries of weathering and erosion.

The site is a major tourist attraction managed by the New Lanark Trust and in 2007 it let a competitive tender for a phased approach to upgrading of the site, with initial work comprising a condition survey of walls and rock slopes, with subsequent phases including a ground investigation, detailed design and construction of remedial works.

3 CONDITION SURVEY

The tender for the phases upgrading of the site was won by Jacobs. The commission commenced with the completion of a detailed condition survey of all the walls and rock slopes, which exist below and around the residential complex. The locations of the walls are shown on the location plan below, Fig. 1.

In order to carry out as detailed a survey as possible, roped access techniques were used to be able to make detailed observations of the fabric of the walls as well as the slopes. The rock slopes were found to comprise grey inter-bedded sandstone with red calcareous fine grained sandstone, which have a laminated structure and are prone to weathering. The beds were found to be sub-horizontal and dip into the face. With the near flat bedding and sub-vertical jointing, the rock slope instability was found mainly to comprise overhanging blocks prone to toppling off the face as a result of ongoing weathering and erosion of the weaker laminated seams.

The retaining walls themselves were found to contain bulging areas, loose blocks of rubble and masonry, cracking of various severities, missing mortar, deterioration of supporting beams and lintels and missing copes.

Drainage was found to be provided through the walls which resulted in water washing from behind the walls down the rock slopes themselves. A risk profiling exercise was completed using a complex risk rating system to categorise the different sections of the walls and slopes, from 'extreme' and 'very high risk' to 'low risk'. Details of the risk rating are shown below, in Table 1.

Pie charts were used to clearly indicate the likely percentages of walls and rock slopes which needed attention (Figure 2), while In order to show clearly the actual risk areas, Jacobs devised a colour coded system to highlight those areas that were considered to lie in each risk category on photo-montages of the various walls and slopes. An example is shown on Figure 3.This system allowed explanation of the various factors to the clients and helped then in their funding applications, as all monies for the stabilisation or upgrading works had to be provided by outside parties like Historic Scotland South Lanarkshire Council and other grant organisations.

4 COLLAPSE AND EMERGENCY WORKS

In 2008, while the Trust was applying for funding for the next phase of the works, i.e. the ground investigation, a collapse occurred in a 'high risk' area of the walls. The extent of the collapse is shown below.

The collapse was a catalyst for works at the site. In light of the potential danger to the public and

Table 1. The risk rating system used.

Qualitative measure of likelihood

Level	Descriptor	Description	Indicative interval	Annual occurrence
A	Almost certain	The event is expected to occur	0 to	2
B	Likely	The event will probably occur under adverse conditions	2 to	5
C	Possible	The event could occur under adverse conditions	5 to	15
D	Unlikely	The event might occur under very adverse circumstances	15 to	50
E	Rare	The event is conceivable but only under exceptional circumstances	50 to	100

Qualitative measure of consequence

1	Catastrophic	Large section of wall damaged or small section destroyed, buildings may be at risk and/or possible serious injury to public
2	Major	Damage to small section of wall requiring reinstatement and stabilisation works and/or significant damage to public property or possible injury to public
3	Medium	Limited or aesthetic damage to moderate section of wall with immediate stabilisation works required and/or minor damage to public property
4	Minor	Limited or aesthetic damage to small section of wall requiring some stabilisation or repair works
5	Insignificant	Minor debris clean up

	Consequence				
Likelihood	Catastrophic	Major	Medium	Minor	Insignificant
Almost Certain	VH	VH	H	H	M
Likely	VH	H	H	M	L-M
Possible	H	H	M	L-M	L
Unlikely	M-H	M	L-M	L	VL
Rare	M-L	L-M	L	VL-L	VL

Risk level	Recommended treatment strategy
VH Very High	Extensive detailed investigation, planning and implementation of treatment options essential to reduce risk to acceptable levels
H High	Detailed investigation, planning and implementation of treatment options required to reduce risk to acceptable levels
M Moderate	Tolerable provided treatment plan is implemented to maintain or reduce risks. May be accepted where public are not at risk. May require investigation and planning of treatment options
L Low	Usually accepted. Treatment requirements and responsibility to be defined to maintain or reduce risk
VL Very Low	Acceptable. Manage by normal maintenance procedures

the trust employees, the ground investigation phase was replaced by an emergency stabilisation requirement. Issues of concern included the exact nature and thickness of the walls, the nature of the soil behind the wall, the condition of the foundations of the residential buildings immediately behind the wall, the bedrock profile and the levels and variations of groundwater.

In order to shed light on these a number of trial excavations were undertaken inside one of the unoccupied buildings in an attempt to find the foundations of the building and get an idea about depths and material type. The foundations, as expected, were found to be very shallow and rest at each corner on a large 'corner stone'—a block of sandstone. This led to initial worries with

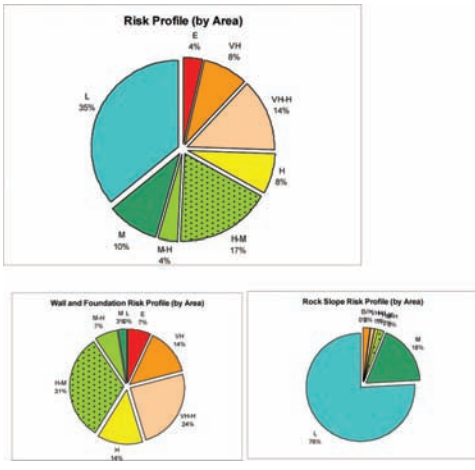

Figure 2. Pie charts breaking down approximate risk profile by area of walls and slopes.

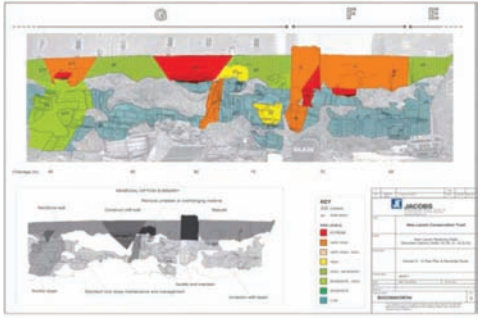

Figure 3. Example of colour coded risk rated condition survey for a typical area of old masonry walls and rock slope.

Photo 3. Collapsed wall section showing 'Double Row' residential building in the background.

regard to the requirement for underpinning of the buildings before any type of remedial works could commence on the retaining walls, as the collapsed section of wall would need to be removed and re-built, exposing soil/fill and potentially affecting the building stability. Further considerations with possible underpinning works was the age and construction of the buildings themselves, with the risk of cracking due to differential settlement becoming an issue. In order to remove this possibility, a cut-off trench was excavated immediately in front of the buildings down to bedrock to act as a temporary barrier and support during the works to the retaining wall. This cut-off wall performed well and throughout the repairs including excavations behind the existing walls and rebuilding of the walls in areas, the buildings themselves do not appear to have been affected.

The design of the repairs to the failed portion had to take into account the sensitivities of this being a world heritage site. While the stability of the wall and rock slope below had to meet current standards, the appearance and thus the high heritage value of the site had to be maintained. In order to stabilise the failed portion of the wall, a rear mass concrete wall, excavated down to bedrock and dowelled into bedrock was

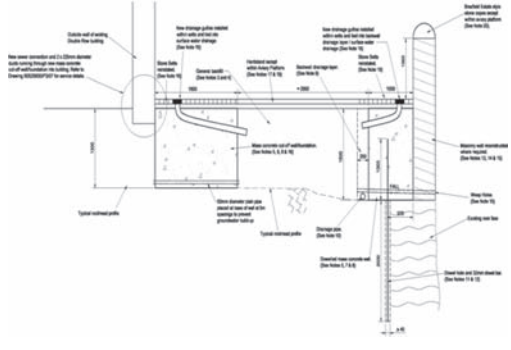

Figure 4. Typical design details for the buried mass concrete wall behind old masonry wall together with cut-off wall next to building.

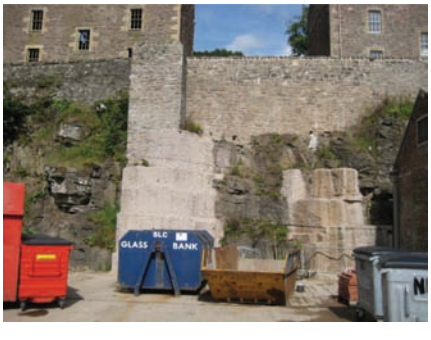

Photo 4. Completed emergency stabilisation works to the failed portion of the wall.

constructed. This mass concrete wall was built in sections and became buried and thus invisible when the road surface was reinstated after the works. The failed portion of the wall was then rebuilt using the same techniques as 250 years ago using as much of the failed stone as possible and employing specialist traditional stone masonry techniques and original lime mortar mixes. A combination of steel wall ties and resin anchor rods were used to tie the masonry to the mass concrete rear wall. The final appearance of the wall had to be agreed with Historic Scotland and whilst the taking down and rebuilding was to be the last resort, in this emergency portion little else could be done.

With regards to the stabilisation of the rock slope below the failed portion, concrete buttresses were the obvious stabilisation technique, based on the condition and characteristics of the rock mass. In order to achieve and maintain an appearance in keeping with the status of the site, these concrete buttresses were 'sculpted' to give the appearance of rock.

This emergency works made up phase 1 of 3 phases of upgrading and stabilisation work completed on the walls.

5 STABILISATION AND UPGRADING OF OTHER WALLS AND ROCK SLOPES

The next two phases of works involved the stabilisation of all the walls in front of 'Double Row' and 'Wee Row' of buildings, as well as upgrading of the 'Aviary' and adjacent walls.

The over-riding design for the walls was a buried mass concrete wall down to bedrock and dowelling into bedrock which stabilised the slope behind but allowed the existing old masonry wall to be pinned and re-mortared, rebuilt locally, to provide a design which stabilised the walls but remained 'invisible' to the public and thus maintained the heritage value of the site.

One area that came under the phase 3 of the Works was an upgrade of the existing area known as the 'Aviary'. While no Aviary structure existed at the site it was thought this area was originally used as a sitting out area for the workers at the mills. The exact condition of the structure was unknown until clearance works got underway.

The two photographs below show a before and after condition of the Aviary area, and similar design were used to stabilise the walls around the Aviary. New walls were built to stabilise the platform areas and the rock slope below the Aviary was stabilised using concrete buttresses.

Where there were no foundations for buttresses, areas of the rock slope were shotcreted to prevent

Photo 5. Staged construction of the buried mass concrete wall constructed to stabilise the old masonry walls.

Photo 6. A completed section of Phased 2 works—showing the upgraded old masonry wall and the concrete buttresses stabilising the rock slope which have been sculptured to reflect the rock mass structure, with bedding and block sizes similar to the rock mass. Rock mass dentition was used in thin weak laminated areas together with passive dowels to pin blocks together, hidden behind areas of sculpted concrete support.

Photo 7. Coloured shotcrete was used on the weathered rock mass—the colour was chosen to 'mimic' the rock mass colour. (Historic Scotland determined the colour used).

Photo 8. Before and after views of the 'Aviary' platforms.

Photo 9. Completed Aviary with 'Double Row' buildings behind.

erosion, with any small overhanging rock slope areas being infilled with shotcrete. Systematic dowels were also installed in highly weathered areas of the rock slope to add support prior to shotcreting.

Over the past four years Jacobs has completed a large number of individual tasks on the site, including the three phases described above, additional walls, bell tower repairs, design and stabilisation of War Memorial walls and slope, design of a new road surfacing for one of the main streets, input into a church options study and examination of an unstable wall near old sluice gates.

Future works may involve a stabilisation of the existing soil slopes, a flood risk assessment and an upgrading and stabilisation of slopes and walls around the existing village church.

6 CONCLUSIONS

Innovative designs for the stabilisation of old masonry walls in a world heritage site have been completed giving a stable site with buried and invisible engineering while maintaining the original appearance of the walls. Rock slope concrete buttresses were sculpted to reflect the rock mass appearance while providing future stability. Our delighted client states '*The Double Row retaining wall is one of the most technically complicated projects that has been tackled, extra care had to be taken to minimise disruption to visitors and guest and to ensure their safety'*. Historic Scotland commented *'It was very challenging but this carefully executed scheme has now secured the cliff setting and fabric of the historic retaining walls'*.

The lesson to be learnt here is that with careful and innovative designs the historic appearance of heritage structures can be maintained for the public to enjoy for many years to come. Early and continued liaison with governing government bodies is a must to provide both input into final appearance requirements at an early stage and thus financial control of construction, with a 'get it right first time' mentality for all parties. For all three phases of the works the same general and specialist contractors were used to provide continuity of site staff and application of knowledge gained during the design and construction of the emergency works, which was applied to the remaining phases of the works.

ACKNOWLEDGEMENTS

This paper is presented with the kind permission of New Lanark Trust. The project team who undertook the work for Jacobs included Fraser Lindsay, Andrew Robbie, Dave Sallis and the author. Their contributions are gratefully acknowledged.

REFERENCES

Sallis, D.K. (2009). *Mixed Stability*. Ground Engineering December 2009.

Sallis, D.K. (2010). New Lanark World Heritage Article published in Jacobs' internal 'Info' Magazine.

Geotechnical Engineering for the Preservation of Monuments and Historic Sites – Bilotta, Flora, Lirer & Viggiani (eds)
© 2013 Taylor & Francis Group, London, ISBN 978-1-138-00055-1

Evaluating the effects of tunnel construction on monuments: The example of the Basilica di Massenzio in Rome

F.M. Soccodato
University of Cagliari, Italy

L. Callisto & S. Rampello
University of Rome La Sapienza, Rome, Italy

G.M.B. Viggiani
University of Rome Tor Vergata, Rome, Italy

ABSTRACT: This paper describes some results of the studies carried out for the Basilica di Massenzio in Rome, potentially affected by the construction of the new C Line of Rome Underground. Displacement fields at foundation level were obtained from three-dimensional soil-tunnel-structure interaction analyses, that included a simplified but realistic model of the structure. The results of the study confirmed the effects of structure stiffness in reducing curvatures, differential settlements and tensile strain in the structure as compared to greenfield predictions. It was seen that the significant weight of the Basilica di Massenzio has an important effect on the settlements, that are significantly larger than those predicted from additional analyses that neglected the weight of the structure.

1 INTRODUCTION

The construction of new underground infrastructures in historical city centres raises a number of issues that must be properly managed in the design. Among others, the evaluation of the effects of tunnel construction on historical monuments, which are often of outstanding archaeological value, represents a key-step of the project.

A study of the effects of the new C Line of Rome Underground, currently at the final design stage, on the existing monumental Roman structures was carried out as part of a research project sponsored by the Municipality of Rome. Along the T3 junction of the C Line, a number of monuments, such as the Basilica di Massenzio, the Vittoriano, the Colosseo and the Aurelian Walls are potentially affected by the construction of the two closed-shield running tunnels. In order to minimize excavation-induced subsidence and avoid direct interferences with the archaeological layer, the tunnel axes run at the relatively large depth of 20–30 m.

A significant joint effort of archaeologists and geotechnical and structural engineers was required in the definition of reliable geotechnical and structural models. In fact, only limited information was available about the geometry of the structures (including their foundations), the mechanical properties of the materials and the history of the ancient monuments in terms of partial collapses, demolitions and reconstructions, and this lack of information is partially due to conservation issues that limit direct structural investigations.

The study of the interaction between tunnels and structures was carried out following stages of increasing complexity and accuracy in order to evaluate the level of approximation introduced in each stage of the analysis. More in detail, displacement fields at foundation level were obtained from soil-structure interaction analyses, in which a simplified but realistic model of the structure was implemented; these displacements were successively applied at the foundation nodes of a refined 3D structural model of the building, in order to improve the evaluation of the expected damage (Rampello et al., 2012; Burghignoli et al., 2005). This paper describes the results of a number of geotechnical three-dimensional (3D) soil-tunnel-structure interaction analyses, specifically referred to the Basilica di Massenzio, that were carried out at an intermediate design stage. While the detail of the tunnel layout varied at the final stage of the design, the approach followed in the present analyses formed the backbone of all the evaluations of the potential damage in the monumental buildings, and served as a guide for the successive development of the design. After a brief description of

the problem under investigation, the paper illustrates the geotechnical characterization of the site and the main geometrical and structural properties of the Basilica. Successively, the numerical model are introduced and the results of the analyses are presented and discussed.

2 THE AREA OF THE BASILICA

Figure 1 shows the plan of the area of the Basilica of Massenzio. According to the preliminary design of the line, the two 10 m outside diameter tunnels run nearly parallel to the main axis of the monument; the distance between the nearest tunnel axis and the NW facade ranges from 20 to 33 m whereas the tunnels, whose axes are 25 m apart, are located about 23 m below the level of the Via dei Fori Imperiali (23.5 m asl).

Over the years, the area of the Basilica had already been the object of studies and investigations; thus, a significant amount of data from archaeological, structural and geotechnical investigations carried out between 1995 and 2008 was available and has been employed for the purposes of this study.

The geotechnical characterization of the area was obtained both from in situ and laboratory tests carried out between 1995 and 2002 (Soccodato & Burghignoli, 2003); a complementary soil investigation was carried out in 2008.

The typical subsoil profile along the T3 junction is shown in Figure 2.

The actual structure of the Basilica consists of three large vaults, forming the aisle parallel to Via

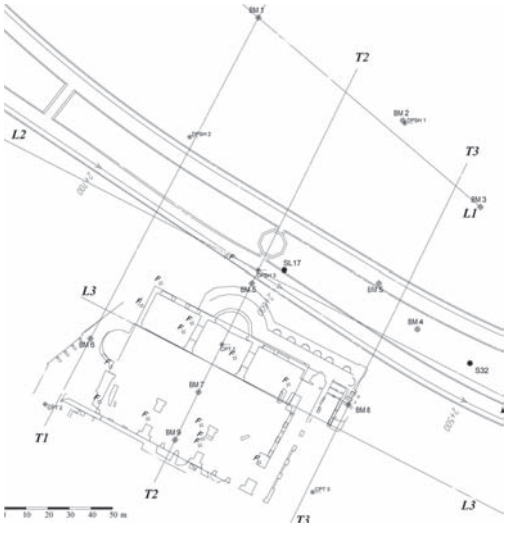

Figure 1. Plan of the area of the Basilica.

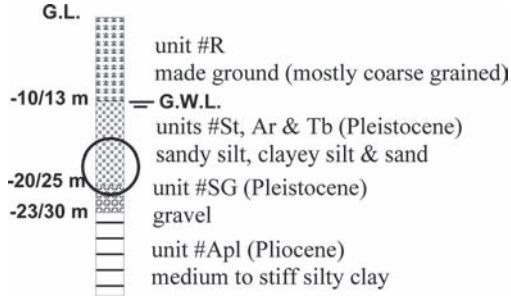

Figure 2. Typical soil profile.

Figure 3. SW view of the Basilica.

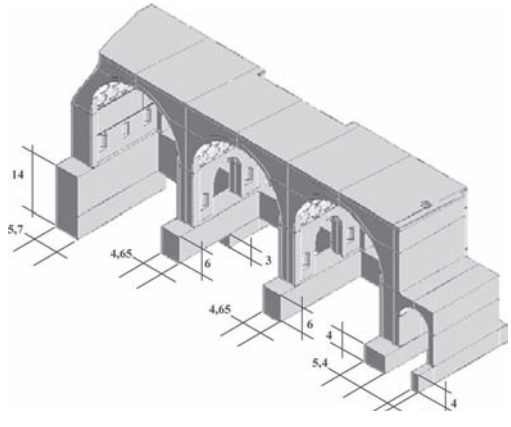

Figure 4. Geometry of the foundations (after CISTeC, 2001).

dei Fori Imperiali: each vault spans 20 m and is supported by massive walls (piers). The two side vaults are closed by a thinner wall on Via dei Fori Imperiali, with two layers of three arched windows, whereas the central vault terminates with an apse constructed by Constantine. Figure 3 shows a view of the Basilica.

The Basilica was built using the *opus caementicium* technique: two-sided masonry walls with an inner filling of roman concrete. Today, the monument exhibits significant cracks due to a variety of events occurred over the last two thousand years.

Figure 4 shows a scheme of the foundations of the Basilica: the depth of the foundations, following the original ground level before the construction of the Basilica, increases moving westwards.

A Roman wall, originally retaining part of the ancient Velia hill, separates the Basilica from the Via dei Fori Imperiali.

3 3D NUMERICAL MODEL

In the 3D numerical model, the real geometry of the problem was simplified as shown in Figures 5 to 7. The analyses were carried out by assuming the presence of a fictitious axes of symmetry between the two tunnels. This assumption, which implies that, in the model, the two tunnels will be excavated at the same time, appears to be reasonable because: a) on the other side of Via dei Fori Imperiali, opposite to the Basilica, there is a high hill (Belvedere Cederna terrace); b) the second tunnel is very far away from the Basilica and its effects are thus negligible.

Furthermore, the tunnel(s) were assumed to be parallel to the longitudinal axis of the Basilica, the real skew angle being about 6°; the distance between tunnel and Basilica was taken equal to the shortest in the actual layout, that is attained next to the Colosseo pier.

The 3D analyses were carried out with the commercial finite-element code Plaxis3D Tunneling v. 3.1 (Plaxis, 2008).

The finite-element mesh used in the analyses is shown in Figure 8. A total length of 204 m was adopted in the longitudinal direction, and of about

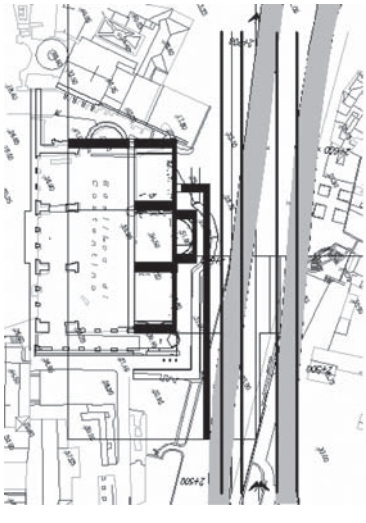

Figure 5. Three-dimensional model geometry: Plan view.

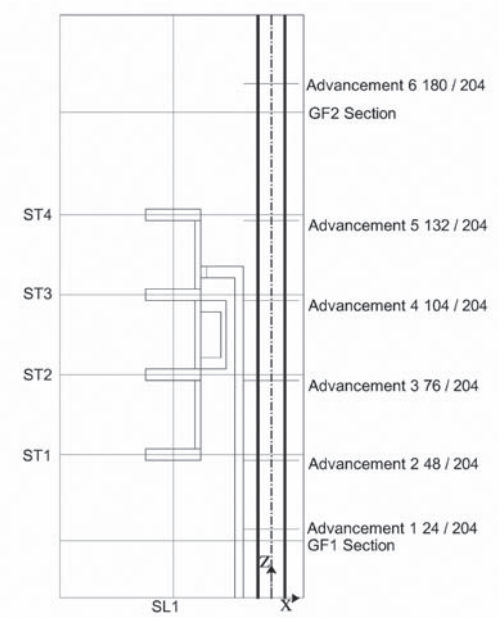

Figure 6. Three-dimensional model geometry: Control sections.

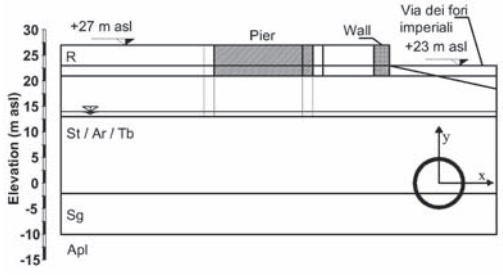

Figure 7. 3D model geometry: Transverse section.

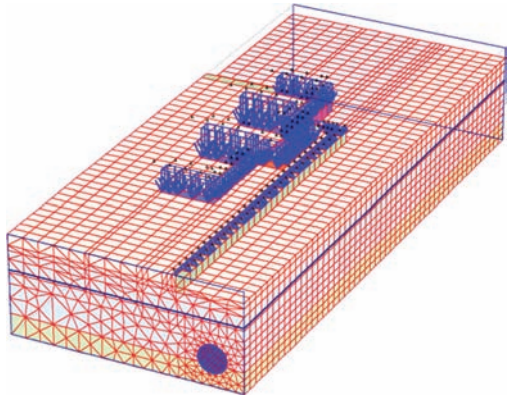

Figure 8. 3D model of the soil, tunnel and structure.

60 m in the transverse section. The top of the stiff clay soil layer Apl was used as the bottom boundary of the mesh, which thus extends from –10 to 27 m a.s.l. Rollers were prescribed on the four lateral vertical boundaries, while the nodes of the bottom boundary were fixed in all directions. The mesh includes about 24.000 tethraedal solid elements. In the direction of the tunnel axis, the size of the elements is constant and equal to 4 m, that corresponds to the excavation step adopted in the analyses.

In the simplified structural scheme, only the underground parts of the Basilica and of the retaining walls were modeled. The weight of the superstructures was modeled as applied vertical loads, as indicated in Figure 8.

Another view of the model, taken form behind, is shown in Figure 9; this view evidences the different foundation levels of the four massive piers of the Basilica.

According to the presence of the coarse-grained SG layer and to the relatively high permeability of the silty sand layer St/Ar, the analyses were carried out in drained conditions; pore water pressure distribution is hydrostatic, with a water table located at +10 m asl.

The steps of the 3D analysis are as follows:

- geostatic equilibrium at +27 m asl;
- activation of elements and loads modelling the Basilica and the retaining wall;
- excavation at +23 m asl in the area of Via dei Fori Imperiali;
- simulation of progressive tunnel construction.

The Hardening Soil Model HSS (Schanz et al, 2000) was adopted for simulating soil behaviour. Tables 1 and 2 summarize the main physical and mechanical properties of the different soil units.

Most of the model parameters were obtained from the interpretation of in situ and laboratory tests. More in detail, the E_{ur} stiffness was linked to the small strain stiffness measured in cross-hole and resonant column tests, as shown in Figure 10. Dilatancy at failure was set equal to zero for all soil units.

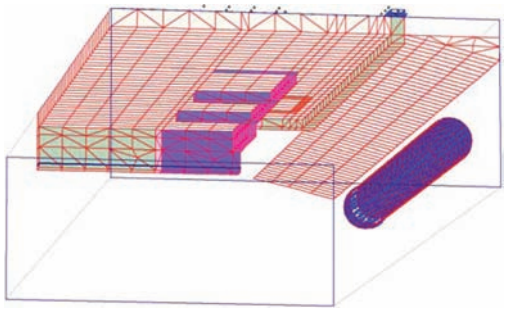

Figure 9. 3D model: View of tunnel and foundations.

Table 1. HSS model parameters: Main properties.

Soil unit	γ (kN/m^3)	K_0 (–)	OCR (–)	ν' (–)	c' (kPa)	φ' (°)
R	17.0	1.0	2	0.20	0.5	31
St, Ar	19.5	0.68	2	0.25	6.0	32
SG	20.0	0.36	2	0.20	0.5	40

Table 2. HSS model parameters: Stiffness properties.

Soil unit	E^{ref}_{ur} (MPa)	m (–)	E_{ur}/E_{50} (–)	E_{oed}/E_{50} (–)
R	240	1.0	10.0	1.0
St, Ar	170	0.7	7.5	1.0
SG	480	1.0	10.0	1.0

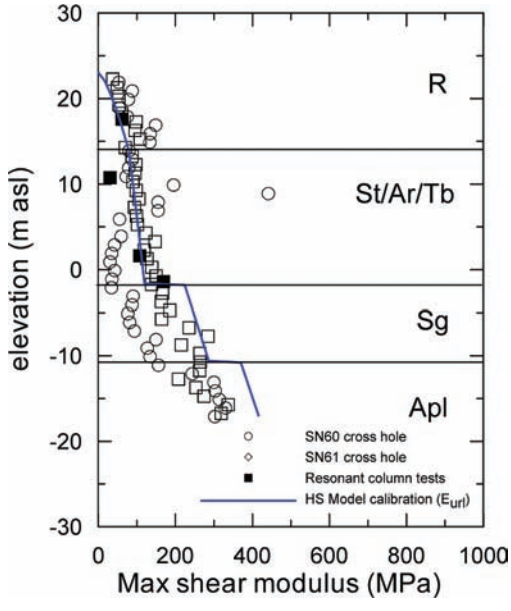

Figure 10. Small strain soil stiffness (based on 2002 soil investigation).

An example of results of model calibration is illustrated in Figure 11, which shows a comparison between experimental results and numerical predictions for a typical triaxial compression tests carried out on St/Ar soil samples.

The agreement between measurements and predictions is reasonable, especially at the low strain levels (Fig. 11d) which are expected to be relevant for the problem under investigation.

Massive piers and walls of the structure were modelled with an isotropic linear elastic—perfectly plastic model; a Mohr-Coulomb strength rule with a limiting tensile stress was used, as shown in

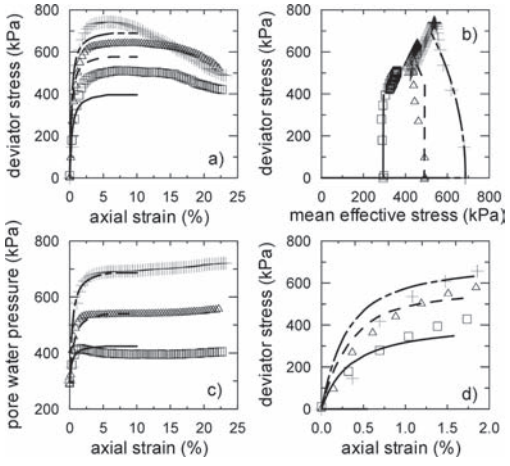

Figure 11. TX-CIU test: Experimental results (symbols) and model predictions (lines).

Table 3. Model parameters for Roman concrete.

	γ (kN/m³)	ν (–)	c (MPa)	φ (°)	σ_t (MPa)
Masonry	18.0	0.15	0.75	37	0.5

Table 4. HSS model parameters: Main properties.

Structure	Foundation level (m asl)	E (MPa)	Load (kN)	Applied pressure (kPa)
Colosseo pier	+23	3000	47,540	456
Central piers	+21	3000	56,190	626
Carinae pier	+13	2000	41,160	374
Arched wall	+21/+18	800	14,730	315
Apse	+23	2700	2260	439
Retaining walls	+21	3000	-	90

Table 3. Foundation level, stiffness (Young modulus), total structural loads and equivalent applied pressures are reported in Table 4.

Closed shield tunnelling was modelled by using a numerical technique capable to reproduce, in greenfield conditions, the typical displacement patterns observed in field monitoring. Basically, the technique consists in applying a given semi-elliptical, vertical displacement profile at the nodes of the tunnel boundary, immediately at the back of the tail of shield (Rampello et al, 2012). This forced displacement profile is released when permanent lining is erected. The value of the maximum displacement that had to be applied at tunnel crown is linked to the design ground loss ($V_L = 0.6\%$) and it was found, for the case at hand, by trial and error.

4 RESULTS OF THE ANALYSES

4.1 *Greenfield conditions*

Empirical predictions were obtained by assuming: i) a superimposition of the effects due to the construction of the two tunnels; ii) a constant value of the ground loss $V_L = 0.6\%$, according to design requirements; iii) a value of the parameter k controlling the width of settlement curve equal to 0.4 at ground level (+23 m asl) and decreasing with depth (Moh et al., 1996), according to soil profile properties.

Figures 12 shows, at different elevations, the profiles of the final transversal settlements w along the two greenfield control sections marked in Figure 6, obtained form the analyses and form the empirical procedure. The increase in maximum settlements with decreasing distance from tunnel is clearly apparent. Computed volume losses were found to be ranging from 0.55 to 0.65%, with a slight tendency to increase with depth. It can also be noted that settlement profiles are in reasonable

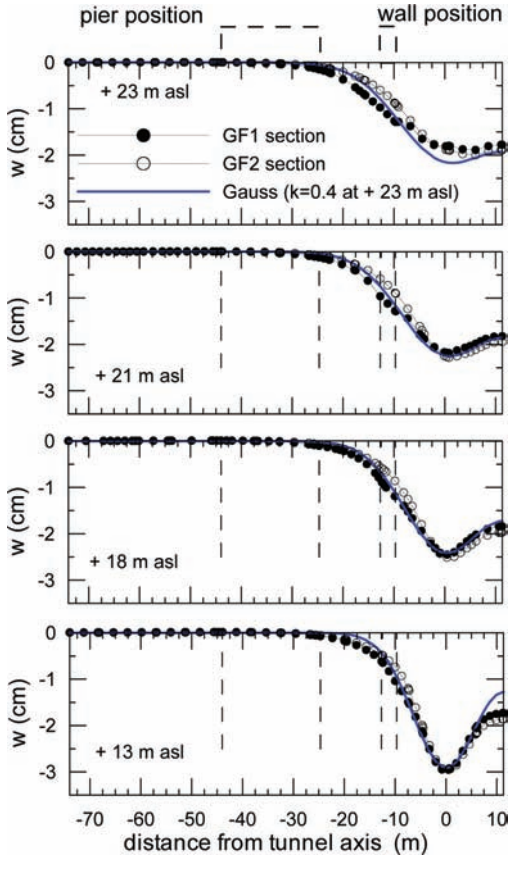

Figure 12. Transverse settlement profiles.

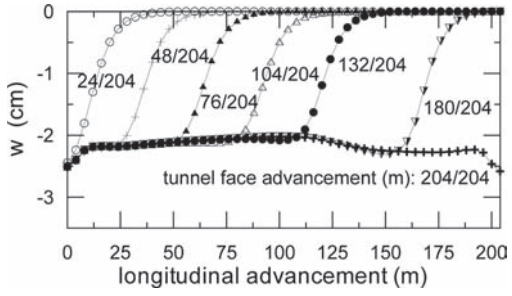

Figure 13. Settlement as a function of tunnel advancement.

agreement with those predicted by the empirical methods.

The settlements computed along the tunnel axis, at the elevation of 21 m asl, are shown in Figure 13 as a function of the tunnel face advancement. A restraining effects produced by the mesh boundary is limited to a distance of about 12 m. The computed settlements increase moving from the area where fill and retaining wall is present (GF1 section in Fig. 6, +27 m asl) to the area where an horizontal ground level exists (GF2 section in Fig. 6, +23 m asl). The settlement in correspondence of the tunnel face position (marked by an arrow in figure) is only about 15% of the final settlement, while the remaining 85% is produced when the tunnel face moves 20–30 m away.

Figure 14 shows, in the plane perpendicular to the tunnel axis and at three different depths, the final horizontal displacements u_X. For the GF2 section, their maximum value is located in correspondence of the inflection point of the settlement profile (see Fig. 6) and decreases with depth, from about 12 to 7 mm.

Along section GF1, soil-structure interaction effects due to the presence of the retaining wall (stiffness and loads) are apparent. Semiempirical methods assume that displacement vectors always point towards the tunnel axis (O'Reilly & New, 1982). The results obtained in this study, according with Grant & Taylor (2000), clearly indicate that displacement vectors are directed towards a 'moving' point that is located above the tunnel axis for shallow depth e below tunnel axis with increasing depth.

Finally, the final longitudinal horizontal displacements v_Z at +23 m asl are shown in Figure 15. Contrary to empirical methods, the longitudinal displacements do not vanish after the passage of the tunnel face: they are always directed towards the advancement direction and their values are similar to the transversal horizontal displacements u_X.

Basically, the trend of v_Z is related to the balance between ground losses at tunnel face and ground losses due to the closure of the gap between shield

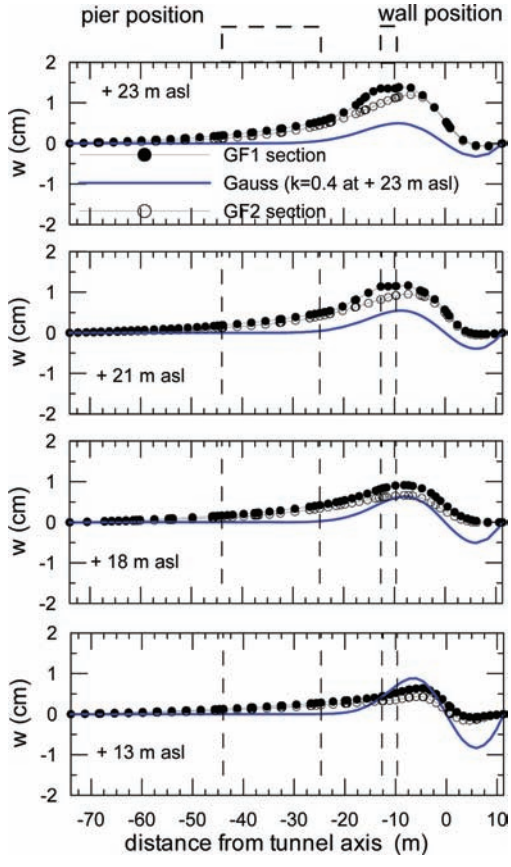

Figure 14. Transverse horizontal displacements.

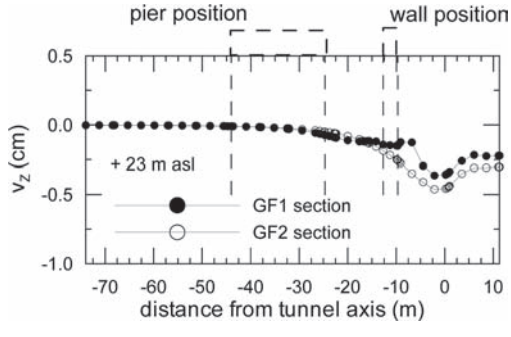

Figure 15. Longitudinal horizontal displacements.

and soil during lining erection. The numerical technique adopted in this study (Rampello et al., 2012) forces ground losses at the tail of the shield, that therefore tend to dominate over the longitudinal displacements occurring at the tunnel face, giving rise to permanent 'negative' longitudinal horizontal displacements.

4.2 *Soil-structure interaction*

In the area of the Basilica, the analysis allowed to evaluate the complete evolution of displacement field as a function of tunnel advancement. Figure 16 shows vertical and horizontal displacements at foundation level (+23 m asl) for the Colosseo pier (section 1 in Fig. 6). The results indicate a progressive rotation of the pier towards the tunnel, with maximum final settlements of about 7 mm (Colosseo pier). It is important to observe that the computed settlements of the foundation are significantly larger than those obtained in greenfield condition (GF1 section). The horizontal displacements are of the same order of magnitude of settlements, even though maximum differential values, due to the effects of structural stiffness, are smaller than 1 mm. Similar results were obtained for the other three piers of the Basilica, with maximum foundation settlements decreasing moving towards the Carinae wall, where the depth of the foundations increases.

Figure 17 shows the evolution of the settlements as a function of with the tunnel face advancement, along a longitudinal section (SL1 section in Fig. 6) that crosses the four piers. The maximum differential settlements for the four walls are smaller than 5 mm, also during the different construction stages.

It is interesting to understand why the soil-structure interaction analyses produce settlements

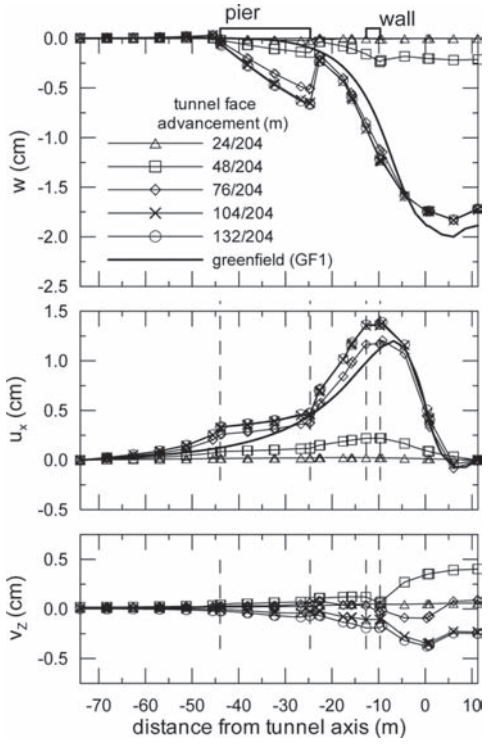

Figure 16. Colosseo pier section (+23 m asl): a) vertical, b) transverse and c) longitudinal horizontal displacements.

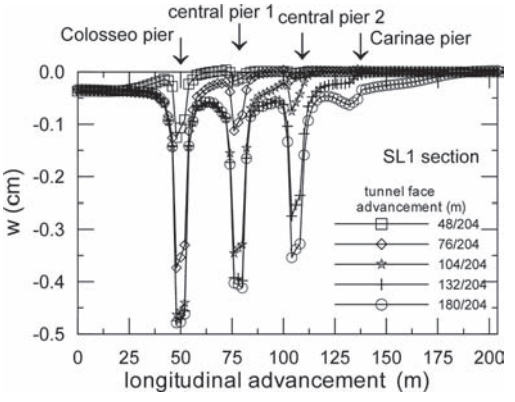

Figure 17. Settlements evolution with tunnel advancement.

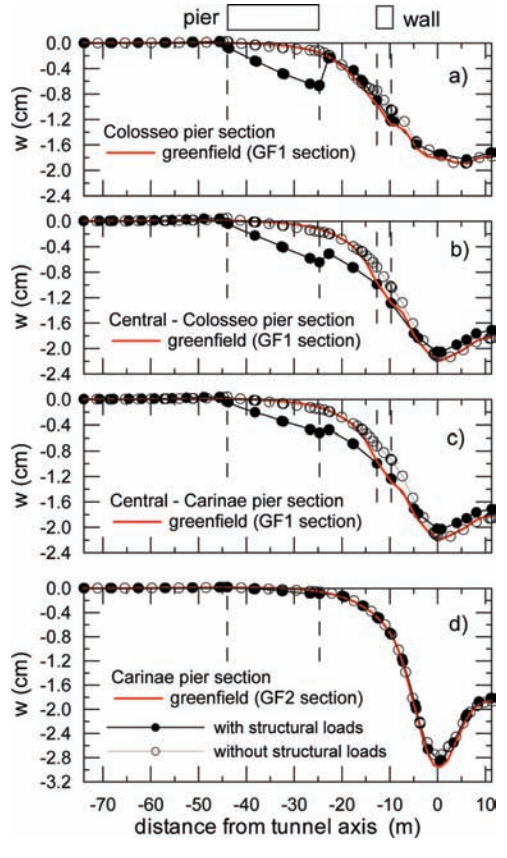

Figure 18. Settlements along a) Colosseo, b) central Colosseo, c) Central Carinae and d) Carinae sections.

that are larger than the free-field ones. The reason of this somewhat unexpected finding becomes apparent when looking at Figure 18 which shows, for all the four walls, the effect of the self-weight of the Basilica on the computed settlements. Neglecting the weight of the structure, the settlements obtained from the soil-structure interaction analyses are quite similar to free-field predictions

The weight of the structure modifies the initial state of stress in the subsoil, producing an increase in the deviatoric stress components; since the constitutive soil model used is non-linear, this change in the initial stress state produces a reduction of the tangent stiffness, and hence an increase of the computed displacements.

The results of the present analyses were used for a preliminary evaluation of the potential damage in the structure, based on the relative deflections computed at the foundation level. In a successive stage, the displacement field computed from these analyses was applied to the base of a refined three-dimensional model of the structure for a more detailed evaluation of the damage.

5 CONCLUDING REMARKS

This paper summarizes some of the results obtained in a study of the effects of tunnel construction on the Basilica di Massenzio in Rome.

The analyses were carried out taking into account information derived from a large archaeological, structural and geotechnical investigation.

A full three-dimensional soil-structure interaction analysis was deemed necessary given the complexity of the structural layout and the outstanding value of the monument. The numerical analyses were carried out adopting simplified but realistic models of the problem. A non-linear soil model was adopted in order to capture the effects of the evolution of soil stiffness with stress and strain levels.

An appropriate numerical technique was developed in order to model closed shield tunnelling, obtaining, in a greenfield condition, numerical predictions of displacements in agreement with typical field observations.

The analyses yielded the evolution of the displacement field as a function of the advancement of the tunnel face. The results confirmed that stiffens of the stiffness reduces the curvatures, the differential settlements and the tensile strain in the structure, as compared to greenfield predictions. However, it was found that the presence of the loads associated to the weight of the structure caused settlements at foundation level significantly larger than those that would be predicted neglecting such loads. This effect is clearly related to dependency of the dependency of the equivalent elasto-plastic stiffness of the constitutive soil model on stress levels. A soil model that neglects this feature of the soil's behaviour may not be able to reproduce this effect, that for the massive Basilica di Massenzio was quite significant.

The displacement fields obtained from the analyses described in this paper were successively applied to a refined structural model of the Basilica, in order to single out the structural components which are likely to suffer the largest damage from the tunnelling activities and that, consequently, will require the most careful monitoring during tunnel construction.

ACKNOWLEDGEMENTS

The Authors wish to acknowledge the contribution of Roma Metropolitane s.r.l. and Metro C S.p.a. that made this study possible; Profs. Michele Jamiolkowski, Alberto Burghignoli and Kalman Kovary, of the steering technical committee, engaged stimulating discussions; Prof. Fabrizio Vestroni and Mr. Adriano De Sortis provided and shared all the necessary information about the structural behaviour of the Basilica. Thanks to Mr David Carlaccini for performing some of the numerical analyses.

REFERENCES

Burghignoli A., Lacarbonara W., Soccodato F.M., Vestroni F. & Viggiani G. 2005. A study of the responce of monumental and historical structures to tunnelling. Proc Int. Symp. on *Geotechnical Aspects of Underground Construction in Soft Ground*, Amsterdam, pp. 487–493.

CISTeC 2001. Rapporto sulle indagini geotecniche nell'area della Basilica di Massenzio. (in Italian)

Mair R.J., Taylor R.N. & Bracegirdle A. 1993. Subsurface settlement profiles above tunnels in clay. *Geotechnique*, 43(2): 315–320.

Moh Z.C., Hwang R.N. & Ju D.H. 1996. Ground movements around tunnels in soft ground. In Mair et al. (eds) *Geotechnical Aspects of Underground Construction in Soft Ground*. London: Balkema.

O'Reilly M.P. & New B.M. 1982. Settlements above tunnels in the United Kingdom—their magnitude and effects. *Tunnelling 82*: 173–181.

Plaxis 2008. 3D Tunnelling v. 3.1 User' manual. Plaxis BV.

Rampello S., Callisto L., Viggiani G. & Soccodato F.M. 2012. Evaluating the effects of tunnelling on historical buildings: the example of a new subway in Rome. *Geomechanics and Tunnelling*, 5(3): 1–25.

Soccodato F.M. & Burghignoli A. 2003. Studio dell'interazione tra terreno, gallerie metropolitane e strutture monumentali. *Incontro Annuale dei Ricercatori di Geotecnica.* IARG 2003. (in Italian)

Geotechnical Engineering for the Preservation of Monuments and Historic Sites – Bilotta, Flora, Lirer & Viggiani (eds)
© 2013 Taylor & Francis Group, London, ISBN 978-1-138-00055-1

The preservation of the historical, archeological and artistic heritage of Orvieto: An interdisciplinary project

F.M. Soccodato
I.A.T. Ingegneria per l'Ambiente ed il Territorio Srl, Roma, Italy

E. Martini
Alta Scuola—Regional Government of Umbria, Casalina di Deruta, Italy

L. Tortoioli
Perugia, Italy

A.M. Mazzi
Municipality of Orvieto, Orvieto, Italy

ABSTRACT: The Orvieto Hill, with its historical and cultural heritage, for its geotechnical peculiarities represents one of the most interesting and analyzed case study in the world, with more than 300 international scientific publications. The happening of the instabilities and the consequent intense activities of consolidation, transformed Orvieto to a one of a kind open sky laboratory for the study of the instability phenomena and for the study of the effects of the remediation works. The town of Orvieto, located 105 km north of Rome, was included in 1937 in the list of inhabited areas threatened or affected by landslides; starting from this date, a number of occasional state interventions took place to tackle the instability of the tuff cliff until Law 25 May 1978 No. 230 was adopted calling for "Urgent actions for the consolidation of the cliff of Orvieto and hill of Todi to safeguard the landscape and historical, archaeological and artistic heritage of the two towns". The law authorized the Umbria Region to carry out studies and interventions on both Orvieto and Todi, historic towns presenting similar problems. The Orvieto Project, started at the end of the Seventies, is one of the first examples in Italy in which it has been adopted an interdisciplinary approach to the drafting of the plan in all its phases, from the study to the carrying out of the remediation works. For over thirty years the activities pushed involved professional from different areas of expertise (archaeology, chemistry, geotechnics, geophysics, hydraulics, transportation engineering, etc.) in a synergistic work.

1 INTRODUCTION

The town of Orvieto, located 105 km north of Rome, was included in 1937 in the list of inhabited areas threatened or affected by landslides; starting from this date, a number of occasional State interventions took place to tackle the instability of the tuff cliff until Law 25 May 1978 No. 230 was adopted calling for "Urgent actions for the consolidation of the cliff of Orvieto and hill of Todi to safeguard the landscape and historical, archaeological and artistic heritage of the two towns" (Fig. 1). The law authorized the Regional Government of Umbria to carry out studies and interventions on both Orvieto and Todi, historic towns presenting similar problems. In the "Orvieto Project" the following interventions were foreseen and completed: strengthening of the cliff, stabilization of slopes and ditches, consolidation of the caves, re-organization of drainage and improvement of the water and ecological systems of the slopes, substitution and completion of the sewage system, paving of streets and waterproofing of the city areas; re-organization of the archaeological

Figure 1. Cannicella landslides 1977.

park areas, implementation of alternative mobility plans, installation of geotechnical and topographic monitoring instruments (Soccodato et al., 2007).

Within the framework of the important interventions for the consolidation of the Orvieto rock and slopes, began in 1978, the Regional Government of Umbria, in coordination with the Municipality of Orvieto, set up an "Observatory for permanent control and maintenance" with the aim of managing the upkeep of the works carried out for the consolidation and structural stabilization of the cliff, as well as managing the protection of the historical and environmentally sensitive sites and the system designed to monitor the structural behavior of the interventions and the potential phenomena of geological instability in the region (Pane & Martini 1997). In addition, the Observatory functions as an operational unit for the prevention of risks, as well as a centre for the control and study of the different problems faced during implementation, and as an experimental centre for the identification of innovative maintenance and monitoring methods.

The monitoring system was installed during the course of the works to constantly control and record the trend of the tuff rock deformation and the movements of the slopes as well as to monitor the effects of the structural remediation works carried out. Such system, that integrates hundreds of geotechnical, structural and topographical instruments, is managed through the SIOR (Sistema Informativo dell'Osservatorio Rupe), a tailor-made Geographic Information System. The SIOR is an operational tool to collect, organize and analyze data related to the activities and works carried out to consolidate the cliff and slopes of Orvieto as well as all informations and data acquired by the monitoring system.

2 ORVIETO'S HERITAGE

The city has one of the richest artistic and cultural patrimonies in Umbria. Orvieto rises on a natural tableland at the summit of a 150-metre-high tufa cliff emerging, much like an island, from the surrounding plains. The city's distinctive feature comes from the particular relationship between this sheer cliff and the fabric of the city dominated by its imposing cathedral (Fig. 2).

Orvieto is of Etruscan origin with the more ancient traces dating back to 9th century BC; the necropolis and other findings indicate however, that the Etruscan settlement reached its peak development only between the 6th and 4th century BC and then declined in Roman times.

During the early Middle Ages, the cliff's strategic importance as a natural fortress was once more appreciated; a new settlement developed around the year 1000 and became a free Commune in 1137. At the centre of a vast territory, Orvieto's social,

Figure 2. The Cathedral, 14th century.

political and economical importance progressed rapidly, inducing important building activities—stately homes, towers and churches—and favouring the development of arts and crafts with the manufacture of refined handicrafts. The city reached its maximum expansion between the 13th and 14th century and its very particular urban structure has since remained basically unchanged.

The Cathedral was built between the end of the 13th century and the first half of the 14th century and marks Orvieto's peak development. The new cathedral was titled to Santa Maria Assunta in Cielo and erected over the ruins of two other churches: the previous mother church and St. Costanzo. The works spanned several centuries and produced one of the more grandiose examples of Italian medieval architecture. The facade, a great triptych built by Lorenzo Maitani in the first years of the 14th century, is certainly the prime masterpiece of Italian decorative Gothic (Fig. 3). Particularly significant in the sober, luminous interior, the chapel built by Andrea Pisano, around 1350 and paintings by Beato Angelico, Benozzo Gozzoli, Perugino and Luca Signorelli.

The "palazzo" surrounding the Cathedral are also noteworthy, namely those built for Pope Urban IV (1262–1264), Pope Gregory X (1272–1276) and Martin IV (1281–1284); they now appear as a single unit although the diverse typology of each one remains clearly identifiable.

The popes frequently took residence in Orvieto and this led also to the construction of Pope Boniface VIII's palazzo, known as Palazzo Soliano; it followed the rhythms of the Cathedral's construction and ended up as its annexe. Palazzo dell'Opera del Duomo was erected in 1359 to house the administration of the Cathedral's works; next to it, Palazzo Faina was built using the structure of the medieval Palazzo Monaldeschi and today houses the Archaeological Museum.

Political events during the Middle Ages were marked by the city's struggle against papal dominion but, in 1354, Cardinal Albornoz conquered Orvieto and submitted it to papal authority. Following

Figure 3. The Cathedral's facade, built by Lorenzo Maitani.

Cardinal Egidio Albornoz's diplomatic and military victory, it was established that, as in all other cities of the Papal States, a fortress would be built also in Orvieto. This fortress was destroyed a few years after it had been completed (1390) and rebuilt by Antonio da Carpi (1450–1452) over the same perimeter with the addition of a circular ravelin; the construction was completed under the supervision of Bernardo Rossellino.

A first urban renewal took place throughout the 16th century when, over the ancient medieval structure, new churches and "palazzo" were built by celebrated architects. A similar phenomenon occurred again during the 19th century architects such as Giuseppe Valadier and Virginio Vespignani enriched the city with new, neo-classical public and private buildings.

The very particular geological characteristics of Orvieto's tableland also determined another of this city's specific features: the presence of an outstanding number of artificial caves dug out following the trend of the city's development. First of all the quarries that, in the course of the centuries, provided tufa, travertine, sand and "pozzolana" first for the Etruscan buildings and later for Medieval and Renaissance "palazzi". There are also several caves created in order to find, draw, store and distribute water; caves were also used as stables, cattle sheds, colombariums and to store grain.

The celebrated Pozzo di San Patrizio or St. Patrick's well deserves special mention; it was commissioned by Pope Clement VII specially for Albornoz's fortress and built by Antonio da Sangallo il Giovane who was also in charge of the defences (Fig. 4). Sangallo took the idea from the Vatican's Chiocciola del Belvedere

Figure 4. St. Patrick's Well.

and created two one-way courses using a double helix pattern around a 53, 15-metre-deep cylinder, more than half of it is dug out in the lithoidal tufa, the rest built in brickwork with 70 large windows to provide air and daylight (Umbria Region, 2006).

3 GEOMORPHOLOGICAL ASPECTS

The Orvieto Hill can be considered as a rocky plate formed by pyroclastic deposits of various consistency, overlaying a middle pliocenic stiif clay deposit, with a thickness of more than 2000 mt (Fig. 5). A layer of alluvional deposits (silty sands and coarse gravels), including also some pyroclastic materials, about 10 m in thickness, represents an intermediate element of the stratigraphical series. The shape of the Rock is nearly elliptic, lengthening along E-NE—W-SW direction, with major and minor axes equal to 1600 and 850 meters, respectively. The faces of the Cliff are subvertical and, in some cases, overhanging; their height raises up to 50 m. Morphogenetical processes caused the progressive reduction of the original volcanic "plateau", the separation of the Cliff from the surrounding areas and the formation of the valleys, where two small rivers flow; these are located in the clay deposit, weathered by natural exogenous agents.

The clay formation is covered by a thick debris deposit originated by the progressive erosion of pyroclastic rocks; this debris cover contains loose elements and rock fragments, with dimension that may reach up to several cubic meters. The thickness of the debris decreases linearly with the distance from the rock faces (Calabresi & Scarpelli 1982). The water table is located inside the debris: springs appear along the contacts with the impervious clay formation all around the slopes Manfredini et al., 1980).

The pyroclastic plate, gently dipping N-NE, is visibly layered, with giant subhorizontal bedding planes. It is possible to distinguish the following levels, more or less wheathered by diagnesis: hard-tuff,

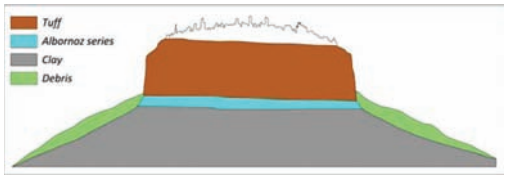

Figure 5. Geological section of the Orvieto Hill.

pomiceous tuff with black scoria, cemented ashes and very soft tuff. The thickness these different formations is variable, and the passage from one level to another is continous. Bedding is influenced by paleomorphology (Conversini et al., 1977).

Tuff is fractured and joints are generally closed. In some cases fractures, which run along the whole height of the rock face, are opened in the upper part of the cliff and tend to close towards the bottom. These systems of joints divide the cliff into columns and pillars. The number of fractures decreases with increasing distance from the rock face (Lembo Fazio et al., 1998).

3.1 *Failures and instability phenomena*

The general conditions of instability of the cliff and of the underlain clay slopes are well known and described since the Middle Age. It is interesting to note that, on the basis of the available historic and iconographic documentation back to 1528, it appears that the areas where most of the failures occur are almost the same (Lembo Fazio et al.,1984). These areas correspond, more or less, to the actual perimeter of the rocky plate, where temperature changes, meteoric waters and, in addition, the effects of man, have been more pronounced.

Failures can be so classified:

- landslides along the slopes (in the pliocenic clays and in the rocky debris)
- earth flows, mud flows and soil creep
- failures in the tuff cliff (along the external boundary): rockfalls, desquamations
- local subsidences due to undermining

Due to their formation process, the debris slopes are potentially unstable: any change of the underground pore water pressure, due to unusual rainfalls or due to losses of the town sewerage system through the pervious tuff strata, may trigger a landslides. The pliocenic clay, has been interested, during the prehistorical and historical times, by many landslides: in fact, the structures of the huge Etruscan necropoli, founded on the pliocenic clay, appear today backtilted, with a path of differential settlements in agreement with the relative distance from the cliff (Ribacchi et al., 1988, Tommasi et al., 2006).

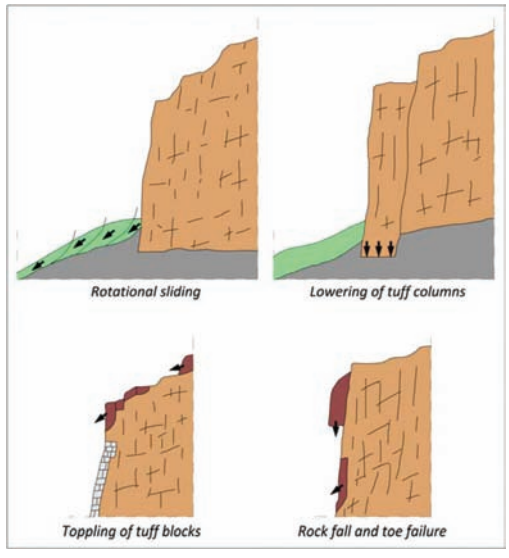

Figure 6. Failures and instability phenomena.

Large instabilities consist of extremely slow translation movements along well defined shear surfaces or bands extending from the slope toe up to the upper third of the slope (at times up to the foot of the cliff) within the softened portion of the in situ clay formation (Fig. 6). These movements are likely to represent a very advanced evolutionary stage of old failures that started under quite different morphologic conditions and propagated retrogressively. Slope failures, characterized by a progressive mechanism, also occurred in more recent times following major man-made changes in slope geometry or hydraulic conditions.

4 THE ORVIETO PROJECT: A MULTIDISCIPLINARY APPROACH

In Italy, State intervention in the "consolidation of landslides threatening residential areas and relocation of inhabited neighbourhoods" began in 1904, and was subsequently confirmed by Law 9 of July 1908, No. 445, which officialises a table containing a list of critical locations. This table was periodically updated by the National Government until the institution of the Regions, which, starting in 1972, took up direct responsibility in this regard.

In 1937, on the basis of the Royal Decree of 4 March 1937 No. 1069, the town of Orvieto was included in the list of inhabited areas threatened or affected by landslides, and, starting from this date, a number of occasional state interventions took place to tackle the instability of the tuff cliff.

Only in 1977, following two major landslides, which affected Orvieto's tuff rock (1972 and 1977), the Regional Government of Umbria Region decided, assuming a new cultural position of great responsibility, not only to stop the landslides, but also to try to understand more in general what was happening in Orvieto. As the landslides became more and more frequent, the Region started to analyse what solutions could be adopted in order to plan and implement permanent and long-lasting interventions. In 1977, a geological and technical study was carried out on the entire Orvieto cliff (Fig. 7). The study clarified that the problem of rehabilitating and consolidating the cliff and the inhabited town centre had to be faced making use of a very expensive large scale multi-disciplinary approach, whose costs couldn't be entirely supported by the regional budget. Thus, following in-depth discussions among the various political groups, Law 25 May 1978 No. 230 was adopted calling for "Urgent actions for the consolidation of the cliff of Orvieto and hill of Todi to safeguard the landscape and historical, archaeological and artistic heritage of the two towns". The law authorized the Region to carry out studies and interventions on both Orvieto and Todi, historic towns presenting similar problems (Barla et al., 1995).

This law was followed by other national administrative measures of a comprehensive character and made it possible to carry out numerous works aimed at achieving a "permanent consolidation", and adopting systems for long-term monitoring and surveillance. As a result of these measures, Orvieto was able to execute the interventions planned within the framework of an International Tender Competition for general consolidation works, as well as implement a parallel rehabilitation of the environmental heritage, which was executed under the aegis of the ministry responsible (Fig. 8).

Worth mentioning is the procedure for the consolidation of the tuff rock cliff, which was developed through the definition of reference tables aimed at choosing and calibrating in the best possible way the dimensions, intensity and distribution of interventions. These were identified on the basis of field test accompanied by theoretical studies, which applied the methods of the extreme allowable equilibrium, as well as analyses of tension stresses aimed at verifying "local" and "global" conditions of stability (Lunardi & Fornaro 1980).

Figure 7. Orvieto Hill during the '70s.

Figure 8. Orvieto Hill during the '90s.

Numerous specialists from academic and research institutions tackled the scientific problems and consolidation approach to be followed in Orvieto. It should be underlined that the interventions carried out for the consolidation and rehabilitation of Orvieto, including those related to the historic and artistic heritage and environment of the town, have had the effect of revitalizing and bringing new attention to an environmental and anthropic context of great value.

The interventions already carried out, and those currently under way for the management of the Observatory for monitoring and maintenance, have followed a distinct path: they emerged from emergency interventions at the beginning of the 1980s, and developed into an entire structural and integrated consolidation of the tuff cliff and its associated anthropic system, and the ongoing management of the entire territorial ensemble through the permanent maintenance of the executed works. All this generated and continues to generate added value to the place, as well as development opportunities for the town, cliff and inner parts of Orvieto's tuff rock.

5 THE REMEDIATION AND REHABILITATION WORKS

5.1 *Hydraulic works in the city areas*

The hydraulic works in the city areas, consisted in the rebuilding and repaving of the water and drainage systems, has been carried out in order to eliminate, or at least to reduce, the circulation and the infiltration of waters inside of the Cliff (the works

have been executed thanks to a previous financing). The rebuilding of the water and drainage systems involved all the historical center resting on the top surface of the cliff, involving more than 24.000 m of drainage pipes (with diameters from 800 to 315 mm), and the connections of approximately 6000 users. At the same time, it has been carried out the new distribution network of drinkable water for approximately 3000 connections and services. Paving (in paving stone and/or porphyry), with appropriate waterproofing, has been reconstructed on all the streets.

These works allowed to drastically reduce the infiltrations of water diffused on all the top of the cliff (Soccodato et al., 1984–1997).

5.2 *Strengthening of the cliff*

The design of remedial works has been inspired by the following issues:

- reducing hazards and dangerous states of the cliff;
- elimination or reduction of other factors which concur to impairment phenomena;
- recovering of the damaged areas.

The main works (Fig. 9) necessary for the completion of the stabilization master plan were:

- the setting up of servicing scaffolding, and the same time, the removal of weeds;
- steel bars/rockbolts used to strengthen the rock faces and joints;
- passive deep rock anchors at the top and bottom of the Cliff (with an additional row at mid height, dependant on the local height of the cliff);
- prestress rock anchors at the base of the Cliff, in those zones where a small cover is present, such as near the Fortress of Albornoz;
- sub-horizontal drainages in order to reduce water pressure due to water infiltration.

Together with the consolidation of the cliff faces, the limit edges of the cliff, close to faces, have been consolidated, where necessary, to limit possible water infiltration inside the Cliff and to avoid the growing of damaging bushes and trees (Diamanti & Soccodato 1981).

5.3 *Stabilisation of slopes and ditches*

These works involved three principal actions: regulation of the running surface waters into five main ditches, their stabilisation and, finally, slope stabilisation by means of deep drainage systems (Fig. 10).

In order to improve surface water flow, slope profiles have been reshaped and grass covered; ditches have been also renewed and consolidated. It is worth noting that this was the first Italian application of geosynthetics (Coluzzi et al., 1995).

For the stabilisation of the slopes, deep drainage shafts (15 m deep and 3.5 m in diameter), interconnected with sub-horizontal drains, have been constructed.

5.4 *Restoration of the historical walls*

These works, typical in areas of historical and archaeological importance, have consisted in the replacing of the foundations of the wall, in the static consolidation of the wall itself by substituting the degraded parts and by nailing and some cement injections.

A particularly relevant work has been made under the Fortress of Albornoz: it was necessary to almost completely rebuild the ancient wall under Lion Fountain road (Fig. 11).

This work required a very detailed historical research in order to carry out a correct reconstruction which took into account the long and ancient evolution of the wall structure.

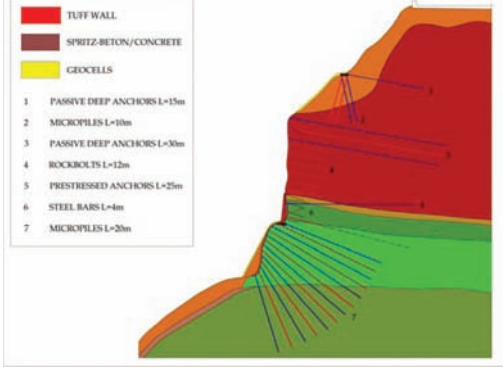

Figure 9. Strengthening of the Cliff.

Figure 10. Stabilization of the slopes.

Figure 11. Fortress of Albornoz during the '80s.

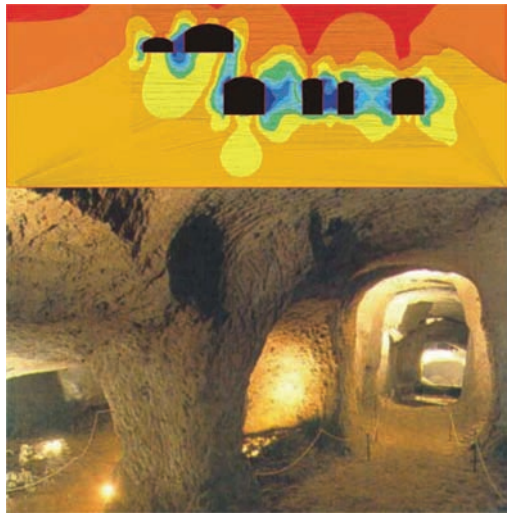

Figure 12. "Grotta delle Macine" geophysical survey.

5.5 *Survey and consolidation of the caves*

In order to map the (at that time) almost unknown location of the caves beneath Orvieto, a geophysical survey (Fig. 12) has been carried out using georadar technology (about 1.000 lines, up to 50 km in total length). The aim of this first phase was to verify the existence of the caves and, then, to accurately map each of them using topographic survey (using both traditional terrestrial and GPS satellite technology). About 450 caves (for a total surface area of 50.000 m^2) were in fact surveyed. All the mapping work was 'tied' to a local base line to accurately register all the cavities features, including their degree of damage and danger.

The works necessary for the consolidation of the cavities under public areas (some cavities were found in very bad conditions and, therefore, dangerous for the public safety), were developed following two directions, according to the historical and cultural value of the cave itself:

Static consolidation by:

- passive nailing (reinforcement with steel bars in the fractured zones);
- building of walls, vaults and arcades made of tuff, for the reinforcement of thin walls and weak columns;
- strengthening of foundation structures.

Caves in critical conditions but not interesting from an historical point of view, were completely filled with coarse grain mixed sized aggregates, and mixture of hydrated lime and bentonite/cement additive.

Conservative consolidation by:

- widespread micro-nailing;
- soaking of degraded and altered zones with low viscosity. chemical products;
- injections of cracks with special mortars (hyper ventilated pozzolana, hydrated lime and La Farge cement).

5.6 *The alternative mobility plan*

The alternative mobility system of Orvieto derives from the feasibility study of the re-establishment of the funicular, promoted by the Regional Government of Umbria in 1980, and consists of an integrated multimodal system providing a complete and articulated answer to the request of access to the city. Indeed the definitive consolidation of the Cliff of Orvieto involves the adoption of ad hoc plans of the automotive traffic (especially that heavy one) on the city centre, from which the problems of degradation of the historical buildings depends.

The Alternative Mobility System was structured so to ensure:

- the elimination of heavy public transportation (city bus and touristic ones) and the drastic reduction of private cars entering and parking in the urban area;
- the abatement of the atmospheric pollution index with the consequent reduction of the degradation and the maintenance of historical monuments;
- the improvement of accessibility and parking facilities for private means of transport of residents.

The general plan of Alternative Mobility foresaw the development of three integrated subsystems (two for infrastructure and one for management and computerisation) and a program of interventions

for the application of advanced technologies to the services of public transport.

The three subsystems were articulated as follows:

Subsystem 1: East side parking and funicular

- parking of Orvieto Scalo;
- underground connection from the Parking to the railway station square;
- funicular;
- funicular stations downstream and upstream;
- special means of transport.

Subsystem 2: West side parking and mechanized connection

- parking in Campo della Fiera (Fig. 13);
- mechanized connection to the Historical Centre through: lift to the edge of the cliff, tapis-roulant and escalator to Piazza Ranieri, pedestrian footpath in via Loggia dei Mercanti.

Subsystem 3: Distribution and parking of the residents of Historical Centre

- underground parking of Piazzale Roma;
- palazzo Crispo pedestrian access from the foot to the top of the Cliff (Fig. 14).

Figure 13. Parking "Campo della Fiera".

Figure 14. "Palazzo Crispo" pedestrian access.

5.7 *PAAO—Archeological and environmental park of Orvieto*

Two slopes at the foot of the Cliff house two important Etruscan necropolis (the necropolis of Cannicella on the South side and the necropolis of the Crocifisso of the Tufo, or Conce, on the North side), as well as other areas that are still under archeological surveys and analysis, are placed around the Cliff.

The idea and the cultural objectives that have inspired the set-up of the Archaeological Park are linked to the necessity not only to improve the accessibility to the two necropolis, connecting them to a series of structures (roads, paths, etc), but above all to the will to create at the foot of the Cliff an area of protection and continuous maintenance of the slopes, thanks to an appropriate use of the territory and the relative cultivations (Martini 2007).

The area occupies the conical declivity of the hill, between the cliff and the street ring surrounding it. The areas are composed of zones with different problems and vocations, hereunder a schematic articulation:

- an area of naturalistic and anthropic interest in its best integrated expression, that assumes meanings and values strongly linked to the orography of the ground;
- a belt, situated close to the tuff plateau on the northeast side, morphologically tied to the Cliff and with the necessity of a strict environmental conservation;
- an area of pre-eminently archaeological interest divided in the two complexes of Cannicella and Crocifisso del Tufo.

As a whole, the area can be recognised as an organic archaeological park. Here, the pedestrian paths that connect the main points of environmental and archaeological interest have been equipped to provide informative, didactic, tourist and scientific services.

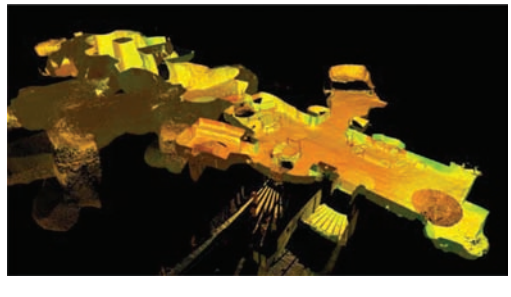

Figure 15. "Grotta delle Macine" Laser Scanner 3d survey.

In the framework of the creation of the Archaeological Park, it has been carried out the pathway that goes up from the Etruscan Necropolis (Fig. 16) to the Cliff, reaching the historical center and crossing the ruins of Porta Vivaria.

The interventions had the following three objectives:

- the strengthening of the Cliff in two areas: the first near to the S. Patrizio Well and the second next to the area named Porta Vivaria;
- the strengthening of two big cavities founded during the works, next to the S. Zero ditch;
- the provision of a pedestrian footpath, partly attached to the Cliff, allowing the connection from the city centre to the slopes and particularly to the areas of archaeological interest.

5.8 *The monitoring system*

The monitoring system, installed during the course of the works to observe over time the various factors that affect the tuff rock and the slopes of the Cliff, and to monitor the behaviour of the structural consolidation works implemented, is also capable of acquiring information on the structural stresses affecting the Cliff, piezometric variations, as well as any instability phenomena affecting the slopes and the consolidation works (I.A.T. Ingegneria & Orvieto Observatory, 1999–2013).

The network of instrumentation and topographic control is articulated into six significant test areas, specially selected to acquire the elements necessary for a definition, both general and localized, of the equilibrium condition of the cliff and surrounding slopes. The system has been carried out with the integration of manual and automatic readings.

Figure 16. Backward-titled Etruscan dice-tombs of the necroplis of "Crocifisso del Tufo" on the northern slope of the Hill.

For the topographical control of the areas subject to potential movement, it was decided to set in place, in conjunction with the necessary instrumentation, a geodetical network organized into a series of control points positioned along the most critical areas of the cliff (using high precision optical prisms) and slopes (using control points fitted with theodolites, GPSs and adapted in the recent years to robotic total stations), including also an external polygonal line used as a reference for the readings carried out from the different observation points. The geodetic surveys are carried out through an integrated method, consisting of topographical surveys on the ground (also with robotic total stations) and GPS satellite surveys (Fig. 17). The integration of these two methods is essential, as the terrestrial topographic surveys are indispensable for the readings carried out through the optical prisms installed on the surfaces of the cliff (and therefore unreachable by the surveyors), while the associated GPS technique has the advantage of expeditious surveys, without the necessity of visual connectivity between the measuring points. The topographic network is made up of 42 optical prisms positioned on the tuff face and 32 control points installed along the slopes (Fig. 18).

To monitor the Cliff's deformation, was installed a number of extensometers with single and triple bases at the foot and edge of the tuff face. For groundwater monitoring, a series of piezometers were installed, both on the plateau and along the slopes so as to be able to correlate variations in the level of the water table resulting from rainfall, measured by a dedicated meteorological station, as well as following possible movements of the terrain occurring along the slopes.

For displacement monitoring of the slopes a series of inclinometers pipes was installed near the peziometers, with some of them fitted with permanent probes on two levels with electrical sensors; all the instruments were associated with topographical reference benchmarks (Fig. 19).

Figure 17. Geodetical survey of the Fortress of Albornoz.

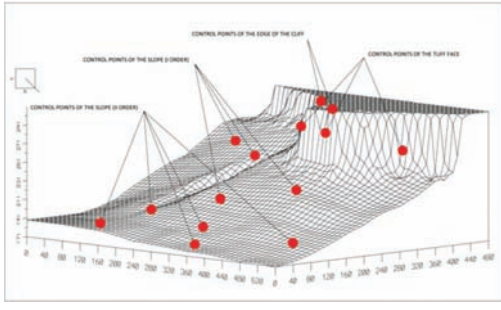

Figure 18. Geodetical instrumented network.

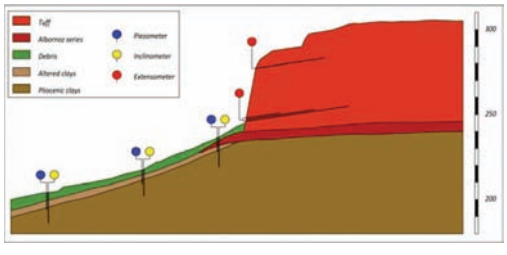

Figure 19. Geotechnical instrumented section.

Finally, an automatic meteorological station was installed on the plateau, containing pluviometric, anemometric, gonioanemometric, barometric and termoigrometric sensors.

The electrical instrumentation (extensometers, piezometers, inclinometers and meteorological sensors) is connected via an 8 km-long cable to fifteen data loggers positioned along the slopes and cliff, which acquire the data on a permanent and automatic basis. The data loggers are connected, through a GSM-GPRS digital communication system, to a remote central computer in the Observatory headquarters at the Municipality, which acquires and archives the data for consultation and analytical purposes within a dedicated developed software. The software allows real-time alerting and advanced data representation, enabling an unlimited number of data views in table, graph or map plots. The monitoring and early warning system supports all the tools to activate automatic alert and alarm procedures.

The geotechnical monitoring system, installed in the early '80s and implemented in the following decade, is actually composed of 221 instruments (91 piezometers at a depth of up to 60 meters; 81 inclinometers with a depth of up to 45 meters; 49 borehole extensometers, of which 24 have a triple base, for a total of 97 instruments, with depths varying from 10 to 60 meters); the data from 119 instruments are acquired both manually and automatically.

The automatic system is composed by 180 sensors, out of which 140 implemented also with temperature sensor. In detail: 32 bi-axial electrolytic inclinometers, 51 vw piezometers and 97 vw extensometers. The measurements collected automatically by the acquisition data units, including the extensometers, are also acquired, checked and calibrated periodically with manual measurements.

The automatic monitoring system also includes the meteorological station, and the seismic station (comprising seismic and vibration sensors). At last satellite SAR Interferometry monitoring is performed within the "Permanent Scatterers Interferometry Project" of the Italian Authority of Environment.

In addition, a number of monitoring subsystems have been put in place during the working phases and, for a brief period, following the development of specific interventions, in order to check the results of the works and their impact on the area in question. In particular, during the construction of the parking area at the "Campo della Fiera" and mechanized escalators connecting the Campo with the city centre, it was decided to install a monitoring system implemented with manual and automatic instruments. These included bi-axial tiltmeters, inclinometers, borehole extensometers, load cells and strain gauges (the latter to check the stresses affecting the steel ribs of the underground tunnel) for the control of the bulkheads and supporting structures built on top of the parking area; the data collected were integrated with topographic surveys (more specifically, high-precision levelling measurements) to check the stability of the buildings located above the area of intervention (Barla & Soccodato, 2000). All of these subsystems, like the above mentioned Campo della Fiera, as well as the near cliff of Rocca Ripesena (Fig. 20), are now managed by the Observatory increasing the total number of the instruments up to 400, out of which 230 support automatic data acquisition (Soccodato 2007).

Figure 20. Rocca Ripesena rockfall on November 1997.

Figure 21. WebGIS-based monitoring system software.

For over 30 years the monitoring system has been continuously collecting set of data. Up to now, more than 15 millions measurements have been stored in the database and have been post-processed and analysed by the SIOR software (Fig. 21).

6 THE ORVIETO OBSERVATORY

"... All masons of Orvieto are obliged once every two years to clean up the cliff and the walls from the twigs, weeds and all sorts of grass and shrubs ...", Pope Urban VIII bull issued in 1628.

"… to keep under observation the area more compromise of the cliff and adjacent parts of the settlement, in order to record the progressive movements of the mass tuff and of the underlying escarpment and to resume the observations." Final report of the "Commission on security conditions of the volcanic tuff cliff on which is built the city of Orvieto", November 1897.

"… it should be noted that any type of work is made on a situation that continues to evolve, despite the retarding action of the intervention ... this therefore must be conceived dynamically, becoming aware of the fact that we need a permanent activity of monitoring with the possibility to operate promptly in order to restore the functionality of the work in a short time and prevent the activation of deterioration process ...", Manfredini et al., in "Stability problems of the Orvieto Cliff" presented at the XIV Italian National Congress of Geotechnics in Florence, October 1980.

These three fragments of history underline as a scheduled maintenance (1628), an observation to record the settlements (1897) and a permanent surveillance in order to provide promptly to the restoration (1980), are concepts already expressed during the centuries in "bulls" and "reports" written for Orvieto, but never taken to be imposed in a legislative measure.

The National Law 545/97 takes these concepts and impose to install in Orvieto constant monitoring and supervision systems.

In order to keep under control the evolution of the various factors influencing the stability of the hill, systems for monitoring and controlling were planned and carried out. Those systems were also made to ensure, with careful maintenance, the behavior of the remediation works. For this purpose and for a constant vigilance on the areas affected by hydrogeological risk, was set up "The Observatory for the permanent monitoring and maintenance of the Orvieto Cliff, in order to operate promptly. The Observatory is managed by the Municipality of Orvieto under the supervision of the Regional Government of Umbria.

6.1 *Activities*

The Observatory schedules and coordinates the activities necessary for the regular and extraordinary maintenance of the works carried out on the plateau, the cliff and the surrounding slopes for the structural consolidation and safeguarding of the territory. In particular, the interventions concern: the roads on the plateau and at the foot of the cliff, the caves in good repair, the cliff's edges, tuff surfaces and slopes, the ditches and trenches for surface water drainage, the restored structures, retention walls, and the water networks (I.A.T. Ingegneria & Orvieto Observatory, 1999–2013).

The information related to the upkeep activities (types, dates, schedule of interventions, geographic locations, and photographic documentation) are digitized and archived by the Observatory's technical personnel in the Information System's data base.

In addition, the Observatory performs the regular and extraordinary maintenance of the entire monitoring system, including test, overhaul, repair, calibration and reconfiguration of the instrumentation and the acquisition data units (Fig. 22). Together with the upkeep, the Observatory is also responsible for the management of the monitoring system. It performs periodically field campaigns to manually read the data gathered by the extensometers, piezometers, inclinometers, and the topographic network.

The Observatory is also responsible, using a tailor-made information system specifically designed for the purpose, for the acquisition, archiving, management and post-processing of data collected by the monitoring system.

Periodically, the Observatory reports the results of the maintenance activities, as well as management of the information system under its care to the Regional Directorate responsible.

Figure 22. Maintenance activities of the monitoring system.

Figure 23. SIOR: Information system for the Cliff Observatory.

6.2 *SIOR—The observatory information system*

The principal support for the operational activities of the Observatory and for the coordination of the different actors involved in the management and maintenance of the territory surrounding the Cliff of Orvieto is the SIOR (Sistema Informativo dell'Osservatorio della Rupe di Orvieto) or Information System for the Cliff Observatory (Fig. 23).

The SIOR is a tailor-made information system which collects all the data and information available related to the structural consolidation of the cliff and slopes, and which provides the tools for the management and analysis necessary to plan and control maintenance activities, as well as run the monitoring system in ways that are standardized and can be used by all concerned.

The system is the result of a logical integration of a territorial information system for the management of structural interventions and a control system monitoring geotechnical, meteorological and climatic data (supporting all types of automatic or manual data, for any type of sensor and measure).

The system therefore acts as an operational tool to collect, organize and process data related to the activities and works carried out during the realization of the remediation interventions, in coordination with municipal, provincial and regional information systems (Soccodato 2008).

Moreover, the system may be considered a single container into which can be poured all data and information related to individual projects and structural interventions, the maintenance activities, the data collected through the monitoring equipment, the activities related to the design and preparation of plans, and the policies for the protection and management of the region.

Within this framework, the system allows the Observatory to discharge, with the necessary consistency of criteria, competency and effectiveness, its technical and operational mandate toward the safeguarding and monitoring of the territory (Fig. 24).

The system provides visibility and access to the activities of the Observatory for scientific cooperation and training in collaboration with research institutes and universities.

Finally publish data and reports of general interest that can be publicly consulted with different level of access.

6.3 *Implementation of innovative monitoring solutions*

During the past decade the Observatory have taken part in the implementation of a number of innovative monitoring solutions. In particular the Observatory is currently cooperating with University Departments and private entities for the integration of the GPS, Robotic Total Station and 3D Terrestrial Laser Scanner surveys with the aim of studying, analysing, modelling and monitoring rock slopes (Fig. 25).

6.4 *Alta Scuola*

The necessity to preserve the patrimony of knowledge and experiences acquired, brought to the idea to constitute, in agreement with the two Municipalities of Todi and Orvieto and the Umbria Region, a no-profit society named "Alta Scuola—Cultural and Scientific Society—Advanced Specialization School and Research Centre for the Maintenance and Preservation of Historical Town Centers in Unstable Areas".

Figure 24. SIOR—Tools preview.

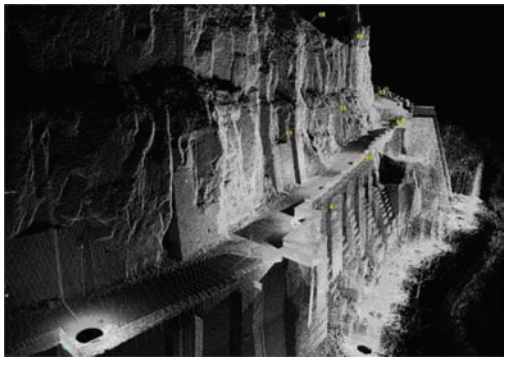

Figure 25. Integration of geodetic technologies.

The Society carried out Masters in "Maintenance and Preservation of Historical Town Centers in Unstable Areas" opened to multidisciplinary degrees, financed by the Umbria Region through European funds. It also organized scientific congresses all around Italy regarding the topics of its own mission with a wide participation of the National and International scientific community interested in the disciplines related to the consolidation of the inhabited unstable areas.

7 CONCLUSIONS

The Orvieto Hill, with its historical and cultural heritage, for its geotechnical peculiarities represents one of the most interesting and analyzed case study in the world, with more than 300 international scientific publications. The happening of the instabilities and the consequent intense activities of consolidation, transformed Orvieto to a one of a kind open sky laboratory for the study of the instability phenomena and for the study of the effects of the consolidation works (Figs. 26–27).

Figure 26. The Orvieto Hill before the remediation works.

Figure 27. The Orvieto Hill after the remediation works.

The Orvieto Project, started at the end of the Seventies, is one of the first examples in Italy in which it has been adopted an interdisciplinary approach to the drafting of the plan in all its phases, from the study to the carrying out of the remediation works. The activities pushed involved professional from different areas of expertise (archaeology, chemistry, geotechnics, geophysics, hydraulics, transportation engineering, etc.) in a synergistic work.

An outstanding characteristic of the Project is the have foreseen, more than thirty years ago, a complex scheme of monitoring system as a support tool for the planning activities, from the surveying phase to the construction of the intervention and the post-operam phase.

In synthesis, the Project has considered the maintenance and the monitoring of works and of the territory as a remediation work itself and in that respect, the Region has set up the Observatory of Orvieto and Alta Scuola.

ACKNOWLEDGMENTS

Past and present manager and technicians of the Orvieto Observatory: C. Casasole, R. Forbicioni,

T. Giuliacci, P. Mattioni, L. Pacelli, R. Sacco and the colleagues at Umbria Region, M. Barluzzi, P. Tamburi, and for Alta Scuola, P. Cerchice.

Technicians of the General Contractors Consortium (Geosonda, Todini, Fioroni, CCC, Grassetto), that carried out the remediation works, for all the precious information, data, support and material courtesy given.

Professors and researchers at Structural and Geotechnical Engineering Department of La Sapienza University of Rome, for their enthusiastic support during the development of the experimentations.

Finally special thanks are due, for their competence and patience in all of these 18 years of in situ tests, field investigations, surveys and activities to all the colleagues from the I.A.T. Ingegneria per l'Ambiente ed il Territorio Srl and in particular to G. Decina, E. Moruzzi, B. Paglia and Andrea Geacata.

REFERENCES

Barla G., Soccodato C. 2000. Pedestrian access to Orvieto through ancient tunnels. Proceedings of the International Conference GeoBen on Geologica and geotechnical influences in the preservation of historical and cultural heritage, National Research Council, GNDCI, Turin.

Barla G., Coluzzi E., Martini E., Soccodato C., Tortoioli L., 1995. *Proceedings of the Conference Orvieto e Todi due città da salvaguardare*, Orvieto.

Calabresi G., Scarpelli G., 1982. Argille sovraconsolidate e fessurate: fenomeni franosi. Progetto Finalizzato Conservazione. Rapporti di sintesi delle ricerche svolte dalle unità operative, EsaEditrice, Roma.

Coluzzi E., Curli G., De Carolis P., Rimoldi P., Soccodato C., 1995. Rinforzo mediante geogriglie delle pareti del fosso della Civetta alla base della Rupe di Orvieto. *Proceedings of the XI I.G.S. National Conference on Geosymthetics*, Bologna.

Conversini P., Sauro L., Martini E., Pialli G., Sabatini P., 1977. Regione Umbria, Rupe di Orvieto—Indagini geologiche tecniche. Regional Government of Umbria, Perugia.

Diamanti L., Soccodato C., 1981. Consolidation of the Historcal Cities of San Leo and Orvieto. *Proceedings of the X International Conference on soil Mechanics and Foundation Engineering*, Stockholm.

I.A.T. Ingegneria per l'Ambiente ed il Territorio Srl, Orvieto Observatory, 1999–2013. Reports and Publications of the Orvieto Observatory, Regional Government of Umbria, Perugia.

Lembo Fazio A., Manfredini G., Ribacchi R., Sciotti M., 1984. Slope failure and cliff instability in the Orvieto hill. *Proceedings of the IV International Symposium on Landslide*s, Toronto.

Lembo Fazio A., Ribacchi R., Sciotti M., Tommasi P., 1998. Problematiche di intervento su versanti naturali per la salvaguardia di abitati ed opere di ingegneria: alcuni esempi in relazione a diversi tipi di dissesto. *Proceedings of the International Conference on Il ruolo della meccanica e dell'ingegneria delle rocce nella protezione del territorio e dell'ambiente*, Turin.

Lunardi P., Fornaro M., 1980. Criteri di scelta per interventi di consolidamento della rupe di Orvieto e proposte operative. *Proceeding of the XIV A.G.I. National Conference,* Florence.

Manfredini G., Martinetti S., Ribacchi R., Sciotti M., 1980. Problemi di stabilità della Rupe di Orvieto. *Proceeding of the XIV A.G.I. National Conference*, Florence.

Martini E., 2007. Consolidation and rehabilitation of the Orvieto Cliff. *Proceedings of the International Symposium on Conservation and Sustainable Devel-opment of the Tuff Towns, World Monuments Fund,* New York.

Pane V., Martini E., 1997. The preservation of historical towns of Umbria: the Orvieto case and its Observatory. *Proceedings of the International Conference on Geotechnical Engineering for the Preservation of Monuments and Historic Sites,* Balkema, Rotterdam.

Ribacchi R., Sciotti M., Tommasi P., 1988. Stability problems of some towns in Central Italy: geotechnical situations and remedial measures. IS Engineering Geology as related to the Study Preservation and Protection of Ancient Works, Monuments and Historical Sites, Springer-Verlag, Berlin.

Soccodato C., Soccodato F.M., 2007. Orvieto e Todi. Città in divenire. Alta Scuola, Regional Government of Umbria, Perugia.

Soccodato C., Soccodato F.M., Spaini F., Ricci M., RPA SpA, SOT Srl, 1984–1997. Preliminary, definitive and final designs of the Orvieto Hill Remediation Works Project, Regional Government of Umbria, Perugia.

Soccodato F.M., 2007. The Orvieto Hill Observatory, *Proceedings of the International Symposium on Conservation and Sustainable Development of the Tuff Towns*. World Monuments Fund, New York.

Soccodato F.M., 2008. Tools for Territorial Maintenance and Monitoring: the S.I.O.R.—Information System for the Cliff of Orvieto. *Proceedings of the International Conference on Sediment disaster prevention technology*, Italian and Japanese National Institutes of Research, Rome.

Soccodato F.M., Tortoioli L., Mazzi A.M., 2011. The Orvieto Hill Observatory*, Proceedings of the Second World Landslide Forum*, Springer-Verlag, Berlin.

Tommasi P., Pellegrini P., Boldini D., Ribacchi R., 2006. Influence of rainfall regime on hydraulic conditions and movement rates in the overconsolidated clayey slope of the Orvieto hill. Canadian. Geotechnical Journal, Vancouver.

Umbria Region, 2006. Submission in the Tentative List of Unesco World Heritage, Regional Government of Umbria, Perugia.

Geotechnical Engineering for the Preservation of Monuments and Historic Sites – Bilotta, Flora, Lirer & Viggiani (eds)
© 2013 Taylor & Francis Group, London, ISBN 978-1-138-00055-1

Landslide risk assessment and management in the archaeological site of Machu Picchu (Peru)

D. Spizzichino, C. Margottini & L.M. Puzzilli
ISPRA, Italian Institute for Environmental Protection and Research, Rome, Italy

ABSTRACT: The archaeological site of Machu Picchu, designated by UNESCO as a World Heritage Site since 1983, is affected by frequent landslides which threaten its security and tourism exploitation. In order to contribute to a proper site management, research activities on a local scale have been developed; these, combined with field surveys, monitoring and analysis, have been transformed into a geotechnical model of selected relevant phenomena, in order to assess the related risk. In the present work the following analysis has been implemented on a local scale: geomechanical characterization, passive seismic technique and stability analysis implementation. Such results allowed the implementation of a general evolutionary model in terms of response to geomorphological stress. The main result of the above mentioned activities is the landslide risk assessment for the entire area and the implementation of a master plan for the definition of mitigation measures and conservation policy for site management.

1 INTRODUCTION

Machu Picchu Inka citadel is affected by frequent landslides that threaten security of inhabitants and tourist exploitation (March 2004, February 2008, January 2010). Different landslide patterns (rock falls and topples, debris flows, rock slides and debris slides) have been recognized and classified according to their kinematics, involved materials and state of activity. During last field survey a site-scale analysis was carried out, consisting mainly in seismic ambient noise measurements, geomechanical classification, structural and kinematical analysis and slope stability modeling (Spizzichino, 2012). In the present work the potential of the single-station passive seismic technique (H/V, Horizontal to Vertical spectral ratio) for the investigation of the subsoil at Machu Picchu has been explored. Passive techniques exploit only the environmental noise, which exist everywhere in nature (Castellaro, 2005), and are therefore to be preferred in Cultural Heritage environments, thanks to their non-invasiveness. The presented technique can both be used be used a) as a preliminary survey to address further investigation and b) to support and spatially extend the results of other techniques.

2 GENERAL SETTING OF THE AREA

The monumental complex of Machu Picchu (Lat. 13° 09' South, Long. 72° 31' West), is located on the top of a graben-like structure at 2.430 m.a.s.l., in the high Eastern Cordillera of the Peruvian Andean chain, approx. 80 km from Cuzco (Peru) (Fig. 1).

The Machu Picchu granitoid pluton, forming part of the larger "Quillabamba granite", is one of a series of plutons intruded along the axial zone of the high Eastern Cordillera Permo-Liassic rift system including a variety of rock types, dominantly granites and granodiorites (Mazzoli et al., 2009). Slope evolution of the area is mainly controlled by tectonic uplift, fluvial erosion operated by the Urubamba river, located at the toe of slopes, and by the geomechanical-structural settings of slope forming materials. The local bedrock of the Inca citadel of Machu Picchu is mainly composed of granite and subordinately granodiorite. Granodiorite is mainly located in the lower part of the slopes (magmatic

Figure 1. Panoramic view of Machu Picchu archaeological site.

layering at the top). Superficially, the granite is jointed in blocks with variable dimensions, promoted by the local structural setting. Soil cover, widely outcropping in the area, is mainly composed of individual blocks and subordinately coarse materials originated by chemical and physical weathering of minerals. Part of the slopes exhibit debris accumulation as result of landslide activity. Talus and talus cones are composed of fine and coarse sediments, depending on the local relief energy (Spizzichino, 2012). Alluvial deposits outcrop along the Urubamba River and its tributaries. They are composed of etherometric and polygenic sediments, that may be in lateral contact with the talus deposits. Anthropogenic fill and terraces (*Andenes*), on the top of the Citadel, reflect the work of Inca activities in the area (Canuti et al., 2008 and 2009).

3 LOCAL GEOMORPHOLOGY AND KINEMATIC CONDITIONS

Rock slides, topples and rock falls recognized and detected in the area, produce blocks with dimensions varying from 10^{-1} to 10^{2} m^3 that form the toe accumulation on steeper slopes. The structural setting of the granite bedrock and some superficial geomorphic evidences have been recently associated to a potential deep rock slide with an estimated volume of $10^4 m^3$, capable to produce severe damage to the archaeological site.

The structural setting is related to the main following dip orientations/dipping: a) 30°/30° in the Machu Picchu hill; b) 30°/60°; c) 225°/65; d) 130°/90°. In the SW cliff, the local morphological setting is governed by the intersection between the systems 225°/65° and 130°/90° which bounds the lateral evolution of the slopes. This kinematic condition causes rock slides with high angle which often evolve in rock falls. The morphological evolution of the NE flank below the Inca Citadel is constrained prevalently by the 30°/30° and 30°/60°

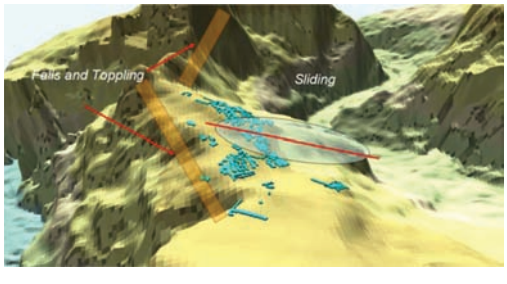

Figure 2. 3D Plot of main potential phenomena affected the citadel area as output coming from kinematic analysis.

systems and marginally the 225°/65° one; the intersection of the first two systems with the slope face is kinematically compatible with the occurrence of planar rock slides (Delmonaco et al., 2010); the intersection of the slope face with 225°/65° systems is kinematically compatible with rock falls (fig. 2).

4 SITE SCALE GEOTECHNICAL CHARACTERISATION

Geo-mechanical characteristics of the Machu Picchu slope-forming rocks outcropping in the study area, have been reconstructed through geotechnical field techniques and laboratory tests (executed in Italy), on rock blocks. A rock mass classification and failure criteria (Hoek, 2007, Hoek and Brown, 1988 and Hoek et al., 1992) have been implemented. In particular, the following activities have been carried out:

- Field survey implementation through scan lines techniques in order to define and reconstruct the main geotechnical and geomechanical parameters and Index (e.g. RMR, GSI, Q system);
- Strength and deformation parameters are collected starting from scientific and technical literature as well as from local technical report;
- Geo-structural analysis (orientation and characteristics of discontinuities);
- Sampling of blocks in the field for implementing laboratory analysis;
- Schmidt-hammer test on joint surfaces and intact rock block for in-situ analysis of UCS;
- Laboratory Point Load test to provide UCS data from sampled blocks and compare them with in-situ data.

The main results are reported in Table 1 and 2.

Table 1. Synthesis of geotechnical parameters carried out from in situ tests.

Geological strength index GSI	Cohesion c′ (Mpa)	Friction angle ϕ′	Elastic modulus E_m (GPa)	UCS from point load test (MPa)
65	0.3–0.4	40°	32.64	77.6

Table 2. Synthesis of geotechnical parameters carried out from laboratory tests.

Unit weight (KN/m^3)	Wave velocity V_p (Km/s)	Wave velocity V_s (Km/s)	Elastic modulus $E_{sec}50$ (GPa)	UCS σ_1 (MPa) triaxial tests
25.9	3.4	1.82	27.2	79.95

5 PASSIVE SEISMIC SURVEY

Site effects associated with local geological conditions constitute an important part of any seismic hazard assessment: furthermore passive seismic techniques uses only environmental noise which exists everywhere in nature (Castellaro et al. 2005). The H/V spectral ratio technique of ambient noise recordings relies on the basic idea that the response of underground structures to such kind of vibrations may provide useful indications about their mechanical behavior under seismic stress, even if it concerns low strain levels. Interest aroused due to the possibility of using such a small amplitude ground motion for the cost effective seismic characterization of subsoil and the parameterization of building dynamical response (Castellaro et al. 2009). In particular, Horizontal-to-Vertical Noise Spectral Ratios (HVNSR) deduced by single station measurement could be considered, in many cases, as an important tool for a very preliminary seismic characterization of shallow subsoil providing two basic pieces of information: identification of seismic resonance phenomena induced by the presence of sharp seismic impedance contrasts in the subsoil and the preliminary estimation of the resonance frequencies F_0 of the subsoil.

In this perspective, during field survey of May 2009 in Machu Picchu, more than 80 ambient noise measurements were conducted inside the Inka citadel and its surrounding areas by using TROMINO Micromed, a three-directional digital tromograph with a sampling frequency of 128 Hz and an acquisition time of 12 minutes, following the procedure described in SESAME European project (SESAME, 2013).

Despite the relatively short duration of measures, the task to cover the entire archeological area in less than 2.5 days were accomplished, together with an high quality of the registrations. It allows to retrieve meaningful information about fundamental resonance frequency of subsoil and about possible double-resonance effects on the main structures of Machu Picchu area as well (figure 3).

All the collected traces have been elaborated by using open source software Geopsy (http://www.geopsy.org) initially developed during above mentioned SESAME project, following the recommendation for data processing and interpretation of the results. Before any attempt of geological/geophysical interpretation, the quality of HVSR curves have been evaluated in agreement with international consensus criteria (SESAME, 2013). The analysis of the raw spectra of each components for every measurement was firstly conducted, to individuate the possible "anthropogenic" origin of F_0, usually characterized by sharp peak on all components (Lermo et al., 1993). Only after this checks,

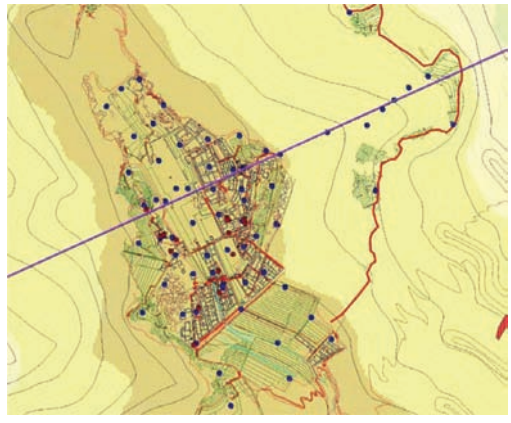

Figure 3. Location of the ambient noise measurements.

frequency peaks on HV curves were referred to the subsoil characteristics. For the application of H/V technique we chose a window length of at least 20 sec, being necessary to investigate the wide range of engineering interest between [0.5, 20] Hz. After elaboration, more than 80% of traces were finally selected to retrieve information about the fundamental resonance frequency of the area: from the HV technique applied to each traces we obtain an average HV curve with its corresponding peak frequency and peak amplitude (F_0 and A_0 respectively) with associated standard deviation values. As all the ambient noise registrations have been georeferenced, value of F_0 have been plotted in order to define a preliminary fundamental frequency contour map (F_0) for the whole citadel as depicted in Figure 4.

Here it can be observed the presence of higher resonance frequency that follows a trend elongated NNW-SSE corresponding to Sacred Plaza whereas in the most elevated areas F_0 value remain between 2-4 Hz. All the frequency peaks (F_0) have been plotted Vs amplitude A_0 with the aim of verifying value distributions and clustering. As shown in Figure 5 a cluster in the frequency range between 2 and 4 Hz it's easy to recognize, whereas other F_0 at upper frequency are poorly clustered from 8 to 12 Hz.

Furthermore, to stress the information derived from HVNSR technique, the citadel has been subdivided into 9 different zones, according to geological, geomorphological and anthropogenic criteria to represent the variety of the many stratigraphical, geological and structural settings (e.g., anthropogenic terraces, bedrock outcrops, intense fracturing, granitic chaos). Ambient noise measurements were reclassified into each zones. All the F_0/A_0 data have been analyzed and re-plotted with respect to the 9 mentioned zones, with the aim of underline the presence of potential clusters (Figure 6).

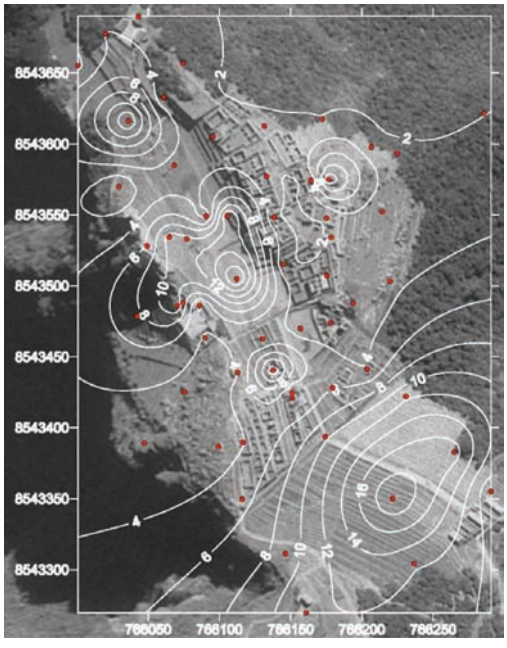

Figure 4. Preliminary contour map of fundamental resonance frequency for the citadel of Machu Picchu derived from HVNSR .

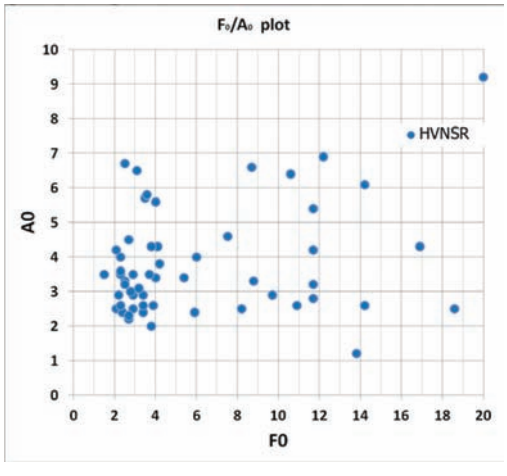

Figure 5. Plots of fundamental frequencies vs amplitude for HVNSR in the Machu Picchu area.

The plot in Figure 6, if compared to the Fig. 4, indicates that for some zone the frequency peaks resulted even more clustered (e.g. Z2 and Z5).

The application of HVNSR technique in this area was used to address further seismic investigation (mainly active) but also to retrieve other useful information together with other geophysical

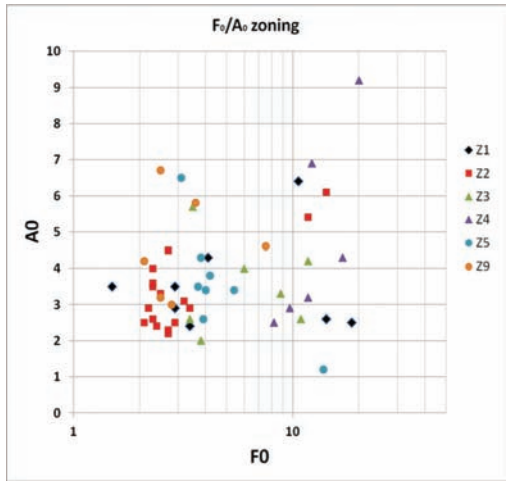

Figure 6. Distribution of F_0 and A_0 ratio for entire dataset overlapping zones and respect to each zone (except Z8).

investigations conducted with GPR and ERT techniques in this area (Best et al. 2009).

For a single soft sedimentary layer over bedrock (1D stratigraphy) the resonance frequency F_0 of the sedimentary cover is linked to the average shear wave velocity (Vs) in the sedimentary cover itself and to its thickness (h) by:

$$F_0 = Vs/(4h) \quad (1)$$

and assuming an appropriate model for the wave field and/or having a-priori information about subsoil, the thickness of the most superficial layer or the Vs average velocity could be estimated.

In this case, a good constraint for the thickness of soft sedimentary layer under Plaza Mayor has been derived from the GPR profile collected during the 2005 geophysical field survey (Best et al., 2009). Here the average Vs value was estimated around 200 m/s, being the resonance frequency around 8–10 Hz.

The most useful information to constrain the average Vs value under the entire archeological area derived from our re-elaboration of the ERT dataset collected by Canadian and Peruvian research team (Best et al. 2009), in order to better describe the shape of 2D contact surface between weathered and un-weathered and/or fractured granite (white dotted line).

The first dotted line is just close the surface of Sacred Plaza and could be surely correlated with the same surface founded with GPR data even, of course, in ERT we have quite a different scale of precision (figure 7). In depth, along the entire section the deepest vertical change in resistivity could be interpreted as the upper surface of un weathered granite rock.

These two surface could be responsible for the presence of two impedance contrast that gave a fundamental resonant frequency of 8–10 Hz in Plaza Mayor (upper surface) and of 2–4 Hz (deepest surface) along all the Machu Picchu area. Being the latter surface at a constant depth of about twenty meters from upper surface, the estimating average Vs velocity varying between 160–320 m/s.

As previously mentioned, an analysis of likely double resonance effects in some of the most important structures has been carried out in order to verify the correspondence between the fundamental frequencies of seismic signal, as transmitted to the surface, and the fundamental frequencies of the archaeological artifacts located in the same place.

From empirical point of view, the resonant frequency of a building is governed primarily by the height and can be approximately calculated (Pratt et al., 1997), as follows: *resonant frequency of a building ≈ 10 Hz/number of floors.*

The coincidence of resonance between soil and structure is particularly dangerous, and should be avoided because it produces maximum amplification: *resonant frequency of a building ≈ resonant frequency of soil.*

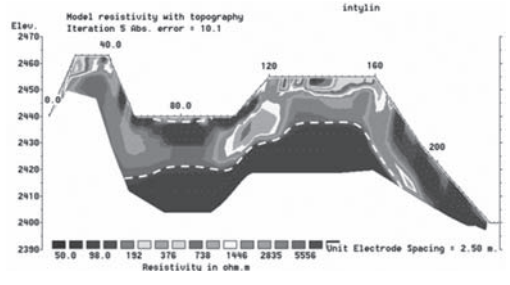

Figure 7. Geo electrical resistivity model from ERT collected by Best et al. 2009 (courtesy of P. Bobrowsky).

Analysis were conducted using the "structure spectrum" plug-in of Geopsy suite, an advanced signal processing tool aiming at estimating the *Transfer function* of a system by computing the spectral ratio between the input and the output signals(http://www.geopsy.org/wiki/index.php/Geopsy:_Structure_spectrum).

The "input signal" were represented by ambient vibrations recordings at bottom of each structure (G_N, G_E) whereas the registrations on top of buildings (T_N, T_E) were considered as "output signal": a third signal represented by the difference of each pair of signals (D_N, D_E) were finally added for the deconvolution. Thus two different spectral ratios were obtained: the ratio between the relative motion and the input signal represented by D_E/G_E and D_N/G_N as an estimate of the transfer function of the soil-structure system and the direct deconvolution between I/O signals represented by T_E/G_E and T_N/G_N.

Main outcome of this analysis was represented by a possible double resonance effect detected in the Main Temple area and in the Industrial Sector close to the Mortar Group.

For the first area the analysis showed a clear peak around 11 Hz (Fig.8) strongly focalized on the NS component, as for the EW component ratio is less sharp. It's worth noting in the E54 registration a secondary resonance frequency around 3 Hz that is the same fundamental resonance frequency of entire citadel.

For the industrial sector we find, as well, a very close range of resonance frequency between 9.5–10 Hz but not focalized, as shown in figure 9

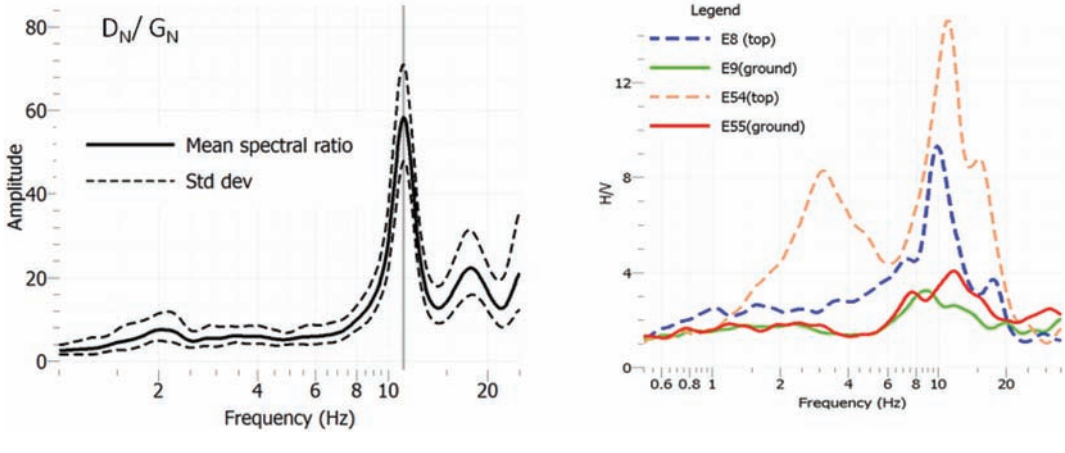

Figure 8. Example of ratio between D_N/G_N for the Main Temple area (E55 and E54 traces) (left) and HVSR of four registrations collected in this area (right).

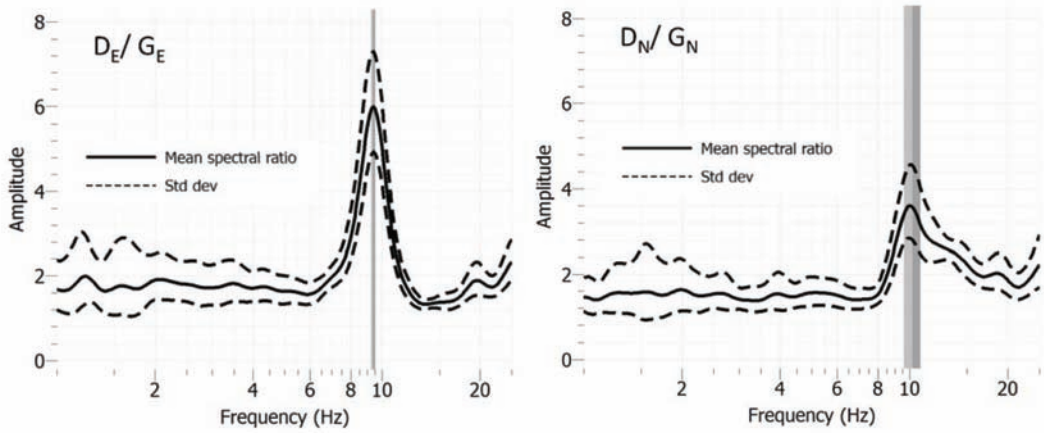

Figure 9. Ratio between DE/ GE (on the left) and DN/ GN (on the right) for the Mortero area.

in which the two D/G ratio for each component were depicted.

6 MOST HAZARDOUS AREAS

In order to identify the phenomena, we have started from the main results of the geomorphological, stratigraphic suggestion of the passive seismic analysis and kinematic analysis (Figs. 2 and 4). We have focused mainly on rock fall and planar sliding typologies, avoiding the treatment of debris flow phenomena (although widely present). Rock falls have been treated according to their frequency and magnitude (involving large areas of the archaeological site), even if the block average dimension is often very small, the risk is amplified by the daily presence of a large number of tourists (Pasuto et al. 1996). Planar sliding, although less frequent, owes its dangerousness to its potential impact due to possibility of involving a big portion of the site just with the triggering of a single disastrous event.

6.1 *Slope stability analysis*

After the identification of the most prone areas from a geomorphological point of view and those most exposed and vulnerable from an archaeological and historical point of view, the analysis has been focused on the area which is most prone to risk. More in detail, the potentially investigated unstable areas are:

- the SW slope and the Wayna Picchu NE slope prone to rock fall phenomena (Fig. 2);
- the NE slope of the citadel prone to planar slide (Fig. 2).

After the definition of deformability and strength parameters of the involved rock masses (Tables 1 and 2), a slope stability analysis has been carried out, in order to define specific and residual landslide risk conditions (Lembo Fazio et al., 1984). Regarding planar slides, two different scales of approach have been taken into consideration:

1. a limited portion of the NE slope (unstable wedge, Fig. 10);
2. the whole NE slope (Fig. 11), not reported in this paper.

In the first analysis, Mhor-Coulomb strength criteria have been adopted in case of limit equilibrium planar conditions. The analysis has been performed by using RocPlane software from RockScience®. Whereas, for the second approach, both Mhor-Coulomb criteria and Hoek-Brown strength criteria have been adopted for the entire rock masses.

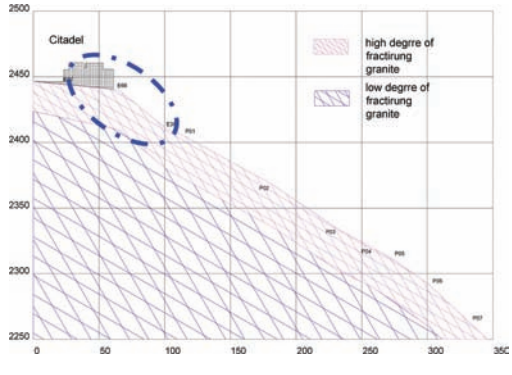

Figure 10. Two different scale of analysis for the potential planar slides. Small and local in the upper part of the slope (blue circle) and the whole NE slope.

6.2 *Slope stability of the potential unstable block of the NE sector*

The potential unstable planar sliding has been detected by the presence of the following sets of joint: the first one parallel to the slope and the second one given by the average of two different set of joints (dip 30°/slope 30°; dip 30°/slope 60°), from whose envelope the potential sliding stepped surface can be furnished (Fig. 12).

The slope stability analysis has been implemented under the following hypotheses:

- planar sliding (static and dynamic conditions) in dry and saturated condition with the presence of a tension crack (Fig. 13);
- planar sliding (static and dynamic conditions) in dry, partially and fully saturated condition without the presence of a pre fixed tension crack figure (Fig. 14).

The analysis has been performed by using Mohr-Coulomb resistance criteria (more conservative than Barton-Bandis and Hoek and Brawn criteria) and the following average geotechnical parameters for the discontinuities:

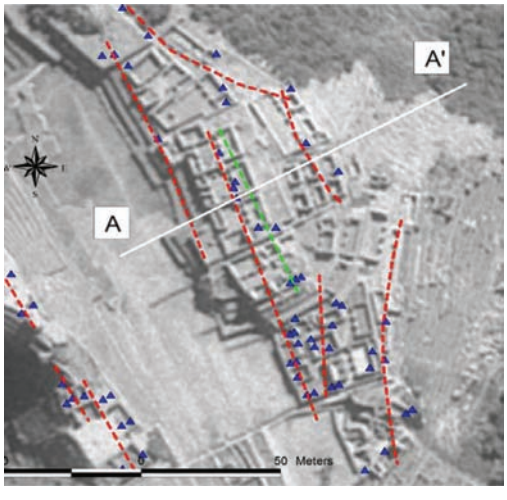

Figure 11. Trace AA' of potential unstable planar slide in the NE flank of the citadel adopted for the model.

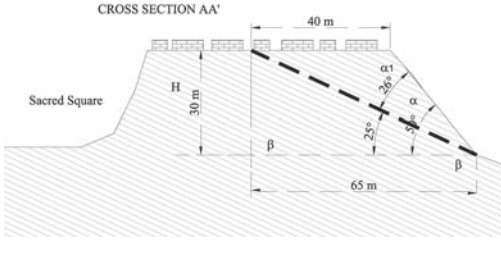

Figure 12. Cross section of potential unstable planar slide in the NE flank of the citadel adopted for the model.

Table 3. Geotechnical parameters used for the discontinuities.

Source	Rock type	Friction angle	Cohesion KPa	Unit weight KN/m^3
GSI	Granite	$\phi' = 40°$	$c' = 305$	$\gamma = 25.4$

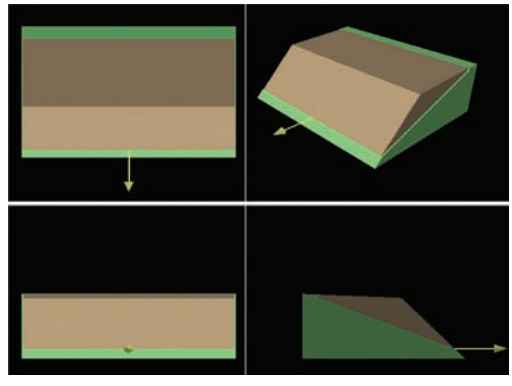

Figure 13. Geometry of the potential unstable planar slide (tension crack distance = 40 m).

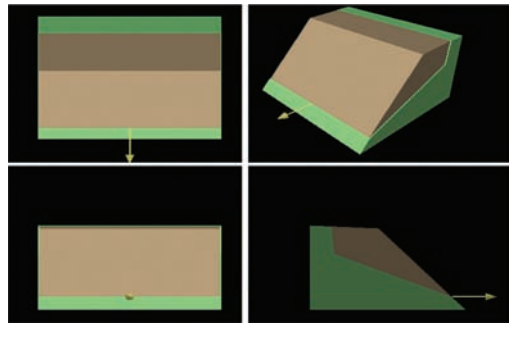

Figure 14. Geometry of the potential unstable planar slide (no pre fixed tension crack).

The main results of the analysis is summarized in the Figure 15.

The analysis shows (under the preliminary hypothesis of a pre-existing tension crack), factor of safety (in static conditions) always major than 1. FOS minor than 1 has been detected in dynamic condition starting from a degree o f saturation along the discontinuity around 70%. Under the hypothesis of absence of pre existing tension crack, the analysis is able to calculate the distance from the crest of the unknown discontinuity which minimized the FOS.

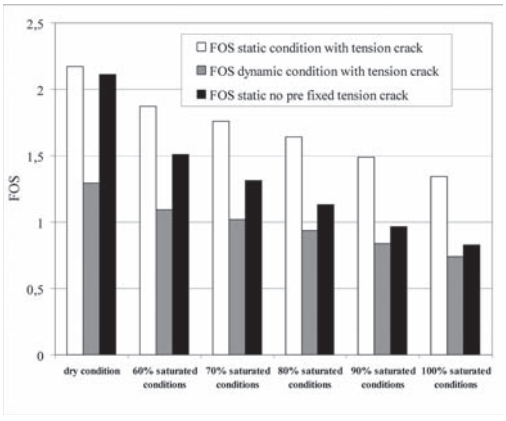

Figure 15. FOS values for the different discontinuities saturations conditions.

6.3 *Machu Picchu rock falls analysis*

In order to perform a complete rock fall analysis, for Machu Picchu's most prone area, the following steps have been developed:

1. source area definition (following the main results and indications from kinematic and geomorphological field survey and analysis);
2. typological section along the W-SW and E-NE slope (in order to take into account the interactions between theoretical paths and exposed elements, including tourist trails);
3. potential paths simulation using Rocfall software from Rockscience®;
4. defining and dimensioning preliminary mitigation measures (barriers).

Concerning the first and the second point, selected source areas are reported in Figure 16 on the basis of field survey and kinematic analysis.

Three sections along the W-SW slope and two sections along the E-NE have been defined and implemented. The selected profiles represent possible path interactions between different typologies of exposed elements (e.g., Intiwuatana, Main Temple, Inka Trail, paths). The analysis has been implemented for a profile along the SW slope and for a profile along the NE slope, as an example of the fully procedure (Fig.17 and 18).

As a first step, slope geometry (2D) must be fixed. Along this geometry, the different lithology must be defined in order to assign the corresponding normal and tangential restitution coefficients (Table 4).

A band (as source area) has been assigned with horizontal initial velocity equal to 1.5 m/s and an average weight of about 10 kN per block.

The probability analysis developed (Fig. 17 and 18), highlights that rock fall phenomena may

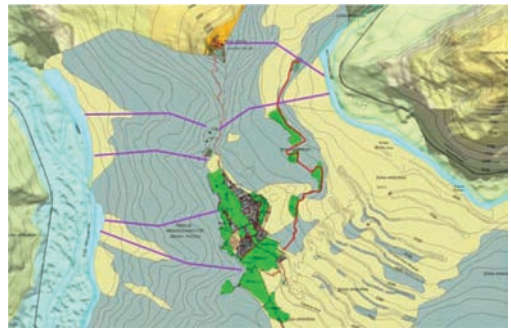

Figure 16. Rock fall source areas and implemented profiles for the stability analysis.

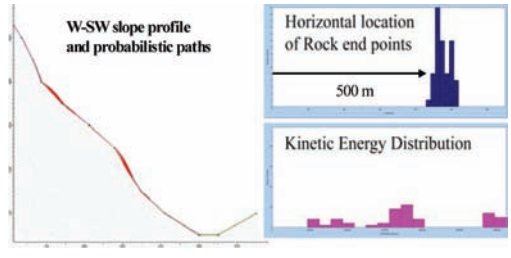

Figure 17. Paths and main results of rock fall probabilistic analysis along profile of the W-SW slope.

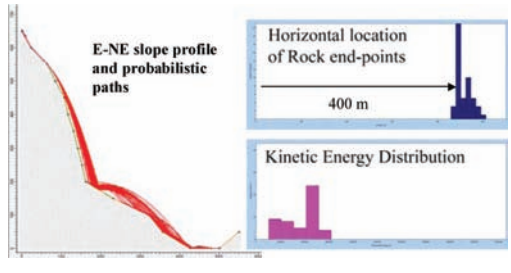

Figure 18. Paths and main results of rock fall probabilistic analysis along profile number 5 of the E-NE slope.

Table 4. Impact restitution coefficient assignement.

Lithotype	Coefficient of normal restitution (K_n)	Coefficient of tangential restitution (K_t)	Friction Angle ϕ (°)
Clean hard bedrock	0.53	0.99	45°
Bedrock outcrop	0.35	0.85	40°
Talus with vegetation	0.33	0.82	35°

interfere both with the structures located behind the sources areas and with specific exposed elements along the rock fall trajectories (e.g., the Inka trail at the toe of the NE slope).

Through the software the potential paths and size of mitigation measures (location and typology), able to reduce the risk impact along the above mentioned trail, have been defined.

7 POLICIES OF RISK REDUCTION AND MANAGEMENT

7.1 *Machu Picchu: Landslides and tourism*

The archaeological site of Machu Picchu is a major (if not the largest) tourist attraction of Peru. The site has ranked fourth among the top seven wonders of the world, in a recent worldwide poll realized via web. The latest data indicate a growth in Peruvian tourism, which is twice the average international tourism. In 2011, according to the provisional data released by Promperú (2012), the arrival of foreign tourists increased by 9.5%. The centenary year of the discovery of Machu Picchu—the symbol of the Inca culture—marked a real tourist boom for the town which aims to increase to 900,000 visitors in 12 months. On average, according to the data provided by Promperú, Machu Picchu is a tourist destination for 1.4 million people every year, both Peruvian and foreign travelers, conveying a turnover of 50 million dollars. By 2012, the IncaRail company, which operates on the Cusco-Machu Picchu Andean railways, expects to carry 225,000 tourists to the Inca citadel of Ollantaytambo, thus increasing by 29% in comparison with 175,000 (passengers in 2011). Approximately 11.8 million passengers, in fact, have passed through Lima airport, with an increase in passengers of about 14.7% (compared to 2010). Between January and November 2011, the only Peruvian airline (LAN) reached a total amount of 5,000,000 passengers, with a growth of 14.93%. For this reason, the exploitation of the archaeological park and tourist sustainability are vitally important for the "induced" tourism of the whole country. Moreover, the above provided data highlight that conservation and management policies of the park are a fundamental tool for the maintenance of such trends. All the results obtained from filed survey, laboratory analysis and stability models have been summarized in a landslide mitigation measure map for the archaeological park (Fig.19). The map has been divide in zones of measures depending on type

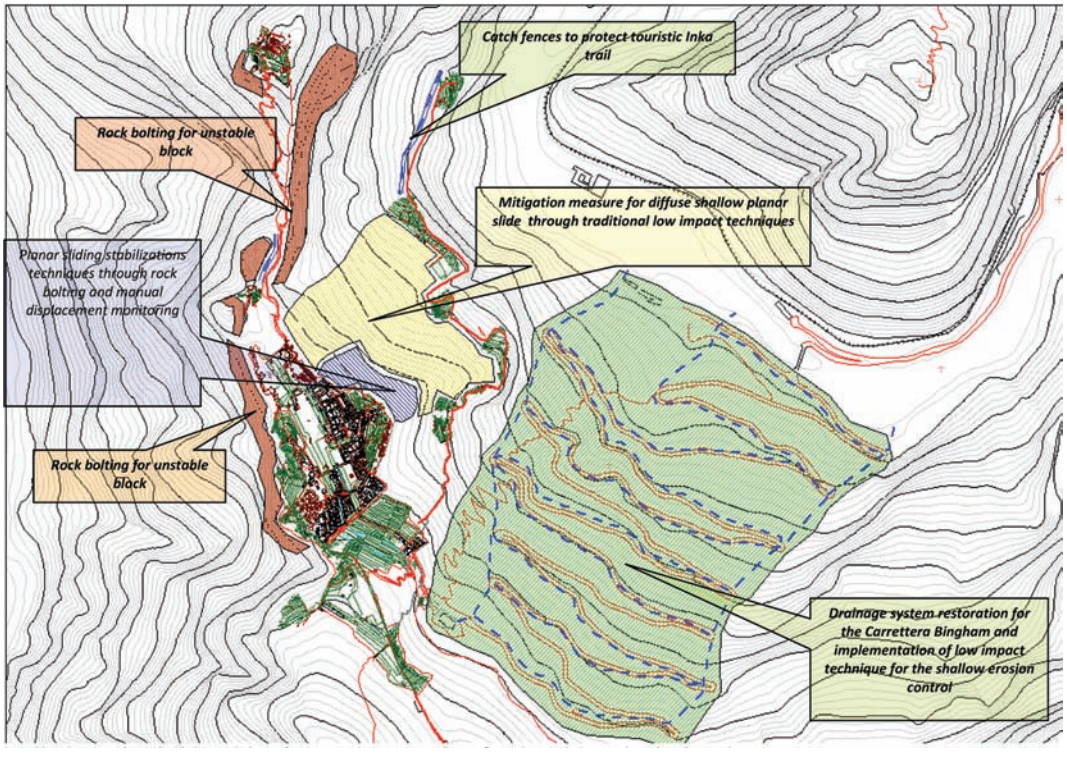

Figure 19. Preliminary landslide mitigation measure zoning for the archaeological park.

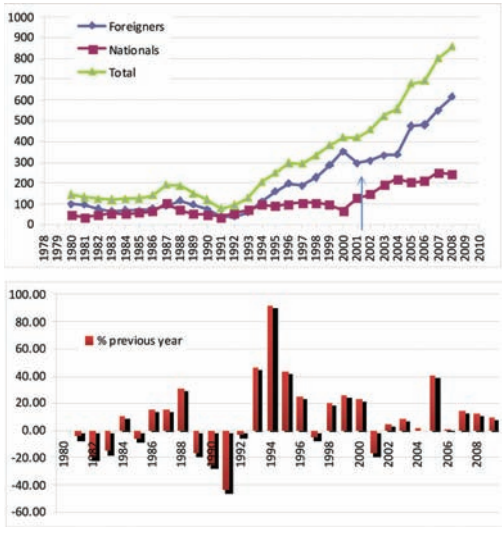

Figure 20. Tourist trend over the past 18 years in Machu Picchu archaeological site.

of landslide. For some of these areas, some preliminary cost-benefit analyses have been provided, which compared the estimated costs of measures with the average daily income deriving from tourism. These analyses are fundamental for developing correct management sustainable development policies. As an example of Machu Picchu archaeological park fragility, the data concerning the stream of visitors to the site over the past 18 years are reported in Figure 20. The sudden collapse occurred in 2001 is evident. The same year in which the mentioned article on New Scientist warned about a potential disastrous landslide. The figure also shows that we have actually exceeded the carrying capacity for the site fixed by UNESCO of 900 visitors/day and by the INC of 2,000 visitors/day and we are quickly reaching the threshold fixed by the Peruvian central government of 2,500 visitors/day (Peruvian Times, 2011).

8 CONCLUSIONS

For all the above described pieces of evidence, a proper policy for the management of the park concerning potential landslide risk and geomorphological process (natural hazards in general) can not be avoided or underestimated (Gill, 1974).The policies of risk reduction and actions to be taken, based on two main pillars, are briefly reported below:

1. Active Policies, by directly acting on the phenomena and physical vulnerability through conservation, maintenance, prevention, monitoring and mitigation measures calibrated for different types of hazard in time and space (Fallsvik, 2007) (long and short term strategies), see the preliminary master plan hypothesis reported in figure 19;
2. Passive Policies, by directly acting on social and economic vulnerability through tourism management and access control, potential reduction of anthropogenic pressure, by avoiding overcrowding in the most risky period (Oct.–Mar. semester), by promoting the archaeological park development only under safety condition constraints, implementation of awareness campaign for the tourist and capacity building and training for the workers of the park (resilience policies).

The economic volume mobilized by Machu Picchu tourist machine (ca 100.000 $/day) could enable an effective and long-term planning of the above mentioned policies. Such policies could avoid the collapse of the stream of visitors or even a temporary closure of the site, due to a triggering of small magnitude phenomena (rock falls or shallow planar slides) but with a high media impact.

ACKNOWLEDGMENTS

Authors are very grateful to Fernando Astete Victoria, Director of P.A. Machu Picchu, for his great experience, profound knowledge on Inca Citadel's dynamics on monuments and territory and cooperation during the local missions and dr. Gilbert Carpio Merino, for supporting field analysis and knowledge-sharing on geological and structural setting of the area. The investigation team was also highly supported and assisted by the INC group during collection of data. We are grateful to the FORGEO project team for their assistance during mission and filed survey and special thanks go to Dr. Luca Falconi and Dr. Claudio Puglisi for their helpful cooperation to the investigation and data collection.

REFERENCES

Amorosi A, Castellaro and S, Mulargia F (2008) Single-Station Passive Seismic Stratigraphy: an inexpensive tool for quick subsurface investigations. GeoActa, vol. 7, 29–39.

Best M, Bobrowsky P, Douma M, Carlotto V and Pari W (2009) Geophysical Survey at Machu Picchu, Peru: Results for Landslide Hazard Investigations. Landslide—Disaster Risk Reduction. Sassa K, Canuti P (eds.) Springer—Verlag Berlin Heidelberg. (978-3-540-69966-8). 265–273 pp.

Canuti P, Margottini C, Casagli N, Delmonaco G, Falconi L, Ferretti A, Lollino G, Puglisi C, Spizzichino D and Tarchi D (2009) Monitoring, geomorphological evolution and slope stability of Inca citadel of Machu Picchu: results from Italian Interfrasi Project.

Landslide—Disaster Risk Reduction. Sassa K, Canuti P (eds.) Springer—Verlag Berlin Heidelberg. (978-3-540-69966-8). 249–257 pp.

Canuti P, Fanti R, Margottini C and Spizzichino D. (2008) Effects of landslides on Machu Picchu Cultural Heritage-Proceedings of The First World Landslide Forum 18-21 November, Tokyo, Japan pp. 411–416.

Castellaro S, Mulargia F, Bianconi L (2005) Passive seismic stratigraphy: A new efficient, fast and economic technique. Journal of Geotechnical and Environmental geology 3: 51–77.

Castellaro S, Mulargia F, (2009) Vs30 Estimates Using Constrained H/V Measurements. Bulletin of the Seismological Society of America, Vol. 99, No. 2A, pp. 761–773, doi:10.1785/0120080179.

Delmonaco G, Margottini C, Spizzichino D (2010) Kinematic analysis for the implementation of landslide mitigation measures. Proceedings of European Geosciences Union 2010 General Assembly. Austria Vienna, Vol. 12, EGU2010-10383, © Author(s) 2010. 535–549.

Fallsvik, J, 2007, Recommendations for planning, surveillance, inspection with LS DTM. Usefulness of LSDTM in landslide hazard mapping and slope management, Deliverable 8, Swedish Geotechnical Institute Varia 580, Linköping 2007, 74p.

Gill J.L., 1974, Risks, legalities and insurance of slopes stability. Symposium on stability of slopes in natural ground—Wellington: 2.1–2.6.

Hoek (2007) Practical Rock Engineering (2007 edition). http://www.rocscience.com (last access 15 June 2011).

Hoek, E., Wood D. and Shah S. (1992) A modified Hoek-Brown criterion for jointed rock masses. Proc. Rock Characterization, Symp. Int. Soc. Rock Mech.: Eurock '92, (Edited by Hudson J.A.), London, Brit. Geotech. Soc., pp. 209–214.

Hoek E., Brown E.T. (1988) The Hoek-Brown failure criterion-a 1988 update. Proc. 15th Canadian Rock Mech. Symp. (ed. J.H. Curran), Toronto: Civil Engineering Dept., University of Toronto, pp. 31–38.

Konno, K. and T. Omachi (1998). Ground-motion characteristics estimated from spectral ratio between horizontal and vertical components of microtremor, Bull. Seism. Soc. Am. 88, no. 1, 228–241.

Lachet C and Bard P-Y (1994) Numerical and theoretical investigations on the possibilities and limitation of Nakamuras technique, J. Phys. Earth 42, 377–397.

Lermo J, and Chavez-Garcia F J (1993) Site effect evaluation using spectral ratios with only one station, Bull. Seismol. Soc. Am. 83, 1574–1594.

Lembo Fazio A., Manfredini G., Ribacchi R., Sciotti M. (1984). Slope failures and cliff instability in the Orvieto hill. 4th Int. Symp. on Landslides, Toronto, 2, 115-120.

Mazzoli S, Vitale S, Delmonaco G, Guerriero V, Margottini C, Spizzichino D (2009)—Diffuse faulting in the Machu Picchu granitoid pluton, Eastern Cordillera, Peru—Journal of Structural Geology Vol. 31, pp. 1395–1408, doi: 10.1016/j.jsg.2009.08.010.

Pasuto A. & Soldati M. (1996) – Landslide hazard. In: M. Panizza (ed.), Environmental Geomorphology. Elsevier, Amsterdam, 64–88.

Pratt, T. L.; Johnson, S. Y.; Potter, C. J.; Stephenson, W. J. (10 December 1997), "Seismic reflection images beneath Puget Sound, western Washington State: The Puget Lowland thrust sheet hypothesis", Journal of Geophysical Research 102 (B12): 27,469–27, 490.

Promperù Comisión de Promoción del Perú para la Exportación y el Turismo http://www.promperu.gob.pe/2012

SESAME project. http://sesame-fp5.obs.ujf-grenoble.fr/ http://www.peruviantimes.com/20/one-million-tourists-visit-machu-picchu-in-2011/14250/

Spizzichino D. (2012). Landslide risk assessment and management in the archaeological site of Machu Picchu Inca citadel (Peru). PhD thesis in Earth System Sciences: Environment, Resources and Cultural Heritage at University of Modena and Reggio Emilia (XXIII Cycle).

This page intentionally left blank

Geotechnical Engineering for the Preservation of Monuments and Historic Sites – Bilotta, Flora, Lirer & Viggiani (eds)
© 2013 Taylor & Francis Group, London, ISBN 978-1-138-00055-1

The rebuilding of San Piero a Grado bell tower

N. Squeglia
University of Pisa, Italy

ABSTRACT: Toward the end of the second World War, many towers have been destroyed in Italy because of their possible use as points of sight; among them, the bell tower of the church of S. Piero a Grado, in Tuscany. During the years following the war the Italian government allocated some funds to the reconstruction of the tower, but the discovery of archaeological remains of previous warship structures stopped the works. A great pressure has been recently exerted by the public opinion to re-start the reconstruction, intended not only as a rebuilding of the medieval bell tower, but also as a sort of "restoration" of the landscape. The geotechnical aspects of the design are reported in the paper, starting from the choice of rebuilding the tower with the same materials and techniques of medieval masons, up to the recovery the original masonry foundation

1 INTRODUCTION

One of the most important tasks for Italians in the third millennium is the management of their outstanding cultural heritage (Settis, 2007). Such a task involves the responsibility of many figures at different levels: politicians, who manage the public resources and take the decisions; officers in charge of the conservation of the monuments, the so called superintendents, who put into effect the decisions of politicians or exert pressure to orient such decisions; designers and restorers, who apply up to date knowledge to restoration problems.

The chain of decisions and responsibilities can be long and tortuous, and as a consequence it often results in inefficiencies of the system.

Sometimes an ad hoc committee has been appointed to solve a particular problem (Jamiolkowski, 2001). The case of the bell tower of San Piero a Grado is one of the examples of low efficiency of the system, due to clumsy decisions of politicians hindering the efforts of officers and specialists.

2 THE BASILICA AND ITS BELL TOWER

The Basilica of San Piero a Grado, in its present configuration (Fig. 1), rises near the ancient mouth of the Arno river. According to an old tradition, this was the site were Saint Peter arrived in Italy, during his travel to Rome.

The construction of the Basilica started at the end of Xth century, in the period of maximum splendor of the Republic of Pisa. It rises above ruins of former places of worship dating back to IVth and VIIth century and recovered by means of archaeological excavations carried out during the whole XXth century.

Figure 1. The Basilica and its bell tower at the beginning of XXth century.

The bell tower (Fig. 2) was built in XIIth century and was about 38 m high with a 7×7 m^2 square base. Because of its height it was a perfect point of sight covering a wide territory all around. During the Middle Age it protected the Republic of Pisa from possible invasions from the sea, but for the same reasons at the end of Second World War it was destroyed by the Wehrmacht to cover the retreat.

On July 22nd, 1944, the explosion of fifty mines installed at the base of the bell tower produced the collapse of the tower itself and a portion of the south aisle (Fig. 3).

Figure 2. The bell tower at the beginning of XXth century.

Figure 3. The tower and the aisle collapsed.

Figure 4. Portion of bell tower rebuilt between 1944 and 1956 in a recent picture.

In the post-war period, some reconstruction works have been carried out (Sodi, Burresi, 2010) but, during an archaeological excavation within the Basilica, the discovery of the remains of former worship structures stopped the reconstruction. The archaeological excavations lasted from 1944 to 1956 and conditioned the reconstruction works started in the meantime. In 1956 the reconstruction of the bell tower was abandoned, six meters above the foundation level (Fig. 4).

3 THE INVESTIGATIONS

3.1 *Structural investigations*

In 2008 the Italian Ministry of Cultural Heritage appointed a geotechnical engineer, a structural engineer and a geologist to design the reconstruction of the tower. The requisite requested by the Ministry was the absolute accuracy in reproducing materials and techniques of the original medieval structure.

A broad study of the materials used by the ancient masons was carried out, bringing to the selection of quarries were a similar material could be recovered. In order to have a sufficient homogeneity of materials, a quantity of stones sufficient for the construction of the whole tower has been purchased.

Four boreholes through the old foundation and an archaeological investigation allowed a sufficiently detailed knowledge of the foundation geometry and its state of conservation (Fig. 5). In the same figure the presence of a concrete slab is reported. This structure consists simply in a concrete finishing without any reinforcement put in place in order to have a smooth surface (Fig. 6). Foundation depth is about 3.1 m below ground surface and the structure of foundation is a masonry mass with a prismatic shape and a 8.6×8.6 m^2 square base. The archaeological

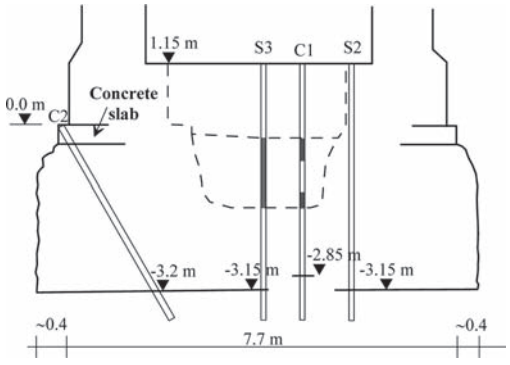

Figure 5. Scheme of foundation as deduced by investigation.

Figure 6. Concrete slab. A portion of the ancient masonry is also visible.

Figure 7. Masonry of foundation.

Figure 8. Present situation of construction.

investigation stated that masonry is a typical medieval one with some voids (Fig. 7). The same investigation revealed the presence of vertical cracks in the foundation mass. These cracks were in a symmetrical position near the edges of the foundation (say 0.5 m). Since the foundation mass is a very rigid body and the cracks were near the edges of foundation, they have been ascribed to stress increase due to soil-foundation interaction.

The reconstruction started in 2009 and in the following year the height of 15 m had been reached. At that time, unfortunately, the available resources were shifted to other projects, and the reconstruction was interrupted. Figure 8 shows the present situation of tower. A roof has been installed for protection purposes, as a consequence of uncertainty in work continuation.

3.2 *Subsoil investigation*

In a preliminary phase of design, subsoil investigations were practically missing and as a consequence a piled foundation had been foreseen for the reconstructed tower. The same conclusions about the necessity of a piled foundation were reached in 1944 by the architect Sanpaolesi (Sodi, Burresi, 2010), even if no explanations have been provided. Anyway the piled foundation was not realized during the reconstruction works of period 1944–1956.

Since there were no traces of any foundation problem during the life of the monument, a suitable subsoil investigation program has been carried out in 2009 to conceive a foundation system possibly more respectful of the restoration principles, though satisfying modern safety requirements.

Besides the two holes through the old foundation, kept to depths of 4.3 and 10 m below ground level, the geotechnical investigation included:

- a borehole in “green field”, to a depth of 31 m below ground level;
- a CPTU in green field up to a depth of 26 m below ground level;

- a CPTU very close the existing foundation to a depth of 11 m below ground level;
- measurement of shear waves velocity by a Down—Hole profile carried out in the first borehole;
- a MASW test and a Seismic refraction test for comparison purposes.

Since the subsoil is composed essentially by sand, no undisturbed sampling and laboratory testing was possible. Laboratory tests have been carried out on remolded samples only for soil classification.

Figure 9 shows the grain size distribution profile. The soil is clearly a sand, with a fine fraction always below 30% and often around 20%; the fine fraction is non-plastic. Down to a depth of 23 m below ground level the subsoil appears quite homogenous; this is not surprising since the depositional mechanism was connected to flood of the Arno river.

Figure 10 and 11 show the profile of normalized values of penetrometer resistance in terms of $N_{1,60}$ and $q_{T,1}$. Between the depths of 9 and 15 m the penetrometer resistance increases indicating the probable occurrence of cementation bonds; this aspect influences the estimate of relative density.

Relative density has been estimated by means of empiric correlation with SPT and CPTU. Standard Penetration Test has been processed by both Cubrinowski & Ishihara (1999) and Skempton (1986) correlations. Tables 1 and 2 report the results of such elaboration. In processing data from borehole S2 the action exerted by the load of the existing structure has been taken into account.

Between 10 and 15 m a very high value of relative density is evident, often above 100%. This evidence corroborates the geological indication on the presence of cementation bonds. Similar indication is obtained from CPTU data, which have been processed by means of Jamiolkowski et al. (2001) suggestions. Figure 12 shows the relative density profile obtained by means of such correlation. Between 10 and 15 m there is again an increase of relative density up to values near 90%.

As a consequence of high values of relative density, a value of 37° for effective shear strength angle is conservatively considered (Schmertmann, 1978).

Figure 13 shows the values of over consolidation ratio deduced by means of the correlation proposed by Mayne (2005). The correlation has been applied to the CPTU performed in green field, far away from the existing foundation, in order to have information about the virgin soil, not affected by the bell tower load. It is clear that the soil is slightly over consolidated and this finding must be taken into account in addition to the unload—reload cycle due to collapse and reconstruction of tower.

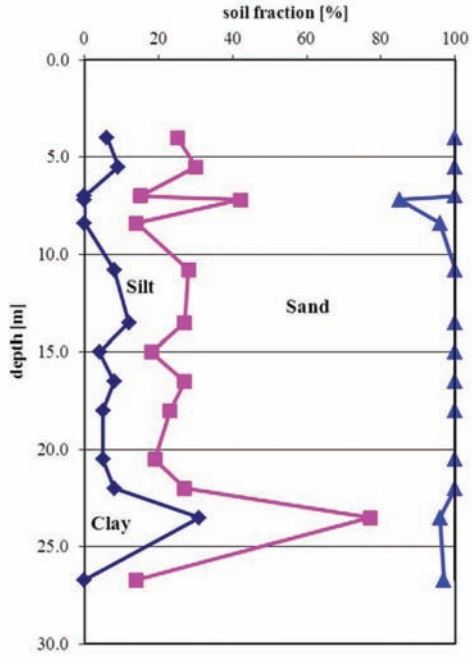

Figure 9. Grain size distribution profile.

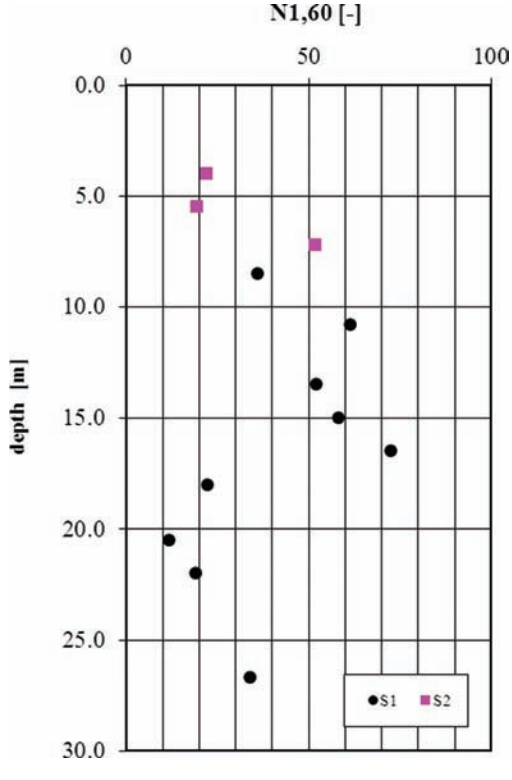

Figure 10. Normalized N_{SPT} profile.

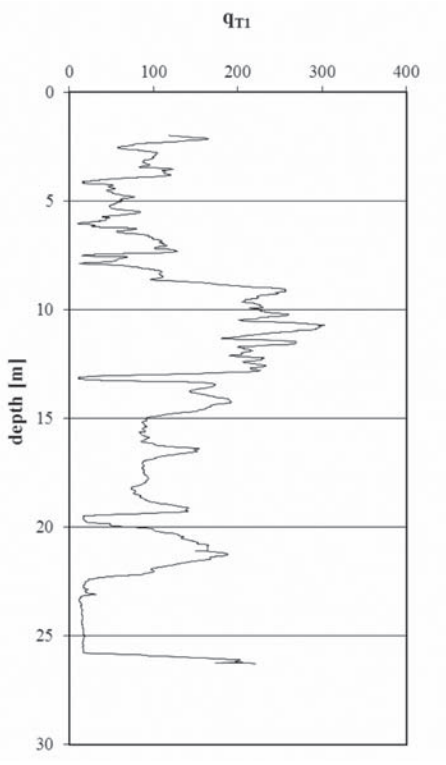

Figure 11. Normalized total penetrometric resistance profile.

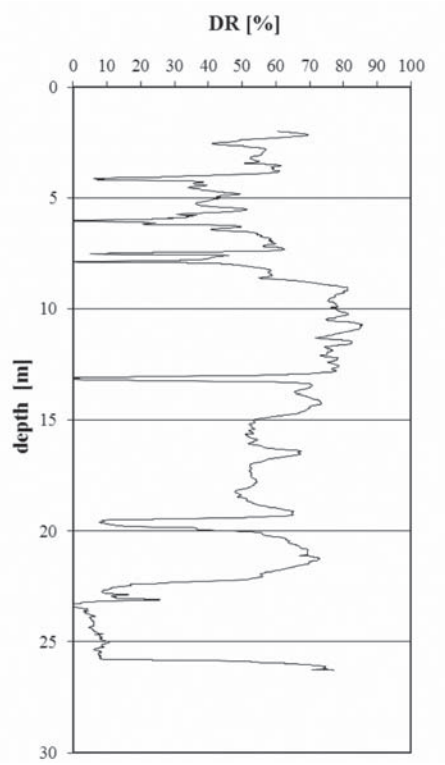

Figure 12. Relative density profile.

Table 1. Processing of SPT data for borehole S1 (green field).

Depth [m]	N_{SPT} [–]	Note	D_{50} [mm]	σ'_{v0} [kPa]	C_N [–]	$N_{1,60}$ [–]	$N_{1,78}$ [–]	$e_{max} - e_{min}$ [–]	C_D [–]	DR_{CI} [%]	DR_{SK} [%]
8.5	38		0.35	110	0.953	36.2	27.9	0.401	42.47	81	78
10.8	71		0.12	133	0.867	61.6	47.4	0.730	15.37	176	101
13.5	66	ref.	0.2	160	0.791	52.2	40.1	0.530	26.48	123	93
15.0	77		0.21	175	0.756	58.2	44.8	0.516	27.74	127	98
16.5	100	ref.	0.18	190	0.725	72.5	55.8	0.563	23.87	153	110
18.0	32		0.22	205	0.698	22.3	17.2	0.503	28.97	77	61
20.5	18		0.17	230	0.659	11.9	9.1	0.583	22.53	64	44
22.0	30		0.14	245	0.639	19.2	14.7	0.659	18.31	90	57
23.5	14	peat	0.01	260							
26.7	58		0.2	292	0.585	33.9	26.1	0.530	26.48	99	75

Table 2. Processing of SPT data for borehole S2 (below the tower foundation).

Depth [m]	N_{SPT} [–]	Note	D_{50} [mm]	σ'_{v0} [kPa]	C_N [–]	$N_{1,60}$ [–]	$N_{1,78}$ [–]	$e_{max} - e_{min}$ [–]	C_D [–]	DR_{CI} [%]	DR_{SK} [%]
4.0	31		0.12	195	0.716	22.2	17.1	0.730	15.37	105	61
5.5	28		0.13	210	0.690	19.3	14.9	0.692	16.85	94	57
7.2	78		0.9	227	0.664	51.8	39.8	0.297	71.02	75	93

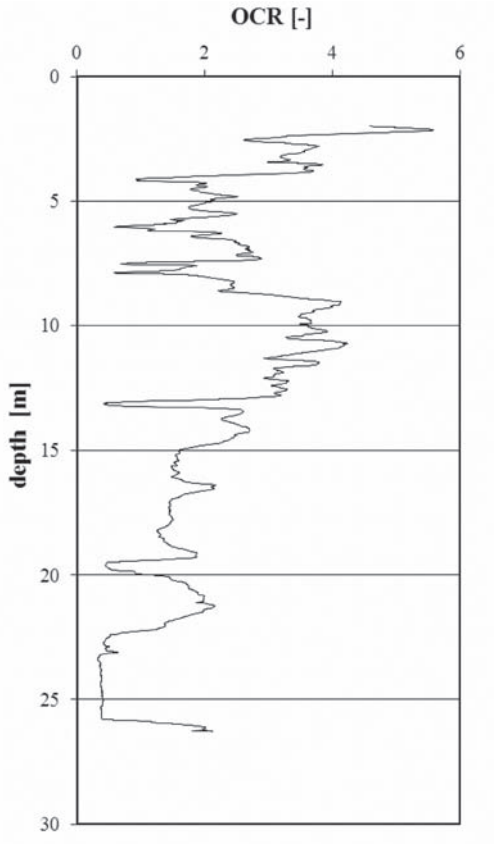

Figure 13. Overconsolidation ratio profile as deduced by CPTU.

4 GEOTECHNICAL ASPECTS

The ancient tower did not experience any structural disease during its history, and its collapse was due to "artificial" reasons, as mentioned above. In fact, the ultimate bearing capacity computed for the existing foundation is above 3.5 MPa, whereas the maximum load acting on it after reconstruction shall be about 0.55 MPa.

Being satisfied by the bearing capacity, the aspects connected to soil deformability have been examined; in particular, the forecast of settlement due to the unload—reload cycle and the estimate of the safety factor against leaning instability (Hambly 1985).

The evaluation of the settlement due to reconstruction has been carried out by means of different methods: Burland & Burbidge (1984), Schmertmann et al. (1978) and elastic solutions. The first and second method are based respectively on SPT and CPT, whereas the application of elastic solution have been carried out by means of elastic parameters deduced by the measurements of in situ shear wave velocity.

The computed settlement ranges between 10 and 28 mm, with elastic method and Burland & Burbidge method in agreement at the lower bound of the interval. Since the method proposed by Schmertmann is known to be conservative (NCHRP, 2007), a forecast of 10 mm has been finally accepted.

About the stability of the tower, it is widely accepted that this phenomenon depends on the stiffness of soil-foundation system rather than its strength (Lancellotta, 1993; Desideri et al., 1994, 1997). Approaching the problem in a simple way, the tower-foundation-subsoil system can be considered as linearly elastic; the safety factor against leaning instability can be expressed by

$$FS_l = \frac{E_{op} B^3}{(1-\nu^2) W \cdot H \cdot I_\alpha} \tag{1}$$

in which E_{op} is the operative elastic modulus (90 MPa), B is the side of the square foundation (8.6 m), W is the weight of the tower (27.6 MN), H is the height of center of gravity of the tower (17.85 m) and I_α is a coefficient of influence depending on the geometry (3.8).

With this set of parameters the safety factor against leaning instability amounts to 31, which indicates that the tower is perfectly stable. In order to take into account non linearity of the soil behaviour and the occurrence of defects, a relatively simple two degree of freedom nonlinear model (Pepe 1995) has been applied, in which the soil has been modeled as a couple of hyperbolic plastic springs.

During unloading the springs have a stiffness equal to the initial one, whereas during increasing load the stiffness decreases continuously. In such a way the model is sensitive to the initial conditions and the following equations which describe the phenomenon are clearly nonlinear:

$$u_m = \frac{u_1 + u_2}{2} \tag{2}$$

$$a = \frac{u_2 + u_1}{2c} \tag{3}$$

$$P = A(1 - e^{-Bu_1}) + A(1 - e^{-Bu_2}) \tag{4}$$

$$Pla = [A(1 - e^{-Bu_1}) - A(1 - e^{-Bu_2})]C \tag{5}$$

$$P = \frac{2C^2}{l} AB e^{-Bu_2} \tag{6}$$

In which P is the total weight of tower, A is the asymptotic value of the nonlinear spring, AB is the initial stiffness of the spring, u is the settlement of the spring, l is the height of the center of mass of the tower, c is the distance between the springs and α is the initial rotation of the tower.

Table 3. Safety factor against leaning instability.

Initial rotation		
[°]	[arcsec]	FS
0.25	900	3.91
0.50	1800	2.98
1.00	3600	2.05
2.50	9000	1.16
5.00	18000	1.03

The solution of the system has been obtained by Levemberg—Marquardt optimization method using the software MATLAB (Bartolomei, 2010).

The solution of the system lead to the evaluation of the stiffness characteristics of the model, as a consequence it is possible to evaluate the Von Karman critical load as

$$P_{cr,k} = \frac{2C^2}{l}\frac{2k_i k}{k_i + k} \tag{7}$$

In which k_i is the stiffness in unload-reload cycle and k is the current stiffness in loading path. Safety factor is defined as ratio between $P_{cr,K}$ and P.

In Table 3 the safety factor against leaning instability has been reported as a function of an initial rotation of the tower foundation, possibly due to constructional defects or soil heterogeneity. As reported in the table, the greater the initial rotation, the lower the safety factor. If the initial rotation equal to 5°, the factor of safety decreases almost to unity. Such a rotation corresponds to an overhang of 3.5 m for a tower with a H/B ratio equal to 4.6; it is indeed a very high rotation, and the result is to be considered quite obvious. It is more interesting to notice, however, that even a rotation of only 0.25°, which correspond to a small overhang of 17 cm, reduces the safety factor by an order of magnitude.

In any case, considering the tight tolerance of modern construction, the solution based on the reuse of the ancient foundation has been considered fully satisfactory.

5 CONCLUDING REMARKS

The paper describes the geotechnical aspect of reconstruction of San Piero a Grado Basilica's bell tower. The tower has been destroyed in 1944 by German army to cover its retreat. The history of tower is free from static or structural diseases, as a consequence the piled foundation provided in the preliminary design seemed inappropriate. The mechanical properties of soil have been described and some geotechnical aspect of reconstruction have been discussed.

From a more general point of view, the case history of S. Piero a Grado bell tower puts into evidence the role of politicians—unfortunately sometimes detrimental—in the management of cultural heritage and the role of specialists in defining the most appropriate solution. Any intervention regarding an historic building has to be based on a deep knowledge of its history and behaviour; without these preliminary considerations, any intervention could be useless or even detrimental.

REFERENCES

Bartolomei, P. 2010. *Analisi della fondazione del nuovo campanile di San Piero a Grado*, MS thesis, Università di Pisa (in Italian).

Burland, J.B., Burbidge, M.C. 1984. *Settlements of foundation on sand and gravel*, Glasgow and West of Scotland Association Centenary Lecture.

Cubrinovski, M., Ishihara, K. 1999. Empirical Correlation between SPT N-value and Relative Density of Sandy Soils, in *Soils and Foundations*. 5: 61–71.

Desideri, A., Viggiani C. 1994. Some remarks on the stability of towers, in *Symposium on development in Geotechnical Engineering, from Harvard to New Delhi 1936–1994*, Bangkok.

Desideri, A., Russo G., Viggiani C. 1997. Stability of towers on compressible ground, in *Rivista Italiana di Geotecnica*, XXXI, n. 1, pp. 5–29.

Hambly, E.C. 1985. Soil buckling and the leaning instability of tall structures, in *The Structural Engineer*, Vol. 63, 3, pp. 78–85.

Jamiolkowski, M. 2001. The Leaning Tower of Pisa: end of an odyssey. Terzaghi Oration, in *XV International Conference on Soil Mechanics and Geotechnical Engineering*, Istanbul, IV, pp. 2979–2996.

Jamiolkowski, M. Lo Presti, D.C.F., Manassero, M. 2001. Evaluation of Relative Density and Shear Strength of Sands from CPT and DMT. *Ladd Symposium*, Boston, ASCE STP.

Lancellotta, R. 1993. Stability of a rigid column with non linear restraint, in *Geotechnique*, XLI, 2, pp. 331–332.

Mayne, P.W. 2005. Integrated Ground Behavior: In-Situ and Lab Tests, *Deformation Characteristics of Geomaterials*, Vol. 2 (Proc. Lyon, France), Taylor & Francis, London, United Kingdom, pp. 155–177.

NCHRP, 2007. Cone Penetration Testing, Synthesis Report 368, Transportation Research Board, Washington DC.

Pepe, M. 1995. La Torre pendent di Pisa, analisi teoricosperimentale della stabilità dell'equilibrio, PhD thesis, Politecnico di Torino (in Italian).

Schmertmann, J.H. 1978. Guidelines for Cone penetration Test Performance and design, Report no. 78–209, US Dpt. Of Transportation, FHA, Washington DC.

Schmertmann, J.H., Hartman, J.D., Brown, P.R. 1978. Improved Strain Influence Strain Factor Diagrams, Technical Note, JGED, ASCE, GT8.

Settis, S. 2007. *Italia S.p.A.,* Torino: Einaudi.

Skempton, A.W. 1986. Standard Penetration Tests Procedures & the Effects in Sands of Overburden Pressure, Relative Density, Particle Size, Ageing and Overconsolidation. *Géotechnique*. 36(3): 425–447.

This page intentionally left blank

Geotechnical Engineering for the Preservation of Monuments and Historic Sites – Bilotta, Flora, Lirer & Viggiani (eds)
© 2013 Taylor & Francis Group, London, ISBN 978-1-138-00055-1

Safeguard stories of living monuments (unstable towns of the region of Umbria)

P. Tamburi
Geologic and Seismic Service, Region of Umbria, Perugia, Italy

E. Martini
Alta Scuola, Casalina di Deruta, Perugia, Italy

ABSTRACT: With the competence passage of the consolidation of villages affected or threatened by landslides from the Italian State to the Regions, the Region of Umbria dealt with problems that have historically plagued towns like Orvieto and Todi with new and in-depth studies, having the support of the National Research Council and of the Universities. Thanks to the resources made available through special laws, it was possible to deal with the issue of hydrogeological risk in a comprehensive and integrated way, combining the mitigation of risk with the valorization of the inhabited centres and the restoration and enhancement of artistic, historical and archaeological sites. The experience gained in Orvieto and Todi inspired all the subsequent action taken by the Region of Umbria in the mitigation of hydrogeological instability. The result is the adoption of a multidisciplinary approach in the studies needed to define the solutions and the monitoring and maintenance of the works and of the areas of intervention.

1 INTRODUCTION

Umbria is the green heart of Italy, where the wealth of natural and artistic wonders coexists with the fragility of a territory affected by hydrogeological risk.

The risk related to landslides and hydrogeological instabilities is prevalently due to the historic development of the towns around castles, towers and medieval villages situated on the top of hills, where the natural evolution of erosion phenomena is aggravated by human activity and causes situations that frequently required the State and Regional intervention. This intervention was formalized by the inclusion of 41 towns threatened by landslides in the "list of towns to be consolidated". These places, always animated by industrious people and tourist destinations for the high artistic and cultural value, could be considered living monuments to safeguard.

The fundamental law of the Region of Umbria (N. 65/1978) for the consolidation of the unstable towns threatened by landslides says: "*Rules on the consolidation and transfer of villages affected or threatened by landslides, and prompt intervention in case of public calamities*" and declares that "*interventions are willing to ensure normal conditions of stability to the villages affected or threatened by landslides and to guarantee normal conditions of safety in order to promote the continuous presence of people in the settlements*" with interventions at the total charge of the Region of Umbria.

Figure 1. Region of Umbria.

In 2006 was also approved Hydro-Geological Arrangement Plan of Tevere River Basin (PAI), in order to protect present and future residential and infrastructural activities from risk. This Plan individualize at present 185 sites characterized by really high (R4) and high risk (R3) of landslides. Today it is the main tool for territorial planning and it is finalized to establish conditions that guarantee equilibrium and compatibility among the

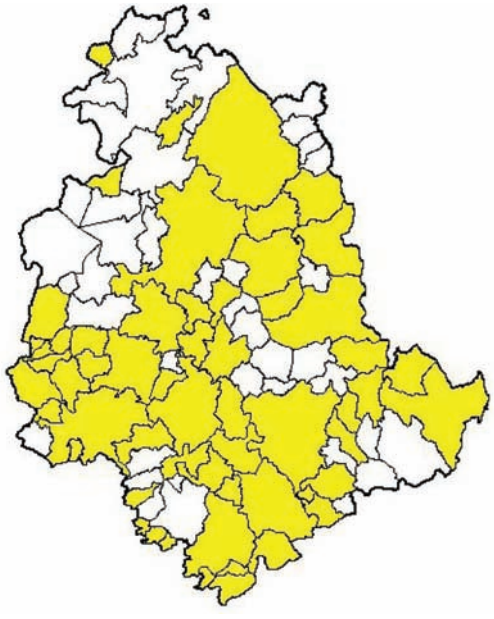

Figure 2. Highlighted in yellow 54 of the total 92 Umbria municipalities, with landslides classified at R3 or R4 risk.

hydrogeological dynamics, the growing anthropogenic pressures on the territory and the safeguard of unstable towns.

In this context, rich in monuments, cultural heritage and archaeological sites, develops the story of the consolidation of unstable towns in Umbria. Orvieto, Rocca Ripesena, Todi, Pale, Sant'Eutizio, Spoleto Giro dei Condotti, Massa Martana and the Marmore Falls are the living monuments protagonists of this story.

2 ORVIETO

"Yesterday and today crucial moments [...] arrived at Orvieto, sited like Salzburg Castle, you ascend with the funicular from the station. City of solid stone, multi-coloured Duomo! Etruscan tombs, bought antique objects, enchanting view [...] Orvieto superb [...] Health very satisfying".

This is what Sigmund Freud wrote about Orvieto to his wife Martha on a postcard from Bolsena dated 9 September 1897.

Orvieto is situated on the borders among Umbria, to which it belongs, Tuscany and Latium. Built on the top of a steep cliff of tuff, it has always been a majestic and fascinating city.

The geological formation of the hill is structured by a bottom layer of pliocene marine clay covered by a series of river and lake deposits made up of sand, clay and volcanic sediments, topped by the tuff of the Orvieto cliff.

The city of Orvieto was included in 1937 in the list of unstable town to be consolidated at the expense of the State. Since 1972 (year of Regions Establishment) the Region of Umbria faced the Orvieto landslides through new and detailed studies, in collaboration with the National Research Council and the University.

After the landslides in the area Gonfaloniera in 1972, near the hospital in 1977, and in the Cannicella area in 1979, thanks to economic resources made available by special laws, the Regional Government of Umbria faced with global approach the issue of instability. To sum up the interventions executed are:

- renovation of the aqueduct and sewage networks;
- waterproofing tuff plateau through the paving of roads and squares;
- reinforcement and anchorage of tufaceous cliff along the whole rock face (4200 m of perimeter for an average of 27 meters in height) by rock bolt, passive and prestress rock anchors;
- consolidation of 54 caves affected by serious stability problems;
- reshaping of the cliff brow and grassing;
- consolidation and restoration of the historic walls of the cliff, even medieval;
- carrying out of deep drains;
- regulation of the running surface waters on the approximately 750,000 m^2 of slopes with transverse structures on the ditches that go down into the valley in order to reduce water energy and capacity to erode.

Expenditure incurred for the mitigation of risk: € 108.8 million.

Figures 3 and 4. Orvieto, Cannicella during and after consolidation works.

3 ROCCA RIPESENA

The village of Rocca Ripesena (Orvieto—TR) is located at the base of the northern side of a tufaceous plate arranged from East to West for a length of about 200 m, a width of about 50 m and a thickness of 15–25 m. It rests on a river and lake deposit under which there is a clayish base.

The rock cliff overlooking Rocca Ripesena results from the erosion of the same volcanic formation that belongs to the most famous Orvieto. The collapse of 1997 led, after the highest urgency intervention, to the definition of a general project for the completion of the consolidation. The collapse still in progress on the opposite side of the village offers a suggestive picture of what would happen also to Orvieto without mitigation works.

The operation performed for the protection of the town provided for:

- rock consolidation by means of passive nails;
- waterproofing of the summit plateau;
- access road construction for the tufaceous plateau maintenance;
- surface runoff water control.

Expenditure incurred for the mitigation of risk: € 0.8 million

Figure 5. Rocca Ripesena landslide, 1997.

Figure 6. Rocca Ripesena after consolidation works.

4 TODI

The Todi hill is essentially formed in the upper part of conglomerates of permeable sandy gravel, and in the lower part of a basement made of sands and silts clayey with low permeability.

Numerous are the historical documents testifying the appearance of instability problems, from the decrees of the General Council of the City of Todi that since the thirteenth century forbade the cultivation of land surrounding the village (prohibitions largely disregarded).

The town was placed among the historic towns to be consolidated at the expense of the State in 1916 but only thanks to the resources made available by special laws, the Region of Umbria approached globally the problem of instability and in 1979 approved the General Plan for the consolidation of the hill.

The stabilization work may be summarized as follows:

- complete reconstruction of the sewerage network and aqueduct;
- waterproofing of the squares and streets of the city by paving;
- rehabilitation and recovery of numerous small historical tunnels which in the past ensured the city water supply and drainage;
- reduction of the ditches slope by transverse structures in order to avoid the erosion of the bottom;
- canalization of runoff water;
- drainage systems along the route of the old ditches;
- large diameter drainage wells, 30 to 20 m in depth, with radial sub-horizontal drain pipes departing from several levels of the wells;
- series of draining ditches that affected an area of about 180 to 190 acres;
- grassing and reforestation of degraded soils;
- reprofiling of slopes.

Expenditure incurred for the mitigation of risk: € 61.7 million.

Figure 7. Todi, stabilization of the slope by draining trenches.

Figure 8. Todi hill, 2006.

Figure 9. Pale, 1997 earthquake.

5 PALE

Pale village (Foligno—PG) is located on the right hand side of the Menotre River, at the foot of the calcareous mountain known as "Sasso di Pale".

During the XIV century, in this village grew up an important paper mill, thanks to the richness in water and so in energy. The first printed version of the Dante's *Divine Comedy* was printed in Foligno (Perugia) on the paper coming from the Pale's factory.

After the heavy earthquake of 1997, many rockfall processes occurred along the travertine cliff, on the west side of the village. Due to these events, all the houses situated in proximity of the edge of the cliff were in a really high risk situation.

The works carried out for the consolidation of the cliff can be summarized as follows:

- unstable rocks removing;
- anchoring of the cliff, by 5 m nails arranged in a grid of 1 m step;
- deep anchoring of the cliff, with a grid of 4 m step;
- sub-horizontal drainage.

Expenditure incurred for the mitigation of risk: € 4.7 million.

Figure 10. Pale during consolidation works.

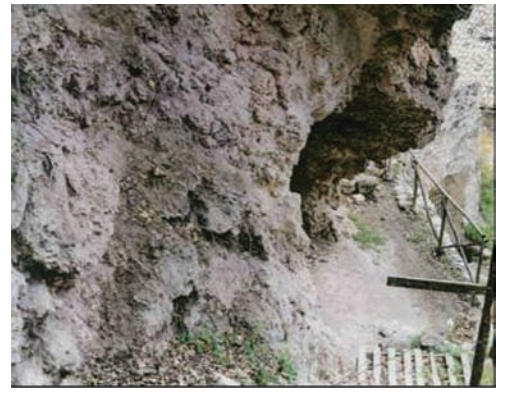

Figure 11. Saint Eutizio Abbey, Preci, 1998, Hermits Caves on the rock wall behind the abbey.

6 SAINT EUTIZIO ABBEY

Saint Eutizio Abbey was founded in the 5th century by the Syrian monks who were the spiritual fathers of San Benedict. Nearby there are the Hermits Caves and an enchanting path that leads to Norcia. In this Abbey the Preci Surgery School was founded, it constitutes one of the first surgery school in the world.

The Abbey is built on the foot of a travertine formation.

After the 1997 earthquake, the incremented risk of rockfall led to the carrying out of prevention and protection works to reduce the risk.

The works carried out can be summarized as follows:

- unstable rocks removing;
- anchoring of the cliff, by nails;
- digging of a well with a diameter of 3, 4 m and 14 m of depth;
- anchoring of the cliff to the well;
- hydraulic works.

Expenditure incurred for the mitigation of risk: € 0.8 million.

Figure 12. Saint Eutizio Abbey, Preci, 2006.

7 GIRO DEI CONDOTTI

Giro dei Condotti area (Spoleto—PG) is classified as SIC—Site of European Community Importance—and it is situated in front of Spoleto, a typical mediaeval city, also known for the "Festival dei Due Mondi". The area is connected to the town by the Towers Bridge (Ponte delle Torri), which amazed Goethe during his Italian Journey.

"I went to Spoleto and also on the aqueduct, which at the same time is a bridge between a mountain and the other. […] This is the third work of the ancient that I have in front of me and I observe the same mark, always magnificent. The architectural art of the ancients is truly a second nature, that works conforms to the uses and civilian purposes. Thus rise up the amphitheater, the temple, the aqueduct."

Giro dei Condotti is a small footpath created for the aqueduct maintenance works and it is classified as really high risk site for rockfalls.

During 2003 and 2004 some landslides caused the temporary closure of the path, which was reopened after the removal of the rocks collapsed.

As a result the area has been classified at higher risk, including 1.3 km of path between the bridge and the S. Leonardo hermitage, characterized by the presence of a high vertical rock face 30 to 60 m above the level of the path.

Due to those reasons and to the artistic and natural peculiarities of the place, the rockfall barriers were positioned appropriately, to minimize the environmental impact.

Expenditure incurred for the mitigation of risk: € 0.5 million.

8 MASSA MARTANA

The town of Massa Martana is located at the foot of the Martani Mountains, on the edge of a travertine plate, thick 25 to 30 m resting on a clay base. The collapses over the years affected the travertine

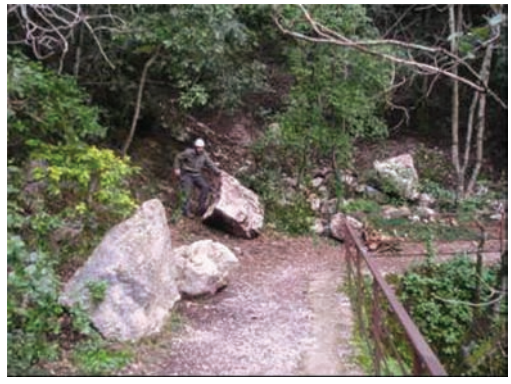

Figure 13. Giro di Condotti, Spoleto, 2004.

Figure 14. Giro di Condotti, Spoleto, 2010.

cliff below the western side and led, since 1929, to include Massa Martana in the list of unstable towns to be consolidated at the expense of the State. First consolidation works were performed between 1972 and 1980.

After the earthquake in 1997 the Regional Government of Umbria approved a general project that faced in an integrated way the problem of hydrogeological risk and the need to repair damaged buildings and redevelop the town.

Even in Massa Martana the works carried out were:

- renovation of the aqueduct and sewerage networks;
- paving of streets and squares in order to reduce the infiltration;
- consolidation of the ditches that run along the sides of the cliff;
- consolidation of the cliff with nails and anchors;
- reinforced concrete coating, covered with stone, of the most degraded parts of the cliff.

Figure 15. Massa Martana, 2008, interventions in progress.

Figure 16. Massa Martana, 2012, interventions in progress.

Expenditure incurred for the mitigation of risk: already contracted € 25.0 million in process of acquisition € 9.0 million.

9 MARMORE WATERFALLS

Marmore Waterfalls does not need to be presented, because we are all aware of the many reasons that make it a unique heritage and a special resource for Umbria and Europe (it is classified as SIC).

The spectacular three leaps, for a total jump of 165 meters, are the result of geological history helped by human actions since 271 bC, when Consul Manlio Curio Dentato, for the reclamation of the Reatina Plain, ordered to dig an artificial canal in the travertine banks that were blocking the course of the Velino River, "the Cavo Curiano". The canal, over 2 kilometres long, ending at the edge of a cliff, gave life to the waterfall.

In the years that followed many other hydraulic structures were carried out until those built in the last twenty years of the nineteenth century for the production of hydroelectric power.

Marmore Waterfalls have always been a tourist destination for travelers: a sculpture placed at the bottom viewpoint shows the verses that Lord Byron wrote after admiring the waterfall:

"The roar of waters! From the headlong height
Velino cleaves the wave-worn precipice.
The fall of waters! Rapid as the light
the flashing mass foams shaking the abyss.

Figure 17. Marmore Waterfalls, 2010.

The hell of waters! Where they howl and hiss,
and boil in endless torture; [. . .] Look! Where it comes like an eternity,
as if to sweep down all things in its track,
charming the eye with dread, a matchless cataract horribly beautiful!"

In 1970 a great portion of the "Campacci" travertine ridge, sited on the right side of the waterfall, collapsed. In the following years numerous investigation put in evidence conditions of remarkable risk because of the tendency of the rock masses towards sudden and rapid collapse.

Consolidation works can be summarized as follows:

- barring of the unstable masses;
- nailing the outer cliff to an average depth of 5 meters;
- coating cortical mesh;
- structural wells of large diameter with elliptical cross-section, major and minor axis 8 m and 5 m respectively, not more than 30 meters deep, located 40–50 meters from the cliff;
- from the wells branch of towards the outer wall of the cliff anchors prestressed, with lengths ranging from 30 to 50 m, arranged in orders variable in number from 11 to 17 for a total of tie rods, depending on the well, variable from 122 to 196.

Expenditure incurred for the mitigation of risk: € 22.5 million.

10 CONCLUSIONS

In addition to the works carried out directly, the Region of Umbria has promoted measures to mitigate the risk in defense of settlements, infrastructure, environmental and historical heritage, through annual action plans, three-year action plans, Framework Programme Agreements for the

Figure 18. Marmore Waterfalls, excavation of a well.

Figure 19. Piazza del Popolo repaved, in the background the Duomo.

protection of soil, or extraordinary plans following states of emergency. Interventions to reduce the risk, although not always decisive, were financed and implemented in more than half of the risk R3 and R4 areas identified in the PAI, with priority given to R4 areas that today are for the most part at least partially secured.

In the last two decades 340 interventions were made for a total amount of € 228 million.

Simultaneously to the great commitment in the implementation of measures for the mitigation of risks, the need to ensure the necessary maintenance and monitoring of interventions and of intervention areas has been underlined also with the birth of Alta Scuola, a Cultural and Scientific Association established by the Region of Umbria and the Municipalities of Orvieto and Todi.

The mission assigned to this Association is "Advanced Specialization School and Research Centre for the Maintenance and Preservation of Historical Town Centres in Unstable Areas".

A Special mention, during the work carried out in Orvieto, Todi and Massa Martana, must be given to the coordination activities with local service providers (electricity networks, telephone networks, gas distribution, public lighting), especially in small and narrow streets of the historical centers, during the complex task of reconstruction of water networks, sewage networks and waterproofing of roads.

This coordination activity allowed that the streets of the city maintained a look closer to their ancient and medieval historical origins.

Together with the consolidation works, has been also completed the restoration and renovation of numerous historic, architectural and archaeological monuments, thanks to the intervention of the competent bodies of the Ministry of Culture.

In Orvieto should be underlined the restoration and renewal of the historic walkway to the city from the north wall (Porta Vivaria—ancient Etruscan

Figure 20. Pedestrian access to the town from Porta Vivaria.

Figure 21. The maintenance and surveillance path, on the edge of Marmore cliff, Campacci area, with a panoramic view on Valnerina (2007).

access) and the gallery of penetration in Orvieto for alternative mobility, which from Campo Boario and relying on an old Etruscan/Roman tunnel, comes within the city near the town hall.

In these cities were made important restoration of churches, historic buildings and archaeological sites.

In the areas of outstanding natural beauty, it has been privileged the requalification of the spaces and the improvement of accessibility, also with the valorization of pathways, including those made for the access to areas of intervention and maintenance, which were then returned to the local and tourist use, as extraordinary itineraries in areas of great historical, natural and environmental importance.

These consolidated towns are now more than ever throbbing of activity and attractors of interest for their renewed beauty and cultural importance.

They are not only the favorite destinations for tourism but also desired places of residence, real living monuments already safeguarded and to be preserved through continuous interventions of monitoring and maintenance of their territory and of the works therein carried out.

ACKNOWLEDGEMENT

Special thanks to Paola Cerchice, secretary of Alta Scuola, for the contribution given to the layout of the article and to the revision of the translation.

Web sites:
www.regione.umbria.it
www.altascuola.org

REFERENCES

Barla G., Coluzzi E., Martini E., Soccodato C., Tortoioli L.,1995. Proceedings of the Conference Orvieto e Todi due città da salvaguardare, Orvieto.

Comastri C., Biondi R., Federici G., Venanti L.D., Faralli L., Gasparri N. e Piccioni R., 22–24 September 2004. XXII Convegno Nazionale di Geotecnica di Palermo, "Lavori di consolidamento abitato di Massa Martana, Umbria, Italia", Palermo.

Conversini P., Lupi S., Martini E., Pialli G., Sabatini P., 1978. Rupe di Orvieto-Indagini Geologico tecniche—Quaderni Regione Umbria, Perugia.

Conversini P., Martini E., Pane V., Pialli G., Tacconi P., Tortoioli L., Ubertini L., 1995. La rupe di Orvieto e il colle di Todi: due casi di città fragili. Geologia Applicata e Idrogeologia, XXX, pp. 211–224, Taormina.

Curli G.,.Martini E., 14–16 May 1986. Rupe di Orvieto, controllo della stabilità dei pendii. Atti XVI Convegno Nazionale di Geotecnica, Bologna.

Felicioni G., Martini E., Ribaldi C., 1995. Studio dei centri abitati instabili in Umbria-Atlante regionale-CNR, Regione Umbria, 418 pp., Catanzaro: Rubbettino Arti Grafiche.

Federici G, Russo L.E., December 2008. "Estabilizacion del barranco de massa martana (italia) mediante el uso multiple de geosinteticos" Camsig XIX Congreso Argentino de Mecanica de Suelos e Ingegneria Geotecnica 2008, Buenos Aires.

Felicioni G. et al., 2007. "Marmore Waterfall a resource for Terni and Umbria", Perugia: Umbria Region.

Giallongo V., Martini E., May 1999 Il dissesto idrogeologico per frana: Spazio Ambiente, n.1, CRIDEA Regione Umbria, Perugia.

I.A.T. Ingegneria per l'Ambiente ed il Territorio Srl, Orvieto Observatory,1999–2011. Reports and Publications of the Orvieto Observatory, Umbria Region, Perugia.

Martini E., 2007. Consolidation and rehabilitation of the Orvieto Cliff. Proceedings of the International Symposium on Conservation and Sustainable Development of the Tuff Towns, World Monuments Fund, New York.

Martini E., February 1995. Osservatorio: strumento per la prevenzione dei rischi e la manutenzione degli interventi-Atti convegno: Orvieto e Todi due città da salvaguardare. Umbria Region. Orvieto and Todi.

Martini E. Margottini C, September 2000. Le frane storiche di Orvieto e Todi CD—Regione Umbria-ENEA, Perugia.

Martini E., 2–13 July 2007. Orvieto, Massiccia città di pietra (City of solid stone. In Umbria Sotterranea (Umbria Underground). IUGG. XXIV General Assembly, Perugia.

Martini E., Cenci M., Salciarini D., Conversini P., Tortoioli L., Tamburi P., 18–21 November 2008. Risk mitigation from landslides for cultural heritage in Umbria Region. First World Landslides Forum—Session 5—Tokyo, Japan.

Martini E., Cenci M., Conversini P., Salciarini D., Tamburi P., 9–11 September 2009. Landslide prevention, monitoring and mitigation in Umbria Region of central Italy: case histories GEOITALIA 2009 VII Forum Italiano di Scienze della Terra, Rimini.

Pane V., Martini E., October 1996. The preservation of historical towns of Umbria. The Orvieto case and is observatory. Proc. Int. Symp. on geotechnical engineering for the preservation of monuments and historic sites, pp. 489–498, Napoli.

Pane V., Martini E., 1997. The preservation of historical towns of Umbria: the Orvieto case and its Observatory. Proceedings of the International Conference on Geotechnical Engineering for the Preservation of Monuments and Historic Sites, Rotterdam: Balkema.

Salciarini D. & Conversini P., Martini E., Tamburi P. & Tortoioli L., June 30-July 4, 2008. Rapid landslides threatening roads: three case histories of risk mitigation in the Umbria Region of central Italy. 10° International Symposium on Landsides and Engineered Slopes, Xi'an-China.

SOT Srl, 1984–1997. Preliminar, definitive and final designs of the Orvieto Hill Remediation Works Project, Umbria Region, Perugia.

Umbria Region, 1998–1999. "Hydrogeological risk Pale Village (Foligno-PG) inhabited mitigation" Preliminar, definitive and final designs, Umbria Region, Perugia.

Umbria Region, 1998–1999. "Hydrogeological risk Rocca Ripesena Village (Orvieto-TR) mitigation" Preliminar, and final designs, Perugia.

Umbria Region, 2005–2006. Hydrogeological risk Giro dei Condotti (Spoleto-PG)—Spoleto Town mitigation "Preliminar, definitive and final designs, Umbria Region, Perugia.

Geotechnical Engineering for the Preservation of Monuments and Historic Sites – Bilotta, Flora, Lirer & Viggiani (eds)
© 2013 Taylor & Francis Group, London, ISBN 978-1-138-00055-1

Geohazards and climate change issues for the preservation of the Saxon Shore in South Britain

D. Tapete
University of Florence, Italy

E.N. Bromhead
Retired, formerly Professor of Geotechnical Engineering, Kingston University, London, UK

ABSTRACT: The former environmental context and current visitors' perception of the Roman Shore Forts in South-East England belonging to the so-called "Saxon Shore" (i.e. the *Litus Saxonicum* firstly mentioned in the *Notitia Dignitatum*, late 4th century AD) were drastically altered by centuries of sea-level rise and siltation phases due to past climate changes, and correlated coastal erosion and landsliding processes. Further threat for conservation is reasonably to be expected as a consequence of the near future climate change scenarios drawn for the UK. In this paper we analyze coastal and inland geohazards and consequent geotechnical instability which chronically affect the Roman Shore Forts, as well as the issues related to the implementation of protection schemes. The current land-locked configuration of sites like Richborough in Kent and Pevensey in East Sussex, makes them relatively or totally secure. Conversely, the direct and persistent exposure to coastal dynamics is a pressing issue for the conservation of the archaeological structures in Portchester, Hampshire and Reculver, North Kent. These sites clearly exemplify the current need of planning targeted conservation initiatives in the framework of an established and shared procedure of coastal risk management. They are assumed here among the demonstrative cases to critically discuss the impacts of climate change and ever-changing coastal environment on the choice of site-specific mitigation/adaptation strategies.

1 HISTORICAL BACKGROUND

The history of Romans in British territory started with the two expeditions made by Julius Caesar in 55 and 54 BC during the Gallic Wars. But it was only almost one century later, in 43 AD, under the Emperor Claudius, that the Roman conquest of Britain actually began. The guarantee of Romans' stable control of the land was always associated, especially for the indigenous population, with the permanent presence of garrisons. Indeed, the definite withdrawn of the troops in 383 AD meant the end of Roman rule in Britain, and marks the beginning of the post-Roman history.

Military garrisons were distributed throughout the country, at the northern frontier facing the Caledonians and Picts tribes in Scotland, and along the southeastern coastline. The latter was the main entrance from the Continent and for trade, and offered sites for sheltered anchorage of ships and construction of several coastal installations thanks to its geomorphology at that time characterized by small embayment and inlets behind natural barriers, up to inner channels running inland.

This historical and geomorphologic perspective is essential to understand the importance of Roman military sites still preserved in the UK, and to infer the consequences on the geotechnical stability of these installations due to their former (and present) location.

This paper focuses on the stone forts built during the late 3rd century AD in East Anglian and southern coasts of England, most commonly known as 'Saxon Shore Forts' or, better, 'Roman Shore Forts'. The first appellation derives from the term 'Saxon Shore' (*Litus Saxonicum* in Latin) firstly mentioned in chapter XXVIII of the *Notitia Dignitatum*, a document dating back to the late 4th century AD which lists the sites under the command of the so-called 'Count of the Saxon Shore in Britain' (*Comes Litoris Saxonici per Britanniam*). Of these eleven coastal installations, we here analyze in detail the sites of Portchester Castle in Hampshire, Pevensey in East Sussex (Figure 1), and Richborough and Reculver in Kent (Figure 2).

All of them are currently properties in the care of English Heritage (EH) and scheduled under the Ancient Monuments and Archaeological Areas

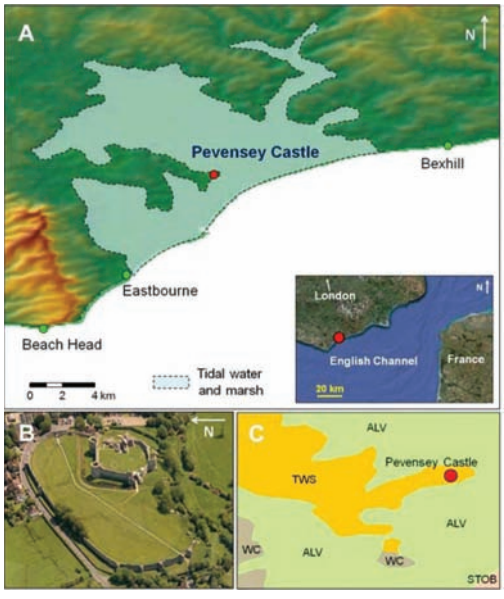

Figure 1. A) Location map of Pevensey Castle, East Sussex, South UK, over SRTM DEM. The present topography still marks the area formerly occupied by marshland surrounding the peninsula over which the Romans built the shore fort. B) Aerial view of Roman fort with the medieval castle on the eastern corner. C) Sketch map showing the local bedrock geology (Turnbridge Well Sand F.—TWS; Weald Clay F.—WC) and superficial deposits (Alluvium—ALV; STOB—Storm Beach Deposits). The shape of the ancient peninsula is perceivable thanks to the distribution of surrounding alluvium.

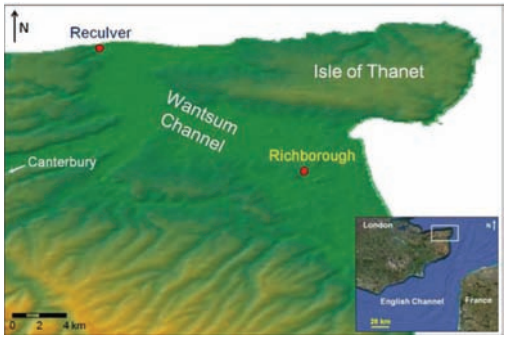

Figure 2. Location map of Reculver and Richborough Forts, Kent, over SRTM DEM. The present topography still marks the area formerly occupied by the Wantsum Channel.

Act 1979. They were formerly located on strategic estuaries, on raised ground or low-elevated well-drained hills overlooking tidal water and marsh (cf. section 2) and, interestingly, preserve features which distinguish one from each other. Nevertheless, according to Wilmott (2011), two groups of forts can be differentiated on a morphologic basis. The 'early group' includes most of the Roman forts sharing the 'playing card shape', e.g. Reculver, the principia and barracks of which were unearthed. Singular plan shape, massiveness of the walls (up to 11.5 feet, around 3.5 m) and semi-circular bastions placed around the perimeter are instead the features of the forts classifiable in the 'main group'. To this type regularly squared Portchester Castle and irregularly oval Pevensey can be referred to. From a structural point of view, it is worth noting that such thicker walls exploit foundations made of chalk and flint rafts overlying timber piles which strengthen the ground beneath (Wilmott, 2011). At Lympne, South Kent, the bastions were formerly founded on ragstone rubble above buried timber piles, and archaeological evidences allowed a reliable back-analysis of the sliding downslope of the masonries due to landslides occurred in the past (Hutchinson et al., 1985).

The early group dates back to the early-mid 3rd century AD, while the main group to the final quarter. About their origin and functions there is still an open debate. The quite common image of the Roman Shore Forts as an organized protection scheme against piracy and seaborne raiders currently appears weaker, since it is not justifiable with an actual large-scale maritime threat to Britain (Pearson, 2002). Conversely, their undoubted defence character and realistic estimations of the number of soldiers employed in each fort seem reasonably to support the hypothesis of military garrisons used by Allectus and Carausius during their rebellions against the central Empire (286–293 AD; cf. Tapete et al., in press). Albeit this aspect lies outside the scope of this paper and is worthy of a separate treatment, it contributes to highlight the strategic position of these shore forts, most of them sited in areas at that time sheltered from the open waters and associated to harbours and safe berths for ships.

Landscape transformations due to climate change and correlated sea-level change had a relevant impact throughout the South-eastern coasts of England and, for our study interests, on the stability and preservation of the Roman Shore Forts. Such changes have long been observed by scholars through centuries and traces are still visible. Despite a first appearance of relative security for land-locked sites like Pevensey and Richborough, coastal erosion and flooding threats are nowadays a real issue to deal with. The macroscopic manifestation at Reculver Fort, as well as the exposure of Portchester Castle to potential future inundation, are only some of the aspects involved in the current context of coastal management in the UK, where the long-established concept of 'defence' and 'protection' from sea (and more generally

from sea-land interactions and coastal hazards) is now flanked by 'adaptation' to coastal change (cf. Hunt, 2011).

2 GEOLOGICAL AND LANDSCAPE SETTING

Referring to Bromhead & Ibsen (2004, 2006) for the geological setting of the whole south-eastern region of England, the area corresponding with the Saxon Shore is characterized by soft Cretaceous and Eocene geological formations quite prone to marine erosion.

In the southern site of Portchester Castle located on the northern edge of Portsmouth Harbour (cf. Figure 3) at approximately 2–4 m above ordnance datum ('mean sea level' in the UK), the bedrock is composed by chalk, overlain with river terrace deposits (undifferentiated) of sand, silt and clay. As also observed by Pearson (2002), Portchester Castle is likely the least-changed of any of the Shore Forts from ancient times, with erosion having affected the promontory of the fort whereas siltation partially the harbour as a response to past sea-level changes.

Conversely, the Roman Fort of Pevensey, nowadays at about 1.5 km from the East Sussex coast, occupies the remnant of an ancient peninsula (from

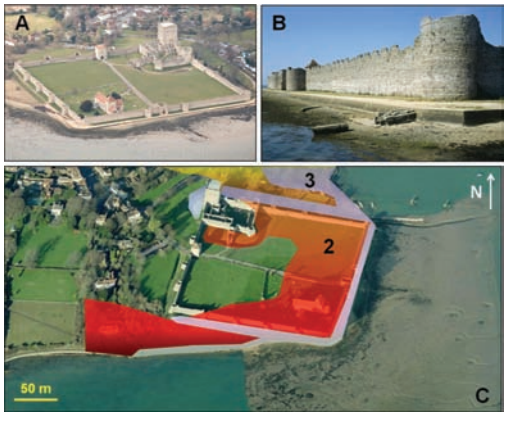

Figure 3. A) Bird's eye view of Portchester Castle (© Air Frame Photography) and B) view from north-west to south-east of the eastern wall of the Roman fort, which shows the pedestrian path for visitors and the concrete seawall. C) Aerial view from which the saltmarsh located offshore within Portsmouth Harbour are clearly visible, as well as the shingle/gravel dominated beach and the seawalls along the coastline (Bing Map, © 2012 Microsoft Corporation). Flood zone 2 and 3 are reported in red and violet colours, respectively (see the numbers. The boundaries refer to the Castle area and are only indicative of the estimated risk; derived from Hunt, 2011).

which scholars claim the name origins) founding on Tunbridge Wells Sand Formation (sandstones, siltstones and mudstones), and overlooks a marshland area known as Pevensey Levels (Figure 1A).

The latter are the product of sequences of coastal accretion and erosion occurred in Flandrian age (Jennings & Smyth, 1990), back to which the silty clay alluvium distributed around the raised ground of the fort dates. It is reasonable to hypothesize that Pevensey was formerly lapped by a shallow coastal marsh, and the site position was selected by the Romans thanks to the presence of a waterway as deep-water channels suitable for navigation and recovery of boats (Figure 1C). Such hypothesis also might explain the dimension of the fort and its orientation, with the main gate located at the west corner and the southern wall (and presumably the northern one too) following the physical borders of the peninsula (Figure 1B). Pearson (2002) suggests that in post-Roman times a shingle barrier formed due to debris sedimentation driven by the eastward longshore drift, and it progressively evolved into the current one stretching from Eastbourne to Bexhill, thereby transforming Pevensey Castle into a land-locked site.

Moving to the eastern sites in North and East Kent, it is proved that Reculver and Richborough Roman Forts were originally located to garrison the south-eastern and northern ends of the now silted up Wantsum Channel respectively (Figure 3). This channel originated after flooding of the shallow basin formed by the syncline on the underlying chalk beds, as a consequence of sea level rise at the end of the last ice age (about 15,000 BP). Regional topography confirms the extent of Flandrian-age alluvium over the previous 3-mile wide channel separating the Isle of Thanet from the pre-Flandrian mainland. Local topography still reflects the former configuration of the Wantsum. Historical documentation confirms that Canterbury (which is today far from the coast of about 23 km) was reachable by sailing till the 15th century, while in the century after navigation was not possible anymore and the channel started to become all dried up. The former island on which Richborough Roman fort was built became a hill, and the River Stour currently flows close to the east-facing slope.

As mentioned above, the regional geology is dominated here by Cretaceous chalk overlain by Eocene deposits (Thanet Sand and Woolwich Formations) and Pleistocene deposits (Head Brickearth). Thanet Sand Formation is the main bedrock of Reculver and Richborough Roman Forts and comprises unconsolidated marine loamy sands. Interestingly, along the eastern side of Richborough hill the BGS 1:50,000 geological map reports sands of the Woolwich Formation belonging to the Lambeth Group, along with a small section of

Harwich Formation. Head Brickearths also cover the bedrock over the areas of the fort and Amphitheatre (Small, 2002).

Looking at the superficial geology, the tidal flat deposits normally consisting of consolidated soft silty clay with layers of sand, gravel and peat, mark the boundaries of Reculver fort and the toe of the ancient island of Richborough. Despite the moderate permeability of these soils, control of groundwater level is possible only with constant pumping and targeted drainage (albeit soils are usually seasonally waterlogged; Small, 2002 and cf. English Heritage, 200b). Conversely, the soil at the hilltop are permeable and naturally well-drained (Small, 2002).

Marine erosion is evidently an actual threat for the coastline of Reculver, as testified by the long history of cliff retreat and consequent cultural heritage loss (cf. section 6). Nevertheless, comparing the map of flood zones in England and Wales by Environment Agency (not taking account of flood defences; NAO, 2007) and BGS map of the areas flooded in the recent geological past (i.e. in the last 10,000 years) published by Jackson (2004), the region of Isle of Thanet and the surroundings of Reculver and Richborough Roman Forts show a non-negligible susceptibility to flooding. This encounters a good fit with the risk rating 'low' (but not 'n/a'!) assigned to both sites by EH Coastal Estate Risk Assessment (CERA; Hunt, 2011), as well as with the 'medium' one reported in EH's Scheduled Monuments at Risk (SM@R) database.

Such hazard, apparently not relevant, may be of some concern in order to protect not only the major archaeological remains but also the cultural landscape and other heritage features, within the frame of the near future implementation of Shoreline Management Plan (SMP) policies.

As being large-scale assessment of the risks associated with coastal processes, it is here to be noted that these high-level documents were produced for each region of the UK and are part of DEFRA strategy for flood and coastal defence as 'route maps' for local authorities and involved decision-makers to manage coastal risks in the short term (0–20 years), medium term (20–50 years) and long term (50–100 years) (i.e. the so-called Epochs 1, 2 and 3). In the following sections implications of SMP policies are also discussed, with specific regard to beneficial, neutral or potentially detrimental impacts they may have on the Roman Shore Forts and their landscape.

3 PORTCHESTER CASTLE

As being located in a ward currently affected by tidal flooding and overlooking a harbour exposed to intertidal mudflats, the Roman Fort of Portchester Castle is likely to be susceptible in near future to inundation (CERA risk level 'medium'), and secondarily to coastal erosion ('low') (Figure 3A). Impacts of past marine attack on the exterior structures are assessable by the repairs still visible over the masonry surface and from the plan comparison of the former distribution of the outer bastions with the present one (cf. Tapete et al., in press).

At this site the solution was the construction of concrete seawall (Figure 3B-C) which undoubtedly prevents seawater directly lapping the archaeological structures, as happened still in the early 1900s. According to the North Solent SMP (2010), this type of defences was recognized as being in fair condition (even good for those located south-east and north of the Castle) and assigned an estimated residual life of 11–20 years. Besides its protection function, this solution also allows the sea-facing frontage to be accessed by visitors, thereby combining site conservation with public opening.

Although the rate and scale of shoreline erosion tend to be less within the harbour than along open coastlines (cf. appendix C5 of North Solent SMP, 2010), the national heritage importance of the site stimulated reviewed flooding risk assessment, to reach the conclusion that maintenance and improvement of the existing flood defences is the best and worthy solution (cf. Tapete et al., in press).

Indeed, as already shown by risk scenario presented by Environment Agency (2008), at least the outer half of the Castle closer to the sea, the medieval keep and the area in front of the northern and southern walls would be included into the Flood Risk Area 2018, considering 0.5% of annual probability event, a predicted sea level rise of 1 m and in absence of any coastal defence. By the way, it is interesting what Hunt (2011) shows in terms of probability of occurrence, reporting the flood zoning distinguished into the flood zone 3, limited to external ditches surrounding the fort and the pedestrian path along the eastern wall, and the flood zone 2, which is actually larger and potentially evolves the eastern part of the fort and the keep (Figure 3C).

In this context it was chosen to implement the EA 'Hold The (existing defence) Line' (HTL) policy, i.e. the construction or maintenance of artificial defences so that the position of the shoreline remains unchanged, whatever the Epoch. SMP maps confirm that this policy is going to be applied not only to Portchester Castle, but also the whole extent of the surrounding coast. Among of the main implications, uniform arrangement and maintenance of protection scheme will be guaranteed, with a direct benefit for the preservation of

the entire historic environment around the archaeological monument.

4 PEVENSEY

Of the four Roman Shore Forts here presented, Pevensey is the only one for which it seems possible not to recognize any specific active geohazard at the present. The silted up valley separating the fort from the sea is a guarantee of site security from coastal threats, while the raised location makes the probability of inland flooding into the fort absolutely low, even negligible. On the contrary, damages to heritage occurred in the past.

As extensively discussed in Tapete et al. (in press), ground movements due to post-Roman landsliding have significantly affected the southern and eastern sides of the enceinte. Fallen Roman masonry blocks can be found sparsely along the ruinous and almost completely disappeared southern wall of the Roman fort (1), at few metres from the towered bailey wall of the Norman Castle (2) at its turn from the southern to the eastern slope of the hill, and at the toe of the eastern slope at approximately 70 m from the East Gate (3) (Figure 4). By the way, a bird's-eye view of Pevensey Castle in ink wash on paper drawn by S.H. Grimm currently accessible at the British Library, gives us an interesting image of the monument as it was in 1773 (British Library Online Gallery, 2012), with clear indication of the main fallen blocks n. 2 and 3 (Figure 4) from previous Roman bastions.

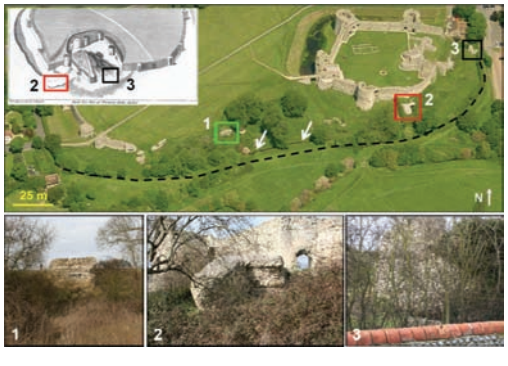

Figure 4. Location of three of the fallen blocks of Roman mansory still visible along the southern and eastern slope of Pevensey hill, among which the n. 2 and 3 (the latter presumably at an early stage of sliding downslope) were already documented in a copperplate engraving printed in 1783 reproducing a 10-year earlier ink wash on paper by S.H. Grimm. The dashed line marks where the sea formerly lapping the raised peninsula, while the arrows the present ditch with a little stream.

The hypothesized fitting of the fortified structures to the former coastal peninsula (cf. section 2) actually was the reason of its instability. Following the historical observations reported by McInnes (2001), the reinforcement of the keep by means of large buttresses, quite unusual for the Norman construction routines, appears an early attempt to solve ground instability already activated at that time. Presumably the same terrain motions which caused the toppling and sliding downslope of the block n. 3 (Figure 4). McInnes (2001) also infers that the loss of the eastern portion occurred in a period after the battle which took place here in 1264 during the castle siege by Simon de Montforte. The author interestingly also suggests reflections about possible climate change-induced triggering of these landsliding processes, in relation to warmer temperature and desiccation conditions in medieval periods (cf. comments on climate and sea-level change connections for the triggering of historical landslides at Lympne Castle discussed by Hutchinson et al., 1985).

The completely changed landscape at Pevensey due to past siltation and landsliding necessarily imply nowadays the promotion of correct interpretation initiatives to virtually restore a reliable image of the Castle in visitors' perception as much close as possible to the former arrangement. Among others, they should include a 360 degree visit of the monument, by walking around the exterior walls, especially along the path running on alluvium soils at the toe of the southern side of Pevensey hill (Figure 5A).

According to BGS lexicon accessed through GeoIndex, these soils are normally soft to firm consolidated, compressible silty clay, with a stronger, desiccated surface zone which may be produced. Field observations performed during winter season (Figure 6) did not highlighted specific degradation of the marshland more than those expectable for a typically wet British country soils. Anyway, these observations are sufficient to raise the question about the potential climate change effects on the stability of visitor carrying capacity of the soils.

Figure 5. Details of A) the southern slope of Pevensey hill and B) little stream showed in Figure 4 (see the arrows).

Figure 6. Pictures taken in February 2010 showing a detail of the marshland of Pevensey Levels and the condition of the public pathways, whose visitor carrying capacity can be affected by near future climate-change impacts.

At a first glance this issue might seem unrelated and far from geotechnical problems of concern for this paper, but recent condition surveys performed along touristic paths, such as that over the Hadrian's Wall Path National Trail (McGlade, 2012), confirm the increasing urgency to deal with these practical problems due to high soil moisture content and poor drainage systems implemented. Interpretation activities and public access to Pevensey Castle should consider in the near future this aspect, especially for the stability and preservation of the southern side (Figure 5A). The latter was affected by past ground movements, and we cannot exclude that it could be also in the near future due to the coactions of ground instability which seem still affecting the southern slope and the erosion potential of the ditch running at the toe of the escarpment (Figure 5B).

5 RICHBOROUGH

Some rough similarities with Pevensey can be found in the archaeological area of Richborough, whose current land-locked arrangement again induces us to consider this site quite secure from coastal threats. Indeed for the hilltop areas, i.e. the Roman fort and amphitheatre, CERA report considers coastal erosion as being a not applicable geohazard, whereas it assigns flood risk level 'low' (Hunt, 2011). Correct understanding of the latter rating has necessarily to take account of the chronic susceptibility to flooding of the regional area of Island of Thanet (cf. section 2). On the other side, actual flooding threat might result for the eastern extremity of the site, the surroundings of Richborough hill and areas of archaeological potential located at the toe of the eastern slope, as a response of the regime of the neighbouring River Stour (Figure 7A). Nevertheless, the presence of the railway line at the foot of this escarpment is claimed as being an anthropogenic factor of protection (Hunt, 2011).

Also for Richborough Fort, the site interpretation help us to back-analyze the effects of past slope instability having affected the integrity of the Roman structures (by the way, reminiscence of the original coastal environment is hidden in the Latin name *Portus Rutupiae* from ancient Celtic term for 'muddy waters' or 'muddy estuary').

In particular the recent archaeological discovery performed during a targeted campaign carried out by EH in 2008 (English Heritage 2008a-b; Wilmott & Tibber, 2009) shed lights on the collapse of the eastern wall of the fort due to gradual erosion of the former peninsula by the River Stour shifting progressively its course westwards (Figure 7B).

EH archaeological and laser scanning-based investigations along the foot of the incline showed that the collapse of the eastern wall occurred in two main steps, with a first downslope rolling and complete flipping of two large masonry segments, followed by a second fall of a further section on its face, which spread in different parts as it reached the ground (Figure 7B). Surprisingly, the re-use of

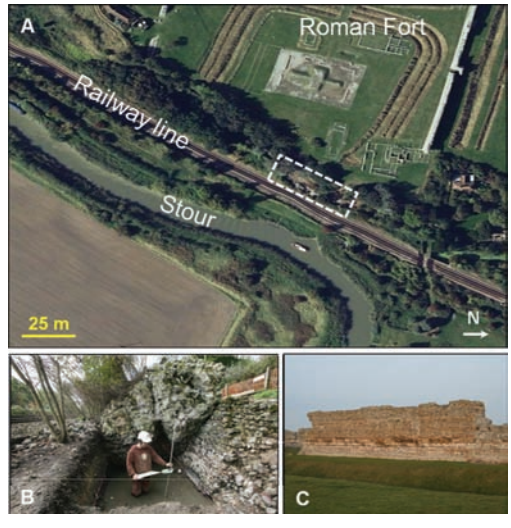

Figure 7. A) Aerial view of Richborough hill, River Stour and the railway line at the toe and the ruins of the Roman Fort at the top (Bing Map, © 2012 Microsoft Corporation). The dashed square indicates the position of archaeological digs carried out in 2008 by EH to investigate the coastline in Roman times and the collapse of the east wall (B; The Guardian, 2008). The latter, we can imagine, was formerly as massive as those still preserved (C).

the collapsed wall in the late 14th century served the construction of an artificial waterfront including a small dock. Besides the confirmation of later occupation of the riverside, this archaeological evidence would suggest a still changing environment at that time.

6 RECULVER

The former perimeter of Reculver Roman Fort is observable in a map dating back to 1685 reported in McInnes (2001), which also clearly draws the cliff profile and waterfrontage of the site. In 1781, i.e. almost one century later, the eroding cliffs had already reached the northern wall and first sections had fallen into the sea.

Loss of land also meant the disappearance of post-Roman structures, such as those belonging to the monastery and medieval church, the latter being also interested by demolitions in 1800s, when the northern wall was definitely lost (cf. Hasted, 1800).

Hence the documentary evidences seem to suggest more an episodic nature of past phenomena against a probably misleading impression of an erosion process developing continuously through time, although there is no doubt that this section of coastline actually was ever-changing since Roman times.

Under the perspective of heritage preservation, much of the site is listed as a Scheduled Ancient Monument and is in the care of EH, together with an approximately 165-m length of coastline.

This confirms that site conservation is not limited to the main monument, but also includes the maintenance of its surrounding historic environment aimed to safeguard the landscape value features and inhibit further progression of ongoing coastal phenomena.

As observed in Portchester Castle (cf. section 3), the chosen solution was the construction of hard coastal defences. A rock-rubble armouring along the shore at the toe of the church ruins prevents rapid erosion and cliff undermining (Figures 8–9).

Indeed coastal protection started here quite early, as a further proof of high awareness of the erosion risk for the Reculver Towers. In 1809 Trinity House undertook the construction of groynes (Murphy, 2010), followed in 1866 by the erection of a facing made of ragstone blocks around the cliffs beneath and west of the church (Figure 10). All of these interventions (e.g., sea walls and groynes, even beach recharge schemes) evidently respond to the concept of 'defence' (cf. section 1), but also foresee and require a practical approach of periodic monitoring and regular maintenance, which is actually performed by EH (Figures 8–9; cf.

Figure 8. Aerial view of Reculver Towers as they appear at the present, with the rock-rubble armouring and ragstone apron immediately to the north of St Mary's Church regularly maintained by EH (Bing Map, © 2012 Microsoft Corporation).

Figure 9. View of the ragstone apron, seawall defences and rock armouring along the coastline east from the Towers.

Periodic Condition Survey Report, Bailey Partnership 2010, cited by Hunt, 2011).

The case of Reculver is also suitable to discuss the impacts due to the coexistence of different owners/responsible bodies for heritage and related different approaches to coastal risk management, such as the above mentioned HTL (cf. section 3) and the so-called 'Managed Realignment' (MR) policies, the latter proposing a managed process of natural shore movement (usually designed for contexts of low-lying areas, but also occasionally proposed in cliff areas). EA supervises the land immediately adjacent to the EH area of competence, as well as a huge area located west of the historic site (i.e. Reculver Country Park) and the eastern stretch from the shellfish hatchery to Plumpudding Island. For both areas SMP2 document for the Isle of Grain to South Foreland (SMP, 2010) propose the implementation of MR. Although a direct impact on Reculver Towers and archaeological site is well far from happening, the MR project still raises criticism, due to the uncertainties on the future coastal changes that it might

Figure 10. Old postcards of Reculver Towers at the early 1900s, showing past protection solutions, i.e. wooden groynes, along both coastal stretches immediately west and east of the archaeological area.

cause and doubts about its long-term effectiveness. This issue is also of landscape concern, since the environmental context in which Reculver Fort is inserted would be certainly subject to modification, together with a loss of local property. Although the risk scenario of a total loss of land on either side of the site mentioned by Hunt (2011) might seem at this stage quite exaggerated especially with regard to a future image of Reculver as isolated site on a newly created promontory, these reflections further confirm the need to achieve a shared coastal strategy harmonizing both the point of views.

In relation to flooding hazard mentioned in section 2 as a non negligible for the entire region of Island of Thanet, it is worth noting here that the height of Reculver fort and church (about 10–13 m above ordnance datum) makes tidal flooding risk very low and unlike to occur at the top. Nevertheless, uncontrolled damages in sea walls and apron due to lacking condition monitoring, as well as erosion at the margins of the maintained defences can actually represent source of actual hazard. On the other side, a flood zone 3, i.e. in conditions of annual probability of flood occurrence higher than 0.5%, can be assigned to the surrounding land of the archaeological area.

7 SUMMARY AND CONCLUSIONS

The comprehensive review carried out on past and present geotechnical problems affecting the Roman Shore Forts of Portchester Castle, Pevensey, Richborough and Reculver due to geohazards and landscape changes is associated here with the discussion of potential threats in the context of a changing environment in response to climate forcing. The surveyed sites show various situations, from relatively secure to highly susceptible to climate change-induced hazards (mainly coastal erosion and flooding, but also ground instability and decrease of soil properties, among which visitor carrying capacity).

The ongoing evolution of risk management concepts (from protection to adaptation) raises practical issues for site preservation, which the different stakeholders involved (e.g., heritage bodies, departmental agencies like EA, and national and local authorities) are trying to deal with. In some cases the proposed solutions can be quite controversial, such as MR policies to be implemented in areas with high archaeological potential and/or landscape value. On the other side, maintenance and monitoring of coastal defences are still preferred in most cases, but they require adequate economic resources.

The current tendency in risk management is to find a balance between the costs of defence and the value of the assets to protect. With specific regard to the Roman Forts belonging to the Saxon Shore, the benefit-cost ratio is undoubtedly favorable to heritage preservation and safe public accessibility. Indeed, in light of the history of geohazards and landscape changes experienced by these archaeological sites, it is absolutely worth guaranteeing their preservation and correct interpretation, taking properly account of their geotechnical issues.

ACKNOWLEDGMENTS

Part of site-specific geological information was retrieved using BGS Onshore GeoIndex datasets (© NERC 2013) available via web map services (WMS, http://www.bgs.ac.uk/geoindex/). SRTM 90 m DEM V4 was provided by NASA via CGIAR-CSI (http://srtm.csi.cgiar.org).

REFERENCES

British Library Online Gallery 2012. A bird's eye view of Pevensey Castle by Samuel Hieronymus Grimm, ink on wash paper, 1773. British Library collections. Accessed at: http://www.bl.uk/onlinegallery/onlineex/topdrawings/a/zoomify84286.html.

Bromhead, E.N. & Ibsen, M-L. 2004. Bedding-controlled coastal landslides in Southeast Britain between Axmouth and the Thames Estuary. *Landslides* 1(2): 131–141.

Bromhead, E.N. & Ibsen, M-L. 2006. Landslide and coast erosion damage to historic fortifications in SE Britain. *Landslides* 3(4): 341–347.

Environment Agency 2008. Planning for the future. Portchester Castle to Emsworth draft coastal flood and erosion risk management strategy. Summary document.

English Heritage 2008a. Richborough Excavation 2008. Update 1: progress for 1–14 September 2008.

English Heritage 2008b. Richborough Excavation 2008. Update 2: progress for 15–26 September 2008.

Hasted, E. 1800 Parishes: Reculver. In The History and Topographical Survey of the County of Kent, Volume 9: 109–125.

Hunt, A. 2011. English Heritage Coastal Estate Risk Assessment. Research Department Report Series no. 68–2011.

Hutchinson, J.N., Poole, C., Lambert, N., Bromhead, E.N. 1985. Combined archaeological and geotechnical investigations of the Roman fort at Lympne, Kent. *Britannia* (16): 209–236, plates XIII-XVI.

Jackson, I. 2004. Britain beneath our feet. Keyworth, Nottingham: British Geological Survey Occasional Publication No. 4.

Jennings, S. & Smyth, C. 1990. Holocene Evolution of the gravel coastline of East Sussex. In: Proc. of the Geologists' Association 101 (3): 213–224.

McGlade, D. 2012. Hadrian's Wall Path National Trail 2012 autumn condition survey. Rainfall, soils, perched water tables. Carrying capacity. Readiness for climate change? 8 November 2012. Accessed at: http://www.hadrians-wall.org/

McInnes, R. 2001. What is the nature of the evidence? http://www.risknat.org/projets/riskydrogeo/docs/guide_pratique/Acivite1_Ateliers/Presentations%20Atelier1/A1P13-Coastal%20changes/programs/nature.html

Murphy, P. 2010. Coastal management infrastructure. In: Conservation Bulletin. Inherited infrastructure, Issue 65, English Heritage: 16–18.

NAO 2007. National Audit Office (NAO). Environment Agency: Building and maintaining river and coastal flood defences in England, ISBN: 9780102945522.

North Solent SMP 2010. Final North Solent SMP Document and Policy Statements. http://www.northsolentsmp.co.uk/

Pearson, A. 2002. The Roman Shore Forts: Coastal Defences of Southern Britain. Tempus Stroud.

Small, F. 2002. Richborough Environs Project, Kent. Aerial Survey Report Series AER/12/2002, English Heritage.

SMP 2010. Isle of Grain to South Foreland SMP Review 2010. http://www.se-coastalgroup.org.uk/wp-content/uploads/2012/02/IGSF-SMP-Report.pdf

Tapete, D., Bromhead, E.N., Ibsen, M-L., Casagli, N. in press. Coastal erosion and landsliding impact on historic sites in SE Britain. In: Margottini, C., Canuti, P., Sassa, K.. (eds.) *Landslide Science and Practice. Volume 6: Risk Assessment, Management and Mitigation*. Springer-Verlag, pp. 451–458, doi:10.1007/978-3-642-31319-6_60

The Guardian, 2008. Unexpected Roman ruin turns history on its head. 2 October 2008 Accessed at: http://www.guardian.co.uk/artanddesign/2008/oct/02/roman.fort.heritage

Wilmott, T. & Tibber, J. 2009. Richborough, a Roman and medieval port! In: Research News. Newsletter of the English Heritage Research Department 12 (2009): 16–18.

Wilmott, T. 2011. Introductions to Heritage Assets. Saxon Shore Forts. English Heritage.

This page intentionally left blank

Geotechnical Engineering for the Preservation of Monuments and Historic Sites – Bilotta, Flora, Lirer & Viggiani (eds)
© 2013 Taylor & Francis Group, London, ISBN 978-1-138-00055-1

Preservation and reconstruction of historic monuments in Saint Petersburg with provisions for soil-structure interaction

V.M. Ulitsky
Chair of TC207 "Soil-Structure Interaction and Retaining Walls" ISSMGE
State Transport University, Saint Petersburg, Russia

A.G. Shashkin, K.G. Shashkin & M.B. Lisyuk
Georeconstruction Engineering Co, Saint Petersburg, Russia

ABSTRACT: Many important historic monuments in Saint Petersburg have been analysed by the authors using a soil-structure interaction (SSI) approach. Among them are the Stock Exchange Building, the Admiralty Building in central Saint Petersburg, and St. Nicholas Naval Cathedral in the town of Kronshtadt near Saint Petersburg. These projects are presented in the paper. It is shown that SSI is a very powerful tool in analysing historic monuments. The potential of this method lies in the complete description of the stress-state of the monuments and in a possibility to develop measures for the monuments' remediation. To fulfil this method successfully, a comprehensive survey of the monuments is needed. Essential parts of such a survey are condition surveying of structural elements and foundations, geophysical research, soil sampling and testing. Influence of geotechnologies on adjacent buildings in congested urban conditions is also discussed in the paper.

1 INTRODUCTION

The lecture deals with preservation and reconstruction of the most valuable historic monuments in St. Petersburg. Generally, analysis of historic buildings condition is very important for projects dealing with preservation or reconstruction of historic monuments and their foundations (Burghignoli, Jamiolkowski and Viggiani, 2007, Powderham, 2003, Ulitsky et al., 2003). Such analysis should include the following major steps:

- Analysis of the actual stress—strain conditions of subsoil of preserved buildings, and, if necessary, of adjacent buildings;
- Estimation of the influence of present vibration background on settlement development;
- Estimation of ongoing settlements of buildings (under own weight and owing to outside factors) that is defined through calculations or observations the location of geodetic marks and gauges;
- Estimation of the allowable additional settlement of the existing buildings during reconstruction works or new development.

In all cases the principle of soil-structure interaction analyses was used with account of joint work of subsoil, foundations and superstructure.

2 ANALYSIS OF THE ADMIRALTY BUILDING IN CENTRAL SAINT PETERSBURG

Historic analysis of a geotechnical problem is very important for projects dealing with preservation or reconstruction of historic monuments and their foundations (Ulitsky et al, 2003).

For important projects it is necessary to perform the following works:

- Historical analysis of foundation behaviour of preserved/reconstructed buildings and buildings adjacent to the object of reconstruction or new development together with substructure behaviour of the existing buildings;
- Calculations of the total assumed deformations and percentage of different causes in settlement development of the existing buildings.

An example of a historical analysis is the Admiralty building in central St. Petersburg (Fig. 1a). The building has well pronounced cracks. The purpose of the historic analysis in this case was to find out the reason of these cracks development to make decision about further strengthening or preservation of the monument.

The Admiralty tower was constructed in 1734 by the architect I. Korobov. In 1811–1823 the

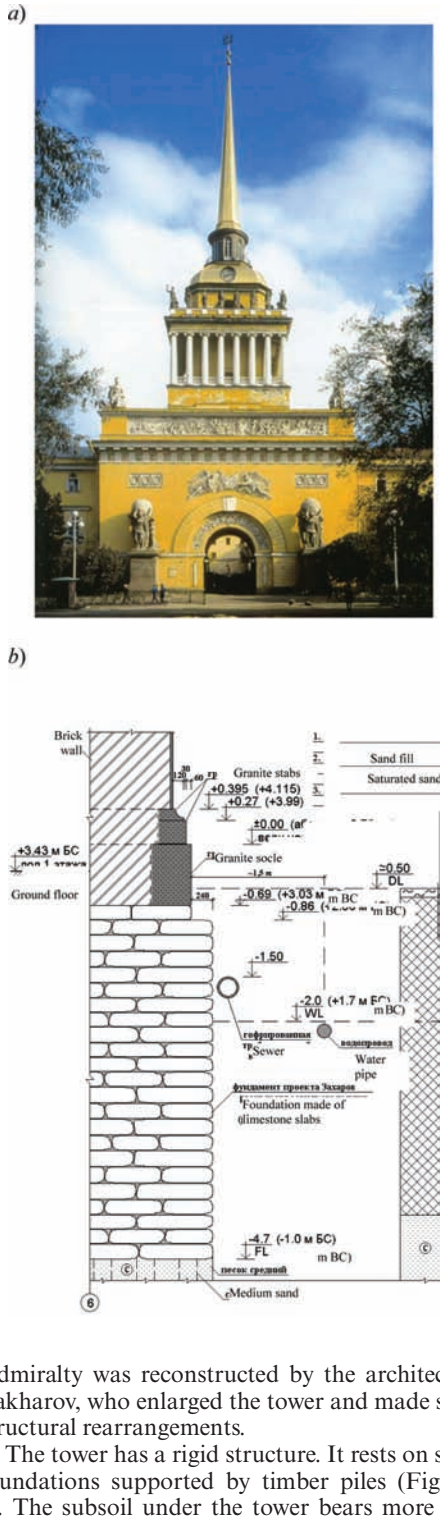

Figure 1. (*a*) The Admiralty Building, (*b*), (*c*) old foundation under the Admiralty tower.

Admiralty was reconstructed by the architect A. Zakharov, who enlarged the tower and made some structural rearrangements.

The tower has a rigid structure. It rests on stone foundations supported by timber piles (Fig. 1b, c). The subsoil under the tower bears more load than the adjacent lower wings of the building; consequently, settlement is bigger in the tower than in the wings. The cracks appeared in the wings near the location of windows.

The subsoil of the Admiralty is comprised of fine-grained saturated sand of medium density and soft clayey sands.

Index properties of soils based on site investigation results are contained in Table 1.

A thorough survey of the foundation was made. The stone foundations were inspected by a mini TV camera lowered down the survey holes predrilled through the stone foundations. All in all, seven 30 mm diameter holes were drilled. Visual survey was conducted down to the ground water level. One such investigation is illustrated in Fig. 2. It was found out that the average percentage of voids in the foundation body was in the range of 1 to 10%. General condition of the foundations was found to be satisfactory, except for one part of the foundation under a transverse walls of the tower. The structural survey of the building made it possible to identify all cracks in the walls. It was discovered that many cracks appeared in the bearing walls of the tower.

To find out the reasons for the cracks developing in the tower, a 3D soil-structure interaction analysis has been performed. All findings made during the geotechnical and structural survey

Table 1. The Admiralty subsoil properties.

Type of soil and thickness of stratum	W	γ, kN/m^3	e	φ°	c, kPa	E, MPa
Made up ground, 3…5 m		16.5				
Silty saturated sand of medium density 0…1.4 m	–	19.4	0.75	25	2.0	18.0
Plastic clayey sand 1.8…2.5 m	0.21	20.5	0.57	23	4.0	16.7
Liquid clayey sand 7.5…7.9 m	0.27	19.7	0.73	19	11.0	10.9
Varved sandy clay 14…17 m	0.35	18.6	0.97	10	7.0	6.7
Plastic clayey sand with gravel and pebbles 0…1.9	0.13	22.4	0.36	25	10.0	10.0
Sandy clay with gravel and pebbles	0.20	20.9	0.56	26	6.0	15.0

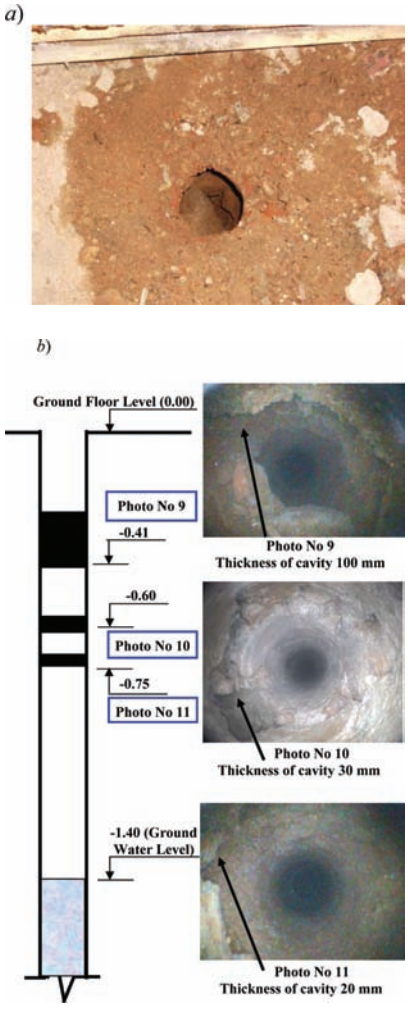

Figure 2. Drilling a borehole (*a*) and fragments of video footage containing cavities in the body of the foundation (*b*).

of the building were then incorporated into the design layout.

Initial construction and consequent reconstruction of the building were modelled. First

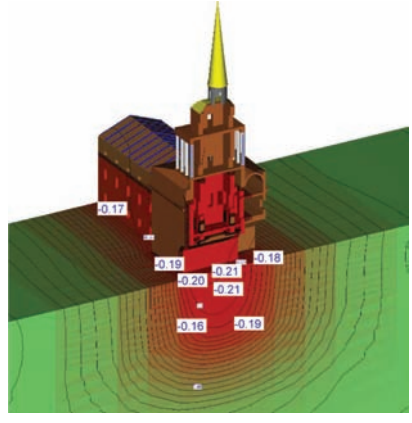

Figure 3. Contours of computed settlements of the Admiralty (cross section along the symmetry axis).

the deformations of old Korobov's Admiralty tower (1732) were assessed, to be followed by modifications of the design layout with account of the added walls (1816) and additional loads (Fig. 3). Thus, the real construction history was simulated.

The contours of settlements accumulated after the reconstruction of the building are shown on Fig. 3. The total estimated settlements have a value of about 20 cm. It should be noted that the soil model used in the analysis can take into account a long-term creep of the Admiralty's subsoil.

The performed analysis made it possible to identify the reasons for the cracks developing in the structural elements of the building. The main crack appeared in the tower wall adjacent to the lower wing. The reason for this crack development is the non-uniform settlement of the building. The settlement development may still go on, which can be explained by long-term creep of the subsoil. The differential settlement leads to generation of shear stresses in the walls with maximum values of up to 235 kPa (Fig. 4a). The shear stresses cause cracks in the tower walls to develop (Fig. 4b). There is a good correspondence between soil-structure

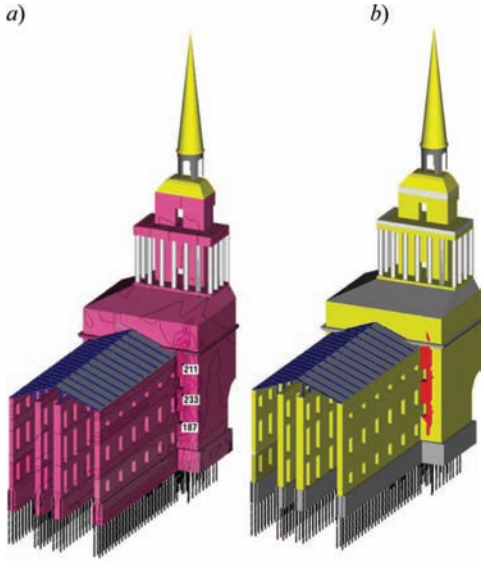

Figure 4. Calculations of the structure of the building: (a) contours of the shear stresses in the masonry (kPa), caused by the differential settlement of the tower and the lower wing; (b) zones of the possible development of the cracks caused by shear deformations of the transverse wall.

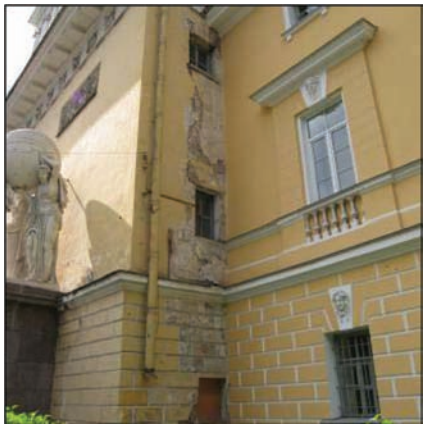

Figure 5. Development of cracks in the Admiralty Tower.

interaction calculation results and behaviour of the building observed in actuality (Fig. 5).

Thus, the conducted historical analysis of this geotechnical problem taking into account joint behaviour of both Admiralty's structure and its subsoil, alongside the construction history, helped to identify the reasons for the deformation of this famous monument in the central Saint Petersburg.

3 ANALYSIS OF ST. NICHOLAS NAVAL CATHEDRAL IN KRONSHTADT NEAR SAINT PETERSBURG

St. Nicholas Naval Cathedral is located in the town of Kronshtadt (Fig. 6). It was built in 1902–1913, as designed by the architect V.A. Kossiakoff. In this cathedral the idea of a classical cruciform church with a domed roof was fulfilled. This idea was realized first in the famous St. Sophia Cathedral in Constantinople.

In fulfilling ancient architectural traditions new structural materials, introduced in the beginning of the 20 century, were used. The main dome is supported by a system of steel beams. The dome is made of reinforced concrete. Four big pillars are the main supporting elements of the cathedral.

Geological investigations were made in 1897 and 1902. Eighteen boreholes were drilled to the depth of 27.7 m. The bearing layer of subsoil is a coarse sand containing pebbles (thickness of the stratum is 1.1–4.3 m). This stratum is underlain by moraine loams with boulders (thickness 6.4 m) and hard clays.

Due to the presence of the boulders the designer decided to construct foundations made of cast-in-place reinforced concrete in order to avoid construction of piles. The depth of foundations is about 4…4.4 meters.

In solid foundations iron girders were installed underneath stairwells and also in juncture areas between the higher and the lower sections of the masonry, as well as in the solid foundation walls underneath individual supports.

Immediately after completion, about 4 cm of differential settlement were recorded.

During the Cathedral's life a lot of cracks developed. In May 2009 an abrupt local increase of a crack in one of the abutments was observed. This endangered the stability of the whole structure.

Figure 6. St. Nicholas Naval Cathedral in Kronshtadt.

A special programme of cathedral structural survey, research and development of salvage measures was put forward. The key issue of this investigation was to find out the reasons for cracks development.

Some dangerous cracks in the cathedral's structures are shown in Fig. 7 and 8.

The scope of the survey was as follows:

- Full structural survey of the cathedral
- 11 holes drilled through the foundation to the subsoil to estimate the condition of both. Scheme of test boreholes is shown in Fig. 9.
- Dynamic sounding of the subsoil
- Taking soil samples from the boreholes; determining main properties of the soil.

It was found out that the conditions of both the subsoil and the foundations were satisfactory.

- A detailed geophysical investigation was then carried out. This investigation identified several zones of local subsoil softening due to leakage of water. These zones are located in the vicinity of existing services. Around the cathedral a partially decayed timber sheet pile wall was found.

Figure 7. Cracks in the vaults of the cathedral.

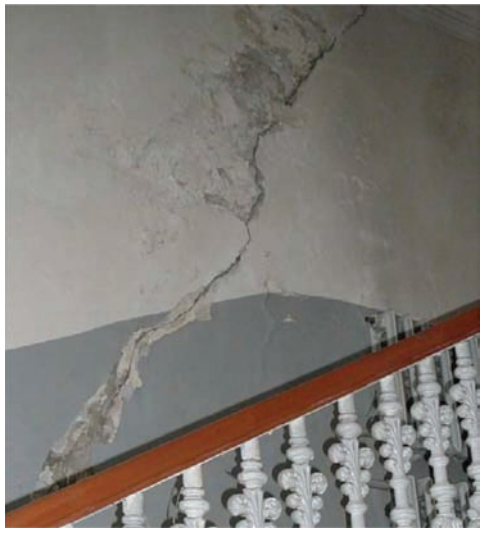

Figure 8. Cracks in the wall of stairwell passage.

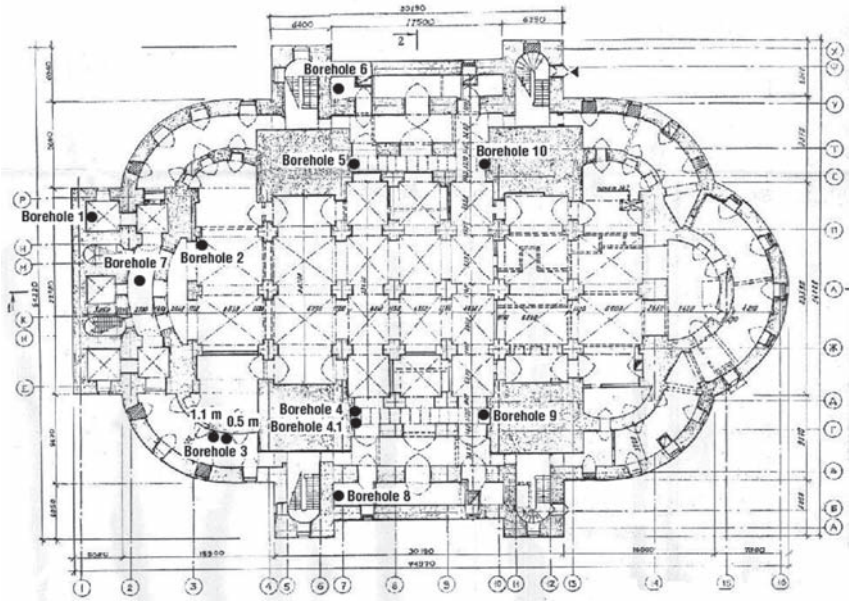

Figure 9. Location of test boreholes drilled through foundation body to the subsoil.

Index properties of soils underneath the Cathedral based on site investigation results are contained in Table 2.

A series of soil-structure interaction computations was performed with the help of *FEM models 2.0* software (Ulitsky V.M. et al, 2003). The computation profile is shown in Fig. 10. All main structural elements, foundations, and subsoil layers were incorporated in the computation profile. All main findings brought to light during the condition survey of structural elements, foundations, and subsoil were accounted for in computations.

Soil-structure analyses showed the cathedral being subject to diferential settlements. The reason for these settlements is a differential load acting on the main bearing structures of the Cathedral (Figs. 11, 12).

Such non-uniformity of loads is quite typical for temples of the cross-cupola structural scheme. The most heavily loaded are the central pillars by which the central cupola is supported. Hence, the pillars are subject to bigger settlements. The calculated differential settlements (Fig. 11) correspond well to the results of the geodetic investigations. The observed settlement differential is about 13–22 mm.

Computations show that the zones of tensile stresses in brickwork well agree with the locations of the actual cracks. In particular, taking into account non-uniform settlements we have a characteristic system of cracks in the semi-domes in the altar and the western parts of the Cathedral (Figs. 13 and 14).

The main conclusion of the investigations and the SSI computations is that currently there is no danger of an immediate collapse of the Cathedral.

Locally, a list of the most endangered structural elements follows below: the main dome, its supporting elements and semi-domes in the eastern and western parts of the cathedral. Local strengthening

Table 2. Main subsoil properties of Kronshtadt Cathedral.

Type of soil and thickness of stratum	W	γ, kN/m^3	e	φ	c, kPa	E, MPa
Made-up ground 1…2 m		16.5				
Plastic clayey sand 2..3 m	0.09	23.0	0.26	31	36.0	12. 0
Silty saturated dense sand 0…0.7 m	–	18.5	0.6	30	4.0	18.0
Medium grain saturated sand, dense, 0..1 m	–	19.7	0.55	38	2.0	20.0
Gravelly saturated sand, dense, 0..0.6 m	–	20.4	0.55	40	1.0	20.0
Hard clayey sand	0.13	21.5	0.40	28	50.0	15.0
Firm dislocated clay						10.0
Firm clay						20.0

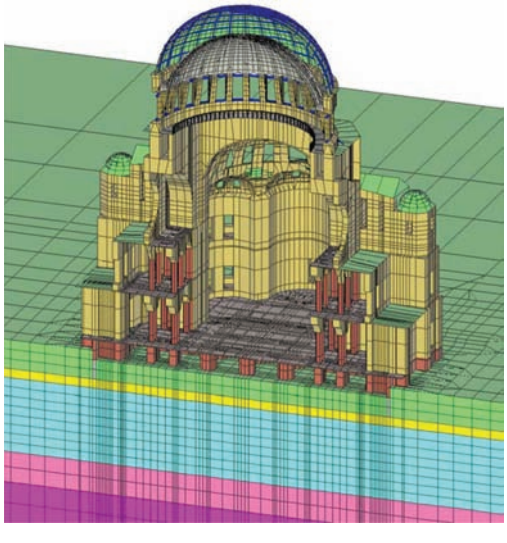

Figure 10. Computation profile of the cathedral.

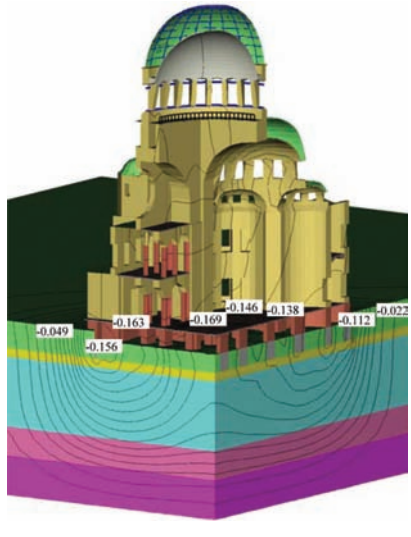

Figure 11. Contours of computed settlements of the Cathedral (cm).

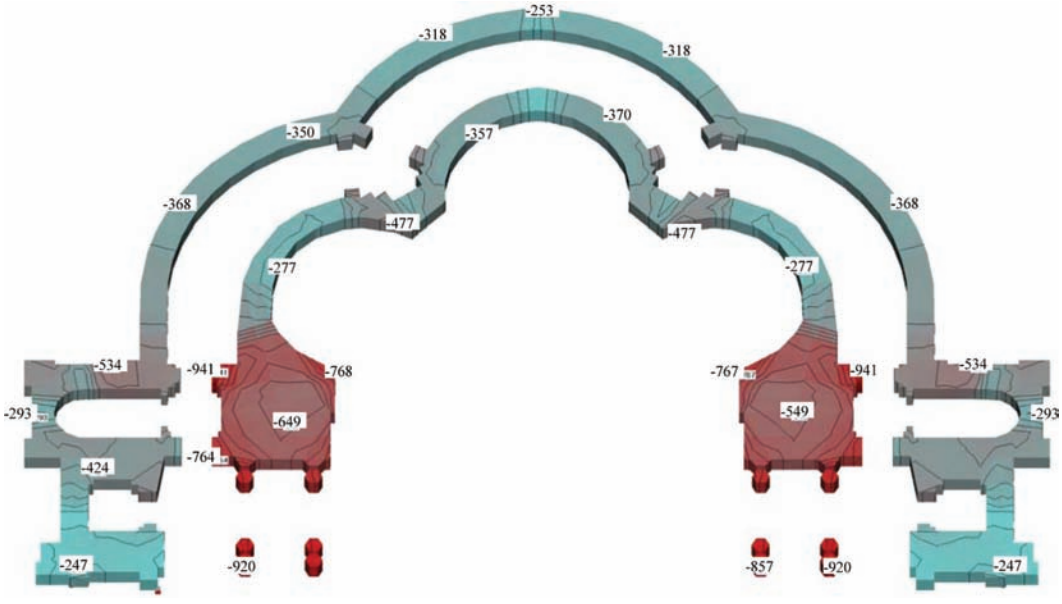

Figure 12. Distribution of vertical stresses (kPa) in the main bearing structures of the Cathedral on the level of the 1st floor. The most heavily loaded are the main pillars, the least loaded are the walls of the outer galleries.

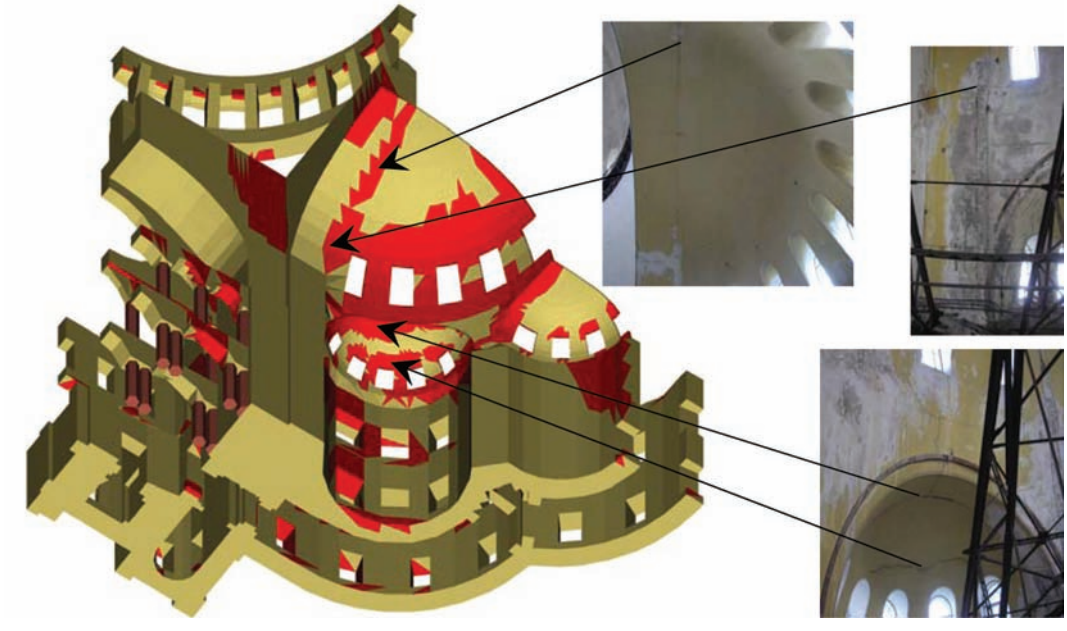

Figure 13. Comparing locations of possible calculated crack development and the real observed crack locations.

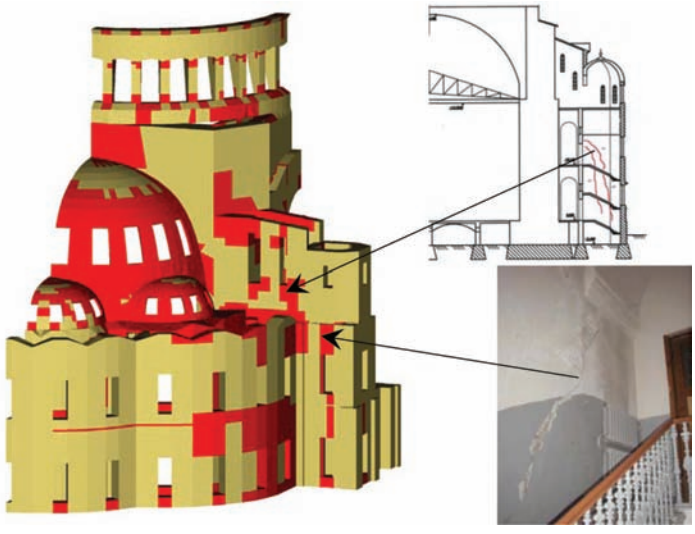

Figure 14. Location of possible cracks development by calculations as compared with the real observed cracks.

must be provided as soon as possible. This strengthening must be based on a detailed analysis.

The computations of the system "subsoil-foundations-superstructure" show that all main cracks in the structural elements of the cathedral are caused by differential settlements of the monument (see Fig. 11), conditioned by the non-uniform loading of the subsoil. The most dangerous cracks caused by differential settlements are the cracks in semi-domes in eastern and western parts of the cathedral.

4 CONCLUSIONS

Two examples of historic monuments are presented in this paper—Admiralty building in central Saint Petersburg and St. Nicholas Naval Cathedral in the town of Kronshtadt near Saint Petersburg.

As these examples show, it is very important to use soil-structure interaction approach in design of monuments preservation and renovation in urban areas. SSI approach is a very efficient at all stages of analyses of monuments. It is very powerful tool in prediction of behaviour of listed buildings and structures.

Successful application of SSI approach requires a very comprehensive survey of the monuments. Essential parts of this survey are: investigation of the structural elements, foundations and subsoil, geophysical research and testing, soil sampling and tesing, in-situ testing of cores. Results of these investigations must be used in SSI analysis.

REFERENCES

Burghignoli, A. Jamiolkowski, M. and Viggiani, C. 2007. Geotechnics for the preservation of historic cities and monuments: components of a multidisciplinary approach. General report. *Proc. of XIV European conference on Soil Mechanics and geotechnical Engineering "Geotechnical Engineering in Urban Environments"*, Madrid, Vol. 1.

Frank, R. 2006. Some aspects of soil-structure interaction according to Eurocode 7 "Geotechnical design", *Engenharia Civil/Civil Engineering*, Universidade do Minho, Portugal, No. 25, pp. 5–16.

Powderham, A. 2003. Protecting historic infrastructure using the Observational Method. *Proceedings of the geotechnical conference "Reconstruction of historic cities and geotechnical engineering"*. St. Petersburg, 16–18 September 2003. Vol. 1, pp. 243–250.

TSN 50-302-2004. *Design of foundations for buildings and structures in St. Petersburg*. Local constructional codes for St. Petersburg. Government of Saint Petersburg, 2004.

Ulitsky, V.M., Shashkin, A.G., Shashkin, K.G. and Lisyuk, M.B. 2003. Soil-structure interaction: methodology of analysis and application in design. ASV Publishers. St. Petersburg—Moscow. 40 p. (in English)

Ulitsky, V. 2003. Geotechnical challenges in reconstruction of historic cities (as may be illustrated by St. Petersburg). *Proceedings of the geotechnical conference "Reconstruction of historic cities and geotechnical engineering"*. St. Petersburg, 16–18 September 2003. Vol. 1, pp. 13–28.

Geotechnical Engineering for the Preservation of Monuments and Historic Sites – Bilotta, Flora, Lirer & Viggiani (eds)
© 2013 Taylor & Francis Group, London, ISBN 978-1-138-00055-1

Localized settlements of an ancient hospital foundation: Analysis of the problem to assess a possible reinforcement intervention

R. Valentino, E. Coïsson, F. Freddi & F. Ottoni
University of Parma, Parma, Italy

ABSTRACT: The paper deals with the study of both structural and geotechnical problems regarding a hospital which was built in the twenties of the past century in Borgo Val di Taro, Province of Parma, in the Northern Italian Apennine. The study is mainly devoted to the description of the great damages suffered by the ancient building after a localized differential settlement of the shallow foundation. The settlement, which had been probably caused by a great and prolonged leak of water from a hydraulic pipe, provoked, in its turn, a large deformation of the structure. The structure, which is made of stone masonry, has been accurately investigated, in order to obtain a complete description of both the crack systems and the deformation mechanism. The structure has been also monitored through the installation of appropriate instruments, such as wire extensometers. The paper describes the survey of the crack pattern and the analysis of one-year monitoring data. Under the geotechnical viewpoint, the study deals with the design of field investigations and in situ measurements, the definition of laboratory test program on the foundation soil, the interpretation of both field and laboratory test results. Moreover, this study stresses the importance of monitoring—combined to geotechnical and structural analysis—in evaluating the most suitable reinforcement intervention, in step with the last Italian law for seismic risk evaluation of historic monuments.

1 INTRODUCTION

Permanent monitoring of monuments is a crucial target in the framework of cultural heritage preservation and conservation. Indeed, it plays a very important role in the diagnostic process, significantly contributing to a better understanding of historic buildings structural behavior.

In step with this, the recent Italian seismic law for cultural heritage states that "*the periodic inspection of the building is a practice highly desirable because it represents the main tool for conservation awareness"* and it adds that *"in some cases, when the possible mechanism of collapse is well understood and can be defined safety thresholds, monitoring can be an alternative to intervention*" (DPCM 2011, Art. 4.1.9).

By relating measurements of movements and deformations to the external actions (winds, earthquakes, temperature variations, fluctuation of the ground water table) it is possible to reconstruct the links between actions and structural response, which is usually the goal of structural numerical calculation. If it's possible to rebuild these correlations, every aspect of the building behavior can be reached, including long term phenomena, which are very significant when, like in the examined case, soil settlements are present. These correlations, the more reliable the longer is the period of data collection, are able to provide two main key information. Firstly, they can provide a real-time control of the structure physiological behavior: in fact, any deviation from the expected response behavior against a given excitation can be immediately detected. Moreover, the monitoring system can be used to verify the effectiveness of either strengthening or reinforcement interventions. Data collected before and after the interventions can be compared, in order to check positive or negative changes in cracks evolution (Rossi & Rossi, 1998). In case of temporary interventions, they can be validated before making definitive works.

Very often, structural problems of old buildings and monuments are determined by geotechnical aspects or, at least, by soil-structure interaction. When a historical building needs for structural reinforcements, in order to recover its lost serviceability, it should be usual analyzing possible geotechnical causes before carrying out any restoration work on the structure. Sometimes, the geotechnical origin of structural instability is so clear that it cannot be disregarded. This is the case of differential settlements.

In the present study, the settlement problems affecting an old building, which houses a hospital since its construction (1920–1928), are analyzed. In the last twenty years, the hospital suffered localized differential settlements, which caused, in turn, considerable structural problems in the building.

In order to evaluate the opportunity of any kind of intervention and, if possible, to design a specific restoration work, a preliminary monitoring activity of the structure deformations and some geotechnical investigations were carried out. In this type of problems, very often the basic question deals with the opportunity of carrying out an intervention or not, even considering costs and benefits.

This paper outlines the adopted methodology to acquire the minimum number of data required for an appropriate assessment of the seasonableness of a possible intervention.

The final aim is to show the importance of the multidisciplinary approach in the analysis of historic structures, which often—as stated by the recent law for seismic protection of cultural heritage (DPCM 2011)—in long monitoring finds the first guarantee of conservation, defining the most suitable intervention and validating its efficiency in time.

2 CHARACTERISTICS OF THE BUILDING

The case study presented in this paper is the hospital of Borgo Val di Taro, Province of Parma, in the Northern Italian Apennine. The whole hospital complex is the result of several construction phases, which took place in different past periods. The portion of the building affected by the most important crack pattern is the oldest one, built in masonry between 1920 and 1928 (Fig. 1). For the Italian regulations (DL 22/01/2004), it is considered an historical building, because it is a public building older than fifty years. For this reason it is under bonds of the Board for Cultural Heritage and Preservation.

In 1964 a new concrete building was added adjoining on the south-west side, another one in 1968 near the north corner (Fig. 1). A further building was added in 1989 about 18 m far from the north west side and, at last, a new portion was inserted adjoining to the north-east side in 2006 (Fig. 1). It is clear that this elaborate history, with subsequent variations of loads on the subsoil surrounding the original building, has had a deep influence on its settlements.

At present, the oldest building, on which this paper concentrates, has an U-shaped plan, about 50 m long and 14 to 24 m large. In height, it develops over four storeys: one is partially below the ground level, two are currently in use as offices, the last one is an unused attic.

The construction is made in thick stone masonry walls all around and two main brick masonry spine walls, marking off a corridor. The floors are mainly made in concrete while the roof structure is wooden.

3 ANALYSIS OF THE LOCALIZED SETTLEMENT PROBLEM

The old masonry building shows a complex crack pattern, which seems mainly related to differential settlements (Fig. 2). The two lateral wings of the building appear to be separated from the main structure by vertical cracks, which start from the first floor and get larger in the attic. This differential settlement has probably to be related with the construction of the nearby buildings after the ancient foundations had set.

Nevertheless, these settlements and consequent cracks are not particularly worrying, both for their limited entity and for their position. The monitoring of their evolution seems sufficient to guarantee the required safety for the building.

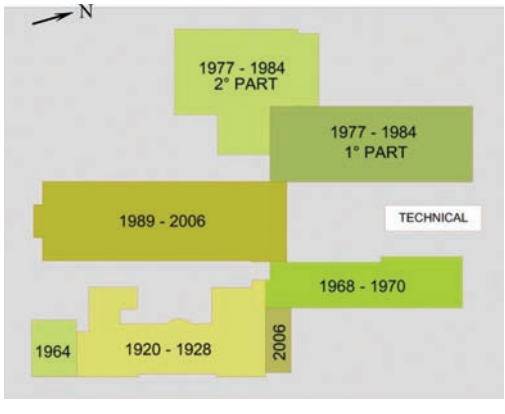

Figure 1. Plan of the entire complex and of construction phases.

Figure 2. Particular of the differential settlement in the main masonry building, on the façade.

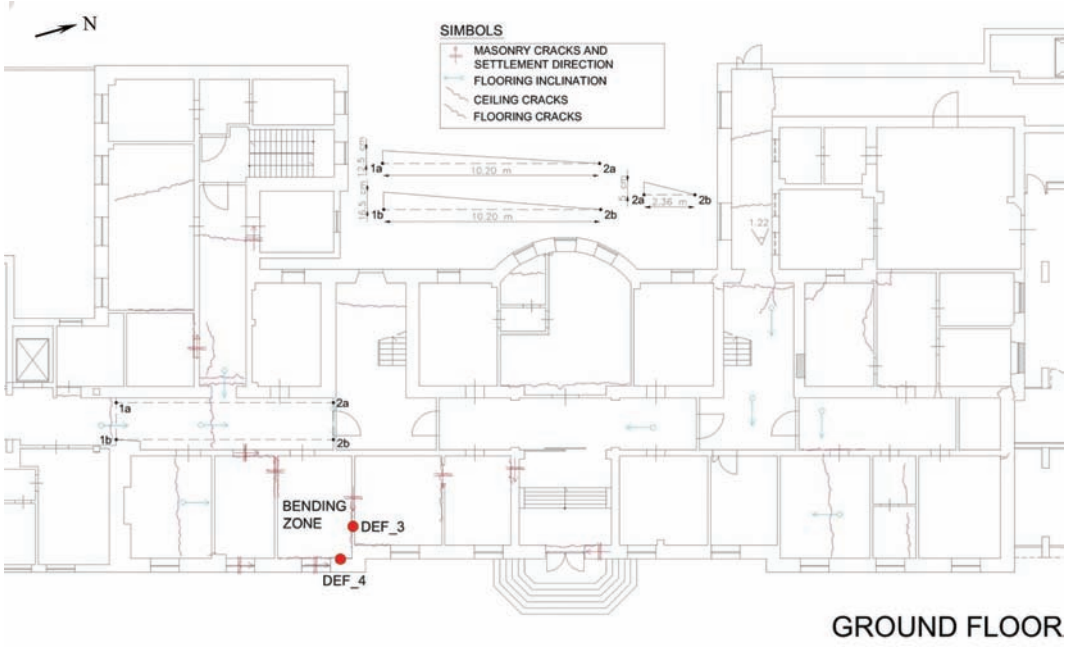

Figure 3. Plant of the building and sketch of cracks.

On the contrary, the south side shows a much more intense and concentrated crack pattern. Indeed, under the adjacent concrete enlargement built in 1964, a large water leak occurred in 1993: about 6 m^3 of water a day came out from the hydraulic system pipes for several months before the leak was discovered and fixed. Nevertheless, the concrete portions (1964 and 2006 blocks in Fig. 1) of the building show no sign of settlements. The adjacent masonry building, on the contrary, was deeply affected by this leak and since it was stopped, cracks and deformations started to develop and increase, causing difficulties in closing doors and windows, which had to be fixed several times in the last two decades.

As shown in Figure 3 the cracks are concentrated in the south-west area of the ancient masonry building, near the joint with the concrete enlargement. More specifically, the crack pattern denounces a settlement under the foundations of the spine walls in the part which is closer to the leak source, while moving eastwards the settlement signs, with inclined cracks, move on the external south-east wall and then disappear after about half the facade. The point of maximum differential settlement appears to be the corner of the external wall, next to the recess. No cracks related to this settlement have been found in the attic: the masonry developed a self-defense mechanism, creating a natural relieving arch, which has its key in the horizontal cracks at the first floor.

The floor at ground level also shows deformations connected to the settlement: along the corridor, a 16.5 cm droop was measured over a 10 m length, while across the corridor the droop reaches 5 cm over a 2.36 m width. It looks like the settlements follow the ground inclination, as probably the water did during the leak (Fig. 3).

4 THE MONITORING SYSTEM AS BASE OF THE "OBSERVATIONAL METHOD"

In order to fully understand the damage observed in the analyzed building, the evolution of its instability and cracking phenomena has been recorded by a digital monitoring system, capable of automatically detecting, with a frequency of 6 hours, even extremely small movements, far below the significance thresholds.

Currently, the movement of the structure is controlled by 7 extensometers, installed on September 2011, on the main cracks (Fig. 4)

Each instrument (displacement transistors inductive types, with a precision of +/–0.02 mm) (DEF_n), has an integrated datalogger, able to store—at predefined intervals—the amplitude of the crack. In addition, the instrument measures

Figure 4. One of the monitored crack, strictly related to the subsidence phenomena (DEF_3 at the ground floor).

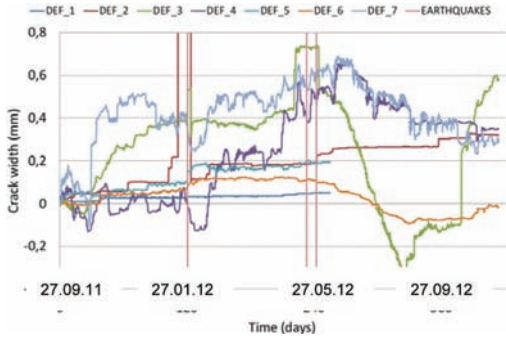

Figure 5. Data recorded by the 7 extensometers installed on the building. Vertical red lines are drawn in correspondence to the traumatic events occurred during the measurement period.

the air temperature (Tam-Dn, with a precision of +/–0.05°C), in order to correlate the evolution of the crack to the well known thermal dilatation phenomena, typical of masonry buildings.

The acquisition system registers data every six hours, starting at 6.00 a.m. every day. At the moment, almost one year data, recorded from September 27, 2011 to date (about 1500 measures/year, for each instrument) are at our disposal.

Despite its simplicity, the above described monitoring system is significant, once referred to other analyses carried out on the monument.

The preliminary analysis of data recorded from September 27, 2011 to November 21, 2012 allows to advance some hypotheses on the behavior of the monitored cracks, also considering some exceptional events occurred during the observation period (in particular, the seismic events on January 27, 2012 and on May 20 and 29, 2012).

Despite the monitoring period is not so long—it reaches the minimum duration of 1 year, which represents the minimum period of observation needed to fully understand the behavior of cracks in relation to temperature variations—the high frequency of measurements and the deep knowledge path carried out on the building, allow to argue some preliminary considerations.

The data recorded by the 7 instruments are plotted in Figure 5. The analysis carried out so far unraveled a steady pejorative increasing in cracks size and, at the same time, a relation with environmental variables (especially temperature).

The registered data have been compared to the traumatic events suffered by the building during the last year (in particular the rainfall event on October 25, 2011, characterized by a rainfall depth of 161 mm in 24 hours, and the earthquakes of January 27, 2012, at 15.53 (M 5.4), and the two followed, on May 20 and 29, 2012).

As represented by diagrams in Figure 5, all the cracks show opening trends, whose gravity is variable in function of their position.

The instruments most directly involved in the settlement phenomenon affecting the south corner of the building are DEF_3, which is positioned near the main entrance, DEF_4 and DEF_7, which are positioned on the east side of the main body, at first floor and at the attic level, respectively. All these extensometers show a pretty significant opening trend of about 0.7 mm/year, which demonstrates that the differential settlement mechanism is still ongoing.

This fact confirms how the foundation settlement is the main cause of the building instability and of the evolution of the cracks.

In particular, the data recorded by the instrument DEF_3, just above the area most affected by settlements (Fig. 6), are very significant for the evaluation of the phenomenon. Despite some anomalies (jumps of measurement), probably due to extraneous agents not imputable to proper mechanical reactions, the analysis of the data shows an overall trend in opening of about 0.3 mm/year.

The same behavior can be retraced for the instruments DEF_4 and DEF_7, both controlling the same movement, at two different levels. It has to be noticed that the cracks do not seem to highlight a significant response to the seismic events occurred during the period of observation, with the exception of the instrument DEF_5, at the first floor, which highlighted a jump of 0.05 mm (on a global trend of about 0.2 mm/year) after the earthquake of January 27, 2012 (Fig. 5).

Longer monitoring (at least two years long) may highlight side effects, certainly present, as the temperature changes, on the performance of lesions allowing a purification of the data and a more precise assessment of the overall trend.

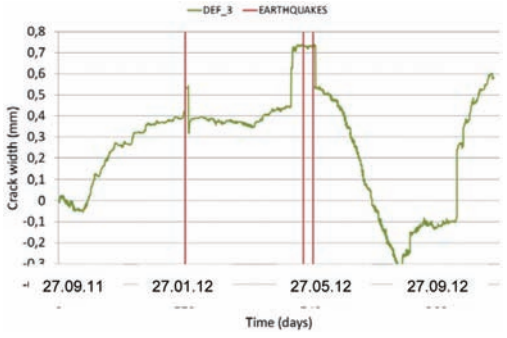

Figure 6. Data recorded by extensometer DEF_3, positioned on the south corner at ground floor. Vertical red lines are drawn in correspondence to the traumatic events occurred during the measurement period. Despite some anomalies, the graph evidences an opening trend of about 0.3 mm/year.

5 GEOTECHNICAL INVESTIGATIONS

The geological formations of the area are defined as clayey-calcareous and have a complex origin. They are generally composed of clay and shales with abundant calcareous, marly or arenaceous inclusions. In order to determine the soil profile and the relevant subsoil mechanical parameters, results of past investigations were gathered and a new site investigation was planned in April 2012. In particular, three soil borings (S2, S3 and S4) had been carried out in 1968, while boring S1 has been performed in April 2012. A sketch of the plan position of the four borings with respect to the studied building is reported in Figure 7. Figure 8 shows the soil profiles obtained by the four borings.

During the S1 boring, samplers producing either disturbed or undisturbed samples have been used. The soil profiles obtained from borings S1 and S2, which are near the area of interest, can be described as follows: beneath a layer made of asphalt pavement, base and sub-base material (as), there is a first level of gray/brown silty clay (from –1.20 up to –4.35 m) with few millimetric gravel inclusions; a second level of wet gray/brown clayey silt (from –4.35 up to –7.10 m) with abundant millimetric gravel inclusions; a third level of stiff clayey silt (from –7.10 up –11 m, with different wet conditions); a level of sandy silt (from –11 up –17 m); a new level of stiff clayey silt (from –17 up –25.7 m); a thin level of sandstone (from –25.7 up to –26.9 m) and a level of shale (from –26.9 up to –30 m). The stone wall building foundation is based at –2.5 m from ground level.

In order to obtain the geotechnical characterization of the subsoil, both field and laboratory tests have been carried out.

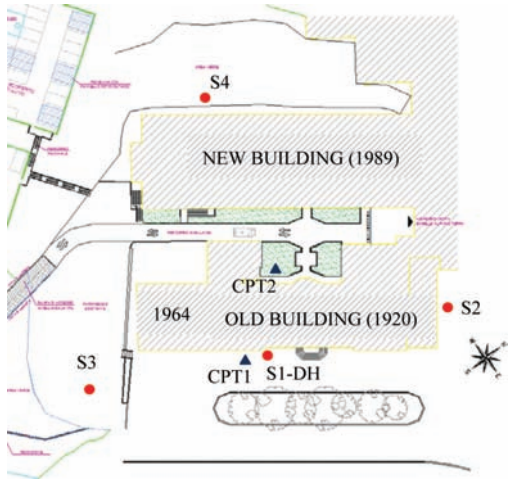

Figure 7. Position of field tests with respect the building.

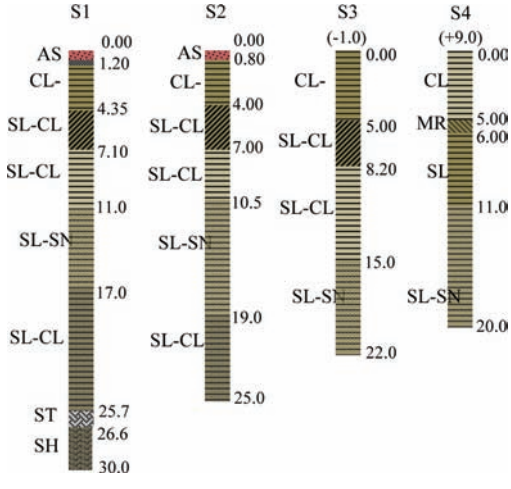

Figure 8. Sketch of the four borings. Asphalt pavement, base and sub-base material (as); gray/brown silty clay (cl-sl); wet gray/brown clayey silt (sl-cl A; sl-cl B and sl-cl C); sandy silt (sl-sn); sandstone (st); shale (sh).

5.1 *Field tests*

The mechanical characteristics of the soil have been investigated through the execution of two cone penetration tests (CPT). Given the stiffness of the subsoil, some technical problems were encountered during the execution of these tests. The position of the two investigation points is reported in Figure 7. The results obtained are reported in Figure 9. By assuming the ground level with z = 0 m in point S1 (Figure 7), the results of CPT1 are not relevant from 0 m down to 1m in depth, since this first layer

is made of asphalt pavement, base and sub-base material; moreover, given the stiffness of the soil, it was impossible to carry on the CPT1 over than 5.5 m in depth. On the back of the old building, the presence of a filling soil 2 m thick, allowed to carry out the CPT2 from the ground level down to 6.5 m (Figure 7). It must be underlined that between the investigation point of CPT2 and that of CPT1 there is a slope and a difference of level equal to 2 m. That's why results of CPT2 reported in Figure 9 include 1.5 m above the reference ground level.

One down hole (DH) test has been also carried out in correspondence of the S1 borehole (Figure 7), in order to obtain the velocity profile of both shear waves (V_s) and compression waves (V_p). The obtained results are reported in Figure 10. It is well known how these measurements are fundamental in the evaluation of the elastic properties of the subsoil.

5.2 *Laboratory tests*

Both undisturbed and disturbed soil samples were taken at different depths in the S1 drilling. In particular, an undisturbed sample (S1C1) and a disturbed sample (S1C2) have been subject to laboratory tests, in order to obtain the geotechnical classification in terms of grain size distribution curves (Figure 11) and Atterberg limits (Table 1). The swelling/shrinking potential has been evaluated on the basis of the activity index (A = PI/CF, where

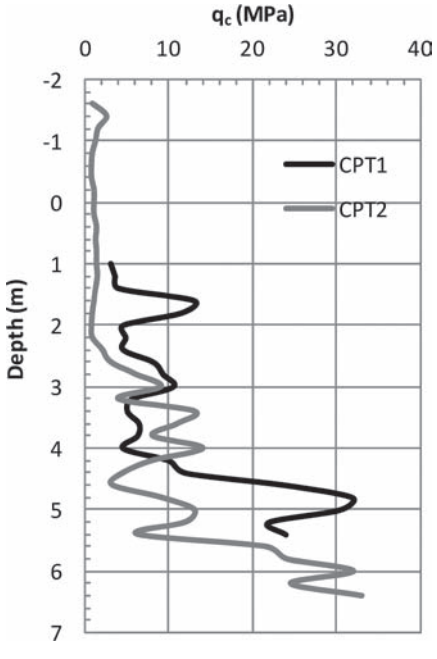

Figure 9. Results of cone penetration tests.

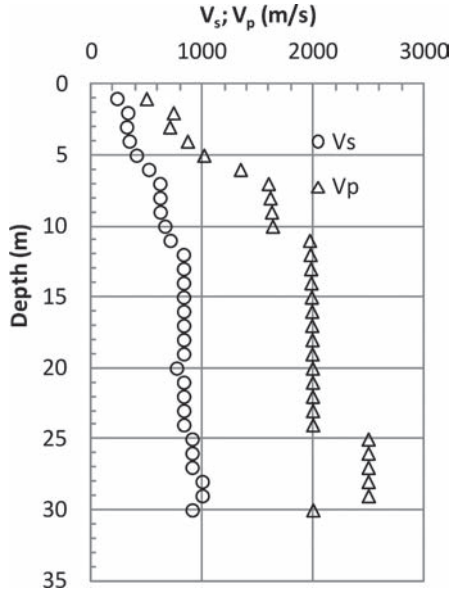

Figure 10. V_s and V_p measurements by down-hole test.

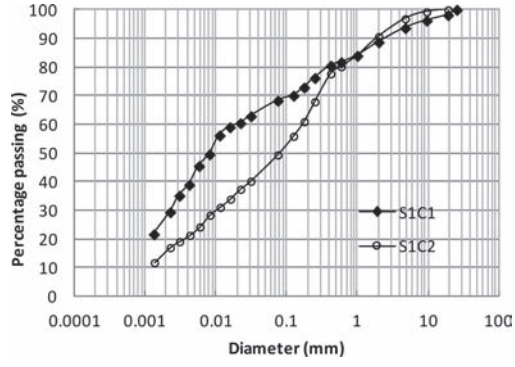

Figure 11. Grain size distribution of samples S1C1 and S1C2.

Table 1. Properties of soil samples.

Sample	z m	Gs –	G %	S %	M %	C %	w_L %	IP %	A –
S1C1	5.10	2.76	11	22	39	28	42	22	0.78
S1C2	14.3	2.75	9	44	31	16	28	11	0.68

CF = Clay Fraction (%)): sample S1C1 presents a medium to high level of activity, while sample S1C2 presents a low level of activity (Lancellotta, 2012). This characteristic can be related to the seasonal fluctuation of crack width observed by DEF_3 (Fig. 6).

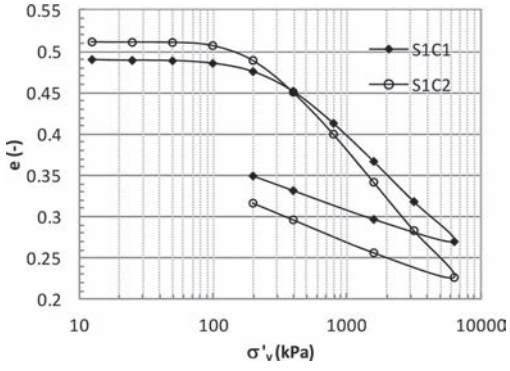

Figure 12. Oedometric test results on samples S1C1 and S1C2.

The two samples have also been subject to oedometric compression tests (Figure 12) and only the undisturbed (S1C1) sample was subject to standard triaxial compression CID tests (Figure 13). In particular, Figure 13b highlights how, during triaxial compression tests, a cycle of unloading and reloading (at $\varepsilon_a = 1\%$) has been carried out, in order to obtain the elastic properties of the material.

Soil profiles (Figure 8) and results of laboratory tests on the soil samples (Table 2) suggest the presence of a slightly preconsolidated soil layer within the first horizon, while the deeper horizon appears normally consolidated. Oedometric parameters obtained are reported in Table 2.

6 CONCLUDING REMARKS

It is more and more evident that, especially for monuments, detecting in time the effectiveness of restoration and strengthening interventions before making them definitive, is really desirable. Too many times, in fact, past interventions have resulted not only ineffective but even dangerous for historical buildings.

In step with this, the monitoring analysis, the more reliable the longer is the period of data collection, is able not only to provide a real-time control of the structure but also to verify the effectiveness of the proposed reinforcement or strengthening interventions. Before making them long-life, designed reinforcements can be validated and calibrated through the well known "observational method".

Indeed, monitoring analysis, joined to a deep knowledge path on the examined building, could represent the first guarantee of the "principle of the minimum intervention", fundamental in the field of restoration. In fact, it is possible to pursue it only using and exploiting the carrying capacities of the existing structures, rather than distorting

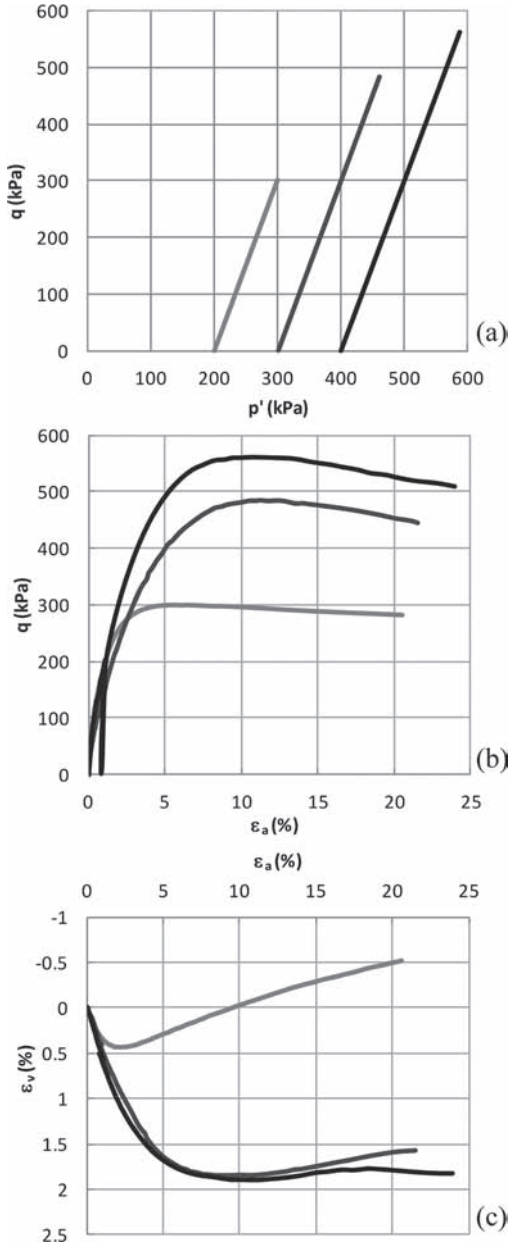

Figure 13. Triaxial test results on sample S1C1.

Table 2. Oedometric properties of soil samples.

Sample	γ kN/m³	e_o –	σ'_p kPa	OCR –	c_r –	c_c –
S1C1	20.8	0.491	350	3.3	0.041	0.159
S1C2	20.7	0.513	300	1	–	0.211

them or substituting them with new elements. In order to do this, a reliable knowledge of the past and present structural behavior of the buildings is needed (Roca, 2004).

The study presented in this paper has been oriented to gather all the information needed for a correct analysis of the damage evolution, in order to later calibrate and validate possible strengthening and reinforcement interventions. It can represent a general methodology, particularly suitable for ancient monument retrofitting strategy, which, in a multidisciplinary approach, finds it primary guarantee of success.

About the choice of the geotechnical investigation tests, it appears fundamental to underline the importance of field geophysical tests. It is well known, in fact, that seismic exploration tests represent a special class of field tests, thanks to their non-invasive character (Lancellotta, 2010). This allows the preservation of the initial structure of soil deposits as well as the mechanical characterization of soils that are difficult to be sampled. Furthermore, soils are tested at small strain level and, for this reason, it appears reasonable to analyze the results of these tests in the light of the wave propagation theory in elastic materials (Lancellotta, 2010).

In the analyzed problem, since undisturbed sampling was possible only for the shallow soil layer, strength and deformation parameters have been obtained partly by laboratory tests, partly by in situ tests.

Notwithstanding a proper design of any reinforcement intervention has not yet carried out for the analyzed case study, the described adopted methodology represents the "ground rule" for a subsequent numerical analysis of the soil-structure interaction. Numerical methods, in fact, are particularly appropriate when, due to the complexity of the problem, an approach based on simplifications is not practicable. Nevertheless, it is of the utmost importance to validate the numerical model through in situ measurements, in order to assess its reliability in capturing the real behavior of the considered engineering problem. Results of the monitoring can also be useful in calibrating and verifying the numerical model.

In perspective, further studies will be focused on finite element numerical modeling of the analyzed problem. The numerical model, in its turn, will be useful, in order to define a possible intervention strategy, also accounting for all the limitations given by the particular conditions of the site and by the conservation of the structure. At last, the physical constrains to the technology to be adopted, such as the need to operate in tight inner rooms at ground level, should not be disregarded.

ACKNOWLEDGEMENTS

The authors would like to express their gratitude to Prof. Carlo Blasi, coordinator of the global research on the building of "Ospedale Santa Maria", and to the USL Agency of Parma, for the financial support of the present research.

REFERENCES

DL 22/01/2004, n. 42 Codice dei beni culturali e del paesaggio (ART.10 L. 6/07/2002, n. 137).

DPCM 2011. Direttiva del Presidente del Consiglio dei Ministri (2011). Valutazione e riduzione del rischio sismico del patrimonio culturale con riferimento alle Norme Tecniche per le Costruzioni di cui al D.M. 14/01/2008.

Lancellotta, R. (2010). Geotechnical aspects related to the preservation of the Ghirlandina Tower. In: Cadignani, R. (edited by) The Ghirlandina Tower: conservation project, Luca Rossella Editore, Roma.

Lancellotta, R. (2012). Geotecnica, Zanichelli, 4th Edition.

Roca, P. (2004). Considerations on the significance of history for the structural analysis of ancient constructions. In: Proc. of 4th Congress Structural analysis of historical constructions, Balkema, Amsterdam, 63–73.

Rossi, P.P. & Rossi, C. (1998). Surveillance and monitoring of ancient structures: recent developments. In: Proc. of 1st Int. Congress on Structural analysis of historical constructions SAHC1998, Barcelona, Spain.

Geotechnical Engineering for the Preservation of Monuments and Historic Sites – Bilotta, Flora, Lirer & Viggiani (eds)
© 2013 Taylor & Francis Group, London, ISBN 978-1-138-00055-1

Geotechnical investigation and stabilization of the foundations of a World Heritage in Portugal, the Guimarães Castle

A. Viana da Fonseca, A. Arêde & E. Paupério
Department of Civil Engineering, Faculty of Engineering, University of Porto, Portugal

A. Costa
Department of Civil Engineering, University of Aveiro, Portugal

ABSTRACT: Conservation and restoration of monuments and historical areas are disciplines that require specific training. The forts and castles are among these monuments that present high complexity due to the elevate nature of the forts. Each fort and castle has distinctive engineering and architectural features that turn its study a challenge. In this paper, the methodologies followed in the studies and investigations on ancient forts carried out at University of Porto are briefly presented. Studies concerning forts with Portuguese legacy are presented. In particular, a specific study is presented focusing on the rehabilitation of foundations and walls of Guimarães castle in Portugal. Preliminary diagnosis of the castle walls has shown important pathologies in two walls, one of them located in the north tower where apparent cracks and joint openings were clearly visible. In the latter, the cracking pattern was consistent with possible foundation movements that were found likely to be responsible for wall corner rotation which induced signs of stones' crushing in the wall base in contact with the foundation rock mass. An assessment of the causes of the appearance signs of holes or torn threads in the exposed face of the wall and tower of the extreme southwest of the castle was done, after the site survey with geotechnical laboratory tests. The intervention performed was focused both on the foundation and the walls, starting by the foundation stabilization by nailing a set of high-strength blocks of rock mass and careful sealing of the massive network of high strength and consolidation of the most altered and fractured. Subsequently, the wall cracks and joint openings should be repaired, but structural monitoring was started beforehand in order to control any possible movements both during the geotechnical works and for a three year long period after repairing cracks and joints. Construction issues including logistics and problems found are described, as well as the main outcome of the monitoring process and the finally adopted structural interventions.

1 THE GUIMARÃES CASTLE

1.1 *The history*

The Castle of Guimarães was founded in the Xth century by the countess Mumadona Dias, on the summit of Mount Latito, for the defense of the monastery of Guimarães and the adjacent roads. The first castle was constructed in the granite mass outcrops overlaying a large plane area. Additional excavation and leveling work contributed to set up a defensive position already very favorable. From this primitive fortress, however, nothing survived to our days. The oldest traces still remaining are of the castle end of the XIth century, contemporary of the Earls Henry and Teresa with a Proto-Romanesque style characterized by an apparatus with large ashlars granite with irregular sizes, all around this area, being the northwest angle the most pronounced, and to an even greatest extent the north side, facing the field of S. Mamede, where, outside the Gate of Treason, there is a great shoe formed by five rows of large blocks.

In an ulterior stage, the in plan architecture definition of the castle was modified to a shield form, with some further changes until present times. During the reign of Afonso Henriques, first king of Portugal (1143) the architecture was Romanesque style, characterized by a more versatile structure than the previous one, using smaller ashlars disposed in regular rows. This fort had not yet Romanesque flanking towers (Figures 1 and 2), nor the donjon, which were built later on, during the reigns of kings Afonso III and Dinis. Eight quadrangular towers were therefore added around the primitive one, as well as the castle that donjon, built by 1258 in the center of the interior courtyard.

In the third (Gothic) phase the southwest corner of the fence was reviewed, by advancing the Castle village walls built between 1265 and 1318. The

Figure 1. A partial view of the medieval Guimarães castle (http://pt.wikipedia.org/).

Figure 3. View of the watchtower in the interior medieval castle of Guimarães (http://pt.wikipedia.org/).

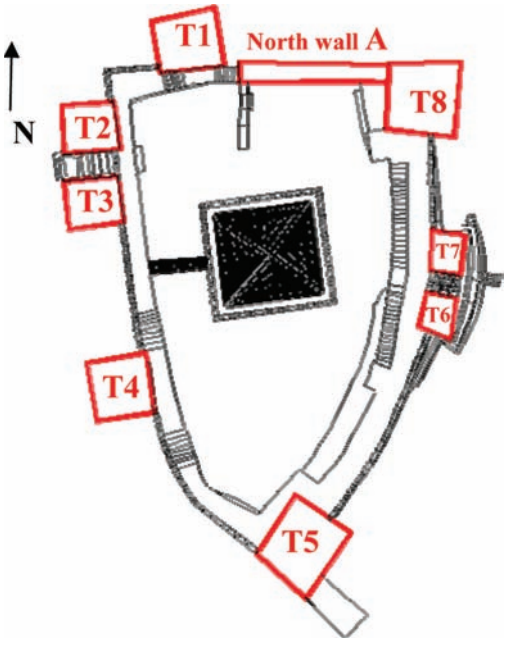

Figure 2. Plan view of the medieval Guimarães castle.

weight of the tower which stood up, forced that door to be closed. For the usefulness to the people, a new door was later opened in the same fence, but on the opposite side of the fortress.

The radical change in military tactics, motivated by the introduction of balistique, determined the beginning of the fortress decay; fortunately, however, such decay was sustained in time. The castle has a shield-shaped plan, with eight square towers flanking the center wall and the keep, also quadrangular and about 7.5 m high, all elements being crowned with triangular merlons in monumental granite. The wall runs along or around almost the entire perimeter, as well as a battlement, only interrupted in the area of the Palace of Mayors. Two ports, each of them flanked by two towers, provide access to the interior courtyard of the castle: the gate of the village, facing the city, and the Betrayal, in open field to S. Mamede. Inside, stone stairs of battlement on the front door of the keep, get close to (around 1 to 2 meters from the ground) a wooden walkway (Figure 3). Also in the donjon and battlements are visible along the stone corbel that originally supported the defensive structures of wood, "hurdes" or blocks. Located in the center of the parade ground, the Watchtower has square plan, with few openings to enlighten the floors which are connected by internal staircases made of wood and stone. The Watchtower, also crowned with pentagonal sharp battlements, allowed for continuous movement and observation at the top of the tower.

1.2 *The pathologies and call for the intervention*

During the last century, starting in 1936, the Portuguese National Directorate for Public Buildings and Monuments (DGEMN, http://www.monumentos.pt) made several restoration works on this monument, a priceless National Heritage piece intrinsically associated with the Portuguese nation foundation in the early days of the XIIth century, whose walls are considered as "*the shell of a soul satisfying love and respect*". The works ended in 1971, having consisted of walls' consolidation, main door restoration, replacement of masonry pieces, demolition of "newly built" elements and reconstruction battlements, stairs, parapets, wall panels, etc.

In November 2008, the Portuguese National Institute for Built Heritage and Culture Preservation

(IGESPAR, http://www.igespar.pt/en/), that replaced the former DGEMN, requested the University of Porto (IC-FEUP) to make a structural appraisal of the Guimarães Castle. In particular, special attention should be given to the apparent cracks and joint openings developed in the North exposed façade wall and tower (Figure 4a), for which a solution should be proposed accounting for damage control and repair.

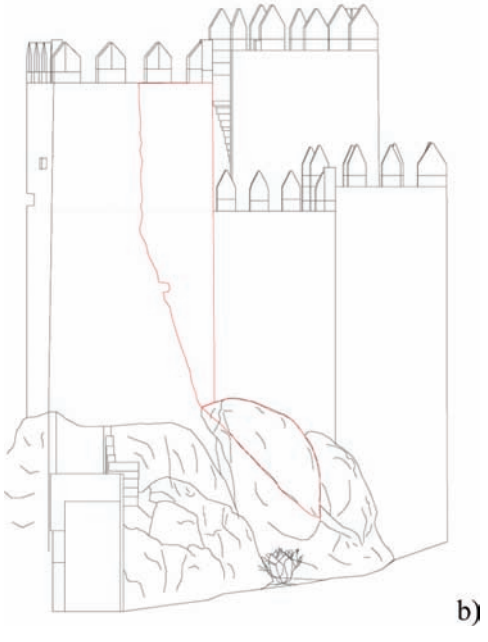

Figure 4. a) Damaged North tower, façade wall (left side of picture) and corresponding foundation; b) scheme of the destabilized foundation discontinuities (Viana da Fonseca, 2008).

Detailed in-situ surveys allowed evaluating the structural pathologies and identifying the inherent causes. The tower illustrated in Figure 4a, presents joints' opening developing from the apex on the rightmost base of the tower, forming a wedge-shape detachment (Figure 4b) consistent with foundation motions composed by vertical sliding with rotation. At the tower structure level, these base motions generated the rotation of the right tower corner along the Northwest direction, as evidenced by a sub-vertical crack with significant expression (Viana da Fonseca, 2008). On the tower North face, joint opening and cracks were quite large, with some losses of stone material and evidencing crushing by compression due to stress increase caused by the wedge rotation.

The ground that supports the foundation of this tower, and specifically of this wedge, is a rocky system with an outcrop of around 3.5 m above the surface which presents a clear fracturing system and a high degree of weathering, more intense in the base. The position and orientation of the system of discontinuities, explains fairly well the orientation of the masonry cracking pattern, especially along vertical joints in the North side of the fort as illustrated in Figure 5. Therefore, from the performed analysis, where the geological-geotechnical studies have played an important role for understanding the structural mechanisms, it was concluded that a previous cutting of the rocky outcrops might have been responsible for the instability verified in some of these outcrops. Historical investigation showed that such operations were made in the 1940's in the framework of urbanistic arrangements to enlarge the view of the fortified masonry. This situation was found particularly serious since these rock

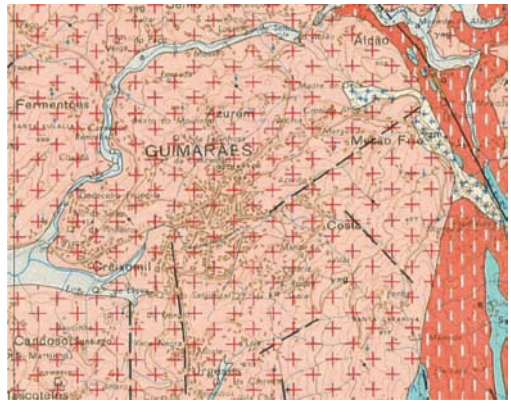

Figure 5. Leaf extract 9 B—Guimarães. Geological map of Portugal.

formations support the foundations of the towers and the adjacent walls of the castle.

In this context, the geotechnical intervention consisted in the insertion of a well selected high resistance nailing system, that could allow for stabilization of blocks and boulders of the rocky ground jeopardized by the unconfinement. The execution of a thorough net of nails sealed in the high resistance rock masses, aimed at avoiding the mobilization of the most weathered and unstable masses, which would be responsible for additional movements and settlements, responsible for the structural damages. The identification of the weak planes and fractures was the main concern of the geological-geotechnical studies, which were developed under the supervision of the geotechnical laboratory of FEUP (Viana da Fonseca, 2008). Both interventions were done, with the purpose of maintaining or recovering the initial repos conditions, without jeopardizing the original 8 century architecture or its structural behaviour, for what it was decided to minimize as much as possible the ulterior works, namely the execution of prebored holes to insert the nails.

2 GEOLOGY

2.1 *Geological features*

Excluding the thin siliciclastic surface deposits of Cenozoic age, all the other mapped lithologies (granite and metamorphic rocks—high grade schist, gneiss and migmatite) are part of the basement which is strongly deformed and metamorphosed during the variscan orogeny (Devono-Carboniferous). In fact, the main features of regional geology are mainly due to the variscan orogeny and strongly marked by the closeness to a main tectonic suture between two geotectonic zones: the Ossa-Morena Zone and the Centro-Iberian Zone, which was a major crustal transcurrent shear zone during the variscan times (e.g. Ribeiro et al., 1990). The pervasive metamorphic foliations in the country rocks and, in some extent in the granites, are consequence of these tectonic events. The schists, gneisses and even migmatites are the metamorphic correspondents of a former thick sedimentary sequence of graywackes, mudrocks and conglomerate levels named Schist and Graywacke Complex. The main granitic body at the site is interpreted as the result of crustal partial melting during the variscan orogeny. The proximity to the major crustal shear zone (Porto-Tomar), a plate boundary of Cadomian age (Viana da Fonseca et al., 2006), separating the NE Central Iberian Zone from the SW Ossa Morena Zone—and its tectonic activity during the variscan orogeny favored the crustal melting and the ascent of granitic magmas.

The upper zone of these basement units are frequently strongly weathered, forming often a saprolite level with variable thickness, overlaid by a thin layer of soil and antropic materials, the most common surface and subsurface material in this region. There are some fresh outcroppings of basement rocks, but usually there is a thin upper layer of soil of varying thickness, overlaying more or less weathered granite contacting an older gneissic migmatite with dominant sub-vertical foliation. However, it is not rare to have some weathered granite zones with wide irregularities, with common blocks of sound or partly weathered granite, with various dimensions involved in high to extremely high weathered masses.

2.2 *Geological particularities*

The presence of those granite blocks is related to geological structures such as fractures, foliation or faults, where water can easily flow into and through, accelerating chemical weathering processes. They can be reasonably determined when a careful and rigorous geological-geotechnical site investigation campaign (involving the all excavated volume, both in area and depth) is carried out into the boreholes net, in order to construct a reliable geological-geotechnical model.

The study area is characterized by granite formations, whose matrix corresponds to a calc-alkaline granite two-mica biotite with predominant porphyritic texture with frequent, sometimes gneissica. The study area is mapped at the scale

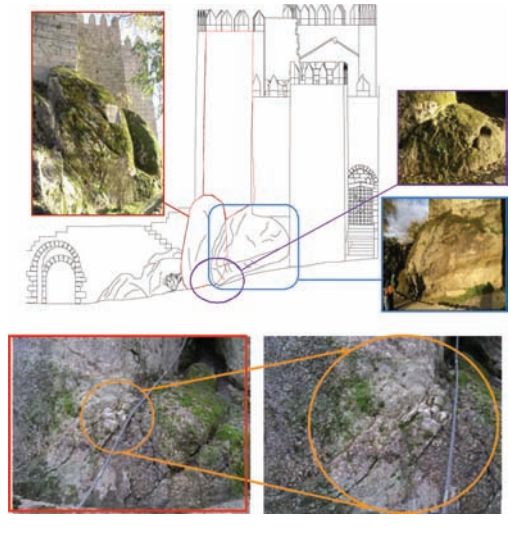

Figure 6. Detail of the fracture system of the rock masses in the foundation (Viana da Fonseca and Cruz, 2010).

1:50 000, the sheet 9 B—Geological map of Guimarães in Portugal, edited the Geological Survey of Portugal (Figure 5).

An emphasis is due to the importance of masses of rounded blocks, consisting of granites low weatherin levels (W2), included in sound granitic masses. The characterization of surfaces of discontinuity contained in the unstable blocks (Figure 6) was first made in a field survey and drilled cores. Details of this characterization are available in Portuguese.

3 STABILIZATION AND REINFORCEMENT

3.1 *Implemented solution*

After studying various solutions that could be implemented in this case and taking into account the constraints of the site, a set of reinforcement measures were proposed that, at first glance, would ensure the stabilization of the rock mass above the large fractured block by nailing the passive feature (in number identified below in the text and spaced 1.5 m in triangular layout). These passive nailing were designed to strengthen the massif, profiting from its self-supporting capacity, attaching with these linear inclusions high strength large and massive blocks. The methodology led to the execution of passive anchors, which tend to tide specifically blocks potentially unstable. These were constituted by steel rods sealed with cement grout in boreholes previously executed. The arrangement of the nailing system was made according to the geometrical distribution of the discontinuities and faults and the corresponding gravity forces involved, and were installed in accordance with the necessary lengths to avoid the development of sliding movements. Their arrangements and lengths were modified by the Project depending on the conditions and quality of rock identified during the borehole coring. Being aware of unforeseen circumstances, additional nailing execution was implemented at certain locations where weak features revealed lack of mass stability. The nailing holes were installed in advance and executed at specified depths in the design drawings. These depths were adjusted in accordance to the rock cores classification. Their diameters had to ensure better handling for filling the holes with grout by injection. The perforations were inclined to the horizontal in accordance with the drawings. The minimum diameter of the holes was 40 mm above the diameter of the nails, then, with a minimum of 87 mm, for high strength steel bars of 47 mm diameter (see below). These high resistance steel nails (high-strength steel, type Y1050H from Dywidag® with a tensile strength of 1050 N/mm^2) were sealed with selective and repetitive injections in the area of fractures and faults, but also in the rest of the involved areas, looking to fill other discontinuities which would be identified in the drilling process for nail installation. To this purpose, the drilling procedure (conducted by rotary core drill with integral sample extraction) enabled the designer to analyze the geomechanical characteristics of the underlying massive ground, including large blocks ("balls" or "boulders" with low weathering degree) to be fixed, and filling weathered rock masses (more altered) or discontinuities (faulty planes) with grout, giving particular relevance to the massive under the walls.

The holes were cleaned of all drill cuttings, sludge and debris displayed during rotary coring, by means of air or water flow injection. The integral rotary technique that was used to make the holes for the inclusion of the steel bars had also the advantage of not transmitting significant vibrations to the structure. This drilling was deep extended so that the sealing lengths could ensure a safe embedment in the sound rock (W_2 to W_3 according to the classification of ISRM, 1981) as defined above, which was decisive for the ongoing monitoring of drilling registration. This was complemented with enough drilling extension to ensure the contiguous block nailing and its attachment to the base. The installation of nailing was performed immediately following the drilling and hole preparation, within a maximum of 3 hours. Finally, the whole mass was sealed with micro-cement underlying the two major granite balls (identified in Figure 6). The space between the two blocks would still be filled with structural material cemented due to capping of the original stone material.

It is considered that nailing subject to cutting forces, should be introduced through the upper surface of the block, near the area of the foundation close to the walls, and that drilling openings should be spaced 1.5 m of the edge line, looking for a layout that was as orthogonal as possible to the gap plane (see schemes in Figure 7).

The nailing elements to be adopted should consist of steel bars of high resistance so that they could establish the safety level imposed by design criteria an in number compatible with the available space.

Bars similar to "Threadbar®" Dywidag 47 mm nominal diameter were adopted, inserted in holes with diameters equal to or greater than 90 mm (drilled by rotation), sealed in its entire length with mortar, carefully filling the fractures and discontinuities with low pressures, but repetitive phases.

The design phase indicated that the minimum lengths should be 10 m.

The bars were single correction protection type, after evaluating the non-aggressive characteristics of the rock massive and the purity of the

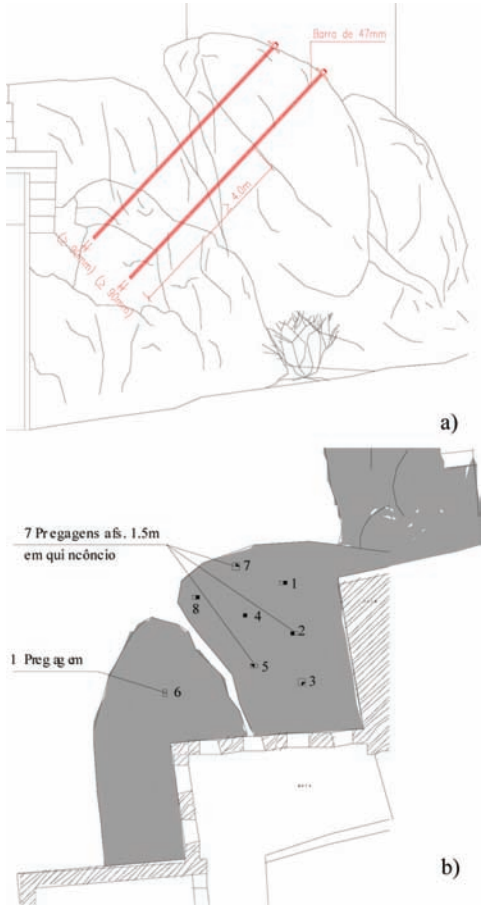

Figure 7. Scheme of nailing positioning: a) elevation and b) plan view.

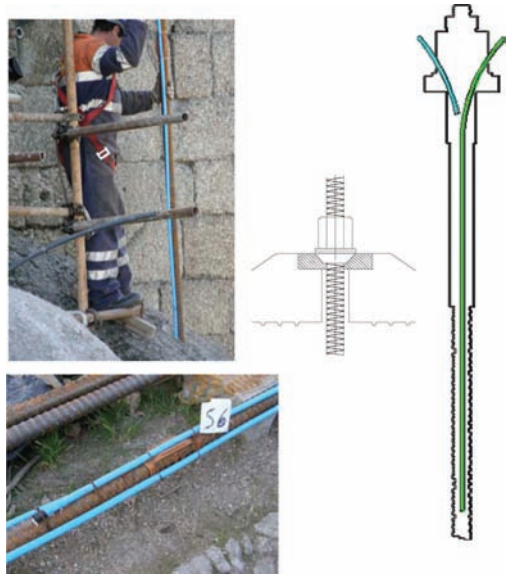

Figure 8. Scheme of the bar and pictures of installation.

underground water (see pictures in Figure 8 and schemes from http://www.dywidag-systems.com/).

These bars are coated with a corrosion inhibitor and, additionally, they were covered with cement grout in fully lengths, as described in what follows.

The injection procedure and inspection criteria are described below. The proposed intervention required continuous monitoring, needed to adjust the solution in terms of bars' length, arrangement and number, depending on the recognition of the solid and weathered rock zones. This monitoring by the designer in works of this kind must be, in fact, an assumption in such of geotechnical works.

3.2 *Execution of the works*

Figures 9 and 10 show some construction phases. Cement admixtures were prescribed to be made using an automatic or semiautomatic central system, comprising the following main components (see Figure 11):

- Electronic scale for the solid parts;
- The water tank;
- Primary high turbulence mixer (min. 1500 revolutions/min);
- Stirred tank and dispenser secondary volume for cement mixtures.

The work should be started by injecting upwards, according to the two following injection steps: a first step run by gravity purge tube up to the hole mouth; the second step, immediately performed, by pressurized injection with volume control (accompanied by a careful check of any upwelling sign). Two different injection types should be considered: injections in rock masses of good quality and injections in very altered rock masses and/or fractured soils.

The injections were performed with cement grout with a water/cement ratio (A/C) between 0.4–0.5 to achieve the pressures that ensured the land consolidation and good sealing of the steel rods.

The first hole injection was used to assess which solution type should be adopted and how the injections should be made. For the treatment of the foundation mass, in the presence of soils or soft soils' areas and highly weathered rock masses, selective and repetitive injections were applied in some specific sections.

The injection pressures should not exert the maximum admissible level and should be reduced as the injection rate increased. The maximum pressure

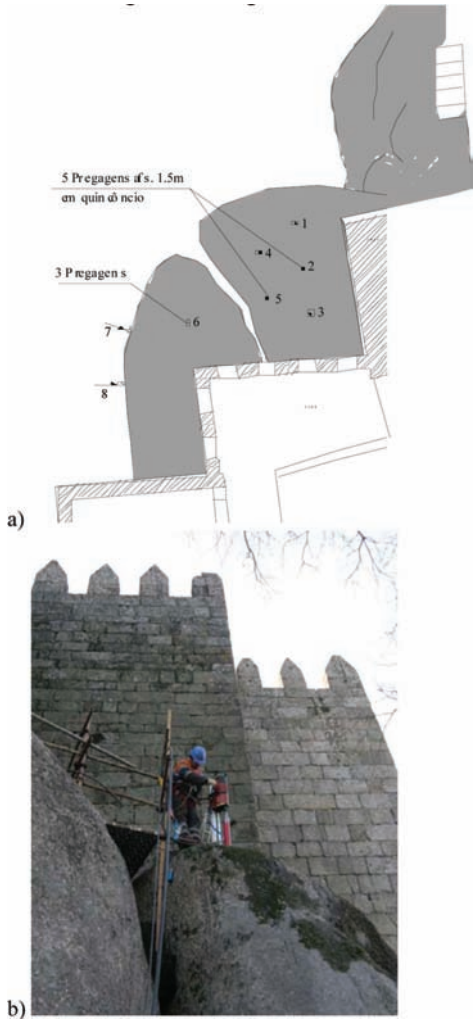

Figure 9. a) Nailing positioning, plan view and, b) drilling nailing 6, crucial for load transfer of this block.

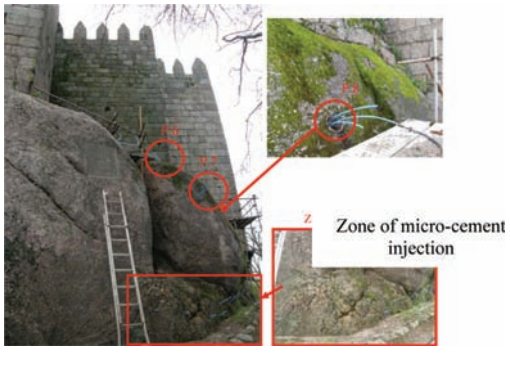

Figure 10. Arrangement of nailings and zone of consolidation with micro-cement.

Figure 11. Central preparation of cement mixtures.

should only be reached when the rate of injection would be very low. Exception to this would be the opening the tubes valves ("manchettes" type) for pressures instantly exceed, less than 5 kg/cm^2, on the demand of the designer, adjust in preliminary tests for different compositions so that they worked within the allowable values.

Special care would be taken to avoid excessive injection pressure and high flow, so that when injecting the ground, the refusal was reached for an absorption maximum pressure, and when the volume filling the hole was less than 0.5 l/min.m for 10 minutes. The maximum pressure was then maintained for 10 minutes and the additional injection could be considered completed. Any limitations of pressure should be reported by the designer according to particular cases or observations made during the work (Figure 12). 24 hours after the sealing operation, all the holes were inspected, checking the depth at which the grout is seated in relation to the mouth of the hole, being refilled until the hole is completely sealed. The rods had a length sufficient to allow their connection by welding rod to a circular plate with 12 mm thick. The plate sat on a surface perfectly equalized, assuring the fixation of the top.

Figure 12. Multiple works in the repetitive injections.

Figure 13. Sealing and application of pre-adjustment force, 40kN, with torque wrench.

Figure 14. Stabilization of the North tower foundation.

3.3 *Pre-adjustment force after nail curing and natural stone closing*

It was further specified that after 14 days (curing time enough for the purpose), the rods would be set with a pre-stressing screw (low load, 40 kN), for the purpose of, firstly, determine the proper mass sealing provided by the adopted injection methodologies and, secondly, to confine the structural elements "sewing" the rock masses (Figure 13). Finally, all the holes' mouths where then closed with 200 mm diameter stone cores that were extracted and kept from the very beginning of hole drilling.

Later on, the space between the two rock masses was filled with large cemented stone blocks (Figure 14 left) which were then faced with dry stone masonry similar to the wall. At the base of the second block, where consolidation had been made with mortar and very fluid micro-cement—see above—a similar procedure was adopted (Figure 14 right).

4 STRUCTURAL MONITORING

The first impression gathered from the detailed survey of both the North tower T1 and the wall A (see Figure 2), suggested that structural interventions should be made to correct and stop the damage process.

However, after the geotechnical stabilization (concluded in February 2009) and before proceeding with any of the foreseen structural corrections, it was decided to monitor the structural behavior of tower T1 and wall A for a considerable period of time (not less than two years) in order to check for any damage evolution or, instead, to decide on its stabilization.

The tower damage was already reported and it was found essentially to involve cracks or joint opening/closure as well as possible global rotation of the northwest corner of the tower. As for the wall A, it was evidencing clear signs of out-of-plane North-South motion towards the castle interior, which was found to be due to lack of connection to the tower T8 and of any type of height wise bracing, thus rendering the wall to behave has a cantilever element.

Therefore, a continuous monitoring system was installed to evaluate and record the relative displacements (using electric crackmeters) and global rotations (resorting to electric tiltmeters) both in the tower T1 and wall A. For the latter, it was monitored the out-of plane displacement relative to the adjacent corner of tower T8, the vertical out-of-plane rotation of the wall and the relative displacement between the two masonry leaves composing the wall.

As for the tower T1, crack opening/closing was measured at four elevation levels (three zones in the North face and one zone in the West face) and the rotation was read by a bi-directional tiltmeter placed at the tower corner. Figure 15 shows the adopted types of sensors, namely the crackmeters

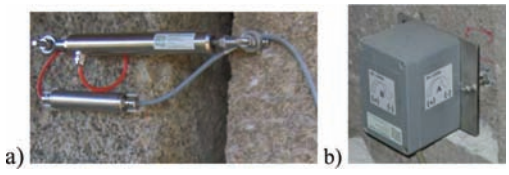

Figure 15. Instrumentation for: a) relative displacement (crackmeter) and b) rotation monitoring (tiltmeter).

(25 mm range) and the tiltmeters (+/– 3º range, relative to the vertical direction in two orthogonal vertical planes).

The instrumentation of the tower is illustrated in Figure 16, both schematically and by a corner picture capturing all the sensors located in the North and West faces. Besides displacement and rotation measurements, temperature sensors were necessarily included to account for thermal variations on sensor readings. Therefore, regarding Figure 16b, different tones ellipses indicate the locations of, respectively, four crackmeters (F1 to F4, in Figure 16a), one tiltmeter (C1) and one temperature sensor (T1).

Since the present paper just focuses on the tower T1 stabilization, only its monitoring is briefly reported herein. In particular, for the assessment of the foundation and cracking pattern stabilization, it is worth showing the main results for the whole monitoring period.

Thus, Figure 16 includes the time variation of readings of the crackmeter F3 (located at the most open crack, Figure 16) and of the tiltmeter C1A (in the West-East direction).

Between May 2009 and March 2011, the measured values are very low (Figure 17), both for relative

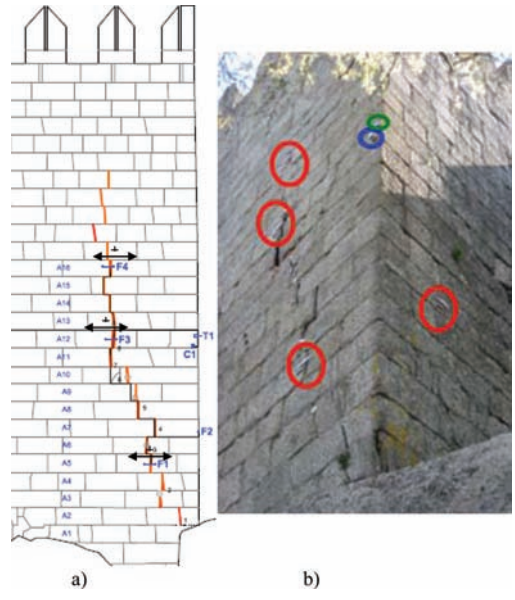

Figure 16. Instrumentation on tower T1 for structural monitoring: a) schematic layout and b) corner view of crackmeters, tiltmeter and temperature sensor.

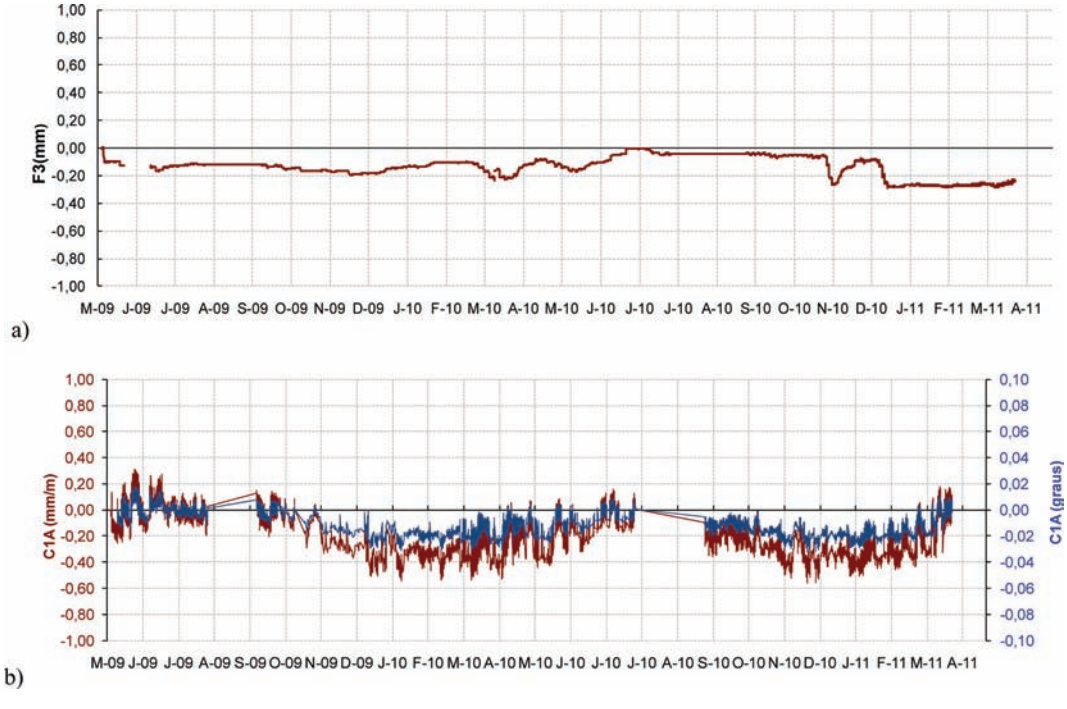

Figure 17. Monitoring readings after the stabilization of the rock masses walls foundations: a) relative displacement (F3) and b) rotation monitoring (C1- West/East).

displacement of F3 (which just read crack closure, less than 0.3 mm, thus with no structural significance) and for global rotation (less than 0.03º, that was found due to thermal effects).

5 CONCLUSIONS

Geotechnical investigations in the Guimarães castle revealed that the main structural pathologies were associated with the degradation of rock masses' quality, which support these medieval walls, mostly due to the softening of the fracturing system and an evolution of the weathered granite masses.

From the analysis of this foundation system, a solution for the reinforcement of these masses was implemented and hereby described, being an excellent example of application of Rock Mechanics concepts for the stabilization of that foundation.

From the tower monitoring using crackmeters, tiltmeters and temperature sensors, the data read by a local data acquisition system and wireless transmitted to FEUP (University of Porto), allowed concluding that the tower did not exhibit meaningful structural motions after the foundation intervention.

ACKNOWLEDGEMENTS

The authors thank the Department for the Cultural Heritage of DRCN (IGESPAR), in Portugal, in the persons of Mrs. Architect Paula Silva and Mrs. Ing. Anabela Carvalho, for creating the conditions for the execution of stabilization solution of the Guimarães Castle and authorization for publication of this work.

REFERENCES

Costa A., Miranda Guedes J., Paupério E., Almeida C., Ribeiro, R. and Lopes V. (2008).Castelo de Guimarães: Diagnóstico Estrutural e Construtivo. IC-FEUP.

Costa A., Arêde, A., Paupério, E. and Coutinho, D.(2009). Castelo de Guimarães—Sondagens: Nota Técnica. IC-FEUP.

Costa A., Arêde, A. and Neves, F. (2009 to 2011). Castelo de Guimarães—Relatórios de Monitorização. IC-FEUP.

Ribeiro, A., Quesada, C. and Dallmeyer, R.C. (1990). Geodynamic evolution of the Iberian Massif. In: Dallmeyer,R.D. & Martinez Garcia, E. (Eds.): *Pre-Mesozoic Geology of Iberia:* 399–410, Springer-Verlag.

Viana da Fonseca, A. and Cruz, N. (2010). Geotechnical interventions in Patrimonium with reinforcement of foundations. The Castle of Guimarães. *Congress "Rehabilitation 2010*. CD-Rom: 31 pages (ISBN:978-972-752-123-4).

Viana da Fonseca, A., Carvalho, J.M., Ferreira, C., Santos, J.A., Almeida, F., Pereira, E., Feliciano, J., Grade, J. and Oliveira, A. (2006). Characterization of a profile of residual soil from granite combining geological, geophysical and mechanical testing technique. *Geotechnical and Geological Engineering*. Vol. 24, Nº. 5, pp. 1307–1348.

Geotechnical Engineering for the Preservation of Monuments and Historic Sites – Bilotta, Flora, Lirer & Viggiani (eds)
© 2013 Taylor & Francis Group, London, ISBN 978-1-138-00055-1

Safeguarding interventions for two historical sites in the Middle East

B. Vingiani
Trevi S.p.A., Cesena, Italy

G. Salerno
Swissboring & Co. LCC, Muscat, Oman

ABSTRACT: The paper deals with two distinct safeguarding interventions on historical sites carried out in the Sultanate of Oman. The first refers to the activities of soil consolidation and foundations underpinning carried out in 1999 at Sohar Fort, a military presidium located on the Batinah coast and dating back to the 8th century AD. The second refers to the activities of stabilization of a vertical cliff, whose instability was jeopardizing the integrity of the archeological site of Shisr, where, in 1991, the remains attributed to the legendary city of Ubar were detected and disclosed.

1 INTRODUCTION

1.1 *Brief historical framework of Oman*

The Sultanate of Oman lies in the south-eastern Arabian Peninsula. Although in the past the definition of "Oman" referred to a much larger area, including that of the present United Arab Emirates, it is the current political territory of Oman to have a major interest from an archeological and historical point of view. Indeed, this land was on route followed by Homo Sapiens during his prehistoric migration from Africa to Asia, believed to have taken place around 100,000 years ago. Recent discoveries of Paleolithic stone tools in caves in the southern and central Oman have supported the archeologists on this hypothesis. Since those distant times, a stable and continuous human presence in the area has been confirmed by survey and archeological findings. Actually, stone, pottery, copper and iron handicraft pieces, discovered in numerous widely-scattered locations in Oman, date back to the Old Stone Age up to the Late Iron Age, being the latter also called Samad Period and representing the end of the pre-Islamic culture in the area. Dealing now with more recent years, we have to mention another specificity that has played a key role in Oman's history and heritage: its geographical location. With 1,700 km of coastline and a "bridge" position between Africa, inland Arabia and Asia, Oman's territory has constantly attracted the attentions and the interests of many foreign commercial, military and colonial powers that have developed, throughout history, both in the near Asia (i.e. Achaemenid, Parthian and Sassanid empires, Buyyids dynasty, Seljuq empire, Ottoman empire) and in Europe (i.e. Portuguese and British colonial empires). Whether these "attentions" led to a strong cultural influence or to an actual occupation of the country, the effects of the multicultural panorama experienced by the country for so many centuries can be clearly perceived in the ancient buildings that are part of Oman's historical heritage.

1.2 *Oman's historical heritage*

Together with some isolated towers, forts and castles are Oman's most remarkable historical symbols, as well as a lively witness of the different cultures and populations that time to time have occupied or imposed their influence on the country. Mainly located along the coastline and traditionally used as defensive bastions and look-out points, they were often also the seat of administrative and judicial authority. The restoration, preservation and opening to the public of these buildings are nowadays one of the priorities of Oman's Ministry of Heritage and Culture. The several prehistoric settlements discovered through survey and archeological excavations are also an important feature of Oman's historical heritage. Although archaeological field work started in the Sultanate only in the mid-seventies, the results have been prolific and significant since the very beginning. Currently, there are ten important archeological sites in the country and new archeological campaigns are in progress or under planning. Among the others, the site of Bat deserves a special mention. In 1976, it was designated by UNESCO the world's most complete and well preserved collection of settlements and necropolis dating back to the 3rd millennium BC.

2 UNDERPINNING OF SOHAR FORT TOWER

2.1 *Historical framework of Sohar Fort*

Located along the Batinah coast at Harat Al Hajara, in front of Iran's coasts, the original structure of Sohar Fort can be dated back to the 8th century AD. It was renovated to its present shape between the 14th and 15th century AD, during the reign of Imam Nasser bin Murshid Al Ya'arubi, who defeated and expelled the Portuguese. The fort was used as administration center till the reign of Al Busaid dynasty. In 1985, the structure was subject to a major restoration intervention and, since 1993, houses an archeological and historical museum (Figure 1).

Alphonso de Albuquerque, the great Portuguese admiral, in 1507, described Sohar Fort as "a fortress of square shape, with six towers, having also over the gate two very large towers".

2.2 *Reasons of the safeguarding intervention*

In 1999, the Government of Oman, through its Royal Court Affairs—Royal Estates Section, issued a tender for an urgent safeguarding intervention on the only structure of the fort that was not touched by the works performed in 1985: the Main Tower. At that time, this portion of the fort was impracticable and in severe structural decay. Since the visible signs of distress (i.e. large vertical and sub-vertical fissures present on the inner and outer walls) were reasonably due to the occurrence of differential settlements affecting the foundations, the tender works were mainly addressed to:

a) investigate tower's foundations dimensions and estimate loads and pressures transmitted by the latter to the underlying soil strata;
b) characterize, from a geotechnical point of view, the soils below the foundations and analyze their capability to withstand the estimated loads without major deformations;
c) propose and perform a long-term reinforcement of the soil-foundation mechanism, preserving the authenticity of the building.

2.3 *Investigation results and analysis*

The investigation carried out as first activity at site, showed that the tower's foundations were made of large stone blocks and had a maximum width of 1.45 m (Figure 2). The soils below the foundations were identified as loose rubble and debris, consisting of broken bricks and stones in a silty matrix (upper 4 ÷ 5 m), followed by a layer of dense to medium dense silty sand (down to 12 m and more). The average pressure induced by the tower to the soil was estimated to be 133 kN/m^2, while the maximum depth affected by significant stresses was calculated to be 9.50 m.

The analysis of these outcomes led to the following conclusions:

a) clear inadequacy of the involved soils strata to withstand the loads induced by the tower;
b) due to the current critical conditions of the structure, necessity to improve the mechanical characteristics of the layer of loose rubble and debris before the execution of any other intervention;
c) long-term intervention requiring, both an improvement of the deeper silty sands and the installation of structural elements capable of transferring the loads to this ameliorated soil layer.

Figure 1. Sohar Fort as it appears at the present time.

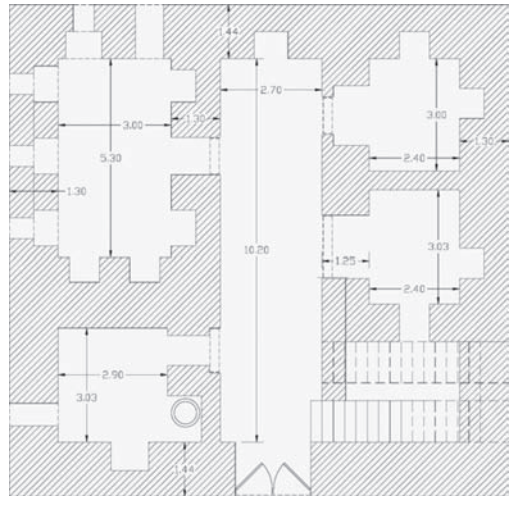

Figure 2. Sohar Fort—main tower foundations.

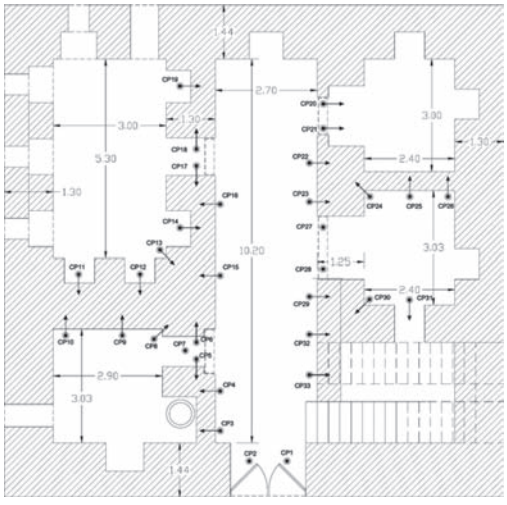

Figure 3. Preliminary low pressure grouting—plan view of the grout holes executed from inside the tower.

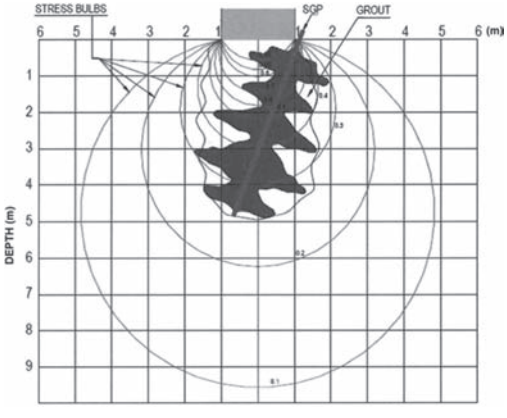

Figure 4. Preliminary low pressure grouting—schematic section at one single grouting location.

Figure 5. Preliminary low pressure grouting—drilling activities from inside the tower in progress.

In the following paragraphs, the different foundations engineering techniques finally applied to fulfill these requirements are described.

2.4 *Low pressure grouting of rubble and debris*

The preliminary treatment of the 4 ÷ 5 m thick layer of rubble and debris on which tower's foundations were resting was reasonably considered as the most critical activity of the whole intervention. As a result of a wide-range analysis of the applicable techniques and technologies, low pressure grouting was finally evaluated as the most effective and less invasive one. Therefore, a series of 5 m long inclined grout holes were drilled and equipped with 2" seamless steel sleeved pipes. For each grout hole, the inclination was adjusted according to the actual width of the foundation, in such a way to have the bottom of the hole at the middle of the wall (Figures 3–4). Drilling and grouting operations were performed by working, both from inside the tower (Figure 5) and from its outer perimeter, over a 3 m high temporary embankment.

From the installed pipes, a sleeve-by-sleeve upstage pressure grouting was carried out by means of a hydraulic inflatable packer. For obvious reasons, the maximum applied pressure was limited to 0,5 MPa. Taking into account the peculiar nature of the formation to be treated and the need to achieve a good final strength, a stable cement-water mix was employed as grouting medium. Grouting operations were carried out following the common split-spacing progressive sequence, thus avoiding the risk of applying excessive localized stresses to the structure. The steel sleeved pipes were left protruding from the wall at the original ground level for the reasons explained later, at Section 2.6.

Upon completion of all operations concerning the improvement of the layer of loose rubble and debris, the situation was considered sufficiently safe, thus allowing to proceed with the implementation of the succeeding phase.

2.5 *Improvement and reinforcement of the silty sand layer*

In order to improve the mechanical characteristics of the deeper soil layer, a different technique was applied: the compaction grouting. Compaction grouting is a method by which a controlled densification of coarse-grained soils is achieved by injecting a "growing" bulb of a stiff grout mix. The bulb acts as a hydraulic jack, thus displacing and compressing the soil radially from the injection axis. In our specific case, in order to cover the volume of soil significantly affected by the stresses induced by the tower, the geometry of compaction grouting boreholes assumed a "fan" configuration.

Each "fan" consisting of six separate boreholes deepened down to a maximum of 10 m (Figure 6).

As for the previous low pressure grouting, the inclination of compaction grouting boreholes had to fit the actual width of the foundation and the operations had to be performed working, both from inside the tower and from its outer perimeter (Figure 7–8).

As common practice, compaction grouting operations were carried out following an up-stage sequence. The grouting mix consisted of a stiff mortar, having a slump value at the Abrams cone ranging between 10 cm and 12 cm. The applied maximum pressure was limited to 2 MPa.

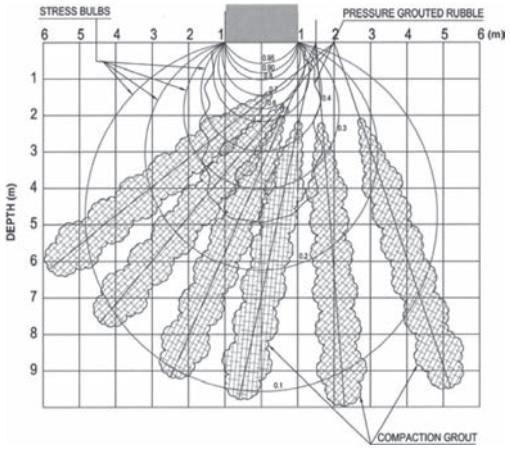

Figure 6. Reinforced compaction grouting—schematic section of one typical grouting "fan".

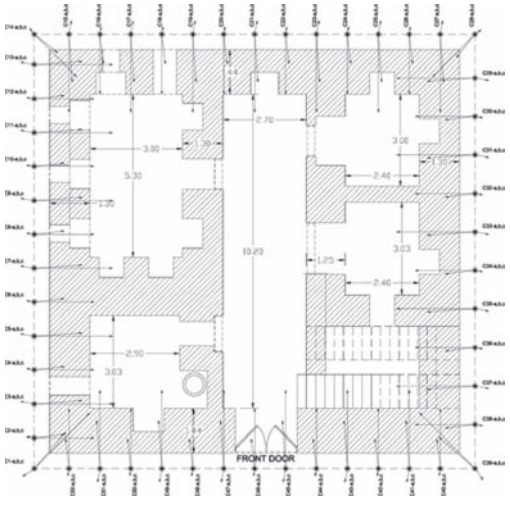

Figure 7. Reinforced compaction grouting—plan view of the boreholes executed from the outer perimeter of the tower.

Figure 8. Reinforced compaction grouting—drilling activities from outside the tower in progress.

It is worth to mention that, as additional soil reinforcement measure, a 40 mm steel bar was installed into each compaction grouting column.

The steel bars were introduced into the borehole casing before starting grouting operations, thus saving time and costs of a possible re-drilling and cementation of the bar.

2.6 *Structural underpinning of the existing foundations*

Upon completion of all previously described operations, the final activity of transferring foundation loads to the deeper and freshly reinforced soil layer could start.

To achieve this target, the 2" seamless steel pipes employed for performing the low pressure grouting, and intentionally left protruding from the walls, played a key role. In fact, after removing the temporary embankment and lowering the original ground level, it was possible to embed the top of the pipes into a wall "belting" reinforced concrete structure.

This structure was constructed by creating a 25 cm thick and 2 m high niche along the original walls, that was sequentially reinforced, shuttered and concreted.

The structure was enlarged at its bottom so as to obtain a trapezoidal shape, which allowed to, both increase the surface resting on the ground and easily house the upper 40 cm of the steel pipe (Figure 9). As common practice in all underpinning works, the reinforcement wall was constructed in 5 m long sections following a split-spacing progressive sequence.

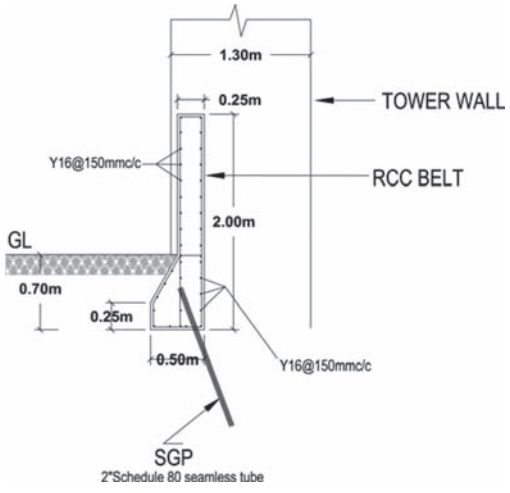

Figure 9. Existing foundations structural underpinning—typical section.

2.7 *Conclusions*

The described safeguarding intervention at Sohar Fort was successfully completed in January 2010 by Swissboring & Co. LCC, a Trevi Group company. No sign of further deterioration of the structure was observed during the execution of the works, despite its critical conditions before the intervention. The main tower is now accessible and open to the public.

3 CLIFF STABILIZATION AT SHISR ARCHEOLOGICAL SITE

3.1 *Historical framework of Shisr archeological site*

The actual existence in the southern Arabian sands of a legendary lost city destroyed by a natural disaster has long been the source of debate among historians, archaeologists and explorers. Although it has been called with different names, the most common being Ubar, Wabar and Iram, the historians agree on the extraordinary wealth of this city. Al-Hamdani, historian living in the 6th century AD, described Ubar as "*first among the treasures of ancient Arabia*". In February 1992, the *New York Times* announced a major archeological find in the following terms "*Guided by ancient maps and sharped-eyed surveys from space, archeologists and explorers have discovered a lost city deep in the sands of Arabia, and they are virtually sure it is Ubar, the fabled entrepôt of the rich frankincense trade thousands of years ago.*" Reference was made to the archeological surveys and excavations in progress at Shisr, in the Dhofar province of the Sultanate of Oman (Figure 10). From that date, the quarrel on the controversial existence of this fabulous city restarted with new fervor. Being or not the vestiges of the "*Atlantis of the Sands*", in 2000, the archeological remains of Shisr/Wubar were recognized by UNESCO as part of the world's heritage, as they "*vividly illustrate the trade in frankincense that flourished in this region for many centuries*".

3.2 *The occurred problem*

The archeological site of Shisr rests at the top of a 15 m to 20 m high vertical cliff facing the Arabian Sea. The rocky formation is eolian limestone. Due to weathering action and some earthquakes occurred in the past, the stability of the cliff looked very critical. Indeed, its face was showing large opened fissures between the stone blocks, most of which were almost totally disconnected from the rocky mass (Figure 11). Numerous piles of stones and debris, resting at the foot of the cliff, were testifying the already occurred collapses. In January 1999, with the aim to preserve the integrity of the archeological area, the Government of

Figure 10. Archeological site of Shisr—general view.

Figure 11. Archeological site of Shisr—close-up of rocky cliff conditions.

Oman, through its Office of the Advisor to His Majesty the Sultan for Cultural Affairs, asked Swissboring & Co. LCC to propose and implement an urgent intervention for a long-term stabilization and protection of the cliff.

3.3 *The implemented solution*

The proposed, and successively applied, solution consisted in the sequential implementations of three different interventions:

a) pressure grouting of the major open joints between the stone blocks;
b) reinforcement of the degraded portion of the cliff by a grid of rock dowels;
c) final protection of the rocky surface by the application of a structural layer of shotcrete.

Due to the height of the cliff, pressure grouting operations of the open joints, as well as all subsequent activities, were carried out, both from scaffolding (Figure 12) and from a specifically conceived aerial platform (Figure 13).

Figure 12. Pressure grouting of rock open joints—grouting operations from scaffolding in progress.

Figure 13. Rock dowels installation—drilling operations from aerial platform in progress.

This activity was preceded by sealing the exposed fissures by means of a high strength quick-setting cement mortar. In few cases, due to the huge dimension of the space between the blocks, stone pieces were also employed for that purpose. The grouting was conducted from 3 m long boreholes in one single phase, by employing a relatively thick and stable cement-water mix.

Location and direction of the grout holes were adjusted at each location according to the visible geometrical configuration of fissures. Once grouting operations were completed, the subsequent safeguarding activity could begin. Starting from the cliff face, a network of 4 m long rock dowels were drilled, installed and grouted.

The spacing of the grid was varied on the spot to match with the actual conditions of the rock mass. An average of 1 dowel per 4 m^2 was finally reached as a result of this visual evaluation. A 25 mm high-strength threaded bar was employed as dowel. The dowel head, was finished by fixing a 20 cm × 20 cm steel plate and a nut. All plates and nuts were made of galvanized steel.

Afterwards, working from the top of the cliff, additional much longer rock dowels were installed (Figure 14). In fact, in order to create the envisaged reinforcement grid, thus restoring the original monoliths of the rocky mass, these vertical dowels had to cross the entire height of the cliff.

To this purpose, 15 m to 20 m long boreholes were drilled by means of down-the-hole (DTH) hammer technology. The diameter of the drilled hole was 75 mm. Inside each hole, a 40 mm high-strength threated bar was installed and successively grouted by using a stiff cement-water mix. The protection of the cliff's vertical face from weathering actions was the last activity carried out at site. Taking into account its key role for a long-term preservation of the whole intervention, the shotcrete mix

Figure 14. Rock dowels installation—drilling operations from the top of the cliff in progress.

design was defined after a comprehensive program of laboratory and field tests. The finally selected mix included the addition of bonding and strength enhancing admixtures and steel fibers to increase ductility and crack resistance. The application thickness was 10 cm (Figure 15).

This structural layer of shotcrete was then followed by a second application. In fact, in order to blend the area of the intervention with respect to the surrounding cliff's face, a second and much thinner (i.e. 20 mm thick) layer of pigmented shotcrete was finally applied. The selected pigment was matching with the typical light brown of the limestone in the area (Figure 16).

Figure 15. Structural shotcrete application—spraying operations from scaffolding in progress.

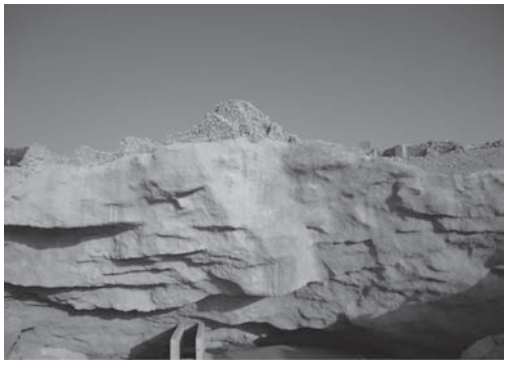

Figure 16. Archeological site of Shisr—the cliff as it appears after stabilization and protection works.

3.4 *Conclusions*

The described safeguarding intervention at the archeological site of Shisr was successfully completed in 2000. Only one maintenance intervention was required, at the beginning of 2011, to reinstate a limited area of the cliff that was showing some new signs of instability.

4 FINAL CONCLUSIONS

As clearly depicted by the two case histories described in this paper, any intervention to safeguard the foundations of historical buildings and sites can rarely be fully and detailed planned during the design phase. Due to the multiple variables and "surprises" always intervening during the progress of the works, a tight and confident cooperation between Employer, Designer, Engineer and Specialized Contractor is of utmost importance and the key of success. On the other hand, few other activities, in the field of foundation engineering, are more challenging and satisfying for the people involved in the project.

ACKNOWLEDGMENTS

The authors are grateful to the management and staff of Swissboring & Co. LCC for the time kindly provided for the preparation of this paper. Special thanks are also given to all Employer's Representatives involved, at any level, in the works, whose cooperation has significantly contributed to their success.

This page intentionally left blank

Geotechnical Engineering for the Preservation of Monuments and Historic Sites – Bilotta, Flora, Lirer & Viggiani (eds)
© 2013 Taylor & Francis Group, London, ISBN 978-1-138-00055-1

Use of jet grouting technique to realize substructures of historic buildings: The example of an apartment building in Warsaw

K. Wanik
Silesian University of Technology, Gliwice, Poland

ABSTRACT: The paper presents the application of jet grouting technology allowing to create a substructure of existing buildings. Neighbouring historic apartment buildings situated in the centre of Warsaw were used as an example. The ideas of the solution consisting in creation of basement walls together with new foundation, formed from cemented soil under existing continuous footings, were analysed. The process of geotechnical engineering construction project implementation was surveyed in all stages of work, starting from preliminary concepts and the designing stage, through basic construction and finishing works. Suggestions have been included regarding the tests and observations required due to the exceptional characteristic of the facility and adopted solutions. Attention has been paid to the necessity of considering specific technological conditions. Additional difficulties related to the execution of works in the very centre of a large urban area and at substantially limited space of premises situated below the ground level have been determined. The issue of specific requirements and limitations resulting from the need to interfere into the structure of a historic building has been raised. The role of execution monitoring has been defined, suggesting the scope of required observations and measurements. Based on the experience gathered during the construction, attention has been paid to especially important issues of geotechnical engineering supervision.

1 INTRODUCTION

Aleje Jerozolimskie is one of the most important and longest arteries of Warsaw, within the city nearly 12 kilometres long. It includes sections of national and regional roads.

At the turn of the 19th and 20th centuries, i.e. in the period of extensive development, the construction of two apartment buildings situated on Aleje Jerozolimskie was finished. These apartment buildings were part of frontage of monumental development, characteristic of the Warsaw city architecture at the turn of centuries (Fig. 1).

Now this frontage is one of few, which survived World War II. It shows the appearance of houses with a characteristic variety of building facades, each of which was designed in a slightly different style.

The described apartment buildings are situated in two fully developed and adjacent plots of shape close to a rectangle. The access to the courtyard was provided by two gateways. Courtyards creating a "well" backyard (Fig. 2).

Buildings were constructed as four-storey basement houses, with habitable attic in the front part and non-habitable attic in outbuildings. Later on one storey and an external lift shaft were added.

Figure 1. Current state of apartment buildings on Aleje Jerozolimskie in Warsaw.

Buildings were constructed using a traditional technology, with brickwork walls. Basement ceilings were constructed as ceramic barrel vaults and arched floors. Timber flooring systems were made

Figure 2. The courtyard of apartment buildings in Aleje Jerozolimskie in Warsaw, creating a "well" backyard, during the refurbishment works.

on higher storeys. Ceramic arched floors existed only in hygienic facilities. Roofs of timber structure were covered with roofing felt on a timber decking. Buildings were equipped with services, which were subject to numerous reconstructions with time.

In 2005 a discussion broken up on the future of both buildings situated on Aleje Jerozolimskie. There were opinions supporting a possibility of apartment buildings demolition due to their poor condition. However, finally after the intervention of monuments conservation officer a decision was made about a major renovation. A decision on reconstructing the destroyed front facades was also taken. Because of buildings condition and of requirements set the refurbishment works comprised numerous construction and conservation works. It included also geotechnical engineering works. The activities carried out were constrained by the need to maintain the historic nature of the building.

2 RENOVATION WORKS

2.1 *General assumptions*

The basic objective of carried out works consisted of restoring the proper condition of buildings together with their adaptation to current requirements. Because of historical value of both apartment buildings special care was devoted to the protection and conservation of preserved historic elements. The reconstruction of façade decorations was also included.

The adaptation works consisted in adapting the buildings to modern requirements set to service-office type buildings. This required performing a number of actions both in the architectural and structural field.

The necessity to equip the buildings with much more expanded building services forced placing

Figure 3. Excavation for the technical room under the courtyard on Aleje Jerozolimskie in Warsaw.

most of technical equipment in the reconstructed substructure. An additional space was obtained by building a technical room under the courtyard and connecting it with the existing basement premises (Fig. 3).

In general, the construction works consisted in strengthening, partial replacement and construction of new elements. Because of numerous cracks the lintels, piers between window openings and walls were strengthened. The timber floorings were replaced with reinforced concrete floors. Also brick floorings above the basement were partially replaced. The top storey was entirely reconstructed and a new roof structure was made. All the works were carried out without changes in external dimensions and maintaining the building's historic nature.

2.2 *Soli profile characterization*

All existing continuous footings had rested on stiff sandy clays prevail in the area in question. A uniform arrangement of layers forming the subsoil with parameters improving with increasing depth substantially simplified the analytical analyses (Table 1). No water level was measured in the investigations. Only water infiltrations were recorded.

2.3 *Geotechnical engineering works*

Typical basements made during apartment buildings construction feature usually low height, ranging from 1.7 to 2.5 m. The depth of continuous

Table 1. Geotechnical properties of soil layers.

Depth below ground surface	Soil layer	Geotechnical properties
0.0–0.5	Top soli	–
0.5–5.0	sandy clays stiff	c_u = 32 kPa, Φ = 18° M = 36 MPa, γ = 21,0 kN/m^3
5.0–12.0	Sandy clays very stiff	c_u = 45 kPa, Φ = 23° M = 60 MPa, γ = 21,5 kN/m^3

footing or base walls foundation is very shallow, between 0.2 m to 0.5 m. Willing to use fully the underground storey it becomes necessary to lower the floor level. It implies the need to perform new, much deeper foundations.

The underpinning must carry increased loads, which values include structural changes and the new way of premises use. Also it is necessary to consider local over excavations related to performance of shaft pits and equipment, in particular technological tanks.

At first, the underpinning using classical methods was considered, with performance of concrete in sections 1.0 to 1.4 m long under the existing continuous footings. This solution required application of reinforced concrete continuous footing 0.4 to 1.2 m wide.

The classical underpinning was related to the hazard of excessive cracks during the occurrence of temporary lack of support. The condition of walls selected for underpinning was variable, both due to their age and influences to which they were subject during the building existence (numerous reconstructions, war operations etc.). The neighbourhood of two apartment buildings was an additional impediment for performance of foundations deepening using classical methods.

After a thorough analysis of the solution, and in particular related hazards, the search started for foundations deepening method, which could exclude or minimise the existing hazards. The predicted long period of works execution, carried out in cramped and low premises, was also important.

At the stage of preliminary consultations a possibility of jet grouting use to underpinning was considered. At a correct performance of works this solution would cancel hazards characteristic of a classical underpinning.

Advantages of the suggested solution contributed to performance of more detailed analyses, which ultimately resulted in jet grouting underpinning within a full scope. This allowed using entirely the existing space, connected with a new technical room situated under the courtyard level (Fig. 3).

3 JET GROUTING UNDERPINNING

3.1 *Stages of designing works*

Preparation of design documents related to works described in this paper, requires planned and coordinated actions. They refer both to the stage of pre-design works and also to later designing and implementation of construction works.

The design works on geotechnical engineering solutions should be started at the stage of concept development or ultimately at the stage of building permit design. It is important that persons responsible for the described issues get involved in the design team work already at that stage. Even working consultations create opportunities to outline preliminary solutions and to determine the scope of required recognition. Proper directing of actions and the awareness of hazards allows carrying out further work efficiently, coordinating activities of individual architect's consultants and working out common, but primarily consistent, solutions (Pieczyrak & Wanik, in press).

Adoption of a correct procedure simplifies the process of a construction project implementation. It allows avoiding unpredicted difficulties resulting from the lack of project coordination. In the case of necessity to introduce changes or of situation occurrence, which requires a quick response, it enables effective activities.

In the considered case the work aimed at developing a underpinning solution was started at the stage of preliminary design. Initially the adoption of a solution using classical technologies was considered. Only partial application of jet grouting was assumed, which would cover continuous footings of walls adjacent to the neighbouring buildings. Also the overall scope of foundations deepening was supposed to be much smaller, which made full utilisation of basement impossible.

The proposal to perform the works in a way limiting the hazards occurring at digging under the existing foundations as well as a possibility to include in them the whole basements was approved. A close cooperation of geotechnical engineer on the contractor side with investor's design team started since that moment.

At the design stage, based on the provided guidelines and approvals, an initial version of the design was prepared. After interdisciplinary coordination and minor corrections the documentation was submitted for external assessment by an independent scientific worker.

The designed solutions obtained a positive opinion. Attention was drawn only to the need of current verification of the brickwork material condition in the bottom part of the foundation. Because there was a justified concern that locally it may have an insufficient strength.

Taking into account the recommendations, an assumption was made on taking core samples from drillings made through the foundation to form jet-grouted columns. Collected samples should be evaluated on a current basis in terms of material quality and strength.

The process of detailed design presented above integrates well with the model schemes. The cooperation between individual members of the design team, comprising various disciplines, is extremely important. Mutual verification of adopted solutions allowed avoiding inconsistencies in the developed documentation, which could result in further execution difficulties.

3.2 *Description of adopted solutions*

Prepared final design assumed performance of foundations underpinning using columns formed in the jet grouting technology (Fig. 4–6). The idea of adopted solution consisted of production of a cemented soil body forming walls of the lowest storey and a new foundation.

In the performed analytical calculations it has been assumed that the jet grouting underpinning will transfer the planned load on the load-bearing layers of the subsoil. An assumption was made that the underpinning would work like the continuous footing without considering friction resistance on the petrified soil body side surface.

On the basis of adopted architectural solutions maximum differences in the bottom of existing

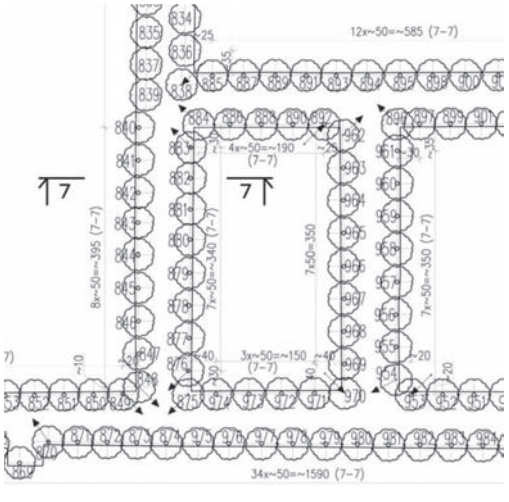

Figure 4. Part of floor projection of jet grouting columns to strengthen and deepen foundations of apartment buildings on Aleje Jerozolimskie in Warsaw.

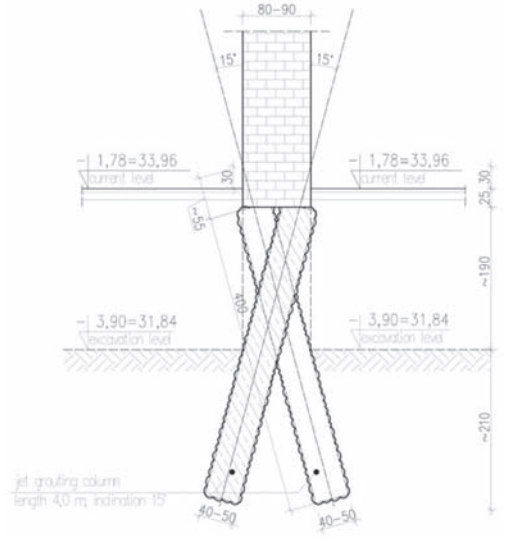

Figure 5. An example of trestle system of foundation underpinning in apartment buildings on Aleje Jerozolimskie in Warsaw.

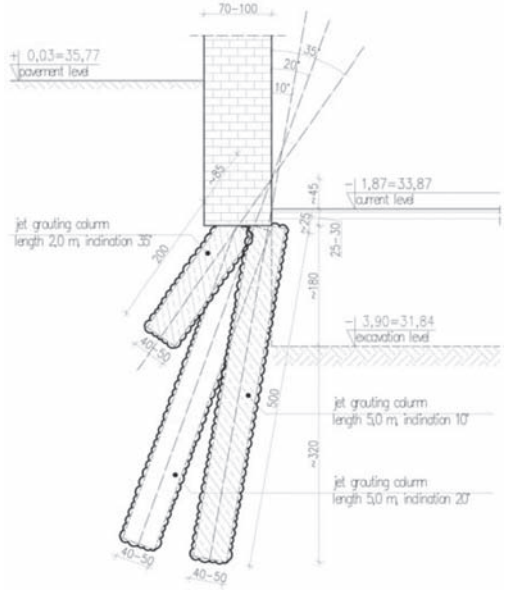

Figure 6. An example of one-sided system of foundation underpinning in apartment buildings on Aleje Jerozolimskie in Warsaw.

foundations and the excavation bottom were determined, ranging from 1.8 to 2.1 m. Locally there were over excavations of height differences reaching 3.25 m, related to the planned technological tank and the lift foundation. Only in these sections jet grouting columns were reinforced using steel tubes 60.3 mm diameter.

Because of hazard connected with temporary lack of support a relatively small diameter of jet grouting columns, equal to 0.5 m, was adopted. Its selection was affected also by the type and condition of soils occurring in the subsoil (Table 1).

Also the order of individual works performance was defined in the documentation. A possibility of forming on one day neighbouring elements of the underpinning was excluded. The necessity to form every third jet grouting column was imposed.

Designing the works, because of adopted technology and site specificity, slightly higher tolerances were assumed. Performance of works using small-dimension equipment is one of factors having an adverse impact on the achievable accuracy. A substantially lower possibility of accurate drilling tube rod running results in a greater sensitivity to various obstacles existing in the subsoil. In the case of encountering boulders and stones, remnants of old buildings, bricks or timber, the drilling tube rod may be pushed away. This results in shifting the performed jet grouting element (Wanik, 2010).

Working levels, from which columns were formed, were assumed on ordinates corresponding to the level of premises finish floors of the lowest storey. Very shallow foundations (Fig. 5–6) excluded a possibility of preliminary lowering the working level. Combined with low premises it caused the need to demolish part of ground floor slabs before starting the works.

Small diameters of jet grouting elements and the requirement of forming a possibly uniform substitute foundation forced the necessity of forming inclined columns. Drillings through brick foundations were made before starting injections. In accordance with guidelines there was an ongoing control of brickwork samples collected from the drill cores.

For safety reasons the performance of test holes was predicted prior to works start to localise unknown underground utilities.

Two types of jet grouting columns were adopted depending on the drilling locations accessibility. In premises, to which a two-side access was possible, trestle systems execution was planned. Columns were formed alternately on both sides of the foundation (Fig. 5). In the remaining cases petrification was carried out on one side, which required increased number of jet grouting elements to ensure a proper support of walls (Fig. 6).

For both apartment buildings performance of in total 2472 jet grouting columns was designed, of overall length of 9921 m. A detailed specification of designed elements is presented in the table 2.

4 SPECIFIC NATURE OF CARRIED OUT WORKS

4.1 *Jet grouting*

Jet grouting consists in destructing the structure of soil forming the subsoil within the range of injection stream action and in its mixing and partial replacement with a grout. Destruction of soil structure and its mixing are obtained as a result of action of a high-energy injection stream of liquid, which usually is also a grout. Elements formed during injection are called jet grouting columns (Fig. 7) or jet grouting walls, depending on their shape. The jet grouting may be performed in a single, double or triple fluid system. These systems differ between themselves in the number of media used for soil loosening and mixing. The most commonly used single fluid system uses one medium, which usually is a cement grout.

The range of injection stream depends on many factors, including the type and condition of subsoil ground and technological parameters of columns forming (Bzówka 2009, Flora et al. in press, Modoni et. al. 2006).

Table 2. Specification of the number of planned columns, Aleje Jerozolimskie in Warsaw.

Column length	Number of columns	Total length
m	units	running metres
Aleje Jerozolimskie 61		
1.0	152	152
2.0	111	222
3.5	64	224
4.0	27	108
5.0	878	4390
Total	1232 pcs	5096 m
Aleje Jerozolimskie 63		
1.0	189	189
1.5	20	30
4.0	718	2872
4.5	8	36
5.0	132	660
6.0	173	1038
Total	1240 pcs	4825 m

Technological effluents originate during columns drilling and forming, being an excess of injection grout mixture with soil. These are wastes flowing out to the ground surface through the free space between the drilling rod tube and the injection hole wall.

In the initial stage of columns forming a hole is drilled to the target depth using drilling rod tube equipped with an injector. The borehole diameter is much smaller than the column diameter and ranges between 90 and 150 mm. This stage is used to reach the required depth, from which column forming starts and possibly to preliminary loosen the soil structure. The soil loosening is aimed at increasing the range of the injection stream forming the column, which ultimately translates to its higher diameter. Then the proper column forming starts from the borehole bottom. The energy of injection stream getting out through injection nozzles situated at the end of drilling rod tube destroys the soil structure and forming a cylindrical column. The column material is the injected grout mixed with the soil, containing in its volume everything, which in the considered subsoil was within its range of action (Wanik, 2010).

The technological line used in the single fluid system comprises: a set of mixers, an high pressure injection pump, a drilling rig with a drilling-injection rod tube equipped with an injector, and a set of tubing connecting individual elements of the system. Depending on the specific nature of drilling and injection this set may be expanded with additional elements.

The use of drilling diameter much smaller than the target diameter of jet grouting elements is one of advantages of described technology (Fig. 8). It translates to a smaller interference in the existing elements, which has a substantial importance for the works carried out within historic buildings.

The lack of vibrations at the execution of drilling and injection work related to columns forming is another important engineering aspect worth noticing. It is particularly important, when we consider the earlier mentioned and frequently existing poor condition of strengthened structures. The need of vibrations introduction may be related only to the use of a hammer drill to pass through obstacles, such as boulders, concrete elements etc. However, even in this case the generated vibrations do not threat the structure, which has been confirmed by numerous implementations in recent years (Wanik, 2009).

In the considered case the main advantage of the technology adopted was a possibility to apply a small-dimension, hydraulically driven drilling rig. The use of a separate power pack and the location of remaining technological elements, i.e. the set of mixers and pump outside the building, had a substantial importance at the limited inside space.

4.2 *Work within the historic building*

Performance of works within historic buildings is related to the necessity of fulfilling much wider scope of requirements. The necessity to perform the works in a way that does not change the

Figure 7. Interpenetrating jet grouting columns of the trestle system of apartment buildings in Aleje Jerozolimskie in Warsaw.

Figure 8. Jet grouting underpinning foundation of the apartment buildings on Aleje Jerozolimskie in Warsaw with removed offsets. Visible places of drilling through brick continuous footings.

building or maintains the historic elements ranks first. It makes that the process of individual design and material solutions approval turns into laborious negotiations. The presented proposals need approval and the process of decision making is usually long.

Specific requirements force the designer and contractor to look for new and unconventional solutions. Performance of simple tasks requires frequently application of incommensurably complex actions. Limitations to technology and materials adoption possibility substantially make the works more difficult or longer. They can have a significant impact on the increase in investment implementation costs.

With respect to the described deepening and strengthening of foundations the conservation requirements focused on ensuring as high as possible safety of the building. It was understood as limiting to minimum the possibilities of creating new or development of the existing damages. This forced searching for new alternative solutions to the initially proposed classical underpinning. The adoption of solution based on jet grouting ensured the required safety level. However, it required allowing demolition of the ground floor slabs and of part of basement walls.

4.3 *Protection works*

Works related to formation of a new foundation are related to transferring the load onto deeper situated layers of subsoil. The process of loads transferring is accompanied by a change of the stress state, which leads to origination of settlements. When using the jet grouting technology, at properly carried out works, the settlements are minute and do not cause origination or development of the existing damages.

In the case of buildings in poor condition, despite limitation of hazard it becomes necessary to undertake additional protective measures. Damaged walls are usually repaired through their rebuilding of masonry or stitching in places of the existing cracks.

Older buildings do not have ring beams and the timber floorings poorly stiffen the structure. Ceiling beams initially supported in shallow holes after a few decades of use do not provide a sufficient guarantee of proper support. In most cases, prior to repair works start, it is recommended to clamp building walls on the floors level. Both steel bars and reinforced concrete perimeter beams are used.

Attention should be paid also to the condition of window and door lintels. Cracks existing within them create a substantial threat for the safety of building and people working inside it. The best solution is to make new elements prior starting the basic renovation works. Frequently, to increase the spatial stiffness, openings are temporarily walled over.

Numerous cracks of walls and piers existing in described buildings and a poor condition of timber floors forced proactive performance of strengthening works. At first, lintels were repaired and piers between window openings were strengthened. Repairs covered mainly walls, on the courtyard side, which were in the worst condition. Rebuilding of masonry and additionally stitching the walls using steel bars were locally performed.

The necessity of ground floor slabs demolishing, required due to making premises available to carry out underpinning, forced a proactive replacement of floors on higher storeys. Works staging was assumed so that demolition works would not be performed in adjacent rooms. New floors were bolted to walls.

Drilling and injection works were started once the strengthening was performed and assuming that above the room, where the works are carried out, reinforced concrete floors have been made.

4.4 *Works in the city centre*

When performing construction works in the centre of a big city it is necessary to take into account additional difficulties, characteristic of urban areas. They result from a dense development limiting the usable space and from significant impediments related to equipment and materials transport.

The location of described works in the very city centre of Warsaw, at one of main arteries, was a major logistic challenge. The equipment was transported and unloaded in early morning hours. Because of lack of pedestrian pavement possession possibility, the site facilities for injection works were situated on the apartment buildings courtyard. The delivery of high-pressure injection pump created the greatest difficulties. Existing gateways did not allow entering the courtyard by the transport (Fig. 9). The pump casing had to be removed and the pump rolled in to the target location using special rollers and a block and tackle.

After performance of the first stage it was necessary to move the grouting point to the courtyard of the neighbouring house, not covered by the renovation works. The transport issues were resolved in a similar way. However, a problem appeared related to the works performance in the surrounding of residential and office premises. To reduce the nuisance caused by the equipment operation, the possessed area was fenced, performing also a temporary canopy roof. Soundproofing was installed on the pump and the exhaust gas was discharged by a duct above houses roofs.

The aforementioned impediments together with limitation of permitted working hours during the daytime to a large extent contributed to extension of the execution.

4.5 *Injection grout punching*

A problem of injection grout punching to premises not related with the performed works occurred during the injection works. In the basement of the adjacent apartment building there was an outflow of the cement grout. This situation did not create a major hazard and the originated damages were immediately removed.

Injection rout punching cases are pretty common and difficult to avoid. They may be caused by a lower level of adjacent premises floor finish, local loosening of the soil and too long period of upper column part forming directly under the foundation. Also the subsoil fracturing due to a temporary loss of the injection opening flow capacity cannot be excluded.

4.6 *Obstacles in the subsoil*

When carrying out drilling works it is necessary to consider a possibility of encountering in the subsoil of obstacles, difficult to drill through.

An especially high probability exists in a developed area and when the works are performed in the place, where earlier development existed. In areas covered with postglacial formations boulders exist in the subsoil.

During the work under foundations erratic boulders of rock material were encountered twice (Fig. 9). Performance of the drilling, due to a small force of drilling rig thrust, required using a dawn the hole drilling hammer.

Apart from the obstacles mentioned above in Warsaw there is a high probability of encountering duds dating back to World War II. They create a hazard for people and buildings safety. If the work is carried out in an area of especially high hazard, usually UXO monitoring is present on the site.

4.7 *Geotechnical engineering monitoring and supervision*

Performance of measurements and observation and also an ongoing verification of assumptions made at the design stage becomes highly important.

The strengthening works, carried out within foundations, create a hazard of originating excessive, but primarily uneven, settlements. If parallel to that wall and header cracks occur, there are no bond beams and floors, which could bind the structure ensuring its spatial stiffness, the hazard scale increases.

Figure 9. Erratic boulder in the underpinning structure in the apartment buildings on Aleje Jerozolimskie in Warsaw.

The design regarding the apartment buildings underpinning contained a provision imposing the necessity to perform land surveying and observations of existing damages development. The measurements should have been initiated before starting the works, carried out during their performance and continued till the completion of works comprising the underground storey.

The soil conditions were verified on a current basis during the drilling works. Also the wall structure condition was assessed, which has been previously mentioned.

Special attention was paid to ongoing assessment of carried out land surveying. During the works performance local increases in settlement, reaching a few millimetres, were observed twice. As it has been shown by later thorough analyses, the reason was in damages of walls structure and in performed demolition of floors.

The jet grouting underpinning did not represent displacements of higher parts of the wall.

Knowing the scale of hazards and being aware of importance of the tasks performed in the case of large and complicated investment projects it is necessary to appoint an experts team. Specialists in the field of geotechnical engineering cannot be missing in the group of persons supervising the course of the construction (Pieczyrak & Wanik, in press).

5 SUMMARY

On the basis of the presented implementation an attempt was made to introduce the possibility

of jet grouting use to create an substructure of a historic building. Important issues related to the construction process, comprising implementation of complex geotechnical engineering works, have been discussed. In particular the importance of proper order of actions has been emphasised.

Attention has been paid to the existing difficulties and to sources of possible threats. The role of strengthening works, performed prior to start of underpinning, has been emphasised, as well as of the later execution supervision.

The presented procedure allowed a safe performance of work. Concerns related to the occurrence of excessive settlements have not been reflected in the actual performance. It is possible to state that the application of larger diameters of jet grouting columns would not have an adverse impact on the building condition. The reduction of jet grouting elements number obtained this way would substantially accelerate the works.

REFERENCES

Bzówka, J. 2009. Interaction of jet grouting columns with subsoil. Monograph. Gliwice: Silesian University of Technology Publishers (in Polish).

Flora A., Modoni G., Lirer S. & Croce P. 2012. The diameter of single, double and triple fluid jet grouting columns: prediction method and field trial results. Geotechnique in press.

Modoni G., Croce P. & Mongiovi L. 2006. Theoretical modelling of jet grouting. Geotechnique 56, No. 5, 335–347.

Pieczyrak J. & Wanik K. Geotechnical engineering requirements for deeply founded investments in developed areas. XXVIII Polish Workshops of Structure Designer Work, Wisła: 2013 PZITB. In press. (in Polish).

Wanik K. 2009. Application of jet grouting to protect and strengthen foundations of close-to-shaft surface facilities. Wiadomości Górnicze 7-8/2009: 443-449 (in Polish).

Wanik K. 2010. Selected design and technological conditions of jet grouting application. Inżynieria i Budownictwo 2/2010: 68–70 (in Polish).

This page intentionally left blank

Geotechnical Engineering for the Preservation of Monuments and Historic Sites – Bilotta, Flora, Lirer & Viggiani (eds)
© 2013 Taylor & Francis Group, London, ISBN 978-1-138-00055-1

Geotechnical and structural investigations of historical monuments of Kazakhstan

A. Zh. Zhussupbekov, T.O. Zhunisov, A.Z. Issina & T. Awwad
Eurasian National University, Astana, Kazakhstan
Damascus University, Damascus, Syria

ABSTRACT: Currently, a total of about 25.000 monuments—basically archeological structures—exist in the territory of Kazakhstan. Such monuments include the ruins of ancient settlements, barrows, burial grounds, as well as constructions dating back to the Middle Age and representing the typical religious architecture of Kazakhstan—mausoleums, necropolises, ancient mosques, madrasah, etc. This paper presents some historical sites in the Southern and Central part of Kazakhstan, describing their typical foundations and the main geological ground features. Some useful survey methods, and an example of technical diagnosis on a historical monumental structure such as the mausoleum of Arystanbab, Hodzha Ahmed Yassaui are also described in the paper. It is argued that geotechnical and structural investigations are important for the conservation of historical culture heritage in Kazakhstan and other territories with similar archeological structures and geological environment as Syria and Egypt.

1 INTRODUCTION

The life of architectural monuments is strongly influenced by the geological environment and by human engineering and economic activities. Problems may be caused in time by the peculiar characteristics of the foundation soil, by their modifications or by man-made works in the soil close to the monuments. Because of these geotechnical problems, critical displacements and even destruction of monuments may take place. Human activities may be therefore detrimental, and as times goes by, their impact will likely increase.

It is therefore important to clearly understand the impact of human activities on architectural monuments, and in case construction works are carried out close to a monument it is essential to determine the induced deformation field, in order to be able to have a diagnosis for possible problems in order to choose the right preservation procedure and, if necessary, a treatment strategy. It must be also noticed that, if not correctly conceived and designed, treatments may happen to be incorrect, with the effect of increasing the then man-caused problems they had to mitigate.

With the aim of monuments preservation, the impact of human activities cannot be ignored. The risk is to become aware of structural and geotechnical problems too late, understanding their causes only during restoration.

What is needed is the diffusion of the culture of preservation, spreading knowledge and technical literature as much as possible to prevent the destruction of monuments which belong to the history of a nation and testify about the evolution of its culture.

2 GEOTECHNICAL AND STRUCTURAL INVESTIGATIONS

The diagnosis of the deformation of architectural monuments requires a clear understanding of its interaction with the geological environment. So, it is necessary to take engineering and geological information into account, the content of which allows solving the issue by finding the cause and explaining the phenomena of the researched object, and deformation of architectural monuments.

The importance of determining the role geotechnical and hydrological factors in preserving architectural monuments is considerable and is of great importance when trying to understand the causes of deterioration or failure of foundations and walls of monuments.

On the other hand, uncertainty on real soil conditions or an inadequate investigation may lead to misunderstand the causes of geotechnical problems of monuments. Such confusion sometimes leads to absurd decisions which can result into interventions that have a negative effect on the construction, making its safety margins even worse than the original ones (Abramov, 1973).

An example of a critical information, sometimes underestimated, is groundwater regime and the degree of saturation of the most superficial

part of the subsoil, which closely interacts with the monument foundations and therefore has a great influence on the monuments behaviour.

As well known, there is a zone above groundwater table which may be saturated because of capillarity and then partially saturated (i.e. with pores not completely filled with water) up to ground level.

Seasonal water table depth variations, and the permeability characteristics of soils, affect the superficial hydraulic regime.

There is usually one aeration zone and one logged zone, but in some cases, two or more zones may exist. If there are two aeration zones, then the lowest zone of aeration is situated between the highest and lowest logged zones. The aeration zone, according to its water content and its circulation, can be divided into three belts: soil moisture zone, internal zone and capillary cover zone (Michailovsky, 1977).

The soil moisture zone is adjacent to the surface zone where water evaporates into atmosphere. The thickness of this zone depends on soil and flora characteristics. Where there is a grass cover consisting of 0.1–0.15 m, and where there are gardens and parks, this portion of soil may be relevant rather higher. The moisture content of the intermediate soil zone depends on its hydroscopic water. Finally, capillary cover determines the zone which is above the logged zone and is in permanent contact with the waterlogged zone. Water of the capillary cover is above this zone and under the influence of capillary drains which rise up along the walls and pro rata to the pore soil diameter. That is why the height of capillary rise depends on soil behaviour and its moisture. For dry sand, the height of capillary rise is only few dozens centimeters. (in non granulated sands—0.15–0.35 m, small granulated sands—0.35–1.0 m). In damp condition the height of capillary rise of sand reaches for 3–4 times higher (Pashkin, 2005). Clay sand reaches 1.0–1.5 m., Uliginose soils—2.4 m., loamy soil—from 3-to 4 m. Capillary water in clay can raise to 8.0 m., and in loess—4.0 m.

Generally speaking, the height of capillary water rising is influenced by loads applied at ground surface. Then, underneath a monument, changes in the local water regime may be expected.

The chemical structure of water also affects the height of capillary rising; particularly as a result of chlorous and sulphureous natrium presence in water in moist integument loam raising these saline through capillaries happens differently. Penetration of these salines brings to that in lower part of loams where sulphates predominate, and in upper one—chlorides, greater maintenance of the latters in upper part of slit is connected also with the fact that chlorides diffuse faster than sulphates. It's especially important to take that into account now, when salt is used against the icy cover of pavements and roads, which then migrates up through seepage of surface water along the capillary.

In this case, water first penetrates into foundation soil capillaries, into the construction materials of the foundation and the walls, consequently it causes the appearance of dampens not only on frame constructions and interiors, but also brings to the penetration of salty ingredients into whitewash, natural building materials, layer and their chemical destruction. Capillary water movement in soil goes not only from bottom to top, but also tends to impact the side of capillary force, which occurs on the boundary of different components: foundation soil and foundation material. On this basis there is molecular interaction of water and air with inner surface of ore space of brick work material, in its wetting and formation of meniscus pores, determining rising force.

Between soil water and capillary cover there is an interim belt of aeration zone. Water occurring onto this zone with its mass goes down to the logged zone or is kept in capillary pores of transition belt and is called water of intermediate belt. Up and down boundaries of internal belt is defined according to local conditions stipulating for the peculiarity of soil dampness regime of aeration zone.

If the aeration zone is missing, capillarity makes the soil fully saturated to ground level.

Possibility of soil humidity changing aeration zone in the time and space depends on the influence of factors that determine distribution of moisture in this zone. Particularly, soil humidity of aeration zone depends on absorbing ability of soil, and that ability primarily depends on its characteristics. The surface infrastructure condition which determines evaporation amount impacts on soil moisture. That is why in usual conditions soil moisture goes down when evaporation takes place. But soil moisture increases after rain. However if the surface is covered with steam-proof materials like concrete or asphalt, evaporation dramatically decreases and soil moisture distinctly increases in spite of atmospheric precipitates seepage exception. In this way natural soil moisture of aeration zone reflects influence both of soil content and seepage, and evaporation conditions. (Pashkin & Bessonov, 1984.)

Architecture monuments have great influence on evaporation way, under which it gets smaller or entirely excluded. The traditional way to avoid water rise into the most superficial soil or even in the constructions is by means of a ventilated zone underneath the building. Such measure is used to provide evaporation of moisture from soil pores and to exclude the capacity of fully absorbing

ability of the grounds. This trick permitted to avoid moisture accumulation in soils under the monument's building and its further penetration into bearing constructions and interiors.

Fig. 1 shows the example of a valuable historical building (Arystan-Bab mausoleum) for which such a ground water protection device was adopted (Massarsh, 2004). Because of the relevance of such a building, it would be necessary to monitor it as follows:

- Supervision of UPV changing before and after dewatering;
- Constant control of old splits on the fronts and lurking of appearance of new ones;
- Geodetic control of vertical and horizontal deformations of longitudinal and cross-cut walls, especially buttresses;
- Registration of ventilation trench and pipes;
- Measurement of TVR parameters to define suitable exploitation parameters;
- Control of measuring salinization of brick walls and foundations;
- Control of change of chemical behaviour of underground water and its link with agriculture land;
- Geo-ecological control of ground and underground space.

To perform these tasks it is necessary to be equipped with modern facilities. We show some examples of pictures of architectural monuments below (Figures 2–6).

Now let's introduce some considerations on geological and hydrogeological conditions of the territories of Hodzha Ahmed Yassaui mausoleum shown in Figure 2.

The mausoleum of Hodzha Ahmed Yassaui is located in historical centre of Turkestan, on the territory of the old city. The territory of the old city towers over other part of the modern city by 2–8 m. The surface of the ancient settlement is a slightly hilly area, in topography of the ancient settlement the direction of streets, ruins of constructions are well seen through planning of the old

Figure 1. Mausoleum Arystan-Bab XIIth century.

Figure 2. Mausoleum of Hodzha Ahmed Yassaui.

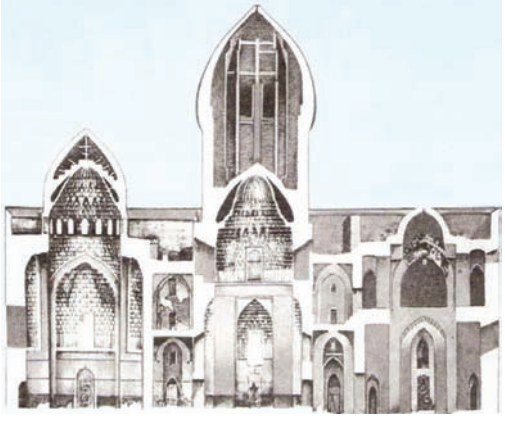

Figure 3. Crosscut of Mausoleum of Kozha Ahmed Yassaui.

Figure 4. Historical monuments of the city Otrar.

Figure 5. Main view of the historical monuments of the city Otrar.

Figure 6. Mausoleum of Kalka-Ishan.

city, in places it is pitted by archaeological holes and excavations, there are trenches, arcs, holes, embankments of soil. Hodzha Ahmed Yassaui's mausoleum is located in the north-east part of the ancient settlement. The old city is crossed by an open drainage collector originating around an underground mosque of Hilvet. Its depth is of about 5 m, being as large as 6 m. The concrete pipeline is laid at the bottom of it.

Within the territory of the monument the following types of soils are widespread: bulk soil, sandy loams, loams, sandy soils, galechnik. Bulk anthropogenous soil is presented generally by sandy loam with inclusion of beaten ceramics, pebble and gravel. Quarternary loams with a thickness of 5–7 m containing lenses of less sandy loams form the basis of the monument. They are spread water containing gravel with the power from 4 to 24 m. Sandy loams are met mainly in the top part of a section.

Maximum liftings of level of ground waters were observed in 1969–1970 and 1982. They caused flooding of some capital structures of the city, including security zone of the historical complex. Thus, the first cycle of the flooding which began after input of ATC in 1964 and reached a maximum in 1969–70 was most considerable both on time of manifestation and amplitude of a raising levels, by 1–2 m more in comparison with 1962. Second rather short-term cycle of lifting of levels (1981–1982) caused increase of level surface by 0,5–1 m on the average. In the monument territory it appeared only 3,5–4 m from earth surface, i.e. above critical mark for capital constructions. Due to the lack of emergence of essential deformations of the monument in the first cycle it wasn't given due consideration though at this moment there was a deep wetting of soil and the basis of the bases of monuments of the complex. The second cycle of lifting of level of ground waters caused external deformations of the building of monument 3, in December 1982 there was a destruction of the top restoration number of stalactites of a dome of Kazanlik.

In the late 1960s and the beginning the 1970s engineering-geological researches were carried out by GPI "Fundamentproyekt" (Moscow).

In 1974, according to GPI "Fundamentproyekt" project 11 drainage wells were drilled, equipped from the mouth with ferroconcrete wells of 4 m in depth. Wells were connected by ceramic pipes with diameter of 250 mm laid in horizontal gallery at the depth of 4 m from the surface of the earth. The created drainage and collector system of an needle purifying drainage paid off on removal of local pressure in subdeep-well waters by means of the drainage wells drilled at the bottom of special wells, with their subsequent outflow on the pipes closed from a surface in the general catchment basin. From there compulsory and self-flowing dumping of water in main drainage the collector was provided. Water drain head of drainage wells tower by 0,5 m over the bottom of the wells—stores therefore having poured out waters from such wells to become possible only at emergence of a piezometric pressure and rising of water up to the depth of 3,5 m and less from the earth surface. Besides, in all the territory of Turkestan intensive water selection by means of a set of operational wells was executed. But the existing drainage and collector system couldn't prevent moistening of walls of the monument. In 1986–1988 level of ground waters went down by more than 3 m and was at the depth of 6–6,5 m, against 2,7–3,3 m in 1982. It occurred due to water inflow reduction in ATC and dry waterless seasons.

According to the decision of Council of Ministers of Kazakh Soviet Socialist Republic No. 17-23/30 (February, 1983) "About some measures for restoration of temperature and moist mode of the building of Ahmed Yassaui complex in Turkestan" SA Presidium of KazSSR assigned

hydrogeology and geophysics institute named by U.M. Akhmedsafin SA KazSSR in 1983–1987 to conduct complex hydrogeological researches on clarification of the reasons and extent of influence of ground waters on the construction and to develop recommendations about their neutralization. Big work was done, collecting field and share materials, generalization and the analysis of results of earlier works, regime supervision on networks of wells and wells, skilled experimental and chemical analysis works was executed. As a result of researches hydro-geological and engineering-geological conditions of the territory of the monument were found out, major forming factors were studied, recommendations about measures of decrease in negative influence of lifting of ground waters were planned. Researches revealed that rather powerful water-bearing complex of allyuv-prolyuvial deposits containing pressure head and free-flow waters and being characterized as high water containing and water carrying out properties is widespread on the territory of security zone of Ahmed Yassaui.

As a whole, an active drainage water intake consisting of a number of interacting wells was installed, the fortifications of the Kokand period located from the outer southeast side, at distance not less than 200 m from the building of the mausoleum of Hodzha Ahmed. According to technical recommendations about the device and operation of water step-down water intake according to the settlement scheme of a water intake it was necessary to drill and equip six prospecting and operational wells with distance between them 140 m. Total length of a water intaking row was 700.

Design depth of wells is 30 m. Diameter of a filter column is 12 inches (outer diameter is 325 mm on the coupling of 351 mm). Length of the filter is accepted depending on a concrete section and on the average makes 9 m. The filter perforated frame and wire with a spiral cast-over, with distance between rounds of a wire of 1–2 mm. Settler length with a deaf bottom not less than 6 m.

Near water wells (at distance of 5 m) there have to be drilled and equipped on one observation well, necessary for studying of a-level and hydrochemical mode of underground waters on the water intake line. For supervision over development of a depression funnel from an average well of a water intake to the mausoleum 2 regime wells remote from water intaking (and being are drilled at it observant a well) at distance of 50 and 125 m. Total of the observation wells which are subject to drilling on a site of a water intake—8. To regime supervision have to be also connected: 4 wells in drainage wells (on one at each of the mausoleum parties) and 2 wells (well Kudukhana in the mausoleum and a well in the territory of an archaeological museum); 1 well at Seed station (in 300 m from the mausoleum from outer side of a water intaking row). The specified wells in process of development of a depression funnel, are subject to careful cleaning and deepening.

The fresh drainage waters extracted by a water intake, can find application for an irrigation and the centralized municipal and drinking water supply. At the first stage when the main objective puts protection of an architectural and historical complex against flooding, calculations pursue creation of an effective water intake capable to cause fall (cut) of level under the mausoleum building almost on 4 m thanks to what the depth of underground waters has to reach here 10 m from a surface. Therefore the recommended water intake provides continuous extraction of nearly 180 p/a of underground waters during the vegetative period (180 days). This water has to be most used first of all for an irrigation of lands that will allow to compensate capital expenditure for construction and the water intake equipment in a certain measure. For this purpose water from the main drainage system can directly be dumped in the Turkestansky collector laid in dense low permeable loams and on it to be taken away by drift to irrigation fields for the subsequent water analysis.

At the second stage, in process of studying of a mode of operation and obtaining the specified hydrogeological parameters, other operating mode of a water intake can be calculated. It can provide, for example, year-round giving of any part of water (from two-three wells) for economic and drinking water supply, and from other wells—only seasonal water selection (120–150 days) for a local irrigation. In this case the water directed for municipal and drinking needs, has to collect previously in the special tank (for example, in the concreted capacity), to be exposed to necessary sanitary processing, and then by means of centrifugal pumps to move in the high-level and distributive water supply system.

In a security zone for the purpose of reduction of filtrational losses in a bed of an artificial reservoir application physical and chemical (argillization) or chemical (osolentsevany, ozhelezneny and oglinizemlivany breeds) ways of technical melioration was recommended.

By calculations of scientists this system would allow to lower level of ground waters in the monument territory to 10 m. It would positively be reflected both other architectural and archaeological monuments being in the territory of a historical kernel. Work of hydrogeologists was highly appreciated by experts and scientific and technical council of RGP of design institute "Kazproyektrestavratsya" of the Ministry of Culture of KazSSR and the positive decision for drawing up

the engineering design and budget documentation was made.

In 1989 "The hydrogeological conclusion and technical recommendations about protection of a security zone of a monument of Ahmed Yasavi in Turkestan from flooding by ground waters" developed by hydrogeology and hydrophysics Institute of U.M. Akhmedsafina of Academy of Sciences KazSSR was approved by Technical Council of «Kazproyektrestavratsya» institute and transferred for drawing up for drawing up technical documentation. The decision of executive committee of the Chimkent regional council of People's Deputies the customer by design and construction actions for fall of ground waters determined regional executive committee Construction Department. Design is assigned to "Soyuzgiproris" institute (Chimkent). Began design—the 2nd quarter 1989. In the early nineties, according to the project, in the territory of a security zone vertical wells are drilled. Unfortunately all planned actions were not completed.

Wells were drilled, established, but the work wasn't completed though now some of wells are used for watering of green plantings in a security zone. The condition of system isn't known, besides in 20 years hydrogeological conditions in the area significantly changed, there are no data on regime supervision, additional researches are required. The problem of flooding of the territory of a monument exists and now.

Most engineering-geological researches in southeast part of the city near the mausoleum were carried out in 1963 by the State leading research design institute "Kazgorstroyproyekt" for the engineering-geological characteristic of Turkestan.

In October and November 1990 to the historic core of the protection zone geological engineering at 1:5000 scale for the complete division of the Institute of Chimkent YuzhGIIZ based on specification of the State Institute "Kazproektrestavratsiya" to develop a detailed plan of the city.

Further geotechnical investigations in the territory of the monument were held, were only local work carried out on the instructions of conservators to determine the moisture content of soils around the monument: in 1997, the Shymkent State Institute of Technical Research and the 2011 LP "Surveying" Shymkent.

3 CONCLUSIONS

As shown by practice, salinization processes in favourable geological and hydro geological conditions may take place on historical monuments, especially in regions with hot climate and with notable temperature oscillations of atmosphere. Cyclic process can cause walls to crack, particularly on weak joint parts. A possible easy starting way to solve this problem is the reduction of the capillary zone below the ground surface.

Preservation of monuments as Arystan-Bab mausoleum is a worldwide problem. In most cases geotechnical and hydro geological conditions play the most important role. Capillary water rise process in clay soil and pore materials with salinization is observed on most historical monuments, particularly in regions with hot climate and with a notable temperature difference of atmosphere.

In order to work out a special project on a regulation moisture regime of ground and underground soil damp of the underground parts of mausoleum frontward (Technological scheme of SR…, cipher 778 g/04) NIPI PMK has offered to use an evaporation method with the help of air ventilation through pore material backfilling outside, inside and particularly the lowest parts of the trench, and brick walls (foundations). Moisture ventilation and evaporation intensity is stimulated with a fixation of vertical asbestos-cement pipes with a diameter of 100 mm (NIPI PMK, 2004).

The most complex problem appeared to be fighting against salinization. There are many ways of finding a solution of the problem, but detailed study of the object might be more useful.

As the geological environment, geotechnical problems and the the typical religious architecture in Syria and Egypt looks similar to the conditions in Kazakhstan, so it is logical to expand this research to include the important archaeological cultural buildings of these areas in the future.

REFERENCES

Abramov, S.K. 1973. *Underground drainage in industrial and urban development*. Moscow: Stroizdat.

Massarsh, K.P. 2003–2004. *Preservation of Egyptian monuments of the pharaoh epoch. Reconstruction of cities and geotechnical construction*. St. Petersburg, Russia.

Michailovsky, E.V. 1977. Architectural monument restoration methods. Moscow: Stroizdat.

NIPI PMK. 2004. *A project work documentation on Mausoleum "Arystan-Bab's"*. Almaty city.

Pashkin, E.M. 2005. *Engineering geology*. Moscow: Architecture.

Pashkin, E.M. & Bessonov, G.B. 1984. *Deformation diagnosis of architectural monuments*. Moscow: Stroizdat.

Geotechnical Engineering for the Preservation of Monuments and Historic Sites – Bilotta, Flora, Lirer & Viggiani (eds)
© 2013 Taylor & Francis Group, London, ISBN 978-1-138-00055-1

The safety of an industrial archaeological heritage: The underground quarries in Marsala (Sicily)

M. Zimbardo, L. Ercoli & C. Cannone
University of Palermo, Italy

A. Nocilla
University of Brescia, Italy

ABSTRACT: The present paper analyses an underground and inactive quarry of calcarenite, which belong to a localised area called *Cave di calcarenite in Contrada Cuccidenna* that has been recognised as a typical example of industrial archaeological heritage. The study of this typical quarry is finalised to the preservation and safe fruition of this site, which represents the history of manufacturing technologies of rocky ashlars. Rock samples from the pillars have been collected and, at first, a petrographic characterisation has been performed. The strength parameters have been estimated by means of triaxial and isotropic compression tests. Through a finite element analysis, the mechanical characterization has been then used to assess the stability and safety conditions of the structure. The influence of several parameters has been considered: e.g. mesostructure of the rock mass, shape of the underground quarry and effects, in close areas, of human interventions.

1 INTRODUCTION

The *Calcarenite of Marsala* is widely outcropping in the western Sicily and it had been used in the historical and monumental buildings since the Punic age, at the beginning as elements of bearings walls and then, after the invention of the reinforced concrete, as masonry facing. An extensive quantity of shafts had been created because of these secular quarries, which are often localised under built-up areas, as under the Town of Marsala. As a consequence of the progressive increase of urban areas, numerous instabilities occurred both on the surface and in the underground quarries and the hazard condition increases consequently. The development of the underground cavities was therefore influenced by the quality of the rock: because of the extraction of the material with good mechanical properties, sometimes in the cavities the ceilings, the pillars and the bearing walls are made of the worse rock material. According to the local quarrymen (Rodolico, 1853), this lithotype can be classified in two main types: the *pietra forte* (strong stone), used for the public housing and monumental buildings, and the *pietra franca* (soft stone), which were avoided during quarrying. The variability of the me chanical characteristics of the material, which have conditioned the morphology of the underground extractions, has been clarified from the researches developed in the last years (Arces et al., 1998, 2000; Zimbardo, 2010). These studies have allowed the authors of the present paper to identify three different textural types, since the texture influences the mechanical properties of the material. In detail, these textural types are characterised by porosity of 50%, 40% and 60% respectively for the type A, B and C (Zimbardo et al., 2010). Successive studies have correlated the mechanical behaviour with the distribution and the type of pores and have leaded to a well-structured classification of Sicilian Calcarenite. From the point of view of its texture, this material has been separated in three classes according to the fabric: A (dense); B1e B2 (sponge), C (house of cards) and, according to this classification, the *Calcarenite of Marsala* belongs to B and C classes (Zimbardo et al., 2011).

The exploiting of the *Calcarenite of Marsala* begins in the VI^{c} b.C, when Phoenicians set up the town and surrounded it with a defensive wall and a moat. During the roman epoch the exploitation increased because of the enlargement of the town and her planning. Nowadays, after many years of intense exploitation, especially during the strong building industry demand of the 70s and the 80s, most of the quarries are abandoned and not in use. After the Second World War, open pit quarries have been most commonly used because of the better profits that arise from the lower costs of delivery and pile and the possibility to extract the whole thickness of the rock bank. Nevertheless the open

pit quarries guarantee a better safety and healthiness working conditions. The extraction galleries show different shapes of typical sections: they can have a plane intrados or, rarely, a toppling flight steps. Rough pillars, based on quadrangular sections of 1 to 9 m^2, support the intrados in one level hypogeous cavities. The sections of these pillars can increase up to 50 m^2 and more for overlapping extraction rooms. Sometimes, for cavities placed side by side, the thin rock septum that separates them is committed to support the stability of the whole structure. Signs of the cutting equipment are evident on the quarry walls: vertical and horizontal cuts have been left by the cutting machine or, in the oldest quarries, by the axe used for the ashlar cut. Hence, it has been possible to recreate the cutting technique used during different historical periods: before the industrial age, ashlars were hand made, and with the passing of time, the extraction process has been mechanized. As a result, the working speed and the areas of exploitation increased. Consequently, the cavity dimensions have increased and the cover of some cavities has reduced to a thickness of few meters. It is worth mentioning that the exploitation of these quarries has been severe at all depths and that sometimes, when the quality of the rock bank allowed it, it has reached very high depth and it has stopped at the groundwater table. The present research regards the study of the *Cave di Calcarenite di Marsala in contrada Cuccidenna,* Figure 1a. The quarries in *Contrada Cuccidenna* summarize all the aspects of this manufacturing activities which have taken place from the beginning up to this day and age, in an amazing, large and complex sequence of open pit (Figure 1b) and underground areas (Figure 1c e Figure 1d).

These last figures show the different cutting techniques. Regarding the cutting technique, the material was removed gradually from the top down to the bottom, following horizontal and consequential planes.

Even more than 10 meters deep shafts guarantee the access to the galleries, the cross-ventilation and the way out for the extracted ashlars. The rock used to be cut laterally, in order to reach the higher quality material. Large rock pillars were left to support the structure that arises from the cutting and that consisted in big cavities, which could penetrate deeply into the rock mass, even hundred meters from the entrance shafts. The waste material was not removed: this end material, which generally represented the 30% of the entire excavated volume, was abandoned in piles in the areas that were already exploited, exactly along the gallery flanks.

The quarries in *Contrada Cuccidenna* are next to a deep artificial depression, confined by a versant created for the extractive activities. This slope

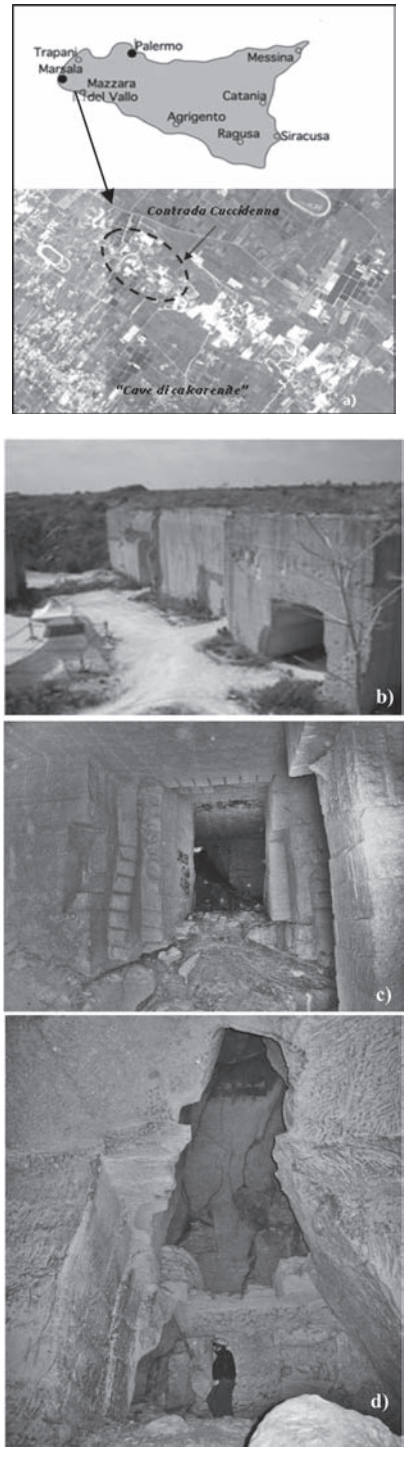

Figure 1. a) Map of "Cave di Calcarenite" b) open pit c) cutting machine signs in an underground d) axe signs in an underground cavity.

is characterized by a spontaneous and luxuriant vegetation, which occurred when the quarries were abandoned and the working activities ended. Nowadays, the deep depression is progressively filled by the waste material, which is partially coming from the closest cavities and partially coming from the close active quarries.

Regarding the site geometry, it is the result of the cutting progression. It consists in numerous crossing cavities, which are large from 6 m to 27 m and high from 8 m to 21 m.

2 ROCK MASS MESOSTRUCTURAL CHARACTERIZATION

The rock formation *Calcarenite di Marsala*, which formed in the lower Pleistocene, crops out in the south-west quadrants of the province of Trapani along a band directed NW-SE upon an area of 300 km^2. This rock formation can even reach thickness of about hundred meters.

The rock banks used for commercial purposes, reach the dimension of more than 10 meters in the middle-northern area. On the contrary the rock banks became extremely thin towards south.

The lithological and particle size characteristics of the rock formation *Calcarenite di Marsala* are extremely variable. This variability, in both direction vertical and horizontal, reflects the multitude of involved depositional mechanisms (Arces et al.,1998) and it is characterised sometimes by sandy, sandy-silty lenses or levels that can be interposed among the cemented levels of *Calcarenite*.

The rock mass mesostructure, which has been detected both at the surface and in the underground, is featured by discontinuities that are normal to the layers. These joints have an high or very high persistence (>10 m) and a wide or moderate spacing (5–7 m). Three families of discontinuities characterised the mesostructure of this rock formation as shown in Figure 2 in which modal values of the dip and the dip direction are given.

If a big scale observation is made, the discontinuities appear lightly waved. On the contrary, at small scale, the joint surfaces appear substantially plane. It is worth noting that the presence of discontinuities does not influence the stability, with the exception of the case in which the natural discontinuity is next to a cut wall. Since the upper cavities are 10–15 m large, the rock mass can be considered as a homogeneous and continuous medium characterised by the mechanical and physical features of the intact rock.

The cavity ceiling is always next to the ground level, which lies 3–4 m above for the youngest quarries and about 10 m above for the oldest ones.

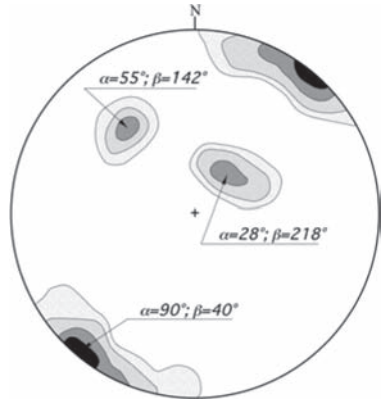

Figure 2. Isodensity diagram of the rock mass.

3 PETROGRAPHIC AND GEOTECHNICAL CHARACTERISATION OF THE INTACT ROCK

For the experimental programme, in the hypogeous cavities, 12 ashlars have been extracted (20 cm large, 18 cm high and 40 cm long). Despite the extreme variability of the texture in the *Calcarenite di Marsala*, in the considered site the rock is very uniform.

To correlate the textural characteristics with the mechanical behaviour, 8 thin sections have been observed in transmitted light by means of a petrographic microscope.

The rock is a biocalcarenite characterized by a uniform composition. The bioclasts are here presented in decreasing order of present percentage: fragments of rhodolithes, fragments of mollusc shells and foraminifera. Briozoa, entrochi and anellida are sporadically present. Lithoclasts, made of fragments of carbonate rocks and monocrystalline or polycrystalline grains of quartz silt, are present at very low percentage.

The particle size distribution of the grains is well graded: the particle size varies between 0.1 mm to 8 mm and the modal value is about 0.8 mm. Sphericity is good for all the bioclasts and lithoclasts except for the fragments of mollusc shells that are flat and elongeted. Roundness is high in the most cases. The grain contacts are, with the same frequency, of tangential or of flattened type. In rare cases, the flat grains show an oriented fabric.

A very thin film (about 10–50 μm thick) of calcite cement wraps totally the grains, as shown in Figure 3. The crystals are microsparitic in size (7–50 μm is the thickness of the cement coating) and appear usually placed side by side in a single level.

If compared to the total volume of grains and pores, cement is of low amount, except for a thin

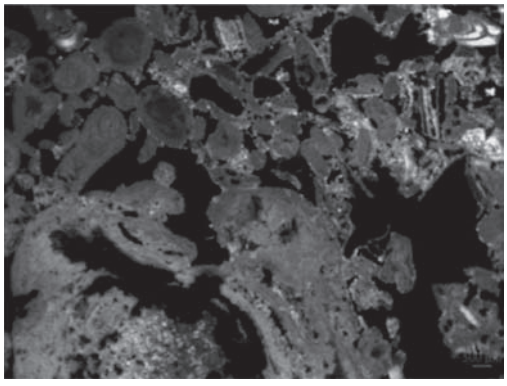

Figure 3. Thin section of the Marsala lithotype.

section referring to a fault surfaces, characterized by micritic cement, which almost fill the interparticle voids. On the contrary all other samples show a low amount of cementation: interparticle and intraparticle porosity is open. As for void volume, the porosity has been evaluated by means of optical comparing tables, and it is about 40–45%. Pores size varies between 0.8 to 0.12 mm.

According to Zimbardo et al. (2011), the pores have been classified as *macropores* when their size is a multiple of the modal size of the grains, *mesopores* when they have about the same size of the modal size of the grains, and *micropores* when the size is lower than the modal size of the grains or like the smallest grains.

Mesopores and micropores are uniformly distributed, macropores are less in volume than the formers and are present in restricted areas. The rock can be described as sponge fabric (lithotype B2, Zimbardo et al., 2011).

The void index is variable between 0.84 and 1.01, the dry unit weight is between 13.4 kN/m^3 and 14.9 kN/m^3 and a modal value of 14.2 kN/m^3 can be estimated. The slaking test results show values of the durability index I_d between 0.83–0.92. These values highlight the strong cementation bond, despite the low percentage of cement and the high porosity.

Regarding the mechanical properties of the rock, the uniaxial rock strength has been investigated for saturated and dry samples and values between 1.2 MPa and 4 MPa have been detected. Although high values have been determined for dry samples, the rock is always classified as a rock with very low strength.

In Figure 4 the Miller diagram shows that the test values are in the average ratio of the tangent elastic moduli. The tangent elastic modulus at the 50% of the ultimate strength is between 300 MPa e 1500 MPa.

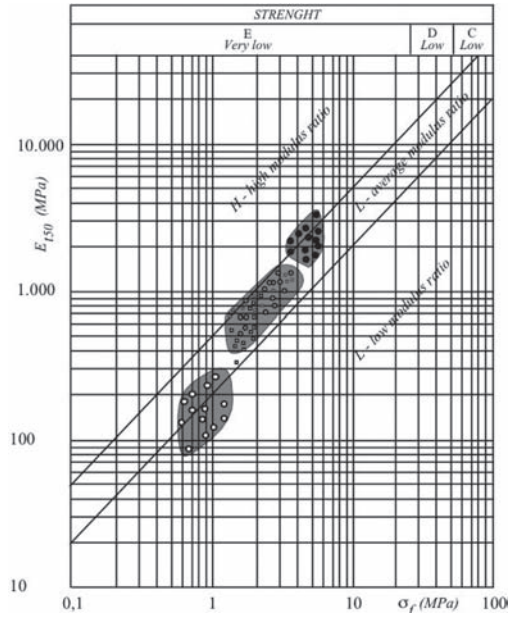

Figure 4. Miller diagram: Uniaxial tangent stiffness at 50% ultimate strength versus uniaxial strength.

These values are intermediate between those typical for lithotype C and lithotype B1, and are similar to values estimated on rock samples coming from close quarries.

The yielding stress obtained by means of isotropic compression tests (Figure 5) is 3 MPa. It is possible to notice that the material mechanical behaviour is typical of strong bonding since the yielding is on the right of the Normal Compression Line (NCL) (Coop & Cuccovillo, 1997).

With the yielding, an elevate decrease of volume occurs and the material becomes progressively denser. As shown in Figure 6, the same behaviour has been observed during triaxial tests and, elaborating the test results, the shear strength parameters at failure ($c' = 0.23$ MPa, $\phi' = 35°$) have been estimated.

According to all tests carried out, both isotropic and triaxial compression, a unique yielding surface has been drawn in Figure 7.

4 NUMERICAL ANALYSIS FOR SAFETY ASSESSMENT

In Figure 8 the geometrical model used for the stability and safety analysis is shown for the quarry site in study in *Contrada Cuccidenna*. The geometrical model consists in a section with cavities next to the depression created for the open pit quarries.

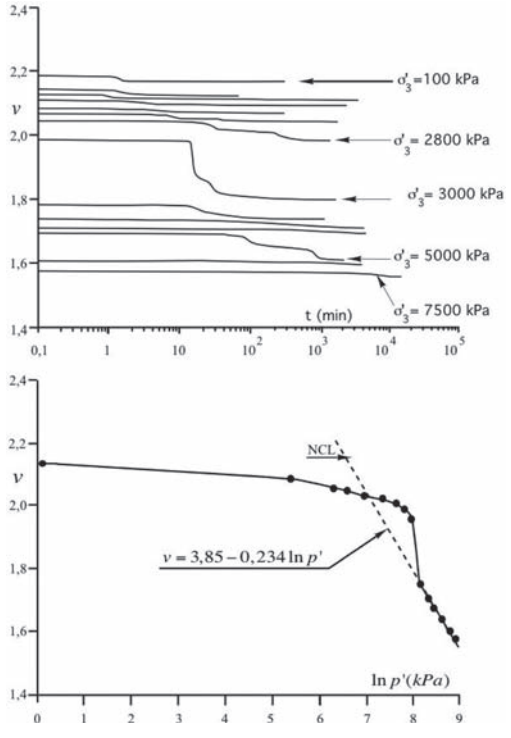

Figure 5. Specific volume changes during isotropic compression for test A1.

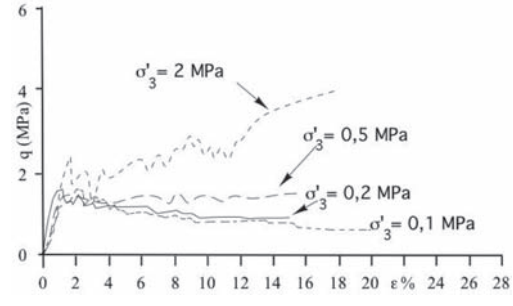

Figure 6. Drained triaxial tests.

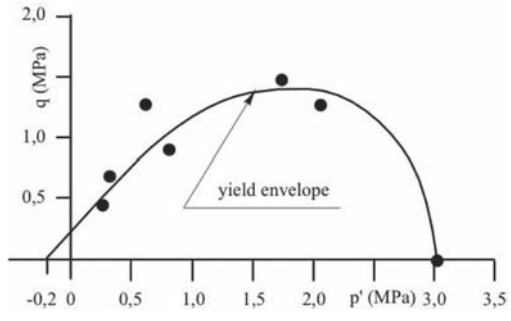

Figure 7. Yielding surface. Data from triaxial and isotropic tests.

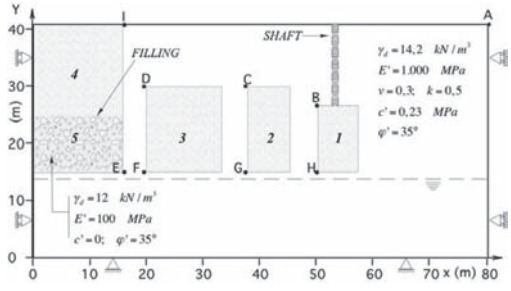

Figure 8. Geometrical definition of the model.

The cavity dimensions have been determined directly in situ by means of a laser distance meter. After the geometrical definition of the model, the numerical analysis has been carried out in a plane deformation state using a finite element program where triangular elements with 15 junctions and 12 Gauss points have been considered.

Considering domains of different extensions (between 80 m and 102 m) it has been demonstrated that the stresses are substantially uninfluenced by the domain length, therefore the lowest extension has been chosen, since the displacement was zero for the boundary point (Fig. 8 point A) at the ground level on the right. Because of the high values of discontinuities spacing (>5–7 m), Mohr Coulomb has been adopted as failure criterion to consider in the numerical analysis.

A lithostatic initial stress state has been considered and a value of 0.5, for the lateral coefficient of earth pressure at rest, has been considered. In the Figure 8, the mechanical parameters obtained by the experimental tests and used in the model are shown. Simulations corresponding to the geometrical configurations of cavities during the different historical periods have been performed. In the same figure, it is possible to observe the cutting sequence estimated on the base of statements of quarrymen descendants and their historical reconstruction has been highlighted with a progressive numeration.

Hence, at the beginning, the stress states has been referred to the quarry state with the realisation of the cavity n°1 only. Developing the analysis, the realisation of successive cavities and the final partial filling of the open pit quarries with the waste material have been taken into consideration, as shown in the Figure 8.

Hence, the presence of only one cavity has been considered in the first cycle of numerical analysis. Dimensions have been assigned to the cavity, which is 7 m large, 11 m high and accessible through a shaft 13 m deep (Fig. 8 phase 1). The cavity has been realised by means of an excavation that stopped at about 1–2 m from the groundwater table. A maximum deviatoric stress of 690 kPa has been reached in correspondence to the edges of the cavity (points B and H of Fig. 8).

During the second phase (phase 2), a septum 5 m thick separates the first cavity and the second. The excavation of the second cavity started at a deepness from the ground level of about 9 m and it stopped at the same deepness of the previous cavity.

The second hypogeous cavity is 7 m large and 15 m high and, even in this case, a maximum deviatoric stress of 720 kPa has been reached in correspondence to the base edge of the cavity (point G of Fig. 8). At the same time, deviatoric stresses in proximity of points H and B have scarcely increased.

As for the third cavity (phase 3) that is 13 m large and 15 m high, the walking floor and the distance from the ground level are at the same depth as the previous cavities. In this cavity, a maximum deviatoric stress of 890 kPa has been reached in correspondence to the edges of the cavity (points D and F). At the same time, the stress state in proximity of the close cavities did not increased. On the contrary, deviatoric stresses in all septa between two close cavities (1–2 and 2–3) have increased up to a maximum value of vertical stresses so that the ratio between the uniaxial resistance and these vertical stresses (σ_c/σ_v) is always more than 3.5 (Evangelista et al., 2000).

Once the excavation in the underground quarries has been ended, the extraction has been proceeded in open pit quarries: a depression with sub-vertical walls has been created in successive steps of excavations, which moves deeply towards the ground water table and crossing somewhere the cavities walls (phase 4 of the numerical analysis).

As much as the open pit excavation proceeds, the deviatoric stresses increase and concentrate both at the open air in proximity of the base of the septum which separates the open pit wall with the third cavity and both in the underground in correspondence of its ceiling.

In these two areas, a high deviatoric stress of 1280 kPa has been reached. On the contrary, in correspondence to the base edge of the cavity, the vertical stress increased so that a reduction of the ratio σ_c/σ_v occurs and a value of 2 is reached. Meantime, an increment of deviatoric stresses between the biggest cavities ceiling and the ground level occurs.

At this phase, the cavity covering starts to be exposed to a deviatoric stress range of 200–400 kPa.

In the ceilings, particularly in the third cavity, this ratio between the mobilized shear strength and the ultimate one can increase up to a value of 0.7 but the stability is still assured. The safety condition, described by this ratio, is confirmed by the stress paths, which developed during excavations.

The septum between the open pit quarry and the third cavity shows localised plasticized areas that indicate that the ultimate shear strength has been reached (Fig. 9).

Indeed the shear strength contours show values of 1 for the ratio between the mobilized shear strength and the ultimate one in correspondence to the bottom of the third cavity and the open pit wall (D stress path in Fig. 10). For all the other points and in every excavation phase, stress paths confirm the safety conditions, as shown in Figure 10 where stress paths for points E, D and F are presented.

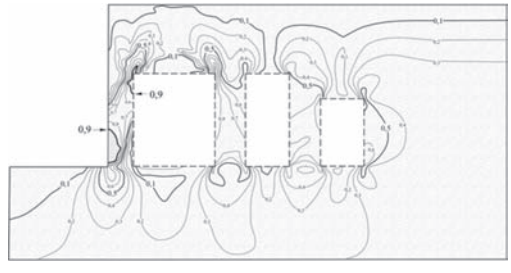

Figure 9. Shear strength contours: Phase 4.

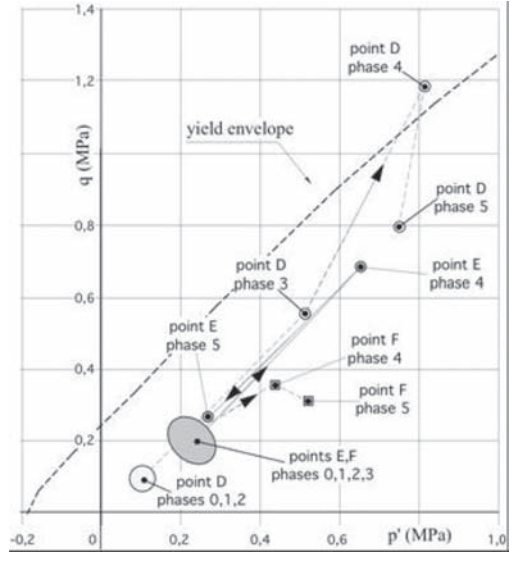

Figure 10. Stress paths and yield envelope.

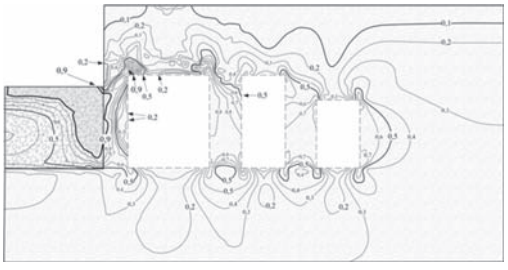

Figure 11. Shear strength contours: Phase 5.

When the open pit is realized, a redistribution of stresses follows and, in correspondence of points D, E and F of the new pillar between the open pit with the third cavity, an increment of the effective mean stress p′ occurs because of the reduction of the section on which the cover weight is applied.

In the same diagram, the yielding envelope is drawn. This curve highlights the passage from the purely elastic behaviour to the elastoplastic behaviour. The D stress path reaches and cross the yielding surface and the plasticization condition occurs. However the ultimate strength stress is not reached, all stress paths point out the possibility for different areas to reach elevate strains which are linked to destructuration processes that can occur in the material. Even if the ratio between the uniaxial strength and the vertical stresses (σ_c/σ_v) is far from 1, the previous results indicate a risk condition, due to the rheologycal behaviour of the *Calcarenite,* that is not negligible for the third cavity.

The last phase of the numerical analysis (phase 5), corresponds to the partial filling of the open pit quarries with the waste material. As shown in Figure 11, stress contours show an improvement of safety conditions, especially in the underground cavities. Also stress paths highlight the described improvement and in Figure 10 it is possible to notice the coming back of the stress paths (see ending points).

As a consequence of the filling procedure, also the end material can be subjected to a stress state close to the plasticization: the material is often throws without an adequate constipation and strains occur in correspondence of the external basements.

5 CONCLUSIONS

The possibility to extract a wide quantity of material in a very high speed is a consequence of progresses in the used technologies, which have allowed the passage from manual methodologies of extraction to industrial techniques. Cavities realised with manual techniques show heights, extension and septum thickness and ceiling thickness that guarantee an high value of the safety factor, which decreased severely when big cavities have been realised by the industrial cutting equipment (steam and after electrical). As a consequence of the enlargement of the cavities, the ceiling thickness has reduced substantially down to values of few meters. Above these cavities, buildings and civil structures have been realised and the safety conditions decreased consequentially.

The better safety and healthiness working conditions have promoted open pit quarries, which used to be realised deep in the ground down to the water table. This procedure creates wide pits in the calcarenite bank, which can be sometimes next to hypogeous cavities.

In the *Cave di Contrada Cuccidenna*, the plasticization of some areas occurs as a consequence of excavations and the safety condition get worse.

Further instability might occur because of the degradation phenomena of the exposed rock or because the ground water table can be very close to the foot of the quarry structure. Indeed, in this case, extremely intense rainfall events can increase the level of the ground water table and a saturation of the lower Calcarenite levels might occur.

If a fruition of the area is planned, both of the above phenomena need to be carefully studied and solved.

At the moment, the partial filling of the open pit quarries with the waste material, in the *Cave di Contrada Cuccidenna*, improves the safety conditions and limited possible destructuration phenomena which might occur at the ceiling edges and at the septum walls or, rarely, at their basement. As a consequence of an inadequate constipation of the filling waste material, differential settlements might occur and endanger the access to the internal and the external areas of the quarry.

The touristic enjoyment of this amusing industrial archaeological heritage is possible and desirable on condition that, besides the necessary studies of instability phenomena, the stability operation project is done after an accurate monitoring of the deformation and stress state processes, particularly for the septa next to the open pit excavations.

ACKNOWLEDGMENT

The authors are grateful to Mr. L. Foderà, owner of the *Cave in Contrada Cuccidenna*, who allowed the access to the area and the rock sampling for the mechanical characterization. The authors would also like to express their gratitude to the speleologist Mr. T. Giordano for his contribution to the sampling and detection of hypogeous

cavities. A thank goes to Professors C. Gullo for his comments on cutting historical techniques and historical data. The authors are indebted to *Soprintendenza BB.CC.AA.* of Trapani for the thematic historical charts supply.

A special thank goes to Professors N. Nocilla for his advice in the interpretation of the data.

REFERENCES

Arces, M., Nocilla, N., Aversa, S., Lo Cicero, G. 1998. Geological and geotechnical features of the "Calcarenite di Marsala". *Proc. 2nd Int. Symp. on "Hard Soils—Soft Rocks", Naples, 12–14 Oct. 1998*. Balkema, Rotterdam, 1, 15–25.

Arces, M., Aversa, S., Nocilla, N., Lo Cicero G. 2000. The Pleistocene "Calcareniti di Marsala: Geotechnical and Sedimentological Characterisation". *Memorie Società Geologica Italiana, 55.*

Coop, M.R. & Cuccovillo, T. 1997. Yielding and pre-failure deformation of structured sands. Géotechnique, 47(3), 491–508.

Corkumb, B.T. 1997. Three Dimensional triangulated boundary element meshing of undergroun excavations and visualization of analysis data. *Thesis of Doctor of Philosophy. Department of Civil Engineering, University of Toronto.*

Evangelista, A, Feola, A, Flora, A, Lirer, S., Maiorano, M.R.S. 2000. Numerical analysis of roof failure mechanism of cavities in a soft rock. *Geoeng, Melbourne.*

Evangelista, A, Flora, A, Lirer, S., De Sanctis, F., Lombardi G. 2002. Studi e interventi per la tutela di una patrimonio sotterraneo: l'esempio delle cavità di Napoli. *XXI Convegno Nazionale di Geotecnica L'Aquila.*

Kavvadas, M.J. 2000. Modelling the soil behaviour—Selection of soil parameters. The Geotechnics of Hard Soils-Soft Rocks—Balkema, Rotterdam.

Rodolico, F. 1953. Le pietre delle città d'Italia. F. Le Monnier.

Zimbardo, M. 2010. Comportamento meccanico di rocce tenere: le calcareniti di Palermo e Marsala, Thesis of Doctor of Philosophy. Department of Civil Engineering, Università degli Studi di Napoli Federico II.

Zimbardo, M., Nocilla, N., Ercoli, L. 2011. Petrographic and textural characteristics and mechanical behaviour of Sicilian calcarenites. *Proceedings of the 15th European Conference on Soil Mechanics and Geotechnical Engineering* (*goetechnics of hard soils/soft rocks*). A. Anagnostopoulos al. (Eds.)

Zimbardo, M., Nocilla, N., Evangelista, A., Ramondini, M., Scotto di Santolo, A. 2010. Destructuration of typical sicilian calcarenites. *Bullettin of Engineering Geology and the Environment,* Ed. Springer.

All the traces of historic heritage are a fundamental part of our environment and reward us in the form of cultural enrichment, with the ability to have a positive effect both on our lifestyle and economy. Therefore, the preservation of ancient monuments, historic towns and sites has increasingly drawn the attention of public opinion, governmental agencies as well as consultants and contractors. This interest must be however carefully controlled and directed, since the conservation of monuments and historic sites is one of the most challenging problems of our age. Careless attempts at preservation can be detrimental not only to their iconic value (formal integrity), but even to their structural characteristics and the materials they are built with (material integrity).

Geotechnical Engineering for the Preservation of Monuments and Historic Sites collects one opening address, four special lectures and 82 contributions from all over the world, giving a unique sample of the geotechnical problems to be tackled, the solutions currently being proposed, and the strategies being carried out to preserve the overall integrity of monuments and historic sites. It is clearly apparent that differences exist around the world not only in terms of the characteristics of the monuments or sites to be preserved, but also in the approaches adopted to achieve this aim. Hence, no unique solution is available to the geotechnical engineer dealing with the delicate structures and sites that represent our cultural heritage, and knowledge of previous experiences may be a unique guide in any technical decision-making process.

Front: Palazzo donn'Anna (Naples), picture by Eugenio Lupoli

ISBN 978-1-138-00055-1

CRC Press
Taylor & Francis Group
an **informa** business
www.crcpress.com

6000 Broken Sound Parkway, NW
Suite 300, Boca Raton, FL 33487
Schipholweg 107C
2316 XC Leiden, NL
2 Park Square, Milton Park
Abingdon, Oxon OX14 4RN, UK

an **informa** business